सत्यमेव जयते

INDIAN AGRICULTURAL
RESEARCH INSTITUTE, NEW DELHI

35835-836

I.A.R .6.
GIP NLK—H-3 I.A.R.I.—10-5-55—15,000

Discussions of the Faraday Society

No. 8, 1950

HETEROGENEOUS CATALYSIS

THE FARADAY SOCIETY
Agents for the Society's Publications:
The Aberdeen University Press Ltd.
6 Upper Kirkgate
Aberdeen

The Faraday Society reserves the Copyright of all Communications published in the "Discussions"

PUBLISHED . . SEPTEMBER, 1950

A GENERAL DISCUSSION

ON

Heterogeneous Catalysis

A GENERAL DISCUSSION on Heterogeneous Catalysis was held in The New Arts Theatre, Liverpool University (by kind permission of the Vice-Chancellor) on the 12th, 13th and 14th April, 1950. The President, Prof. Sir John Lennard-Jones, K.B.E., F.R.S., was in the Chair and about 250 members and visitors were present.

Among the distinguished overseas members and guests welcomed by the President were the following :—

> Dr. O. Beeck (U.S.A.), Dr. Behrens (Uruguay), Mrs. Behrens (Uruguay), Mr. Bevington (Holland), Dr. J. J. A. Blekkingh (Holland), Prof. J. H. de Boer (Holland), Dr. H. de Bruijn (Holland), Dr. E. W. Cook (U.S.A.), Ir. A. Cranendonk (Holland), Dr. J. K. Dixon (U.S.A.), Mrs. J. K. Dixon (U.S.A.), Dr. V. Haensel (U.S.A.), Dr. G. D. Halsey (U.S.A.), Dr. H. Hoog (Holland), Prof. G. F. Huttig (Austria), Prof. G. H. Jura (U.S.A.), Dr. S. Kruyer (Holland), Mr. J. Mignolet (Belgium), Dr. J. A. Morrison (Canada), Dr. A. G. Oblad (U.S.A.), Mrs. A. G. Oblad (U.S.A.), Prof. L. J. Oosterhoff (Holland), Mr. A. Orzechowski (Poland), Dr. L. L. Reyen (Holland), Dr. G. C. A. Schuit (Holland), Prof. G.-M. Schwab (Greece), Prof. P. W. Selwood (U.S.A.), Mr. K. Sutherland (Australia), Dr. G. J. Szasz (U.S.A.), Dean H. S. Taylor (U.S.A.), Dr. E. W. Thiele (U.S.A.), Dr. J. R. Vinograd (U.S.A), Dr. S. El. Wakkad (Egypt), Dr. A. E. R. Westman (Canada), Dr. R. Westrik (Holland), Prof. E. Wicke (Germany).

The President addressed a special welcome to Dean H. S. Taylor (Princeton University, N.J.) on calling upon him to give the Fifth Spiers Memorial Lecture, " Surface Catalysis : Retrospect and Prospect ".

The President recalled that the Spiers Memorial Lecture was founded in honour and memory of the Society's first secretary, Frederick Solomon Spiers, and that the interest on the Memorial Fund was available for the payment of an honorarium to a lecturer on some subject of physical chemistry.

The first lecture was given on the occasion of the Silver Jubilee of the Society in 1928. The subject was " Some Debatable Problems in Physics ", and the lecturer was Sir Oliver Lodge. The second was given in 1938 by Sir Robert Ludwig Mond on " Faraday ". Subsequent lectures were by Sir William Bragg in 1934 and Dr. W. T. Astbury in 1937.

In 1939, the Council decided that future lectures should take the form of an Introduction to one of the Society's Discussions but, owing to the war, this was not brought into effect. Recently the Council re-affirmed its intention of instituting these lectures from time to time in connection with its Discussion and accordingly invited Prof. Taylor, one of the leading exponents of the subject of Heterogeneous Catalysis, to give the first of these lectures on the occasion of the present Discussion. The lecture is published in full in the present volume.

Contents

PAGE

General Introduction 3

5th Spiers Memorial Lecture : Catalysis : Retrospect and Prospect. By Hugh S. Taylor 9

I. Theories of Adsorption and Properties of Surface Layers—

Behaviour of a Molecule near a Metal Surface. By K. Huang and G. Wyllie 18

On Conditions for the Existence of Surface States. By C. A. Coulson and G. R. Baldock 27

A Calculation of Heats of Chemisorption. By D. D. Eley . 34

The Activated Complex in Chemisorption and Catalysis. By Henry Eyring, Charles B. Colburn and Bruno J. Zwolinski 39

The Activated Complex in Heterogeneous Catalysis. By Keith J. Laidler 47

The Role of Heterogeneity in Adsorption and Catalysis. By G. D. Halsey, Jr. 54

Statistical Aspects of Chemisorption. By A. R. Miller . . 57

The Kinetics of Catalytic Reactions on Inhomogeneous Surfaces. By H. de Bruijn 69

General Discussion.—Dr. J. G. M. Bremner, Prof. G.-M. Schwab, Dr. A. R. Miller, Mr. N. Thomas, Dr. G. Wyllie, Dr. K. W. Sykes, Dr. K. G. Denbigh, Dr. D. M. Young, Dr. F. C. Tompkins, Prof. D. H. Everett, Prof. R. M. Barrer, Dr. G. D. Halsey, Jr., Dr. G. H. Twigg, Prof. K. J. Laidler, Mr. A. E. J. Eggleton, Dr. O. Beeck, Prof. J. H. de Boer, Mr. R. S. Bradley, Mr. C. Kemball, Dr. H. de Bruijn, Dr. A. F. H. Ward 79

II. Adsorption and Catalysis on Metals—

Introductory Paper (i). By Eric K. Rideal. 96

Introductory Paper (ii). By D. D. Eley 99

Studies in Contact Potentials—

Part I.—The Adsorption of Some Gases on Evaporated Nickel Films. By J. C. P. Mignolet 105

The Mechanism and Temperature Coefficient of the Para-Hydrogen Conversion. By E. K. Rideal and B. M. W. Trapnell 114

Hydrogenation Catalysts. By O. Beeck 118

On the Existence of Active Centres in Chemical Adsorption and Contact Catalysis. By A. Eucken 128

The Relationship between Sensitivity to Poisoning and Catalytic Surface. By E. B. Maxted, K. L. Moon and E. Overgage 135

CONTENTS

PAGE

The Mechanism of Ammonia Oxidation and certain Analogous Reactions. By J. Zawadzki 140

The Mechanism of the Catalytic Hydrogenation of Ethylene. By G. H. Twigg 152

The Effect of Crystal Parameter on Hydrogenation and Dehydrogenation. By O. Beeck and A. W. Ritchie . 159

Alloy Catalysts in Dehydrogenation. By George-Maria Schwab 166

The Parahydrogen Conversion on Palladium-Gold Alloys. By A. Couper and D. D. Eley 172

Some Reactions over Alloy Catalysts. By D. A. Dowden and P. W. Reynolds 184

General Discussion.—Dr. D. D. Eley, Dr. B. M. W. Trapnell, Sir Charles Goodeve, Dr. O. Beeck, Dr. P. A. Wright, Dr. F. S. Stone, Prof. W. E. Garner, Mr. A. E. J. Eggleton, Mr. P. R. Rowland, Mr. P. Zwietering, Prof. G.-M. Schwab, Prof. E. Wicke, Dr. J. J. A. Blekkingh, Mr. P. F. Tiley, Dr. F. C. Tompkins, Prof. A. R. Ubbelohde, Mr. A. S. Porter, Mr. D. A. Dowden, Dr. G. C. A. Schuit, Prof. R. M. Barrer, Prof. J. H. de Boer, Dr. N. Uri 191

III. Adsorption and Catalysis on Oxides—

Introductory Paper. By W. E. Garner 211

Catalytic Activity and Composition of Oxide Systems. By G. F. Hüttig 215

Structure of Oxide Catalyst Systems. By P. W. Selwood and Lorraine Lyon 222

The Use of ^{18}O in Studies of the Reactivity of Solid Oxides. By E. R. S. Winter 231

Electronic Conductivity and Surface Equilibria of Zinc Oxide. By D. J. M. Bevan and J. S. Anderson 238

Reactions on the Surface of Copper Oxide. By W. E. Garner, T. J. Gray and F. S. Stone 246

Part I.—Semiconductivity Measurements. By T. J. Gray and S. D. Savage 250

Part II.—Surface Processes and Heats of Adsorption. By F. S. Stone and P. F. Tiley 254

The Physical Properties of Promoted Molybdenum Dioxide Catalysts. By R. H. Griffith, P. R. Chapman and Miss P. R. Lindars 258

Some Notes on Oxide Catalysts for Dehydrocyclization. By H. Steiner 264

Chemistry of the Surface and the Activity of Alumina-Silica Cracking Catalyst. By M. W. Tamele 270

The Chemical Characteristics and Structure of Cracking Catalysts. By T. H. Milliken, Jr., G. A. Mills and A. G. Oblad 279

PAGE

The Mechanism of the Catalytic Cracking of Unsymmetrical Diarylethanes. By D. R. May, K. W. Saunders, E. L. Kropa and J. K. Dixon 290

General Discussion.—Mr. D. A. Dowden, Dr. U. R. Evans, Prof. G.-M. Schwab, Prof. W. E. Garner, Dr. G. C. A. Schuit, Dr. R. H. Griffith, Dr. E. R. S. Winter, Dr. H. de Bruijn, Dr. P. H. Given, Dr. J. Weiss, Dr. A. G. Oblad, Dr. D. D. Eley, Dr. Alwyn G. Evans, Dr. Herman E. Ries, Jr., Dr. John S. Melik, Dr. Marvin F. L. Johnson, Dr. J. K. Dixon, Dr. J. S. Anderson, Dr. P. W. Selwood, Mr. N. W. Luft 296

IV. Techniques—

Introductory Paper. By J. W. Mitchell 307

The Adsorption of Gases on Copper Films. By J. A. Allen and J. W. Mitchell 309

Determination of Heats of Adsorption using Metal Films. By O. Beeck, W. A. Cole and A. Wheeler 314

The Measurement of the Thermal Properties of Gases and Vapours Adsorbed on Solid Surfaces. By J. A. Morrison and J. M. Los 321

Studies in Contact Potentials—

II.—Vibrating Cells for the Vibrating Condenser Method. By J. C. P. Mignolet 326

Semi-Conductivity and Catalysis. By T. J. Gray. . . . 331

Proton Relaxation and Catalyst Accessibility. By P. W. Selwood and F. K. Schroyer 337

Study of Catalysts by Scattering of X-rays at Small Angles. By A. Guinier 344

Electron Microscopy and Small Angle X-ray Scattering. By John Turkevich, Harry H. Hubbell and James Hillier . 348

Stable and Unstable Isotopes in Catalytic Research. By John Turkevich, Francis Bonner, Donald Schissler and Peter Irsa 352

General Discussion.—Mr. J. A. Allen, Mr. A. S. Porter, Dr. J. W. Mitchell, Mr. B. M. W. Trapnell, Mr. P. F. Tiley, Dr. J. S. Anderson, Dr. D. D. Eley, Mr. P. R. Rowland, Prof. J. H. de Boer, Dr. T. J. Gray, Dr. A. F. H. Ward . 357

Author Index 366

5th SPIERS MEMORIAL LECTURE

CATALYSIS: RETROSPECT AND PROSPECT

By Hugh S. Taylor

The finest memorial to the first secretary of the Faraday Society is the maintenance of the General Discussions at the highest level of excellence. Wherever physical chemistry is prosecuted, wherever students are acquiring physicochemical science, there the record of the discussions which Secretary Spiers initiated and organized for so many years will be found indispensable.

There is a curious discrepancy in the archives of the Society concerning the General Discussions. In the index of Volume III for 1907 two general discussions are recorded, one on " Osmotic Pressure," one on " Hydrates in Solution ". Sir Oliver Lodge was then President of the Society. In the index to the first twenty volumes of the *Transactions* the earliest recorded General Discussion is in Volume IV, on " The Constitution of Water ". I am at a loss to account for such a discrepancy unless it is a simple oversight. The last General Discussion organized by Secretary Spiers was in October 1925 on " Photochemical Reactions in Liquids and Gases " and was held in Oxford. I was present on that occasion, which marked, as the General Discussions so frequently do, a milestone in the development of the particular phase of physical chemistry then under consideration. For such reasons, and with a peculiar sense of privilege and honour, I am happy on this occasion to introduce a general discussion on " Heterogeneous Catalysis " as the Spiers Memorial Lecturer, in my own University, where, as a student in the departmental library, I first learned to appreciate how greatly these General Discussions can contribute to the definition of the present state of science and in what direction progress may develop.

The present Discussion is the third in a sequence which includes two famous predecessors. In 1922 the Discussion on Catalysis brought forward two basic concepts, that of Lindemann on the nature of unimolecular kinetics and that of Langmuir on reaction at surfaces between adjacently adsorbed reactants, with adsorption restricted to monolayers. The discussion on " Adsorption " in 1932 was concerned, in the main, with slow processes of sorption and evoked, from our President, a definition of van der Waals' and of chemisorption in terms of the potential energies between an impinging molecule and a surface. The diagram brought out clearly the manner in which activation energy of adsorption might be involved, and sharply differentiated physical and chemical processes of adsorption, the differences between which had been indistinct up to that time. It emerged that physical adsorption had little relevance to catalysis at surfaces; the chemisorbed monolayers of Langmuir were the loci of such reactions.

It is pertinent here to emphasize that the Langmuir formulation of surface kinetics was restricted to those surface reactions in which the velocity of interaction on the surface was the rate-determining process. This condition was indeed fulfilled in the classic researches of Langmuir and in further developments by Hinshelwood, Rideal, Schwab and others.

It is useful, however, to recall an example which does not conform to this condition, the decomposition of ammonia on doubly-promoted iron synthetic ammonia catalysts as studied by Love and Emmett.[1] They found a kinetic equation,

$$-\frac{d[NH_3]}{dt} = k\frac{[NH_3]^{0 \cdot 6}}{[H_2]^{0 \cdot 9}},$$

which, on the Langmuir basis, would suggest a strong adsorption of hydrogen on the iron surface and a moderate ammonia adsorption on the surface bare of hydrogen, with nitrogen an inert constituent. We now know that such a view is erroneous; the slow step is the desorption of nitrogen from the surface, the slow sorption being rate-determining in synthesis. This example alone would have justified the emphasis on slow sorption in the monolayer, first discussed by the Society in 1932. The availability of isotopic forms of a given molecular species has revealed the variation in temperatures at which these species will interact on surfaces which still further emphasizes the necessity for the concept of activation energy accompanying their chemisorption on catalyst surfaces. Some examples are cited in Table I.

TABLE I.—INTERACTION OF ISOTOPIC MOLECULES ON SURFACES

Catalyst	Isotope Reaction	Temp. ° C. for Measurable Rates	Reference
Fe synthetic ammonia catalyst, doubly promoted	$H_2 + D_2$	−195	1
,, ,, ,,	$NH_3 + ND_3$	+ 25	2
,, ,, ,,	$N_2^{14} + N_2^{15}$	+450	1, 3
Rhenium	$H_2 + D_2$	+ 25	3
,,	$NH_3 + ND_3$	+100	3
,,	$N_2^{14} + N_2^{15}$	+500	3
Nickel	$H_2 + D_2$	−195	4
,,	$CH_4 + CH_4$	+150	5
Osmium	$N_2^{14} + N_2^{15}$	+250	6

[1] Kummer and Emmett, *Brookhaven Conference Report* (Dec. 1948), p. 1.
[2] Taylor and Jungers, *J. Amer. Chem. Soc.*, 1935, **57**, 660.
[3] McGeer, *Thesis* (Princeton, 1949).
[4] Sadek and Taylor, *J. Amer. Chem. Soc.*, 1950, **72**, 1168.
[5] Wright and Taylor, *Can. J. Res. B*, 1949, **27**, 303.
[6] Guyer, Joris and Taylor, *J. Chem. Physics*, 1941, **9**, 287.

It is important for the further argument that these variations found with technical catalysts are also to be found with the idealized catalysts produced by the Beeck method of evaporating metals to form oriented or non-oriented films. In these cases, also, where purity and cleanliness of surface have been raised to the highest attainable standards, similar variations in the temperature at which chemisorption occurs are found, although there will be differences between films and technical catalysts in the actual temperature range involved. Thus, on nickel films, Beeck has shown chemisorption of hydrogen even at 15° K, but examines interaction between ethane and nickel films only in the temperature range 200-250° C. In contrast to Beeck's measurements on nickel films are those of Eucken and Hunsmann [2] with reduced nickel from the oxide where the adsorption at 20° K shows a heat of van der Waals' adsorption. Chemisorption with 5 kcal. of heat of adsorption is found only at 50° K. While iron films chemisorb nitrogen (as molecules ?) at liquid-air temperatures there is a slow activated adsorption of nitrogen, with a much higher heat of adsorption, around room temperatures. This latter fact is to be contrasted with the studies of Emmett and Brunauer with iron synthetic ammonia catalysts [3] where the slow sorption of nitrogen was measured in the temperature interval from 224 to 449° C.

---

[1] Love and Emmett, *J. Amer. Chem. Soc.*, 1941, **63**, 3297.
[2] Eucken and Hunsmann, *Z. physik. Chem. B*, 1939, **44**, 163.

This example takes us at once to the heart of a problem which it ought to be the objective of this Discussion finally to resolve. In 1925, a concept of the catalytic surface was formulated which emphasized heterogeneity or, as it came to be expressed, the concept of "active centres". A variety of evidence on the properties of technical catalysts, which were the only catalysts then extensively studied, contributed to this concept of active centres. This evidence included observations on adsorption by catalysts both active and inactivated by heat treatment. It attempted to account for the great influence of poisons and promoters, present in minimal amounts, and invoked the existence of centres of high activity, very sensitive to poisoning. The quantitative measurements of poisoning by Pease in the hydrogenation of ethylene and by Almquist and Black on the poisoning action of oxygen on water vapour in ammonia synthesis on iron catalysts were conspicuous examples of such studies. Over the 25-year period, and largely due to the work of Balandin in Russia, of Roberts on the properties of a clean tungsten wire surface and of Beeck and his co-workers on evaporated films, a contrary view has emerged which has sought the interpretation of catalysis solely in terms of the properties of plane faces of crystalline materials, which, by specialized techniques, could be studied in a "clean" condition. It is my purpose to attempt a reconciliation of these two points of view in a more generalized and unifying concept.

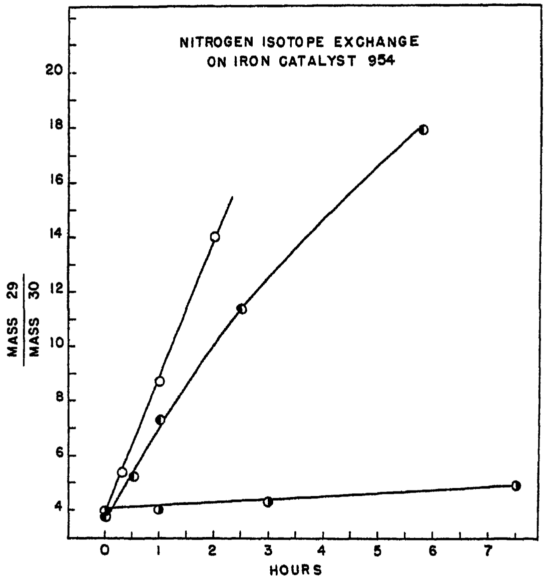

FIG. 1

A recent research by McGeer [4] on the exchange reaction between light and heavy nitrogen on iron synthetic ammonia catalysis and on rhenium surfaces at 450° C provides a clue to such an attempt. The velocity of reaction was shown to be very sensitive to the reduction process to which the catalyst was submitted prior to the velocity measurements. In Fig. 1 the slowest rate is that of an iron-alumina catalyst (No 954, 1·5 % Al_2O_3) which had been prepared by reduction at 450° C with a fast stream of tank hydrogen containing 0·15 % oxygen. The intermediate rate shows the rate of exchange when the same catalyst was subjected to reduction in a stream of hydrogen from which oxygen and water vapour had been removed by the normal techniques of oxygen removal and drying of the gas stream. The residual water vapour was probably well below 0·01 %. The fastest rate of exchange was obtained when excessive precautions were taken to ensure dry, oxygen-free hydrogen for reduction. Similar findings resulted with the rhenium catalyst. The data suffice to show how very sensitive the exchange reaction is to the residual traces of oxygen that are left on an iron surface even with good reduction techniques. In the terminology of 20 years ago this is a typical example of "active centres" on a technical catalyst. It parallels entirely, as it should, the quantitative data obtained by Almquist and Black[5] on an iron-alumina catalyst in ammonia synthesis in presence of water vapour as a poison. The data in Table II recall some of these results.

---

[3] Emmett and Brunauer, *J. Amer. Chem. Soc.*, 1940, **62**, 1732.

[4] McGeer, *Thesis* (Princeton, 1949).

TABLE II.—AMMONIA YIELD AT A SPACE VELOCITY OF 25,000, 444° C AND 1 ATM. PRESSURE

Mg : O_2 retained by catalyst . .	0	5·5	13
% NH_3 produced . . .	0·22	0·06	0·03

The very marked effect of the first 5 mg. of oxygen retained is the more striking since, from B.E.T. measurements of the surface area of this catalyst, only 10 to 15 % of the total surface would be covered by this oxygen. Because the ammonia synthesis reaction is determined in rate by the slow step of chemisorption of nitrogen it is apparent that we must seek the interpretation of the "active centres" or quasi-heterogeneity in the effect of adsorbed oxygen on the surfaces of the iron crystallites. The presence of oxygen results in an increased energy of activation of nitrogen adsorption on the iron surface.

A generalization of this point of view for technical catalysts makes possible a reconciliation between the findings of those who have worked with clean tungsten wires and evaporated metal films and those whose attention has centred on the properties of technical catalysts. In each case one is concerned with the properties of one or more crystal faces of a particular catalytic species. In the case of technical catalysts, however, these properties may be profoundly modified by the presence of poisons as adsorbed oxygen or added ingredients such as alumina in the case just considered.

Our knowledge in this area is being rapidly increased by reason of the studies of electron emission from hot wires and by studies of the properties of semi-conductors. One need only cite the beautiful studies of Müller[6] and of Jenkins[7] relative to the emission of electrons from fine tungsten points as revealed by the field-emission projection electron microscope, and the influence of adsorbed oxygen, barium, thorium and sodium on the emission process. The varying activity of different crystal faces, the preferential adsorption of the poison on particular faces and the migration of poisons at definite temperatures can be visually demonstrated. Especially, however, the data accumulating on semi-conductors demonstrate how profoundly the conducting properties of a pure substance can be modified by traces of a prescribed impurity. One may cite in this respect the recent data of Pearson and Bardeen[8] on the activation of silicon as a semi-conductor by additions of boron. The addition of 0·0013 atomic per cent of boron significantly changes the energy required to release an electron, whilst a concentration of 0·013 atomic per cent lowers this energy to zero. As Mott pointed out recently in the Kelvin Lecture[9] impurity centres may be imagined as " great swollen 'atoms' extending over 10-20 lattice parameters ", a concept pertinent to the whole problem of interaction between adsorbed species on a surface. We must assume, in the case of the iron-synthetic ammonia catalyst already discussed, that the presence of impurity centres raises the activation energy of adsorption of nitrogen as oxygen would raise the activation energy of conduction in zinc oxide semi-conductors. In this manner the findings of Beeck on evaporated iron films can be correlated with those of Emmett and Brunauer and of McGeer with the technical iron catalysts. It is, on this basis, the impurity centre randomly distributed over the plane face of a crystal which would confer on such a crystal face quasi-heterogeneity.

---

[5] Almquist and Black, *J. Amer. Chem. Soc.*, 1926, 48, 2814.

[6] Müller, *Z. physik.*, 1949, 126, 642.

[7] Jenkins, *Reports Prog. Physics*, 1943, 9, 177.

We can draw from the data on semi-conductors further analogies to problems of surface catalysis. Verwey,[10] cited by Mott, has prepared semi-conducting NiO by dissolving in the lattice Li_2O, the radii of the Li^+ and Ni^{++} being practically identical. On heating in air, Li^+ replaces Ni^{++} in the lattice and for each Li^+ introduced a Ni^{+++} ion is formed. The latter are carriers of current by electron displacement. The magnetic measurements carried out by Selwood and his co-workers on valence induction in nickel and other oxides are illustrative of the same effect.[11] Magnetic measurements, on nickel oxide impregnated on γ-alumina supports, indicate that the nickel is present in the trivalent form. On magnesia, the isomorphous divalent oxide is present. On the rutile structure of titania the nickel assumes a valency of four, the oxide being bright yellow in colour. Manganese and iron oxides behave similarly. The relation of valence induction to semi-conductors and to the whole problem of promoter action in catalysis is illuminated by such studies. Let us recall that the activation energy of adsorption of hydrogen by zinc oxide is markedly diminished by incorporating chromium oxide in the preparation.

On the viewpoint here presented poisons and promoters become impurity centres in the normal lattice of the catalyst, the former tending to raise the activation energy of adsorption, the latter to lower it.

A further factor which can be influenced by such impurity centres in a catalyst surface is the heat of adsorption. The data are scanty but what data are available tend to indicate that the measured heats of chemisorption are markedly less on technical catalysts than on the corresponding evaporated films. The data of Beeck recorded for this Discussion on a variety of metal films for hydrogen, ethylene and nitrogen are conspicuously higher heats of adsorption than have been recorded by Beebe, Eucken and others with technical catalysts. Indeed, the high heats of adsorption on evaporated films constitute a grave disadvantage of these films regarded as catalysts. They are, indeed, clean, but they " die " after brief experimentation because they are self-poisoned owing to the high heats of adsorption of one or more of the reactants. The technical catalysts, though " dirty ", at least " live ", largely because of the lower heats of binding to surfaces having " impurity centres ". From such circumstances it can result that a technical catalyst may have a higher activity than an evaporated film. Wright[12] has made one such concrete comparison. With 27 mg. of a nickel-chromia (80 % Ni) catalyst in a reaction volume of 350 cm.^{3}, i.e. 0·077 mg. catalyst per cm.^{3} gas, containing an equimolar hydrogen-ethylene mixture Wright found a half-life of $t_{1/2} = 4$ min. at −78° C. From Beeck's data and his temperature coefficient one computes a half-life of 45 min. at −78° C with 30 mg. nickel film in a reaction volume of 400 cm. or 0·075 mg. catalyst per cm.^{3} of reacting gas. On this basis, the technical catalyst is 11 times as efficient as the evaporated film. The cause is obvious from an examination of Beeck's paper to this Discussion on the reactions of hydrocarbons. Most of his surface is covered with "acetylenic residues" by reason of the high heat of chemisorption of ethylene, thereby becoming ineffective for the catalytic interaction. Beeck's data on the heat of adsorption of hydrogen on clean tantalum, 45 kcal., and on a nitrided tantalum film, 27 kcal. are evidence for a lower heat of adsorption on metal surfaces covered in part with other constituents. Another method of formulating the same idea is that, with technical catalysts, the areas responsible for the high initial heats of adsorption found with metal films are already occupied by impurity centres.

---

[8] Pearson and Bardeen, *Physic. Rev.*, 1949, **75**, 865.

[9] Mott, *Proc. Inst. Electr. Eng.*, 1949, **96**, 253.

[10] Verwey, Haayman and Romeyn, *Chem. Weekblad*, 1948, **44**, 705.

[11] Selwood, *Bull. Soc. chim. France D*, 1949, 489.

[12] Wright, *Thesis* (Princeton, 1949).

Beeck's data for heats of adsorption of hydrogen on his metal films vary directly with the change in *d*-band character of the metals. Boudart has recently[13] shown that Beeck's measurements of activities in the hydrogenation of ethylene on metal films increase with increasing *d*-band character of the metallic bond as given by Pauling, with rhodium of maximum activity. This suggests that "the lattice parameter is not to be considered solely as a cause but as an effect. The primary cause has to be sought in the electronic structure of the metal and a deeper insight into the latter may be obtained by means of Pauling's theory." From this point of view there is a notable discrepancy between the findings with films and technical catalysts in the case of copper. Beeck reports no hydrogen adsorption on films of copper whose *d*-band is filled. Technical copper catalysts have revealed chemisorption of hydrogen from the earliest studies of adsorption on catalysts, with a heat of adsorption of some 10 kcal. It is pertinent to ask whether this discrepancy is to be associated with the intrinsic nature of technical copper catalysts, to what extent it may be a function of a mixed Cu^+—Cu^{++} structure deriving from impurity centres of a promoting character.

Similar considerations, involving activation energy or heat of adsorption or both, animate the research work on catalysis by metal alloy systems. Schwab associates the catalysis in the decomposition of formic acid, on alloys of silver and of gold,[14] with a variety of metals giving both homogeneous and heterogeneous phases, with an entry of protons into the interlattice planes and electrons dissolving in the electron gas of the metal, the required activation energy depending on the degree of completion of Brillouin zones which define the allowed electron energies in the metallic structure. Similarly Couper and Eley[15] have associated the increase in activation energy of the hydrogen-deuterium exchange with the filling of the partly empty *d*-band of palladium by alloying with gold. Dowden[16] has treated the problem in detail theoretically and Reynolds[17] has applied the treatment to experimental findings on homogeneous solid solution binary alloys of Group VIII metals with copper. In all such cases both activity and activation energy should be studied; it is preferable also to study exchange reactions between isotopic molecules in order to minimize the influence of other factors such as displacement effects when two different molecular species are competing for a given surface. In this area there is a wealth of experimental opportunity.

[13] Boudart, *J. Amer. Chem. Soc.*, 1950, **72**, 1040.
[14] Schwab, *Trans. Faraday Soc.*, 1946, **42**, 689.
[15] Couper and Eley, *Nature*, 1949, **164**, 578.
[16] Dowden, *Chem. and Ind.*, 1949, 320; *J. Chem. Soc.*, 1950, 242.
[17] Reynolds, *Chem. and Ind.*, 1949, 320; *J. Chem. Soc.*, 1950, 265.

Parallel studies with oxide systems will be equally interesting. In these, the properties of the catalytic oxide viewed as a semi-conductor will be useful aids to understanding. One example is copper oxide, recently examined by Garner, Gray and Stone,[18] in terms of the electrical conductivities of thin films during formation, on reduction and after adsorption of gases. Oxygen enhances, hydrogen and carbon monoxide depress the conductivity of the Cu_2O—CuO surface. The conductivity is interpreted in terms of a movement of electrons across an array of Cu^+ and Cu^{++} ions. In contrast to cuprous oxide which is an oxidation semi-conductor, zinc oxide is a reduction semi-conductor losing oxygen in a vacuum, the conductivity increasing and the excess zinc atoms entering interstitially into the lattice as ions, the electron being held in the field of the positive charge. In this way the oxide acquires the characteristics of a metal, hydrogenating in character. Foreign ions can enter the lattice substitutionally and interstitially, electrons being trapped in their fields, the radius of the orbit of the trapped electron extending over several interatomic distances. The conductivity of the semi-conductors varies with the temperature and there is evidence that a whole spectrum of energies may be involved.

Our knowledge of the properties of solid catalysts conferred by impurity centres or admixtures of two or more constituents is still very much in the qualitative stage. It is known that the admixture of aluminium oxide in magnetite increases considerably the difficulty of reduction of the iron oxide. On the other hand the admixture of alumina has little influence on the dissociation pressure of copper oxide, but increases considerably the oxygen dissociation pressure with cerium oxide, CeO_2. Chromium oxide admixture strongly increases the dissociation pressure of copper oxide. These findings on dissociation pressure are paralleled by the results of Rienäcker [19] on the catalytic activity of such mixed oxides in the oxidation of carbon monoxide. The added oxide influences both activity and activation energy of the basic catalyst, with marked lowering of the activation energy in those cases where admixture of the second oxide increases the oxygen dissociation pressure, and with increase of activation when the added oxide decreases the reducibility of the basic catalyst.

In the older literature there are many such examples. The old data of Kendall and Fuchs [20] on the influence of added oxides on oxygen release from barium peroxide, silver and mercuric oxides need to be recalled. The influence of added oxides on the slow sorption of hydrogen as illustrated by the accelerating influence of chromium oxide and the retarding effect of molybdenum oxide on the adsorption of hydrogen by zinc oxide is an example in another area. Such material should now be re-examined in the light of data revealed by Selwood on valence induction and with the newer techniques stemming from the study of semiconductors. The catalyst itself, rather than the reactions which occur on it, seems to be the principal objective for future research in the coming years.

This is not to deny the importance of a study of such reactions, since they, also, can reveal the nature and action of the catalyst surface. An excellent example in this respect is the recent work on the nature and functions of cracking catalysts, as exemplified by the recent conclusions of Greensfelder, Voge and Good [21] based on earlier work and newer investigations of the cracking of cetane, cetene and other hydrocarbons thermally and over catalysts such as activated carbon, alumina, silica and alumina-silica commercial cracking catalysts. Two fundamental types of cracking emerge, characteristic both as to the type of primary and secondary reactions. Two types of mechanism are involved. The one involves free radical fragments and the pattern of cracking is described by the Rice-Kossiakoff theory of cracking. This mechanism is characteristic of thermal cracking. The other mechanism is ionic in nature conforming closely to acid-activated, carbonium ion mechanism. Commercial acid-treated clays and synthetic silica-alumina catalysts are of the latter type. Activated carbon, an active, non-acidic catalyst gives a product distribution which can be interpreted as a free-radical type of cracking, quenched, as compared with thermal cracking, by reaction of free radicals with chemisorbed hydrogen on the catalyst to yield the corresponding normal paraffin. With silica-alumina, acidic-type catalysts, isomerization accompanies cracking to yield its particular spectrum of products. Such acidic surfaces are poisoned specifically by organic bases such as quinoline and by potash, ammonia and other alkalis. Oblad and his co-workers indicate that some 4 % of the total surface is involved in such catalyses.

---

[18] Garner, Gray and Stone, *Proc. Roy. Soc. A*, 1949, **197**, 294.

[19] Rienäcker, *Z. anorg. Chem.*, 1949, **258**, 280.

[20] Kendall and Fuchs, *J. Amer. Chem. Soc.*, 1921, **43**, 2017.

[21] Greensfelder, Voge and Good, *Ind. Eng. Chem.*, 1949, **41**, 2573.

Volkenstein [22] has recently analyzed the concepts of adsorption and of adsorption kinetics from the standpoint of the solid catalyst viewed as a structure containing a certain concentration of lattice defects, two-fold in nature. On the one hand, there are macro-defects, such as cracks, whose perturbations exceed those of the crystallographic unit. On the other hand, there are micro-defects which exercise perturbations of the order of the unit cell, the periodic structure being re-established at a distance of a few lattice parameters. In the terminology of semiconductors, these defects include holes or vacant sites, interstitial atoms or ions, ions in a heteropolar lattice with normal position but anomalous charge, or foreign atoms in substitional or interstitial positions. Such defects deform a region of the lattice and it is the region which should be regarded as the defect. It is with the properties of such regions that catalysis may well be associated. Volkenstein introduces into his considerations the concept of mobility of micro-defects with an associated activation energy determined by the nature of the defect and the lattice and by the direction of migration. These micro-defects may react, attract or repel each other, dependent on the charges involved. Two defects may interact to produce a new defect with different properties.

Volkenstein envisages the " disorder " in terms of the total number of defects which is small compared with the total number of unit cells. Disorder may be " biographical ", that which is present at 0° K and arising from the circumstances of the catalyst preparation or it may be " thermal " or that which results from the effect of temperature. The biographical disorder x, at 0° K will increase progressively with temperature to a maximum y at $T = \infty$, the thermal disorder at any temperature varying from 0 at $T = 0°$ K to $y-x$ at $T = \infty$. The relative importance of biographical and thermal disorder depends both on the temperature and the " biography ".

In the older theories of adsorption one assumes (*a*) constancy of adsorption centres, (*b*) immobility of adsorption sites, and (*c*) invariance of sites with coverage. None of these assumptions enter necessarily into Volkenstein's treatment. Volkenstein assumes that adsorption occurs in the defect region. With one kind of defect the surface is energetically homogeneous. With differing defects there will be heterogeneity. Adsorption creates new centres. Increase of temperature increases the number of adsorption centres up to but not beyond the maximum, y. Volkenstein shows that the Langmuir isotherm results when the whole disorder is biographical. When, however, the defect is thermal involving an absorption of energy u, then, depending on the nature of the process producing the new defect whether unimolecular or by bimolecular interaction of two defects, the mathematics shows that, with no heterogeneity of sites and without interaction between adsorbed atoms, the adsorption isotherm may conform to the Freundlich equation, $v_{ads} = kp^{1/n}$, and the differential heat of adsorption can fall from an initial value q to a minimum $q - u$. The curve obtained is reverse sigmoid falling at first slowly, then rapidly and finally asymptotically to $q - u$ at complete coverage. The adsorption centres on the crystal surface operate as a kind of plane gas the concentration of which increases on filling up and the change of energy of which is measured by the differential heat of adsorption.

---

[22] Volkenstein, *Zhurr. Fiz. Khim.*, 1949, **23**, 917.

For the kinetics of adsorption the bimolecular production of sites can be shown to yield either a rapid Langmuir kinetics determined by the rate at which molecules strike the surface or an adsorption proportional to the square root of the time. For a unimolecular production of sites the kinetic expression for adsorption is that typical of the so-called activated adsorption, $k = k_0 \exp(-E_{act}/RT)$. In the theory of activated adsorption a potential barrier between adsorption sites and impinging molecule is assumed. In Volkenstein's treatment it is the number of sites which increases with temperature and proportionally to $\exp(-u/RT)$. No potential barrier is assumed. An alternative method of stating the same is to say that the number of sites remains constant but the number of excited centres which are able to absorb increases as observed.

There are several observations from the older literature on activated adsorption which can readily be interpreted on the bases of the Volkenstein concepts. In the General Discussion for 1932 it was pointed out that the velocity of activated adsorption of hydrogen as measured on zinc oxide was very much smaller than the number of molecules striking the surface with the necessary activation energy. Our subsequent knowledge, from B.E.T. measurements, of surface area indicates that the discrepancy between calculation and observation was of the order of 10^8. A similar discrepancy was noted by Emmett and Brunauer [3] in their careful measurements of the velocity and activation energy of adsorption of nitrogen on synthetic ammonia catalysts. In this case the discrepancy was at least of the order of 10^6. From Volkenstein's point of view these data would involve both the concentration of defect centres and the activation energy of adsorption of the molecule. In the case of doubly-promoted ammonia synthesis catalysts this might well be associated with the iron-potassium-oxide-aluminium oxide centres where the varying valency of iron, the univalent potassium and the trivalent aluminium ions suggest at once the possibility of lattice defects, as was pointed out to me by Boudart. Boudart has also emphasized in this regard the observations of Pace and myself [23] on the identity in the velocities of adsorption of hydrogen and deuterium on oxide catalysts which led to the conclusion that " the activation energy necessary is required by the solid adsorbent ". Other data on the influence of pressure on the velocity of chemisorption of hydrogen on oxides such as chromium oxide gel are also in agreement with the view that velocity is not determined by the number of molecules striking the surface. To account for the slow sorptions observed it was earlier suggested that interaction must occur between the adsorbent and van der Waals' adsorbed gas. The Volkenstein concept represents a mechanism by which such would be achieved.

The apparent saturation capacity of an oxide surface for hydrogen adsorption at a given temperature and the large change to a new apparent saturation at another temperature, facts familiar to all who have studied the slow sorption processes on oxides, should be re-studied in reference to Volkenstein's assumption that the sites available for adsorption, the " thermal " sites, vary with temperature. On this view the measurements of Shou-Chu Liang [24] and the writer would gain new significance. In brief, measurements of slow sorption on oxide surfaces need to be

[23] Pace and Taylor, *J. Chem. Physics*, 1934, **2**, 578.
[24] Taylor and Liang, *J. Amer. Chem. Soc.*, 1947, **69**, 1306.

re-examined from the standpoint of the entropy as well as the energy of activation.

In retrospect, three decades of scientific effort devoted to the science of catalytic phenomena have revealed a wealth of detail and understanding not available to the technologist in the empirical developments of the nineteenth and early twentieth centuries. The background of scientific theory and data that has been accumulated since Mr. Spiers first organized a General Discussion on Catalysis has led to a surer and swifter attack on any new catalytic problem that emerges. Out of the discussions which will ensue, here in Liverpool, we may anticipate a reconciliation of the several attitudes that sometimes have appeared to divide us, but are, in reality, a spur to further and continued effort towards the mastery of our science in an era which is of deep significance in all human affairs. In prospect, therefore, the future of our science is both challenging and bright.

Chemistry Department,
Princeton University,
Princeton, N.J.

I. THEORIES OF ADSORPTION AND PROPERTIES OF SURFACE LAYERS

BEHAVIOUR OF A MOLECULE NEAR A METAL SURFACE

By K. Huang * and G. Wyllie

Received 18th November, 1949

An account is given of the energy changes associated with electron transfer to or from a molecule at distances from the metal surface such that quantum-mechanical tunnel effect may be neglected. A self-consistent treatment of the image field is used to find the distribution of charge on a large adsorbed molecule.

The modification in electronic structure of an adsorbed molecule in consequence of the formation of a weak covalent bond with the metal is treated in terms of a very simple model. A possible semi-empirical approach to treatment of the catalytically active surface is examined.

It is of interest in a number of applications to consider the interaction between a molecule and a metal surface. At large distances, this interaction is of the same nature as the van der Waals' interaction between molecules, being attractive in character. This attractive potential has been discussed by a number of authors, especially Lennard-Jones,[1] and Margenau and Pollard.[2] The short-range interaction is of a more complicated character, and has only received a satisfactory discussion for the case in which the short-range forces are due to electron exchange and are purely repulsive.[3]

---

* Now at Department of Theoretical Physics, Liverpool University.

[1] Lennard-Jones, *Trans. Faraday Soc.*, 1932, **28**, 334.

[2] Margenau and Pollard, *Physic. Rev.*, 1941, **60**, 128.

[3] Pollard, *ibid.*, 1941, **60**, 578.

Experimentally, it is usual to distinguish between physical adsorption and chemisorption, according as the binding energy between the adsorbed molecule and the solid surface is small or large. In physical adsorption the binding energy is of the order of the cohesive energy of a molecular crystal: in chemisorption it is of the order of the energy of an ionic or homopolar chemical bond. In the past, chemisorption has frequently been called "activated adsorption," since, in many cases it occurs comparatively slowly, and the temperature dependence of the rate corresponds to the necessity of a thermal activation energy. It seems, however, that chemisorption occurs instantly in those cases where experiments have been carried out with thoroughly clean metal surfaces (e.g. hydrogen on tungsten[4]), so it is at least possible that the observed activation characterizes the displacement of a previously chemisorbed layer rather than the simple process of adsorption.

It is generally observed that heterogeneous catalysis is accompanied by chemisorption of at least one of the reactants on the catalyst surface. It is thus of interest to enquire what changes in molecular structure may be expected to accompany chemisorption. The object of the present paper is to outline the relevant considerations and draw some qualitative conclusions.

1. A number of workers (e.g. Nyrop,[5] Dowden,[6, 7]) have suggested electron transfer in one direction or the other as the essential process in catalytic action. We shall consider first of all the energy changes associated with such transfer, where the separation of molecule and metal is such that we may neglect the influence of quantum-mechanical tunnel effect on this energy.

Suppose that the work function, which is both the first ionization potential and the electron affinity of the metal, is χ, that the electron affinity of the free molecule is A and that its first ionization potential is I. Then if molecule and metal are at a great distance from each other, the work done in transferring an electron from metal to molecule is

$$W_- = \chi - A,$$

and from molecule to metal

$$W_+ = I - \chi.$$

Typical values of the quantities concerned are $\chi = 2$ to 5 eV, $A = 0$ to 1 eV, $I = 9$ to 12 eV, so that in general $W_+ > W_- > 0$.

Let us suppose an electron to have been transferred in one direction or other. There now exists an electrostatic attraction between metal and ionized molecule. We discuss first the simple case in which the molecule consists of a single atom. The ion will polarize under the influence of the charge induced by itself on the metal surface, and so long as its interaction with that charge is sufficiently described by the image field, the electrostatic energy of the system when the ion is at a distance r from the surface is given by

$$E_s = -\frac{e^2}{4r} - \frac{Ke^2}{64r^4} - \frac{3K^2e^2}{896r^7},$$

where K is the polarizability of the ion in E.S.U.

The approximation of the image field breaks down for static charges under two conditions, (i) if the surface charge density on the metal approaches the value of one electron per surface atom; (ii) if the value of r diminishes below the effective diameter of a metal atom or of the ion, whichever is larger.

The value of $e^2/4r$ is 2 eV for $r = 2\frac{1}{2}A$; the second term in E_s is generally smaller. Thus, if W_- has the rather small value of 2 eV, it is possible to form a negative ion near the surface at such a distance that the exchange interaction is negligible, without expenditure of energy. The ion will, of course, only be in equilibrium at such a distance if there is already some sort of obstructing layer (e.g. of previously adsorbed atoms) between it and the metal surface.

---

[4] Roberts, *Some Problems in Adsorption* (Cambridge University Press, 1939).

[5] Nyrop, *The Catalytic Action of Surfaces* (Copenhagen, 1937).

[6] Dowden, *Research*, 1948, **1**, 239.

[7] *Nature*, 1949, **164**, 51.

A larger molecule cannot be characterized electrostatically by a point charge and point dipole when it is at a distance from the surface comparable with its own dimensions. We shall treat in some detail the case of a relatively large conjugated system, in which the charge transferred to the molecule is small compared with the total charge of the mobile electrons in the normal molecule, using a method developed by Coulson and his co-workers.[8]

In a molecule of this type there are vacant molecular orbitals separated by only a small energy interval from the highest orbitals occupied by the mobile electrons in the ground state of the normal molecule. The charge transferred from the metal will enter such vacant orbitals.

The molecular orbitals of the mobile electrons are constructed as linear combinations of atomic orbitals ϕ_s, $s = 1, \ldots N$; we make the usual simplifying assumption that only one orbital on each atom need be considered. Coulson has defined polarizability coefficients

$$\pi_{st} = \frac{\partial q_s}{\partial \alpha_t}, \qquad . \quad . \quad . \quad . \quad . \quad . \quad (1)$$

where q_s is the number of mobile electrons on the atom s and α_t is the Coulomb integral for the atom t. Under the condition mentioned above, i.e. that the fractional change in the q_s is small, we may in a first approximation treat these coefficients as having the same values in the adsorbed as in the normal molecule.

In the final configuration of the molecule near the metal surface, there is an electrostatic field arising from the charge distribution on the molecule and its electrical image in the surface. This potential enters into the Coulomb integrals α_s, causing a change $\Delta\alpha_s$ as compared with the values in the normal molecule. If then ϵ be the average number of electrons per atom (concerned in mobile orbital formation) transferred to the molecule, and $\epsilon + \Delta q_s$ the actual excess on atom s, we have from (1) in a first approximation

$$\Delta q_s = \pi_{st}\,\Delta\alpha_t, \qquad . \quad . \quad . \quad . \quad . \quad . \quad (2)$$

where the repetition of the dummy index t implied summation.

In the model used, the charge $\epsilon + \Delta q_s$ must be supposed distributed according to the atomic orbital ϕ_s. Thus we have the charge distribution

$$-(\epsilon + \Delta q_s)e\,|\phi(r - r_s)|^2$$

where r_s is the position vector of the sth nucleus, and this together with its electrical image gives rise to a potential distribution which is everywhere proportional to $\epsilon + \Delta q_s$. The potential occurs linearly in the integrand of the Coulomb integral α_t, so we have the strictly linear relation,

$$\Delta\alpha_t = a_{tu}(\epsilon + \Delta q_u). \qquad . \quad . \quad . \quad . \quad . \quad (3)$$

The a_{tu} depend on the form of wave function involved and the geometrical configuration of the system. An example of their calculation for a particular simple case is given in the Appendix A.

Eqn. (2) and (3) together determine Δq_s and $\Delta\alpha_t$ for given ϵ, for they can be combined to give the systems of linear equations

$$\Delta q_s = \pi_{st}\,a_{tu}(\epsilon + \Delta q_u), \qquad . \quad . \quad . \quad . \quad . \quad (4)$$

and

$$\Delta\alpha_t = a_{tu}(\epsilon + \pi_{us}\,\Delta\alpha_s). \qquad . \quad . \quad . \quad . \quad . \quad (5)$$

---

[8] Longuet-Higgins and Coulson, *Trans. Faraday Soc.*, 1947, **43**, 87; *Proc. Roy. Soc. A*, 1947, **191**, 39.

These may be more neatly expressed in terms of the column matrices $\{\Delta q\}$ $\{\Delta\alpha\}$ and the square matrices $\{\pi\}$ $\{x\}$. Then we have

$$\{E - \pi a\}\{\Delta q\} = \{\pi a\}\{\epsilon\}, \qquad . \quad . \quad . \quad (4a)$$

$$\{E - a\pi\}\{\Delta\alpha\} = \{a\}\{\epsilon\}, \qquad . \quad . \quad . \quad (5a)$$

where $\{E\}$ is the diagonal unit matrix and $\{\epsilon\}$ is ϵ times the unit column matrix $\{I\}$.

There are two physically interesting possibilities. If the molecule is, as discussed above, too far from the metal surface for tunnel effect to be of importance, ϵ is simply an integral multiple of the reciprocal of the number of atoms sharing the mobile orbitals (e.g. 6 in benzene). If however, the molecule is close to the metal surface but not too much distorted, the above calculation may give a good description of the charge distribution except in those atoms which are directly bound to the surface. In this case, ϵ is to be determined by the consideration that the highest occupied level in the molecule must now coincide in energy with the highest occupied level in the metal.

As the energy ϵ_0 of the highest filled level in the molecule is a function of the Coulomb integrals α_s, Coulson has introduced the derivatives $\partial\epsilon_0/\partial\alpha_s$ which we shall denote by the row matrix

$$\{\xi\} = \{\xi_1, \xi_2 \, . \, . \, . \, \xi_s \, . \, . \, . \, \xi_n\}$$

where $\xi_s = \partial\epsilon_0/\partial\alpha_s$.

Then in first approximation we must have

$$I - \chi = \frac{\partial\epsilon_0}{\partial\alpha_s}\Delta\alpha_s = \{\xi\}\{\Delta\alpha\} \qquad . \quad . \quad . \quad (6)$$

at equilibrium. It follows from (5*a*) that

$$I - \chi = \{\xi\}\{E - a\pi\}^{-1}\{a\}\{\epsilon\} \qquad . \quad . \quad . \quad (7)$$

and hence

$$\epsilon = \frac{I - \chi}{\{\xi\}\{E - a\pi\}^{-1}\{a\}\{I\}}. \qquad . \quad . \quad . \quad (8)$$

This in conjunction with (4*a*) gives the charge distribution in the adsorbed molecule.

II. In the above calculation we have treated the image field in a self-consistent manner; in particular we have considered the electrons of the molecule as moving in the field of the electrical image of the average electron distribution rather than in the field of the image of the "instantaneous" electron configuration (we are here concerned with the fictitious classical configuration used in setting up the Hamiltonian of the system). It appears, however, from experiments on the emission of electrons from metal surfaces that electrons of energy sufficient to escape from the metal move when near the surface in a field which is at least very closely approximated by the image field. This is the result of the correlation between the movements of the electron considered and those of the other electrons in the metal, which can be quantitatively expressed in terms of the density matrix of the metallic electrons.[9, 10]

The correlation is less important the higher the kinetic energy of the electron. Crudely speaking, the conduction electrons of the metal no longer have time to adapt themselves to its motion. Thus the "instantaneous" rather than the average electrical image will be of importance only for the molecular orbitals of high energy (and so of low average kinetic energy). These are precisely the orbitals which are responsible for chemical binding. However, the difference between this and a self-consistent treatment can only become significant when the molecule is dealt with by a more precise method than that of linear combination of atomic orbitals used in § I.

---

[9] Wigner and Seitz, *Physic. Rev.*, 1934, **46**, 509. Wigner, *ibid.*, 1934, **46**, 1002.

[10] Herring and Nichols, *Rev. Mod. Physics*, 1949, **21**, 185.

Bosworth[11] has attempted to treat the adsorption of a hydrogen atom to a metal surface by a variational method, regarding the image potential as a perturbation. He assumes a perturbed wave function of the form

$$\Psi = a_1 \psi_{1s} + a_2 \psi_{2s} + a_3 \psi_{2px}$$

and chooses the coefficients so as to minimize the energy of the system for a given distance R of the nucleus from the surface. The difficulty of the calculation is that the integral of the Hamiltonian diverges at the surface unless the image field is correctly cut off. Bosworth evades the difficulty by assuming the analytic form, $-e^2/4x$, for the potential energy of the image force for positive and negative x, then integrating straight through the surface and taking the principal value of the resulting improper integral. This device is more ingenious than valid. In any case, a variation calculation which neglects exchange effects can in these circumstances claim little accuracy.

A treatment of the exchange interaction between an atom and a metal surface by the Heitler-London method has been given by Pollard[3] who obtains the energy of interaction in terms of a series of integrals involving the density matrix of the metal and atom. He imposes, however, a restriction on the wave function of the system which is only justified by the supposition that the electrons of the metal are in pairs of opposite spin with identical space wave-functions. By doing so, he denies the possibility of covalent bond formation, which is essentially associated with spin exchange, and in consequence his results are only valuable for the repulsive exchange force in physical adsorption, which was the problem in which he was interested.

An immediate corollary of Pollard's work[12] is that it is not possible by the Heitler-London method to predict important binding by exchange forces between an adsorbed radical and the free conduction electrons. It is necessary in this model that an electron of the metal should have a localized wave-function, more nearly approximating an atomic orbital than a Bloch wave, for formation of a covalent link. On the other hand, it is evident from consideration of the usual LCAO molecular-orbital treatment of the addition of an atom to a linear chain of similar atoms, each contributing one binding electron, that in this model it is just the lowering in energy of all the electron waves by the altered boundary condition that gives rise to the binding of the new atom. A distinction between the two approximations in a given case may be made by magnetic determinations, as one would expect a stronger suppression of paramagnetism if the Heitler-London picture is in better accord with the physical facts.

In order to have some indication of the effects of a covalent link between molecule and metal, we have used the LCAO molecular-orbital method to discuss the simplest model which can be expected to give relevant results. We consider two linear chains of identical atoms, coupled end to end, and examine the electron distribution in one of them when the number of atoms in the other tends to infinity. This constitutes a reduced model of a polyolefine free radical interacting end on with a metal surface. The calculation will merely be outlined here, details being given in Appendix B.

For convenience, we consider the number of atoms in each chain to be even, $2m$ in the first, $2r$ in the second, and allow r to tend to infinity. The secular equation is set up in the usual way, and with some manipulation reduces to the form

$$(\cos\theta + \sin\theta \cot 2m\theta)(\cos\theta + \sin\theta \cot 2r\theta) = 0.$$

Evidently this equation has a root θ_t in each interval between successive singularities of cot $2r\theta$, and two roots in any such interval which also contains a zero of $\sin(2m+1)\theta$. The regularity of this distribution is sufficient to ensure that if $f(\theta)$ is a function analytic in the interval

---

[11] Bosworth, *Proc. Roy. Soc., New South Wales*, 1941, 74, 538.

[12] Pollard, *Physic. Rev.*, 1939, 56, 324.

$$a < \theta < b,$$

$$\sum_{a<\theta_i<b} f(\theta_i) \to \frac{1}{\pi}\frac{2r}{b-a}\int_a^b f(\theta)\mathrm{d}\theta \text{ as } r \to \infty.$$

Examination of the coefficients in the orbitals of the whole system for varying values of θ_i shows that we may regard the orbitals of the whole system, which are regularly spaced in θ, as divided into bands centred on the levels for the short chain by itself (corresponding to the zeros of $\sin(2m+1)\theta$), the electronic charge in an orbital diminishing sharply with increasing separation in energy from the centre of its band (for the short chain of $2m$ atoms).

The electronic charge on a given atom due to all the orbitals in the band corresponding to a single level of the short chain may then be evaluated by integration in the limiting case. After some approximation, we find for the number of electrons on the sth atom, counting from the free end of the chain, contributed by the lth band

$$\frac{}{2m+1}\left\{1-(1-\delta^2)^{-\frac{1}{2}}\exp\left[-\pi\left(\frac{s\sqrt{1-\delta^2}}{2m+1}\frac{\sin^2[l\pi/(2m+1)]}{\phi_l}\right)^2\right]\right.$$
$$\left.\times\cos\left[\frac{2s}{2m+1}\left(l\pi-\frac{(1-\delta^2)\sin[2l\pi/(2m+1)]}{2\phi_l}\right)\right]\right\},$$

where $\phi_l = \delta^{-2} - 2\cos^2[l\pi/(2m+1)] + \delta^2\cos[2l\pi/(2m+1)]$, and δ is the ratio of the exchange integral between the two atoms at the coupled ends of the chains to the exchange integral between neighbouring atoms in either chain. The approximations used are valid for small δ; for sufficiently small δ the above rather clumsy expression is quite well approximated by

$$\frac{1}{2m+1}\left\{1-\exp\left[-\frac{\pi s^2}{(2m+1)^2}\delta^4\sin^4\left(\frac{l\pi}{2m+1}\right)\right]\cos\frac{2sl\pi}{2m+1}\right\}.$$

The corresponding expression for the free chain is

$$\frac{1}{2m+1}\left(1-\cos\frac{2sl\pi}{2m+1}\right).$$

It thus appears that the effect of coupling to a long similar chain is to smooth out the charge variations in each orbital towards the coupled end of the short chain, the effect being most marked for the occupied levels of higher energy (l approaching m). The importance of geometrical factors for this type of binding is indicated by the high power of δ appearing in the exponential, δ being itself a very steeply varying function of the atomic separation.

A similar calculation carried through for the case that the two chains consist of different atomic species proved the inadequacy of the simple LCAO method. The difficulty is of the same type as arises in the discussion of heterocyclic compounds.[8]

Unfortunately, it is much easier to obtain a reasonable approximation to the charge distribution, by methods of the sort discussed above, than to obtain a sufficient approximation to the energy of the system to be able to choose reliably between different, *a priori* reasonable, molecular configurations. In order to approach this latter problem, it will be necessary to consider a specific system and use a much more empirical method. However, we may, from the point of view developed here, estimate what might be a profitable approach.

The heterogeneous catalytic reactions which have been most extensively studied under well-controlled conditions are the ortho-para-hydrogen conversion, hydrogen-deuterium exchange, and various hydrogenation reactions catalyzed by transition metals, especially of the nickel, tungsten, palladium, platinum family. These metals have high work functions which are nevertheless considerably lower than the first ionization potentials of the molecules concerned. It is therefore not possible to account for their catalytic effectiveness in terms of simple electron transfer in either direction, which we have discussed in § I. They have unfilled *d* levels, which lend themselves, according to the Pauling picture of directed valence [13] to the formation of complex bond-systems. They are strongly paramagnetic, and the paramagnetism of the powdered metals is strongly influenced by the chemisorption of a catalytic poison.[14] A preliminary account of experimental work on the relation between catalytic properties and the electronic band structure of the catalyst is given by Couper and Eley.[15]

It thus appears probable that a representation of electronic conditions at the catalytic metal surface in terms of Pauling's resonating bond theory of the metal structure, with the formation of largely covalent bonds between definite metal atoms and the adsorbed reactants, should give a reasonable physical approximation to the real situation.

The authors are indebted to Dr. D. D. Eley, Prof. C. A. Coulson and Prof. N. F. Mott for illuminating discussion of various aspects of the subject-matter of this note. One of us (G. W.) is indebted to the Anglo-Iranian Oil Co. Ltd., for a grant which made this work possible.

Appendix A.—Calculation of $\{a\}$ in a Concrete Case.

As an example, we shall consider an ideal model most suited for our treatment. It consists of a linear molecule perpendicular to the metal surface. The interatomic distance and the distance of the first atom from the metal surface is assumed to be both equal to *d*.

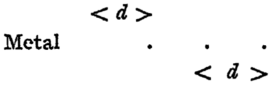

The atomic orbitals are the usual *p* function which we assume to be given by the Slater type of function :

$$\sqrt{\frac{\alpha_p^5}{\pi}}\, r \cos\theta\, e^{-\alpha_p r}. \qquad . \quad . \quad . \quad . \quad (12)$$

Since the rigorous integration to obtain a_{st} in the manner we have described above is not possible analytically for $s \neq t$, we shall suppose that the distribution $|\phi|^2$ which consists of the two well-known symmetric loops can be replaced by two points at the charge-centres of the loops. The distance of the charge centre from the symmetry plane is given by

$$2\int_0^\infty r^2 dr \int_0^{\pi/2} \sin\theta d\theta \int_0^{2\pi} d\phi\, |\psi|^2 r \cos\theta$$
$$= \frac{15}{8} \cdot \frac{1}{\alpha_p}. \qquad . \quad . \quad . \quad . \quad . \quad (13)$$

This value leads immediately to the following expression for a_{st}

$$a_{st} = \tfrac{1}{2}e^2\left\{\left[(u+t)^2 d^2 + 4\left(\frac{15}{8\alpha_p}\right)^2\right]^{-\frac{1}{2}} + (u+t)^{-1}d^{-1}\right.$$
$$\left. + \left[(u-t)^2 d^2 + 4\left(\frac{15}{8\alpha_p}\right)^2\right]^{-\frac{1}{2}} + |(u-t)d|^{-1}\right\}, \quad s \neq t. \quad (14)$$

---

[13] Pauling, *Proc. Roy. Soc. A*, 1949, **196**, 343.
[14] Dilke, Eley and Maxted, *Nature*, 1948, **161**, 804.
[15] Couper and Eley, *ibid.*, 1949, **164**, 578.

For $s = t$, we have the contribution from the image and the density itself; the former contribution can be obtained with the similar approximation as before

$$(a_{ss})_1 = \tfrac{1}{4}e^2\left\{\left[s^2t^2 + \left(\frac{15}{8\alpha_p}\right)^2\right]^{-\frac{1}{2}} + (sd)^{-1}\right\} \quad . \quad . \quad . \quad (15)$$

For the contribution of the density itself the above approximation obviously breaks down. But we shall find the rigorous integration can be carried through in this case. In accordance of the procedure we have described above $(a_{ss})_2$ is given by the following integral:

$$e^2\frac{\alpha_p^{10}}{\pi^2}\int_0^\infty r^2\mathrm{d}r\int_0^\infty r'^2\mathrm{d}r'\int_0^\pi \sin\theta\mathrm{d}\theta\int_0^\pi \sin\theta'\mathrm{d}\theta'\int_0^{2\pi}\mathrm{d}\phi\int_0^{2\pi}\mathrm{d}\phi'\frac{r^2r'^2}{\quad}\quad \mathrm{s}^2\,\theta\cos^2\theta'\mathrm{e}^{-2a_p(r+r')}$$

The angular parts as they stand are not convenient for integration, but they may be readily converted to the desirable form. The integrand is seen only to involve the relative angles between the fixed p-function axis and the two vectors r and r', and the integrations over the angles are just uniform integration over all directions of r. Clearly we may replace them by integrating over all directions of the p-function axis and that of r', whereas regarding r as fixed in direction. The integral becomes then

$$(a_{ss})_2 = e^2\frac{\alpha_p^{10}}{\pi^4}\int_0^\infty r^4\mathrm{d}r\int_0^\infty r'^4\mathrm{d}r'\int_0^\pi \sin\theta\mathrm{d}\theta\int_0^\pi \sin\theta'\mathrm{d}\theta'\int_0^{2\pi}\mathrm{d}\phi'$$
$$\times\left[\frac{2\pi\cos^2\theta'\,(\cos\theta\cos\theta' + \sin\theta\sin\theta'\cos\phi')^2}{\sqrt{(\mathrm{r}^2 + r'^2 - 2rr'\cos\theta)}}\mathrm{e}^{-2\alpha_p(r+r')}\right],$$

where the ϕ integration of r is carried out.

All the successive integrations can be carried out by elementary means, and the final result is

$$(a_{ss})_2 = \frac{21}{10}\alpha_p e^2; \quad . \quad . \quad . \quad . \quad . \quad (16)$$

(15) and (16) combined give:

$$a_{ss} = e^2\left\{\frac{21}{10}\alpha_p + \frac{1}{4}\left[s^2d^2 + \left(\frac{15}{8\alpha_p}\right)^2\right]^{-\frac{1}{2}} + \frac{1}{4sd}\right\}. \quad . \quad . \quad (17)$$

Appendix B.—Consider a chain of $2m + 2r$ similar atoms, of which the first $2m$ are evenly spaced, while the successive $2r$ are also evenly spaced with the same interval but the space between the $2m$th and $(2n + 1)$th atoms is different from the others. Let the wave function for a valence electron in a single atom separated from the rest be ψ the corresponding energy E_0, and the exchange integral between neighbouring atoms at the normal separation be β, while that between the $2m$th and $(2m + 1)$th atoms is $\delta\beta$. Then if the wave function of an electron in the chain be represented by a linear combination of the available wave functions of lowest energy of the different atoms

$$\Psi_j = a_1^j\psi_1 + a_2^j\psi_2 \ldots,$$

and if we neglect all interactions except that of nearest neighbours, the energies $E (= E_0 + \epsilon)$ of the states available for the electrons are given by the secular equation:

$$\begin{vmatrix}
\epsilon & -\beta & & & & & \\
-\beta & \epsilon & -\beta & & & & \\
 & \ddots & \ddots & \ddots & & & \\
 & -\beta & \epsilon & -\delta\beta & & & \\
 & & -\delta\beta & \epsilon & -\beta & & \\
 & & & \ddots & \ddots & \ddots & \\
 & & & -\beta & \epsilon & -\beta & \\
 & & & & -\beta & \epsilon &
\end{vmatrix} = 0$$

where all the elements not on the three middle diagonal lines are zero. If now we substitute $\epsilon = 2\beta \cos \theta$, this equation reduces to

$$\frac{\sin (2r + 1)\theta \sin (2m + 1)\theta}{\sin 2r\theta \sin 2m\theta} \quad \delta^2,$$

which may be written in the form

$$(\cot \theta + \sin \theta \cot 2m\theta)(\cos \theta + \sin \theta \cot 2r\theta) \quad \delta^2.$$

Evidently this equation has a root θ_t in each interval between successive singularities of $\cot 2r\theta$, and two roots in those of these intervals which also contain a zero of $\sin (2m + 1)\theta$. The regularity of this distribution is sufficient to ensure that, if $f(\theta)$ is a function analytic in the interval $a \leqslant \theta \leqslant b$

$$\sum_{a \leq \theta_s \leq b} f(\theta_s) \to \frac{1}{\pi} \frac{2r}{b - a} \int_a^b f(\theta) d\theta \text{ as } r \to \infty.$$

Again, for a given value of θ, the coefficients a_n are determined by the set of linear equations:

$$\begin{array}{lr}
-2 \cos \theta a_1 \quad + a_2 & 0 \\
a_1 \quad - 2a_2 \cos \theta + a_3 & 0 \\
\\
\ldots - 2a_{2m} \cos \theta + \delta a_{2m+1} & 0 \\
\delta a_{2m} - 2a_{2m+1} \cos \theta + a_{2m+2} & 0 \\
\\
a_{2m+2r-1} - 2a_{2m+2r} \cos \theta & 0.
\end{array}$$

Hence
$$a_s = A_s \left\{ \sum_{s=1}^{2m+2n} A_s^2 \right\}^{-\frac{1}{2}}$$

where $A_s = \sin s\theta$, where $s = 1, 2, \ldots 2m$.

$A_{2m+n} = (\delta \sin \theta)^{-1}[\sin (2m+1)\theta \sin n\theta - \delta^2 \sin 2m\theta \sin (n-1)\theta]\ n = 1, \ldots 2r.$
The denominator in a_s reduces to

$$\begin{aligned}
\Big\{ m - \frac{1}{2} \frac{\sin 2m\theta}{\sin \theta} \cos (2m + 1)\theta \\
+ (\delta \sin \theta)^{-2}\Big[\sin^2 (2m + 1)\theta \left(r - \frac{1}{2} \frac{\sin 2r\theta}{\sin \theta} \cos (2r+1)\theta \right) \\
- \delta^2 \sin 2m\theta \sin (2m + 1)\theta \left(2r \cos \theta - \frac{\sin 4r\theta}{2 \sin \theta} \right) \\
+ \delta^4 \sin^2 2m\theta \left(r - \frac{1}{2} \frac{\sin 2r\theta}{\sin \theta} \cos (2r - 1)\theta \right) \Big] \Big\}^{\frac{1}{2}}.
\end{aligned}$$

If r is large, this may be approximated by

$$\phi + r/\sin^2 \theta[\delta^{-2} \sin^2 (2m + 1)\theta - 2 \cos \theta \sin (2m + 1)\theta \sin 2m\theta + \delta^2 \sin^2 2m\theta]\}^{\frac{1}{2}},$$

where ϕ is of the same order of magnitude as m.

The factor to be multiplied by $r/\sin^2 \theta$ is a positive definite form, so for very large r the denominator in a_s tends to

$$\begin{aligned}
\{r[\delta^2 + \sin^2 (2m + 1)\theta \sin^{-2} \theta(\delta^{-2} - 2 \cos^2 \theta + \delta^2 \cos 2\theta) \\
+ \sin (2m + 1)\theta \cos (2m + 1)\theta \sin^{-2} \theta \sin 2\theta(1 - \delta^2)]\}^{\frac{1}{2}}.
\end{aligned}$$

If, then, we suppose δ to be small, we see that the coefficients of the atomic wave functions in the group $1, \ldots 2m$ will be small unless $\sin (2m + 1)\theta$ is also small.

Thus for the first $2m$ atoms we may regard the almost uniformly spaced energy levels of the system as divided into bands centred on the levels for the $2m$ chain by itself (the zeros of $\sin (2m + 1)\theta$), with the degree of occupation of the levels in any band falling off with distance from the centre.

Within a given band, then, the electronic charge on the sth atom ($s \leqslant 2m$) due to a given orbital may be approximated by

$$\frac{\sin^2 s\theta}{r(\delta^2 + a_1 \sin^2 (2m + 1)\theta + a_2 \sin (2m + 1)\theta \cos (2m + 1)\theta},$$

where a_1, a_2 are constant, since the circular functions of θ, 2θ vary only slowly with θ in comparison with those of $(2m + 1)\theta$. The total electronic charge on this atom due to orbitals within the band is then the sum of all the similar terms for which θ lies between $(l - \frac{1}{2})\,w$ and $(l + \frac{1}{2})w$, where $w = \pi/(2m + 1)$, l being some integer. Then, as observed above, if we make r tend to infinity, this sum can be replaced by the integral,

$$\frac{2}{(2m+1)\pi}\int_{(l-\frac{1}{2})\pi}^{(l+\frac{1}{2})\pi}\frac{\sin^2[s\theta'/(2m+1)]\,d\theta'}{\delta^{-2}+a_1\sin^2\theta'+a_2\sin\theta'\cos\theta'},$$

where we have replaced $(2m + 1)\theta$ by θ' in the above expression.

If s is so small that $\sin^2[s\theta'/(2m + 1)]$ may be taken as constant, the integral can be evaluated at once, giving $\sin^2 slw/(m + \frac{1}{2})$ in precise agreement with the expression for the charge on the sth atom due to the corresponding orbital in the isolated $2m$ chain. For larger s, however, the integral cannot be so simply evaluated. If we replace $\sin\theta'$ by x and approximate to the quadratic denominator by $A\,e^{B^2(x-a)^2}$ extending the range of integration in x from $-\infty$ to $+\infty$, and choosing the constants A, B, a to give the correct minimum value of the denominator at the correct place, and the correct value of the integral for small s, we obtain for the charge on the sth atom due to the lth band

$$\frac{1}{2m+1}\left\{1-(1-\delta^2)^{-\frac{1}{2}}\exp\left\{-\pi\left[\frac{s\sqrt{(1-\delta^2)}}{2m+1}\,\frac{\sin^2(l\pi/2m+1)}{\phi_l}\right]^2\right\}\right.$$
$$\left.\times\cos\left[\frac{2s}{2m+1}\left(l\pi-\frac{1-\delta^2}{2\phi_l}\sin\frac{2l\pi}{2m+1}\right)\right]\right\},$$

where $$\phi_l = \delta^{-2} - 2\cos^2\frac{l\pi}{2m+1} + \delta^2\cos\frac{2l\pi}{2m+1}.$$

H. H. Wills Physical Laboratory,
University of Bristol.

ON CONDITIONS FOR THE EXISTENCE OF SURFACE STATES

By C. A. Coulson and G. R. Baldock

Received 13*th February*, 1950

The existence or non-existence of surface states on the boundary of a monovalent metal is investigated fully for simple cubic models in 1, 2 and 3 dimensions, using the molecular modification of Bloch wave functions. Limiting values are found for the necessary changes required at the surface atoms, both for their Coulombic (electronegativity) terms α and their resonance integrals β. It is shown that surface states may be induced by the perturbation caused by the approach of a polar, or ionic, group; and that such surface states are more easily produced close together than separately. In certain non-cubic systems, e.g. graphite, surface states exist even without any necessary changes in α or β on the boundary. Finally, a series of recent theorems on the charge distribution in large molecules is applied to a study of the alternating charge distribution sometimes associated with surface states.

From the earliest recognition that there were sometimes surface states associated with a metal, their importance for all types of surface reactions has been appreciated. But very few attempts have been made to see under what conditions such states appear. It is our intention in this note to present some preliminary results which we have just obtained in this field. Since a more complete account of this work will be presented later, we shall be content here merely to summarize our conclusions, without giving many details of the procedure by which they have been obtained.

After we have described the model and our notation, it will be convenient to report our results first for the simple cubic lattice in one, two or three dimensions, and then for other lattices. We conclude with a short discussion of the validity and relevance of the idea of surface states, using for this purpose some known results in the theory of molecular structure.

Notation.—As is usual, we treat a metal by the Bloch method or, more properly, by the "molecular" modification of it which recognizes the existence of one or more boundaries of the metal, and therefore replaces the progressive waves of Bloch's treatment by stationary waves such as (1) below, in which all the coefficients are real. This is simply the familiar molecular-orbital method extended to much larger molecules than those normally found in chemistry, and occupying one, two or three dimensions. This link with molecules will enable us to make use of several quite general theorems recently established in this field (the so-called LCAO approximation).[1]

As in the work of Goodwin [2] and others, the metal is supposed to consist of a large, but finite, number of positively charged atoms which provide an effective field for the conduction electrons. Each conduction electron is governed by the same Hamiltonian H. Its motion is described by stationary de Broglie waves, which are solutions of the wave equation $H\psi = E\psi$. The tight-binding approximation [3] is used to represent the appropriate single-electron wave functions, so that, if the atoms are suitably ordered, any such orbital is

$$\psi = \Sigma c_r \phi_r, \qquad . \quad . \quad . \quad . \quad . \quad (1)$$

where the c_r are constants to be determined by a variational calculation and ϕ_r is the atomic orbital which would be used by the conduction electron if it were in the presence of atom r only. We are implicitly neglecting any of the hybridization recently proposed for metals by Pauling,[4] and we concentrate for the moment on systems where all, or nearly all, of the atoms contribute one metallic electron. This model is essentially the same as that used by Goodwin, though we differ from him in the way we deal with the boundary of the array and also in our inclusion of certain overlap integrals.

Let us put

$$\begin{aligned} \alpha_r &= \int \phi_r^* H \phi_r \mathrm{d}\tau, \\ \beta_{rs} &= \int \phi_r^* H \phi_s \mathrm{d}\tau, \qquad . \quad . \quad . \quad . \quad . \quad (2) \\ S_{rs} &= \int \phi_r^* \phi_s \mathrm{d}\tau. \end{aligned}$$

Then α_r may be called, in molecular language, the Coulomb term of atom r, and β_{rs} and S_{rs} are the resonance and overlap integrals between atoms r and s. Without loss of generality we may take each ϕ_r to be real; this makes both β_{rs} and S_{rs} real also, and symmetric in r and s. The coefficients c_r and the energy E of the orbital (1) are now related by means of the secular equations:

$$c_r(\alpha_r - E) + {\sum_s}' c_s(\beta_{rs} - ES_{rs}) = 0, \quad r = 1, 2, \ldots . \quad . \quad (3)$$

The summation in (3) is taken over all the atoms of the metal except r, and there is one equation for each atom r. If we decide to retain β_{rs}

---

[1] Coulson and Longuet-Higgins, *Proc. Roy. Soc. A*, 1947, **191**, 39; 1947, **192**, 15; 1948, **193**, 447, 456; 1948, **195**, 188.

[2] Goodwin, *Proc. Camb. Phil. Soc.*, 1939, **35**, 205.

[3] Mott and Jones, *Theory of the Properties of Metals and Alloys* (Oxford Univ. Press, 1936).

[4] Pauling, *Proc. Roy. Soc. A*, 1949, **196**, 343.

between adjacent atoms only, relatively few terms survive in (3). As a rule we shall do this by supposing that interactions between all other pairs of atoms are negligibly small. In at least one of our calculations, however, we consider interactions between next-to-nearest neighbours also.

Some explanation is needed regarding the inclusion of the overlap integrals S_{rs}. It is true, as Chirgwin and Coulson [5] have recently shown, that there are many cases in which charge distributions and interatomic distances are entirely unaffected by its inclusion. But the energies are always slightly changed and, particularly in the upper half of the conduction band, as Coulson and Rushbrooke [6] showed for graphitic layers, the shape of the band is strongly dependent on the value of this overlap integral.

Now if all the atoms are entirely equivalent, we may put

$$\begin{aligned} &\alpha_r = \alpha \quad \text{for all } r, \\ &\left.\begin{aligned} \beta_{rs} &= \beta \\ S_{rs} &= S \end{aligned}\right\} \text{for all neighbouring pairs } rs. \end{aligned} \qquad . \quad . \quad (4)$$

But it soon follows that for simple cubic crystals, this precludes the possibility of surface states. We shall therefore accept (4) for internal atoms, and be prepared to characterize the surface atoms by a different value of α_r, and different values of β_{rs} and S_{rs}. The details of these new values vary from model to model, and are described for each case as it occurs.

The questions that we ask are: For what values of the parameters α, β, S are there solutions of the secular equations that may be interpreted as surface states? And do the energies of these states lie inside or outside the band of continuous distribution of energy?

But there are other related questions. Although the existence of surface states is undoubtedly an aid to catalytic action, it is by no means inconceivable that, even if such states do not exist at first, they are nevertheless brought into existence by the approach of some other group, particularly polar groups, toward the metal surface. There is a close parallel here to some work by Coulson and Longuet-Higgins,[1] who studied the perturbations induced in large aromatic molecules by the approach of some charged ion. In our present case, we could approximately describe such activity by a change in the α_r of one surface atom. And we ask the question: if one surface atom is changed in this way, will there be a surface state induced in the metal, which was not there before? A supplementary question, to which we can give only an incomplete answer, is: in such a case, how will two such surface states, associated with two distinct surface atoms, behave towards each other? Questions of this sort are clearly very important in discussing the variation of catalytic activity with fraction of surface occupied.

Results.—We must now define a surface state more precisely. If, in one of the single-electron wave functions (1), $c_r \rightarrow 0$ as the distance of atom r from atom m increases, and if this occurs at a rate independent of the total number N of atoms in the crystal (N being assumed large), then ψ is said to be a point state associated with atom m. This implies that an electron in the orbital ψ is effectively restricted to a region close to atom m. The extent of this restriction depends on the rapidity of the convergence of the sequence (c_r) to zero. This convergence is not necessarily monotonic, and there may be local increases as well as decreases near to atom m.

We shall also encounter orbitals for which c_r is relatively high in the regions of atoms $m, n, p, \ldots$, tending to zero away from these atoms.

---

[5] Chirgwin and Coulson, *Proc. Roy. Soc. A*, 1950 (in press).

[6] Coulson and Rushbrooke, *Proc. Roy. Soc. Edin., A*, 1948, **62**, 350.

Such states will be termed multiple point states associated with atoms m, n, p, ... The definitions of line states and surface states can obviously be formulated in precisely analogous ways.

We shall first consider three simplified types of crystal: the one-dimensional linear chain, the two-dimensional square lattice, and the simple cubic lattice. For these models we shall outline some of the conditions under which these special states may occur. Throughout the following summary, the assumptions (4) are made for all the atoms except for those specifically mentioned.

(I) LINEAR CHAIN.—Let there be N atoms in a chain numbered consecutively from 1 to N, and let

$$\alpha_1 = \alpha_N = \alpha' \qquad \text{for the end atoms,}$$

$$\beta_{12} = \beta_{N-1,\ N} = \eta\beta \text{ for the end bonds,}$$

where β is the resonance integral for all other adjacent pairs and η is a multiplier which may be either greater than or less than unity. In most cases η will be greater than 1. We have thought it proper to allow for the end resonance integrals having a different value from the internal ones, partly because detailed calculations for the linear case of polyene hydrocarbon chains[7] shows that the end links are appreciably shorter than the others, and also because in some unpublished work we have shown that variations may also be anticipated near the surface, and also in the surface, of three-dimensional aggregates.

In this model we include possible next-nearest-neighbour interaction by writing

$$\beta_{24} = \beta_{35} = \ . \ . \ . = \beta_{N-3,\ N-1} = \omega\beta,$$

where ω will usually be quite small. For the end interactions of this type we write

$$\beta_{13} = \beta_{N-2,\ N} = \omega\eta\beta.$$

Following the suggestion of Mulliken for molecules, and developed by Chirgwin and Coulson[5] and by de Heer,[8] we suppose that all overlap integrals S_{rs} are proportional to the corresponding β_{rs}.

It is convenient to define

$$\gamma = \beta - \alpha S, \quad \lambda = (\alpha - \alpha')/\gamma, \qquad . \quad . \quad . \ (5)$$

and to put

$$\sigma = \lambda/(1 + \lambda S), \ 1 - \mu = \eta^2/(1 + \lambda S). \qquad . \quad . \ (6)$$

These substitutions enable us to express the condition for point states quite simply in terms of σ, μ, and ω. If $\sigma = 0$, the end atoms have the same Coulomb term as the internal atoms; if in addition $\mu = 0$, then $\eta = 1$, so that $\beta_{12} = \beta_{23}$, etc.

(i) $\sigma = \mu = 0$. There are no point states, whatever the value of ω.

(ii) $\omega \ll 1$. If ω^2 is neglected we find that the condition for point states depends only on σ and μ, and not at all on ω (second-neighbour interaction).

There is a point state whose energy is below the continuous band if $\sigma + \mu < -1$ and one with energy above the band if $\sigma - \mu > 1$.

If $\sigma = 0$ the conditions become $\eta > \sqrt{2}$.
If $\eta = 1$ the conditions become $\sigma < -1/(1 + S)$,
or $\sigma > 1/(1 - S)$,

and the states correspond to those found by Goodwin.

Both these states are doubly degenerate. They are double point states associated with the end atoms.

---

[7] Coulson, *Proc. Roy. Soc. A*, 1939, **169**, 413.

[8] de Heer, *Phil. Mag.*, 1950 (in press).

(iii) $\alpha_m = \alpha'$. We now consider the possibility of point states occurring when nothing but the Coulomb term of the mth atom is changed. This atom may perfectly well be an internal or boundary atom. In this case the overlap integral S is ignored. The condition for a point state associated with atom m is $|\lambda| > 1/m$. Thus in the interior of the chain, any deviation of α_m from α gives rise to a point state.

(II) SQUARE LATTICE.—(i) In a square lattice the next-to-nearest neighbours are separated by a distance $\sqrt{2}$ times the lattice constant. If we take into account the corresponding resonance integral $\omega\beta$ (without changing any of the other parameters), we find that no point or line state emerges for any value of ω.

(ii) We now consider the effect of altering the Coulomb term of only one atom (m), on the boundary of the rectangular array, from α to α'. In this case we shall neglect the overlap integral S altogether and write $\lambda = (\alpha - \alpha')/\beta$ instead of (5).

We assume that atom m is not near the corner of the rectangle, and we find that if $|\lambda| > 2{\cdot}8$ (approx.) there is a state whose energy lies outside the continuous band. This state is a point state associated with atom m.

(iii) Suppose now that two atoms, m and n, separated by p atomic distances along one of the edges, have an altered Coulomb term α'. If p is large, the condition for the existence of double point-states associated with these atoms is $|\lambda| > 2{\cdot}8$. As p is reduced, the limiting value of $|\lambda|$ steadily decreases. For example, when $p = 2$, so that the altered atoms are separated by only one intervening atom, the condition is $|\lambda| > 2{\cdot}3$; and when $p = 1$, so that they are neighbours, it is $|\lambda| > 2$. Since $|\lambda|$ measures the difference in electronegativity of the affected atoms, we infer that induction of surface states is made easier by the presence of a perturbation already existing on the surface; and that such surface (point) states will tend to be associated together in groups rather than distributed at random over the whole surface. It is possible that we have here a little insight into the nature of the active centres so frequently postulated for catalytic activity.

(III) SIMPLE CUBIC LATTICE.—(i) Let us denote any atom in the crystal by (r, s, t), where

$$1 < r < L, \quad 1 < s < M, \quad 1 < t < N.$$

Evidently there are LMN atoms in the crystal. We shall consider the effect of a change in the parameters for all the atoms on the two opposite faces $r = 1$, $r = L$ of the crystal. For these surface atoms

$$\alpha_{1st} = \alpha_{Lst} = \alpha' \text{ (for all } s, t).$$

Also we suppose that the resonance integrals between all neighbouring atoms in these two planes have the value $\kappa\beta$, and that the resonance integrals such as $\beta_{1st,\ 2st}$ between one atom in the surface and the adjacent one inside the crystal, have the value $\eta\beta$. All other non-vanishing resonance integrals are equal to β, and we suppose that in every case the overlap integral is proportional to the corresponding resonance integral.

We define λ, σ, μ as in the case of the linear chain (eqn. (5), (6)), and we also introduce ν and ρ defined by

$$1 - \nu = \kappa\eta/(1 + \lambda S)$$
$$\rho = \sigma + 2\nu(\cos\phi + \cos\psi),$$

where

$$\phi = k\pi/(M + 1) \qquad k = 1, 2, \ldots M$$
$$\psi = l\pi/(N + 1) \qquad l = 1, 2, \ldots N.$$

The conditions for surface states will now depend on μ and ρ.

There is a band of surface states of low energy if $\rho + \mu < -1$, and one of high energy if $\rho - \mu > 1$. These bands consist of levels depending on μ and ρ, and since ρ may take MN different values for fixed σ and ν the conditions may be fulfilled for part of one band but not for all of it. Each level is doubly degenerate and all the states are double surface states associated with the faces $r = 1$, $r = L$. There is one such orbital for each of the modified surface atoms. These bands of surface states may overlap the continuous band of energy levels.

(ii) If only one atom (m) on the surface has a different Coulomb term α' and if we neglect overlap, we find the condition for an energy level outside the continuous band is $|\lambda| > 4\cdot5$ (approx.). This state is a point state associated with atom m.

IV. Other Crystal Structures.—Our previous examples have all been associated with the simple cubic structure, in which the unit cell only contains one atom. But as soon as we go to more complicated structures in which two or more atoms comprise the unit cell, the situation is quite different. For now surface states may appear even without any perturbation of the edge atoms. This is because not all surface atoms are equivalent geometrically (as they were in the earlier cubic crystal), and the differences in environment produce the same effect as a change in α in the simpler model.

An example will illustrate this effect. Fig. 1 shows a part of a single layer of graphitic carbon, in which the atoms are arranged in regular hexagonal form. The electronic wave functions for such a layer have been discussed fully by Bradburn, Coulson and Rushbrooke,[9] who obtained the energies in terms of the numbers n and m which determine the size of the layer. These energies are obtained from the secular determinant, which may be factorized, corresponding to nodes of the wave function parallel to the m and n directions. A combination of eqn. (9) and (12) in their paper, together with some rather tedious analysis which we shall not reproduce, shows that in a large layer such as Fig. 1 there are $2n/3$ surface states. Application of the argument developed by Coulson [10] shows that in a layer of this kind all the energies are in the range $E_0 \pm 3\beta$, which is known to be the range covered by the continuum of two-dimensional orbitals. Thus none of the surface states lie outside the continuum. In Fig. 1 the surface states are associated with the atoms on the extreme left- and right-hand edges, and not those on the top or

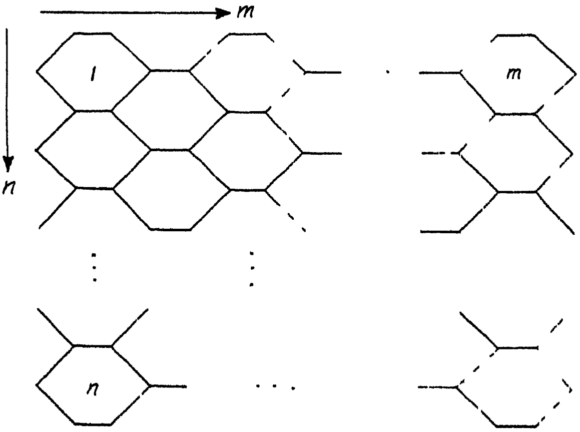

Fig. 1.

---

[9] Bradburn, Coulson and Rushbrooke, *Proc. Roy. Soc. Edin. A*, 1948, **62**, 336.
[10] Coulson, *Proc. Camb. Phil. Soc.*, 1950, **46**, 202.

bottom. This is linked with the fact that in a graphitic layer the unit cell contains two atoms. Those atoms on the left are all crystallographically equivalent, and so are those on the right, but those at the top and bottom are not.

It may be presumed that similar surface states will appear in other such lattices. We are making further calculations to investigate this in more detail. One conclusion, however, is quite clear from the graphite example: surface states are quite liable to occur even without any changes in Coulomb terms or resonance integrals, but simply on account of the geometrical structure of the boundary.

General Molecular Considerations.—It is perhaps worth stressing that certain quite general results may be obtained by treating a crystal as a large molecule and using the general theory developed by Coulson and Longuet-Higgins.[1] For example:

(i) The existence of surface states does not necessarily imply an uneven distribution of charge. Thus, in the graphite example in (IV) we are dealing with an "alternant molecule", and there will therefore be a precisely equal number of electrons associated with each atom. The excess of charge near the edges due to the surface states is compensated by a corresponding excess in the body of the crystal due to the other electrons.

(ii) In the same way, as Chirgwin and Coulson have shown,[5] if there are no changes in Coulomb terms, but only in resonance integrals, the net charge is uniform.

(iii) But if the Coulomb term of one atom is changed in the direction of increasing its electronegativity, it will carry a final net negative charge, and as we proceed away from this atom, other atoms will have an alternating positive and negative charge. In the case of a surface layer with increased α-values, the alternation of charge occurs as between one layer and its neighbours.

There are still one or two further molecular considerations that we may "carry over" to crystal lattices. Thus:

(iv) There is considerable uncertainty regarding the validity of using the same Hamiltonian operator H for each electron. These operators are not strictly self-consistent, and as Chirgwin and Coulson have shown in some unpublished work, we ought really to use a different operator for each electron. The resulting errors are not likely to be so serious in crystals as in molecules.

(v) A more serious difficulty arises from the fact that the so-called "lowest configuration" is not, by itself, a sufficiently good wave function. As Miss Jacobs[11] has shown for naphthalene, there is often considerable configurational interaction, which results in a slight unevenness of charge, more particularly at the edges of the molecule, i.e. at the surface of the crystal. We are investigating this matter more carefully at the moment, in this Department using a simplified model.

Conclusion.—To some extent all the models that we have discussed above are largely formal. And consequently our conclusions are not immediately applicable to any real problem. But we believe that they do illustrate tendencies and situations likely to be found in actual surfaces, and may serve to "point the way" to further specific calculation.

Wheatstone Physics Laboratory,
King's College,
London.

---

[11] Jacobs, *Proc. Physic. Soc. A*, 1949, **62**, 710.

A CALCULATION OF HEATS OF CHEMISORPTION

By D. D. Eley

Received 3rd April, 1950

Heats of chemisorption are calculated by Pauling's equation for covalent bonds. Quite good agreement is secured for hydrogen on tungsten, copper and nickel. Calculations for oxygen on tungsten and ethylene on nickel enable us to rule out certain mechanisms of chemisorption.

There are a number of good reasons for believing that in many cases the chemisorptive bond is of a covalent type.[1, 2] It is a matter of some interest that this hypothesis allows a calculation of heats of chemisorption. Consider, for example, the chemisorption of hydrogen on tungsten. We write this as

$$2W + H_2 \rightarrow 2W\text{—}H.$$

The differential heat of chemisorption per mole of hydrogen, Q_0, is to be calculated, when the fraction of surface covered $\theta \rightarrow 0$ and we may neglect effects due to neighbour interactions in the monolayer. The result may be obtained in terms of bond energies E,

$$Q_0 = 2E(W\text{—}H)\text{—}E(H\text{—}H) \quad . \quad . \quad . \quad (1)$$

Considerable success has attended the recent application of electron-pair theory to metals.[3] Therefore I shall assume that the energy of the surface W—H bond may be calculated from Pauling's equation,[4]

$$E(W\text{—}H) = \tfrac{1}{2}\{E(W\text{—}W) + E(H\text{—}H)\} + 23{\cdot}06\,(x_W - x_H)^2. \qquad (2)$$

To evaluate eqn. (2) we first need to obtain E(W—W). We shall assume that each metal atom has 12 nearest neighbours. This result is true for face-centred cubic lattices, but not strictly for body-centred cubic lattices, where there are 8 nearest and 6 next nearest neighbours. In the latter case, however, no great error is involved in treating the lattice as one with 12 nearest neighbours. Since two atoms are involved in each bond we can write

$$E(W\text{—}W) = \frac{2}{12}S,$$

where S is the sublimation energy of the metal, listed in Landolt-Bornstein.[5]

The term involving the difference in electronegativities $x_W - x_H$ is estimated by Pauling's approximate rule[4] that it is equal to the dipole moment of the bond in debyes, μ. If the measured contact potential of a complete monolayer is V volts, then we may write

$$\mu = V/2\pi 300 C_s,$$

where C_s is the number of sites per cm. of surface, taken here as the mean of the (110) and (100) surfaces, i.e. $1{\cdot}2 \times 10^{15}$ for W and $1{\cdot}38 \times 10^{15}$ for Ni. This value of μ for an atom in a full layer can only be equated to μ_0 for a dilute layer if we assume depolarization effects to be small.

---

[1] Couper and Eley, this Discussion.

[2] Eley, *Amer. Chem. Soc. Symposium*, June, 1950 (to be published in *J. Physic. Chem.*).

[3] Pauling, *Proc. Roy. Soc. A*, 1949, **196**, 343.

[4] Pauling, *The Nature of the Chemical Bond* ((New York, 1939).

[5] Landolt-Bornstein, *Tabellen, Erg.* IIIc, 2709.

The calculations have been made for systems where modern experimental data are available, and the results presented in the Table. The bond energy values used are due to Pitzer.[6] For nitrogen and carbon bonds, two values are possible, " high " and " low " values, depending on the values chosen for the heats of atomization of carbon and nitrogen. The situation is well presented by Coates and Sutton.[7] Pitzer's values are high values, and for the —N=N— bond, we have also taken the high value given by Coates and Sutton.[7] The low values give the results which are very little different from those listed.

In applying the equation to multiple bonds, we are making a definite assumption, since the equation was deduced for single bonds. In particular, it is not at all clear that the equation will give a correct estimate of the ionic term. Also, depolarization effects are probably more important for dipoles such as W = o, 1·76 V contact potential, compared with W—H which has the smaller value of 1·04 V.

System	V, Volts	μ, D $= x_M - x_A$	E(M - M) kcal.	E(A A) kcal.	$23(x_M - x_A)^2$	E(M - A) kcal.	$Q_{calc.}$ kcal.	$Q_{expt.}$ kcal.	Experimental Specimen
$2W + H_2$ $\rightarrow 2W—H$	−1·04[8]	−0·46	33·8	103·2	4·9	73·4	43·6	45[11] 45[12] 46[13]	Wire Film Powder
$2Ni + H_2$ $\rightarrow 2Ni—H$	−0·34[9]	−0·13	16·4	103·2	0·39	60·2	17·2	31[12] (21[14])	Film Powder
$2Cu + H_2$ $\rightarrow 2Cu—H$	?	?	13·6	103·2	?	58·4	13·6	9[15]	Powder
$2W—O$ $\rightarrow 2W{=}O$	−1·76[10]	−0·78	2 × 33·8	117·2	14	106·4	95·6	139[11] 150[10] 147[16]	Wire " "
$2W + N_2$ $\rightarrow 2W{\equiv}N$	−1·38[10]	−0·61	3 × 33·8	225·1	8·5	171·8	118·5	28[10] (75[17])	Wire Powder
$2Ni + C_2H_4$ 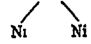	+0·83[9]	+0·32	16·4	80(σ) 65(π)	2·4	50·6	36·2	58[12]	Film

Discussion

The agreement between calculation and experiment is good for W—H and Cu—H. For Ni—H, the calculated result is lower than the value of 31 kcal., which since it was obtained with an evaporated film is more likely to correspond to the true value for a clean surface than the value of 21 kcal. for a powder. The differences in electronegativities are what one might expect from Pauling's thermochemical values for similar bonds.

---

[6] Pitzer, *J. Amer. Chem. Soc.*, 1948, **70**, 2140.

[7] Coates and Sutton, *J. Chem. Soc.*, 1948, 1187.

[8] Bosworth, *Proc. Camb. Phil. Soc.*, 1937, **33**, 394.

[9] Mignolet, this Discussion.

[10] Bosworth and Rideal, *Physica*, 1937, **4**, 925.

[11] Roberts, *Proc. Roy. Soc. A*, 1935, **152**, 445.

[12] Beeck, *Rev. Mod. Physics*, 1945, **17**, 61.

[13] Frankenburg, *J. Amer. Chem. Soc.*, 1944, **66**, 1827.

[14] Eucken and Hunsmann, *Z. physik. Chem. B*, 1939, **44**, 163.

[15] Ward, *Proc. Roy. Soc. A*, 1931, **133**, 506.

[16] Johnson and Vick, *ibid.*, 1935, **151**, 308.

[17] Davies, Jr., *J. Amer. Chem. Soc.*, 1946, **68**, 1395.

Thus for the nearest example, Al, $x_M = 1{\cdot}5$ and for H, $x_A = 2{\cdot}1$, so that $x_M - x_A \sim - 0{\cdot}6$. For $W{=}O$ and $2W{=}C_2H_4$, the calculated values are markedly lower than the observed values. However, the calculations reproduce the general features of the observed results quite well, and the discrepancies may be associated with changes in hybridization and loss of resonance energy on adsorption at the surface. The experimental values for ethylene may be too high because of a certain amount of self-hydrogenation.[12] The calculated oxygen value may be low because we have under-estimated the ionic term. Thus Pauling's table[4] would give $x_{Al} - x_0 = - 2{\cdot}0$ and one should not expect tungsten-oxygen to be very different.

The nitrogen value is much higher than the preferred experimental value of 28 kcal. The relatively low stability of nitrogen films as compared with ethylene films has been qualitatively demonstrated by other methods,[18] adding weight to the low values for Q_{expt}. This discrepancy may be connected with the relatively large ratio $E(N{\equiv}N)/E(N - N)$ compared with $E(C{\equiv}C)/E(C{-}C)$.* Another possibility for chemisorption is

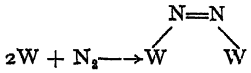

$$2W + N_2 \longrightarrow \overset{N=N}{W\quad W}$$

but the calculated value is $Q_{\text{calc.}} = - 38$ kcal. which rules this out.

Beeck has suggested that the chemisorbed film of ethylene consists mainly of acetylenic complexes. We have calculated three possible processes of formation, the third one being that favoured by Beeck.

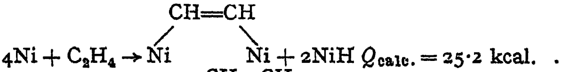

$$4Ni + C_2H_4 \rightarrow \overset{CH=CH}{Ni\quad Ni} + 2NiH \quad Q_{\text{calc.}} = 25{\cdot}2 \text{ kcal.} \quad . \quad . \quad (1)$$

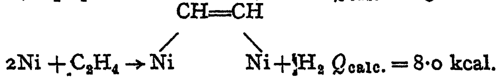

$$2Ni + C_2H_4 \rightarrow \overset{CH=CH}{Ni\quad Ni} + \tfrac{1}{2}H_2 \quad Q_{\text{calc.}} = 8{\cdot}0 \text{ kcal.} \quad . \quad (2)$$

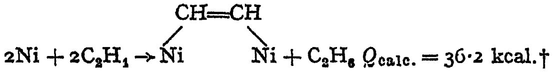

$$2Ni + 2C_2H_4 \rightarrow \overset{CH=CH}{Ni\quad Ni} + C_2H_6 \quad Q_{\text{calc.}} = 36{\cdot}2 \text{ kcal.}\dagger \quad . \quad (3)$$

The first process is a possible one energetically, although obviously not as likely as the associative adsorption calculated in the Table. However, it is ruled out by the observation that hydrogen deuteride formation is inhibited by ethylene, so that there is no chemisorbed hydrogen in the film.[19] The second process is clearly unlikely but the third process is a possible one. Finally, there is the process of dissociative chemisorption suggested by Farkas,[20]

$$Ni + C_2H_4 \rightarrow Ni{-}CH{=}CH_2 + \tfrac{1}{2}H_2 \quad Q_{\text{calc.}} = 4,$$

which gives too small a heat. The associative process given in the Table yields the best value of $Q_{\text{calc.}}$.

All the calculations for ethylene and nitrogen have been repeated using low values of the carbon and nitrogen bond energies concerned with very little difference in the calculated heat values. This is because the changes effect both the bonds disrupted and the bonds formed to metal in the same way.

---

[18] Eley and Rideal, *Proc. Roy. Soc. A*, 1941, 178, 429.

* It has been possible subsequently to solve this problem, cf. the following discussion.

† I.e. 18·1 kcal. mole of ethylene.

[19] Twigg and Rideal, *Proc. Roy. Soc. A.*, 1939, 171, 55.

[20] Farkas, *Trans. Faraday Soc.*, 1939, 35, 906.

In one of his later papers, Roberts [21] indicated a new view that possibly the oxygen film on tungsten is *not* atomic. The only simple alternative to the process in the Table is

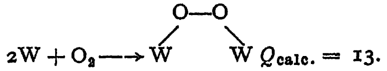

$$2W + O_2 \longrightarrow \overset{O\text{—}O}{W \quad\quad W} \quad Q_{calc.} = 13.$$

Clearly this mechanism is ruled out because of its low heat value.

It is hoped to improve this approach to chemisorption in future by a theoretical consideration of the type of bond involved, but even at its present stage, the method offers an approach to the heat of adsorption, which, while it is of great importance in chemical kinetics, is difficult to determine experimentally. The calculations support strongly the notion that the chemisorption bond is an electron pair bond, rather than a completely ionic bond.

I should like gratefully to acknowledge that the two values for nickel contact potentials are taken from the paper by J. Mignolet (Liège),[22] and communicated personally to me beforehand.

ADDENDUM.—It is possible to extend the calculations in my paper to all the new data reported by Beeck in his paper on Hydrogenation Catalysts. The Table compares calculated values (kcal./mole gas) with the values observed by Beeck.

Gas	Metal	Rh	Ni	Fe	Ta	W	Cr
H_2	obs.	28	31	32	39	45	45
	calc.	23	17	17	32	44	15·7
C_2H_4	obs.	50	58	68	138	102	102
	calc.	42	36	36	51	64	34·7
%*d*		50	40	39·7	39	43	39

The calculated values for C_2H_4 are for associative chemisorption, i.e. M—CH_2—CH_2—M. The heats of sublimation of Ta and Rh are not available, but I have found a good linear relation exists between sublimation energy and melting point for the related metals, from which I have interpolated the values for Ta, $S = 184$ kcal., and Rh, $S = 130$ kcal. I have assumed the surface dipoles for H adsorption are the same for Rh, Fe and Ta as for Ni, and for C_2H_4 adsorption the same for Fe, Ta, W, Rh as for Ni. It seems likely that there will not be any large *variations* in the ionic term, for one gas with the range of metals, i.e. we should not expect very large variations in surface dipoles. Nevertheless, I would point out that this calculation strictly requires data on contact potentials at low surface coverings of gas, which are not available at present.

The fundamental significance of the success of the calculation is this, that the surface M—H bond is closely similar to the M—M bond in the solid, i.e. it may be treated as a covalent bond, but of the metallic type, resonating below the surface of the metal with all the nearest neighbour metal atoms. It assumes that the hybrid orbitals are the same as in the bulk metal, essentially d^3sp^3 metal orbitals. This, of course, can only be an approximation and for the last two years, Mr. Crowne in my laboratory has been building up the technique to test this hypothesis, by measuring the *change*, if any, in the surface paramagnetism of tungsten when hydrogen (and other gases) chemisorb. We know that when dimethyl sulphide is adsorbed on palladium, atomic *d* orbitals are pressed into service to form surface bonds, but in this case we have a *co-ordinate* link formed to the metal, rather than the simpler bond we are here considering.

---

[21] Roberts, *Some Problems on Adsorption* (Cambridge University Press, 1939), pp. 88, 113.

* I.e. ignoring the possibility of a π bond.

[22] This Discussion.

Calculations on the nitrogen data of Beeck, Cole and Wheeler enable us to give some quantitative support to views advanced by these authors, and originally by Taylor [23] as to the *nature* of these films. I give the arithmetic so that the method of calculation is clear. The value for N_2 on Ta observed is $Q_0 = 135$ kcal. Just as for tungsten we calculate

$$N_2 + 2Ta \rightarrow 2Ta \equiv N \quad Q_{calc.} = 109 \text{ kcal.}$$

Now we calculate

$$H_2 + 2Ta \equiv N \rightarrow 2Ta = N - H \begin{cases} Q_{calc.} = 17 \text{ kcal.} \\ Q_{calc.} = 25 \text{ kcal.} \end{cases}$$

The steps are

$$\begin{aligned} E(Ta \equiv N) &= \tfrac{1}{2}(3 \times 30{\cdot}7 + 225{\cdot}1) + 8{\cdot}5 = 167{\cdot}1 \\ E(Ta = N) &= \tfrac{1}{2}(2 \times 30{\cdot}7 + 100{\cdot}3) + 8{\cdot}5 = \underline{135{\cdot}2} \end{aligned}$$

$$\therefore Ta \equiv N \rightarrow Ta = N\text{—} \qquad Q = -31{\cdot}9 \text{ kcal.}$$

The N—H bond is 92·2, the H—H, 103·2.

$$\therefore Q_{calc.} = 2(92{\cdot}2 - 31{\cdot}9) - 103{\cdot}2 = 17{\cdot}4 \text{ kcal.}$$

The agreement here is such as to convince us that our models are probably right. The observed heats of N_2 on Fe (10 kcal.) and on W (28 kcal.) must be low because the chemisorption largely gives some species such as M=N—N=M, (for W=N—N=M, $Q_{calc.} = -3{\cdot}1$) and the production of the atomic nitrogen films may well be inhibited by an activation energy as suggested by Taylor and Beeck.

Finally may I refer to one way in which aromatic resonance energy may *lower* heats of chemisorption. For benzene

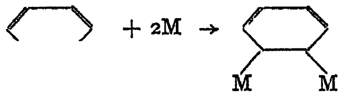

To a first approximation

$$Q_{calc.} = Q_{calc.}(C_2H_4) + R_4 - R_6,$$

where $R_4 - R_6$ is the *difference* in resonance energies between butadiene and benzene, i.e., -39 kcal. Thus $Q_{calc.} = 36 - 39 = -3$ kcal. and benzene should be weakly chemisorbed, compared to ethylene, in line with the different kinetic behaviour in exchange and hydrogenation reactions.[24]

Note added in proof.—Beeck in *Advances in Catalysis, Vol II* (*New York, 1950*), p. 183, gives for nitrogen on evaporated tungsten films Q_0(expt.)=95 kcal./mole. This is in good agreement with the calculated value for atomic nitrogen films, and is probably to be preferred to the value based on rates of desorption.

The University,
Bristol.

[23] Joris and Taylor, *J. Chem. Physics*, 1939, **7**, 893.
[24] Eley, *Quart. Rev.*, 1949, **3**, 221.

THE ACTIVATED COMPLEX IN CHEMISORPTION AND CATALYSIS

BY HENRY EYRING, CHARLES B. COLBURN AND BRUNO J. ZWOLINSKI

Received 6th February, 1950

The basic assumptions underlying the theory of absolute reaction rates have been analyzed in terms of recent studies. A general treatment of chemisorption and catalysis is given in terms of the activated complex theory of chemical kinetics. A mechanism is proposed for the hydrogenation of ethylene which appears to be in agreement with the available data.

Through the efforts of investigators such as Rideal, Taylor, Schwab, Langmuir, Hinshelwood and others, the broad outlines of the field of catalysis have been defined and the importance of parameters like extent of surface, nature and condition of surface, coverage, active sites, geometry put in their proper perspectives. However, one is still not in the desirable position whereby for any one case one may predict and calculate the extent of a surface reaction from first principles. In this regard it may be worth while to re-examine the assumptions underlying the theory of absolute rates of reaction and show its applicability in the interpretation of heterogeneous reactions.

In formulating the rate of any chemical reaction, consider reaction complexes passing from one region of configuration space to another. Along any one reaction path there will always be a region of phase space corresponding to a maximum free energy separating the initial and final states. The number of reaction complexes passing through this region is given by

$$- \mathrm{d}C/\mathrm{d}t = \sum_{n,i} \mathscr{K}_{ni} C_{ni} \nu_{ni}, \quad . \quad . \quad . \quad . \quad (1)$$

where C = total number of complexes in initial state at any time t,
$\mathscr{K}$ = probability that the reaction complex crosses the barrier in any one attempt,
ν = frequency with which the complexes cross the energy barrier.

The subscripts n and i refer to the quantum numbers associated respectively with the degree of freedom along the reaction co-ordinate and with the remaining internal degrees of freedom of the reaction complex. The above equation applies exactly to any rate process under any set of conditions. Assuming a normal distribution of energy among the internal degrees of freedom of the complex or the equivalent idea of an equilibrium existing between the reactants and the activated state at the top of an energy barrier, the well-known expression obtained for the specific rate constant for a reaction of any order is :

$$k' = \mathscr{K} \frac{kT}{h} \frac{F^{\ddagger}}{\Pi_i F_i} \mathrm{e}^{-\frac{\epsilon_0}{kT}} \quad . \quad . \quad . \quad . \quad . \quad (2)$$

Here, $\mathscr{K}$ is the average transmission coefficient, $F^{\ddagger}$ the partition function of the activated complex, F_i the partition functions for the reactants and ϵ_0 the activation energy of the reaction at the absolute zero of temperature. Although the strict validity of the equation rests on the establishment of an equilibrium, the interpretation of many varied rate phenomena in terms of the above relation lends support to its applicability to most irreversible processes. The concept for which one could wish more definite proof before proceeding to a study of the mechanics of heterogeneous processes is the equilibrium postulate.

For adiabatic reactions involving a rearrangement of matter as embodied in the idea of a reaction complex surmounting an energy barrier, it appears to be sufficient to ascribe $\mathcal{K}$, the transmission coefficient, a value of unity. Hirschfelder[1, 2] and Wigner[1] have considered more closely the shape of the potential energy surfaces in the region of the activated state to find that only in rather exceptional cases can one expect the $\mathcal{K}$ to deviate from unity. Born and Weisskopf[3] formulated a mechanism of surface reactions based on the idea of tunnelling through the potential barrier which would be reflected in values of $\mathcal{K}$ less than unity. At the present time there is little evidence to indicate that this may be an important step in catalysis.

The Equilibrium Postulate.—Consider a unimolecular decomposition of a molecule on a surface. For a surface to be effective, it is imperative that a much closer and more specific interaction takes place between the molecule and the surface atoms than can be ascribed to dispersion forces. Regarding this intermediate as the reaction complex assume that reaction consists in the complex passing as a result of molecular collisions or vibrations into a set of levels corresponding to the activated state or the final state of the products. The following set of linear equations with constant coefficients is obtained :

$$\frac{dC_i}{dt} = \sum_{j \neq i}^{n} (\nu_{ji}C_j - \nu_{ij}C_i) \quad . \quad . \quad . \quad . \quad (3)$$

for the n possible energy levels of the system. The ν_{ij}'s are the specific rates of transition from the level i to the level j, which, in principle at least, can be calculated. Solution of the above set of linear differential equations can be carried out readily and takes the following form

$$C_i = \sum_{k=1}^{n} A_k B_{ik} e^{b_k t}, \quad . \quad . \quad . \quad . \quad (4)$$

where A_k are the arbitrary constants in the general solution determined by the initial values of the C_i's ; B_{ik} and b_k are functions of the transition constants ν_{ij}, which arise from solution of the secular or characteristic determinant. Each C_i is now a completely determined function of time and an overall rate of reaction can be calculated under any set of equilibrium conditions.

To compare the actual rate with the equilibrium rate as determined by a Maxwell-Boltzmann distribution of reacting complexes, a function Γ is defined whose deviation from unity with the extent of reaction provides a measure of the validity of the equilibrium postulate in chemical rate theory. The actual rate for the forward reaction is given by

$$v_a = \sum_{i=1}^{k} \sum_{j=k+1}^{l} \nu_{ij}C_i ; \begin{cases} k < l \\ k + l = n, \end{cases} \quad . \quad . \quad . \quad (5)$$

where k and l refer to the levels of the initial and final states, respectively. Assuming a Maxwell-Boltzmann distribution function, the equilibrium rate for the forward process is then given by the following :

$$v_e = \frac{C_0}{\sum_{i=1}^{k} e^{-\frac{\varepsilon_i}{kT}}} \left\{ \sum_{j=k+1}^{l} (\nu_{1j} e^{-\frac{\varepsilon_1}{kT}} + \nu_{2j} e^{-\frac{\varepsilon_2}{kT}} + \ . \ . \ .) \right\}, \quad . \quad (6)$$

---

[1] Hirschfelder and Wigner, *J. Chem. Physics*, 1939, 7, 616.

[2] Hulburt and Hirschfelder, *ibid.*, 1943, 11, 276.

[3] Born and Weisskopf, *Physik. Chem.*, 1931, 12, 206.

where C_0 is the total concentration of complexes in the levels of the initial state at any time t. Hence, the ratio of the actual rate to the equilibrium rate is

$$\Gamma = \frac{\sum_{i=1}^{k} \sum_{j=k+1}^{l} \nu_{ij} C_i}{\frac{C_0}{\sum_{i=1}^{k} e^{-\frac{\varepsilon_i}{kT}}} \left\{ \sum_{i=1}^{k} \sum_{j=k+1}^{l} \left(\nu_{ij} e^{-\frac{\varepsilon_i}{kT}}\right) \right\}} ; \quad \left\{ \begin{array}{l} k < l \\ k + l = n \end{array} \right. . \qquad (7)$$

Calculations of this nature[4] have been carried out for an extremely simple model of reacting system (with n equals 4) based on chosen values of proper magnitudes for the transition constants. The results are shown graphically in Fig. 1. Though the calculations were made on an oversimplified model under rather extreme conditions of non-equilibrium, only an error of 20 % occurs in the specific rate constant as determined by the theory of absolute rates of reaction for 1 % of the material reacted. Essentially similar results were obtained by Kramer[5] who employed classical diffusion theory. Hulburt and Hirschfelder[6] in a recent study regarded the reaction complexes in configuration space as a compressible fluid and employed hydrodynamic theory to show qualitatively the correctness of the equilibrium postulate. In view of the above studies, a complete rate theory is available which, except for minor refinements, can be applied with confidence to all rate processes.

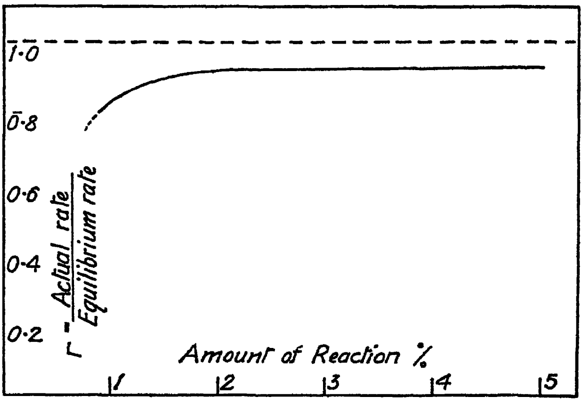

FIG. 1.

General Treatment of Chemisorption and Catalysis.—The application of the activated complex or transition state theory to surface reactions was carried out by Kimball,[7] Temkin,[8] Eyring[9, 10, 11] and more recently by Laidler.[11, 12, 13] A slightly more generalized approach will be developed in the following paragraphs.

---

[4] Zwolinski and Eyring, *J. Amer. Chem. Soc.*, 1947, **69**, 2702.

[5] Kramer, *Physica*, 1940, **7**, 284.

[6] Hulburt and Hirschfelder, *ibid.*, 1949, **17**, 964.

[7] Kimball, *ibid.*, 1938, **6**, 447.

[8] Tempkin, *Acta Physicochim.*, 1938, **8**, 141.

[9] Eyring, *J. Chem. Physics*, 1935, **3**, 107.

[10] Glasstone, Laidler and Eyring, *The Theory of Rate Processes* (McGraw-Hill Book Co., Inc., New York, 1941).

[11] Laidler, Glasstone and Eyring, *J. Chem. Physics*, 1940, **8**, 659, 667.

[12] Laidler, *J. Physic. Chem.*, 1948, **53**, 712.

[13] Schuler and Laidler, *J. Chem. Physics*, 1949, **17**, 1212.

The following assumptions are made :

(1) In every surface process, the activated complex consists of the reactants and the catalyst. In certain specific cases, where—except for the catalyst atoms—the activated state contains the same number and kind of atoms of the reactants as the homogeneous reaction, the difference in energies of activation between the homogeneous and heterogeneous reactions is ascribed to the heat of adsorption of the homogeneous activated complex to the surface of the catalyst.

(2) The surface reaction is considered as a homogeneous reaction between the gaseous reactants and the atoms, molecules or ions of the catalyst. In this analysis, we are neglecting volume phenomena, such as solution of reactants, and the effect of reverse reactions.

Consider a reacting system consisting of two different gaseous species and a catalyst. The following mechanism can be written based on a model of the two different gaseous reactants interacting with the surface. The kind and number of atoms in the activated complex will determine the kinetics of the overall process, so as to agree with experimental data. Thus one obtains

$$nC_i + mC_j + S_k \rightleftharpoons (C_{ni}C_{mj}S_k)^{\ddagger} \rightarrow C_{i+1} + C_{j-1} + S_k,$$

$$\text{where the}\quad \left.\begin{aligned} C_i,\ C_j &= \text{gaseous concentration of reactants,} \\ C_{i+1},\ C_{i-j} &= \text{gaseous concentrations of products,} \\ S_k &= k^{\text{th}}\ \text{surface site.} \end{aligned}\right\} \quad . \quad (8)$$

The subscripts *n* and *m* in the activated complex are used to denote any fragmentation or dissociation of the original reactants.

As is well known, the rate-determining step in catalysis can be one of a number of different processes, e.g. diffusion to the surface, diffusion on the surface (excluding solubility in catalyst), adsorption of reactants, surface dissociation, combination of radicals on the surface and desorption of products. Assuming no alteration in surface characteristics with reaction, it is possible to write, in the most general form, for the initial velocity of reaction, the following equation without assuming any one specific activated complex for the mechanism :

$$v = \mathscr{K}(C_{n_i}C_{m_j}S_k)^{\ddagger}\nu \quad . \quad . \quad . \quad . \quad (9)$$

Expressing the concentration of activated complex in terms of the reactants, one has the result

$$v = \mathscr{K}C_i^nC_j^mS_k\frac{\dfrac{F^{\ddagger}}{A}}{\left(\dfrac{F_i}{V}\right)^n\left(\dfrac{F_j}{V}\right)^m f_k}e^{-\frac{\varepsilon_0}{kT}} \quad . \quad . \quad . \quad (10)$$

$$v = \mathscr{K}C_i^nC_j^mS_a\frac{f^{\ddagger}}{f_i^nf_j^mf_k}e^{-\frac{\varepsilon_0}{kT}} \quad . \quad . \quad . \quad . \quad (11)$$

By proper choice of an activated complex, i.e. specifying the values of *n* and *m* the rate equation for any kind of a surface process is obtained. If it is assumed that all the products and reactants establish equilibrium concentrations on the surface, the effect of pressure and poisons can readily be accounted for by modification of the above equation with the appropriate adsorption isotherms.

Mechanism of Ethylene Hydrogenation.—To illustrate more fully the application of the above theory the procedure appropriate to the determination of the mechanism of the hydrogenation of ethylene may here be outlined. This reaction was chosen because a successful mechanism for the catalytic hydrogenation has not been proposed, even though the reaction has been studied extensively by a number of workers.

(Beeck[14, 15, 16] and co-workers investigated this reaction on numerous catalysts such as chromium, iron, cobalt, nickel, rhodium, palladium, platinum, tantalum and tungsten; Twigg[17] on nickel; Taylor and co-workers[18, 19] on various oxides; A. Farkas,[20, 21] L. Farkas[20, 21] and Rideal[22] on nickel; Toyama[23, 24] on nickel at temperature of 0° C and in the temperature range 99-165°; Pease[25] on copper; Wheeler and Pease[26] have studied the relative rates of hydrogenation by deuterium and hydrogen on copper. Many other workers have also contributed much to the understanding of the mechanism of hydrogenation. Roberts'[27] work on the nature of adsorbed layers is fundamental to the knowledge of all surface processes.)

From these studies the following facts will have to be explained by or be in agreement with any proposed mechanism:

(1) H_2 and C_2H_4 are rapidly adsorbed by metallic surfaces even at liquid air temperatures, however, in the case of the hydrogen about 20 % of the H_2 can be removed by pumping at room temperature.

(2) ΔH_{ads} for H_2 varies from 30 to 18 kcal. per mole on Ni; ΔH_{ads} for C_2H_4 varies from 60 to 23 kcal. per mole on Ni. The larger value is the heat of adsorption on a clean metal surface and the smaller value is the heat of adsorption on a nearly complete monolayer.

(3) The activation energy of the hydrogenation is 10·7 kcal. on Ni, Rh, Co, Fe, Pd, Pt, W, Ta.

(4) The value for the average heat of adsorption of ethylene on nickel is 41·5 kcal.

(5) The reaction rate may be expressed as $v \propto P^1_{H_2} P^0_{C_2H_4}$ at low temperatures.

(6) The reaction rate may be expressed as $v \propto P^1_{H_2} P^1_{C_2H_4}$ at high temperatures.

(7) The overall heat of reaction is 32 kcal. per mole.

(8) The hydrogenation appears to be molecular in hydrogen.

These observations which must be explained are apparently satisfied only by the following mechanism. Both ethylene and hydrogen are adsorbed on the surface but ethylene being much more tightly held tends to displace hydrogen molecules. The activated complex is an ethane just desorbed from its two positions on the surface. Suppose that for an adsorbed ethylene there are b neighbouring positions which a hydrogen molecule can occupy and still react with the ethylene to form ethane. We let a represent the number of positions per square centimetre accessible to both hydrogen or ethylene and we take σ_1 and σ_2 as the fraction of these positions covered by ethylene and hydrogen respectively; k' is the specific rate of reaction of an adsorbed ethylene with an adsorbed hydrogen molecule. We shall not take explicit account of the co-operative forces which tend to make adsorbed molecules bunch on the surface. Then the velocity of reaction v in molecules per square centimeter is

$$v = a\sigma_1\sigma_2 bk'. \qquad (12)$$

[14] Beeck, Smith and Wheeler, *Proc. Roy. Soc. A*, 1940, **177**, 62.
[15] Beeck, *Rev. Mod. Physics*, 1945, **17**, 61.
[16] Beeck, *ibid.*, 1948, **20**, 127.
[17] Twigg, *Trans. Faraday Soc.*, 1935, **35**, 934.
[18] Woodman, Taylor and Turkevich, *J. Amer. Chem. Soc.*, 1940, **62**, 1397.
[19] Woodman and Taylor, *ibid.*, 1940, **62**, 1393.
[20] Farkas, Farkas and Rideal, *Proc. Roy. Soc. A*, 1934, **146**, 630.
[21] Farkas and Farkas, *J. Amer. Chem. Soc.*, 1938, **60**, 22.
[22] Rideal, *Chem. and Ind.*, 1943, **62**, 335.
[23] Toyama, *Rev. Phys. Chem., Japan*, 1937, **11**, 152.
[24] Toyama, *ibid.*, 1938, **12**, 115.
[25] Pease, *J. Amer. Chem. Soc.*, 1923, **45**, 1196, 2235.
[26] Wheeler and Pease, *ibid.*, 1936, **58**, 1665.
[27] Roberts, *Proc. Roy. Soc. A*, 1935, **152**, 445.

To calculate the σ's we define a partition function f_1 for ethylene such that $\mu_1 = -kT \ln f_1$, where μ_1 is the chemical potential of ethylene.

Thus
$$f_1 = \frac{(2\pi m_1 kT)^{3/2}}{h^3}\frac{V}{n_1}\frac{8\pi^2(8\pi^3 ABC)^{1/2}(kT)^{3/2}}{4h^3}\prod_{i=1}^{12}\frac{1}{1 - e^{-\frac{h\nu_i}{kT}}} \quad . \quad (13)$$

Here V is the total gaseous volume which contains n_1 molecule of C_2H_4 so that $V/n_1 = kT/p_1$, where p_1 is the partial pressure of ethylene. The other quantities in (13) have their usual meaning. f_2 is defined analogously for hydrogen gas. f_s represents the partition function for the surface atoms before they combine with hydrogen or ethylene; f_{s1} and f_{s2} represent the partition functions for the compound ethylene-surface and hydrogen-surface respectively. Then

$$\sigma_1 = \frac{f_{s1}f_1}{f_s f_1 f_2 + f_{s1}f_2 + f_{s2}f_1},$$

and
$$\sigma_2 = \frac{f_{s1}f_2}{f_s f_1 f_2 + f_{s1}f_2 + f_{s2}f_1}.$$

Thus substituting in (12) gives

$$v = ab\frac{f_{s1}f_{s2}f_1 f_2}{(f_s f_1 f_2 + f_{s1}f_2 + f_{s2}f_1)^2}\mathscr{H}\frac{kT}{h},\frac{f_{3ss}}{f_{s1}f_2}, \quad . \quad . \quad (14)$$

or
$$v = ab\mathscr{H}\frac{kT}{h}\frac{f_3^{\ddagger}}{f_1 f_2}\left(1 + \frac{f_{s1}}{f_1 f_s} + \frac{f_{s2}}{f_2 f_s}\right)^{-2} \quad . \quad . \quad . \quad (15)$$

Here f_{3ss} is the combined partition function for activated ethane with all the surface atoms involved in reaction and $f^{\ddagger} \equiv f_{3ss}f_s^{-2}$. Since under all experimental conditions v is proportional to the pressure of hydrogen we must suppose the quantity $K_2 p_2 \equiv \frac{f_{s2}}{f_s f_2}$ may always be neglected in comparison with 1 and with $\frac{f_{s1}}{f_s f_1} \equiv K_1 p_1$. Further, if we write $f_1 = C/p_1$

$$v = ab\mathscr{H}\frac{kT}{h}p_1(1 + K_1 p_1)^{-2}\frac{f_3^{\ddagger}}{Cf_2}.$$

At low pressures of ethylene $v \propto p_1$ and at high pressures $v \propto 1/p_1$ in agreement with experiment. By setting $\frac{d}{dp_1}(p_1(1 + K_1 p_1)^{-2}) = 0$ we find that for $K_1 p_1 = 1$ the value of v is independent of p_1. Substituting $p_1 = 1/K_1$ gives

$$v = \frac{ab}{C}\mathscr{H}\frac{kT}{h4K_1}\frac{f_3^{\ddagger}}{f_2}.$$

Substituting for C and K_1 gives

$$v = \frac{ab}{4}\frac{kT}{h}\mathscr{H}\frac{f_3^{\ddagger}f_s}{f_2 f_{s1}}.$$

We now substitute for these quantities. We assume $b = 2$ corresponding to two neighbouring hydrogen molecules being able to combine with an adsorbed ethylene. Then

$$v = 170/4 \times 10^{15} \times 2 \times 5\cdot 6 \times 10^{12}$$

$$\frac{\displaystyle\prod_{i=1}^{20}\frac{1}{1 - e^{-\frac{h\nu_i^{\ddagger}}{kT}}}\frac{8\pi^2(8\pi^3 ABC^{\ddagger})^{1/2}(kT)^{3/2}}{6h^3}e^{-\frac{E_0}{RT}}}{\displaystyle\frac{(2\pi m_{H_2}kT)^{3/2}}{h^3}\frac{kT}{p_2}\frac{8\pi^2 I_{H_2}kT}{2h^2}\frac{1}{1 - e^{-\frac{h\nu}{kT}H_2}}\prod_{i=1}^{18}\frac{1}{1 - e^{-\frac{h\nu}{kT}C_2H_4}}} \quad (16)$$

Here E_0 is the energy required to pass from gaseous hydrogen and absorbed ethylene to gaseous ethane. This is the heat of adsorption of ethylene minus the heat of reaction of gaseous hydrogen with gaseous ethylene to make gaseous ethane and agrees with the experimental activation energy $E_0 = 10{,}700$ cal. as nearly as we can estimate it. This point is discussed further below. The internal degrees of freedom of ethane plus its rotational degrees have an entropy of 18·46 cal./mole deg. at 300° K. The internal vibrations of ethylene at 300° have the value of 0·57 cal./mole deg. If we use these values and the known values for hydrogen the only things left undetermined in (16) are the two vibrations associated with the motion of ethane tangent to the surface and these same two vibrations for ethylene plus its motion normal to the surface. Thus we obtain for the velocity of reaction

$$v = 1{\cdot}4 \times 10^{-4} p_2 \frac{\dfrac{1}{\left(1 - e^{-\frac{h\nu}{kT}}\right)^2}}{\prod\limits_{i=1}^{3} \dfrac{1}{1 - e^{-\frac{h\nu_i}{kT}}}} \text{ mole/cm.}^2 \text{ sec.} \quad . \quad . \quad (17)$$

This is to be compared with $v = 1{\cdot}2 \times 10^{-4} p_2$ found by Beeck for unoriented nickel where the surface roughness was found to have the value 170 which we used in our calculation. Thus, if we assume the vibration frequencies in (17) cancel agreement is too good since many things including the experimental values may be slightly different. Quite apart from the numerical agreement it does appear that this must be the reaction mechanism.

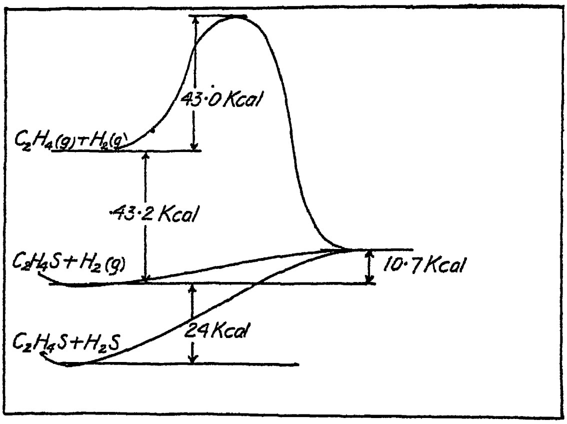

FIG. 2.

If we had an exact value for the heat of adsorption of ethylene our postulated mechanism would enable us to calculate a value for E_0 to compare with the experimental value $E_0 = 10{,}700$ cal./mole. The situation is as follows. The homogeneous hydrogenation of ethylene requires an activation energy of 43 kcal. together with a ΔH of reaction of 32·5 kcal. and occurs readily on the surfaces of metals of Group VII such as Rh, Fe, Ni, Pt, Pd as also W, Ta and Cr, with a constant energy of activation at 10·7 kcal. Whereas the ΔE^{*} remains constant, the temperature-independent factor of the rate constant shows variation by a factor of 10,000 as we progress from W to the much more active Rh. This has been shown by Beeck and co-workers[14, 15, 16] who studied this reaction on evaporated films of the above metals. The average heat of adsorption of ethylene is 41·5 kcal. whereas that of hydrogen is 24 kcal. on prepared Ni evaporated films; thus, the more strongly adsorbed ethylene preferentially covers the surface of the metal catalyst in the place of the hydrogen. The 10·7 kcal. of energy represents the amount of work necessary to form the gaseous ethane from the adsorbed ethylene and the gaseous hydrogen for the condition where the rate of reaction was measured independent of the ethylene pressure. The temperature coefficient for the reaction will take on different values depending on the magnitudes of the pressure of the two reactants. This is shown in Fig. 2, where the potential energy changes are shown along the reaction coordinate.

Such specific considerations of the energies of the process are limited to the specially prepared catalytic surfaces as employed by Roberts and by Beeck. One has only to observe the variations in the heats of adsorption of ethylene, as summarized in Table I, to realize the importance of catalyst preparation, as is well known. Changes that have been measured in the heat of adsorption indicate the heterogeneity of the catalysts, whose activity is conditioned by the sintering, crystallization and impurities, e.g. hydrogen and oxygen resulting from the mode of preparation of catalysts from their salts. Such catalysts, however, as pointed out by H. S. Taylor, are of prime importance in industrial application and will remain a constant challenge to the chemist.

TABLE I.—HEATS OF ADSORPTION OF ETHYLENE

Metal	Heat (kcal./mole) †	Reference
Au	8·8- 6·9	Beebe—Schwab *
Fe	16 - 8	,,
Ni	12	,,
Cr_2O_3	10·8	,,
Cu	16	,,
Pt	9	,,
ZnO	25 -19	,,
ZnO—Cr_2O_3 (reduced) . .	11 -10	,,
ZnO—Cr_2O_3 (oxidized) . .	20 -17	,,
Pt—Black	9	Maxted, Moon
Ni	15	Toyama [23]
Ni	60 -20	Beeck [14]

*Schwab, *Handbuch der Katalyse* (Springer, 1943).
† Variation of heats of adsorption with extent of surface coverage.
Maxted and Moon, *Trans. Faraday Soc.*, 1936, **32**, 1375.

The authors wish to acknowledge a grant from the United States Naval Research Office which made this investigation possible. Special thanks are due to Dr. R. B. Parlin for reading the paper in manuscript and for helpful discussions during the course of the study.

Department of Chemistry,
University of Utah,
Salt Lake City, Utah.

THE ACTIVATED COMPLEX IN HETEROGENEOUS CATALYSIS

By Keith J. Laidler

Received 16th February, 1950

The evidence that certain surface reactions proceed by interaction between an adsorbed molecule and a gas-phase molecule is reviewed briefly, with special reference to the para-ortho hydrogen conversion and the combination of atoms and free radicals. On the basis of absolute rate theory, general rate expressions are developed for reaction between two molecules A and B, of which A is more strongly adsorbed, assuming the following alternative mechanisms; (1) interaction between adsorbed A and adsorbed B, (2) interaction between adsorbed A and gaseous B, (3) interaction between adsorbed B and gaseous A. According to mechanism (1) the rate passes through a maximum and later decreases as the concentration of A is increased, but according to (2) and (3) a limiting rate is reached at high concentrations of A. It is shown that at the maximum according to mechanism (1) the frequency factor is approximately the same as at high A concentrations according to (2) and (3).

The rate expressions are compared with special reference to the reaction between ethylene and hydrogen, for which it is shown that the data appear to favour mechanism (1). The low frequency factor for the reaction ($\sim 10^{-6}$) is explained quantitatively on the basis of the theory, being due to the loss of translational and rotational freedom in forming the activated complex.

The close analogy between surface and enzyme reactions is discussed, and it is shown that many enzyme processes can be interpreted on the basis of mechanism (1). The initial step in the dehydrogenation of lactic acid, the urease-catalyzed hydrolysis of urea and other reactions are considered briefly from this point of view.

From the standpoint of the theory of absolute reaction rates[1] the central problem in the theoretical treatment of the rates of chemical and physical processes is the determination of the configuration of the activated complex. The manner in which the activated complex is composed of the reactant molecules controls the way in which the rate depends upon the concentrations of the reactants (i.e. the order of the reaction), and the entropy and energy of the complex with respect to the reactants control the rate of the reaction. In principle the structure and energy of the activated complex can be calculated by the methods of quantum mechanics, and hence the rate obtained: in practice this cannot be done satisfactorily, and an empirical method must be used. This has usually consisted of obtaining information as to the configuration of the activated complex from the experimental order of the reaction, and deriving the energy of the complex (corrected to 0° K) from the experimental activation energy. It is then possible to calculate frequency factors and rates for postulated mechanisms, and to decide between various possibilities on the basis of the agreement with the experimental data.

This type of treatment has been applied successfully to adsorption and desorption processes at surfaces,[2] to a variety of chemical processes on surfaces,[3] and to the para-ortho hydrogen conversion.[4] In the present paper we discuss further examples, and in particular extend the treatment to a somewhat different type of surface activated complex, in which only one of two reacting molecules is attached to the surface. Langmuir[5] and Hinshelwood[6] have formulated the theory of bimolecular surface reactions on the assumption that in order for reaction to occur it is necessary for the two reactant molecules to become adsorbed side by side, and the calculations referred to above (except for the ortho-para hydrogen conversion) were a development of this idea. There seems to be little doubt that such mechanisms are applicable to most, if not all, of the reactions to which they have been applied. However, there are a few reactions, which have been the centre of recent interest, in which it appears to be more likely that the activated complex is formed not from two adsorbed molecules but from an adsorbed molecule or atom and a molecule or atom in the gas phase or in a van der Waals' layer. This type of mechanism was first propounded by Rideal,[7] and was applied by him and Eley[4] to the para-ortho hydrogen conversion, the activated complex for which may be represented as being formed by the process

---

[1] Eyring, *J. Chem. Physics*, 1935, 3, 107.

[2] Laidler, Glasstone and Eyring, *ibid.*, 1940, 8, 659.

[3] Laidler, Glasstone and Eyring, *ibid.*, 1940, 8, 667.

[4] Eley and Rideal, *Proc. Roy. Soc. A*, 1941, 178, 429.

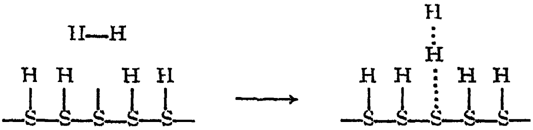

(activated complex)

Such a mechanism seems necessary in this case, since the alternative explanation[8] that the conversion involves an adsorption process followed by rearrangement and desorption,

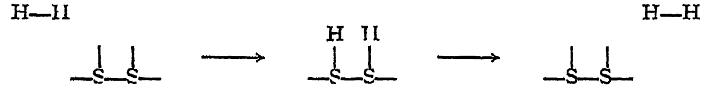

is excluded by Roberts' result[9] that the observed rates of desorption are much too slow. Further support for the Eley-Rideal mechanism is provided by the fact that a quantitative treatment[10] gives good agreement between observed and calculated rates.

Another class of reactions for which it seems necessary to assume that the activated complex is formed directly from a gas-phase species and a surface species comprises the recombinations of atoms and free radicals on surfaces.[11] These are almost always first-order processes, and one mechanism that would explain this behaviour is surface adsorption of the atoms or radicals followed by recombination on the wall; however, this is again excluded by the facts with regard to the stability of the adsorbed layer. An alternative explanation, and the most probable one, is that the reaction involves interaction between a surface-adsorbed atom or radical and a gaseous one; thus the recombination of hydrogen atoms on clean glass surfaces may be represented as

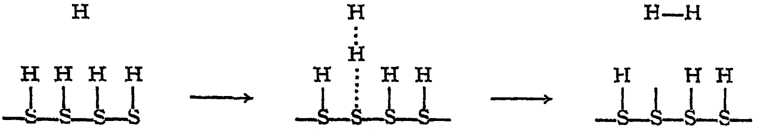

(activated complex)

---

[5] Langmuir, *Trans. Faraday Soc.*, 1921, **17**, 621.

[6] Hinshelwood, *Kinetics of Chemical Change* (Oxford University Press, 1926), p. 145; (1940), p. 187.

[7] Rideal, *Proc. Camb. Phil. Soc.*, 1939, **35**, 130; *Chem. and Ind.*, 1943, **62**, 335.

[8] Farkas, *Z. physik. Chem. B*, 1931, **14**, 371.

[9] Roberts, *Trans. Faraday Soc.*, 1939, **35**, 941.

[10] Eley, *Trans. Faraday Soc.*, 1948, **44**, 216; K. J. Laidler and G. W. Castellan, (unpublished results).

[11] Shuler and Laidler, *J. Chem. Physics*, 1949, **17**, 1212, 1356.

Detailed calculations on the basis of such a mechanism again give satisfactory agreement with the experimental results.

In view of the importance of Rideal mechanisms in processes of this kind it is natural to inquire whether similar mechanisms are applicable to reactions which have conventionally been regarded as controlled by interaction between two adsorbed molecules. In the general case of a reaction between two molecules A and B we can formulate the Langmuir-Hinshelwood mechanism as follows :

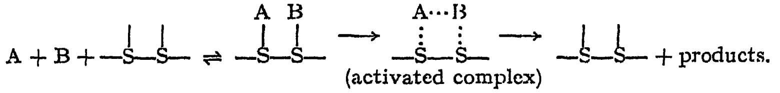

$$\mathrm{A + B + {-}\overset{|}{S}{-}\overset{|}{S}{-} \rightleftharpoons {-}\overset{\overset{A}{|}}{S}{-}\overset{\overset{B}{|}}{S}{-} \longrightarrow {-}\overset{\overset{A\cdots B}{\vdots\quad\vdots}}{S{-}S}{-} \longrightarrow {-}\overset{|}{S}{-}\overset{|}{S}{-} + products.} \qquad (1)$$

With the Rideal mechanism there are two distinct possibilities : in the first, reaction occurs between a gas phase molecule of A and an adsorbed molecule of B, e.g.

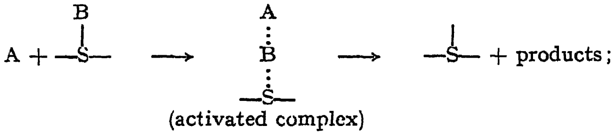

$$\mathrm{A + {-}\overset{\overset{B}{|}}{S}{-} \longrightarrow \underset{\underset{-S-}{\vdots}}{\overset{\overset{A}{\vdots}}{B}} \longrightarrow {-}\overset{|}{S}{-} + products;} \qquad (2)$$

in the second, A is adsorbed and B is in the gas phase ;

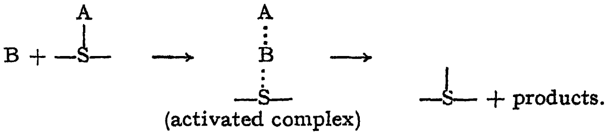

$$\mathrm{B + {-}\overset{\overset{A}{|}}{S}{-} \longrightarrow \underset{\underset{-S-}{\vdots}}{\overset{\overset{A}{\vdots}}{B}} \longrightarrow {-}\overset{|}{S}{-} + products.} \qquad (3)$$

In mechanism (2) it is not necessary that A is not at all adsorbed, but rather that an adsorbed A does not contribute directly to reaction ; however, it may be noted that if A is adsorbed more than very weakly it will indirectly affect the rate by influencing the concentration of adsorbed B molecules.

With a view to contributing to the problem of distinguishing between the three mechanisms (1), (2) and (3) in any instance we will now formulate the rate laws in each case. It will be assumed throughout that A is much more strongly adsorbed than B, i.e. that there are more adsorbed A molecules than B ; however, no other restriction is placed on the degree of adsorption. The equations will then be applied briefly to the kinetics of the hydrogenation of ethylene, with A = C_2H_4 and B = H_2. Beeck[12] has suggested that this reaction proceeds by mechanism (2), gaseous ethylene reacting with adsorbed hydrogen ; A (ethylene) is strongly adsorbed but the adsorbed ethylene molecules do not interact directly with adsorbed hydrogen molecules. The data certainly exclude mechanism (3), but it will be seen that the formulation of the rate laws leads us to the conclusion that the data are more consistent with mechanism (1) than with mechanism (2).

Interaction Between Two Adsorbed Molecules (Mechanism (1)).— The concentration c_a of adsorbed A is given by

$$\frac{c_a}{c_s} = Kc_g, \qquad . \quad . \quad . \quad . \quad . \quad (1)$$

where c_s is the concentration (in molecular units) of bare surface sites and

---

[12] Beeck, *Rev. Mod. Physics.*, 1945, **17**, 61.

* The derivations given here and in the following two sections employ the same notation and general assumptions as in Glasstone, Laidler and Eyring, *The Theory of Rate Processes* (McGraw-Hill Book Company, New York, 1941), Chap. VII.

c_g that of A in the gas phase; K is the equilibrium constant, given by

$$K = \frac{f_a}{F_g f_s} e^{\epsilon/kT}, \quad \cdot \quad \cdot \quad \cdot \quad \cdot \quad \cdot \quad (2)$$

where the f are the partition functions and ϵ the energy of adsorption. Similarly, for the adsorption of B, denoting the quantities by primes,

$$\cdot \quad \cdot \quad \cdot \quad \cdot \quad \cdot \quad (3)$$

$$\upsilon_s$$

where K' is now given by

$$K' = \frac{f_a'}{F_g' f_s} e^{\epsilon'/kT} \quad \cdot \quad \cdot \quad \cdot \quad \cdot \quad (4)$$

In addition,

$$c_a + c_a' + c_s = L, \quad \cdot \quad \cdot \quad \cdot \quad \cdot \quad (5)$$

where L is the concentration of sites when the surface is completely bare. Eqn. (1), (3) and (5) give rise to

$$c_a = \frac{LKc_g}{1 + Kc_g + K'c_g'}, \quad \cdot \quad \cdot \quad \cdot \quad \cdot \quad (6)$$

and

$$c_a' = \frac{LK'c_g'}{1 + Kc_g + K'c_g'} \quad \cdot \quad \cdot \quad \cdot \quad \cdot \quad (7)$$

The condition that $c_a \gg c_a'$ implies that $Kc_g \gg k'c_g'$; these equations thus reduce to

$$c_a = \frac{LKc_g}{1 + Kc_g}, \quad \cdot \quad \cdot \quad \cdot \quad \cdot \quad \cdot \quad (8)$$

and

$$c_a' = \frac{LK c_g'}{1 + Kc_g} \quad \cdot \quad \cdot \quad \cdot \quad \cdot \quad (9)$$

The fraction θ' of surface covered by B is clearly c_a'/L, i.e.

$$\theta' = \frac{K'c_g'}{1 + Kc_g} \quad \cdot \quad \cdot \quad \cdot \quad \cdot \quad \cdot \quad (10)$$

The rate can now be formulated as follows. The average number of adsorbed B's adjacent to any given adsorbed A is $s\theta'$, where s is the maximum possible number of near neighbours; the total number of adsorbed A—B pairs is thus $c_a s\theta'$, which equals

$$(1 + Kc_g)^2.$$

If these react with an activation energy (at the absolute zero) of ϵ_0, the rate is given by

$$v = \frac{sLKK'c_g c_g'}{(1 + Kc_g)^2} \cdot \frac{kT}{h} \cdot \frac{f^{\ddagger}}{f_{aa}'} e^{\epsilon_0/kT}, \quad \cdot \quad \cdot \quad \cdot \quad (11)$$

where $f^{\ddagger}$ and f_{aa}' are the partition functions for the activated complex and for the adsorbed pair of molecules. Expressing the K and K' in the numerator using eqn. (2) and (4) gives

$$v = \frac{sLc_g c_g'}{(1 + Kc_g)^2} \cdot \frac{kT}{h} \cdot \frac{f^{\ddagger} f_a f_a'}{F_g F_g' f_s^2 f_{aa}'} \exp((-\epsilon_0 + \epsilon + \epsilon')/kT) \quad (12)$$

It is seen that the rate is always proportional to c_g' (provided that the condition $Kc_g \gg K'c_g'$ holds), but that when c_g is increased the rate at first increases linearly, later goes through a maximum, and finally decreases. The maximum rate corresponds to $c_g = 1/K$, and is equal to

$$v = \frac{sLc_g}{4K} \cdot \frac{kT}{h} \cdot \frac{f^{\ddagger} f_a f_a'}{F_g F_g' f_s^2 f_{aa}'} \exp((-\epsilon_0 + \epsilon + \epsilon')/kT) \quad \cdot \quad (13)$$

$$= \frac{sLc_g'}{4} \cdot \frac{kT}{h} \cdot \frac{f^{\ddagger} f_a'}{F_g' f_s f_{aa}'} \exp((-\epsilon_0 + \epsilon')/kT) \quad \cdot \quad \cdot \quad (14)$$

The activation energy of the reaction increases with increasing concentration of A owing to the positive heat of adsorption of A, i.e. to the fact that K varies with temperature as $e^{\epsilon/kT}$, where ϵ is positive. At low concentrations of A, when $1 \gg Kc_g$, it is seen from eqn. (12) that the activation energy at the absolute zero * is $\epsilon_0 - \epsilon - \epsilon'$; at the maximum eqn. (14) shows it to be $\epsilon_0 - \epsilon'$, while at high concentrations it is $\epsilon_0 + \epsilon - \epsilon'$. Eqn. (12) also predicts that the activation energy will decrease with increasing temperature, owing to the decrease in the importance of Kc_g compared with unity in the denominator. In view of these variations the importance of measuring activation energies under well-defined conditions is obvious; unfortunately this has not always been done.

Interaction Between an Adsorbed Molecule A and a Gaseous Molecule B (Mechanism (2)).—The concentration of adsorbed A is given by eqn. (1), and the rate of reaction with a gaseous B molecule is therefore given by

$$v = c_g{'}c_a \cdot \frac{kT}{h} \cdot \frac{f^{\ddagger}}{F_g{'}f_a} e^{-\epsilon_0'/kT} \quad . \quad . \quad . \quad . \quad (15)$$

$$= \frac{LKc_gc_g{'}}{1 + Kc_g} \cdot \frac{kT}{h} \cdot \frac{f^{\ddagger}}{F_g{'}f_a} e^{-\epsilon_0'/kT} \quad . \quad . \quad . \quad (16)$$

$$= \frac{Lc_gc_g{'}}{1 + Kc_g} \cdot \frac{kT}{h} \cdot \frac{f^{\ddagger}}{F_gF_g{'}f_s} e^{-(\epsilon_0'-\epsilon)/kT} \quad . \quad . \quad (17)$$

The rate now varies with the concentration of A in a different manner, increasing linearly at first and finally reaching a constant value. The activation energy is $\epsilon_0' - \epsilon$ at low concentrations of A and ϵ_0' at high ones.

Interaction Between an Adsorbed Molecule of B and a Gaseous Molecule of A (Mechanism (3)).—The rate is now given by

$$v = c_gc_a{'}\frac{kT}{h} \cdot \frac{f^{\ddagger}}{F_g{'}f_a{'}} e^{-\epsilon_0''/kT} \quad . \quad . \quad . \quad . \quad (18)$$

$$= \frac{LK'c_gc_g{'}}{1 + Kc_g} \cdot \frac{kT}{h} \cdot \frac{f^{\ddagger}}{F_gf_a{'}} e^{-\epsilon_0''/kT} \quad . \quad . \quad . \quad (19)$$

$$= \frac{Lc_gc_g{'}}{1 + Kc_g} \cdot \frac{kT}{h} \cdot \frac{f^{\ddagger}}{F_gF_g{'}f_s} e^{-(\epsilon_0''-\epsilon)/kT} \quad . \quad . \quad (20)$$

This mechanism predicts the same type of variation of the rate and activation energy with the concentration of A as does mechanism (2).

Comparison of the Mechanisms.—An interesting feature of the treatments given above is that at low concentrations of A all three mechanisms correspond to approximately the same frequency factor. Moreover, in the region of the maximum rate mechanism (1) predicts the same frequency factor as is given by mechanisms (2) and (3) at high concentrations of A, when the rate is no longer dependent upon the pressure of A. This conclusion could hardly have been reached without the detailed treatment, and indeed other conclusions have been arrived at on intuitive grounds. Thus Beeck [12] implies that the low experimental frequency factor for the ethylene-hydrogen reaction is in favour of mechanism (3), the argument being that since the surface is sparsely covered with hydrogen only a small fraction of the sufficiently energetic collisions of ethylene molecules will be effective. The reason that this argument is not valid is that the concentration of adsorbed hydrogen varies with the temperature, so that the effect appears in the activation energy and not in the frequency factor. We shall see later that the low frequency factor is due to the loss of translational and rotational freedom in forming the adsorbed activated complex. The same assumption as

---

* This differs slightly from the value at experimental temperatures owing to the temperature dependence of kT/h and the partition functions.

Beeck's is also implicit in Eley's discussion [13] of the factors determining whether a reaction will proceed by a Langmuir-Hinshelwood or by a Rideal mechanism.

Since the frequency factors are the same the question must be determined by the relative activation energies for the three possible mechanisms. In general this factor will favour mechanism (1), since adsorbed molecules are more reactive than gaseous ones. Mechanisms (2) and (3) may, however, involve lower activation energies than mechanism (1) if the product of the reaction is strongly adsorbed on the surface, so that a considerable energy of activation is required for its removal. This would seem to be the only factor which will cause a reaction to proceed by mechanism (2) or (3). This situation particularly arises when the product of reaction is a hydrogen molecule.

Our general conclusion is therefore that the Langmuir-Hinshelwood mechanism is probably the general rule, and that the Rideal mechanism would seem to apply only when the reaction product is strongly adsorbed on the surface.

The Reaction Between Hydrogen and Ethylene.—The hydrogenation of ethylene has been very thoroughly investigated, on a variety of surfaces,[14] and will now be discussed briefly in the light of the conclusions derived above. Ethylene is more strongly adsorbed than hydrogen on the surfaces employed, so that A = C_2H_4 and B = H_2. The product, ethane, is very weakly adsorbed, so that we should expect the reaction to proceed by the Langmuir-Hinshelwood mechanism (1). Support for this conclusion is provided by the fact that the rate decreases at high ethylene concentrations, a result that is predicted by mechanism (1) but not by mechanisms (2) and (3). That the reaction is frequently stated to be of zero order with respect to ethylene is probably due to the fact that the measurements were made in the neighbourhood of the maximum.

We may now consider whether the frequency factor predicted by mechanism (1) at the maximum rate is consistent with the experimental data. Beeck [12] has found on nickel a steric factor of $\sim 10^{-6}$; this is the ratio of the rate to the number of ethylene molecules striking the surface with the required energy of activation. According to eqn. (14) the frequency factor at the maximum is

$$B_1 = \frac{sL}{4} \cdot \frac{kT}{h} \cdot \frac{f^{\ddagger} f_a'}{F_g' f_s f_{aa}'}, \qquad (21)$$

$$= \frac{sL}{4} \cdot \frac{kT}{h} \cdot \frac{1}{\frac{(2\pi mkT)^{3/2}}{h^3} b_g}, \qquad (22)$$

where m is the mass of the ethylene molecule and b_g is the rotational and vibrational contribution to the partition function. The frequency factor for striking the surface is [15]

$$B_2 = \frac{kT}{h} \frac{1}{\frac{(2\pi mkT)^{1/2}}{h}} \qquad (23)$$

The steric factor for the reaction is therefore

$$\frac{B_1}{B_2} = \frac{(1/4)sL}{\frac{(2\pi mkT)}{h^2} b_g} \qquad (24)$$

---

[13] Eley, *Advances in Catalysis* (Academic Press, New York, 1948), Vol. 1, p. 157; *Quart. Rev.*, 1949, 3, 209.

[14] For full references see Eley.[13]

[15] Laidler, *J. Physic. Chem.*, 1949, **53**, 712.

For ethylene at 300° K, $(2\pi mkT)/h^2$ is $2{\cdot}6 \times 10^{17}$ and b_g is $2{\cdot}2 \times 10^3$; with $s = 4$ and $L = 5 \times 10^{14}$ the steric factor is found to be

$$B_1/B_2 = 0{\cdot}9 \times 10^{-6}, \quad . \quad . \quad . \quad . \quad (25)$$

in excellent agreement with the experimental value of $\sim 10^{-6}$. This low steric factor is seen to be due to the loss of translational and rotational freedom in forming the activated complex, and there is no need to assume that only a fraction of the surface is active.

Certain arguments have been invoked by Beeck [12] in favour of mechanism (3). His thermochemical objection to mechanism (1), the main argument, has been answered by Eley,[13] while the point with regard to the frequency factor is covered above. Our conclusion is therefore that mechanism (1) is entirely consistent with all the data that have been recorded, and that the evidence favours it strongly in comparison with mechanisms (2) and (3).

Reactions Catalyzed by Enzymes.—The above considerations have direct application to the kinetics of enzyme-catalyzed reactions, which may now be considered very briefly. Enzymes are in some ways easier to treat than inorganic surfaces, since the sites at which adsorption can occur are more clearly defined, a fact that can be inferred from the very high specificity. Enzymes can be divided into two classes, according to whether they have one or two different types of surface sites which are concerned in reaction. The former comprises many of the protolytic enzymes, the latter all of the hydrogenases, in which one site interacts with the substrate and the other with the coenzyme. We have elsewhere [16] formulated the kinetic laws applicable to the two-site systems, and will here only indicate the analogies between them and the surface reactions considered above.

One example is the reaction :

lactic acid + coenzyme I → pyruvic acid + reduced coenzyme I,

which is catalyzed by the apoenzyme of lactic dehydrogenase ; we have recently studied this reaction experimentally from the present standpoint.[17] The rate is found to increase at first linearly with increasing concentrations of lactic acid and of coenzyme. At higher concentrations of lactic acid the rate reaches a constant limiting value, while at higher concentrations of coenzyme the rate passes through a minimum and then diminishes. This may be interpreted by a mechanism which is similar to mechanism (1) for the hydrogenation of ethylene. For reaction to occur it is supposed that a lactic acid molecule must be adsorbed on a site of type 1, and a coenzyme molecule on a site of type 2. The inhibition at high coenzyme concentrations must be due to the fact that a coenzyme molecule can also be attached to a site of type 1, replacing a lactic acid molecule. However, lactic acid presumably cannot displace a coenzyme molecule on site 2, since there is no inhibition at high lactic acid concentrations.

A somewhat similar situation appears to exist in the urease-catalyzed hydrolysis of urea, the rate of which passes through a maximum as the urea concentration is increased. Here it is supposed [18] that for reaction to occur a urea molecule must be adsorbed on one type of site and a water molecule on the second type ; urea may, however, exclude the water by becoming adsorbed on a site of type 2. A similar situation exists in the decomposition of hydrogen peroxide catalyzed by catalase, a reaction that is also inhibited at high substrate concentrations ; presumably two sites are again involved, although a detailed mechanism has not been worked out. When there is no such inhibition, as with the majority of protolytic enzymes, it may be supposed that it is not necessary for the water to be attached to a site on the enzyme, so that here the situation resembles mechanisms (2) and (3).

---

[16] Laidler and Socquet, *J. Physic. Chem.* (in press).

[17] Socquet and Laidler, *Arch. Biochem.* 1950, **25**, 171.

[18] Laidler and Hoare, *J. Amer. Chem. Soc.*, 1949, **71**, 2699.

Department of Chemistry,
The Catholic University of America,
Washington, D.C.,
U.S.A.

THE ROLE OF HETEROGENEITY IN ADSORPTION AND CATALYSIS

BY G. D. HALSEY, Jr.

Received 9th January, 1950

Data on adsorption almost always deviate from the Langmuir equation. These deviations often can be formally explained equally well by interaction between absorbed molecules or non-uniformity of the adsorbing surface. The author has emphasized the second of these explanations, and a discussion is given of various proofs or indications that it is a valid one.

In some cases, notably physical adsorption near the saturation pressure, interaction plays an important role in determining the isotherm. The author has shown that a refined treatment of a uniform surface does not lead to the BET equation but leads to the conclusion that heterogeneity and interaction operate simultaneously. The BET surface area determination using nitrogen as adsorbate, seems completely satisfactory. The reasons that explain this validity in the face of the unreality of the isotherm equation are discussed.

The rate of reaction on a non-uniform catalyst surface is formulated, and it is pointed out that the assumption that some one reaction is the rate-determining step is no longer valid. Because a group of sites that are of overwhelming importance catalytically may not contribute appreciably to adsorption, there is no very direct information about catalysis to be gained from adsorption studies. Also, on a non-uniform surface, the rate of the forward reaction cannot be determined from the equilibrium constant and the rate of the backward reaction, except at equilibrium.

Adsorption on Tungsten.—Frankenburg's data for the adsorption of hydrogen on tungsten powder have been interpreted on the basis of a non-uniform adsorbing surface by Taylor and Halsey.[1] We showed that an exponential distribution of adsorption energies over the surface would account for the Freundlich type isotherms discovered by Frankenburg. We maintained that interaction on a uniform surface alone could not account for the strongly varying heat of adsorption, which declined exponentially (excepting for a small amount of constant heat Langmuir adsorption at below 2 % coverage).

Miller [2] has criticized the conclusion that Frankenburg's data are explained by the non-uniform surface. He remarks that interaction was rejected by us because the relation between q and θ was not the linear one, required by simple theory. Actually we considered a more general case (our eqn. (8)) with higher terms in θ, to allow the energy of a cluster to differ from the sum of the isolated pair interactions involved. We thus did not assume a fixed interaction energy. We could confine our attention to the crude approximation of random distribution because refinements such as the quasi-chemical approximation lessen the effect of repulsive interaction, making the $q - \theta$ curve convex to the axes, while Frankenburg's heats were strongly concave to the axes. Similarly, Roberts'[3] model for the immobile film leads to curvature in the wrong sense. The rejection of interaction as a sole explanation of the q against θ curve was based not on the shape of the curve, but its slope at low θ, where the contributions to the repulsive interaction would come almost entirely from isolated pair interactions. The repulsive energy required would then be many times RT. Therefore the random arrangement of atoms on the surface would be far from the most stable configuration, thus causing the heat curve for a uniform surface to become strongly convex to the axes. In short, the chief reason for the rejection of the interaction theory as a complete explanation is the magnitude of the repulsive energy, coupled with the overall concavity of the q against θ curve.

---

[1] Halsey and Taylor; *J. Chem. Physics*, 1947, **15**, 624.

[2] Miller, *ibid.*, 1948, **16**, 841.

We do not imply that interactions are not also operating, especially at larger θ ; it is true, however, that it is not *necessary* to invoke interactions to explain the data on tungsten. It should be pointed out, nevertheless, that the loophole in our argument is the neglect of other than nearest neighbour interactions. Using an arbitrary function for repulsion against separation, and assuming random distribution over the surface, any desired heat curve can be reproduced.

It is apparent, that for large repulsions, and the so-called immobile film randomly distributed, that the configuration is far from equilibrium, and that no equilibrium isotherm, free energy or entropy can be derived. In view of the complexities of the problem, it seems wise to confine attention to the equilibrium state, experimentally verified by the reversibility of the isotherm measurements, and the agreement of isosteric heats with those measured calorimetrically.

Physical Adsorption.—An analysis of adsorption on a uniform surface,[4] using the quasi-chemical theory of interaction, has shown that the refined hypotheses of the Brunauer-Emmett-Teller (BET) theory lead to substantially no adsorption beyond the first layer, if the energy of condensation in the second layer equals the energy of liquefaction of the bulk liquid. On a uniform surface even if $E_2 > E_3 \ldots E_n > E_L$, a refined treatment predicts an isotherm composed of a series of steps. Non-uniformity of the surface smooths these steps out, explaining the curves observed experimentally. It is apparent that when the monolayer portion of an isotherm in the region of physical adsorption is considered by itself, it may not be easy to choose between repulsion or heterogeneity. This difficulty arises because the required repulsion potentials may not be large compared to kT. Nevertheless the imminence of the *attractive* interactions that cause multilayer formation, coupled with the necessity of a slightly non-uniform field to smooth out the later part of the isotherm suggest that heterogeneity cannot be neglected. The formidable problem of considering interaction on a heterogeneous surface has recently been attacked by Hill,[5] but as yet, no experimental case has been quantitatively analyzed.

The BET Surface Area.—Although the BET isotherm equation has been shown to be invalid, the surface areas estimated using the equation seem to be remarkably satisfactory. A number of reasons can be given.

1. In so far as the isotherms on two similar catalyst preparations are geometrically similar, the ratio of any two corresponding points, for any pressure, will be a constant, giving the relative surface area.

2. The BET plot, although based on a " theoretical " equation, can be looked upon as a graphical method of selecting the " point B " of the isotherm, having no essential connection with the BET theory.

---

[3] Roberts, *Some Problems in Adsorption* (Cambridge, 1939), § 2.6, Fig. 14.
[4] Halsey, *J. Chem. Physics*, 1948, **16**, 931 ; Hill, *ibid.*, 1949, **17**, 106.
[5] Hill, *ibid.*, 1949, **17**, 762.

3. The nitrogen isotherms have been found the most "reliable" for estimating surface area; and, in general, nitrogen gives by far the best-defined point B.

4. Point B is located where the affinity of the surface for the gas is changing most rapidly; it is reasonable to identify this change in adsorptive power with the completion of the first layer.

5. When a well-defined point B is absent (Type III isotherm), although a BET plot can be made, no reliable surface area can be assigned.

6. It is possible to have a completely false point B when a portion of the surface is much more active than the rest, leading to an apparent saturation that does not represent the surface as a whole.

7. The Harkins-Jura absolute method[6] based on heats of wetting will give a true surface area for a plane surface, but their relative method is only strictly true when the isotherm of the unknown, and the isotherm for the powder used in the absolute method are geometrically similar.

Interestingly enough, only an isotherm which certainly will not give a BET plot can be relied on to give a true monolayer volume. For if an apparent point B is followed by an inflexion point, leading to another point B, the second apparent saturation must involve co-operation. In order to involve co-operation, the adsorbate molecules must be close together, almost touching, and one has real proof of a monolayer being formed.

Nitrogen isotherms never show this behaviour; but co-operative adsorption must obtain near $p/p_0 = 1$; no inflexion is noted between high p/p_0 and low p/p_0; so presumably, co-operative adsorption must have started before point B, where the inflexion would be masked by the strongly heterogeneous surface. Thus the nitrogen point B gives a true monolayer volume.

Catalysis.—The rate of reaction on a non-uniform surface[7] has been investigated, and the general conclusions only will be summarized here. The catalyst is presumed to function by strongly adsorbing a reaction product or products, thereby lowering the activation energy for reaction. Then, the reaction product must be desorbed to make way for a second unit reaction to take place. If the adsorption energy is too large, the actual reaction will proceed, but the desorption of products will be so slow that the site will be effectively poisoned. On the other hand, if the energy of adsorption is too small, the reaction will not take place, although the products would be easily desorbed. If the adsorption energy is distributed continuously, it is clear that on the optimum sites these two reactions would be equally difficult. Therefore, the usual assumption that a particular step in a reaction is the rate-determining one is inapplicable. The rate of reaction on other than optimum sites falls off rapidly with energy, and the location of the optimum site depends on the pressure. Therefore, although a very small proportion of the sites contribute to reaction at a given pressure, no group can be selected and treated as if it were effectively uniform. Data for adsorption and rate of adsorption involve a wide range of sites, and the catalytically active sites may contribute negligibly to adsorption. It is clear, then, that there is little direct connection between adsorption and catalysis on a continuously non-uniform surface.

In addition, away from equilibrium, the backward reaction will proceed on entirely different optimum sites than the forward reaction, and therefore the forward and backward rates cannot in general be determined from one another and the equilibrium constant.

Mallinckrodt Chemical Laboratory,
Harvard University,
Cambridge, Mass., U.S.A.

---

[6] Harkins and Jura, *J. Amer. Chem. Soc.*, 1944, **66**, 1362.

[7] Halsey, Jr., *J. Chem. Physics*, 1949, **17**, 758.

STATISTICAL ASPECTS OF CHEMISORPTION

BY A. R. MILLER

Received 7th March, 1950

The basis of the statistical mechanical account of adsorbed monolayers is discussed, and the way in which the properties of the monolayer can be deduced is indicated. The physical distinction between immobile and mobile monolayers of particles adsorbed on localized or fixed sites is emphasized and important differences in the properties of these two types of films are examined. The way in which the experimental results for adsorption on to clean surfaces can be interpreted in the light of these ideas is described. For oxygen films adsorbed on tungsten it is shown that these ideas lead to a consistent picture of the way in which successive layers of the film can be built up. The application to hydrogen films adsorbed on tungsten is also examined. More recent measurements of the variation of the heat of adsorption of these films suggest that the earlier interpretation of them was oversimplified, although the basic ideas are vindicated. It now appears that hydrogen films adsorbed on tungsten pass through an intermediate region when the surface is about three-quarters covered, and their behaviour changes from that of an immobile film to that of a mobile film adsorbed on localized sites.

---

1. Introduction.—The classical experiments of Langmuir [1] showed that when a clean surface of a solid or a liquid is exposed to a gas or a vapour, a monomolecular layer of the gas is often formed on the surface. An adsorbed monolayer of this sort is of considerable importance in the study of surface properties and surface reactions, as well as in the study of the interchange of energy between a solid surface and a gas.

The purpose of this paper is to give a review of some statistical aspects of chemisorbed monolayers. Many of these topics are dealt with in my monograph [2] to which the reader is referred for the mathematical details of the argument. Here, I shall restrict myself to considering the basis of the statistical mechanical theory of adsorbed monolayers, and the interpretation of the available experimental data in the light of the theoretical deductions. In particular, I want to examine some of the ideas of the statistical theory in the light of experimental results which have become available since my book was written.

2. Physical Model.—Both experimental and theoretical studies have shown that a solid surface provides a periodic potential field for an atom or molecule incident on the surface. The potential field near a crystal surface was determined in a number of cases by Lennard-Jones and his collaborators.[3] These calculations provide a potential map of the space as experienced by a gas molecule approaching the surface. The potential field consists of a periodic array of positions of minimum potential energy. The structure of this array is determined by the crystal structure of the surface. This work provides a firm basis for the idea of localized sites for adsorption which was advanced by Langmuir.

---

[1] Langmuir, *J. Amer. Chem. Soc.*, 1912, **34**, 1310; *ibid.*, 1915, **37**, 417; *Gen. Elect. Rev.*, 1926, **29**, 153.

[2] Miller, *The Adsorption of Gases on Solids* (Cambridge University Press, 1949).

[3] Lennard-Jones and Dent, *Trans. Faraday Soc.*, 1928, **24**, 92; Lennard-Jones, *ibid.*, 1932, **28**, 333.

More recently, it has also received direct experimental confirmation. The experiments of Crawford and Tompkins,[4] for instance, on the adsorption of a number of gases on barium fluoride crystals have shown that the amount of gas adsorbed in a complete monolayer is independent of the particular gas. Even though ammonia and nitrous oxide molecules differ in cross-section by about 50 %, the same amount of each was adsorbed in a complete monolayer. The number of molecules in a monolayer depends not on their size, for they do not form a close-packed structure on the surface, but on the localized sites for adsorption defined by the potential field provided by the solid surface.

This idea of the adsorption of molecules on localized sites is the basis of the examination of adsorbed monolayers using the methods of statistical mechanics. This was initiated by Fowler [5] who derived the adsorption isotherm statistically on the assumptions that

(i) there is a definite number per unit area of localized sites for adsorption,
(ii) one gas molecule or atom is adsorbed on each site,
(iii) the vibrational states of any adsorbed particle are independent of the occupation of neighbouring sites, and
(iv) there is no interaction between the adsorbed particles.

It was clearly necessary to extend the theory by taking account of the interactions between the adsorbed particles.[6] In this case, assumption (iv) is discarded, but then the regular arrangement of the sites becomes an essential feature of the argument.

3. Statistical Theory.—In using the methods of statistical mechanics to study adsorbed monolayers, the equilibrium between the gas phase and the adsorbed phase is considered. We first consider the case covered by assumptions (i), (ii), (iii) and (iv) of § 2. If there are N_a particles adsorbed on the surface and each is in its lowest state, the energy of the surface layer is $-N_a\chi$, where χ is the difference in energy between the ground state of a particle in the adsorbed phase and the lowest state in the gas phase. If a particle adsorbed on a particular site can occupy a set of states of energy ϵ_r and weight ω_r, its vibrational partition function is

$$v_a(T) = \sum_r \omega_r \exp\left(-\epsilon_r/kT\right).$$

Let there be N_s sites for adsorption on the surface. In the absence of interactions between the adsorbed particles, the energy of the adsorbed phase depends only on the number of adsorbed particles and not on their arrangement on the surface. The partition function of the monolayer can then be written

$$\Xi = g(N_s, N_a) \exp\left(N_a\chi/kT\right)\{v_a(T)\}^{N_a}, \qquad . \quad . \quad (1)$$

where $g(N_s, N_a)$ is the number of ways in which N_a adsorbed particles can occupy the N_s sites available for adsorption. That is $g(N_s, N_a)$ is the weight of the adsorbed state of the whole assembly of energy $-N_a\chi$; for it, we have

$$g(N_s, N_a) = \frac{N_s!}{N_a!\,(N_s - N_a)!}.$$

The contribution of the adsorbed layer to the Helmholtz function of the assembly is

$$F_a = -kT\log\Xi.$$

---

[4] Crawford and Tompkins, *Trans. Faraday Soc.*, 1948, **44**, 698.

[5] Fowler, *Proc. Camb. Phil. Soc.*, 1935, **31**, 260.

[6] (*a*) Fowler, *ibid.*, 1936, **32**, 144; (*b*) Peierls, *ibid.*, 1936, **32**, 471; (*c*) Roberts, *Proc. Roy. Soc. A*, 1937, **161**, 141.

Consider the gas phase containing N_g particles in a volume V in equilibrium with the adsorbed monolayer. The Helmholtz function of the gas phase is

$$F_g = -kTN_g\left\{1 + \log \frac{(2\pi mkT)^{3/2}}{h^3}\frac{V}{N_g}v_g(T)\right\}, \quad . \quad . \quad (2)$$

where $v_g(T)$ is the partition function for the internal degrees of freedom of a particle in the gas phase and the other symbols have their usual meanings.

The condition for equilibrium between the gas phase and the monolayer is

$$\left(\frac{\partial F_g}{\partial N_g}\right)_{T,\,V} = \left(\frac{\partial F_a}{\partial N_a}\right)_{T,\,V}. \quad . \quad . \quad . \quad . \quad (3)$$

This leads immediately to the adsorption isotherm, which can be written in the form

$$\frac{\theta}{1-\theta} = \frac{h^3 \exp(\chi/kT)}{(2\pi m)^{3/2}(kT)^{5/2}} \cdot \frac{v_a(T)}{v_g(T)} \cdot p, \quad . \quad . \quad . \quad (4)$$

where $\theta = N_a/N_s$, has been introduced for the fraction of the surface covered.

So far we have neglected the interactions between the adsorbed molecules. Suppose that the interaction between two particles adsorbed on a pair of closest neighbour sites has a fixed value, and neglect the interactions between more distant adsorbed particles. Theories of this sort will be referred to as *fixed interaction* theories. The energy of adsorption of a layer of particles is then

$$-N_a\chi + XV, \quad . \quad . \quad . \quad . \quad . \quad (5)$$

where V is the interaction energy between two particles adsorbed on a pair of closest neighbour sites and X is the number of such pairs. The interaction energy now depends on the arrangement of the particles on the adsorbing surface. In other words, the weight of the state having a particular energy depends on the arrangement of the particles on the surface; and the partition function is

$$\Xi = \sum_X g(N_s, N_a, X) \exp\{(N_a\chi - XV)/kT\}\{v_a(T)\}^{N_a}. \quad . \quad (6)$$

In this expression, $g(N_s, N_a, X)$ has been written for the number of arrangements of N_a particles on the N_s available sites for adsorption so that there are X closest neighbour pairs.

This expression has not been evaluated exactly. An approximate value can be found for Ξ by assuming either (i) that the interaction energy has its average value [6a] for the number of adsorbed particles, or (ii) by using the method of local configurations [6b, c] in order-disorder theory. Fowler using the former approximation, and Peierls using the latter, showed that critical adsorption could occur only when there were strong attractive forces between the particles in the monolayer.

If we use the former approximation, the adsorption energy becomes

$$-N_a(\chi + \tfrac{1}{2}\theta V).$$

The only term in Ξ which involves X is then $g(N_s, N_a, X)$ and Ξ can be evaluated since

$$\sum_X g(N_s, N_a, X) = N_s!/N_a!\,(N_s - N_a)! \quad . \quad . \quad (7)$$

The equilibrium states are again determined by eqn. (3), and the adsorption isotherm is

$$\frac{\theta}{1-\theta}\exp\left(-\frac{\theta V}{kT}\right) = \frac{h^3 \exp(\chi/kT)}{(2\pi m)^{3/2}(kT)^{5/2}}\,\frac{v_a(T)}{(v_g T)}p. \quad . \quad . \quad (8)$$

Fowler showed that his results were in qualitative agreement with the critical phenomena observed by Cockroft[7] in studying the deposition of metallic vapours on to insulating surfaces. However, in systems in which chemisorption occurs, the forces between the adsorbed particles are generally repulsive. In this case, critical conditions do not arise.

Once the equilibrium conditions have been determined in this way, other quantities of interest can be calculated. The heat of adsorption and the way in which it varies as the fraction of the surface covered changes, has been studied widely. The heat of adsorption per molecule is defined as the fall in the energy of the system when one molecule is adsorbed. It is given, as a function of the fraction of the surface covered, by the relation

$$q = u - \frac{\partial U(\theta)}{\partial (N_s\theta)}, \qquad (9)$$

in which u is the energy of a molecule in the gas phase and $U(\theta)$ is the total energy of the adsorbed film. If $\overline{X}$ is the average number of closest neighbour pairs for a given value of θ then

$$U(\theta) = -N_s\theta\chi + \overline{X}(\theta)V. \qquad (10)$$

Consideration of the experimental results in relation to simple theoretical considerations led to an important distinction between the different types of monolayer that can be adsorbed on an array of localized sites. It is necessary to examine these types of adsorbed film, before calculating the variation of the heat of adsorption.

4. Types of Adsorbed Monolayers.—The idea of the distinction between immobile and mobile films adsorbed on fixed or localized sites was introduced by Roberts.[8] In his experiments on the adsorption of hydrogen and oxygen on tungsten wires, Roberts found heats of adsorption of the order of 2×10^5 joule/mole. Taking the vibrational frequency for the adsorbed particles to be of the order of 10^{13} sec.$^{-1}$, the frequency of evaporation at room temperature is of the order of 10^{-23} sec.$^{-1}$. These films must therefore be very stable at room temperature. On the other hand, for heats of adsorption of the order of 10^4 joule/mole, the rate of evaporation would be of the order of 10^{10} sec.$^{-1}$, and quite different behaviour would be expected. In this case, the evaporation of the film, and consequent re-condensation, is so rapid that the particles adsorbed on the surface could be expected always to assume an equilibrium (Boltzmann) distribution. For an intermediate value of the heat of adsorption, say, 8×10^4 joule/mole, the rate of evaporation is 0·1 sec.$^{-1}$. When the heat of adsorption of a system is in this neighbourhood, it is in a transition state between the two extreme cases represented by the other values which have been considered.

These orders of magnitude illustrate the two kinds of film adsorbed on localized sites. They can be given formal definitions[8] in the following way. By a mobile film is meant one in which the energy of activation necessary to enable an adsorbed particle to move from a given site to a neighbouring vacant site is much less than kT, so that the particles move freely from one site to another. This free movement from one localized site to another ensures that the film takes up equilibrium configurations during the occurrence of any process. By an immobile film is meant one in which the energy of activation necessary to enable a particle to move from one site to another is so much greater than kT that, for the times which are concerned in any experimental procedure, the particles may be treated as remaining on the sites on which they are first adsorbed. The particles in such a film will not assume an equilibrium distribution;

---

[7] Cockroft, *Proc. Roy. Soc. A*, 1928, **119**, 293.

[8] Roberts, *Proc. Camb. Phil. Soc.*, 1938, **34**, 399; see also Miller, *ibid.*, 1947, **43**, 232.

the occupation of sites by the adsorbed particles will be random. It should be noted that not only free mobility on the surface, but also evaporation and re-condensation will also set up an equilibrium distribution. The conditions under which evaporation can occur are roughly the same as those under which the adsorbed particles are freely mobile over the surface from one localized site to another.

As has already been pointed out there will be intermediate cases. In these, the particles can be looked upon as being able to move from site to site on the surface but so slowly that there is an appreciable time lag in establishing equilibrium again if it is disturbed in any way.

5. Statistical Theory of the Heat of Adsorption.—The two extreme cases which have been specified in § 4 can be dealt with theoretically. The methods of statistical mechanics can be used to examine the equilibrium distribution in the mobile film and to examine some properties of the immobile film. Here, we shall determine the equilibrium conditions and show how the variation of the heat of adsorption with the fraction of the surface covered can be determined.

For an immobile film in which the particles from the gas phase are adsorbed on single sites, the heat of adsorption varies directly as the fraction of the surface covered. This follows immediately from the fact that in such a film there is a random occupation of single sites. In the adsorption of hydrogen on tungsten, it is probable that each molecule occupies two sites, one for each atom in the molecule. An immobile film of this sort consists of a random distribution of *pairs of sites* on the surface. There is not an exactly linear relation between the heat of adsorption and the fraction of the surface covered in this case, but the departure from linearity is not very great.

The heat of adsorption of a mobile film is quite different from this. The exact shape of the heat curve depends on the interaction between the adsorbed particles but in all cases it shows a rapid fall in the vicinity of $\theta = 0{\cdot}5$. We now show how these results can be obtained by the use of the grand partition function.

The grand partition function of the adsorbed layer can be written in the form

$$\Xi = \sum_{Na}\sum_{X} g(N_s, N_a, X) \exp\,(-XV/kT)\{\lambda_a v_a(T) \exp\,(\chi/kT)\}^{N_a}, \qquad (11)$$

where λ_a is the absolute activity of the particles in the adsorbed phase. It is related to the partial or chemical potential μ_a by the relation

$$\mu_a = kT \log_e \lambda_a,$$

The other symbols in eqn. (11) have the meanings which have been ascribed to them in earlier sections of this paper. Without serious error, as far as finding average values is concerned, the sum in eqn. (11) can be replaced by its maximum term. Denote the values of the parameters in the maximum term by asterisks. Then the grand partition function can be replaced by

$$\begin{aligned}\Xi^* &= g(N_s, N_a^*, X^*) \exp\,(-X^*V/kT)\{\lambda_a v_a(T) \exp\,(\chi/kT)\}^{N_a^*} \qquad (12)\\ &= g(N_s, N_a^*, X^*) \exp\,(-X^*V/kT)\xi^{N_a^*},\end{aligned}$$

where ξ has been written for $\lambda_a v_a(T) \exp\,(\chi/kT)$.

The essence of the method of local configurations is to deal with a small group of sites in detail and to represent the effects of particles adsorbed on sites outside this group by average values. For definiteness, we shall consider a square array of sites, as is provided by the (100) plane of a tungsten crystal, and examine the occupation of a particular site (the central site) and its z closest neighbours (the first shell sites).

We introduce average quantities in the following way. Let ξ_{AV} be the geometrical mean contribution per site of the array to the factor

$$\{\lambda_a v_a(T) \exp\,(\chi/kT)\}^{N_a^*};$$

let ζ be the geometrical mean contribution per pair of occupied sites to the term involving the interaction energy; and let γ be the geometrical mean contribution per site of the array to the combinatory factor. Thus, we define

$$\left.\begin{aligned} \xi_{\mathrm{AV}}^{N_s} &= \{\lambda_a v_a(T) \exp(\chi/kT)\}^{N_a^*}, \\ \zeta^{\frac{1}{2}zN_s} &= \eta^{X^*} = \exp(-X^* V/kT), \\ \gamma^{N_s} &= g(N_s, N_a^*, X^*). \end{aligned}\right\} \quad . \quad . \quad (13)$$

Consider a particle adsorbed on a particular first shell site. If the central site is occupied, its interaction with that particle is allowed for by a factor η. It occupies a site which is a closest neighbour also to $z - 1$ other sites; its possible interactions with particles which may be adsorbed on these sites is represented by a factor ζ^{z-1}, obtained by taking the average value defined in the second of eqn. (13). Each arrangement of particles adsorbed on the group of $z + 1$ sites can be considered in detail in this way. Examining the detailed occupation of this group of sites, and using the average values defined in eqn. (13) with regard to the occupation of the $N_s - z - 1$ sites outside the selected group, the partition function is represented by

$$[\xi(1 + \eta\xi\zeta^{z-1})^z + (1 + \xi\zeta^{z-1})^z]\gamma^{N_s - z - 1}\xi_{\mathrm{AV}}^{N_s - z - 1}\zeta^{\frac{1}{2}zN - z^2}, \quad . \quad (14)$$

where ξ has been written for $\lambda_a v_a(T) \exp(\chi/kT)$. In considering different modes of occupation of the array, we are concerned only with the ratios of terms in eqn. (14). The last three factors in the right-hand member of this equation can therefore be omitted, without affecting the results which are obtained. Thus, the expression

$$\xi(1 + \eta\epsilon_1)^z + (1 + \epsilon_1)^z, \quad . \quad . \quad . \quad (15)$$

in which ϵ_1 has been written for $\xi\zeta^{z-1}$, is used for the partition function. This method[9] is equivalent to that used by Roberts.[6a] The argument given here is more formal than the physical considerations on which Roberts based his deduction of the essential results. Their equivalence becomes clear on reflecting that successive terms in the right-hand members of eqn. (11), (14) and (15) give the relative probabilities of different modes of occupation of the sites on the surface.

Having constructed an expression for the partition function, the derivation of any quantities of interest can be proceeded with. The equilibrium relations for particles on the surface are obtained by using the fact that each site must be an average site. If a fraction θ of the sites on the whole array is occupied by adsorbed particles, then the average occupation of both the central and the first shell sites must also be θ. This leads to relations

$$\frac{\theta}{1 - \theta} = \frac{\epsilon_1(1 + \eta\epsilon_1)}{1 + \epsilon_1}, \quad . \quad . \quad . \quad . \quad (16)$$

$$\xi = \epsilon_1\left(\frac{1 + \epsilon_1}{1 + \eta\epsilon_1}\right)^{z-1}, \quad . \quad . \quad . \quad (17)$$

the detailed derivation of which can be found in § 2.3 of my monograph.

When equilibrium is established with a gas phase in contact with the surface, the absolute activity of an adsorbed particle must be equal to that of a particle in the gas phase. The latter is given by

$$\lambda_g = p\frac{h^3}{(2\pi m)^{3/2}(kT)^{5/2}v_a(T)},$$

while the former is given by

$$\lambda_a = \xi \exp(-\chi/kT)/v_a(T).$$

---

[9] Guggenheim, *Proc. Roy. Soc. A*, 1938, 169, 134.

When equilibrium between the adsorbed and gas phases is reached, λ_a is therefore proportional to the pressure in the gas phase. Eqn. (16) and (17) then give the adsorption isotherm.

The value of $\overline{X}$ is determined by the average occupation of the first shell sites when the central site is occupied. This can be found from the first term of relation (15) to be $\eta\epsilon_1/(1 + \eta\epsilon_1)$. If we use eqn. (9) and (10) with this result, we obtain finally [10] for the heat of adsorption

$$\frac{q - q_0}{zV} = -\frac{1}{2}\left[1 - \frac{1 - 2\theta}{\{1 - 4(1 - \eta)\theta(1 - \theta)\}^{\frac{1}{2}}}\right]. \quad . \quad . \quad (18)$$

If the adsorbed particles are diatomic molecules which dissociate on adsorption so that a mobile film of adsorbed atoms is formed, the only difference in the expression for the heat of adsorption is that the factor $\frac{1}{2}$ must be omitted from the right-hand member of eqn. (18).

The way in which the heat of adsorption varies with the fraction of the surface covered, according to eqn. (18), is shown by curve (*a*) of Fig. 1.

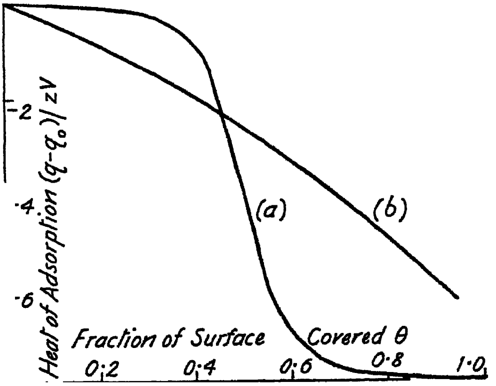

FIG. 1.—Variation of the heat of adsorption with the fraction of the surface covered, calculated from the statistical theory. Curve (*a*) is for a mobile film on localized sites, and curve (*b*) is for an immobile film.

This has been calculated for $V = 2{\cdot}3 \times 10^{-13}$ erg per pair of particles and 300° K. This interaction energy corresponds to the difference between the heat of adsorption on a bare surface and on an almost filled surface for hydrogen adsorbed on tungsten.

Now let us examine the case in which each particle from the gas phase occupies a pair of closest neighbour sites when it is adsorbed. The grand partition function is again replaced by its maximum term, and we consider the same group of $z + 1$ sites as in the other case. Each adsorbed particle can occupy either the central site and one first shell site, or a first shell site and an outer site, or a pair of outer sites. Geometrical mean contributions are introduced by equations which are formally the same as eqn. (13), but now N_a^* refers to the number of pairs of closest neighbour sites that are occupied by adsorbed particles, and X^* refers to the number of closest neighbour interactions between *different* adsorbed particles. The maximum term is then represented by

$$[\xi\zeta^{2z-1}(1 + \eta\xi\zeta^{2z-3})^{z-1} + (1 + \xi\zeta^{2z-3})^z]\gamma^{N_s-z-1}\xi_{AV}^{N_s-z-1}\zeta^{\frac{1}{2}zN_s-2z^2}.$$

Again, in considering the ratios of terms in the partition function, the last three factors can be omitted without affecting the results which are obtained. Thus, the expression [11]

$$z\epsilon_0(1 + \eta\epsilon_1)^{z-1} + (1 + \epsilon_1)^z, \quad . \quad . \quad . \quad (19)$$

---

[10] Wang, *Proc. Roy. Soc. A*, ., 1937, 161, 127.

[11] Roberts and Miller, *Proc. Camb. Phil. Soc.*, 1939, 35, 293.

in which ϵ_0 has been written for $\xi\zeta^{2z-1}$ and ϵ_1 has been written for $\xi\zeta^{2z-3}$, is used for the partition function.

To determine the heat of adsorption it is necessary to determine the probability that if the central site is occupied, a given first shell site is occupied by some other molecule. This is

$$\frac{z-1}{z}\,\frac{\eta\epsilon_1}{1+\eta\epsilon_1},$$

and the expression obtained[12] finally for the heat of adsorption is

$$\frac{q-q_0}{zV} = -\frac{z-1}{z}\,\frac{\eta\epsilon_1}{1+\eta\epsilon_1} - \left(\frac{z-1}{z}\right)^2\left(\frac{1+\epsilon_1}{1+\eta\epsilon_1}\right)^2\frac{\eta}{1+2\eta\epsilon_1+\eta\epsilon_1^2}\,\frac{\theta}{(1-\theta)^2} \quad . \quad (20)$$

This formula applies where there is adsorption as molecules to form a mobile film and each molecule occupies a pair of closest neighbour sites on the surface.

If an *immobile* film is formed by the dissociation of molecules, the sites are occupied in pairs, and formula (20) can be applied to this case. An immobile film of this sort corresponds to a random selection of pairs of closest neighbour sites; a random distribution corresponds to the case $\eta = 1$. The heat of adsorption of an immobile film is therefore given by

$$\frac{q-q_0}{zV} = -\frac{(z-1)^2\theta(2z-\theta)}{z\;(z-\theta)^2} \quad . \quad . \quad . \quad (21)$$

This is shown by curve (*b*) of Fig. 1, and it is seen that it departs only slightly from a linear relation and is far different from the heat curve for a mobile film. The heat of adsorption of an immobile film in which each particle from the gas phase occupies a pair of closest neighbour sites on the surface was first obtained by a numerical method using a model of the surface[13] and gave a curve in good agreement with eqn. (21).

6. Structural Discontinuities in the Final Immobile Film.—There is another feature of immobile adsorbed films of the kind which we have been considering which must be examined before we consider the interpretation of the experimental results. This is the existence of structural discontinuities or gaps[14] in the immobile film when adsorption into the first layer is completed.

We have seen that when each particle from the gas phase occupies a pair of closest neighbour sites on the surface to form an immobile film, there is a random distribution of *pairs* of sites. As the surface becomes covered, there will be some sites on it which remain bare while all of their closest neighbour sites are occupied. In an immobile film of this sort, such unoccupied sites can never become available for adsorption into the first adsorbed layer, and remain bare when adsorption into the first layer is complete. A surface film of this sort therefore necessarily has structural discontinuities or gaps in it.

The extent of these gaps can be determined either numerically using a model of the surface[15] or statistically.[11] In the statistical determination it is necessary to determine the probability that the central site is unoccupied while each of its first shell of neighbours is occupied. It is found that the number of single unoccupied sites completely surrounded by occupied sites, in the final film is about 8 % of the total number of sites. This means that about 92 % of the surface can become covered in the first surface film.

---

[12] Miller, *ibid.*, 1947, **43**, 232.

[13] Roberts, *ibid.*, 1938, **34**, 399, § 4.

[14] Roberts, *Nature*, 1935, **135**, 1037; *Proc. Roy. Soc. A*, 1935, **152**, 445; *ibid.*, 1937, **161**, 141; *Proc. Camb. Phil. Soc.*, 1938, **34**, 399.

[15] Roberts, *Proc. Roy. Soc. A*, 1935, **152**, 464, § 5.

Structural discontinuities of a similar kind occur in any adsorbed film in which each adsorbed particle occupies more than one site on the surface. Another possible case is that in which the occupation of a site precludes the occupation of its shell of closest neighbours by any other particle. In this case,[16] the coverage in the final film is reduced by about 20 %.

The properties of adsorbed films which have been obtained in this and the preceding section have proved particularly useful in the interpretation of the experimental results. We now consider the data on hydrogen and oxygen films formed on clean tungsten surfaces.

7. Oxygen Films Adsorbed on Tungsten.—An oxygen film adsorbed on tungsten has a very high heat of adsorption. That on a bare surface is about 500,000 joule/mole of oxygen; and it would be expected from the considerations advanced in § 2, that here we have to deal with an immobile film. We have seen that the final film will then have gaps in it. These might be expected to provide preferential sites for adsorption into a second film. There would be no such preferential sites if the film adsorbed immediately on the metal surface were a mobile film adsorbed on localized sites. The detailed structure of the adsorbate built up of successive layers can then provide information about the nature of the film.

The structure of the oxygen film adsorbed on tungsten was determined by the measurements of Morrison and Roberts.[17] The basis of their method is the sensitiveness of the accommodation coefficients [18] of neon and helium against tungsten to traces of adsorbable impurity. Changes in the accommodation coefficient thus provide a sensitive test of the presence of adsorbed films on the surface and also of any changes in them.

The results which were obtained for oxygen adsorbed on tungsten can be indicated briefly. The accommodation coefficient of neon for a bare tungsten surface is 0·057. When oxygen is admitted, it rises to a final steady value which depends on the partial pressure of oxygen in contact with the surface. This can be plotted as a function of pressure and extrapolated to low pressures of oxygen; this gives a value 0·226, which apparently corresponds to a layer of oxygen adsorbed on the tungsten. The higher steady values of the accommodation coefficient, which depend on the partial pressure of oxygen, are apparently due to the adsorption of a second layer of oxygen. The rise in the final value of the accommodation coefficient with the partial pressure of oxygen, indicates that when adsorption into the second layer is completed, the accommodation coefficient has reached a value 0·36.

It is also found that the accommodation coefficient varies with the pressure in much the same way as the fraction of the surface covered does; it can therefore be used as a measure of the fraction of the surface covered in the second adsorbed layer. The adsorption isotherm determined from the experimental results in this way agrees well with that calculated statistically.[16] This agreement justifies the determination of the coverage in the *second* layer from the accommodation coefficient by the formula which Morrison and Roberts used.

There is one other point to be noted. When the wire carrying the adsorbed layer corresponding to an accommodation coefficient of 0·226 is heated to 1100° K, the accommodation coefficient falls to 0·177, but no further evaporation occurs until it is heated to 1700° K. This indicates that the first layer is itself composite and consists of two distinct films. Furthermore, comparison of the changes in the accommodation coefficient suggests that the fall in it from 0·226 to 0·177 corresponds to the evaporation of much less than a complete monolayer. This would not be possible if we were dealing with mobile monolayers on an array of localized sites; but it is possible if the more stable film in the first layer is immobile. Its intense stability to heating up to 1700° K lends weighty support to this view, as also do the very high heats of adsorption which are observed.

---

[16] Roberts, *Proc. Camb. Phil. Soc.*, 1938, **34**, 577, § 7; see also Miller, ref. 2, eqn. (6.4).

[17] Morrison and Roberts, *Proc. Roy. Soc. A*, 1939, **173**, 1.

[18] Roberts, *ibid.*, 1930, **129**, 146; 1932, **135**, 192; 1933, **142**, 518.

We are led to the following consistent picture. The first adsorbed layer of oxygen on tungsten consists of a very stable immobile film. This film is probably atomic and formed by the dissociation of an oxygen molecule and the adsorption of its two atoms on a pair of closest neighbour sites. It therefore has 8 % vacant sites; and these provide preferential sites for further adsorption. The first layer is completed by the adsorption of molecules in these gaps; corresponding to this, the accommodation coefficient rises from 0·177 to 0·226. On top of this composite layer a second layer is then adsorbed. It probably consists of molecular oxygen adsorbed on the array of localized sites determined by the tungsten substrate, and its coverage depends on the partial pressure of oxygen.

These experiments about oxygen films on tungsten provide conclusive evidence for the existence of mobile and immobile films adsorbed on localized sites. The differences in the behaviour of these two kinds of film and of their structure indicate the importance of the distinction. The application of these ideas in the present instance, as it was developed largely by the late Dr. J. K. Roberts, indicates also their power and utility in the interpretation of otherwise complex data.

8. Hydrogen Films Adsorbed on Tungsten.—The heat of adsorption of hydrogen on tungsten wires which were cleaned by flashing at about 2000° C before each experiment, has been measured by Roberts.[14a] The heat of adsorption varied from about 180,000 joule/mole of hydrogen for a bare surface to 80,000 joule/mole of hydrogen for a filled surface. The relative values of the heat of adsorption for successive admissions of hydrogen to the surface could be determined much more accurately than the absolute values which would be needed to compare the results obtained in different experiments. This uncertainty can, however, be overcome by plotting relative values of the heat of adsorption Q/Q_0, where Q_0 is the heat of adsorption for a bare surface. Accordingly, I have re-plotted Roberts' results for the adsorption of hydrogen on tungsten and they are shown by the points in Fig. 2. The values obtained in each separate run are shown by a different symbol. The full line shown in Fig. 2 is the curve obtained theoretically for the variation of the heat of adsorption of the immobile film which is obtained when a diatomic molecule dissociates on adsorption, and its two atoms occupy a pair of closest neighbour sites on the surface, given by eqn. (21).

The agreement between the experimental points and the theoretical curve is good. The important point is that these experimental results could not be fitted to a curve such as (*a*) of Fig. 1, which is the other possible theoretical curve. These experiments appear to establish that the hydrogen film adsorbed on tungsten is an immobile film on localized sites, as we have defined it in § 4.

Similar results have been obtained by Beeck and Wheeler [19] who have examined the adsorption of various gases on evaporated metal films at liquid air and room temperatures. Their results for hydrogen adsorbed on nickel show a variation of the heat of adsorption from 130,000 joule/mole of hydrogen for a bare surface to 60,000 joule/mole of hydrogen for the filled surface. The experimental points (Fig. 3) show an almost linear variation over this range, and this suggests that the hydrogen film adsorbed on nickel is also an immobile film, formed by the adsorption of the two atoms of a hydrogen molecule on a pair of closest neighbour sites.

---

[19] Beeck and Wheeler, *J. Chem. Physics*, 1939, **7**, 631; Beeck, *Rev. Mod. Physics*, 1945, **17**, 61.

The question is not, however, quite so clear cut as these results suggested at first. So far, we have considered what I have called a fixed interaction theory. However, the interactions between the adsorbed particles ensure that for a surface which is only partly covered, the adsorbed particles will be displaced from the potential minima provided by the surface. When this factor and the variation of the interaction between two particles with their distance apart are taken into account, it can be expected that the heat curves will be changed.

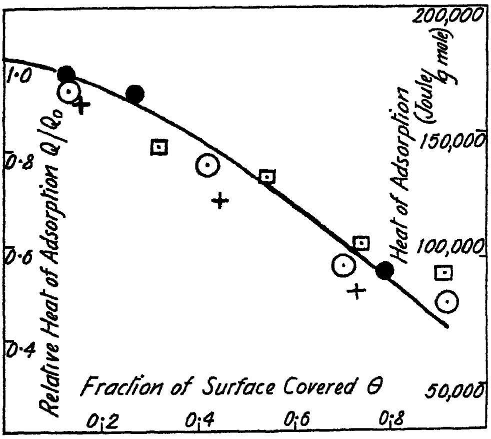

FIG. 2.—Experimental values of the relative heats of adsorption of hydrogen on tungsten (Roberts) as a function of the fraction of the surface covered compared with the theoretical curve for an immobile film

These effects have been considered only for a linear chain.[20] The calculations are tedious and there is no immediate extension to the two-dimensional case. As far as they go, they indicate that there is a less marked difference between the heat curves for mobile and immobile films than is obtained with the fixed interaction theory. However, the heat curve for the immobile film is still much more nearly linear than that for a mobile film. The theoretical curve for the immobile film represents the experimental results for hydrogen films adsorbed on tungsten and nickel better than does the curve for a mobile film.

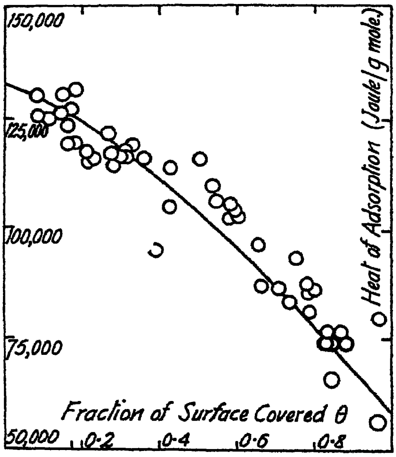

FIG. 3.—Experimental values of the heat of adsorption of hydrogen on nickel (Beeck and Wheeler) as a function of the fraction of the surface covered, compared with the theoretical curve for an immobile film.

More recently, Trapnell[21] has obtained experimental results for the adsorption of hydrogen on tungsten which differ from those obtained by Roberts. As he is to present his results later in this Discussion, I shall say merely that they suggest that in Roberts' experiments the surface of the wire was never more than about seven-tenths covered. If this be so, it would require a reconsideration of the data. This is reinforced by the fact that at his highest coverages, Trapnell obtains a flattening of the heat curve, which is more typical of a mobile film adsorbed on localized sites than it is of an immobile film.

---

[20] Miller and Roberts, *Proc. Camb. Phil. Soc.*, 1941, **37**, 82.

[21] Trapnell, this Discussion.

It should also be noted that at these highest values of θ, the heat of adsorption has fallen to a value at which one would expect appreciable evaporation and re-condensation in the time required to make a measurement. It may be that in this region, the behaviour of the film is changing from that typical of an immobile film to that typical of a mobile film; this is, in fact, the intermediate region spoken of in § 4. The point is that the two types of adsorbed film which we have described are characterized by heats of adsorption which differ by a factor of four or five. But the change in the heat of adsorption of hydrogen on a tungsten surface as it becomes fully covered is sufficiently great, and it is in such a range of values, that it overlaps regions typical of each kind of film.

The nature of the hydrogen films on tungsten must at present be regarded as obscure, and the original view that it forms an immobile film needs some qualification. While it has not been refuted, it is perhaps an over-simplification.

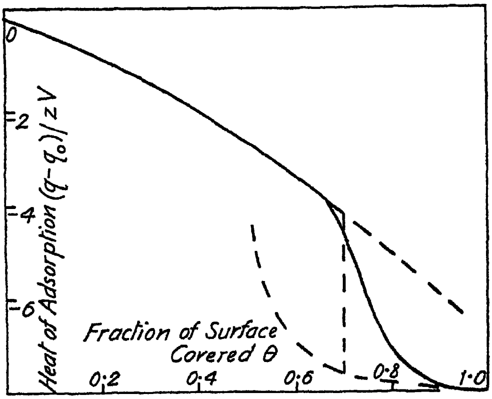

FIG. 4.—Drop in the heat of adsorption in the neighbourhood of a region in which a film adsorbed on localized sites changes from immobile to mobile in character. The full line represents the likely shape of the heat curve if this change takes place at about $\theta = 0{\cdot}75$.

It is possible that the new results which appear to cast some doubt on the original interpretation of Roberts' measurements, strongly vindicate the essential ideas—which have been developed in the statistical theory given in earlier sections—on which it was based. Consider what happens if both the facters which have just been mentioned are operative. That is, we assume that the lowest heats of adsorption of hydrogen on tungsten measured by Roberts referred, for some reason not at present known, to a film covering seven-tenths of the surface. At this stage, the heat of adsorption is about 80,000 joule/mole, and evaporation and re-condensation are approaching the rate at which a mobile film would be set up. If it be assumed that there is a sudden change at this point from an immobile to a mobile film, there would be a sudden drop in the heat of adsorption as is shown by the dotted vertical line in Fig. 4. Allowing for the fact that the change in behaviour could not be absolutely sudden, and that the film would pass through a region of intermediate behaviour, the complete heat curve would show a drop of this sort but rounded off a bit. A curve such as that shown by the full line in Fig. 4 would then result. This is very like the results obtained by Trapnell.

This is why these latter results which at first sight appear to cast doubt on the detailed interpretation of Roberts' results for hydrogen films on tungsten, also appear to vindicate the basic ideas on which it was based. For only a view of adsorption phenomena which contains the possibility of two kinds of behaviour would appear to have much hope of explaining these results. On this view, even the later measurements provide support for the basic ideas which have been developed in the statistical theory.

9. Conclusion.—The conclusion to be drawn from all these experimental results is, I think, as follows. For adsorption on an array of localized sites, the distinction between mobile and immobile films is important. These two kinds of film show markedly different behaviour as far as the variation of the heat of adsorption is concerned, and the statistical theory leads to ideas about the structure of immobile films which can play a major role in the interpretation of the experimental data about oxygen films adsorbed on tungsten, and which make it possible to give a consistent picture of the way in which successive layers are built up on the surface. While the original interpretation of the behaviour of hydrogen films adsorbed on tungsten appears now to be only partly correct, the essential validity of the ideas on which it was based appears to be vindicated.

Cavendish Laboratory,

THE KINETICS OF CATALYTIC REACTIONS ON INHOMOGENEOUS SURFACES

BY H. DE BRUIJN

Received 3*rd February*, 1950

A theory has been developed for the kinetics of catalytic reactions on inhomogeneous surfaces in which we started from an entirely arbitrary distribution of the more or less active sites on the surface. The ammonia synthesis was used as a model process. It was assumed that the adsorption of the velocity-determining reactant (in this case nitrogen) is of an atomic character and that an unrestricted migration may occur on the surface. The influence of simultaneous adsorption of the second reactant and the reaction product has been discussed. An essential factor of the theory is the occurrence of a so-called inhomogeneity factor in the reaction-rate relation. The value of this factor is determined by the frequency of those active sites which are really active under synthesis conditions. What active sites (characterized by their heat of adsorption) are really active depends on the temperature, total pressure and gas composition.

In this paper particular attention is paid to the influence which the total pressure and the gas composition have upon the value of the inhomogeneity factor. Thus it was possible to give an explanation for a well-known practical rule for the testing of catalysts used in high pressure synthesis. In practice it will in many instances (in the absence of important side reactions) be best to test the activity of the catalyst for the decomposition reaction at 1 atm., taking care to establish a certain mixing ratio between the reaction product and the synthesis gases (in the ammonia synthesis 300 atm. at 425° C, corresponds to 4·6 % NH_3).

The Inhomogeneity of a Catalyst Surface.—Many authors hold different views as to the importance of the inhomogeneity of the surface.

Whereas Taylor,[1] Cremer,[2] Emmett,[3] Temkin,[4] Zeldovitch,[5] Roginskiĭ,[6] Sips[7] and Fricke[8] *et al.* support the opinion that this inhomogeneity of the surface is a very important factor in the kinetics of catalytic processes, other investigators such as Roberts,[9] Beeck,[10] Volkenstein[11] and Eucken[12] advocate a different view. The latter consider the interaction between adsorbed molecules or atoms as a far more important factor.

We may safely assume that there are catalysts whose surfaces may be considered as homogeneous. On account of the fact that equivalent adsorption sites are located close together, it will be necessary in this case to reckon with an interaction effect. Sometimes, however, the quantitative examination leads to unsatisfactory results. Following the method indicated by Roberts,[9] Rideal[13] calculated a far smaller interaction energy than had been found in careful experiments and could only assume that the repulsion is considerably increased by the underlying layer (the catalytic surface).

On the other hand it may likewise be assumed that on account of their preparation (cp. Fricke[8]) many catalysts have a pronounced inhomogeneous surface. Even though, owing to geometric factors, a certain type of crystal faces has the greatest catalytic activity (cp. Beeck[10]), it may nevertheless be expected that not all adsorption sites of this type of face are equivalent. Either as a result of crystal deformations, starting from the interior of the crystallites or owing to missing and extraneous structural elements in the surface of the crystallites, the energy of the adsorption sites will differ considerably.

As a strong argument in favour of the assumption that the inhomogeneity is an important factor, we may refer to the deformation of the molecules in chemisorption. Wright and Taylor[14] for instance proved the occurrence of each of the methane fragments CH, CH_2, CH_3 in the chemisorption of methane on nickel. From desorption tracer experiments with CO, Emmett and Kummer[3] concluded that the bond between CO and Fe is not equally strong for all adsorbed molecules. The CO molecules which have been adsorbed first prove to have the stronger bond and in desorption these molecules are the last to leave the Fe surface. (The suggestion for this criterion for the inhomogeneity was made by Roginskii[15].)

The iron catalyst used in the ammonia synthesis could be adequately used as a model for a catalyst with an inhomogeneous surface. It is very likely indeed that only the (111) face of the α-Fe has a great catalytic activity (Brunauer and Emmett[16]) but in the adsorption of ammonia Taylor and McGeer[17] unmistakably found N, NH and NH_2 radicals on the surface which points to inhomogeneity. The latter fact need not seem odd when it is borne in mind that small admixtures in the magnetite used for the preparation of these catalysts are highly concentrated on the surface (Brunauer and Emmett [16]) where they will give rise to dislocations.

---

[1] Taylor, *Colloque sur l'Adsorption et la Cinétique heterogene* (Lyon, Sept., 1949).
[2] Cremer, *J. Chim. Physique*, 1949, **46**, 411.
[3] Emmett and Kummer, cf. ref. 1.
[4] Temkin, *Levin Uspekhi Khimii*, 1948, **17**, 174.
[5] Zeldovitsch, *Acta Physicochim.*, 1934, **1**, 961.
[6] Roginskiĭ, *ibid.*, 1947, **22**, 61.
[7] Sips, *J. Chem. Physics*, 1948, **16**, 490.
[8] Fricke, *Z. Elektrochem.*, 1949, **53**, 264.
[9] Roberts, *Proc. Roy. Soc. A*, 1935, **52**, 445.
[10] Beeck *Rev. Mod. Physics*, 1945, **17**, 61.
[11] Volkenstein, *Levin Uspekhi Khimii*, 1948, **17**, 174.
[12] Eucken, *Z. Elektrochem.*, 1949, **53**, 285.
[13] Rideal and Trapnell, cp. ref. 1.
[14] Wright and Taylor, *Can. J. Res.*, 1949, **27**, 303.
[15] Roginskiĭ, *Acta Physicochim.*, 1946, **21**, 537.
[16] Brunauer and Emmett, *J. Amer. Chem. Soc.*, 1937, **59**, 310, 1553.
[17] Taylor and McGeer, Princeton Univ., 1949.

A priori little can be said about the distribution of the more or less active sites. The distribution is probably of the Gaussian type (a frequency curve with a maximum (Fig. 1)). The equipartition of sites with different adsorption energies as postulated in Temkin's [18] theory is most unlikely.

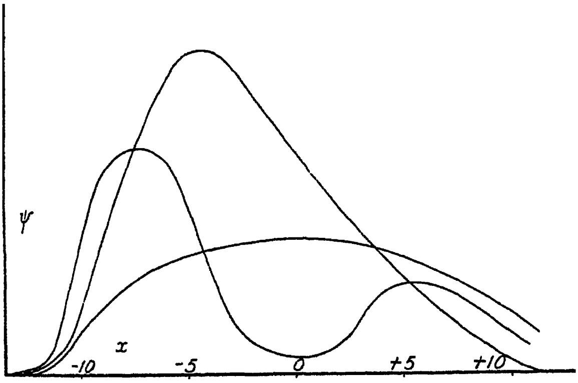

FIG. 1.—Different types of inhomogeneous surface.

The Slowest Reaction Step.—The advantage of selecting the ammonia synthesis as a model for our discussions chiefly lies in the relative simplicity of the mechanism. Hardly any side reactions occur and all reaction steps are reversible.

Nevertheless, this mechanism is still rather complicated :

$$N_2 + [\ ] \rightleftharpoons [2N] \quad \ldots \quad (1)$$

$$3H_2 + [\ ] \rightleftharpoons [6H] \quad \ldots \quad (2)$$

$$[2N] + [6H] \rightleftharpoons [2N + 6H] \quad \ldots \quad (3)$$

$$[2N + 6H] \rightleftharpoons [2NH + 4H \rightleftharpoons 2NH_2 + 2H \rightleftharpoons 2NH_3] \quad (4)$$

$$[2NH_3] \rightleftharpoons 2NH_3 + [\ ]\ ; \quad \ldots \quad (5)$$

there are three adsorption processes (1), (2) and (5), a migration process and a chemical reaction.

Temkin [18] supposed that with heterogeneous catalytic processes all reaction steps, except the first (adsorption of nitrogen) are in *equilibrium* because they proceed so rapidly. It should, however, be remembered that the velocity of a step is not solely determined by so-called intrinsic factors such as activation energy and frequency factor, but also by a factor containing fugacity terms of reactants and products which depends on conditions. As soon as the reaction has reached a point at which it deviates considerably from total equilibrium (high space velocities), the next slow step will become rate-determining. In any case, the latter can no longer be considered as being in equilibrium.

For this reason we shall restrict ourselves to reactions occurring in a differential reactor in which the gas composition differs but slightly from the total equilibrium composition.

ATOMIC OR MOLECULAR ADSORPTION OF THE VELOCITY DETERMINING REACTANT (NITROGEN).—Temkin [18] suggests a molecular nitrogen adsorption. Having regard to the then available data this was a natural assumption, since Taylor and Joris[19] had found that the exchange of the ^{14}N–^{15}N isotopes on iron catalysts only proceeded at a velocity comparable to that of the N_2 adsorption, if hydrogen was present.

---

[18] Temkin and Pyzhev, *Zhurn. fiz. khim.*, 1939, **31**, 851.

Recent investigations by Emmett and Kummer[8] have clearly proved, however, that if the experiments are carried out with sufficient care, the isotope exchange does proceed at a sufficiently high rate, even in the absence of hydrogen. On account of these results it will be more correct to regard the adsorption of nitrogen as an atomic adsorption.

SIMULTANEOUS ADSORPTION PROCESSES.—In his theory on the kinetics of the ammonia synthesis Temkin[18] did not take into account the simultaneous adsorption of hydrogen and ammonia. This omission is allowed as far as the adsorption of hydrogen is concerned since Brunauer and Emmett[20] have stated that under conditions of synthesis nitrogen and hydrogen are adsorbed on different types of sites.

In addition, Brunauer and Emmett found, however, that after adsorption of nitrogen the hydrogen adsorption increases. When repeating these experiments in our laboratory we not only confirmed this result but moreover observed that, although the additional binding of hydrogen below ~ 250° C may be considered as adsorption, at higher temperatures, however, this increased adsorption is fictitious and due to the formation of ammonia. After we had made a correction for the amount of ammonia formed, the hydrogen adsorption proved to be normal

The increased hydrogen adsorption, occurring in the presence of nitrogen on the surface, may therefore be considered as a chemisorption of ammonia in the form of NH or NH_2 radicals (cf. also Taylor and McGeer[17]). Even though at a low NH_3 pressure (i.e. at a low total pressure) this adsorption will be of minor importance, it is quite possible that at a high pressure part of the sites where nitrogen adsorption may occur, will be covered with ammonia radicals.

Reaction Rate on Arbitrary Inhomogeneous Surfaces.—As Temkin did, we characterize the adsorption sites with the adsorption energy for nitrogen ϵ as a parameter, and as a characteristic for the catalytic surface we adopt a function $\Psi(\epsilon)$. In general this function will have an arbitrary form which may possibly be derived from adsorption measurements (Roginskiĭ and Todes,[21] Sips[7]). In the first instance we shall neglect the adsorption of ammonia, and later show to how far our considerations must be altered when this adsorption is taken into account.

Following Temkin's treatment and assuming that all the processes, except the slowest, may be considered as being in equilibrium, we write

$$P^*_{N_2} = \frac{P_{NH}}{KP^3_{H_2}}, \qquad . \quad . \quad . \quad . \quad (2.1)$$

which implies that the fugacity of the adsorbed nitrogen is determined by the normal total equilibrium constant K, the hydrogen fugacity and the fugacity of the ammonia contained in the gas mixture. (In this paper the fugacities are supposed to be equivalent to the partial pressure of the gas phase components.)

Using the subscript o for the most active sites, and i for an arbitrary site, it follows from the customary assumed linear relationship between activation energy E and binding energy ϵ that

$$E_i - E_0 = n(\epsilon_0 - \epsilon_i), \quad . \quad . \quad . \quad . \quad (2.2)$$

where n is a constant.

Assuming atomic adsorption and unrestricted migration the rate of adsorption on sites of the i-type is

$$V_i = P_{N_2}(1 - \theta_i)^2 k'_a e^{-[E_0 + n(\varepsilon_0 - \varepsilon_i)]/RT} \quad . \quad . \quad (2.3)$$

(k'_a also includes the constant entropy factor).

---

[19] Taylor and Joris, *J. Chem. Physics*, 1939, **7**, 893.
[20] Brunauer and Emmett, *J. Amer. Chem. Soc.*, 1940, **62**, 1732.
[21] Roginskii and Todes, *Acta Physicochim.*, 1947 **15**, 624.

Since $P^*_{N_2}$ is the fugacity of the adsorbed nitrogen, we may write

$$\theta_i = \frac{(aP^*_{N_2})^{\frac{1}{2}}\, e^{\varepsilon_i/2\boldsymbol{R}T}}{1 + (aP^*_{N_2})^{\frac{1}{2}}\, e^{\varepsilon_i/2\boldsymbol{R}T}}, \quad . \quad . \quad . \quad (2.4)$$

where $a = k'_a/k'_d$,

i.e. the ratio between the frequency constants for adsorption and desorption (including the entropy factor).

Integrating over all types of adsorption sites we find for the average rate of adsorption :

$$V = k'_a P_{N_2}\, e^{-(E_0+n\varepsilon_0)/\boldsymbol{R}T} (aP^*_{N_2})^{-n} \, . \, \frac{\int \left[\dfrac{(aP^*_{N_2})^{\frac{1}{2}n} e^{n\varepsilon/2\boldsymbol{R}T}}{1 + (aP^*_{N_2})^{\frac{1}{2}}\, e^{\varepsilon/2\boldsymbol{R}T}} \right]^2 \Psi(\epsilon)\, d\epsilon}{\int \Psi(\epsilon)\, d\epsilon},$$

or

$$\overline{V} = k'_a P_{N_2}\, e^{-(E_0+n\varepsilon_0)/\boldsymbol{R}T} (aP^*_{N_2})^{-n} \overline{[\theta^n (1-\theta)^{1-n}]^2}. \quad . \quad (2.5)$$

In an analogous manner we find for the rate of desorption :

$$\overline{W} = k'_d\, e^{-(E_0+n\varepsilon_0)/\boldsymbol{R}T} (aP^*_{N_2})^{1-n} \overline{[\theta^n (1-\theta)^{1-n}]^2}. \quad . \quad . \quad (2.6)$$

Since the reaction rate is determined by

$$-\frac{dP_{N_2}}{dt} = \overline{V} - \overline{W}$$

we consequently find that

$$\frac{dP_{N_2}}{dt} = k_a'^{\,1-n} k_d'^{\,n} \overline{[\theta^n (1-\theta)^{1-n}]^2}\, e^{-(E_0+n\varepsilon_0)/\boldsymbol{R}T}$$
$$\times\, P_{N_2}{}^{1-n} \left[\left(\frac{P^*_{N_2}}{P_{N_2}} \right)^{-n} - \left(\frac{P^*_{N_2}}{P_{N_2}} \right)^{1-n} \right]. \quad (2.7)$$

With the exception of the factor,

$$F = \overline{[\theta^n (1-\theta)^{1-n}]^2}, \quad . \quad . \quad . \quad . \quad (2.8)$$

this relation contains the same factors as the equation derived from Temkin's theory.*

In view of this result it is useless to examine the relation as a whole. Therefore we shall restrict ourselves to a discussion of the factor F which we have termed the inhomogeneity factor since it represents the inhomogeneity of the catalytic surface in the rate equation.

We note, however, that the entire reaction rate equation, for the interpretation of the experimental results, can be appropriately transformed to the equation :

$$\frac{d \ln (1-\eta^2)}{dt} = k'' \frac{P_{N_2}{}^{\frac{1}{2}-n}}{P_{H_2}{}^{3/2}} \eta^{1-2n} \quad . \quad . \quad . \quad (2.9)$$

after substituting the efficiency η (defined as

$$\left(\frac{\text{actual concentration of the reaction product}}{\text{concentration after establishing the equilibrium state}} \right).$$

For the ammonia synthesis the last factor η^{1-2n} may be assumed to be practically equal to 1, since (i) n differs only very slightly from $\frac{1}{2}$

---

* If, contrary to our assumption, the nitrogen adsorption should not be of an atomic but of a molecular character, the resulting change in the above relation will be restricted to the factor F which in that case will read

$$\overline{[\theta^n (1-\theta)^{1-n}]}.$$

(Temkin) and (ii) we shall only consider reaction rates in the neighbourhood of the equilibrium state $\eta \rightarrow 1$. (All constants inclusive of the temperature factors have been included in the constant k''.)

Inhomogeneity Factor *F*.—The inhomogeneity factor is in the first place determined by the value of exponent n. The latter originates from the relation between activation and binding energy. Most probably the value for n ranges between $n = \frac{1}{2}$ and $n = 1$. When $n = 1$ and we are dealing with molecular adsorption of the rate-determining reactant, the inhomogeneity factor becomes equal to θ which in a separate experiment may consequently be determined as a function of P_A^* (A = rate-determining reactant). (In atomic adsorption and $n = 1$, the value for F becomes $F = \overline{\theta^2}$, which is not identical with $(\overline{\theta})^2$.)

The case $n \approx \frac{1}{2}$, which according to Temkin[22] occurs in the ammonia synthesis, is more interesting. In eqn. (2.8) for $n = \frac{1}{2}$ and $\theta = \frac{1}{2}$, the function F reaches its maximum and decreases rapidly with lower and higher degrees of occupation.

From this it may be concluded that in the latter case the reaction rate is almost exclusively determined by those adsorption sites having an intermediate degree of occupation. Of the entire " surface energy spectrum " consequently only a narrow band (corresponding with adsorption sites with an intermediate degree of occupation) is active. This does not imply that under all conditions always the same energy band is active.

Apart from the adsorption energy the degree of occupation depends on the fugacity $P_{N_2}^*$ and the temperature T, e.g. where

$$\theta = \tfrac{1}{2},\ P_{N_2}^* = \frac{1}{a}c^{\epsilon/RT} \quad . \quad . \quad . \quad . \quad . \quad (3.1)$$

We now introduce $\epsilon_{\frac{1}{2}}$ for the adsorption energy of those sites which under normal conditions (e.g. $T = 427°$ C, $P = 1$ atm., $\eta = 1$) have a degree of occupation of $\theta = \frac{1}{2}$. Adopting the new variable

$$x = \frac{\epsilon - \epsilon_{\frac{1}{2}}}{2RT},$$

then for $n = \frac{1}{2}$ we may write

$$F = \overline{[\theta^n(1 - \theta)^{1-n}]^2} = \frac{\displaystyle\int \frac{(aP_{N_2}^*)^{\frac{1}{2}}\, c^{\epsilon/2RT}}{[1 + (aP_{N_2}^*)^{\frac{1}{2}}\, c^{\epsilon/2RT}]^2}\, \Psi(\epsilon)\mathrm{d}\epsilon}{\displaystyle\int \Psi(\epsilon)\mathrm{d}\epsilon},$$

$$F = \frac{\displaystyle\int_{-\infty}^{+\infty} \frac{e^x}{(1 + e^x)^3}\, \Psi(x)\mathrm{d}x}{\displaystyle\int_{-\infty}^{+\infty} \Psi(x)\mathrm{d}x} \quad . \quad . \quad . \quad . \quad . \quad . \quad . \quad (3.2)$$

We have already observed that $\theta(1 - \theta)$ rapidly converges for values of $\theta \lesseqgtr 1/2$ or in other words that the function $\frac{e^x}{(1 + e^x)^2}$ will rapidly converge for energy values of $\epsilon >$ or $< \epsilon_{\frac{1}{2}}$ (Fig. 2*a*, 2*b*).

So if the value of the energy distribution function $\Psi(x)$, does not change too rapidly in the neighbourhood of $\epsilon_{\frac{1}{2}}(x_0 = 0)$ we may write:

$$F = \Psi(x_0) \quad . \quad . \quad . \quad . \quad . \quad (3.3)$$

---

[22] Temkin and Kiperman, *Zhurn. fiz. khim.*, 1947, **21**, 927.

since $$\int_{-\infty}^{+\infty} \frac{e^x dx}{(1+e^x)^2} = 1 ;$$

in other words the inhomogeneity factor is consequently a direct measure of the frequency of those adsorption sites having a degree of occupation $= \frac{1}{2}$.

When the conditions deviate from those mentioned above, $\theta = \frac{1}{2}$ will hold for other adsorption sites, since $\epsilon_{\frac{1}{2}}$ depends on the fugacity $P^*_{N_2}$.

It will be seen that the value of the inhomogeneity factor $F = \Psi(x_0)$ will change to a greater or less extent with pressure according to the shape of the energy distribution function $\Psi(x)$. Also a change in the efficiency of the synthesis η entails a shift of $x_0(e)$. However, as long as we do not know at what η values deviations from the theory will occur, the latter shift is less interesting since we are not sure whether the next slow step will also play a part.

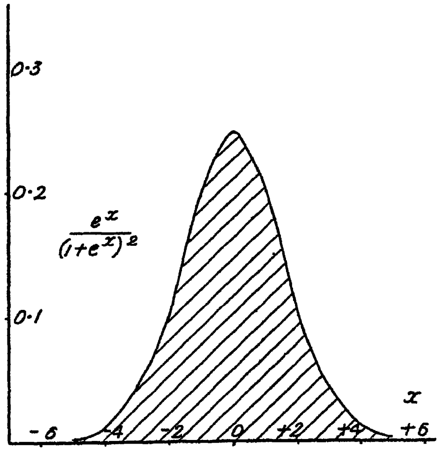

FIG. 2*a*.—Active area determining inhomogeneity factor *F*.

When we consider the decomposition of ammonia at 1 atm., for which case (in accordance with the postulated reversibility of the reaction) the general reaction rate equation also holds, we see that the same value of *F* at 100 atm. corresponds with a gas mixture containing 2·9 % of ammonia (at 300 atm. 4·6 % NH_3, at 3000 atm. 9·2 % NH_3).

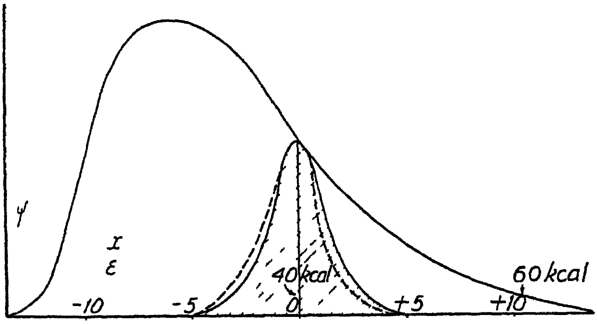

FIG. 2*b*.—— - - distortion of active area by curvature of ψ.

Simultaneous Adsorption.—In the introduction we pointed out that the adsorption of the reaction product cannot be ignored. The adsorption of ammonia should now be considered in the same way as, for example, the adsorption of methane on nickel described by Wright and Taylor.[14] The most active radical will be found on the most active sites, i.e. the N atoms on the most active and NH and NH_2 radicals on the less active sites. From this it follows that the NH and NH_2 radicals are adsorbed on the sites of intermediate activity which sites, as stated in the preceding paragraph, determine the reaction rate.

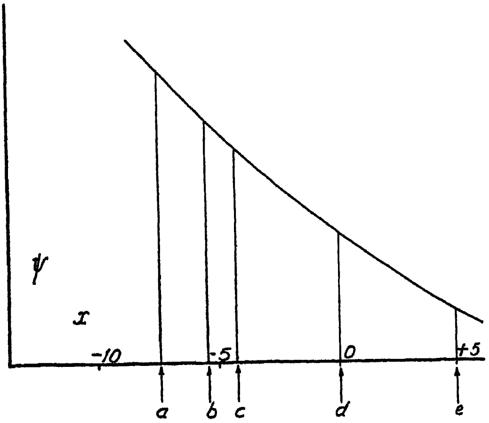

FIG. 3.

	P (atm.)	η	Equiv. % NH_3 at 1 atm.
a	3000	1	9·2
b	300	1	4·6
c	100	1	2·9
d	1	1	—
e	1	0·1	—

The shifting of x_0 with respect to its location under standard conditions if only the total pressure is modified, is indicated by arrows *a*, *b*, *c*.

So, if the conditions are favourable for ammonia adsorption, a simultaneous and competitive adsorption of nitrogen and ammonia will occur on the sites of intermediate activity. Part of the adsorption sites located in the " active energy band " are then blocked by the adsorbed NH and NH_2 radicals.

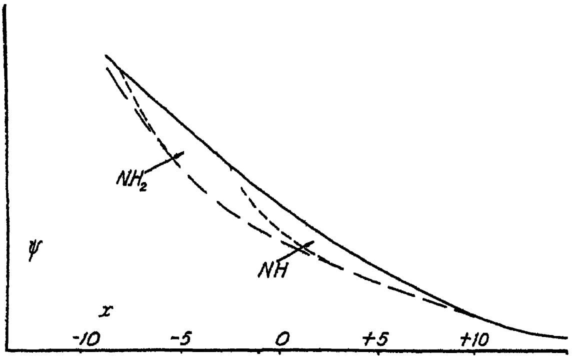

FIG. 4.—Radical adsorption of ammonia.

If now the equilibrium ammonia pressure is highly dependent on the total pressure as is the case in the ammonia synthesis, it is quite possible that the simultaneous adsorption of ammonia will decrease the reaction rate at high but not at low pressures. The influence of the ammonia adsorption is illustrated in Fig. 4. The occupation by nitrogen molecules has, as it were, reduced the frequency of the sites where nitrogen adsorption may occur.

Now since the ammonia radicals have a polar character, the adsorption of these may be influenced by dipole interaction or polarization effects caused by polar molecules present on the surface, such as the so-called first promoters Al_2O_3, MgO and the like. For the same reason, however, it may also be imagined that the second promoter such as K_2O, CaO may, at least in principle, act as antagonists. (At the moment the latter point is under investigation in our laboratory so that it is only mentioned briefly.)

Testing of the Activity of Catalysts.—Due to the peculiar behaviour of the inhomogeneity factor in the reaction rate equation, it is not surprising that for the testing of catalysts used in high pressure processes the " synthesis test " at 1 atm. may in many cases lead to wrong conclusions, whereas the decomposition test at 1 atm. will frequently yield a more accurate result. Thus at atmospheric pressure another part of the inhomogeneous catalyst (another band in the energy distribution spectrum) will be active than at a pressure of 300 atm. and generally $\Psi(\epsilon)$ will not have the same value for two different catalysts.

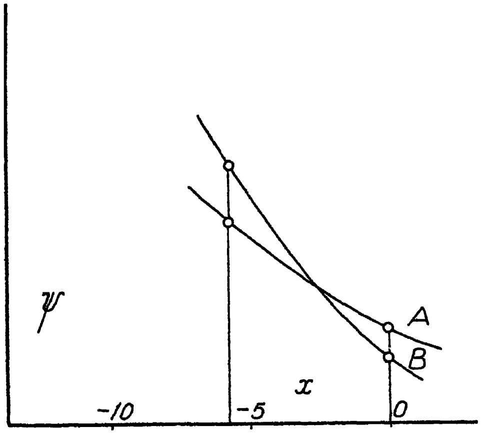

FIG. 5.—Different sequence of catalysts at different pressures.
At 1 atm. A, the most active. At 300 atm. B, the most active.

It is by no means impossible that the $\Psi(\epsilon)$ curves intersect (Fig. 5, catalyst A is the best at atmospheric pressure and catalyst B at a pressure of 300 atm. although the latter possesses a far smaller number of very active sites.) Moreover, it is quite possible that even if, in the absence of ammonia, the distribution functions do not intersect in the range between 1 and 300 atm., one catalyst adsorbs the ammonia far better than another. (Fig. 6. catalyst A, being the best at atmospheric pressure, is far more sensitive to ammonia adsorption than catalyst B.) We think for instance of the typical behaviour of singly and doubly promoted catalysts.

If, however, in performing the test, the rate of decomposition of the ammonia under normal conditions is used as a criterion for the catalytic activity and provisions have been made for the appropriate ammonia content of the gas mixture we are able :

(i) to examine the same energy band of the inhomogeneous catalysts as is active at high pressure and

(ii) to find whether a possible simultaneous adsorption of ammonia will exert an influence.

Although in practice the most efficient testing procedure had been known for a long time, it was not known why it had to be performed in this way.

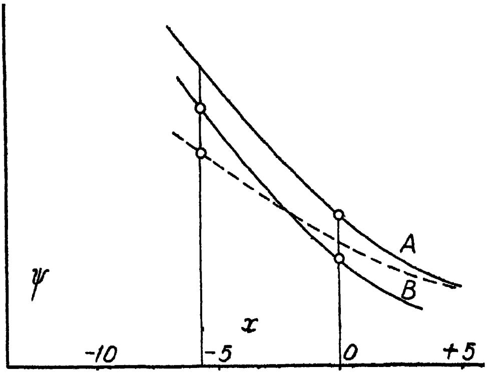

FIG. 6.—Different sequence of catalysts at different pressures. At 1 atm. A, the most active; at 300 atm. B, the most active . . . effect of NH_3 adsorption on A.

Concluding Remarks.—In this paper our considerations of the kinetics of catalytic reactions on inhomogeneous surfaces, are still of a qualitative nature.

This is due to:

(i) the uncertainty as to the shape of the distribution function $\Psi(\epsilon)$;
(ii) the uncertainty as to what extent the migration of the adsorbed nitrogen atoms and ammonia radicals can proceed without restriction;
(iii) the lack of knowledge of the intrinsic rate factors (activation energy and frequency factor) for the next slow step;
(iv) the fact that the quantitative description of the adsorption of ammonia in the form of NH and NH_2 radicals cannot as yet be given.

It may be that in the near future the application of the theories of Roginskii and Todes [21] and Sips [7] will enable us to obtain a better idea of the shape of the distribution function $\Psi(\epsilon)$ from exact data on the chemisorption of nitrogen.

Even the extent to which the migration of nitrogen atoms and ammonia radicals proceeds unrestrictedly, as has been suggested here, is open to doubt. The great difference between the experimental activation energies of synthesis and decomposition reactions (with many catalysts about 20 kcal. after elimination of the heat of reaction) as well as the influence of the temperature on the activation energy in the decomposition reaction (cf. Love, Emmett and Brunauer,[23, 24] and Chrizman [25]) must presumably be ascribed to restricted migration. Knowledge of the intrinsic rate factors of the next slow step is also lacking. Both these points are being investigated in our laboratory.

In conclusion it may be remarked that an extensive examination of the chemisorption of nitrogen, hydrogen and ammonia both separately and in combination (i.e. an extension of the investigation by Brunauer

---

[23] Love and Emmett, *J. Amer. Chem. Soc.*, 1941, **63**, 3297.
[24] Love and Brunauer, *ibid.*, 1942, **64**, 745.
[25] Chrizman, *Acta Physicochim.*, 1936, **4**, 899.

and Emmett [20] will probably enable us to complete our knowledge of the chemisorption of ammonia.

I wish to express my gratitude to my collaborators, particularly Dr. Kruyer and Mr. Zwietering.

Central Laboratory,
Staatsmijnen,
Geleen, The Netherlands.

GENERAL DISCUSSION

Dr. J. G. M. Bremner (*Billingham*) (*communicated*) : In connexion with the calculations of Huang and Wyllie on the interaction of adsorbed molecules with a surface, I have applied the method of molecular orbitals to a simple model of a chemisorbed unsaturated molecule e.g. acetylene, ethylene or benzene and have derived relative adsorption heats in this way. On this model, the π-electrons, by tending to fill the empty holes in the *d*-band, become delocalized and, moreover, as interaction of these electrons in the metal surface is also postulated, the structure for chemisorbed benzene is as shown. Geometrical considerations will affect the length and consequently the exchange integral of the carbon–metal, (C—M), bond. In this way, the model implies a correlation between the spatial and electronic factors. If the adjustments for the unknown integrals are allowed to accumulate in the C—M bonds, the secular equation takes the form shown in which the top-left and bottom-right quarters correspond to the circulant for benzene, , while the exchange integral for the C—M bond, $n\beta$, occupies the leading diagonals in the two remaining quarters.

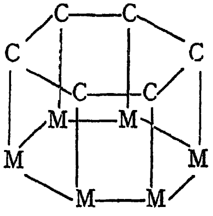

The 12 roots of this equation are obtained by adding $\pm n\beta$ to the 6 roots of the circulant for benzene. In consequence, the 3 lowest roots become

$$-\beta(n+2)\,; \quad -\beta(n+1)\,; \quad -\beta(n+1).$$

The π-electron energy for the adsorbed molecule is now $\beta(8+6n)$ compared with 8β for the unadsorbed molecule. The difference, $6n\beta$, corresponds to the heat of adsorption. In general, such calculations give an adsorption heat of $Zn\beta$, where Z is the number of electrons delocalized at the surface.

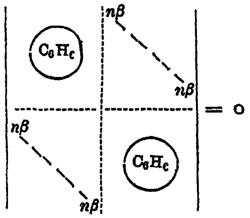

	C_2H_4	C_2H_2	C_6H_6
Heat of adsorption kcal. ($n = 1$)	36	72	108

The heats of ethylene adsorption given by Beeck [1] cannot be used to evaluate n because of the unknown heat change in the side-reactions which accompany the adsorption process. If we take $n = 1$ and put $\beta = 18$ kcal., we obtain the heats of adsorption shown. The higher heat of C_2H_2 adsorption compared to C_2H_4 accounts energetically for the dehydrogenation reactions which C_2H_4 undergoes on adsorption, as well as for the selective hydrogenation of C_2H_2 in C_2H_4 mixtures.[1] It is further evident that the heat of benzene adsorption becomes very large on this model as the delocalization effect easily outweighs the resonance energy of the unadsorbed molecule.[2]

Prof. G. M. Schwab (*Athens*) said: The remark of Mr. Huang that "activated adsorption" possibly is merely an activated displacement of surface contaminations, is rather revolutionary in view of the more recent development of the aspect of catalysis and would lend support to the older view that adsorption is never rate-determining.

---

[1] Beeck, this Discussion.

[2] Cp. Eley, *Quart. Rev.*, 1949, 3, 209.

Dr. A. R. Miller (*Cambridge*) (*communicated*) : In his communication to the Discussion about changes in the accommodation coefficient of neon against tungsten bearing adsorbed oxygen Dr. Wyllie appears to neglect an important consideration. An essential condition that the conclusion in his opening paragraph should be valid is that there exists a linear relation between the accommodation coefficient and the amount of gas adsorbed *irrespective of the layer into which the gas is adsorbed.* There seems to be no *prima facie* reason why this should be so and consideration of the detailed picture postulated by Roberts to explain his experimental results suggests that it may be far from the case. For oxygen adsorbed on tungsten Roberts suggested that the first process was a random distribution of molecules occupying pairs of sites with 8 % unoccupied sites in the final film ; the second process was molecular oxygen adsorbed " end on " in the vacant sites ; and the third process was the adsorption of a second layer on top of this substrate.

The accommodation coefficient for the first process was 0·18, for the second process it changed to 0·23 and for the third to 0·36. I suggest that the explanation of Dr. Wyllie's apparent difficulty is that the change in accommodation coefficient for these different processes depends not only on the amount adsorbed but also on the substrate. In other words, in the third process we are concerned with the accommodation coefficient of neon on a tungsten surface covered with one layer of oxygen and not of a bare tungsten surface as in the first process.

The point is that the changes in the accommodation coefficient observed experimentally indicate that three distinct processes take place in succession. Any discussion must succeed in identifying these distinct processes ; the explanation put forward by Roberts does this. Dr. Wyllie's discussion of the changes in the accommodation coefficient appears to neglect this.

I agree with the remarks by Dr. Beeck. In mentioning his results for hydrogen adsorbed on nickel, I did not appreciate how small a fraction of the sites on which adsorption takes place are directly exposed to incident gas molecules.

In reply to Dr. Wright, it should be stated that the possibility of molecules lying " end on " on the 8 % vacant sites of a random distribution of pairs of sites has been considered in other connections. It would be inadequate to account for the difference of surface coverage obtained in the experiments of Roberts and of Rideal and Trapnell since the latter obtain a surface coverage greater by 40 or 50 % than that of Roberts.

Mr. N. Thomas (*Imperial College, London*) said : I have developed an approximate treatment of the problem treated by Dr. Wyllie.

Firstly, we note that " co-ordinate complexes " formed by various metals are due to the formation of hybridized bonds by unpaired *d*-electrons in the outer shell of the metal. This suggests that chemisorbed complexes on the metal surface are held by co-ordinate bonds, since catalytic activity and ability to form complex ions seem closely correlated.

Such a bond involves donation of an electron to the metal by the adsorbate. This process can be simp'y treated using the following model :

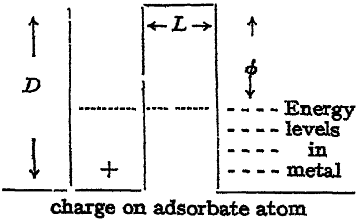

ϕ—thermionic work function.

L—interatomic distance.

D—energy needed to break bond of adsorbate molecule.

A potential valley of depth D approaches the metal and the electron has to pass out of it. It will do so in two stages; it will become statistically excited to the upper energy level of the metal and will then penetrate the barrier as a penetration wave. The transparency of a rectangular barrier is readily obtained by the Jeffreys approximation. Combining the "penetration factor" and the statistical factor, we finally get for the rate of adsorption

$$K_{ads} = AT^2 \exp\left(-(D-\phi)/kT\right) . \exp\left(-2(2\phi)^{\frac{1}{2}}L\right) \quad . \quad (1)$$

L, the barrier width, must be estimated from X-ray values. Eqn. (1) can be modified to allow for the effect of an applied electric field, thus:

$$K_{ads} = AT^2 \exp\left([-(D-\phi) - \sqrt{E\epsilon^{3/2}}]/kT\right) \exp\left(-(2\sqrt{2}\phi^{\frac{1}{2}}L\right). \quad (2)$$

This expression involves two terms, one temperature-dependent, the other temperature-independent; one varies as $\phi^{\frac{1}{2}}$, the other as $(D-\phi)$. If D is constant, they will obviously vary in opposite directions (cf. Schwab).

The work function of the metal ϕ is dependent on the cohesive energy of the crystal. Now a portion of the crystal elevated above the surface level is already partially removed from the main crystal, and since the cohesive energy is that required to remove an isolated atom from the crystal to infinity, the mean cohesive energy of the detached group will be much less than that of the crystal. Hence ϕ may be reduced. In our new model, the electron still has to rise through the range of energy levels of the metal $D-\phi$, but instead of penetrating a barrier of height ϕ it would have to penetrate one of height $\phi - \Delta E_c$, where ΔE_c is the change in cohesive energy. The lowest energy level in the metal "moves up" ΔE_c. Calculation of ΔE_c for any given configuration is very difficult, but the method of Onsager, applied by Frank[3] to a similar problem, may prove useful. Again, differences in the spacing of atoms in a surface plane may be reflected in the value of ϕ, which includes a term in $1/r_s$ (r_s = radius of the Wigner sphere). Thus a wider crystallographic spacing would reduce r_s, and hence ϕ.

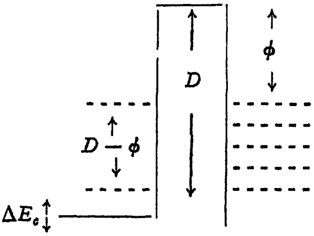

The overall reaction rate for a process such as we have discussed above would be given by combining our expression for the adsorption process with a kinetic expression, such as that used by Eyring and by Temkin.

We get an expression of type

$$v = kT/h\left\{\frac{(2\pi mkT)^{3/2}/h^3 . 8\pi^2 I_p kT/h^2 . 1/\sigma_p}{8\pi^2 I_c kT/h^2 . 1/\sigma_c}\right\}e^{-\phi E/kT}$$

for emission of product; here ϕ_E = effective work function and the suffixes c, p, refer to complex and product respectively.

Similarly for rate of adsorption

$$v' = kT/h\left\{\frac{8\pi^2 I_c kT/h^2 . 1/\sigma_c}{(2\pi mkT)^{3/2}/h^3 . 8\pi^2 I_R kT/h^2 . 1/\sigma_R}\right\}\exp\left(-(D-\phi)/kT\right)\exp\left\{-2(2\phi)^{\frac{1}{2}} . L\right\},$$

the notation being as before.

The main problem, now, seems to me to be the determination of ϕ_E for the groups of atoms which form "active centres", but any relation between ϕ_E and the configuration of these groups would certainly be very complicated.

---

[3] *Faraday Society Discussion*, 1949, 5.

Dr. G. Wyllie (*Bristol*) (*communicated*) : The process described by Mr. Thomas is that of thermal ionization of an atom close to the surface rather than formation of a co-ordinate link. He appears to neglect the interaction of the resulting ion with the metallic electrons, which may be roughly approximated by the image potential, and I am not clear how this is justified. This process may be important as a stage in some catalytic reactions, but it is an excitation, not directly involved in adsorption, though it may be in some cases a preliminary to it.

Mr. N. Thomas (*Imperial College*) (*communicated*) : The process assumed involves donation of an electron by the adsorbate to the metal, but this does not necessarily imply that the interaction between adsorbate and metal can be described only by Coulomb forces. The electron may be spatially localized to some extent in forming a co-ordinate bond.

Dr. K. W. Sykes (*Swansea*) said : A recent theory of the catalysis of the oxidation of carbon might briefly be mentioned here, because it suggests a useful approach to some of the problems under discussion. It has long been known that the reactions of carbon with gases such as steam, carbon dioxide and oxygen are catalyzed by many of the metals which may be present as impurities in the carbon. All the explanations proposed hitherto involve an alternative reaction path in which the catalyst acts as an intermediate ; the oxidizing gas reacts with the catalyst which in turn oxidizes the carbon. Some recent experimental work[4] has shown, however, that the reaction mechanism is unchanged by the catalysts, which merely alter the rates of certain of the individual stages. The new theory consequently deals with the general energy levels of the reacting system.

A common feature of all reactions in which carbon is oxidized at high temperatures is the conversion of adsorbed oxygen into gaseous carbon monoxide ; this process takes place at some of the less firmly bound carbon atoms at the edges of graphitic lattice planes. When an oxygen atom is adsorbed at such a site, two types of distribution of the π-electrons may be distinguished :

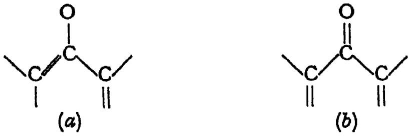

Type (*b*) is the more favourable for the evolution of carbon monoxide, because the carbon-carbon links which must be broken are weaker and the carbon-carbon bond approximates more closely to that in the carbon monoxide molecule. It is suggested, therefore, that the catalysts make the bond distribution less like (*a*) and more like (*b*) by interacting in some way with the π-electrons.

Molecular-orbital theory[5] shows that the necessary changes can, in fact, be produced by electron transfer between the carbon and the catalyst. To avoid the difficulties associated with calculations on the rather complex system under discussion, the phenoxyl radical, derived by removing a hydrogen atom from the hydroxyl group of the phenol molecule, serves as a simple model which contains the essential features of the real situation. The calculated π-bond orders in the neutral radical, and also in its singly charged positive and negative ions are as follows :

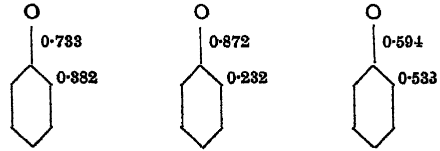

---

[4] Long and Sykes, *Int. Cong.* (Nancy, 1949), *J. Chim. Physique*, 1950, **47**, 36.

[5] Coulson, *Trans. Faraday Soc.*, 1946, **42**, 106.

These figures indicate that the removal of an electron should result in appreciable catalysis, since in the positive ion the carbon-oxygen bond is strengthened and the adjacent carbon-carbon bonds are weakened; the total change in the energy of these bonds is about 30 kcal. Similar calculations for the α-naphthoxyl and β-naphthoxyl radicals show that the effect is a perfectly general one. It is suggested, therefore, that this is the mode of operation of those catalysts which are able to accept an electron from the carbon. Transition metals, which can readily change from an upper to a lower valency state, appear to be good examples of this class.

Although the detailed comparison of the theory with experiment has been discussed in the reference given above, one particular aspect might be emphasized here. The mobility of the π-electrons provides a means whereby catalysts situated at various points in the carbon lattice can influence events at the active sites. This point seems to be especially interesting in view of what Prof. H. S. Taylor, and indeed other contributors, have said about the way in which the catalytic effect of an impurity atom may spread over the surface.

The application of this type of theory to other heterogeneous reactions can now easily be appreciated. The whole of the reacting system, i.e. the adsorbed molecules and the appropriate orbitals of the catalyst, should be regarded as one large molecule, and the molecular orbital method, or, if preferred, a valence-bond approach, applied to it. That is essentially the procedure recommended by Dr. Huang and Dr. Wyllie. By varying the number of electrons placed in the orbitals of the reacting system, one may represent the effect of an alloy constituent and so deal with the type of situation discussed by Mr. Dowden, Dr. Eley, Prof. Schwab and others. It should thus be possible to combine many of the newer ideas in a consistent manner without undue elaboration.

Dr. K. G. Denbigh (*Cambridge*) (*communicated*): Under conditions where there are large temperature gradients over the surface, it seems probable that the mobility of an adsorbed layer may be appreciably enhanced due to thermal migration. Such an effect on the surface would be analogous in two dimensions to the well-known thermal diffusion process in gases or to the Soret effect in liquids and solids. The isothermal mobility of an adsorbed layer has, of course, already been demonstrated experimentally by Volmer and others.

Consider an ideal system in which the migrating species has a certain low concentration c. The flow along the x-axis due to the concentration gradient is given by

$$- D \cdot \frac{\partial c}{\partial x},$$

which defines D, the diffusion coefficient. The corresponding flux due to the temperature gradient is given by

$$- D' \cdot c \frac{\partial T}{\partial x},$$

which defines D', the coefficient of thermal diffusion. The total flow along the x axis is thus given by

$$J_x = - D \cdot \frac{\partial c}{\partial x} - D' c \frac{\partial T}{\partial x}.$$

The relative degree of ordinary diffusion and of thermal diffusion is dependent on the ratio D'/D, the Soret coefficient. The magnitude of this quantity is larger in condensed phases than in gases and may attain a value of 10^{-2}. Its sign may be either positive or negative, according to whether the particular species tends to move towards lower or higher temperature. Although D' is always much smaller than D, the actual magnitude of the thermal flux may exceed the magnitude of the ordinary diffusion if the term $c \cdot \partial T/\partial x$ is very much greater than $\partial c/\partial x$.

Turning to the case of the adsorbed layer, c is now the surface concentration of the particular species and $\partial T/\partial x$ is the temperature gradient in a particular direction over the surface. If a catalytic reaction is strongly exothermic and takes place on localized regions it seems probable that there will be very steep gradients of temperature. It may occur, therefore, that the surface mobility due to the thermal effect may exceed that due to the concentration gradient and may be in the reverse direction.

Other thermal diffusion effects which are to be borne in mind in the discussion of non-uniform catalysts are concerned with the migration of lattice defects or charged species within the solid itself. In principle such effects could give rise to differences of electric potential, although it is to be doubted whether they are appreciable.

Dr. D. M. Young (*Dundee*) said : Dr. Halsey has pointed out that although the B.E.T. theory has been shown to be invalid, the surface areas estimated by the " point B " method appear to be remarkably satisfactory. He has given a number of qualitative reasons to account for this. In view of the importance of surface areas in catalysis, it seems worth while to attempt to account for the validity of the B.E.T. surface areas in a quantitative manner.

The B.E.T. theory, as Halsey pointed out in 1948,[6] is based on the quite untenable hypothesis that an isolated adsorbed molecule can adsorb a second molecule on top, yielding the full heat of liquefaction. It is far more likely that adsorption into the second layer takes place over square arrays of first layer molecules. In what follows we shall take essentially the B.E.T. model and insert a clause to this effect. If we confine our attention to the lower part of the isotherm we may neglect adsorption in the third and higher layers. Thus we may write

$$N = \frac{N_s b_1 p}{1 + b_1 p} + \left(\frac{b_1 p}{1 + b_1 p}\right)^4 \cdot \frac{N_s b_2 p}{1 + b_2 p},$$

where N is the number of molecules adsorbed and N_s is the number of

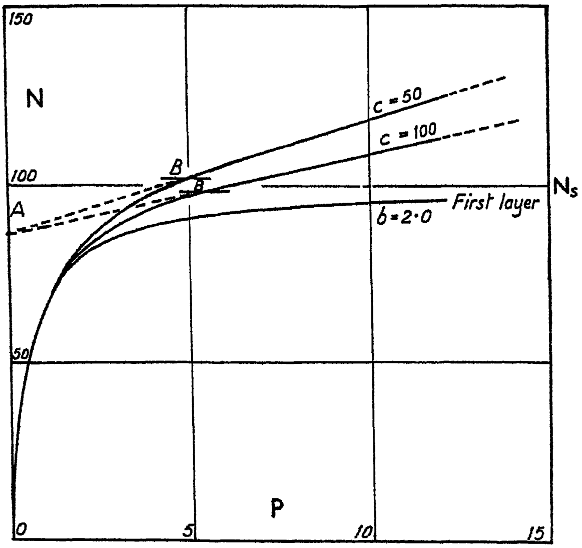

FIG. 1.

---

[6] Halsey, *J. Chem. Physics*, 1948, **16**, 931.

sites on the adsorbing surface. The ratio b_1/b_2 is analogous to the B.E.T. c constant. This equation neglects the shielding effect of the second layer, impeding the evaporation of first-layer molecules ; for the two cases to which the equation has been applied this effect has been shown to be negligible. I have applied the equation to a lattice of 100 sites, using an arbitrary value of b_1. Two values of b_2 have been considered, corresponding to values of the B.E.T. c constant of 50 and 100 (values of this order being usual for nitrogen at its boiling point). The lowest curve is the adsorption isotherm for the first layer ; the upper curves represent the total adsorption for the two values of b_2 chosen. These isotherms become linear at higher pressures, as found experimentally for a number of systems. Application of the "point B" technique gives values of the monolayer capacity within 3 % of the value required by the above equation, namely $N_s = 100$. Point A, for both values of b_2, occurs at 87 % of the theoretical monolayer capacity. These few preliminary results show that the addition of this one refinement to the B.E.T. theory causes no substantial change in the calculated value of the monolayer capacity (see Fig. 1).

Dr. F. C. Tompkins (*Imperial College, London*) (*communicated*) : It is true that some of the unreality of the B.E.T. model can be removed in the manner described by Dr. Young, but the experimental fact is that v_m is determined by a B.E.T. analysis of physical adsorption—chemisorption can in fact, as Dr. Beeck [7] has shown, lead to spurious values. In physical adsorption the distribution can rarely, if ever, be a random (i.e. non-equilibrium) one. The important point is that on a uniform surface if c is large ($>$ 100) the 1st layer is practically complete before 2nd layer adsorption is significant.[8] Adsorption proceeds therefore virtually on an *adsorbate* surface with a heat not largely different from the heat of liquefaction of the adsorbate, and moreover the number of possible adsorption sites in the 2nd layer (neglecting small edge effects) is practically the same as on the original surface. If therefore we confine attention to the range of $p/p_s < 0.3$, then as we have shown previously,[9] the amount in the 2nd layer is $N_s \, . \, p/p_s$ (where N_s = the number of adsorbent sites, p = equilibrium pressure, and p_s = saturated vapour pressure of adsorbate) to within 10 % irrespective of whether we adopt B.E.T. or Hüttig's evaporation conditions, whether we assume adsorption on square or hexagonal arrays or on single molecule sites, or whether we apply a "pure" Langmuir mechanism on a covered layer. All these must lead to a linear portion as Dr. Young has indicated in his particular case.

Dr. D. M. Young (*Dundee*) (*communicated*) : Prof. Taylor has suggested the use of the Hüttig equation for evaluating surface areas, since it describes multimolecular adsorption data over a much wider range than the B.E.T. equation. While this may be true for certain systems, as shown by the comparison of the two equations given by Ross,[10] it is by no means general. In the accompanying diagram the results of Arnold [11] for the adsorption of nitrogen and oxygen on anatase at liquid-air temperatures are fitted to the two equations. In this particular case the B.E.T. describes the results over a slightly greater range than the Hüttig equation. Similar comparisons using other published isotherms suggest that analytically there is little to choose between the two equations. Like Ross, we find that the Hüttig equation usually gives larger values of the monolayer capacity, but rarely more than 10 % higher than those given by the B.E.T. equation.

[7] Beeck, *Advances in Catalysis*, Vol. II (Academic Press).
[8] Halsey, this Discussion.
[9] Crawford and Tompkins, *Trans. Faraday Soc.* (in press).
[10] Ross, *J. Physic. Chem.*, 1949, **53**, 383.
[11] Arnold, *J. Amer. Chem. Soc.*, 1949, **71**, 104.

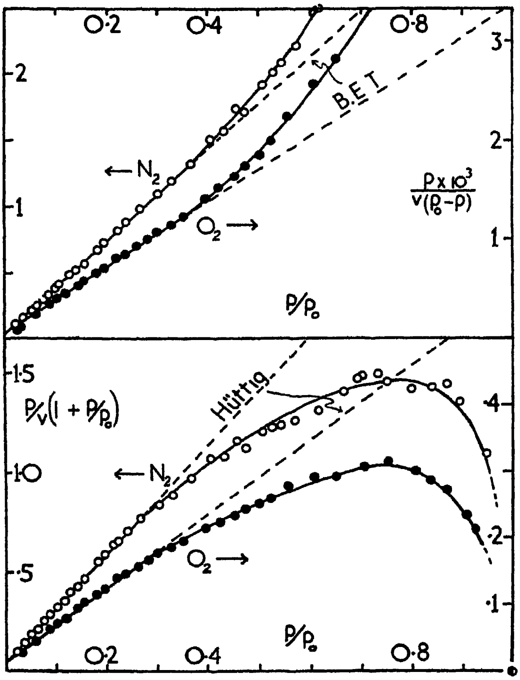

FIG. 2.

Prof. D. H. Everett (*Dundee*) said : I wish to mention some evidence which, while not conclusive, does imply that surfaces may not be as heterogeneous as some authors have suggested recently. The use of entropies of adsorption to examine surface heterogeneity has been suggested recently by Hill,[12] and an independent study of the thermodynamics of surfaces which we have carried out[13] shows that thermodynamic studies may assist in solving this problem.

Essentially our procedure has been to use methods analogous to those of solution thermodynamics and to compare actual systems with a hypothetical " ideal " system. For monolayer adsorption the Langmuir model of a localized non-interacting monolayer seems to be the most useful ideal reference system. For this model the partial molar entropy of adsorption includes a configurational term $- R \ln \frac{\theta}{1-\theta}$. We may write the partial molar entropy change (from the standard gas state to the surface) as

$$\overline{\Delta S} = \overline{\Delta S}^* - R \ln \frac{\theta}{1-\theta},$$

where $\overline{\Delta S}^*$ is the entropy change associated with changes in translational and rotational degrees of freedom of the adsorbed molecule on adsorption from the standard gas state, together possibly with similar changes induced in the atoms of the surface.

We have analyzed data for a large number of systems and find evidence for a linear relation between $\overline{\Delta S}^*$ and $\overline{\Delta H}$, the differential heat of adsorption. For adsorption on charcoal at 0° C this relation is identical with the Barclay-Butler relation between heats and entropies of condensation; similar relations appear for the H_2-tungsten system at higher temperatures, and for adsorption of gases on charcoal and glass at very low temperatures. Unfortunately in the absence of suitable published data we have not been able (except for the H_2—W system) to extend our examination to chemisorption.

---

[12] Hill, *J. Chem. Physics*, 1949, 17, 762.

[13] *Trans. Faraday Soc.*, submitted for publication.

The detailed interpretation of these heat-entropy relationships need not concern us at the moment, but, if we attach any significance to them, their existence suggests strongly that the term $- R \ln \frac{\theta}{1 - \theta}$ (or something very near to it) plays a fundamental role in adsorption equilibrium in the systems we have studied. This term only arises when all the adsorption sites are of equal energy, and so have equal probability of being occupied. This equal probability will be upset if the surface is heterogeneous, and some sites are much more active than others: the term $- R \ln \frac{\theta}{1 - \theta}$ will no longer appear. If interaction occurs between molecules so that the heat of adsorption varies with coverage on this account, the term $- R \ln \frac{\theta}{1 - \theta}$ is still separable from the expression for the entropy.[14] We believe therefore that our analysis indicates that the surfaces we have examined are less heterogeneous (as regards variation of adsorption energy from site to site) than is often supposed.

We still have to answer Halsey's objection that the variation of $\overline{\Delta H}$ with θ is too great and of the wrong form to be accounted for by interaction forces. I believe that this reflects our ignorance of the energetics of surface phases, especially on metals and charcoal where the orbitals of the electrons in the surface may extend over considerable areas. As stressed by Prof. Taylor an adsorbed molecule may influence a very large area of surface, and the contributions of Huang and Wyllie, and of Coulson and Baldock, represent perhaps the first steps in a more complete theory of interaction between adsorbed molecules.

Dr. A. R. Miller (*Cambridge*) (*communicated*): The linear relation which Prof. Everett has found between the experimentally determined quantities $\overline{\Delta S}^*$ and $\overline{\Delta H}$, as defined by him, is of interest. Essentially, this implies that there is a linear relation between $\partial f/\partial T$ and $\partial (f/T)/\partial (1/T)$ where f is the partial molar free energy, that is, f is defined as $\partial F/\partial \theta$ where F is the Helmholtz free energy of the adsorbed monolayer. This will be so provided f is the sum of a configurational term and an interaction term which depends linearly on T.

An expression for F can be derived from the statistical theory. In fact

$$F = \overline{\overline{\overline{X}}} V,$$

where
$$\overline{\overline{\overline{X}}} - \partial \overline{\overline{\overline{X}}}/\partial T = \overline{X},$$

with $\overline{X}$ defined by eqn. (2.15) in my monograph on adsorption. It is very complicated, and there is no reason to suppose that it (or f) necessarily has the form required. It therefore appears that the observed linear relation is essentially empirical and apparently arises fortuitously.

That there is such an empirical relation is, however, important. I agree with Prof. Everett that it suggests that the configurational term $- R \log \theta/1 - \theta)$ has a fundamental role in the adsorption equilibria considered; and that it lends support to the idea that each site for adsorption on the bare surface has the same energy.

---

[14] Fowler and Guggenheim, *Statistical Thermodynamics* (C.U.P., 1939), p. 441.

Prof. R. M. Barrer (*Aberdeen*) (*communicated*) : I wish to emphasize a point which is no doubt realized by those directly concerned in sorption studies, but which may not be appreciated by others, interested less closely in sorption phenomena. This is the diversity in meaning of the term " heterogeneity " as applied to surfaces. Thus a heterogeneity in a sorption process based on dispersion forces may operate in the opposite sense when sorption is due to electrostatic forces. In the figure, A, B and C are three possible positions a sorbed molecule might occupy on a rough surface. As regards dispersion forces, the affinity lies in the order A <B <C but for a heteropolar surface and electrostatic forces the sequence in affinity tends to be A> B> C.[15]

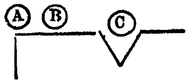

Again, in a chemical adsorption in which the adsorbed molecule in any of the positions A, B or C forms a chemical bond with one atom of the sorbent, it does not necessarily follow that the energy of formation of the bond will differ essentially whether it is formed at position A, B, or C. One should moreover differentiate between heterogeneity in a *heat* of chemisorption and in an apparent or true *energy of activation* for chemisorption. In a research carried out some years ago[16] a considerable heterogeneity was observed in the apparent energy of activation for chemisorption of hydrogen by partially graphitic carbon. It was suggested that the hydrogen molecule was chemisorbed as atoms, one atom on an edge carbon of a graphitic lamella and the other on an edge carbon of a second lamella just above or below the first. In partially crystalline carbon there is some disorder in the stacking of graphitic lamellae and variability in inter-laminar spacing, responsible for variations in energy of activation. But there seems no reason in such a case for the overall *heat* of chemisorption to differ. Indeed this heat was as nearly as could be ascertained constant. Both in kinetic and equilibrium studies therefore some care must be taken to define the sense in which the term " heterogeneity " is employed.

Dr. G. D. Halsey, Jr. (*Harvard*) said : The current emphasis on the role of surface impurities and surface heterogeneity, coupled with the realization that the adsorption on such surfaces may be far from equilibrium indicates that extreme caution is required in making theoretical calculations. The possibility of calculating configuration energy and rates from first principles seems remote indeed. Even the use of semi-empirical theories must wait for the complete formulation of mechanism. Thus, the comparison of catalytic activity and lattice parameter can be done only if one assumes identical mechanisms, or else isolates the step involved. We may recall that the (homogeneous) decomposition of N_2O_5 was attacked with most sophisticated theories, only to find, as Ogg has pointed out, that it proceeds by a complex mechanism.

Prof. G. M. Schwab (*Athens*) said : A treatment of catalytic kinetics with a rearrangement velocity not small compared with desorption velocities can also be given in terms of the usual Langmuir-Hinshelwood formalism, using Bodenstein's principle of stationary intermediate concentrations. For the simple sequence :

$$\mathrm{A}_{\text{gas}} \underset{2}{\overset{1}{\rightleftharpoons}} \mathrm{A}_{\text{ads.}} \xrightarrow[3]{} \mathrm{B}_{\text{ads.}} \underset{5}{\overset{4}{\rightleftharpoons}} \mathrm{B}_{\text{gas}},$$

this leads to

$$v = \frac{-\,\mathrm{d}P_{\mathrm{A}}}{\mathrm{d}t} = \frac{+\,\mathrm{d}P_{\mathrm{B}}}{\mathrm{d}t} = \frac{k_1 k_3 k_4 P_{\mathrm{A}}}{k_1 P_{\mathrm{A}}(k_3+k_4)+k_5 P_{\mathrm{B}}(k_2+k_3)+k_4(k_2+k_3)}.$$

---

[15] E.g. de Boer, *Electron Emission and Adsorption Phenomena* (C.U.P.), p. 48.
[16] Barrer, *Proc. Roy. Soc. A*, 1935, **149**, 253.

Assuming $k_3 \ll k_4, k_2$, this reduces to the usual expression for the rate-determining rearrangement,

$$\frac{k_3 b_A P_A}{1 + b_A P_A + b_B P_B},$$

and assuming desorption to be rate-determining ($k_4 \ll k_3, k_2$) to

$$v = \frac{k_4 b_A P_A}{b_A P_A + (k_5/k_3)P_B + k_4/k_3 + k_4/k_2}.$$

The apparent reaction orders are about the same (< 1 for A and > -1 for B) in the limiting and the intermediate cases. For inhomogeneous surfaces, instead of k_2, k_3, k_4 integral mean values according to energy distribution functions must be introduced. The most active centres will have increased k_3 and diminished k_2 and k_4, which shows (as k_3 always occurs as an addendum to desorption constants) that a certain compensation takes place, the reaction order depending on heterogeneity much less than the actual velocity. It is probably because of this compensation that the simple Constable treatment ($k = k_0 . \exp (q/h)$) is approximately true, although the change in the rate determining process has been neglected.

Dr. G. H. Twigg (*Epsom*) (*communicated*) : In considering the hydrogenation of ethylene, Prof. Laidler states that the zero order with respect to ethylene may be due to measurements having been made in the neighbourhood of the maximum, i.e. that an insufficient range of conditions has been covered. This is not so, however. The zero order is found over the temperature range −80° C to +150° C, and with any reasonable value for the heat of adsorption, a change in kinetics would have been evident.

The simple Langmuir-Hinshelwood mechanism for the hydrogenation of ethylene can be excluded by the following argument. If adsorption equilibrium is established, as assumed by this theory, and reaction occurs between adsorbed ethylene and an adsorbed hydrogen atom, the rate of reaction can be expressed as

$$\text{Rate} = k_1 p_1^n p_2^m \equiv k_0 \theta_1 \theta_2,$$

where p_1 and p_2 are the pressures of ethylene and hydrogen and θ_1 and θ_2 are the fractions of the surface covered by ethylene and hydrogen. It is a simple deduction from the theory that

$$n = 1 - 2\theta_1$$
$$m = \tfrac{1}{2}(1 - 2\theta_2).$$

Now, since the ortho-para hydrogen conversion is inhibited during hydrogenation, we know that θ_1 is very close to unity, so that the order of reaction with respect to ethylene should be -1. That this is not so is evidence either that the two gases do not compete for the same surface (Laidler's mechanisms (2) and (3)) or that adsorption equilibrium is not maintained in the way envisaged by the Langmuir-Hinshelwood scheme. The latter is now thought to be correct.[17]

Prof. G.-M. Schwab (*Athens*) said: As pointed out by Laidler and previously by Hinshelwood, the Langmuir-Hinshelwood mechanism for a bimolecular surface reaction predicts a denominator in the velocity expression of the form $(1 + Kc_g)^2$, provided both reactants are adsorbed on the same kind of sites. This leads to a maximum velocity at an optimal pressure ϕc_g. Besides enzyme reactions (wherein the maximum is mostly to be explained by a self-displacement of the reactant due to adsorption of two molecules on one site [18]), the only clear example of this maximum is Hinshelwood's reaction, $CO_2 + H_2 \rightarrow CO + H_2O$ over platinum.

---

[17] Twigg, this Discussion.

[18] Schwab, Bamann, Laeverenz, *Z. physiol. Chem.*, 1933, **215**, 121.

However, we showed[19] that under pure conditions (freezing out water vapour rather than absorbing it in sulphuric acid) the maximum disappears. Thus, it has been concluded[20] that the square term in the denominator does not generally occur. This can be explained either by a Rideal mechanism, or by an adsorption on adjacent sites of the reactants. Both possibilities have been formulated by myself and Pietsch in 1928.[21] In ethylene hydrogenation we preferred the second possibility. We had observed[22] that the maximum is definitely absent; the decrease of velocity at high ethylene concentrations is an almost irreversible poisoning and not due to reversible adsorption. We already concluded[23] from a classical kinetic treatment that a distinction of mechanisms from frequency factors will hardly be possible, at least as long as detailed knowledge of the absolute active surface and of the degrees of freedom of the adsorbed molecules is lacking.

Dr. G. H. Twigg (*Epsom*) said: I am very interested in the results which Turkevich *et al.* have obtained on the reactions between ethylene and deuterium. The ability to analyze the individual hydrocarbons should add greatly to our knowledge. The result that light ethane is an early product of the reaction of ethylene and deuterium at 90° C is in agreement with some results that Rideal and I obtained on this reaction.[24] We found that up to *ca.* 150° C the hydrogen that was returned to the gas phase from the catalyst was largely H_2. This is due to the fact that on the catalyst there is a fast reaction:

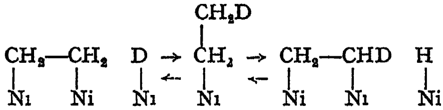

$$\underset{\mathrm{Ni}}{\underset{|}{\mathrm{CH_2}}}\text{—}\underset{\mathrm{Ni}}{\underset{|}{\mathrm{CH_2}}}\quad\underset{\mathrm{Ni}}{\underset{|}{\mathrm{D}}}\rightleftarrows\overset{\mathrm{CH_2D}}{\overset{|}{\underset{\mathrm{Ni}}{\underset{|}{\mathrm{CH_2}}}}}\rightleftarrows\underset{\mathrm{Ni}}{\underset{|}{\mathrm{CH_2}}}\text{—}\underset{\mathrm{Ni}}{\underset{|}{\mathrm{CHD}}}\quad\underset{\mathrm{Ni}}{\underset{|}{\mathrm{H}}}$$

which exchanges the adsorbed hydrogen atoms with those in the ethylene. The exchange reaction is not controlled by this reaction, but by the return of the adsorbed hydrogen to the gas phase so that the hydrogen present on the catalyst is mostly H, and the ethane produced by the addition of this hydrogen is correspondingly largely C_2H_6.

Prof. K. J. Laidler (*Washington*) (*communicated*): It is evident from the divergent views expressed by Twigg, Schwab and myself that there is still need for a great deal of further evidence with regard to the important matter of whether the rates of certain reactions fall off at higher pressures. For the ethylene-hydrogen reaction, Pease[25] found that there was such a falling-off on copper. Since at these high pressures the general evidence is that desorption occurs more readily than at lower pressures, it does not seem likely that the irreversible effects referred to by Schwab can be occurring here. It therefore seems to be more likely that the falling-off in this system is due to the necessity for the reacting molecules to be adsorbed side by side.

The fact, stated by Twigg, that the reaction remains of zero-order with respect to ethylene over a wide range of *temperatures* is not convincing evidence that there is no falling-off at higher *pressures*. The ethylene pressure at the maximum has been seen to be equal to $1/K$, where K is the equilibrium constant for the adsorption of ethylene. Now K varies with temperature largely as $e^{q/RT}$, where q is the heat of adsorption. If q is quite small, as is the case when the surface is fairly fully covered,[26] is it clear that K may vary very little with temperature.

---

[19] Schwab and Naicker, *Z. Elektrochem.*, 1936, **42**, 670.
[20] Schwab, *Advances in Catalysis*, 1950, vol. 2.
[21] Schwab and Pietsch, *Z. physik. Chem. B*, 1929, **1**, 385.
[22] Schwab and Zorn, *ibid.*, 1936, **32**, 169.
[23] Schwab and Drikos, *ibid.*, 1942, **52**, 234 and ref. (3).
[24] Twigg and Rideal, *Proc. Roy. Soc. A*, 1939, **171**, 55.
[25] Pease, *J. Amer. Chem. Soc.*, 1923, **45**, 1196.
[26] Rideal and Trapnell, this Discussion.

Consequently the position of the maximum may vary only very slightly over a wide range of temperatures, so that zero-order kinetics will be found over such a range.

An example of just this type of behaviour is to be found in the results of some work now being done by Prof. J. Weber and myself at the U.S. Naval Ordnance Laboratory. The system being studied is the ammonia-deuterium exchange on an activated iron catalyst. As the ammonia concentration is increased the rate of this reaction goes through a maximum, the falling-off at higher pressures being due to a reversible adsorption of ammonia. The position of the maximum varies only very slightly with the temperature so that rate measurements at a pressure corresponding to the maximum would give zero-order kinetics over a wide range of temperatures, and on the basis of Twigg's argument would have been interpreted as indicating no falling-off at higher pressures.

Prof. G.-M. Schwab (*Athens*) said: Using the same mechanism for the ethylene hydrogenation as that proposed by Eyring, we evaluated [27] from our kinetic data on Raney catalysts the adsorption energies of hydrogen and ethylene and calculated a " true " activation energy for the transition of adsorbed ethylene and *adsorbed* hydrogen to adsorbed ethane of about 22 kcal. on the assumption that the directly observed values around 10·7 kcal. are lowered by the adsorption energy of hydrogen. This result agrees with Maxted's figures for a series of other hydrogenation reactions. It would be of interest to examine whether the author's treatment also accounts for the most general result of a temperature optimum of the hydrogenation velocity.

Dr. G. Wyllie (*Bristol*) (*communicated*) : It may be profitable to take the consideration of the adsorption of hydrogen and oxygen on tungsten a little further. Examination of the results quoted by Miller for the accommodation coefficient of neon on tungsten surfaces bearing adsorbed oxygen shows that an increase in the accommodation coefficient by 0·05 is on the accepted interpretation ascribed to the adsorption of oxygen at sites occupying 0·08 of the surface. This requires, on the simple supposition that meaning may be attached to the accommodation coefficient at a site, that the coefficient at these sites should rise to about 0·7. But its value for a complete second layer of oxygen is only 0·36. It seems more natural to describe the observed increase in terms of a smaller increment over something approaching quarter of the total surface, and there seems then to be a possible analogy with the results obtained by Rideal and Trapnell for the chemisorption of hydrogen on tungsten.

An effect which may be expected to be common to all monatomic chemisorbed films on a metal surface is a tendency at high film densities to adopt a configuration which continues the lattice structure of the metal. The principal reason for this is that the electrons of the partially covalent chemisorption bonds obey the Pauli exclusion principle, and the forces involved are precisely analogous to those which tend to maintain a constant bond angle in e.g. the water molecule. In the adsorbed film, the effect would be expected to appear as a short-range many-body interaction among the adsorbed atoms. It will not be very easy to estimate it theoretically, but it seems clear that it will be more important the greater the extent to which *p* and *d*-orbitals of the metal atoms partake in the chemisorption bond.

However, on the (110) surface of a body-centred cubic crystal, a position at which an adsorbed atom would continue the crystal lattice is co-ordinated with only two nearest neighbours in the plane below it, but with four in its own plane. In a film of low density, on the other hand, it is more likely that an adsorbed atom will find a position equidistant from three nearest neighbours in the metal surface. If the interaction described in the last paragraph is important, as indeed it must be inside the metal to force it into the body-centred cubic rather than a close-packed structure, then at some density there will occur an allotropic change in the film, the energy of which will be reflected in a drop in the heat of adsorption with increasing θ.

---

[27] Schwab and Zorn, *Z. physik. Chem. B*, 1932, 19, 169.

If in the experiments of Roberts and Trapnell an important fraction of the metal surface lay in (110) planes, the results might bear an interpretation on these lines. As Johnson has shown that appropriate treatment can develop the (100) faces of tungsten, on which the geometrical effect should not appear, some experimental check should be possible.

Dr. J. G. M. Bremner (*Billingham*) (*communicated*) : Dr. Miller mentions various conclusions that can be drawn from the work of Roberts but it has now [28] been shown that a reassessment of much of this work is necessary. Roberts' object in introducing the flashing procedure was to free the surface of the wire from impurities. He found this procedure reduced the heat loss from a tungsten wire immersed in a gas at low pressure and accounted for this reduction by a fall in the accommodation coefficient. That this interpretation is incorrect has been shown in a number of ways. Thus, as the effect produced by flashing is found to be independent of the temperature at which measurements are carried out, the reduction in accommodation coefficient is apparently greatest when the wire temperature approaches that of the gas. Measurements made at 5° above the gas temperature will, in consequence, respond to the Roberts treatment very much more than when working with an increment of 50°. The effect is, moreover, more apparent as the gas pressure is lowered and, indeed, at a given time interval after flashing, is greatest when working *in vacuo*. That the Roberts effect is due mainly to the warming of the internals of the vessel in which the wire is mounted is shown by the nature of its dependence on the duration and temperature of flashing, its increase on platinizing the walls of the vessel and also by its duplication on flashing a similar wire adjacent to the one under examination.

Mr. A. E. J. Eggleton and Dr. F. C. Tompkins (*Imperial College, London*) (*communicated*) : We are unable to agree with Dr. Bremner "that a reassessment of much of (Roberts') work is necessary". We

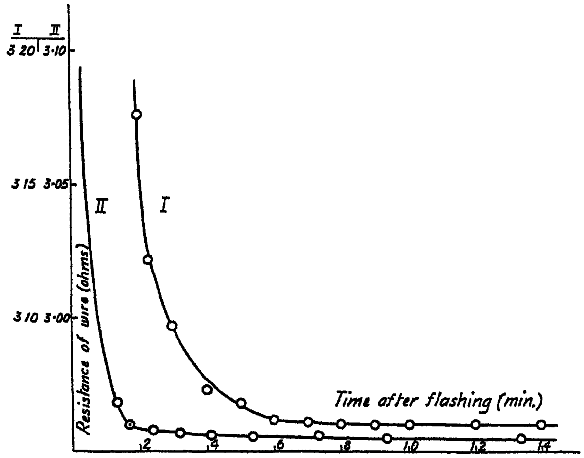

FIG. 3.

I.—Cooling curve of tungsten wire after flashing to 2300° C for 1 minute.
II.—Cooling curve of experimental wire after flashing auxillary wire to 2300° C for 15 min.

---

[28] Bremner, *Proc. Roy. Soc. A* (in press).

have measured the accommodation coefficient α using a W wire (0·07 mm. diam., 19 cm. long) in neon circulating at a pressure of 0·1 mm. Hg in an apparatus identical in design with that of Roberts. The wire was flashed at 2300° C for 1 min. and the resistance then measured using a small current of 2mA. Fig. 3 (I) gives a typical curve; after 8 min. the resistance is constant and within 0·02 % of its original value. In measurements a current of 20 mA was used in order to maintain the wire at *ca.* 20° above that of its surroundings; there is then a slow drift consistent with increasing contamination of the surface and α obtained 30 min. after flashing *without* extrapolation to zero time is still below 0·1. Variation of time of flashing and change in temperature excess of the wire over its surroundings had no effect on α values obtained using Roberts' extrapolation method (see Table I). This is consistent with the conclusion that the drift is due to contamination (Roberts) but not in accord with the non-attainment of thermal equilibrium (Bremner).

TABLE I

Expt. No.	5	6	9	12
Excess temp. (°C) of wire α = 0·1	27·0	36·0	16·7	18·0
Extrapolated value of α . .	0·059	0·057	0·051	0·055

Dr. Bremner kindly sent us details of his work mentioned in his remarks. In later experiments we used a central iron wire in a tube containing two auxiliary W wires which were flashed at 2300° C for 15 min. As shown in Fig. 3 (II) the resistance returns to its former value within 5 min. Using a *contaminated* iron wire, which had been maintained previously at 1200° C for considerable periods and had given an evaporated iron film on the walls of the tube, we again find that there is attainment of thermal equilibrium within 5 min. and moreover there is *no* drift at all. This result would be expected if Roberts' explanation were correct.

We are forced, therefore, to the conclusions (i) that Roberts' value of 0·06 for α is a true one, (ii) that his flashing procedure did clean his W wire, and (iii) that the drift is due to contamination. We are also equally convinced that Dr. Bremner's explanation of his own results in his apparatus of *different design* from that of Roberts is also correct.

Dr. O. Beeck (*Emeryville, California*) said: Dr. Miller quotes our values of the heat of adsorption of hydrogen on nickel as an example for an immobile film, while we quote the same values as indicative of a mobile film. This apparent discrepancy should be clarified. While Dr. Miller is correct that curves of this nature will result if molecules hit a plain surface randomly from the gas phase, this type of curve is not to be expected for porous evaporated films, whose surface is entirely internal and can only be reached through pores from the outside of the film. Under these conditions a curve, showing a decrease of heat of adsorption with fraction of surface covered, can only result if the adsorbed atoms are mobile, as discussed in the paper by Beeck, Cole and Wheeler,[29] where further references are quoted.

Prof. J. H. de Boer (*Geleen and Delft*) said: The question whether adsorbed molecules are attached to localized sites or whether the surface spaces which they occupy are only governed by their mutual forces and their two-dimensional kinetic movements as a two-dimensional gas which condenses to a two-dimensional condensed phase, is of some importance for the estimation of surface areas by the B.E.T. method. In addition to the experimental evidence for localized sites in some cases, as mentioned by Dr. Miller, viz. the experiments of Crawford and Tompkins, I would like to mention that some 20 years ago I was studying the adsorption of various molecules on films of inorganic salts, obtained by evaporation in high vacuum. The surface area was measured by a surface reaction with alizarin and—to mention the case of CaF_2 films—was about 240 m.^{2}/g. Water molecules and *atoms* of hydrogen occupied one crystallographic site, when adsorbed in a unimolecular layer, iodine molecules occupied two sites, *p*-nitrophenol four sites.[30]

---

[29] This Discussion.

These molecules, though bound to definite sites, are nevertheless quite mobile over the surface and form two-dimensional condensed states which may act as a new surface for multimolecular adsorption. As, however, the mutual distances differ from those in the liquid, one may not expect the heat of adsorption of the 2nd and higher layers to be equal to the heat of liquefaction. This conception leads to a slight alteration of the B.E.T. equation, mainly to the effect that the saturation pressure p_0 has to be replaced by a, mostly somewhat higher, pressure q. This explains why in practical cases the adsorption isotherm does not approach the axis $p/p_0 = 1$ asymptotically, but intersects it at a definite point. I hope to publish the consequences of this and other views shortly in a new book.

Although the upper part of the isotherm is highly effected by this behaviour, the lower part is not and one can still use the method for an estimation of surface areas, provided one does not claim a too high degree of accuracy.

We have compared the B.E.T. method with another method, based on the adsorption of fatty acids from pentane solutions. The adsorption of fatty acids can easily be worked out as a micro-method, when one estimates the change in concentrations of the fatty acid by spreading on water. Pentane or another saturated aliphatic hydrocarbon have to be used as solvents. Benzene is not allowed because of its own adsorption. Details of the method will be published later.[31]

The smooth character of the isotherms, experimentally found in most practical cases, point to a heterogeneous character of most surfaces for physical adsorption. On a homogeneous surface step-wise adsorption would occur rather than adsorption showing a smooth isotherm. Absorption spectra of adsorbed molecules point in the same direction. The fall of adsorption energies with increasing degree of occupation can partially be understood in this way.

In adsorption of atoms or molecules on metal surfaces, however, one may expect a decrease of the heat of adsorption, even on smooth surfaces, if the formation of positive or negative ions plays a role. These ions decrease or increase the work function and therefore lower the heat of adsorption for further atoms. This is experimentally known from photoelectric and thermionic measurements.[32]

Even if the bond of the adsorbed atom with the metal is mainly of homopolar or of metallic character, there is, nevertheless, a small dipole moment left which alters the work function gradually when the degree of occupation increases.

Mr. R. S. Bradley (*Leeds*) (*communicated*) : In support of Prof. de Boer's contention that the B.E.T. adsorption isotherm should become asymptotic at pressures greater than the saturation value, we have the fact that supersaturated vapours may be kept in vessels on the walls of which there must be a multimolecular layer, and yet condensation to bulk liquid does not occur.

Dr. C. Kemball (*Cambridge*) said: Dr. de Bruijn mentioned that the existence of the methane fragments CH, CH_2, CH_3 found by Wright and Taylor [33] in the chemisorption of methane on nickel and also of the radicals N, NH and NH_2 found by Taylor and McGeer [34] in the adsorption of ammonia on an iron catalyst indicated inhomogeneity of the surface. It is important to emphasize that it is the way the radicals behave on change of temperature which may indicate heterogeneity of the surface but that their existence is mainly controlled by the composition of gas mixture admitted to the surface. Methane admitted to a nickel surface will yield a larger proportion of carbon atoms and CH radicals on the surface than if a mixture of hydrogen and methane is used. An example of this type was given by the study of the rupture of the C—C bond of ethane on a nickel catalyst both in the presence and the absence of hydrogen.[35] The results indicated that the slow step was the rupture of the C—C bond of adsorbed ethylene which is formed by the dissociative adsorption of ethane :

---

[30] A survey of these studies can be found in J. H. de Boer, *Electron Emission and Adsorption Phenomena* (Cambridge, 1935).

[31] C. M. M. Houben, *Thesis* (Delft).

[32] J. H. de Boer, *Electron Emission and Adsorption Phenomena* (Cambridge, 1935).

$$C_2H_6 \rightleftarrows \underset{\cdot}{C}_2H_5 \quad \underset{\cdot}{H} \rightleftarrows \underset{\cdot}{H} \quad \underset{\cdot}{C}H_2\text{—}\underset{\cdot}{C}H_2 \quad \underset{\cdot}{H}$$

The presence of hydrogen tended to shift the equilibrium to the left and in fact the rate of decomposition depended inversely on the 1·3 power of the hydrogen pressure. In the absence of hydrogen small amounts of ethane decomposed quantitatively according to the equation :

$$2C_2H_6 \rightarrow 3CH_4 + C,$$

and this implied that a large number of radicals must have existed on the surface during the reaction. It was found that the adsorbed carbon could be removed quantitatively by hydrogen :

$$C + 2H_2 \rightarrow CH_4.$$

These results indicated that a large variety of radicals can exist on the same catalyst surface but that the proportion of the different types depended markedly on the composition of the gas admitted.

Dr. H. de Bruijn (*Geleen, Netherlands*) (*communicated*) : I quite agree with Dr. Kemball that the occurrence of different fragments of adsorbed molecules on the surface of a catalyst as such is no proof of inhomogeneity of the surface. In my paper I probably mentioned the experiments of Wright and Taylor too briefly. They found on hydrogenation of the fragments with deuterium that each of the species required a specific temperature. The equilibrium which exists between the different species on a homogeneous surface is disturbed as soon as one of the species is hydrogenated. On a inhomogeneous surface, however, the amount of the other species will not be altered unless one chooses a higher temperature. This is what Wright and Taylor actually found. Apart from this, the strongest argument for inhomogeneity remains the result obtained by Emmett and Kummer in their experiments on the adsorption and desorption of labelled carbon monoxide on iron catalysts.

Dr. A. F. H. Ward (*Manchester*) said : The question has been raised of the extent to which it may be necessary to attribute to active centres an important influence in catalysis. It would appear that a decision on this matter could be reached by a study of catalytic reactions on *liquid* metal surfaces. Many years ago, Williams [1] attempted to catalyze the reduction of nitrobenzene to aniline on a liquid tin surface. He was unable to detect any reaction, although the oxides of tin catalyzed the reaction readily. One might, of course, expect some difficulty in observing catalysis on a liquid surface on account of the much smaller area. However, it seems important to establish whether catalysis will take place at all on a liquid surface, and if so, to study kinetics on such surfaces in the detail that has been used with solid surfaces. If, in a comparison with equal areas of solid and liquid surfaces the latter gives a smaller (or zero) rate of reaction, it would imply that the catalysis must be attributed to some property characteristic of the solid state, not shown by the liquid, and not merely dependent on the type of metal used. This method of approach should allow a discrimination between the effects of non-uniformity of the surface and interaction between adsorbed molecules.

---

[33] Wright and Taylor, *Can. J. Res.*, 1949, **27**, 303.

[34] Taylor and McGeer (Princeton Univ., 1949).

[35] Kemball and Taylor, *J. Amer. Chem. Soc.*, 1947, **70**, 345.

II. ADSORPTION AND CATALYSIS ON METALS

INTRODUCTORY PAPER (i)

By Eric K. Rideal

We are indebted to our Spiers Memorial Lecturer, Dean H. S. Taylor, for the clear recognition that on a metallic surface gas adsorption may take place by two distinct methods—by the operation of the dispersive forces giving physical adsorption and by means of an electron switch by which a heteropolar or covalent bond is formed between adsorbent and adsorbate.

It is nevertheless a matter of some difficulty to identify in any particular case which type of adsorption is operating. In very many cases slow activated processes ascribed to the operation of chemical adsorption have been found to be due to the process of solution in the substrate requiring marked energies of activation. Again slow surface reactions have been found involving displacement and replacement of one chemisorbed species by another. The two general methods of preparing unquestionably clean metal surfaces for these studies are by utilizing a wire or ribbon capable of being cleaned by flashing and by deposition of metallic mirrors.

In the former case the surface areas are small and the building-up of surface phases is best followed by indirect means such as by observing changes in the accommodation coefficient of a rare gas, the thermionic or photoelectric work functions or even by electric capacity measurements. On mirrors the specific surfaces can be made large enough to permit of direct volumetric measurement of the adsorption very accurately up to pressures of about 10^{-1}mm. Hg. In chemisorption we have evidence that complex molecules are frequently broken down to form surface compounds of simpler constitution, e.g. molecular hydrogen to form surface hydrides, which can be detected by the ortho-para hydrogen conversion or by exchange with deuterium. These methods unfortunately do not permit us to find out how far a hydrogen-containing complex molecule undergoes surface decomposition in chemisorption, e.g. in the chemisorption of ammonia, whether a nitride, imide or amine is the residue. Therefore, attempts have been made to identify these residues by indirect means, e.g. by chemical attack by another gas or by direct volatilization into a mass spectrometer.

Chemical reaction may proceed by interaction between two different chemisorbed species, or between a chemisorbed species and a physically adsorbed molecule, or by collision from the gas phase with a chemisorbed species. Energetically at first sight the latter processes seem preferable to the former, since reaction schemes can be set up in which bond exchange, i.e. a chemical for a physical, alone is involved with no rupture of primary bonds leaving an unsaturated metal atom but the first operation may take place if a fresh molecule of reactant displaces one of the chemisorbed reacting species to react with its neighbour.

It is usual to differentiate between chemisorption and physical adsorption by the high heat of adsorption involved in the former process, but it must be noted that in those cases which have been examined over a sufficient range the $\Delta H - \theta$ curve for chemisorption falls as the surface becomes more closely packed. By some this has been attributed to surface heterogeneity. This involves the assumption of surface mobility so that redistribution can take place within the experimental time period. In many cases this does not appear to occur. Even if surface mobility occurs at high temperatures the fall in the $\Delta H - \theta$ curve is noted even at very low temperatures.

This fall may be accounted for by assuming a progressive weakening of the bond strength between substrate and ad-atom or ad-radical as the surface fills up. If this bond is heteropolar then the dipole moment of the bond will change and the mutual interactions, i.e. the repulsive forces between the ad-atoms or ad-radicals likewise change.

I can quote the following data that Bosworth and I obtained for the spreading pressures, i.e. the two-dimensional osmotic pressures for potassium chemisorbed on tungsten in comparison with formic acid physically adsorbed on mercury.

θ Molecules/sq. cm. $\times 10^{14}$	F (dynes/cm.)	
	K on W	HCOOH on Hg
0·5	9	9
1·0	22	16
2·0	70	28
4·0	190	48

We note how great a contribution the dipole repulsion makes to the spreading pressure as the surface packing increases.

At the same time the apparent adhesion to the tungsten decreases as the surface packing increases. This is reflected in a lowering of the heat of adsorption and an increase in the rate of evaporation—in fact the logarithm of the rate changes linearly with the heat of adsorption. The weakening of the bond is reflected in a decrease in the apparent dipole moment of the ad-atom. I cite some values of Langmuir for caesium on tungsten:

θ	$\mu \times 10^{18}$ e.s.u.
0	16·16
0·5	8·28
0·9	6·06

It is clear that as the composition of the electric double layer at the surface of the metal changes with increasing or decreasing adsorption the work involved in the transition of an electron from the internal levels to the double layer or vice-versa, likewise changes. Atomic spacing, the electron work function and the electron levels in the metal are thus three factors playing a part. These considerations imply that the heat of adsorption may fall to such low values as θ increases that (*a*) surface mobility may set in at some value of θ, (*b*) θ may never obtain the value $\theta = 1$ even at relatively high pressures, (*c*) physical adsorption may set in before $\theta = 1$ and a mixed film will result, e.g. an ortho-para hydrogen conversion in the Bonhoeffer-Farkas scheme. If at some value of θ the bond strength to the substrate may be so weakened that some ad-atoms may rise to a mobile level, migration and chemical action may then occur. The mechanism of the chemical catalytic action may thus change between small and large values of θ.

The evidence for the hydrogen-deuterium exchange in olefines taking place through the medium of the half-hydrogenated state or the organic alkyl metallic radical complex seems to be fairly convincing, whether the latter is produced by some mechanics of one of the following types :

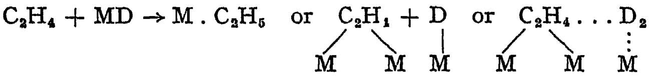

(i) (ii) (iii)

or not. It is certain that hydrogenation of a double bond does not go via the same path. Evidence is presented that gaseous ethylene can remove chemisorbed hydrogen to form ethane and that chemisorbed ethylene can, like other hydrogen-containing molecules, break down further on chemisorption. In reactions involving hydrogenation of double bonds the interatomic spacing of the catalyst on the various crystal facets plays a dominant role in the catalytic process. However, in ring closure and in the hydrogenation and dehydrogenation of aromatic substances we believe that it is the double bond that is attacked by two-point contact through the medium of the π electrons. This at once raises the issue whether there are two mechanisms for the hydrogenation of ethylene, the removal of two chemisorbed hydrogen atoms suitably spaced by gaseous or van der Waals' adsorbed ethylene or the addition of van der Waals' hydrogen to chemisorbed ethylene.

We must note that on the catalytically active facets of crystalline catalytic metals the spacing is suitable for two-point contact,

i.e.

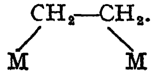

The change in carbon-carbon spacing to yield surface acetylenic complexes would not take place readily in these facets but on other crystal facets acetylenic compounds can be retained with ease and it is possible that these facets only are responsible for the dehydrogenation of ethylene. The fact that ring closure also takes place through double-bond two-point contact likewise supports the view that olefine hydrogenation involves the chemisorption of the olefine. The fact that ΔH varies with θ suggests that the bonding energy to the substrate is a function of the surface covered we should thus anticipate that the energies of activation for catalytic processes which involve simple electron transfer reactions should be related to the electron work function provided that the relative changes in the bonding energies due to the degree of packing are identical for the cases under consideration. This seems to be the case for the following in which Wansbrough-Jones and I found the following values :—

		E volts	ϕ	$\phi - E$
Oxidation of NH_3 . . .	Pt	2·74	6·35	3·61
	W	0·87	4·48	3·61
	C	0·52	4·31	3·79
Decomposition of NH_3 on .	Pt	3·5	6·35	2·85
	W	1·7	4·48	2·78
	Mo	1·39	4·36	2·97

In conclusion I might again draw attention to the valuable information to be gained in exploring the mechanism of gas adsorption and heterogeneous catalysis on metals by a comparison with the thermionic and photoelectric behaviour of these metals when monolayers are present on their surfaces.

Davy-Faraday Laboratories,
The Royal Institution,
Albemarle St., W. 1.

INTRODUCTORY PAPER (ii)

By D. D. Eley

With one exception, the papers in this section deal with the activation of hydrogen and particularly the hydrogenation of ethylene. I shall first consider them from the viewpoint of reaction path, starting with the simple case of adsorption. I shall then discuss the factors underlying the fundamental mechanism of catalysis, i.e. electronic and lattice spacing factors. Thus the various papers may be referred to more than once under each heading, and where necessary, reference will be made to papers in other sections.

Chemisorption of Gases on Metals.—Roberts established that the surface of a tungsten wire cleaned by flashing at 2500° K *in vacuo,* chemisorbed hydrogen,[1] oxygen [1] or nitrogen [2] with immeasurably fast velocity even at − 183° C. The heats of adsorption on the bare surface ($\theta = 0$) are 45,[1] 139 [1] and 28 [3] kcal./mole gas respectively, and the indications are that one atom occupied one metal site. Many of the results gained further support from the contact potential work of Bosworth and Rideal.[4, 5] Roberts found the heats of adsorption (in particular he studied H_2—W) fell off with surface covering. He indicated that certain cases of slow adsorption of gases on metals may result from displacement of impurities. Dr. Beeck [6] has confirmed these results in all essential respects, with evaporated metal films of area 10^5 times that of a wire, and in addition extended them to other gases, such as ethylene, and numerous other metals. The only case where a true *slow* adsorption is known to exist is nitrogen on iron, where the activation energy is doubtless associated with the rupture or partial rupture of the triple bond.[7] We had also confirmed many of Roberts' results on tungsten by using the para-ortho hydrogen conversion to detect adsorbed films and by the use of evaporated films of the metal.[8, 9] There are good grounds for believing that the chemisorbed atoms are held by largely covalent bonds. The study of contact potentials, and the new calculations of heat of chemisorption presented at this Discussion,[10] establish this view beyond much doubt. Thus the primary chemisorbed layer of atoms is understood in general, though many points of *detail* await further experimental work. In the potential energy diagram given by Lennard-Jones,[11] the height of the energy hill between van der Waals' and chemisorption is 1 kcal. or less when approached from the "gaseous" side. The paper of Rideal and Trapnell,[12] however, raises the point that Roberts was concerned only with 70 % of the surface. According to them, the heat of chemisorption on the last 30 % falls rapidly from 14 kcal. to 3 kcal. and this hydrogen is easily pumped off. Couper and I can confirm that easily removable hydrogen is present at ordinary pressures, and indeed the effect is mentioned in the first paper by Beeck.[13] The fundamental question for the discussion may well be how far this hydrogen is held in a *second* layer. Mignolet [14] has shown how the primary hydrogen layer on nickel has a *negative* contact potential, but that afterwards a second weakly bound layer is formed with a *positive* contact potential. Since Xe—Ni also has a positive contact potential, we may assume this hydrogen in the second layer is also held by van der Waals' forces. If so, the heats of adsorption are rather larger than those usually attributed to this kind of adsorption; but we should not reject the hypothesis out of hand on this account in the absence of further theoretical work on the subject.

---

[1] Roberts, *Proc. Roy. Soc. A*, 1935, **152**, 445 ; *Some Problems in Adsorption* (London, 1939).
[2] Roberts, *Nature*, 1936, **137**, 659.
[3] Bosworth and Rideal, *Physica*, 1937, **4**, 925.
[4] Bosworth and Rideal, *Proc. Roy. Soc. A*, 1937, **162**, 1.
[5] Bosworth, *Proc. Camb. Phil. Soc.*, 1937, **33**, 394.
[6] Beeck, this Discussion.
[7] Beeck, Cole and Wheeler, this Discussion.
[8] Eley and Rideal, *Proc. Roy. Soc. A*, 1941, **178**, 429.
[9] Eley, *ibid.*, 1941, **178**, 452.
[10] Eley, this Discussion.
[11] Lennard-Jones, *Trans. Faraday Soc.*, 1932, **28**, 333.

Besides forming van der Waals' and chemisorbed layers, hydrogen may penetrate the lattice, giving true solutions such as those examined by Sieverts, or being held on intercrystalline boundaries. Long ago this was suggested as a mechanism for activated adsorption [15] and Beeck's work on sintering nickel films supports this most strongly.[16] From the catalysis point of view, dissolved hydrogen may poison the catalyst as Couper and Eley [17] have shown for the parahydrogen conversion on palladium. Quite a number of cases of poisoning found in the literature may be tentatively ascribed to this effect.

The paper by Eucken [18] describes results on the adsorption of hydrogen on nickel powder, the pre-treatment of which is not stated. Eucken gives evidence for two kinds of adsorption, one with a peak in the isobar at 200° K and the other at 280° K. The heat in the first case is estimated as 6 kcal./mole, which Eucken attributes to the chemisorption of an H_2 molecule to give two atoms side by side. The second maximum corresponds to the atoms having diffused apart into positions of minimum energy. Beeck, Cole and Wheeler [7] with evaporated nickel films state that hydrogen atoms are mobile at $-183°$ C and that the heat of adsorption against θ curve is the same as at 23° C. The reduced powder may of course not only differ physically from an evaporated film, but may even contain dissolved hydrogen and oxygen. Evaporated films are much more likely to possess an uncontaminated surface. A comparison of results in two cases such as these may eventually yield valuable generalizations for technical catalysts, as indicated by Prof. Taylor in his opening lecture.

The Parahydrogen Conversion.—The heterogeneous parahydrogen conversion [19] by the *chemical* (as opposed to magnetic) mechanism, is identical in rate and kinetics with the hydrogen deuteride reaction in cases known at present. The original Bonhoeffer mechanism involved dissociation and recombination of atoms in a loosely-bound chemisorbed layer,

$$p\text{—}H_2 + 2M \rightarrow 2MH \rightarrow 2M + o\text{—}H_2$$

but as a result of surface interchange experiments on evaporated films of tungsten,[9] for this case the following mechanism was substituted.

---

[12] Rideal and Trapnell, this Discussion.

[13] Beeck, Smith and Wheeler, *Proc. Roy. Soc. A*, 1940, **177**, 78.

[14] Mignolet, this Discussion.

[15] Ward, *Trans. Faraday Soc.*, 1931, **28**, 339.

[16] Beeck, Ritchie and Wheeler, *J. Colloid Sci.*, 1948, **3**, 504.

[17] Couper and Eley, this Discussion.

[18] Eucken, this Discussion.

[19] Reviewed by Eley in (*a*) *Advances in Catalysis*, Vol. I, 157; (*b*) *Quart. Rev.*, 1949, **3**, 209.

A p—H_2 molecule in the van der Waals' layer was supposed in some way to exchange an atom for one in the underlying chemisorbed layer

$$p\text{—}H_2 + HW \rightarrow H_3W \rightarrow WH + o\text{—}H_2.$$

This work was confirmed for the metal nickel.[20] Trapnell and Rideal, assuming the loosely-bound hydrogen on tungsten exists in the chemisorbed layer, once again suggest that in this case the Bonhoeffer mechanism is valid. Neither must we neglect here the suggestions of A. and L. Farkas [20] for the metals platinum and palladium. Dr. Couper, Mr. Hulatt and myself have further unpublished work which we hope will help in the discussion of this matter.

The adsorption work of Beeck, and of Rideal and Trapnell raises again the question of the determination of surface areas. The usefulness of the B.E.T. method is now beyond dispute, but undoubtedly other methods are to be sought and the paper by Maxted *et al.*[21] shows how the phenomena of catalyst poisoning may be brought to bear upon the problem, with most hopeful results.

Hydrogenation of Ethylene.—While dispute can still occur concerning the mechanism of the parahydrogen conversion, the chances of agreement on the mechanism of ethylene hydrogenation must seem remote at present. Let us remind ourselves of the general facts of ethylene hydrogenation as they stood in 1940 when Beeck commenced to add the large number of striking new data on films, summarized in his papers to this Discussion. The reaction had been investigated on many catalysts, particularly copper and nickel powder, produced by reduction of oxides, or wires activated by oxidation and reduction. References are given in a recent review.[19b] In the range 100-150° C, the reaction is first order in hydrogen and zero order in ethylene. A marked excess of ethylene has sometimes been ascribed an inhibiting effect. At 200° C and higher the reaction is second order, i.e. first order in both gases. At room temperature Beeck reports that the reaction is first order in hydrogen and zero order in ethylene, while for butene-1 at 50° C. Twigg reports $u \sim p_{H_2}{}^{0.5} p_{Et}{}^{0.5}$. On transition metal catalysts, the activation energy is usually 5-10 kcal. Beeck reports $E = 10{\cdot}7$ kcal. for many metals investigated, exceptions being tungsten and tantalum. A marked feature of the reaction is that as the temperature increases the activation energy falls to zero, at 150° C for nickel catalysts, and much higher temperatures for nickel-silicon skeleton catalysts, as pointed out by Schwab. This effect in the past has been attributed to desorption of ethylene ; but desorption of hydrogen must first be considered, since it starts at a lower temperature.

Any theory advanced has to take account of these facts and also the many new facts advanced by Beeck, of which two are outstanding : [22]

(*a*) Ethylene gas admitted to a clean metal film is strongly adsorbed, probably as acetylenic complexes 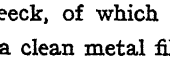 $Ni\diagup^{CH=CH}\diagdown Ni$ which largely cover the surface. The hydrogen atoms are removed by further ethylene forming ethane in the gas phase. Such a pre-adsorbed film is only *slowly* removed on exposure to hydrogen gas.

(*b*) A hydrogen film pre-adsorbed on nickel is rapidly removed by gaseous hydrogen giving ethane.

The main modern theories in the field may be considered in chronological order.

(1) THE HALF-HYDROGENATED STATE THEORY OF HORIUTI AND POLANYI.[23]—In this, two hydrogen atoms are added on independently

---

[20] A. Farkas and L. Farkas, *J. Amer. Chem. Soc.*, 1942, **64**, 1594.

[21] Maxted, Moon and Overgage, this Discussion.

[22] Beeck, *Rev. Mod. Physics*, 1945, **17**, 61.

[23] Horiuti and Polanyi, *Trans. Faraday Soc.*, 1934, **30**, 1164.

and successively. The ethylene is held by "associative" chemisorption, i.e. by opening of the double bond.

$$\overset{*}{C}H_2—\overset{*}{C}H_2 + \overset{*}{H} \rightleftharpoons \overset{*}{C}H_2CH_3 + \overset{*}{H} \rightarrow CH_3—CH_3$$

(an asterisk indicates a chemisorption bond to a metal site).

(2) THE ADDITION OF A MOLECULE OF HYDROGEN :

(*a*) $H_2 + \overset{*}{C}H_2—\overset{*}{C}H_2 \rightarrow CH_3—CH_3$ (Twigg and Rideal [24])

(*b*) $H_2 + CH_2=\overset{*}{C}H \rightarrow CH_3—\overset{*}{C}H_2 + \overset{*}{H} \rightarrow CH_3CH_3$ (Farkas [25])

(*c*) $\overset{*}{H} + CH_2=CH_2 + \overset{*}{H} \rightarrow CH_3CH_3$.

Farkas favours dissociative adsorption, while Twigg and Rideal favour associative adsorption of ethylene.

Mechanism (2*a*) may possibly be brought into line with (1) if we realize [19b] that the simultaneous addition of $2\overset{*}{H}$ atoms from one H_2 molecule comes to the same thing, (2*c*). Mechanism (2*c*) is expected to occur when the hydrocarbon is very strongly adsorbed as with ethylene, i.e. when the chemisorbed hydrogen cannot diffuse on the surface. Benzene, on the other hand, is more weakly adsorbed and the resultant high concentration of $\overset{*}{H}$ favours independent $\overset{*}{H}$ from separate H_2 molecules.

(3) Beeck's mechanism is that the surface is largely covered with ethylene molecules held as acetylenic complexes and only slowly removed by adsorbed hydrogen

$$2\overset{*}{H} + \overset{*}{C}H=\overset{*}{C}H + 2\overset{*}{H} \rightarrow CH_3—CH_3$$

On the spaces set free Beeck visualizes two possible mechanisms. Firstly, *hydrogen* is chemisorbed and reacts with gaseous ethylene, this reaction determining the hydrogenation reaction

$$\overset{*}{H} + CH_2=CH_2 + \overset{*}{H} \rightarrow CH_3—CH_3.$$

Originally suggested by Beeck for the nickel group of metals, he now retains it only for the tungsten group. For nickel he now favours interaction between chemisorbed hydrogen and chemisorbed ethylene, i.e. presumably some mechanism related to (1) or (2*c*) above. A good case has been made out for (1) or (2) on thermochemical grounds,[19b] in contradiction to some earlier arguments of Beeck.[23] It is now a matter of great interest that Eyring [26] and Laidler [27] both base their transition state treatments on formal schemes related to (2*a*), (2*b*) and (2*c*) and can show that the low steric factor for the reaction calculated by Beeck (and also by Eucken [18] from the results of Toyama) is due to loss of translations and rotations on adsorption of the reacting gases. It does, however, appear that a number of mechanisms must have the same calculated frequency factor, so that really we are not much further ahead. Also (as Schwab has pointed out) the treatments give a maximum rate at a definite pressure which is not found in practice.

The extensive and important researches of Twigg and Rideal,[24] and Farkas [25] on the exchange of deuterium atoms between deuterium molecules and ethylene molecules have been recently reviewed.[19] Twigg and Rideal showed :

(1) The exchange and hydrogenation have identical kinetics on a nickel wire at 156° C. The activation energy for exchange is 18·6 kcal., and falls off in an identical fashion with increase of temperature, being at all temperatures 4-5 kcal. greater than that for the hydrogenation reaction.

[24] Twigg and Rideal, *Proc. Roy. Soc. A*, 1939, **171**, 55.

[25] Farkas, *Trans. Faraday Soc.*, 1939, **35**, 906.

[26] Eyring, Colburn and Zwolinski, this Discussion.

[27] Laidler, this Discussion.

Farkas obtained similar results on platinum foil. The $H_2 + D_2$ reaction is effectively inhibited by the presence of the ethylene. Twigg and Rideal suggested the rate-determining step to be the first of the following reactions :

$$\overset{*}{C}H_2—\overset{*}{C}H_2 + D_2 \rightarrow \overset{*}{C}H_2—CH_2D + \overset{*}{D} \rightarrow \overset{*}{C}H_2—\overset{*}{C}HD + HD.$$

(2) Conn and Twigg found *no* exchange between C_2D_4 and C_2H_4 even at temperatures as high as 360° on a Ni filament which favours adsorption as $\overset{*}{C}H_2—\overset{*}{C}H_2$ rather than $CH_2{=}\overset{*}{C}H\ \overset{*}{H}$. The calculations of heat of chemisorption by Eley also tend to support the first kind of chemisorption.

The paper by Turkevich, Bonner, Schissler and Irsa [28] brings forward similar data to Twigg, but by the mass spectrometer they can distinguish the various isotopic species. They also note that in the initial stages of reaction of $D_2 + C_2H_4$, light C_2H_6 is produced. This result is the same as that of Baxendale and Warhurst [29] who found appreciable quantities of light methyl elaidate produced by deuterogenation of methyl oleate on platinum black. This is very strong evidence for the occurrence of Beeck's reaction outlined above, but it would appear from Turkevich's result, as we would expect, that the rate of production of C_2H_6 soon decreases to zero, and that this reaction plays no part in the stationary hydrogenation process. Thermochemical reasons support this view, since

$$2CH_2{=}CH_2 \rightarrow CH_3—CH_3 + CH{\equiv}CH$$

has $\Delta H = +\ 17{\cdot}2$ kcal. and since $\Delta S \sim 0$ it will be thermodynamically impossible, and can only occur at all because the acetylene is chemisorbed on the catalyst.

My own tentative viewpoint is that a large part of the catalyst may be covered by the so-called acetylenic complexes, *particularly* if pure ethylene is admitted to a clean catalyst, but that the catalyst settles down to a stationary state in which a fair part of the catalyst is covered by chemisorbed ethylene, which reacts by (2*a*) or (2*c*). It is difficult to see how (3) could give the observed kinetics, but there is clearly a need for a great deal more work before a definite decision can be reached, and the lines of investigation should come out of this Discussion.

It might be convenient finally to raise one new suggestion at this time. The solubility of hydrogen in metals such as nickel increases strongly with increase of temperature. If hydrogen dissolved in the metal does exert a poisoning action, it might well lead to the activation energy falling off to zero. It is well known that ethylene does not desorb off nickel below 200° C, but it is exceedingly unlikely, since the reaction is first order in hydrogen gas at relevant temperatures, that desorption of *this* gas can affect the activation energy. If desorption were a factor, one would expect Ni—Si catalysts to have a *lower* temperature of maximum rate, but if solubility comes in a *higher* temperature. This is only a very tentative suggestion as we have no experiments to show a poisoning action of dissolved hydrogen on this system, but only on the palladium —p—H_2 system.

Other reactions discussed include dehydrogenation,[30] and the oxidation of ammonia.[31]

There would seem to be no special problem in the kinetics of dehydrogenation comparable with the hydrogenation reaction, probably because the former occurs at much higher temperatures. Zawadzki's paper reviews the impressive body of work done on the ammonia reaction, much of which is not easily available to workers in this country.

---

[28] Turkevich, Bonner, Schissler and Irsa, this Discussion.

[29] Baxendale and Warhurst, *Trans. Faraday Soc.*, 1940, **36**, 1186.

[30] Schwab, this Discussion.

[31] Zawadzki, this Discussion.

Lattice Spacing Factor.—Beeck's work on the increased activity of oriented films of nickel is well known.[13] He has now [32] developed this work showing that the actual activity is associated with an increased area of exposed (110) plane, and not merely increased orientation. This is so for ethylene hydrogenation and ethane dehydrogenation. On the other hand, there is no difference between oriented and non-oriented nickel films for benzene hydrogenation. Oriented (110) films of platinum were less active than non-oriented films in cyclohexane dehydrogenation. This latter result Beeck associated with the Balandin criterion of 6-point adsorption on the octahedral (111) faces. Beeck associates the maximum activity of rhodium for ethylene hydrogenation and palladium for acetylene hydrogenation with the need for a lattice spacing in the metal to fit the substrate, but qualifies his view for metals like chromium, where he believes bond-type, in particular percentage *d* character plays a part, as emphasized recently by workers both in Billingham and Bristol, and discussed in the next section.

Electronic Factors.—Schwab [30] has summarized his work on the dehydrogenation of formic acid on a wide range of alloys of monovalent with multivalent metals. He has quite convincingly demonstrated that the activation energy is proportional to the square of the electron concentration, and argues that the rate-determining step is the loss of 2 electrons from the formic acid molecule into the lowest unfilled level in the metal. This is a particularly thorough and satisfying piece of work. He has also raised again the question of the linear relation between the logarithm of the frequency factor and the activation energy. Couper and Eley [11] have shown how the activation energy of the parahydrogen conversion on palladium is suddenly increased when gold is alloyed at the right concentration to fill up the holes in the *d* band. In other words, unpaired *d* electrons, presumably at the surface, are a necessary condition for a strongly bound activated complex. Dissolved hydrogen exerts a similar poisoning action. The clear cut nature of the result is probably associated with the simple nature of the system they examined. Dowden and Reynolds,[33] with a similar objective, examined Ni—Cu and Ni—Fe alloys. The general picture is that a high activity is associated with a partly empty *d*-band (not only for the hydrogenation of styrene, but also for the decomposition of methanol and formic acid). On the other hand, the decomposition of hydrogen peroxide is favoured by a full *d*-band, which they believe is due to the slow step being electron donation from metal to substrate [34]

$$M + H_2O_2 \rightarrow M^+ + HO + OH^-.$$

They have also produced evidence that in Ni—Fe alloys the catalytic activity increases with $g(E)$, the energy density of electron levels. For one range of compositions while the number of holes in the *d*-band are decreasing, nevertheless there is a strong increase in hydrogenation activity in the composition region where specific heat data indicates an increase in $g(E)$.

It is quite clear that with the application of the relatively novel ideas and techniques outlined in these papers that the subject of metal catalysis is going to enter a long period of fruitful development.

The University,
Bristol.

---

[32] Beeck and Ritchie, this Discussion.
[33] Dowden and Reynolds, this Discussion.
[34] Weiss, *Trans. Faraday Soc.*, 1935, **31**, 1547.

STUDIES IN CONTACT POTENTIALS

PART I.—THE ADSORPTION OF SOME GASES ON EVAPORATED NICKEL FILMS

BY J. C. P. MIGNOLET

Received 2nd February, 1950

Surface potentials have been determined for a number of gases on unoriented evaporated nickel deposits. The chemical films studied are: Ni—H: − 0·345 V; Ni—C_2H_2: + 1·0 V; Ni—C_2H_4: + 0·83 V. Contact potential appears to be suitable for directly studying surface reactions involved in the catalytic hydrogenation of C_2H_2 and C_2H_4 on nickel. Van der Waals' films of non-polar gases may exhibit considerable surface potentials: Ni—Xe: + 0·85 V; Ni—N_2: + 0·21; Ni—C_2H_6: + 0·77 V. Surface potential appears to afford a criterion of limited applicability for distinguishing between van der Waals' adsorption and chemisorption.

Surface potential (S.P. in short) has a number of qualities which make it an interesting physical quantity in the field of adsorption and catalysis on solids. It is a true surface property simply related to the electric moment of the adsorbed particles and to their concentration on the outer surface.

Experimentally contact potential techniques are available which enable S.P. (or S.P. variations) to be measured in an extraordinarily wide range of conditions. It seems possible with them to study reactions between adsorbed films and gases and to observe the films on catalysts in operation. Apparently, little has been done in this direction.[1] In the case of the catalytic dissociation of H_2 on tungsten, Bosworth has been able to choose between two mechanisms on the basis of a contact potential determination. In a study of the catalytic para hydrogen conversion on a tungsten wire poisoned with an oxygen film, Eley and Rideal[2] have used a contact potential technique to determine the relation between catalytic activity and concentration of the poison film. The main object of this investigation was to examine the films of H_2, C_2H_2, C_2H_4 and C_2H_6 on nickel, as a first step towards a study of the catalytic hydrogenation of C_2H_2 and C_2H_4. In the course of this investigation, it has emerged that van der Waals' films of non-polar particles could exhibit appreciable S.P. Since this raises questions as to the interpretation of S.P., films of such typically non-polar particles as N_2 and Xe have also been studied.

Experimental

The apparatus used is shown schematically in Fig. 1. The cell[3] and the micro-introductors[4] are described elsewhere. Before starting an experiment, the apparatus is degassed thoroughly, baking the cell and trap 1 at 500° C in an oven, torching out the tubings and heating the filament for 2 hr. just under evaporation point. An additional precaution has been found advisable, i.e. to pump impurities of intermediate volatility out of the traps. Otherwise, virtual leaks may occur and cause, for instance, variations of 0·1 to 0·2 V when the condenser tube is cooled to − 196° C. These fractional distillations are carried out by temporarily warming-up traps 1 and 3 to − 160° C as shown in Fig. 1. Such slight warming-ups are also useful when handling "vapours," e.g. C_2H_4.

---

[1] Bosworth, *Proc. Camb. Phil. Soc.*, 1937, **33**, 394.

[2] Eley and Rideal, *Proc. Roy. Soc. A*, 1941, **178**, 429.

[3] Mignolet, Part II, this Discussion.

[4] Mignolet, *Trans. Faraday Soc.*, 1949, **45**, 271.

Vacuum-tight tests showed that, with the cut-off shut, the pressure remained of the order of 10^{-6} mm. Hg for a few hours and rose overnight to 1 or 2 × 10^{-5} mm. Hg. In normal working conditions, a bare nickel deposit will not exhibit any appreciable drift in contact potential for 2 hr.

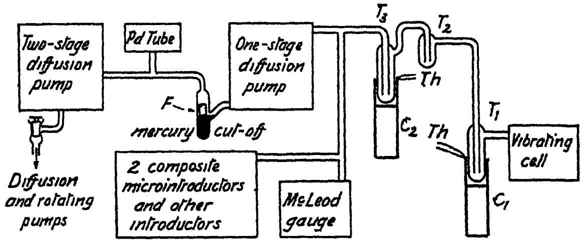

FIG. 1.—Apparatus.

F : iron cylinder enclosed in glass tube.

T_1, T_2, T_3 : traps normally cooled in liquid nitrogen. T_1 outgassed with the cell at 500° C in an oven ; T_2 cooled temporarily before removing oven.

C_1, C_2 : copper tubes sealed to traps with alcohol; warmed to − 160° C (indicated by thermocouple Th) for fractional pumping-out of impurities. Long lower part prevents temperature from rising owing to evaporation of liquid nitrogen.

Three cells were used : a simple type I cell in series E, F and G ; a type I cell of a somewhat different design in series H, . . . N ; a type II cell in series O, . . . W. The second cell incorporated two filaments—one opposite each "area"—and a screen to meet secondary requirements enabling, for instance, evaporations to be made without condensation on either "area". The result was worse, however, because increased crowding caused the S.P. values to be about 15 % too low.

Much attention has been paid to avoiding and detecting possible variations of the auxiliary surface. In series E to N, controls were systematically made, fully using the possibilities of the two "areas" (see discussion in Part II). These controls have shown that the surface of the auxiliary electrode—such as results from the outgassing—is extremely inert chemically. The situation is very favourable too with van der Waals' films at low temperatures because the temperature of the auxiliary electrode remains much higher than that of the vibrating electrode. Actually, with the condenser tube in liquid nitrogen, the temperature of the auxiliary electrode *in vacuo* is roughly − 10° C. Of course, the temperature sinks as the gas pressure is raised, but since it reaches its final values within a few minutes, adsorption on the auxiliary surface would be detected. Actually, such effects as have been observed never exceed 0·02 V. They probably result from a thermal variation in the work function. The stability of the auxiliary surface being satisfactory, and since controls are a source of small errors, it was decided to drop them after series N and choose the best possible conditions for the measurements proper. As a result, a better reproducibility of the S.P. values was obtained (see below).

Materials.—NICKEL DEPOSITS. Evaporation was produced by heating a nickel filament (0·3 mm. diam.) electrically (2·8 to 3·0 A) *in vacuo*. Nickel wire of two sorts were used, i.e. 99 % Ni + 0·5 % Co and after series M, spectroscopically pure Ni. No difference was detected. With the first two cells, the nickel was deposited on a nickel foil (vibrating plate) at − 196° C. With the third cell, the base was Pyrex glass cooled externally in ether. Apparently, there was no difference between the two sorts of deposits. An X-ray diffraction test * showed that the latter method yields microcrystalline unoriented deposits as stated by Beeck, Smith and Wheeler.[5] With the thick opaque deposits used, no influence of thickness was apparent.

---

* Kindly carried out by Dr. H. Lambot and Dr. J. Toussaint.

[5] Beeck, Smith and Wheeler, *Proc. Roy. Soc. A*, 1940, 177, 62.

HYDROGEN : electrolytic ; purified by diffusion through a palladium tube.
NITROGEN : from a steel cylinder ; purified by bubbling through $Na_2S_2O_4$ + KOH.
ACETYLENE : prepared and purified according to Moser.[6]
ETHYLENE : prepared and purified according to Moser[6] ($C_2H_5OH + H_3PO_4$).
ETHANE : prepared by the reaction $C_2H_5MgBr + H_2O$; washed with $KMnO_4$.

All three hydrocarbons were fractionated *in vacuo* in the apparatus itself and sent directly into the introductors.

ARGON : 99·9 % + 0·1 % N_2.
XENON : supplied by Matheson Co. According to mass spectrometer analysis, the only impurity was krypton (0·25 %).

Results

HYDROGEN FILMS.—Two kinds of hydrogen film have been observed. They are easily distinguished as their S.P. are of opposite signs, i.e. negative * for the chemical (atomic) film, positive for the van der Waals' film (see Fig. 2).

A few S.P. (in volt) of the negative film at 20° C are :

Experiment	Oa	Ra	Sa
In vacuo ($p \sim 10^{-6}$ mm. Hg) .	− 0·304	− 0·266	− 0·306
At saturation ($p > 2$ mm. Hg) .	—	− 0·327	− 0·359

The S.P. for a complete chemical hydrogen film may be taken as −0·345 ± 0·02 V.

At − 196° C, addition of hydrogen to a nickel surface already covered with the negative film leads to the formation of a volatile positive film, as shown in Curves 2 and 3. Curve 2 was obtained with an incomplete negative film prepared by pumping at 20° C and cooling, and Curve 3 with a complete film prepared by cooling in hydrogen (50 mm. Hg) and pumping. Except for a constant difference of about 0·06 V due to the negative film, the two curves do not differ appreciably. A maximum S.P. of + 0·1 V is obtained in both cases. This value is not accurate. It contains a possible contribution of thermal origin from the auxiliary surface (+ 0·02 V at most).

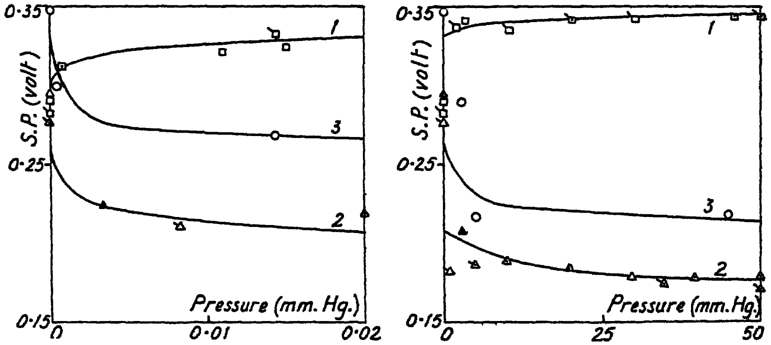

FIG. 2.—Surface potentials of hydrogen films as a function of pressure (plotted at two different pressure scales).

Curve 1 : at 20° C ; chemical film.
Curve 2 : at − 196° C ; van der Waals' film on incomplete chemical film.
Curve 3 : at − 196° C ; van der Waals' film on complete chemical film.
□̍ △̍ : Expt. Ra ; □ △ ○ : Expt. Sa.

Points from Expt. Ra have been raised by 0·016 V and those from Expt. Sa, lowered by the same quantity so as to make the S.P. coincide for a complete negative film.

---

[6] Moser, *Die Reindarstellung von Gasen* (F. Enke, Stuttgart, 1920), pp. 140 and 137.

* Negative films increase the work function.

Bare nickel at − 196° C adsorbs hydrogen very rapidly ($t < 1$ min.). The negative film (somewhat incomplete) is formed first. Measurements of adsorbed volumes on larger nickel films prepared in the same way have shown that, at about 4×10^{-3} mm. Hg, the ratio of quantity of H_2 in 2nd film/quantity of H_2 in 1st film is about 0·03, whereas the ratio of the corresponding S.P. is about 0·25. Therefore, the electric moment of the hydrogen particles is much higher in the van der Waals' film than in the chemical one. Preliminary experiments give evidence that the S.P. of the negative film is proportional to the amount of hydrogen adsorbed, i.e. that the electric moment is independent of the fraction of surface covered. No similar indication is available for the positive film. In particular, it has not been possible to determine whether the adsorption isotherm exhibits a saturation as does the S.P. isotherm.

C_2H_2, C_2H_4 and C_2H_6 Films.—The adsorption of these gases on bare nickel has not been studied in detail. The values given are only preliminary ones. Expt. Ta and Wb give 0·94 and 1·10 V for the S.P. of a chemical C_2H_2 film at 20° C in good agreement with the value 1·046 V obtained from the displacement reaction, $Ni—H + C_2H_2 \rightarrow Ni—C_2H_2 + \ldots$ Expt. Va gives 0·835 V for the S.P. of a chemical C_2H_4 film at 20° C, in qualitative agreement with other less accurate values obtained either directly or from the reaction,

$$Ni—H + C_2H_4 \rightarrow Ni—C_2H_4 + \ldots .$$

There seems to be little doubt that the S.P. of the C_2H_4 film is in fact 0·2 V lower than that relative to C_2H_2.

At − 183° C, C_2H_2 and C_2H_4 films exhibiting approximately the same S.P. as at 20° C. have also been observed. It is not clear whether they are van der Waals' or chemical films because it has not yet been possible to desorb them and restore the bare surface. With C_2H_2, a desorption from 0·943 to only 0·766 V was observed during warming up (with appropriate precautions to pump out the C_2H_2 quickly at a low temperature) to 20° C. With C_2H_4, desorption was apparently complete, but the surface would no longer adsorb hydrogen at 20° C.

As regards C_2H_6, a series of adsorptions at − 183° C gave the values + 0·62 ; + 0·80 and + 0·74 V. Addition of C_2H_6 at 20° C has no effect. Heating in contact with C_2H_6 to 250° C produces a variation of − 0·3 V. A few observations have been made on the reactions between adsorbed hydrogen and gaseous C_2H_2 or C_2H_4, and also on the reverse reactions. They are insufficient to justify amplification. Yet, in view of their interest as regards the possibilities of contact potentials in catalysis, it is perhaps as well to give a few indications. At room temperature and low pressures, C_2H_2 and C_2H_4 react rapidly ($t < 1$ min.) with an adsorbed H film. The measured S.P. jumps are equal to the difference in the S.P. given above for films on bare nickel. The reverse reactions are extremely slow at room temperature but rapid at 250° C. Again, a jump of about 1 V is observed. Alternate displacement reactions can be repeated several times and the kinetics with C_2H_2 and C_2H_4 compared. It appears that the rates are not very different.

Van der Waals' Films.—The results are collected together in Table I.

The S.P. recorded are those for complete films except in those cases discussed below. Films on bare Ni are stable *in vacuo*, S.P. variations of about 5 % being sometimes observed by pumping. The S.P. are often considerable, comparable in magnitude with those obtained for chemical films. One of the most significant is perhaps that of Ni—Xe where there is no possibility of chemical interaction. The effect observed must therefore be ascribed to polarization in the field existing near the surface ; and clearly, the same cause is operating in the other cases. Incidentally, the agreement between the S.P. values for Ni—Xe (+ 0·840 and + 0·866 in Expt. Va ; + 0·849 in Expt. Wa) shows the degree of reproducibility that can be reached when no complication arises from the film itself. The case of argon shows that the observed S.P. are really due to adsorption and not to the presence of gas between the electrodes. At − 196° C, argon is very slightly adsorbed as was shown by a special volumetric test. As should be, it gives a negligible S.P. Pre-adsorbed hydrogen increases the surface potential of nitrogen (Table I) but decreases the fraction of surface covered. The latter point is shown clearly by the isotherms of Fig. 3.

The isotherms are numbered in the order in which they were taken. Since the nickel deposit had been kept at a temperature somewhat higher than 20° during deposition, no sintering can have occurred between isotherms 1 and 3 and it must be concluded that (i) only 20 % of the hydrogen-covered nickel surface are capable of adsorbing nitrogen ; (ii) the electric moment of the adsorbed N_2 molecules is about 10 times greater on a Ni—H than on a Ni substrate.

All surface potentials on Ni and Ni—H being positive, it is interesting to examine the adsorption on positive pre-adsorbed films to see whether the second film would not be negative. Results for Ni—C_2H_4 and Ni—C_2H_2 show very small S.P., indicating that either there is no adsorption or that the adsorbed particles are weakly polarized. In Expt. Wa, enough xenon to produce a polymolecular layer was added to a nickel surface covered with a chemical C_2H_2 film at — 196° C, care being taken to warm the traps to $-183°$ C. A contact potential variation of about — 0·06 V occurred. Such small effects might result from a compensation between two effects arising : one from the nickel surface, the other from the pre-adsorbed film. It is more probable that they are a result of the short range of the forces involved. In this respect, the adsorption of Xe on Ni—N_2 affords favourable conditions for a test, since there is, so to speak, a + 0·65 V reserve for polarization if the range is sufficient.*

TABLE I.—SURFACE POTENTIAL OF VAN DER WAALS' FILMS ON NICKEL BARE OR COVERED WITH PRE-ADSORBED CHEMICAL FILMS

Base Surface	Gas	T (° C)	p mm. Hg	S .P. (volt)	Expt.
Bare nickel	N_2	-196	10^{-3}	$+0·21 \pm 0·01$	Oa
„	Ar	-196	1	$\leqslant +0·03$	Ta ; Va
„	C_2H_6	-183	3×10^{-4}	$+0·77$	Ua
„	Xe	-196	2×10^{-3}	$+0·85 \pm 0·01$	Va ; Wa
„	„	-183	„	$+0·80$	Wa
Ni—H	H_2	-196	10	$+0·09 \pm 0·01$	Ra ; Sa
„	C_2H_4	-190	10^{-6}	$+0·88$*	Kb
Incomplete Ni—H :—					
(S.P. = — 0·072)	N_2	-196	5×10^{-3}	$+0·36$	Oa
(S.P. = — 0·28)	„	„	„	$+0·45$	„
(S.P. = — 0·30)	„	„	„	$+0·41$	„
Ni—C_2H_4	C_2H_4	-183	2×10^{-4}	$+0·07 \pm 0·01$*	He
„	H_2	„	2×10^{-3}	$-0·02 \pm 0·01$	Hf
„	Xe	-196	2×10^{-3}	$0 \pm 0·02$	Va
Ni—C_2H_2	N_2	-196	6×10^{-3}	$-0·006$	Ne

† Value obtained with the second cell (see Experimental) and therefore 15 % too low.

Discussion

From the results presented here, it is clear that contact potential can be used to study the catalytic hydrogenation of ethylene and acetylene on nickel and the related surface reactions. A discussion is undoubtedly premature now but, perhaps, we can say a few words in relation to the problem of active centres. S.P., being proportional to the concentration of adsorbed particles, will not detect changes in the adsorption on sparse array of active centres. Hence, for a reaction occurring only at active centres, there will be no parallelism between the behaviour of the films observed by contact potentials and that expected for the films through which the catalytic reaction proceeds. Of course, a close parallelism does not prove that the surface is homogeneous. In the case studied here, the films seem to behave as would be anticipated from the catalytic data.

The adsorption of hydrogen on nickel has been studied at room temperature by v. Duhn[7] who reports a positive (with the convention of signs adopted here) S.P. varying from 0·3 V at 10^{-2} mm. Hg to 0·7 V at 10 mm.

---

† A negative surface potential is not excluded. The experiment has not yet been carried out.

[7] v. Duhn, *Ann. Physik*, 1943, **43**, 37.

Hg. Since both v. Duhn and the writer find a negative oxygen film,* a systematic error in the signs is excluded. It is suggested that part of the discrepancy results from a difference in the condition of the surfaces before contact with H_2. The nickel surface was not bare in v. Duhn's experiments because of inadequate technique. On the other hand, v. Duhn's measurements were made *in vacuo*, after the upper electrode had been in contact for some time with the gas at the pressure given. Therefore, his curves are not ordinary isotherms and indeed, it is not clear how, in most cases, the pressure could have had an effect at all.

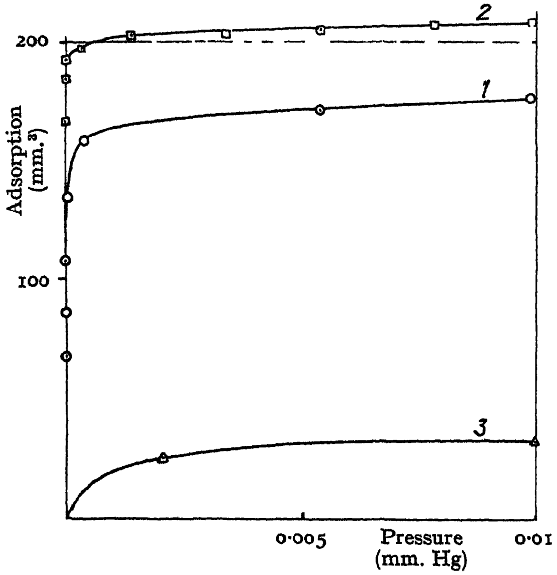

FIG. 3.—Adsorption isotherms at − 196° C.

Curve 1 : N_2 on bare nickel.
Curve 2 : H_2 on bare nickel.
Curve 3 : N_2 on nickel covered by an incomplete H film (prepared by pumping at 20° C and cooling).

S.P. of van der Waals' films of non-polar gases have been reported previously. There must have been van der Waals' films in those examined by v. Duhn, though the distinction with chemisorption was not made. In another direction, Frost and Hurka [8] obtained S.P. of about 0·1 V for a few films, e.g. CCl_4 and C_6H_6 on collodion.

In several of the cases studied here, the effects are much greater. This raises the question of the interpretation of S.P. So far, it has been customary to interpret them in terms of chemical polar bonds, either within the adsorbed molecules or between adsorbate and metal. It is clear that induced polarization must be taken into account too. For the chemical films of C_2H_2 or C_2H_4 on Ni, for instance, it is able to account for more than half the effect. The writer has held the view that the second H_2 film is a " film in the gaps ".[9] Curve 3 in Fig. 2 brings strong evidence against this view, since the film is still present although the gaps have been filled.[10] It is not proposed to discuss possibilities as to the seat of adsorption before experiments are made at intermediate temperatures and on oriented films.

---

* In series E, a S.P. of −1.6 V has been found for the oxygen film on nickel at − 190° C, in satisfactory agreement with Bosworth's determination (−1·4 V; *Trans. Faraday Soc.*, 1939, **35**, 397).

[8] Frost and Hurka, *J. Amer. Chem. Soc.*, 1940, **62**, 3335.

[9] Roberts, *Some Problems on Adsorption* (Cambridge University Press, London, 1939). Rideal, *Chem. and Ind.*, 1943, **62**, 335. Rideal and Trapnell, *Colloque sur l'adsorption et la cinétique hétérogène* (Lyon, Sept., 1949).

Perhaps, for the present, the main interest of the curves of Fig. 2 lies in another direction. We have here a striking example of the ability of S.P. to distinguish between van der Waals' adsorption and chemisorption by virtue of its having a sign. Examining the meagre data of Table I from a purely empirical point of view, one will notice that the van der Waals' films on bare nickel examined (Xe, N_2, C_2H_6) exhibit positive S.P. The positive sign may well be a feature common to all van der Waals' films of non-polar gases on bare metals. If this turns out to be true, a negative S.P. on a bare metal will point to chemisorption; and perhaps, when more is known about induced polarization, it will be possible to develop the criterion for positive films on a bare metal by taking the value of the S.P. into account. It is hoped in another paper to present additional data on induced polarization and discuss the matter in detail.

I wish to express my deep gratitude to Prof. L. D'Or for help, encouragement and advice. I also wish to thank Messrs. J. Haesen and J. Sarlet for skilful technical help and Dr. J. Serpe and Dr. J. Pirenne for useful discussions.

Laboratoire de Chimie générale,
Liége,

ADDENDUM—**On the Origin and Nature of "Induced Polarization".**— How is it that van der Waals' films of non-polar particles exhibit surface potentials? The effect might be one of compression of the electric double layer at the metal surface by the adsorbed particles, without the latter being polarized, but this is very improbable. Therefore, it has to be assumed that the adsorbed particles are polarized and our problem is to understand the origin and nature of the electric field responsible for the effect.

Let us first consider the films on bare metals. A model based on image forces has been frequently used in the past to account for properties of films. Bosworth [11] has used it to calculate the heat of adsorption and electric moment of a H atom on an ideal metal. Besides the negative moment, he finds a positive moment at greater distance from the surface. Although the case treated by Bosworth is one of chemisorption, it might be thought that the explanation lies in that direction. However, this can hardly be so. With xenon, for instance, the image has nearly spherical symmetry. Therefore, the electric field produced in the xenon atom is negligible, and insufficient to polarize the latter appreciably.

Clearly, the electrical field responsible for the effect must be the one existing within the electric double layer at the metal surface.* A number of theoretical studies [12] have been concerned with the electric double layer but, apparently, it has not been realized that the field near the surface may be of such magnitude as to induce important electric moments in adsorbed particles.

---

[10] Couper and Eley (unpublished); cited by Eley, *Quart. Rev.*, 1949, **3**, 216.

[11] Bosworth, *Trans. Roy. Soc. N.S.W.*, 1941, **74**, 538.

[12] Mrowka and Recknagel, *Physik. Z.*, 1937, **38**, 758. Bardeen, *Physic. Rev.*, 1936, **49**, 653. Huang and Wyllie, *Proc. Physic. Soc.*, 1949, **62**, 180.

* *Added in proof:* Frost (*Trans. Electrochem. Soc.*, 1942, **82**, 259) has foreseen and briefly discussed this cause of induced polarization.

Consider a simplified model neglecting the atomic structure of the surface. There is an electric double layer at the surface, due to electrons of the metal projecting a short distance outside. The electric field H in empty space, within the double layer, is directed as shown in Fig. 4.

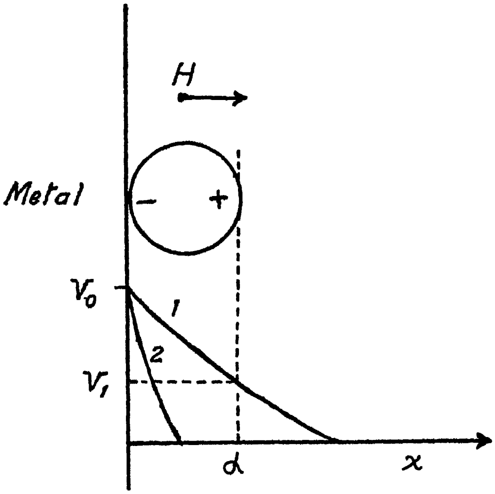

FIG. 4.

Let now a film of non-polar particles be adsorbed. The particles are polarized with the positive charge outwards. Accordingly, the surface potential of the film is positive. Thus, the model accounts for the positive sign found for the three films studied (Ni—Xe, Ni—N_2, Ni—C_2H_6). Moreover, the positive sign appears to be a property of the type of film considered here. Can the model also account for the order of magnitude? Since the characteristics of the double layer of nickel are not known, we examine that point from the experimental side. The electrostatic potential V decays rapidly with increasing distance x from the surface. Let Curves 1 and 2 represent V against x for double layers thicker and thinner respectively than the film. Knowing the surface potential v of the film, we propose to estimate V_0 (see Fig. 4) and compare it with the work function of nickel.

Let us first consider a double layer thicker than the film. Provisionally, it is assumed that the field is constant. Then $(V_0 - V_1)$ and v are defined by

$$V_0 - V_1 = Hd \quad . \quad . \quad . \quad . \quad . \quad (1)$$

$$v = 4\pi nM = 4\pi n\sigma h, \quad . \quad . \quad . \quad . \quad (2)$$

where d, M and σ are the diameter, induced electric moment and polarizability of the particles, and n is their number per unit surface. h represents the field within the film.

Hence

$$V_0 - V_1 = \frac{d}{4\pi n\sigma} \cdot \frac{H}{h} \cdot v. \quad . \quad . \quad . \quad . \quad (3)$$

The difference between h and H results from two effects, i.e. a depolarization due to the film and a polarization of the electric double layer itself by the film. The first effect is easily taken into account using, after Topping,[13] a depolarizing field given by

$$- 9Mn^{3/2}.$$

---

[13] Topping, *Proc. Roy. Soc. A*, 1927, 114, 67; see also Roberts, *Some Problems in Adsorption* (Cambridge University Press, 1936), p. 103

The second effect arises because $(V_0 - V_1)$ and H refer to the electric double layer at the bare surface. Since it is not clear at present how it could be taken into account, we neglect it and, therefore, content ourselves in determining $(V_0 - V_1)$ for the film-covered surface. With this new definition,

$$h = H - 9Mn^{3/2}, \qquad (4)$$

or

$$h = \frac{H}{1 + 9\sigma n^{3/2}}, \qquad (5)$$

since

$$M = \sigma h. \qquad (6)$$

Formula (3) becomes

$$V_0 - V_1 = \frac{1 + 9\sigma n^{3/2}}{4\pi n\sigma} \,.\, dv\,^{*} \qquad (7)$$

Hence

$$V_0 > \frac{1 + 9\sigma n^{3/2}}{4\pi n\sigma} \,.\, dv \qquad (8)$$

The same result is arrived at if the electric double layer is thinner than the film (curve 2). For, while in this case, V_0 is used completely $(V_1 = 0)$, only part of the polarizability is effective.

With the inhomogeneous field existing in the electric double layer relations (1) and (2) may still be used to define mean values of H and h, but formulae (4) and (6) are not strictly valid. It is, however, probably safe to use formula (8) as a first approximation.

Let us tentatively apply eqn. (8) to a complete xenon film on nickel for which

$$\sigma = 4 \times 10^{-24}\ \text{cm.}^3;\ d = 3{\cdot}5 \times 10^{-8}\ \text{cm.}$$

$$n = 1/d^2 = 8{\cdot}17 \times 10^{-14}\ \text{atom./cm.}^2;\ v = 0{\cdot}85\ \text{V.}$$

We get

$$V_0 > 1{\cdot}57\, v = 1{\cdot}33\ \text{V.} \qquad (9)$$

Thus we find a quite reasonable lower estimate of the strength of the electric double layer, lower—as it should be—than the work function of nickel.

In spite of the approximations made, it is felt that this result is strong evidence for the scheme developed above. In the absence of an essentially different explanation, it may be considered that the positive surface potentials found for van der Waals' films of non-polar particles on bare metallic surfaces are to be ascribed to a polarization of the adsorbed particles by the field existing in the double layer at the metal surface.

Accordingly, result (9) may be taken as experimental evidence that the electric double layer is just a few Å thick. It is clear, therefore, that the atomic structure of the surface cannot be neglected. At the moment, it is difficult to see how important structural effects may be.

Finally, a few words about double films. The results reported show important positive surface potentials for second films on negative films and small surface potentials on positive first films. The explanation seems to be somewhat as follows. Due to van der Waals' forces, the particles of the second film tend to locate themselves into depressions in the first film where they are polarized with the opposite sign. Thus, the effects produced by the metal and by the film reinforce (destroy) each other for negative (positive) first films. In the case of H_2 and N_2 on Ni—H, it seems necessary to assume a deep penetration of the second film into the substrate. Would this imply that the hydrogen atoms of the first film are on top of the nickel atoms and not in between ? This may well be so.†

---

* Consideration of a model treating the film as a dielectric leads to a result practically identical with formula (7) viz. :

$$V_0 - V_1 = \frac{\epsilon}{\epsilon - 1} v = \frac{1 + 8/3\pi\sigma n^{3/2}}{4\mu n\sigma} dv \qquad (7')$$

where ϵ is the dielectric constant of the film.

† In that case, the (110) faces may well play an important part because of the large available spaces between rows of nickel atoms, which can easily accommodate the molecules of the second film (N_2 for instance ; cp. the 20 % of surface covered at saturation, and Couper and Eley, this Discussion).

To sum up, van der Waals' films can be used to explore the electric field at the surface of metals and used to obtain information about the electrical double layer. Moreover, they may well yield information about the structure of primary pre-adsorbed films.

THE MECHANISM AND TEMPERATURE COEFFICIENT OF THE PARA-HYDROGEN CONVERSION

By E. K. Rideal and B. M. W. Trapnell

Received 2nd February, 1950

The results of a volumetric study of the chemisorption of hydrogen by evaporated tungsten films are summarized. These indicate that the probable mechanism of the parahydrogen conversion by tungsten surfaces is the condensation and re-evaporation of chemisorbed gas. The significance of the temperature coefficient of the conversion rate is discussed.

Using a tungsten filament as adsorbent, which was cleaned by flashing, and following the uptake of hydrogen volumetrically, thermally and by measurement of the change in neon accommodation coefficient on adsorption, Roberts [1] made important discoveries concerning the nature of chemisorption processes. Two of the results that he claimed have particularly influenced theories of the parahydrogen conversion and hydrogen-deuterium exchange. Firstly, that the chemisorbed layer was complete at pressures of 3×10^{-4} mm. Hg at 0° C. Secondly, that evaporation of hydrogen from the chemisorbed layer took place at an immeasurably slow rate until temperatures of over 400° C had been reached.

On the other hand, the parahydrogen conversion proceeds readily through a chemical mechanism at tungsten surfaces at room temperatures and even at liquid air temperatures.[2] Rideal [3] therefore rejected the mechanism of reaction suggested by Bonhoeffer and Farkas,[4]

$$2W + p.H_2 \rightleftharpoons 2WH \rightleftharpoons 2W + o.H_2 \quad . \quad . \quad . \quad (1)$$

and postulated that reaction proceeds through interaction of a chemisorbed atom and a molecule held by van der Waals' forces either in a second layer or in a so-called gap site [1]

$$p.H_2 + WH \rightarrow HW + o.H_2 \quad . \quad . \quad . \quad (2)$$

Later work by Eley [5] showed that deuterium, chemisorbed by an evaporated tungsten film, could exchange with gas-phase hydrogen even at 77° K. If the chemisorbed deuterium was unable to evaporate below 400° C, the exchange must have been described by eqn. (2). Eley also disproved a suggestion by Farkas [6] that the hydrogen was converted by the mechanism of eqn. (1), but only on a very small number of lattice sites, too few to be detected by Roberts' technique.

---

[1] Roberts, *Proc. Roy. Soc. A*, 1935, **152**, 445.
[2] Eley and Rideal, *ibid.*, 1941, **178**, 429.
[3] Rideal, *Proc. Camb. Phil. Soc.*, 1939, **35**, 130.
[4] Bonhoeffer and Farkas, *Z. Physik. Chem. B*, 1931, **12**, 231.
[5] Eley, *Proc. Roy. Soc. A*, 1941, **178**, 452.
[6] Farkas, *Trans. Faraday Soc.*, 1939, **35**, 943.

Roberts,[1] and Beeck[7] who has as a result of a study of the adsorption by evaporated films reached similar conclusions to those of Roberts, agree that the heat of chemisorption can fall to values of about 15,000 cal. as the layer becomes more densely packed. For such heats, a measure of reversibility for the adsorption would be expected at room temperatures; irreversibility up to 400° C, as Roberts claimed, would certainly not be expected. Moreover, reflection shows that Roberts' statement that the adsorbed layer only became complete at the finite pressure of 3×10^{-4} mm. at room temperatures itself implies that the adsorption is to a degree reversible under these conditions.

It was therefore decided to investigate the adsorption volumetrically using evaporated metal films to decide under what circumstances and to what extent the chemisorption is reversible, and to consider how the present views of the parahydrogen conversion and hydrogen deuterium exchange would have to be modified.

The Chemisorption of Hydrogen by Evaporated Tungsten Films.—The experimental study covers the temperature range 0° C to − 183° C and has been made at pressures up to 10^{-2} mm. It will form the substance of a forthcoming publication, and has given the following results.

(i) For smaller adsorbed amounts, the equilibrium gas pressure is immeasurably low, as found by Roberts. When, however, the adsorbed layer has passed a certain density of packing, the equilibrium pressure rises to sensible values, so that reversible adsorptions are observed, with isothermal heats falling from 14,000 cal. to some 3,000 cal. for the largest adsorbed amounts. Heats of van der Waals' adsorption of hydrogen do not seem to exceed 2,000 cal., so that these adsorptions must be of the chemical type.

(ii) Confirmation of this conclusion was obtained in the following manner. Areas of evaporated metal films may be controlled and repeated, and determination of the area of a given film type has been made by measurement of both the oxygen and carbon monoxide chemisorptions. The relative amounts of oxygen chemisorption, carbon monoxide chemisorption and saturation hydrogen adsorption on films of equal area have been found to be very nearly 1/2/1. This is taken as proof that the reversible hydrogen adsorptions described above essentially refer to a first-layer process, and are chemisorptions.

(iii) From the results, rough values of fractional surface coverages under various conditions of temperature and pressure have been obtained. These are plotted as isotherms in Fig. 1. It is seen that the coverage varies extremely slowly with temperature and pressure. This is believed to be the reason for Roberts' failure to detect these phenomena with his accommodation coefficient technique.

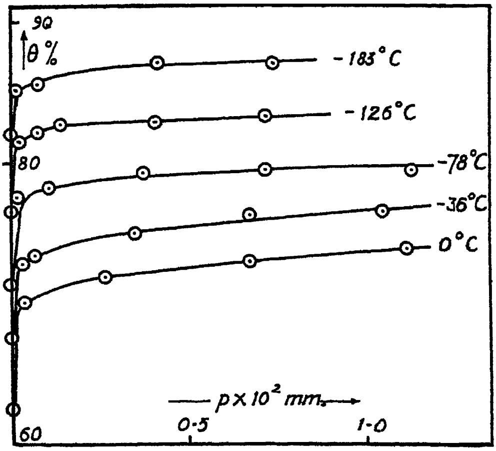

FIG. 1.

---

[7] Beeck, *Rev. Mod. Physics*, 1945, 17, 61.

The Mechanism of the Parahydrogen Conversion at Tungsten Surfaces.—The heat of adsorption of the process

$$2\text{W} + \text{H}_2 \rightarrow 2\text{WH}$$

falls to far lower values than hitherto believed, so that the adsorption is partly reversible, even at − 183° C. This result caused us to reconsider the mechanism of the parahydrogen conversion.

The kinetics of the conversion have been investigated in detail by Eley and Rideal.[2] The features are as follows:

(i) The energy of activation, as measured by a temperature coefficient of reaction velocity, is low. Reported values vary between 1,000 and 3,800 cal., the average value of those obtained by Eley and Rideal being 1,950 cal.

(ii) The conversion at constant volume is always first order.

(iii) Representing the rate of reaction as kp, k is found to depend on pressure, and between − 78° C and − 100° C and at pressures between 1 and 20 mm.,

$$kp = \text{const. } p^n,$$

where n varies between 0·1 and 0·5.

(iv) At pressures around 1 mm., and between 0° C and − 196° C, the number of molecules reacting per second per sq. cm. of catalyst

$$= 2{\cdot}6 \times 10^{20} e^{-E/RT}.$$

These characteristics of the reaction may then be calculated from the adsorption data, assuming the mechanism of eqn. (1), and compared with the experimental values. Now the adsorbed layer is mobile in the presence of a finite equilibrium gas pressure if only because molecules are continually evaporating and condensing, thereby enabling the pattern of the adsorbed phase to alter and achieve a state of minimum energy. In this case, the expression for the rate of condensation of molecular hydrogen as atoms on pairs of adjacent sites is given[8] by the expression

$$R = \alpha p/\sqrt{2\pi mkT}\,.\frac{(1-\theta)}{1+\epsilon}, \qquad (3)$$

where θ is the fractional surface coverage, α the condensation coefficient and ϵ is given by the equation

$$\frac{\theta}{1-\theta} = \frac{\epsilon(1+\eta\epsilon)}{1+\epsilon},$$

$$\text{where} \qquad \eta = e^{-V/RT},$$

V being the energy of repulsion of atoms adsorbed on adjacent sites. Assuming the mechanism of eqn. (1) to be correct, the rate of conversion can then be calculated from the rate of condensation, and using Lennard-Jones and Devonshire's[9] value of 0·3 for the condensation coefficient, and a value 1200 cal. for V, it is found that

(i) the temperature coefficient of the condensation rate gives an activation energy of some 1800 cal.;

(ii) the order at constant volume is unity, and at varying pressures less than unity;

(iii) the calculated absolute rate of conversion agrees with the experimental.

These results make it probable that the conversion proceeds by the path of eqn. (1)

---

[8] Peierls, *Proc. Camb. Phil. Soc.*, 1936, **32**, 471.

[9] Lennard-Jones and Devonshire, *Proc. Roy. Soc. A*, 1936, **156**, 6.

Experiments performed with evaporated nickel films have shown that the adsorption of hydrogen is very similar to that described for tungsten, the equilibrium gas pressure being appreciable when the surface coverage exceeds a certain value at room temperatures and below. Calorimetric work by Beebe and his collaborators [10, 11] has yielded a similar result for the surfaces of iron and of chromic oxide, for hydrogen is chemisorbed on both with a heat change of some 5000 cal. With these catalysts it may be concluded that the parahydrogen conversion and hydrogen deuterium exchange may also proceed by the condensation and re-evaporation of chemisorbed hydrogen, and it is probable that the mechanism will prove to be general.

The Temperature Coefficient of Velocity of the Conversion.—The activation energy of adsorption is at most a few hundred calories. The activation energy of desorption is therefore effectively equal to the heat of adsorption. On the basis of eqn. (1) the true energy of activation of the conversion must hence be the heat of adsorption. This is very much greater than that derived from a measurement of the temperature coefficient of the velocity of the conversion. For example, under conditions where the heat of adsorption is 11,000 cal., the activation energy derived from the temperature coefficient is only 16 % of this figure.

Now, the temperature coefficient of reaction is, from eqn. (3),

$$\sqrt{T_2/T_1} \,.\, (1 - \theta_1) \,.\, (1 + \epsilon_2)/(1 - \theta_2) \,.\, (1 + \epsilon_1)$$

where the suffixes 1 and 2 refer to the two temperatures of measurement. The temperature coefficient therefore gives an apparent energy E which is determined by the change of θ with T, and as indicated in Fig. 1, this is very small. The reason is that in the particular region of surface coverage studied, the heat of adsorption is falling very rapidly as the surface fills. This may be seen in a general way by the following consideration. Imagine a surface 70 % covered by an adsorbate under given conditions of temperature and pressure, and then let its temperature be lowered. If the heat of adsorption ΔH is independent of surface coverage, let the drop in temperature increase the surface coverage to 80 %. If, however, the heat falls very rapidly with increasing coverage, cooling the adsorbate, though causing condensation of gas, will cause less than in the above case as the condensation itself has the effect of weakening the binding of the adsorbate. The coverage will therefore not increase to such a high value as 80 %. This is what is happening in the above case, and is responsible for the great disparity between E and ΔH. E has no relation to the true activation energy, being determined by the manner ΔH changes with increasing θ. It is certainly no measure of catalytic power.

The following two points arise from these considerations.

(i) The activation energy of a heterogeneous reaction is invariably obtained from a temperature coefficient of velocity at constant pressure. It has been shown the figure derived in this way may be quite unrelated to the energetics of the surface processes involved in reaction. A true energy of activation is only definitely obtained if the temperature coefficient is measured at constant surface coverage of reactants, and this is not, of course, experimentally attainable.

(ii) Smith and Taylor [12] have measured the quantity E at different temperature ranges of working on zinc oxide surfaces, and have found considerable variations. Between 143 and 178° K, E has the value 600 cal. In the range 195 to 373° K, E is roughly constant, but with the value 7000 ± 2000 cal. Above 373° K it is larger, and except for the interval 405 to 430° K, where $E = 0$, has the rough value 12,000 cal.

[10] Beebe and Dowden, *J. Amer. Chem. Soc.*, 1938, **60**, 2912.

[11] Beebe and Stevens, *ibid.*, 1940, **62**, 2134.

[12] Smith and Taylor, *ibid.*, 1938, **60**, 362.

These results were cited as proof of the marked heterogeneity of the surface for chemisorption. The above analysis shows that the results may be due to varying rates of fall in θ with increasing temperature, and it must first be decided whether these differences, and the differing rates of change of ΔH with θ which they indicate, require the concept of a non-uniform surface.

The Royal Institution,
21 Albemarle Street,
London, W.1.

HYDROGENATION CATALYSTS

By O. Beeck

Received 7th February, 1950

The rate of the hydrogenation of ethylene over evaporated porous metal films of the transition elements is strongly depending on the heat of adsorption of ethylene, which (except for much higher absolute values) parallels that of hydrogen. When plotted against the *d*-character of the metallic single bond (Pauling), both the heats of adsorption of ethylene (or hydrogen) and the rates of hydrogenation fall on smooth curves, such that the greater the *d*-character, the lower are the heats of adsorption and the higher the rates. Since the *d*-character is closely related to the atomic distances in the crystal lattice, especially in Group VIII elements, the dependence of catalytic activity on crystal parameter is largely, but not solely, a consequence of the nature of the metallic bond.

The following mechanism for the hydrogenation is suggested. Depending on the heat of adsorption for ethylene, initial irreversible poisoning by acetylenic adsorption complexes, formed by self-hydrogenation of ethylene, renders the surface more or less inactive for hydrogenation. On the remaining part of the surface the overall rate of reaction is determined by the reaction of adsorbed ethylene (non-dissociative) with adsorbed hydrogen with an apparent activation energy of 10·7 kcal. for metals of Group VIII. Strong evidence is presented that a third type of a fast reaction with low activation energy is also involved. This reaction is thought not to necessitate empty crystallographic sites for the separate adsorption of ethylene, but of being able to form the activated state on a surface already covered with hydrogen.

Related phenomena, such as the cracking of ethane in the presence of hydrogen, the hydrogenation of acetylene, and the reaction of preadsorbed ethylene and acetylene with hydrogen, are also discussed.

A systematic study of the catalytic hydrogenation of ethylene and other hydrocarbons on evaporated porous metal films has been carried out by the author and his collaborators during the past years. The experimental observations, which are briefly reviewed and discussed here, illustrate the surprising complexity of this apparently simple reaction, and demonstrate the difficulty of arriving at any simple theory of catalytic activity in terms of any one kinetic scheme or any one property of the catalyst surface. It will be shown how chemical properties (electronic configuration) and the resultant physical properties (crystal parameter) of the catalyst surface influence the rate of reaction.

Earlier results published by Beeck, Wheeler and Smith [1] with oriented and unoriented films suggested that the (110) plane is much more active as a catalyst for this reaction than any other simple plane of metallic nickel. Direct calorimetric measurements of the heats of adsorption have also been made.[2]

---

[1] Beeck, Smith and Wheeler, *Proc. Roy. Soc. A*, 1940, 177, 62.

Recently, new and direct experimental proof was obtained by Beeck and Ritchie[3] that gas evaporated nickel films, showing (110) orientation parallel to the backing, actually expose (110) planes to the gas phase. By determining the surface through low-temperature adsorption using the B.E.T. method and dividing the surface area obtained by the number of hydrogen atoms adsorbed on the same surface, the crystallographic site of the oriented film was found to be 8·65 Å^2 in surprisingly good agreement with the X-ray value of 8·70 Å^2. Correspondingly the area of the site of unoriented films was found to be 6·17 Å^2 which again agrees well with the X-ray value for the (100) plane of 6·15 Å^2. The latter agreement may be fortuitous, however, since the average size of the three major planes is 5·84 Å^2, very close to the value for the (100) plane. If, therefore, a number of planes along the cube edges were (110) planes and another number at the corners were (111) planes, an overall value close to that of the (100) plane would be expected.

Beeck, Wheeler and Smith[1] have found that (110) oriented nickel films have at least five times the specific activity of oriented films for the hydrogenation of ethylene. In continuation of this work it was of great interest to investigate how far crystal geometry considerations could be used to explain the greatly different activities of other metals for this reaction. It was expected that metals with different chemical properties would show differences in activity for reasons of their specific electronic configurations which in turn must be related to the crystal geometry in the sense that the former is the cause of the latter; This statement needs the further qualification that the catalyst must be able to chemisorb hydrogen and that in the absence of this prerequisite crystal geometry considerations become meaningless. (Pure copper, for instance, will not chemisorb hydrogen although its crystal parameter is very close to that of nickel; it also will not produce porous films except when evaporated at very low temperature.) Aside from these considerations, however, the distance at which two hydrogen atoms are chemisorbed should in itself for purely geometrical reasons affect the rate at which hydrogen is adsorbed and the rate at which the ethylene molecule picks up two hydrogen atoms from the surface especially if this reaction takes place without the adsorption of ethylene itself as will become apparent later.

Beeck and Wheeler investigated the rate of hydrogenation of ethylene over evaporated films of iron, platinum, palladium, rhodium, chromium, tungsten and tantalum, in addition to nickel. The results of this investigation have been published already in a preliminary report by Beeck[4] in which Fig. 5 shows the logarithm (used merely to accommodate the data) of the specific velocity constant against the crystal parameter of the various metals investigated. A smooth curve was obtained showing a maximum for rhodium at 3·75 Å, this metal being several hundred times more active than nickel and 10^4 times more active than tungsten, based on the same hydrogen adsorption.

In order to investigate the influence of the electronic structure of the different metals, Beeck, Cole and Wheeler[2] measured the heats of adsorption of hydrogen and ethylene (and other gases) on evaporated metal films. Of immediate interest is a comparison of oriented and unoriented nickel films. The results of this investigation have been briefly reported in Fig. 6 and 7,[4] and Fig. 14,[5] and are also shown in Fig. 1 of this paper without the experimental points. The heats of adsorption at 23° C for both hydrogen and ethylene are the same for the two film types (with perhaps the heat of adsorption of hydrogen on oriented films 2 to 3 % greater than on unoriented films). The heat of adsorption of hydrogen is 31 kcal. for the sparsely covered surface and decreases to 15 kcal. for the completely covered surface. The conclusion was reached that this decrease is due to interaction of adsorbed atoms via the crystal lattice and that hydrogen atoms are mobile at 23° C in the sense that they can easily migrate from site to site, except perhaps for tungsten where mobility seems to be somewhat impaired. At − 183° C hydrogen is still mobile on nickel and is adsorbed with the same heat of adsorption as at room temperature, while on iron at − 183° C it is immobile, with a constant incremental heat of adsorption (average value of the heat of adsorption at 23° C) which drops to very low values when the surface is completely covered. For further information the reader is referred to ref. 5 where the adsorption of hydrogen on metal films is discussed in great detail.

---

[2] Beeck, Cole and Wheeler, this Discussion.

[3] Beeck and Ritchie, this Discussion.

[4] Beeck, *Rev. Mod. Physics*, 1945, **17**, 61.

[5] Beeck, *Advances in Catalysis*, Vol. II (Academic Press, New York, 1950).

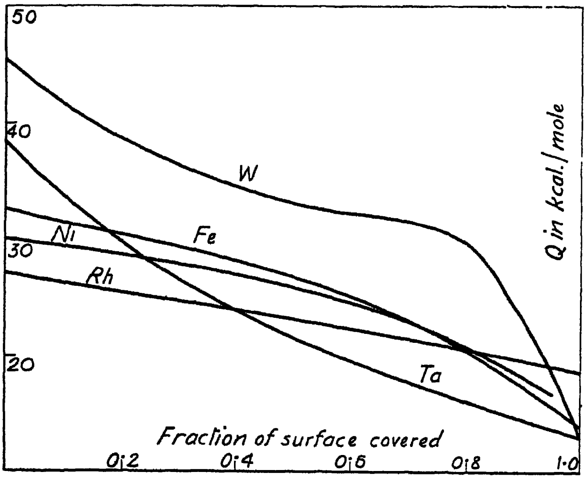

FIG. 1.—Heats of adsorption of hydrogen. *

The heat of adsorption of ethylene at 23° C decreases rapidly from 58 kcal. to lower values with increasing adsorption. When ethylene is adsorbed at 23° C, only about 5 × 10^{18} molecules per 100 mg. of unoriented film (to be multiplied by 2 for oriented films) will be adsorbed practically instantaneously and irreversibly. On addition of more ethylene, ethane will appear in the gas phase and when 12·5 × 10^{18} molecules are adsorbed the same number of ethane molecules will be in the gas phase, leaving an adsorbate of acetylenic nature on the surface. This process is still very fast, in agreement with the immeasurably fast rate when adsorbed hydrogen reacts with ethylene from the gas phase. Apparently ethylene adsorption leads to dissociation of the ethylene molecule into two hydrogen atoms and an acetylenic residue, which, however, as will be mentioned later, does not behave like acetylene itself. Upon adding more ethylene the process of self-hydrogenation will proceed more slowly, and the composition of the adsorbate for very large admissions (80 × 10^{18} molecules per 100 mg.) becomes $C_nH_{0\cdot4n}$. The molecules in the adsorbate also polymerize, as will be discussed later.

Fig. 1 shows the heats of adsorption of hydrogen on Rh, Ni, Fe and W as a function of fraction of surface covered where the adsorption at

---

* Subsequent re-evaluation has shown that the initial value for Ta is likely to be at least as high as that for W— see also Fig. 3.

0·1 mm. pressure is taken to represent total coverage. Tantalum showed strong exothermic absorption into the structure, with 860 × 10^{18} molecules of hydrogen adsorbed and absorbed at 1·3 mm. The original curve for tantalum shows a clear break where adsorption is complete and this point was used for complete coverage. Fig. 2 shows the heats of adsorption of ethylene as a function of number of molecules adsorbed for 100 mg. of film. All films were high vacuum evaporated.

An especially careful study was made of the rate of reaction and of reaction products when hydrogen from the gas phase reacts with ethylene that is pre-adsorbed on oriented and unoriented nickel films. Reaction rates and products are identical for both types of film. At 23° C, 20 % of the adsorbed residue can be reacted off in 1 hr. The product is about 90 % saturated polymers (C_4 to C_8 and higher) and 10 % ethane. Similar experiments with rhodium at 23° C yield 60 % of the adsorbate in 1 min. (and nearly 100 % with long contact times), the product being primarily ethane with only a few per cent. polymer.

When ethylene is pre-adsorbed on nickel, the initial rate of hydrogenation at 0° C is decreased by 60 %; when pre-adsorbed on tantalum or tungsten the rate is decreased by factors of ten and five, respectively; however, a decrease of only a few per cent. is noted when ethylene is pre-adsorbed on rhodium or platinum. Pre-adsorbed acetylene cannot be hydrogenated off nickel at 23° C but 40 % of pre-adsorbed acetylene can be hydrogenated off rhodium in 1 hr.

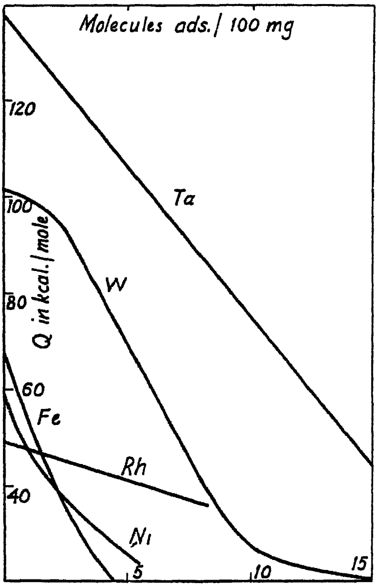

FIG. 2.—Heats of adsorption of ethylene.

It has been shown in ref. 4 (p. 69, Fig. 9) that the apparent activation energy for the hydrogenation of ethylene over nickel films is 10·7 kcal. and identical for (110) oriented and non-oriented films, although the activity of the former is at least 5 times that of the latter. In the figure referred to, the rate values for the two film types were adjusted to be identical at 0° C for easy comparison. It is of particular interest that the activation energy for the same reaction over rhodium was found to be 10·7 kcal. also, although the rate over this metal is several hundred times faster than over nickel. In contrast to this, the activation energy over tungsten was found to be only 2·4 kcal. although the rate over tungsten is 20 times lower than over non-oriented nickel. However, the initial rate over tungsten when an equal molar gas mixture is admitted is 10 times faster than the final rate which is strictly first order and which was used for comparison with other metals. The initial rate (about 20-30 sec. after admitting the gas mixture) was therefore 0·1 times that of non-oriented nickel films. Tantalum is similar in its behaviour.

Another series of experiments (Beeck, Ritchie and Wheeler) was concerned with the cracking of ethane on evaporated metal films at about 200-250° C. If pure ethane is admitted to a nickel film, the rate of this reaction decreases to zero within a short time with only a very small amount of the ethane having reacted. With equal molar mixtures of ethane and hydrogen the reaction $C_2H_6 + H_2 \rightarrow 2CH_4$ proceeds on nickel with zero order and an activation energy of 48·4 kcal. The rate is 6 times faster on (110) oriented than on unoriented nickel films. The rate over rhodium is 60,000 times faster than over unoriented nickel films. If residues are formed on both nickel and rhodium by admitting ethane to the films at 225° C, these residues can be removed by hydrogen from the gas phase with methane formation only, the rate being much faster in the case of rhodium. Residues thus formed cannot be removed by hydrogen at 23° C, except for a very small amount of methane formation in case of rhodium. If residues formed on both metals at 23° C are heated to 225° C, hydrogen and a little methane evaporate from the nickel film and methane with a little hydrogen evaporate from the rhodium film. When the remaining residues are contacted with hydrogen at 225° C, methane only is formed.

Some experiments were also carried out (Beeck and Ritchie) to investigate the influence of crystal geometry on benzene hydrogenation and cyclohexane dehydrogenation. Both oriented and unoriented nickel films were equally active for the benzene hydrogenation at 58° C. The rates were very low (independent of the benzene pressure and proportional to the 0·44th power of hydrogen pressure) and hydrogenation proceeds most likely through the adsorbed state of benzene. The apparent activation energy was 8·7 kcal. Nickel was found to be 2·3 times more active than iron.

Cyclohexane dehydrogenation proceeds fast at 325° C over unoriented platinum films, partially (110) oriented films being 10 times less active. An activation of 9·3 kcal. was found for this reaction, which in its first half is first order with respect to cyclohexane but is increasingly poisoned by benzene in the second half.

Beeck and Wheeler have also carried out experiments on acetylene hydrogenation with the result that iron and tungsten were found to be inactive at 23° C; nickel was mildly active (2×10^2 to 2×10^3 less active than for ethylene hydrogenation), rhodium and platinum were 10 times more active than nickel, and palladium 20 times more active. Maximum activity is found for palladium and not for rhodium as in the case of ethylene. The activation energy for acetylene hydrogenation on all four metals was 6 to 7 kcal. A thorough kinetic study was made of the acetylene hydrogenation also in the presence of ethylene where selective hydrogenation of acetylene takes place.

Discussion.—It has been suggested already (Beeck [4]) that the overall rate of hydrogenation is proportional to the fraction of surface not covered by adsorbed ethylene and to the ethylene pressure itself. This not only accounts for the observed kinetics:

$$\frac{dp_{C_2H_4}}{dt} = kp_{C_2H_4}\frac{p_{H_2}}{p_{C_2H_4}} = kp_{H_2},$$

but offers a satisfactory explanation for all other experimental facts. According to this mechanism the fast process is the reaction of adsorbed hydrogen with ethylene from the gas phase without adsorption of the ethylene itself. The high rate of this process is substantiated by the experimental fact that the reaction of pre-adsorbed hydrogen with ethylene at very low pressure and at − 79° C is practically instantaneous. At this temperature ethylene does not self-hydrogenate. The slow and rate-determining process is the removal of adsorbed ethylene from the surface by hydrogenation with adsorbed hydrogen. The rate of this reaction will, under steady state conditions, determine the surface available for the fast reaction. The initial step of poisoning the surface with ethylene proceeds most likely through the adsorption of ethylene on two crystallographic sites but does not lead to formation of acetylenic complexes except when four adjacent sites are empty to accommodate the two hydrogen atoms. The heat of adsorption of ethylene on two sites is not directly known but must be relatively low, perhaps of the order of 10 to 15 kcal. The heat of adsorption of hydrogen on a well-covered surface may be taken as 15 to 20 kcal. Reaction between the two reactants with an activation energy of 10·7 kcal. may reasonably be expected. Once ethylene adsorption has led to the formation of acetylenic complexes and to polymerization, the surface is irreversibly poisoned since the rate of removal of these materials by hydrogen was found to be very low. This explains why surfaces initially contacted with ethylene (and successive runs over the same catalyst) have lower activities. In the case of tungsten with its high heat of adsorption for ethylene the poisoning process is actually observable and proceeds apparently to a point where the formation of acetylenic complexes becomes impossible due to the fact that four adjacent sites are no longer available. Under these conditions the surface available becomes constant and the rate of removal of adsorbed ethylene is no longer rate determining. The rate is now primarily determined by the fast reaction of adsorbed hydrogen with ethylene from the gas phase. The low activation energy of the fast reaction should therefore prevail. An intermediate stage must, of course, be expected. This mechanism not only explains satisfactorily the low activation energy of the slow reaction on tungsten but also represents an indirect proof for existence of the fast hydrogenation reaction.

In order to explain the (at least) five-fold activity (based on the same hydrogen adsorption) of (110) oriented nickel films over unoriented films, both having the same activation energy, it must either be concluded that the rate-determining surface reaction between adsorbed hydrogen and adsorbed ethylene has a higher frequency factor for geometrical reasons or that the fraction of surface initially poisoned by acetylenic complexes and polymers is larger for unoriented films due to the higher metal atom density in the surface of these films, which may facilitate the formation of these complexes and of polymers. It is possible, of course, that both factors are involved. However, the latter factor, i.e. the formation of acetylenic complexes and polymer formation, seems to outweigh the former when different metals are compared since it was shown that the heats of adsorption of ethylene differ largely, rhodium having the lowest heat, the least polymer formation, and the fastest rate for removal of adsorbed residues by hydrogen. In fact, if the specific activities of the different metals studied are plotted against the heats of adsorption of either hydrogen or ethylene (Figs. 1 and 2), it is seen that the lower the heats of adsorption, the higher are the activities.

The tenfold activity for the dehydrogenation of cyclohexane by unoriented platinum films in comparison with partially (110) oriented films could be explained on geometrical grounds following the hypothesis of Balandin,[5] according to which the simultaneous removal of 6 hydrogen atoms from the cyclohexane molecule is facilitated by the octahedral faces (111 planes) of face-centred cubic lattices. It appears likely that the influence of surface geometry should be particularly large for this reaction and the observed kinetics favour the dehydrogenation reaction proper to be rate determining.

The six-fold activity of (110) oriented nickel films for the cracking of ethane in the presence of hydrogen at 225° C in comparison to unoriented films is of particular interest since in this zero-order reaction the rate must be determined by the formation of methane on the surface from radicals produced by ethane. The activation energy for hydrogenation of these radicals, which is equal to that of the over-all reaction, was found to be about 48 kcal., almost five times greater than the activation energy for the removal of adsorbed ethylene. This shows clearly that ethylene cannot have been adsorbed as a true radical but has formed partial bonds only. This conclusion is in agreement with the fact that acetylenic complexes formed by the adsorption of ethylene behave chemically differently from adsorbed acetylene. It does not seem likely that the rate of methane formation from a singly-bonded radical should be increased materially by the wider spacing in the (110) plane especially since the

(110) plane is the plane of highest surface energy (although this is only borne out by a marginal increase of the heat of adsorption of hydrogen, almost within the limits of experimental error). Conversely it will be more difficult to remove CH_2, CH and C radicals from the denser planes since multiple bonds of carbon with the metal atoms in the surface are more likely to be formed, which would lead to a preferential poisoning of unoriented films.

It is of interest to note that palladium is more active for the hydrogenation of acetylene than rhodium, although the reverse is true for ethylene. In this case the geometrical factor seems to outweigh the over-all heat of adsorption picture, probably because the bond-forming character of the two metals is very nearly the same.

It has been pointed out repeatedly by the author that geometric considerations are meaningless in catalysis unless the prerequisite of adsorption is fulfilled. However, if the surface is capable of making chemical bonds with the adsorbate, the distance of the atoms in the surface must influence the activation energy in cases such as the adsorptive dissociation of hydrogen,[6, 7, 8] the hydrogenation of the double bond, polymerization on the surface, etc. Both hydrogen adsorption and hydrogenation of gas phase ethylene by adsorbed hydrogen have extremely low activation energies and are not rate determining. Small differences in heat of adsorption of hydrogen cannot therefore influence the rates. Rate determining in the broadest sense is the poisoning of the surface by adsorbed ethylene and its degradation products. This poisoning depends in general on the ability of the metal surface to make strong bonds with carbon. The simplest and most direct way to measure the energy of these bonds is by measuring the heats of adsorption of the ethylene or acetylene. Fig. 2 shows how the heat of adsorption increases from rhodium to tantalum, this increase corresponding to a decrease in catalytic activity by a factor 10^4. The heats of adsorption of hydrogen and ethylene on chromium (not shown in the Figures) are almost identical with those for tungsten and correspondingly the catalytic activities are nearly the same. This is of interest because chromium, which has a lattice spacing almost identical to one of the spacings in iron, did not fall on the smooth curve of activity against lattice distance (ref. 4 Fig. 5) showing clearly that the nature of the chemical bond can outweigh completely any geometrical effect. The apparent correlation of catalytic activity with the interatomic spacing of different metals may well arise from two causes, of which the electronic configuration is the more important one and is reflected by the crystal parameters of the metals. The geometrical factors can outweigh the purely chemical factors, however, when different planes of the same metal are considered, in which case the resulting differences in chemical bonding of the adsorbate on the surface have their cause in crystal geometry.

The next step in any attempt to further elucidate the phenomenon of heterogeneous catalysis must involve the correlation of heats of adsorption (strength of surface bonds) with the nature of the chemical bond in metals, intermetallic compounds, oxides, etc. This was pointed out appropriately in a recent note[9] where work by Dowden and Reynolds, Eley, Maxted, and Anderson is briefly reported. In the absence of a general theoretical picture of surface states, Beeck *et al.* (this work was started in 1940) have preferred to measure heats of adsorption rather than to derive them from theoretical considerations, although the time is probably ripe now to do both, as the encouraging results reported[9] would indicate, both in the light of the older band theory of metals and in the newer resonating-valence-bond theory (Pauling). According to

[6] Belandin, *Z. physik. Chem. B*, 1929, **2**, 289; 1929, **3**, 167.

[7] Sherman and Eyring, *J. Amer. Chem. Soc.*, 1932, **54**, 2661.

[8] Okamoto, Horiuti and Hirota, *Sci. Pap. Inst. Phys. Chem. Res., Tokyo*, 1936, **29**, 223.

[9] *Nature*, 1949, **164**, 50.

Pauling,[10] the number of empty atomic orbitals decreases as the *d*-band is filled. Assuming that the surface states are, qualitatively at least, related to the electron configuration of the bulk of the metal, one may expect that metals with a large *d*-character of their metallic bond will have less orbitals available for bonding with the adsorbate than those with a small *d*-character. This is borne out by the measured heats of adsorption of hydrogen and especially of ethylene on the series of metals investigated where the heat of adsorption decreases with the increasing *d*-character of the bond. This was correctly anticipated by Dowden and Reynolds[9] and was independently and indirectly suggested by Boudart,[11] who relates the *d*-character of the metallic bond directly to the activities reported by Beeck *et al.*[4] without having had knowledge of the correlation between activity and heats of adsorption of ethylene first reported in this paper. The discrepancy in the relation of *d*-character and activity which Boudart points out for tungsten does not apply, however, to the heats of adsorption measurements which were shown in this paper to be almost identical for tungsten and chromium.

The short report,[9] as well as a more recent letter by Couper and Eley,[12] takes the view of minimizing the importance of crystal parameter considerations. While this is possibly true for the ortho-para hydrogen conversion (if adsorption of the hydrogen molecule by a single surface atom of palladium is sufficient for this conversion), the crystal parameter can certainly not be neglected when dissociation (or partial dissociation) of a hydrogen molecule through a two-point adsorption is an apparently necessary prerequisite for hydrogenation at low temperature.

It was pointed out[1] already in 1940 that pure copper films do not adsorb hydrogen at − 183° C (at which temperature they could be prepared with a large surface) and do not show any activity at room temperature or higher unless they were prepared by evaporation in hydrogen at − 183° C, and then only to the extent of 10^{-6} of the activity of nickel films for the same weight. This was taken as proof that pure copper does not chemisorb hydrogen. It is quite plausible therefore that if copper and nickel atoms were to occupy alternate positions in the surface lattice, the dissociative adsorption of hydrogen could be impaired. If in addition the valency electrons of copper fill up the holes in the 3*d*-band of nickel, both processes may have to be considered simultaneously, and this may well be the reason why in the work of Dowden and Reynolds[9] 30 to 40 atomic per cent. of copper decrease the activity of the copper-nickel alloy to very low values while the magnetic measurements show that 60 atomic per cent. are necessary to fill up the 3*d*-band of nickel. Such considerations are of course not necessary when activation through the formation of a singly-bonded activated complex is sufficient as for instance in the isomerization and deuterium exchange of hydrocarbons catalyzed by aluminium chloride or bromide, or sulphuric acid[13] where the activated complex (carbonium ion type) is formed by a single bond.

A good indication that even hydrogen atoms are using *d*-character bond energy for adsorption on metals is shown by the decrease of heats of adsorption as a function of fraction of surface covered, especially with metals which have metallic bonds of a low *d*-character. The hydrogen bonding energy and the bonding energy in general of these metal surfaces can be lowered substantially by pre-adsorption of nitrogen. Such a " nitrided " surface is in principle equivalent to an intermetallic compound or alloy but is more easily prepared with evaporated metal films. As an example, Fig. 3 in the paper by Beeck *et al.*[14] shows the heat of adsorption at room temperature of nitrogen on tantalum and the heat of adsorption of hydrogen on a nitrogen-covered surface. The initial heat of adsorption of hydrogen on the nitrogen-covered surface (27 kcal.) can be compared with that of pure tantalum in Fig. 1 of the same paper (45 kcal.).

---

[10] *Proc. Roy. Soc. A*, 1949, **196**, 343.

[11] *J. Amer. Chem. Soc.* (in press).

[12] *Nature*, 1949, **164**, 578.

[13] Beeck, Otvos, Stevenson and Wagner, *J. Chem. Physics*, 1949, **17**, 418 and 419; 1948, **16**, 225 and 745.

[14] This Discussion.

Shell Development Company,
Emeryville,
California.

ADDENDUM.—Additional Figures (3 to 8) were presented at the Discussion. Fig. 4 and 5 show the heats of adsorption (initial heats, sparsely covered surface) for ethylene and hydrogen respectively plotted against the logarithm of the velocity constant of the hydrogenation reaction. Of particular interest is the large increase in rate from iron to rhodium for the relatively small decrease in heat of adsorption. This fact is borne out more strongly when the heats of adsorption of ethylene are plotted against % *d*-character of the metallic single bond (Fig. 5). Noteworthy is the fact that a much smoother curve is obtained in this correlation as well as in the plot of % *d*-character against log *k* shown in Fig. 7. The value for tungsten shown in the Figure refers to the usually body-centred cubic structure ($a = 3{\cdot}15$ Å), whereas tungsten evaporated on to a cold surface will crystallize in a face-centred cubic form [15] ($a = 4{\cdot}17$ Å). This consideration brings the points for tungsten in Fig. 6 and 7 back on the curve. Of further interest is the fact that the point for oriented nickel falls definitely outside the smooth curve, indicating that this parameter effect is a purely geometrical one, especially since the *d*-character of the metallic bonds of the surface atoms could not be larger in this plane, but only smaller, a fact that is borne out by the slightly higher heats of adsorption for hydrogen on the (110) plane. Since the *d*-character of the metallic bond is closely associated with the distance between nearest neighbours (especially in Group VIII elements), it is not surprising that a plot of log *k* of the hydrogenation reaction against crystal parameter (the long distances were chosen since they appear to be operative in this reaction for geometrical reasons) reflects both the measured heats of adsorption (total bond energies) as well as the % *d*-character as shown in Fig. 8, where the % *d*-character value for tungsten falls actually on the curve as explained above.

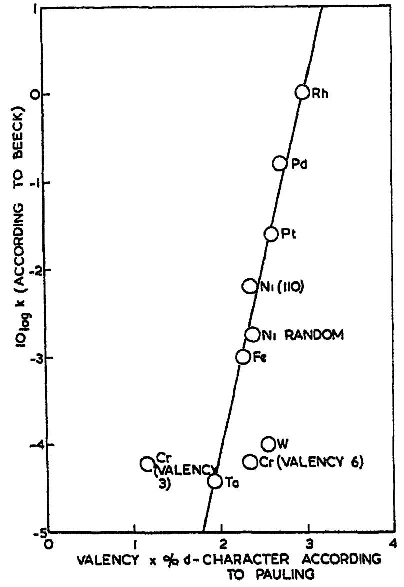

FIG. 3.

A further interesting correlation was suggested by Dr. G. C. A. Schuit of the Koninklijke/Shell-Laboratorium, Amsterdam, in this Discussion.

---

[15] Private communication by F. H. Horn, General Electric Co., Schenectady.

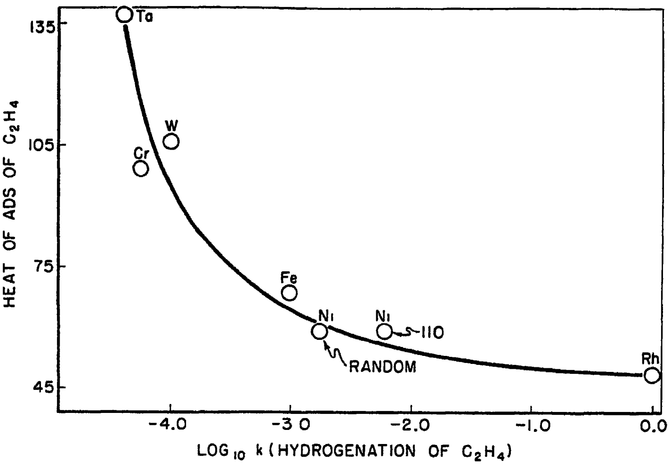

FIG. 4.

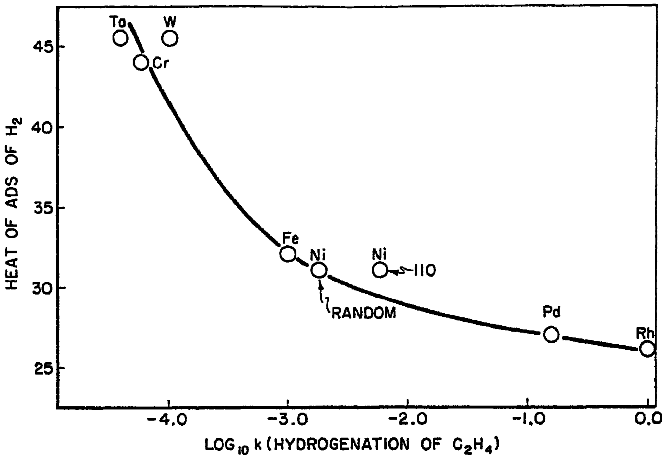

FIG. 5.

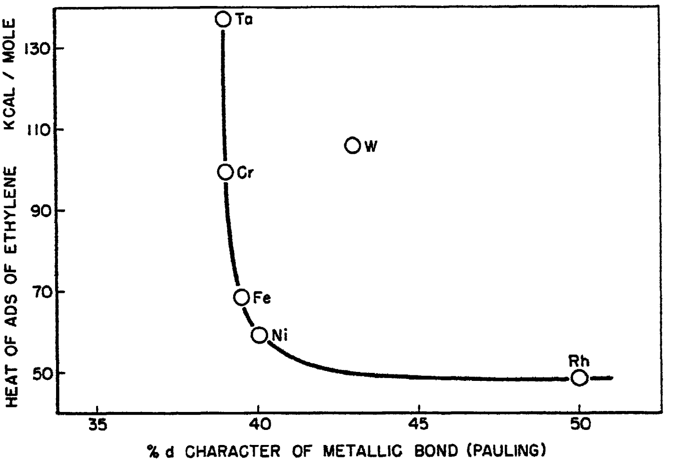

FIG. 6.

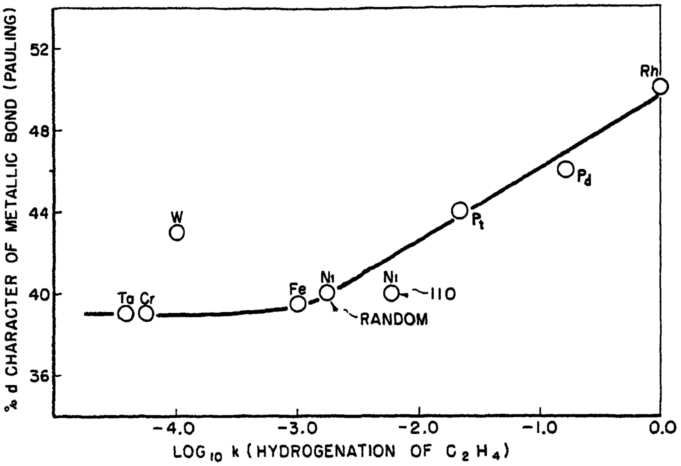

FIG 7.

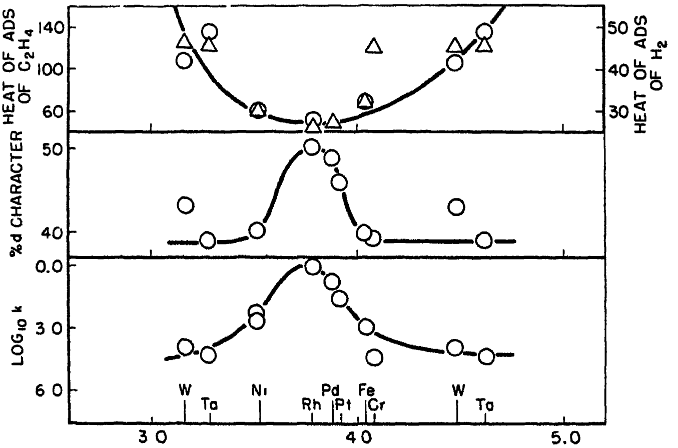

FIG. 8.

ON THE EXISTENCE OF ACTIVE CENTRES IN CHEMICAL ADSORPTION AND CONTACT CATALYSIS

BY A. EUCKEN

Received 25th January, 1950

The problem as to whether chemisorption and catalytic reaction occur over the whole available surface of a catalyst or only at active centres is discussed. The apparent heterogeneity arising from mutual interaction of adsorbed particles and the possibility of different states of the adsorbate on the surface are considered in detail for the adsorption of hydrogen on highly activated nickel. It is concluded that the supposed effect of active defects should be rejected and that the essential part is played by the active intermediate states of the adsorbed reactant.

A final answer has not yet been given to the question as to whether chemical adsorption or catalytic reaction occurs on the whole available surface of the solid adsorbent or catalyst, or only at certain places (active centres). It is, however, doubtful having regard to the complexity of this field, whether this question can ever be completely answered. It should therefore be noted that the conclusions obtained here depend on a limited number of facts, and that different conclusions might be obtained with different types of adsorption processes or catalytic reactions.

It is advisable to consider the existence of active centres in chemical adsorption separately from contact catalysis since, contrary to a view held earlier, it appears that the chemical adsorption of any particle is frequently, but by no means always, connected with an increase of its chemical reactivity (for this reason the term "activated adsorption", which is frequently used, is not considered suitable).

Chemical Adsorption.—Two cases of the inhomogeneity of solid surfaces in regard to chemical adsorption can *a priori* be distinguished.

(i) The heat of adsorption and also the activation energy often varies considerably with coverage, and this has led to the conception of the *existence of a continuous spectrum of adsorption centres* of different activity, which might be identified with the lattice defects of the contact surface.

(ii) On heating, the adsorption isobar frequently shows two maxima which, following H. S. Taylor, are considered as an indication of the existence of two (homogeneous) regions, whose adsorption capacity differs from that of the bulk. No details are given as to how this comes about. We can consider these two regions as crystal planes having different arrangements. Fundamentally, however, at least with the ionic type of adsorbent, it is possible to consider this difference as being determined by the individual lattice units, for example, the one as an adsorption on the cations, and the other on the anions. An alternative interpretation of these two adsorption effects which will apply to monatomic adsorbents (pure metals) and in part also to salts (oxides, etc.), can be proposed.

(i) THE SURFACE IS PERFECTLY HOMOGENEOUS IN REGARD TO ITS ADSORPTION PROPERTIES.—The apparent inhomogeneity (the existence of a spectrum of active centres) then arises from the influence of the adsorbed particles on each other, since a particle is less tightly held in the immediate environment of another adsorbed particle than on a completely clean surface.[1] If we assume this kind of mutual interaction[2] it is clear that the heat of adsorption continually decreases with increasing coverage of the surface.

(ii) DIFFERENT STATES OF THE ADSORBATE CAN EXIST ON THE HOMOGENEOUS SURFACE, i.e. the steps in the adsorption isobars are not associated with the regions of different activity of the surface. These two theories will be discussed in detail for the adsorption of hydrogen on highly active nickel.

The shape of a typical adsorption isobar is shown in Fig. 1. Two maxima occur with heating, the first being not strongly marked and only observed at relatively low pressures (approximately 10^{-2} mm. Hg). It can be shown thermodynamically for the adsorption equilibrium above 273° K that the hydrogen is essentially atomically bound to the surface.

---

[1] For example in the chemical adsorption of hydrogen atoms on a metal (e.g. Ni) the interaction between adsorbed hydrogen atoms occurs in the following way. As the metal surface possesses a certain electron affinity, the hydrogen atoms become positively polarized, and consequently there is coulombic repulsion between them. Furthermore as more hydrogen atoms become available as electron donors, the electron affinity of the metal surface becomes satisfied. At the same time the binding energy of the individual hydrogen atoms decreases.

[2] Recently this point of view has been expressed by Beeck (*Rev. Mod. Physics*, 1945, **17**, 61); cf. also Herington and Rideal (*Trans. Faraday Soc.*, 1944, **40**, 505).

Thus the first maximum of the adsorption isobar can be ascribed to an adsorption of molecules, similar in type to an atomic adsorption of a chemical nature, since physical (van der Waals') adsorption is only observed at much lower temperatures (in the region of liquid hydrogen). The heat of adsorption is estimated to be about 6 kcal./mole, i.e. it is relatively small, so that on heating, desorption occurs at about 200° K, and at 273° K the fraction of the surface covered by molecules falls to about 1 %. However, one would have to assume, not only at this temperature but also at higher temperatures, that the hydrogen is primarily adsorbed as molecules. The adsorbed molecules subsequently dissociate more or less rapidly into atoms, which are initially closely packed but later diffuse apart (slowly at the lower temperatures and more rapidly at higher temperatures), since according to the above consideration a uniform distribution of the atoms over the whole surface corresponds to minimum potential energy.

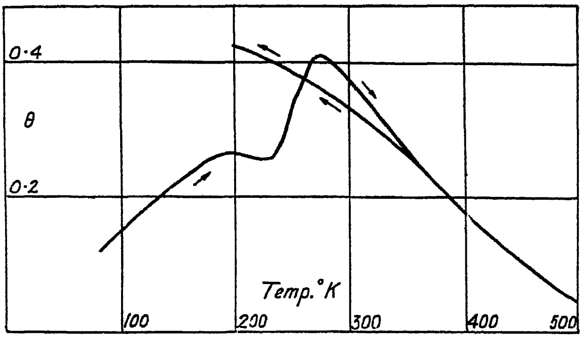

FIG. 1.

Isobars of adsorption velocities (schematically).

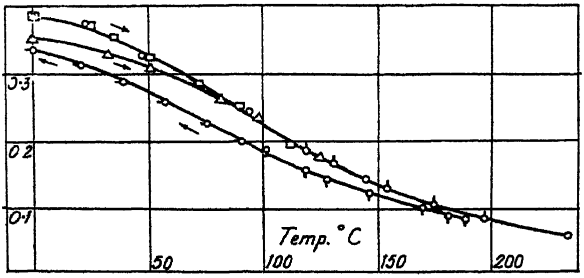

FIG. 2.

H_2 adsorption isobars at 10^{-2} mm. Hg on 28·8 g. Ni powder.

Desorption graphs.

○ Expt. 16 } Adsorption at 0° C on completely pure Ni surface.
□ Expt. 34 }
△ Expt. 35. Previous covering at 100° C after adsorption at 0° C.
$\overset{|}{\text{O}}$ Expt. 33. Adsorption at 100° C.

Adsorption graphs.

$\underset{|}{\text{O}}$ Expt. 33 from 200 to 100° C.
—O Expt. 36 from 100° to 0° C.

The shape of the isobar on subsequent cooling is abnormal. Contrary to a number of other investigators, a smaller amount of material is adsorbed in the range 260° K to 360° K on subsequent cooling, than on heating (Fig. 1 and 2). The effect becomes clearer on comparing the two velocity isotherms at 0° C (Fig. 3). Here, the adsorption was in some cases on pure nickel and in others on a nickel preparation which had been previously covered with hydrogen at 100° and 200° C respectively.

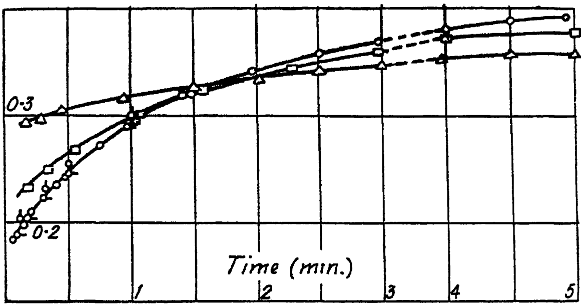

FIG. 3.

○ Expt. 28 ⎫
○— Expt. 31 ⎬ Adsorption without previous covering.
⦶ Expt. 37 ⎭
△ Expt. 29. Adsorption after previous covering at 100° C.
□ Expt. 32. Adsorption after previous covering at 200° C.
Isotherms of adsorption velocities at 0° C (23·0 g. Ni).

This result can hardly be explained by the assumption of two separate regions (independent of each other), since in such circumstance there is no reason to expect previous covering to cause a decrease in the adsorption velocity. On the contrary, it can be regarded as a *poisoning of the total surface* by the adsorbed atomic hydrogen. On the basis of the assumption previously made, we can visualise this effect as follows.

Since the atoms adsorbed at 100° C are almost uniformly distributed over the surface, then during cooling only those places with relatively small adsorption activity are available for adsorption. Moreover the dissociation and diffusion of the newly-formed atoms will be greatly hindered by atoms already present in stable positions, so that establishment of the final stable state, which is characterized by the most uniform distribution of hydrogen atoms over the total surface, is made much more difficult than on a surface initially completely unoccupied.

One might expect to find similar effects during the adsorption of hydrogen on other metals; in the experiments of Emmett and Harkness (1935) adsorption isobars with two maxima are obtained for the system Fe—H_2. Unfortunately, in the isobars as yet determined for other metals and gases, the decreasing temperature branches are lacking in almost every case.

The results obtained with the Ni—H_2 system will probably not be directly comparable with those obtained with salt-type catalysts, as conditions with these vary considerably from case to case. In Fig. 4 the full line shows an isobar recently obtained for the adsorption of hydrogen on WS_2. The quantities of gas chemically adsorbed (near saturation) are approximately the same as for physical adsorption; therefore the total surface is active in the chemical adsorption. Evidently two processes are superimposed which correspond to the dotted lines 1 and 2 in the graph. It is probable that the first graph corresponds to a chemical (atomic) adsorption and the second, to a solution of hydrogen. The heat of adsorption (approximately 17 kcal./mole) changes relatively little with coverage, at least within the region where measurements could be made. The influence of the adsorbed particles on each other is in this case smaller than for a metallic surface. A number of other salt-type solid surfaces show analogous behaviour to that of the metal and WS_2, as here again the physically and chemically active surfaces practically coincide.

One of the few exceptions is γ-Al_2O_3 for which only about 10 % of the physically active surface is shown to be reactive in the adsorption of steam and alcohols. Here the lattice defects must be responsible for the preferred chemical adsorption. This can easily be understood as the lattice of γ-Al_2O_3 is known to be of the spinel type in which the Mg^{2+} ions are replaced by an equivalent number of Al^{3+} ions ; to maintain electroneutrality 33 % of the original sites occupied by Mg^{2+} ions (a total of about 10 % of the cation lattice sites of the spinel) must remain unoccupied. In the environment of such " holes " there are regions of excess negative charge, which can now interact with the hydrogen atoms of the hydroxyl groups of water and the alcohols, and thus cause strong adsorption. Apparently we are concerned here with a reinforced hydrogen-bridge binding.

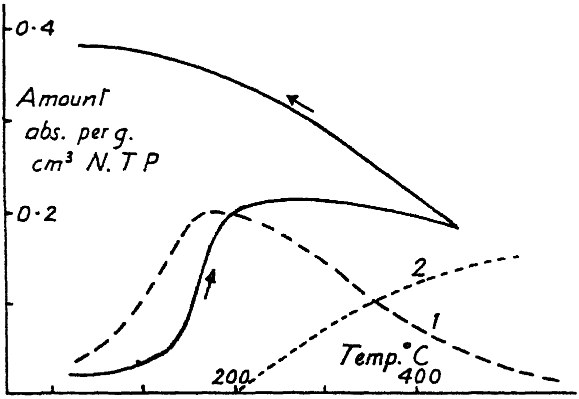

FIG. 4.
H_2 adsorption isobar of H_2 on WS_2 at 100 mm. Hg.

CONTACT CATALYSIS.—We shall confine ourselves to the discussion of a typical example of low temperature catalysis, since in high temperature catalysis (e.g. the catalytic combination of H atoms to molecules on metals) there is no doubt that the total surface is catalytically active.

However, it may at first appear as though in low temperature catalysis, e.g. the hydrogenation of unsaturated hydrocarbons in the region of 0° C, the chemical change occurs only on a negligibly small fraction of the contact surface, i.e. as if the assumption of the existence of active centres cannot be avoided.

As an example we may quote an experiment by Toyama (1937) and its interpretation. It deals with the hydrogenation of ethylene on the surface of a Ni powder at a pressure of about 1 mm. Hg. The reaction is zero order with respect to ethylene, and first order with respect to hydrogen.

Taking the reaction velocity as

$$-\frac{dn}{dt}\cdot\frac{1}{p_{H_2\,(gas)}}\left(\frac{\text{no. of moles}}{\text{sec. mm. Hg. cm.}^2}\right),$$

a value of the order of 1×10^{-11} per cm.² of the contact surface was obtained. Assuming that every H_2 molecule from the gas phase, colliding with sufficient energy with the ethylene adsorbed on the surface leads to a reaction, an activation energy of 5000 cal./mole and a value of $2{\cdot}5 \times 10^{-7}$ for dn/dt are obtained. The collision factor is approximately 4×10^{-5}, which may be taken to mean that only a very small part of the total surface is catalytically active.

This and similar results support the view that the reaction only occurs on a relatively few small centres of the surface; but the problem can by no means be regarded as finally solved. Some experiments undertaken with a view to a solution of the problem showed first of all that ethylene at normal pressures has a strong poisoning effect [3] on the reaction. Starting with a carefully cleaned surface and allowing the reactants to react simultaneously at low pressures (of about 10^{-3} to 10^{-1} mm. Hg), values 100 times greater are obtained for the reaction velocity. In order to remove the possibility of any poisoning effect remaining even at low pressures, an attempt was made to replace the ethylene by a hydrocarbon the poisoning effect of which would be much less. It was shown that cyclohexene served this purpose, and was also very suitable for use in other contact catalytic hydrogenation experiments.

The real clue to the understanding of the processes occurring in the low-temperature hydrogenation on Ni was found in experiments with a relatively large amount of solid, on which one of the reactants was adsorbed; the other was subsequently added and allowed to react from the gas phase. If cyclohexene was adsorbed, and then hydrogen allowed to react in this manner, only a negligibly small amount of C_6H_{12} was formed. If, however the hydrogen was adsorbed and the cyclohexene subsequently added, a considerable change was obtained. This surprisingly depended to a great extent upon the time interval between adsorption of the hydrogen and addition of the C_6H_{10}. It was also of importance whether the hydrogen was adsorbed at 0° C or 100° C.

TABLE I.—HYDROGENATION EXPERIMENTS. SURFACE PREVIOUSLY COVERED WITH HYDROGEN

Ni powder (670 mg.); reaction temperature: 0° C

Expt. No.	Relative Covering of Surface with H_2	Temp. of Previous Covering (° C)	Time between Covering and Start of Reaction	Duration of Reaction (min.)	Yield of C_6H_{12} (%)
1	0.200	0	35 sec.	5	86
2	0·172	0	35 ,,	5	80
3	0·143	0	20 min.	5	17
4	0·404	0	20 ,,	5	45
5	0·400	0	20 ,,	15	66
6	0·286	100	20 ,,	2	12
7	0·286	100	20 ,,	5	19
8	0·306	0	20 ,,	5	35
9*	0·310	—46	10 ,,	5	68

* At — 46° C for reaction temperature.

The results are summarized in Table I. It can be seen that the atomically adsorbed hydrogen, distributed over the whole surface, is apparently not capable of reaction. The fact that the reactivity of the hydrogen adsorbed at 0° C for a short duration of adsorption is rather large but decreases rapidly with time, may mean that the adsorbed *molecules* cause the reaction, prior to their dissociation and subsequent diffusion as atoms. A more detailed quantitative calculation of the reaction kinetics indicates that the adsorbed molecules as such most

[3] Pease (1923) was the first to point this out.

probably do not determine the kinetics of the reaction. Finally we may suppose that a characteristic maximum of the reactivity is reached immediately after their dissociation i.e. in a state where two hydrogen atoms are still close together or form a H-atom pair.

On the basis of this picture it is possible to calculate the course of the catalytic hydrogenation of C_6H_{10} from the gas phase on Ni, if we assume that the change of coverage per unit time θ_{HH} is proportional to the number of H atom pairs and to the number per sec. colliding with C_6H_{10} molecules from the gas phase. The adsorption velocity of the hydrogen also enters into the process, but for this a sufficiently accurate empirical expression is available.

In the final expression for the reaction velocities we have to include the collision factor, the activation energy and the ratio A/v of the active contact surface to the reaction volume. Taking all the experiments into account, a collision factor of about 0·1 was obtained, which is of a reasonable order of magnitude. The activation energy was calculated in the usual manner from the temperature dependence of the reaction velocity. The ratio A/v can be estimated with an accuracy of at least ± 50 %, as the effective surface was always determined by physical adsorption experiments.

The experiments were carried out with a series of different Ni surfaces (nickel-powder from carbonate and formate, nickel-foil, Raney-Nickel from $NiAl_3$ and $NiSi_2$, evaporated nickel films) at pressures of 10^{-2} to 10^{-1} mm. Hg. The observed variation of the reaction velocity with time was on the whole given satisfactorily by the final equation; as a rule, however, it was found that the reaction velocity decreased rather more rapidly within the individual series of experiments than demanded by the equation. This can be explained by the fact that a small amount of adsorbed hydrogen is not used up during the reaction but distributes itself over the surface in the atomic form and thus poisons it. It is remarkable to find that the final expression remained quantitatively valid for *all* the Ni preparations employed, provided they had not been previously heated above 280° C.[1]

One gains the impression therefore, that on *pure* nickel planes irrespective of the method of preparation, the same hydrogenation mechanism always occurs, and thus the supposed effect of active defects, which should necessarily show some difference in the compounds prepared differently, must be rejected.

This must not, however, be taken to mean that at very instant the total surface is catalytically active. It seems more reasonable to regard the sites instantaneously occupied by H-atom pairs as temporary centres of catalytic activity, their position on the surface being subject to continuous change. From the above, the function of the surface covered with these temporary centres, θ_{HH}, may easily be calculated; in our experiments values between 5×10^{-3} and 1×10^{-1} (maximum) according to the magnitude of the ratios of p_{HC}/p_{H_2} were obtained. In fact, at any instant, only a relatively small fraction of the surface is taking part in the reaction, whereas the major part of the stably adsorbed reactants (C_6H_{10} and H atoms) covering the surface, are not at all, or only to a very small extent, capable of reaction. It may be expected that similar conditions exist for other low temperature catalytic processes and that an essential part is played by the active intermediate states of the adsorbed reactants.*

Institut für Physikalische,
Chemie der Universität Göttingen,
Göttingen, Bürgerstrasse 50,
Germany.

---

* The results communicated here are given in detail in *Naturwiss.*, 1949, **36**, 74; *Z. Elektrochem.*, 1949, **53**, 285, and 1950, **54**, Heft 2.

THE RELATIONSHIP BETWEEN SENSITIVITY TO POISONING AND CATALYTIC SURFACE

By E. B. Maxted, K. L. Moon and E. Overgage

Received 6th February, 1950

The expected inverse variation of sensitivity to catalyst poisoning with the surface area of a catalyst has been confirmed experimentally for platinum hydrogenation catalysts poisoned with methyl sulphide, a relationship of the type: $\alpha_1 s_1 = \alpha_2 s_2$, in which α is a measure of the sensitivity and s is a measure of the surface area, being obtained. This relationship apparently holds even when the variation in the area of a constant weight of platinum is induced by sintering. A characteristic value for the product αs has been obtained which should make possible the calculation of the surface area of platinum catalysts in general by sensitivity tests carried out on small quantities of platinum.

In connection with measurements of the specific catalytic activities of metals of the platinum and palladium groups, it became necessary to try to develop a method by means of which the relative surface area of finely divided metal catalysts could be measured with amounts of catalyst which are too small for a determination of the surface by Brunauer-Emmett low-temperature adsorption isotherms. This preliminary work has been done with platinum, which—unlike some of the rarer metals of the group—was available in sufficient quantities also for area determinations by the low-temperature adsorption method. The main object of the present work has been to examine the degree to which the sensitivity of a catalyst to poisoning, which can be determined with a fraction of a gram of material, can be used as a measure of the surface of catalysts.

It would be expected on first principles that the sensitivity of a catalyst to poisoning would be inversely proportional to the surface area, this inverse relationship being derivable both for a catalyst having a catalytically uniform surface and for a catalyst containing points or areas of special activity, provided that the ratio of specially active area to the total surface is not changed by the method used for varying the surface area. In the present work the surface area of a platinum hydrogenation catalyst has been varied in two ways: firstly, by using different weights of the same catalyst and, secondly, by using a constant weight of a second stock of platinum, the surface area of which was varied by sintering. In the latter case, it was necessary to determine the relative surface independently by the Brunauer-Emmett method.

Experimental

The catalysts consisted throughout of platinum black which had been made by the reduction of chloroplatinic acid with alkaline formate solution. The measurements of the sensitivity to poisoning were made by the general method which has already been described in previous papers [1] and which is applicable either for the determination of the relative toxicity of different poisons or, by using a standard poison, for the determination of the relative sensitivity of different catalysts. Methyl sulphide was used as the poison; and the standard charge taken for each hydrogenation test consisted of 10 ml. of a 10 %

---

[1] Maxted and Evans, *J. Chem. Soc.*, 1937, 603, 1004 and later papers.

solution of cyclohexene in cyclohexane, together with known amounts of platinum and of methyl sulphide. The hydrogenation reaction, which was carried out in a shaker under standardized conditions at 30°, was, as is usual, of zero order ; and the approximately uniform rate of absorption of hydrogen, in any test, up to the stage at which the cyclohexene approaches saturation, made possible a direct and accurate reading of the hydrogenation velocity, which was taken as representing the activity of the catalyst.

On plotting the hydrogenation rates against the poison content, the usual type of graphs [2] consisting of a linear or very nearly linear portion followed by a region of inflexion were obtained, the course of the main linear portion being expressible by an equation of the type :

$$k_c = k_0(1 - \alpha c),$$

in which k_0 is the orginal unpoisoned activity, k_c is the activity in the presence of a concentration c of the poison and α is the poisoning coefficient.[3] It will be seen that α represents the fraction of the original activity which is suppressed by each unit of poison present and that the values of α, for a series of catalysts poisoned by the same poison under similar conditions, can be used as a measure of the relative sensitivity of the catalysts to poisoning.

Sensitivity Tests Involving a Variation of the Surface Area by Varying the Amount of Catalyst.—This is the simplest method of studying the variation of the sensitivity with the surface, in that the surface area is obviously directly proportional to the weight of catalyst used and accordingly no independent determination of the relative surface, within the series, is necessary. In the present paper, for reasons of space, a summary only of the results obtained can be given ; but a more detailed account of the work is in course of publication.[4] The graphs for various weights of the stock of platinum used for this series (Platinum A) are given in Curves I to IV of Fig. 1. From these, the corresponding values of α can be calculated and are given in Table I. If the sensitivity varies inversely with the surface area of the catalyst (which is proportional, within the series, to the weight of the platinum used), the product αs, where s is the relative surface, should be constant. The experimentally observed degree of this constancy is shown in the last column of the Table. This constancy also follows directly from the geometry of Fig. 1, since the initial linear portions of all the graphs are approximately parallel to one another.

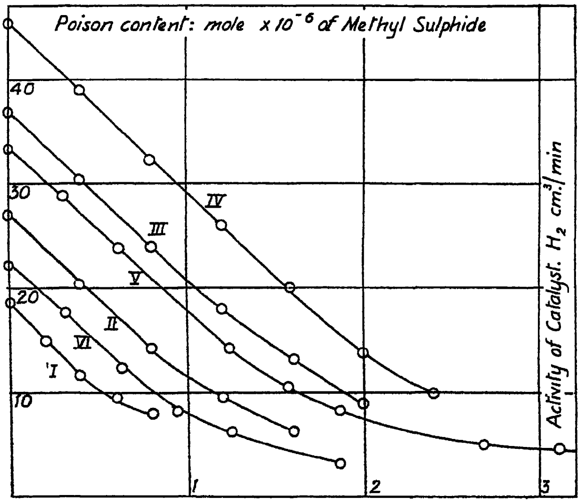

FIG. 1.

---

[2] Maxted, *Trans. Faraday Soc.*, 1945, 41, 406.

[3] Maxted and Stone, *J. Chem. Soc.*, 1934, 26.

[4] Maxted and Overgage (in course of publication).

TABLE I

Platinum A

Wt. Platinum g.	Relative Surface Area, s	Activity (k_0 in cm.^{3} H_2 per min.)	$\alpha \times 10^{-6}$	$\alpha s \times 10^{-6}$
0·025	1·0	18·7	0·901	0·90
0·0375	1·5	27·4	0·599	0·90
0·05	2·0	37·1	0·435	0·87
0·0625	2·5	45·7	0·355	0·89

Sensitivity Tests Involving a Variation in the Surface Area by Sintering.—This work was carried out by reducing the surface area of a fresh stock of platinum black (Platinum B) by sintering at 400-410°. The change in the surface area per unit of weight caused by the sintering was followed by means of Brunauer-Emmett isotherms and was compared with the corresponding change in the sensitivity to poisoning by hydrogenation tests on samples of the platinum taken before and after sintering.

The measurements of surface area were made with nitrogen at − 183°, helium being used as the calibration gas. The isotherms obtained on plotting the nitrogen adsorption against the resulting pressure were of the normal Brunauer-Emmett type [5, 6] having a long linear portion, by the extrapolaton of which to zero pressure a value could be obtained for the volume of nitrogen required to form a monolayer and consequently for the surface area. This zero-pressure extrapolation method was adopted for its simplicity in place of using the more complicated Brunauer-Emmett-Teller equation.[7] It is perhaps open to some doubt whether the figure obtained by any method of extrapolation corresponds very exactly to the adsorption of a monolayer, although Emmett, in a recent critical review [8] of the reliability of all the proposed extrapolation methods (including the use of the Brunauer-Emmett-Teller equation), states, " It must be admitted that this zero pressure extrapolation method certainly will yield areas which are of the correct order of magnitude and which are probably capable of yielding fairly reliable relative areas for various finely divided solids ".

The results for the relative surface of the platinum before and after sintering are contained in Table II, from which it will be seen that about one-third of the original surface area has been lost by the heat treatment.

TABLE II

Platinum B

State of Platinum	Wt. of Pt Taken (g.)	N_2 Required for Monolayer at − 183° (cm.^{3} N.T.P.)	N_2 for Monolayer Corrected to Original Wt. of Platinum (cm.^{3})	Relative Surface Area of Pt per Gram
Unsintered .	38·71	104	104	1
Sintered . .	34·59	63	71	0·68

The corresponding graphs for 0·05 g. of the unsintered and sintered platinum are given in Curves V and VI of Fig. 1. It will be seen that these curves agree, from the standpoint of their position and slope, with what would be expected if they had been based on poisoning tests carried out with catalysts of the first series having an equivalent unpoisoned activity, in spite of the fact that Curves

[5] Emmett and Brunauer, *J. Amer. Chem. Soc.*, 1937, **59**, 1553.

[6] Brunauer and Emmett, *ibid.*, 1935, **57**, 1754.

[7] Brunauer, Emmett and Teller, *ibid.*, 1938, **60**, 309.

[8] Emmet, *Advances in Catalysis* (Academic Press, New York, 1948), Vol. I, p. 75.

V and VI have been obtained with a different stock of platinum and that the change in the surface area has been induced by sintering ; and it is evident that all the graphs of Fig. 1 are closely interconnected and that some simple relationship connects all these platinum catalysts, irrespective of whether they have been drawn from different stocks or whether the surface has been sintered or not. From Curves V and VI the relative sensitivity to poisoning of the unsintered and of the sintered Platinum B can be calculated as before : further, on the basis of the low-temperature isotherms, approximate values for the surface areas of the amount of Platinum B (0·05 g.) used in the poisoning tests can also be inserted. These are included in Table III.

TABLE III

0·05 g. Platinum B

State of Platinum	Surface Area for Monolayer at 183° (cm.^{3} N_2 N.T.P.)	Surface Area s (m^2.)	Uupoisoned Activity k (cm.^{3} H_2 per min)	¦Sensitivity $\alpha \times 10^{-6}$	$\alpha s \times 10^{-6}$ (s in m.^{2})
Unsintered .	0·134	0·59	33·41	0·459	0·271
Sintered .	0·0917	0·40	22·22	0·680	0·272

From the above figures, $\alpha_1/\alpha_2 = 0{\cdot}67$, $s_2/s_1 = 0{\cdot}68$, and $k_2/k_1 = 0{\cdot}67$, in which the subscripts refer respectively to the unsintered and to the sintered platinum. Accordingly, within the limit of the accuracy of the measurements,

$$\frac{\alpha_1}{\alpha_2} = \frac{s_2}{s_1} = \frac{k_2}{k_1},$$

this inverse variation of the sensitivity with the surface area, and the direct variation of the rate of working with the surface, being similar to the results obtained in the first series with Platinum A.

Discussion

If all the curves of Fig. 1 can be treated as a connected series, it should be possible, by applying the relationship, $\alpha_1 s_1 = \alpha_2 s_2$, to calculate the surface area of all the catalysts used in the Figure, provided that the area is known in at least one case. This area in m.^{2} is known in two cases, namely for the 0·05 g. of unsintered Platinum used in Curve V ($s = 0{\cdot}59$ m.^{2}) and for the 0·05 g. of sintered Platinum ($s = 0{\cdot}40$ m.^{2}) used in Curve VI : furthermore both of these catalysts give approximately identical values ($0{\cdot}271 \times 10^6$ and $0{\cdot}272 \times 10^6$) for the sensitivity-area product, which can be used as one side of the αs equation, the surface area of any of the catalysts of Table I being obtained by dividing this product by the value of α for the catalyst in question. It can in this way be shown that the surface area of Platinum A is about 12·1 m.^{2}/g. This conversion of the arbitrary scale of relative surface used in Table I into areas expressed in m.^{2} gives Table IV, in which the areas of all the catalysts used in both series are consequently expressed on a directly comparable scale. The above conversion could also, in principle, have been carried out by using the alternative surface-to-rate relationship, $s_1 k_2 = s_2 k_1$, but this method is less accurate in practice than the use of the αs relationship, in that it is influenced more by any traces of impurities, the effects of which tend to cancel out in the ratio k_c/k_0, which determines α, since k_0 and k_c are affected proportionately : further, the αs relationship is of special interest since α has a direct coverage component due to the poison.

The product αs for the figures in the last two columns of the Table is, of course, in each case $0{\cdot}27 \times 10^6$, which—since it was given by two independent and direct measurements of surface on two rather widely different catalysts, i.e. both for the unsintered and for the sintered Platinum B—seems to be a characteristic sensitivity-area product, which can be used for calculating the surface area in m.^{2}, not only of Platinum A, but also of other platinum catalysts, merely by measuring the valuc of the sensitivity α of the catalyst in question and dividing the above

TABLE IV

Platinum Stock	Wt. of Pt (g.)	Sensitivity, $\alpha \times 10^{-6}$	Surface Area s (m.^{2})
A	0·025	0·901	0·30
B (sintered) . . .	0·050	0·680	0·40
A	0·0375	0·599	0·46
B (unsintered) . .	0·050	0·459	0·59
A	0·050	0·435	0·61
A	0·0625	0·355	0·76

characteristic product by the observed value for α. In more general terms, it should be possible, after an initial calibration of a hydrogenation apparatus for a single catalyst by means of a single low-temperature isotherm, subsequently to use the apparatus for the determination of the area in m.^{2} of any other specimen of platinum catalyst without the necessity for further Brunauer-Emmett isotherms.

Rate of Working of the Platinum Surface.—Finally, the rate of working per unit of area of the various platinum surfaces used may be considered briefly. If the two series are combined by expressing the areas in m.^{2}, as in Table IV, Fig. 2 is obtained on plotting these areas against

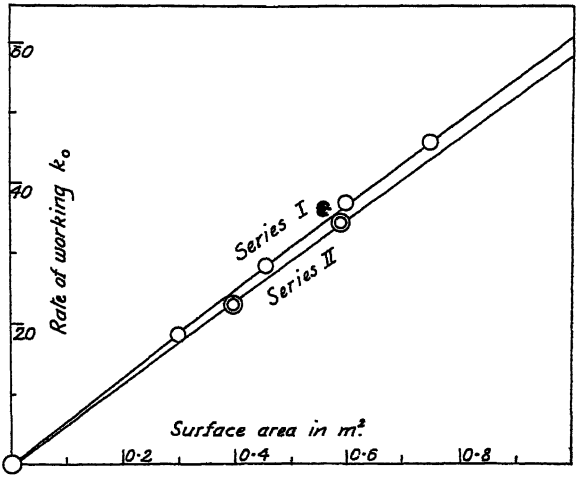

Fig. 2.

the unpoisoned catalytic activities k_0. It will be seen that the rate of working of unit surface area in all the catalysts taken is approximately, although not exactly, the same in both series, the slight difference being, however, possibly due to a change in the cyclohexane stock from Series I to Series II, since, as has already been stated, the values for the actual velocities of hydrogenation are found in practice to be far more sensitive to such changes than the ratio of velocities used for calculating α. From the results given in the Figure, each square metre of platinum surface in Series I works at a rate corresponding to the insertion of about 61 cm.^{3}

H_2 per min. into cyclohexene. In Series II the corresponding rate of fixation of hydrogen was 57 cm.^{3} per min. in each case, in spite of the fact that in one case the surface of the platinum had been sintered. The very close correspondence of the rate of working per square metre of this sintered and unsintered platinum—for which the comparison of surface area was not dependent on a conversion factor but on direct measurements by low-temperature isotherms—as well as the degree of the agreement of the rate of working by each square metre of platinum catalysts generally, are obviously of interest in connection with the nature, and with the resistance to sintering, of active points or of specially active crystal planes of the surfaces of Pt catalysts and work is in progress to investigate this aspect more systematically.

One of the authors (E. B. M.) wishes to acknowledge the help given by a Leverhulme Research Fellowship in the carrying out of the above work.

Department of Chemistry,
University of Bristol.

THE MECHANISM OF AMMONIA OXIDATION AND CERTAIN ANALOGOUS REACTIONS

BY J. ZAWADZKI

Received 30*th January,* 1950

The characteristic feature of the reaction of catalytic ammonia oxidation is its great velocity; in favourable conditions nearly every one of the NH_3 molecules striking the surface of the platinum catalyst gives NO as a final product. The attainment of the high efficiency of the oxidation to the desired product depends on the velocities of a number of successive and simultaneous reactions, which take place in the system NH_3—O_2—catalyst, as well as on the suppressing of the reactions between reagents, intermediate and final products of reaction before and after the catalyst.

From experiments on various catalysts (Pt, oxides) under such conditions that N_2O appears as one of the main products a scheme of the most probable mechanism of reaction is given. Certain assumptions are made concerning the elementary processes and the chemisorption of O_2 on the catalyst which proceeds with great velocity.

1. Preliminary Remarks. — Recent experiments on the ammonia oxidation [1-4] at temperatures below 550° clearly proved that N_2O was one of the main products of reaction on oxide catalysts and on platinum. The results of these experiments enabled us to make a step towards a better understanding of the mechanism of this reaction (cp.[5]).

The extensive experimental material collected by several authors [6] was critically reviewed in 1922-1927.[7-10, 12] Although it was not known that N_2O was present in the products it was shown that:

---

[1] Zawadzki, *Roczniki Chem.*, 1948, **22**, 220.

[2] Tuszynski, *ibid.*, 1949, **23**, 397.

[3] Marczewska, *ibid.*, 1949, **23**, 406.

[4] Winnicki, *ibid.*, 1949, **23**, 388.

[5] Ostwald, *Berg.-u. Hüttenmän. Rundschau*, 1906, **3**, 71.

[6] Gmelin, *Handbuch der anorganischen Chemie (Stickstoff)*, 1936, 639.

[7] Zawadzki and Wolmer, *Roczniki Chem.*, 1922, **2**, 158.

[8] Zawadzki and Lichtensteinowa, *ibid.*, 1926, **6**, 824.

[9] Zawadzki and Narkiewicz, *ibid.*, 1927, **7**, 369.

[10] Andrussow, *Z. angew. Chem.*, 1926, **39**, 321; 1927, **40**, 166.

(i) It is necessary to distinguish between the reactions which occur on the catalyst itself and those which take place before or after the catalyst bed.

(ii) There is no optimal temperature for a given catalyst. The greater the gas velocity the higher the temperature at which the maximum yield is obtained.

(iii) Consequently we can obtain [10] high yields of NO even at 1200°, provided the time of contact is sufficiently short.

(iv) In connection with (i) it was pointed out [10] that at low flow rates a countercurrent diffusion of gases was an important factor. The processes which took place either before or after the catalyst bed were demonstrated by carrying out the oxidation in a platinum capillary tube.[11]

The final products of ammonia oxidation are N_2 and H_2O and NO is an intermediate (non-equilibrium) product, which under suitable conditions can be recovered with high yields. In the oxidation we have to distinguish between successive and simultaneous reactions. Only one of the simultaneous reactions gives the desired product; others (e.g. $2NH_3 \rightleftarrows H_2 + 3H_2$, or reactions of NH_3 with intermediate or final products) are detrimental to high yields of NO. Another source of loss is the successive reactions in which final products take part (e.g.

$$2NO \rightleftarrows N_2 + O_2,$$

or reactions of NO and NO_2 with NH_3, etc.).

In these elementary processes there are involved not only the original reagents (NH_3, O_2) and final products, but also various intermediate products and by-products (e.g. NH_2OH, NH, HNO, HNO_2, N_2O, etc.). By considering the results of the latest experiments (where high proportions of N_2O were formed at low temperatures) it is possible to explain the nature of losses occurring in the NH_3 oxidation on platinum as well as on oxide catalysts.

(*a*) AT HIGH TEMPERATURES. (i) The velocity of decomposition of NH_3 to N_2 and H_2 at sufficiently high temperatures is comparable to that of its oxidation to NO. The extent of loss is thus controlled by temperature and not by the rate of flow of gases, except when this is too low when there are losses due to NO decomposition. These rise with increasing temperature and decreasing rate of flow. (ii) Losses are developed also when unconverted ammonia passes through the catalyst bed and beyond it due to reaction with NO and other intermediate products. Too large or uneven mesh of the Pt gauze catalyst or too high a rate of flow may be responsible for the passage of unconverted ammonia. (iii) When the rate of flow is too low the reaction before the catalyst bed causes additional losses.[7, 10]

(*b*) AT TEMPERATURES BELOW 500°. (i) N_2O is present in considerable proportions in the reaction products. The amount depends on temperature and rate of flow. The formation of N_2O accounts for the decrease in yield of NO. N_2O decomposes easily into N_2 and O_2. The higher the temperature and the longer the time of contact, the greater is the proportion of decomposed N_2O. (ii) When the rate of flow is low the losses before the catalyst bed are caused by the countercurrent diffusion. (If, e.g. NO passes into the space before the catalyst bed, it is oxidized to NO_2, which reacts with NH_3 giving free nitrogen through formation of NH_4NO_2). (iii) There are losses on the catalyst itself when conditions are such that the first intermediate product of reaction (e.g. NH) is formed slowly and can react with undecomposed ammonia, the product being free nitrogen. Nitrogen is also produced when NH_3 reacts with intermediate products formed in the next stage of the process. (iv) When the rate of flow is high, the unchanged NH_3 can pass beyond the catalyst bed, where analogous reactions take place, although probably they proceed at a lower rate. The course of these reactions depends on the space available and temperature.

2. Proposed Schemes of Mechanism of the Reaction.—To explain the mechanism of ammonia oxidation we have also to consider the HCN oxidation, and the reaction of NO with hydrogen. At first it was assumed that NH_3 and O_2 decomposed to atoms and that the yield of NO depended on a proportion of the N atoms combining with O atoms. Only that part of the hypothesis concerned with the role of atomic oxygen is true.

---

[11] Andrussow, *Ber.*, 1927, 60, 2005.

Contrary to Andrussows'[10, 11] (nitroxyl) hypothesis the formation of HNO is not an intermediate reaction; it is a side reaction, which is responsible for formation of N_2O in the final products. The weak point of this hypothesis is the assumption that a reaction of NH_3 with molecular oxygen proceeds on Pt surfaces. The work of Langmuir,[16] Cassel and Glückauf[17] and others definitely proved that the adsorption of atomic oxygen does occur and that it is a fundamental process in oxidation of CO or H_2 on platinum. In Langmuir's experiments each molecule of CO or H_2 striking the platinum surface with adsorbed atomic oxygen enters the reaction. Similarly in the NH_3 oxidation, nearly every NH_3 molecule, which strikes the catalyst surface, gives ultimately a molecule of NO, provided the conditions are favourable. In a process of such a high velocity as that of NH_3 oxidation to NO we cannot assume the primary reaction to be $NH_3 + O_2$, as the heat of activation would have to be considerable. In our studies on NO decomposition on platinum[18] we have postulated a stronger inhibiting action of atomic oxygen formed in the reaction itself than of molecular oxygen introduced to reacting mixture.

Numerous experiments carried out at low pressures and at high temperatures by Bodenstein and Krauss[21] and their collaborators, and also investigations on various reactions of hydroxylamine, have led Bodenstein[14, 19] to the following reaction mechanism:

$$NH_3 + O = NH_2OH. \qquad (1)$$

Reactions leading to NO:

$$NH_2OH + O_2 = HNO_2 + H_2O \qquad (2)$$

$$HNO_2 + O_2 = HNO_4 \qquad (2a)$$

$$HNO_4 = NO + O_2 + OH \qquad (2b)$$

$$2OH = H_2O + O \qquad (3)$$

Reactions leading to N_2O:

$$NH_3O + O = HNO + H_2O \qquad (4)$$

$$2HNO = N_2O + H_2O \qquad (4a)$$

Reactions leading to N_2:

$$HNO_2 + NH_3 = 2H_2O + N_2 \qquad (2a')$$

$$HNO + NH_2OH = 2H_2O + N_2 \qquad (4a')$$

and the decomposition of NO and N_2O.

However, we consider Bodenstein's hypothesis unfounded. Thus the reaction

$$NH_{3\,ads.} + O_{ads.\,Pt} = NH_2OH_{ads.}$$

is endothermic[20] as Bodenstein admits. Similarly, the reaction of NH_3 with oxides such as MnO_2 or Fe_2O_3 are appreciably endothermic.

---

[12] Adadurow, *Proizwodstwo azotnoj kistoty, Leningrad*, 1934; *Zurnal chimicheskoj promyshlennosti*, 1933, **10**, 37.

[13] Bodenstein, *Z. angew. Chem.*, 1927, **40**, 174.

[14] Bodenstein and Büttner, *Trab. IX Congr. Int. Quim. Pura Aplicata. Madrid*, 1934, **3**, 475; Bodenstein, *Trans. Electrochem. Soc.*, 1937, **71**, 353; *Helv. chim. Acta*, 1935, **18**, 758.

[15] Nagel, *Z. Elektrochem.*, 1930, **36**, 754.

[16] Langmuir, *Trans. Faraday Soc.*, 1922, **17**, 607, 621.

[17] Cassel and Glückauf, *Z. physik. Chem.*, 1930, **9**, 435; 1932, **17**, 380; **18**, 347; 1932, **19**, 47.

[18] Zawadzki and Badzynski, *Roczniki Chem.*, 1931, **11**, 15. Zawadzki and Perlinski, *Compt. rend.*, 1934, **158**, 200.

[19] Bodenstein, *Z. Elektrochem.*, 1941, **47**, 517.

[20] Bichowsky and Rossini, *The Thermochemistry of the Chemical Substances* (Reinhold Publishing Corp., New York, 1936).

It is clear that an endothermic reaction cannot be the first step in a process, in which practically every impact of NH_3 molecule with the catalyst surface is effective, because the heat of activation, being at least equal to the endothermic heat of reaction, should be equal to or very nearly zero; this does not agree with calculations.

Yields of NH_3O and HNO_2 in Bodenstein's [14] and Krauss' [21, 23] experiments rise with increasing temperatures (from 1050° to 1350°). The yield at 1050° is still comparatively low and would be lower at temperatures below 1000°. Bodenstein [22] admits that if platinum used had not been heated to a very high temperature, hydroxylamine would not have been found in the reaction products.

On the other hand under certain conditions it is possible to obtain high yields (well over 90 %) of NO from NH_3, even at temperatures slightly higher than 500°, and that the reaction proceeds with a very high velocity. Hydroxylamine has never been discovered except under special conditions at very high temperature, and it is well known, that hydroxylamine is unstable well below 500°. The combination of NH_3 with atomic oxygen may result in a transition state or activated complex (catalyst . O . NH_3). In Bodenstein's and Krauss' experiments this activated complex probably gives hydroxylamine, which is then desorbed from the catalyst. The higher the temperature, the greater is the probability of formation and desorption of NH_2OH. At lower temperatures it is probable that the activated complex gives NH which stays on the surface of the catalyst, and H_2O which is set free.

We shall now discuss the imide theory and thereby try to explain the results of ourselves and other authors for the NH_3 oxidation on Pt and on oxide catalysts. Several of the facts can be explained by both the hydroxylamine and the imide theory; however, using the latter, the explanation is simpler and, what is more important, it is in agreement with energy calculations.

AUTHOR'S SCHEME OF REACTION MECHANISM.

$$NH_3 + O = NH + H_2O \tag{1}$$

Reactions leading to NO:

$$NH + O_2 = HNO_2 \tag{2}$$
$$HNO_2 = NO + OH \tag{2a}$$
$$2OH = H_2O + O \tag{2a'}$$

or,

$$2HNO_2 = NO + NO_2 + H_2O \tag{2b}$$

or reactions (*2a*), (*2b*), (3) of Bodenstein's scheme.

Reactions leading to N_2O:

$$NH + O = HNO \tag{3}$$
$$2HNO = N_2O + H_2O \tag{3a}$$

Reactions leading to N_2:

$$NH + NH = N_2 + H_2 \tag{4a}$$
$$NH + NH_3 = N_2H_4 \text{ and decomposition of } N_2H_4 \tag{4b}$$
$$NH + HNO = N_2 + H_2O^* \tag{5}$$
$$NH_3 + HNO_2 = N_2 + 2H_2O \text{ (decomposition of } NH_4NO_2\text{)} \tag{6}$$
$$2NO = N_2 + O_2 \tag{7}$$
$$2N_2O = 2N_2 + O_2, \text{ also reactions between } NH_3 \text{ and } NO_2. \tag{8}$$

---

[21] Krauss, *Z. physik. Chem. B*, 1938, **39**, 83.

[22] Bodenstein, *Z. Elektrochem.*, 1935, **41**, 466.

[23] Krauss and Neuhaus, *Z. physik. Chem. B*, 1941, **50**, 323.

* Andrussow gives also:

$$NH_3 + HNO = N_2H_2 + H_2O \text{ and } N_2H_2 + 1/2\, O_2 = N_2 + H_2O.$$

All these reactions proceed on the catalyst surface; in the gas phase probably only the reaction of NH_3 with NO_2 takes place.

The regeneration of atomic oxygen (2a′) (of this scheme or (3) of Bodenstein's) gives, at best, half of the amount of O necessary for reaction (1), and the rest must then be supplied by the dissociation of O_2 on Pt, i.e. $O_2 = 2O_{ads.}$

The following arguments have been proposed in favour of the imide as the first product of oxidation:

(i) An unstable NH is found in several reactions in which N_2 and H_2, or compounds of nitrogen with hydrogen, take part. The characteristic spectrum of NH has been found and its occurrence has been proved by optical methods.[24] (For imide formation in the catalytic decomposition of NH_3, see Mittasch and Frankenburger,[25] Frankenburger and Hodler,[26] Christiansen [27] and others.)

(ii) Hydrazine has been identified among the products of various reactions in which NH_3 takes part. It is probably formed by the reaction,

$$NH_3 + NH = N_2H_4.^{28, 29, 30}$$

(iii) Raschig [29] has explained the occurrence of N_2 and H_2 in a ratio of 1/1 and also of N_2H_4 in ammonia-oxygen flames (with NH_3 in excess) by assuming NH as an intermediate product.

(iv) Hofmann and Korpium [30] have similarly found N_2 and H_2 in a ratio of 1/1, when carrying out the oxidation of NH_3 in excess in presence of a fine copper wire. Hydrazine was identified on Ni—NaOH catalysts.

In my opinion the first elementary process in the NH_3 oxidation on platinum or oxide catalysts is the reaction of NH_3 with atomic oxygen:

$$\begin{array}{lcccc} & NH_3 + & O_{ads.} = & NH + & H_2O^{20} \\ \Delta H \text{ (kcal.)}: & 11 & 21{\cdot}7 & -39{\cdot}9 & 57{\cdot}8. \end{array}$$

Assuming gaseous NH to be the product, it follows that the reaction is endothermic ($\Delta H = 8{\cdot}8$ kcal.). If, however, we take into account the heat of adsorption of NH on platinum, the result is different. This heat of adsorption is undoubtedly much higher than the heat of adsorption of NH_3 or NH_3OH, and is probably of the order found in the adsorption of atoms such as O, H or N. (The heat of adsorption of O on Pt calculated from the data of Cassel and Gluckauf = 80·8 kcal.[17])

However, it follows that the heat of adsorption of NH on Pt is higher than 8·8 kcal., and that the reaction is exothermic. The heat of adsorption of NH undoubtedly greatly exceeds this limiting value, i.e. the reaction of NH_3 with adsorbed oxygen is highly exothermic.

It is difficult to calculate the energetics for all the elementary processes proposed in the scheme because of the lack of thermochemical data. A rough estimate indicates that the NH_3 oxidation is composed either of exothermic or of slightly endothermic elementary processes. Hence the assumption of low heats of activation of all elementary processes involved is justified.

3. Discussion of Experimental Data in Terms of the Proposed Scheme of Reaction.—We shall now discuss the results of experiments reported in the present and previous papers, and of other authors,[15, 23, 25] which were carried out at temperatures below 600°. Our experiments, the results of which are given in Fig. 1, 2 and 3, have been performed in manner analogous to that described by Tuszynski[2] and Marczewska.[3] Information on experiments concerning Fig. 4 and 5 can be found in a paper by Winnicki.[4] In Fig. 4 has been plotted a curve for constant temperatures from the data obtained in experiments performed at various temperatures and at constant flow rates.

---

[24] Gaydon, *Spectroscopy and Combustion Theory* (Chapman Hall, London, 1942), 71, 157, 173.

[25] Mittasch and Frankenburger, *Z. Elektrochem.*, 1929, **35**, 927.

[26] Frankenburger and Hodler, *Trans. Faraday Soc.*, 1932, **28**, 289.

[27] Christiansen, *Det Kgl. Danske Videns. Selsk. Mat. fys. Medd.*, 1935, **13**, 12.

[28] Bredig, Koenig and Wagner, *Z. physik. Chem.*, 1928, **139**, 211.

[29] Raschig, *Z. angew. Chem.*, 1927, **40**, 1183; 1928, **41**, 265.

[30] Hofman and Korpium, *Ber.*, 1929, **62**, 3001.

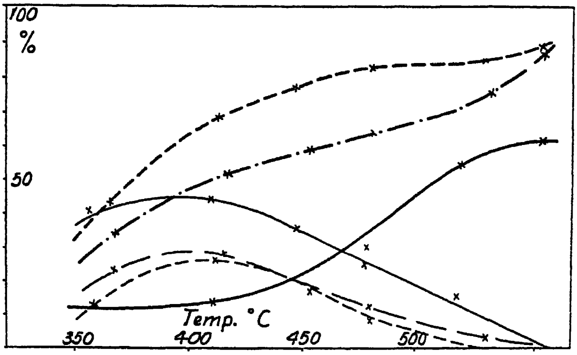

FIG. 1.—Catalyst : Pt gauze 3600 mesh per cm.², double-folded.
Incoming gases : 10 % NH_3+90 % air
Flow rates : 6 l./hr. ———— N_2O
━━━━ NO
12 l./hr. —·— N_2O
━·━ NO
24 l./hr. - - - - N_2O
▬ ▬ ▬ ▬ NO

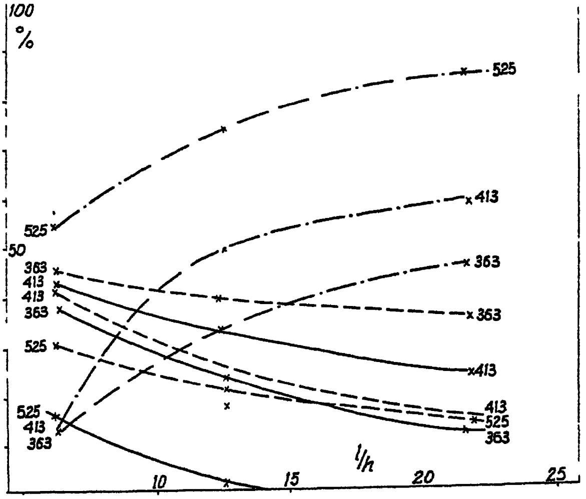

FIG. 2.—Catalyst : Pt gauze 3600 mesh per cm.², double-folded.
Incoming gases : 10 % NH_3+90 % air,
———— N_2O
— . — . — NO
- - - - - - N_2

In experiments recently carried out by Kepinski and Witczynski (Fig. 6, 7 and 8), NO, NO_2 and NH_3 were absorbed in concentrated H_2SO_4 as described in a paper by Zawadzki and Wolmer.[7] Special care was given to the complete removal of NO and NO_2. From the gases deprived of NO, NO_2 and NH_3 nitrous oxide was removed by cooling in liquid air.

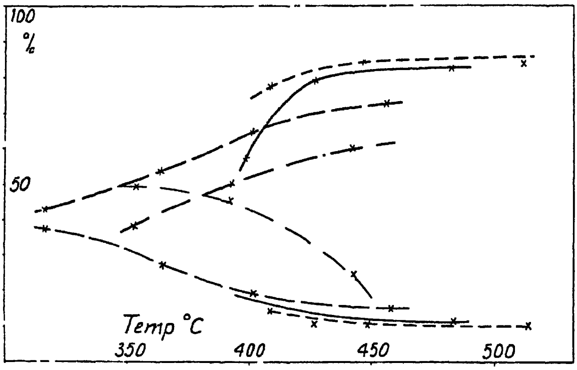

FIG. 3.—Catalyst : Pt gauze 3600 mesh per cm.^{2}, double-folded. Incoming gases : 12 % NH_3 + 29 % O_2 + 59 % N_2.

Flow rates : 4 l./hr —— · —— N_2O
—— · —— NO
8 l./hr. —— —— N_2O
—— —— NO
16 l./hr. ———— N_2O
———— NO
24 l./hr. – – – – N_2O
– – – – NO

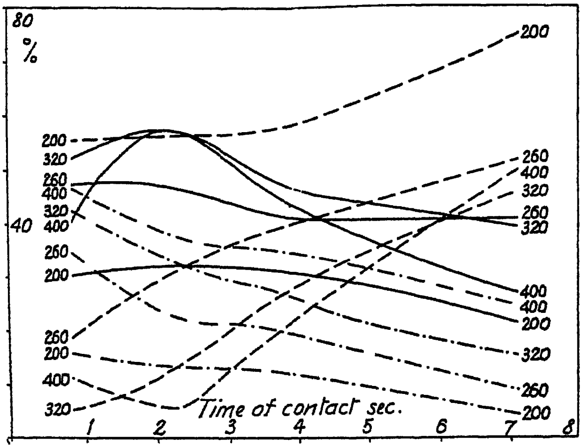

FIG. 4.—Catalyst : 35·58 % CuO + 65·62 % MnO_2. Incoming gases : 10 % NH_3 + 90 % O_2.

———— N_2O
— · — · — NO
– – – – N_2

The method of estimation of N_2O by the change of volume after passing over Pt is far from perfect. Some N_2O, though small in amount, is decomposed to NO + N_2 and the NO is then oxidized to NO_2.

In our latest experiments this error did not appreciably exceed 1 %. (Detailed data will be published by Kepinski at a later date.)

These results can be explained in terms of the reaction mechanism, given above. NH (formed by (1)), which is adsorbed on the catalyst, can react either with another NH radical, or NH_3 molecule ((4*a*) and (4*b*)), or with atomic oxygen ((3), and further conversion to N_2O), or even with HNO (5), or with molecular oxygen (2). This last reaction, giving NO as final product, undoubtedly has the greatest heat of activation due to the necessity of loosening the bond between oxygen atoms in a O_2 molecule in order to form HNO_2. This heat of activation is different for various catalysts and depends on their structures. This accounts for the different tempeıatures at which this reaction starts and the various rates of reaction observed at the same temperature for various catalysts. It follows that the formation of NO will be favoured but reaction (3) diminished by increasing temperature.

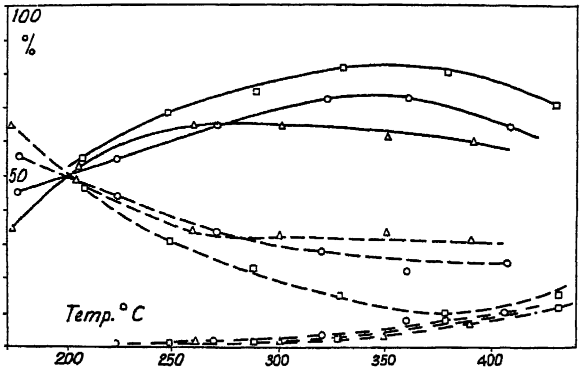

FIG. 5.—Catalyst: 79·45 % Fe_2O_3 + 11·53 % Bi_2O_3 + 7·21 % MnO_2.
Incoming gases: 10 % NH_3 + 90 % air.
————N_2O, ——.——NO, — — — N_2.
△ 100 l./hr., ○ 200 l./hr., □ 300 l./hr.

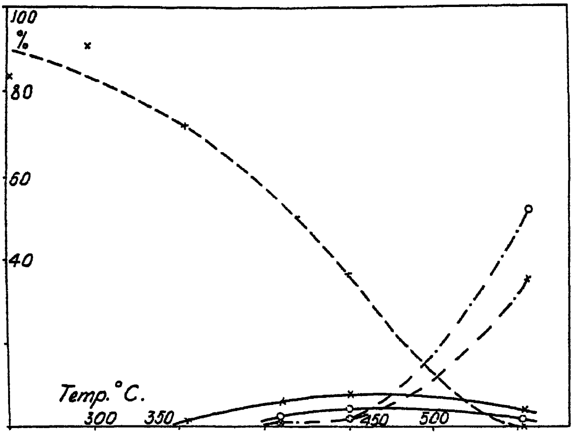

FIG. 6.—Catalyst: Bi_2O_3.
Incoming gases: 10 %NH_3 + 90 % air.
————N_2O, ——.——NO, — — — NH_3.
× 10 l./hr., ○ 20 l./hr.

There are several reasons why the yield of NO increases with increasing rates of flow. Naturally the decomposition of NO to elements is negligible, but at low rates of flow there is a possibility of a counter-current diffusion and consequently of a reaction of NO_2 with NH_3 which takes place before the catalyst bed and, at low temperatures, even in the first part of the bed. This leads to loss of NO already formed.

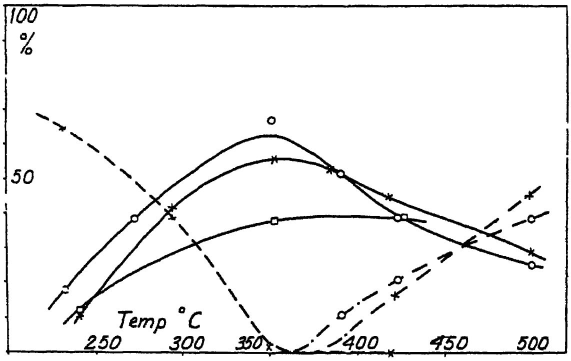

FIG. 7.—Catalyst : 45 % CuO, + 45 % MnO_2 + 10 % $CaCO_3$.
Incoming gases : 10 % NH_3+90 % O_2.
————N_2O, ——.——NO, — — — NH_3.
○ 5 l./hr., × 10 l./hr., □ 20 l./hr.

Some influence on the acceleration in formation of NO (as well as N_2O) from NH_3, is undoubtedly exerted also by the increasing rate of desorption of reaction products with the increase of the rate of flow. In the reaction on oxide catalysts yields of NO are considerably increased, when oxygen is used in place of air.

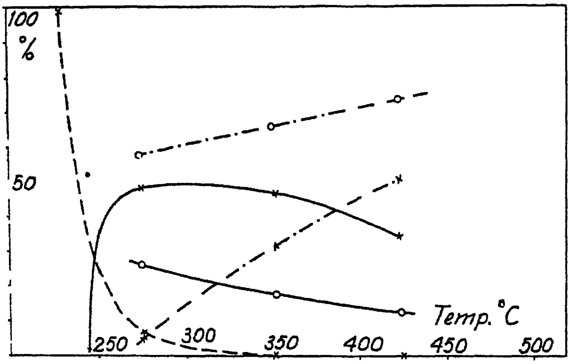

FIG. 8.—Catalyst : Pt gauze 1039 mesh per cm.^{2}, triple-folded.
Incoming gases : 10 % NH_3+90 % O_2.
————N_2O, ——.——NO, — — —NH_3.
× 4 l./hr. ○ 16 l./hr.

Moreover, there are other factors connected with the fact that the course of reaction is not uniform on the whole length of the catalyst bed. If we suppose the catalyst bed to be divided into a number of sections of equal width in the direction of gas flow, the reaction may practically cease after the gases have passed the first section, provided the rate of flow is sufficiently low. A two-fold increase of the rate of flow may result in reaction proceeding also in the second section, etc. Further sections of the bed are then inactive and only at high temperatures are they responsible for partial decomposition of previously formed NO.

The migration of adsorbed NH_3 molecules on the catalyst surface (Volmer [31]) could not alone explain these observations. Reagents are being consumed on their way through the catalyst bed : in the first part of it, more NH_3 and O_2 molecules strike a given area of catalyst surface in unit of time than in further parts where the reacting gases contain less NH_3 and O_2. The amounts of NH_3 and O_2 consumed, as well as the amounts of NH, etc. produced, then gradually diminish as the gases flow through the bed. Accordingly the concentration of adsorbed NH is greatest at the beginning. This exerts an influence on the velocity of reactions since the processes are exothermic and the amount of heat evolved at the beginning is greater than in the rest of the bed. The temperature therefore should be higher than that measured after the bed. This has been well illustrated in several experiments.[1, 8, 9] The higher the rate of flow, the greater the difference is. Now, as the yield of NO is strongly increased by increasing temperature, the influence exerted by flow rate on temperature prevailing in the bed constitutes another reason why the high rates of flow favour the good yields of NO.

The occurrence of N_2 in the products before the formation of NO is ascribed to reaction (6). Possibly another reason is the hypothetical reaction: $NH + HNO_2 = N_2O + H_2O$. At high temperatures, when NH_3 and NH are consumed rapidly, these reactions play no part at all, but they must be considered when unconverted NH_3 is present or when NH slowly reacts to HNO_3.

N_2O has been found on all catalysts. Although Krauss and Neuhaus [23] have not found it using Bi_2O_3, our own experiments, the results of which are shown on Fig. 6, prove that yields of N_2O on this catalyst are not insignificant. N_2O appears only at temperatures up to about 550°. The main cause is a rapid decomposition of N_2O, which takes place even below this temperature, and which was shown to be present in experiments on catalysts such as MnO_2, Mn_2O_3 and NiO,[23] by Kepinski on $CuO + MnO_2$, and by many authors on platinum.[6] With increasing temperature and constant rate of flow the yield of N_2O first rises to a maximum, then falls to zero. The difference between Pt and oxide catalysts is qualitative rather than quantitative. The yield diminishes at higher temperatures: because of (i) the decomposition of N_2O, and (ii) the increasing rates of reactions leading to NO.

The rising part of the yield against temperature plot is explained by reaction (3), and especially by (3*a*), which has a definite heat of activation though smaller no doubt than that of reaction (2). As a result of (3), comparatively small amounts of HNO are formed at low temperatures, since the chance of (3*a*) occurring is less at higher temperatures. This favours (5) and also a reaction between unconverted NH_3 and HNO giving N_2. This is an additional reason for the appearance of free nitrogen as a reaction product at the lowest temperatures.

The differences in the action of various oxide catalysts constitute an important argument that the process of N_2O formation goes through stages (1), (3) and (3*a*).

A BaO_2 catalyst [23] which decomposes to BaO and oxygen at comparatively low temperatures, gives N_2O as almost the sole product of NH_3 oxidation. Reaction proceeds in the same direction and with nearly equal yields, independently of whether the usual mixture of NH_3 and O_2 or one of NH_3 with N_2 is used. BaO too gives high amounts of N_2O and, as atomic oxygen is available in smaller quantities, large proportions of free nitrogen are formed. All the oxides which easily undergo conversion to lower stages of oxidation give high yields of N_2O, as atomic oxygen is here available for reactions (1) and (3). Especially interesting are experiments with NiO.[23] In NiO lattice an excess of oxygen is present and an excess proportionality of N_2O to amount of oxygen has been found.

---

[31] Volmer and Adhikari, *Z. physik. Chem.*, 1926, **119**. Adhikari and Felman, *ibid.*, 1928, **131**, 34. Volmer, *Trans. Faraday Soc.*, 1932, **28**, 359.

The examination of changes of N_2O yield with varying rates of flow on different catalysts is important for better understanding of the mechanism of reaction. There are considerable differences in the action of Pt and oxides, though some of the latter approach Pt in their behaviour.

The results of our experiments on oxide catalysts, where one can expect high amounts of atomic oxygen to be available, are shown in Fig. 4, 5 and 7. Analogous results were obtained by Winnicki[4] and Nagel.[15]

These experiments prove that the yields of N_2O, within the wide range of temperatures under consideration, increase with diminishing time of contact. This can be explained by an increased rate of desorption of N_2O, and by the fact that in the first part of the catalyst bed, where the main portion of NH_3 reacts, we have to deal with high concentrations of NH on the catalyst only when the rates of flow are high. Because atomic oxygen is available in considerable proportions, the concentration of NH on the catalyst surface constitutes the rate-controlling factor. Deviations observed in Fig. 4 at very short times of contact can be due to the true temperature in the first part of the bed being higher than that actually read on a milivoltmeter. In Fig. 7, we have also to note that reactions (3*a*) and (3) are not so rapid as reaction (1), and that consequently, when rates of flow are high, conditions can arise such that the influence of a reaction of NH with HNO on the final result is considerable.

When there is less atomic oxygen available, as with Bi_2O_3, the dependence of N_2O yield is similar to that observed on Pt. On Pt the yield of N_2O at constant temperature decisively diminishes with increasing flow rates (Fig. 1, 2, 3, 8). In this case oxygen is only adsorbed on the catalyst surface, probably forming a unimolecular layer. The regeneration of atomic oxygen which can take place only by surface adsorption, is then much more difficult than with oxides, where the typical reaction is $MeO_2 = MeO + O$. From the proposed scheme it follows that the atomic oxygen is necessary for a very rapid reaction (1), as well as for the slower reaction (3). When small proportions of oxygen are available the chances of N_2O formation diminish. This explains why we cannot obtain as high yields of N_2O on Pt or Bi_2O_3 as on the oxides of the type Fe_2O_3 or MnO_2, which easily undergo regeneration in oxidizing atmosphere.

It can be seen from the scheme that half of the atomic oxygen needed for reaction (1) is regenerated in reaction leading from HNO_2 to NO. This is independent whether we consider the mechanism to be represented by eqn. (2*a*) and (2*a*′), or by (2*b*), or even by (2*a*), (2*b*), (3) of Bodenstein's scheme. The remaining atomic oxygen has to be supplied either by way of adsorption of O_2 from the gas phase, or by oxidation of a lower oxide formed in reaction (1). The situation is worse in reactions leading to N_2O. The atomic oxygen is not regenerated at all, nor is it in reactions which give N_2. In addition we must have atomic oxygen not only for reaction (1), but also for (3), i.e. twice as much as when NO is the product.

The higher the rate of flow of gases through the catalyst bed, the more ammonia reacts in unit time on a given area of catalyst surface, and the more atomic oxygen is needed for reaction (1). When it is available only in limited amounts, as with Pt, it is primarily consumed by reaction (1), because it is more rapid than (3) and because it precedes it. We see then, that by high flow rates, unfavourable conditions for (3) and (3*a*) arise. On the contrary, favourable ones arise for (2), especially at high temperatures, as molecular oxygen is always available. When the flow is low, chances of formation of HNO and N_2O are higher, because less atomic oxygen is necessary, particularly at low temperatures. Free nitrogen appearing in NH_3 oxidation may be formed in reactions (4*a*) and (4*b*), as well as in (5) to (8).

An assumption that imide is the first intermediate product of reaction explains the oxidation of HCN and also the reduction of NO by excess hydrogen up to 90 % yield. Neumann and Manke[33] in work on HCN oxidation consider NH to be an intermediate product, and some of our experiments lead to the same conclusion. When HCN is oxidized on Pt and oxygen is available in insufficient proportions, we find in the "post-reaction" gases considerable quantities of NH_3 and carbon is deposited in the catalyst bed. When HCN with N_2 is passed through the Pt gauze in absence of oxygen, $(CN)_2$ is in the reaction products.

These facts are explained by the following reactions:

$$2HCN = (CN)_2 + H_2;$$
$$3HCN + O_2 = NH + H_2 + 2CO + N_2 + C$$
$$NH + H_2 = NH_3.$$

Evidently the normal oxidation of HCN by oxygen adsorbed on Pt gives a complex HCNO which immediately decomposes into $NH_{ads.} + CO$.

In the reduction of NO,[1, 32] when hydrogen is used in excess, a film of atomic hydrogen is formed on Pt, and this reacts as follows:

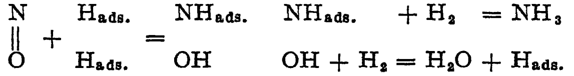

$$\begin{array}{ccccl} N & & H_{ads.} & & NH_{ads.} \\ \| & + & & = & \\ O & & H_{ads.} & & OH \end{array} \qquad \begin{array}{l} NH_{ads.} + H_2 = NH_3 \\ \\ OH + H_2 = H_2O + H_{ads.} \end{array}$$

4. The Effect of Temperature on the Rate of Reaction.—The oxidation of NH_3 to NO is rapid[1] in spite of its complicated course. Reactions such as the catalytic synthesis of ammonia proceed at a much lower rate. This needs an explanation as does a sudden increase of the velocity which occurs on Pt within a small range of temperatures. Studying NH_3 oxidation on oxide catalysts, we found in numerous experiments that the difference of temperatures at which reaction starts and at which NH_3 has practically completely disappeared is from about 100° to 400° or more (cp. also [23, 15]). This difference on Pt does not generally exceed 50° (e.g. Fig. 6, 8).

With the oxide catalyst the increase of rate with temperature can be roughly explained in terms of the factor $e^{-A/RT}$ (A = heat of activation), but with platinum it is more difficult.

It is also difficult at first to understand a high velocity of adsorption of O_2 as atomic oxygen on platinum. Now in the formation of $CaCO_3$ from CaO and CO_2, or $CdCO_3$ from CdO and CO_2 etc., the process proceeds without activation at pressures not far from the equilibrium pressure.[34] In the reversed process (endothermic) the heat of activation is equal to the heat of reaction. When conditions are chosen so that the interface F, at which reaction occurs, remains practically constant, then k from $v = kF(p - p_0)$ is independent of temperature.[34, 36] There is, however, a powerful influence of a comparatively small change of temperature when F does not remain constant because of the formation of nuclei i.e. new centres of reaction, when the system is far from equilibrium (high values of $p - p_0$) and the temperature is high.[35]

This may be explained as follows. When a two-dimensional nucleus has been formed, the building-up of a layer of the new phase goes on rapidly (each of the CO_2 molecules striking the solid phase reacts with CaO to form $CaCO_3$). This is a mechanism analogous to that of a chain reaction and is a result of deformation connected with the liberation of energy in an exothermic process. A point situated near the place where reaction has just occurred is ready to take up another CO_2 molecule without hindrance.

---

[32] Andrussow, *Ber.*, 1927, **60**, 536.

[33] Neumann and Manke, *Z. Elektrochem.*, 1929, **35**, 751.

[34] Zawadzki and Bretsznajder, *ibid.*, 1935, **41**, 215.

[35] Zawadzki and Bretsznajder, *Trans. Faraday Soc.*, 1938, **34**, 951; *Z. physik. Chem. B*, 1933, **22**, 79.

[36] Zawadzki, *Fetskrift Tillägnad I. Arvid Hedvall, Göteborg*, 1948, 611; *Roczniki Chem.*, 1934, **14**, 823; 1938, **18**, 892.

A CO_2 molecule reaches this point not only directly from the gas phase, but possibly also as one of loosely adsorbed CO_2 molecules, which move over the surface (Volmer [31]). In ammonia oxidation it is probably easier for atomic oxygen to move over an oxide catalyst surface than over a platinum one and consequently the regeneration of atomic oxygen would be easier. On Pt there is a chemosorption of oxygen which can, by analogy, be considered as the formation of two-dimensional crystals. The points of the surface from which oxygen atoms are released, as result of a number of exothermic processes, can easily take up more oxygen from the gas phase and this chemosorption does not need any activation energy.

This is a qualitative hypothesis and is not yet definitely proved. I think, however, that a more precise analysis of this hypothesis can contribute to the explanation of the enormous velocity of such processes as the NH_3 oxidation on Pt, as well as of the rapid increase of velocity within a small range of temperature.

Laboratory of Inorganic Technology,
Institute of Technology,
Warsaw.

THE MECHANISM OF THE CATALYTIC HYDROGENATION OF ETHYLENE

By G. H. Twigg

Received 1st *May*, 1950

Ethylene has been hydrogenated on a nickel catalyst at −78° C with (*a*) a mixture of $H_2 + D_2$, and (*b*) the equilibrium mixture of $H_2 + HD + D_2$. Infra-red spectroscopic examination showed that the mixtures of ethanes produced in the two experiments were identical, and were different from an equimolar mixture of C_2H_6 and $C_2H_4D_2$. This is direct proof that in hydrogenation the hydrogen is first dissociated into atoms on the catalyst.

This result and the existing knowledge concerning the hydrogenation and exchange reactions are reviewed, and a mechanism for hydrogenation is proposed which accounts for all the known facts, and in particular for the temperature dependence of the energy of activation. Hydrogen is not adsorbed directly on the catalyst, but only through reaction with a chemisorbed ethylene molecule to form an adsorbed ethyl radical and an adsorbed hydrogen atom ; hydrogenation takes place through the addition of a further hydrogen atom to the ethyl radical, while exchange is controlled by the reverse of the first step. A further fast reversible reaction occurs in exchange between adsorbed ethylene and a hydrogen atom to form an adsorbed ethyl radical.

The mechanism of the hydrogenation of ethylenic double bonds on metal catalysts such as nickel has been the subject of much investigation. The determination of the kinetics alone has not thrown much light on this problem, but the discovery of the exchange reaction between ethylene and deuterium [1] appeared to offer a fresh approach. Horiuti and Polanyi [2] proposed the following reaction schemes :

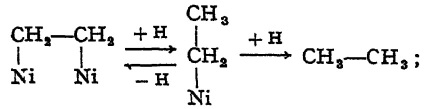

$$\begin{array}{c}CH_2—CH_2\\ |\qquad\quad |\\ \text{Ni}\qquad \text{Ni}\end{array} \underset{-\text{H}}{\overset{+\text{H}}{\rightleftharpoons}} \begin{array}{c}CH_3\\ |\\ CH_2\\ |\\ \text{Ni}\end{array} \xrightarrow{+\text{H}} CH_3—CH_3\,;$$

the first reaction and its reverse gives rise to exchange, whilst the addition of a second hydrogen atom to the "half-hydrogenated state" completes the hydrogenation. Farkas[1, 3] proposed different mechanisms, and suggested that the first step in exchange was loss of a hydrogen atom from the ethylene, and that hydrogenation was independent of exchange and proceeded through the simultaneous addition of a pair of hydrogen atoms.

---

[1] Farkas, Farkas and Rideal, *Proc. Roy. Soc. A*, 1934, **146**, 630.
[2] Horiuti and Polanyi, *Trans. Faraday Soc.*, 1934, **30**, 1164.

A fuller investigation of the exchange reaction with ethylene[4, 5] and with higher olefines,[6] and of the migration of the double bond in butene-1 which occurs simultaneously[7] with exchange, has provided a great deal of evidence that the exchange reaction did in fact proceed by the "associative" mechanism of Horiuti and Polanyi. The difference in order of reaction between exchange and hydrogenation predicted by Horiuti and Polanyi[2] did not, however, materialize, and the fact that both reactions were of the same kinetic order, and yet had different energies of activation, led Twigg and Rideal[4] to suggest that in both reactions the rate-determining step was reaction of a van der Waals' adsorbed hydrogen molecule with a chemisorbed ethylene molecule to produce on the one hand an adsorbed ethyl radical and an adsorbed hydrogen atom (exchange), and on the other hand a non-adsorbed ethane molecule (hydrogenation).

Farkas[8] pointed out that in many cases *cis*-addition of hydrogen took place, even though the product was not the more stable. Greenhalgh and Polanyi,[9] however, showed that this was not proof of the simultaneous addition of a pair of hydrogen atoms, since the attachment of the ethylene molecule to the catalyst prior to the formation of the half-hydrogenated state automatically means that addition of single atoms would occur in the *cis*-position.

It was realized that it would be possible to distinguish between these two mechanisms by a direct experiment in which ethylene was hydrogenated with a mixture of H_2 and D_2. The addition of single atoms would produce ethane of composition

$$\tfrac{1}{4}CH_3—CH_3 + \tfrac{1}{2}CH_3—CH_2D + \tfrac{1}{4}CH_2D—CH_2D,$$

whereas the simultaneous addition of a pair of atoms would produce a mixture of

$$\tfrac{1}{2}CH_3—CH_3 + \tfrac{1}{2}CH_2D—CH_2D.$$

These experiments were begun in 1938, but the analytical technique —infra-red spectroscopy—was not then sufficiently developed to distinguish easily these two mixtures. The development of automatically recording spectrometers of good resolution has enabled this experiment to be made.

Experimental

Hydrogenation must be carried out with a minimum of exchange, which means as low a temperature as possible. A supported catalyst was therefore used made by impregnating Kieselguhr pellets with nickel nitrate, igniting and then reducing in hydrogen at 300° C. The rest of the apparatus used was similar to that described previously.[4] With 7 g. of this catalyst in a reaction vessel of 400 ml. volume, the half life of a typical hydrogenation was about ¾ hr. at − 78° C.

Cylinder ethylene was given three single-plate distillations to remove high and low boiling impurities. C_2H_6 was prepared by reacting $C_2H_4 + H_2$ at −78° C for 15 hr. $C_2H_4D_2$ was prepared by reacting $C_2H_4 + D_2$ at −78° C. The relative importance of exchange with respect to hydrogenation declines as the temperature is lowered, and at −37° C on a similar catalyst it was shown that after the addition of deuterium to a sample of ethylene only 2 % of the hydrogen of the ethylene had been exchanged. The $C_2H_4D_2$ obtained should thus have been of over 95 % purity.

---

[3] Farkas and Farkas, *J. Amer. Chem. Soc.*, 1938, **60**, 22.
[4] Twigg and Rideal, *Proc. Roy. Soc. A*, 1939, **171**, 55.
[5] Conn and Twigg, *ibid.*, 1939, **171**, 70.
[6] Twigg, *Trans. Faraday Soc.*, 1939, **35**, 934.
[7] Twigg, *Proc. Roy. Soc. A*, 1941, **178**, 106.
[8] Farkas, *Trans. Faraday Soc.*, 1939, **35**, 906.
[9] Greenhalgh and Polanyi, *ibid.*, 1939, **35**, 520.

Two experiments were carried out :

Expt. 11. $C_2H_4 + H_2 + D_2$. The catalyst was treated with H_2 at −78° C for 6 hr. and the H_2 pumped off. To prevent the reaction $H_2 + D_2 \leftrightarrows 2HD$ occurring, the ethylene (107 mm.) was admitted first to the reaction vessel, and an additional 120 mm. of a 50–50 mixture of $H_2 + D_2$ added. Reaction was allowed to proceed for 18 hr., and the ethane produced was separated from residual hydrogen by passage through a trap cooled in liquid N_2.

Expt. 12. $C_2H_4 + H_2 + HD + D_2$. This experiment was carried out to obtain a product similar to that anticipated if addition proceeds atom by atom. A 50–50 mixture of $H_2 + D_2$ (120 mm.) was admitted to the catalyst at −78° C after the previous experiment. The reaction vessel was allowed to reach room temperature and kept there for 6 hr. before cooling to −78° C. Ethylene (107 mm.) was added and reaction allowed to proceed for 16 hr. The product was separated as before.

Analysis.—Infra-red spectra were recorded on a Perkin-Elmer Spectrometer Model 12B, at medium resolving power in the region 650-4000 cm.$^{-1}$ and at the highest resolving power over the range 670-890 and 1027-1450 cm.$^{-1}$. The cell length was 10 cm., and the pressure 700 ± 5 mm. Fig. 1 and 2 are photographs of relevant parts of the records obtained for (*a*) a mixture of 50 % C_2H_6 + 50 % $C_2H_4D_2$, (*b*) products of Expt. 11, and (*c*) products of Expt. 12.

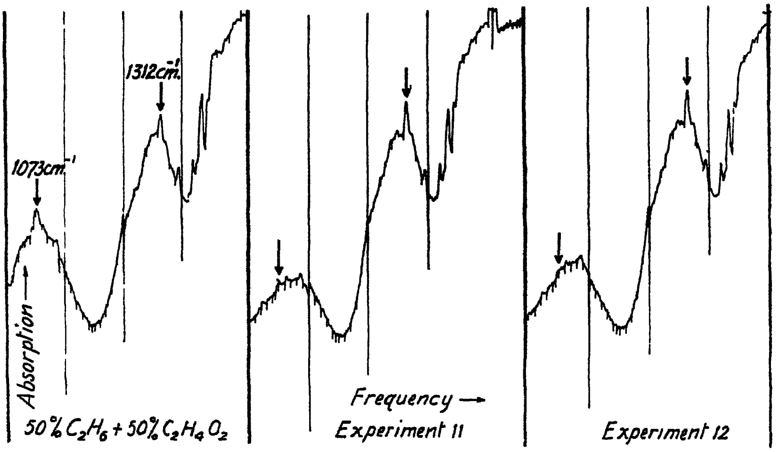

Fig. 1.—1027-1450 cm.$^{-1}$.

Infra-red spectra of deuterated ethanes,

(*a*) 50 % $CH_3—CH_3$+50 % $CH_2D—CH_2D$;
(*b*) from Expt. 11 ;
(*c*) from Expt. 12.

Note: The arrows mark the same wavelength on the other two spectra.

It is very clear that the ethanes from Expt. 11 and 12 are identical and different from the mixture of C_2H_6 and $C_2H_4D_2$. The identity was complete over the whole spectral range. No residual ethylene was observed (< 0·1 %).

In order to check that the reaction $H_2 + D_2 \rightleftharpoons 2HD$ was inhibited during the hydrogenation, the ortho-para hydrogen conversion was examined. Ethylene (48·9 mm.) was admitted first to the reaction vessel at − 78° C, and $p - H_2$ (75·8 mm.) added. Samples were removed at various times, ethylene and ethane separated, and the hydrogen analyzed in a coiled-coil type microthermal conductivity gauge [10] immersed in liquid N_2. The results are shown in the table.

---

[10] Bolland and Melville, *Trans. Faraday Soc.*, 1937, **33**, 1316.

Time (min.)	Residual Ethylene %	Conversion %
15	73	1
25	60	2
46	38·5	5
85	5·8	13
119	0·0	92

The half-life of the conversion in the absence of ethylene was 13 min.

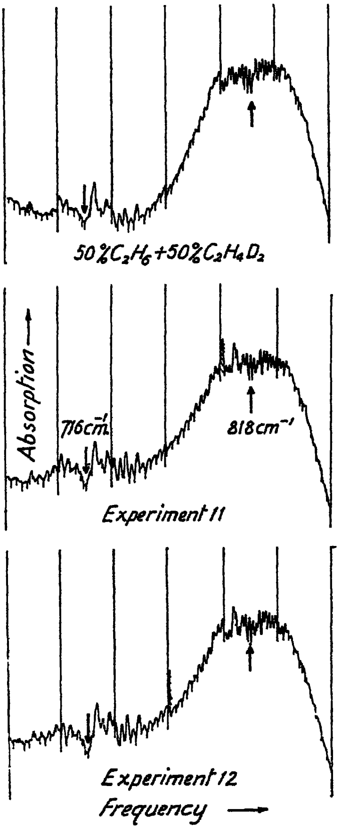

FIG. 2.—670-890 $cm.^{-1}$.

Infra-red spectra of deuterated ethanes,

(*a*) 50 % CH_3—CH_3+50 % CH_2D—CH_2D ;
(*b*) from Expt. 11 ;
(*c*) from Expt. 12.

Note: The arrows mark the same wavelengths on the other two spectra.

Discussion

The experiments show unequivocally that addition of hydrogen to the double bond does not take place in a single act, but that the hydrogen molecule is first split into atoms which then add one at a time.

The previous work has shown that exchange proceeds through attachment of ethylene to the catalyst at two points and the formation of the half-hydrogenated state. In considering the mechanism of hydrogenation, the following salient facts will be taken into account :

(*a*) The order of reaction is identical in exchange and hydrogenation, the rate being given by $p^0_{C_2H_4} \times p^n_{H_2}$ from − 78° C to + 150° C, where n is unity or slightly less.

(*b*) The energy of activation for exchange is greater than for hydrogenation.

(*c*) The energy of activation for both exchange and hydrogenation decreases with increasing temperature above about 100° C, although the order of reaction is unchanged and the reaction $H_2 + D_2 \rightleftharpoons 2HD$ is still inhibited.

(*d*) The ortho-para conversion and the reaction $H_2 + D_2 \rightleftharpoons 2HD$ are inhibited by ethylene except in so far as they proceed via exchange with the ethylene.

(*e*) The hydrogen returned to the gas phase during exchange between ethylene and deuterium is very largely H_2 molecules.

(*f*) Hydrogen is dissociated into atoms before hydrogenation.

Fact (*d*) means that the available surface is almost entirely covered with ethylene. The fact that the reactions are of zero and not negative order with respect to ethylene then means [11] either that the two gases do not compete for the same surface or that adsorption equilibrium by the Langmuir mechanism, is not achieved. The previous mechanism proposed for hydrogenation,[4] and that of Beeck,[12] take the former alternative. Beeck's mechanism, that gaseous ethylene reacts with adsorbed hydrogen, does, with certain assumptions, fit the kinetics, but is unsatisfactory in that it does not explain the exchange reaction, and particularly the close connection between the two reactions.

We are left, therefore, with the second alternative, that adsorption equilibrium is not maintained, and it is now proposed that up to 150° C the reaction $H_2 \rightarrow 2Ni{-}H$ is of no significance because the free surface available is too small; in other words, the adsorption of the ethylene is much faster than that of the hydrogen on the available bare surface. Also, in accordance with (*e*) above, the interchange of ethylene between the gas and the catalyst is much faster than that of the hydrogen. The present experiments have shown that hydrogen must be dissociated, and therefore adsorbed, before hydrogenation, and the following scheme is proposed:

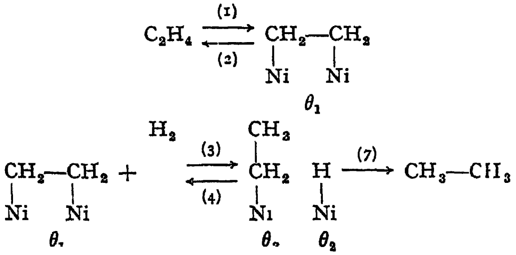

$$C_2H_4 \underset{(2)}{\overset{(1)}{\rightleftharpoons}} \underset{\theta_1}{\begin{array}{cc} CH_2 & \!\!-\!\! CH_2 \\ | & | \\ Ni & Ni \end{array}}$$

$$\underset{\theta_1}{\begin{array}{cc} CH_2 & \!\!-\!\! CH_2 \\ | & | \\ Ni & Ni \end{array}} + \overset{H_2}{} \underset{(4)}{\overset{(3)}{\rightleftharpoons}} \underset{\theta_3}{\begin{array}{c} CH_3 \\ | \\ CH_2 \\ | \\ Ni \end{array}} \; \underset{\theta_2}{\begin{array}{c} H \\ | \\ Ni \end{array}} \xrightarrow{(7)} CH_3{-}CH_3$$

Ethylene is adsorbed by opening of the double bond. The adsorption of the hydrogen takes place by reaction of a van der Waals' adsorbed molecule with an adsorbed ethylene molecule. Since exchange and hydrogenation have different energies of activation, this step (3) cannot be the rate determining one. Since both reactions have identical kinetics, the rate-determining step must proceed from the same adsorbed state, and therefore reaction (4) controls exchange while reaction (7) controls hydrogenation. Because the hydrogen returned to the gas phase during exchange between ethylene and deuterium is largely H_2, and reactions (3) and (4) would only give HD, we must add another and faster reaction

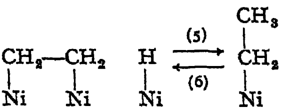

$$\begin{array}{cc} CH_2 & \!\!-\!\! CH_2 \\ | & | \\ Ni & Ni \end{array} \; \begin{array}{c} H \\ | \\ Ni \end{array} \underset{(6)}{\overset{(5)}{\rightleftharpoons}} \begin{array}{c} CH_3 \\ | \\ CH_2 \\ | \\ Ni \end{array}$$

---

[11] Twigg, this Discussion (comment on Prof. Laidler's paper).

[12] Beeck, *Rev. Mod. Physics*, 1945, **17**, 61; this Discussion.

These steps can be shown to explain all the features of the exchange and hydrogenation reactions.

If the fractions of the surface covered by the different species are as indicated, steady-state equations can be set up, the solutions to which give

$$\theta_2 = \left[\frac{k_3k_6}{k_5(k_4 + k_7)}p_{\mathrm{H}_2}\right]^{\frac{1}{2}},$$

$$\theta_3 = \left[\frac{k_3k_5}{k_6(k_4 + k_7)}p_{\mathrm{H}_2}\right]^{\frac{1}{2}}\theta_1.$$

The expression for θ_1 is more complex, but is in agreement with the fact that θ_1 is close to unity for the temperature range considered. Then:

$$\text{Rate of hydrogenation} = k_7\theta_2\theta_3,$$

$$= \frac{k_3k_7}{k_4 + k_7} \cdot p_{\mathrm{H}_2}\theta_1.$$

$$\text{Rate of exchange} = k_4\theta_2\theta_3,$$

$$= \frac{k_3k_4}{k_4 + k_7} \cdot p_{\mathrm{H}_2}\theta_1.$$

These expressions show both reactions to be of the same kinetic order, i.e., rate proportional to the first power of the hydrogen pressure, and independent of the ethylene pressure (since $\theta_1 = 1$). The term p_{H_2} should strictly be replaced by the concentration of hydrogen in the van der Waals' layer, so that at low temperatures the order of reaction is reduced slightly below unity.

The ratio, exchange/hydrogenation $= k_4/k_7$ and therefore the difference in energies of activation of the two reactions $(E_4 - E_7)$ should be constant over the entire temperature range, as was found.[4]

The above expressions for the rates of reaction now provide an explanation of the long-known fact that the energy of activation for hydrogenation,[13, 14] and for exchange,[4] decreases with increasing temperature above *ca.* 90° C, and even becomes negative. Previous explanations [14] have attributed the phenomenon to desorption of the ethylene, but it has been shown that this does not occur until temperatures above 150° C. There are two extreme cases:

(*a*) Low Temperatures. Hydrogenation faster than exchange, i.e.

$$k_7 > k_4.$$

$$\text{Rate of hydrogenation} = k_3p_{\mathrm{H}_2}\theta_1, \qquad E_{\mathrm{H}} = E_3;$$

$$\text{Rate of exchange} = \frac{k_3k_4}{k_7} \cdot p_{\mathrm{H}_2}\theta_1, \qquad E_X = E_3 + E_4 - E_7.$$

(*b*) High Temperatures: Exchange faster than hydrogenation, i.e.

$$k_4 > k_7.$$

$$\text{Rate of hydrogenation} = \frac{k_3k_7}{k_4} \cdot p_{\mathrm{H}_2}\theta_1, \qquad E_{\mathrm{H}} = E_3 + E_7 - E_4;$$

$$\text{Rate of exchange} = k_3p_{\mathrm{H}_2}\theta_1, \qquad E_X = E_3.$$

On proceeding from low to high temperatures, both energies will decline by the term $E_4 - E_7$.

---

[13] Rideal, *J. Chem. Soc.*, 1922, **121**, 309. Tucholski and Rideal, *ibid.*, 1935, 1701. Maxted and Moon, *ibid.*, 1935, 1190.

[14] Schwab, *Z. physik. Chem. A*, 1934, **171**, 421. zur Strassen, *ibid.*, 1934, **169**, 81.

Taking the value previously determined[6] for

$$E_X - E_H = 9{\cdot}0 \text{ kcal.} = E_4 - E_7,$$

and taking $E_3 = 11$ kcal., and noting[6] that rate of exchange = rate of hydrogenation at 90° C, a curve was constructed of log rate of hydrogenation against $1/T$. It showed the typical behaviour associated with this reaction and the apparent energies of activation at different temperatures were as tabulated.

T °C	E_H (kcal.)
21	10·4
40	9·8
84	7·3
143	3·4
203	2·5

At temperatures above about 150° C, it has been shown[4] that desorption of ethylene begins to set in, and the apparent energy of activation will decline further, and become negative. There is, however, a partial compensation as the uncovering of the surface now permits direct entry of the hydrogen ($H_2 \rightarrow 2Ni{-}H$).

Numerical values for the individual energies of activation can be estimated. Making the not unreasonable assumption that the heats evolved (x) in the following two reactions are equal:

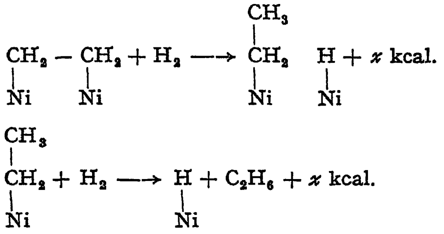

$$\underset{\displaystyle\text{Ni}}{\underset{|}{CH_2}} - \underset{\displaystyle\text{Ni}}{\underset{|}{CH_2}} + H_2 \longrightarrow \overset{\displaystyle CH_3}{\overset{|}{\underset{\displaystyle\text{Ni}}{\underset{|}{CH_2}}}} \quad \underset{\displaystyle\text{Ni}}{\underset{|}{H}} + x \text{ kcal.}$$

$$\overset{\displaystyle CH_3}{\overset{|}{\underset{\displaystyle\text{Ni}}{\underset{|}{CH_2}}}} + H_2 \longrightarrow \underset{\displaystyle\text{Ni}}{\underset{|}{H}} + C_2H_6 + x \text{ kcal.}$$

and taking the heats of adsorption for hydrogen (17 kcal.) and ethylene (36 kcal.) calculated by Eley,[15] one finds $x = E_4 - E_3 = 7$ kcal., and $E_5 - E_6 = 10$ kcal. Using Beeck's values for heats of adsorption on covered surfaces, $x = 11$ kcal. and $E_5 - E_6 = 1$ kcal. Assuming $E_3 = 11$ kcal. from low-temperature hydrogenation, $E_4 = 18$ kcal. (Eley) or 22 kcal. (Beeck), and $E_7 = 9$ kcal. (Eley) or 13 kcal. (Beeck).

It should be possible to estimate E_5 and E_6 from data on double bond migration, since this reaction is mainly effected by the faster processes (5) and (6) above. On this scheme,

$$\begin{aligned} \text{Rate of double bond migration} &= k_6\theta_3 \\ &= \left(\frac{k_3k_5k_6}{k_4 + k_7}\right)^{\frac{1}{2}} \cdot p_{H_2}^{\frac{1}{2}}\theta_1. \end{aligned}$$

However, experiments[16] showed that all three reactions were of the same order ($p_{H_2}^{\frac{1}{2}} \cdot p_{\text{butene}}^{\frac{1}{2}}$) and that the olefine did not completely cover the surface.[16] The above equations cannot therefore be applied, since it is probable that direct adsorption of the hydrogen was taking place.

---

[15] Eley, this Discussion.

[16] Twigg and Rideal, *Trans. Faraday Soc.*, 1940, 36, 533.

I am pleased to record my indebtedness to Messrs. A. R. Philpotts and W. Thain who carried out the infra-red spectroscopic analyses. My thanks are also due to Mr. R. D. Richards for assistance with the experiments, and to the Directors of the Distillers' Company Limited for permission to publish this work.

The Distillers' Company Limited,
Research and Development Department,
Great Burgh, Epsom, Surrey.

THE EFFECT OF CRYSTAL PARAMETER ON HYDROGENATION AND DEHYDROGENATION

By O. Beeck and A. W. Ritchie

Received 7th February, 1950

Through measurement of the surface of oriented and unoriented evaporated porous nickel films by the B.E.T. method, using neon, krypton, methane and butane, and by measuring the number of crystallographic sites through the adsorption of hydrogen at liquid nitrogen temperature, direct proof has been obtained that (110) oriented nickel films do also expose (110) planes to the gas phase.

A study of the hydrogenation of benzene over oriented and unoriented nickel and iron films showed no difference in rate in contrast to the previously reported 5-fold rate for the hydrogenation of ethylene over (110) oriented nickel films in comparison to unoriented films. It is concluded that the observed slow hydrogenation, which kinetic considerations show, proceeds through the adsorbed state of benzene, is not influenced by the crystal geometry of the substrate.

In contrast, the dehydrogenation of cyclohexane over unoriented platinum, was found to be 10 times faster than over partially (110) oriented platinum films, indicating that the geometrical factor is of great importance in this reaction, the kinetics of which is in agreement with the assumption that cyclohexane loses 6 hydrogen atoms simultaneously when colliding with the catalyst surface.

Following the hypothesis of Balandin, this reaction should be facilitated by (111) faces, which should be more abundant in unoriented than in (110) oriented films.

I. Experimental Proof for Surface Exposure of (110) Planes in Gas-induced Orientation of Nickel Films.—In an earlier publication Beeck, Smith and Wheeler [1] have shown that by controlling the pressure of an inert gas during evaporation of metals such as nickel, iron and others, unoriented and oriented porous metal films could be produced at will. Completely oriented nickel films were obtained with an inert gas pressure of about 1 mm., the (110) plane, the least dense of the planes, lying parallel to the backing and the two remaining planes showing random distribution. Films evaporated in high vacuum were found to be unoriented. The oriented nickel films were found to have twice the surface for hydrogen adsorption per gram of metal and were about ten times as active as catalysts for the ethylene hydrogenation than the unoriented films. The oriented films therefore had five times the intrinsic activity of unoriented films. Oriented and unoriented films were found to have approximately the same thickness for the same weight, that is the same density. This demands that the oriented films have smaller pores (or a pore size distribution favouring smaller pores) since the internal surface for hydrogen adsorption per gram of metal is twice that of unoriented films.

---

[1] Beeck, Smith and Wheeler, *Proc. Roy. Soc. A*, 1940, **177**, 62.

Several arguments were presented [1] (which will not be repeated here) why the crystallites of gas evaporated nickel films showing (110) orientation parallel to the backing should also actually expose (110) planes to the gas phase. No direct experimental proof was offered at that time, although all indirect proof, especially the catalytic experiments, pointed to the correctness of this deduction, particularly the fact that films evaporated in an inert gas pressure of 10 mm. were unoriented but had the intrinsic activity of oriented films. This was explained by the assumption that under conditions of high gas pressure small crystallites of nickel would form in the gas phase with (110) planes exposed and that these crystallites would then be deposited randomly to form the unoriented film of not only the intrinsic catalytic activity of oriented films but also of an especially large specific surface.

It is the purpose of Part I of this paper to bring a direct proof that gas-induced orientation of evaporated nickel films produces (110) planes as the metal-gas interface.

Experimental

It is generally accepted that when hydrogen is chemisorbed on a clean metal surface, such as a nickel surface, that each hydrogen atom occupies one crystallographic site. This has been shown by electron diffraction,[2, 3] but is also borne out by adsorption experiments [1] and by the fact that the heat of adsorption is high, 30 kcal. per mole for the sparsely covered nickel surface and 15 kcal. for the completely covered surface.[5] Thus measurement of the number of hydrogen atoms adsorbed affords a means of measuring the number of crystallographic sites irrespective of size. Beeck, Ritchie and Wheeler [4] (see also [5]) have shown recently that such measurements have to be done cautiously, having in mind that hydrogen is also *ab*sorbed into the interior of the metal structure. Initial adsorption at liquid nitrogen temperature of − 196° C and 0·1 mm. pressure represents a true measure of the number of sites available for adsorption, although, as has been shown,[3] the total sorption at room temperature as measured shortly after admission of the gas is in close agreement with the value for adsorption at − 196° C.

The total surface, irrespective of the number of crystallographic sites, can be measured by the Brunauer, Emmett, Teller (B.E.T.) method.[6] However, this method will give correct results only when no chemisorption of the gas employed takes place. The author and his co-workers have found [5] that nitrogen which is generally used in the B.E.T. method cannot be used with clean nickel, iron and many other metal surfaces because nitrogen is adsorbed on nickel at − 196° C with a heat of adsorption of 10 kcal. for the sparsely covered surface decreasing to 5 kcal. for the completely covered surface.[3, 5] The nitrogen molecule occupies two crystallographic sites and is probably only partially dissociated. This chemisorption, which cannot be detected by the usual B.E.T. procedure using nitrogen at liquid nitrogen temperature, causes the surface to appear too large by a factor of 1·55 in the case of nickel. Accordingly, gases have to be used whose adsorption is of known van der Waals' type at the temperature of measurement. Neon, krypton and butane were used in this investigation at such temperatures as to make the number of molecules in the gas phase of nearly the same order of magnitude as the number adsorbed on the small surface studied. This is necessary in order to obtain the desired high accuracy and can be achieved by using suitably small saturation pressures. The use of krypton at − 196° C for the measurement of small surfaces comparable with those of the metal film has been previously described by Beebe.[7] By measuring the number of sites relative to the total surface in cm.^{2} for oriented and unoriented nickel films, the average size of the site for each type of film can be established.

[2] Rupp, *Z. Elektrochem*, 1929, **35**, 586.

[3] Germer, *Z. Physik*, 1929, **54**, 408.

[4] Beeck, Ritchie and Wheeler, *J. Colloid Sci.*, 1948, **3**, 505.

[5] Beeck in *Advances in Catalysis*, Vol. II (Academic Press, New York, 1950). Beeck, Cole and Wheeler, this Discussion.

[6] Brunauer, Emmett and Teller, *J. Amer. Chem. Soc.*, 1938, **60**, 309.

[7] Beebe, Beckwith and Honig, *ibid.*, 1945, **67**, 1554.

It will be seen that for unoriented films the surfaces measured by the B.E.T. method using molecules of different sizes agree well within the limits of experimental error. The oriented films, however, with their larger surfaces and smaller pores gave surfaces markedly dependent of the size of molecule used, making it necessary to extrapolate to the size of the hydrogen molecule since the chemisorption of hydrogen is used for comparison. For this purpose the area of the hydrogen molecule was taken as 1 Å². This figure may be somewhat arbitrary because adsorbed hydrogen atoms have been shown [3, 5] to migrate from site to site and the pore size necessary for this fast migration (as distinguished from the slow diffusion into the crystal lattice) would be difficult to evaluate. It will be seen, however, that whatever the choice of this figure, within the possible limits, it has little bearing on the quantitative conclusions to be drawn.

The surface measurements with neon were carried out at 16° K in a Collins helium cryostat. A full description of the experimental details will be published later.

The cross-sectional areas of methane, krypton and neon were calculated by means of the formula $A = 1{\cdot}52 \times 10^{-16} (M/\rho)^{2/3}$, where ρ is the liquid density and M the molecular weight. The area of n-C_4H_{10} was calculated by the method of Livingston [8] assuming that the molecule lies flat on the surface as a cylinder with the diameter of 4·75 Å (the distance of nearest approach between two hydrocarbons) and with a length of 1·29 Å per carbon atom.

The procedure of producing the evaporated metal films has already been described in detail.[1]

Results

The experimental results are presented in Table I and in Fig. 2. Fig. 1 shows the B.E.T. plots for Expt. 7, 8 and 9, where the hydrogen adsorption at − 196° C and the B.E.T. surface measurements with neon, krypton and butane were done on the same oriented film. The hydrogen adsorption was carried out first after experimental proof was obtained that adsorbed hydrogen had no measurable effect on the B.E.T. surface measurements. Expt. 5 and 6 were made with two different oriented films, the hydrogen adsorption at − 196° C preceding the B.E.T measurements. Numbers 2, 3 and 4 are averages of measurements on several different unoriented films. In these experiments the hydrogen adsorption at 23° C was used, while Expt. 1 was preceded by a hydrogen adsorption measurement at − 196° C. The average value for the area per H atom site for the unoriented films is 6·17 Å² and is independent of the size of molecule used for the B.E.T. measurement.

TABLE I

No.	Film Type	Ads. Temp. °C	Gas	Unilayer Molecules Per 100 mg. Ni × 10⁻¹⁸	Area per Molecules Å²	Surface Area m.²/g.	H_2 Ads. per 100 mg. Ni Molecules × 10⁻¹⁸	Area per H Atom Site Å²
1	Unoriented	−196	Kr	6·15	14·6	9·00	7·28	6·18
2	Unoriented	−196	Kr	5·85	14·6	8·55	6·9	6·18
3	Unoriented	−196	CH_4	5·40	15·68	8·46	6·9	6·14
4	Unoriented	−78	n-C_4H_{10}	3·48	24·5	8·53	6·9	6·18
5	Oriented	−196	Kr	11·70	14·6	17·09	13·33	6·42
6	Oriented	−257	Ne	15·00	9·95	14·92	10·35	7·25
7	Oriented	−196	Kr	12·08	14·6	17·64	13·85	6·37
8	Oriented	−78	n-C_4H_{10}	5·29	24·5	12·95	13·85	4·68
9	Oriented	−257	Ne	20·00	9·95	19·90	13·85	7·18
10	Dep. Temp. −183° C Unoriented	−196	Kr	3·68	14·6	5·37	6·9	3·9

---

[8] Livingston, *J. Amer. Chem. Soc.*, 1944, **66**, 569.

Extrapolation to 1 Å^2 for the oriented film is obviously best done by a curve through the points from Expt. 7, 8 and 9, where the same film was used. This happens to be a straight line and extrapolation leads to the value 8·65 Å^2 for the (110) oriented films.

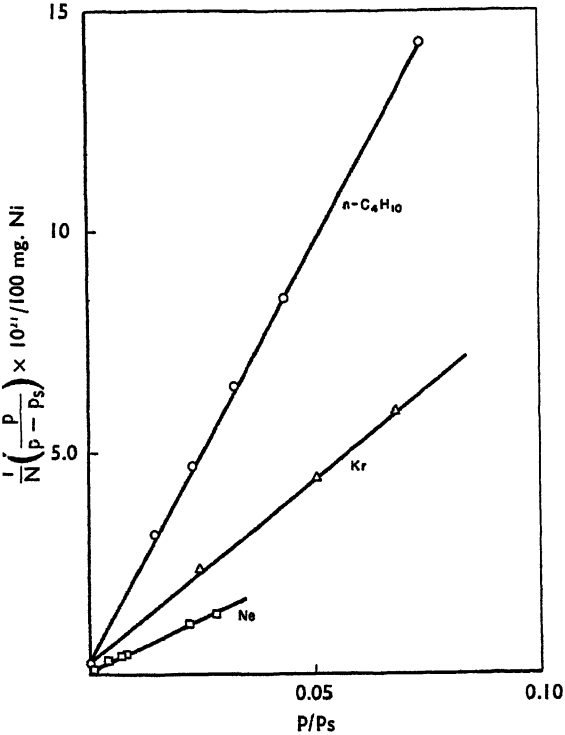

FIG. 1.

Discussion

The X-ray values for the short and long distances in the face-centred cubic nickel lattice are 2·48 Å and 3·51 Å, respectively. The (110) site area is therefore 2·48 × 3·51 = 8·70 Å^2 in unexpectedly good agreement with the experimental value of 8·65 Å^2. The area of the (100) site is $2{\cdot}48^2 = 6{\cdot}15$ Å^2, again in excellent agreement with the experimental value of 6·17 Å^2. Since planes involving higher indices would undoubtedly adsorb more than 1 H atom per site, it may be safely concluded that (110) oriented films exhibit only (110) planes to the gas phase. In the case of the unoriented films the agreement with the (100) site area may be more fortuitous since the average size of the three major planes including the (111) plane is $\bar{A} = 5{\cdot}84$ Å^2 very close to the (100) value. If, therefore, only a small number of planes along the cube edges were (110) planes and another small number at the corners were (111) planes, one would expect an overall value close to that of the (100) plane. It was also shown [1] that relatively heavy high vacuum films (film weights of several hundred mg. were used in these experiments) showed a tendency to slight (110) orientation with increasing thickness, if deposited at 23° C. Since such films showed also a slightly increased activity per unit weight, it must be concluded that heavy high vacuum films expose a certain unknown fraction of (110) planes also for this reason. One film (Expt. 10) was deposited at — 183° C and the size for the site derived from this measurement is 3·9 Å^2 indicating that (111) planes with an area of 2·66 Å^2 are fairly abundant. The straight line relationship between the surface of the oriented films and the size of the molecules employed for its measurement shows perfect randomness of pore size.

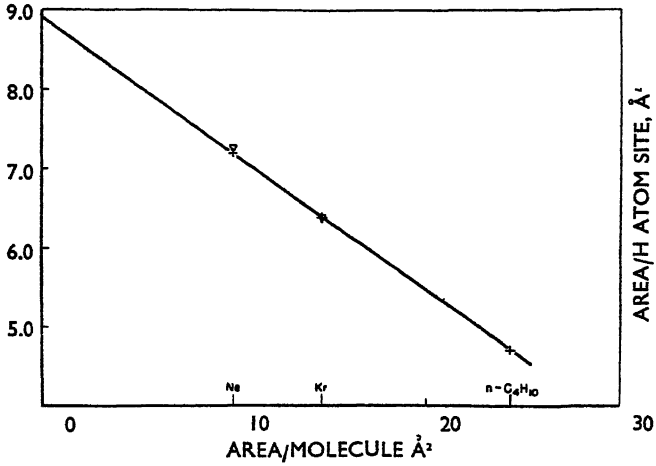

FIG. 2.

The dependence of surface on pore size makes it also necessary to adjust the ratio of the intrinsic activities of the two film types. It was earlier reported [1] that the intrinsic activity of oriented nickel films for the hydrogenation of ethylene was about five times greater than for unoriented film. If it is assumed that the surface available for ethylene hydrogenation in oriented films is the same as that measured by methane adsorption (which would be the lower limit), the new factor becomes 5 × 1·4 = 7, as can readily be deduced from Fig. 2, since the earlier comparison was based on hydrogen adsorption only. Oriented evaporated nickel films are, therefore, at least about seven times more active than unoriented films.

II. Hydrogenation of Benzene and Dehydrogenation of Cyclohexane.—After having demonstrated that (110) planes are exposed in oriented evaporated nickel films and are at least five, but possibly seven times more active (see Part I) as catalyst for the hydrogenation of ethylene than the planes exposed by unoriented films (which may either be (100) planes only or contain some (110) and (111) planes also) it was tempting to test such films for the hydrogenation of benzene or the dehydrogenation of cyclohexane for the latter of which Balandin [3] has proposed his "multiple adsorption" hypothesis. According to this hypothesis dehydrogenation of cyclohexane takes place on the octahedral face, i.e. (111) planes, of a face-centred cubic metal lattice. He further specified that the lattice constant must lie between those of nickel and palladium. Since at the temperature necessary for dehydrogenation (about 300° C) nickel and iron films sinter to the extent that they lose nearly completely their internal surface [4] only the hydrogenation of benzene at 23° C and at about 60° C was studied over these two metals. Dehydrogenation of cyclohexane was carried out over tungsten, nickel and platinum films. No systematic study was attempted in these experiments.

---

[3] Balandin, *Z. physik. Chem. B*, 1929, **2**, 289; *ibid.*, 1929, **3**, 167.

Experimental

The experimental technique was that used previously [1] except that metal valves were used instead of greased stopcocks in order to avoid solution [9] of benzene and cyclohexane in the grease. The benzene was Merck Reagent, thiophene-free and was used without further purification, except for removal of air by repeated freezing at liquid nitrogen temperature and pumping to high vacuum. The cyclohexane was an A.P.I.-N.B.S. spectrographic standard sample of better than 99 % purity. All metal films were sintered at the reaction temperature at which they were to be used and the hydrogen adsorption at 23° C was used for a measure of the surface available for the reactions to be studied.

Results

Benzene Hydrogenation.—Both oriented and unoriented nickel films were active for the benzene hydrogenation at 58° C. The initial rates were slow, i.e. of the order of 1 mm. pressure decrease per minute for a benzene-hydrogen ratio of 1/3 at the initial total pressure of about 240 mm. The reaction was found to be independent of the benzene pressure and proportional to the 0·44th power of the hydrogen pressure at 58° C and proportional to the 0·56th power at 100° C. The rate at 19° C was six times lower than that at 58° C, corresponding to an activation energy of 8·7 kcal. for this temperature interval. The specific reaction rate per unit surface was found to be greater for the oriented films than for the unoriented film by a factor of 1·24.

Comparative experiments on nickel and iron were carried out at 23° C on unoriented films and the specific activity of nickel was found to be 2·3 times that of iron. All measurements are tabulated in Table II.

TABLE II

Run	Metal	Film Type	Reaction Temp. °C	$\overset{\circ}{p}_{H_2}$ (mm.)	$\overset{\circ}{p}_{C_6H_6}$ (mm.)	$-dp/dt$ per 100 mg. Corrected to $\overset{\circ}{p}_{H_2}$ = 183·0 mm. (mm./min.)	H_2 Ads./100 mg. at 23°C Molecules × 10^{-18} (Sintered at 23°C)	H_2 Ads./100 mg. at 23°C, Molecules × 10^{-18} Sintered at Reaction Temp. (Calc.)	Relative Activity	Remarks
1	Ni	Oriented	58	181·0	57·5	1·48	8·42	6·31	0·234	Evaporated at 0° C
2	Ni	,,	58	183·0	58·0	1·83	10·10	7·56	0·239	Evaporated at 0° C
3	Ni	Un-oriented	57	171·5	58·5	1·03	6·91	5·18	0·199	Film evaporated at −183° C
4	Ni	,,	58	159·5	40·5	1·02	7·51	5·63	0·181	,, ,,
5	Fe	,,	23	318·5	67·0	0·46*	11·90	11·90	0·039	Evaporated at 0° C
6	Ni	,,	21·5	342·0	63·0	0·52*	5·95	5·95	0·091	,, ,,

* Corrected to $\overset{\circ}{p}_{H_2}$ = 318·5.

Cyclohexane Dehydrogenation.—The cyclohexane dehydrogenation was investigated over tungsten and platinum films and was attempted over palladium. Those three metals sinter much less than nickel (see Table II). In spite of this fact tungsten was found to be inactive at 324° C. Platinum and palladium were both very active, although proper evaluation in the case of palladium was impossible due to the high rate of solution of hydrogen in this metal. The measurements on platinum are set forth in Table III.

[10] Beeck, this Discussion.

TABLE III

Run	Film Type	Reaction Temp. °C	p° Cyclohexane (mm.)	$\frac{dp/dt}{100\text{ mg.}}$ Corrected to 57·0 mm. Cyclohexane	H_2 Ads. 23° C After Sintering Molecules $\times 10^{-18}$	Relative Activity
1	Unoriented	324	57·0	14·8	0·57*	13·0
2	,,	324	58·0	7·48	0·34* (1·34†)	11·0
3	,,	324	29·5	10·60	0·45	11·6
4	,,	324	29·0	10·41	0·46	11·5
5	,,	324	32·5	6·63	0·31	12·1
6	,,	324	32·0	8·06	0·37	12·2
7	,,	324	32·0	7·98	0·36*	11·0
8	Partially oriented	325	57·0	1·06	0·37*	1·4
9	,,	322	57·0	0·57	0·37*	0·8
10	,,	324	57·0	0·85	0·37* (1·46)†	1·1

* Calculated (see text). † H_2 adsorption before sintering.

As shown in Fig. 3, where the logarithm of cyclohexane pressure is plotted against time, the initial reaction rate over platinum is first order with respect to the partial pressure of cyclohexane which allows for easy normalizing of the measured rates. From the temperature coefficient of the rates at 326° C and 356° C an activation energy of 9·3 kcal. was calculated. In Expt. 2 and 10 adsorption of hydrogen was measured at 23° C before sintering, and in agreement with previous findings there is little difference in the adsorption of oriented and unoriented films. In Expt. 3 to 10, hydrogen adsorption at 23° C after sintering was measured showing that one-third of the surface is still available after sintering at 325° C. In Expt. 1, 2, 7, 8, 9 and 10 hydrogen adsorption was not measured after sintering, and the values were calculated for 1, 2 and 7 from a plot of the figures in column 5 against those in column 6 for Expt. 3 to 6. The values for the oriented films 8, 9 and 10 were assumed to be the same and adjusted through the adsorption measurements of the unsintered films 2 and 10. From the ratio of the averages in column 8 it is seen that the unoriented films are more active by a factor 11·9/1·1 = ~ 11 than the oriented films. This figure is likely to be much greater since electron diffraction studies showed the " oriented " films to be partially oriented only.

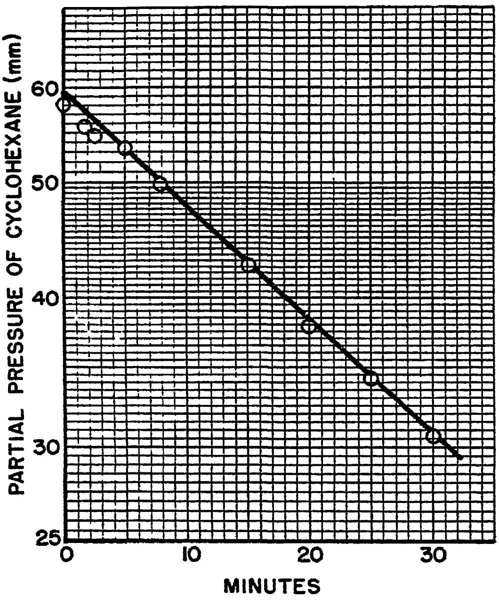

Fig. 3.

All that can be said with regard to palladium films is that a high-vacuum film which was not strictly unoriented but showed mixed orientation under electron diffraction study was for the same film weight 2·5 times more active than a (110) oriented film deposited in 1 mm. of nitrogen.

Discussion

Because of the zero-order reaction rate with regard to benzene it must be concluded that the benzene hydrogenation proceeds through the adsorbed state of benzene and is therefore possibly not subject to influence by the size of the crystallographic sites but is simply a function of total surface available which, as has been shown in Part I, is 1·4 times larger for oriented than for unoriented films for the same hydrogen adsorption. This should make the rate on oriented films 1·4 times faster. A smaller factor would be expected since benzene may not be able to enter the smallest pores. Within the experimental limtis the rates may be regarded as equal. If the same argument were applied to the comparison of unoriented iron and nickel films, iron should be 2·7 times more active than nickel if one assumes that the large (100) face is exposed. Actually the activity for the same hydrogen adsorption is half as large. Further discussion of this point will be postponed until after Part III.

The tenfold activity of unoriented films even over only partially oriented films suggests that Balandin's hypothesis may be operating if the assumption is made that unoriented films expose, in part at least, (111) planes. In the later stage of this reaction the adsorption of benzene poisons the reaction, reducing the initial rate of a second run on the same film by a factor 20.

It is likely that the inactivity of tungsten films (the surface of which after sintering at 325° C is still about 1/2 of that at 23° C) is due to poisoning by a reaction product with the surface. Experimental proof of a highly unsaturated residue was obtained by admitting small amounts of cyclohexane to both platinum and nickel films at 250° C. In both cases 4 hydrogen molecules appeared in the gas phase for each cyclohexane molecule admitted. Even at room temperature cyclohexane is strongly adsorbed on tungsten and nickel with evidence that dissociation to benzene and hydrogen takes place. This strongly suggests that poisoning by residues is responsible for the inactivity of tungsten.

For further discussion of the results presented in Parts I and II of this paper in connection with other aspects of metal film catalysis see (10).

Shell Development Company,
Emeryville,
California.

ALLOY CATALYSTS IN DEHYDROGENATION*

BY GEORGE-MARIA SCHWAB

Received 24th October, 1949

In homogeneous Hume-Rothery alloys the activation energy of the formic acid dehydrogenation increases in proportion to the square of the increase of the electron concentration caused by the multivalent solute metal. Amongst the intermetallic Hume-Rothery phases, the γ-phase shows a maximum activation energy. In general, activation energy and electric resistance run parallel. It is concluded that the catalytic activation consists in an entrance of substrate electrons into empty levels of the first Brillouin zone of the metal. It is suggested that in alloys containing polar or covalent bonds the conductivity electron concentration is lowered. Catalytic experience confirms this view. The frequency factors of the dehydrogenation reaction on different catalysts increase logarithmically with increasing activation energy. The mechanical hardness of alloys runs parallel with the activation energy, and it is concluded that the hardness is a function of the saturation of the Brillouin zone. This is confirmed catalytically for martensite.

---

* Contribution from the Dept. of Inorganic, Physical and Catalytic Chemistry of the Institute Nicolaos Canellopoulos, Piraeus, Greece.

It has often been suggested [1, 2] that the catalytic action of metals, where the cycle is not a simple oxidation-reduction one, is connected with their electronic structure. Only recently, direct proofs for this view are appearing, e.g. in Bockris's [3] connection between overvoltage and work function. In this case, however, it is not yet clear if a discharge of ions or a catalytic recombination of atoms is rate-determining. A direct comparison of catalytic action and electronic structure has been found in our laboratory by the systematic study of the dehydrogenating action of alloy catalysts. In the present work, the activation energy of the dehydrogenation of formic acid vapour has been measured in presence of homogeneous alloys of varied electron concentration and intermetallic phases.

Kinetics.—In all cases of simple catalytic reactions, the Arrenhius equation

$$k = k_0 \, . \, e^{-q/RT},$$

or

$$\log k = B - q/4{\cdot}57T, \quad . \quad . \quad . \quad . \quad . \quad (1)$$

represents fairly well the experimental temperature dependence of the velociy constant k, q being known as activation energy. Only in zero-order reactions proceeding on entirely saturated active surfaces (centres), is k free from a temperature-dependent adsorption factor, so that q may be considered as the true activation energy required by the adsorbed molecules. The formic acid decomposition has been shown to be of this type.[4] As k_0 or its logarithm B contains the unknown active proportion of the geometrical surface, a determination of q is possible only by measuring the temperature coefficient

$$\frac{d \log k}{d(1/T)} = q \; 4{\cdot}57. \quad . \quad . \quad . \quad . \quad . \quad (2)$$

Special care is needed in such measurements so as not to confuse accidental activity alterations with the true temperature coefficient of k. Only complete coincidence of temperature-velocity curves, repeated at rising and falling temperatures, can yield reliable values of q. As a secondary result, empirical values of the frequency number, k_0 (or of B), are obtained, whose dependence on various factors form the object of separate study (see below).

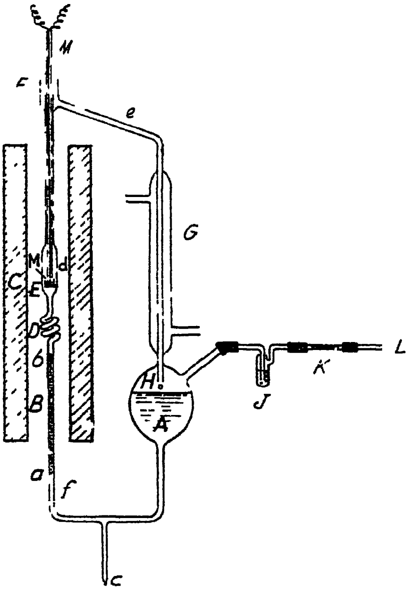

FIG. 1.

Experimental

The experimental arrangement developed for this purpose and used in most of the work, is shown in Fig. 1.[5] Liquid formic acid is contained in the vessel A which communicates with the evaporator B, filled with glass particles or fine capillaries. In that particular zone of B which, by means of the electric furnace C, is maintained just at the boiling point, the liquid is evaporated smoothly and the vapour at atmospheric pressure passes over the catalyst in E. Undecomposed acid is recirculated by G, H, and the gaseous reaction products (CO_2+H_2) purified in J and K, enter a flowmeter at L. MM is the outer tube of a

---

[1] Goldschmidt, *Ber.*, 1927, **60**, 1263.

[2] Russell, *Nature*, 1926, **117**, 47.

[3] Bockris, *ibid.*, 1947, **159**, 539.

[4] Hinshelwood, *J. Chem. Soc.*, 1923, **123**, 1014, and ref. [11].

[5] Schwab and Theophilides, *J. Physic. Chem.*, 1946, **50**, 427.

thermocouple, removable by a ground joint at the top of the apparatus. By this arrangement, the reaction velocity can be directly obtained for every temperature of the catalyst in runs at rising and falling temperatures. Always, after a short period of " formation " of the catalyst, coincident curves are obtained and evaluated in the form of log k — $1/T$ diagrams according to eqn. (1) and (2).

The alloys were prepared from chemically pure metals in porcelain crucibles under suitable molten salts in a gas blast-furnace, and the phases present were found by X-ray analysis. Ductile metals were used as foils, brittle alloys as pieces, and the total geometrical surface of the pieces estimated by measuring their dimensions.

Homogeneous alloys.[6, 7]—Silver dissolves most of the metals of Groups II-V of the Periodic Table to form Hume-Rothery's α-phases, without a change of the cubic face-centred lattice type, up to an electron concentration (EC) = 1·33 in the period VB (Cd, In, Sn, Sb) and EC = 1·1 in the period VIB (Hg, Tl, Pb, Bi). Thus, in these systems, it is possible to alter the EC at will without a radical change of the chemical and crystallographic character of the catalyst. The results of the kinetic measurements show that the activation energy using pure silver (17·6 kcal./mole) is always increased, by a few kcal./mole by " addition " of Cd, In, Sn, Tl, Hg, but by amounts up to 20 kcal./mole by Sb, Pb, Bi. The increase is not always strictly proportional to the concentration of the solute metal, but for small additions the results can be approximately represented by

$$q = q_{\mathrm{Ag}} + Ax(n - 1)^2, \quad \ldots \quad (3)$$

x being the atomic fraction of the solute metal, n its Group number or valency, and A a constant, amounting to 11 in the 5th and 100 in the 6th period if q is expressed in kcal. Similar results were obtained with elements of the 4th period ($A \sim 100$) and with solutions of thallium, lead, cadmium[8] and iron[9] in gold.

Hence, in homogeneous α phases the activation energy is increased when the EC is raised by dissolution of a multivalent solute, and this increase, exactly as is the electric resistance, is proportional to the square of the EC increase per solute atom. Likewise, within the domain of the densest hexagonal ϵ phase of Ag—Sb,[10, 7] the activation energy rises with increasing Sb content or EC.

Heterogeneous alloys and intermetallic phases.—In binary alloys consisting of two phases (Ag + Cu,[11] $\alpha + \gamma$, $\gamma + \epsilon$ and $\epsilon + \eta$ Cu-Sn,[7, 10] $\alpha + \beta$ and $\beta + \gamma$ Au-Cd,[8] Al + ϵ Ag-Al,[11] Au + Fe,[9] Cu + Cu_2Mg, Cu_2Mg + $CuMg_2$,[9]) the activation energy is generally found to lie between those of the component phases. The intermetallic phases or compounds themselves show different values. For the system Cu-Sn [7, 10] these are shown in Fig. 2, and for Au-Cd [8] in Fig. 3. Generally, the cubic face-centred phase β, the hexagonal densest phase ϵ and the hexagonal layer phase η show values not very different from

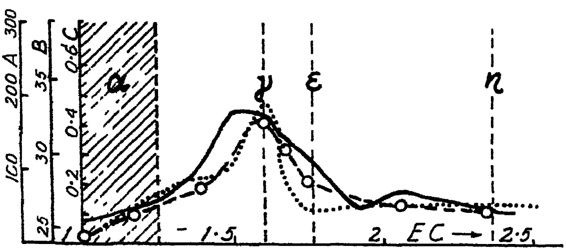

A ——— hardness: kg. mm.$^{-2}$
B – – ○ – act. energy: kcal. mole^{-1}
C …… resistance: Ω cm. 10^4

FIG. 2.

---

[6] Schwab and Holz, *Z. anorg. Chem.*, 1944, **252**, 205.
[7] Schwab, *Trans. Faraday Soc.*, 1946, **42**, 689.
[8] Schwab and Pesmatjoglou, *J. Physic. Chem.*, 1948, **52**, 1046.
[9] Schwab and Petroutsos, *ibid.*, 1950, **54** (in press).
[10] Schwab and Karatzas, *Z. Elektrochem.*, 1944, **50**, 204.
[11] Schwab and Schwab-Agallidis, *Ber.*, 1943, **76**, 1228.

that of the corresponding saturated α phase, while the more complicated cubic phase γ always gives a very distinct maximum of the activation energy. As Fig. 2 shows, and as can be shown for numerous other systems,[12] this exceptional behaviour of the γ phases concerns also the electric resistance and the hardness.

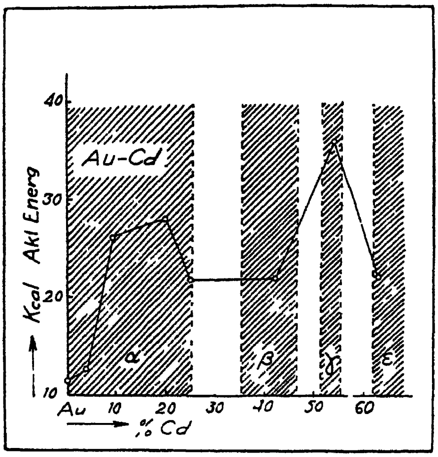

FIG. 3.

Theory of the electron influence.—According to the theory of Mott and Jones [13] the upper limit of stability of a purely metallic (Hume-Rothery) phase is given by that electron concentration at which the co-ordinated material waves of the fastest electrons just begin to be reflected by the most intensely reflecting lattice planes according to Bragg's law. At this limit, the surface of a sphere, constructed with the reciprocal half wavelength of the fastest electron as radius, touches from within planes of a polyhedron enclosed by planes parallel to the above lattice planes at distances from the centre of the sphere reciprocal to the respective lattice distances. This polyhedron is called the volume of the first Brillouin zone in the *k*-space. This theory permits a satisfactory theoretical calculation of Hume-Rothery's electron concentrations of the stable phases α, β, γ and ε. It is important that the volume of the first Brillouin zone at the stability limit is not filled by the sphere ; the corners of the polyhedra, amounting to about 30 % of the total zone volume α, β and ε, remain empty. It is in these corners that electrons, acquiring energy from an external field, can move, and this accounts for the fact that even saturated phases α, β and ε are still good conductors, although poorer than a pure monovalent metal with a half-empty zone. A remarkable exception is the γ phase. Its zone, as represented in the *k*-space, is, because of the complicated lattice structure, of a highly polyhedric, nearly spherical shape, and thus in the state of saturation it is almost completely (i.e. 88·5 %) filled by the sphere. Little room is left for accelerated electrons, and this at once accounts for the high resistance of γ alloys.

Now, our experimental results for the activation energies, for homogeneous alloys as well as for intermetallic phases, can be expressed in terms of the zone theory as follows. The activation energy increases within the domain of one phase according as the Brillouin zone approaches the saturation limit, and, comparing different phases, it is highest in the γ phase where there is the highest degree of zone completion. Thus, generally, empty levels in the zone favour the catalytic reaction. We are led to the conclusion that, to form an activated adsorbed formic acid molecule, electrons from it must intrude into the metal, and that this entry needs more thermal energy the more the metal is already saturated with electrons. Most probably the two protons of the formic acid molecule occupy extra lattice sites in the catalyst surface, while their electrons are " dissolved " in the electron gas of the metal.

[12] Schwab, *Experientia*, 1946, 2, 103.

[13] Mott and Jones, *The Theory of the Properties of Metals and Alloys* (O.U.P. 1936).

This picture of the activated state of dehydrogenation (and, of course, also of hydrogenation) agrees fully with the views generally accepted for the dissolution and activated adsorption of hydrogen. It gives, at the same time, a concrete interpretation, based on experiments, to the concept of a homopolar substrate-catalyst bond, by supposing a sharing of *substrate* electrons.

Theory of polar and covalent alloys.—The zone theory of metals and alloys is based on the assumption that the valency electrons of the metal atoms form a degenerated gas distributed according to Fermi statistics over the levels of the Brillouin zone. This is the extreme case of a purely metallic bond, as it occurs in typical metals and Hume-Rothery alloys. The same picture, however, has been successfully applied by Mott and Jones [13] to the description of lattices, which, from the crystallochemical point of view, are not purely metallic. E.g. in graphite, the four electrous per atom can be placed in one common Brillouin zone, and likewise in selenium, the six electrons per atom. However, many arguments suggest that in graphite three electrons per atom are localized in covalent bonds, and only one is a conductivity electron, and that in selenium two electrons per atom are localized in covalent bonds between neighbouring atoms of endless chains parallel to the *c*-axis, and only four electrons are conductivity electrons. This picture suggests a different treatment, viz. the electrons belonging to covalent bonds are placed in fully complete zones and only the conductivity electrons in a Brillouin zone of smaller *k*-volume. In fact, it has been shown [9] that a zone containing one electron per atom can be constructed from reflecting planes of the graphite lattice, and most probably a similar procedure is possible for selenium and other semi-metals.

This viewpoint is important in discussing the degree of saturation of the conductivity zone in alloys other than of the Hume-Rothery type, containing covalent or polar bonds in addition to the metallic bond. In these, probably, the number of free electrons to be placed in a conductivity zone, taken from X-ray data, is less than the total number of valency electrons of the constituent atoms, because electrons are used in forming covalent bonds or anions. From this point of view, a relatively low activation energy will be an argument in favour of non-metallic bonds.

Different alloy systems have been examined. In the Au-Fe system, on dissolution of a few atomic per cent. of iron in the gold lattice, the activation energy and specific resistance are higher due to the two valency electrons contributed by the iron atom. At higher percentages, however, the magnitude of both properties decrease again, indicating, in agreement with magnetic data, that valency electrons now enter the gaps of the incomplete iron shell and disappear from the conductivity zone. Gold and antimony form a compound $AuSb_2$ having the lattice type of iron pyrite FeS_2. Its activation energy was found to be nearly equal to that of a saturated solution of antimony in gold. This reveals a relatively low degree of saturation of the first Brillouin zone. Apparently, the covalent bond between the pair of antimony atoms uses most of the valency electrons of antimony. In the compound Cu_2Sb, the antimony atoms are isolated from each other. Nevertheless, this compound shows the same activation energy as the Sb-poorer ϵ phase, an energy only slightly higher than that of pure copper. Hence, even here, the antimony electrons do not fill the conductivity band, the antimony atoms being anions or at least neutral. In the system Cu-Mg, the ordered cubic compound Cu_2Mg has a much increased activation energy. This, together with the lattice data, show that the binding is almost entirely metallic, as in Hume-Rothery alloys. The other compound $CuMg_2$ shows an activation energy much lower even than that of copper itself. As the lattice data indicate a purely metallic bond, the first Brillouin zone must have an extremely low degree of saturation. This is not due to chemical bonds in this case, for the X-ray diagram of this phase reveals that the polyhedron representing the zone volume is far from spherical in shape and very sparsely filled by the inscribed sphere. The result with Cu_2Mg was confirmed by the behaviour of the isomorphous compound Au_2Pb. This, also, does not exhibit an increase of activation energy, as compared with lead-saturated gold.

Frequency numbers.—Hitherto, only the activation energy, the term q in eqn. (1), has been considered. The actual absolute reaction velocity is determined by this and the temperature-independent frequency factor k_0 or its logarithm B. This factor, in a zero-order reaction, ought to be a lattice frequency of $\nu \sim 10^{13}$ sec.$^{-1}$, multiplied by the number of moles covering the unit surface. Expressed in flow rate of the reaction products, this product has been calculated [5] to be 10^{11} to 10^{12} cm.^{3} min.$^{-1}$ cm.$^{-2}$. The experimental evidence [14] shows that this value gives an upper limit only for fully active surfaces. In real systems, the measured B-values are much less, and the smaller this is, the lower is the activation energy. The empirical relation

---

[14] Schwab, *Proc. XI Int. Congr. Pure Appl. Chem.* (London, 1947).

$$B = B_0 + q/h \quad . \quad . \quad . \quad . \quad . \quad (4)$$

has been shown [14] to be a general law of heterogeneous catalysis. It indicates that a low activation energy is always, at least in part, compensated by a low B-value. Eqn. (4) is explained by assuming that centres with high activation energies at a catalytic surface are more frequent than very active centres with low activation energies. The magnitude h is a parameter determining the distribution law of the active centres in the surface. It often [15] depends on the temperature at which the distribution equilibrium has been established. Fig. 4

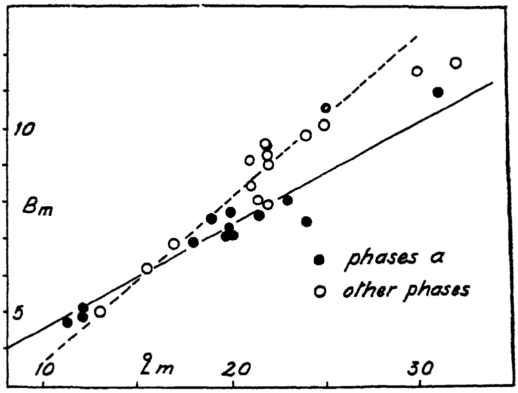

FIG. 4.

shows that eqn. (4) is valid for alloy dehydrogenation catalysts. B has been plotted against q, and two straight lines represent the results approximately, one for the cubic face-centred metals (α phases) and another one for other lattice types. We assume, at least preliminarily, that this does not signify a different h-value, but that it is due to the greater hardness of alloys other than α phases. This results in a greater roughness of the broken surfaces of the pieces, while B refers to the geometrical minimum surface.

Mechanical hardness.—The increase of hardness with increasing activation energy is a general feature of dehydrogenating alloys and very generally the hardness [12] shows the same dependence electron concentration and lattice type as do electrical resistance and activation energy. This is illustrated in Fig. 2 which contains the three curves for the Cu-Sn system. It has been shown [16] that the hardness increase is due to an increased formation energy of atom dislocations and it was suggested that this in turn is due to the greater resistance against increases in local atomic distance (zone volume decreases) found in phases with a nearly full Brillouin zone. From this point of view, the question whether an observed high hardness is of electronic or of structural nature, can be checked by measuring the activation energy of dehydrogenation. The hardness of carbon steel or of martensite may be due to the increased electron concentration of martensite as compared with ferrite (α iron), as similar hardness increases are observed in other alloy systems of similar EC. A direct proof is to be seen in the fact [9] that hardened steel dehydrogenates formic acid with an activation energy of 25 kcal./mole whereas soft pure iron or annealed steel requires 20 kcal./mole only.

Thus, it appears possible to utilize the dehydrogenation catalysis on the basis of its clear-cut electronic mechanism as a useful auxiliary method for alloy research.

Dept. of Inorganic, Physical and Catalytic Chemistry,
Institute Nicolaos Canellopoulos,
Piraeus,
Greece.

---

[15] Schwab and Pesmatjoglou, *Hedvall-Festskrift*, Göteborg, 1948, 533.
[16] Schwab, *Trans. Faraday Soc.*, 1949, **45**, 385.

THE PARAHYDROGEN CONVERSION ON PALLADIUM-GOLD ALLOYS*

By A. Couper and D. D. Eley

Received 30th January, 1950

The activation energy of the parahydrogen conversion on palladium-rich alloys is 3·5 kcal./mole and increases abruptly between 40 and 30 atomic per cent. palladium to the value of 8·5 kcal. found for gold-rich alloys. Magnetic measurements have identified this composition as corresponding to the complete filling of the *d*-band, or atomic *d*-orbitals, with electrons. Vacant *d*-orbitals are therefore essential for the low-temperature catalysis, and it is suggested that they bond the chemisorbed hydrogen atoms M—H. The reaction goes through a triatomic H_3 complex formed by entry of an H_2 molecule from the van der Waals layer,

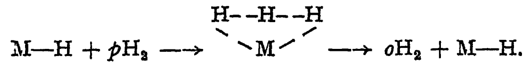

$$M{-}H + pH_2 \longrightarrow \overset{H--H--H}{\diagdown M \diagup} \longrightarrow oH_2 + M{-}H.$$

It is postulated that each site exerts two bonds to the activated complex, employing " atomic " d and hybrid $d^{2.56}$ $sp^{2.22}$ metallic orbitals. The values of temperature-independent factor found agree with earlier calculations for this mechanism. The *d*-band of palladium may also be filled by electrons from dissolved hydrogen atoms which cause a similar increase in activation energy.

This work [1] was initiated in Bristol University in 1945 in an attempt to relate the activity of transition metal catalysts to their electronic structure. In the past various efforts have been made to provide a theoretical basis for catalyst activity, by relating catalytic activity to lattice spacing. Thus, on the experimental side there are the papers by Balandin,[2] Long *et al.*,[3] Twigg, Herington and Rideal,[4, 5] and Beeck and his co-workers.[6, 7] On the theoretical side, calculations of the chemisorption of hydrogen molecules by the Eyring-Polanyi method indicate a marked effect of the lattice-spacing in the surface on the activation energy of the process.[8, 9] Recent advances in our knowledge of the metallic state now make it possible to begin a more fundamental approach to the problem, and to attempt to relate catalyst activity to the nature and occupation of the electronic energy levels of the catalyst.

All those metals active as hydrogenation catalysts fall into the group of transition elements, with the exception of copper which, in general, has a higher activation energy than the others. The atoms of these elements possess partly empty *d*-shells and the theory of the bulk metal may be treated by either of two methods. The first method, due to Mott and

---

* Part I in a series of papers on the Electronic Basis of Catalyst Activity.

[1] Couper and Eley, *Nature*, 1949, **164**, 578.

[2] Balandin, *Z. physik. Chem. A*, 1927, **126**, 267; *B*, 1929, **2**, 289; *B*, 1929, **3**, 167.

[3] Long, Frazer and Ott, *J. Amer. Chem. Soc.*, 1934, **56**, 1101.

[4] Twigg and Rideal, *Trans. Faraday Soc.*, 1940, **36**, 533.

[5] Herington, *ibid.*, 1941, **37**, 361.

[6] Beeck, Smith and Wheeler, *Proc. Roy. Soc. A*, 1940, **177**, 62.

[7] Beeck, *Rev. Mod. Physics*, 1945, **17**, 61.

[8] Sherman and Eyring, *J. Amer. Chem. Soc.*, 1932, **54**, 2661. Sherman, Sun and Eyring, *J. Chem. Physics*, 1934, **3**, 49.

[9] Okamoto, Horiuti and Hirota, *Sci. Papers Inst. Phys. Chem. Res., Tokyo*, 1936, **29**, 223.

Jones,[10] is an extension of the free-electron theory of Bloch, and considers that the "valency" electrons lie in two energy bands, a broad *s*-band overlapping a narrow *d*-band. The *s*-band can accommodate at most two electrons per atom and the *d*-band 10 electrons per atom, and thus there is a relatively high density of energy states in the *d*-band. The electrons fill up both bands to the same energy level. Hence in the element palladium, of the 10 valency electrons approximately 9·4 enter the *d*-band and 0·6 enter the *s*-band. Thus, there are 10 − 9·4 = 0·6 positive holes in the *d*-band. Alloying this metal with approximately 60 atomic per cent.* of silver or gold lowers the paramagnetism to zero, in agreement with the above model, which requires that the *s*-electron of the added monovalent element goes to fill the 0·6 holes in the *d*-band of the palladium. Besides paramagnetism, positive holes in the *d*-band give rise to high heat capacity, electrical resistance, and other properties. On this view we should be inclined to associate the catalytic activity of the transition metals with their partly empty *d*-band,[11] and a promising line of investigation should be the catalytic activity of an alloy such as that of palladium with gold, where changes in lattice spacing are small. That it is not entirely possible to separate lattice spacing from electronic structure effects in metals is shown by the valence bond treatment due to Pauling.[12] This author, also arguing from the magnetic data, considers that the bonds between atoms in a transition metal are electron pair bonds using hybrid metal orbitals built up from 2·56 $4d$ orbitals, the $5s$ and 2·22 $5p$ orbitals, viz. $(d)^{2\cdot56}\,s(p)^{2\cdot22}$. The remaining 2·44 d orbitals are "atomic" orbitals. Of the valency electrons available in the transition metals, 5·78 are supposed to be used for bonds, so that in palladium with 10 electrons 4·22 are left to enter the atomic orbitals, leaving $2 \times 2{\cdot}44 - 4{\cdot}22 = 0{\cdot}66$ unpaired electrons in the atomic orbitals.

The 5·78 bonds resonate between the 12 neighbours surrounding the centre atom. Thus, what are holes in the *d*-band on the free electron theory are unpaired *d*-electrons on the Pauling theory. These actual numbers were developed to explain the chromium-copper series, but are approximately applicable to palladium.

In any attempts to apply such theories to catalysis, it is easiest to assume, in the first instance, that the electronic structures of the bulk metal persist unchanged into the surface layer where catalysis occurs. Investigations of the theory of surface energy levels have been made on the basis of the free electron model [13, 14, 15] but are not yet sufficiently developed to apply to transition metals. From the point of view of valence bond theory this means assuming that there is no change in orbital hybridization at the surface, either alone or in the presence of the reacting substrate.

While this work was in progress, our attention was drawn by the note by Dowden [16] to the interesting work of Rienäcker, who has made extensive investigations of the catalytic properties of alloys, though not from the theoretical viewpoint adopted here. His latest paper with Sarry,[17] will be discussed later. Magnetic and crystallographic data support the suitability of palladium-gold and palladium-hydrogen systems for the present work. Nickel has the complicating feature of ferromagnetism, and some of the other alloys show departures from the simple theory.

---

[10] Mott and Jones, *The Properties of Metals and Alloys* (London, 1936).

* All the alloy compositions in this paper are given as atomic percentages.

[11] Eley, *Research*, 1948, **1**, 304.

[12] Pauling, *Physic. Rev.*, 1938, **54**, 899; *J. Amer. Chem. Soc.*, 1947, **69**, 542. Pauling and Ewing, *Rev. Mod. Physics*, 1948, **20**, 112.

[13] Lennard-Jones, *Trans. Faraday Soc.*, 1932, **28**, 333.

[14] Shockley, *Physic. Rev.*, 1939, **56**, 317, and references cited therein.

[15] Pollard, *ibid.*, 1939, **56*y***, 324.

[16] Dowden, *Research*, 1948, **1**, 239.

[17] Rienäcker and Sarry, *Z. anorg. Chem.*, 1948, **257**, 41.

In palladium-gold the evidence [18] indicates that the lattice constant increases from 3·88 Å (Pd) to 4·07 Å (Au) almost linearly, all the alloys being homogeneous, face-centred cubic systems. No information is available on phase-separation in palladium-gold, but since no special heat treatment was given we may assume that all the alloys are in the " disordered " state, a view supported by the electrical resistance data given in the next section. For palladium-hydrogen there is the complication of two phases, α and β.[19, 20] For the α phase the lattice constant varies scarcely at all from 0 to 56 atomic per cent. hydrogen, being about 3·88 Å. Between 3 and 10 atomic per cent. hydrogen, however, the β phase appears, with a lattice spacing varying upwards from 3·97 Å. The existence of this second phase is little understood.

Experimental

The palladium-gold alloy wires, 42 S.W.G., 0·1032 mm. diameter, were obtained from Johnson Matthey, Ltd. A satisfactory check on their homogeneity and composition is given by values of the specific resistance. As shown in Fig. 1, these agree very well with the earlier data of Geibel.[21] The catalyst consisted of a 15 cm. length of wire sealed down the axis of a cylindrical Hysil reaction vessel. This was connected via a liquid air trap and mercury cut-off to an apparatus essentially the same as that used in the work on tungsten wires.[22] The apparatus was baked out initially and the resistance-temperature relation established for the catalyst wire. The reaction vessel was then immersed in liquid oxygen, parahydrogen admitted, and at zero time the catalyst filament was heated electrically to the required temperature. The hydrogens used were all purified by passage through a palladium thimble and stored over sodium films. Analyses were made with a microPirani gauge.[23]

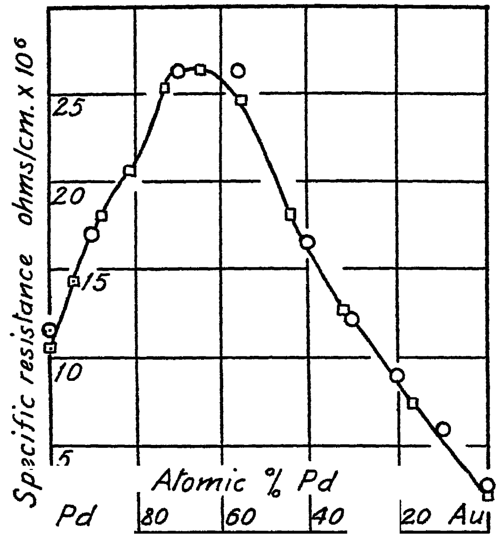

FIG. 1.—The specific resistance of the alloy wires used as catalysts, compared with the data of Geibel.

□ W. Geibel ; ⊙ Alloys used as catalysts.

---

[18] Mundt, *Ann. Physik*, 1934, 19 (5), 721.

[19] Linde and Borelius, *ibid.*, 1927, 84 (4), 747.

[20] Kruger and Gehm, *ibid.*, 1933, 16 (5), 174.

[21] Geibel, *Z. anorg. Chem.*, 1911, 69, 38.

[22] Eley and Rideal, *Proc. Roy. Soc. A*, 1941, 178, 429.

[23] Bolland and Melville, *Trans. Faraday Soc.*, 1937, 33, 1316.

A new method was used to clean the filaments from oxygen, since heating *in vacuo* to a high temperature was precluded by the low melting points of the alloys. The reaction vessel was surrounded by a coil of five turns of wire connected to an oscillator, immersed in liquid oxygen, and filled with 0·1 mm. hydrogen gas. On switching on the oscillator a current of 2·9 A at a frequency of 15 Mc./sec. passed through the coil, giving a luminous discharge which was continued for 5 min. The work of Johnson [24] and tests with the homogeneous parahydrogen conversion [25] showed that the concentration of hydrogen atoms in the discharge was quite adequate to clean the filament. It was essential to heat the wire *in vacuo* subsequently at 700-900° K to remove dissolved hydrogen atoms. This method was used with all the wires from pure gold to 90 atomic per cent. palladium, namely, Au, 10 % Pd, 20 % Pd, 30 % Pd, 55·2 % Pd, 70 % Pd. The solubility of hydrogen atoms in 90 % Pd and Pd was so high that it was found better to clean these wires by heating in *molecular* hydrogen at 600° K, followed by a period of outgassing at 700-900° K.

Activation Energy and Frequency Factor in Palladium-Gold Alloys.—A series of experiments was made for each wire at 1·2 mm. Hg pressure over as wide a range of temperatures as possible. In many cases the results were checked with a second specimen of wire. The reaction velocities were expressed in terms of the first-order constant k_e, defined below, which has frequently been found,[25, 22] and again in the present investigation, to describe accurately the course of the reaction. Here

$$k_e = \frac{1}{t}\ln\frac{C_0}{C_t},$$

where $C_0(C_t)$ is the concentration of parahydrogen in excess of the equilibrium value at time zero (t). A set of typical results in Fig. 2 shows that the effect

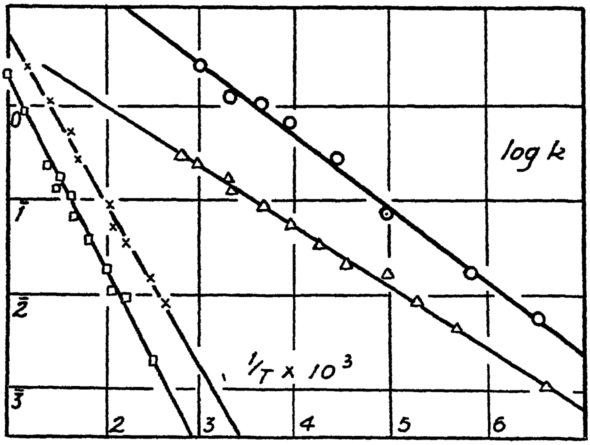

FIG. 2.—Typical Arrhenius lines for the parahydrogen conversion on Pd/Au alloys of smaller Pd content.

○ 55·2 atomic % Pd. × 30 atomic % Pd.
△ 40 ,, % Pd. □ 20 ,, % Pd.

of temperature is given by the Arrhenius equation, $k_e = Be^{-E/RT}$. In general, the activation energy E may be obtained with a maximum uncertainty of ± 0·3 kcal., with a corresponding uncertainty in B of a factor 4. To correct for differences in reaction volume V and catalyst area A, we employ $B^0 = B(V/A)$, the value of the frequency factor for unit volume and unit area, usually given in units of cm. min.$^{-1}$. The results are collected in Table I.

---

[24] Johnson, *Proc. Roy. Soc. A*, 1929, **123**, 603.

[25] Farkas, *Orthohydrogen, Parahydrogen and Heavy Hydrogen* (Cambridge, 1935).

TABLE I.—ACTIVATION ENERGY E AND FREQUENCY FACTOR B^0

Atomic % Pd in Alloy	Temp. °K	E cal. mole^{-1}	B min.$^{-1}$	B° cm. min.$^{-1}$
100 (*a*)	170-330	3640	$4{\cdot}68 \times 10^2$	$2{\cdot}75 \times 10^5$
100 (*b*)	170-330	3960	$1{\cdot}20 \times 10^3$	$7{\cdot}05 \times 10^5$
100 (*c*)	170-330	3980	$4{\cdot}90 \times 10^2$	$2{\cdot}59 \times 10^5$
100 (*d*)	170-330	3140	$6{\cdot}74 \times 10$	$3{\cdot}96 \times 10^4$
90	180-350	3980	$8{\cdot}51 \times 10^2$	$4{\cdot}82 \times 10^5$
70 (*e*)*	200-500	3470	$1{\cdot}15 \times 10$	$5{\cdot}40 \times 10^3$
70 (*f*)*	150-330	3170	$1{\cdot}02 \times 10^3$	$4{\cdot}80 \times 10^5$
70 (*g*)	150-330	2820	$7{\cdot}58 \times 10^2$	$3{\cdot}56 \times 10^5$
70 (*h*)	150-330	3190	$7{\cdot}59 \times 10^2$	$4{\cdot}10 \times 10^5$
55·2	170-330	3520	$6{\cdot}30 \times 10^2$	$2{\cdot}99 \times 10^5$
40	150-350	2960	$2{\cdot}04 \times 10$	$1{\cdot}14 \times 10^4$
40 (*j*)	200-400	3180	$2{\cdot}95 \times 10$	$1{\cdot}82 \times 10^4$
30	400-800	8000	$2{\cdot}34 \times 10^2$	$1{\cdot}18 \times 10^5$
20	370-1000	8950	$1{\cdot}51 \times 10^2$	$7{\cdot}41 \times 10^4$
20 (*k*)	370-1000	7850	$1{\cdot}31 \times 10^2$	$6{\cdot}35 \times 10^4$
10	300-750	8600	$6{\cdot}45 \times 10$	$3{\cdot}72 \times 10^4$
0 (*l*)	500-800	17500	$1{\cdot}25 \times 10^2$	$2{\cdot}06 \times 10^4$
0 (*m*)*	500-770	17500	$5{\cdot}83 \times 10^2$	$8{\cdot}31 \times 10^2$

* indicates not plotted in Fig. 3, 4.

Notes.—(*a*) First specimen—first determination. (*b*) First specimen—second determination. (*c*) Second specimen. (*d*) After "activation" by oxidation and reduction. (*e*) First specimen, heated at 600° K in hydrogen and then *in vacuo*. (*f*) First specimen, heated at 900° K in hydrogen and then *in vacuo*. (*g*) First specimen, discharge applied, outgassed at 800° K. (*h*) Second specimen, discharge applied, outgassed at 750° K. (*j*) Second specimen. (*k*) Second specimen. (*l*) Gold wire, 60 cm. long. (*m*) Gold foil in vessel, walls at catalyst temperature.

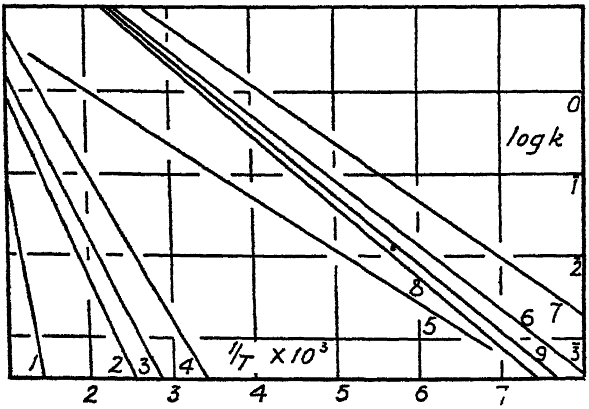

FIG. 3.—The parahydrogen conversion on the Pd/Au alloys (points omitted).

1. Pure Au.	4. 30 at. % Pd.	7. 70 at. % Pd.
2. 10 at. % Pd.	5. 40 ,,	8. 90 ,,
3. 20 ,,	6. 55·2 ,,	9. Pure Pd.

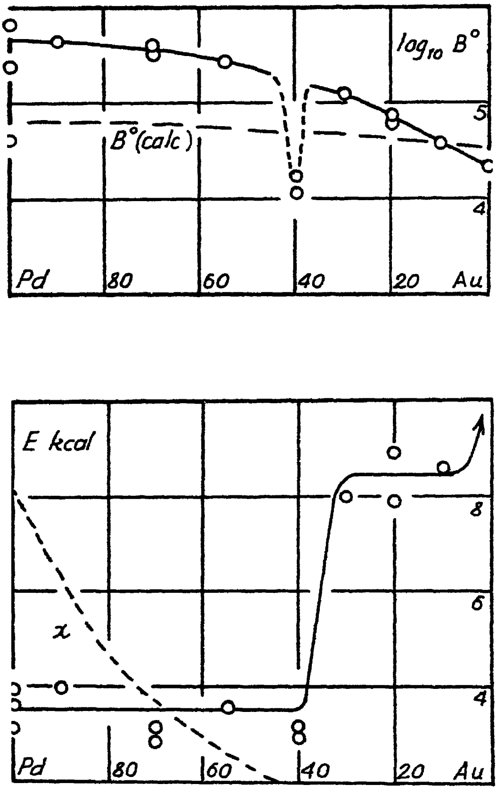

FIG. 4.—Activation energy and B° as a function of composition. The broken line x denotes the paramagnetic susceptibility in arbitrary units (Vogt, *Ann. Physik.*, 1932, 14 (5), 1).

The catalysts fall into two groups in a most striking fashion, as shown particularly in Fig. 3, or in Fig. 4 in which E and $\log_{10} B^{0}$ are plotted as a function of atomic composition.

The data in Table I are completely described by the footnotes, but one or two further points are of importance. Thus, as noted by Farkas,[26] a palladium wire heated at 573° K successively in oxygen, hydrogen and vacuum, has a more than usually active surface. The effect is seen to be due to a decrease in E, and there is also a decrease in B^{0} below the usual value, which would rule out the view that this treatment increases the surface area of the catalyst. Arguing from our results, described later, on the poisoning effect of hydrogen dissolved in palladium, we suggest tentatively that the effect of the initial oxygen treatment is to remove dissolved hydrogen atoms. This would imply that the wires prepared simply by heating in hydrogen, that is, the first three examples, still contained, even after prolonged outgassing, a little (perhaps 0.5 atomic per cent.) dissolved hydrogen.

The surface oxygen film seemed to vary somewhat in its reducibility by molecular hydrogen, from alloy to alloy. Thus, palladium remained inactive until it was heated to at least 320° K in hydrogen, while the oxygen film on 90 % Pd was removed at 250° K. 55·2 % Pd could not be activated by molecular hydrogen even at 850° K and the discharge method was essential for these alloys.

A paramagnetic conversion was detectable on a gold foil at low temperatures, and will be discussed in another paper.

---

[26] Farkas, *Trans. Faraday Soc.*, 1936, **32**, 1617.

Reaction Order.—Let the reaction vessel, volume V, having its walls at T_V (here 90° K), contain n molecules of hydrogen, and the surface area of catalyst be A cm.^{2} and contain f adsorption sites per cm.^{2}. We suppose that a fraction σ of the sites are occupied, and that $k_p(k_0)$ are the first-order constants for the change para → ortho (ortho → para). It may be shown that

$$k_e = \frac{Af\sigma}{n}(k_0 + k_p)$$

and substituting $n = pV/kT_V$, where p is the pressure of hydrogen gas,

$$k_e = \frac{AfkT_V}{V}(k_0 + k_p)\frac{\sigma}{p}.$$

Some time ago Eley [27] remarked that the data then available supported the view that $\sigma \propto p^{1/n}$, the Freundlich isotherm, over wide ranges of pressure. We have now made specific investigations on this point for wire catalysts, and have found that tungsten wires and the 40 % Pd wire accurately obey the Langmuir isotherm, so we write

$$\sigma = bp\,/(1 + bp)$$

and

$$k_e = \frac{AfkT_V}{V}(k_0 + k_p)\frac{b}{1 + bp}.$$

We have tested pure gold and 40 % Pd at their average working temperatures of 600° K and 350° K respectively. The gold catalyst gave a truly first-order reaction, that is, k_e independent of p so that $bp \ll 1$, and the 40 % Pd catalyst was very nearly first-order at 1 mm. Hg pressure. Attempts to obtain a pressure dependency experiment on pure palladium failed for the reason below.

Hydrogen-charged Palladium Catalysts.—In Fig. 5 we show the effect of simply raising the pressure from the standard value of 1·2 mm. to 6·1 mm. pressure. The result is an increase in activation energy to 6500 cal. This effect can only be due to an increased concentration of dissolved hydrogen atoms in the palladium, and so a palladium wire was charged wth atoms produced by the electrodeless discharge until no further solution took place, as judged by measuring the resistance of the wire at 90° or 298° K. Thus, in one series the resistance of the wire increased from 2·542 Ω to 2·766 Ω at 298° K. The data of Sieverts and Danz [28] allow us to calculate that this wire has a hydrogen content of 8 atomic per cent., though the hydrogen is not necessarily distributed uniformly. It was found possible to carry out a series of parahydrogen conversions on this wire in the range 290-400° K, since the wire did not lose dissolved hydrogen at any appreciable rate. The effect of temperature on k_e

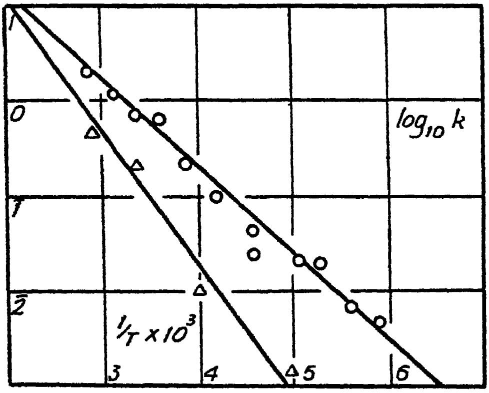

FIG. 5.—Variation of conversion velocity on palladium with pressure.
⊙ 1·2 mm. △ 6·1 mm.

---

[27] Eley, *Trans. Faraday Soc.*, 1948, 44, 216.
[28] Sieverts and Danz, *Z. physik. Chem. B*, 1937, 38, 61.

at 1·2 mm. Hg pressure is shown in Fig. 6, from which we calculate the approximate values $E \sim 11{,}000$ cal. and $B^0 = 1{\cdot}17 \times 10^9$ cm. min.$^{-1}$.

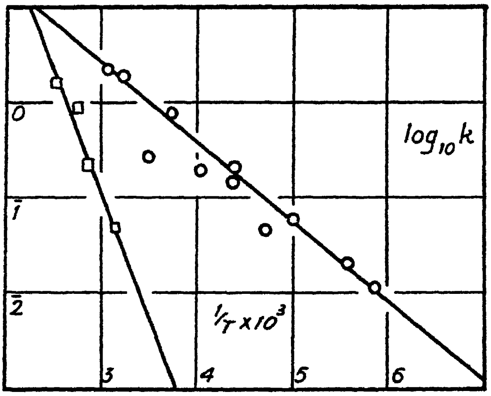

FIG. 6.—Effect of hydrogen dissolved in palladium upon the activation energy.
⊙ Pd outgassed at 600° K *in vacuo*.
□ Pd with dissolved hydrogen.

The applicability of the Sieverts resistance against dissolved hydrogen relationship was confirmed in some solubility experiments on the 70 % Pd wire. The solubility effects described above were reversible, but after a certain amount of this kind of working, irreversible changes in the wire occurred.

Discussion

The Activation Energy, *E*.—From Fig. 4 we see that the activation energy for the conversion is about 3·5 kcal. for pure palladium and remains the same for all alloys down to 40 at. % Pd. Between 40 at. % Pd and 30 at. % Pd, the activation energy increases to 8·5 kcal., which is also the value for the 20 at. % Pd and 10 at. % Pd alloys, beyond which it increases to the value of 17·5 kcal. for pure gold. The *exact* point at which the *d*-band of palladium becomes filled has an uncertainty to an atom percentage of about 5 %. The recent magnetic work of Sieverts and Danz [28] on the palladium-hydrogen system would put the point of zero susceptibility at 64 %, which would agree closely with the results of our catalytic work. Clearly we are justified in associating a low activation energy with the presence of holes in the *d*-band (free electron theory) or vacant atomic *d*-orbitals (valence bond theory). It is also clear that a bulk concentration of *d*-vacancies of 5 atomic per cent. or even less suffices to maintain the activity of the catalyst. There must therefore be a mechanism by which *d*-vacancies corresponding to a layer 33 atoms thick can be made available to hydrogen atoms adsorbed on the surface. Such behaviour is presumably implicit in the free electron theory, or in the resonance of valence bonds. Catalytic activity, a surface property, is quite different from magnetic susceptibility, a bulk property, which decreases linearly with the concentration of gold or dissolved hydrogen, as shown in the dotted line in Fig. 4. The lattice spacing change over 40 to 30 at. % Pd will only be 0·02 Å. We may use Eyring's calculations [8] to give an idea of the magnitude of the change in activation energy resulting from such a change in lattice spacing. In the neighbourhood of optimum spacing the result is 0·01 kcal., and at the worst 0·8 kcal., which is much less than the observed change of 5·0 kcal.

The results are a little different for the palladium-hydrogen system in that the initial activation energy for pure palladium of 3·5 kcal. is increased to 6·5 kcal. by the solution of a very small amount of hydrogen.

An overall concentration of 8 at. % hydrogen, produced by electrical discharge, gave $E \sim 11{\cdot}1$ kcal., which is larger than the E value for 60 at. % Au. In the first place we are of the opinion that the hydrogen atoms are concentrated in the outer layers of the wire. Such a skin effect always occurs in the solution of hydrogen in palladium unless special precautions are taken.[29] Thus, an overall concentration of 8 at. % in our wire is easily shown to correspond to 64 at. % in the outermost 30,000 atomic layers. Secondly, it is quite possible that the presence of the β phase with relatively large spacing gives rise to an increase in E additional to that arising from the filling of the d-band. A non-homogeneous distribution of hydrogen in the wire would explain the disrupting effect of continual solution and removal of hydrogen.

It is a matter for some satisfaction that these results are qualitatively similar, both for E and $B°$, to the results recently published by Rienäcker and Sarry [17] for the parahydrogen conversion on copper-platinum foils, except that the change in E in their work occurs at 16 at. % Pt, that is, some way from the 40 % value, and is less abrupt.* Thus, some of the remarks we make here may be applicable to their work also.

The Frequency Factor $B°$.—In a previous paper Eley [27] gives a calculation of $B°$ for the exchange mechanism, viz.,

$$pH_2 + HM \longrightarrow MH + oH_2,$$

conversion occurring by an exchange of atoms between a parahydrogen molecule in a van der Waals' layer and a hydrogen atom in an underlying complete chemisorbed layer, indicated by MH. For a dilute van der Waals' layer, as found here, palladium at 297° K and a reaction volume of 400 cm.^{3}, the calculated value was $B = 200$. Thus, the value of $B°$ is $200 \times 300 = 6 \times 10^4$ cm. min.$^{-1}$. This value is calculated for $f = 1{\cdot}2 \times 10^{15}$ sites per cm.^{2} and it is better to take a more exact value of f so as to allow for the variation from palladium to gold. Accordingly we use the formula $B° = 8{\cdot}61 \times 10^{-10}\, f/T^{\frac{1}{2}}$, which follows from eqn. (20) of ref. 27. We obtain the values in the Table below, taking as f the mean values for the (110) and (100) planes.

TABLE II.—CALCULATED VALUES OF $B°$

Alloy	Av. T °K	f per cm.^{2}	$B°$ calc.	$B°$ expt.
Pd	250	$1{\cdot}15 \times 10^{15}$	$6{\cdot}26 \times 10^4$	$\sim 4 \times 10^5$
40 % Pd	300	$1{\cdot}07 \times 10^{15}$	$5{\cdot}32 \times 10^4$	$1{\cdot}1 \times 10^4$
Au	600	$1{\cdot}02 \times 10^{15}$	$3{\cdot}58 \times 10^4$	$2{\cdot}1 \times 10^4$

The calculated $B°$ values are shown in Fig. 3 by a dotted line. The agreement is good, considering the difficult nature of the problem and bears out the conclusions of the earlier work based on data available in the literature. However, later, so far unpublished, calculations show that the Bonhoeffer-Farkas mechanism may possess the same value of $B°$, so that we cannot have a decision on mechanism on this ground alone. In this connection we have to qualify the remarks in an earlier paper (ref. 22, p. 449).

***d*-Levels and Catalysis.**—The only certain conclusion from the present experiments is that d-vacancies are essential in bonding the activated complex of the conversion reaction. It is, however, well worth postulating a detailed reaction path so as to take the analysis further. The original exchange mechanism [30] for the conversion involved the adsorption of the hydrogen molecule over empty sites in the chemisorbed layer, but we have found no evidence for these sites (cf. remarks in a review [31]), so we prefer to formulate the mechanism using a single site in the metal surface. This involves a departure from the usual Langmuir postulate, at least for activated complexes. We write

---

[29] Kruger and Gehm, *Ann. Physik*, 1933, 16 (5), 190.

* Rienacker and Gaubatz (*A.C.S. Abstr.*, 1941, **35**, 3944) gave magnetic data which indicate that the d-band is filled at about 50% Pt in Pt—Cu alloys.

[30] Rideal, *Proc. Camb. Phil. Soc.*, 1938, **35**, 130.

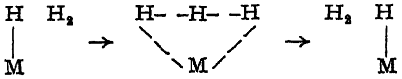

and for the equivalent formation of hydrogen deuteride,

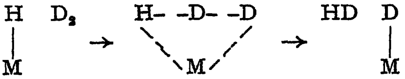

There is a little evidence that the *d*-vacancies, i.e. unpaired *d*-electrons, are concerned with the initial MH bond. Thus, copper, which has no unpaired *d*-electrons, has a heat of chemisorption of hydrogen of only 9 kcal./mole [32] compared with average values of 30 kcal. for tungsten [33] and 24 kcal. for nickel.[7] The hydrogen on copper, and presumably gold also, will then be held by the $d^{2 \cdot 56} sp^{2 \cdot 22}$ orbitals * relatively weakly because a large part of the bonding power will be concerned with the metal itself. For palladium the hydrogen atom is either bonded by the unpaired *d*-electron, the simplest view to take, or the atomic *d*-orbitals are used to form a metal hybrid *surface* orbital containing more *d* than the usual 2·56. This notion that the atomic *d*-electrons hold the hydrogen is in accordance with the qualitative evidence that hydrogenation catalysts adsorb hydrogen strongly. The H_3 activated complex will then be held by a *d*-bond and a metal hybrid bond to the metal site, and resonance between the three or more canonical states will be fundamental in lowering the energy of the complex. When the *d*-band becomes full, there may possibly occur a change over to the Bonhoeffer-Farkas mechanism for the conversion,

$$2MH \rightleftharpoons 2M + H_2$$

when the activation energy will be related to the heat of desorption of the chemisorbed hydrogen as molecules. The B° factor would not necessarily show any marked change in value, according to a transition state analysis of the recombination mechanism, to be published later. It seems quite certain that the Bonhoeffer-Farkas mechanism must set in at a certain relatively high temperature for all metals, and measurements of chemisorption on the alloys which we have planned should enable this temperature to be calculated.

The value of $E = 17 \cdot 5$ kcal. for pure gold requires a little discussion. Unlike the alloys, for gold the log k_s against $1/T$ plot is markedly curved, E increasing continuously as T increases. The upper temperature of 800° K for the gold wire is approaching the temperature at which the homogeneous conversion of parahydrogen through hydrogen atoms is observed. In this region we shall have to anticipate yet a *third* mechanism for the parahydrogen conversion, that is, a reaction in the gas phase set off by hydrogen *atoms* desorbed from the gold surface,

$$Au—H \rightarrow Au + H;$$
$$H + pH_2 \rightarrow oH_2 + H.$$

Returning now to the exchange mechanism which is the fundamental process at low temperatures, the question whether or not the H_3 complex may be formed will depend largely on steric conditions within the chemisorbed layer. Fig. 7 shows that linear and possibly triangular complexes are sterically possible on the (110) plane of palladium, but scarcely so on the (100) plane. The linear complex would be analogous to the complex found in the gaseous reaction.[34] It may be hoped that other simple reactions will fit into a similar picture, and in this connection the least dense lattice planes of nickel and other metals have been stated to be the most effective lattice planes for the hydrogenation of ethylene.[6]

---

[31] Eley, *Quart. Rev.*, 1949, **3**, 209.
[32] Ward, *Proc. Roy. Soc. A*, 1931, **133**, 506.
[33] Roberts, *ibid.*, 1935, **152**, 445.
* Hereafter called metal hybrid orbital.

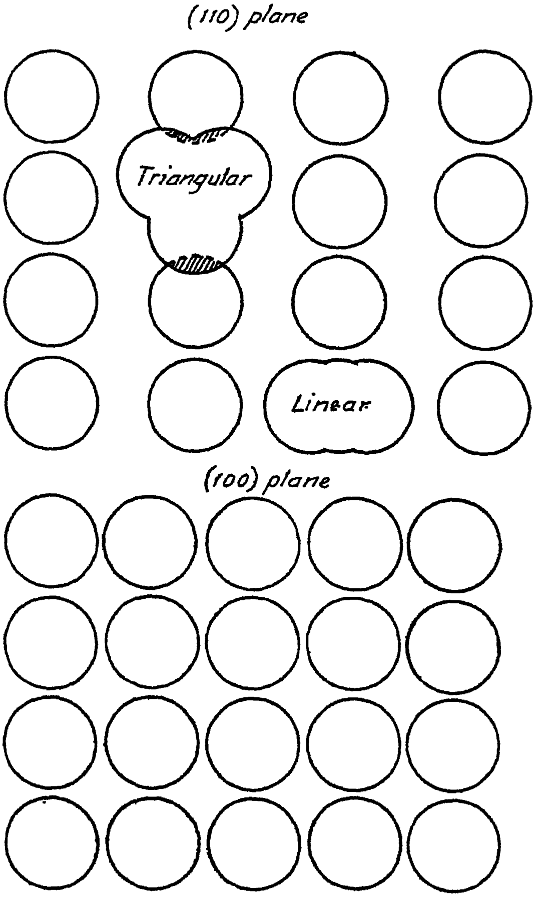

FIG. 7.—Hydrogen atoms on sites in the 110 and 100 planes of palladium. 3-atom complexes are easily formed on the (110) plane.

Besides lowering the energy of the activated state, the resonance energy of the initial state may influence the reaction. Following up an earlier suggestion,[35] Eley [31] has shown how the chemisorption of benzene most probably takes place by opening of the double bond. In this way we get a low heat of adsorption due to loss of resonance energy, and a consequent exchange reaction with hydrogen sensitive to benzene pressure and with a low activation energy of 9 kcal. By contrast, the reaction with ethylene is zero order in the ethylene and has an activation energy of about 20 kcal.

[34] Eyring and Polanyi, *Z. physik. Chem. B*, 1931, **12**, 279.

[35] Smith and Meriwether, *J. Amer. Chem. Soc.*, 1949, **71**, 413.

As pointed out in our note [1] the 20-fold decrease in B° from palladium to gold (100-fold from platinum to copper [17]), is in accordance with Dowden's suggestion that the entropy of activation may be influenced by the density of electronic states. In our calculation of B° we, in effect, assumed that the ratio of electronic weights in initial and activated states was unity. Until we have further investigated the much more marked changes in B° that arise from other factors, as in the effect of dissolved hydrogen, we reserve any further comment on this point.

Bond Type in Chemisorbed Hydrogen.—We shall conclude with an explicit statement of our views on the hypothesis [16, 36, 37] that chemisorbed hydrogen atoms are ionized on the surface of transition metals. On the theoretical side, our objections are essentially the same as those of Emmett and Teller.[38] Let I denote ionization potential, E electron affinity, ϕ_w work function, r the spacing from the chemisorbed ion to the surface, and e the electronic charge. Then there are three possible processes, for which we wish to calculate $\Delta E_{\text{ads.}}$ the internal energy change on chemisorption from hydrogen molecules. D_{H_2} is the dissociation energy of a hydrogen molecule.

$$\text{W} + \tfrac{1}{2}\text{H}_2 \longrightarrow \text{W}^- \ldots \text{H}^+$$

$$\Delta E_{\text{ads.}} = \tfrac{1}{2}D_{\text{H}_2} + I_{\text{H}} - \phi_w - \frac{e^2}{4r}. \qquad (1)$$

$$\text{W} + \tfrac{1}{2}\text{H}_2 \longrightarrow \text{W}^+ \ldots \text{H}^-$$

$$\Delta E_{\text{ads.}} = \tfrac{1}{2}D_{\text{H}_2} + \phi_w - E_{\text{H}} - \frac{e^2}{4r}. \qquad (2)$$

$$\text{W} + \text{H}_2 \longrightarrow \text{W}^- \ldots \text{H}_2^+$$

$$\Delta E_{\text{ads.}} = I_{\text{H}_2} - \phi_w - \frac{e^2}{4r}. \qquad (4)$$

Data and results are listed in Table III and from this it is quite clear that all the ionization processes are prohibitively endothermic, involving $\Delta E_{\text{ads.}} \sim 10$ eV ~ 230 kcal. No assistance is to be expected from the entropy change.

TABLE III

Bond.	r (Å)	I eV.	ϕ_w eV.	E eV.	$e^2/4r$ eV.	D_{H_2}, eV.	$\Delta E_{\text{ads.}}$, eV.
$\text{W}^- \ldots \text{H}^+$	1·41+0 = 1·41	13·59	4·54	—	2·52	4·46	10·99
$\text{W}^+ \ldots \text{H}^-$	1·41+2·08=3·49	—	4·54	0·7	1·02	4·46	7·28
$\text{W}^- \ldots \text{H}_2^*$	1·41+0·60=2·01	16·2	4·54	—	1·78	4·46	9·88

On the experimental side, Bosworth's [39] value for the W—H contact potential of − 1·04 V corresponds to the small dipole of 0·4 D, i.e. about one-tenth of an electronic charge (negative) on the H atom. Oatley's [40] value for Pt—H of + 1·17 V corresponds to a similar small *positive* charge, on the hydrogen atom. Both bonds are essentially covalent bonds of low polarity, such as a single electron [15] or electron pair [13] bond might be. It is our belief that many misconceptions have been based on Coehn's demonstration [41] of the positive nature of hydrogen atoms dissolved in palladium. Calculation, however, shows that the positive charge per hydrogen atom is only one-fiftieth of an electronic charge.[42]

[36] Schmidt, *Chem. Rev.*, 1933, **12**, 363.

[37] Nyrop, *The Catalytic Action of Surfaces*, 2nd Edn. (London, 1937).

[38] Emmett and Teller, *12th Report Comm. on Catalysis* (New York, 1940), p. 68.

[39] Bosworth, *Proc. Camb. Phil. Soc.*, 1937, **33**, 394.

[40] Oatley, *Proc. Physic. Soc.*, 1939, **51**, 318.

[41] Coehn and Specht, *Z. Physik.*, 1930, **62**, 1.

[42] Duhm, *ibid.*, 1935, **94**, 434.

Dissolved Hydrogen as a Catalyst Poison.—The results of this paper help to throw light on a number of obscure points in the literature. Thus, we have Willstatter's [43] observations on the loss of activity of hydrogenation catalysts which might be reactivated with oxygen, and the loss of activity of platinum cathodes with continual discharge of hydrogen.[44] Films of platinum and palladium formed by sputtering *in vacuo* are good catalysts, but formed in hydrogen are quite inactive.[45] The active films did not contain occluded oxygen, which argues against the Roginsky hypothesis [46] that pure metals are inactive, but may be activated by the merest traces of dissolved oxygen or other gas. Most striking of all are the results of Farkas [27] on the parahydrogen conversion on the inlet and outlet sides of a palladium disc and a palladium tube through which hydrogen is diffusing. The activation energy for the conversion is notably higher on the inlet side where the concentration of dissolved hydrogen atoms will naturally be higher than on the outlet side. This experiment definitely shows that only energy states in a piece of metal in the *immediate* neighbourhood of the surface can influence the catalytic effect. On this view the activation of platinum catalysts by oxidation, e.g. platinum foil by anodic polarization (Faraday [47]) or by chromic acid, or platinum black by oxygen [43] is due, at least in part, to removal of hydrogen atoms dissolved or " embedded " in the surface. That the effect of dissolved hydrogen is a complex one is shown by the fact that while E is raised, $B°$ is also raised powers of ten above the normal value. Abnormally high values of $B°$ may be associated with the presence of a distribution of sites of activity,[27] but further comment is reserved for a future paper.

Our best thanks are due to the Chemical Society and the Anglo-Iranian Oil Company for financial help in the purchase of the alloy wires, to the Royal Society for an optical pyrometer, and to the D.S.I.R. for a research grant to A. C.

The Chemistry Department,
The University,
Bristol, 8.

---

[43] Willstatter and Jacquet, *Ber.*, 1918, **51**, 767. Willstatter and Waldschmidt-Leitz, *ibid.*, 1921, **54**, 113.

[44] Hammett, *J. Amer. Chem. Soc.*, 1924, **46**, 7.

[45] Bredig and Allolio, *Z. physik. Chem.*, 1927, **126**, 41.

[46] Roginsky, *J. Phys. Chem. U.S.S.R.*, 1941, **15**, 1. Ablesowa and Roginsky, *Z. physik. Chem.*, 1935, **174**, 449.

[47] Faraday, *Experimental Researches in Electricity* (London, 1914).

SOME REACTIONS OVER ALLOY CATALYSTS

By D. A. Dowden and P. W. Reynolds

Received 2nd February, 1950

Analysis of the " electronic factor " in heterogeneous catalysis suggests that activity of Ni—Fe alloys in multiple bond hydrogenation should increase rapidly in the region where the energy density of electron levels at the Fermi surface rises; moreover, that reactions controlled by the rate of transfer of an electron from metal to substrate should, in the Ni—Cu alloys, decrease in rate as the 3*d*-band begins to empty. Experiments on styrene hydrogenation over Ni—Fe catalysts and hydrogen peroxide decomposition on Ni—Cu alloy foils provide general confirmation of these predictions. Methanol and formic acid decompositions on the Ni—Cu alloys decrease in speed as the 3*d*-band

holes are filled, following the pattern of multiple bond hydrogenation over supported Ni—Cu catalysts and further emphasize the role of the electronic factor in catalysis.

Catalysis at the interface between solids and fluids is a complex phenomenon, the energetics of which are functions of a number of parameters as yet insufficiently defined to provide the industrial chemist with a basis for fruitful calculation. However, it has proved useful to divide the parameters (somewhat arbitrarily) into two sets, one set being called the "geometric factor"[1] the other the "electronic factor",[2] and to seek experimental correlations between the catalytic activity of solids and their other physical properties supposed to depend chiefly on the same factors. Thus the edge of the unit cell of metal catalysts with cubic lattices might be the gauge of the geometric factor and the magnetic properties the measure of the electronic factor. The early qualitative success of covalent bond theory as applied to the study of the activated complex,[3] and the newness of the theory of the solid state, resulted in most emphasis being placed on the geometric factor almost to the complete neglect of the effect of electron characteristics.

Recent researches[4, 5, 6] have re-established the practical value of the electron characteristics of solids as a guide to their catalytic activity whilst semi-empirical theory has provided a firmer footing for future endeavour. According to a new view[5, 7] the activity of a metal depends on the values of the electronic exit work function θ, the energy density of electron levels at the Fermi surface $[g(E)_{E=-\theta}]$ and the gradient of the latter $[\mathrm{d}g(E)/\mathrm{d}E]_{E=-\theta} = G$. Reactions proceeding at a velocity affected by the rate of formation or the concentration of a chemisorbed positive ion or radical appear to be favoured by an increase in the value of each of these (when G is positive). When negative ions assume the dominant role reaction velocity should increase as θ and $g(E)$ decrease and when G decreases (especially to negative values).

In particular, for the series of binary solid solutions containing one of the group 8 elements (Ni, Pd or Pt) together with one of the Group 1 elements (Cu, Ag or Au) and the binary alloys of iron, cobalt and nickel, the efficacy in multiple bond saturation or in dehydrogenation depends largely on the number and the characteristics of the holes in the *d*-bands of the alloys. The activity diminishes as the number of holes falls to zero.[4, 8] For instance[8] the specific activity of a series of supported nickel-copper catalysts in styrene hydrogenation at 20° C decreased from a maximum at pure nickel to zero at the alloy of approximately the equi-atomic composition; this fall was paralleled by the gradual decline of ferromagnetic properties to zero at the same composition. Now the low-temperature electronic specific heat data of Keesom and Kurrelmeyer[9] indicate, not only a sharp fall in $g(E)$ at about the equi-atomic composition in the nickel-copper series of solid solutions but a sharp rise in the iron-nickel series somewhere between the binary alloys of composition 80 Ni + 20 Fe and pure nickel. Theory suggests therefore that activity in multiple bond hydrogenation over the nickel-iron alloys should increase rapidly at some point in this composition range. By way of contrast the decomposition of hydrogen peroxide, on the basis of the Haber-Weiss [10, 11] mechanism for the ferrous ion catalyzed reaction, should involve electron transfer with anion formation according to the equation

---

[1] Griffith, *Recent Advances in Catalysis*, Vol. I (Academic Press Inc., New York, 1948), p. 91.

[2] Roginsky and Schultz, *Z. physik. Chem. A*, 1928, **138**, 21; Russell, *Nature*, 1926, **117**, 47.

[3] Sherman and Eyring, *J. Amer. Chem. Soc.*, 1932, **54**, 2661.

[4] Rienäcker, *Z. anorg. Chem.*, 1938, **236**, 252; *ibid.*, 1939, **242**, 302; *ibid.*, 1941, **248**, 45; *J. prakt. Chem.*, 1941, **158**, 95.

[5] Dowden and Reynolds, *Nature*, 1949, **164**, 50.

[6] Couper and Eley, *Nature*, 1949, **164**, 578.

[7] Dowden, *Research*, 1948, **1**, 239; *J. Chem. Soc.* (in press).

[8] Reynolds, *J. Chem. Soc.* (in press).

[9] Keesom and Kurrelmeyer, *Physica*, 1940, **7**, 1003.

$$H_2O_2 + \text{metal electron} \rightarrow OH^- + OH$$

and requires that the decomposition rate over alloy catalysts should decrease as holes appear in the *d*-band. This paper presents experimental results on styrene hydrogenation over supported nickel-iron catalysts and methanol, formic acid and hydrogen peroxide decomposition over nickel-copper foils, which are in general accord with these conclusions.

Experimental

Undoubtedly the best metal surfaces for catalytic work are those prepared by evaporation *in vacuo*.[12] The difficulty of preparing homogeneous alloy films of this type leads instead, in these preliminary studies, to the choice of metal foils and supported metals closer to the orthodox, industrial model.

Reactants: HYDROGEN was prepared by electrolysis and purified by diffusion through a palladium thimble preceded and succeeded by liquid nitrogen traps. Hydrogen peroxide and methanol were both A.R. grade, the latter very low in sulphur content (3 parts per 10^6). Pure styrene was vacuum-distilled, made up in methanol solution and treated with activated Raney nickel to remove residual poisons. A 90 % solution of pure formic acid was dried with phthalic anhydride and distilled to yield a formic acid feed containing only 0·2 % of water.

NICKEL–IRON CATALYSTS.—The nickel and iron were co-precipitated as carbonates upon a specially purified kieselguhr (specific area ~ 5 m.^{2} g.$^{-1}$) using aqueous solutions of the pure nitrates and ammonium carbonate; each catalyst contained a total weight of metal equal to 15·5 % of the weight of kieselguhr present. The products were dried, calcined for 4 hr. at 400° C, sieved through a 100 B.S.S. mesh and small lots (~ 1 g. in thin layers) reduced by pure hydrogen during 40 hr. at 500° C. All measurements were done on the reduced catalysts which were kept either under pure hydrogen or for very short times under the de-oxygenated liquid substrates. Specific areas were estimated by the Brunauer-Emmett-Teller [13] method with argon (area $14{\cdot}4 \times 10^{-16}$ cm.^{2}) as the sorbate. X-ray examinations confirmed the presence of metal crystallites with face-centred cubic structure and showed the crystal size distribution to be similar in each catalyst. Specific activities were therefore calculated using the specific areas from gas absorption.

NICKEL–COPPER FOILS.—Nine alloys, which together with the pure metals covered the whole composition range at 10 % intervals, were prepared by Johnson Matthey and Co. Ltd. from spectroscopically standardized nickel and copper; they and the pure metals were rolled into foils of 0·003 cm. thickness spectroscopic analysis of which showed only faint impurity lines of silver, calcium, silicon, magnesium, iron and cobalt. The area of each foil was measured by a modification, due to Wooten and Brown,[14] of the Brunauer-Emmett-Teller [13] method using ethylene (area $17{\cdot}55 \times 10^{-16}$ cm.^{2}) as the substrate. It was found that the area by gas adsorption was only 85 % of the geometric area in accord with some recent observations of Davis, De Witt and Emmett.[15] However, this factor was the same for all the foils and since microscopic methods showed little variation in grain size over the series, the geometric area was used to obtain the specific activity. The magnetic susceptibilities of the copper-rich alloys were obtained with a Gouy balance and checked, in part, with a Sucksmith balance.

Normal cleaning of the metal surfaces by treatment with pure hydrogen followed by extensive outgassing, both at 500° C, resulted in the deposition of a metal film on the walls of the Pyrex container. This treatment was in consequence abandoned in favour of a high frequency discharge in hydrogen

---

[10] Haber and Weiss, *Proc. Roy. Soc. A*, 1934, **147**, 332.

[11] Weiss, *Trans. Faraday Soc.*, 1935, **31**, 1547.

[12] Beeck, Smith and Wheeler, *Proc. Roy. Soc. A*, 1940, **177**, 62.

[13] Emmett, Brunauer and Teller, *J. Amer. Chem. Soc.*, 1937, **59**, 1553.

[14] Wooten and Brown, *ibid.*, 1943, **65**, 113.

[15] Davis, De Witt and Emmett, *J. Physic. Chem.*, 1947, **51**, 1232.

(~ 2 mm. Hg) prolonged intermittently for 12-24 hr. in a system containing a liquid nitrogen trap and alternating with pumping out at 10^{-6} mm. Hg. The sole internal check of the success of this technique lies in the reproducibility of the results so obtained. Foils used in the decomposition of hydrogen peroxide were pre-treated by immersion in 5 % nitric acid for 30 sec. followed by thorough washing with distilled water. As used the foils all possessed their bright metallic sheen without sign of thick (> 300 Å) oxide film formation.

Decomposition of Hydrogen Peroxide and Hydrogenation of Styrene.—The rate of evolution of oxygen from neutral hydrogen peroxide (H_2O_2 = 0·058 g. cm.$^{-3}$) and the rate of adsorption of pure hydrogen by styrene in methanol (10 cm.^{3} of a 10 % solution) were followed with a soap-film flow-meter at atmospheric pressure and temperatures of 20° C to 80° C in a static system shaken at high speed (2000 c./min.). The hydrogenation over ~ 0·1 g. catalyst was observed at the maximum shaking rate where the reaction velocity was almost independent of this rate. The decomposition of hydrogen peroxide over the foils (area 16 cm.^{2}) showed for a given foil a maximum at an intermediate shaking rate which coincided with that giving the best contact, assessed visually, between foil and substrate; the activity of each foil was measured at its optimum shaking rate.

Decomposition of Formic Acid and Methanol.—The decomposition of the vapours of formic acid and methanol over nickel-copper alloy foils was effected at atmospheric pressure in an apparatus similar to that described by Schwab [16] but modified to permit pre-treatment of the foils with hydrogen in the electrodeless discharge and to permit vacuum out-gassing. The flow of reactant vapours was maintained at a constant value (90 cm.^{3} sec.$^{-1}$) for a foil area of 40-120 cm.^{2}. and the exit gases, substantially carbon monoxide or carbon dioxide and hydrogen measured with a soap-film flow-meter. The reactor temperature could be varied from 20° C to 520° C as recorded by a thermocouple, sheathed in thin glass and placed in contact with the foil. Blank runs gave small gas rates which necessitated very minor corrections to the rates of the metal catalyzed reactions.

Results

Styrene Hydrogenation.—Fig. 1 contains the specific activity of the nickel-iron catalysts, in styrene hydrogenation at 20° C plotted against the atomic fraction of nickel in the metal crystals. Each point is the mean of at least ten tests with fresh catalysts and the vertical line represents the probable

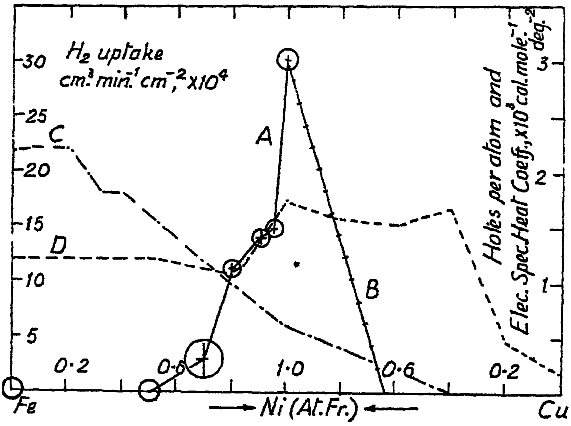

FIG. 1.—Effect of nickel content on the rate of hydrogenation of styrene by alloy catalysts.

Curve A: Ni—Fe catalysts, H_2 uptake cm.^{3} min.$^{-1}$ cm.$^{-2}$, × 10^4.
Curve B: Ni—Cu catalysts, H_2 uptake cm.^{3} min.$^{-1}$ cm.$^{-2}$, × 10^4.
Curve C: Number of holes per atom in the 3*d*-band.
Curve D: Coefficient of the electronic specific heat term; × 10^3, cal. mole^{-1} deg.$^{-2}$.

---

[16] Schwab, *J. Physic. Chem.*, 1946, **50**, 427.

error. The pattern is completed by inclusion of results for a corresponding series of nickel-copper catalysts taken from an earlier paper and "normalized" to give the pure nickel members of both series the same specific activity. Also depicted is the variation with nickel content of the number of holes per atom in the alloy 3*d*-bands [17, 26] and the density of electron levels *g*(*E*), taken to be proportional to the electronic specific heat coefficient according to Keesom and Kurrelmeyer. Separate experiments showed that hydrogenation stopped at the ethyl benzene stage.

Hydrogen Peroxide Decomposition.—Fig. 2 shows the specific activity of the nickel-copper foils. Each point is the mean of at least ten experiments with new foils and the vertical lines indicate the probable error.

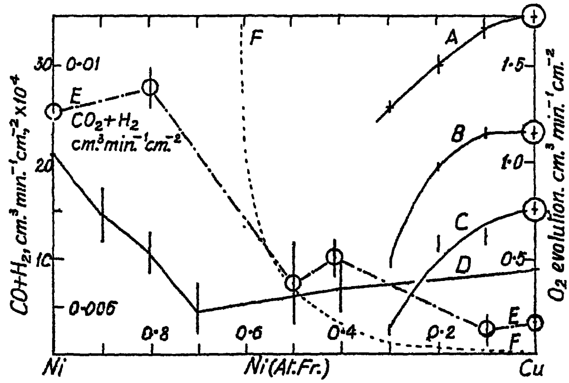

FIG. 2.—Specific activity of Ni—Cu alloys in hydrogen peroxide, formic acid and methanol decomposition.

Curves A, B, C: O_2 evolution from H_2O_2 at 80° C, 70° C and 60° C respectively, $cm.^3$ $min.^{-1}$ $cm.^{-2}$.
Curve D: Total $CO_2 + H_2$ exit gases from HCOOH at 253° C $cm.^3$ $min.^{-1}$ $cm.^{-2}$.
Curve E: Total $CO + H_2$ exit gases from CH_3OH at 253° C $cm.^3$ $min.^{-1}$ $cm.^{-2}$, $\times 10^4$.
Curve F: Magnetic susceptibility of the foils in arbitrary units.

The rates recorded are the constant values observed immediately after the attainment of steady shaking (within 15-30 sec. of zero time) and while the foils retained their pristine sheen without change of colour. In runs prolonged to 15 min. or more, the rates frequently showed a slow rise from the initial constant values but this was always accompanied by a loss of lustre and the appearance of a dirty red-brown colour indicative of thick oxide films; such effects have been neglected as not representative of metal or metal plus the thinnest films. Omission of the pre-treatment with dilute nitric acid did not change the character of the results but caused some loss of reproducibility. The activity at 60° C and 70° C of alloys containing more than 40 % of nickel was too small to estimate. The measured magnetic susceptibilities are given in arbitrary units; a small field-dependence due to ferromagnetism, is already apparent at 30 at. % nickel and becomes greatly magnified with increasing nickel content.

The apparent activation energies (kcal./mole) and frequency factors (molecules $sec.^{-1}$ $cm.^{-2}$) are respectively for pure copper 10·3, 1·0 × 10^{23}; 90 at. % copper, 10·9, 2·1 × 10^{23}; 80 at. % copper, 11·0, 2·4 × 10^{23}; 70 at. % copper, 23·7, 1·3 × 10^{31}.

Formic Acid and Methanol Decomposition.—Included in Fig. 2 are the specific activities of the foils in the decomposition of the vapours at 253° C. Each point on the formic acid curve is the mean of six determinations on the same foil with intermediate treatment in the hydrogen discharge and the probable error is shown. The activation energy of formic acid decomposition (250° C-300° C) varies from 30 kcal./mole over pure nickel to 36 kcal./mole over pure copper but although our variation is of the same kind as found by Rienäcker [4] in a static system, our values are approximately twice as great suggesting poisoning of our foils.

Discussion

Since there are no phase changes or magnetic transitions at room temperature in the face-centred nickel-iron alloys covering the range 30Ni + 70Fe to pure nickel, Fig. 1 shows quite clearly, in accord with expectation, the general parallelism between the rate of hydrogenation of styrene and the variation of electron-level density $g(E)$. Together with the earlier results in the nickel-copper series, it yields the complete activity pattern as the Fermi surface approaches and passes under the peak of $g(E)$ in the overlapping $3d$- and $4s$-bands and emerges into the $4s$-band. In the nickel-iron alloys a rising $g(E)$ accompanies an almost linear decrease in the number of d-band holes but in the nickel-copper alloys $g(E)$ remains almost constant, until the holes are quite full at the critical composition (0·61 atomic fraction of copper) and then decreases rapidly. The rise in activity between the alloy 75Ni + 25Fe and pure nickel must therefore be attributed to the great increase in $g(E)$, whereas the decline between pure nickel and the alloy 40Ni + 60Cu is due both to the disappearance of $3d$-band holes and to the fall of $g(E)$. The order-disorder changes which are only sluggish at 500° C around the composition Ni_3Fe do not appear to affect the activity since the activity curve possesses no symmetry with respect to this composition.

Fig. 2 shows that the decomposition rates of formic acid and methanol vapours over Ni—Cu alloys decrease as the $3d$-band holes fill up and the trend is quite similar to that for styrene hydrogenation. On the other hand, the rate of hydrogen peroxide decomposition falls off as the $3d$-band begins to empty, as is to be expected for a process controlled by the rate of transfer of an electron from the metal to the substrate.

The correlation between the electron characteristics of metals and their catalytic properties depends inevitably on the physical data available. Especially important to the topics of this paper are the values of θ, $g(E)$ and G, whose variations across the two alloy series are known in form but not in detail.[17] Simple band-theory, using early values for the saturation magnetization of the ferromagnetic alloys, gave a clear-cut picture of the d-band holes in the nickel-copper solid solutions and although recent studies [18] of associated phenomena are not always in exact accord with this model, the divergences are not sufficient to invalidate our conclusion. Again, it is possible that the number and properties of d-band holes differ in the bulk and the surface but if so the effect is not sufficient to disturb significantly the relationship with bulk properties.

Beeck and co-workers,[19] in a purely geometric interpretation of ethylene hydrogenation by pure metals, correlate activity with crystal parameter (closest spacing in the plane of least packing density) and find 3·75 Å to be its optimum value. For the face-centred cubic alloys of nickel here examined, this suggests an increase in activity as iron and copper are alloyed with nickel in direct contradiction of the results given. Many reactions,[4, 20, 6] not only multiple-bond saturation, appear to depend on the presence of d-band holes in approximately the same way and the pattern, viewed broadly, is independent of any particular interatomic distance in the substrates.

The effect of intramolecular environment on the rate of a catalyzed reaction at an unsaturated group is illustrated by the styrene hydrogenation. Under mild conditions the reaction proceeds only as far as ethylbenzene ; more severe treatment is required to produce ethylcyclohexane, yet each step in the reaction is favoured thermodynamically and exhibits the same dependence of rate on the holes in the *d*-bands (ethylbenzene can hardly differ from benzene [5, 8] in this respect). From the geometric standpoint the resistance of the aromatic ring to hydrogen addition might be associated with differing multiple-bond lengths; electronically the resonance energy could be the significant factor. In truth only the summation of such influences can represent the facts.

---

[17] Mott and Jones, *Properties of Metals and Alloys* (Oxford Univ. Press, 1936), 1st ed., chap. 6.

[18] Stoner, *Reports Prog. Physics*, 1946-47, **11**, 43.

[19] Beeck, *Rev. Mod. Physics*, 1945, **17**, 61.

[20] Tammann, *Z. anorg. Chem.*, 1920, **111**, 90.

Although the results on hydrogen peroxide decomposition are in harmony with the Haber-Weiss [10, 11] mechanism, it is necessary to consider an alternative formulation of Bray and Gorin [21] for the initiation of the ferrous ion catalysis, i.e.

$$Fe^{2+} + H_2O_2 \rightarrow FeO^{2+} + H_2O.$$

Adapted to alloy catalysts this becomes

$$\text{metal} + H_2O_2 \rightarrow (\text{metal, O}) + H_2O,$$

where the symbols in parentheses denote a chemisorbed complex. Certainly thin oxide films must be formed on the alloys during reaction and both theory and the work by Pilling and Bedworth,[22] on the high-temperature oxidation of nickel-copper alloys, suggest that the uptake of oxygen should be most rapid for the copper-rich alloys. However, on completion of the oxide film, the short-range forces of the covalent bonds in the ferroxyl analogue will depend only on the oxide layer, not on the base metal, and the apparent dependence on the electron structure of the alloy must be accounted for. None of the recorded phase boundaries [23] in the nickel oxide-cupric oxide system can account for the changes in activity, moreover Hickman [24] has found by electron diffraction that the low temperature oxidation of nickel copper-alloys produces only cuprous oxide and cupric oxide in the oxide layer over a wide range of alloy composition. Thus the use of the Bray and Gorin mechanism for the alloy catalysis requires one or more postulates: (*a*) the oxide film is not complete, (*b*) there is a change in the structure or composition of the oxide film as the 3*d*-band begins to empty, (*c*) the electron levels in the oxide film undergo some systematic change parallel to that occurring in the metal; none of these appears to be true. The electron-transfer process of the Haber-Weiss mechanism is not likely to be greatly affected by a thin oxide film.

Formic acid decomposition might be formulated in several ways since its behaviour over the alloy series suggests electron donation to the metal (cf. Schwab),[25]

$$HCOOH \rightarrow HCOOH^+ + e,$$

followed by

$$HCOOH^+ \rightarrow CO_2^+ + H_2 \text{ and } CO_2^+ + e \rightarrow CO_2,$$

or reaction with a positive ion, e.g.

$$HCOOH + H^+ \rightarrow H_2 + HCOO^+ \text{ and } HCOO^+ \rightarrow CO_2 + H^+,$$

together with its free radical counterpart.

Imperial Chemical Industries Limited,
Billingham Division,
Billingham,
Co. Durham.

---

[21] Bray and Gorin, *J. Amer. Chem. Soc.*, 1932, **54**, 2124.

[22] Pilling and Bedworth, *Ind. Eng. Chem.*, 1925, **17**, 372.

[23] Rigamonti, *A.C.S. Abstr.*, 1947, **41**, 7192; unpublished work from this laboratory.

[24] Hickman, *Metals Tech.*, 1948, **15**, (Tech. Publ. 2483).

[25] Schwab, *Trans. Faraday Soc.*, 1946, **42**, 689.

[26] Peschard, *Compt. rend.*, 1925, **180**, 1836.

GENERAL DISCUSSION

Dr. D. D. Eley (*Bristol*) (*partly communicated*) : Firstly, I shall give new evidence in favour of my assumed mechanism. Dr. Couper and Mr. Hulatt in my laboratory have carefully examined the effect of pressure on the first-order constant K_e of parahydrogen conversion on wires of W, Pd–Au and Pt. All these data satisfactorily fit the equation

$$1/K_e = A + Bp$$

meaning that the adsorbed reactants are obeying the Langmuir isotherm, which on the simplest view means that they are being adsorbed on a uniform surface. The results fit over the whole range of surface fractions covered 0 to 1. The effect of temperature on the constants A and B for Pt leads to a value of 2300 cal. for the heat of adsorption uniform from $\theta = 0$ to 1. This is rather larger than the value of 1000 cal. calculated by Lennard-Jones in 1932 for the van der Waals' adsorption of H_2 on Cu. But it does suggest a second layer held by predominantly dispersion forces on top of the primary layer held by predominantly exchange forces.[1] It is indeed difficult to see how the Trapnell-Rideal mechanism can give a Langmuir isotherm for the hydrogen atoms over the whole range of surface covered with apparent heat of 2300 cal., yet this is what would be required by the above results.

The interchange mechanism was based on the observations that on W [2] and Ni [3] the conversion had a rate closely similar to the rate of atomic exchange between gaseous D_2 and pre-adsorbed hydrogen,

$$D_2 + H{-}M \rightarrow M{-}D + HD.$$

Again it was found [4] that a considerable part of the chemisorbed oxygen film on W may be removed, corresponding to a fall in the negative value of the contact potential from 1·76 to 1·22 V, before any parahydrogen conversion sets in. Both these results are easily reconciled with these interchange mechanism but not, I think, with that advanced by Trapnell and Rideal. I might also refer to the result that on a surface partially poisoned by oxygen the rate of conversion is reduced in proportion approximately as the amount of chemisorbed exchangeable hydrogen.

For these reasons the interchange mechanism is still in my view the probable mechanism for the parahydrogen conversion for cases such as W at low temperatures. An alternative explanation of the loosely adsorbed hydrogen is that it is held in a second layer, but the published details of the experimental methods and results are insufficient to make a discussion worthwhile at present. If we assume that the surface orbitals are the ordinary metallic orbitals one can at least see the possibility of a small amount of exchange interaction between the metal and a second adsorbed layer, which might account for the extra few kcal. of energy beyond that expected for strictly dispersion forces.

Dr. B. M. W. Trapnell (*Royal Institution, London*) (*communicated*) : Dr. Eley has unfortunately only provided us with quantitative heat data for platinum, and it is possible that hydrogen chemisorption by platinum is so strong even at high coverages that it is effectively irreversible, in which case the interchange mechanism would be the more important.

With tungsten, the experimental result indicating the impossibility of the interchange mechanism is that the reaction order is between 0·1 and 0·5 at −100° C and 1 mm. If this is to be interpreted in terms of varying coverages in a van der Waals' adsorbed layer, use of the Langmuir isotherm shows that the fraction covered must lie between 0·45 (order 0·5) and 0·8 (order 1·0). Now for an adsorbed layer of a small molecule to be so densely packed under these conditions the heat would have to be some 7000 cal. My results show, however, that at this heat, the adsorbed amount corresponds to considerably less than 1 atom per site, so that there is no second layer present at all, let alone a concentrated one. Even at 2900 cal. heat, the adsorption cannot exceed one atom per site by more than a few per cent. We must conclude that the fractional order or reaction is not explicable by the interchange mechanism : it is, of course, readily explicable by the older mechanism.

---

[1] *Trans. Faraday Soc.*, 1929, **25**, 447.
[2] Eley, *Proc. Roy. Soc. A*, 1941, **178**, 452.
[3] A. and L. Farkas, *J. Amer. Chem. Soc.*, 1942, **64**, 1594.
[4] Eley and Rideal, *Proc. Roy. Soc. A*, 1941, **178**, 429.

Eley's other objections are less easy to understand. Provided the heats of chemisorption of H_2 and D_2 are not very different, the older mechanism would predict near equality of conversion and exchange rates, as the expression

$$R = \frac{K(1 - \theta)}{1 + \epsilon}$$

would be nearly the same in the two cases. And as regards the experiments on oxygenated wires, we cannot, I think, discuss these until we know whether the oxygen was mobile under the conditions of evaporation, the heat of chemisorption of hydrogen into a partial oxygen layer and so on.

Sir Charles Goodeve (*B.I.S.R.A., London*) (*contributed*) : A useful approach to this problem of chemisorption and surface reaction lies through a consideration of metallic solutions. Hydrogen and nitrogen, in particular, are soluble to some extent in most metals and exist in solution as single atoms (or ions) lying interstitially in the metallic lattice. Indeed, in some metals the concentration of the non-metallic element can be increased up to a point or points, where phase changes or shifts in the lattice dimensions or a slight rearrangement take place. These new phases are commonly called hydrides or nitrides, despite the fact that the resulting phases are essentially metallic ; e.g. they have metallic electrical conduction. The high heats of solution (of the atom) signify chemical bonding, but the high diffusion coefficients of these atoms compared with those of other atoms in the solid metallic lattice, show that this bonding energy is related to the solid state, rather than to a position, or to a phase. The whole range of compositions can be looked upon as states of solid solution.

I know of no evidence so far, that the state of chemisorption of these elements on a surface differs in any way from that of solution except in so far as the different co-ordination number of an atom just at the surface may lead to a lower, or a higher energy level. In other words, if one breaks a metallic crystal containing hydrogen or nitrogen in solution, the atoms of these elements so disclosed on the new surfaces will be in the same state as atoms produced by chemisorption, except that their surface concentration may be greater or less.

Such a picture gives strong support for Beeck's reminder[5] that more attention should be paid to penetration from the chemisorbed state into the substrate. Trapnell's contention[3] that this can be ignored in the para-hydrogen conversion on tungsten should be supported by quantitative data on the solubility and/or the diffusion coefficient of hydrogen in tungsten showing that these are very low at the particular temperatures used.

Another consequence of this approach is the conclusion that the lateral mobility of chemisorbed atoms must be as great as, and probably many times greater than, the diffusion rate of these in solution in the metal.

Finally, experimental studies of surface reactions based on this approach can lead to a much more rigorous comparison with theory. In the simplest of heterogeneous catalytic reactions one has at least three processes in series, the adsorption, the surface reaction and the desorption, with the resulting latitude in fitting in a particular theory. If, however, one chooses conditions where the reservoir of the reactants is in solution and the rate of diffusion is known to be high enough to maintain the surface concentration at a fixed level, then a very much simplified situation results.

---

[5] This Discussion.

Such experiments have been done[6] with a solution of nitrogen in iron (ϵ-iron nitride) which when placed in a vacuum (or in an atmosphere of nitrogen) at 350 to 500° C gives up its gas at an easily measurable and reproducible rate. The reaction is found to be bimolecular with respect to N concentration in the solution and to have a constant energy of activation of 42 kcal. There is ample evidence to prove that diffusion to the surface is much faster than the over-all liberation of gas.

From a knowledge of the behaviour of N atoms in the crystal we know that there is a repulsion between the atoms and that this rises rapidly when two approach to a distance less than 5 Å. In order for a physically adsorbed N_2 molecule to be formed the N—N distance has to come nearly down to 1 Å and the Fe—N distance of 1·94 Å must be nearly doubled. It is, therefore, consistent with our general knowledge of energy–spatial relationships to associate the 42 kcal., with the peak of a barrier between the chemical and physical adsorbed states which will lie somewhere near a N—N distance of 1·5 Å.

What is much more important is that, on the assumption that the heat treatment of the particles used gave smooth surfaces and that the nitrogen atom concentration on the surface is the same as in the bulk, a calculation of the expected surface reaction velocity agrees well (within a factor of two) with the observed velocity.

Such agreement in experiments of this type is probably fortuitous, particularly as the theory ignores the effect of surface contamination, say, of oxide. The agreement does, however, suggest that experiments should be done on other systems using metals with hydrogen or nitrogen where similar simple conditions may lead to further tests of theory. It might even be possible to deduce an expected value of the energy of activation from force constants of the N—N and the Fe—N link. At all events, further experiments should show how far this approach can be usefully followed.

Dr. B. M. W. Trapnell (*Royal Institution, London*) said : I should like to discuss two points in connection with my paper.[7] The first is the suggestion by Dr. Beeck that the reversible uptakes of gas which we have observed are not chemisorption, as we have claimed, but are solution, which is known to proceed with a low heat. The suggestion implies that the conversion might proceed through evolution of dissolved gas rather than chemisorbed gas. Now we have investigated the solution of hydrogen in tungsten films, and have found that the dissolved amount is so small that the reversible uptakes of gas must almost entirely be chemisorption. Moreover, if we consider the rate of evolution of gas from surface and bulk under specified conditions, clearly the rate of evaporation of chemisorbed hydrogen will be much larger than the rate of evolution of dissolved hydrogen as the solution process requires an appreciable energy of activation whereas chemisorption is non-activated, and because the chemisorbed amount is some 20 times the dissolved amount. The conversion therefore will proceed almost entirely through the reversibility of chemisorption, as we have said.

Secondly, it should be noted that the θ values of Fig. 1 were derived assuming that when the heat of adsorption is zero, $\theta = 1$. This now appears a rather artificial method of procedure, and in the detailed publication of the work, oxygen chemisorption will be used as the basis of determination. The new method alters none of our conclusions.

Dr. O. Beeck (*Emeryville, California*) said : While I am inclined to agree that the probable mechanism of the para hydrogen conversion by tungsten surfaces proceeds through condensation and re-evaporation of chemisorbed gas, I believe that this process is still somewhat more complicated than the authors assume.

---

[6] Goodeve and Jack, *Faraday Soc. Discussions* 1948, 4, 82.

[7] Rideal and Trapnell, this Discussion.

It has now been conclusively shown [8] that on many metal films, including tungsten, hydrogen will be dissolved to some degree in the metal structure, after the surface is covered with a monolayer, and that this solution is of the activated type with a heat of sorption considerably lower than the lowest heat of adsorption. This phenomenon will even take place at very low temperatures and is most likely responsible for the para-ortho hydrogen conversion or the hydrogen-deuterium exchange at low temperature. Solution of hydrogen can be shown to be responsible for the easily reversible part of the hydrogen isotherm on nickel and can be shown to take place even if the surface is irreversibly covered with carbon monoxide. By subtracting the hydrogen isotherm on a carbon monoxide covered nickel surface from the isotherm obtained with hydrogen alone, the resultant true adsorption isotherm is completely flat over the pressure range from 10^{-3} to 10^{-1} mm. While the mechanism for solution is not clear in detail as yet, it must be assumed to proceed through a second layer adsorption on that very small part of the surface where the heats of adsorption are the lowest. Taking this view, the ideas of Rideal and Trapnell as well as those of Couper and Eley may in fact be very closely related.

Dr. P. A. Wright (*Bedminster Smelting Works, Bristol*) (*communicated*) : A possible explanation of the difference in surface coverage achieved in the experiments of Roberts and of Rideal and Trapnell lies in the 8 % of sites left vacant after random covering of the surface by H_2 molecules. If we imagine that these sites are filled by H_2 molecules lying " end on ", we shall then achieve a surface coverage of " 108 " % ; this latter addition would be expected to yield a smaller heat of adsorption and consequently some degree of mobility.

Dr. F. S. Stone (*Bristol*) (*partly communicated*) : With reference to Eucken's observations on the reaction of cyclohexene with adsorbed hydrogen, it is of interest to quote details of a parallel case of the time-dependence of the adsorbed state of oxygen. Carbon dioxide can only be taken up on our copper oxide catalyst provided adsorbed oxygen is present with which it can form a CO_3 complex.[9] If oxygen has been pre-adsorbed, carbon dioxide will subsequently adsorb to give a ratio of 0·7 $CO_2/1\ O_2$ on the adsorbent. If a 1/1 mixture of $CO_2 + O_2$ is admitted, the gases are taken up in a 1/1 ratio, and if a 2/1 mixture of $CO_2 + O_2$ is admitted, the gases are taken up in a 1·5/1 ratio. With mixtures in which the CO_2 is in large excess, e.g. a 6/1 mixture, the uptake ratio is 2/1, indicating total capture of oxygen by CO_2. It therefore appears that quite a large fraction of the oxygen adsorbed loses its ability to react with CO_2 in a *very short time,* since merely by increasing the ratio of CO_2/O_2 admitted the percentage of oxygen reacting increases sharply. A similar loss of yield is found in the reaction of CO with adsorbed oxygen. In neither case, however, does the total loss exceed 60 % even over long periods of time. This behaviour is analogous to that reported for oxygen on porous nickel films.[10] In the present case the adsorbed oxygen is lost either by oxidation or by diffusion into the porous interior : indeed, the uptake of oxygen on cuprous oxide,[9] manganese oxide [11] and nickel oxide,[12] obeys a diffusion equation.

Prof. W. E. Garner (*Bristol*) said : The nature of the adsorption of hydrogen on nickel appears to vary with the method of preparation of the nickel. Euchen finds that the heat of adsorption on metal prepared from oxide is 6 kcal. at 100-200° K and is 17 kcal. above 300° K, whereas Beeck finds a heat of adsorption of 30 kcal. at −183° K. A possible explanation of these discrepancies is that there are two types of atomic hydrogen films, one formed within the nickel lattice and the other outside. The formation of a hydrogen film within the lattice is supported by the negative surface potential of atomic hydrogen films.

---

[8] Beeck in *Advances in Catalysis,* Vol. II.

[9] Garner, Gray and Stone, this Discussion.

[10] Beeck, Smith and Wheeler, *Proc. Roy. Soc. A,* 1940, **177**, 62.

[11] Sakai, Kurimura and Okura, quoted in ref. (1).

[12] Roginsky and Tsellinskaya, *J. Phys. Chem. U.S.S.R.,* 1947, **21**, 919.

It is suggested that the presence of foreign atoms of greater dimensions than the metal atoms, e.g. oxygen, in the surface of the nickel causes a compression of the atoms in the surface of the metal over considerable areas, thereby hindering the penetration of the surface by the hydrogen atoms. Thus in Euchen's experiments at low temperature, the hydrogen film is on the outside of the lattice, and on raising the temperature, this passes into the surface. In Beeck's films, being relatively free from foreign atoms, there is no hindrance to the formation of the internal film even at liquid-air temperatures.

Mr. A. E. J. Eggleton (*Imperial College, London*) (*communicated*): Using an apparatus[13] similar to that of Roberts, the accommodation coefficient α of neon on iron has been determined. After flashing the wire (0·05 mm. diam.) to 1200° C *in vacuo* or in neon at a pressure of *ca.* 0·1 mm. Hg for periods up to 1 hr. α was 0·2 and there was no drift with time after the thermal disturbance due to flashing had died away (8 min.) as is the case with tungsten. (Clean metal wires, using Roberts' technique, have values of α of 0·06; when contaminated by adsorbed gas α is normally $> 0{\cdot}15$.) Admission of hydrogen to a pressure of 1×10^{-3} mm. had no effect on the value of α (ct. clean W). Flashing the wire at lower temperatures gave higher values of α, up to 0·29. Heating the wire in hydrogen before flashing had no effect. In one experiment the wire, after preliminary outgassing, was heated at 1100° C for 45 min. in 0·1 mm. of hydrogen, left overnight at 700° C *in vacuo*, followed by 20 min. at 1200° C in 2×10^{-3} mm. H_2 and a further 30 min. *in vacuo* and finally 20 min. at 1200° C in neon which had been left standing over charcoal immersed in liquid nitrogen for 1 hr. (The hydrogen was circulated past the wire and through liquid nitrogen traps during the reduction.) After this treatment sufficient of the iron had evaporated to form a visible film on the walls of the tube surrounding the wire but α did not fall below 0·2 and again admission of hydrogen had no effect. Heating the wire to higher temperatures or for longer periods was not possible since the evaporation from the iron wire seriously alters the physical constants of the wire.

In view of these results compared with those of Roberts and my own results on tungsten it seems improbable that a clean iron surface can be prepared by reduction of iron oxide with hydrogen or by outgassing of iron powders at high temperatures *in vacuo* and that workers who have used this method for preparing iron surfaces for adsorption, are in fact dealing with a surface that is already contaminated.

More recently a clean surface has been prepared by subjecting the iron wire to positive ion bombardment in a gas discharge.[14] Treatment with positive neon ions (1000 V and 1 mA) reduced the value of α from 0·2 to 0·16. However, if the wire was first subjected to a discharge in nitrogen for 15 min. and then to a neon discharge for 2 min. the value of α was reduced to approximately 0·07. There was a small drift with time indicating slow contamination. Admission of a small amount of hydrogen caused α to rise to approximately 0·12.

These results are of some interest in connection with the remarks of Prof. Garner. It seems most likely that failure to clean the iron wire by flashing treatment alone was due to the rapid diffusion of impurities

[13] *Proc. Roy. Soc. A*, 1930, **129**, 146.

[14] Cp. Mitchell, this Discussion (Introductory paper).

from the interior of the wire to the surface after the cleaning treatment. Now it is suggested that the treatment with positive nitrogen ions forms a barrier which prevents the diffusion of impurities from the interior. Subsequent treatment with neon ions removes the surface layer of nitrogen exposing a clean surface. The nitrogen may act simply by blocking the gaps between iron atoms, or, as suggested by Prof. Garner, by compression of a layer of atoms in the lattice, in this case below the surface.

Oatley[15] found similar behaviour with platinum: the work function of a surface prepared by bombardment with oxygen followed by argon was the same as that of a surface cleaned by flashing. Treatment with argon alone gave a value approaching that of a clean surface, but which rapidly altered, indicating contamination.

In connection with Dr. Bremner's communication[16] it may be noted that the bombardment treatment only raises the temperature of the wire to 400° C. The first values of α are obtained about 5 min. after the treatment has ended and there is a continual slow drift lasting 40 min. or more. It seems very unlikely that the low value of α and the slow drift can be due to thermal disturbance particularly since the same wire in a contaminated condition had been flashed at 1200° C after which α was 0·2 and there was no drift at all after thermal disturbance had died away ($\sim$ 8 min.).

Mr. P. R. Rowland (*Guy's Hospital, London*) said: When discussing the positions of adsorbed atoms on a metal surface evidence taken from the adsorption of hydrogen is perhaps the most unfortunate to consider since on adsorption it is probable that the orbital electrons of hydrogen enter the metal leaving protons which imbed themselves in the electron gas of the metal. It is difficult to attribute a size to such particles which cannot themselves be regarded as simply substituting for metal atoms at adsorption sites in the Langmuir sense but may wander through the lattice with high mobility. Electronegative atoms on the other hand are more likely to attach themselves to the surface by bonds resembling those in solid salts, i.e. to surround themselves with as many metal atoms as possible by substitution of metal atoms at Langmuir sites. It is interesting to note that in the presence of electronegative atoms the most stable metal crystal faces are those on which every adsorption site is identical so that the adsorbed atoms all lie in one plane. This suggests that such adsorbed layers together with the metal surface atoms may be regarded as two-dimensional compounds or adsorption complexes.

Mr. P. Zwietering (*Geleen, Netherlands*) (*communicated*): The results of Dr. Maxted's measurements[17, 18] were invariably expressed as the activity A of the catalyst depending on the amount of poison c added to the reaction mixture. The greater part of this amount c will be adsorbed on the catalyst; however, a small portion must remain in solution to build up the equilibrium concentration corresponding with the amount adsorbed on the catalyst.

Therefore we may write:

$$c = \alpha\theta + \beta p, \quad . \quad . \quad . \quad . \quad . \quad (1)$$

where θ = fraction of surface covered with poison, and p = equilibrium conc. in the solution.

The relation between p and θ can simply be expressed by the equation of Langmuir:

$$p = \frac{\theta\gamma}{1 - \theta}$$

so that

$$c = \alpha\theta + \frac{\beta\gamma\theta}{1 - \theta} \quad . \quad . \quad . \quad . \quad (1a)$$

---

[15] *Proc. Phys. Soc.*, 1939, **51**, 318.

[16] This Discussion.

[17] *Trans. Faraday Soc.*, 1945, **41**, 406.

[18] This Discussion.

From this it follows:

$$\frac{c(1-\theta)}{\theta} = (\alpha + \beta\gamma) - \alpha\theta \quad . \quad . \quad . \quad (2)$$

Assuming that the activity A of the catalyst is proportional to the fraction of the surface not covered by poison we may write

$$A/A_0 = 1 - \theta, \text{ or } \theta = 1 - A/A_0.$$

From (2) it follows then

$$\frac{cA/A_0}{1 - A/A_0} = (\alpha + \beta\gamma) - \alpha(1 - A/A_0). \quad . \quad . \quad (3)$$

Consequently there must exist a linear relationship between

$$\frac{cA/A_0}{1 - A/A_0} \text{ and } (1 - A/A_0).$$

In Fig. 1 and 2 the experimental figures, obtained from the published curves, have been plotted according to eqn. (3). Obviously the experimental data are very well described by this equation. The deviations at high values of A/A_0 must be attributed to the limited accuracy with which the experimental data can be obtained from the published curves.

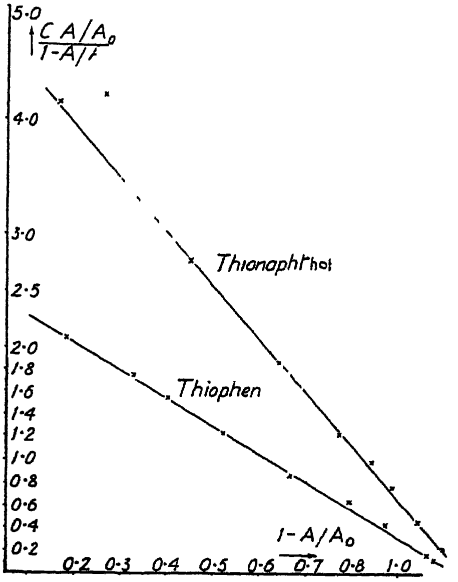

Fig. 1.

It follows from the theory that the slope α of the straight lines must be determined by the total area of catalytic surface, so that for the series I to IV a proportionality may be expected between α and the amount of catalyst used, whereas for the series V and VI, α must be proportional to the surface area.

Finally also A_0 must be determined by the area of the catalytic surface, so that α must also be proportional to A_0. In Fig. 3, 4 and 5 the values for α derived from the linear plots have been plotted against the above-mentioned quantities. The result does not entirely come up to expectations. Instead of the expected straight lines through the origin, linear plots are found which intersect the ordinate at a constant negative value of α_0. Probably this negative value of α_0 can be explained if the adsorption of the reactants and/or the reaction products is also taken into account.

In this case eqn. (1*a*) must be replaced by

$$c = \alpha\theta + \beta\gamma\frac{\theta_g}{1 - \theta_g - \theta_r},$$

where θ_g = fraction of surface covered with poison and θ_r = fraction of surface covered with reactants and/or reaction products. From this it follows:

$$\frac{c(1-\theta_g)}{\theta_g} = (\alpha - \alpha\theta_r + \beta\gamma) + \left(\alpha - \frac{c\theta_r}{\theta_g^2}\right)\theta_g,$$

or
$$\frac{cA/A_0}{1 - A/A_0} = (\alpha - \alpha\theta_r + \beta\gamma) + \left(\alpha - \frac{c\theta_r}{\theta_g^2}\right)\left(1 - A/A_0\right),$$

where $\frac{c\theta_r}{\theta_g^2}$ is a correction term for the slope which in a first approximation may be considered as a constant.

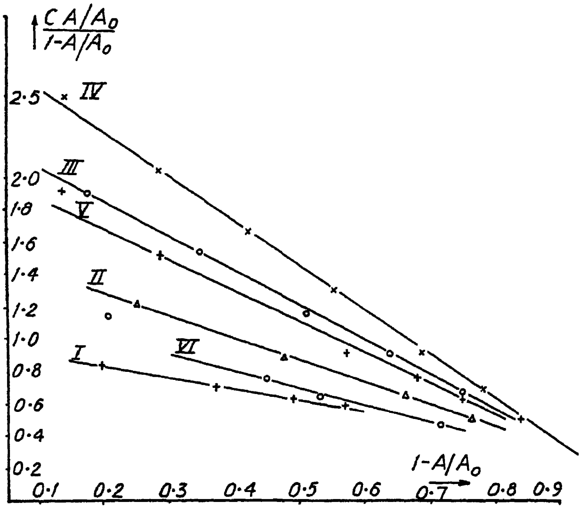

FIG. 2.

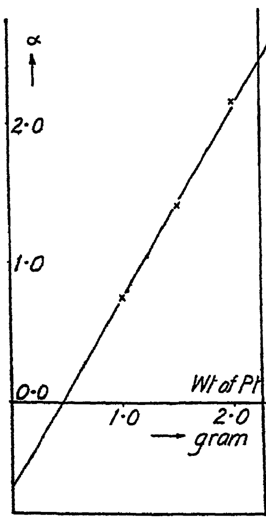

FIG. 3.

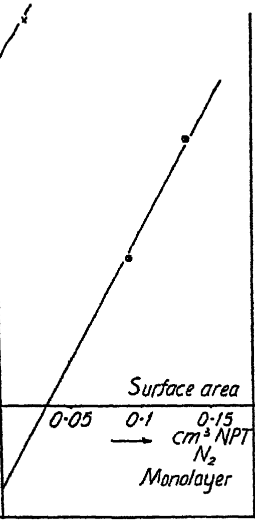

FIG. 4.

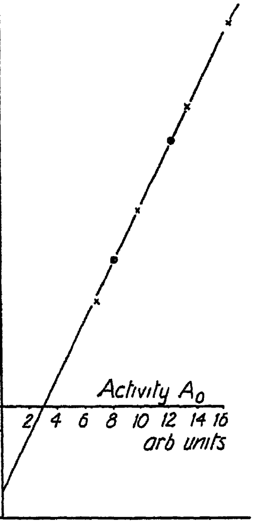

FIG. 5.

Prof. G.-M. Schwab (*Athens*) (*communicated*) : We made some years ago[19] a series of measurements of the action of poisons on platinum catalysts, using the hydrogenation of cinnamic acid, poisoned by ethyl mercaptan. We found that on progressive poisoning (within the steep

[19] Schwab and Photiades, *Ber.*, 1944, 77, 296.

quasi-linear branch of Dr. Maxted's curves) the activation energy increases considerably. From this we concluded that there was an energy distribution between active centres and were able to deduce from this distribution a surface equilibrium temperature coinciding in fact with the temperature of preparation of the catalyst. In view of these and Maxted's present results it is interesting to observe that a poison eliminates the most active centres first, whereas sintering decreases their extent in the same proportion as it does the total surface. A possible explanation would be that, during preparation, a certain crystal habitus is established, wherein the ratio of different faces in the surface depended on the method of preparation (and temperature), and that during sintering this habitus is preserved, perhaps simply by the elimination of the smallest crystals without a change in shape of the larger ones.

Prof. E. Wicke (*Göttingen*) said : With our calorimetric values of the adsorption heat of H_2 on reduced Ni powder, i.e. $Q(\theta) = 21{\cdot}2 - 18{\cdot}0\,\theta$ kcal./mole H_2 (θ = covered surface fraction ranging from 0 to 0·5) one may calculate adsorption equilibrium data for atomic adsorption using the well-known formula (based on Langmuir's theory) :

$$\theta = \frac{p^{\frac{1}{2}}}{p^{\frac{1}{2}} + \exp\{1/2R(-Q(\theta)/T + \Delta S)\}},$$

where ΔS is the entropy difference of gaseous (molecular) and adsorbed (atomic) hydrogen, the latter being nearly negligible. These calculations are in complete agreement with measured isotherms, isosteres and isobars in a temperature range 50-250° C where adsorption equilibrium is established. Hence there is no sign of solution.

If one adsorbs C_2H_4 and H_2 together on a Ni surface (reduced Ni powder) around 0° C and at such a low concentration ($\theta < 0{\cdot}2$) that the pressure in the gas phase is negligibly small ($p < 10^{-4}$ mm. Hg), then no hydrogenation occurs at all. If one pre-adsorbs C_2H_4 and immediately lets H_2 impinge on the surface from the gas phase, hydrogenation, though incomplete, takes place, decreasing in velocity and completeness with increasing time between pre-adsorption of C_2H_4 and inlet of H_2; this poisoning, as is well known, is caused by the polymerization of C_2H_4. If finally H_2 is pre-adsorbed, and C_2H_4 introduced from the gas phase, the hydrogenation is fast and nearly complete. But again the reaction proceeds more slowly, with increasing time after the pre-adsorption of H_2. This sort of poisoning, not previously reported, is caused by the H atom " dissipation " along the Ni surface rendering the distance from one another too large for fast hydrogenation at lower temperatures. This effect is especially marked with pre-adsorption around 100° C (where there is rapid " dissipation " of H atoms), followed by C_2H_4 at about 0° C. I do not see how these results can be understood in terms of the mechanisms of C_2H_4 hydrogenation hitherto proposed, but they confirm conclusively the idea of the catalytically active atom-pair state.

Dr. D. D. Eley (*Bristol*) (*communicated*) : I should like to congratulate Dr. Beeck on the numerous stimulating contributions he has made to ethylene hydrogenation and to catalysis as a whole. It may be worthwhile at this time to mention one or two points of detail. I am very glad to see that Dr. Beeck now believes the reaction is one between adsorbed ethylene and adsorbed hydrogen on the surface left bare from acetylenic complexes, as I do not believe it is possible to reconcile the reaction between gaseous ethylene and adsorbed hydrogen with the usually observed kinetics (zero order in ethylene, first in hydrogen). Since he wishes to retain his old mechanism for tungsten, I think it will be of great interest to check on the kinetics in this case. I doubt, however, that there can be *any* hydrogen chemisorbed in the ethylene film on tungsten, as the para-hydrogen conversion is completely poisoned up to relatively high temperatures.[20]

[20] Eley and Rideal, *Proc. Roy. Soc. A*, 1941, 178, 429.

I wonder whether it is worth pursuing the idea that percentage *d*-character determines interatomic spacing, and thus correlating percentage *d*-character with catalyst activity (Boudart) or heat of chemisorption (Beeck). The strength of the chemisorption bond is determined not only by the extent of orbital overlap (therefore % *d*-character), but also by the number of metallic electrons involved, and other factors. To a first approximation, all these are allowed for in my calculation by the way the sublimation energy is used as a measure of the strength of the metallic bond. The orders are :

Obs. Heat H_2 Rh < Ni < Fe < Ta < W, Cr
Obs. Heat C_2H_4 Rh < Ni < Fe < W, Cr < Ta
% *d* Cr, Ta < Fe < Ni < W < Rh[21]
Heat Calc. (Eley) Cr < Fe, Ni < Rh < Ta < W.

My calculations put Cr at the wrong end and Rh too high. The % *d* series, if it were completely reversed and W placed at the top, would exactly fit the experiment. This is what Dr. Beeck has done. It seems to me Beeck believes that the surface bond is *different* from the metallic bond and can only use the *d* orbitals *left over* from the metallic bond, i.e. the higher the % *d* in the metal-metal bond, the weaker the metal-gas bond. To reconcile the position of W in the series, Beeck notes an unpublished result that in evaporated films, its lattice parameter is different from the wire state, i.e. face-centred cubic with a greater distance which leads to a lower % *d* character. If this is so, I find it most difficult to understand why both W wires (Roberts) and W films (Beeck) should have the same heat of chemisorption for hydrogen. In my view it is incorrect to distinguish the surface orbitals M—H from the " under-surface " orbitals M—M.

Dr. J. J. A. Blekkingh (*Rotterdam*) (*communicated*) : A nickel hydrogenation catalyst in contact with hydrogen has the property of transmitting molecular hydrogen to double bonds in normal hydrogenation reactions and also of changing molecular hydrogen into atomic hydrogen. Adsorbed molecular hydrogen can be physically replaced by other substances ; this is not so with absorbed atomic hydrogen. The amount of atomic hydrogen in a nickel catalyst can be in proportion of 1 atom H to about 3 atoms of nickel.

It is because of the presence of atomic H that there is—amongst other things—a shifting of the double bonds in unsaturated fatty acid derivatives, a side-reaction (isomerization) occurring in addition to the normal hydrogenation. This side-reaction takes place already at room temperature. The isomerization with atomic H in the nickel catalyst can be represented diagrammatically by the following steps:

(i) A partial hydrogenation, in which 1 atom H is added to 1 CH group of a double bond. A radical with a free valency is formed. There are two possible radicals.

(ii) A partial dehydrogenation, in which 1 atom H is given to the nickel. A double bond is formed again. There are three possibilities for the position of the double bond.

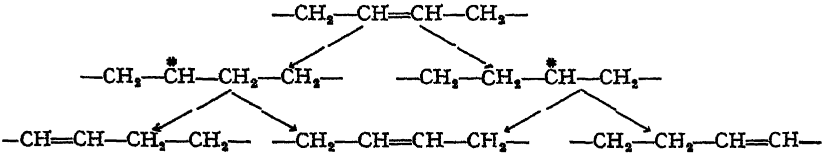

In this way we have found that a double bond can shift along the whole chain rather quickly.

---

[21] Pauling, *Proc. Roy. Soc. A*, 1949, **196**, 343.

It may be that the second step is not a partial dehydrogenation, but again a partial *hydrogenation*. In this case we may speak of *atomic* hydrogenation, with addition of H + H in the *trans* position to the double bond (addition to both sides of the plane of the double bond).

The ordinary hydrogenation may be called *molecular* hydrogenation, with addition of $H_2 = 2H$ in the *cis* position to the double bond (addition to one side of the plane of the double bond).

In practice, we suppose, isomerization with atomic hydrogenation (including 1 : 4 addition to conjugated double bonds) and molecular hydrogenation take place more or less together, and this may be the reason for different hydrogenation velocities with different nickel catalysts, or with oriented and unoriented nickel films. Selectivity of fatty oil hydrogenation may be favoured by the formation of conjugated double bonds in linoleic and linolenic, and successive atomic hydrogenation to isolated double bonds. In our opinion atomic H will not be able to poison the nickel hydrogenation catalyst, at least not above room temperature.

Mr. P. F. Tiley (*Bristol*) said: The results of Beeck and Ritchie on the use of krypton, butane and other g ses in the B.E.T. surface area measurements of metal films cannot escape comment in view of the results which have been obtained with these gases on adsorbents in other physical forms. For example, I would refer to the work of Davis, De Witt and Emmett [22] who found from B.E.T. studies with krypton and butane on silver foil and monel ribbon that the areas determined were only 80-90 % of the geometric areas. In the same work the authors found that, on adsorbents such as glass spheres, zinc oxide, tungsten powder and silica gel, the surface areas as measured by krypton and butane adsorption were less than the nitrogen values by some 30-40 %. Beebe, Beckwith and Honig [1] observed a similar phenomenon on comparing krypton and nitrogen adsorptions on anastase. In all the results quoted, the values for the cross-sectional areas of the adsorbate molecules were those calculated by the usual formula, viz: N_2, 16·2; Kr, 15·2; C_4H_{10}, 29·7 Å^2 (Dr. Beeck uses Kr, 14·5; C_4H_{10}, 24·5).

The results of Emmett and Beebe cannot be interpreted in terms of pore size nor is chemisorption of nitrogen likely on these adsorbents. The problem which faces us (discussed fully by Emmett [23] and Livingston [24]) is that, having determined the number of adsorbate molecules in the monolayer by the B.E.T. isotherm, it is still necessary to employ a suitable value for the cross-sectional area in order to calculate the absolute surface area. The value of 16 (± 0·5)Å^2 for N_2 has been generally accepted in view of confirmation by other methods of surface area determination. Emmett suggested that the empirical values of approx. 21 and 44 Å^2 for Kr and C_4H_{10} produce more satisfactory results, but as yet no fundamental explanation of these discrepancies has been established.

The surface area measurements of Dr. Beeck are extremely interesting as they are among the first to have been made on evaporated metal films and may throw some light on this problem. However, until this problem is satisfactorily elucidated it is felt that the determination of absolute surface area by B.E.T. methods must still involve uncertainties of the order of 20-30 %, particularly if gases other than nitrogen are used.

Dr. F. C. Tompkins (*Imperial College, London*) (*communicated*): I think that Mr. Tiley expects too much of B.E.T. surface area determinations. Accepting all the postulates of the B.E.T. model there is no reason why we should introduce the cross-sectional area of the adsorbate molecule—it is the lattice parameter, or the area of the crystallographic site, which is important. When the adsorbate molecule is larger than the site, one has to make decisions based on energy considerations as to what is the stable packing in the layer—if it does happen to be hexagonal close-packing it is then and only then legitimate to use the cross-sectional area of the molecule. Normally up to 70 to 80 % 1st layer coverage, it is a good approximation at low temperatures to assume localized adsorption—when there are attractive lateral interactions there can be, and often is, a transition to hexagonal packing ; but where there are repulsive interactions the localized array is approximately retained. Furthermore, analysis shows that the B.E.T. eqn. merely corrects the Langmuir eqn. for 2nd higher layer adsorption by the term $(p_s - p)/p_s$. Consequently where the B.E.T. c term is high we are virtually using only the 1st layer adsorption on a uniform surface for the evaluation of v_m, and the above considerations are important.

---

[22] Davis, de Witt and Emmett, *J. Physic. Chem.*, 1947, **51**, 1232.

[23] Beebe, Beckwith and Honig, *J. Amer. Chem. Soc.*, 1945, **67**, 1554.

[24] Livingston, *J. Colloid Sci.*, 1949, **4**, 447.

Finally, the evaluation of v_m by the B.E.T. eqn. carries with it the assumption of the equality of the internal partition functions of the adsorbed molecules in the 1st and 2nd layer—provided the same gas is used for different adsorbents and the heats of adsorption are approximately the same no trouble arises in comparing areas. With different gases on the same adsorbent, the ratio of such partition functions though of the order of unity will be somewhat different and, particularly where c is not large, different v_m values can be expected. It seems therefore profitless to concern oneself with the precise values to be taken for the cross-sectional area of molecules in the adsorbed state. The trouble is more acute when a non-uniform surface is considered—the transition from 1st to 2nd layer adsorption is then less abrupt and all the uncertainties and inaccuracies associated with low c values on uniform surfaces are again present.

Mr. P. F. Tiley (*Bristol*) (*communicated*) : In the last few years, both theory and experiment have demonstrated the shortcomings of the B.E.T. model, particularly with regard to heats of adsorption. However, the value of the standard B.E.T. technique, in providing a reasonable estimate of surface area, has not been disproved. In so far as an assessment is possible, the errors (using N_2 as adsorbate) are not as great as would be expected from Dr. Tompkins' contentions concerning the invalidity of the B.E.T. isotherm for non-localized adsorption and the irrevelance of the dimensions of the N_2 molecule in localized adsorption. With krypton, which may be used for low surface areas, consistently good agreement with the N_2 values is obtained, using the " corrected " value for $\sigma_{Kr} \approx 20$ Å^2. Whether the reason for this " correction " lies in the method of evaluation of v_m, or in the packing of the adsorbate molecules is, I suggest, a matter for conjecture. It is felt that, whilst Beeck and Ritchie have drawn rather bold conclusions from their experimental results, yet the logical outcome of Dr. Tompkins' arguments is to underrate the empirical value of the B.E.T. method.

In connection with these low pressure B.E.T. studies at liquid air temperatures, few workers seemed to have mentioned the question of thermo-molecular flow. From the experimental details given, it is difficult in some cases to discover if there is justification for thus ignoring this effect. Mr. Porter in Section IV of this Discussion gives an excellent quantitative treatment of this phenomenon.

Dr. F. C. Tompkins (*Imperial College, London*) (*communicated*) : It is my contention that the B.E.T. method cannot be expected to give results of absolute surface area determinations to better than 10-20 %. I know of no experimental data of measurements obtained by methods not involving adsorption where the agreement with the B.E.T. method is of higher concordance. Nor can I be convinced by the fact that N_2 and Kr (using an *arbitrary* value of σ_{Kr}) give consistent values ; O_2 and A for example often give quite different values than does N_2. My criticism was concerned with the excessively high accuracy implied by giving values of σ_{N_2} as 16·2 Å (or 16 ± 0·5 Å^2) ; it would be more consistent if this were written as 16 ± 2 Å.

Prof. A. R. Ubbelohde (*Belfast*) said : The terminology of the electron band theory of metals has not been adapted in any quantitative way to catalysis, and there is a risk that rather vague concepts may hinder real progress in interpreting catalytic phenomena.

Starting with the Pauling theory as an alternative to the electron band theory of metallic binding, it is possible to formulate a more concrete model for the binding of atoms such as H, O, N to the metal atoms M of the catalyst. This "pseudometallic bonding" model postulates that a group of atoms such as (M—H_n) behaves as regards external electronic behaviour like the atom *n* places to the right in the periodic system. For example, the grouping Pd—H behaves electronically like Ag, and in particular forms metallic bonds to neighbouring atoms similar to those which would be formed by Ag.

There is considerable experimental foundation for the pseudometallic bonding of groups (M—H_n). For example, when hydrogen is dissolved in alloys Pd—Ag_x in certain ranges of composition [25] the electrical resistance is actually lowered, as would be expected of the "pseudosilver group" (Pd H), compared with Pd, when alloyed with Ag. Again, the wetting of metals by mercury, which almost certainly involves the formation of metallic bonds between Hg and the surface atoms of the metal, is changed by dissolution of hydrogen in the sense to be expected from the pseudometallic model. Thus whereas Hg wets Pd only slowly, it wets Ag with avidity and recent experiments have shown that it likewise amalgamates with great avidity with Pd $H_{0.6}$, forming "palladium hydride" amalgams. Mercury also wets iron after the surface has been cathodically charged with hydrogen.

This concept of the pseudometallic bonding of hydrides can explain a number of features of hydrogenation catalysis, such as the poisoning by mercury. It leaves the possibility open that on isolated peaks on the catalyst hydrogen might be bonded by an ordinary covalent bond, less stable than the pseudometallic mode of binding in which (M—H_n) is alloyed with the neighbouring atoms.

Properties of ions such as VO^{++} and UO_2^{++} suggest that the grouping M—O_n should also be able to act as a pseudometallic unit similar to the metal *2n* places to the right in the periodic system. And the concept can be extended in obvious ways, when experimental evidence suggests that such extension is fruitful.

Mr. A. S. Porter and Dr. F. C. Tompkins (*Imperial College, London*) (*communicated*) : The admission of mercury vapour at 0° C to an evaporated iron film covered with hydrogen has been found to cause rapid desorption of most of the hydrogen, followed by a further slow desorption. After 1 to 2 hr., desorption was complete (within 1 % of the amount of gas originally put on the film). On admission of H_2 again, no further adsorption of hydrogen could be detected on this film, even at $-195°$ C and 10^{-2} cm. H_2. Similarly, a film prepared in the presence of mercury vapour was found to take up less than 1/2000 of the normal amount of hydrogen. It is clear, from these observations, that any Fe—H—Hg alloys which may exist are far less stable than the Pd—H—Hg alloys mentioned by Prof. Ubbelohde.

Mr. D. A. Dowden (*Billingham*) said : In a discussion of the possible correlation of the catalytic activity of metals with their electronic structure, both the electronic models in current use should be exhausted of their possibilities since it appears [26] that some situations can best be described by one of these models and with difficulty or not at all by the other. The band theory suggests effects connected with changing electronic exit work function, inner potential, electron-level density, etc., and emphasizes electron mobility while Pauling's transitional metal valencies encourage ideas more closely allied to the chemical, directed bond.

[25] See Ubbelohde, *J. Chem. Soc.*, 1950, 1143.

[26] Mott, *Proc. Physic. Soc.*, 1949, **62**, 416.

Mott[27] has given a qualitative explanation of the variation in cohesive energy of the transitional metals as the *d*-bands are filled up. Where the metals possess vacant *d*-levels the increased cohesion can be ascribed to the decrease of the average electron energy on removal of *s*, *p*-electrons into lower-lying *d*-levels. If a chemisorbed particle is considered, in a crude approximation, as just another lattice surface atom then the change in chemisorptive bond strength of a given substrate at the surface of transitional metals should parallel the change in cohesive energies of the metals. An old rule[28] expresses this trend by including a factor, proportional to the square root of the sublimation energy of the metal, in the binding energy of the chemisorbed substrate.

This interpretation assumes that the electron levels remain almost unchanged in the series of metals and focuses attention on the behaviour at the top of the Fermi distribution. In fact there may be variations at the bottom of the distribution leading to changes in the centre of gravity of the occupied *d*-levels[29] and hence to changes in cohesive energy and heats of chemisorption but the parallelism between these two remains unchanged.

Prof. A. R. Ubbelohde (*Belfast*) said : The discontinuous change in catalytic activity of PdH_x, or of $PdAu_x$, at the critical compositions which are just no longer paramagnetic, may have more than one cause. A factor for which insufficient allowance may have been made is the highly strained two-phase structure of the alloys up to the critical compositions, when they contain hydrogen. For example, as more hydrogen is dissolved in Pd, α and β Pd H phases with approximate composition $PdH_{0.03}$ and $PdH_{0.65}$ coexist in the solid, and the hydrogen-rich phase merely grows at the expense of the other as the total hydrogen content increases. A significant point for catalytic activity is that the coexistence of these two phases which have different specific volumes induces a high state of strain in the solid. This strain persists, as can be shown by X-ray studies and in other ways, till all the solid has been converted to the β phase, after which it is much smaller. Two-phase structures are also formed by $PdAu_x$ with $x < 0{\cdot}6$, when these alloys have dissolved hydrogen. The resultant lattice strains may likewise affect catalytic activity.

Mr. D. A. Dowden (*Billingham*) (*communicated*) : Experiment indicates that the idiosyncrasies of particular alloy systems, remarked by Prof. Ubbelohde, do not disturb the general activity pattern of a decline in hydrogenation activity as holes in *d*-bands are filled up. The notion of " a hole in the *d*-band " or its counterpart " a vacant *d*-orbital " should be neither less useful nor more confusing than was the idea of " an incomplete Lewis-Kossel octet " a generation ago.

The fall in magnetic susceptibility of palladium as it dissolves hydrogen is the over-riding criterion of activity changes in the presence of hydrogen ; phase changes and strain effects appear to be of secondary importance. It should have been a clear indication that in some temperature ranges reactions involving palladium must be hydrogen-poisoned. These solution effects occur only on a smaller scale in catalysts of nickel and platinum consequently the nickel-copper alloy series, being free from order-disorder transitions and immiscibility gaps is, despite its ferromagnetism, the best for general study.

The geometric path of adsorbed hydrogen atoms during the transition from the chemisorbed to the dissolved state must surely include interstitial sites in the surface lattice just as solution involves interstices in the bulk. These surface sites, being directly accessible from the gas phase, are in the chemisorption zone, possess the largest number of surface-metal nearest neighbours, should have the largest heats of adsorption and should be filled first. Such a surface phase might undergo transitions analogous to those of the bulk phases. More important, as Prof. Ubbelohde implies, since the ratio palladium/hydrogen atoms ~ 1, for instance in a stoichiometric, surface phase on a (100) plane then that phase has electronic properties more like a layer of copper or silver than palladium.[30] Further adsorption above this phase, e.g. above the palladium atoms, can occur only by much weaker bonds. In fact because of diffusion to the interior this surface phase is usually non-stoichiometric under catalytic condition and is never as inactive as copper except at very low temperatures. No doubt these details could be resolved by a careful study of solution and chemisorption in series of binary alloys of the type described.

---

[27] Mott and Jones, *Properties of Metals and Alloys* (Oxford, 1936).

[28] Eucken, *Z. Elektrochem.*, 1922, **28**, 6.

[29] Seitz and Johnson, *J. Appl. Physics*, 1937, **8**, 84, 186 and 246

Dr. G. C. A. Schuit (*Koninklijke/Shell Laboratorium, Amsterdam*) (*communicated*) : Dr. Beeck's remarkable correlation between the character of the metallic bond according to Pauling and his velocity constants for the hydrogenation of ethylene can be still improved upon by taking into account the valency of the metal as stated by Pauling. To effect this, $10 \log k$ is plotted against valency × % *d*-character.[31]

It is seen that the decrease in activity for Ta, which originally could not be accounted for by the decrease in *d*-character, is effected by the decrease in valency and that Ta falls on the same straight line as the metals with valency 6. Cr, which, according to Pauling, should have a valency between 6 and 3, indeed seems to be situated in valency between these two extremes. Only W appears definitely to fall out of the correlation, but as Dr. Beeck reported the metal-film structure to be face-centred, and thus abnormal, this deviation seems explainable.

Both an increase in valency and in *d*-character tend to strengthen the total bonding strength between the metal atoms ; this correlation seems to indicate that the catalytic activity runs parallel to the strength of the bonding between the metal atoms.

Dr. D. D. Eley (*Bristol*) said : The calculations on heats of chemisorption[32] assume that the metal orbital used to bond the surface hydrogen is, in all cases, the ordinary metallic (here symbolized as $d^{2.56}sp^{2.22}$) orbital. This would point to a second extreme hypothesis to explain our results, viz. the chemisorbed H atoms are held by $d^{2.56}sp^{2.22}$ and the atomic *d* orbital is only required to bind the H_3 activated complex strongly. Obviously, to decide between these closely similar possibilities requires further work.

In reply to Prof. Ubbelohde, the question of phase separation was most carefully considered by us with the conclusions given in our paper, viz. that there is no phase separation in the Pd—Au system, but that a part of the increase in activation energy in the Pd—H system may arise from the large spacing of the β-phase. We do not want to ignore his suggested effects of lattice strain on electron energy levels, but we believe the main results described in our paper may be described in terms of the simple band or orbital picture.

Prof. G.-M. Schwab (*Athens*) (*communicated*) : It would be of interest to study the parahydrogen conversion on Hume-Rothery alloys of Group I metals where *d*-gaps are absent and the occupation of the conductivity band is an important factor. The parahydrogen conversion ought to fall in one class with hydrogenation and dehydrogenation reactions, and an increase of electron concentration or formation of a γ-phase, it is predicted, should increase the activation energy.

I agree with Dr. Eley's view, that the adsorption of hydrogen " as a positive ion " does not really mean complete ionization, but rather a covalent bond by means of electrons shared between the proton and the conductivity band.

---

[30] See Beeck, this Discussion

[31] Data taken from Pauling, *Proc. Roy. Soc. A*, 1949, **23**, 196.

[32] Eley, this Discussion.

Prof. R. M. Barrer (*Aberdeen*) (*communicated*): I wish to support the observation by Couper and Eley concerning the frequently supposed positive charge on hydrogen dissolved in Pd. The calculation of the +ve charge per H-atom of 1/50 of the protonic charge must if correct lead to the conclusion that nearly all the H-atoms are substantially neutral. I pointed this out two years ago,[33] and indicated also that the frequently postulated protonic character of the dissolved hydrogen was hardly compatible with the well-known clustering of the hydrogen atoms in the metal when a critical concentration of dissolved hydrogen was reached. If the H atoms are protonic, they should repel one another.

I would also like to raise a point concerning Table I in the paper by Eley and Couper. All the larger apparent energies of activation E_a are measured in a much higher temperature range than the small energies and there is an abrupt change in the temperature range at the point where E_a also changes abruptly. Since one has only apparent energies of activation to go by, and since such apparent energies may themselves be dependent on temperature (the last two paragraphs in the paper by Rideal and Trapnell[34] emphasize just this point) I would like to ask whether we can in fact be sure that *true* energies of activation would vary in any similar way? This it seems may have to be answered satisfactorily before the electronic effect on the true energy of activation can be regarded as established.

Prof. J. H. de Boer (*Geleen and Delft*) said: The decomposition of H_2O_2 is enormously catalyzed by the presence of small amounts of ions of e.g. Co^{2+}, Cu^{2+} etc. Is it to be excluded that a small amount of Cu^{2+} are formed locally when H_2O_2 is in contact with copper? If this were true, curves A, B, and C of Fig. 2 of Dowden and Reynold's paper would denote a decrease of surface attack by H_2O_2 on copper, by increasing amounts of nickel. This might be important for corrosion problems; the explanation of such a behaviour would follow the same lines as given by these authors.

Mr. D. A. Dowden (*Billingham*) (*communicated*): Early in our experiments we considered the possibility noted by Dr. de Boer, that the whole or a part of the activity in hydrogen peroxide decomposition observed on the copper-rich foils might be due to a homogeneous catalysis by metal ions dissolved from the foils. However, analysis showed no significant differences in metal content between fresh and spent substrate. Moreover, if an otherwise normal experiment was halted during the steady state (well before the exhaustion of the hydrogen peroxide) the foil removed and the experiment continued, no activity was observed in the second stage. These tests dispose of the possibility of a homogeneous catalysis.

Mr. D. A. Dowden (*Billingham*) (*communicated*): It has been suggested by Prof. H. S. Taylor that some of our results might arise from bulk diffusion phenomena and indeed the effects noted by him occur quite frequently in the comparison of liquid with vapour-phase hydrogenations on the industrial scale. However, in these experiments the inter-phase contact is immeasurably better than can be found in a normal liquid-phase converter. Inspection of the shaking vessel (photography with a flash of duration one microsecond) confirmed the intimate mixing at shaking speeds where the reaction rate was already independent of shaking speed and showed the absence of any peculiar resonance effects. Attention should be drawn to the fact that the vapour-phase reaction over the same catalysts shows activity trends with increasing copper content which parallel those found in the liquid-phase reaction. This indicates conclusively that the activity pattern is a result of variation in electronic structure and not of complicated diffusion processes. Since the absolute activities of the iron-nickel alloys are of the same order of magnitude as those of the nickel-copper alloys and all linear dimensions, concentrations and shaking speeds remain constant, the same conclusion applies to the activity pattern of the iron-nickel alloys.

---

[33] *Faraday Soc. Discussions*, 1948, 4, 77, 120.

[34] This Discussion.

Dr. N. Uri (*Manchester*) (*communicated*) : Dowden and Reynolds point out that it is necessary to consider the reaction

$$Fe^{2+} + H_2O_2 \rightarrow FeO^{2+} + H_2O$$

as an alternative to the Haber-Weiss [35] reaction

$$Fe^{2+} + H_2O_2 \rightarrow Fe^{3} + OH + OH^-$$

which adapted to alloy catalysts becomes

$$\text{metal} + H_2O_2 \rightarrow (\text{metal, O}) + H_2O.$$

Although this mechanism, first suggested by Bray and Gorin,[36] has been recently revived by Kolthoff and Medalia,[37] who show that it is in agreement with the reaction kinetics of the hydrogen peroxide decomposition, it would appear that the formation of FeO^{2+} ion is unlikely for the following reasons.

(i) Whereas the Haber-Weiss reaction can be interpreted as one involving the breaking of the O—O bond in H_2O_2 and electron transfer from the Fe^{2+} ion to one of the OH radicals, the Bray-Gorin reaction would require a complicated rearrangement of atoms. In the latter case one would expect a considerable activation energy. Experimentally, however, the activation energy is found to be comparatively small, viz. of the order 5-10 kcal.[38] and, indeed, corresponds closely to the endothermicity of the Haber-Weiss reaction (in accordance with the energy values estimated by Evans and Uri [39] and Evans, Baxendale and Uri [40] for the O—O bond in H_2O_2, the ionization potential of ferrous ion and the electron affinity in solution of the OH radical).

(ii) Baxendale, Evans and Park [38] have shown that OH radicals produced in the Haber-Weiss reaction initiate the polymerization of vinyl compounds. No one has as yet observed the inclusion of iron atoms in the polymers, although these systems have been thoroughly investigated. In this connection I would like to mention that I have recently postulated the formation of radicals derived from tungstic and molybdic acid :[41] it would also be interesting to establish experimentally whether such radical endings could be detected in polymers formed in systems like $Fe^{2+} + H_2WO_4 + H_2O_2$ + vinyl monomer.

Prof. G.-M. Schwab (*Athens*) (*communicated*) : It is rather satisfactory that two so entirely independent approaches to the influence of the electronic factor, as Mr. Dowden's and ours, lead to so complete agreement of results. The only difference is that Mr. Dowden, working with electron-defect metals, considers the electron gaps in these elements as decisive, whereas we, working mainly on Group I metals, have to do with the empty conductivity levels.

A sphere of contact is given in our study of iron-gold alloys. There, in the concentration range where the iron gaps are filled up, Mr. Dowden would probably expect a decrease in formic acid dehydrogenation, whereas an increase is found. However, this difference can easily be explained by the fact that gold is a much more powerful catalyst than iron or copper, in a way that its conductivity band is of much more importance than the iron " gaps ".

[35] Haber and Weiss, *Proc. Roy. Soc. A*, 1934, **147**, 334 ; *Naturwiss.*, 1932, **20**, 948.

[36] Bray and Gorin, *J. Amer. Chem. Soc.*, 1932, **54**, 2124.

[37] Kolthoff and Medalia, *J. Polymer Sci.*, 1949, **4**, 377.

[38] Baxendale, Evans and Park, *Trans. Faraday Soc.*, 1946, **42**, 155.

[39] Evans and Uri, *ibid.*, 1949, **45**, 224.

[40] Evans, Baxendale and Uri, *ibid.*, 1949, **45**, 236.

[41] Uri, *J. Physic. Chem.*, 1949, **53**, 1070.

As for the formic acid reaction on nickel and copper, the most reliable values for the activation energies, as found in our laboratory, are 15 and 18 kcal. respectively, which is one-half of the figures given by him. The explanation by poisoning is probably correct. In Rienaecker's early work values as high as 26 kcal. instead of 17 for silver and 29 kcal. instead of 12 for gold were given.

One remark is in order concerning the frequency factors of the hydrogen peroxide decomposition. Their logarithms, expressed for 15 cm.^{2} surface and a product flow in cm.^{3}/min. are 2·1 for $q = 10$ kcal. and 8·8 for $q = 24$ kcal. For formic acid vapour over any catalyst whatsoever the respective values are 3·1 and 7·3 kcal. Thus, as to the general relationship of activity and activation energy, the two reactions, externally so different and internally so opposite, do not differ essentially.

Lastly, it is of interest to note that Wagner and Himmler found that the completion of the electron band decreases the (de)hydrogenation, but enhances the nitrogen adsorption, thus indicating the adsorption of nitrogen in the form of an anion or at least at the expense of the metal electrons. The importance of this in ammonia catalysis is obvious.

Mr. D. A. Dowden (*Billingham*) (*communicated*) : It is especially important now, in view of the successes of the carbonium-ion theory in other fields, to keep an open mind about the presence of positive ions at metal surfaces. As Huang and Wyllie [42] have pointed out, simple image force calculations provide no conclusive answer to this problem. In systems where hydrogen chemisorption is accompanied by a positive dipole layer there is no difficulty in applying an old established model used in the study of thermionic emission [43] and considering a small fraction of the surface to be covered by positive ions or strong positive dipoles. Moreover, any chemisorbed hydrogen, whatever the polarity of the bond, may function as a proton under those conditions where the presence of another species of large proton affinity (e.g. olefines, alcohols) can lead to the production of strongly adsorbed carbonium and oxonium ions. Bremner [44] has given evidence suggesting that the hydrogenolysis of esters and alcohols is controlled by reactions involving carbonium ions at the surface of metallic copper catalysts. If this analysis is correct then one must admit the presence of adsorbed species which are essentially positive ions not only at copper surfaces but at all active metal surfaces.

Prof. J. H. de Boer (*Geleen and Delft*) said : Prof. Schwab's remarks that there is a linear relationship between the logarithm of the frequency factor and the activation energy reminds me of a similar relationship between the work function ϕ of a metal and the logarithm of the constant A of the Richardson equation for thermionic emission :

in cases of adsorption of gases on metal surfaces. An increase of ϕ by the chemisorption of, e.g. oxygen, is accompanied by a large increase of A, whilst a decrease of ϕ by the adsorption of, e.g. alkali metals or thorium or, in many cases, hydrogen, gives rise to a substantial decrease of A. Richardson himself noticed already that both A and ϕ depend amongst other things, upon the degree of occupation with adsorbed material θ and that a relationship :

$$\phi_\theta = \phi_0 + k \ln A_\theta$$

holds. The cause of the change of the constant A was later ascribed by Schottky and by others to the temperature dependence of the dipoles which the adsorbed atoms have formed on the metal surface. This temperature effect gives rise to a temperature dependent term in $\Delta\phi$, which term when substituted in Richardson's equation cancels its proportionality with T against the T of kT, the result being that part of the exponent is independent on temperature and will automatically be combined with A. The effect gives indeed the right order of magnitude for the changes in A which are observed.[1]

---

[42] This Discussion.

[43] de Boer, *Electron Emission and Adsorption Phenomena* (Cambridge, 1935).

[44] Bremner, *Research*, 1948, 1, 281.

If now in a catalytic reaction the formation of a *positive* ion plays a dominant role, and we can alter the work function of the metal independently, we may expect:

(i) An increase of the work function to give a decrease of the energy of activation and a decrease of the frequency factor;

(ii) a decrease of the work function to give an increase of the activation energy and an increase of the frequency factor. If the formation of a *negative* ion on the surface plays a dominant role, we expect:

(iii) an increase of the work function to increase the activation energy and to increase the frequency factor; and

(iv) a decrease of the work function to decrease the activation energy and to decrease the frequency factor.

I would not be surprised if double layers of either positive or negative sign play a role at the surface of alloys. I do not think it improbable that, e.g. in a silver-cadmium alloy, the distribution of the cadmium atoms and the silver atoms at the surface results in a small double layer with its positive side pointing away from the metal. The formic acid decomposition on such a surface would then represent case (ii), giving an increase of both the activation energy and the frequency factors, as Prof. Schwab has found.

Mr. P. Rowland (*Guy's Hospital, London*) said: I wish to call attention to the work of Gwathmey and his collaborators.[45] The essential properties of heterogeneous catalysts are mainly the chemical properties of the surfaces of crystallites and it is therefore valuable to study the chemistry of the surfaces of single crystals. Two main types of experiment have been carried out on electro-polished single crystal spheres, slices, etc.

(*a*) The rates of reaction of the different faces with O_2, Cl_2, etc., have been studied and found to vary markedly with the indices of the surface planes.[46]

(*b*) Catalytic reactions have been studied, e.g. the reaction of H_2 with O_2 in the neighbourhood of 400° C on copper and nickel.[47] In many cases rearrangement of surface atoms of the metal occurs during the catalytic reaction to give microfacets parallel to certain crystal planes, e.g. the reaction between H_2 and O_2 on copper exposes mainly (111) microfacets. Gwathmey has further shown that different faces have different catalytic activities (e.g. for $H_2 + O_2$ on copper at 400° C the activities of (001) and (111) are in the appropriate ratio 1 : 2) and has shown some correlation between the catalytic properties of a face and its oxidation rate.

The author has extended the oxidation technique by studying reactions such as

$$\mathrm{Cu}\ (cryst.) + \mathrm{I_2}(g) \rightarrow \mathrm{Cu_2I_2}(g)$$

under conditions such that bulk halide is not built up.[48] These reactions etch the surface so that only certain microfacets appear (i.e. (001), (011), (111) and (012)). It is the author's opinion that these microfacets appear because they are stabilized by chemisorbed monolayers of halogen. It is also suggested that in the reactions between H_2 and O_2 studied on metal surfaces by Gwathmey, the rearrangement of the surface metal atoms is ordered by relatively stable adsorbed layers of oxygen on the faces concerned. There is strong evidence that in the presence of electronegative substances at moderate temperatures the mobile surface atoms of a metal rearrange to give definite microfacets.'[49]

---

[45] Cp. de Boer, *Electron Emission and Adsorption Phenomena* (Cambridge, 1935).

[46] Benton and Gwathmey, *J. Physic. Chem.*, 1942, **46**, 969.

[47] Gwathmey and Leidheiser, *J. Amer. Chem. Soc.*, 1948, **70**, 1200, 1206.

[48] Rowland, *Nature*, 1949, **164**, 1091.

These experiments have an important bearing on the production of metal catalysts either by reduction of oxy-compounds or by leaching out one component of an alloy as in the manufacture of Raney nickel. Thus, in the later stages of the reduction of CuO with hydrogen, conditions closely resemble those in the reaction of H_2 with O_2 on copper crystals. In both cases copper atoms migrate freely through the vapour phase.[50] It will be expected, therefore, that the copper crystallites produced will present mainly (111) facets as in Gwathmey's experiments. Also, unless exceptionally pure hydrogen is used nearly all metals will retain a monolayer of oxygen and their catalytic properties are those of surfaces so contaminated. On the argument given above it is probable that, beside altering the work function, etc., these layers stabilize the facets of the crystallites and inhibit sintering (e.g. pure copper sinters at room temperature and is non-catalytic[51]).

Similar considerations apply to experiments on " flashed " tungsten wires. The cleaning process at high temperature should leave a smooth surface[52] but heating in the presence of oxygen should produce microfacets and hence a change in the surface.

There is strong evidence that etching in solution is also controlled by chemisorbed layers[53] and this may be important in the production of Raney nickel by leaching out Al from Ni + Al alloy. The nickel atoms must re-aggregate since they are too widely spaced in the original alloy to form a structure after removal of the aluminium. The adsorbed layers will play an important part in determining which facets predominate in the nickel crystallites and will also remain to modify the catalytic properties of the metal. Studies of the electrochemical properties of metal crystals are therefore essential to an understanding of Raney type catalysts.

The chief criticism of the single crystal method is the impossibility of obtaining a clean surface. However, as indicated above, most metal catalysts are contaminated with oxygen. In any case, the state of the surface which is important is that which obtains during catalysis and it is not practical (or even possible in some cases) to work with reagents which are completely free from oxygen. The chemistry of catalysts is therefore, in the main, the chemistry of contaminated surfaces and for this reason the study of the behaviour of known crystal surfaces, under well-defined conditions of contamination (e.g. oxidation, $H_2 + O_2$ catalysis, etc.) is of fundamental importance. The results of Gwathmey and of the author together with those of electron emission experiments show that the adsorptive properties (and hence the effective chemical properties) of metal surfaces are very dependent on the crystal plane concerned. By applying single crystal techniques in conjunction with those of electron diffraction and electron emission further insight may be gained into the processes involved in the production of metal catalysts, the types of surface which predominate and the chemical properties of those surfaces.

Mr. D. A. Dowden (*Billingham*) (*communicated*) : Our magnetic apparatus could not be used to determine Curie points and it was not therefore of use as a test of homogeneity in the ferromagnetic alloys. The supported alloy catalysts are not completely homogeneous because the susceptibilities of the nickel-copper series from 0·6 to 0·9 atomic fraction of copper are somewhat larger than for the corresponding annealed foils

[49] Chalmers, King and Shuttleworth, *Proc. Roy. Soc. A*, 1948, **193**, 465.

[50] See also Dowden and Reynolds, this Discussion.

[51] Beeck, Smith and Wheeler, *Proc. Roy. Soc. A*, 1940, **177**, 62.

[52] But only if alternating current is used ; see Johnson, *Physic. Rev.*, 1938, **54**, 459.

[53] Tamman and Sartorius, *Z. anorg. Chem.*, 1928, **175**, 97.

and show a slight field dependence between 2000 and 4000 oersted. Nevertheless the close parallelism between the decline in susceptibility (at a fixed field strength) and activity in the region where the 3 *d*-band is filling establishes the main point for the bulk of the catalyst. The inferences drawn from the results on the iron-nickel series must be true in a similar approximation.

III. ADSORPTION AND CATALYSIS ON OXIDES

INTRODUCTORY PAPER

By W. E. Garner

The principal catalytic reactions occurring on oxides are those concerned with hydrogenation, dehydrogenation, dehydration and oxidation, and subsequent molecular rearrangements such as isomerization, polymerization, etc. The basic processes therefore involve the exchange of hydrogen, oxygen and water, and in some cases carbon monoxide, between the adsorbent and the substrate. It is clear that the nature of these elementary processes must be understood before the kinetics of oxide catalysis can be placed on sound foundations. With this in mind, considerable attention has been paid in recent years to the study of the basic processes by physical and chemical methods.

The Substrate.—The oxides act as catalysts in a region of temperature where there is believed to be relatively little mobility of oxygen atoms in the lattice itself, although, as shown by the rates of oxidation of metals at low temperatures, there may be appreciable movement of metal ions under the electrical fields which are set up during the oxidation.[1, 2] On the surfaces of oxides, however, there must be greater freedom of movement, and the mobility of the oxygen atoms must be considerably greater on the surface than in the bulk of the oxide. The work of Hüttig[3] on the interaction between mixtures of oxides shows that the first process on raising the temperature is the flow of the more mobile oxide over the surface of the less mobile oxide. Experiments by Winter[4] on the exchange of O^{18} with the oxygen atoms of Al_2O_3, MgO and Cr_2O_3 show that there is a very considerable mobility of oxygen from the first layer of atoms into the adsorbed state and vice versa.

In this Discussion, Winter describes further work on oxygen exchange with thorium oxide (440-540° C), chromium oxide (323-527° C) and magnesium oxide. In all cases the exchange reaction is kinetically first order. The interesting result is obtained that for chromium oxide the activation energy is 29·5 kcal. up to 410°, and 1-4 kcal./mole above this temperature. The rate-determining step is ascribed to desorption below 410° and to exchange between adsorbed oxygen and the oxygen atoms of the lattice above this temperature. If this interpretation is correct, then the oxygen ions in the surface of Cr_2O_3 are mobile at catalytic temperatures.

The oxide catalysts may be classified into two groups, semiconductors and insulators. In semiconductors there is a higher mobility within the lattice than occurs with insulators, as a result of which lattice defects are the more readily produced. There are two principal kinds of defect in oxides, one due to an excess of metal and the other due to an excess of oxygen within the lattice, and both kinds may arise during the oxidizing and reducing processes that occur in catalytic reactions at high temperatures. However, within the range of temperatures at which catalytic

---

[1] Mott and Gurney, *Electronic Processes in Ionic Crystals*, 1940.
[2] Anderson, *Trans. Faraday Soc.*, 1948, **44**, 163.
[3] Hüttig, *Z. anorg. Chem.*, 1935, **224**, 225 ; see also this Discussion.
[4] Houghton and Winter, *Nature*, 1949, **164**, 1130.

processes are carried out, the formation of defects by oxidation and reduction is confined, in general, to the surface layers, since the diffusion of defects within the lattice possesses a high temperature coefficient. The importance of these defects for catalysis lies in the fact that around the defects there are produced a variety of surface energy levels, some of which may lie in the range required (*a*) for electron exchange reactions between the absorbent and the lattice and (*b*) for the facilitation of chemical bonding of molecules and atoms with the surface. Dowden[5] has analyzed the position from this point of view, and has indicated the ways in which defects can facilitate adsorption processes. Since the basic reactions occurring on the surface of semiconductors may modify the semiconductivity, measurement of this property during adsorption and catalytic reactions yields useful information.[6, 7]

Chemisorption.—There has been much discussion as to whether chemisorption and catalytic reactions occur on the whole available surface or on active centres. As Eucken[8] points out, it is important to separate adsorption from catalysis, since there may be reasons of a statistical character why, on a completely covered surface, only a part of the adsorbed film is effective catalytically. There seems to be little doubt from the studies of tungsten and nickel surfaces, that the whole surface is involved in the chemisorption of hydrogen, and there also seems to be little doubt in the case of some of the catalytic reactions involving hydrogen. There is, however, no reason why this should be generally true. The energetics of the catalytic activation of hydrogen have been discussed by Polanyi,[9] who finds that on a good hydrogen catalyst the strength of the hydrogen bond with the surface must lie within narrow limits. This is probably true generally with regard to the relationship between the strength of the bonds of chemisorbed substances and catalytic activity. The conditions for the formation of a chemical bond with the characteristics required for catalysis may be just as likely to be met at a defect, a Frenkel step, or a dislocation as at a plane surface. There is therefore no *a priori* reason why catalysis should not proceed as rapidly at defect structures as on the plane surface, except that the numbers of defects are necessarily limited compared with the total number of surface atoms. Many observers working with oxide surfaces have found it necessary to postulate the presence of "active" centres. A striking example is that of catalysis on alumina-silica, where the activity is proportional to the number of structural acid groups on the surface.[10]

One of the stages in a catalytic reaction involves the dissociation of molecules, which requires the breaking of strong chemical bonds (H_2, 102, and O_2, 117 kcal.). This is, however, balanced by the simultaneous formation of strong bonds with the surface of the solid. There is, however, a lower limit of temperature below which the dissociation occurs very slowly. This varies from case to case; for example, it occurs at $\sim 150°$ K for hydrogen on nickel[8] and at $\sim 300°$ K for hydrogen on manganous chromic oxide.[11] There is considerable evidence available (cf. Eucken[8]) that hydrogen may be chemisorbed as molecules as well as atoms. Taylor has summarized the evidence bearing on the dissociation of hydrogen and other gases on solid surfaces.[12]

In many of the catalytic reactions involving oxides, adsorbed hydrogen would appear to be dissociated into atoms at temperatures below those at which catalytic reactions involving hydrogen occur. Therefore, in the majority of cases, the dissociation of hydrogen may be ruled out as a rate-determining step.

---

[5] Dowden, *J. Chem. Soc.*, 1950, 242.

[6] Garner, Gray and Stone, this Discussion; Gray, this Discussion.

[7] Anderson and Bevan, this Discussion.

[8] Eucken, this Discussion.

[9] Polanyi, *Sci. J. Roy. Coll. Sci.*, 1937, **7**, 21.

[10] Millikan, Mills and Oblad, this Discussion.

[11] Taylor and Williamson, *J. Amer. Chem. Soc.*, 1931, **53**, 2168.

[12] Taylor, *ibid.*, 1931, **53**, 578; *Advances in Catalysis* (1947), p. 1.

On oxides, hydrogen may be reversibly or irreversibly chemisorbed. The occurrence of reversibly adsorbed hydrogen on oxides is of interest because it resembles the adsorption of hydrogen on metals. The adsorption of hydrogen on metals can be visualized as giving M—H linkages, the hydrogen being bonded possibly with the electrons of the *d*-shell. On zinc oxide, which possesses interstitial zinc atoms, the reversible adsorption of hydrogen of this character on the defects offers no difficulty, nor does its adsorption on the lower oxides of the transition elements, where not all of the metal atoms are directly linked to oxygen. In promoted oxides, where one of the oxides is easily reduced to metal (for example, Cu in CuO . ZnO) or on promoted iron-ammonia catalysts, the metallic type of bonding with hydrogen must be present.[5] Oxides showing reversible adsorption of hydrogen at low temperatures, on heating may evolve hydrogen, which is re-adsorbed irreversibly on raising the temperature to give OH groups on the surface.[13] This explains the fact that at still higher temperatures, the hydrogen can be desorbed only as water. The adsorption of hydrogen atoms on oxides may thus be effected in at least two ways, in one of which it is held as M—H and in the other as M—OH. Many catalytic processes may involve the switch of hydrogen from one position to the other. Further investigation may, however, show that hydrogen is adsorbed in other ways in addition to the two mentioned above.

Work described in this Disucssion[6] indicates that the oxygen molecules adsorbed on Cu_2O surfaces undergo the following series of reactions :

$$O_2 \overset{1}{\rightleftharpoons} \underset{/}{O}\text{—}\underset{/}{O} \overset{2}{\rightleftharpoons} 2O \overset{3}{\rightleftharpoons} 2O^- .$$

Stage 1, giving a chemisorbed molecule, is apparently a rapid process, as is also the case with hydrogen, but it has not been found possible to decide whether 2 or 3 is the rate-determining step. There is considerable mobility of the adsorbed oxygen atoms on cuprous oxide, so that on porous surfaces some of the oxygen may escape reaction with other gases, possibly due to diffusion down narrow channels. Thus, in the reaction between CO_2 and adsorbed oxygen, the gases must be admitted simultaneously with the carbon dioxide in large excess in order that each oxygen atom may enter into reaction. A similar time dependence of the reactivity of adsorbed hydrogen is found by Eucken in studies of the reduction of cyclohexene, which he ascribes to the separation of the hydrogen atom pairs formed on dissociation by a process of surface diffusion.

The chemisorption of carbon monoxide is very similar to that of hydrogen. The heats of adsorption and behaviour on desorption indicate that there are two types of bonding which can be represented as M——CO and $MOCO_2$.[14] In this connection it will be noted that carbon dioxide can react with adsorbed oxygen to give surface carbonate ions held by electrovalency to the surface.

In the chemisorption of hydrocarbons on oxide surfaces, there is a rupture of carbon-carbon and carbon-hydrogen bonds. There are two theories of the cleavage process, in one of which radicals are produced which adhere to the surface by homopolar bonds ; according to the other, carbonium ions are produced which adhere to the surface by electrovalency. In order to explain the nature of the final products of hydrocarbon alkylation, isomerization and cracking, and the yields in which the products are obtained, it has been convenient in recent years to postulate the formation of fugitive intermediates containing the carbonium

[13] Garner and Kingman, *Trans. Faraday Soc.*, 1931, **27**, 322.

[14] Garner, *J. Chem. Soc.*, 1947, 1329.

ion. The presence of a positively charged carbon atom in the hydrocarbon chain is regarded as facilitating scission, and the transference of hydrogen atoms and methyl groups along the carbon chain. There appears as yet to be no independent physical evidence supporting the carbonium mechanism, which is highly desirable.

Promotion and Poisoning.—The types of promotion and poisoning are at least as numerous as the ways in which solid substances can interact with one another. Mixtures of solids can give rise to solid solutions or chemical compounds. Also, additives can modify the network structure of glasses and colloidal aggregates, or can produce various types of interface when adsorbed on a solid surface.

Solid solutions are of considerable importance in the semiconducting oxides, especially if the cations and anions entering into solid solution have different valencies from those of the lattice. It is possible to vary the number and nature of the anionic and cationic vacancies by the addition of appropriate ions which will lead to modifications in catalytic activity. Again, vacancies can be poisoned by the adsorption of strongly adsorbing ions on the defect structures. The alkali metals may play this role in a number of catalysts.

In the formation of chemical compounds between oxides (as in the formation of spinels from oxides), Hüttig [8] has shown that labile intermediate states are first formed on the surface of the less mobile oxide which are more effective in catalysis than the final compound. The characteristics of mixed oxide films on the surface of solids and their nucleation to give a second solid phase form an interesting subject for further research. The new surface lattice structures may be geometrically more useful for catalysis than those of either component, and they may, on energetic grounds, enter more readily into chemical reaction with adsorbents. The nature of the defects may be modified by compound formation, and from this point of view Anderson has studied the semiconductivity of the spinels. The importance of the structural acids produced by the interaction of alumina and silica gel is emphasized in this Discussion in the employment of cracking catalysts.

Selwood and his co-workers have employed magnetic susceptibility measurements to study the structure of the transition metal oxides, for example, of chromium, manganese, nickel and iron, when dispersed on supporting oxides such as magnesia, γ-alumina and rutile. It was shown that above a certain surface concentration the transition metal oxides aggregate into islands of several layers thick which have high magnetic susceptibilities and high catalytic activity. The support may confer its own structure and induce its own valency on the transition metal oxide : thus nickel on magnesia has a valency of two, on γ-alumina a valency of three, and on rutile a valency of four. Selwood and Lyon [15] extend this work in this Discussion to other oxides on the same supports. The stabilization of different valencies on the supported oxide obviously must play an important part in catalysis, and the magnetic susceptibility results indicate that the *d*-shell is involved in the surface reactions.

Griffiths, Chapman and Linders [16] have studied the promotion of molybdenum oxide catalysts by silica, making measurements of changes in composition, surface area, crystal structure, electrical conductivity and thermoelectric potential of the catalysts. It is shown that the area and activity of the catalyst for hydrocarbon decomposition is at a maximum when the maximum amount of silica is incorporated in the lattice. There is some reduction to metal with hydrogen when the silica exceeds 3 %. The molybdenum metal produced is not, however, believed to play much part in the catalysis, which is mainly due to MoO_2. Evidence is brought forward that MoO_2 is an electron-excess conductor.

---

[15] Selwood and Lyon, this Discussion.

[16] Griffiths, Chapman and Linders, this Discussion.

Insulators as Catalysts.—Insulators, of which silica-alumina and aluminium chloride are examples, bring about the dehydration, isomerization, polymerization and the cracking of organic molecules. Since the mechanisms of the processes which are involved resemble those occurring in the homogeneous phase with strong acids, it is generally concluded that the sites responsible for the catalysis are strongly acidic. It is also on similar grounds maintained that organic carbonium ions, and oxonium ions, are formed as intermediates during cracking processes, and that an exchange of protons occurs between the adsorbed molecules and the surface. Water present as OH and H ions is regarded as being the source of the protons, since the activity decreases with fall in the water content of the catalyst. In agreement with these hypotheses, the acidity of the surface, as determined by chemical methods, in many cases runs parallel with the catalytic activity and also, as anticipated, poisons of a basic nature are found to lead to a decrease in activity.

These questions are discussed in a number of papers in this Discussion. Millikan, Mills and Oblad [10] have studied the nature of the structural acidity and conclude that structural acids do, in fact, exist at catalytic temperatures but are unstable at the higher temperatures. They suggest that in some cases structural acids are not actually needed for all catalytic cracking reactions. Since hydrocarbons are weak Lewis bases, all that is needed is an active polar complex of aluminium oxide and silica capable of undergoing change of co-ordination. It is suggested that these complexes are formed at the points of contact of silica and γ-alumina grains. May, Saunders, Kropa and Dixon [17] have studied the cracking of 1 : 1-diaryl ethanes on silica-alumina catalysts, using the production of ethyl toluene and methyl styrene as a measure of the total cracking. It is shown that the rate of cracking decreases as the electronegativity of the hydrocarbon increases, the order being the same as in Hammett's reactivity series. This supports a carbonium ion mechanism in which there are interchanges of protons between structural acids and the adsorbed molecules. Tamele [18] ascribes the activity to changes in the co-ordination number of an aluminium-silica complex by the addition of water. This complex in a fully dehydrated state is a Lewis acid and an electron pair acceptor. He ascribes various methods of determining acid strengths of catalysts, and in particular the titration of the solid immersed in benzene with *n*-butylamine, using *p*-dimethylaminobenzene as indicator. The activity of the catalysts for a number of processes runs parallel with the acidity. In the polymerization of *iso*propylene the activity varies linearly with the surface acidity.

The University,
Bristol.

---

[17] May, Saunders, Kropa and Dixon, this Discussion.
[18] Tamele, this Discussion.

CATALYTIC ACTIVITY AND COMPOSITION OF OXIDE SYSTEMS

By G. F. Hüttig

Received (in German), 19th January, 1950

Intermediate states in the transformation from an oxide mixture to a chemical compound are important in the theory of catalysts. The transformation does not proceed discontinuously but through individual characteristic states ; it takes place by the diffusion of the mobile component, i.e. the oxide

of lower melting point, over the surface of the less mobile component, the former later becoming strongly bound and localized. Other stages of activation include internal diffusion of the mobile oxide, the formation of disordered crystalline aggregates and finally the filling of crystal defects. The various stages are linked with the changes of catalytic activity during activation for binary oxide systems.

The activity of a catalyst composed of several oxides depends primarily upon its chemical nature, which can be determined by qualitative and quantitative analysis. As a general rule it is valid to suppose that an observable catalytic activity can only be expected if there is some chemical affinity between at least a component of the catalyst and a component of the substrate which, however, in the conditions under consideration, will just be sufficient to bring about a chemical reaction between the catalyst (or part of it) and the substrate.

The complexity of catalytic phenomena in this field is even greater, since systems of the same chemical nature show different catalytic characteristics according to their previous history. The cause of this may be the difference in the *magnitude of the reactivity*. We shall define the chemical reactivity as the free energy which 1 mole of the catalyst system in the state considered contains in excess of that in its thermodynamically stable state. In general there is little error if one equates the chemical reactivity to the thermodynamic activity which, according to the above consideration, is related to the difference in the total energy. The cause of activity in catalysts consisting of a single oxide lies either in the high degree of dispersion, or irreversible lattice defects, or less often, in the existence of a thermodynamically unstable modification. For catalysts consisting of several oxides, a *further* possible cause of the activity is the potential energy of the oxide mixture compared with that of its reaction products. Thus, for example, although each oxide alone shows no activity, a mixture of ZnO and Cr_2O_3 will react slowly (perhaps after a very long period) to form the compound $ZnCr_2O_4$, and here the activity of the mixture is larger than that of the product by an amount equal to the affinity of this reaction. From experience we know that the process above does not proceed discontinuously, but passes through a number of intermediate states, which can no longer be regarded as being the original mixture nor yet the final product. A mixed catalyst will thus change continuously in the catalytic furnace to a greater extent than a single oxide. Since it is a fundamental postulate of thermodynamics that a series of successive states indicate also a series of free energies in decreasing order of magnitude, it is possible to reduce the changes which occur in a catalyst consisting of an oxide mixture, to the following scheme.

The arrangement of decreasing reactivity is of course related only to the total free energy content per mole of catalyst, and not at all to how this free energy is distributed over the individual molecules. Thus, in principle, we can have in any state, molecules or regions with a high free energy content and others with small energy content. Regions of especially high free energy content are expected at or near the phase boundaries. Every *active* substance must take part in *every* reaction or *every* chemical equilibrium which has an affinity larger than the reactivity by an amount which would be attributed under similar conditions to the stable metals.[1] This is, of course, also valid for the transient reactions and processes which take place between catalyst and substrate. Thus, under similar conditions the catalytic activity will be the greater, the higher the reactivity. It is therefore not impossible that the total catalytic activity of any one of the intermediate states may be greater than that of the original mixture, since in some of the intermediate states, the activity of the sites accessible to the substrate, and perhaps their number, is greater than in the original mixture. It is a well-known experimental fact that many catalysts require a certain time before reaching their optimum catalytic activity.

---

[1] Thus for example, a stable ZnO in contact with liquid water is in equilibrium with stable $Zn(OH)_2$ at 39° C, whereas ZnO of thermochemical activity of 930 cal. is in equilibrium with it at 140° C. Hüttig and Möldner, *Z. anorg. Chem.*, 1933, **211**, 368.

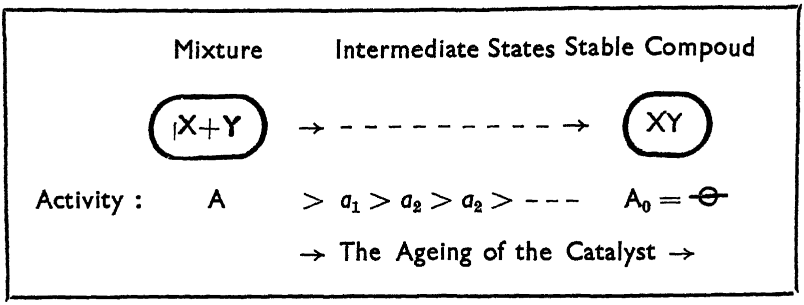
Mixture
Intermediate States Stable Compoud
X+Y
XY
Activity :
A
> a_1 > a_2 > a_2 > - - -
A_0 = 0
→ The Ageing of the Catalyst →

FIG. 1.

This definition of the activity in terms of energy is insufficient for an unambiguous description of such a state. It is possible for two catalysts identical in chemical composition and free energy content to behave differently in regard to catalytic activity because of differences in kind and spatial arrangement of lattice defects or constitutional characteristics. In modern chemistry, especially using colloid principles, one can obtain an almost infinite number of states in one and the same chemical compound. Such states (in some cases confined to the surface) can be caused by partial or complete differences in the position of the atoms or molecules or ions. This causes a number of singularities in the fields of force between atoms, which in turn affect in different ways the extent and selectivity of the catalyst. With single oxides there exist as many series of states as there are reactions in which an oxide is involved. Every active state of the solid will still have the characteristics of the solid from which it has been formed. It is clear that the possibilities of preparation will increase as we pass from a single oxide to systems built up from two or more oxides. The variations in preparation most frequently made use of include the following: the stable oxides are ground separately or together to a more or less finely dispersed system, or one can use as starting material reactive oxides with certain properties, or alternatively compounds are put into the catalyst furnace (e.g. hydroxides or carbonates) which at the temperature employed are transformed into oxides. Often, small alterations in the method of preparation (as for instance the capacity of the furnace, or the method of stirring, or mixing [2]) may cause essential differences in the catalytic properties of the resultant preparation. The gaseous atmosphere in which the catalyst is formed has also a considerable influence. To obtain a certain selective activity, it is especially favourable to prepare the catalyst in an atmosphere of the same gas (e.g. by thermal decomposition of an oxy-salt) whose change is to be effected catalytically. Thus, for example, one would prepare the iron catalyst, required for ammonia synthesis, by reduction of an iron oxide with the mixture ($3H_2 + 1N_2$). The phenomena encountered in this field are comparable in their enormous complexity with those found in organic chemistry. In the literature of catalysis, the development of theory has dealt relatively little with this aspect, in contrast to the predominant part given to it in kinetic problems. The

[2] Hüttig and Heinz, *Z. anorg. Chem.*, 1948, **255**, 223.

majority of the innumerable empirical observations found in the patent literature are almost ignored by those engaged in fundamental research. An attempt by Hüttig[3] to introduce some theoretical order, on the basis of a comprehensive system of reaction types, has remained almost unnoticed.

An example of the fundamental dependence of the properties of the catalyst upon its history is shown in Fig. 2. Two different compounds were prepared, both having the composition $1ZnO + 1Fe_2O_3$. One compound (*a*) was prepared by mechanical disintegration and admixture of the two oxides, while the other compound (*b*) was formed by precipitation of the Zn and Fe hydroxides from a common solution. As is well known, these hydroxides are transformed into oxides at moderate temperatures. Various samples of each compound were heated in the same way, to different high temperatures T_1 and, after cooling, their magnetic mass susceptibility χ was measured. In Fig. 2 the temperatures of preheating are plotted as abscissae and corresponding values of $\chi \times 10^6$ as ordinates. Graphs (*a*) and (*b*) refer to the compounds mentioned above. It can be seen that the magnetic character of the two series of compounds is completely different, and the same might be expected of their catalytic properties.

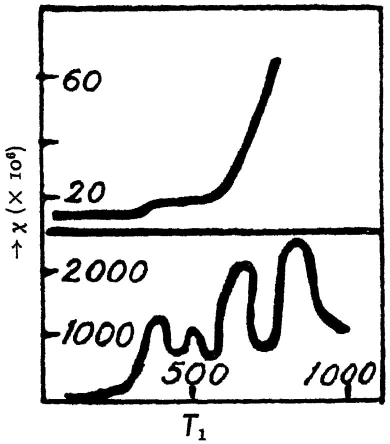

FIG. 2.

In the theory of catalysts, those intermediate states in the transformation from the oxide mixture to the chemical compound will be of special importance. Preliminary information about this is obtained from the experimental results given in Fig. 2. Various samples of the mixture $1ZnO + 1Cr_2O_3$ were heated for the same time in a stream of pure nitrogen to different high temperatures. After cooling, determinations were made of the solubility of ZnO at 40° C in 10 N hydrochloric acid and that of Cr_2O_3 in boiling hydrochloric acid of maximal concentration. The amounts of ZnO and Cr_2O_3 dissolved at any instant are plotted as a function of the preheating temperature (ordinates are on a different scale for ZnO and Cr_2O_3). In the upper half of Fig. 3, the full line corresponds to the amount of Cr_2O_3 dissolved and the dotted line to that of ZnO. In the lower half of this Figure are given the results of X-ray examination of the compounds prior to solution.

From these results, one can draw the following conclusions. Firstly, the transformation of the mixture into the chemical compound does not occur discontinuously but through individual, characteristic, intermediate states which, however, are not substances with specific X-ray diagrams. For example in Fig. 3, such intermediate states predominate for the two compounds preheated between 550° C and 900° C. The mode and extent of catalytic capacity are characteristic of the corresponding system of mixed catalysts.

Secondly, in the course of this transformation, both oxides fulfil different functions, often marked by opposite behaviour. Thus increase in the solubility of one component always corresponds to a decrease in the solubility of the other, or vice versa. It is only when the final product $ZnCr_2O_4$ is present that any further alteration is associated with a decrease in the solubility of both components. We shall therefore distinguish between a "mobile" component, that with the lower melting point (in this case, Cr_2O_3), and the "less mobile" component (ZnO).

---

[3] Hüttig, *Kolloid-Z.*, 1941, **94**, 258.

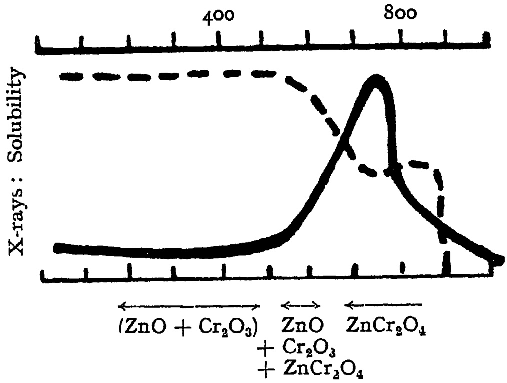

FIG. 3. --- ZnO ——Cr_2O_3

It is clear that the existence of these intermediate states and the phenomena associated with them, are of special interest in the theory of catalysts composed of two or more oxides. Naturally one cannot expect to solve this problem simply on the basis of catalytic and related phenomena but rather on the broadest possible phenomenological basis.

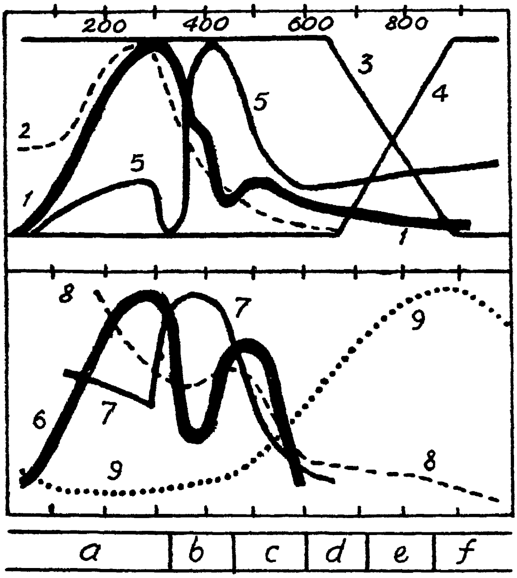

FIG. 4

The experimental methods employed here are the same as those referred to in Fig. 3. The change of some arbitrarily chosen properties of the system 1ZnO + $1Cr_2O_3$ are shown in Fig. 4. The results unless otherwise stated have been obtained by Hüttig and his co-workers.

Graph (1) shows the catalytic activity of the system for the CH_3OH decomposition; (2) refers to the same process observed by Jander and Weitendorf, while (3) gives the intensity of the strongest line of Cr_2O_3 in the X-ray diagram, and (4) the strongest line of $ZnCr_2O_4$.

Graph (5) represents the magnetic susceptibilities, and (6) the amounts of water taken up in constant time intervals and water vapour pressures; (7) shows the adsorption capacity compared with $Pb(NO_3)_2$ dissolved in CH_3OH as observed by Starke by means of radioactive indicators. Graph (8) gives the adsorption capacity for eosin solution; (9) shows the velocity with which compounds become oxidized to $ZnCrO_4$.

As these results were obtained by different authors with compounds of not always the same previous treatment, they can only serve a qualitative purpose. Especial use may, however, be made of the adsorption isotherms of any suitable gas as the interpretation of these by Langmuir and by Zsigmondy, allows us to estimate quantitative and qualitative changes in the surface and also in the distribution of the radii of capillaries. Systems which have been investigated from this point of view are:

Al_2O_3 with Cr_2O_3; with Fe_2O_3; with SiO_2.
BaO with Fe_2O_3; MoO_3; WO_3.
BeO with Cr_2O_3; Fe_2O_3.
CaO with Al_2O_3; Cr_2O_3; Fe_2O_3; SiO_2; TiO_2.
CdO with Cr_2O_3; Fe_4O_3.
CoO with MnO_2.
Cr_2O_3 with Fe_2O_3; SiO_2; TiO_2.
CuO with Al_2O_3; Cr_2O_3; Fe_2O_3; Mn_2O_3; WO_3; ZnO.
Cu_2O with Cr_2O_3; Mn_2O_3.
Fe_2O_3 with SiO_2; TiO_2.
MgO with Al_2O_3; Cr_2O_3; Fe_2O_3; GeO_2; SiO_3; TiO_2; V_2O_5; WO_3.
Na_2O with SiO_2.
NiO with Al_2O_3; Fe_2O_3.
PbO with Fe_2O_3; SiO_2
SrO with Fe_2O_3.
ZnO with Al_2O_3; Cr_2O_3; Fe_2O_3; SiO_2; TiO_2; WO_3.

Only in a few cases have systems of salts or organic materials been examined with regard to their intermediate states. However, it should be pointed out that the investigation of catalysts and of powder metallurgy, now in a most important stage of their development, have the same scientific interest in regard to the intermediate states.[4]

The problem is now one of setting up general rules and laws and, if possible, a model on the basis of the large number of observations. In particular, one can see that at low temperatures (i.e. the initial stages of the transformation) only those changes which are a function of the *surface* occur. Only later are changes in the crystal lattice observable. In addition, it seems feasible to distinguish 6 stages in the life-time of an oxide mixture (denoted by the letters (*a*) to (*f*) for the system $ZnO + Cr_2O_3$; cp. also foot of Fig. 4).

STAGE (*a*): This starts almost always with the mixing of oxides at room temperature and is slightly changed by a moderate increase of temperature. It is mainly distinguished by the mixing which causes an intimate surface contact of the two compounds, such that the surface available to the larger molecules is considerably reduced. Here the main characteristic is a mutual covering of surfaces; we shall term this the " covering " stage.

STAGE (*b*): This stage is one of activation and is due to the formation of *Zwitter*-molecules and to molecular covering of surfaces. The molecules of the mobile component (e.g. Cr_2O_3) diffuse over the surface of the less mobile component (e.g. ZnO), covering it with a molecular layer. Observations by Roulston[5] also indicate the possibility of surface migration of loosely held particles. The original interpretation of the apparent surface migration of atomic groups in reactions in the solid state was due to Hedvall,[6] who assumed that it was concerned with sites of energy disturbance, which only become appreciably mobile structures at the crystal surface. In systems where stage (*b*) predominates a relatively high catalytic activity is to be expected.

---

[4] Cf. e.g. the report of the Symposium held by the Sylvania Electric Products Inc., Bayside, New York, on " The Physics of Powder Metallurgy " (Aug., 1949).

[5] Roulston, *Proc. Camb. Phil Soc.*, 1941, **37**, 440.

STAGE (*c*) : This comprises a stage of deactivation of the *Zwitter*-molecules and of molecules covering the surfaces. The foreign molecules migrating over the surface of the less mobile component finally become strongly bound and localized. This process can be regarded as similar to Taylor's switch from van der Waals' adsorption to activated adsorption. Thirsk and Whitmore[7] observed film formation and the transition into ordered arrangements in the system MgO + Fe_2O_3. It was observed by Holm[8] that coagulation of the oxide film on metals led to structures with regular geometrical boundaries. In any case a decrease in chemical reactivity of the molecules involved occurs in this state and with it a decrease in catalytic activity. From the viewpoint of colloid chemistry we can consider this " solidification " as the protective action associated with some protective colloids (Thiesen[9]). According to Schenk[10] molecules of Ag_2S which have migrated on solid ZnS are less reactive than solid Ag_2S.[12]

STAGE (*d*) : This is a stage of activation due to internal diffusion : as the temperature is further increased, molecules of the mobile oxide diffuse into the crystal lattice of the less mobile oxide. The loosening necessarily associated with this causes an increase in catalytic activity and for the first time the molecules of the less mobile component actually contribute to this activity.

STAGE (*e*) : This stage is the formation of less ordered crystalline aggregates of the addition compound.

STAGE (*f*) : Finally there is the filling of the crystal defects. The processes occurring in the two latter stages are linked with diminution in catalytic activity.

It is possible that a part of the action of the mixed catalyst is based upon the Hedvall effect through the continuous transformation within the rigid system, causing an increase in the catalytic effect. Related to this is Schwab's[11, 13] treatment of the existence of " coupled gas-solid-body-catalysis ". Such an effect has actually been found for the reactions BaO + $CuSO_4$ and BaO + $ZnSO_4$. It would be very desirable to extend these investigations not only to processes which in the classical sense go to completion, but to the more subtle transformations among the intermediate states.

Of the results obtained by varying the ratio of the two components in the mixture, we may note the observation on the ZnO + Fe_2O_3 system. Here minute amounts of Fe_2O_3 added to ZnO promote great catalytic activity, increased adsorption capacity and increased magnetic mass susceptibility. The effect is more marked with smaller than with larger concentrations.

The discussion has so far assumed that the two oxide components possess for each other a large affinity which is sufficient for the formation of a classical compound. However, this is not always so ; for example, BeO + Fe_2O_3 do not chemically combine and do not form solid solutions.

---

[6] Hedvall, *Chalmers tekn. Högskolas Handl.*, 1942, No. 4.

[7] Thirsk and Whitmore, *Trans. Faraday Soc.*, 1940, **36**, 862.

[8] Holm, *J. Res. Nat. Bur. Stand.*, 1942, **28**, 569. See also Schwab, *Trans. Faraday Soc.*, 1947, **43**, 715. [9] Thiessen, *Kolloid-Z.*, 1942, **101**, 241.

[10] Schenck, *Chemie*, 1943, **56**, 279.

[11] Schwab and Karatzas, *J. Physic. Chem.*, 1948, **52**, 1053.

[12] Cf. the lectures given in the Discussion of the *Deutsche Bunsen-gesellschaft* on contact catalysis, especially the lecture by R. Fricke which refers to the research of Rienäcker.

[13] Schwab and Schwab-Agallidis, *Kemisk Tidskrift*, 1946, **58**, 161.

In spite of this, changes particularly in catalytic activity, may be observed at elevated temperatures. Analogous stages labelled *a*, *b* and *c*, are traversed as before, after which the process comes to a halt. Thus, in this case, the less mobile oxide remains essentially unchanged, while the mobile oxide, or part of it, is found in some crystallographic form on the surface of the less mobile oxide. In a similar manner, we can explain the specific action which a promoter is known to exert on a catalyst (e.g. an oxide).

Recently attempts have been made to incorporate the phenomena of intermediate states into a general theory of chemical kinetics.[14] The usual definition of reaction velocity, i.e. the amount of reaction products formed per unit time, cannot be applied. Instead, one has to replace the velocity by the reciprocal of the time τ required to reach a characteristic state with certain properties at a given temperature. Where different reaction mechanisms are not superimposed we may expect Arrhenius' relation to be valid,

$$-\ln \tau = -q/RT + \ln k_0.$$

Thus, in 1946 Hüttig, Ehrenberg and Kittel[15] calculated from some results on the system $ZnO + Fe_2O_3$ at lower temperatures, where the processes are practically determined by surface diffusion, a value $q(=$ activation energy$) = 30{,}000$ cal. For higher temperatures where the diffusion of Fe_2O_3 into the ZnO lattice is the rate-determining step, $q = 70{,}000$ cal.

According to the most recent views[14, 4] it might be permissible to identify these values with the activation energy for diffusion of Fe_2O_3 over the surface and diffusion into the interior of the ZnO lattice, respectively. Where the intermediate states are compounds which can actually be prepared, it follows from isothermal considerations, that the last-formed state must be formed at a lower velocity than all the previous states. A discussion of the role of q and k_0 in the velocity of formation has been given by Roginski.[16]

A comprehensive description of the theory of mixed catalysts up to 1943, was given by the author in the *Handbook of Catalysis*.[17]

Institute für Anorg. und Physikal. Chemie,
der Technischen Hochschule.
Graz, Rechbauerstrasze 12.

---

[14] Hüttig, *Z. Elektrochem.*, 1950, (in press).
[15] Hüttig, Ehrenberg and Kittel, *Z. anorg. Chem.*, 1936, **228**, 112.
[16] Roginski, *J. Phys. Chem. Russ.*, 1947, **21**, 1143.
[17] Contribution by Hüttig in the *Handbook of Catalysis*, edited by Schwab.

STRUCTURE OF OXIDE CATALYST SYSTEMS

BY P. W. SELWOOD AND LORRAINE LYON

Received 4th January, 1950

Magnetic methods, in general, reveal the oxidation state and the atomic environment of active oxides of the transition group elements. Susceptibility isotherms have been determined for all these elements, and their interpretation falls into three categories: change of exchange interaction, change of oxidation state, and intercation covalency.

There is no obvious relation between magnetic susceptibility and catalyst activity. The susceptibility is a tool for the elucidation of structure, which in turn, determines activity. Nevertheless, it is not infrequently possible to predict catalyst activity from susceptibility measurements, especially when these are considered together with surface area determinations.

These methods are applicable not only to supported oxides but to the same oxides in self-supported, or gel-like systems.

The susceptibility isotherm method has been shown to yield information concerning the structure of supported transition group oxides.[1] This information includes (*a*) the oxidation state of the metal ion in the supported oxide, (*b*) the possible existence of overlapping wave-functions leading to partial covalent bonds between adjacent positive ions, and (*c*) the " paramagnetic neighbourhood," i.e. the approximate number of paramagnetic neighbours possessed by each paramagnetic ion.

Susceptibility isotherms obtained for the several oxides of the transition elements, when supported on a diamagnetic high area oxide such as γ-alumina, fall into several classes, depending on which of the factors mentioned above is dominant, or on which combination of factors the susceptibility depends. Thus, the supported system chromia + alumina [2] gives a typical result in which all the change of susceptibility depends on a modified exchange interaction, or paramagnetic neighbourhood. The system $Fe_2O_3 + Al_2O_3$ gives an isotherm the shape of which depends both on the paramagnetic neighbourhood, and the existence of intercationic bonds.[3] The system consisting of manganese oxide [4] supported on alumina, through moderate temperature ignition of alumina impregnated with manganous nitrate, has an isotherm dependent on change of oxidation state, as well as change of paramagnetic neighbourhood.

The purpose of the present paper is to extend these observations to supported oxides of vanadium and of ruthenium, and to several other systems not previously investigated. The method, in brief, consists of preparing oxides on high area supports by methods which are, in general, familiar to catalytic chemists, and then to measure the magnetic susceptibility of the product as a function of concentration of the supported oxide, and as a function of temperature.

Experimental

Magnetic, surface area, and X-ray methods have all been described earlier in papers from this Laboratory. Preparation and analysis of samples is more conveniently described *seriatim* below.

Results

Preparation of Samples.—VANADIA + ALUMINA.—Samples were prepared by impregnation of γ-alumina with ammonium metavanadate solutions of varying concentrations. The alumina had a surface area of 224 m.^{2}/g. (BET, nitrogen). In general, 10 g. of alumina was impregnated with 100 cm.^{3} of solution for 1 hr. The yellow samples were then suction-filtered, dried at 110° C, and reduced in hydrogen for 60 hr. One series was reduced at 800° C, another at 650° C. All samples were analyzed as follows: the sample was dissolved in 1/1 sulphuric acid, with heating. The solution was titrated with N/10 potassium permanganate. The sample was then reduced with sulphur dioxide, after which titration with permanganate was repeated. The two titrations gave, respectively, the average oxidation state and the total vanadium.

A reduction temperature of 800° C gave samples which contained about 80 % of the vanadium in the + 3 state; the 650° reduction gave about 70 % of the vanadium in the + 3 state. In both cases there was no evidence to suggest that the remaining vanadium was in any state but + 4. It may be wondered why reduction was not continued until all the vanadium was in the same (+ 3) oxidation state. But complete reduction to the + 3 state is difficult without causing irreversible changes in the alumina support, and in the distribution of the vanadia.

---

[1] This is the eighth paper on the susceptibility isotherm from this Laboratory. The seventh, by Hill and Selwood, appeared in *J. Amer. Chem. Soc.*, 1949, **71**, 2522.

[2] Eischens and Selwood, *ibid.*, 1947, **69**, 1590.

[3] Selwood, Ellis, and Wethington, *ibid.*, 1949, **71**, 2181.

[4] Selwood, Moore, Ellis, and Wethington, *ibid.*, 1949, **71**, 693.

Results on the samples reduced at 800° C are shown in Table I and those at 650° in Table II. These Tables give the measured susceptibilities at several

TABLE I—MAGNETIC DATA FOR VANADIA + ALUMINA SERIES REDUCED AT 800° C

% V	$\chi \times 10^6$				Δ	μ
	298° K	229·5° K	183·9° K	127·5° K		
2·5	1·1	1·5	1·8	2·3	86	3·0
	56·0	71·6	83·0	103		
3·3	1·3	1·7	2·6	2·6	84	2·8
	48·5	59·7	69·7	87·5		
4·1	1·6	2·2	2·5	3·1	90	2·7
	46·8	60·0	67·4	84·0		
4·7	2·1	2·4	2·9	3·6	84	2·7
	50·0	57·8	69·0	83·5		
4·9	2·2	2·8	3·2	4·4	84	2·8
	50·1	61·9	71·2	95·5		
*5·1	4·2, 4·1, 3·9	5·3, 4·8, 4·6	5·6, 5·1, 4·9	6·5, 6·0, 5·8	210	3·8
	76·5	82·5	86·4	102		
5·2	2·3	2·7	3·2	4·3	80	2·8
	49·1	57·2	66·6	87·7		
5·5	1·9	2·4	2·8	3·7	90	2·6
	40·0	49·0	56·6	73·0		
6·7	2·0	2·5	2·9	3·3	180	2·6
	34·0	41·4	48·3	53·6		
8·8	2·4	3·1	3·3	3·7	222	2·6
	30·7	38·8	41·2	45·7		
9·5	2·6	3·0	3·4	3·8	280	2·7
	30·4	34·8	38·9	43·1		
13·4	3·2	3·6	4·0	4·4	340	2·6
	25·7	29·0	31·9	35·2		

* Sample slightly ferromagnetic.

TABLE II.—MAGNETIC DATA FOR VANADIA + ALUMINA SERIES REDUCED AT 650° C

% V	$\chi \times 10^6$				Δ	μ
	298° K	229·5° K	183·9° K	127·5° K		
2·5	0·9	1·2	1·5	2·1	24	2·5
	46·5	58·5	72·5	98·2		
3·3	1·1	1·4	1·8	2·5	36	2·4
	41·8	53·0	64·4	85·4		
4·1	1·4	1·8	2·1	2·7	76	2·5
	40·4	51·5	57·8	73·1		
*4·9	1·7	2·44, 2·42, 2·39	3·09, 2·98, 2·97	3·84, 3·70, 3·72	84	2·7
	41·7	53·0	56·0	67·8		
*5·1	4·2, 4·1, 3·9	5·3, 4·8, 4·6	5·6, 5·1, 4·9	6·5, 6·0, 5·8	210	3·8
	76·5	82·5	86·4	102		
5·2	1·9	2·5	3·0	3·9	90	2·7
	42·0	54·5	63·1	80·0		
5·7	1·7	2·3	2·7	3·6	90	2·4
	35·2	45·6	52·6	66·6		

* Sample slightly ferromagnetic.

temperatures, the calculated susceptibilities per gram of vanadium, the Weiss constant in °C, and the magnetic moment in Bohr magnetons. For instance, the sample containing 2·5 % vanadium had a susceptibility at 25° C of $1{\cdot}1 \times 10^{-6}$ per gram. The susceptibility per gram of vanadium was then 56×10^{-6}. The reciprocal susceptibilities thus obtained gave a straight line when plotted against temperature. From this plot the Weiss constant is found, and the moment is then given by

$$\mu = 2{\cdot}84\sqrt{\chi_M(T + \Delta)}.$$

Normally, the magnetic susceptibility is independent of field strength, although measurements are invariably made at several fields. In a few cases the vanadia + alumina samples exhibited a slight field strength dependence of susceptibility. Where found, this is indicated in the Tables by including measured susceptibilities at 3630, 4710, and 5450 oersteds, in that order. In such cases the susceptibility per gram of vanadium has been calculated by first extrapolating the measured susceptibilities to zero reciprocal field. But this dubious procedure is further discussed below.

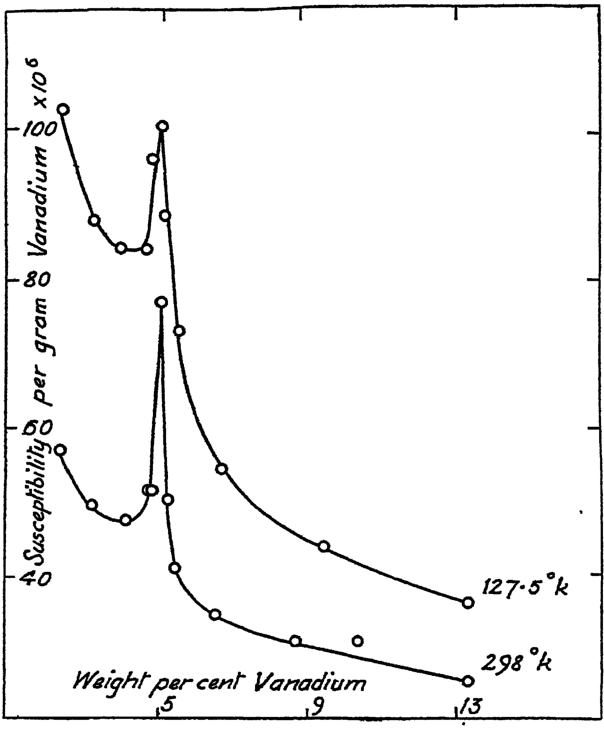

FIG. 1.—Susceptibility isotherms for vanadia + alumina.

Susceptibility isotherms are shown in Fig. 1 for the 800° C reduction vanadia + alumina series. Chemical analyses for oxidation state, which are not very accurate, are as follows. For the 650° reduction series the average oxidation state was independent of concentration (at ~ 70 $\%V^{+3}$) except in the region, referred to below, of the peculiar peak in the susceptibility isotherm. In the region of this peak the average oxidation state was ~ 66 $\%V^{+3}$. For the 800° reduction series the average oxidation state was also independent of concentration (at ~ 80 $\%V^{+3}$) except in the region of the peak where it was again ~66 $\%V^{+3}$

Vanadia + Rutile.—Samples were prepared by the ignition of high area rutile with ammonium metavanadate solutions of varying concentrations. In general, 10 g. samples of rutile were soaked for one hour in 100 cm.³ of solution.

The samples were then filtered with suction, dried at 100° C and reduced in hydrogen at 350° C for 18 hr. This reduction temperature was found to yield products containing about 95 % V^{+4} and 5 % V^{+3}. Lower reduction temperatures did not give consistent results. It will be noted that the high concentration of V^{+4} found does not constitute evidence for valency inductivity because more V^{+3} could be obtained by raising the reduction temperature.

Analyses were performed as described for the vanadia + alumina series.

The data obtained are shown in Table III and Fig. 2. A few attempts were made to obtain higher total vanadium concentrations in the vanadia + rutile series. But these gave erratic results, as was not unexpected in view of the strong dependence of susceptibility on the vanadium/oxygen ratio in this range, as reported by Hoschek and Klemm.[5]

TABLE III.—MAGNETIC DATA FOR VANADIA + RUTILE SERIES

% V	× 10⁶				Δ	μ
	298° K	229·5° K	183·9° K	127·5° K		
	1·05	1	1·58	2·22		
3·3	29·1		41·5	58·5	+34	1·9
	1·12	1·48	1·90	2·37		
3·8	26·8	34·0	43·0	55·0	+34	1·9
	1·11	1·59	1·96	2·38		
4·1	26·0	34·1	43·2	51·0	+38	1·9
	1·25	1·58	1·90	2·46		
5·0	23·1	27·8	34·2	43·4	+60	1·8
	1·65	1·80	2·11	2·62		
6·6	23·6	24·4	29·2	35·4	+100	1·8

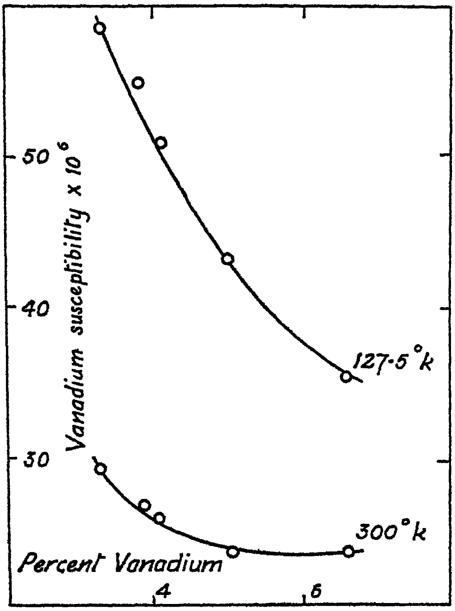

FIG. 2.—Susceptibility isotherms for vanadia + rutile.

---

[5] Hoschek and Klemm, *Z. anorg. Chem.*, 1939, **242**, 63.

Chromia + Rutile.—This supported oxide system was investigated to see if any valency inductivity occurred. It was realized that, because of the easy oxidation to chromate, the results might be difficult to interpret.

Samples of high-area rutile were impregnated with chromium nitrate solutions of several concentrations. The impregnated samples were filtered, dried at 110° C, and then ignited for 4 hr. at 200-250°, except as noted below. The resulting samples ranged from yellow-brown to dark brown as the chromium concentration increased. They were analyzed by fusion with sodium peroxide. The mixture was dissolved and filtered from some hydrous titania, neutralized and boiled to destroy excess peroxide, acidified and titrated with permanganate after the addition of excess ferrous ammonium sulphate.

The magnetic susceptibilities first obtained showed the surprising result of an isotherm which turned up with increasing chromium concentration. The reason for this was obviously because the lower chromium concentrations contained increasing proportions of chromate, which is diamagnetic. It was found that somewhat similar results could be obtained by impregnating γ-alumina with chromium nitrate, and igniting, but omitting the usual reduction step.

Chromia-rutile samples were prepared through an ignition step at 165° C for 7 days. These samples were then leached with water until the washings showed no trace of chromate. Two of the resulting samples contained 5·6 % and 2·6 % of chromium. Some of the preparations showed a slight trace of ferromagnetism, which was not unexpected in view of the well-known occurrence of ferromagnetism in some intermediate oxide of chromium.

The magnetic susceptibilities of these two samples indicated gave moments as follows: for the 5·6 % sample, $\mu = 3{\cdot}8$, $\Delta = -28°$; for the 2·6 % sample, $\mu = 2{\cdot}8$, $\Delta = -27°$. These results seem to indicate that the 5·6 % sample had all its chromium in the + 3 state, and that the 2·6 % sample had all its chromium in the + 4 state.

Copper Oxide + Magnesia.—The system copper oxide + alumina had already been studied in this Laboratory. It was thought worth while to prepare one sample of copper oxide on each of the two supports, magnesia and rutile.

A solution of copper nitrate was used for the impregnation of high-area magnesia. The samples were filtered, dried and ignited at 190° C for 60 hr. The black sample was analyzed by solution in nitric acid, followed by conversion to the sulphate, and electrolysis. It contained 21·7 % copper. The magnetic susceptibilities were as follows:

Temperature . . .	229° K	184° K	127·5° K
$\chi \times 10^6$ per g. sample . .	3·9	4·8	6·4
$\chi \times 10^6$ per g. Cu . . .	19·4	23·5	30·9

From these data the magnetic moment was found to be 1·6 and the Weiss constant 40°

Copper Oxide + Rutile.—Preparation and analysis were similar to those described above. The sample contained 2·9 % copper, and was green. Magnetic results were as follows:

Temperature . . .	229° K	184° K	127·5° K
$\chi \times 10^6$ per g. sample . .	1·1	1·2	1·5
$\chi \times 10^6$ per g. Cu . . .	31·0	38·0	51·7

These data give a moment of 2 and a Weiss constant of about 26°. The data are less accurate than usual because of the low concentration and the presence of only one unpaired electron per Cu^{+2} ion.

Ruthenia + Alumina.—Choice of a solution suitable for use in the impregnation step is somewhat more complicated for ruthenium than for other elements studied. Ammonium chlororuthenate, the sulphate, and the chloride were each used. Effective impregnation was achieved only with the chloride, as follows. The metal was fused with sodium hydroxide and sodium peroxide, the fusion mixture was dissolved in hot water, unreacted metal was removed by filtration, and hydrous ruthenium dioxide was precipitated by digestion after addition of alcohol. The washed oxide was then dissolved in conc. HCl.

After impregnation on high-area alumina the samples were ignited at several temperatures from 400° to 660° C. Analyses of the samples, which proved difficult, was achieved by dissolving the samples in 1/1 sulphuric acid, followed by precipitation of the ruthenium at a controlled pH = 5. The ruthenium was finally weighed as metal, after reduction.

Samples were thus prepared ranging in ruthenium content from about 2 to about 17 %. Magnetic measurements were made at room temperature and at − 150° C, but in all cases the samples proved to be diamagnetic with a susceptibility indistinguishable from that of the pure support.

Silica-supported Samples—Almost all the work previously reported has involved alumina or titania as the diamagnetic support. Some measurements were made on silica-supported samples.[6] There seemed no justification for an extensive series for any of these systems, but a few representative samples were made for copper, nickel, chromium, and iron oxides, all prepared through an impregnation on silica.

Two batches of silica were prepared. The first, silica I, was obtained by hydrolysis of dilute sodium silicate solution with 10 % HCl. The susceptibility was $-0{\cdot}2 \times 10^{-6}$, approximately independent of temperature. The second batch of silica, silica II, was obtained by the hydrolysis of ethyl orthosilicate in alcohol with the addition of water and a little HCl. The surface area was 845 m.^{2}/g., and the susceptibility $-0{\cdot}3 \times 10^{-6}$.

A pale green sample of copper oxide on silica II, prepared and analyzed in the usual way, contained 7·9 % copper. The copper was found to possess a magnetic moment of 1·9, and the Weiss constant was 30°. A black sample of nickel oxide on silica II, similarly prepared and analyzed, contained 4·3 % nickel and showed a moment of 2·0 and Weiss constant of 26°. Another sample contained 4·4 % nickel, $\mu = 2{\cdot}1$, $\Delta = 26°$. A sample of silica II supported chromia prepared by impregnation with chromic acid solution, followed by ignition and reduction contained 9·5 % chromium. The moment was 3·7 and the Weiss constant 190°.

A sample of iron oxide supported on silica I was prepared by impregnation with concentrated ferrous ammonium nitrate solution. The deep red ignited sample showed no measureable ferromagnetism. Three samples similarly prepared on silica II showed a slight ferromagnetism. The data for these four samples of supported iron oxide are shown in Table IV.

TABLE IV

% Fe	Susceptibility × 10^6				Δ	μ
	300° K	23° K	184° K	128° K		
3·2	2·9	3·9	4·6	6·0	70	4·2
	100	130	150	200		
1·1	1·03, 1·13, 1·10*	1·82, 1·76, 1·80	2·12, 2·26, 2·19	3·08, 2·95, 2·83	50	4·9
	127	191	228	300		
2·0	—	3·84, 3·77, 3·70	4·57, 4·55, 4·55	6·55, 6·40, 6·24	50	4·9
		195	230	300		
2·5	3·89, 3·76, 3·74*	6·33, 6·22, 6·08	7·35, 7·16, 7·10	10·30, 9·90, 9·55	100	6·0
	156	244	286	356		

* These susceptibilities obtained at 3630, 4710, and 5450, respectively. The susceptibilities per g. of iron were found by extrapolation to zero reciprocal field.

The above data are given in some detail because they illustrate an important point which is often overlooked in magnetochemical studies.

Electron Microscope Investigation.—Magnetic susceptibility data on supported oxides give a clear indication that exchange effects persist to quite low concentrations. The surface areas show that at these low concentrations there is insufficient supported oxide to cover the support by any continuous aggregation. It was concluded early in this work that the supported oxides must be aggregated into microcrystals which are separated from each other by large areas of bare support.

One picture of the surface which is consistent with the view expressed, is that the surface consists of large uncovered areas with rather regular aggregations of supported oxide in somewhat the way that mesas appear on a desert. If this view were correct, then it might be possible to obtain electron microscope pictures of these aggregates. An electron microscope study of several supported chromia + alumina samples failed to yield any indication of such structures. A similar study on uranium dioxide supported on alumina likewise gave negative results.

---

[6] Selwood, *J. Amer. Chem. Soc.*, 1948, **70**, 883.

Discussion

Interpretation of New Data.—All the new magnetic data fall into patterns previously established for other supported oxide systems. The vanadia + alumina susceptibility isotherms are much like those previously reported for chromia + alumina, and for several other supported oxide systems. Valency inductivity plays no part in this system. There is one major difference, however, and that is the astonishing peak shown at about 5 % vanadium. This peak is related to an apparent increase of, moment, but, as will be pointed out below, this effect is probably spurious. The peak is almost certainly due to a trace of ferromagnetic component, or at least to the great increase of susceptibility reported by Hoschek and Klemm[5] for the stoichiometric ratio $VO_{1.71}$, which corresponds to the formula V_3O_5, near which the peak occurs. Absence of the peak for the vanadia + rutile system is doubtless due to the high V^{+4} concentration, which makes it difficult for the system to revert to V_3O_5. Otherwise the isotherm is the normal chromia + alumina type.

The system chromia + rutile seems to show evidence of valency inductivity, which puts it somewhat in the class of manganese oxide supported on alumina (as prepared by low-temperature ignition).[4] Copper oxide supported on magnesia and on rutile gives a normal moment and a normal degree of dispersion. The situation is not unlike that previously reported for copper oxide on alumina.[7] Ruthenia + alumina is an addition to the small group consisting of supported oxides of molybdenum and of rhenium which give zero moment. If our interpretation is correct, this means that valency bonds between adjacent rutheniums are such that the moment is quenched entirely.

The several oxides supported on silica appear to offer no feature not previously encountered. Copper, nickel and chromium give moments and dispersions almost exactly similar to those found for the same oxides on alumina. Iron oxide gives the same rather low moment as found on alumina, but this is not true if the sample shows some ferromagnetism.

It appears from these results that the main observational characteristics of the susceptibility isotherm, as a tool in catalyst research, have now been found. Some details of interpretation await further development. This is especially true of the need for a more quantitative interpretation of the relation between moment, Weiss constant, and structure.

It may be worth while to summarize the several cases in which valency inductivity does or does not appear. The cases reported from this Laboratory are as follows.

VALENCE INDUCTIVITY

Found	Not found
Chromia + titania	Vanadia + alumina
Manganese + alumina	Vanadia + titania
Iron + titania	Copper + alumina
Nickel + alumina	Copper + titania
Nickel + titania	Silver + alumina.

These results suggest that the effect will not be found if the radius of the supported ion (in its induced form) differs from that of the corresponding diamagnetic ion in the support by more than about 30 %.

---

[7] Selwood and Dallas, *J. Amer. Chem. Soc.*, 1948, 70, 2145.

We shall conclude this section with a remark concerning the failure of electron microscopy to show any aggregates of the supported oxides. It may be that the precise conditions for viewing the aggregates have not yet been obtained. But it will be noted that the magnetic and surface area data do not require any particular shape for the aggregates. It is possible that the supported oxides are present as long fibres, only a few atoms thick. This view is that commonly held for the structure of so-called hydrous oxides, to which class several of the supporting oxides undoubtedly belong.

The Ferromagnetic Correction.—Attention is drawn to the high apparent susceptibilities and moments in each case (e.g. vanadia + alumina, iron oxide + silica) in which a trace of ferromagnetism was present. Traces of ferromagnetism are often present in inorganic solids; it is particularly common to find them in solids containing iron. Such substances may contain magnetite or γ-iron sesquioxide in proportions not over a few parts per million, but this is more than enough to give a measureable dependence of susceptibility on field strength. Our policy in all this work on solid oxides has been to make measurements at three fields, so that a trace of ferromagnetism would be detected. The importance of this procedure cannot be over-emphasized. But it has also been our policy to reject samples in which such ferromagnetism is found, unless, as for vanadia + alumina, the occurrence of the ferromagnetism is of primary interest for its own sake.

A procedure commonly used for samples containing traces of ferromagnetism has been to plot the apparent susceptibilities as a function of reciprocal field strength, and to extrapolate to $1/H = 0$ for the true susceptibility. This procedure seems to give reliable results if all the sample at all times during the measurement is maintained in a saturating field. For spherical particles the demagnetization factor is so large, that the field must apparently be at least 7000 oersteds. The Faraday method for susceptibility measurement generally fulfils this condition. But the Gouy method suffers from the major systematic error that part of the sample is in a field which is far from saturating, indeed it may be near zero. This difficulty has been pointed out by Knappwost,[8, 9] but it has not received adequate attention. The presence of a trace of ferromagnetism in samples measured by the Gouy method will definitely lead to erroneous and very high apparent susceptibilities, even though the usual correction procedure is employed. The apparent high moments reported for certain concentrations of vanadia + alumina, and for one sample of iron oxide + silica should be ignored. They are included to draw attention to this frequently overlooked source of error.

This work was done under contract with the Office of Naval Research.

Department of Chemistry,
Northwestern University,
Evanston, Illinois, U.S.A.

---

[8] Knappwost, *Z. physik. Chem. A*, 1941, **188**, 246.

[9] Knappwost, *ibid. A*, 1942, **191**, 261.

THE USE OF ^{18}O IN STUDIES OF THE REACTIVITY OF SOLID OXIDES

BY E. R. S. WINTER

Received 22nd February, 1950

An experimental technique is outlined for following continuously with a mass spectrometer ^{18}O exchange between solid oxides and oxygen gas. Preliminary results are presented and discussed for thorium and chromic oxides. The apparent activation energy for oxygen exchange is 27 ± 0·5 kcal./mole for thorium oxide between 440° and 540° C. With chromic oxide two processes are operative, one at temperatures below 410° C with an activation energy of 29·5 ± 0·5 kcal./mole and one above 410° C with an activation energy of 1 ± 4 kcal./mole. The high activation energy is ascribed tentatively to a limiting process governed by the rate of desorption of oxygen from the oxide surface. The low activation energy is believed to be associated with the true exchange reaction. The kinetics of these two limiting cases are discussed.

As is well known, considerable progress has been made in the investigation and understanding of some heterogeneous reactions by the employment of the isotopes of hydrogen and of ortho- and para-hydrogen.[1] Recently the carbon isotopes have been used to study the transformations of certain organic compounds upon catalyst surfaces,[2] while Joris and Taylor[3] have investigated some aspects of ammonia synthesis, using ^{15}N upon iron and tungsten catalysts. These and other investigations have shown that many catalytic reactions involve dissociative adsorption of the reactants and it is clearly of interest to determine to what extent such a step is important in other heterogeneous catalytic reactions.

Suitable reactions for such a study include oxidations taking place upon oxide surfaces, since if dissociative adsorption does occur it is very likely to involve some exchange of oxygen between the reactants and the surface of the oxide. Such exchange could be detected and followed by use of the isotopes of oxygen. Similar exchange might be found in the decompositions and transformations of oxygen-containing organic compounds upon solid oxides. In general we would expect a detailed study of oxygen exchange to give useful information upon the nature and reactivity of oxide surfaces and upon heterogeneous reactions. This paper presents some preliminary observations upon the exchange of ^{18}O between gaseous oxygen and certain solid oxides.

Experimental

The reaction system is shown in Fig. 1.* T is a cold finger designed to prevent any condensible impurities from reaching the mass spectrometer. During the present work it was not found necessary to use this trap, and after a few experiments it was discarded. A weighed amount of the oxide was placed in the bulb R (capacity about 85 ml.) and outgassed overnight (10^{-5} to 10^{-6} mm. Hg) at a suitable temperature. The furnace temperature was then rapidly adjusted to that at which the exchange reaction was to be studied and allowed to reach constant conditions over 1½-2 hr. The enriched oxygen gas was introduced in known amount through T, and a very small quantity of the gas ($< 10^{-5}$ g./hr.) continuously bled off through the capillary leak L into the ionization region of the mass spectrometer. A record was taken of the change with time of the ^{18}O content of the gas. The apparatus is described more fully elsewhere ;[4] the method has been used by Urey and Brandner[5] who discuss in sufficient detail the errors inherent in the use of a mass spectrometer in this fashion to obtain kinetic data. The results are quoted as velocity constants calculated in min.$^{-1}$. The mass spectrometer is a Nier-type 60° sector instrument ; the masses were brought into focus by voltage scanning.

---

[1] Eley, *Advances in Catalysis* (Academic Press Inc., 1948), p. 157; *Quart. Rev.*, 1949, **3**, 209.

[2] Beeck, Otros, Stevenson and Wagner, *J. Chem. Physics*, 1948, **16**, 255.

[3] Joris and Taylor, *ibid.*, 1939, **7**, 893.

* Reproduced by courtesy of the Editors of the *J. Chem. Soc.*

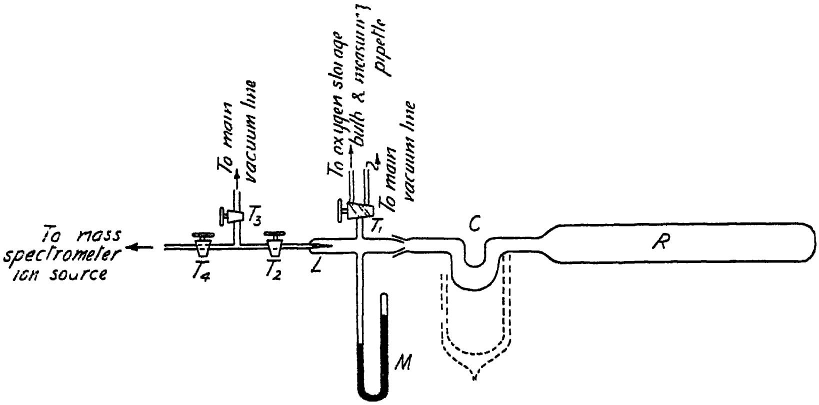
To main vacuum line
To oxygen storage bulb & measuring pipette
To main vacuum line
To mass spectrometer ion source
T_3
T_1
T_4
T_2
L
C
R
M

FIG. 1.

The oxides used were : a sample of thorium oxide of ordinary reagent grade and unknown history ; chromic oxide prepared by the method given by Anderson *et al.* ;[6] magnesium oxide prepared by heating the carbonate in air to about 850° C. The chromium and magnesium oxides were of A.R. quality. The enriched oxygen contained in general 1·2 to 1·3 % ^{18}O, although a sample containing about 1 % ^{18}O was used for some experiments.

Kinetics of the Exchange Reaction.—We have shown elsewhere [4, 7] that the exchange consists of two processes occurring with different speeds, and that it is possible to separate the fast reaction from the slower. We are here concerned only with the former, which we consider to be exchange between the gas and oxygen ions lying in the surface of the oxide. The slow reaction, which has been found to continue at approximately constant rate through at least five ionic layers, we believe to be a measure of the rate of diffusion of oxygen through the solid lattice. An investigation of this reaction is proceeding.

The surface exchange reaction has been found for all oxides so far examined to be kinetically first order with respect to residual ^{18}O content in the gas, i.e. we may define the experimental rate constant, k_s by the equation

$$-\,d\alpha/dt = k_s(\alpha - \alpha_\infty), \qquad \text{(1)}$$

where α is the atom fraction of ^{18}O in the gas at time t and α_∞ that at the end of the surface exchange. We may regard the exchange as being represented by the equilibrium

$$^{18}O_g + {}^{16}O_s \underset{k_{-1}}{\overset{k_1}{\rightleftharpoons}} {}^{16}O_g + {}^{18}O_s,$$

where O_s and O_g refer to the reacting species from the solid and gas respectively. A plausible assumption, which we make use of here, is that O_g refers to chemisorbed, most probably mobile, oxygen atoms, and O_s to oxygen ions in the oxide surface. There is no evidence as to what proportion of the surface oxygen

[4] Winter, *J. Chem. Soc.*, 1950 (in press).
[5] Brandner and Urey, *J. Chem. Physics*, 1945, **13**, 351.
[6] Bevan, Shelton and Anderson, *J. Chem. Soc.*, 1948, 1729.
[7] Houghton and Winter, *Nature*, 1949, **164**, 1130.

ions is active in this connection and indeed the proportion probably depends upon the temperature of the exchange reaction and upon the thermal history of the oxide specimen. Extended speculation upon the details of the exchange mechanism is not profitable as yet since correlation is first needed with other experimental figures, notably with the heats and rates of adsorption and desorption of oxygen at the temperatures involved, and with studies of semiconductivity such as those of Anderson *et al.*[6] and Garner *et al.*[8] Nevertheless, the preliminary results so far obtained do indicate the power of this method of approach to the problems of catalysis and of gas-solid interaction, and emphasize the need for other experimental work so that a proper interpretation can be made of the present observations.

We can divide the process with some certainty into three stages : (*a*) chemisorption of oxygen, (*b*) exchange with the oxide surface, (*c*) desorption of oxygen ; (*a*) probably involves the formation of atoms and, (*c*) conversely, their desorption as molecules. Any of these stages may be rate-determining. We can find no published data which would enable us to decide between (*a*) and (*c*) as rate-determining processes and experimental work is therefore proceeding along these lines in these laboratories. Preliminary results indicate that chemisorption of oxygen is, for chromium and magnesium oxides, and at our temperatures, much more rapid than the observed rates of exchange ; we therefore examine here the cases which arise when (*b*) or (*c*) are rate-determining.

CASE (1). EXCHANGE REACTION RATE-DETERMINING.—In addition to the notation already introduced we use the following :

α_0 = the initial ^{18}O content of the gas ;

β_0 = initial ^{18}O content of the exchangeable portion of the oxide surface (assumed to be the normal ^{18}O abundance) ;

β = the corresponding ^{18}O content at time t from the start of the reaction ;

β_∞ = the value of β at the completion of the surface exchange (the α and β terms being expressed as atom fractions of ^{18}O) ;

n_s = number of exchangeable oxygen ions in the oxide surface/g. of oxide, (i.e. of the species O_s) ;

w = wt. of oxide used in g. ;

n_g = quantity of oxygen gas (expressed as the number of atoms) in the gas phase in the reaction system (including the amount involved in the C_g term) ;

C_g = concentration of the species O_g in the reaction zone, expressed here as a number of atoms/g. of oxide.

We may then write the velocity of the exchange reaction, given as the number of atoms undergoing exchange in the reaction system in unit time, as

$$v = -n_g\,d\alpha/dt = n_g k_s(\alpha - \alpha_\infty) \quad . \quad . \quad . \quad . \quad . \quad (2)$$
$$= k_1 w(n_s)(C_g)\alpha(1 - \beta) - k_{-1}w(n_s)(C_g)(1 - \alpha)\beta ;$$

we may also put with sufficient accuracy for our purpose

$$k_1 = k_{-1},$$

so that

$$v = k_1 w(n_s)(C_g)(\alpha - \beta), \quad . \quad . \quad . \quad . \quad . \quad (3)$$

Now at any time during the reaction

$$(\alpha_0 - \alpha)n_g = wn_s(\beta - \beta_0), \quad . \quad . \quad . \quad . \quad . \quad (4)$$

while at the end of the reaction

$$(\alpha_0 - \alpha_\infty)n_g = wn_s(\beta_\infty - \beta_0), \quad . \quad . \quad . \quad . \quad . \quad (5)$$

and since we have put $k_1 = k_{-1}$,

$$\alpha_\infty = \beta_\infty. \quad . \quad . \quad . \quad . \quad . \quad . \quad . \quad (6)$$

Eqn. (2)-(6) give us

$$k_1 C_g = k_s\left(\frac{\alpha_\infty - \beta_0}{\alpha_0 - \beta_0}\right). \quad . \quad . \quad . \quad . \quad . \quad . \quad (7)$$

CASE (2). DESORPTION RATE-DETERMINING.—The kinetic law governing the desorption is not known although it seems probable from the worker of Garner, Gray and Stone [8] (cf. also Goodeve and Jack [9]) that it will be second order, being governed by the speed of recombination of the atoms at the surface :

$$O + O \rightarrow O_2.$$

---

[8] Garner, Gray and Stone, *Proc. Roy. Soc. A*, 1949, **197**, 294. Gray, *ibid.* 1949, **197**, 314. [9] Goodeve and Jack, *Faraday Soc. Discussions*, 1948, **4**, 82.

If this is the case the rate of desorption, expressed as atoms in unit time, is

$$v' = k_2 w(C_g)^2, \qquad (8)$$

or in general if the desorption depends upon the nth power of the concentration of chemisorbed atoms,

$$v' = k_3 w(C_g)^n, \qquad (9)$$

where k_2 and k_3 are velocity constants.

We can then write

$$n_g k_e(\alpha - \alpha_\infty) = k_3 w(C_g)^n(\alpha - \beta) \qquad (10)$$

which, using eqn. (4)-(6), gives

$$k_3(C_g)^n = n_s k_e\left(\frac{\alpha_\infty - \beta_0}{\alpha_0 - \beta_0}\right). \qquad (11)$$

The proper use of eqn. (7) and (11) depends upon determination of C_g; this is being attempted by adsorption measurements, making the assumption that C_g will at least be proportional to the quantity of chemisorbed oxygen/g. of oxide.

Results and Discussion

The results are expressed as values of k_0, where

$$k_0 = k_e\left(\frac{\alpha_\infty - \beta_0}{\alpha_0 - \beta_0}\right) \qquad (12)$$

The reasons for this method of presentation are given below.

Eqn. (7) and (11) involve two quantities, namely C_g and n_s, of which the former is difficult to measure. Both would be expected to depend upon the previous thermal history of the oxide; thus heating to a high temperature, in air or *in vacuo*, will produce sintering which will reduce the number of active sites in unit area of the surface and so lower both C_g and n_s. Whether C_g and n_s are associated with *the same* active sites is not at present determinable. Similarly, different times and temperatures of outgassing will leave on the surface varying amounts of any strongly adsorbed impurities, which again could lead to changes in n_s and C_g. In the latter connection it is regrettable that the present experimental technique does not permit the use of films of oxide formed *in situ* in an all-glass apparatus by oxidation of metal films, such as have been used by Garner, Gray and Stone.[8] This is because at least 10^{20} atoms of exchangeable surface oxygen atoms are needed, and this number of atoms will (as close-packed ions of radius $\sim 1{\cdot}4$ Å) occupy an area of about 8 m.[2] In what follows we discuss the rate of oxygen exchange making allowance for probable or known changes in n_s and C_g.

(*a*) **Variation of Exchangeable Surface (n_s) with Temperature.**—With thorium oxide (as the results of Table I reveal) (cf. also γ-alumina [4]), there was no significant variation of n_s, calculated from eqn. (5), over the temperature range studied, viz., 446° to 535° C (γ-alumina 400°-592° C). There was no alteration in n_s, determined at a fixed temperature, when the temperature of outgassing of these two oxides (normally 590° C in both cases) was lowered by 75° C.

Chromium oxide showed greater lability, as is seen from Table I, referring to experiments in which 18-20 hr. outgassing was given. Allowing for experimental error it is evident that n_s remains independent of the reaction temperature over the range 323° to 527° C; a sharp decrease in n_s occurs when the outgassing temperature is increased from 567° to 600° C, whereas between 387° and 567° C, n_s is independent of outgassing temperature. This change in n_s is unlikely to be due to alteration in the amount of chemisorbed normal oxygen remaining on the oxide at the end of the outgassing since when the chromium oxide was outgassed for only 1½ hr. at 495° C, it gave a value of $1{\cdot}9 \times 10^{20}$ for n_s. If, as seems very probable, n_s refers to highly reactive centres on the oxide surface, this drop in n_s will be paralleled by a drop in catalytic activity and determinations of n_s should provide a sensitive test of the onset of sintering. Similar, but more extensive, changes of n_s have been found with magnesium oxide.[10]

TABLE I

Oxide	Temp. ° C		$n_s \times 10^{-20}$ atoms/g.
	Outgassing	Exchange Reaction	
Cr_2O_3	387	386	1·98
	455	323	1·94
	455	345	1·92
	455	365	2·00
	455	391	1·73
	455	410	1·99
	455	441	2·04
	527	527	2·20
	567	345	1·92
	600	367	1·28
	600	374	1·58
ThO_2	590	445	5·8
	590	472	6·1
	590	502	5·9
	590	535	6·4

(*b*) **Dependence of Rate of Exchange upon Oxygen Pressure.**—Insufficient work has yet been done to determine properly this relationship; the range of experimental conditions is limited by the difficulty of making capillary leaks which will work satisfactorily at high pressures, and by the need to adjust the oxygen/oxide ratio in the reaction system so that neither $(\alpha_0 - \alpha_\infty)$ nor $(\alpha_\infty - \beta_0)$ are too small. The latter restriction has been imposed hitherto by difficulties in ^{18}O analysis and will eventually be removed by the use of greater enrichments of ^{18}O. We have already reported [7] that values of k_e for magnesium and chromium oxides are independent of the oxygen gas pressure in the reaction system; this is also approximately true for γ-alumina.[4] The figures given in Table II show that k_0 (eqn. (12)) increases with oxygen pressure for magnesium oxide (cf. also γ-alumina where a similar effect is observed [4]) but is approximately constant for chromic oxide; this probably means that, at least for the first two oxides, C_g is still increasing over the pressure range used. It should be noted that these experiments upon pressure-dependence were performed before it was found that there are two possible limiting processes (cf. (*d*) below); the figures for magnesium oxide refer to the region of low activation energy, and those for chromium (and aluminium) oxide to that of high activation energy. We do not consider the independence of k_e and oxygen pressure previously reported [7] and shown in Table II to have any significance.

TABLE II

Oxide	P_{O_2} (mm. Hg.)	k_e	k_0	Temp. ° C	
				Reaction	Outgassing
MgO	40·7	0·028	0·0124	491	510
	79·7	0·029	0·0161	491	510
	83·5	0·029	0·0170	493	510
Cr_2O_3	69·5	0·037	0·023	386	387
	139·4	0·035	0·022	385	387

---

[10] Houghton and Winter (in course of publication).

(*c*) **Influence of Outgassing Temperature upon Reaction Velocity.**—The figures inset against the experimental points in Fig. 2 are the temperatures of outgassing in °C. With the exception of the points for 387° C outgassing, which are those given in Table II, and the two points for 600° C outgassing which are discussed in the next section, all the runs were performed at oxygen pressures between 5·7 and 6·4 cm. Hg so that the effect of pressure may be disregarded (cf. below). It is seen that k_0 increases slightly as the outgassing temperature is raised from 387° to 455° C, but that a further increase to 567° C has no effect (cf. below for discussion of the effect of outgassing at 600° C). We may remark that γ-alumina also appears to be relatively insensitive to outgassing temperature,[4] but that the sample of magnesium oxide used by us is very sensitive.[10]

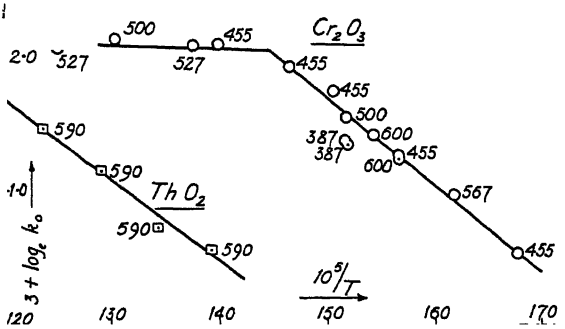

FIG. 2.

(*d*) **Temperature Coefficient of the Velocity of Exchange.**—The results plotted in Fig. 2 clearly indicate that there are two limiting processes for exchange with chromium oxide; only one has so far been found with thorium (and aluminium [4]) oxide, but an extensive examination of magnesium oxide [10] has demonstrated the presence of two processes here also, with activation energies very similar to those for chromium oxide. The activation energy for thorium oxide obtained from Fig. 2 is 27 ± 0·5 kcal./mole., while for chromium oxide the two values are 29·5 ± 0·5 and 1 ± 4 kcal./mole. The large error estimated for the last figure is due to the rapidity of the exchange reaction in this temperature range. In the absence of experimental data from other methods of approach we tentatively assign the lower activation energy for chromium oxide to the exchange reaction proper and the higher activation energy to the desorption of oxygen from the oxide surface. This is done on the grounds that (*a*) by analogy with somewhat similar systems the energy of activation for the desorption of chemisorbed oxygen is is likely to be moderately high; (*b*) the exchange reaction involves the switch of electrons between two very similar nuclei, in similar but not identical environments, and is likely to need a smaller activation energy than (*a*). Work upon the adsorption and desorption of oxygen is in progress, together with an examination of the influence of lattice defects upon the initial exchange velocity.

If the above interpretation of the results is correct, then the rate constants in the region of low activation energy should be plotted using eqn. (7), but those obtained in the region of high activation energy should be expressed in terms of eqn. (11). In practice eqn. (12) has been used throughout. However, with thorium oxide the four experiments were performed at oxygen pressures between 6·5 and 7·0 cm. Hg, so that C_g will not vary appreciably, assuming other conditions are fixed, unless it is very sharply dependent upon oxygen pressure. The latter seems unlikely since C_g must be closely related to the quantity of oxygen adsorbed under the conditions of the reaction, and preliminary observations of oxygen adsorption do not reveal a strong pressure dependence. Also, the values of n_s obtained in the thorium oxide experiments remained sensibly constant (Table I) so that under these conditions and assumptions eqn. (11) reduces to eqn. (12).

Considering the results for chromium oxide, excluding for the moment the four runs involving 387° and 600° C outgassing, we note from Table I that n_s remains approximately constant for all the experiments. Since these experiments were performed at oxygen pressures lying between 5·8 and 6·4 cm. Hg, while k_0 for this oxide (in the region of high activation energy) shows no variation with oxygen pressure, it is evident that on the above argument both eqn. (7) and (11) reduce to eqn. (12). Now, both n_s and C_g are measures of the chemical reactivity of the oxide surface, and it is reasonable to assume that $n_s = f(C_g)$; we will also assume that if n_s is unchanged by a change in outgassing conditions, then C_g, referred to a fixed temperature of reaction, is also unaltered. If this is true the reason for the two results for 387° C outgassing falling below the rest of the results in Fig. 3 is that the value of k_3 (eqn. (11)) is lower, and conversely k_3 is constant (at a fixed temperature) for outgassing temperatures between 455° and 567° C. Referring now to the two results for 600° C outgassing, we see that although n_s has fallen appreciably, the points (plotted according to eqn. (12)) lie entirely in accord with the others. Assuming that k_3 has not changed (at constant reaction temperature) we see from eqn. (11) and (12) that this agreement will occur if

$$(C_g)^n \propto n_s$$

This argument is, however, open to criticism since we have no direct knowledge of k_3 and it is quite possible that this does change when sintering sets in.

The above discussion shows that a considerable amount of further work is necessary upon oxygen exchange and more particularly upon the adsorption and desorption of oxygen upon these oxides before an unambiguous interpretation of the results, and an evaluation of k_1 and k_3 is possible. This will then permit the measurement of the activation energies associated with the two limiting processes, since those quoted here are affected to an unknown extent by the variation of C_g with temperature. It is pleasing that this investigation completely confirms the views of Anderson[6, 11] that at temperatures below about $T_m/2$ only the surface of these solids reacts with the gas phase, the exchange with underlying oxygen ions being very low. In this connection it is interesting to note that the inflection point in the activation energy plot for chromic oxide (Fig. 2) is about 410° C, a figure in good agreement with that observed by Anderson *et al.*[6] from conductivity measurements upon sintered discs of chromic oxide. Anderson made no comment upon the inflection points he found for several oxides and spinels in his plots of log (conductivity) against $1/T$, but if our views are correct these changes of slope are connected with a change in the limiting process concerned.

Acknowledgement is made to Prof. H. V. A. Briscoe for his interest and encouragement, to Messrs. I.C.I. for financial assistance towards the expenses of running the mass spectrometer, and to the Central Research Fund of London University for a grant for the purchase of equipment.

Department of Inorganic and Physical Chemistry,
Imperial College,
London, S.W.7.

[11] Anderson, *Faraday Soc. Discussions*, 1948, 4, 163.

ELECTRONIC CONDUCTIVITY AND SURFACE EQUILIBRIA OF ZINC OXIDE

By D. J. M. Bevan and J. S. Anderson *

Received 30*th January*, 1950

The electronic conductivity of zinc oxide at 500-1000° C, in air, varied widely according to the mode of preparation of the oxide. At low oxygen pressures the conductivity is quasi-metallic, and fairly reproducible for different samples, irrespective of their origin. It is suggested that the differences between samples arise largely from the variation in relative importance of surface-conduction and bulk-phase conduction processes.

For any one sample, the conductivity in oxygen at pressures greater than 0·01-0·1 mm. varies with oxygen pressure in readily reversible fashion, according to the law $K = A \,.\, p_{O_2}^{-\frac{1}{4}}$, as required for impurity conduction arising from the reaction $O^{2-} = \frac{1}{2}O_2 + 2e$ occurring at the surface. At low oxygen pressures, however, the conductivity becomes independent of oxygen pressure; equilibrium is attained under these conditions by a process which is slow, structure sensitive and attended with hysteresis. It is suggested that this involves a diffusion process, which gives rise to a heterogeneous surface at low pressures. The bulk-phase conductivity of zinc oxide is probably high, but electrons are trapped by chemisorption of oxygen on the surface.

It has been found that the conductivity of ferric oxide at 500-600° displays similar features, a pressure-independent conducting state preceding the dissociation to Fe_3O_4.

The measurements reported in this paper were undertaken, in the first place, to clear up some anomalies in the behaviour of zinc oxide as an electronic semiconductor. In the course of the work it became apparent that the semiconductivity was controlled, under the conditions of the experiments, almost entirely by surface reactions. An investigation of the phenomena over a wide range of conditions disclosed some features not previously described, and although these cannot yet be fully explained they are undoubtedly relevant to the problem of the nature of an oxide surface under reducing conditions.

As a typical electronic (excess) semiconductor, zinc oxide has previously been studied by a number of workers. Jander and Stamm [1] and Miller,[2] working with powder compacts, found the oxide to have a very low conductivity at ordinary temperatures, with a high temperature coefficient (activation energy of the conduction process of 0·71 eV [2]). Fritsch,[3] to eliminate as far as possible the effects of contact resistances between particles, fused or sintered zinc oxide at high pressures and high temperatures; his material was described as markedly coloured, and was a relatively good conductor, with a very small or negative (quasi-metallic) temperature coefficient. Although the properties of this oxide may have been modified—by introduction of impurities or by freezing in some stoichiometric unbalance during the sintering process—they may, alternatively represent true bulk phase properties of zinc oxide. In the latter case the low conductivity of polycrystalline material, as ordinarily prepared, must be ascribed to resistances arising at the surface of the grain.

* Present address: Atomic Energy Research Establishment, Harwell.

[1] Jander and Stamm, *Z. anorg. Chem.*, 1931, **199**, 165.

[2] Miller, *Physic. Rev.*, 1941, **60**, 890.

[3] Fritsch, *Ann. Physik.*, 1935, **22**, 375.

In the investigations cited, the conductivity was measured in air over a narrow [3] or wide [1, 2] temperature range. Wagner,[4] in developing the statistical concept of lattice defect equilibria, showed that the semiconductivity of oxides must, in general, be a function of the oxygen pressure; in the case of ZnO, if the conductivity be proportional to the concentration of impurity centres (neutral zinc atoms, or electrons trapped near interstitial zinc ions) then $K \propto p_{O_2}^{-\frac{1}{4}}$. The assumption, which may not be justified, is thereby made that the electronic mobility and the activation energy E are independent of the stoichiometric excess of zinc. The conductivity of zinc oxide was, indeed, found by von Baumbach and Wagner [5] to follow the expected law over a limited range of experimental conditions ($p_{O_2} = 10 - 1000$ mm.; $T = 550°$ and $650°$ C).

More recently we have found [6] that, whereas the results of Jarder and Stamm and of Miller are typical of the behaviour of zinc oxide in air, at low oxygen pressures ($p_{O_2} < 10^{-2}$ mm.) the conductivity is high and has a small positive or even a negative temperature coefficient. It became necessary, therefore, to make a systematic study of the variation of conductivity with oxygen pressure, and of the range over which Wagner's hypothesis is valid. This paper summarizes the results that have been obtained.

Experimental

Preparation of Material.—Preliminary measurements were made on zinc oxide prepared from the oxalate [7] as described in our previous paper.[6]

For the preparation of further specimens, very pure zinc was deposited electrolytically from zinc sulphate (Merck, *pro analysi*). The acid solution was first treated with hydrogen sulphide to precipitate heavy metals, a few milligrams of pure copper sulphate being first added so that copper sulphide could serve as a scavenger. The acidity of the solution was adjusted, and electrolysis commenced at low current density and 2·9 V potential difference, to deposit metals more noble than zinc. After 3 hr. a fresh aluminium cathode was substituted, and the potential difference raised to 4·6 V. The zinc was finally washed with distilled water, stripped from the cathode, melted in a Pyrex tube, and finally distilled at 600° and 10^{-4} mm. pressure. The product was converted to oxide by three processes.

(i) The metal was burned in oxygen in a silica tube. The residue was subsequently ignited in air at 950°, a fresh surface being periodically exposed by stirring the powder. At 950° it may be expected that diffusion should take place freely enough to preclude the persistence of any unoxidized zinc. This oxide had a pronounced yellow colour, which showed no tendency to revert to white, even after the most prolonged ignition at 900-1100°.

(ii) A portion of the metal was dissolved in the minimum quantity of pure HCl; basic zinc carbonate was then precipitated by adding an excess of freshly sublimed ammonium carbonate and was ultimately converted to the oxide at 800°. This oxide was distinctly off-white in colour.

(iii) A further portion of metal was dissolved in HCl and precipitated as zinc oxalate. The oxalate, ignited in air at 800°, gave a pure white oxide.

Hüttig and his co-workers have shown [8] that the physical properties and chemical reactivity of zinc oxide may vary markedly, according to the mode of preparation of the material. Although the three samples prepared by the methods cited should have been of similar chemical purity, they varied widely both as to the magnitude and the activation energy of their semiconductivity (Fig. 1), although the conductivity *in vacuo* was markedly reproducible for all samples. In the course of the measurements the oxides were heated to 950-1000°. This should have permitted the healing of lattice disorder, but not necessarily of bulk recrystallization. Each sample was quite stable in behaviour, and the

[4] Wagner, *Z. physik. Chem. B*, 1933, **22**, 181.

[5] von Baumbach and Wagner, *ibid.*, 1933, **22**, 199.

[6] Bevan, Shelton and Anderson, *J. Chem. Soc.*, 1948, 1729.

[7] Rosencranz, *Z. physik. Chem. B*, 1931, **14**, 407.

[8] Hüttig, Kostelitz and Feher, *Z. anorg. Chem.*, 1931, **198**, 206; Hüttig, *Kolloid-Beihefte*, 1934, **39**, 277; Hüttig and Goerts, *Z. anorg. Chem.*, 1937, **231**, 249.

differences in colour and conductivity may perhaps be associated with differences in particle size, and with the consequent variation in importance of surface and bulk phase conduction.

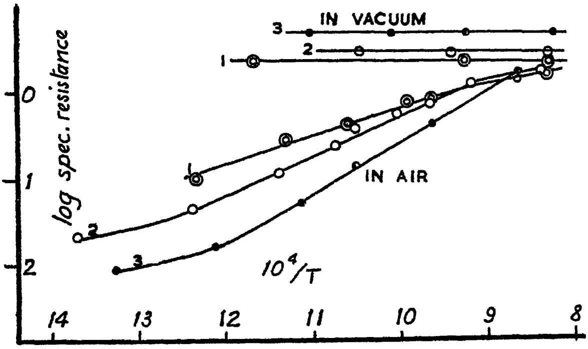

FIG. 1.—Conductivity of ZnO in air and in vacuum. 1. ZnO from ignition of ZnC_2O_4. 2. ZnO from ignition of metal. 3. ZnO from ignition of basic zinc carbonate.

Conductivity Measurements.—The general technique of conductivity measurements has been described in our previous paper.[6]

To provide atmospheres of steady, controlled oxygen content, down to $p_{O_2} = 10^{-5}$-10^{-6} mm., a flow method was used. Oxygen, or commercial nitrogen containing 0·5 % of oxygen, was allowed to flow from storage reservoirs A (Fig. 2), through any selected one of a battery of capillary leaks B, and through the conductivity apparatus C to the pumping system. The steady-state pressure was measured by means of a multi-range McLeod gauge. With the leaks used it was possible to expose the specimen for prolonged periods to well-defined and reproducible oxygen pressures between 2·0 and 4×10^{-6} mm. By suitable manipulation of taps and by-pass connections a smooth and rapid change of oxygen pressure could be achieved. For higher oxygen pressures to 1 atm., static conditions were permissible, since at such pressures, the "gettering" action of metal parts is unimportant.

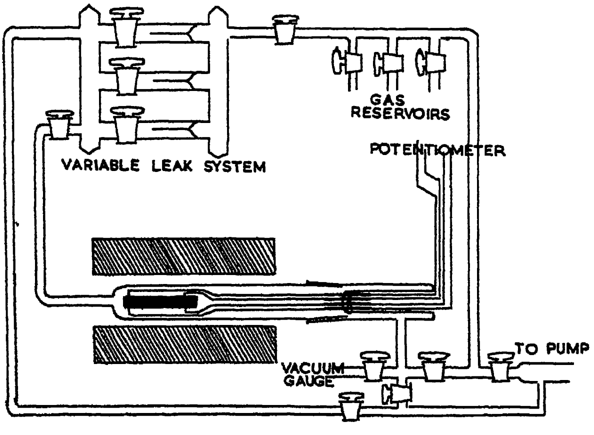

FIG. 2

Satisfactory constancy of temperature between 500° and 900° was attained by means of a Sunvic energy regulator controlling the primary of the autotransformer which supplied the heating current of the furnace. Temperatures were measured with a chromel-alumel thermocouple and potentiometer.

Preparation of Pellets.—Plates 25 mm. × 5 mm. × 1-2 mm. were pressed at 5-10 tons/in.². These were too fragile to use without sintering. "Fully-aged" specimens were sintered at 1000° for up to 20 hr. and can have undergone little subsequent recrystallization. To study phenomena associated with changes in specific surface, later pellets were sintered at 500-600° for 1-4 hr.; these had sufficient strength for careful manipulation.

General Technique.—The dependence of conductivity upon oxygen pressures was first systematically studied at each of a series of temperatures from 500-800°. It was observed that the behaviour under low oxygen pressures was complicated by irreversible processes of ageing—changes in specific surface, or in the area and perfection of inter-crystalline contacts. The effect of repeated cyclic variations of oxygen pressure at 592° C was studied accordingly, using a plate of zinc oxide that had previously been sintered at 600° in air for only 4 hr., so that subsequent ageing processes would show up. To standardize conditions as far as possible, one sample of oxide was separated by sedimentation into fractions of fairly uniform particle size, and the fraction $< 8\ \mu$ was used for subsequent work. With this, the rate of attaining equilibrium at low oxygen pressures was investigated, and pressure-conductivity isotherms were obtained under conditions approaching true equilibrium.

Results and Discussion

Fig. 3 summarizes the pressure-conductivity relations obtained at a series of temperatures, using the same plate of zinc oxide throughout. At all temperatures, and over a considerable range of pressures, the conductivity κ is given by the relation (1)

$$\kappa_{p,T} = Ap^{-B}, \quad . \quad . \quad . \quad . \quad . \quad (1)$$

where $B = 0{\cdot}25 \pm 0{\cdot}02$. The result of Wagner and von Baumbach is thus confirmed, and found to be valid down to $P_{O_2} = 0{\cdot}01$ mm. or lower.

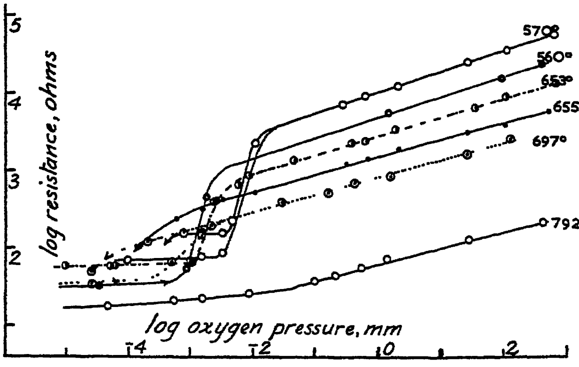

Fig. 3.

Under these conditions Wagner's interpretation appears formally valid; the concentration of conduction electrons could be regarded as determined entirely by the shift of equilibrium in the reactions (2*a*) (as envisaged by Wagner, involving interstitial zinc) or (2*b*) (involving vacant oxygen sites):

$$Zn_l^{2+} + O_l^{2-} \rightleftarrows \tfrac{1}{2}O_2 + Zn_i^0 \quad . \quad . \quad . \quad (2a)$$

$$Zn_l^{2+} + O_l^{2-} \rightleftarrows \tfrac{1}{2}O_2 + \square + Zn_l^{2+} + 2e, \quad . \quad . \quad . \quad (2b)$$

where Zn_l^{2+}, O_l^{2-} represent ions on lattice positions, Zn_i^0 represent an interstitial zinc atom, and □ a vacant oxygen site. Whatever the details of the mechanism, the ionizable impurity centres presumably consist of electrons trapped in the neighbourhood of the lattice defects.

Equilibrium in reaction (2) is rapidly attained, as is shown by the establishment cf a steady and reproducible conductivity within 15-30 min. of changing the oxygen pressure, even at temperatures below 600° C. The melting point of zinc oxide is about 2100°, and the Tammann temperature would accordingly be about 900° C. It appears probable, therefore, that under all conditions summarized in Fig. 3, the rapidity of equilibrium implies that the processes of reaction (2) can involve only the superficial sheets of atoms in, at most, a layer a few unit cells thick in the zinc oxide crystal. The phenomena will, therefore, be regarded as essentially *surface* processes.

At pressures below about 10^{-2} mm. (for the sample used in experiments summarized by Fig. 3) the conductivity is no longer uniquely determined by the shift of equilibrium in reaction (2) : the conductivity becomes independent of the pressure of oxygen, and but little dependent upon temperature.* This state corresponds to the reproducible conductivity *in vacuo*, with a very small temperature coefficient, shown in Fig. 1. Its attainment differs completely from the ready reversibility observed at high pressures ; the transition to the vacuum condition is slow, and attended with considerable hysteresis, with both increasing and decreasing pressures. The resulting step in the log κ — log p isotherms is a structure-sensitive property, which shows signs of shifting to lower oxygen pressures on successive heatings. Because the conductivity at higher oxygen pressures has a large temperature coefficient, the magnitude of the difference between high-pressure and low-pressure conducting states diminishes as the temperature is raised, and at high temperatures (e.g. 800°) there is a smooth transition, with no hysteresis, between the pressure-dependent and the pressure-independent conducting states.

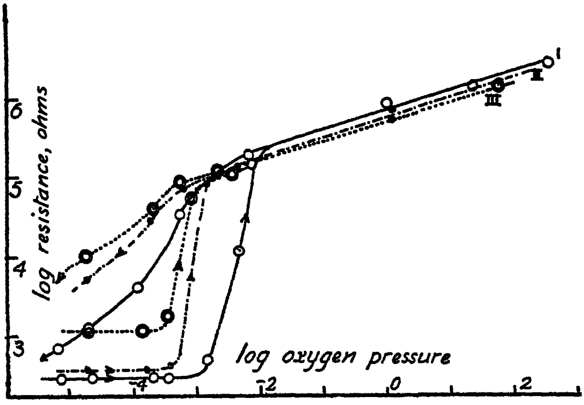

FIG. 4

The effect of successive cycles of pressure changes upon the lower pressure state is shown in Fig. 4. In this experiment the plate was maintained for 1 hr. at each pressure in cycle I, and for 2 and 3 hr. at each pressure in cycle II and III respectively. Instead of eliminating hysteresis effects, the more prolonged experiments indicate the occurrence of an irreversible process which displaces the step towards lower pressures, and produces a smaller but significant increase in conductivity at higher pressures. The latter fact, taken in conjunction with what is known of the phenomena of fritting and reaction processes (e.g. the work of Hüttig, Jander and others) indicates that one factor, at least, in the irreversible ageing is a surface recrystallization, which improves the conductivity of intergranular resistances and effectively changes the relative importance of surface conduction and bulk-phase conduction.

---

* In a series of experiments such as those of Fig. 3, fortuitous changes of contact resistance, etc. (due to shrinkage of the plate) make it difficult to derive a $(\kappa, T)_p$ plot from the $(\kappa, p)_T$ isotherms given, or to obtain satisfactorily reproducible isotherms when the apparatus is cooled to room temperature between experiments.

Hysteresis in the transition from pressure-independent conduction is more marked with decreasing pressures than with increasing-pressures. To study the rate of the processes involved, a plate of oxide was brought to the pressure-independent state by heating it at a high temperature (800°) in vacuum ($p_{O_2} < 2 \times 10^{-6}$ mm.). The temperature was then lowered to 608° and the pressure of oxygen was increased to, and held steady at, a value which just sufficed to bring about a decrease in conductivity. The change of resistance was observed as a function of time in three such experiments, at $p_{O_2} = 4{\cdot}5 \times 10^{-5}$, $1{\cdot}05 \times 10^{-4}$ and $4{\cdot}4 \times 10^{-4}$ mm. respectively; the results are summarized in Fig. 5. This change of resistance was not merely that arising from the relatively rapid shift in equilibrium (2); the rate-determining process was that responsible for the transition from the low-pressure state to the high-pressure state. The resistivity rose asymptotically to a steady value, and the form of the resistance-time curves is suggestive of a diffusion-controlled process.

It is of interest to compare these results with observations made recently by Garner, Gray and Stone [9] on the rate of increase in resistivity of cuprous oxide, a positive hole conductor, as oxygen was stripped from the surface by evaporation into a hard vacuum. The resistivity of cuprous oxide increased according to the relation $\Delta R = Kt^{\frac{1}{2}}$ which can be interpreted as indicating that positive holes are destroyed by a bimolecular process in which oxygen atoms, mobile over the surface, recombine to form oxygen molecules which are subsequently desorbed. The fundamental processes observed on our zinc oxide are just the converse of this: conducting centres are destroyed by the dissociation of adsorbed oxygen molecules, and conversion of oxygen atoms to oxide ions (eqn. (3)).

$$\left.\begin{array}{l} O_2 \text{ gas} \rightleftharpoons O_2 \text{ adsorbed} \\ \qquad O_2 \text{ adsorbed} + 4e \rightleftharpoons 2O^{2-} \end{array}\right\} \quad . \quad . \quad . \quad (3)$$

These processes are operative over the entire pressure range, and are probably rate-controlling for the linear segments of the log R — log p curves; the kinetic data of Fig. 5 refer to a slower process, superimposed on these, when the population of chemisorbed oxygen atoms becomes small.

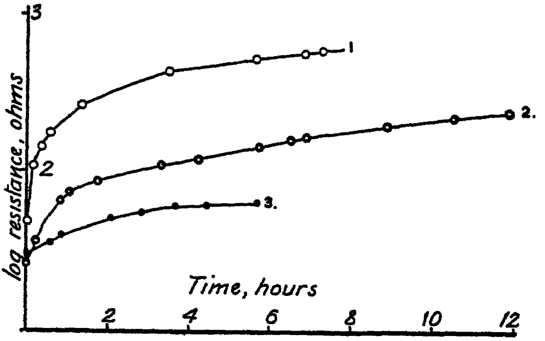

FIG. 5.

The results described in the preceding sections may be summarized as follows: whereas equilibrium between a zinc oxide surface and oxygen is readily mobile at temperatures such that mobility within the crystal is still very small (evidence of conductivity at $p_{O_2} > 10^{-2}$ mm.), a different surface state is attained at low pressures by a much slower process. The characteristics of this process (e.g. pressure of onset of the step, hysteresis) are structure sensitive, and change as grain growth, and fritting proceed. Whereas the conductivity in air varies widely for different zinc oxide preparations, the conductivity is surprisingly reproducible when the surface is in the low pressure state, and is comparable with that reported by Fritsch for macrocrystalline material.

---

[9] Garner, Gray and Stone, *Proc. Roy. Soc. A*, 1949, **197**, 294.

It appears to us that these results can be interpreted only in terms of a difference in semiconducting properties between the surface and the three-dimensional crystal. The conductivities measured were those of granular aggregates, and even apart from the fact that the true conducting cross-section between grain and grain is unknown, and changes as fritting proceeds, the resistance may reside almost entirely in barriers at the contacts between grains if there is, in fact, a difference in stoichiometric composition between the surface and the interior of each particle. In such a case the overall resistance is likely to be highly sensitive to chemical reactions and chemisorptive processes involving the surface layers of atoms.

As has been stated, the linear segments of the curves in Fig. 3 and 4 clearly reflect the maintenance of equilibrium in reaction (3) at the surface of the zinc oxide; this equilibrium leads directly to the observed relation $K = Ap^{-\frac{1}{4}}$, irrespective of the attainment of inner equilibrium in the crystal. The propagation of reaction (3) into the interior of the crystal when equilibrium is disturbed, proceeding through the creation and migration of lattice defects as envisaged by Wagner, is contingent upon sufficiently free diffusion. As such, it certainly occurs at higher temperatures and over a much wider range of oxygen pressures than were used in our experiments. Thus Kitchener and Dancy[10] have informed us that the stoichiometric excess of zinc in solid solution in zinc oxide at 1300° is quantitatively controlled by the oxygen pressure as is required by Wagner's model. At the much lower temperatures used in this work the problem is rather to interpret what happens when the surface layers are partially stripped by evaporation of oxygen. That the $\log R - \log p$ curves are quite linear over the whole range studied shows that the surface, in presence of 1 atm. of oxygen, is still not saturated. What is not assured is that in either the surface or the bulk phase there is a perfect stoichiometric balance between zinc atoms and oxygen atoms.

Several possible models for the relation between surface and bulk phase suggest themselves; an assessment of their validity must be made in the light of further work.

(i) If the crystal of zinc oxide approximates to the ideal composition ZnO, de-oxygenation of the surface in vacuum must give rise to surface atom layers that are richer in zinc than is the interior of the crystal lattice. On this model the conductivity of the surface *in vacuo* should be greater than that of the bulk phase, but the consequences of the model are worth considering in relation to dissociation, reduction and surface reactions proceeding at very low partial pressures of oxygen. The resulting surface state could equally well be regarded as attainable by the chemisorption of zinc atoms on the zinc oxide surface; the concentration of ionizable impurity centres would then be the surface concentration of zinc atoms N_{Zn}, which could be related to the dissociation equilibrium of the oxide (4), by an adsorption isotherm of the Langmuir type (5)

$$ZnO_s \rightleftharpoons Zn_g + \tfrac{1}{2}O_{2g} \quad . \quad . \quad . \quad . \quad (4)$$

$$p_{Zn} = kp_{O_2}^{-\frac{1}{2}}$$

$$N_{Zn} = \frac{ap_{Zn}}{1 + bp_{Zn}} = \frac{aK}{p_{O_2}^{\frac{1}{2}} + bK.} \quad . \quad . \quad . \quad (5)$$

---

[10] Kitchener and Mrs. Dancy (private communication).

The conductivity κ measures the concentration of free electrons, and so is proportional to $\sqrt{N_{\mathrm{Zn}}}$, i.e.

$$\kappa = \frac{C}{(p_{O_2}^{\frac{1}{2}} + B)^{\frac{1}{2}}}, \quad . \quad . \quad . \quad . \quad (6)$$

whence R, the measured resistance of the specimen at the pressure p is related to the limiting resistance R_0 at very low pressures, by the expression

$$R^2 - R_0^2 = \text{const.} \times p_{O_2}^{\frac{1}{2}}. \quad . \quad . \quad . \quad (7)$$

No such relation can give rise to a stepped curve, but (7) represent reasonably well the form of the 800° isotherm, with a smooth transition from the pressure-dependent to the pressure-independent states.

(ii) Several lines of evidence suggest that the three-dimensional crystal of zinc oxide is a good semiconductor, with a quasi-metallic temperature coefficient of conductivity. If—as has generally been considered—this conductivity is an impurity conduction process, it follows that the interior of the crystal must be oxygen-deficient to some slight extent (ZnO_{1-x}) whereas at the surface the chemisorption of oxygen forms almost stoichiometric, non-conducting zinc oxide. The low conductivity of a sintered plate of oxide would then be attributable entirely to barrier resistances at the contacts between grains. The displacement of equilibrium between oxygen molecules and chemisorbed oxygen would then lay bare the substrate of conducting oxide. Over the free surface attainment of equilibrium could readily be reached; the behaviour of material in the inter-granular bridges might be associated with the step in the $\log R - \log p$ curves. This point is considered further below.

(iii) The assumption that zinc oxide is an impurity semiconductor may be at fault; the conductivity may be intrinsic, arising from the excitation of electrons from the d levels of the Zn^{2+} ions to the conduction band. At the surface the chemisorption of oxygen would, in this case, trap electrons from the conduction band by converting oxygen atoms to O^{2-} ions, on surface lattice points. This behaviour would parallel the effect of sulphur upon the conductivity of α-Ag_2S, as interpreted by Reinhold[11] (though in this instance the high diffusion rates and the tendency of silver towards true bivalency lead to a bulk effect, and not merely a surface reaction).

Whatever model be accepted for the conductivity of zinc oxide, the behaviour described in this paper, at low oxygen pressures, seems to require some heterogeneity of surface. Hysteresis in attaining equilibrium at low pressures might in itself be explainable in terms of diffusion along inner surfaces—e.g. in the material bridging inter-granular contents. The ultimate equilibrium conductivities should, however, fit the $\kappa = A \, . \, p^{-\frac{1}{4}}$ relationship. This is not the case, and as an alternative hypothesis we would suggest that the slow process associated with the step of Fig. 3 and 4 represents the creation, by surface diffusion, of a heterogeneous surface. This could either be regarded as consisting of regions of a normal zinc oxide surface with zinc-rich regions (2-dimensional metal), or as regions of exposed, conducting substrate with patches richer in chemisorbed oxygen. Whether the change is regarded as brought about by an increase in population of chemisorbed zinc atoms, or a decrease in population of chemisorbed oxygen atoms, the process could be envisaged as a separation, by a diffusion-controlled process, into two surface phases.

This model is suggested purely as a working hypothesis, to be rejected or modified in the light of further experimental evidence. To examine how far the experimental facts were typical of other instances, a few experiments were carried out on α-Fe_2O_3, at temperatures such that no chemical conversion to magnetite could occur. The results, indicated in

---

[11] Reinhold and Schmitt, *Z. physik. Chem. B*, 1939, 44, 75.

Fig. 6, show that in this case also, at low oxygen pressures, the conductivity becomes independent of the oxygen pressure and (at the lower temperatures) higher than is explicable in terms of the equilibrium which governs the conductivity at high oxygen pressures. Irrespective of the validity of our tentative model this state of the surface is not without significance for the properties of oxides under the conditions obtaining during their action as catalysts for a variety of gas reactions.

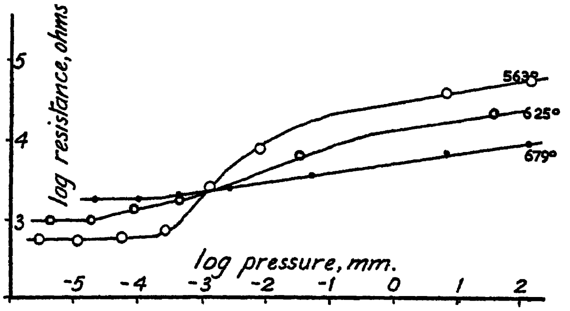

FIG. 6.—Conductivity of ferric oxide as function of oxygen pressure.

University of Melbourne,
Australia.

REACTIONS ON THE SURFACE OF COPPER OXIDE

BY W. E. GARNER, T. J. GRAY AND F. S. STONE

Received 19*th January*, 1950

The absorption of oxygen increases the semiconductivity of the Cu_2O—CuO system, giving a surface energy level of 4·96 kcal. The rate of development of conductivity on the adsorption of oxygen at 140-200° C obeys the relationships $d\lambda/dt = k_1p_{O_2}(\lambda_\infty - \lambda_t)$ and $d\lambda/dt = k_2p_{O_2}(\lambda_\infty^2 - \lambda_t^2)$ over the low pressure range. The rate-determining step is thus first order. It is, however, uncertain whether this relates to the dissociation of oxygen or to the formation of O^- from oxygen atoms. At room temperature, 50 % of the adsorbed oxygen reacts with CO to give CO_2, whereas there is little or no reaction with an evacuated film. A similar reaction occurs between CO_2 and adsorbed oxygen, giving a CO_3 complex. On porous oxide, the rate of adsorption appears to be controlled by the " activated " diffusion of oxygen atoms. These results indicate that in the dissociation of molecular oxygen one oxygen atom enters the lattice, and the other is free to move over the surface. In the catalytic reaction between CO and adsorbed oxygen at room temperature, CO is first adsorbed, and this is followed by a slow reaction to give CO_2. The heat of adsorption of oxygen is 54, of carbon monoxide 20, and of carbon dioxide 23 kcal./mole. The adsorption of CO between 20-200° C reduces the conductivity due to adsorbed oxygen, probably by the formation of a CO_3 complex. At the higher temperature the formation of CO_2 is a three-stage process.

Catalytic reactions consist in a number of successive stages, of which the following are the more important: (*a*) chemisorption of reactants, (*b*) dissociation of reactants into molecular fragments, (*c*) reactions of the molecular fragments, (*d*) association to molecules, and (*e*) desorption of chemisorbed molecules, although not all of these stages will be present in every case. In the present investigation attempts have been made to elucidate the nature of the various stages occurring in the interaction of carbon monoxide and oxygen on the surface of copper oxide. For this purpose two techniques have been combined, one based on measurements of changes of surface conductivity [1, 2] due to the adsorption of gases, and the other on measurements of heats of adsorption. By combination of the two techniques, a more penetrating analysis can be made of the kinetics of the reaction than by either technique separately. Since the changes in electrical conductivity within the range of temperatures investigated are mainly limited to the surface[3] the experiments give information about the surface energy levels of the adsorbed states.

The copper oxide is employed in the form of a thin film on glass in the conductivity measurements,[4] and as a thin film on the copper discs used in the adsorption calorimeter. In order to obtain information not obtainable with the disc calorimeter, measurements on heats of adsorption have been carried out on copper powder coated with a layer of oxide.

Adsorption of Oxygen

The copper oxide film on glass shows its minimum conductivity when present as Cu_2O. There is an increase in conductivity on oxidation to CuO, but at approximately 0·5 % of excess oxygen this reaches a stationary value, as measured in a hard vacuum, not much affected by further oxidation.[5] The activity of a film towards oxygen depends on its thickness and structure. The activity on either copper or glass can be increased by the "embrittlement" process with hydrogen, and can be reduced by annealing above 240° and by treatment with carbon monoxide. Inactive films, which are only very slowly reduced by hydrogen gas, can be reduced and activated by atomic hydrogen. These changes in activity can be explained as due to alterations in the surface area, and to changes in the number and type of adsorbing centres.

At 200° C, after continued evacuation at 10^{-7} mm., a film containing excess oxygen gives a stationary value for the conductivity which is not much affected by the percentage of oxygen or by several weeks' evacuation. Such a film, however, develops a slight gas pressure, 10^{-6} mm., on shutting off the pumps for periods of 12-24 hr. From this behaviour it is judged that this stationary state represents a balance between the rate of removal of oxygen from the surface into the gas phase and the rate of its replacement from the $CuO—Cu_2O$ interface (the system not being in true thermodynamic equilibrium).

On an active film at 200° C, the conductivity was increased 10-fold by the addition of oxygen gas, and the increase was independent of the oxygen gas pressures between 10^{-4} and 0·3 mm. The reaction with oxygen therefore proceeds to the saturation of specific centres of activity. The area of the film on which conductivity measurements are made is too small to measure the surface coverage; but in the disc calorimeter, where the area was approximately 6000 cm.^{2}, the measurements showed that only a few per cent. of the surface was covered with oxygen at saturation. On cuprous oxide the active centres are therefore probably arranged along Frenkel steps or other surface discontinuities.

Surface Energy Levels.—The work of Anderson and Greenwood on the semi-conductivity of copper oxide cylinders[6] shows the presence of two levels at 7 and 23 kcal./mole respectively. The former is operative

[1] Garner, Gray and Stone, *Proc. Roy. Soc. A*, 1949, **197**, 314.
[2] Gray, *ibid.*, p. 294.
[3] Dubar, *Ann. Phys. Paris*, 1938, **9**, 5.
[4] Gray, *Trans. Faraday Soc.* (in press).
[5] Jusé and Kurtschatow, *Physik. Z. Sowjet.*, 1932, **2**, 453.
[6] Greenwood and Anderson, *Nature*, 1949, **164**, 346.

in the range 0-300° C and is probably a surface level. The latter, which is found at higher temperatures, is probably a bulk level. Over the whole temperature range, the current is carried by positive holes. Similar results have been obtained by Wright and Andrews[7] for nickel oxide. Despite the fact that it contains an incomplete $3d$ zone, stoichiometric nickel oxide is an insulator, but NiO containing excess oxygen is a semiconductor. Wright and Andrews find two levels, $E = 7$ kcal./mole and $E = 24$ kcal./mole, and in each case the semiconductivity is due to positive holes. As with copper oxide, the former level is probably a surface level and the latter a bulk level.

From the temperature coefficient of the conductance of thin films of cuprous oxide in the region 20-250° C, the activation energy for the conductivity process has been determined. For an evacuated surface, relatively free from adsorbed oxygen, $E = 5{\cdot}8$ kcal. On the adsorption of oxygen, the semiconductivity is considerably increased and E becomes slightly smaller, 4·96 kcal. Since these two values are of the same order as that of Anderson and Greenwood,[6] it is reasonable to conclude that the conductivity due to the adsorption of oxygen is also +ve hole conductivity.

The conductivity of cuprous oxide is associated with oxygen excess either in the interior or on the surface of the crystals. Since electrical neutrality must be maintained, the presence of an excess of oxygen ions implies that some of the cuprous ions are converted into cupric ions. The adsorption of oxygen on the surface can thus be represented as

$$O + Cu^+ \longrightarrow O^- + Cu^{++},$$

the negative oxygen ion and the cupric ion forming a localized ion pair bonded together near the surface. The positive hole conductivity is associated with this pair of ions. On this picture, the activation energy for the semiconductivity is that required to remove a positive charge from the field of the Cu^+ ion. That the value for an evacuated film is higher than for an oxygenated film may be interpreted as due to the ion-pair being more deeply embedded in the surface in the former case.

Rate of Adsorption of Oxygen.—The rate of increase of electrical conductivity on adsorbing oxygen on an evacuated surface can vary by several powers of ten according to the surface activity; but the rate of disappearance of conductivity (" desorption ") on evacuation is not so much affected by the activity of the surface. The desorption is, however, materially slower than the adsorption in all cases so far studied. The adsorption is first order over the range 100-270° C for varying oxygen pressures and varying activities of surface, and the following equations hold for the low pressure region,

$$d\lambda/dt = k_1 p_{O_2}(\lambda_\infty - \lambda_t), \quad . \quad . \quad . \quad . \quad (1)$$

or

$$d\lambda/dt = k_2 p_{O_2}(\lambda_\infty^2 - \lambda_t^2), \quad . \quad . \quad . \quad . \quad (2)$$

where p_{O_2} is the oxygen pressure, λ_∞ is the conductivity at saturation, which is independent of p_{O_2} within wide limits, and k_1 is the velocity constant, the numerical value of which is dependent on the state of activity of the surface. The linear relationship with p_{O_2}, however, breaks down at the higher pressures (see later). From these results it is deduced that the rate-controlling step in the adsorption of oxygen is first order.* It is significant in this connection that, although the oxidation of Cu_2O to CuO is appreciable at 200° C, the rate at which it occurs is slow compared with the rate of development of electrical conductivity when oxygen is added. It can thus be left out of account when considering the rates of adsorption.

Mechanism of the Adsorption of Oxygen.—The dissociation of molecular oxygen in the gaseous phase requires 117 kcal., and yet the

[7] Wright and Andrews. *Proc. Physic. Soc.*, 1949, 446.

* This is applicable only to plane surfaces. On porous oxides the rate is controlled by diffusion.

process occurs very rapidly on the copper oxide surface. The most probable places for the dissociation to occur are (1) at the localities where oxygen atoms are missing from the plane surface or (2) at the "repeatable step" of a growing face of CuO or Cu_2O. The relevant thermal data are:

$$O_2 = 2O - 117 \text{ kcal.}$$
$$Cu_2O + \tfrac{1}{2}O_2 = 2CuO + 35 \text{ kcal.}$$
$$Cu_2O + O_2 = 2CuO + O - 23{\cdot}5 \text{ kcal.}$$

It is therefore not ruled out on thermal grounds that the dissociation of oxygen molecules can occur at an anionic vacancy in the surface, which permits one oxygen atom to enter the lattice and the other to be free to move over the surface until it is trapped at a discontinuity to form a semiconductivity ion-pair. The evidence in favour of this mechanism is presented later.

The various steps in the reaction path would then be

$$O_{2\text{gas}} \rightleftharpoons O_{2\text{ads.}} \rightarrow O_L + O^{\pm},$$

where O_L forms part of the lattice and $O^{\pm}$ is held more loosely and gives rise to a semiconducting ion pair. The second stage would appear to be the rate-determining step, but further work is needed to settle this point.

Active Oxygen at Room Temperature.—The adsorption is sufficiently rapid for equilibrium to be established within a reasonable time, but the rate of "desorption" under vacuum becomes negligibly slow. Thus, at room temperature the adsorbed oxygen neither evaporates nor does it materially contribute to the oxidation of Cu_2O. Its chemical properties can be studied, and it has been shown to react with carbon monoxide and also carbon dioxide at room temperature. The heat of adsorption of oxygen on an evacuated surface has been measured in a calorimeter containing copper powder, coated with a thin layer of oxide. It ranges from 56-48 kcal./mole O_2, the values depending on the fraction of the surface covered, and is considerably less than the heat of formation of CuO from Cu_2O (70-75 kcal./mole). If the heat for O^{+} is 35 kcal./g. atom, then $O^{\mp}$ in forming the ion pair will liberate 25 kcal. or less. The reactivity of this oxygen atom with other gases is therefore readily understandable.

Reactions of Carbon Monoxide

When carbon monoxide is added at room temperature to a film which has been evacuated at 200° C, the adsorption is accompanied by a decrease in conductivity which, however, rapidly returns to its initial value on evacuation.[1] The process, in so far as it affects the conductivity, is reversible, and the heat of adsorption of this form is 18-20 kcal. The change in conductivity indicates that carbon monoxide forms a chemical bond with the surface in the neighbourhood of a semiconducting ion-pair. It is possible that CO^{+} is formed, but it is more likely that the carbon monoxide forms a CO_2 or CO_3 complex, this being dissociable to give carbon monoxide. The study of the adsorption of carbon monoxide on a larger area of evacuated surface has shown that at temperatures above 100° C, the adsorbed gas undergoes further reaction with the surface and carbon dioxide is liberated.

No carbon dioxide is evolved at room temperature on admitting carbon monoxide to an evacuated plane surface, although considerable quantities of carbon monoxide are adsorbed. The complex formed under these conditions is therefore stable at room temperature. On the oxygenated surface, about 50 % of the adsorbed oxygen is converted into carbon dioxide, confirming the mechanism given on page 250, which suggests that the two oxygen atoms produced on the dissociation of the oxygen molecule are not held in the same way on the surface.[8]

The adsorbed oxygen atoms are thus more reactive than those left on the surface after evacuation. When carbon monoxide, or carbon monoxide and oxygen, is admitted to an oxide surface, whether evacuated or not, the first process is always the saturation of the surface with carbon monoxide. The removal of the active oxygen as carbon dioxide occurs subsequently as a slower process. The following mechanism is tentatively suggested to explain the steps in the process :

$$2O^- + CO \longrightarrow CO_3^=$$
$$CO_3^= + CO \longrightarrow 2CO_2,$$

the CO_2 not being desorbed until the $CO_3^=$ complex formed reacts with excess of carbon monoxide.

The reaction between gaseous carbon monoxide and gaseous oxygen has been studied on a surface which had previously been saturated with carbon monoxide.[1] The reaction proceeded catalytically with a heat corresponding to the reaction $2CO + O_2 = 2CO_2$. The rate of this reaction was shown to be independent of the pressure of the carbon monoxide and proportional to the oxygen pressure. This reaction has been followed in the conductivity apparatus, and the measurements confirm the conclusions that the carbon monoxide–oxygen reaction occurs on a surface saturated with carbon monoxide.

The reactions between carbon monoxide and oxygen have not been systematically studied at higher temperatures since the activity of the film is partially destroyed by the desorption of adsorbed carbon monoxide as dioxide. It was, however, shown that the conductivity of an evacuated film on adding carbon monoxide changed in three stages : (i) there was a rapid fall in conductivity which was followed by (ii) a spontaneous rise and (iii) a slower fall to a final value less than the initial value. The process of conversion of carbon monoxide to carbon dioxide at 200° is therefore a three-stage process. More work is needed before these processes can be understood, but it will be noted that the mechanism given suggests a possible three-stage process.

The new experimental work is given in the sections below.

PART I.—SEMICONDUCTIVITY MEASUREMENTS

By T. J. Gray and S. D. Savage

Experimental

In the previous investigation,[1] the adsorption of oxygen was so rapid that a study of the reaction kinetics of the adsorption could not be attempted. Less active films have now been obtained by forming the copper films slowly, restricting the film thickness to 500-1,000 Å, and preparing the oxide film directly by oxidation of copper. The oxidation is stopped as closely as possible to stoichiometric cuprous oxide. The rates of adsorption of oxygen have been followed by measurements of the changes in conductivity of the film. Reproducible results are obtained at 200° C only if more than 0·5 % excess oxygen is present in the cuprous oxide. It would appear that nuclei of CuO must be present for consistent results to be obtained.

In the measurements of rates of adsorption, the film is returned to the stationary state between successive adsorptions by prolonged evacuation at 200° C. In any series of experiments, the temperature of the film is not raised much above 200° C, since it has been found that treatment at higher temperatures decreases the activity of the film. The deactivation by annealing does not affect the nature of the kinetics, although it reduces the velocity of the adsorption of oxygen. In the earlier work, relatively thick films were employed, 1,200-2,000 Å, and these presented little difficulty in reduction by molecular hydrogen. With the thinner inactive films, reduction with molecular hydrogen is sometimes impossible within a reasonable time. In these cases reduction by atomic hydrogen, produced by a high frequency discharge, proceeds much more rapidly. The atomic hydrogen, however, penetrates the walls of the reaction tube, and makes it impossible to produce high *vacua* at temperatures in the region of 200° C, so that atomic hydrogen cannot be effectively used in the preparation of the films. The reduction by atomic hydrogen activates the film in the same way as molecular hydrogen.

Temperature Coefficient of the Conductance.—In Fig. 1 are given the plots of the log of the conductivity against $1/T$, for films evacuated at 200° C and for films saturated with oxygen gas. The procedure adopted in the case of oxygenated films varied. Usually, the film was saturated with oxygen at 200-250° and cooled from that temperature in an atmosphere of oxygen. Readings were taken both on a cooling and on a rising temperature and no differences were found. Also, if the oxygenated film was evacuated at a low temperature and the temperature coefficient determined upwards, this was found to be the same as with the normal procedure up to the temperatures at which oxygen began to be desorbed. It was therefore concluded that the temperature coefficient was that of a film on which a constant amount of oxygen was adsorbed. The activation energies are calculated on the assumption that there is a simple proportionality between the number of defects (adsorbed oxygen atoms) and the conductivity. It is uncertain in the present stage of the theory of surface conductivity what is the correct assumption that should be made. If it should be shown later that the conductivity varies as the square root of the oxygen concentration, then the activation energies would have to be doubled. The following values have been obtained:

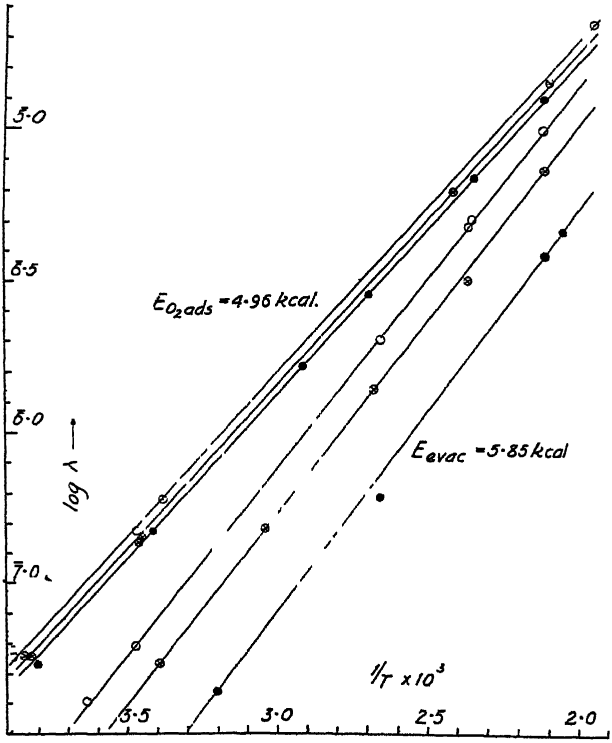

FIG. 1.—Temperature coefficient of conductivity of evacuated and oxygenated Cu_2O films.

Evacuated film, 5·85 kcal./mole; oxygenated film, 4·96 kcal./mole.

The values for the activation energies are not affected by variations in the activities of the films.

Rate Measurements.—Assuming that the conductivity is proportional to the amount of oxygen adsorbed, then if the rate of adsorption is first order,

$$\frac{d(O_2)}{dt} = k(\lambda_\infty - \lambda_t),$$

where λ_∞ is the conductivity at saturation and λ_t the conductivity at time t. A plot of log $(\lambda_\infty - \lambda_t)$ against t should give a straight line. If, however, the oxygen concentration is proportional to λ^2, then log $(\lambda^2_\infty - \lambda^2_t)$ against t should give a straight line. Such plots are shown in Fig. 2 for a range of initial pressures, and both relationships are seen to fit the results. Straight lines are obtained within experimental error up to about 90 % saturation. It is thus not possible, on the basis of these results, to obtain a lead with regard to the relationship between the conductivity and the oxygen concentration on the surface. They, however, make it highly probable that the rate-determining step for the reaction is first order.

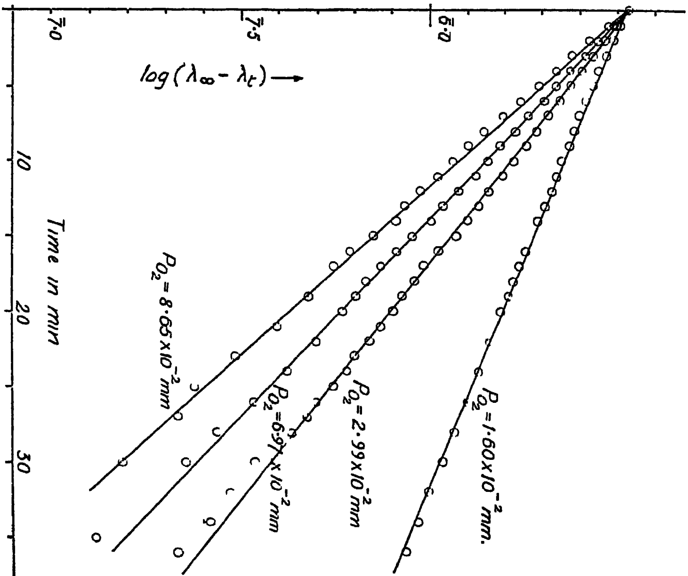

Fig. 2B.—Adsorption of Oxygen on Cu_2O at 200°C.

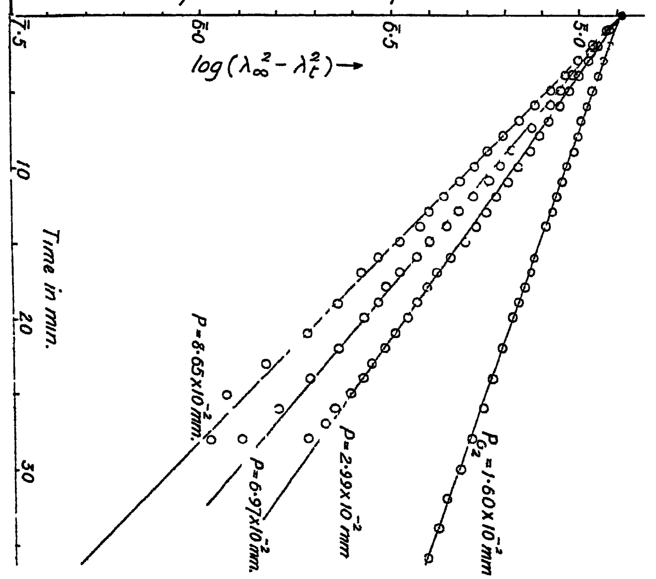

Fig. 2A.—Adsorption of Oxygen on Cu_2O at 200°C.

These relationships do not hold if the composition of the films is very near that of stoichiometric cuprous oxide, or if the film has been previously treated with hydrogen. Also, irregularities in the rate curve occur if the film is maltreated by opening to the air or by being seriously overheated.

It has been observed that the rate of adsorption of atomic oxygen produced by radio frequency discharge is very much greater than for molecular oxygen, 20-30 times in a typical case. This is in agreement with the work of Cubicciotti, Dravnicks and Blevitsky[14] who have found an increase in the rate of oxidation of copper using atomic oxygen. In addition, it is found that the final conductivity λ_∞ on adding atomic oxygen is the same as with molecular oxygen.

The pressure changes during a run are too small to measure. Some measurements have been made of the rate of desorption of oxygen into a high vacuum but the kinetics have not been thoroughly investigated. The rate, however, obeys a fourth order law initially, for 30-40 % of the desorption process, passing into a second-order law which holds for the main period of the desorption (Fig. 3).

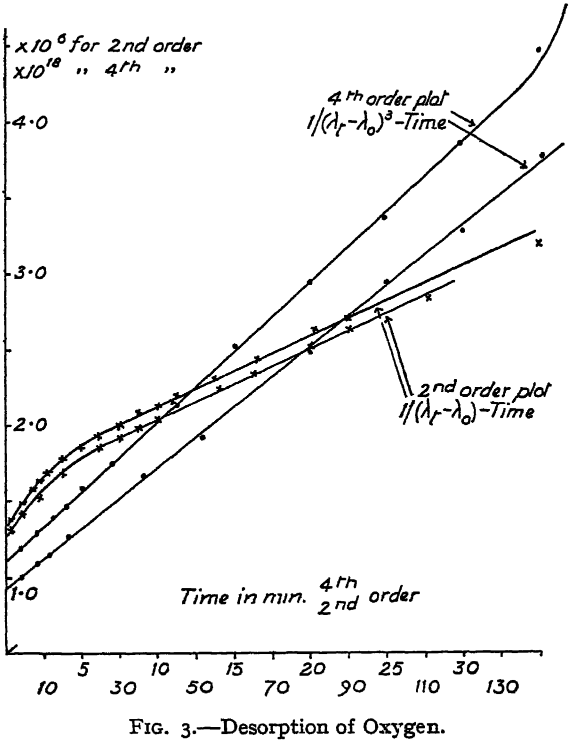

FIG. 3.—Desorption of Oxygen.

The second-order law would be expected since two oxygen atoms would need to collide to form an oxygen molecule. The initial high order, however, indicates that there are probably two independent mechanisms.

Effect of Oxygen Pressure..—In Fig. 4 are given curves showing the variation in the velocity constant with the pressure of oxygen at 200° and 139° C. The copper oxide films are not very stable, there is occasionally a drift in the initial and final conductivity during a series of adsorptions. During the series shown in Fig. 4, the increment in conductivity, at constant temperature, was found to be independent of pressure, although the rate was dependent on pressure; that is, the activity of the film remained constant. At low pressures, the velocity constant is proportional to the pressure, but at the higher pressures, the velocity constant approaches a constant value. The form of the curves resembles that of a Langmuir isotherm, and the constancy of k at the higher pressures may be interpreted as due to the saturation of the effective sites on the surface with oxygen. The rate at which oxygen molecules are converted into atoms on the surface would therefore appear to be proportional to the adsorbed molecular oxygen which obeys a Langmuir adsorption isotherm.

If this interpretation of the results be substantiated, it should be possible to derive values for the heat of adsorption of oxygen molecules, and the activation energy for their dissociation. It is hoped as a result of further investigation to obtain more accurate values than can be derived from the present data.

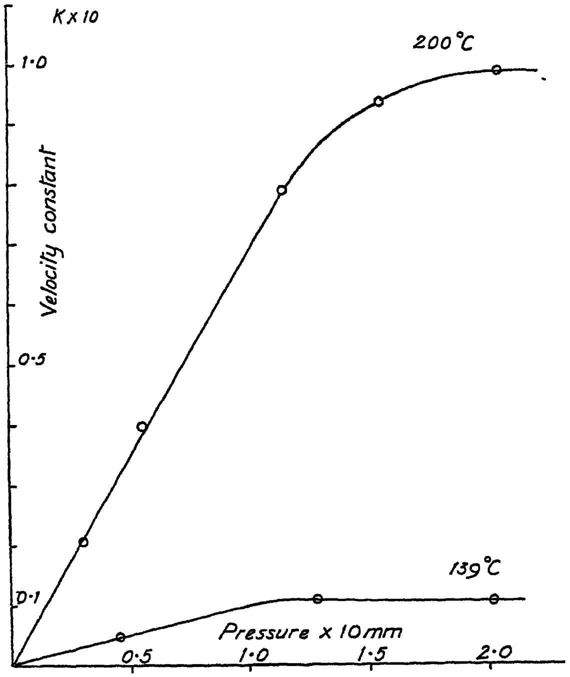

FIG. 4.

PART II.—SURFACE PROCESSES AND HEATS OF ADSORPTION

BY F. S. STONE AND P. F. TILEY

Measurements of heat of adsorption have been made calorimetrically using a thermocouple calorimeter of the type described by Garner and Veal.[8] The weight of adsorbent used was 6·54 g. and the water equivalent of the calorimeter was 0·868 cal. The usual precautions [1, 8] were taken and the galvanometer sensitivity used was 20 cm. per degree. The remainder of the apparatus has been described in a previous publication.[1]

The copper, on which the oxide films were produced, was prepared by dissolving Johnson and Matthey Specpure copper sulphate in distilled water and by reducing with excess hydrazine hydrate in alkaline solution. The spongy precipitate of metallic copper so formed was filtered, washed and dried *in vacuo*. The oxide coating was reduced *in situ* with hydrogen and a thin oxide film (< 500 Å) was formed by oxidation with a known volume of oxygen at 100° C. Several methods have been investigated, but the above method was found to produce the most active catalyst. It also possesses the advantage that the reducing agent is volatile.

Adsorption of Oxygen.—The adsorption of oxygen has been studied at a series of temperatures; the uptake of gas is relatively slow and the fall of pressure with time in a closed system can easily be followed. The adsorption obeys accurately a $\sqrt{p}$ — $\sqrt{t}$ relationship in the initial stages (up to 40 min.) and the results of six adsorptions at constant volume are shown in Fig. 5.

---

[8] Garner and Veal, *J. Chem. Soc.*, 1935, 1437.

Ward's equation[9] for activated diffusion is of this form provided the equilibrium concentration on the surface is proportional to $\sqrt{p}$, as is usually assumed for a gas which dissociates on adsorption. The equation becomes

$$p^{\frac{1}{2}} = -\frac{A\beta}{\alpha V}\left(\frac{Dt}{\pi}\right)^{\frac{1}{2}} + \text{const.}$$

where α, β and A are constants, V is the volume of the system and D is the diffusion coefficient. However, it is not possible at this stage to state decisively that the rate-determining mechanism is one of activated diffusion rather than activated adsorption. The Arrhenius line for the above equation gives an apparent activation energy of 8·5 ± 1·5 kcal./mole.

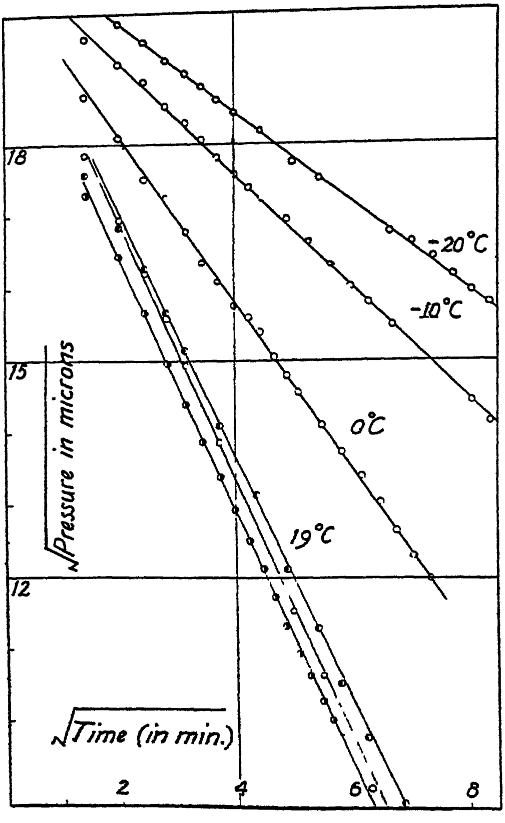

FIG. 5.

Some support for the diffusion mechanism is obtained from the fact that at constant temperature the gradients of the $\sqrt{p} - \sqrt{t}$ plots are found to be proportional to $1/V$, which is a requirement of the above equation. Furthermore, the value of E compares with the value of 9·5 kcal./mole found by the oxidation of copper under conditions where the rate-determining step was believed to be the diffusion of oxygen molecules through cracks in the oxide layer.[10] Finally, the Ward equation has been found to be obeyed in the adsorption of oxygen on manganese oxide.[11]

The occurrence of $p^{\frac{1}{2}}$ in the observed relationship does indicatet hat dissociation occurs before the rate-determining step, and that an equilibrium $O_2 \rightleftharpoons 2O$

[9] Ward, *Proc. Roy. Soc. A*, 1931, **133**, 506.

[10] Wilkins and Rideal, *ibid.*, 1930, **128**, 394.

[11] Sakai, Kurimura and Okura, *J. Soc. Chem. Ind. Japan*, 1943, **46**, 1011 ; *A.C.S. Abstr.*, 1949, 1623.

is established on the surface. The integral heat of adsorption, measured at room temperature for a surface which has been baked out at 200° C, is 53-56 kcal./mole.

The adsorbed oxygen is stable on the surface at room temperature over periods of at least 24 hr., showing that oxidation processes are extremely slow. The adsorbate reacts readily at room temperature with carbon monoxide[1] and the carbon dioxide formed evaporates into the adjacent liquid oxygen trap. It was found, however, that after 24 hr., by which time the reaction has virtually stopped, only about 50 % of the oxygen which had been adsorbed could be removed in this way (see Table I).* The conclusion is drawn, therefore, that about a half of the oxygen adsorbed is " mobile," whilst the remainder is unreactive.

TABLE I

Vol. of O_2 Adsorbed (cm.³)	Vol. of CO Admitted (cm.³)	Vol. of CO_2 Formed After 24 hr.	% O_2 Removed
1·02	3·45	0·83	41
1·88	4·60	1·72	46
0·70	2·15	0·84	56
0·55	1·82	0·65	59

Adsorption of Carbon Monoxide.—The adsorption of carbon monoxide at 20° C is characterized by a rapid uptake of gas, many times faster than the rate of adsorption of oxygen at the same pressure (compare Curve I with III and IV of Fig. 6).

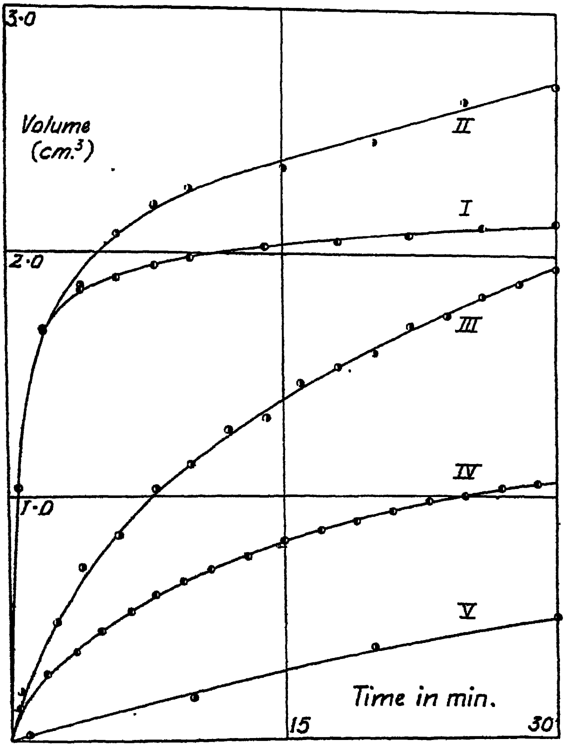

FIG. 6.
I. CO on an evacuated surface.
II. CO on an oxygenated surface.
III. O_2 on an evacuated surface.
IV. O_2 on an evacuated surface.
V. CO and O_2 on a CO-covered surface.

Initial
p = 1·10 mm.
p = 0·73 mm.
p = 1·02 mm.
p = 0·39 mm.
Partial pressure of O_2 = 0·41 mm.

---

* A small amount of CO_2 is obtained under these conditions when CO is applied to a surface which has not previously been exposed to oxygen; these amounts have been deducted before compiling the table.

The heat of adsorption is reproducible and constant throughout an experiment at 20 kcal./mole, as compared with a value of 28 kcal./mole found on larger thicknesses of oxide films.[1] Confirmation of this difference is provided by the desorption characteristics. With a heat of adsorption of 28 kcal./mole, only about 15 % of the gas could be desorbed as carbon monoxide below 100° C; the remainder desorbed as CO_2 at a higher temperature. In the present case, however, where the heat is 20 kcal./mole, the desorption properties are summarized in Table II.

TABLE II

Temp. °C	% Described as CO	% Described as CO_2
20	30	Negligible
20-100	20	25
Above 100	Negligible *	25*

* In the region of 100° C and above, any CO reacts with the surface, producing CO_2.

An estimate of the rate of desorption of a gas may be obtained from the equation [12]

$$\text{Rate of desorption} = c_A \, . \, \frac{kT}{h} \frac{f^{\ddagger}}{f} e^{-E/RT},$$

where $f^{\ddagger}$ is the partition function of the transition complex and f that of the initial state, and c_A is the concentration of the adsorbate.

Assuming $f^{\ddagger} = f$, this shows that, provided no activation energy is required for desorption ($E = Q$, heat of adsorption), the period of half-desorption is 2 min. at 20° C if $E = 20$ kcal., but 24 hr. if $E = 24$ kcal. Thus, for a gas the heat of adsorption of which is 20 or less, some desorption can be expected at room temperature, but if the heat is higher, then appreciable desorption will not occur until the temperature is raised. The fact that, in this case, some 30 % is desorbable at room temperature is in agreement with the fact that the heat of adsorption is 20 kcal./mole.

The heat of adsorption of carbon monoxide on an " oxygenated " surface, that is, one on which oxygen has already been adsorbed, has been measured and the expected exaltation of the heat due to reaction is observed. The heat produced per mole of CO disappearing is as high as 35 kcal. in some cases. It is significant to record that the desorption of CO_2 is not at all rapid, and it is believed that an intermediate CO_3 complex is involved, with the result that the desorption of CO_2 requires a small activation energy. The rate of uptake of CO on an " oxygenated " surface is shown in Curve II of Fig. 6.

Adsorption of Carbon Dioxide.—No appreciable adsorption of carbon dioxide occurs on a reduced or on a baked-out surface (0·005 cm.^{3} in 12 min.). If, however, CO_2 is admitted to a surface on which oxygen has been adsorbed, there is an immediate adsorption of CO_2 (0·2 cm.^{3} in 12 min.). Over a period of 24 hr., about 70 % of the volume of the previously-adsorbed oxygen can be taken up. The heat of adsorption of CO_2 in these circumstances is reproducible at 23 kcal./mole. As is to be expected, a small amount of the gas can be desorbed *in vacuo* at room temperature, and the remainder is easily desorbed on raising the temperature. If, however, a gas mixture of equal volumes of carbon dioxide and oxygen are adsorbed together on an evacuated surface, they are taken up in the ratio 1/1. The initial heat is 41 kcal./mole, falling to 37 kcal./mole, in agreement with the conclusion that oxygen is adsorbed first. This steady value of 37 kcal./mole for the integral heat compares with 38·5 kcal./mole, as calculated from the uptake of equal volumes of oxygen (54 kcal.) and carbon dioxide (23 kcal.).

It follows, therefore, that CO_2 is stable on the surface only in the form of a complex with oxygen, and that this complex is most readily formed with the " mobile " oxygen obtained by the adsorption of oxygen. The fact that 1 volume of oxygen (which gives one reactive and one unreactive O atom) permits the adsorption of 1 volume of CO_2 suggests that the formula of the complex is CO_3, and that it is probably negatively charged. The discrepancy between

---

[12] Glasstone, Laidler and Eyring, *The Theory of Rate Processes* (1941).

70 % and 100 % may be due to blocking, since a CO_3 complex will cover a considerable area.

On admitting carbon monoxide to the complex at room temperature, reaction occurs and two volumes of carbon dioxide are produced for each CO taken up. This is in accord with the equation,

$$CO + CO_3^{=} \longrightarrow 2CO_2 + 2e.$$

The Reaction between Mixtures of Carbon Monoxide and Oxygen.—It has been shown earlier that, for the catalyst in question, the reaction between CO and oxygen occurs on a CO-covered surface,[1] and the fact that the first process is the adsorption of CO was also confirmed by the present work, where the initial (approximate) heat was 29-30 kcal./mole. The combination reaction has now been studied on a CO-covered surface (see Fig. 6, Curve V), and it has been found that the uptake of oxygen is in some cases greater than that expected from the stoichiometry ($1O_2/2CO$), being as high as 1/1 in some cases.

The experimental results of van Cleave and Rideal [13] in the investigation of the H_2—O_2 combination reaction over this type of catalyst show a similar effect. They used a temperature range 170-250° and a catalyst which consisted of copper wire covered with a layer of oxide. At low oxide thicknesses, the gases disappeared in a 1/1 ratio, whereas at higher thicknesses the gases disappeared in the 2/1 ratio which is expected from the stoichiometric equation.

The authors wish to express their thanks to Imperial Chemical Industries, Ltd., and Distillers Company, Ltd., for grants.

Department of Physical and Inorganic Chemistry,
The University, Bristol.

[13] van Cleave and Rideal, *Trans. Faraday Soc.*, 1937, **33**, 635.

[14] Cubicciotti, Dravnieks and Blevitsky (private communication through Dr. G. Szasz).

THE PHYSICAL PROPERTIES OF PROMOTED MOLYBDENUM DIOXIDE CATALYSTS

By R. H. Griffith, P. R. Chapman and Miss P. R. Lindars

Received 1st February, 1950

The physical properties of molybdenum dioxide catalysts, promoted by the addition of small amounts of silica, have been examined. Great changes in the surface area take place as the silica content increases, but these do not alone account for the differences in the activity for hydrocarbon decomposition. Measurements of the composition, crystal structure, electrical conductivity and thermoelectric potential of the catalysts are also recorded and the results suggest that MoO_2 rather than Mo metal is the catalyst, and that the function of the promoter is to increase the surface of the dioxide. This is effected to the greatest degree when the maximum amount of silica is incorporated into the MoO_2 lattice.

The addition of small amounts of promoters to molybdenum dioxide catalysts is known to produce striking changes in their activity for the decomposition of hydrocarbons.[1] The quantity of promoter giving the maximum effect is highly critical and the chemisorption of hydrocarbons, at or near the reaction temperature, follows similar changes.[2] No fundamental reason was found for these relations.

The present paper reports some preliminary results of measurements of the physical properties of catalysts prepared by the reduction of molybdic acid to which known amounts of silica have been added. Surface

[1] Griffith and Plant, *Proc. Roy. Soc. A*, 1935, **148**, 191.

[2] Griffith and Hill, *ibid.*, 1935, **148**, 194.

area, electrical conductivity, thermoelectric potential, crystal structure and chemical composition of the reduced catalysts have been determined.

Experimental

Preparation of Catalysts.—Silica sol, containing about 1 % SiO_2, was added to molybdic acid of A.R. quality, the resulting paste being warmed and stirred until the sol coagulated. The mixture was then dried, powdered, and reduced in pure hydrogen at 450° for 50 hr., a gas rate of 220 cm.^{3}/min. being used with 2 g. catalyst. The reduced material was then evacuated to below 5×10^{-4} mm. for 8 hr. Strict precautions were always taken to prevent access of air to the catalysts after reduction.

Surface Areas were measured with nitrogen by the method of Brunauer, Emmett and Teller.[3]

Electrical Conductivity and Thermoelectric Potential were determined in the apparatus shown in Fig. 1, which is a modified form of that described by Reichardt.[4] The catalyst was placed in the bulb A, the whole apparatus being purged with pure hydrogen before the outlet at F is sealed. With the side arm in a horizontal position, the catalyst was reduced at 450°, escape of powder being prevented by the sintered-glass disc; the tube E was sealed when reduction was complete. The catalyst was tipped into the tube B (int. diam. 6·5 mm.), the weight C being held up by means of an iron strip manipulated by a magnet, and was then packed between the fixed sintered disc G and the movable disc H. The stainless steel weight C was finally lowered to compress the catalyst column. Electrical contact was made by platinum discs, welded to platinum wires, inside each glass disc. The pressure on the catalyst powder due to the weight was 0·78 atm.

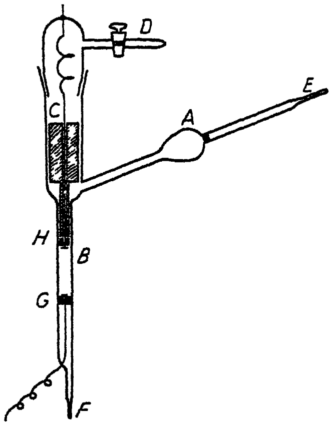

FIG. 1.

For measurement of conductivity, the tube was heated in a small furnace so that the whole catalyst specimen was at a known temperature; for determining the thermoelectric potential, the junction H was kept at 0° by an ice jacket while the junction G was heated to a known temperature. This resembles the technique of Hockberg and Seminski.[5] The whole specimen was evacuated at 450° before measurements were started and was connected by the side tube D to a McLeod gauge and mercury vapour pump through a trap cooled in liquid nitrogen.

As the results given by this apparatus were purely comparative, a strict sequence of operations was followed. After one day's evacuation, the tube was cooled overnight and by connecting the electrodes to a Wheatstone bridge the conductivity was measured at a series of temperatures up to 450°. One hour was allowed at each temperature before taking any readings. After again cooling overnight, the thermoelectric potential at the junction with Pt was determined by measurement of the potential difference and the resistance across the catalyst column when one end was at 0° and the other at a known temperature. This series of measurements was repeated on the following day after admission of hydrogen to a pressure of 100 mm.

Analysis of Reduced Catalyst.—Earlier work [2] failed to detect significant differences in the extent of reduction of MoO_2 as the silica content was altered. But these observations were based on the amount of water produced and this procedure has grave shortcomings in view of the presence of silica gel. Moreover, no precautions were taken to prevent oxidation of the reduced catalyst on exposure to air. A new series of analyses has therefore been carried out on samples prepared and weighed in pure hydrogen.

[3] Brunauer, Emmett and Teller, *J. Amer. Chem. Soc.*, 1938, **60**, 309.

[4] Reichardt, *Grenzflächen Katalyse* (ed. Kröger) (Hirzel, Leipzig, 1933), p. 18.

[5] Hockberg and Seminski, *Physik. Z. Sowjet.*, 1938, **13**, 198.

About 0·5 g. catalyst was reduced for 48 hr. in a glass bulb at 450°, then tipped into a small side-arm which was sealed off without exposure to air. This tube was scratched at a constriction which could be easily broken, then weighed and broken. The contents were tipped into dilute nitric acid and the pieces of tube weighed, corrections being made for the original content of hydrogen. The molybdenum content of the catalyst was determined gravimetrically as lead molybdate.

X-Ray Examination was carried out on specimens of the reduced catalysts sealed in Lindemann glass tubes without exposure to air, by Dr. F. A. Bannister and Dr. G. F. Claringbull, of the Mineralogy Department, Natural History Museum, to whom we are greatly indebted for their assistance and advice. The radiation used was Cu K_{α}.

Results

The surface areas of the catalysts are given in Fig. 2 and the compositions of the reduced catalyst are shown in Table I; these latter are given on a silica-free basis and include figures showing the excess of Mo above that required for the exact composition MoO_2.

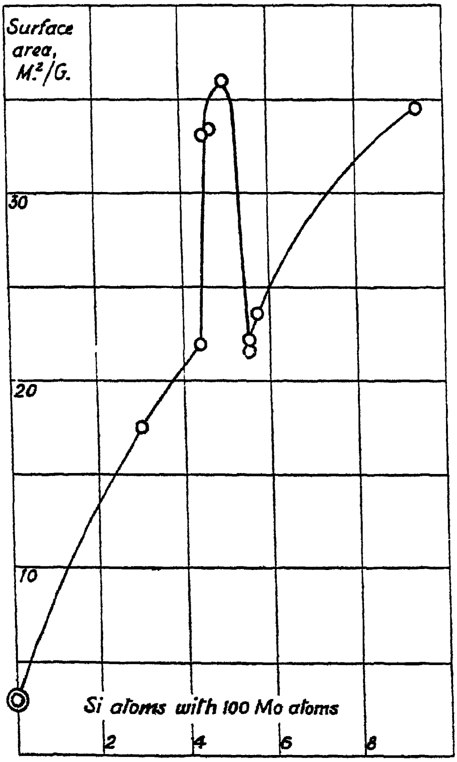

Fig. 2.

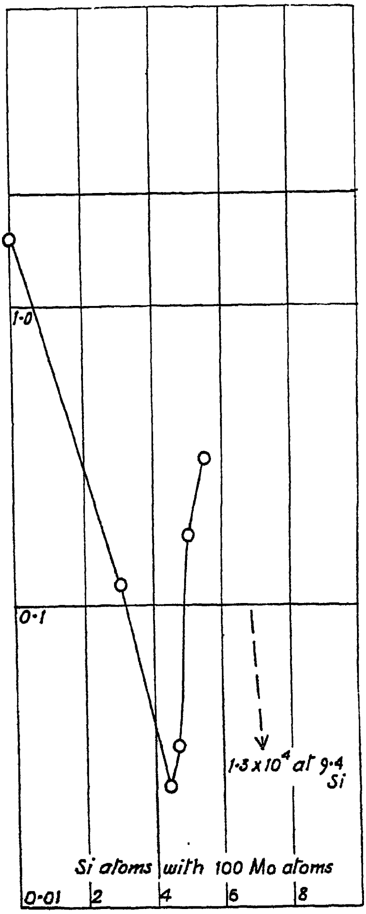

Ordinates: Ω^{-1} (cm.) at 400°C.

Fig. 3.

TABLE I.—COMPOSITION OF REDUCED MoO_2 CATALYSTS

Silicon Atoms with 100 Mo Atoms	% by Weight		
	Mo	Oxygen	Excess Mo
0	76·5	23·5	6·0
3·0	77·9	22·1	11·6
4·4	79·4	20·6	17·6
5·0	81·4	18·6	25·6
5·5	78·0	22·0	12·0
9·4	81·6	18·4	26·4

Crystal Structure.—The crystal structures revealed by the X-ray diagrams are summarized in Table II.

TABLE II.—X-RAY EXAMINATION OF REDUCED CATALYSTS

Si Atoms with 100 Mo Atoms	MoO_2	Mo Metal
0	+	Absent
3·0	+	Absent
4·4	+	Faint
5·0	+	Faint
5·5	+	Faint
9·4	+	Very faint

The relation between the silica content and conductivity at 400° is shown in Fig. 3. Similar differences were observed at other temperatures. With increasing temperature, the conductivity of each mixture up to a silicon content of 4·4 Si atoms to 100 Mo atoms showed a steady fall, indicating that metallic conduction predominated. But with 4·4 Si the curve flattened above 370° and with higher concentrations of silica there was a distinct rise in conductivity above 300°, although at lower temperatures metallic conduction was still dominant. When hydrogen was added, the conductivity of the catalyst increased slightly. Part of this increase may be due to the longer time of compression, but it is also partly caused by lowering of the partial pressure of oxygen. The influence of small additions of oxygen to one catalyst is shown in Table III.

TABLE III.—EFFECT OF OXYGEN ON CONDUCTIVITY OF REDUCED CATALYST CONTAINING 5 Si ATOMS TO 100 Mo ATOMS

O_2 Pressure, mm.	Conductivity/cm.
0·9	0·553
1·5	0·546
3·2	0·540
4·0	0·534
4·7	0·487
5·0	0·330

These results are characteristic of an electron-excess conductor. A similar conclusion is to be drawn from measurements of thermoelectric potential, the heated end of the catalyst being positive with respect to the platinum. The effect of temperature on the thermoelectric potential is summarized in Table IV and the potential developed at 450° is shown in Fig. 4.

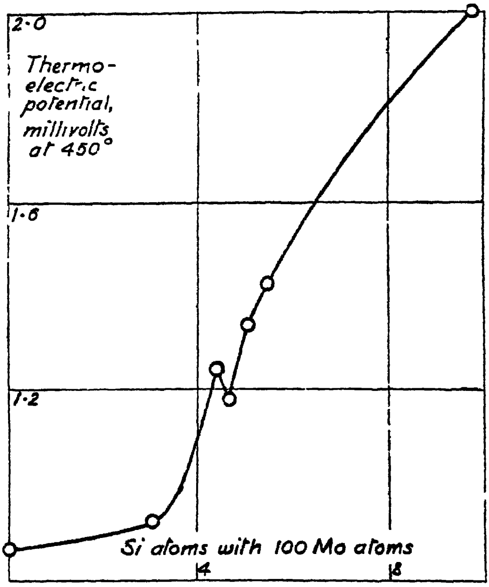

FIG. 4.

TABLE IV.—THERMOELECTRIC POTENTIAL OF PROMOTED MoO_2 CATALYSTS

Si Atoms to 100 Mo	mV/deg. at Junction with Pt., 350-450°
0	0·0038
3·0	0·0038
4·4	0·0055
4·7	0·0059
5·0	0·0062
5·5	0·0051

Discussion

The catalyst activity-promoter concentration curve originally described[1] rose to a sharp maximum when the ratio Si/Mo was 4·4/100. The measurements now recorded must be considered with reference to that curve.

The analyses of the reduced catalysts show that they all contain an excess of molybdenum above that required for the composition MoO_2, even when allowance is made for the statement that this oxide exists in the range $MoO_{1\cdot97}$ to $MoO_{2\cdot08}$, as recorded by Glemser and Lutz.[6] X-ray examination also reveals the presence of Mo metal as well as the MoO_2 in all specimens containing more than 3·0 Si to 100 Mo.

The effect of oxygen on the conductivity and the direction of the current generated at the thermo-electric junction show that all the catalysts are electron-excess solids. This is in agreement with the view of Roginskii[7] that reactions involving hydrogenation, dehydrogenation or ring-closure of hydrocarbons are catalyzed by solids with mobile electrons, often strongly coloured oxides or sulphides which are very sensitive to the presence of impurities. The catalysts do not, however, conform to the Friederich-Meyer rule[8, 9] as they are not derived from the highest valency state of molybdenum. But a similar exception can be found in the results of Klemm and Pirscher[10] for the vanadium oxide series where different individual oxides showed very low conductivities which were greatly increased by either deficiency or excess of oxygen.

---

[6] Glemser and Lutz, *Naturwiss*, 1947, 34, 215.

In the absence of silica, the product contains a mixture of MoO_2 and a little Mo; its conductivity is high and its surface area very small, so that the metal is probably present largely on the surface. The addition of silica in amounts up to the ratio of 4·4 Si/100 Mo produces an increase in surface area in almost direct proportion to its concentration. The conductivity decreases sharply, much more rapidly than can be accounted for on the grounds of the smaller particle size alone. Although excess molybdenum is present it does not appear in crystalline form when only 3·0 Si to 100 Mo atoms are present. If uniformly spread over the surface there would only be enough, at this concentration, to give 2- or 3-atom layers and the excess metal is therefore likely to follow the rutile lattice.

When 4·4 Si atoms are present with 100 Mo atoms, the surface area is again higher but the conductivity has fallen to a minimum in spite of the presence of crystalline Mo metal as well as MoO_2. The system appears to resemble very closely that described by Johnson and Weyl[11] in which ZrO_2 was added to partly reduced TiO_2. The mobility of electrons resulting from the presence of Ti^{3+} ions, which exist under reducing conditions, was greatly restricted by the presence of irreducible foreign ions. Similarly the mobility of the excess electrons in the MoO_2 lattice, which also has the rutile lattice, is decreased as SiO_2 is added to the lattice. The conductivity would thus be expected to be lowest when the lattice had its greatest content of silica.

As still more silica is added, the system becomes strained; the silica now facilitates the formation of metallic Mo and the conductivity increases. But the system is not stable until silica is rejected from the metal crystal: this silica is evidently of great surface area but does not contribute to the catalytic activity or to the X-ray pattern.

This effect, however, is soon outweighed as the molybdenum metal content becomes so high that it forms large aggregates with relatively small surface and maximum conductivity. If the silica content is even higher it provides a gradually increasing total surface largely due to silica alone. These observations suggest that the catalyst for hydrocarbon decomposition is MoO_2, not metallic Mo; this is in agreement with the view of Herington and Rideal[12] that the oxide is essential for the production of aromatic hydrocarbons from paraffins.

The amount of promoter required to give the highest catalytic activity and the maximum chemisorption of hydrocarbons is therefore chiefly a characteristic of the MoO_2 lattice. This agrees with the observation[13] that many other promoters have their maximum effect in about the same concentration as that found with silica. The conditions of preparation of the catalyst are such that its formation from molybdic acid is relatively fast; the first dehydration stage is very quick and the reduction of MoO_3 is largely completed in a few hours. The melting point of MoO_2 is not known but it has now been found to exceed 1600°; at 450°, therefore, the surface must be in a state of frozen equilibrium so that even prolonged heating at that temperature will not result in rejection of the foreign atoms. As the evidence now provided is still somewhat indirect, these views on the mechanism of promoter action with MoO_2 catalysts need confirmation by other methods. Among these the measurement of dielectric properties and power loss should be most informative. Work along these lines is already in progress and will be reported later.

---

[7] Roginskii, *Compt. rend. U.R.S.S.*, 1949, **67**, 97.

[8] Friederich, *Z. Physik*, 1925, **31**, 813.

[9] Meyer, *ibid.*, 1933, **85**, 278.

[10] Klemm and Pirscher, *Optik*, 1948, **3**, 75.

[11] Johnson and Weyl, *J. Amer. Ceram. Soc.*, 1949, **32**, 398.

[12] Herington and Rideal, *Proc. Roy. Soc. A*, 1945, **184**, 434.

[13] Griffith, *Trans. Faraday Soc.*, 1937, **33**, 407.

These observations call attention to the value of chemisorption in determining the effective surface of a catalyst, at least in instances where only one reactant is involved.

The Fulham Laboratory,
North Thames Gas Board,
King's Road,
London, S.W.6.

SOME NOTES ON OXIDE CATALYSTS FOR DEHYDROCYCLIZATION

By H. Steiner

Received 3rd March, 1950

The evidence available on the nature of the catalysts used in the dehydrocyclization reaction is reviewed. It is shown that the active centres catalyzing the three steps which form the reaction sequence, namely, dehydrogenation, cyclization, and also isomerization, are largely identical. The evidence for the mechanism of cyclization based on adsorption of the intermediate olefine by way of opening the double bond, and subsequent formation of a carbon-carbon bond to effect ring closure, is discussed. It is shown that there are important differences in the structures of catalysts using Al_2O_3 as support and Cr_2O_3 and MoO_2 respectively as active oxides.

The catalytic cyclization of paraffins to aromatics was first discovered by Moldawski and Kamuscher in 1936.[1] Since then the mechanism and the kinetics of the reaction have been investigated in considerable detail, and as a result a good deal is known about these aspects of the reaction.[2-6] However, the information on the structure and mode of action of the oxide catalysts used in the cyclization reaction is much more limited. It is intended in the present notes to review shortly this evidence, and to discuss the conclusions regarding the nature of the active centres and the mode of attachment of the substrate to the catalyst, which can be drawn from the kinetics and the mechanism of the reaction.

Before doing this it seems appropriate to recall the most important features of the cyclization reaction. In a temperature range from 450-600° C certain oxide catalysts cyclize and simultaneously dehydrogenate paraffins and olefines containing six or more carbon atoms to the corresponding aromatic compound. Cyclization is not restricted to straight chain hydrocarbons, but generally straight or branched chain compounds react, provided they incorporate within their structure a straight chain of at least five successive links, so that a six-membered ring can be formed without breaking of carbon-carbon bonds. In the great majority of cases we can expect the aromatic compounds resulting from this simple scheme to be formed, e.g. *n*-hexane gives benzene, *n*-heptane and 2-methyl-hexane form toluene.

---

[1] Moldawski and Kamuscher, *Compt. rend., U.S.S.R.*, 1936, **1**, 355; *A.C.S. Abstr.*, 1936, **30**, 6713.

[2] Taylor and Turkevich, *Trans. Faraday Soc.*, 1939, **35**, 921.

[3] Hoog, Verhuis and Zuiderweeg, *ibid.*, 1939, **35**, 993.

[4] Pitkethly and Steiner, *ibid.*, 1939, **35**, 979.

[5] Herington and Rideal, *Proc. Roy. Soc. A*, 1945, **184**, 434.

[6] Herington and Rideal, *ibid.*, 1945, **184**, 447.

In certain cases isomerization reactions take place in addition to simple cyclization. For instance, *n*-octane, in addition to ethyl-benzene and *o*-xylene, the two compounds to be expected from the mechanism outlined above, also forms *p*- and *m*-xylene. The latter compounds can only be formed if an isomerization step is included in the reaction. In a higher temperature range hydrocarbons having at least six carbon atoms but only four successive links in the chain also undergo cyclization to form benzene derivatives. In these cases it is clear that an isomerization as well as a cyclization step forms an essential link in the reaction sequence.

Starting from a paraffin a certain amount of the corresponding mono-olefine is always found in the reaction products. It has been shown that this olefine is an intermediate product, which is subsequently transformed to the aromatic compound. It is most likely that cyclization takes place from the olefine. Neither cycloparaffins nor cyclo-olefines could be found in the products, and it must be assumed that they are dehydrogenated so rapidly to the corresponding aromatic compound that they cannot be formed in appreciable concentration. It has also been shown that where isomerization is necessary this takes place simultaneously with the cyclization itself. It is clear from all this evidence that cyclization, dehydrogenation and isomerization are intimately connected.

Composition of Catalysts.—A survey of the published information on the oxide catalysts used in the cyclization reaction (see Table I) reveals that they belong almost exclusively to those of the 4th, 5th and 6th sub-groups of the Periodic Table. The exception is cerium oxide, which does not belong to these groups, and molybdenum sulphide, the only non-oxide which has shown catalytic activity for cyclization.* Various promoters and catalyst stabilizers not belonging to these groups of the Periodic Table have been tried, but invariably they have been associated with one or other of the oxides mentioned in Table I.

Alumina is the preferred carrier for most of the oxides listed, but by itself it has no catalytic activity. It is noticeable from the preparation of all active catalysts that they must be present either in an amorphous or at least micro-crystalline state. Typical examples are the chromium oxide gel catalysts. On the other hand, crystalline Cr_2O_3, for instance, was shown to be inactive.[7] Alternatively, active catalysts can be prepared by precipitation on or impregnation of supports like activated alumina. Oxides in the gel or microcrystalline form usually have a large surface area. The same is true of supports like activated alumina.

In some cases the alumina, in addition to acting as a suitable support of large surface area, has additional functions. Thus, MoO_2 by itself is inactive, but supported on Al_2O_3 it is one of the most active and stable catalysts. It has been shown that this is connected with the reduction of MoO_2 under the reaction conditions to the inactive molybdenum metal. Alumina retards this reduction to such an extent that the supported catalyst shows activities for sufficiently long periods.[5]

It will be noted that all the active oxides belong to transition elements with incompleted inner electron shells. Oxides of these elements in most cases can be present in several states of valency, and it has been suggested that the active oxide is obtained by reduction under reaction conditions from a higher to a lower valent oxide.[5] The metallic ions of the reduced oxide would contain unpaired electrons, and it would be plausible if these were to interact with the electrons of the double bonds of the olefines which, as has been stated, play a key role in cyclization. However, the fact that ThO_2 and ZrO_2 show cyclization activity does not fit into this picture. There is practically no evidence for the existence of oxides of these elements in a lower state of valency; particularly there is no reason to believe that either ThO_2 or ZrO_2 could be reduced by hydrogen or hydrocarbons under the reaction conditions (450-550° C). On the other hand, the quadrivalent ions of Th and Zr have rare gas electron shells, and an interaction of unpaired electrons with those of the double bond of olefines is not possible in these cases. It could be argued that the activity of ThO_2 is considerably below that of chromium oxide or molybdenum oxide (reaction temperature, 550°, as compared with 475° C, see Table I), but ZrO_2, though less active than CrO_2, compares at least as to order of magnitude with the latter.

---

* In a lower temperature range (*ca.* 300°) platinum on charcoal was also shown to promote cyclization to a limited extent (Kazanski and Plate, *Ber. B*, 1936, **69**, 1862).

[7] Turkevich, Fehrer and Taylor, *J. Amer. Chem. Soc.*, 1941, **63**, 1129.

TABLE I.—OXIDE CATALYST USED IN CYCLIZATION REACTION

Composition	Feed	Reaction Temperature (° C)	Approx. Contact Time (sec.)	Activity, Amount in Products of		Ref.
				% Aromatics	% Olefines	
Cr_2O_3 gel	*n*-Heptane	475	20	15	15	Taylor and Fehrer, *J. Amer. Chem. Soc.*, 1941, **63**, 1385; 1941, **63**, 1387.
Cr_2O_3 gel	”	475	—	41·5	13·5	
10 % Cr_2O_3 on alumina	”	475	120	27	15	
10 % Cr_2O_3 on alumina	”	510	120	60·8	12·3	
10 % V_2O_5 on alumina	”	510	120	29·1	12·7	
10 % ThO_2 on alumina	”	555	120	16·3	11·7	
CeO_2 gel	”	510	120	12·8	5·4	
ZrO_2	”	475	20	8	12	
10 % MoO_2 on alumina	50 % *n*-Heptane +*n*-heptene	475	12	24	?	Herington and Rideal *Proc. Roy. Soc. A*, 1945, **184**, 434.
MoS_2	*n*-Heptane	475	—	Activity comparable with that of Cr_2O_3		Moldawski and Kamuscher, *Compt. rend, U.S.S.R.*, 1936, **1**, 355; *A.C.S. Abstr.*, 1936, **30**, 6713.
10 % UO_3 on alumina	Synthine* fraction boiling 83°-138° C	500	—	11·4	11·2	Kazanski, Sergienko, and Zelinski, *Compt. rend.*, *U.S.S.R.*, 1940, **27**, 664; *A.C.S. Abstr.*, 1941, **35**, 1387.

* Synthine, synthetic gasoline fraction, containing mainly *n*-paraffins (octane rating 10).

The view described, which assumes the metallic cation to be the main active centre of the catalyst, ignores a possible role of the oxygen anions. A possible function of these may be their conversion into a hydroxyl ion by interaction with a hydrogen of a hydrocarbon ; the residual alkyl radical may then interact with the metallic cation to form a bond, as suggested previously. Such a reaction may possibly take place on the surface of a catalyst, even if it is not possible that such a reduction could take place in bulk.

Identity of Catalytic Centres for Cyclization, Dehydrogenation and Isomerization.—The kinetic studies of the cyclization reaction lead one to several interesting conclusions regarding the nature of the catalytic centres and the mode of attachment of the substrate to the catalyst. It has been mentioned already that starting from a paraffin the corresponding olefine is formed as intermediate product of the cyclization reaction.[4] This is demonstrated by the following scheme referring to the cyclization of *n*-heptane to give toluene :

$$n\text{-heptane} \longrightarrow n\text{-heptene} \longrightarrow \text{toluene.}$$

Assuming equilibrium between adsorbed substrate and the substrate in the vapour phase, it can be shown that, within a certain range of contact times, the olefine (*n*-heptene) is present in a stationary concentration, and the ratio of cyclization to dehydrogenation rate is then given simply by

$$\frac{\text{dehydrogenation rate}}{\text{cyclization rate}} = \frac{k_1}{k_2} = \frac{p(\text{heptene})}{p(\text{heptane})}, \quad . \quad . \quad (1)$$

where k_1 and k_2 are rate constants, p(heptene) and p(heptane) are the partial pressures of *n*-heptene and *n*-heptane respectively. Thus, as previously stated, the olefine (*n*-heptene) is an intermediate in the reaction. It has also been shown that the olefine represses the dehydrogenation of the paraffin, by displacing it from the catalytic surface due to its stronger adsorption on the catalyst.[8] Thus identical parts of the catalytic surface are involved in the adsorption of olefines and paraffins, which makes it likely that the active centres for dehydrogenation and cyclization are also identical. A stronger support for this view can be obtained from poisoning effects which occur in prolonged runs extending over a period of hours.[9] Under these conditions, the cyclization activity of all oxide catalysts declines at varying rates, due to the accumulation of surface polymers which block the access to the catalytic centres.

Using eqn. (1), it can be shown that this self-poisoning effect reduces the dehydrogenation rate to very nearly the same extent as the cyclization itself. The relevant data are collected in Table II, where the cyclization activity is measured by the amount of the aromatic compound formed, and the ratio of cyclization to dehydrogenation rate, as calculated from (1), is given as a function of the duration of the run.

It will be seen that whilst the cyclization rate declines by a factor of four, the ratio of cyclization to dehydrogenation rate does not alter by more than 20 %. One must conclude therefore, that the poisoning effects reduce both rates to very nearly the same degree, and that identical catalytic centres are involved in both reactions.

Equally it has been shown that isomerization takes place simultaneously with cyclization.[6] The relevant experiments were carried out with *n*-octane which, on cyclization gives, in addition to *o*-xylene, some ethylbenzene, *m*-xylene and *p*-xylene. Whilst *o*-xylene and ethylbenzene are to be expected by the simple cyclization process, the *m*-xylene and *p*-xylene can be formed only if an isomerization step is included in the sequence of the reactions. It has been shown that neither *o*- or *p*-xylene, nor ethylbenzene, nor the corresponding di-methyl-cyclohexanes, are isomerized under reaction conditions; therefore isomerization cannot take place after cyclization of the paraffin. On the other hand, cyclization of octane and octane-octene mixtures, at two different temperatures and with different catalysts, leads to identical products; therefore isomerization cannot precede the dehydrogenation step. These results taken together would indicate that isomerization is simultaneous with cyclization, and this again strongly suggests that identical catalytic centres are involved in both reactions.

---

[8] Taylor and Fehrer, *J. Amer. Chem. Soc.*, 1941, **63**, 1387.

[9] Steiner, *ibid.*, 1945, **67**, 2052.

TABLE II.—PROGRESSIVE POISONING OF CYCLIZATION CATALYST (Cr_2O_3 + 10 % ZrO_2)

Reaction Period	Mole % of Liquid Product			$\frac{\text{Heptene}}{\text{Heptane}}$
	Heptane	Heptene	Toluene	
1st half-hour . .	48	12	40	0·25
2nd half-hour . .	59	14	27	0·24
3rd half-hour . .	68·5	14·5	17	0·21
4th half-hour . .	74	15	11	0·20

One fact which emerges clearly from the experimental data available, and which is in line with general experience, is the much stronger adsorption of olefines, as compared with paraffins. This is shown by the fact that in the case of a paraffin being cyclized this has to compete with the olefine for the available surface, and is actually largely displaced by it.

One must conclude that the stronger adsorption of olefines is due to the presence of a double bond in the hydrocarbon chain. It is then plausible to assume that adsorption takes place by two-point attachment involving opening of the double bond and formation of links with the catalyst.

This mechanism has been put forward by Twigg and has been supported by further evidence.[10] According to Twigg's scheme, which is demonstrated below by the example heptane to toluene, the intermediate olefine (heptene) is adsorbed on the double bond of carbon atoms 1 and 2 of the chain (Fig. 1*a*), and cyclization would then occur between carbon atoms 1 and 6, with simultaneous splitting of the hydrogen atom from carbon atom 6. Similarly, adsorption on carbon atoms 2-3, and cyclization between atoms 2 and 6, could then take place (Fig. 1*b*).

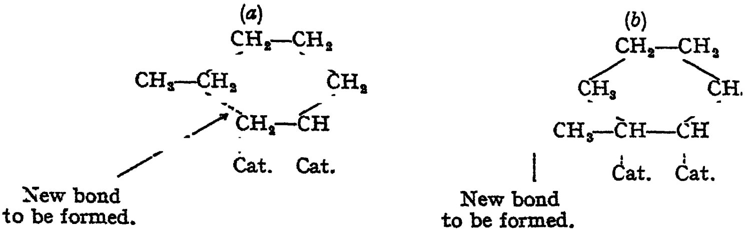

FIG. 1.

Further support for this view, or at any rate for an attachment via the double bond and not via a single carbon atom only, was obtained by Herington and Rideal.[5] Comparing a number of paraffins by the simple cyclization mechanism described previously, it could be shown that the relative rates of cyclization on a chromium oxide-alumina catalyst are given simply by the number of two-point attachments which, according to Twigg's picture, are favourable for cyclization, over the total number of possible two-point attachments, that is, the number of bonds.

---

[10] Twigg, *Trans. Faraday Soc.*, 1939, **35**, 934.

Structure of Supported Oxide Catalysts.—Many of the most active catalysts for cyclization are obtained by supporting an active oxide like chromium-oxide, or molybdenum-oxide, on alumina, which by itself is not active. The alumina used has to have a large internal surface, as measured by nitrogen adsorption, and for highest catalytic activity has to be present in the γ-form.[11]

Considerable light on the structure of these catalysts has been obtained recently by Selwood and Eischens,[12] as reported in this Discussion. In this paper use will be made of one conclusion reached by Selwood in his work on chromium oxide. By comparing the catalytic activity, magnetic susceptibility and internal surface of catalysts having varying quantities of chromium oxide on an alumina support, Selwood came to the conclusion that the chromium oxide, instead of spreading over the internal surface of the alumina in a mono-layer, rather forms clusters, which build up in thicknesses of two, or even three, layers situated on top of each other.

It is of interest to compare with this picture, and with the results obtained by Selwood, the work of Russell on molybdenum oxide deposited on alumina.[13] Russell in comparing the activity of such catalysts of known internal surface, found that the activity increased with increasing molybdenum concentration up to a point where the concentration of active oxide is such that, spread out in a monolayer, it covers approximately the entire surface of the alumina. When this point is reached the activity remains practically constant.

It must be noted that Russell's way of plotting his results differs from that of Selwood. Selwood carried out his experiments in such a way that in every run the same quantity of *active catalytic substance* was present; that is, in case a more concentrated catalyst was used this was diluted by mingling it with alumina which had not been impregnated with active oxide. As a result his activities are based on a unit weight of catalytically active oxide, and are comparable with Russell's only if the latter are calculated on the same basis. If this is done the very interesting result emerges that the catalytic activity of Russell's M_0O_2—Al_2O_3 catalysts is constant until a monolayer is formed, and after that declines in proportion to the increasing concentration.

We have, therefore, here a contrast between chromium oxide catalysts, which appear to form clusters—the catalytic activity of which declines in proportion to their growth—and the molybdenum oxide catalysts, where the active material spreads out in the form of a monolayer, the catalytic activity of which is constant until the monolayer is approximately complete.

In this connection it is worth while recalling the mode of preparation of these catalysts. Generally, a concentrated solution of the water-soluble salt of the active substance is absorbed by the alumina, and it is then heated to some 600-800° C. In most cases the salt is in a higher oxidation state. With chromium this is the chromate, with molybdenum, the molybdate.

On calcination chromium trioxide decomposes, leaving Cr_2O_3, but molybdenum trioxide is stable and remains in this oxidation state.

Cr_2O_3 has an extremely low vapour pressure at the calcining temperature, whilst that of molybdenum trioxide is appreciable (0·1 mm. Hg at 600° C). Thus it is probable that molybdenum trioxide is able to spread out over the total surface by evaporation and re-adsorption, whereas this is not possible with chromium oxide. It seems reasonable, therefore, that by this mechanism molybdenum trioxide can distribute itself over the entire surface of the support, in contrast to Cr_2O_3.

---

[11] Archibald and Greensfelder, *Ind. Eng. Chem.*, 1945, **37**, 356.

[12] Eischens and Selwood, *J. Amer. Chem. Soc.*, 1948, **70**, 2271; 1947, **69**, 1590; 1947, **69**, 2698.

[13] Russell and Stokes, *Ind. Eng. Chem.*, 1946, **38**, 1071; 1948, **38**, 520.

Petrocarbon Ltd.,
Twining Road,
Manchester 17.

CHEMISTRY OF THE SURFACE AND THE ACTIVITY OF ALUMINA-SILICA CRACKING CATALYST

By M. W. Tamele

Received 7th February, 1950

Alumina-silica cracking catalyst owes its activity primarily to a number of acid sites located in the catalyst surface. These sites are formed in the preparation of catalyst by the condensation of the surface hydroxyl groups of the incompletely polymerized silica hydrogel with the hydroxyl groups of the hydrolyzed aluminium ions. The formation of acid is explained by the known tendency of the aluminium atom to acquire a pair of electrons, enhanced by the displacement of electrons in the Al—O—Si bonds towards the silicon atom carrying four positive charges. The electron pair is donated by water, the hydroxyl group becomes part of the structure, and the hydrogen ion is held by electrostatic attraction. The activity of the catalyst is thus reduced to the same general basis as the activity of aluminium halides.

The acidity (acid strength) of the surface of the catalyst has been shown to be in the range of strong acids known to promote hydrocarbon reactions. A linear relationship was found between the activity of the catalyst for polymerization of propylene and the number of acid sites in the surface. A more complex relationship was observed in the cracking of *iso*propylbenzene.

Because of the great importance of the catalytic cracking process to the petroleum industry, investigation of cracking catalysts has been a subject of study in the Emeryville Laboratories of Shell Development Company for some ten years. Alumina-silica cracking catalyst has received most attention although it is not the most active, nor the most stable catalyst that can be prepared. However, the process employing this catalyst has proved, in many instances, to be the most satisfactory when various industrial factors, such as cost and availability of raw materials and design of existing cracking units, are taken into consideration.

In the cracking of petroleum, the alumina-silica catalyst performs many functions besides cracking in the sense of breaking the carbon-to-carbon bonds. Thus, at the usual temperatures of *ca.* 450-550° C, besides the cracking of paraffins and naphthenes concomitant reactions occur, such as double-bond shift in the olefins formed, cyclization and skeletal isomerization, hydrogen transfer, and polymerization (probably of diolefins and of higher aromatics) to coke-like polymeric material. At temperatures below those of cracking, alumina-silica catalyst promotes various other hydrocarbon reactions, such as polymerization of olefins, and certain alkylation reactions.

All these varied reactions have one feature in common, that is, they are all promoted by a variety of acid catalysts. It should be noted, however, that most of these reactions do not take place by an acceleration of thermal cracking reactions by the catalyst, but are brought about by the specific capacity of the cracking catalyst to promote these reactions qualitatively different from thermal cracking reactions.[1] It is further to be considered that the catalyst is a physical, solid body with a characteristic structure and a definite boundary surface, and cannot be satisfactorily represented by one or two of the molecular units of which it is composed ; the chemical composition and the architecture of the accessible surface are of great importance.

Physical and Chemical Properties of Alumina-Silica Catalyst.—Some ten years ago alumina-silica was considered by many to be a combination of two oxides, alumina and silica ; [2] and since it has been known for some time that both silica and alumina alone have low activity for cracking, it was not readily obvious which physical or chemical properties of the combination of the two oxides should be responsible for its high activity.

Alumina-silica catalyst is an amorphous material, not convertible into the crystalline state without a substantial loss of activity and profound chemical alteration, and thus it is not accessible to study by methods applicable to crystalline materials. It was hoped, therefore, that by a careful study of the chemistry of its preparation and of its physical and chemical properties, some clues would be found to its rather surprising catalytic activity.

It was established first that silica gel in any known physical form is practically inactive. For these studies silica gel was prepared by Mr. L. B. Ryland in this laboratory in a great range of physical forms by a wide variation of the conditions of preparation of silica hydrogel and by various treatments of the dried gel. The variations in physical structure were established by a study of the low-temperature nitrogen-adsorption isotherms, and the specimens tested were found to range in surface areas from a few to 800 m.^{2}/g., and in average pore diameter from less than 10 to 150 Å.[3]

Minor variations in activity were soon found to be traceable to incidental variations in the content of impurities, principally aluminium, which appears to accompany all available silicates. When a method was found to remove such impurities, silica gel was shown to be completely inactive for acid-catalyzed reactions.[4]

Alumina was then prepared in a number of physical forms by variation of the conditions of preparation, but no substantially active material was discovered. Some activity, although low, was found even in the most carefully purified materials. It is conceivable that this low activity is characteristic of pure alumina.[5]

It appeared reasonably safe to conclude at this time that the physical characteristics do not contribute substantially to the activity of either silica or alumina, and that this conclusion would hold as well for a mixture of the two substances.[6] It was decided then to examine the possible chemical interaction of the two oxides. The following observations are based mostly on Mr. Ryland's experimental work.

---

[1] Greensfelder, Voge and Good, *Ind. Eng. Chem.*, 1949, **41**, 2573.

[2] However, the acidity of alumina-silica catalyst was recognized early by the workers at the Universal Oil Products Company during their development of industrial methods of manufacture. Cf., e.g., Thomas and Ahlberg, *U.S. Pat.* 2,229,353, also, Thomas, *Ind. Eng. Chem.*, 1949, **41**, 2564.

[3] Tamele, Byck, Ryland and Vinograd, " The Influence of Certain Preparative Variables on the Pore Structure of Silica Gel ". Paper presented at 110th Meeting, Americal Chemical Society, Chicago, Illinois, September, 1946. (Cf. Abstracts of Papers, p. 21E.) Tamele, Byck, Ronay and Vinograd, " The Influence of Steam and Anhydrous Calcination on the Pore Structure of Silica Gel ". Paper presented at 112th Meeting, American Chemical Society, New York, N.Y., September, 1947. (Cf. Abstracts of Papers, p. 4F.)

[4] Schlaffer, Rampino, and Ryland, unpublished results.

[5] Vinograd, Ronay and Schlaffer, unpublished results.

In spite of many variations in the existing industrial processes, the essential step appeared to be the precipitation of alumina from an aluminium salt in presence of an excess of silica hydrogel. Thus, for instance, an active alumina-silica catalyst can be obtained by suspending silica hydrogel in aluminium sulphate solution, and adding enough ammonia calculated to precipitate all alluminium present, but leaving the final slurry slightly acidic. The precipitate is then thoroughly washed to remove electrolytes, dried, and calcined at *ca.* 500° C; the amount of aluminium usually is cl
finished dried catalyst.

It appeared soon that this sequence of operations was essential in order to obtain an active catalyst and that various admixtures of previously prepared pure oxides resulted in catalysts of substantially lower activity. The possibility was therefore considered that freshly prepared silica gel may even in acidic medium interact in some way with fresh alumina, just as sodium silicate may react with sodium aluminate in strongly alkaline environment with formation of complex alumino-silicates. It was then observed qualitatively that upon addition of an aluminium salt to a silica sol (of pH 4·5) the mixture becomes strongly acid. Upon mixing fresh, neutral silica sol with fresh, neutral alumina sol, strong acid reaction developed.

It was likewise observed that the materials prepared by precipitation of aluminium hydroxide by sodium hydroxide in presence of approximately neutral silica gel retained substantial amounts of sodium, even after thorough removal of sodium chloride. The sodium held in this manner was very readily replaced by H^+ ions, or by NH_4^+ ions, as well as by cationic dyes, e.g. methylene blue. It was concluded that the precipitate contained, besides an excess of silica and some free aluminium hydroxide, some acidic material, essentially water-insoluble, and capable of a rapid cation exchange. It was considered probable that the reaction was taking place between the fresh silica gel and the intermediate hydrolysis products which normally precede formation of insoluble alumina.

Precipitation of aluminium hydroxide by hydrolysis of aluminium salts is readily traceable by the potentiometric method and has been found to occur within a narrow range of pH values, dependent on the concentration of the solution.[7] It appeared, therefore, likely that if there is any interaction between silica gel and aluminium ions or aluminium hydroxide in the process of preparation of the catalyst, it would be readily detected by the potentiometric method.

It was found in this way that in the presence of an excess of silica sol, no free aluminium hydroxide is precipitated by the addition of a base to aluminium salt solutions. Instead, at an acidity level higher (*ca.* 1 pH unit lower) than corresponds to the precipitation of aluminium hydroxide, the primary products of hydrolysis of aluminium ions are consumed by the interaction with silica sol particles. One equivalent of acid is produced for each atom of aluminium consumed in this reaction, indicating the formation of an alumino-silicic acid, so that ultimately four equivalents of a base are required to reach neutrality for each aluminium atom present. All aluminium ions are consumed by this reaction if an excess of silica sol is present (cf. Fig. 1). No visible precipitate is formed and the insoluble alkali salt remains in the sol form; it can be converted to gel or coagulated by a decrease of acidity to pH 5 or higher.[8] This reaction proceeds equally well with freshly formed silica gel, less readily with aged gels, and only very slowly with thoroughly aged silica gel.

---

[6] Physical structure of cracking catalyst is, nevertheless, of industrial importance. Cf., e.g., Ryland and Tamele, *U.S. Pat.* 2,469,314.

[7] Cf. e.g. Britton, *Hydrogen Ions*, 2nd Edn. (D. van Nostrand Company, Inc., New York, N.Y., 1932), p. 305.

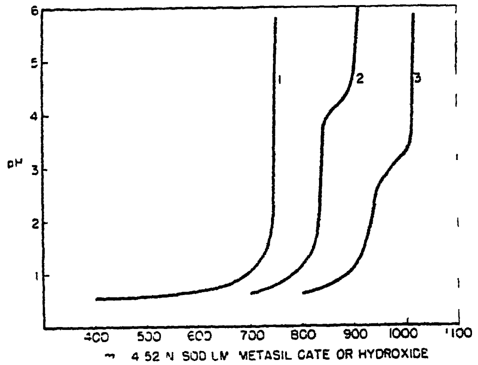

FIG. 1.—Formation of alumina-silica complex.

1. Titration of hydrochloric acid with sodium silicate (silica sol formed).
2. Titration of hydrochloric acid, containing a small amount of aluminium chloride, with sodium hydroxide (aluminium hydroxide precipitated).
3. Titration of hydrochloric acid, containing the same amount of aluminium chloride as in 2, with sodium silicate (alumina-silica complex formed).

When sodium hydroxide was used for neutralization in presence of fresh silica sol, the solid separated by coagulation was found to contain one equivalent of sodium per atom of aluminium for a wide range of compositions (Fig. 2). The stoichiometric relation to silica appeared indefinite, and the efforts to prepare a definite compound by various alternative procedures were unsuccessful, although a minimum of some four silicon atoms to one atom of aluminium appears necessary. The dry, solid sodium salt almost instantaneously exchanges sodium for other cations (e.g. hydrogen, ammonium ions, cationic dyes), and it is considered, therefore, that all sodium and aluminium ions are on the available surface of the solid.

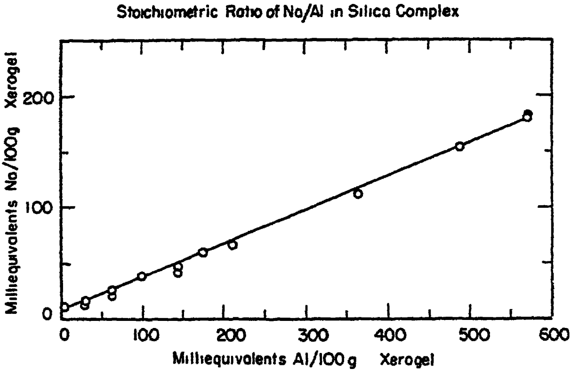

FIG. 2.—Stoichiometric ratio of sodium to aluminium in alumina-silica complex.

---

[8] Tamele and Ryland, " The Acidity of Alumina-Silica Cracking Catalysts ". Paper presented at the 115th Meeting, American Chemical Society, San Francisco, Calif., March, 1949. (Cf. Abstract of Papers, pp. 70-00.)

All this indicates that the complex acid is formed by condensation of the hydroxyl groups of the primary hydrolysis products of aluminium ions with the hydroxyl groups of the incompletely polymerized silica sol or gel particles, and in such a way, that at the point of attachment of aluminium copolymerization ceases and a deficiency of positive charge is created which is compensated by the attachment of a monovalent cation to this point to preserve electrostatic neutrality. Since in acid medium the aluminium ion (co-ordination number 6) can carry at the most only three hydroxyl groups, a neutral condensation product would be expected. The appearance of acidity is undoubtedly traceable to the known tendency of aluminium atom to acquire a pair of electrons to fill its *p*-orbital, enhanced in this case by co-ordinating aluminium atoms carrying three positive charges with oxygens attached to silicon carrying four positive charges. In the extreme case of combination of three such groups with central aluminium atom, the surface group could be pictured as follows:

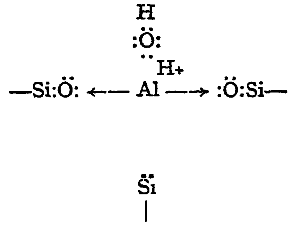

$$\begin{array}{c} \mathrm{H} \\ :\ddot{\mathrm{O}}: \\ \cdot\cdot\ \mathrm{H}^{+} \\ -\mathrm{Si}:\ddot{\mathrm{O}}: \longleftarrow \mathrm{Al} \longrightarrow :\ddot{\mathrm{O}}:\mathrm{Si}- \\ \\ \ddot{\mathrm{Si}} \\ | \end{array}$$

the arrows indicating the displacement of electrons by the proximity of silicon ions. In aqueous medium, the electron pair is donated by water, the hydroxyl group becomes a part of the solid structure, with hydrogen ion held not too strongly by electrostatic attraction. In the thoroughly dehydrated state the catalyst surface becomes a Lewis acid—an electron pair acceptor.

It was considered probable that such acid groups located on the surface of the catalyst are related to the activity. The prospect that the activity of alumina-silica catalyst may be reduced to the same general basis as the activity of aluminium halides was rather encouraging. Aluminium halides exhibit acidity, being electron pair acceptors, and structures such as $HAlCl_4$ or $HAlCl_3OH$ are often postulated by workers in this field to account for the catalytic activity.

In order to examine the possible relation of the acidity to activity two things were needed: firstly, an estimate of the acid strength of the alumina-silica complex, since only strong acids are known to promote hydrocarbon reactions; and secondly, techniques of counting the number of acid centres on the catalyst surface in order to relate activity with acidity quantitatively.

Estimate of the Acid Strength.—An exact evaluation of the acid strength of a solid acid is by no means a simple problem, and we are now engaged in this work. It can be expected that sorption of ammonia, a gaseous base, should provide some information. If the acid can be converted into an ammonium salt, the vapour pressure of ammonia from the ammonium salt could be used, under certain circumstances, as a measure of acid strength, since in the decomposition of the ammonium salt, the major processes are the liberation of ammonia and the return of the proton to the acid anion. The weaker the acid, the more energy will become available to accomplish the decomposition, owing to the ready acceptance of the proton by the acid. Much more energy should be required to decompose an ammonium salt of a strong acid. Fig. 3 shows the smoothed curves of all available data on ammonia vapour pressures of ammonium salts of a number of acids. The data for ammonium sulphate were obtained in this laboratory. It is seen that the relative position of the curves with respect to the temperature axis agrees qualitatively with known or estimated acid strengths.

For non-protonic or Lewis acids, the energy of chemisorption of ammonia should be a measure of acid strength. The adsorption of ammonia on catalysts is being studied by Mr. E. E. Roper and appears to be a very complex phenomenon since besides chemisorption, physical adsorption and capillary condensation may occur simultaneously. Nevertheless, the uptake of ammonia by chemisorption is readily evident upon exposure of a catalyst to ammonia vapours and, in some favourable instances, can be separated from the accompanying complications. Fig. 4 shows the uptake of ammonia by a cracking catalyst and by a silica gel of similar physical structure. The cracking catalyst retained a larger amount of ammonia than silica gel, and the excess, although it is not constant over the whole range of temperature owing to the complicating factors mentioned above, is a rough measure of the amount chemisorbed. An exact quantitative treatment of these and similar measurements cannot be dealt with in this paper.

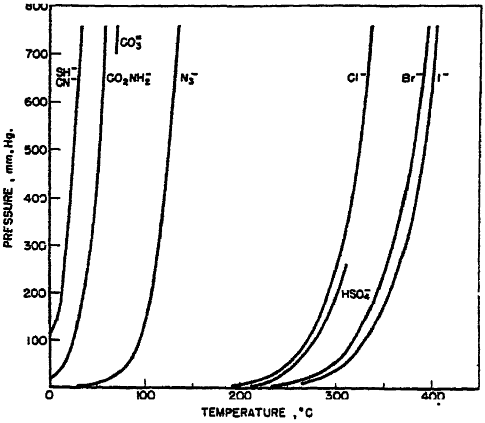

FIG. 3.—Vapour pressure of various ammonium salts as a function of temperature.

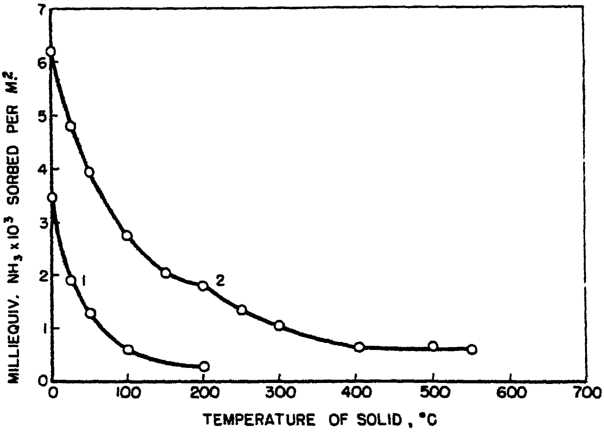

FIG. 4.—Surface concentration of ammonia on pure silica gel (1) and on an alumina-silica catalyst (2) as a function of temperature. NH_3 pressure 7·5 cm. Hg.

For the present purpose of estimating the acid strength of the alumina-silica gel complex, the behaviour of the ammonium salt of the complex as observed by Mr. Roper will be described. This salt was obtained by Mr. Ryland by the treatment of the sodium salt, described earlier, with aqueous ammonium chloride. The ammonium salt contained 3·5 mequiv. of ammonia per gram of dry solid. Following drying at 120° C, the salt was exhaustively outgassed at temperatures increasing in steps of *ca.* 20-50°, and the amounts of water and of ammonia given off after 2 hr. of exhaustive evacuation at each stage were determined. This treatment was found to be sufficient to collect substantially all the water and ammonia available at each stage from the salt. Fig. 5 shows that at about 180° C, the physically adsorbed water was substantially removed. At this point the evolution of ammonia began, accompanied by water escaping somewhat ahead of ammonia; nevertheless ultimately an equimolar amount of water and ammonia was obtained above 180° C.

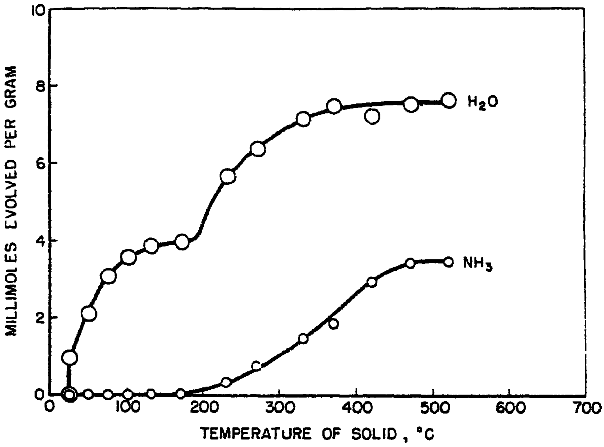

Fig. 5.—Evolution of water and ammonia from an ammonium salt of alumina-silica complex as a function of temperature.

This experiment is believed to represent decomposition of the ammonium salt with formation of the corresponding Lewis acid which retards liberation of ammonia by strong chemisorption via the electron pair of nitrogen. The progressively increasing difficulty of the decomposition of the ammonia complex, the last traces of which can be removed only by exhaustive evacuation at 500° C, demonstrates the high " acidity " attained by the solid at and above 500° C. These observations suggest that the apparent acidity of the solid is dependent on the composition of the solid; this can be expected, considering that the ammonia-alumina-silica complex is an integral part of the surface and no new phase appears during its decomposition. The phenomenon is analogous to chemisorption of hydrogen on the surface of a metal, where only one surface phase is present. Exact quantitative interpretation has not been attempted since, as yet, the reversibility of these phenomena has not been established.

Counting of Acid Groups on Catalyst Surface.—Since no general method of titrating solid acids has ever been devised, a number of methods was studied. Titration with aqueous alkali metal hydroxide was found inadequate since no definite endpoint could be reached. The titration with a weak base in anhydrous medium designed and used here by Mr. O. Johnson has been found quite satisfactory. It follows in the main the procedure devised by G. N. Lewis for titrating acid-base systems in carbon tetrachloride. The method consists of titrating the surface of the solid (suspended in benzene) with *n*-butylamine, using *p*-dimethylaminoazobenzene as indicator. This indicator is sorbed by the solids and gives a red colour to a number of strong solid acids, but does not colour pure silica gel or pure alumina. The titration is carried to the disappearance of red colour on the solid. *n*-Butylamine was chosen since it is not too volatile, and yet it is not too large a molecule to enter the small pores of the catalysts.

In order to estimate the extent of neutralization of the catalysts with *n*-butylamine and the selected indicator a number of solid acids of known strength in aqueous solutions were titrated in the same system. It was found that this method detects acids the dissociation constants of which are *ca.* 10^{-6} or more in aqueous solution.

Relation of Acidity to Activity.—As has been mentioned before, cracking catalysts promote a number of reactions besides breaking carbon-to-carbon bonds. The " cracking " process is a complex process consisting of a number of such reactions and the purpose is to produce a gasoline of certain desirable characteristics from higher boiling petroleum fractions (e.g. gas oils). For examination of activity in relation to acidity, a number of reactions of pure hydrocarbons which proceed as much as possible without side reactions were found more suitable,[1] and some observations of Mr. W. G. Schlaffer on cracking of *iso*propylbenzene at 500° C and Mr. O. Johnson on polymerization of propylene at 200° C are described here. The catalysts used contained progressively larger amounts of alumina and were prepared by the interaction of one silica gel with measured amounts of alumina sol; thus they would not be expected to differ radically in physical properties. The same catalysts were used in both series of measurements. The acidity of each sample was determined by the above described method, following calcination at 200° C and 500° C.

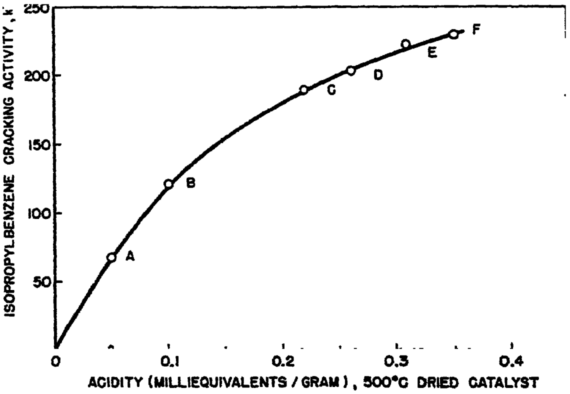

FIG. 6.—Dependence of *iso*propylbenzene cracking activity at 500° C on acidity for a series of alumina-silica catalysts.

Catalyst	A	B	C	D	E	F
Al_2O_3, %	0·12	0·32	1·04	2·05	3·56	10·3

Cracking of *iso*propylbenzene was carried out by passing the hydrocarbon vapours over the catalysts in a stainless steel tube at 500° C at various space velocities. The gaseous product was almost pure propylene; the liquid product, a mixture of benzene and *iso*propylbenzene, was separated by distillation for determination of conversion. Since the conversion is not a linear function of activity, and reaction constants could not be calculated from conversions without knowledge of the kinetics of the reaction, values of k' were calculated from the experimentally derived relationship between space velocity and conversion. These values are proportional to the space velocities necessary to effect an equal conversion by the various catalysts. Since these values are directly proportional to the reaction rate they have been used as a measure of activity (cf. Fig. 6).

The polymerization rate of propylene was studied by a static method. The apparatus was an all-glass reaction system which included a mercury manometer, and a tube containing 0·1 g. of the catalyst, kept at 200° C. A given amount of propylene was introduced to the catalyst (400 mm. Hg), and the pressure drop determined at frequent time intervals. The data were found to follow the equation

$$dx/dt = k(a - x)/(1 + bx),$$

corresponding to a first-order reaction retarded by the products. (a = pressure of propylene, x = pressure drop at time t.) Fig. 7 shows the constants k, determined for the series of alumina-silica catalysts, plotted against the observed acidity. Fig. 8 shows a similar graph of activities

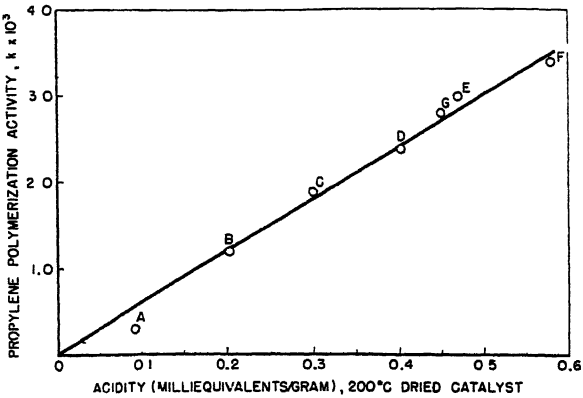

FIG. 7.—Dependence of propylene polymerization activity at 200° C on acidity for a series of alumina-silica catalysts.

Catalyst	A	B	C	D	E	F	G
Al_2O_3, %	0·12	0·32	1·04	2·05	3·56	10·3	25·1

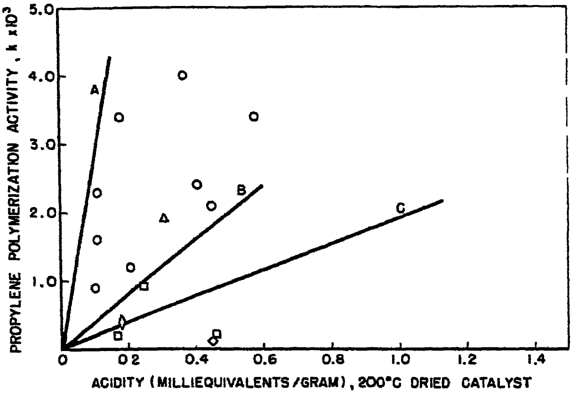

FIG. 8.—Propylene polymerization activities for materials of varying acid strength. (A, perchloric acid; B, silicotungstic acid; C, potassium acid sulphate or arsenic acid. Boric, oxalic, and phthalic acids show no activity.)

○ Alumina-silica catalysts.
□ Magnesia-silica catalysts.
△ Alumina-boria catalyst.
◇ Zirconia-silica catalyst.
◇ Iron-silica catalyst.

against acidity for a number of experimental catalysts as well as various types of acids mounted on silica gel. The influence of acid strength on activity is apparent.

In the propylene polymerization a simple linear relationship exists between the activity and the number of acid sites on the catalyst surface. Apparently the amine method measures adequately all the acid sites of catalytic significance for polymerization at 200° C. In the cracking of *iso*propylbenzene at 500° C the reaction rate appears to be directly proportional to the square root[9] of the number of acid sites.

The above results leave little doubt that the acid strength and the number of acid sites are the major factors determining the activity of alumina-silica catalysts.

Shell Development Company,
Emeryville,
California.

---

[9] A square-root dependence of reaction rate upon catalyst concentration has been observed for the stannic-chloride-catalyzed polymerization of *iso*butylene: Norrish and Russell, *Nature*, 1947, **160**, 543.

THE CHEMICAL CHARACTERISTICS AND STRUCTURE OF CRACKING CATALYSTS

BY T. H. MILLIKEN, JR., G. A. MILLS AND A. G. OBLAD

Received 30*th January*, 1950

A fundamental study of the silica-alumina gel system was carried out to investigate the chemistry and structure of cracking catalysts and determine, if possible, the critical chemical attributes of silica-alumina which are responsibe for catalytic activity. It is the object of this paper to present the results of this study. The various studies carried out to establish the important chemical properties are reviewed. This is followed by a summary of the work showing the relationship between these chemical properties and the ability of silica-alumina to function as a catalyst. Experimental results relating to the structure are presented and the probable structure of the calcined form of the catalyst is discussed. Finally, the probable mechanisms of hydrocarbon reactions in light of the conclusions on the nature of the "active centres" of cracking catalysts, is discussed.

Chemical Properties of Silica-Alumina.—By analogy with other catalysts which catalyze hydrocarbon reactions, it was suspected that silica-alumina catalysts possess acidic characteristics. A number of tests were carried out to demonstrate whether or not such catalysts had acid properties. These tests were (i) reaction with carbonate solutions to evolve carbon dioxide, (ii) titration with solutions of bases, (iii) hydrolysis of sucrose, (iv) reaction with volatile bases such as ammonia and organic nitrogen bases, and (v) reaction with Zerewitinoff reagent.[1, 2] These tests demonstrated unequivocally that the catalyst possessed "acidic" properties.

---

[1] Oblad, Milliken, Mills, to be published in *J. Amer. Chem. Soc.* (presented at the Gordon Research Conference, Colby College, June, 1949).

[2] Mills, Boedeker and Oblad, to be published in the *J. Amer. Chem. Soc.* (presented at the San Francisco meeting of the Amer. Chem. Soc., April, 1949).

Several publications [3, 4, 5, 6] recently have appeared in which other workers have reached a similar conclusion. The presence of an active acid in the catalyst has its counterpart in the base exchange properties of zeolitic materials. The base exchange capacity of materials similar in composition to cracking catalysts has been related to the " acidity " of these materials.[7]

Relationship between Acidity and Catalytic Ability.—The activity of the catalyst to crack a hydrocarbon mixture in the CAT—A, test,[8] and to crack cumene,[2] was found to correlate with the amount of carbon dioxide evolved by a catalyst from a carbonate solution,[1] the amount of CH_4 formed from CH_3MgBr, the amount of acid indicated by base titration,[1] the rate of sucrose hydrolysis by a given amount of catalyst,[1] and the amount of ammonia or nitrogen base (quinoline) chemisorbed from the vapour phase.[2] The correlation of the cracking activities of different catalysts with mequiv. of quinoline chemisorbed at 315° per g. of catalyst is given in Fig. 1. Caution must be exercised in interpreting the acidity measured, particularly when measurements are in aqueous medium. A further demonstration of the dependence of catalytic activity on acidity was found in the observation that a large number of other nitrogen bases and potassium and other basic ions [2, 9] are effective poisons for the cracking reactions mentioned. A detailed consideration of the adsorption and poisoning effect of basic nitrogen compounds leads to the conclusion that a small fraction of the total surface is involved in catalytic activity.

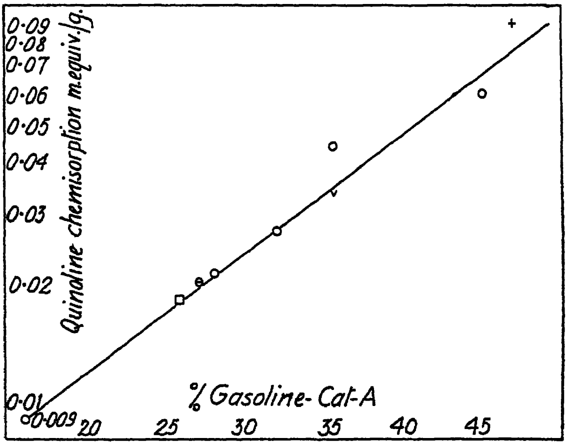

FIG. 1.—Quinoline chemisorption at 316° C as a function of activity for cracking light East Texas gas oil. ⊙ = SiO_2—Al_2O_3 (Houdry type S) ; ⊖ = SiO_2—1 % Al_2O_3 ; ⊡ = clay catalyst (Filtrol) ; + = SiO_2—MgO ; V = SiO_2—ZrO_2.

Structure of the Acid.—A number of investigators [1, 2, 3, 4, 5] have suggested that aluminium in a four-co-ordinated position is a source or the cause of the acid character of silica-alumina catalysts. Very little information has been published, however, which will substantiate this

---

[3] Thomas, *Ind. Eng. Chem.*, 1949, 41, 2564.

[4] Weil-Malherbe and Weiss, *J. Chem. Soc.*, 1948, 2164.

[5] Tamele (presented at Gordon Research Conference, Colby College, N.H., June, 1949).

[6] Grennall, *Ind. Eng. Chem.*, 1949, 41, 1485.

[7] Kelley, *Cation Exchange in Soils* (Reinhold Publishing Co., New York, 1948).

[8] Alexander, *Proc. Amer. Petrol. Inst.*, 1947, 27, (III), 51.

[9] Bitepazh, *J. Gen. Chem. Russ.*, 1947, 17, 199.

suggestion. Ordinary calcined silica-alumina catalysts do not show structure to X-rays. Likewise, there is little published information on the structural chemistry of synthetic zeolitic materials. In order to shed light on this subject, a study was made of the chemical characteristics of silica-alumina hydrogels and subsequent dry and heat-treated gels.

The structure of the complex acids possible in a system of silica and alumina has been developed by Pauling.[10] According to this theory isomorphous substitution of a positive ion of different valency for a given ion in a crystal lattice results in a charge. Thus, if an aluminium ion is substituted for a silicon ion in the four-co-ordinated silica lattice, a positive deficiency of unit charge is developed for each aluminium ion so substituted. Many such silica-alumina structures exist in nature and in all cases the induced negative charge is satisfied by the presence of a positive ion in the immediate vicinity of the point of substitution. Such materials as natural zeolites, montmorillonite and feldspars are examples of this.

Proof of the applicability of the ideas of structural acids to silica-alumina hydrogels and catalysts was obtained in experimental work which consisted of studying the physical-chemical properties of the silica-alumina system as a function of silica-alumina weight ratio. Samples were prepared in hydrogel form by co-precipitating sodium silicate with either aluminium sulphate or sodium aluminate. Sulphuric acid or sodium hydroxide was added during the gel-forming stage to maintain the desired pH levels. (For a complete description of the methods used, see ref. 11.) Physical processing of the hydrogels was closely controlled. Usually the gels were aged at 55° for 4 hr., washed, exchanged with ammonium ion, dried and calcined. The properties studied were base exchange, loss by calcination of water and ammonia, density and crystal structure. A plot of the excess mequiv. of Na^+ per g. of silica-alumina required to maintain the gel system at pH 7 against weight % alumina is shown in Fig. 2. The initial part of the curve from 0 to 30 % alumina is a straight line. The line has a slope which is equivalent to 1 mole of Na^- for each mole of aluminium. Thus, in silica-alumina gel mixtures containing up to 30 % alumina, each aluminium ion is effectively acting as one equivalent of acid. From 30 to 40 % alumina, the ratio of Na to Al drops off and above 40 % alumina the number of aluminium ions holding Na^+ drops rapidly to zero at 100 % alumina. On washing the hydrogel, Na^+ is retained by the gel and may be exchanged for other cations.

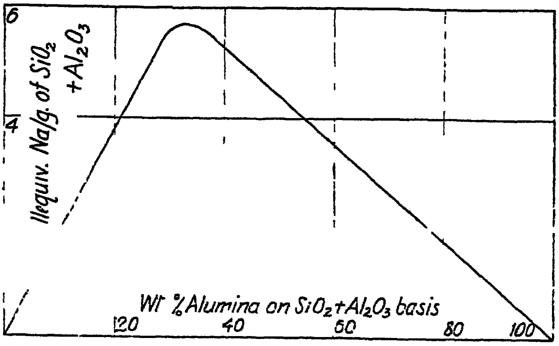

FIG. 2.—Excess sodium ion required to maintain pH of 7 with varying alumina content silica-alumina hydrogels.

---

[10] Pauling, *The Nature of the Chemical Bond* (Cornell University Press, New York, 2nd Edn., 1948).

A second similar series of gels was prepared at pH 9. The hydrogel was washed, base exchanged with NH_4Cl at pH 5 and dried. The dried gels were analyzed for NH_4^+ and Na^+. The total ignition loss at 950° (in flowing dry air) was determined for the gels dried at 100°. Both NH_4^+ and H_2O are lost upon calcination. The results are shown in Fig. 3.

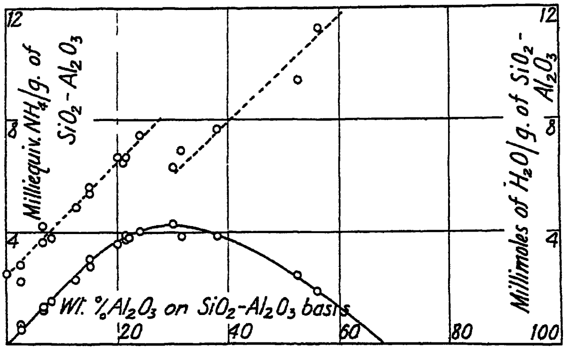

Fig. 3.—Base exchange capacity and water content as a function of weight % alumina. - - - - H_2O loss between 100-950° ; ———NH_4^+ exchange capacity.

It can be seen that there is a close correlation between water content and zeolitic capacity of gel mixtures containing up to 20 % alumina. Over this range the dried gel retains one equivalent of NH_4^+ per mole of aluminium and with this NH_4^+ there is associated one mole of water per mole NH_4^+. As the alumina content increases above 30 %, the zeolitic capacity falls below one equivalent per mole aluminium and the water content becomes irregular. Above 30 % alumina, the zeolitic capacity of the gel mixture drops as before and a new water content line is found which shows no apparent correlation with the NH_4^+ content of the material.

Na^+ zeolites containing up to 20 % alumina prepared in the same manner possessed base exchange capacity and water contents exactly the same as the NH_4^+ exchanged gels. For the Na zeolites containing up to 20 % alumina the slope of the zeolite capacity and water content lines indicates that each aluminium has associated with it one equivalent of Na^+ and one mole of H_2O. An empirical formula of dried (100°) synthetic zeolite may be written as—

$$\begin{array}{l} NaAlO_2(SiO_2)_y(H_2O)_x. \\ H_2O \end{array}$$

While these data show that complexes involving metal cations or NH_4^+ and four-co-ordinate aluminium exist in the silica-alumina gel system, the existence of the same complex involving H^+ must be proved.

Additional work [11] indicates that such acids, if formed at all, are extremely unstable and few, if any, even survive the temperatures reached in drying the hydrogels (100°). The H^+ exchanged gels upon drying lose zeolitic properties and the water content shifts.[11] The incremental water content as a function of increasing Al_2O_3 content of the acidified gels was found to be 1·5 H_2O per Al. This water content corresponds to 3(OH) per aluminium. This was interpreted to mean that the bulk of the alumina in the acidific gel shifted to hydrargillite or bayerite ($Al(OH)_3$). Through this transformation the gel loses its " acid " properties.

It, thus, has been deduced that salt-like complexes of silica-alumina gel mixtures in which the aluminium is four-co-ordinated, can exist in the presence of cations such as Na^+, K^+ and NH_4^+, but that the removal of such ions in the hydrogel results in a loss of the acidic property. The so-called acid exchanged synthetic zeolites are not acids at all. The acid form is not stable even at room temperature. Furthermore, the NH_4^+ exchanged silica-like alumina (the usual end-product in catalyst manufacture prior to calcination) loses NH_3 over a fairly wide temperature range. Ammonia is first detected as coming off at 220° and is lost steadily up to 550°. At this temperature, all the NH_4^+ has been lost. What are the transformations that occur during the loss of NH_4^+?

---

[11] Milliken and Cornelius, *J. Amer. Chem. Soc.*, (to be published).

X-ray spectra of silica-alumina mixtures containing up to 25 to 30 % alumina indicate that the gel mixtures are amorphous. Elkins *et al.*[12] studied mixtures of silica and alumina hydrogels which had been calcined at 120° and 540°. They concluded that those mixtures having alumina contents up to 26 % were amorphous to X-rays. Above this percentage these authors found mixtures of boehmite ($Al_2O_3 . H_2O$) and hydrargillite ($Al_2O_3 . 3H_2O$) present in the gels heated to 120° and γ-alumina in mixtures heated to 540°. They also determined particle sizes of the mixtures by low-angle X-ray scattering. The maximum particle size was found to be between 30 and 65 Å for gels having alumina contents up to 19·8 % alumina.

It is well known that crystal structures of particles much under 100 Å cannot be determined by X-ray diffraction. Therefore, other methods of determining the structure of the catalyst after heat treatment must be used. The authors have measured the density (using water displacement) of the skeletal solids in silica-alumina gels heat treated to 760° in dried air. The density increases linearly with increasing alumina content (Fig. 4). The slope of the line in Fig. 4 for alumina contents less than 20 % indicates that the added alumina has a density of 3·65 g. per ml. This compares closely with the density of 100 % γ-alumina prepared in the same fashion as the gel mixtures, 3·8 g. per ml. Actually, the density of four-co-ordinated alumina should be slightly less than that of silica. It was deduced, therefore, that the decomposition product of the ammonium zeolite is a mixture of γ-alumina and silica, with all or nearly all the alumina existing in the γ-alumina form. The discontinuity shown in the curve at 22 % to 38 % aluminium falls in the same range as the break in the base exchange capacity curves discussed earlier. It also corresponds to the percentage alumina at which Elkins *et al.*[12] found detectable amounts of alumina in silica-alumina gel mixtures by X-ray examination.

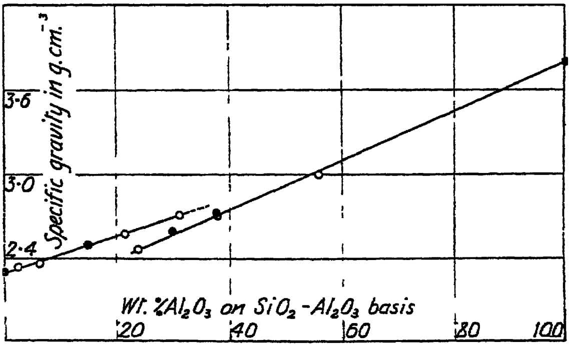

FIG. 4.—Effect of alumina content on specific gravity of heat-treated silica-alumina catalysts.

---

[12] Elkins, Shull and Roess, *Ind. Eng. Chem.*, 1945, **37**, 327.

If the same series of silica-alumina gels is heated to 1160° and then examined by X-ray, relatively strong patterns are obtained.[1] The silica containing no alumina gives a weak pattern of cristobalite. Kreji and Ott [13] and Schulman [14] also found weak cristobalite patterns in heated silica gels. The existence of cristobalite at this temperature is remarkable since the expected form is tridymite. In a calcined silica-alumina mixture containing about 2 % alumina, the pattern of cristobalite is greatly strengthened and the full cristobalite pattern becomes visible. In mixtures containing more alumina, the cristobalite pattern becomes weaker. At 15 % alumina the pattern is lost altogether. From 15 % to 36 % alumina the predominant pattern of the silica-alumina mixture is that of mullite. Above 50 % alumina, α-alumina or corundum are apparent. The most significant fact is the great strengthening of the cristobalite pattern in silica induced by small amounts of alumina. The full significance of this observation will be discussed later. On reviewing the data, a calcined silica-alumina mixture was concluded to be simply a mixture of silica and alumina particles with silicon and aluminium ions sharing oxygen ions at the points of contact.

Alumina is an amphoteric substance and can act like an acid or a base depending upon its environment. Under conditions that cause the alumina to act as an acid it is in a four-co-ordinate state. Sodium aluminate and potassium aluminate are ring structures of six alumina tetrahedra with an enclosed potassium or sodium ion.[15] This structure is not formed in solutions below pH 12. Sodium aluminate solutions, unless stabilized, tend to deteriorate to bayerite and sodium hydroxide.[16] The low temperature forms of alumina are generally boehmite, bayerite and hydrargillite. In these substances the aluminium ion is six-co-ordinate, sharing valency bonds with six oxygens.[17, 18] The ability of aluminium ions to exist in both the four-co-ordinate and six-co-ordinate crystalline state is related to its small ionic radius 0·5 Å, which is small enough to allow an aluminium ion to fit between four close-packed oxygens or six close-packed oxygens. The various crystal forms of alumina are arrangements involving one or both of the co-ordination states of aluminium. In γ-alumina a complex state is found which probably is made up of both four- and six-co-ordinate aluminium ions and combined water as OH. γ-Alumina upon heating loses OH and gradually shifts to α-alumina. This shift is complete at 1000°. The γ-alumina existing at temperatures between 400° and 700° is the most interesting from the viewpoint of hydrocarbon catalysis. Jellinek *et al.* were unable to define the structure of γ-alumina.[19]

Silica occurs in four major modifications—quartz, tridymite, cristobalite and vitreous. The silicon crystal ion is four-co-ordinate in all forms. The various crystal structures of silica are merely different arrangements of the tetrahedra. The structures of most interest to investigators of catalysts are cristobalite and vitreous silica. There is reason to believe that cristobalite or a structure very close to it exists in silica gel. Since cristobalite has the same structure as potassium aluminate without the potassium ion in the centre of the ring of aluminium tetrahedra, the influence of the silica on the crystal habit of alumina is probably great. When mixtures of alumina and silica hydrogel are made (by coprecipitation or by mixing wet gels) interbonding of silicon and alumina ions occurs. Interbonding is brought about by the condensation of the hydroxyls existing at the interface between silica and alumina particles. The tetrahedral structure of the silica being extremely stable will influence the co-ordination of the oxygen around the aluminium ion. If bases are present, they will stabilize aluminium in the four-co-ordinate or aluminate structure. In the aluminate structure the tetrahedra require more rigorous orientation than those in the silica gel structure in order to accommodate the large positive ions. The aluminate structure, in its turn, affects the orientation of the silica tetrahedra adjoining the aluminate structure. At the interparticle interface it is expected that well-defined cristobalite rings exist. This crystallizing influence probably only extends a few molecules deep into the silica particle. However, it could affect the whole particle and not be detectable by means of X-rays. Cristobalite is more stable than vitreous silica. The tetrahedra in silica gel remain in the cristobalite configuration during subsequent heat treatment of the gel mixture. These cristobalite nuclei act as seeds for the crystal growth observed when catalysts of low alumina content are heated to 1150°.[1]

---

[13] Kreji and Ott, *J. Physic. Chem.*, 1931, **35**, 2061.

[14] Schulman, Claffy and Ginther, *Amer. Miner*, 1949, **34**, 68.

[15] Barth, *J. Chem. Physics*, 1935, **3**, 323.

[16] Thibon, *Bull. Soc. Chim.*, 1948, 870.

[17] Reicherts and Yost, *J. Chem. Physics*, 1946, **14**, 495.

[18] Megaw, *Z. Krist.*, 1934, **87**, 185.

[19] Jellinek and Fankuchen, *Ind. Eng. Chem.*, 1949, **41**, 2259.

The stabilizing effect that silica exhibits for the aluminate structure probably is dependent on four factors. These four factors are: relative micelle size of the silica and alumina components, amount of alumina present, pH of the wet silica-alumina gel mixtures, and the electropositive nature of the positive ion required for the stablization of the aluminate structure. Data in the literature show that the particles of silica-alumina mixtures are quite small (of the order of 30 Å). No method has been devised that determines relative sizes and which differentiates small particles of silica from the small particles of alumina in a mixture. However, the effects of the three other factors are demonstrated by the data already presented. Increasing the alumina content reduces the relative amount of alumina in contact with silica. Thus, much of the alumina in silica-alumina mixture of high alumina content cannot be influenced by the silica. At about 15 % alumina, the capacity of the weakly electropositive ammonium ion for stabilizing the aluminate structure, NH_4AlO_2 (at pH 6 or below) begins to be surpassed. The normal crystal structure of alumina at these conditions begins to appear and is accompanied by a concomitant change in the water content. Sodium ion being more strongly electropositive can maintain the aluminate structure (at pH 6) in silica-alumina mixtures containing up to 30 % alumina.[11] By raising the pH to 9 the ammonium ion can stabilize the aluminate structure in mixtures containing up to 30 % alumina. Above an alumina content of 30 % the amount of aluminate that can be formed becomes entirely dependent on the silica content, and therefore decreases steadily as the percentage of silica approaches zero. The alumina not present as aluminate in a silica-alumina mixture is present as boehmite and hydrargillite. This was deduced from the water content given in Fig. 3 and the information given by Elkins *et al.*[13]

If the positive stabilizing ion of a synthetic silica-alumina zeolite is " exchanged " for H^- by mild treatment at pH 3 to 4, the H^+ zeolite is not believed to form. The H^+ is too small to fit in the space left by the exchanged NH_4^+. To be large enough to take the place of the NH_4^-, the H^+ must be associated with a water molecule and become a hydronium ion H_3O^+. By comparing the probable structure of H^- zeolite with the structure of hydrargillite, it was deduced that by a slight shift in crystal arrangement, the hydrogen aluminate structure can change to a hydrargillite structure and lose its acid properties.[11]

The amphoteric character of aluminium is not lost when alumina is combined with silica. However, the pH level at which the amphoteric or co-ordination shift of aluminium takes place is changed from 10 to 12 for silica-free alumina to 3·8 to 4·0 for aluminium in silica-alumina mixtures.

The behaviour of a synthetic silica-alumina ammonium zeolite upon heat treatment is illustrated by Fig. 4 and 5. It is deduced that as the ammonium aluminate is destroyed, γ-alumina is formed. γ-Alumina is the expected structure at the temperatures of decomposition. The character of the curves in Fig. 4 and 5 seems to indicate a distribution of " acid " strengths in the synthetic NH_4^+ zeolite. This distribution of " acid " strengths is only apparent, however. The acid or aluminate form of the zeolite exists in various degrees of stability which depend on the proximity of silica. The farther an aluminate is displaced from a silica interface, the more readily it decomposes. In natural zeolites, such as natrolite, where each alumina tetrahedron shares its oxygens with silicon, the " acid " is expected to be in its most stable form. As

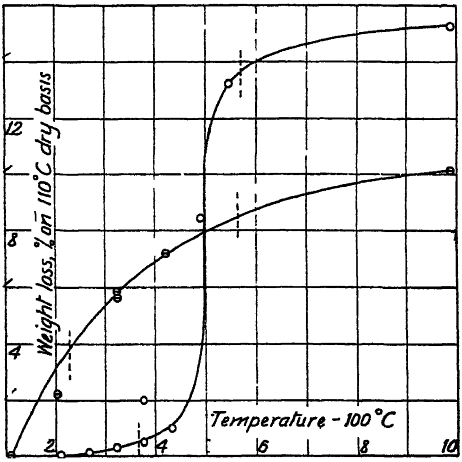

FIG. 5.—Decomposition of natural and synthetic ammonium zeolites on heating. ⊙ NH_4 natrolite ; ⊖ 12·5 % Al_2O_3 synthetic NH_4 zeolite.

shown in Fig. 5 ammonium natrolite, $2(NH_4AlO_2)3SiO_2$, does not decompose at temperatures below 500°. This is to be compared with the decomposition of the synthetic ammonium zeolite which occurs between 220° and 500°. It is proposed that the following reactions take place in the decomposition of NH_4 zeolites :

$$NH_4AlO_2 \, . \, XSiO_2 \longleftrightarrow NH_3 + HAlO_2 \, . \, XSiO_2$$
$$2HAlO_2 \, . \, XSiO_2 \longrightarrow H_2O + Al_2O_3 \, . \, XSiO_2 .$$

The decomposition by heat and by the acid treatment of NH_4 zeolites results in a loss of the acid form of the zeolite. The aluminate structure on losing the stabilizing positive ion shifts into the six-co-ordinate crystalline form of alumina which is stable at the conditions of the experiment.

The reactions of alumina in the presence of silica are, to a large extent, reversible. The reconstruction or reconstitution of the alumina to the aluminate crystal form follows essentially the same mechanism described for the creation of the " acid " from mixtures of silica and alumina hydrogel. The reconstitution of mixtures which have been calcined is more difficult because both the alumina and silica in the calcined mixture are in more rigid crystalline networks. The loss of water upon calcination of a mixture and the concomitant change of the alumina to γ-alumina result in a much more rigid network than that existing in the corresponding hydrogels.

Therefore in order to reconstitute a calcined silica-alumina mixture, the structure of the mixture must be rehydrated by breaking oxygen linkages and substituting two hydroxyl groups for each link so broken. This reaction is accomplished readily with OH^- ions present. Strong caustic solutions will attack and destroy calcined silica and silica-alumina structures. The concentration of hydroxyl ions will, to a large extent, determine the degree of rehydration and, thus, dictate the amount of alumina that can assume the aluminate structure. Titration of silica-alumina mixtures with basic solutions has been employed by several investigators,[6, 3, 9] to study silica-alumina catalysts. It should be pointed out that data obtained by this method can be misleading. The quality being measured during titration is not " acidity ". The property being measured is a capacity to react with a base that can be created at the conditions of the experiment. Such a measure of " acidity " may have little or no relation to the amount of " acids " involved in catalytic reactions.

The nature of the solid remaining after high temperature heat treatment of silica-alumina synthetic zeolites can be deduced from the preceding discussion. The authors have concluded that the calcined solid is essentially a mixture of γ-alumina and silica particles in which the silicon and aluminium ions at the interparticle interface share oxygen ions. The exact structure of the aluminium ions at the interface cannot be deduced. However, these aluminium ions can be considered to be in a three-co-ordinate state. Such a structure corresponds to the anhydride of the acid, $HAlO_2$. The potential acid in such a structure can be viewed as a Lewis acid. During the thermal destruction of highly crystalline ammonium " natrolite ", $2(NH_4 . AlO_2)3SiO_2$, NH_3 and one-half mole of H_2O per mole of NH_3 is lost.

The water must be formed by reaction of the " acid " hydrogens from two alumina tetrahedra with an oxygen ion. In this process the tetrahedral aluminate structure is believed to revert in the manner already described to the " anhydride " structure. The decomposition of ammonium " natrolite " is not reversible in the sense that it is possible to attain the original highly crystalline state. Since the silica-alumina mixtures used in catalytic cracking are invariably subjected to temperatures of about 500°, it is concluded that the acid $H^+\left[\begin{array}{l}\ \ O\\ OAl—OSi\\ \ \ O\end{array}\right]^-$ in an active catalyst (as proposed by Thomas [3] and Tamele [5]) cannot be present in amounts sufficient to account for the activity of silica-alumina mixtures.

It is believed that in all cases the reaction of a " base " with the silica-alumina mixture involves an instantaneous creation of the required " acid ". How this happens for silica-alumina mixtures in hydrous media has already been discussed. The creation of " acids " happens even at elevated temperatures in the dry state. By exposing a silica-alumina mixture to the vapours of a base such as quinoline, more or less of the alumina will become " acidic ". The amount of " acid " created is believed to depend on three factors: (i) the amount of interfacial sharing of oxygen ions between silicon and aluminium ions, (ii) the hydroxyl content of the γ-alumina present, and (iii) the base strength or polarizing capacity of the base. The aluminium ions sharing oxygens with silica, being in the state of greatest electrostatic force deformation, will be the first to react with the basic material. The result of such reaction is the formation of a four-co-ordinate alumina by the shift of an oxygen or a hydroxyl group from the γ-alumina structure. A series of different bases, upon reaction with a silica-alumina nucleus, give widely differing apparent amounts of " acid ". The amount of " acid " formed will depend, as stated, on the base strength of each particular base. The thermal history of the γ-alumina particles will determine the ultimate limit of reconstitution since the hydroxyl content of γ-alumina is dependent on the temperature to which it has been heated.

That the surface atoms are highly mobile and in particular that the oxygen in such structures is capable of shifting, has been demonstrated by the exchange of oxygen between water and various silica-alumina catalysts [20] using O^{18}.

Mechanism of Hydrocarbon Reactions on a Cracking Catalyst.—Using the concept that silica-alumina intrinsically contains a strong acid, several authors have proposed detailed reactions involving carbonium ion mechanisms to account for the products obtained in catalytic cracking.[3, 21, 22, 23] The general agreement between fact and theory in these proposed mechanisms is strong proof that the basis of the reactions is sound.

How then is it possible to reconcile the need in silica-alumina of the strong Bronsted acids required for the carbonium ion reactions proposed, with the conclusions of the authors presented earlier in this paper; i.e. that these required strong acids do not exist.

To reconcile these differences, a mechanism will be proposed which apparently not only applies to silica-alumina, but also it is believed it will have wide application in the field of catalysis. It is proposed that the reversible shift in co-ordination (which was deduced in the earlier part of this paper to explain the many experimental facts in connection with base exchange, density, water content, etc.) is fundamental to the activity of the catalyst.

It is apparent to the authors that the presence in a catalyst of a strong Bronsted acid is not a required intermediate for carbonium ion formation. It is only necessary that the catalyst has the ability to form stable carbonium ions. In reactions involving Friedel-Crafts catalysts, the aluminium halides and boron trifluoride do not form stable Bronsted acids but they do form stable carbonium ions in the presence of certain co-catalysts and substrates. The formation of carbonium ions from olefins and aromatics does require an available proton. This is provided by the co-catalyst. In the case of silica-alumina, the stable carbonium ions (or polarized complexes) are created by structural changes brought about in the catalyst by the presence of the substrate. Thus, the substrate is mutually responsible for the creation of an active intermediate and, likewise, the catalyst must be capable of undergoing structural changes in order to accommodate the substrate. Those sites predisposed to react with the substrate as explained, are " active centres ". Such active centres consist of aluminium ions in the immediate vicinity of the tetrahedral silica. These strategically located aluminium ions are predisposed, by the induction of the four-co-ordinated silica, to shift co-ordination and need only weak bases to stabilize them in the four-co-ordinate or " acid " form. Such a co-ordination shift, as induced by silica and substrate, is represented in the following two important reversible reactions :

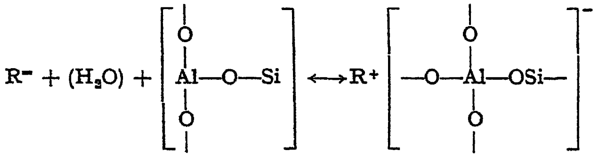

$$R^- + (H_2O) + \left[\begin{array}{c} | \\ \text{O} \\ | \\ \text{Al—O—Si} \\ | \\ \text{O} \\ | \end{array}\right] \longleftrightarrow R^+ \left[\begin{array}{c} | \\ \text{O} \\ | \\ \text{—O—Al—OSi—} \\ | \\ \text{O} \\ | \end{array}\right]^- \quad . \quad (1)$$

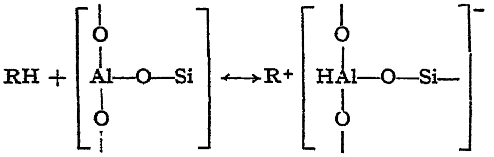

$$RH + \left[\begin{array}{c} | \\ \text{O} \\ | \\ \text{Al—O—Si} \\ | \\ \text{O} \\ | \end{array}\right] \longleftrightarrow R^+ \left[\begin{array}{c} | \\ \text{O} \\ | \\ \text{HAl—O—Si—} \\ | \\ \text{O} \\ | \end{array}\right]^- \quad . \quad . \quad . \quad (2)$$

---

[20] Hindin and Mills, to be published in *J. Amer. Chem. Soc.* (presented at Detroit meeting of Amer. Chem. Soc., April, 1950).

[21] Hansford, *Ind. Eng. Chem.*, 1947, **39**, 849.

[22] Greensfelder, Voge and Good, *ibid.*, 1949, **41**, 2573.

[23] Bremner, *Research*, 1948, **1**, 281.

The instability of the free Bronsted acid is recognized in the first reaction by the necessity of the presence of the basic substrate for stability. The " water " may come from the catalyst where it is a constitutional part, existing as hydroxyl groups. These equations are illustrative only of the stoichiometry of the reactions taking place. It should be realized that these reactions involve crystalline substances and, therefore, rather widespread changes must occur in the micro-structures around any one active centre. Many aluminium ions around a given point may be involved in this shift.

Once it is visualized how carbonium ion complexes can be formed by the catalyst without the existence of a strong acid, then most of the chemistry of catalytic cracking can be explained on the basis of the carbonium ion theory. Since this has been amply dealt with by others previously referred to, it will not be discussed here. In the existing carbonium ion theory, however, it must be realized that the mechanisms so proposed are highly idealized. While there is strong evidence which substantiates the existence of carbonium ions, such ions only exist in intimate association with the catalyst. The ions are, in fact, the product of the interaction of substrate and catalyst, and being such, must have a strong effect on the electronic character of each other, and, therefore, on their mutual chemical behaviour.

Two factors which are not very well understood are proton transfer and hydride ion transfer as they concern the catalyst. Both of these factors are important steps in the reactions which have been proposed to explain the chemistry of catalytic cracking. How can these be accounted for on the basis of the structural dynamics proposed in this paper ? It is believed that the transfer of protons can occur on the surface of the catalyst by minor structural changes in γ-alumina. The catalyst being largely a network of oxygen ions can accommodate and, thereby, transfer protons somewhat in the same way that water does. For hydride ion, it is believed that it can be accommodated as depicted in reaction (2). The six-co-ordinated aluminium ion is a potential Lewis acid. Paraffin hydrocarbons, being weak Lewis bases, are able to form polar complexes with catalyst through a similar co-ordination shift of the aluminium ion. In this case no " water " is involved in the complex. Lewis acids probably play an important role in the alkylation and isomerization of paraffins by other catalysts (($HF)_xH_2SO_4$ and Al_2X_6). All these catalysts possess potential Lewis acids; viz., HF, SO_3, AlX_3 (monomer). The exact manner by which the catalyst brings about the important proton and hydride ion transfer forms an interesting and vital field for additional study. A knowledge of the precise structure of γ-alumina would shed considerable light on these two problems.

The reversibility of the reactions (1) and (2) should be stressed in understanding the concept presented. The ability of the catalyst *to react reversibly* with a substrate in the formation of the polar complexes, is essential, in the authors' opinion, for catalytic activity. If these reactions were not readily reversible at the temperature of reaction being carried out, the substance would not be a catalyst. If one considers the relative stability of a primary, secondary and tertiary carbonium ion, the act of isomerization of an existing primary carbonium ion to a tertiary would result in the formation of an even stronger complex between substrate and catalyst than that existing in the beginning. Hence, the altered complex, in this case, would be less likely to desorb. It is this tendency of the aluminium to go back to its six-co-ordinated environment which provides the driving force for desorption. These substances which form stronger complexes than the substrate being reacted, will act as poisons for the particular reaction in question. Such substances as NH_3, nitrogen bases, alkali metal ions, etc., at the ordinary temperatures of catalysis, tie up all the available aluminium ions in a stable four-co-ordinate form and, thus, act as poisons for the reaction. The reversibility of the silica-alumina complexes has its analogy in such catalysts as aluminium halides, boron fluoride and even in the strong acids, sulphuric and hydrofluoric. Aluminium halides and boron fluoride have a tendency to revert to their usual structural form from the four-co-ordinated complexes. The competition of water in the strong acid catalysts (all of which must contain some water in order for them to act as catalysts) for the proton of the polar complex, provides a driving force for the decomposition of the complex in this case.

In conclusion, the authors believe that the concepts developed can be applied generally to heterogeneous catalysis. A catalyst is looked upon as a surface, the ions of which are disposed to move to a certain extent. In their own environment, the ions of the catalyst are arranged in a pseudo-stable equilibrium state. Depending on the catalyst, certain substrates are able to induce a structural shift in the component atoms or ions of the surface, creating, thereby, complexes which undergo reaction. The decomposition of the complex involves a reverse of the previous reaction. These structural shifts involve co-ordination changes of strategically located ions. It is a well-known fact that very few ions of a particular catalyst are available for catalysis. The apparent heterogeneity of a catalyst surface is real for the reason that the ions active for adsorption, as explained, are not *all* exactly predisposed in the same way. There is a distribution of availability for the dynamic structural change and, consequently, it is more difficult to cause co-ordination shifts of some of the surface ions than it is others.

The authors express their appreciation to Mr. C. G. Kirkbride for his interest and co-operation. The contributions of P. J. Blatz, E. R. Boedeker, E. B. Cornelius, J. J. Donovan and S. G. Hindin of the Houdry Laboratories and H. M. Hulbert of Catholic University of America are gratefully acknowledged.

Houdry Laboratories,
Houdry Process Corporation,
Linwood, Pennsylvania.
Houdry Process Corporation,
Marcus Hook, Pa., U.S.A.

THE MECHANISM OF THE CATALYTIC CRACKING OF UNSYMMETRICAL DIARYLETHANES

By D. R. May, K. W. Saunders, E. L. Kropa and J. K. Dixon

Received 30*th January*, 1950.

The catalytic cracking of substituted 1 : 1-diarylethanes on siliceous catalysts to form a substituted styrene was studied as a function of temperature, contact time, diluent, catalyst particle size and area. At suitable low contact times of 0·001-0·1 sec. at 500° C the reaction is essentially without side reactions, hence is ideal for cracking studies. The reaction has a low temperature coefficient. In contrast with most catalytic reactions the rate of cracking is dependent on the number of collisions of the diarylethane with the *external* area of the catalyst particles and on this basis the variables affecting the rate are correlated. The true internal surface area is not an important factor in the cracking rate.

The rate of cracking decreases as the electronegativity of the substituents increases and the order observed for this effect is apparently the same as in Hammett's *reactivity series*. Because of this correlation it appears that a carbonium ion mechanism is involved in this fast reaction. About one collision in every thousand with the catalyst surface is effective and it is suggested that during an effective collision the consecutive steps in the carbonium ion mechanism take place essentially simultaneously.

It has not been possible for earlier investigators to work out many of the details of the kinetics of hydrocarbon cracking reactions because of the complexity of the mechanism and the products formed by cracking. The catalytic cracking on siliceous catalysts of 1 : 1-*bis* (4-methylphenyl)-ethane (referred to as ditolylethane), a compound which is a typical example of an unsymmetrical diarylethane, forms methylstyrene and toluene with but little tendency to yield numerous or complex by-products. Therefore, this type of reaction has proven to be suitable for a quantitative study of a number of variables affecting the kinetics.

The cracking of substituted unsymmetrical diarylethanes to form a substituted styrene and the aromatic hydrocarbon was discovered and investigated by Sturrock and Lawe.[1] These two workers initially pointed out and interested us in the unique features of this cracking reaction and have co-operated in the development of the studies reported herein. Their work and the later report of Morton and Nicholls [2] indicated the nature of certain variables affecting the cracking rate without relating these factors in the more quantitative manner described in this paper. Greensfelder, Voge and Good have published an important series of papers [3] on the cracking of pure hydrocarbons, and Thomas [4] has recently presented a theory of the mechanism, which will be of importance in discussing the results of this paper.

Experimental

Materials.—The 1 : 1-*bis* (substituted phenylethanes) were usually prepared by condensation of acetylene or acetaldehyde with a substituted aromatic compound in the presence of a Friedel-Craft's catalyst such as aluminium chloride and anhydrous hydrofluoric acid, zinc chloride, etc. For example, 1 : 1-*bis*-(4-methylphenylethane) was synthesized by condensation of toluene with acetaldehyde using a 3-5-fold molar excess of the hydrocarbon at 0-5° C with anhydrous hydrofluoric acid as catalyst.

Cracking Procedure and Analyses.—The cracking of the diarylethane was carried out in conventional equipment. The liquid diarylethane was metered and flash-vapourized. The vapour was mixed with a metered flow of steam and the resulting mixture passed through an electrically heated stainless steel tube maintained at a controlled temperature. The products were quenched and the water layer separated. The off-gas was always negligible. The catalyst decreased in activity during each run but could be restored to the original activity by " burning off " with air in the presence of steam.

The oil layer from the products was stripped at reduced pressures to obtain low boilers. In the case of ditolylethane, for example, these consisted of toluene, ethyltoluene, and methylstyrene. In most cases only 0·1-5 % of the substituted styrene was recovered with the vinyl group in the hydrogenated state. Probably this side reaction occurs by hydrogen transfer from the tar on the catalyst to the vinyl group. The moles of methylstyrene plus ethyl derivative is, however, an accurate measure of the total cracking of the diarylethane.

Extensive distillation or crystallization work, carried out with the aid of infra-red analyses, led to preparation of pure substituted styrenes and the ethyl derivatives. This permitted setting up of quantitative infra-red analytical procedures for the multi-components in the low boilers from the cracking. Samples were adequately analyzed by use of a combination of infra-red, bromide-bromate titration for substituted styrene, and distillation.

[1] Sturrock and Lawe, *U.S. Pat.* 2,373,982, April 17, 1945, to the Dominion Tar and Chemical Company.

[2] Morton and Nicholls, *Can. J. Res. B*, 1948, **26**, 581.

[3] Greensfelder, Voge and Good, *Ind. Eng. Chem.*, 1949, **41**, 2573.

[4] Thomas, *ibid.*, 1949, **41**, 2564.

Pellets made from Merck's kaolin were used as catalyst. This clay had a surface area as measured by the low temperature nitrogen adsorption of around 10 m.²/g. It contained 44 % SiO_2, 42 % Al_2O_3, and 14 % H_2O. A highly active commercial petroleum cracking catalyst containing 90 % SiO_2-10 % Al_2O_3, surface area 500 m.²/g., was also employed.

Results

The rate of cracking of ditolylethane was studied as a function of the contact time, temperature, molar ratio of steam as diluent to ditolyethane, and the diameter of the kaolin catalyst pellets. After reactivation of the kaolin the rate was determined as a function of the time of operation from which the value at zero time was found by extrapolation. Table I summarizes the data obtained.

TABLE I—CATALYTIC CRACKING OF 1 : 1-DI-*p*-TOLYLETHANE, DILUTED WITH STEAM, OVER A KAOLIN CATALYST AT 525° C

(Pressure 1·1 ± 0·1 atm.)

Run No.	Catalyst Particle Diameter cm.	Catalyst Volume, V_a in cm.³	Contact Time, V_a/V, sec.	Collision Frequency Factor, X	% Cracked to Low Boiling Fraction		% Ethyl-toluene Based on Methyl-styrene
					Extrapolated to Start	For 2 g. per cm.³ Passed Catalyst	
10/1 mole Dilution of Steam to 1:1-Di-*p*-tolylethane							
42	0·20	15	0·014	0·07	29	27	0·9
40-2	0·062	6	0·0064	0·12	50	47	0·2
39-3	0·11	15	0·015	0·16	56	53	0·4
34	0·20	60	0·067	0·36	61	58	1·6
43	0·11	60	0·088	1·1	68	64	2·3
132	0·11	100	0·59	5·6	—	62	16
126	0·11	100	0·86	8·1	—	44	40
127	0·11	100	2·0	19	—	30	60
100/1 mole Dilution of Steam to 1 : 1-Di-*p*-tolylethane							
37	0·11	6	0·0064	0·06	30	28	0·0
41	0·20	15	0·016	0·08	34	32	0·4
40-1	0·062	6	0·0066	0·12	51	48	0·2
39-1	0·11	15	0·017	0·17	65	62	0·0
35	0·20	60	0·067	0·35	78	76	0·0
38	0·062	15	0·024	0·48	82	78	0·0
44	0·11	60	0·083	0·93	92	87	0·8
122	0·11	67	0·13	1·3	—	84	6·3
129	0·11	100	0·56	6·6	—	85	*15

* The ditolylethane passed was 1·0 g. cm.$^{-3}$ catalyst. Therefore, this value is high.

The contact time is calculated for the average pressure over the catalyst in atmospheres, and at the reaction temperatures. The collision frequency factor in column 5 will be explained below. The percentages of ditolylethane converted to methylstyrene and ethyltoluene are shown in columns 6 and 7 at the start of the run and after passing 2 g. cm.$^{-3}$ catalyst. The last column shows a negligible formation of ethyltoluene up to 60-90 % conversion.

Experiments in Table I show that if only one factor (contact time, particle size and dilution) is varied at a time, then the converson increases with contact time, dilution and smaller particle size. These variables affecting the conversion are best related by means of the kinetic analysis presented below.

It was observed that the conversion was the same for solid pellets of kaolin as on a non-porous carborundum carrier coated with 16 % kaolin containing 2 % sodium silicate. In a private communication Dr. M. G. Sturrock has informed us that the weight of kaolin on the carrier need be only some 5-10 % in order to achieve the same conversion, yields, etc., as were obtained with the solid kaolin, and any further increase in coating over 10 % had no effect. This indicated that the external (geometrical) area of the pellets and not the true internal surface area, was the important factor. This suggested that the number of collisions of the diarylethane with the external area was important and explained the observed effect that a decrease in catalyst particle diameter increased the conversion.

If we assume that the rate of cracking over any element of length of the catalyst is dn mole sec., and that the rate is dependent on the number of collisions with the external area of the catalyst, then

$$dn = -kZdS, \quad . \quad . \quad . \quad . \quad . \quad (1)$$

where Z = number of collisions per sec. and dS the external area of catalyst in the element under consideration. At the high dilutions of steam used here the change in volume on reaction may be neglected and the pressure P is essentially constant at one atmosphere. Z is proportional to the partial pressure of diarylethane, which is nP/V, where V = initial volume space velocity of vapour passing over the catalyst in cm.^{3}/sec. This volume includes the steam added as diluent. The external area of the catalyst is $S = k_2V_a/d$, where k_2 = constant, V_a the volume of catalyst and d = particle diameter. By integration

$$\ln n/n_0 = -k_1X, \quad . \quad . \quad . \quad . \quad . \quad (2)$$

where X, the collision frequency factor, is V_aP/Vd, and n_0 is the number of moles/sec. of diarylethane fed.

Values of the collision frequency calculated in this way are given in Table I and are plotted in Fig. 1 against the logarithm of the fraction unconverted.

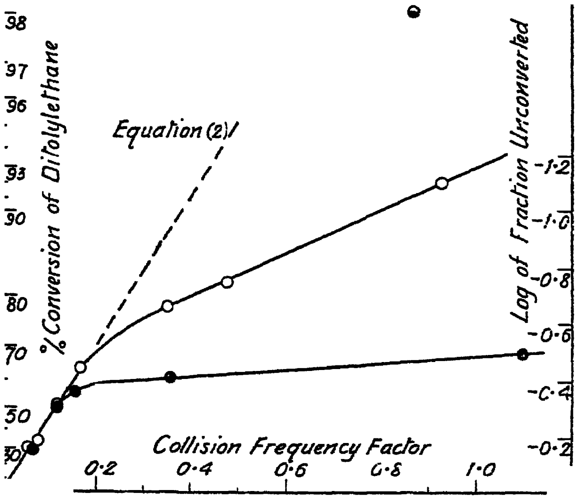

FIG. 1.—Conversion of Ditolylethane against collision frequency factor.
● Dilution, 10/1. ○ Dilution, 100/1. ◓ Dilution, 265/1.

The resulting curve should by eqn. (2) be a straight line. The correlation of the three variables involved in the collision frequency is reasonably good. With a high collision frequency factor the observed conversion is lower than predicted presumably because of an approach to an equilibrium or to a dependence on diffusion which lowers the conversion and makes the extrapolation to zero time less accurate.

Temperature Coefficient.—The conversion of ditolylethane to methylstyrene was determined at several temperatures under comparable conditions on kaolin catalyst. Conversion was obtained at the start of the run and after 10 g. of ditolylethane had been passed per g. of catalyst. The results are shown in Fig. 2, from which it is calculated that the apparent activation energy is 5000 cal./mole.

Effect of Substituents on Cracking Rate.—Using the relation

$$\log n/n_0 = -k_1X,$$

the ratio of collision frequency factor for any substituted diarylethane to that for ditolylethane, at equal values of conversion, gives the ratio of velocity

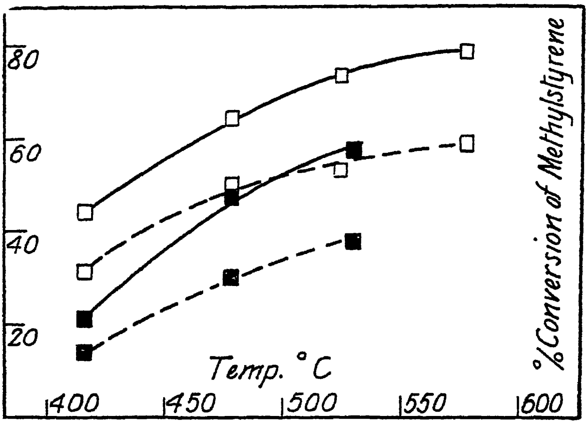

FIG. 2.—Variation in the conversion of 1 : 1-di-*p*-tolylethane to *p*-methylstyrene with temperature of pyrolysis.

Full lines : Conversion at start. Broken lines : conversion at 10 g. ditolylethane passed per g. catalyst.

Contact time : 0·08 sec. Catalyst pellet size : 0·203 cm.

Molar dilutions of ditolylethane vapour.

■ Dilution, 10. □ Dilution, 100.

constants k_1. In some cases the velocity constants were estimated from limited data, but the approximation involved would not change the order of effectiveness of substituent groups. Table II summarizes data for kaolin pellets, and for the petroleum cracking catalyst containing 90 % SiO_2-10 % Al_2O_3.

It is evident from Table II that an increase in electronegativity of the substituent in the nucleus of the diarylethane decreases the rate of cracking.

TABLE II—RELATIVE RATE CONSTANTS OF SUBSTITUTED DIARYLETHANES USING KAOLIN AND 90 % SILICA–10 % ALUMINA CATALYSTS

Substance (a)	Relative Rate Constant on (b)	
	Kaolin	SiO_2–Al_2O_3
1 : 1-*bis* (4-Hydroxyphenyl)ethane . .	(< 5)*	—
2 : 2-*bis* (4-Aminophenyl)propane . .	(< 5)*	—
1 : 1-*bis* (2 : 4-Dimethylphenyl)ethane .	1·4	3·8
1 : 1-*bis* (4-Methylphenyl)ethane . .	1·0	4·2
1 : 1-*bis* (2-Thienyl)ethane . . .	(1)*	—
1 : 1-*bis* (4-Aminophenyl)ethane . .	(1)*	—
1 : 1-*bis* (4-Dimethylaminophenyl)ethane .	(1)*	—
2 : 2-*bis* (4-Hydroxyphenyl)propane . .	(1)*	—
1 : 1-*bis* (2-Naphthyl)ethane . . .	0·5	—
1 : 1-Diphenylethane	0·3	1·0
1 : 1-*bis* (4-Chlorophenyl)ethane . .	0·04	0·5
1 : 1-*bis* (3 : 4-Dichlorophenyl)ethane .	0·01	0·2
1 : 1-*bis* (2 : 5-Dichlorophenyl)ethane .	—	0·1
1 : 1-*bis* (4-Cyanophenyl)ethane . .	Very small	0·05*

(*a*) Structure essentially as designated. In some cases, isomers were present.
(*b*) Ditolylethane over kaolin is the reference standard.
* Only estimated from limited data.

The relative order shown is in qualitative agreement with that given by Hammett[5] in his reactivity series. A mixed diarylethane containing no substituents on one ring and chlorine on the other, i.e. 1-phenyl-1-(chlorophenyl)ethane was synthesized and cracked. The resulting styrenes contained chlorostyrene and styrene in mole ratio of 4/1, thus again indicating an increase in electronegativity decreases the tendency of the bond between phenyl ring and the ethanoid carbon to crack. These results indicate an ionic type and more specifically a carbonium ion mechanism is involved in the cracking of these diarylethanes.

---

[5] Hammett, *Physical Organic Chemistry* (McGraw-Hill Book Co., 1940), Chap. 7.

Discussion

Mechanism of Cracking Reaction.—The mechanism of the cracking of hydrocarbons on alumina-silica catalysts has been described in a recent paper by Thomas [4] and also by Greensfelder, Voge and Good.[3] They represent siliceous cracking catalysts as acids which are capable of donating their protons to the hydrocarbon, thus forming a carbonium ion which then rearranges or decomposes to form the products of the cracking reaction. If we apply the above concepts to the cracking of substituted diarylethanes, and represent the catalyst by HA, then the equations for reaction are as follows :

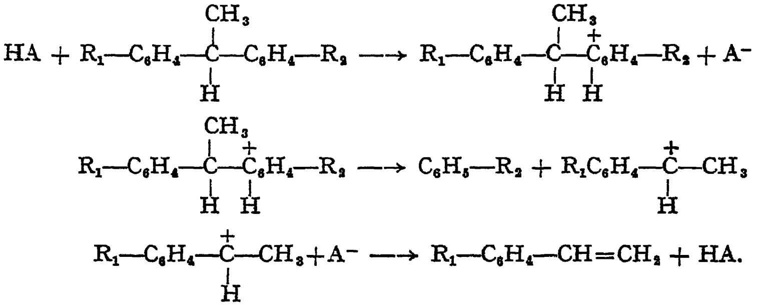

$$HA + R_1—C_6H_4—\overset{\overset{CH_3}{|}}{\underset{\underset{H}{|}}{C}}—C_6H_4—R_2 \longrightarrow R_1—C_6H_4—\overset{\overset{CH_3}{|}}{\underset{\underset{H}{|}}{C}}—\overset{+}{\underset{\underset{H}{|}}{C}}{}_6H_4—R_2 + A^- \tag{3}$$

$$R_1—C_6H_4—\overset{\overset{CH_3}{|}}{\underset{\underset{H}{|}}{C}}—\overset{+}{\underset{\underset{H}{|}}{C}}{}_6H_4—R_2 \longrightarrow C_6H_5—R_2 + R_1C_6H_4—\overset{+}{\underset{\underset{H}{|}}{C}}—CH_3 \tag{4}$$

$$R_1—C_6H_4—\overset{+}{\underset{\underset{H}{|}}{C}}—CH_3 + A^- \longrightarrow R_1—C_6H_4—CH{=}CH_2 + HA. \tag{5}$$

The catalyst is regenerated and starts the cycle again.

If R_1 and R_2 are the same, and their electronegativity is increased, the tendency to form a carbonium ion in eqn. (3) is decreased and the cracking rate is also decreased because of the increase in positive charge at or near the bond between the ring and the ethanoid group. It is suggested that reactions (3)-(5) take place consecutively but essentially simultaneously, a proton from one part of the catalyst taking part in eqn. (3), and another part of the catalyst accepting the proton liberated in eqn. (5). This concept is analogous to that which has been proposed by Turkevich [6] and by Hansford.[7]

A calculation shows that at zero time the number of collisions of diarlyethane with the surface is around 1000 times the experimental number of molecules decomposed. The observed activation energy would account for 40 out of the 1000 and steric factors could easily explain the remainder of the difference. The use of internal rather than external areas in calculating the number of collisions would make the discrepancy considerably larger. Experimental evidence favours the use of external area.

This cracking reaction is unusual because (1) the thousand-fold difference is unusually low for most catalytic reactions, (2) there is no need for requiring activated adsorption of the diarylethane with a prolonged residence time on the surface in order to account for reaction, (3) the external geometric surface of the catalyst is a controlling factor, and (4) the effect of chemical structure on reactivity is predictable.

[6] Turkevich and Smith, *J. Chem. Physics*, 1947, **16**, 466.
[7] Hansford, *Ind. Eng. Chem.*, 1947, **39**, 849.

We are indebted to our many colleagues in this laboratory for valued assistance and especially to the Infra-red group for analyses. Messrs. M. G. Sturrock, Kemp and Lawe of (or formerly of) the Dominion Tar and Chemical Company, Montreal Canada, have provided assistance through discussion and co-operative work.

American Cyanamid Co.,
Stamford Research Laboratories,
1937 West Main St.,
Stamford, Conn., U.S.A.

GENERAL DISCUSSION

Mr. D. A. Dowden (*Billingham*) said : Because both conductivity and substrate-surface reactions must depend upon the electronic structure of the solid surface one feels that Dr. Mitchell should have no hesitation in correlating conductivity with catalysis in the general case. The precise relationship will depend upon the nature of the rate-controlling step.

The complexity of such a simple catalyst as zinc oxide lends point to Dr. Mitchell's comments on the choice of systems most suitable for study. Here the substrate can react with Zn^{2+} and O^{2-} in the complete stoichiometric lattice, with the same ions in the environs of cation and anion vacancies in the defective stoichiometric lattice and with all of these and the lattice analogues of Zn^+ and Zn in the excess semi-conductor.

The division of catalysts into metals, semi-conductors and insulators is a convenience which should not be allowed to obscure the continuity inherent in the reactions of a given substrate on each of these types; this continuity is most readily traced with the band model of electronic structure. Thus if methanol decomposition is controlled by electron donation to the solid, the reaction rate decreases in the nickel-copper alloys with increasing electron/atom ratio until the 3*d* band is full. Addition of zinc to copper gives the Hume-Rothery brass phases with characteristic oscillation of activation energy at the phase boundaries [1, 2] until a point is reached at which zinc oxide is formed. As an excess semi-conductor zinc oxide does not favour the electron donation step but addition of Cr_2O_3 or Al_2O_3 decreases the zinc excess and in the former case may yield a defect semi-conductor, $ZnCr_2O_4$,[3] where electron addition is more easy. Further addition of these "irreducible" oxides up to pure Cr_2O_3 permits the electron transfer in the former but inhibits it in the latter so that over Al_2O_3 the reaction adopts a different path based upon proton exchange.

Dr. U. R. Evans (*Cambridge*) (*communicated*): The idea that catalytic activity in oxides is connected with lattice defects suggests that recent work on protection by oxide films may be helpful in explaining variations in catalytic behaviour. The presence of traces of copper and silver greatly diminish the protective character of alumina films [4] by the introduction of lattice defects, the changes being related to the increase in conductivity in accordance with Wagner's equations. This may be read in connection with Steiner's observations that, whereas Al_2O_3 and MoO_2 have no catalytic power for certain reactions, MoO_2 supported on Al_2O_3 is highly active, and also with the cases of ZnO + Fe_2O_3 and BeO + Fe_2O_3 discussed by Hüttig. It remains uncertain whether any particular effect is attributable to defects associated with foreign atoms in one or other

---

[1] Schwab, *Trans. Faraday Soc.*, 1946, **42**, 689.
[2] Dowden, *J. Chem. Soc.*, 1950, 242.
[3] Bevan, Shelton and Anderson, *ibid.*, 1948, 1729.
[4] Price and Thomas, *J. Inst. Metals*, 1938, **63**, 21, 29.

phase, or those arising from misfit along the plane separating two phases, a matter important in electro-deposition.

It is well known that great changes in the conductivity of oxides can be brought about by heating in a reducing or oxidizing atmosphere, the conductivity falling or rising according as the composition is brought nearer or further from the stoichiometric value; it is reasonable to expect alteration in catalytic activity after such treatment. But the removal or introduction of defects can be brought about in other ways. Pryor and the writer[5] found that so-called "ferric oxide" invariably contains a small amount of matter readily soluble in dilute HCl, the amount depending on the previous heat treatment; when this readily soluble trace has been removed, dissolution becomes extremely slow. There is little doubt that the readily soluble portion is connected with lattice defects present at places where a ferrous ion occupies a site properly belonging to a ferric ion, since the acid extract is found to contain much ferrous, as well as ferric, iron. After the readily soluble fraction has been removed, storage for 15 days at 25° C does not replenish it, but treatment for 24 hr. at 385° C (which doubtless permits a slow diffusion of fresh defects from the interior) leads to the reappearance of some readily soluble material, whilst ignition at 1000° C produces complete recovery. In cases where catalysis depends on the type of defects suggested above, it may be expected that washing with acid would adversely affect the activity of an oxide catalyst.

In other cases, suitable electrochemical treatment may "manufacture" defects. When iron oxide powder is floated on mercury and subjected to cathodic treatment in dilute acid, there is an enormous increase in the rate of dissolution. This is, of course, the reason why on immersing heat-tinted iron in dilute acid the films of oxide responsible for the interference colours are removed in a few seconds or minutes, whereas the same films, after separation from the metallic basis, can withstand the same acid for long periods. In the first case, the ferric oxide suffers reductive dissolution at every discontinuity where the cell Fe | Acid | Fe_2O_3 is set up; a tinted metal specimen can preserve its colours in dilute sulphuric acid over long periods if the liquid also contains chromic acid, or if the specimen as a whole is subjected to anodic treatment, thus preventing the reduction.[6] It is conceivable that catalytic processes carried out in aqueous solution might in some cases be influenced favourably by cathodic polarization of the catalytic mass.

In seeking to correlate catalytic activity with physically measureable properties, most contributors to this Discussion have used electrical conductivity or magnetic susceptibility. Thermoelectric force has also been studied and deserves special consideration, if only for the reason that its measurement involves no knowledge of the geometrical dimensions of the test specimen, so that it can presumably be measured on the actual surface which is subsequently to form the catalyst. Thermoelectric force depends in part on the same factors which determine conductivity, but in semi-conductors containing two carriers of opposite charge thermo-electric force will in the simplest case involve the *difference* between their contributions, and conductivity the *sum*;[7] by measuring both properties two equations should be obtainable instead of one, thus increasing the information provided. The variation of thermo-electric effect as well as conductivity in semi-conductors has of course received much study from Anderson and his colleagues.[8] In alloy catalysts, the thermo-electric effect may be instructive, because, like catalysis, it presents special features[9] in the range of composition where the inner electron band is filling up.

---

[5] Pryor and Evans, *J. Chem. Soc.*, 1949, 3330; also two further papers, *ibid.* 1950 (in press).

[6] Evans, *ibid.*, 1930, 478.

[7] Fowler, *Statistical Mechanics* (Cambridge Univ. Press, 1936), p. 427.

[8] Anderson and Morton, *Trans. Faraday Soc.*, 1947, 43, 185, 194.

Conductivity measurements are complicated, even in a specimen of accurately known external dimensions, by doubts about the internal surface, the true area of contact between the " grains ", and the respective contributions of surface and bulk conductivities. The measurement of the velocity constants governing film growth, which are in general related to conductivity by Wagner's equations, deserves attention, since here several simple methods are available although sometimes doubts about the true surface area introduce difficulties ; good agreement has been obtained when three different methods have been used to measure film thickness on a single specimen.[10, 11] Here the curves of Allen and Mitchell on the oxidation of pre-fused copper beads are of interest. Their form shows a general resemblance to the curves for the oxidation of abraded copper sheet at similar temperature obtained electrometrically by Miley and the author.[12] Comparison is difficult since, as noted above, the value to be adopted for the effective surface area of abraded metal is open to doubt, but the new research shows that the formation of an oxide film of sensible thickness at ordinary temperature does not require the structural damage associated with abrasion.

Prof. G.-M. Schwab (*Athens*) (*communicated*) : It has been found in our laboratory [13] that the combination of carbon monoxide and oxygen on cupric oxide at 280°-400° C and at pressures of a few mm. Hg is first-order for carbon monoxide and independent of the oxygen pressure. This was explained by a rate-determining reaction of carbon monoxide with oxygen atoms and an instantaneous re-oxidation of the surface by oxygen. The frequency factor observed is in agreement with this picture. This kinetic scheme is just the opposite to that reported by Prof. Garner *et al.* who gave evidence for a CO-covered surface. Do they find that at our higher temperatures this layer is removed as carbon dioxide at a rate much higher than that of its formation ?

Prof. W. E. Garner (*Bristol*) (*communicated*) : In reply to Prof. Schwab, it should be pointed out that the mechanism of the reaction between carbon monoxide and oxygen on Cu_2O may occur by different mechanisms at 280-400° C and at room temperature, respectively. On a surface which is free from adsorbed oxygen, carbon monoxide is strongly adsorbed at room temperature, and on evacuation the adsorbed gas is desorbed mainly as carbon monoxide, as would be expected from a heat of adsorption of 20 kcal./mole. At 80° C, however, carbon monoxide interacts readily with the surface to give carbon dioxide, so that there is probably no appreciable reversible chemisorption of carbon monoxide above this temperature. At 200° C the surface will be practically free from adsorbed gas, either in the form of CO or CO_3^{-}. On the other hand, oxygen is more strongly adsorbed, and at 200° C it requires 24 hr. evacuation to remove it from the surface.

The low temperature mechanism consists in an interaction between adsorbed carbon monoxide, and oxygen atoms, to give a CO_3 complex on the surface, which then dissociates. The reaction appears to proceed in three steps :

$$\mathrm{CO_{ads}} + \mathrm{O_{ads}} \rightarrow \mathrm{CO_2}^{\cdot} \quad . \quad . \quad . \quad . \quad (1)$$

$$\mathrm{CO_2} + \mathrm{O_{ads}} \rightarrow \mathrm{CO_{3\,ads}} \quad . \quad . \quad . \quad . \quad (2)$$

$$\mathrm{CO_{3\,ads}} \rightarrow \mathrm{CO_2} + \mathrm{O_{ads}}, \quad . \quad . \quad . \quad . \quad (3)$$

the oxygen and CO_3 complex probably existing as ions. The heat of desorption of CO_2 from the CO_3 complex is only 23 kcal., so that it is relatively unstable. At higher temperature, carbon monoxide removes oxygen from the surface of the lattice to give CO_2, thereby producing holes in the surface which can be filled by oxygen if this gas is present. The process will be first order with respect to carbon monoxide if the rate of reaction is proportional to the rate of collision of the carbon monoxide with the surface, which is kept intact by adsorbed oxygen. There is an appreciable adsorption of oxygen at 280° C. All that is needed is that the rate of repair of the surface by oxygen should exceed the rate of reduction by carbon monoxide. The high temperature reactions would appear to consist in alternate reduction and oxidation of the surface as suggested by Prof. Schwab. These reactions are not in much evidence at room temperature with Cu_2O, because reduction of the surface by carbon monoxide is much slower than its interaction with adsorbed oxygen.

---

[9] Mott, *Proc. Roy. Soc. A*, 1936, **156**, 368.
[10] Evans and Bannister, *ibid.*, 1929, **125**, 380.
[11] Price and Thomas, *Trans. Electrochem. Soc.*, 1939, **76**, 332.
[12] Evans and Miley, *Nature*, 1937, **139**, 283.
[13] Schwab and Drikos, *Z. physik. Chem. B*, 1942, **52**, 234.

Dr. G. C. A. Schuit (*Koninklijke/Shell Lab., Amsterdam*) said : A series of observations has been made on one binary Ni catalyst, $NiO + SiO_2$, prepared by coprecipitation. These observations tend to stress some points raised by communications made earlier in this Discussion.

(*a*) There is not *one* but a series of unreduced catalysts with the composition, $NiO—SiO_2$, consisting of a gradual change via three types :

$$Ni(OH)_2 \rightarrow Ni\ \text{kaolinite} \rightarrow Ni\ \text{mortmorillonite}$$

The sequence is important because the reduction becomes gradually more difficult in this direction, $Ni(OH)_2$ being completely reducible below 200° C, but Ni montmorillonite necessitating a temperature $> 500°$ C.

(*b*) In all cases, however, the product of the reduction is a finely dispersed Ni in a SiO_2 structure.

(*c*) Depending on the completeness of reduction the H_2 adsorption changes in type. Partially reduced catalysts show beautiful examples of activated adsorption ; completely reduced samples, however, are comparable to Ni films. However, for these catalysts complete coverage necessitates about 10 times the amount of H_2 observed for Ni films by Dr. Beeck. They are thus more finely dispersed.

(*d*) The H_2 coverage as a function of pressure (0·01-100 mm.) and temperature (−80° C to 400° C) has been measured in the same manner as has been done by Frankenburg for $W—H_2$. The results are, however, different and comparable to the results of Beeck and Rideal and Trapnell when analyzed according to the Clausius-Clapeyron equation. The plot of ΔH-coverage is concave and not convex to the abscissae. Frankenburg's results accordingly seem not of general value. Arguments based on his results, therefore, do not necessarily apply to other systems.

(*e*) The activity of the fully reduced catalysts for $C_2H_2 + H_2$ is *ca.* 5 to 10 times that of Beeck's Ni films (just as Prof. Taylor mentioned for $NiO + Cr_2O_3$). However, as their surfaces from the total H_2 adsorption seems likely to be higher, it appears that the activity per unit of surface area is about equal to that of the Ni films.

(*f*) For benzene hydrogenation preliminary measurements tend to indicate likewise a constant activity per unit of surface area. There are, however, some peculiar points worth further investigation, e.g. :

(i) partial reduction seems to provide somewhat more active catalysts which is rather surprising because at least a part of the surface is probably covered by oxygen.

(2) Reduction of a montmorillonite catalyst furnishes catalyst samples which are a factor of 10 less active. No explanation of this can be given as yet.

Dr. R. H. Griffith (*N. Thames Gas Board, London*), said : Although this section is strictly concerned with oxide catalysts, it may be permitted to extend the discussion to include sulphides, for in some instances these provide interesting information. This is particularly so in certain oxidation reactions. For example, if oxygen is admitted to NiS it forms a chemisorbed layer which is not removed by evacuation but which reacts at room temperature with H_2S to give H_2O and chemisorbed S.[14] These chemisorptions can occur to a very large extent and produce a slight increase in the lattice parameters of β-NiS. Again, when COS is oxidized on Ni_3S_2 the reaction is known to occur by collision of the sulphur compound with chemisorbed oxygen by a first-order reaction retarded by SO_2. Here, then, are two examples where the change occurs by collision of one molecular species with the other in a chemisorbed state, in which there can be no possible confusion with oxygen initially present as part of the catalyst.

It is to be expected that chemisorbed oxygen and sulphur would produce large changes in the electrical properties of sulphide catalysts of this type, and such measurements are now being made in our laboratory.

Dr. E. R. S. Winter (*Imperial College, London*) said : Dr. E. Whalley and I [15] can provide independent confirmation that the surfaces of oxides are very labile and will exchange oxygen with $H_2{}^{18}O$ vapour.[16] Thus γ-Al_2O_3, MgO, ThO_2, TiO_2 and ZnO have been examined, and show ready exchange of oxygen with water vapour at temperatures as low as 120° C (γ-Al_2O_3 will exchange at room temperature). These temperatures are all much lower than those at which exchange of the same oxides with gaseous oxygen is significant, and this indicates the manner in which the hydrogen atom promotes oxygen lability at the surface.

The number of readily-exchangeable atoms of oxygen/g. of oxide, as determined by the $H_2{}^{18}O$ exchange, is of the same order as that found (at higher temperatures) from exchange with oxygen gas : both these quantities are similar in magnitude to those calculated from low-temperature nitrogen isotherms by the B.E.T. or Harkins-Jura method, as is shown in the Table.

Oxide	Exchangeable O, Atoms/g. of Oxide		
	From H_2O Exchange	From O_2 Exchange	From N_2 Isotherms
Al_2O_3	$1{\cdot}32 \times 10^{21}$ (200° C)	$1{\cdot}3 \times 10^{21}$ (550° C)	$1{\cdot}35 \times 10^{21}$
ThO_2	$3{\cdot}48 \times 10^{20}$ (120° C)	$5{\cdot}9 \times 10^{20}$ (500° C)	$4{\cdot}9 \times 10^{19}$
TiO_2	$9{\cdot}3 \times 10^{20}$ (120° C)	$3{\cdot}1 \times 10^{20}$ (400° C)	$9{\cdot}1 \times 10^{19}$

The use of ^{18}O, incorporated into the catalyst surface by exchange with $H_2{}^{18}O$ vapour, to study the extent to which the surface takes part in heterogeneous reactions is demonstrated by the recent work of Karpacheva and Rozen.[17]

Dr. H. de Bruijn (*Geleen, Netherlands*) (*communicated*) : What has struck me particularly in the paper presented by Dr. Winter is that there exist two temperature regions in the case of Cr_2O_3 and MgO, with largely different activation energies. A similar effect of temperature on the activation energy is found with the decomposition of ammonia on an iron catalyst singly-promoted with aluminium or magnesium oxide, a region with an activation energy of 0-15 kcal. and another region with $E = 40$-50 kcal. As yet no explanation has been given for this change of activation energy with temperature.

---

[14] Badger, Griffith and Newling, *Proc. Roy. Soc. A*, 1949, **197**, 184.
[15] Whalley and Winter, *J. Chem. Soc.*, 1950, 1175.
[16] Milliken, Mills and Oblad, this Discussion.
[17] *A.C.S. Abstr*, **44**, 917.

It occurs to me that there is a certain analogy between both cases. In both cases we have :

(1) a chemical surface reaction, one of the reactants being mobile

$$\begin{array}{lcl} O_{18} + [O_{16}^{-}] \rightleftarrows [O_{18}^{-}] + O_{16} & [NH_3] \rightleftarrows & [NH_2] + H \\ & & \downarrow\uparrow \\ & & [NH] + H \\ & & \downarrow\uparrow \\ & & [N] + H \end{array}$$

(2) a desorption process of molecules, originally adsorbed as atoms.

It might perhaps be possible to find out whether this analogy is real from the following experiments :

(*a*) Extension of the temperature region in Dr. Winter's experiments. (In the NH_3 decomposition the higher value of the activation energy is again found at high temperatures.)

(*b*) A study of the kinetics. In the low activation energy region the kinetics are totally different from those prevailing in the high activation energy region.

(*c*) Addition of potassium ions. This inhibits the region of low activation energy in the decomposition of ammonia (a doubly promoted catalyst does not show regions of different activation energies).

Dr. P. H. Given (*Leatherhead*) said : If the reactions of hydrocarbons on the surface of cracking catalysts proceed through the intermediate formation of carbonium ions and are analogous to corresponding reactions in solution, one would expect in the surface reactions the strong dependence of the rate of reaction on the nature of hydrocarbon system that is found in solution ; the very wide variation of the rates of the substitution reactions of aromatic systems in solutions are particularly well known.[18] In their study of the cracking of diarylethanes, May, Saunders, Kropa and Dixon [19] found the relative rate constants to decrease with increasing electronegativity of substituents, as would be expected if the critical reaction is an attack of a positive ion on the aromatic compound, but the overall decrease for the series they studied is small (about 100-fold). We have found a similar small dependence of reaction rate on the nature of the aromatic system in the reaction of dimethyl ether with aromatic compounds to give (mainly) monomethyl derivatives.[20] When the reactants were passed over a silica-alumina catalyst at 450°, the conversion to monomethyl derivatives in moles % was as follows (the contact time being the same in all cases) :

Aromatic Compound Reacted : . . .	pyridine	benzene	toluene	thiophene	*p*-xylene
Moles % Monomethyl Product . . .	3·5	13·5	16	16·5	21

These figures may be taken as an approximate measure of the relative rates of reaction. The thiophene figure is probably too low, because some decomposition occurred. With this exception, the figures are certainly in the order expected, if, as is probable,[21] the reaction involves attack of a positive (methyl) ion on the aromatic ring ; but there is surprisingly little difference between them. This fact may be connected with the different processes by which a molecule becomes activated in reactions in solution and on a surface. Presumably in aromatic structures the contribution of those canonical states that bear integral charges (which are responsible for orienting effects, etc.) to the resonance hybrid varies with temperature and also with adsorption, but one cannot at present suggest how; the surface reactions considered take place at a temperature some 400° higher than the solution reactions. These points draw attention to an aspect of the mechanism of reactions on cracking catalysts that requires further study.

---

[18] See, for example, Wheland, *The Theory of Resonance and its Application to Organic Chemistry*, 1947.

[19] This Discussion.

[20] Hammick and Given, *J. Chem. Soc.*, 1947, 928 ; 1948, 2154 ; and unpublished data.

[21] Bremner, *Research*, 1948, 1, 281 ; Greensfelder, Voge and Good, *Ind. Eng. Chem.*, 1949, 41, 2573.

Dr. J. Weiss (*Durham*) (*communicated*): We have found recently [22] that a number of substances (e.g. dicinnamylidene acetone) which possess a system of conjugated double bonds give colour reactions in which the surface of the alumino silicate assumes the role of an acid. We have studied this acid function in some detail in relation to the adsorptive properties of the alumino silicates. We have now had an opportunity to study also a number of commercial alumino silicate cracking catalysts and we find that the relative catalytic activities are correlated to the intensity of the colour produced by these reagents so that this might serve perhaps as a rapid test to assess the activity of these catalysts.

Dr. A. G. Oblad (*Marcus Hook, Pa.*) said: I should like to re-emphasize that point pertaining to the detailed structure of a silica-alumina catalyst which we have made in our paper and which is contrary to the suggestions of Dr. Tamele, Dr. Beeck, Dr. C. H. Thomas and others. We do not believe that a structural acid of either the Lewis of Brønsted type exists in the catalyst. Our point is that the catalyst has a potential to act as an acid and does so when placed in the vicinity of a base. This distinction is to us an important point because it has immediate bearing on the structure of the catalyst. To say that the catalyst contains structural acids of the Brønsted or Lewis type means that the alumina and silica are disposed in a particular manner. The presence of a Brønsted acid implies that aluminium exists in a four-ordinate form stabilized by a proton. On the other hand, the presence of a Lewis acid implies that aluminium is three-co-ordinated and surrounded by only three oxygen atoms. Both these structures to us are hypothetical and are not in accordance with the chemistry of the catalyst. These structures cannot exist unless some agent other than a proton is present to stabilize aluminium in these forms. It is our conclusion for calcined catalysts that the aluminium exists entirely as γ-alumina and that some of the aluminium ions are capable, in the presence of the silica, to shift to the four-co-ordinate or " acid " form. This it does, however, only in the presence of stabilizing agents. The reversible shift of the active aluminium ions is an integral part of the catalytic action of silica-alumina.

Dr. D. D. Eley (*Bristol*) said: Dilke, Sheppard and myself [23] have recently obtained preliminary values for the bond energy $RN \rightarrow AlCl_3$ over a range of substances nitrogen bases RN. The energy varies in an interesting fashion with the nature of RN. I believe it would be a matter of great interest to heats of adsorption of nitrogen bases on silica-alumina catalysts, for then a conelation with our data on $AlCl_3$ might yield a valuable indication of the nature of the " active centres ".

Dr. Alwyn G. Evans (*Manchester*) said: I should like to describe some experiments which Dr. Hamann and I have carried out on the olefin, 1 : 1 diphenylethylene, $\phi_2C{=}CH_2$. We chose this olefin because it does not polymerize further than the dimer, and we could thus study its behaviour in the presence of acid catalysts without the formation of high polymers. We have treated this olefin with acid catalysts to see if carbonium ions are formed by proton addition to the double bond.

The ultraviolet absorption spectrum of the carbonium ion $\phi_3\overset{\oplus}{C}$ gives a marked absorption peak at 431 mμ (e.g. ϕ_3CHSO_4 in conc. H_2SO_4).[24] We find that the solution of $\phi_2C{=}CH_2$ in conc. H_2SO_4 shows a very similar spectrum with a peak at 434 mμ. This spectrum is quite different from that of $\phi_2C{=}CH_2$ itself, and we attribute it to the presence of the carbonium ion $\phi_2\overset{\oplus}{C}CH_3$, formed by the transfer of a proton from H_2SO_4 to $\phi_2C{=}CH_2$. We also find that $\phi_2C{=}CH_2$ gives an almost two-fold depression of the freezing point of H_2SO_4, and this confirms the occurrence of the proton transfer reaction

---

[22] *J. Chem. Soc.*, 1948, 2164.

[23] *Trans. Faraday Soc.* (in press).

[24] Hantzsch, *Ber.*, 1921, 54, 2573; Anderson, *J. Amer. Chem. Soc.*, 1930, 52, 4567.

$$H_2SO_4 + \phi_2C{=}CH_2 \rightarrow HS\overset{\ominus}{O_4} + \phi_2\overset{\oplus}{C}CH_3$$

under these conditions.

This absorption peak was also obtained (at 430 mμ), when $\phi_2C{=}CH_2$ was brought into contact with a solution of BF_3 in benzene. The benzene had not been subjected to any rigorous drying, and the solution therefore contained the strong acid F_3BOH_2. In this case too, we attribute the absorption peak to the presence of the ion $\phi_2\overset{\oplus}{C}CH_3$ formed by proton transfer from F_3BOH_2 to the olefin.

We also studied the action of a clay on the olefin. Activated floridin was suspended in paraffin and $\phi_2C{=}CH_2$ was added. This suspension showed an absorption peak at 430-440 mμ. In this case the colour was located on the surface of the clay particles. We attribute the spectrum to the presence of the ion $\phi_2\overset{\oplus}{C}CH_3$ at the surface of the clay particles formed by proton transfer from the floridin to the olefin.

Dr. Herman E. Ries, Jr., Dr. John S. Melik and Dr. Marvin F. L. Johnson (*Harvey, Illinois*) (*communicated*) : Low-temperature nitrogen adsorption techniques have been used for determining surface area, pore volume, pore radius and sintering characteristics of representative cracking catalysts and related materials (Table I). Significant differences in structure characteristics have been demonstrated for silica-magnesia, silica-alumina and clay cracking catalysts as well as for several widely different forms of silica. The virgin silica-magnesia catalysts studied have practically their entire area contributed by the very smallest of pores in the 10 to 15 Å pore radius range. The synthetic silica-alumina catalysts are composed of pores appreciably larger but still amost exclusively in the small pore range, 15 to 25 Å radius. The clay catalysts have a considerably wider pore size distribution which includes pores having much greater radii. In general, surface area values for the synthetic catalysts are greater than for the clays.

Vacuum sintering properties of the silica-magnesia, silica-alumina and clay catalysts are also quite different. The silica-magnesia catalysts studied sinter to zero area at 800° C (1472° F). The silica-alumina synthetic materials fall to zero area in the neighbourhood of 1000° C (1832° F). The clay catalysts approach zero area in an intermediate region. 850-900° C (1562-1652° F).

In the presence of steam the sintering process is accelerated for the three types of catalysts. Apparently the silica-magnesia catalysts are somewhat less sensitive to steam than the silica-alumina and clay catalysts. Steam sintering effects a reorganization of the silica-alumina and clay structures in a relatively profound manner to increase pore size whereas the pore structure of the silica-magnesia catalysts is not changed significantly. For the vacuum-sintered silica-alumina catalysts the structure of the pores remaining is effectively the same as their initial structure. Use of the catalysts in commercial cracking processes causes an increase in pore radius and structure changes that are strikingly similar to those produced by small scale steam treatments. It thus appears that steam at elevated temperatures may be the principal factor in the deterioration of the physical structure of cracking catalysts.

Adsorption-desorption isotherms demonstrate the sharp contrast between the small pore Davison silica gel (r = 11 Å) and the large pore

TABLE I.—AREA, PORE VOLUME AND AVERAGE PORE RADIUS FOR RREPRESENTATIVE CRACKING CATALYSIS IN THE VIRGIN, STEAM TREATED AND USED STATES

	Sample No.	Expt. No. (Hysteresis)	V_m, cm³ Adsorbed in Monolayer on 1 g. (ign. wt.) Adsorbent (BET)	B.E.T. Area, sq. m./g. ign. wt.	% Volatile Matter	V_s, Gas Adsorbed at P_0, cm³/g.	P_g, Pore Volume (from V_s) cm.³/g.	Average Pore Radius, Å ($r = 2P_g/A$)
Nalco, silica-magnesia microspheres	400A449	2575	144·7	630	4·6	292	0·451	14·3
Nalco, used, equilibrium (U.O.P.)	400B4127	3537	72·7	317	8·9	210	0·325	20·5
Nalco, steam treated (1150° F, 400 psig, 24 hr.) . .	400B5541	2858	73·8	322	4·9	183	0·283	17·6
DA-5 silica-magnesia	400B999	4611	151	656	20·9	236	0·365	11·1
DA-5 silica magnesia (calcined)	400A4047	2674	71·8	312	3·4	134	0·207	13·3
DA-5 silica magnesia (calcined) steam-treated (1175° F, 400 psig, 24 hr.)	400B5561	302	34·7	151	5·0	68	0·105	13·9
Socony TCC beads, silica alumina	9335X6147	745	101·3	440	1·3	310	0·479	21·8
Socony TCC beads, used	9335X6134	716	62·2	270	7·2	290	0·448	33·2
Socony TCC beads, steam-treated (1000° F, 28 hr. ; 1050° F, 10 hr. ; atm.)	400C20743	3665	70·3	306	2·5	282	0·436	28·5
Socony TCC beads, steam-treated (1000° F, 28 hr. ; 1050° F, 22 hr. ; 1100° F. 40 hr. ; atm.)	400C21362	3690	55·2	240	0·1	274	0·424	35·3
Socony TCC beads, vacuum-sintered (1780° F, 16 hr. after earlier sintering in vacuum	9335X6147	754	43·3	188	1·3	135	0·209	22·2
Houdry porous beads	400C10151	3658	57·0	248	2·2	334	0·516	41·6
Aerocat, silica alumina microspheres	9416C9363	2620	160·9	700	27·4	375	0·580	16·6
Aerocat, steam-treated (1150° F, 75 psig, 24 hr.) . .	400B5543	2828	16·5	72	0·6	326	0·504	140·0
Diakel, silica alumina	9416C6022	2022	95·6	416	6·7	281	0·435	21·2
Diakel, silica alumina, used	9416C6545	2035	29·9	130	0·5	191	0·284	43·7
Houdry synthetic, silica alumina	9416C6016	537	56·8	291	16·0	240	0·371	25·5
Fluid filtrol, clay	400B5397	2790	77·9	339	21·0	265	0·410	24·2
Fluid filtrol, used, equilibrium (A)	400A4054	217	31·3	136	3·7	250	0·386	56·8
Fluid filtrol, used, equilibrium (E)	400B4761	4059	32·5	141	2·5	215	0·332	47·1
Fluid filtrol, used, equilibrium (G)	400A5530	2857	31·1	135	1·9	240	0·371	55·0
Fluid filtrol, steam-treated (1058° F, 75 psig, 24 hr.) .	400B5454	4052	38·7	169	3·1	248	0·383	45·4
Fluid filtrol, steam-treated (1160° F, 75 psig, 24 hr.) .	400B5437	2821	25·9	113	2·8	244	0·377	66·1
TCC clay pellets	400B4094	2636	63·5	276	7·5	235	0·363	26·3
Houdry type I	400A9294	2611	52·2	227	1·0	230	0·356	31·4

aerogel ($r = 98$ Å). Their areas are similar, 809 and 796 sq. m./g., respectively. The isotherm for non-porous Linde silica resembles that of the aerogel although its area, 180 sq. m./g., is considerably smaller. It has been observed qualitatively that the smallest pore systems show practically no hysteresis, and that adsorbents with larger pores have broader hysteresis loops. For still larger pore systems the hysteresis loop begins to diminish and finally disappears for extremely large pore materials or non-porous particles.

Extension of these and related studies to catalysts deactivated by various treatments will improve our understanding of catalyst deterioration and lead to improved preparations.

Dr. J. K. Dixon (*Stamford, Conn.*) (*communicated*): It was suggested that in the cracking of ditolylethane to produce methyl styrene the reaction may be controlled by diffusion processes. Dr. Glueckauf has asked whether an explanation based on a diffusion-controlled process is compatible with the results shown in Table II where the structure of the diarylethane has an influence on cracking rate. The influence of the particle size of the catalyst on cracking rate has not been studied extensively with all of the diarylethanes containing electronegative constituents, but it was found to be still evident in the cracking of the dichlorophenylethanes. Dr. E. W. Thiele, who was present at the meeting, presented an analysis of the relation between particle size and catalytic activity a number of years ago.[25] Above a certain particle size the catalytic activity depends upon the total external surface of the catalyst particles, and with large particles the reaction is completely diffusion controlled. For smaller sizes the catalytic activity is proportional to the internal surface area (amount) of the catalyst. Thiele's analysis shows there is not necessarily any sharp transition from the case where external area rather than internal surface area controls. In the transition region both factors are important. Our paper indicates that in the cracking of ditolylethane the diffusion process appears to govern the cracking preponderantly. As the reaction rate decreases for other diarylethanes, as shown in Table II, the effect of chemical structure requires that the internal surface become of more importance and the overall rate less dependent on diffusion. The data at hand do not permit a quantitative analysis of the problem.

Dr. J. S. Anderson (*Harwell*) (*communicated*) : Prof. Selwood's work seems to fit very neatly on to the results obtained by Prof. Hüttig, over many years, in his studies of reacting oxide systems. It suggests that the changes in magnetic susceptibility observed during that phase of the reaction attributed by Hüttig to surface migration (stage (*b*)) reflect the changes in magnetic environment of diffusing paramagnetic ions, and possibly valence induction effects also.

Selwood stated in this Discussion that he had observed evidence neither for surface diffusion nor for the formation of " monolayers " of supported oxide. His mode of preparation may, however, consistently give stabilized surfaces. There is no doubt at all that surface migration does occur : that is well attested by the work of Hüttig, Jander, Schröder and others, and indeed by the very occurrence of reactions between solid oxides. The formation of Selwood's islands of supported oxide may, however, correspond to the change from stage (*b*) to stage (*c*) in Hüttig's reaction scheme. It would be most interesting to know whether in his collection of experimental results Prof. Hüttig has data for the *temperature dependence of magnetic susceptibility* at successive stages in the interaction of some of his oxide systems, so that this could be analyzed along the lines developed by Selwood. If no suitable results are extant, data of this sort would be worth obtaining.

Mr. D. A. Dowden (*Billingham*) said : The oxides of three-valent aluminium, manganese and iron exist not only in the stable rhombohedral form but also in the defective spinel lattice or in lattices very similar to it. Radius ratios suggest that chromium sesquioxide may under some conditions possess a defective lattice of the same type.[26] Such extensively defective lattices may possess considerable importance in catalysis by oxides. Has Dr. Selwood any evidence from his work for the induction of the γ-spinel lattice in oxides, particularly Cr_2O_3, supported upon γ-alumina or for lattice induction, as opposed to valence induction, in general ?

---

[25] *Ind. Eng. Chem.*, 1939, 31, 916.

Dr. P. W. Selwood (*Northwestern University, Illinois*) (*communicated*): We have no evidence for lattice induction. The induction of valence probably never occurs beyond one, or at the most two, atom layers.

Mr. N. W. Luft (*Waltham Abbey, Essex*) (*communicated*) *: The catalytic oxidation of NH_3 is a typical example of so-called high-efficiency catalysis in the sense of Wagner [27] and Todes.[28] If the temperature in the reactor is not exceedingly high homogeneous processes are of little importance. The consumption of NH_3 is controlled by the rate of diffusion or transport of NH_3 molecules from the gas flow to the catalyst surface. Allowing for longitudinal diffusion in the incoming gas and using average values of the physical properties and usual values for the coefficients of material transfer,[29] the theoretical NH_3 conversion in a Pt gauze, calculated with this assumption, agrees well with known experimental results. The fraction f of non-converted NH_3 (in terms of initial NH_3 concentration) at any point is :

$$f = 1 - (1 - f_0) \exp (Ux/D) \; ; \quad x < 0 \; ; \qquad (1)$$

$$f = (1 + a_v jD/U)^{-1} = f_0 \; ; \quad x = 0 \; ; \qquad (2)$$

$$f = f_0 \exp (- a_v jx) \; ; \quad 0 < x < x_e \; ; \qquad (3)$$

x = co-ordinate in direction of flow; the catalyst bed extends from $x = 0$ to $x = x_e$; U = linear velocity of flow ; D = diffusion coefficient ; a_v = surface area of catalyst per unit volume of bed ; j = transfer factor.[28] This shows that the main decrease of the NH_3 concentration takes place in the incoming gas in front of the catalytic gauze. Comparatively simple assumptions lead to a maximum of the NO concentration for very small contact times, i.e. near the entrance of the catalyst bed and to a subsequent maximum of the N_2O concentration, which has already been observed experimentally.

It seems difficult to support convincingly any particular one of the three alternative intermediates NH, HNO and H_2NOH by the available experimental data. On thermodynamic and kinetic grounds both NH and HNO, and to a lesser extent also H_2NOH, might occur as primary intermediates. The formation of HONO and $HOONO_2$ according to Zawadzki's mechanisms is improbable for steric reasons, and that of NO by way of HONO is considered as being too slow in comparison with experimental findings.

Many steps will presumably follow the Eley-Rideal mechanism [30] for reactions between gaseous molecules and adsorbed radicals. Probably OH radicals, which in Zawadzki's scheme are only allowed to recombine, play a major part in the process, e.g. by

$$NH + O_2 \rightarrow NO + OH \qquad (4)$$

$$HNO + O_2 \rightarrow NO + OH + O \qquad (5)$$

$$HNO + OH \rightarrow NO + H_2O \qquad (6)$$

$$HNO + NO \rightarrow N_2O + OH \qquad (7)$$

Then the concentrations of OH, O, O_2H, NH and HNO may be regarded as characteristic constants for a given catalyst and working conditions.

---

[26] Visser, *Chem. Weekblad*, 1946, **42**, 127.

* A detailed account will be published later.

[27] Wagner, *Chem. Technik.*, 1945, 18, 1.

[28] Todes, *Izvestia Akad. Nauk. U.S.S.R.*, 1947.

[29] Hougen and Watson, *Chem. Process Principles* (London, 1948).

[30] Eley, *Advances in Catalysis* (New York, 1948).

Together with Wicke's [31] hydroxyl theory of catalytic dehydrogenation processes, these assumptions lead to a unified kinetic explanation of the catalytic activity of Pt and metal oxides in NH_3 oxidation.

---

[31] Wicke, *Angew. Chem.*, 1947, **59**, 34.

IV. TECHNIQUES

INTRODUCTORY PAPER

By J. W. Mitchell

Experimental investigations on heterogeneous catalysis and related problems have, in recent years, fallen into two main groups. In the first group, laboratory scale experiments have been made with catalytic materials under conditions approximating as closely as possible to those of corresponding industrial plant processes, and much valuable information has been obtained. The catalyst system is, in these investigations, usually regarded as a whole; the experimental conditions are complicated, many variables being involved, and the results are not often amenable to theoretical analysis in terms of detailed models of the reacting system. In the second group, emphasis is placed on the elucidation of the mechanism of chemical change in catalytic systems, the ultimate aim being to evolve a sound theory of catalysis. Only the most simplified theoretical models can be used to represent the interaction between gas molecules and adsorbing surfaces and as many variables as possible must therefore be eliminated from experimental work done with the aim of stimulating and assisting parallel theoretical research.

This section on experimental techniques is concerned mainly with investigations in the second group, from among which the following may be mentioned: measurements of the adsorption and of the heats of adsorption of gases on catalytic surfaces; measurements of the work functions of gas covered surfaces from which deductions may be made about the state of the adsorbed molecules; measurements of the change in electrical conductivity which occurs when a film or thin slab of catalytic material is exposed to gases; and finally, studies of reactions which proceed at low temperatures such as, for example, the *o*- to *p*-hydrogen conversion.

All these techniques depend upon the preparation of catalytic or adsorbing surfaces of reproducible initial behaviour. When the properties of metallic surfaces are being investigated, this may be done by evaporating layers on to thoroughly outgassed substrates under the best attainable vacuum conditions. The properties of such evaporated films depend upon their thermal history but heat treatment cycles can be evolved which allow them to be reproducibly conditioned for work at a given temperature. The evaporated films have not the robustness of the commercial forms of the metallic catalysts; their behaviour is liable to change irreproducibly during the course of experiments and they are not usually stable at high temperatures. Many results of great value for the development of fundamental ideas have nevertheless been obtained with them. It does not appear possible at present to out-gas, sufficiently thoroughly for the most critical work, metals in the form of wires or sheets apart from those of the highest melting points such as tungsten. Clean surfaces which will give satisfactory results in many investigations can, however, be produced by exposing massive metals to atomic hydrogen or to positive ion bombardment. Surfaces prepared in this way have the advantage of being more stable than those of evaporated films.

Beeck and his collaborators have demonstrated that orientated metallic films may be produced by depositing metals by evaporation in low pressures of inert gases, and a number of special techniques are available for converting thin sheets of massive metals into single crystals of certain preferred orientations. These orientated surfaces should prove particularly valuable for fundamental investigations.

Far greater difficulties are experienced in preparing surfaces of oxide catalysts of known orientations and reproducible characteristics. Evaporation techniques cannot be generally employed because they are liable to lead to the deposition of material having a variable defect structure. Thorough outgassing in vacuum of a massive specimen may also result in a loss of oxygen. Despite these difficulties there have been many valuable studies of the adsorption of gases and of the heats of adsorption of gases on oxide systems.

In the present group of papers, Allen and the writer describe the results of gas adsorption measurements on thin copper films deposited by evaporation under good vacuum conditions. Quantitative adsorption measurements of this kind necessarily precede more detailed work on heats of adsorption and related properties. The measurement of the heat of adsorption on a known surface provides a most powerful method for determining the strengths of the bonds formed between the adsorbed molecules and the substrate. Beeck, Cole and Wheeler describe a calorimeter with which they have obtained reproducible results for the incremental heats of adsorption of gases on evaporated metallic films. Morrison and Los have developed a precision low temperature adiabatic calorimeter which will be used for the investigation of the adsorption of argon on titanium dioxide. The interpretation of the results of measurements of the incremental heats of adsorption must depend on the initial gas coverage of the specimen. It appears that this requires careful consideration.

The measurement of the change in the work function of a surface which is caused by the adsorption of a gas on the surface allows the calculation of the electric dipole moment of the surface layer, from which it is possible to draw conclusions about the nature of the adsorbed layer. These measurements are most conveniently made by the Kelvin method and for this purpose an ingenious apparatus in the form of a hollow cell tuning fork has been developed by Mignolet. The changes in work function are determined by measuring the changes in contact potential difference between two electrodes, one of which is used as a reference electrode and upon the other of which a metallic layer is deposited by evaporation and exposed to the gas whose effect is being studied. In practice, the gas will also be adsorbed by the reference electrode and the fact that two work functions are changing simultaneously must complicate the interpretation of the results. The possible use of well-aged tungsten in the form of sheet or strip as a standard reference electrode for experiments in this field merits careful consideration. It may be readily outgassed or reconditioned by being heated to a high temperature by electron bombardment and its work function is accurately known.

Deductions concerning the interaction of adsorbed gas molecules with the substrate may be made from observations of the change in the electrical conductivity of a thin film of the substrate which occurs as a result of the adsorption. Measurements on thin metallic films have been made by Allen and the writer and on oxide films by Gray. Gases which are only physically adsorbed on the substrate do not produce resistance changes in such measurements, and the method thus allows physical adsorption to be clearly differentiated from chemisorption or chemical reaction.

Selwood and Schroyer report on the measurement of proton relaxation times in water adsorbed on iron oxide supported on alumina by the nuclear induction method of Bloch, Hansen and Packard. This introduces another useful technique for estimating the effective reactivity of a quantity of supported paramagnetic material.

Two papers dealing with the dispersion and morphology of the catalytic material follow. The low angle X-ray scattering method described by Guinier gives otherwise inaccessible information on the internal heterogeneity of catalytic materials and permits particle size estimations to be made within a limited range of sizes. Turkevich, Hubbell and Hillier examine the correlation between particle sizes of gold sols and catalysts determined by the electron microscope and by small angle X-ray scattering.

Stable and radioactive isotopes will be extensively used in the future for the investigation of the adsorption of gases on solids, for studying exchange phenomena between the gas phase and adsorbed layers and diffusion in solids, all these processes having an immediate bearing on the problems of heterogeneous catalysis. This important field is reviewed by Turkevich and his collaborators who give many examples of the use of isotopes for elucidating the mechanisms of catalytic reactions.

H. H. Wills Physical Laboratory,
University of Bristol.

THE ADSORPTION OF GASES ON COPPER FILMS

By J. A. Allen and J. W. Mitchell

Received 10*th February*, 1950

A simple experimental technique for investigating the adsorption of gases on evaporated metal films is described. Troublesome dead space corrections have been eliminated and the method of preparation ensures that the free surface of the film will be initially uncontaminated by adsorbed gas layers.

The results of an investigation of adsorption and subsequent reaction of oxygen with copper films in the temperature range from − 183° C to 74° C are presented, and the adsorptive properties of the films at low temperatures and their behaviour at the higher temperatures are shown to be strongly dependent on the thermal history of the films.

The adsorption of gases on tungsten has been studied extensively by many investigators among whom Roberts [1] and Eley [2] may be mentioned. For adsorption work tungsten has the great advantage that a surface free from adsorbed gases and oxide films may be produced and renewed at will by heating a wire of this metal to 2800° C in a good vacuum. Clean surfaces may not be prepared in this way with lower melting point metals. They may, however, be conveniently formed by evaporating the metal under the best attainable vacuum conditions from thoroughly outgassed beads and condensing a thin film of the metal upon a glass substrate. This method has been used in the work reported in this paper, the object of which was to study the adsorption and subsequent reaction of oxygen with a series of copper films which were prepared under varied temperature conditions. The investigation forms part of a series of parallel studies by different methods,[3] the general purpose of which is to elucidate the mechanisms underlying the low-temperature oxidation of copper in the light of the theories recently advanced by Mott and Cabrera.[4] Its relevance to the present discussion lies mainly in the information which is obtained on the surface properties of clean copper films which have been subjected to different temperature treatments. It is of interest to compare the results obtained here with those of Beeck, Smith and Wheeler [5] on nickel films similarly deposited on to glass substrates at room temperature, and on evaporated copper films prepared in various ways.

---

[1] Roberts, *Some Problems in Adsorption* (Cambridge Univ. Press, 1939). See also Miller, *The Adsorption of Gases on Solids* (Cambridge Univ. Press, 1949).

[2] Eley, *Recent Advances in Catalysis.* Vol. I (Academic Press, New York, 1948), p. 157.

Experimental

The copper films used in these experiments were deposited over the surface of a spherical glass bulb by evaporating copper from a thoroughly outgassed bead mounted on a tungsten filament at the centre of the bulb. This arrangement ensures that the deposited film will be very nearly of uniform thickness. The amount of oxygen adsorbed and its subsequent reaction with the film were determined from pressure measurements made with a Pirani gauge. Corrections were made for the thermomolecular flow when the temperature of the bulb differed from that of the gauge.

This procedure has the great advantage of providing in a sealed evacuated bulb a self-gettering system, the slow evaporation during deposition renewing the free copper surface which can thus continuously clean up residual gases. The surface of the film formed by the evaporation of the last traces of copper is probably as free from initial gas contamination as possible. Calculations show that a negligible amount of tungsten would evaporate from the filament itself at the working temperature. The inner surface of the bulb is almost completely covered by the copper film and, because of this, contamination of the free copper surface by gases diffusing from the glass will be reduced to a minimum.

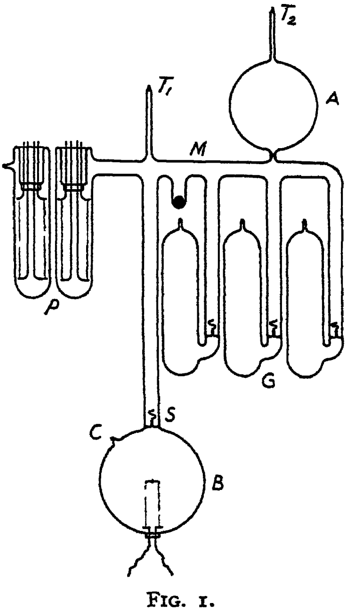

FIG. 1.

The oxygen for the experiments was stored in the Pirani gauge used for making the pressure measurements and also in a series of bulbs provided with breakable tips. It has been assumed, as is likely, that the walls of the gauge and the connecting tubes remain covered with a constant film of adsorbed oxygen throughout an experiment. This system has the advantage of completely eliminating troublesome dead space corrections and thus has the further advantage that accurate measurements can be made in cases in which the amount of gas adsorbed is small.

Apparatus.—This is shown in Fig. 1 and consists of four parts. The spherical bulb B was 8 cm. diam. and was provided with a sealing-off constriction C and a glass stem S in which there was a breakable gas seal, the base of which was approximately level with the contour of the bulb. Diametrically opposite the stem a two-lead tungsten-glass button seal formed part of the bulb wall. A 0·2 mm. diam. tungsten filament was mounted on the two tungsten leads and this filament carried, at the centre of the spherical bulb, a bead of spectroscopically pure copper which had been prefused in hydrogen. The bulb was pumped out through its constriction and, during the evacuation, the copper bead

[3] Allen and Mitchell (in press).
[4] Mott and Cabrera, *Reports Prog. Physics*, 1948-49, **12**, 163.
[5] Beeck, Smith and Wheeler, *Proc. Roy. Soc. A*, 1941, **177**, 62.

was outgassed several times. Just before sealing off at a pressure of less than 10^{-7} mm. Hg, the bead was again thoroughly outgassed and a small amount of copper was evaporated. The details of the vacuum system and of the baking and pumping schedule employed have been described elsewhere.[3] The evacuated bulb was later sealed to the manifold.

The gas tubes G each of about 80 ml. volume, had breakable gas seals and sealing-off constrictions. Before being filled with oxygen they were evacuated to a pressure of less than 10^{-6} mm. Hg and during the pumping they were baked at a temperature of 400° C for several hours. The pressure and temperature of the gas with which they were filled were measured with a McLeod gauge and mercury thermometer, respectively. The Pirani gauge P was constructed according to the specifications given by Reimann.[6] Accurate pressure measurements could be made in the range from 10^{-1} to 10^{-4} mm. Hg and the calibration curves obtained immediately before each experiment were extremely reproducible.

The manifold M to which the bulb, gauge and gas tubes were attached served with the gauge as a gas holder. The auxiliary bulb A which could be sealed off during an experiment was attached to the manifold when necessary in order to increase its volume. The ball bearing used to break the gas seals was not enclosed in glass, but was baked in hydrogen before use.

Volume Measurements.—Since, at the end of an experiment, the pressure in the apparatus was usually $\sim 10^{-3}$ mm. Hg, it could conveniently be filled with water by breaking the tip of T_1 below the surface of a weighed quantity of the liquid. The total volume was thus determined. The bulb and gas tubes were cut off and their volumes measured by weighing them full of water and empty. The volume of the manifold and Pirani gauge together was obtained by difference. If the auxiliary bulb had been used it would have normally been sealed off during the course of the experiment; its volume could be measured afterwards in a similar manner, T_2 being provided for this purpose.

The Preparation and Purification of the Oxygen.—The oxygen was prepared from potassium permanganate by the method outlined by Farkas and Melville.[7] Standard high vacuum methods in all glass apparatus were used and the pure oxygen was stored at a pressure of about 15 cm. Hg in small sealed ampoules provided with breakable tips. The gas tubes and the manifold were filled from these ampoules after thorough outgassing.

Estimation of the Film Thickness.—The geometric surface area of the copper film was calculated from the measured volume of the bulb. At the conclusion of an experiment the evaporated film was dissolved in nitric acid and a volumetric estimation of the total evaporated copper was made using the standard potassium iodide–sodium thiosulphate method.[8] As the bead had been mounted at the centre of a sphere the film was assumed to be of uniform thickness and the weight of copper per cm.^{2} could therefore be calculated.

For each experiment the size of the bead necessary to give the required amount of copper per cm.^{2} was estimated in advance and the evaporation was continued until all the copper had been removed from the filament. The shadows cast by the mounting of the tungsten leads and by the filament had particularly sharp boundaries, and their area did not exceed 0·2 % of the total area.

Experimental Procedure.—The apparatus was assembled and connected to the pumping system through T_1 for the purpose of exhausting the Pirani gauge and manifold. During the evacuation it was baked at a temperature of 400° C for several hours and a pressure of less than 10^{-6} mm. Hg was obtained. The filaments of the Pirani gauge were then flashed, the compensator bulb clamped on to the gauge and the two immersed in a bath at room temperature. The Wheatstone bridge constituting the Pirani gauge measuring circuit was then balanced. Oxygen was admitted to a pressure of 10^{-1} mm. Hg and by reducing the pressure in stages the Pirani gauge was calibrated against a McLeod gauge. This served two purposes, firstly, to maintain a close check on the gauge calibration and, secondly, to ensure that the walls of the manifold and the gauge were saturated with oxygen. The manifold was then filled to the desired pressure and, the pressure and temperature of the gas having been measured, the apparatus was sealed off from the pumping system.

---

[6] Reimann, *Phil. Mag.*, 1933, **16**, 673; 1934, **18**, 1117.

[7] Farkas and Melville, *Experimental Methods in Gas Reactions* (Macmillan, London, 1939), p. 156.

[8] Scott, *Standard Methods of Chemical Analysis* (Van Nostrand, New York, 1917), 2nd Edn., p. 163.

The bulb was then immersed in a bath at the desired temperature and the copper was evaporated by passing a current of 2·4 A through the filament. Copper films prepared in three different ways have been used :

(i) deposited with the bulb at room temperature and then cooled to − 183° C ;

(ii) deposited with the bulb at − 183° C, annealed for 2 hr. at room temperature and then cooled again to − 183° C ;

(iii) deposited with the bulb at − 183° C and maintained at this temperature.

In all the experiments the oxygen was admitted with the film at − 183° C and the temperature of the bath was changed successively to − 78° C, 20° C and 74° C, the film being kept at each temperature for a time sufficient to ensure that the rate at which further gas was being taken up had become very small. The oxygen was admitted in the first instance by breaking the seal on the bulb and the pressure was maintained between any desired limits by opening further gas tubes. The initial pressure and temperature of the oxygen in the manifold and gas tubes were known ; after breaking the tip of the spherical bulb, the pressure in the manifold was measured with the Pirani gauge at suitable time intervals ; and the volumes of the various components were measured at the end of the experiment. The number of molecules taken up per cm.^{2} by the copper film could then be calculated from these results in the following manner.

Calculation of Results.—With the exception of the measurements made with the bulb at room temperature, the Pirani gauge with which the pressure measurements were made was not at the same temperature as that of the bulb. In view of the magnitude of the pressures used, corrections must be made for the thermomolecular flow. This subject has recently been reviewed by Dushman[9] who concludes that, provided the ratio of the diameter of the aperture between two vessels at different temperatures to the mean free path of the gas molecules is of the same order of magnitude as, or less than 0·1, the simple law due to Knudsen[10] can be applied. In the present work this condition has been satisfied and the true pressure P_2' in the bulb at a temperature T_2 is related to the pressure reading on the Pirani gauge, P_2, at a temperature T_1 by the equation

$$P_2'/P_2 = (T_2/T_1)^{\frac{1}{2}}. \qquad \ldots \qquad (1)$$

If P_1 and T_1 are respectively the pressure and temperature of the oxygen initially in the manifold before the seal to the bulb is broken, V_1 and V_2 the volumes of the manifold and bulb respectively, and P_2 is the pressure reading of the Pirani gauge at a temperature T_1 when n molecules of oxygen have been taken up by the copper film with the bulb at a temperature T_2, n is given by the equation

$$n = N/R\{V_1(P_1 - P_2)/T_1 - P_2V_2/T_2(T_2/T_1)^{\frac{1}{2}}\} \qquad \ldots \qquad (2)$$

where N is the Avogadro number and R is the gas constant per mole. The experimental results have been calculated on the basis of this equation.

Results and Discussion

The results are summarized in Table I. The methods of preparation of the films in the first column refer, respectively, to the methods indicated in the previous section of this paper. The figures prefixed by the sign, >, arose from the fact that in these experiments the supply of oxygen was insufficient and the pressure fell to values too low to be measured with the Pirani gauge.

It is clear from these results that the adsorptive properties of the films at low temperatures and their subsequent behaviour at room temperature and at 74° C are strongly dependent on the thermal treatment to which the films have been subjected. In addition, there are marked changes in appearance of films of comparable weight per unit area prepared under different conditions. Films deposited at room temperature have the normal copper-red appearance ; those deposited at − 183° C are bronze in colour and, if such films are annealed in vacuum at room temperature, this appearance changes to the normal copper-red. If, on the other hand, films deposited at − 183° C are saturated with oxygen at − 183° C and then warmed to room temperature, practically no oxygen is evolved and their appearance does not change.

---

[9] Dushman, *Scientific Foundations of Vacuum Technique* (Wiley, New York, 1949), p. 65.

[10] Knudsen, *Ann. Physik.*, 1910, **31**, 205, 633.

TABLE I

Method of Preparation	Film Thickness g. per cm.^{2} × 10^5	Number of molecules taken up per cm.^{2} × 10^{-15} of the geometrically calculated surface at:			
		− 183° C	− 78° C	20° C	74° C
(i)	6·2	1·1	1·0	2·6	—
	6·5	1·3	1·3	3·1	10·3
	6·4	1·5	1·4	3·0	9·4
(ii)	6·9	1·8	1·9	5·0	6·6
	7·0	2·4	2·0	6·0	7·5
(iii)	4·7	8·1	10·6	12·9	12·6
	6·6	10·7	12·1	12·0	11·7
	6·9	10·0	>10·0	10·0	9·9
	10·8	15·0	>15·0	14·9	12·6
	15·5	22·2	26·0	26·0	26·0

Behaviour of this kind has also been observed by Beeck, Smith and Wheeler.[5] They have reported that copper films evaporated in a good vacuum and condensed on a glass substrate at room temperature sinter immediately. Films evaporated in argon or nitrogen and deposited on a surface at − 183° C are blackish in appearance and, on warming to room temperature, completely release the gas and become more coppery. In addition, these authors have stated that copper films of small but measurable catalytic activity can be prepared by evaporating in hydrogen on to a surface at − 183° C and that such films, on warming to room temperature do not sinter entirely because they retain some of the adsorbed hydrogen.

The present observation, that films which are deposited in vacuum on a surface at − 183° C and saturated with oxygen at this temperature give up practically no oxygen on being warmed to room temperature, is clearly an extreme case of the behaviour described by them, arising from the greater chemical affinity of oxygen compared with that of argon, nitrogen or hydrogen.

They have also shown that the amount of carbon monoxide taken up at − 183° C by nickel films deposited in a good vacuum on a glass surface at room temperature increases linearly with increasing weight of the film. The straight line given by them for the adsorption of carbon monoxide has a slope of 1·25 × 10^{20} molecules per gram.* The present measurements with oxygen admitted to copper films deposited and maintained at − 183° C show a similar relation. The straight line obtained by plotting the results has a slope of 1·4 × 10^{20} molecules per gram. It is clear, therefore, that the surface area of a copper film deposited at − 183° C and maintained at this temperature is comparable with that of a nickel film of the same geometric area and weight deposited at room temperature. These results are of considerable relevance to discussions of the catalytic activity of copper films.

---

* In these graphs the number of molecules adsorbed on a given geometric area is plotted against the weight of metal in the film of the same area, and the slope has, therefore, the units of molecules per gram.

The results obtained with films deposited at room temperature are of particular interest in connection with recent ideas on the low-temperature oxidation of metals. At − 183° C and at − 78° C the number of molecules taken up per cm.^{2} is approximately equal to the number which would correspond to a single adsorbed monolayer assuming free (111) copper surfaces, but at 20° C and at 74° C the number of molecules taken up per cm.^{2} strongly suggests that oxidation is actually proceeding. This is also borne out by an examination of the curves in Fig. 2 in which the number of molecules taken up per cm.^{2} is plotted against time for the temperatures − 183° C, 20° C and 74° C. The equilibrium values at 20° C and 74° C correspond respectively, to oxide thicknesses of 24 Å and 76 Å if the density of the cuprous oxide is taken as 6 g. cm.$^{-3}$.

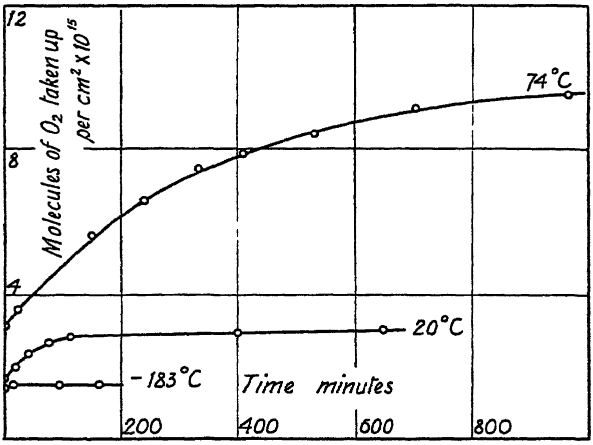

FIG. 2.

We are greatly indebted to J. H. Burrow and D. A. Jones who made the glass apparatus used in these experiments. We also wish to acknowledge a research scholarship granted to one of us (J. A. A.) by the Australian National University.

H. H. Wills Physical Laboratory,
University of Bristol.

DETERMINATION OF HEATS OF ADSORPTION USING METAL FILMS

BY O. BEECK, W. A. COLE * and A. WHEELER †

Received 15*th February*, 1950

A calorimeter is described suitable for the determination of heats of adsorption of gases and vapours on evaporated porous metal films. The heats of adsorption of hydrogen as a function of fraction of surface covered are given for nickel and iron films at room temperature and at liquid air temperature. A criterion for mobility of the adsorbed layer is presented and the value of heat of adsorption measurements in the study of catalysis is discussed.

---

* Now on the teaching staff of Los Angeles High Schools.

† Now with E. I. du Pont de Nemours and Company, Experiment Station, Wilmington, Delaware.

Since heterogeneous catalysis always involves adsorption in one or several ways, e.g. of reactants, activated complex, products or poisons, measurement of heats of adsorption offers a powerful tool to measure the interaction of catalyst and adsorbate. In fact, in the absence of a quantitative extension of the present theories of the solid state to surface states, experimental heats of adsorption are the most direct and reliable measure of the strength of bonds in the adsorbed state.

In continuation of the work with metal films [1] the apparatus and method to be described was developed in 1940 and has since been used in numerous investigations.

Experimental

Apparatus and Method.—The calorimeter employed is shown in Fig. 1. The lower part of the inner tube, the calorimeter proper, is made from a very thin glass tube and is further etched with hydrofluoric acid to make the tube as light as possible (low heat capacity). Tubes of about 1·5 to 2 cm. diameter were used with a weight of 3 to 5 g. for 10 cm. length. About 4·5 m. of 3 mil. platinum wire (about 100 ohms) were wound over the last 10 cm. of tube right to the bottom and cemented on with a thin layer of sodium silicate (or better with the commercial product Sauereisen, which has the same heat capacity). This wire served as a resistance thermometer. The metal film was deposited on the inside of the tube from an electrically heated hairpin-shaped wire. The weight of the film was determined by weighing this wire before and after the experiment. The weight of the total assembly was determined by cutting the glass tube as close as possible to the upper end of the platinum resistance thermometer windings. From the known weights and specific heats of the components (film, glass, thermometer wire, and cement), the total heat capacity was computed and could easily be kept below 1 cal./°C.

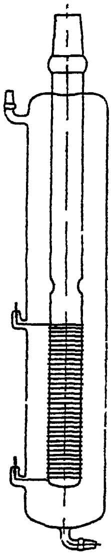

FIG. 1.—Schematic sketch of heats of adsorption calorimeter.

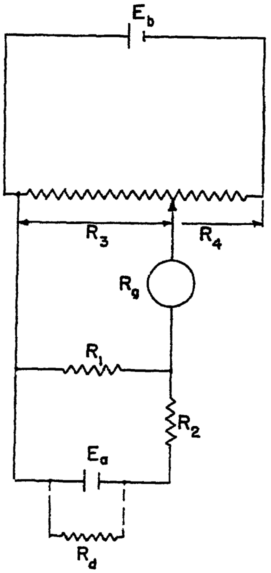

FIG. 2.—Circuit diagram for calorimeter.

Fig. 2 shows the measuring circuit for the Pt thermometer. E_a and E_b are batteries, R_1 is the resistance of the thermometer, R_2 a resistance to regulate the measuring current through the thermometer, R_g the resistance of the galvanometer (Leeds and Northrup Type HS, 16 ohms), R_3 and R_4 are the arms of a

---

[1] Beeck, Smith and Wheeler, *Proc. Roy. Soc. A*, 1940, 177, 62.

Leeds and Northrup Type K_2 potentiometer, and Rd a resistance across E_a which can be adjusted to equalize small drifts of the two batteries.

It can be shown that if S is the sensitivity of the balanced circuit, i.e. the galvanometer deflection d in mm. caused by changing the potentiometer reading 10^{-4} off balance, the heat of adsorption

$$H = \frac{60{\cdot}6C(R_1 + R_2)d}{aR_2nS},$$

where n is the number of molecules adsorbed times 10^{-18}, C the heat capacity of the calorimeter tube, and a the temperature coefficient of resistance of pure platinum which is $3{\cdot}52 \times 10^{-3}$ at room temperature (23° C) and $1{\cdot}76 \times 10^{-3}$ at $-$ 183° C, but which was actually experimentally determined for each of the several calorimeters constructed.

There is some uncertainty as to the heat capacity of Pyrex glass at $-$ 183° C; but since the heat capacity of this glass is very close to that of sodium silicate (or Sauereisen) at room temperature, its specific heat at $-$ 183° C was taken to be equal to that of sodium silicate at $-$ 183° C which is 2·5 times lower than at room temperature.

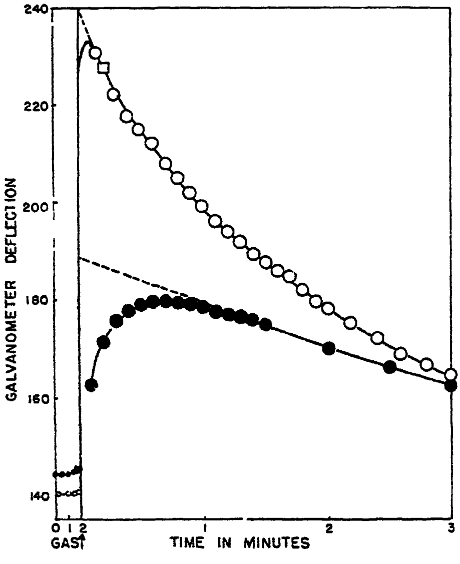

FIG. 3.—Typical calorimeter cooling curves.

In a typical experiment the apparatus is evacuated at 500° C for 2 hours, cooled and the metal film deposited with cooling water running through the outer jacket. After the electrical connections are made (enclosed in glass tubes), the outer jacket is evacuated, thus turning the apparatus into a vacuum calorimeter. A thermostat is then raised immersing the entire calorimeter and filament assembly. The thermostat temperature is adjusted to room temperature ± 0·1° C. After equilibrium is established, admission of 0·1 mm. helium should cause less than 1 mm. galvanometer deflection. If, for instance the heat of adsorption of hydrogen is studied, this gas is stored in a reservoir connected with a McLeod gauge at about 0·1 mm. pressure (McLeod bulb and connecting line is usually sufficient for capacity). In the beginning of the experiment the galvanometer drift is followed by frequent readings for several minutes. Then a small amount of hydrogen is admitted to the evacuated catalyst tube by opening a stopcock for a few seconds. Galvanometer readings are now taken as often as possible (about every 0·1 min.) until the galvanometer has returned to its starting equilibrium position. Fig. 3 shows the resulting cooling curve (circles). Hydrogen is adsorbed instantaneously for several increments admitted leaving no residual pressure in the catalyst tube as indicated by a Pirani gauge connected to it. With subsequent addition of hydrogen, pressure will build up in the catalyst tube and is taken into account in computing the number n of hydrogen molecules adsorbed as calculated from the known volumes and pressures of both the reservoir and the catalyst chamber. The sensitivity S is determined after each experiment, although S remained constant to ± 1 % over long periods. In general the films were saturated to a final equilibrium pressure of 0·1 mm. (final coverage or total coverage, see Discussion).

Since in most cases the heats of adsorption decrease with fraction of surface covered and since gas increments admitted give average heat values for each increment, average coverages were calculated. If three increments gave 30 %, 50 % and 100 % (0·1 mm. equil. pressure), the average coverage for these adsorption increments was taken as 15 %, 40 %, and 75 %

$$\left(\text{i.e. } \frac{30}{2}\ \%,\ \frac{30+50}{2}\ \%, \text{ and } \frac{50+100}{2}\ \%\right),$$

and these values were plotted against the heat of adsorption. With ethylene, self-hydrogenation and polymerization made definition of total coverage meaningless and in this case the heats of adsorption were plotted against total number of molecules adsorbed minus 1/2 the molecules of the last increment.

Extrapolation of the galvanometer cooling curves presents no difficulty if adsorption is fast ($<$ 0·1 min.) and can be made graphically with an accuracy better than ± 1 %, as with hydrogen in Fig. 3 (circles). If adsorption is slow, however, as for nitrogen on iron at room temperature * (Fig. 3, black points), extrapolation can be done more accurately by fitting the experimental cooling curve to the analytical expression

$$D = \frac{a}{b-c}(e^{-ct} - e^{-bt}),$$

which was derived by representing the rate of heat input by an exponential term and the rate of heat loss by a term proportional to the galvanometer deflection D, so that

$$dD/dt = ae^{-bt} - cD.$$

The constant c can be evaluated from the theoretical cooling curve of the calorimeter which is satisfactorily represented by the experimental case of fast adsorption, while b can be evaluated from rate of adsorption data.

Discussion

Fig. 4 shows the heat of adsorption of hydrogen as a function of surface covered. This example gives a good idea of the accuracy and reproducibility of the method since 16 different films were used, half of them oriented and half unoriented.

Space does not permit to discuss fully here the present state of our knowledge of hydrogen adsorption. Beeck, Ritchie and Wheeler[2] and Beeck, Ritchie and Givens[3] have shown that two types of sorption of hydrogen exist—adsorption which is very fast even at 15° K (low activation energy), and *ab*sorption into the structure which is slow and whose rate is temperature dependent (high activation energy). It has also been shown that the low-temperature adsorption of hydrogen at 80° K, which is practically constant between 10^{-4} and 10^{-1} mm. pressure, is a true measure of the surface[2] since no measurable *ab*sorption takes place at this temperature, although the total sorption at room temperature and 0·1 mm. pressure shortly after admission was found to be almost identical with the adsorption at 80° K. This means that at room temperature and 0·1 mm. a small amount of hydrogen is *ab*sorbed, making the heat of adsorption too large. The heat of *ab*sorption of hydrogen into the nickel lattice was further studied on sintered nickel films with a small surface and was found to be considerably lower than the heat of adsorption (see

---

* It is of interest to note that this is the only case of slow " activated " adsorption that was observed in studies of many gases on many metals, all others being too fast (very low activation energy or less than 1 kcal./mole) or definitely proven to be *ab*sorption into the structure (see also [4]).

[2] Beeck, Ritchie and Wheeler, *J. Colloid Sci.*, 1948, **3**, 505.

[3] Beeck, Ritchie and Givens, *ibid.*, (in press).

the comprehensive discussion of this subject by Beeck [4]). It would thus be expected that the heat of adsorption at − 183° C (where no *ab*sorption takes place) would decrease to much lower values for 100 % coverage

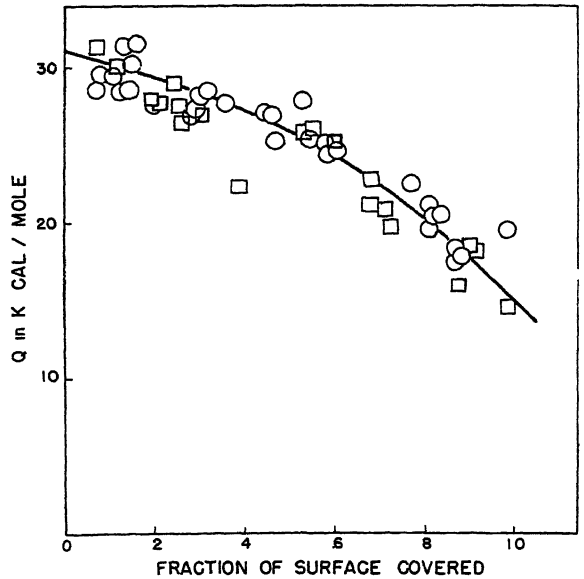

Fig. 4.—Heat of adsorption at 23° C of hydrogen on evaporated nickel films as a function of surface covered.

○ Oriented films ; ☐ Unoriented films.

at − 183° C than at room temperature. This is fully borne out by the data in Fig. 5, which not only show that the original estimate of extent of surface of the metal films [1] is well founded, but that the heats of adsorption at room temperature and at − 183° C are identical and that

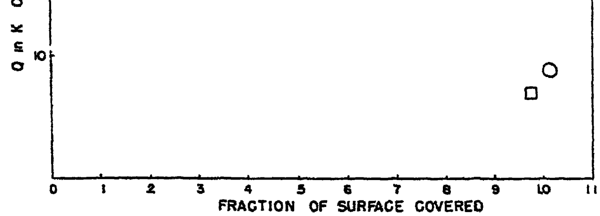

Fig. 5.—Heats of adsorption of hydrogen at − 183° C on evaporated nickel films (points) in comparison with the heat of adsorption at 23° C (curve) as a function of surface covered.

---

[4] " Catalysis and Adsorption of Hydrogen " by Beeck in *Advances in Catalysis*, Vol. II (Academic Press, New York, 1950).

the *ab*sorption or solution does not take place at room temperature until 75 % of the surface is covered.

The heats of adsorption of hydrogen as a function of fraction of surface covered and those of ethylene as a function of molecules adsorbed are shown in Fig. 1 and 2 of this Discussion.* It is seen that the initial heats of adsorption on a sparsely covered surface increase from rhodium to tungsten. All heats decrease with fraction of surface covered and the slopes of the curves are steeper for metals with high initial heats than for

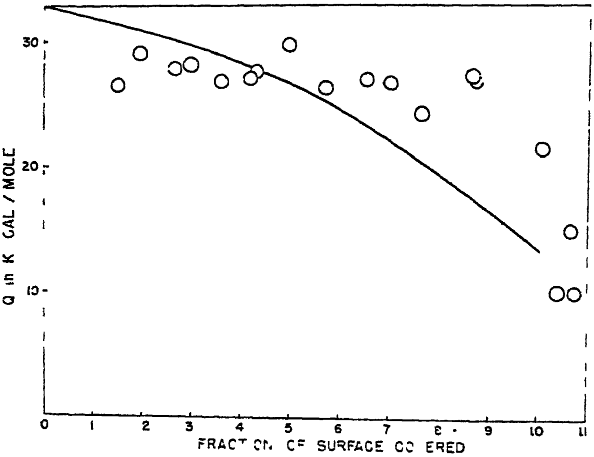

FIG. 6.—Heats of adsorption of hydrogen on evaporated iron film at − 183° C (points) in comparison with the heats obtained at 23° C (curve) as a function of surface covered.

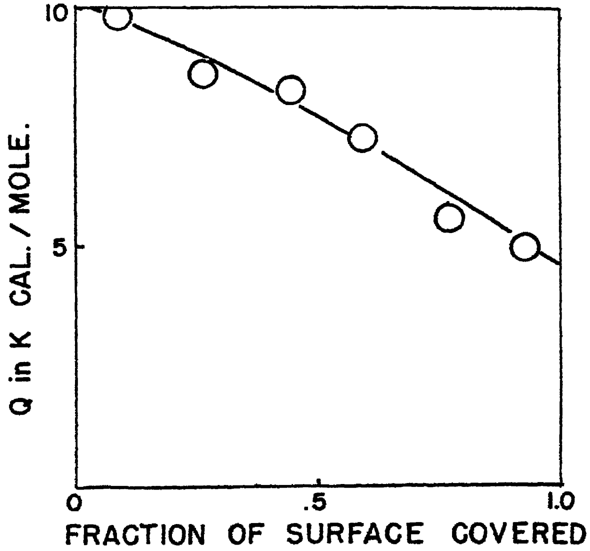

FIG. 7.—The heat of adsorption on iron at − 196° C as a function of surface covered.

---

* *Hydrogen Catalysis*, This Discussion.

those with low heats. (The slope of the curve for hydrogen on tantalum is especially steep due to relatively large absorption into the structure, and the shape of the ethylene adsorption curves is influenced by self-hydrogenation and polymerization.) It has been concluded that the decrease of heat of adsorption of hydrogen is due primarily to the interaction of adsorbed atoms with neighbouring sites and not due to intrinsic energetic heterogeneity of the sites, although such heterogeneity can easily be produced by foreign atoms on the surface (poisons) or will certainly be present in surfaces of substances which contain several atomic species (alloys, oxides, etc.) where different atoms might be exposed by the surface. Arguments in favour of this conclusion have been discussed in great detail by Beeck,[4] where a criterion for mobility (migration from site to site) of adsorbed atoms is also given.

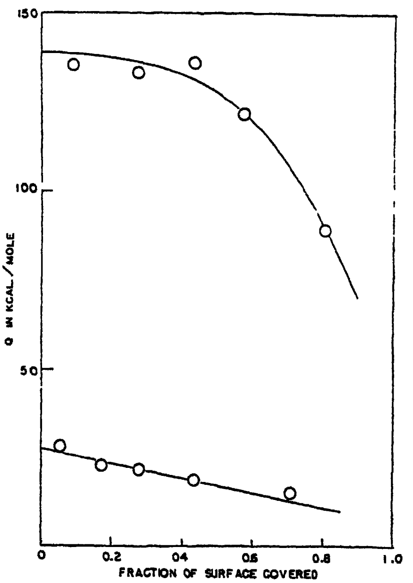

FIG. 8.—Heats of adsorption on tantalum (upper curve nitrogen, lower curve hydrogen on top of nitrogen).

This criterion for mobility is based on the reasoning that if the heats of adsorption decrease with fraction of surface covered, atoms adsorbed on a sparsely covered surface must have taken positions far apart from each other in spite of the fact that all molecules make their access to the internal surface through the same pores from the outside of the film and would be expected to be adsorbed on the first free sites available so that the heats of adsorption on a well-covered surface are high. If these heats were relatively low, distribution of adsorbed atoms could of course proceed through evaporation and readsorption. This, however, is not possible for hydrogen on nickel at − 183° C, so that migration alone must in this case be the reason for deposition of the atoms far enough apart for maximum energy of adsorption.

The behaviour is different for hydrogen on iron (Fig. 6) where the initial heats of adsorption at room temperature are only slightly higher than on nickel, but where the heats of adsorption at − 183° C are constant over the whole surface until a sharp decrease occurs when the surface is completely covered. In this case (no migration) the incremental heats represent average values, each new increment filling up completely a new section of the internal surface of the film.

Fig. 7 shows the heat of adsorption of nitrogen on iron at − 183° C. Similar results were obtained with nickel. The unexpected high heat is in excellent agreement with the fact that the adsorption isotherm at this temperature has a relatively flat portion between 10^{-3} and 10^{-1} mm. pressure.[1, 4] As a consequence, nitrogen cannot be used for these and other clean metals in the evaluation of their surface by the B.E.T. method. A detailed discussion of this subject has already been given.[4]

Fig. 8 shows the heat of adsorption of nitrogen and of hydrogen on top of nitrogen on tantalum at room temperature. As previously mentioned, hydrogen itself is not only strongly adsorbed but also *ab*sorbed into the structure to so large an extent that 860×10^{18} molecules per 100 mg. film (deposited at room temperature) are sorbed at 1·3 mm.

gas pressure. However, when nitrogen with its high heat of adsorption is pre-adsorbed ($11{\cdot}5 \times 10^{18}$ molecules per 100 mg.), only 73×10^{18} molecules of hydrogen per 100 mg. of tantalum are adsorbed with a much lower heat of adsorption than on clean tantalum. Slow *ab*sorption into the structure is absent in this case, the surface adsorption of nitrogen blocking completely the solid structure for *ab*sorption. Tungsten and iron, which also adsorb nitrogen, do not adsorb hydrogen on top of nitrogen at room temperature unless the surface is not completely covered, in which case the rest of the surface can be covered with hydrogen.

Shell Development Company,
Emeryville,
California.

THE MEASUREMENT OF THE THERMAL PROPERTIES OF GASES AND VAPOURS ADSORBED ON SOLID SURFACES

BY J. A. MORRISON AND J. M. LOS

Received 16th January, 1950

A description is given of a low-temperature adiabatic calorimeter suitable for the measurement of thermal properties of gases and vapours adsorbed on solid surfaces. The calorimeter was designed particularly for the determination of the heat capacity and the heat of adsorption of adsorbed films with rather high precision.

An interest in the measurement of the thermal properties of adsorbed films arises from a consideration of the utility of a knowledge of the thermodynamic properties in evaluating theories of adsorption. In addition, direct information may be obtained concerning the state of the adsorbed film, and the magnitude of the interaction between the elementary particles of the adsorbate and the adsorbent may be construed. Recently, Hill[1] has given an extensive treatment of the thermodynamics of adsorption. While some of the quantities used in this treatment are not ordinarily measured calorimetrically, for example, one usually measures C_p rather than C_v, by appropriate rearrangement of the relationships one can arrive at other thermodynamic quantities from the experimentally determined values. Of some interest is the entropy, from a knowledge of which may come information concerning the distribution of energy of adsorption sites.[2]

For the heat capacity measurements the assumption is made that the thermal properties of the adsorbent are unchanged by the adsorption process. While there is no experimental evidence concerning the point, it seems likely that the assumption is valid for physical adsorption provided that the specific surface of the solid is not too large, but it may be seriously in error for chemisorption.

To be used in testing theories of adsorption, the measurements should be performed with as high accuracy as is possible. In the heat capacity measurements, where the heat capacity of the film is obtained as a difference, the requisite precision is only obtained at quite low temperatures where the contribution of the heat capacity of the film to the total is a reasonable fraction. While this factor necessarily makes the experimentation somewhat more difficult, it leads to the use of simple

[1] Hill, *J. Chem. Physics*, 1949, **17**, 520.

[2] Hill, *ibid.*, 1949, **17**, 762.

gases such as argon and nitrogen as adsorbates, which is desirable from the viewpoint of interpretation of results. It would be equally desirable to use a very elementary solid as adsorbent, but here one is limited by requiring a total surface such that the effects being measured are sufficiently large. So far it has not been possible to obtain simple solids with a sufficiently high specific surface and recourse is had to titanium dioxide (rutile) of reasonably high chemical purity.

In what follows is described the calorimeter assembly which is being used to investigate the adsorption of argon on titanium dioxide.

Experimental

A number of adiabatic low-temperature calorimeters have been described in the literature. While in principle all are similar, in detail there are rather important differences which depend upon the specific purpose for which the calorimeter is to be used. The measurement of the heat capacity and the heat of adsorption of vapours adsorbed on solids places some special requirements upon the calorimetric apparatus, and in particular upon the calorimeter vessel itself. The adiabatic design is certainly the most suitable since the adsorption processes taking place in the calorimeter vessel may require a rather long time to reach equilibrium due to unfavourable heat conduction between the particles of the solid or to slow changes taking place on the surface of the solid. With the adiabatic type of low-temperature calorimeter, properly designed, it is possible to determine total heat capacities with a precision of 0·1 % or better even if a half hour or longer is required for equilibrium to be reached. The requirement of outgassing the solid adsorbent in place in the calorimeter vessel at an elevated temperature makes it necessary that the vessel be easily accessible and that surrounding components be detachable. This is not ordinarily necessary in calorimetry where condensable substances are studied.

In a previous investigation Morrison and Szasz [3] described a calorimeter which was used to measure the heat capacity of adsorbed nitrogen. Several features of that design have been incorporated in the present one particularly in the design of the calorimeter vessel. However, the present design embodies sufficient departures to warrant an adequate description. Since the amount of liquid hydrogen available for the work was small, advantage was taken of a cryostat design used by Yost *et al.*[4]

Cryostat.—The cryostat assembly and details of the calorimeter vessel and associated parts are illustrated in the sectional drawings in Fig. 1. The main assembly is hung within the Dewar flask 2, in which liquid nitrogen is kept normally. The flask rests inside the outer case 1, the lower part of which is detachable from a flanged joint. The upper part of the case is held in a frame a sufficient distance from the floor to enable removal of the lower section without disconnection of electrical leads and vacuum lines. Not shown in the drawing are tubes set into the brass top plate which permit the introduction of the liquid nitrogen to the Dewar flask and the connection of the case to a high-capacity Kinney oil pump used for reducing the temperature below 77° K by pumping on the liquid nitrogen. Liquid hydrogen is introduced through the syphon 5 into the container 4 which is supported inside a vacuum space enclosed by the can 3. Gaseous hydrogen which is evolved is led through tube 7 to a vent system. Connection is also possible between this tube and the Kinney pump when it is desired to reduce the temperature to that of solid hydrogen. The heat leak into the hydrogen container is reduced by making all connections to it with thin-walled stainless steel tubing.

Adiabatic Shield and Calorimeter Vessel.—The adiabatic shield 15 which is made of copper sufficiently thick to have a uniform temperature, is of the form commonly used in low-temperature calorimeters. The top and bottom are detachable from the cylindrical side at flanged joints. The shield and the calorimeter vessel 17 are hung by Nylon cords within a vacuum space enclosed by the container 10, which is fastened to the hydrogen container with low-melting solder. Evacuation of the space is accomplished with a high capacity vacuum line connected to tube 6. A similar vacuum line is connected to the space surrounding the hydrogen container through a tube not shown in the

---

[3] Morrison and Szasz, *J. Chem. Physics*, 1948, **16**, 280.

[4] Yost, Garner, Osborne, Rubin and Russel, *J. Amer. Chem. Soc.*, 1941, **63**, 3488.

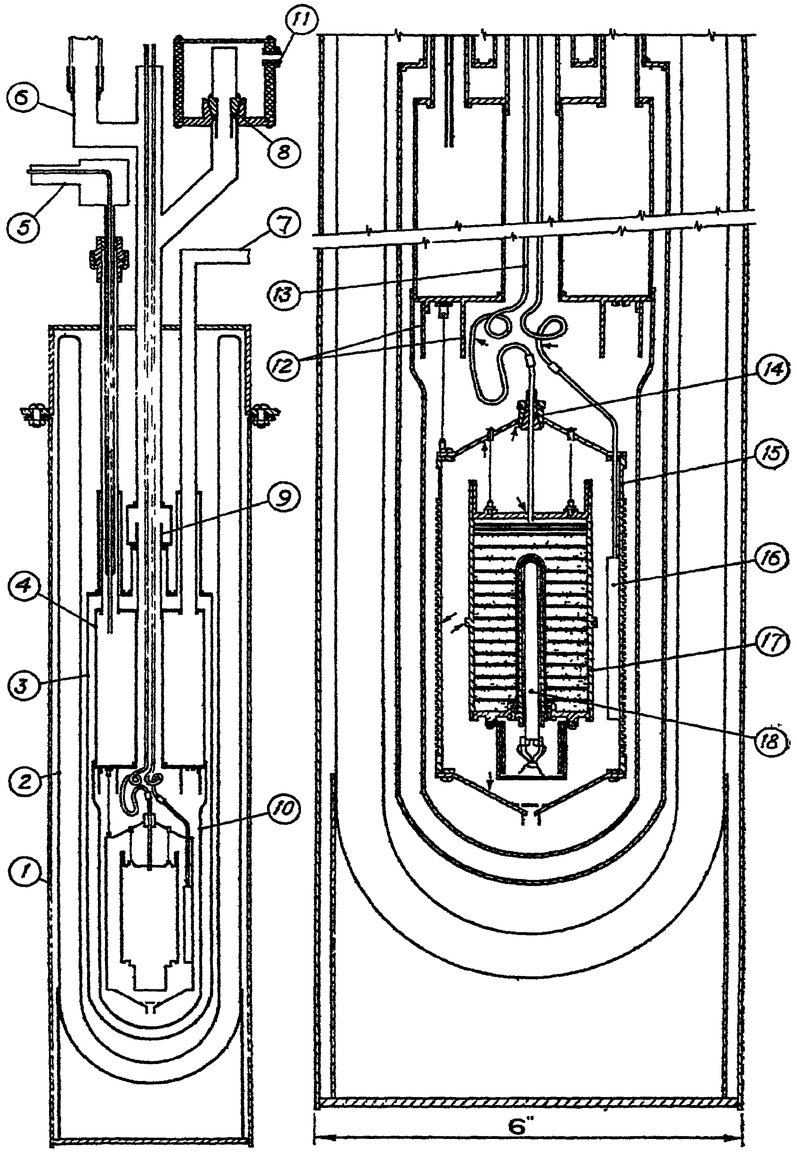

FIG. 1.—Low-temperature adiabatic calorimeter assembly.
1. Monel metal case. 2. Silvered Pyrex Dewar flask, $4\frac{1}{4}$ in. int. diam. × 24 in. inside depth. 3. Brass container (3/64 in. wall thickness). 4. Brass liquid hydrogen container, 680 cm.^{3} volume. 5. Vacuum-jacketed metal syphon. 6. Vacuum line connection. 7. Hydrogen vent line. 8. Vacuum seal for lead wires. 9. Brass anchoring ring at liquid nitrogen temperature. 10. Copper container (1/32 in. wall thickness). 11. Brass clamps for lead wires. 12. Anchoring rings at temperature of hydrogen container—inner ring $\frac{1}{8}$ in. thick brass, outer ring 1/32 in. thick copper. 13. Copper nickel filling tube (2 mm. ext. diam. and 1 mm. int. diam.). 14. Brass tapered joint. 15. Adiabatic shield, 1/16 in. thick copper. 16. Vapour pressure thermometer bulb, 7 cm.^{3} volume. 17. Calorimeter vessel, 1/16 in. thick aluminum, 90 cm.^{3} volume. 18. Platinum resistance thermometer.

drawing. Cooling of the assembly is accomplished by admitting a small pressure of helium, 1 or 2 mm. of mercury, to these spaces. When liquid hydrogen is used the parts within the container 3 are first cooled to the temperature of solid nitrogen. The helium is then removed from the space between containers 3 and 10 and the liquid hydrogen admitted to the container 4. When the calorimeter reaches the desired temperature the helium is removed from the space inside container 10. With the vacuum lines used the pressures of helium can be reduced to less than 1×10^{-5} mm. of mercury within 3 min.

The cylindrical calorimeter vessel is made of pure aluminum, and is sealed by electric welding of the rim of the dished lid. The powdered solid adsorbent is packed not too tightly between thin perforated aluminum discs which make a sliding fit with the cylindrical wall. The dished top construction permits changing of the solid adsorbent in that the vessel may be opened by cutting off the welded seam in a lathe and may be resealed subsequently by welding. The resistance thermometer 18 enclosed in a platinum thimble (5 mm. diam., 70 mm. long and 0·2 mm. wall thickness) is cast into a brass tube with Woods metal. The calorimeter heater of glass-covered manganin wire is wound on the outer surface of the platinum thimble near the upper end and is thus held in the Woods metal. The outer surface of the brass tube is accurately machined with a 1° taper which fits closely a similar taper on the inner surface of the re-entrant well of the calorimeter vessel. A threaded piece at the lower end of the thermometer assembly engages a ring on the brass tube in such a way that it will either tighten or loosen the tapered connection. This design has the distinct advantage of providing a metallic conducting path between the thermometer and heater and the calorimeter vessel. The leads from the thermometer and from the heater are wrapped around a cylindrical aluminum shield surrounding the glass cap of the thermometer to ensure their departure at the temperature of the calorimeter. The calibration of the resistance thermometer may be checked periodically by direct comparison of the thermometer with a vapour pressure thermometer. The bulb of the vapour pressure thermometer 16 is attached to the adiabatic shield, and into it may be condensed pure oxygen or pure hydrogen.

Electrical Wiring.—The electrical leads enter the cryostat through a vacuum seal 8. Forty-two leads of 30 AWG silk-covered copper wires rest in shallow grooves cut longitudinally in a brass male plug which fits a female piece of similar taper, and the small space remaining around the wires is filled with Apiezon wax. Heavier leads from the measuring system which are soldered to the leads coming out of the cryostat are brought in through ten brass clamping pieces 11. The assembly was first used for the intercomparison of resistance thermometers where twelve extra leads were required, so for calorimetry only thirty leads are used. The wires are wrapped twice around the brass ring 9 and held in place with Glyptal lacquer, which step serves to bring the wires to the temperature of liquid nitrogen and hence to minimize the loss of liquid hydrogen due to heat leaking along the leads. The loss could be further reduced by using finer wires but in the present instance where considerable manipulation of the lower part of the wire assembly was necessary the use of sturdy leads seemed desirable. Contact of the wires with the hydrogen container is made by wrapping the wires individually on two rings 12 attached to the bottom of the hydrogen container. The assembly was first tried with just the inner ring but this did not provide a sufficient path to reduce the temperature of the wires and the second ring was added. From the rings 12, the wires are carried in a series of loops to the adiabatic shield. The thermocouple, thermometer and calorimeter heater leads going to the inside of the shield are wrapped in spiral grooves around the cylindrical side of the shield starting near the top and enter through hard rubber insulators near the bottom. The outer surface of the three components of the shield, the top, bottom and side, are covered with electrical heaters close wound and held in place with Glyptal lacquer. Electrical heaters are also wound on the two tubes leading to the calorimeter vessel and to the vapour pressure thermometer bulb, and on the bundle of lead wires just before it reaches the top part of the side of the shield.

The positions of the difference thermocouple junctions are indicated by arrows on the drawing. Single junction difference thermocouples of Chromel P and constantan extend between the side of the adiabatic shield and five other parts, the two capillary tubes, the bundle of leads, the top and the bottom of the shield. Between the side of the shield and the calorimeter vessel is placed a three junction Chromel P constantan couple. A similar three junction couple is placed between the junction of the tube with the shield 14, and the point where the tube is attached to the calorimeter vessel. These latter two are the most important of the difference thermocouples and hence are made of greater sensitivity.

Filling Tube Assembly.—Gases or vapours are admitted to the calorimeter through the capillary tube 13. Control of the temperature of the tube is attained by balancing the heater wound on the tube against a thermal shunt (5 cm. of 18 AWG copper wire) fastened between the tube and the inner of the two rings 12. Connection of the shunt to the tube is made above the upper loop shown in the drawing and in such a way as to avoid having a cold spot on the tube. The shunt is placed under the winding of the tube heater and insulated from the tube with paper for a distance of 2 cm. before being soldered to the tube. A similar shunt is attached to the tube leading to the vapour pressure thermometer bulb 16. However, for calorimetric measurements this latter tube is left disconnected. Thermal contact of the calorimeter tube with the adiabatic shield is made with a tapered connection 14, which is tightened with a screw device. This joint may be undone to permit raising of the top part of the shield when a furnace is placed around the calorimeter vessel for degassing the adsorbent.

Since much better control of the temperature of the assembly may be exercised by heating rather than cooling it is desirable to measure heats of adsorption rather than heats of desorption. In the measurement of the heat of adsorption it is necessary that the gas be at the same temperature as the calorimeter vessel before adsorption. An estimation of the heat exchange between the gas and the tube indicated that sufficient exchange was obtained in 15 cm. of the tube. Such a length is provided in a loop just above the adiabatic shield.

Operation.—Adiabatic conditions within the assembly are maintained by manual adjustment of the energy admitted to the electrical heaters on the three components of the adiabatic shield, on the two tubes and on the bundle of leads. The control of the energy put through the various components is made in such a way that the indications of the array of difference thermocouples are kept at zero. The potentials of the thermocouples are read from two galvanometers of such sensitivity that for the triple junction couples temperature differences of 0·002° at 15° K or 0·0005° at 90° K can be detected. With maintenance of the indications of the thermocouples as near to zero as possible, the temperature of the calorimeter vessel may be held constant within 0·001° for lengthy periods at all temperatures 0·5° or more above the temperature of the hydrogen container.

The resistance of the thermometer and the energy admitted to the calorimeter heater are determined with a White double potentiometer. Standard resistors used in the circuits are checked periodically against standards calibrated at the National Bureau of Standards. The establishment of a temperature scale for a series of resistance thermometers, one of which is used for the calorimetry, will be described elsewhere. The time of energy input to the calorimeter heater is determined with a synchronous clock run on a controlled frequency power supply and operated with a switch coupled directly to the heater switch. Calibration of the clock is made by direct comparison with time signals from the Dominion Observatory.

Liquid hydrogen is made from compressed hydrogen in cylinders with a liquefier of the type used by Andrews [5] at a rate of about 1 l. hr. A single filling of the liquid hydrogen container in the cryostat is sufficient for 5 hr. of experimentation.

For most measurements two operators are required, one of whom adjusts the adiabatic controls continuously. When pressure measurements are also required, a third operator is necessary.

The authors are indebted to Mr. G. Clement of the Central Workshops who made most of the component parts of the assembly. Thanks are due to Mr. R. Reid and Mr. G. Ensell of the Laboratories for technical assistance.

Division of Chemistry,
National Research Laboratories,
Ottawa, Canada.

---

[5] DeSorbo, Milton and Andrews, *Chem. Rev.*, 1946, **39**, 403.

ADDENDUM.—The calorimeter has been designed for the purpose of examining systems involving physical adsorption only, but in its present form it could be used for some particular measurements of heats of chemisorption. The modification of the assembly for other experiments involving chemisorption would require, principally, alteration of the design of the calorimeter vessel.

The operation of the calorimeter has been tested by a rather extended series of measurements of the heat capacity of the calorimeter vessel plus the solid adsorbent only, the heat capacity ranging from 0·6 joules/deg. to 60 joules/deg. The average precision as determined by the deviation of some 40 experimental heat capacity values from a smoothed C_p against T relationship for the temperature range 12° to 92° K was found to be 0·04 %. Below 30° K the precision falls to about 0·1 % due to lowered sensitivity of the resistance thermometer. It seems reasonable to expect that for a limited temperature range above 30° K a precision of 0·01 % could be achieved, which compares favourably with any other form of precise calorimetry. In most of the heat capacity measurements a small correction, 0·02 % on the average, was made for heat exchange between the calorimeter vessel and the adiabatic shield. About 98 % of this heat exchange takes place across the section of the filling tube between the calorimeter vessel and the shield, and the correction is calculated from the indications of the sensitive difference thermocouple placed across this section.

Some measurements have been made of the heat capacity of adsorbed argon at a concentration corresponding to a coverage of the surface of about 0·4. The absolute increment in the heat capacity due to the adsorbed argon varies from 0·25 joules/deg. at 14° to 0·7 joules/deg. at 75° K, and the precision of the calorimeter is such as to permit the measurement of the increment to approximately 1 % of its value. Only a limited number of measurements of heats of adsorption have been made at low coverages of the surface but the values so far obtained appear to be internally consistent to better than 0·5 %. The results of these thermal measurements and their significance will be discussed elsewhere.

STUDIES IN CONTACT POTENTIALS

II. VIBRATING CELLS FOR THE VIBRATING CONDENSER METHOD

By J. C. P. MIGNOLET

Received 2nd February, 1950

Cells are described for measuring surface potentials of films adsorbed on evaporated metal deposits using the vibrating condenser method of Zisman.[1] Essentially they are electrically-driven, hollow tuning forks. Sources of error are pointed out and precautions to be taken, given. The accuracy is ± 1 or 2 mV on individual contact potential measurements and ± 10 or 20 mV on surface potential determinations.

A number of cells for the vibrating condenser method have been described.[1, 2, 3] Two of them are suitable for work in vacuum, but neither is adapted for work with metal deposits prepared *in situ* by thermal evaporation. The Zisman cell can certainly be developed in that direction. However, the writer had preferred to start from a new type of basic cell.

---

[1] Zisman, *Rev. Sci. Instr.*, 1932, **3**, 367.

[2] Potter, *Physic. Rev.*, 1940, **58**, 623.

[3] Frost and Hurka, *J. Amer. Chem. Soc.*, 1940, **62**, 3335. Rosenfeld and Hoskins, *Rev. Sci. Instr.*, 1945, **16**, 343.

Experimental

The Hollow Vibrating Fork Cell.—This cell is essentially a hollow tuning fork. One of the condenser plates is fixed to the inner wall of one limb and vibrates with it. The immobile plate is fixed to the top of the cell (Fig. 1). The second limb, bearing a piece of iron sheet, serves for the electrical excitation of the vibration. The fork is made asymmetrical to allow easy introduction and removal of the non-vibrating electrode. A T-shaped cell would do as well. A very rigid fixation of the fork tail is necessary. This is achieved by a series of 5 side tubes sealed with Picein in an iron block of about 40 kg.

For a cell in Pyrex having the dimensions given in Fig. 1, the fundamental frequency parallel to the plane of the **h** is about 450 c./sec. The length of the side limb is not critical for good resonance. Hence, the fundamental frequency can be slightly modified by altering the length of the side limb and leaving the condenser limb untouched. The glass cells stand an amplitude of 0·7 mm. or more. Since the condenser plates are 0·1 to 0·3 mm. apart there is no risk of the cell breaking in normal operating conditions. We have adapted the hollow fork cell for studying adsorption on metal deposits prepared by thermal evaporation. In this case, the metal must be deposited on one of the condenser plates and not on the other. Accordingly one of the plates has to be removed during deposition and brought back for measuring. Two types of cell have been used in which the non-vibrating plate is displaced magnetically.

Type I Cell.—Here, the non-vibrating plate moves in its plane by flexion of its support (Fig. 2). The plate bears a long iron rod fixed to the tungsten lead by a pair of parallel thin tungsten wires disposed in a plane perpendicular to that of the plate. The displacement is actuated by a magnet which attracts the iron rod and thus bends the two parallel tungsten wires. Two non-overlapping positions are determined by two stops. Fig. 3 shows a cross-section of the condenser limb. The non-vibrating plate is a little less than half as wide as the vibrating plate and defines two distinct " areas " on the latter. A metal film can be deposited on either area by passing a current through a hair-pin

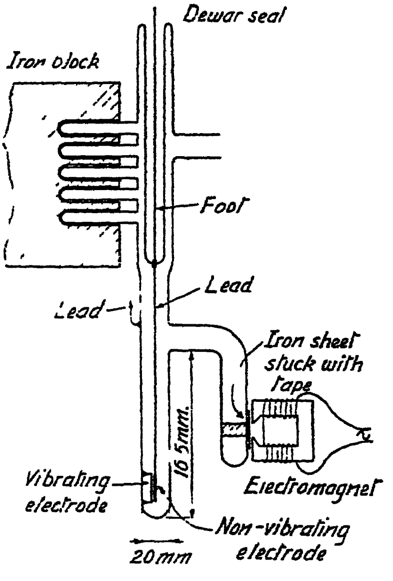

FIG. 1.—Basic cell.

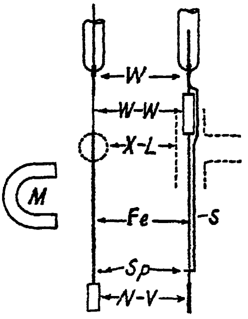

FIG. 2.—Interior of type I cell (filament and filament leads not shown).

W,	tungsten lead
WW,	pair of tungsten wires, diam. 0·3 mm.
XL,	excitation limb
S,	support of the stops
Fe,	iron rod ; M, magnet
Sp,	stops
N—V,	non-vibratingplate.

filament, the leads of which (not shown) are sealed in the foot. The vibrating electrode consists of a nickel foil 0·3 mm. thick welded to two tungsten strips, the ends of which are sealed to the wall. The lead is a 0·3 mm. tungsten wire. It is welded on the upper strip. It crosses the wall a little higher and is stuck on to the external wall (through a glass sheath) on a length of about 10 cm.

The condenser tube is covered from the junction with the side limb to the bottom with a metallic (nickel) deposit. This shield is prepared by thermal evaporation in a preliminary operation, the vibrating plate being protected by a screen.

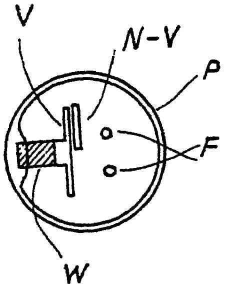

FIG. 3.—Type I cell.

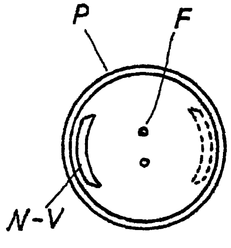

FIG. 4.—Type II cell.

P, Pyrex tube, diam. 20 mm. ; W, tungsten strip ; F, filament ; V, vibrating plate ; N—V, non-vibrating plate.

Broken line represents second position of N—V (Fig. 4).

Type II Cell.—In this, the metal is deposited on the glass wall (Fig. 4). The non-vibrating electrode is moved by rotation around the axis of the tube. The axle is a long, straight tungsten rod (diam. 1·5 mm.) sealed in the foot (Fig. 5).

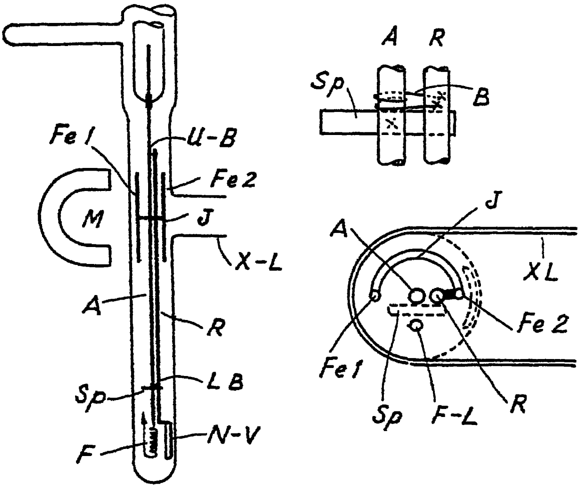

FIG. 5.—Type II cell.

Details of lower buckle and stop (crosses indicate welds).

Cross-section of condenser tube at level of junction with excitation limb.

Dotted lines are vertical projections of lines not in the plane.

A, axle ; R, rotating tungsten rod ; U—B and L—B, upper and lower buckles ; Fe 1 and Fe 2, main and secondary iron rods ; J, junction between Fe 1, Fe 2 and R ; Sp, stop ; F, filament (second lead not shown) ; F—L, filament lead ; N—V, non-vibrating electrode ; M, magnet; X—L, excitation limb.

It also serves as a lead for the filament. The rotating system includes a tungsten rod (diam. 1·5 mm.) to which are spot-welded :

(*a*) the non-vibrating electrode (through a nickel strip) ;

(*b*) two molybdenum wire buckles fitting snugly around the axle for guiding the rotation. The lower buckle rests on a small horizontal piece of tungsten rod welded to the axle and serving a double purpose : (i) it prevents the rotating system from falling ; (ii) it acts as a stop, limiting the rotation of the tungsten rod to half a turn and thus defines two positions of the non-vibrating electrode;

(*c*) two iron rods which, together with an external magnet, produce the rotation. The main iron rod is the one at 180° of the non-vibrating electrode. Since the axle is slightly flexible, pushing the magnet nearer to the main iron rod draws the electrode away from the wall. This has two advantages : (i) it provides a means of adjusting the distance between the electrodes ; (ii) during the rotation from one position to the other, the electrode is held apart from the metal deposit and does not scratch it. The second iron rod helps to reduce the condenser spacing in case of an inaccurate adjustment of the axle.

In one of the two positions of the magnet, the excitation limb is in the way. This difficulty is obviated by choosing a magnet with a gap wide enough for the excitation limb to pass through. The condenser tube is covered internally with a nickel deposit (shield) from the junction with the excitation limb to about 2·5 cm. of the bottom. The lower part is metallized during the experiment proper. Electrical contact with the vibrating electrode is effected through the shield and a small tungsten helix sealed about 1 cm. below the junction.

Sources of Error and Perturbating Effects

Induction from the Electromagnet on the Cell and Amplifiers.—Shielding and grounding eliminates electrostatic but not magnetic induction Fortunately, there is a simple way of obviating this based on frequency doubling, i.e. the property of a non-polarized electromagnet to excite the vibration of a mechanical system at double the frequency of the current. Since the induction has the frequency of the excitation current, and the signal due to contact potential has the frequency of the mechanical vibration, separation can be effected by selective amplification. Actually, we use a band-pass filter which eliminates induction from the mains as well. Of course, the second harmonic of the excitation current must be small.

Triboelectricity.—Friction between the leads and glass or rubber gives rise to irregular, and sometimes enormous, effects. Since even apparently immobile parts of the cell may vibrate a little, it is advisable to avoid loose contact between the leads and non-conductors. They must be sealed or kept apart. For instance, the leads in the foot tube cannot be isolated with either glass or rubber sheaths. They are kept at a distance from one another and from the glass wall only by the seal and by a Pyrex bead at the top. For the same reason, in type I cell the lead of the vibrating plate has to be stuck on to the glass wall.

Electrostatic Effects.—The inner wall of the condenser tube must be metallized, otherwise the measured contact potential varies with the hygrometric or electric state of the outer wall. As an extreme case, rubbing the tube with a cloth produces an effect equivalent to that of a contact p.d. of a few hundred volts. The shield also eliminates effects due to the inner glass wall which would not be detected so simply. So far, it has not been necessary to metallize the inner wall of the foot, but it would probably be a good precaution in very accurate work.

Stray Vibrating Capacities.—Clearly, the capacity between the immobile electrode and the opposite area is only part of the capacity of the system connected to the grid of the amplifier. No error is caused provided that the surfaces forming the stray capacities do not vibrate appreciably. The question is primarily one of crowding. From that point of view type II cell is better than type I cell. Edge effects are also present and as a test the distance between the electrodes can be changed when the measured contact potential should not vary.

Miscellaneous Details.—The equipment used comprises the following items : (i) for exciting the vibration, an oscillator and a push-pull amplifier when 18 W secure ample reserve of energy ; (ii) for amplifying the signal, a pre-amplifier (one 4060 Philips triode, battery operated), a three-stage amplifier (three 1T4 pentodes, battery operated), a band-pass filter for 450 c./sec. and finally an oscillograph.

In good operating conditions, successive measurements agree to ± 1 or 2 mV, but the sensitivity may fall to ± 10 mV or worse in some conditions (scaling-off the deposit, excessive frosting around the condenser tube in experiments at low temperatures, etc.). The accuracy obtained for surface potentials is ± 10 or 20 mV as judged from the results on H and Xe films (see Part I). The same cell can be used for several series of experiments. For cleaning and replacing of the filament, the cell is cut just under the Dewar seal.

Discussion

The problem of designing a cell for the Zisman method is firstly one of vibration. Zisman makes a plate vibrate in an immobile tube. We prefer the reverse solution, i.e. make a tube vibrate with an immobile plate in it, because then there is no need to introduce the vibration into the cell. The hollow vibrating cell is perhaps simpler as regards construction and production of the vibration. It seems more suitable for work in high vacuum since it contains no thin metallic diaphragm liable to cause trouble during the outgassings at 500° C. It has one weakness, it does not work with the condenser tube immersed in a viscous bath. This drawback, though real, is not important for fluid baths, e.g. liquid-air at low temperature, vapour baths at high temperatures, are available. In adsorption studies it is normal to study the variation of single surfaces, but since contact potential techniques require two surfaces, an auxiliary surface * has to be introduced. Then it is essential that its work function be known and above all remain constant. This may be a problem in itself or indeed the major problem. The value of contact potential as a tool[4] in surface reactions on solids depends much on the practical possibilities of eliminating the auxiliary surface or of preventing it from changing. Perhaps a discussion of this question in relation with the cells described here is not superfluous. A surface undergoes a certain change and we propose to determine the difference in work function between the initial and final states. An interesting possibility exists if two surfaces, one in the initial and the other in the final state can be prepared and kept side by side in the same atmosphere (vacuum or gas). Then either they may be used directly as the condenser surfaces or two contact p.d. measurements may be made, using the same auxiliary surface. The stability of the latter can be controlled by measuring alternately with the two surfaces. For instance, for non-volatile films, a metal layer may be deposited on one area of a cell of type I or II and covered with gas ; another metal layer deposited on the area and left bare. The difference between the two yields the surface potential of the film.

When the change in the state of a surface is to be observed directly, care must be taken to prevent a simultaneous variation of the auxiliary surface. Once again, the case of non-volatile films is fairly simple. Measurements can be made in a vacuum and a bare metal (mostly tungsten which can be cleaned at will) chosen for the auxiliary surface. This is the solution adopted in the two-filament methods of Langmuir and Kingdon,[5] Reiman[6] and Bosworth and Rideal.[7] It would be worth while developing vibrating cells offering that possibility too.†

---

* The non-vibrating electrode in cells of type I and II.

[4] Bosworth : *Proc. Roy. Soc. N. S. W.*, 1946, **79**, 53.

[5] Langmuir and Kingdon, *Physic. Rev.*, 1929, **34**, 129.

[6] Reiman, *Phil. Mag.*, 1935, **20**, 594.

[7] Bosworth and Rideal, *Proc. Roy. Soc. A*, 1937, **162**, 1.

† Incidentally, a hair-pin ribbon hanging near the wall could serve both as a source of metal and as an auxiliary surface. The ribbon could be drawn away from the wall for deposition and brought back for measuring.

The case where the surfaces have to be in a gas is more difficult, at least theoretically. In the author's opinion the situation is as follows. There is no general, satisfactory way of preventing the auxiliary surface from changing when the temperature, pressure or composition varies. In actual practice, however, since inert, poisoned surfaces are more readily obtained than active surfaces, it will be frequently possible to find a surface that, in a limited range of conditions, varies much less than the surface under investigation, e.g. massive nickel outgassed at 500° C and a bare nickel deposit relative to additions of H_2, C_2H_4 or C_2H_2, etc. As a first approximation, the effects observed may be attributed to the bare surface.

A limited control is possible with the two-area cells, where one area is available for it. The control area should be poisoned too but in a different way so as to get a control measurement different from zero. Then good constancy of the control measurement during an experiment is strong evidence that the auxiliary surface has not changed appreciably. Eventually, the experiment will have to be repeated with a chemically different auxiliary surface.

Sometimes, it will be possible to get a control at some stage by freezing the film and applying methods available for non-volatile films.*

I wish to express my deep gratitude to Prof. L. D'Or for help, encouragement and advice ; and to Prof. M. Dubuisson for facilities in the early stage of this research. I also wish to thank Messrs A. Debot, J. Haesen, and J. Sarlet for skilful technical help.

Laboratoire de Chimie générale,
Université,
Liége,
Belgique.

* This would be an additional reason for developing cells with a hair-pin ribbon (of tungsten) as the auxiliary surface.

SEMI-CONDUCTIVITY AND CATALYSIS

By T. J. Gray

Received 19*th January*, 1950

The adsorption and interaction of gases on semi-conductors leads to a variation in semi-conductivity which can be successfully applied to the study of adsorption catalysis. Fundamental information is simultaneously furnished regarding the semi-conductivity process. An experimental technique is described for a study of the adsorption of gases by variation in semi-conductivity.

Although von Auwers and Kerschbaum [1] observed the effect of oxygen adsorption on copper oxide systems, the significant work on this system was due to Jusé and Kurtschatow,[2] Wagner and co-workers,[3, 4, 5] and Dubar.[6] The work of Anderson [7] extended the observations of the effect of adsorbed gases to various other systems.

---

[1] von Auwers and Kerschbaum, *Ann. Physik*, 1930, **7**, 129.
[2] Jusé and Kurtschatow, *Physik. Z. Sowj.*, 1932, **2**, 453.
[3] Wagner, *Z. physik. Chem.*, 1933, **22**, 181.
[4] Dunwald and Wagner, *ibid.*, 1933, **22**, 212.
[5] Wagner and Hammen, *ibid.*, 1938, **40**, 197.
[6] Dubar, *Ann. Physique*, 1938, **9**, 5.
[7] Anderson, *Proc. Roy. Soc. A*, 1945, **184**, 83.

The application of the effect of adsorbed gases on semi-conductivity to a study of catalysis has already been described.[8, 9, 10] A technique has been developed whereby semi-conductors can be examined during the adsorption, desorption or interaction of gases under conditions for which a high degree of reproducibility is possible.

The current theory of semi-conductivity [11, 12] relates the conductivity at any temperature to a function of the number of defects. The variation of conductivity with temperature is related to the activation of electrons either into surface levels with the production of a positive hole carrier, or into the conduction band from impurity levels in the case of intrinsic semi-conductors. The variation of conductivity during the adsorption and desorption of gases can, therefore, be taken as directly related to the amount of gas present on specific sites on the surface contributing to the conduction process.

A study of the adsorption of gases requires a consideration of the initial adsorption of gas molecules, dissociation, surface diffusion and final interaction with the surface. Some or all of these stages may be involved and the overall rate of adsorption may be dependent on one or several stages. Although measurements of semi-conductivity may be considered as related to the final stage, a study of the kinetics of adsorption of oxygen on the copper oxide system has demonstrated the suitability of the method in helping to elucidate the various steps in the adsorption mechanism.

Simultaneously the temperature coefficients of conductivity of the systems under varying conditions of adsorbed gas yields inormation relating to the surface energy levels associated with the conduction process and any variation which may occur in these levels from interaction or other cause. This leads to general information relating to the surface which is of particular significance in the general problem of adsorption.

Orthodox methods of investigation of adsorption processes have normally introduced the measurement of the amount of gas adsorbed and frequently an estimate of the surface area by the B.E.T. or other method. The areas involved in semi-conductivity measurements on films are of the order 50 sq. cm. superficial area, so that special methods are essential for the measurement of amounts of gas adsorbed. Expansion from calibrated bulbs at low pressure into accurately calibrated apparatus has been unsuccessful. It may be possible to measure the amount of adsorption by controlled diffusion of hydrogen or oxygen into the system through palladium or silver thimbles respectively. This particular method is applicable to those systems where the incremental change of semi-conductivity on the adsorption of a gas is independent of pressure within certain limits for any particular temperature.

The technique to be described covers the development of a greaseless reaction system containing the catalyst in the form of a glass-supported oxide film between conduction electrodes formed from an evaporated film of metal. The gas handling system has been developed with special attention to the measurement of very small quantities of gas adsorbed and desorbed. Resistance measurements are described for D.C. and A.C. by equipment capable of high accuracy with maximum speed of operation.

Experimental

Several forms of reaction tube have been designed and described. The general form comprises a glass cylinder on to which a uniform metal film can be evaporated from a metal plated tungsten filament at the axis of the cylinder. The

---

[8] Garner, Gray and Stone, *Proc. Roy. Soc. A*, 1949, 197, 294.
[9] Gray, *ibid.*, 1939, 197, 314.
[10] Garner, Gray and Stone, *Trans. Faraday Soc.*, 1949, 00, 000.
[11] Mott and Gurney, *Electronic Processes in Ionic Crystals* (Oxford, 1948).
[12] Seitz, *Modern Theory of Solids* (McGraw-Hill, New York, 1940).

inner surface of the hard glass cylinder carries a series of conduction electrodes in the form of rings of thermal pure platinum foil fused into the surface at suitable intervals. The leads for the conduction electrodes are of 26 S.W.G. platinum

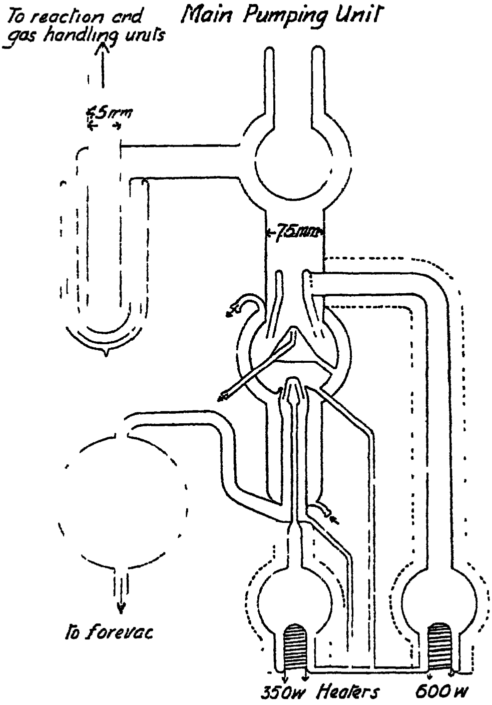

FIG. 1.

and lead out through intermediate seals (C 9 to C 19) to the resistance measuring apparatus. Thermocouples are connected to several of the conduction electrodes.

The pumping system for this investigation requires special attention since very high pumping speeds are required to enable the pressure in the reaction

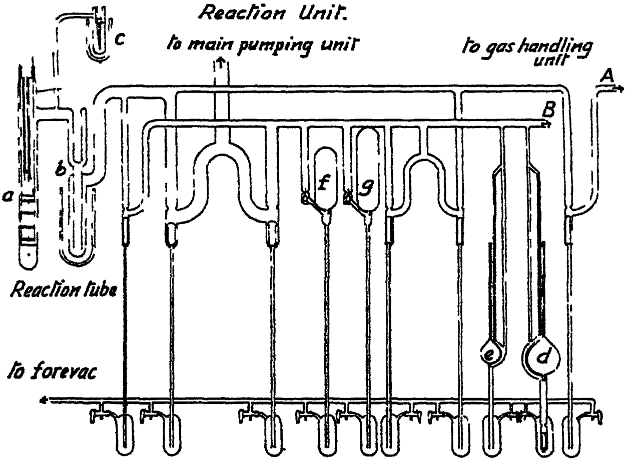

FIG. 2.

system to be reduced from 0·5 mm. to 10^{-7} mm. in 10-15 sec. A two-stage mercury vapour pump, Fig. 1, has been developed with separate boilers for the primary umbrella jet and the secondary high pressure annular ring jet. The use of inner and outer cooling surfaces for the annular ring jet materially improves the pumping speed. Twin liquid oxygen traps are employed as protection for the reaction system. The unit is backed by a two-stage rotary oil pump.

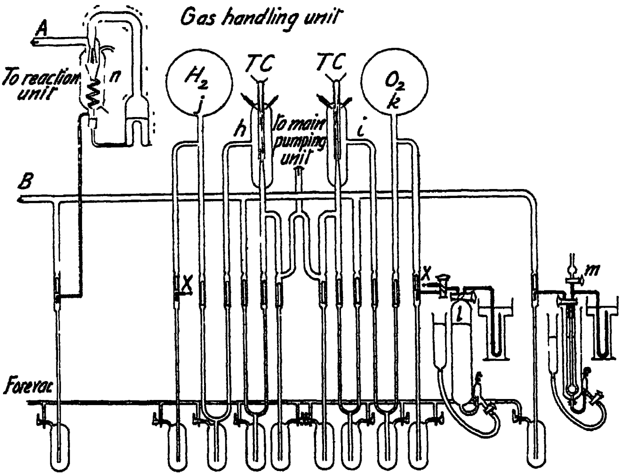

FIG. 3.

The main reaction system is illustrated in Fig. 2. The reaction tube *a* is protected from mercury vapour by dual liquid oxygen traps *b*. Large bore mercury cut-offs connect the tube with the main pumping lead or with the measuring and gas handling sections. A Pirani gauge *c* is included in the reaction tube unit. The measuring unit includes two McLeod gauges *d*, *e*, covering the range 10^{-6} mm. to 15 mm., and two expansion bulbs of calibrated volume *f*, *g*. This unit, together with the associated mercury cut-offs, is housed in an air thermostat and can be operated externally. At one end it connects with the reaction tube system and at the other with the gas handling and desorption unit which is externally mounted (Fig. 3). This unit provides facilities for admitting

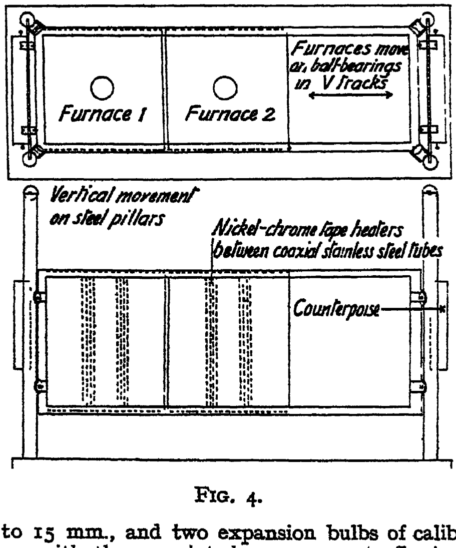
Furnace 1
Furnace 2
Furnaces move on ball-bearings in V tracks
Vertical movement on steel pillars
Nickel-chrome tape heaters between coaxial stainless steel tubes
Counterpoise

FIG. 4.

hydrogen or oxygen through the heated palladium or silver thimbles respectively *h*, *i*, these gases being stored in the reservoirs *j*, *k*. A gas inlet system *l* is provided and a calibrated gas burette *m*. The desorption mercury vapour diffusion pump *n* is of the triple jet variety and returns the desorbed gas to the measuring system inside the air thermostat.

The furnace unit (Fig. 4) incorporates two separate temperature regulated furnaces arranged to permit horizontal and vertical motion. Each furnace is constructed of two heavy walled stainless steel tubes with an exponentially wound nickel-chrome heater between the tubes insulated by asbestos and alundum. These are heavily lagged with asbestos and mounted in angle iron frames. Horizontal movement is facilitated by the use of large ball-bearings in V tracks with precision location of the furnace bores. Vertical movement is taken on four steel columns with a counterweight system. The furnace temperature is controlled by A.C. resistance thermometer controller operating from a nickel resistance thermometer adjacent to the reaction tube. The control is better than 0·05° C at all operating temperatures, although the control unit operation limit is better than 0·001° C and maintains heavier furnace units to ± 0·01° C cycle as measured by a Smith's Difference Bridge.

Measurements of Resistance.—A review of the methods previously employed in the measurement of the resistance of semi-conductors revealed no one method completely satisfactory for the projected measurements. The range of resistance to be covered is 10^{-2}-10^{12} ohms, with an accuracy of 0·1 % to 10^7 ohms and 1 % to 10^{12} ohms. In addition, the readings must be extremely rapid, variations of 5×10^5 to 5×10^4 ohms in less than one minute being encountered with active films. It is also desirable to have A.C. and D.C. measurements available to ensure the absence of any rectifying action. Two units have been developed, the first an A.C. Wheatstone bridge and the second an electronic potentiometer for D.C. measurements.

A.C. Resistance Bridge.—Many A.C. Wheatstone bridges have been described, mainly in relation to conductance measurements, important contributions being due to Jones and Joseph,[13] Shedlovsky[14] and Luder.[15] In general, satisfactory precision was obtained by controlling phase relationships, electrostatic and electromagnetic coupling by suitable screening circuits and the use of the Wagner earth. However, the bridges so far described are relatively slow in operation and have not the range coverage for the study of semi-conductors. The bridge which has been developed employs normal ratio arms but the standard arm is replaced by two precision helical potentiometers (0·05 % accuracy), each having 15 revolutions rotation covering 5400°. The value of these is 1000 ohms and 100,000 ohms. The bridge is fed at mains frequency with an adjustable metered voltage up to 10 V. The output from the bridge is taken by cathode follower, a high-gain amplifier and phase splitter, to the *Y* plates of a cathode ray tube with the *X* sweep operated at mains frequency. After adjustment of the amplifier, a horizontal line is obtained for zero signal input, signal input being visible as inclination of the trace. The system has the additional advantage that phase shift in the bridge circuit immediately appears as an elliptical trace instead of a line and immediate correction may be made. Very satisfactory bridge balancing is obtained up to 10^8 ohms. Although a higher frequency of operation for the bridge would have been preferred, the relatively high and varying inductance of the 100,000 ohm helical potentiometer prevents its use above about 200 c. sec. In practice the bridge gives an accuracy of 0·1 % up to 10^7 ohms with a deterioration to 0·5 % between 10^7 and 10^8 ohms; this is combined with extreme rapidity of measurement.

D.C. Resistance Measurements.—Although for preliminary work a precision Köhler potentiometer was used with standard resistances for D.C. resistance measurements, it was found that the time required for measurements was prohibitive. An electronic potentiometer has been developed with direct indication of 1 to 10 mV full scale deflection. This, in conjunction with a potential source and standard resistors, gives direct readings of resistance from 0·01 ohm to 10^{12} ohms. The instrument is illustrated in Fig. 5. It consists of two bridge circuits, the first being tubes V_1 and V_2 and the resistor train R, while the second bridge is the current amplifying bridge V_3A, B and V_4A, B connected across the output of the first. The first bridge acts as a Schmitt voltage amplifier, while the second bridge acts as a current amplifier to permit connection to a current

[13] Jones and Joseph, *J. Amer. Chem. Soc.*, 1928, **50**, 1049.

[14] Shedlovsky, *ibid.*, 1930, **52**, 1793.

[15] Luder, *ibid.*, 1940, **62**, 89; *Rev. Sci. Instr.*, 1943, **14**, 1.

measuring instrument. Output is either by a pointer instrument or by galvanometer and scale, the accuracy of the final resistance measurement being limited by the method of display. By suitable design the input tube is operated at a grid current of less than 10^{-12} A and normal operation gives an output of 100 μA for 10 mV input, although this can be increased 10-fold when required, with some sacrifice of stability. The potential drop across standard resistors is measured using the standard as a grid resistor with the unknown in series and with a suitable applied potential. With the maximum standard grid resistor normally employed, 5×10^6 ohms, the current in the resistor is greater than 100 times the grid current for a resistance of 10^{12} ohms, which can thus be measured to 1 %.

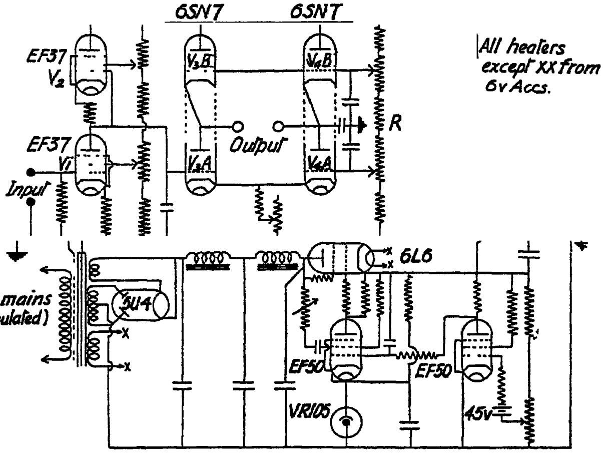

FIG. 5.—Electronic Millivoltmeter.

The unit is spring mounted and supplied from a two-stage degenerative power supply with a stability of 1 in 25,000 ; all heaters are supplied by accumulator. After the initial warm-up period of one hour an accuracy of better than 1 % can be indefinitely maintained in the higher resistance region with considerably improved accuracy up to 10^8 ohms.

General Method of Study.—The initial requirement in the present method of investigation is the successful plating of the parent metal of the oxide under investigation on to the 0·25 mm. tungsten evaporation filament. It is found that no difficulties are encountered in plating tungsten providing the wire is cleaned by A.C. electrolysis in 10 % caustic soda, washed carefully and immediately plated. A wide variety of cells have been used with the tungsten wire at the axis and the anode in the form of a cylinder or several rods distributed on the circumference of a circle with the tungsten wire at the centre ; diaphragm cells have been used where applicable. Normal plating technique is employed except that the current density is increased from 2-5 times and agitation is obtained by nitrogen fed through the glass tube supporting the filament.

The plated wire is carefully washed and spot welded into the reaction tube with the minimum delay. The reaction tube is thereafter rapidly reconnected to the reaction system and evacuated. After thorough degassing, the filament is raised to just below evaporation temperature in the presence of atomic hydrogen obtained by high frequency discharge. This treatment cannot be unduly prolonged as the atomic hydrogen rapidly penetrates the glass.

Evaporation is then performed in hard vacuum by controlled heating at very slow evaporation rates. Uniformity is judged by the simultaneous appearance of the first transmission colour over the entire surface and by comparison of resistances between electrodes immediately measurement becomes possible. Thickness control is by resistance although actual thickness estimates are obtained subsequently by chemical analysis of the film after removal from the reaction system.

The evaporated metal film is next oxidized to the appropriate condition and the oxidation process followed by resistance measurements and pressure change. Frequently atomic oxygen obtained by high-frequency discharge is employed. The oxide film is processed to a semi-conducting condition and is then subjected to prolonged evacuation at 10^{-7} mm. at a suitably selected temperature until a stationary value of resistance has been established. This stationary value is afterwards used as a reference value and the film is normally returned to this reference condition between successive adsorptions.

The general procedure is to determine the temperature coefficient of the evacuated film and investigate any variation with oxidation state. Thereafter the characteristics of the adsorption of oxygen are determined over a range of temperatures and pressures, with particular attention to any modification of the surface resulting in non-reproducible results. During this investigation a maximum temperature is normally established, above which the state of the surface is liable to change. A suitable temperature can then be selected to obtain the greatest range of investigation. Temperature coefficients of the conductivity for varying states of adsorbed gases are determined, together with the kinetics of the processes concerned. Although desorption is studied at various temperatures, the final desorption of the film is always carried out at the reference temperature. A detailed account of the results obtained for the adsorption of oxygen on the copper oxide system has already been given. The effect of variations of pressure is studied in detail and measurements of the amounts of gas adsorbed and desorbed made where possible.

When the characteristics of the adsorption and desorption are determined, interaction of gases can be followed as described for carbon monoxide on copper oxide and the reaction between carbon monoxide and oxygen. Difficulty is, however, experienced in that the effect of such interaction may affect the surface, as does, in fact, occur in the above case at 200° C.

The author wishes to express his thanks for grants from Imperial Chemical Industries Ltd. and from Distillers' Company Limited.

Dept. of Inorganic and Physical Chemistry,
The University,
Woodland Road,
Bristol 8.

PROTON RELAXATION AND CATALYST ACCESSIBILITY

BY P. W. SELWOOD AND F. K. SCHROYER

Received 24th January, 1950

The *accessibility* of a solid catalyst may be defined as the ratio of activity shown by a fixed weight of solid catalyst to that of the same weight of catalyst in true solution in the reacting medium. This quantity may readily be evaluated by the nuclear induction experiment. The proton relaxation time in water is determined, for example, for supported iron oxide on alumina. Catalyst accessibility is then found by relating the measured relaxation time to that observed in solutions of ferric sulphate in water. The accessibility is further corrected for 180° shielding on the under side of the surface. The accessibility then becomes $a = 2M_0/M$, where M and M_0 are the apparent molar concentrations of promoter in supported form and in true solution respectively.

This paper is a further progress report on application of the nuclear induction experiment to problems in heterogeneous catalysis.[1] The results given below supplement to some degree the information from magnetic susceptibility measurements on similar systems. In particular, the nuclear induction experiment may be used to compare the extent to which, in different catalyst samples, supported transition group oxides are accessible to the molecules of a reactant. The supported systems studied were ferric oxide, chromic oxide, and cupric oxide, all on high-area γ-alumina. Susceptibility data and some catalytic activity data have already been reported for these systems.[2-4]

---

[1] Spooner and Selwood, *J. Amer. Chem. Soc.*, 1949, 71, 2184.

35835

Experimental

The nuclear induction experiment is that of Bloch, Hansen, and Packard.[5] Their procedure was modified as follows. A raised rim was added to the flat pole pieces of the magnet. This compensates for the radial inhomogeneity of the simple gap.[6] In place of the paddle used by Bloch to regulate the flux linkage between the primary and secondary coils this experiment employs an auxiliary coil, wound coaxially both with the primary and secondary coils which is in parallel with a variable resistance and a variable capacitance. A simple phase shifting network has been added to the external synchronizing signal circuit, and a square-wave generator and an audio oscillator are used to calibrate the oscilloscope sweep. The modulation of the direct current field is accomplished by either a 60-cycle signal from the mains or by an audio oscillator and power amplifier, if other frequencies of modulation are desired. There is no radio frequency amplification in the part of the circuit containing the secondary coil.

Preparation and analysis of samples have been described.[2,4] Preparation consists, in brief, of impregnation of the support by a nitrate solution, followed by ignition. Catalyst samples of different active oxide concentrations were obtained by varying the concentration of the impregnation solution.

For reasons described elsewhere,[7] the catalytic activities of supported oxides are most easily compared at constant space velocity. This is achieved by using the technique of mechanical dilution. To compare the activities of a series of chromia-aluminas of varying chromia content, each sample except the most dilute is mixed mechanically with pure support until all samples contain the same percentage of chromia. A series of samples ranging from 2 to 30 % chromium content would thus all be reduced to 2 %, but they would differ in the proportion of alumina used as a support to that used merely as a mechanical diluent.

For the first results to be given below a sample containing 17·1 % iron as iron oxide supported on alumina was progressively diluted mechanically with alumina. The proton relaxation times were determined as a function of weight of iron in the several samples. The remaining results on supported oxides of iron, chromium, and copper were obtained on samples all diluted to a fixed percentage of active oxide. The actual percentage of supported element in each case is indicated in the Tables. Proton relaxation times are reported as a function of original concentration before mechanical dilution.

In all relaxation studies, 1 g. of catalyst sample was moistened with 1 cm.^{3} of water. Water was chosen as the proton source in all these experiments, which must be regarded as preliminary to studies involving the use of gaseous proton sources.

Results

In Table I there are given relaxation times as a function of iron concentration for a series of iron oxides supported on alumina, and prepared by progressive

TABLE I

PROTON RELAXATION TIMES ON IRON OXIDE–ALUMINA DILUTED FROM 17·1 % IRON

Actual % Fe	T (sec. × 10^3)
17·1	3·90
12·8	5·00
8·55	7·00
4·27	10·8
2·14	15·5

---

[2] Selwood, Ellis and Wethington, *J. Amer. Chem. Soc.*, 1949, **71**, 2181.

[3] Eischens and Selwood, *ibid.*, 1947, **69**, 1590.

[4] Selwood and Dallas, *ibid.*, 1948, **70**, 2145.

[5] Bloch, Hansen and Packard, *Physic. Rev.*, 1946, **70**, 474.

[6] Rose, *ibid.*, 1938, **53**, 715.

[7] Eischens and Selwood, *J. Amer. Chem. Soc.*, 1948, **70**, 2271.

TABLE II

PROTON RELAXATION TIMES ON IRON OXIDE-ALUMINA DILUTED TO 0·2 % Fe

Original % Fe	*T* (sec. × 10³)
0·37	6·9
0·70	8·2
1·0	7·3
2·5	10·7
3·0	12·0
5·8	14·5
9·5	19·5
17·1	30·1

TABLE III

PROTON RELAXATION TIMES ON COPPER OXIDE-ALUMINA DILUTED TO 1·2 % Cu

Original % Cu	*T* (sec. 10³)
1·2	3·55
2·1	5·39
3·3	5·87
4·9	8·80
10·0	12·9

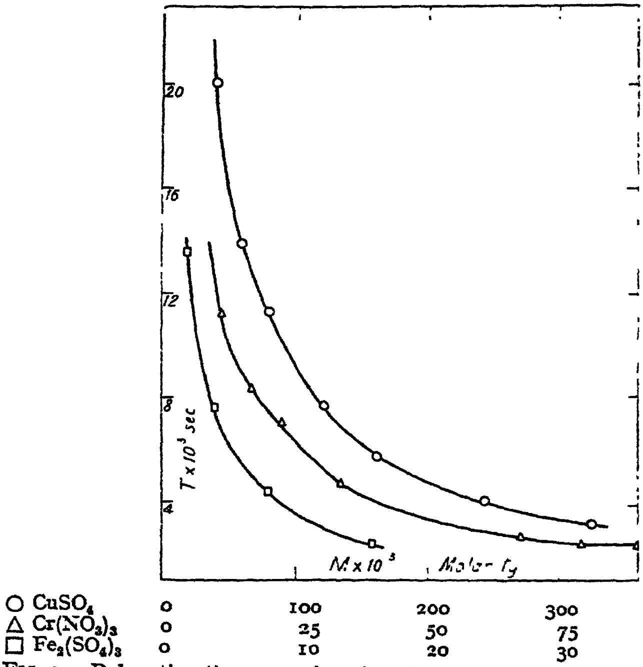

FIG. 1.—Relaxation times as a function of concentration for aqueous solutions of $Fe_2(SO_4)_3$, $Cr(NO_3)_3$, and $CuSO_4$.

mechanical dilution of a sample containing 17·1 % iron. The members of this series differ only in percentage of iron actually present during the measurements.

In Tables II, III, and IV there are given relaxation times for supported oxides of iron, chromium and copper, respectively. These results were obtained by the method described above of diluting the various members of a series down to a fixed concentration. The members of all these series differ in the ratio of alumina used as support to that used as a mechanical diluent.

For reasons to be indicated below it was necessary to remeasure proton relaxation times as a function of concentration for aqueous solutions containing the ions Fe^{+++}, Cr^{+++}, and Cu^{++}. These data are all given in Fig. 1.

Discussion

We shall first compare the relaxation times found over the heterogeneous catalysts with those found for solutions. A convenient method for doing this is to compare molar concentrations of paramagnetic ions necessary to give equal relaxation times for the two cases of heterogeneous and homogeneous catalysis. Thus, we shall say that M is the concentration of supported paramagnetic ions in moles of ions per litre of the water used as a proton source. The concentration is found to give a relaxation time of T. Then M_0 is the molar concentration of an aqueous solution which will also give a relaxation time T. It is assumed that the paramagnetic species is the same in each case ; but if the moment of a supported ion is different from that of the same ion in true solution,[2] then a correction which may be made is

$$T_{\text{corrected}} = T_{\text{measured}}\ (\mu_{\text{supported}})^2/(\mu_0 \text{ in solution})^2.$$

It will be noted that the relaxation time varies inversely as the square of the moment. The only important case in which μ_0 and μ are notably different is for iron oxide where μ is about 70 % of μ_0.

A final term will correct for the fact that a dissolved ion is accessible to protons from all sides, but a supported ion may be reached from one side only. We have then $a = 2M_0/M$, where a may provisionally be referred to as the catalyst *accessibility*.

In Fig. 2 there are given accessibilities for supported iron oxide on alumina, calculated from the data of Table II. It will be noted that the accessibility shows an expected increase as the original iron concentration is diminished. Fig. 2 bears a superficial resemblance to a plot of susceptibility against original iron concentration, but it must be remembered that the measured susceptibility is the average susceptibility of all iron

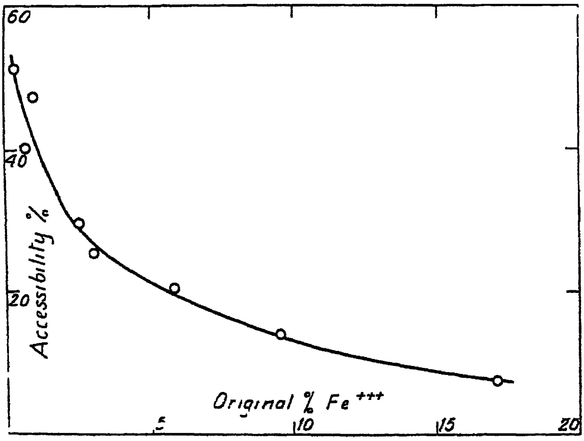

FIG. 2.—Accessibility of iron oxide supported on alumina.

ions in the system, while the relaxation time depends on the moment of those iron ions exposed on the surface, and thus accessible to incoming molecules of reactant.

For supported chromia there are already available catalytic studies on the dehydrocyclization of *n*-heptane.[7] In Fig. 3 there is plotted

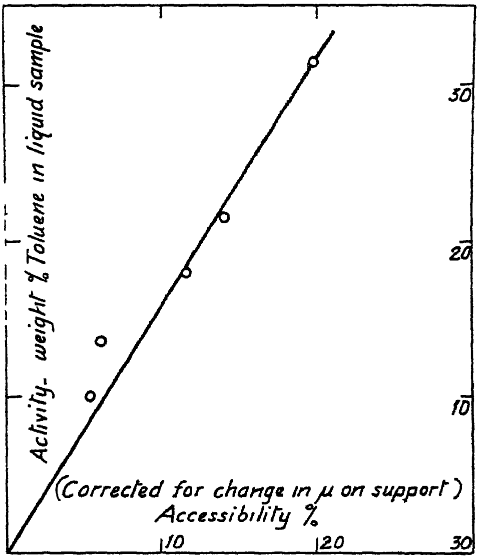

FIG. 3.—Catalytic activity as a function of accessibility for chromia-alumina.

catalyst activity against catalyst accessibility. It is clear from the linear relation observed that for this system and reaction it is possible to predict activity from a measurement of nuclear relaxation.

In Fig. 4 there is plotted the accessibility of supported copper oxide

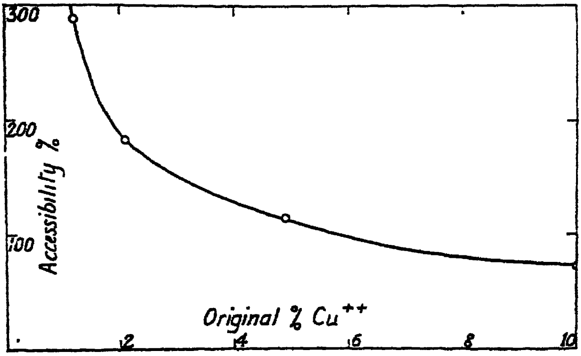

FIG. 4.—Accessibility of copper oxide supported on alumina.

as a function of original concentration. Here we have the anomaly of accessibilities considerably greater than 100 %. This at once illustrates the crudeness of our approach to catalyst accessibility, and suggests how the approach may be refined. Turning to the paper of Bloembergen, Purcell, and Pound,[8] we have reference to their eqn. (54), which is as follows :

$$\frac{1}{T} = \frac{12\pi^2\gamma^2\eta N\mu^2}{5kt}, \quad . \quad . \quad . \quad . \quad . \quad (1)$$

where γ is the gyromagnetic ratio, η the viscosity, N the number of paramagnetic ions per cm.^{3}, μ the effective moment, k the Boltzmann constant, and t the absolute temperature. It is clear from this equation and from the results reported here that the viscosity environment of a water molecule near the surface of a catalyst must be considerably larger than that in normal water. This conclusion is, of course, entirely consistent with current speculations concerning the nature of adsorbed films of water on the active surface. A preliminary measurement of η/η_0 gives the value of 3, (where η is the viscosity factor for the supported ions, and η_0 for the true solution).

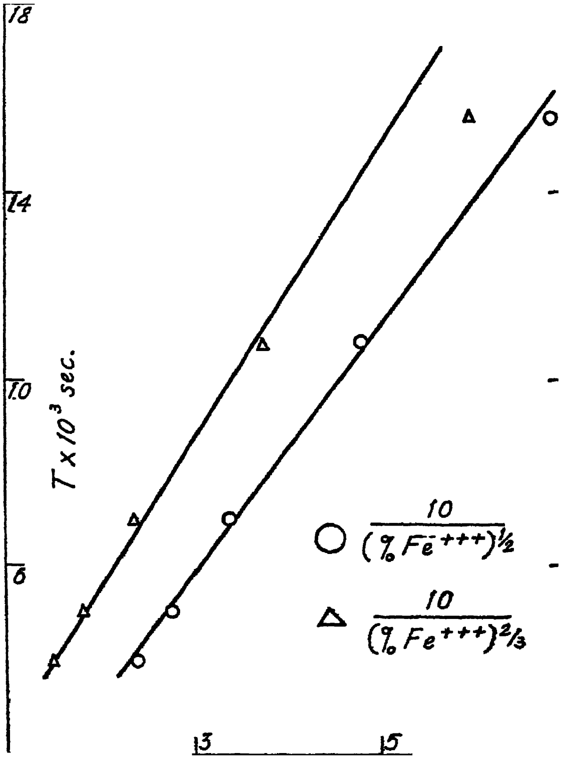

FIG. 5.—Relaxation time as a function of $(\% \text{Fe})^{2/3}$ and of $(\% \text{Fe})^{1/2}$ for iron oxide–alumina.

There will now be presented a provisional theory by which the relaxation times may be predicted for different members of a catalyst series. It will be noted from eqn. (1) above that $1/T \sim N$. The experimental results of Bloembergen, Purcell, and Pound as well as those reported here show that this relation is obeyed over a wide concentration range for iron, chromium, and copper salts in solution. But it is also to be noted that at very low concentrations there is a deviation which is better represented by $1/T \sim N^{3/4}$. The reason for this deviation is not known, but it is believed to be significant in the interpretation of the results on supported oxides given below.

---

[8] Bloembergen, Purcell and Pound, *Physic. Rev.*, 1948, 73, 679.

Examination of the data of Table I where any interaction between adjacent iron ions is constant, shows that $1/T \sim (\%\ \text{Fe})^{2/3}$ over a wide concentration range, but that $1/T \sim (\%\ \text{Fe})^{1/2}$ is obeyed over a wider concentration range. These observations are shown in Fig. 5. It will be noted that $[(\%\ \text{Fe})^{2/3}]^{3/4} = (\%\ \text{Fe})^{1/2}$, and also that the total surface of iron ions exposed must be proportional to $(\%\ \text{Fe})^{2/3}$. Hence it may be said that the exposed surface of the iron particles behaves in the heterogeneous nuclear relaxation experiment in exactly the same way that ionic concentration behaves in the homogeneous experiment.

Let it be assumed then that the function of paramagnetic ions per cm.^{3} in solution is taken by ions per cm.^{2} in the surface of the solid catalyst. We shall further assume that the concentration of such ions in the surface is proportional to the total surface. Take two samples of differing paramagnetic ion content and dilute them mechanically to the same concentration by the addition of pure support. Susceptibility measurements have shown that such supported oxides are aggregated into particles, even though the concentration of active oxide be very small. Let n_1 and n_2 be the number of such particles of radius r_1 and r_2 respectively, and of density ρ in the two samples. Then

$$\rho\, n_2 r_2^3 \pi^{4/3} = \rho\, n_1 r_1^3 \pi^{4/3} \text{ or } n_1\ n_2 = r_2^3\ r_1^3.$$

The surfaces of supported oxide S_1, and S_2 will be related by

$$S_2\ S_1 = (4\pi\, n_2 r_2^2)\ (4\pi\, n_1 r_1^2),$$

then, substituting for $n_2\ n_1$, we have

$$S_2\ S_1 = (r_1^3 r_2^2)\ (r_2^3 r_1^2) = r_1\ r_2.$$

Going back to our original assumption that $T_1\ T_2 = S_2/S_1$, we have

$$T_1\ T_2 = r_1\ r_2 = C_1^{1/3}\ C_2^{1/3},$$

where C_1 and C_2 are the original percentages of paramagnetic ion present in the undiluted samples. The conclusion is, therefore, that the relaxation time should be proportional to the cube root of the original concentration in a series of catalysts all members of which are diluted mechanically to a fixed concentration.

Fig. 6 shows relaxation time plotted as a function of the cube root of the original concentration for supported oxides of iron, chromium and copper. The data are derived from Tables II, III and IV. In general

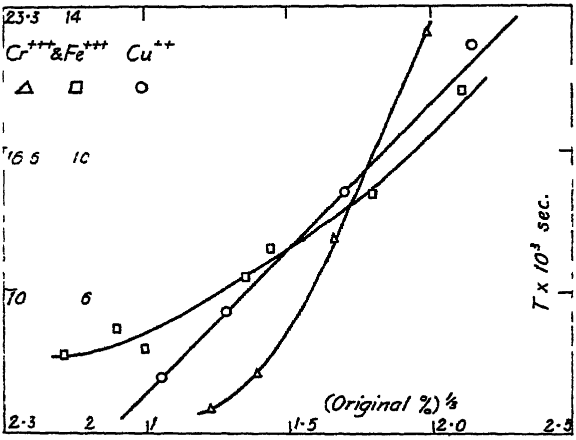

FIG. 6.—Relaxation time as a function of the cube root of original concentration for supported oxides of iron, chromium and copper on alumina.

it is confirmed that relaxation time in these systems is roughly linear with the cube root of original concentration. At extremes of concentration some deviations may be expected parallel to the deviations from $1/T \sim N$ noted above. At high concentration deviations may be noted owing to increasing exchange interaction between adjacent ions. The agreement is best for supported copper oxide which, according to susceptibility measurements, is the most magnetically dilute.

In conclusion it may be observed that the nuclear induction experiment gives the same kind of information as may be obtained from susceptibility measurements on the same systems, but that the nuclear induction effects are related to the surface ions rather than to the whole mass of paramagnetic ions. The information obtainable by nuclear induction is similar to that from ortho-para hydrogen conversion studies. But the nuclear experiment has a much wider range of applicability.

This work was done under contract with the Office of Naval Research.

Departments of Chemistry and Physics,
Northwesterm University,
Evanston, Illinois, U.S.A.

STUDY OF CATALYSTS BY SCATTERING OF X-RAYS AT SMALL ANGLES

By A. Guinier

Received 30*th January*, 1950

The possibilities of using small-angle scattering of X-rays for the determination of the degree of dispersion of catalysts are discussed. It is concluded that these measurements cannot alone provide precise information about the different size and shape of an irregular array of particles of a powder catalyst, but in simple cases or when they are supplemented by information obtained by other methods, such as by electron microscopy, the quantitative use of X-ray data is possible.

One of the essential factors which determine the properties of a catalyst is its mean grain-size, or the total area of the grains. The object of this paper is to show the possibilities of using small-angle scattering of X-rays for the experimental determination of the degree of dispersion of matter in catalysts.

Experimental

It may briefly be recalled that the occurrence of scattering of X-rays at small angles (Fig. 1) is characteristic of the heterogeneous state of the specimen; it does not occur unless the specimen shows local variations of electron density. The scattering is limited to an angle of approximately λ/d, λ being the wavelength of the primary beam and d the mean diameter of the grains.

With current experimental techniques it is difficult to study scattering at angles less than 10′ from the primary beam; consequently, with readily accessible wavelengths, particles of diameter greater than 600 Å cannot be studied. If, on the other hand, the particles are too small, scattering occurs over a larger angle, but becomes too weak to be detected.

The conditions for convenient study of a specimen of a fine powder by the low-angle scattering method are as follows:

(*a*) the particles should be immersed in a medium of considerably different electron density;

(*b*) the dimensions of the particles should be of the order 20 to 500 Å. The first condition is usually realized in powder catalysts; the second limits the use of the method to the most finely divided materials.

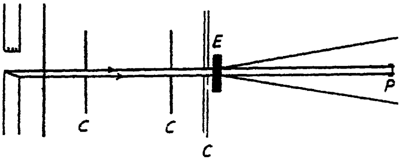

FIG. 1.

Results and Discussion

The results of the experimental work is a curve relating the intensity I of scattered X-rays to the angle of scattering ϵ. Consideration must now be given to the deduction from this curve of the size of the particles. It is known [1] that when the particles are identical and sufficiently far removed from each other for interparticular interferences to be neglected, the "radius of gyration", a quantity representing the size of the particles, can be determined from the experimental data. (The radius of gyration is the root-mean square ofthe distances from all the electrons in the particle to its centre of gravity.) The radius of gyration is deduced by plotting log I against ϵ^2; the plot tends towards a straight line as ϵ tends to zero, and the limiting gradient of the curve gives the radius of gyration.

This result has been satisfactorily verified [2] by comparison of an electron-microscope photograph and an X-ray scattering photograph for a colloidal gold preparation containing very uniform grains. When the preparation is somewhat less homogeneous, calculation of radius of gyration from the scattering curve still gives a good approximation to the mean value for the particles.

It should be noted that a knowledge of the radius of gyration is not sufficient for determination of the dimensions of a particle, which requires some assumption as to its shape. For example, a sphere and a series of elongated ellipsoids, which may have the same radius of gyration, cannot be distinguished by the scattering method.

The case of a specimen with identical and widely dispersed particles, allowing accurate application of the low-angle scattering technique, is unfortunately rare in the study of catalysts. Often there is reason to believe that the grains are of widely varying size and shape; moreover, in powder catalysts the grains are in contact, and distortion of the scattering curve by interparticular interferences may be expected.

Heterodisperse Specimens.—Consideration may first be given to the case in which the grains are dispersed but of varying size. Evidently the observed intensity of scattering will be the sum of the scattering intensities from different groups of particles of given size. For each of these groups the plot of log I against ϵ^2 will tend to become linear at small angles, but the log $I - \epsilon^2$ plot will show greater curvature and be concave upwards.

Several authors [3, 4, 5] have attempted to analyze these complex curves in order to determine the *distribution* of particle sizes from low-angle scattering data. The most correct method is that of Shull and

---

[1] Guinier, *J. Chim. physique*, 1943, **40**, 133.

[2] Turkevich and Hubbell, *Physic. Rev. A*, 1948, **73** (ii), 1250.

[3] Hosemann, *Z. Elektrochem.*, 1940, **49**, 535.

[4] Jellinek and Fankuchen, *Ind. Eng. Chem.*, 1945, **37**, 158.

[5] Shull and Roess, *J. Appl. Physics*, 1947, **18**, 295, 308.

Roess[3]; a particular particle shape is assumed, all particles in the specimen being similar in this respect, and a distribution law (e.g. a Maxwellian distribution) of sizes about a specified mean value is introduced, this mean value being an arbitrary parameter. An *a priori* calculation of the diffusion curves as a function of the parameter is then possible, and the parameter is determined by selecting the curves corresponding most closely with the experimental data. This procedure certainly provides a solution to the problem but it depends on two assumptions—the shape of the particles, and the size-distribution law. If it is desired to determine a mean or integral value (giving, for example, the total surface area), these assumptions may affect the result, and the scattering technique alone does not give a unique solution. It may be used if the assumptions made are justified by other available information about the catalyst, in such a way that the possible results lie in a rather narrow range. Thus Fankuchen *et al.*[4] and Shull and Roess[5] have obtained results for total surface areas of alumina catalysts which agree with values determined by other methods.

Compacted Powders.—The influence of interparticular interferences is particularly important with particles of very uniform shape and size, the significant factor being the regularity of disposition of the particles. We have verified that solutions of macromolecules of known identity give scattering curves which change considerably with concentration.[6]

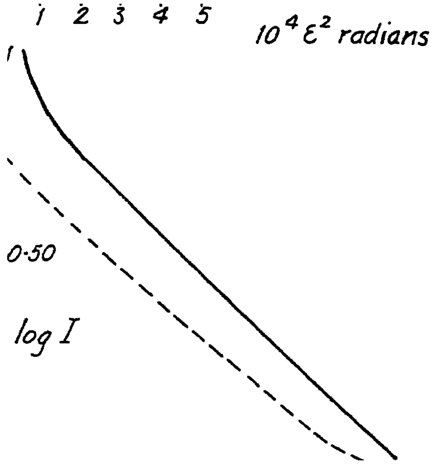

FIG. 2*a*.—Curves of scattering intensity; log I plotted against ϵ^2. Continuous curve: colloidal solution of silver. Dotted curve: flocculated colloidal silver. (The radii of gyration deduced from the linear portions of these curves are, respectively, 48 and 50 Å. The mean grain diameter measured on the electron micrograph is 120 Å, which, in the case of a sphere, corresponds to a radius of gyration of 47 Å.

A ring appears, instead of a central maximum, in diagrams for concentrated solutions. However, if the particles are of different sizes, even if they come into contact, there is no frequently repeated value of the distance between neighbouring particles; under these conditions a ring should no longer occur in the diagram. We have found, in fact, that the same scattering curve is obtained from a dilute colloidal solution of silver and the same colloid after flocculation, although in the latter case the density of the silver is considerably increased (Fig. 2). We consider that this result shows theories applying to dilute solutions to remain roughly valid, in general, for powder catalysts.

---

[6] Fournet and Guinier, *Compt. rend.*, 1947, **224**, 1848.

FIG. 2b.—Electron micrograph of the colloidal silver (magnification × 82,000).

[*To face page* 346.

In conclusion, a low-angle scattering measurement is carried out in the following way. The intensity of scattering is measured as a function of the scattering angle, and log I is plotted against ϵ^2. If the curve has a linear portion of appreciable length, the particles are sufficiently uniform in dimensions, and the radius of gyration may be deduced. If the contrary is observed, the particle sizes are widely dispersed, and an analysis of the size distribution can be made with certainty only if assumptions are made, the validity of which determines the value of the results.

Comparison with the Debye-Scherrer Method.—Low-angle scattering depends only on the dimensions of the unit domain of matter, and not on the internal arrangement of atoms in that domain. Thus the measurement of width of Debye-Scherrer lines for crystalline materials may indicate a smaller grain-size than the scattering method, if each grain comprises several crystallites of different orientation or if the crystal lattice is distorted. We have examined two carbon-black samples, one of which gave broad Debye-Scherrer lines and the other lines so diffuse that they resembled rings from an amorphous material; low-angle scattering from both samples was similar in extent. This shows that the grains were of similar size in both cases, but that the state of crystallization was different; one sample was almost amorphous carbon, whereas the other approached graphite in structure.

This example shows how study of the central part of the diffraction diagram augments information given by classical techniques, and prevents erroneous interpretations based only on the study of Debye-Scherrer line-width.

Comparison with the Electron Microscope.—From a comparison of X-ray data with results given by the electron microscope, it becomes evident that the latter instrument gives much more precise information about the specimen. The electron microscope does not suffer from restrictions inherent in the X-ray method, and the distribution of particle sizes in a heterogeneous sample can be analyzed. The X-ray method, however, offers two advantages; firstly, the specimen can be examined while in suspension in a liquid. For electron-microscopic examination the specimen must be dried; the drying may alter the particles or produce coagulation, so that the true free particle in the system is not actually observed in the microscope. The second advantage is in the examination of porous materials containing minute cavities; these produce regions of heterogeneous electron density which, if of appropriate size, cause strong low-angle scattering. Active charcoal, for example, produces strong scattering, although prior to activation, scattering from the same sample is only weak. This is attributed to the formation of porosities some tens of Ångstroms in size. In general, the electron microscope shows only the apparent contour of the grain and does not disclose internal cavities. It is just such porosity that may be important in the action of catalysts.

Conclusion.—For systems as complex as an irregular array of particles of different size and shape, such as a powder catalyst, the X-ray scattering method above cannot give a precise and complete answer to the problem of granulometry. Nevertheless, in simple cases, or when complementary information secured by other physical methods is available, quantitative use of X-ray data is possible.

It should not be forgotten that, even in the general case, low-angle scattering may be used qualitatively; two catalysts of the same material may be compared, the form of the log $I - \epsilon^2$ curves showing which is the more dispersed or more homogeneous. We have shown that the qualitative selection of two varieties of carbon black used as rubber fillers was the same as that made by study of the filled rubber. In such a case X-rays provide a convenient and practical test of the quality of the product.

Conservatoire National des Arts et Métiers,
292 *Rue Saint-Martin,*
Paris 3eme.

ELECTRON MICROSCOPY AND SMALL ANGLE X-RAY SCATTERING

By John Turkevich[a] Harry H. Hubbell[b] and James Hillier[c]

Received 27th February, 1950

The application of the electron microscope to the study of catalytic substances is discussed. The substances commonly used as heterogeneous catalysts reveal under electron microscope examination a diversity of form: amorphous materials, small spherical bodies, fibres and plates. Applications are cited in the use of the electron microscope for the study of catalyst preparation and sintering. The difficulties of this method of the examination of the fine structure are presented. An apparatus for small angle scattering of X-rays for particle size determination is described. Correlations are presented on the particle size determinations by the electron microscope with those obtained from the low angle scattering of X-rays.

Examination of the fine structure of catalysts is a matter of some importance in any comprehensive study of heterogeneous catalysis. One aspect of such a study has been the thorough investigations carried out on the adsorptive characteristics of surfaces for gases. Van der Waals' adsorption, activated adsorption and heat of adsorption measurements have all been utilized for characterizing the extent, the chemical character and the heterogeneity of catalytic surfaces. Another aspect of such an examination of fine structure is the study of solids by X-ray diffraction.[1] Application of this tool using the Bragg equation for powders is, however, limited since most catalytic bodies are so finely divided that they either give no lines or at best produce diffuse diffraction bands. Crystallite size may often be determined from the width of such bands and in recent years the diffuseness of the central spot of the usual X-ray powder diagram, the low-angle X-ray scattering, has been used to characterize in a semi-quantitative way the particle size of specimens. The applicability of the small angle X-ray scattering has not been fully tested by the direct correlation with the results of electron microscopy.

The invention of the electron microscope offered an opportunity to determine the morphology of catalyst preparations with a resolution which approaches 15 Å under most favourable cases. A survey of various catalytic solids [2-8] disclosed amorphous materials such as activated alumina (Fig. 1), silica gel, cracking catalyst; spherical metal particles such as colloidal platinum; fibrous materials as vanadium pentoxide

---

[a] Chemistry Department, Princeton University, Princeton, New Jersey.

[b] Physics Department, Middlebury College, Middlebury, Vermont.

[c] R.C.A. Laboratories, Princeton, New Jersey.

[1] Jellinek and Fankuchen in *Advances in Catalysis* (Academic Press, New York, 1948, p. 256.

[2] Ruska, *Kolloid-Z.*, 1940, **92**, 276.

[3] Rampino, Kavanaugh and Nord, *Proc. Nat. Acad. Sci.*, 1943, **29**, 247.

[4] Shekhter, Roginski and Isalo, *Acta Physicochim.*, 1945, **20**, 217.

[5] Turkevich, *J. Chem. Physics*, 1945, **13**, 135.

[6] Roginski, Shekhter and Sakharova, *Compt. rend. U.R.S.S.*, 1946, **52**, 687.

[7] Turkevich and Hillier, *Ind. Eng. Chem.* (*Anal.*), 1949, **21**, 475.

[8] Roginski, Tret-yakov and Shekhter, *J. Physic. Chem. Soc. Russ.*, 1949, **23**, 50, 1152.

(Fig. 2), asbestos (Fig. 3); plate-like substances such as aluminium oxide hydrate, tungsten oxide, activated charcoal, kaloin, bentonite clay. Supported catalysts such as platinum on asbestos or platinum on charcoal show well-recognizable dense particles scattered along a fibre or distributed on the surface of the plates. Sintering process is readily visualized as an agglomeration and fusion of fine particles while steam deactivation of activated alumina can be morphologically recognized as the formation of lath-like growth with a concomitant decrease in the surface area. Electron microscopy also furnishes the catalytic chemist with a powerful tool to investigate the ageing of many hydrous oxides. In the alumina sol this phenomenon expresses itself in the aggregation of fine granules into flexible fibrils which ultimately combine to form crystallites while in the vanadium pentoxide sol the short fibrils lengthen into long rods which coalesce to form successively elliptical tactoids and rectangular crystallites.[9] The general conclusion that can be drawn from an electron microscope examination of catalysts and related colloid systems is the presence of diversity of form and a rather wide distribution of particle size. A clear cut correlation between particle size and catalytic activity is therefore difficult.

A programme was therefore initiated by Dr. P. C. Stevenson[10] and one of us (J. T.) on the electron microscope examination of the various modes of preparation of the classical colloidal system, finely divided gold. It was found possible to separate the nucleation process from the growth process in such a way as to produce particles whose average radius can be varied from 100-1000 Å while the deviation from the mean radius was at most 12 %. While such colloidal gold is unsuited for preparation of catalytic material its study has not only furnished samples for calibration of other methods for the determination of particle size but has also given an insight into the mechanism of nucleation and growth of finely divided particles.

There are several difficulties involved in the use of the electron microscope for catalyst examination. The material studied must be so dispersed that each morphologically significant body stands out as a separate unit. This is often difficult to attain especially when the intermolecular forces are great as in the case of the forces between graphite plates or when the elementary particles are fused together by previous treatment at high temperatures. Another difficulty is associated with the fact that significant structure is revealed only at a resolution close to the limiting one attained by the present-day microscopes. Thus an examination of a material with a resolution of only a 100 Å often yields information of limited value. Further difficulty is the demand made on the specimen, that it withstand high vacuum and not be excessively thick (less than 4000 Å). Finally, it must be emphasized that the electron microscope presents us with a silhouette of the inorganic material on the collodion mounting screen and if there is an internal sub-structure it will not be revealed unless fortuitously obtained by the process of dispersion. It was therefore felt desirable to invoke the aid of small angle X-ray scattering to reveal whether there is any sub-structure in the particles which appear in the electron microscope as compact units and whether there are particles in the specimen which are invisible because they fall in size below the resolution limit of the microscope. The first step in this programme was a study of the experimental aspects in the determination of the small angle scattering of X-rays and a calibration of the method using citrate colloidal gold as the specimen.[11] This sample of gold is quite uniform in size at 100 Å radius and 12 % deviation from the mean. A value of 107 Å was obtained from the slope of the linear portion of the logarithm of the intensity against the angle squared of the scattering curve This is in good agreement with the prediction of the exponential curve suggested by Warren [12] Fankuchen [1] Guinier [13] and others The experimental scattering curve also revealed a flat portion which could be interpreted as evidence of the maximum predicted by Guinier [13] but modified to give a flat portion because of the use of slits instead of pin holes and because of the finite distribution in the size of the colloidal particles The small but significant distribution in the gold particle size did not express itself in a curvature of the above-mentioned linear portion of the scattering curve plotted as the logarithm of intensity against the angle squared It is proposed in the present communication to examine the correlation between particle size as determined by the electron microscope and small angle X ray scattering

---

[9] Watson, Heller and Wojtowicz, *J. Chem. Physics*, 1948, **16**, 998.

[10] Stevenson, *Some Experiments on Colloidal Gold* (Princeton University Thesis, 1949).

[11] Turkevich and Hubbell, submitted to *J. Amer. Chem. Soc.*

Experimental

The apparatus is illustrated in Fig 4 and consists of a North American Phillips X ray unit a long collimating system and a small angle camera adapted both for photographic survey work and careful intensity measurements by

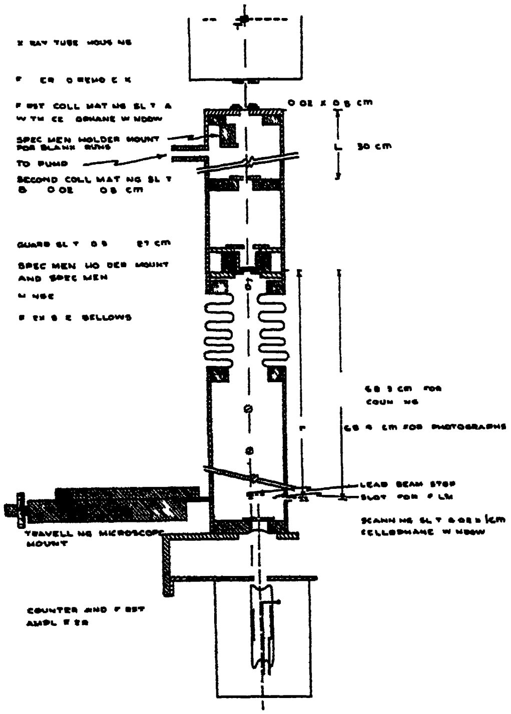

FIG 4 —Small angle X-ray scattering apparatus (½ actual size)

scanning with a Geiger-Muller counter tube The experimental results were plotted as the logarithm of intensity against the scattering angle squared Filtered chromium, copper and iron K_α radiation was used The particle size distribution was obtained using the method of resolution of such curves proposed by Fankuchen, Jellinek and Solomon [14]

---

[12] Biscoe and Warren, *J Appl Physics*, 1942, 13, 364
[13] Guinier, *Ann Physique*, 1939, 12, 161
[14] Jellinek, Solomon and Fankuchen, *Ind Eng Chem* (*Anal*), 1946, 18, 172

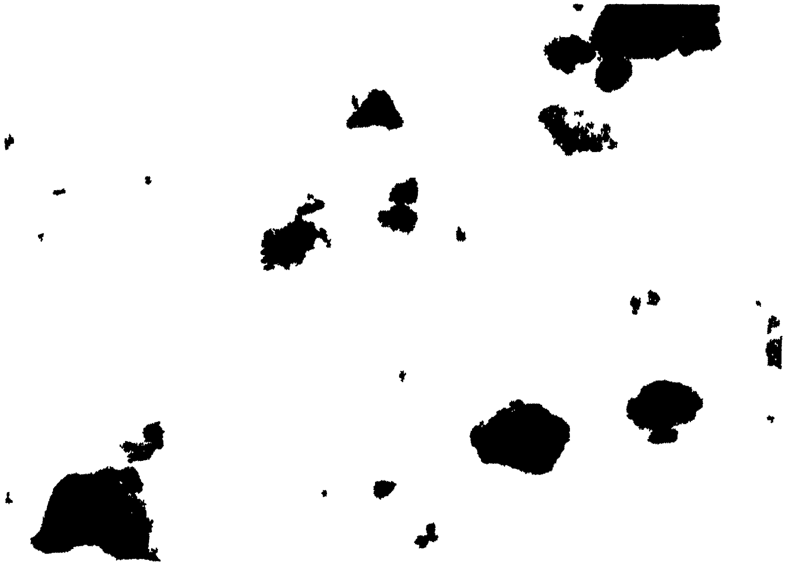

FIG. 1.—Electron micrograph of Alorco activated alumina (1[illegible]500)

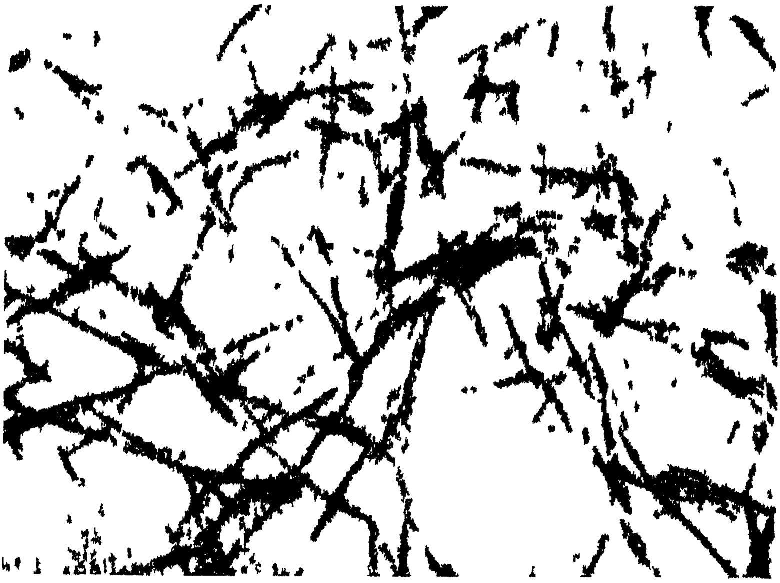

FIG. 2.—Electron micrograph of vanadium pentoxide sol (204 000)

[*To face page* 350

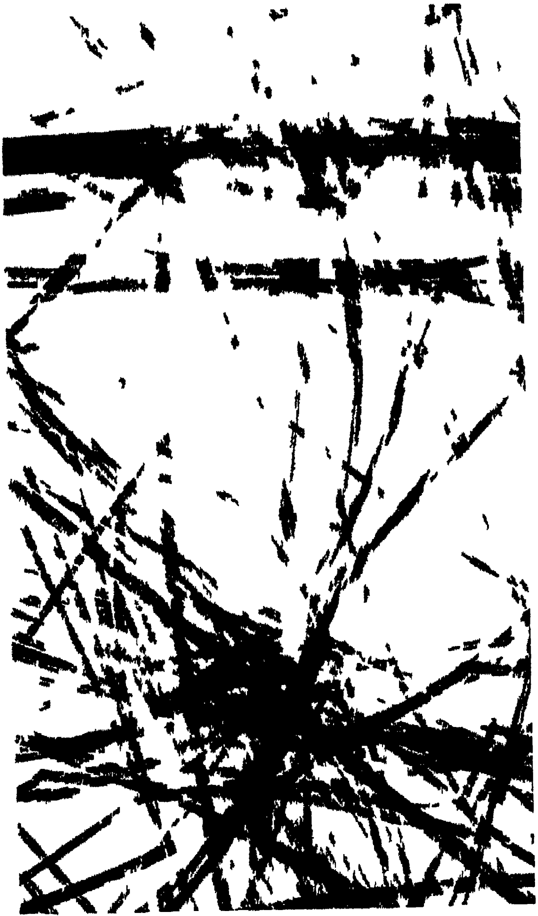

Fig. 3—Electron micrograph of chrysotile asbestos
(31 000)

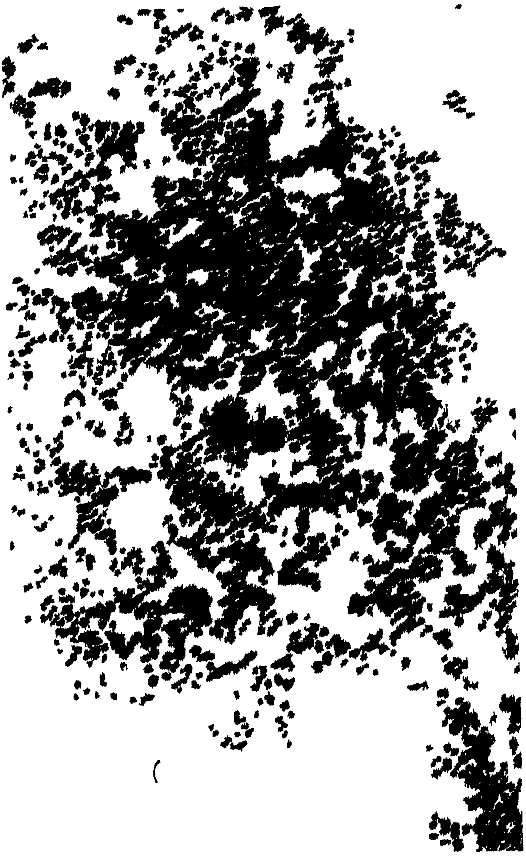

FIG 5—Faraday gold sol (100 000)

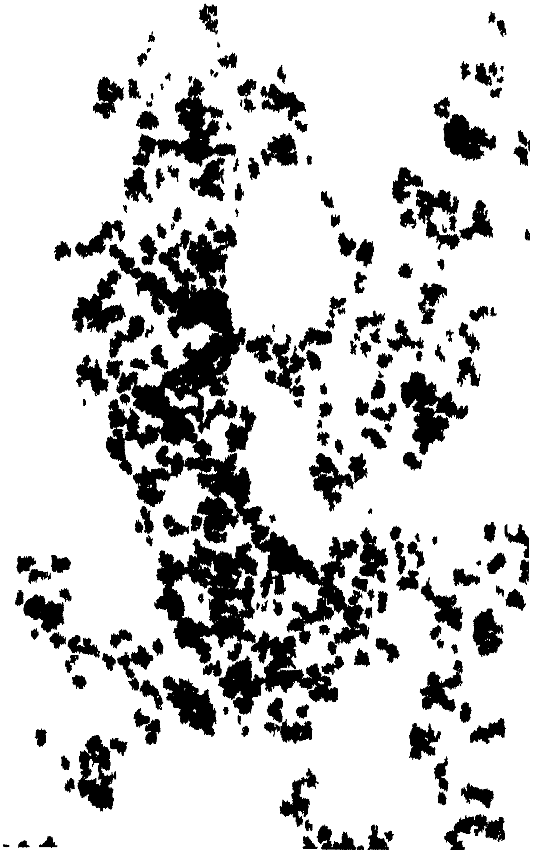

FIG. 6.—Tannin gold sol (124,000).

The sodium citrate gold sol was prepared by adding 45·0 ml. of water to 50·0 ml. of chlorauric acid solution containing 0·1 mg. of gold per ml. and bringing the solution to the boiling point. 5·0 ml. of 1 % sodium citrate solution was added to the boiling solution and the boiling continued with good mechanical stirring for about 7 min. The final colour of the colloid was deep wine-red.

Faraday sol was prepared by treating 100 ml. of chlorauric solution containing 0·5 mg. of gold and 0·5 milliequivalents of potassium carbonate with 2·0 ml. of a saturated solution of yellow phosphorus in diethyl ether and stirring continuously at room temperature. When the reaction was judged to be complete from the depth of colour developed, the deep ruby-red colloid was heated to the boiling point and filtered air was drawn through the solution to oxidize any remaining phosphorus.

Tannin gold sol was made by neutralizing to litmus 110 ml. of auric chloride solution containing 0·01 mg. of gold per ml. with sodium carbonate solution and then heating it to the boiling point. A fresh 1 % tannin solution was added dropwise until no further development of colour resulted.

Activated alumina was the commercially available Alorco alumina. Unactivated charcoal was a coconut char. It was steam activated at 1000° C to give the activated charcoal. It was then impregnated with chlorplatinic acid and heated to give 10 % platinum by weight.

Discussion

The results are presented in Table I. For sodium citrate sol the agreement between the radius of the particles as determined from the small angle scattering with the result of 100 Å as determined with the electron microscope, is excellent. In the case of the Faraday sol and the tannin sol the electron microscope reveals a wide spread in particle size, the size ranging from 15 to 40 Å with a most probable value of 25 Å for the Faraday sol (Fig. 5), and 15 to 75 Å with a most probable value of 55 Å for the tannin sol (Fig. 6). The results of the X-ray scattering do not reveal the same type of heterogeneity in the samples but do indicate a preponderance of particles of radius close to the maximum radius as revealed by the electron microscope. Activated alumina reveals under

TABLE I.—PARTICLE SIZE DISTRIBUTION AS DETERMINED BY X-RAY SCATTERING

Material	Radius (Å)	%
Sodium citrate gold sol	107	—
Faraday gold sol	38	91
	61	7
	107	2
Tannin gold sol	75	95
	170	5
Activated alumina	56	61
	68	28
	100	9
	208	2
Unactivated charcoal	91	69
	120	28
	246	3
Activated charcoal	34	88
	105	10
	169	2
10 % Platinum on charcoal	29	61
	33	29
	36	10

the electron microscope a porous structure which is difficult to characterize in terms of pore and particle size. The latter may be estimated as close to 20 Å in radius. The small angle scattering indicates larger particle size and an apparent distribution in size which may be associated with the porous structure. The X-ray data on the three charcoals is consistent within the group in that steam activation results in the production of particles of smaller " radius " and impregnation with metallic platinum not only increases the total scattering curve by a factor of ten but reveals particles of a radius of 29-36 Å. The electron micrographs disclose that these samples are aggregates of plates that are difficult to disperse and therefore difficult to characterize quantitatively.

In conclusion we wish to state that mere examination of the X-ray scattering does not reveal the morphology of the specimen nor the distribution in size, but must be supplemented by electron microscope examination.

Chemistry Department,
Princeton University,
R.C.A. Laboratories,
Princeton, N.J.

STABLE AND UNSTABLE ISOTOPES IN CATALYTIC RESEARCH

By John Turkevich,* Francis Bonner,** Donald Schissler * and Peter Irsa **

Received 6th February, 1950

A discussion is given of the advantages and disadvantages of the use of stable and unstable isotopes in catalytic research. The application of radioactive carbon to the study of the reduction of carbon dioxide by carbon is presented. The results of the use of radioactive hydrogen for the study of the catalytic double bond migration are cited as evidence for the theory of a hydrogen switch mechanism. A discussion is given of the use of deuterium and mass spectrometry to determine the number and position of the deuterium atoms in molecules containing varying amount of the deuterium atoms. This use of the stable isotope of hydrogen is illustrated by examples of the analysis of the reaction of ethylene and deuterium on a nickel wire catalyst.

The number of radioactive isotopes available to the catalytic chemist and of particular use to him is limited. There are the exceptionally weak β-emitting tritium, the weak β-emitting ^{14}C, a sulphur isotope and one of phosphorus. On the other hand, there are no radioactive isotopes of nitrogen and oxygen of convenient life. Definite advantages are gained in the use of radioactive isotopes in that they may be employed in minute amounts and still be detected by inexpensive counting equipment. Furthermore, in many cases it is possible to monitor continuously the activity during the course of an experiment. It should be pointed out, however, that the use of a radioactive isotope gives only an overall picture of the exchange reactions that take place when there are two or more non-equivalent atom positions in a complex molecule. To determine the position of the radioactive tracer atom in such a molecule, one must chemically degrade the molecule in well-defined steps and determine in what fragment the radioactivity persists. Such chemical degradations

---

* Chemistry Department, Princeton University.
** Chemistry Department, Brookhaven National Laboratory.

may be subject to rearrangements and exchanges and are, at best, time-consuming. Not only is the specific radioactivity of the sample independent of the position of the tracer atom in the molecule, but it is also independent of the distribution of the tracer atoms among several molecules. Thus, the specific radioactivity will be the same if there is one molecule with two tracer atoms and another with no tracer atom, or if two molecules are present each with one tracer atom.

The availability of stable isotopes, deuterium, ^{13}C, ^{15}N, ^{18}O, together with the use of the mass spectrometer for analysis, offers a method for solving the problem of determining the distribution of the tracer atoms among and within molecules. In the mass spectrometer the molecule is broken down by electron impact to give a pattern characteristic of the molecule. The mass spectrum so obtained is governed in its main features by the rupture of valency bonds in the molecule. A number of model deuterium-substituted compounds, not only chemically pure but isotopically pure, have been prepared to determine the pattern relationship between the protium model compounds and the various deuterium model compounds. The spectra of the model compounds are used to convert the positive ion currents for the various masses obtained on the mass spectrometer, into composition of the various polydeuterated compounds.

An Example of the Use of ^{14}C.—As an illustration of the use of a radioactive tracer atom in a heterogeneous reaction, consider the reaction between carbon dioxide containing ^{14}C and charcoal which was investigated at the Brookhaven National Laboratory by Bonner and Turkevich. The apparatus is illustrated in Fig. 1. The radioactive carbon dioxide was generated from the Oak Ridge barium carbonate by mixing it with lead chloride and heating it to 400° C.[1] The charcoal granules were placed in one arm of a thermal syphon E, made in part out of quartz, so that it could be heated to 1000° C. The other arm of the thermal syphon contained a trap for freezing out the carbon dioxide F, a manometer for measuring the pressure changes D and a counter G. The latter was a bell-jar counter with a compartment sealed next to the mica window so that the gases flowing by could be monitored continuously. The counter was calibrated for self-adsorption and a coincidence correction applied. The dead space of the system was measured with

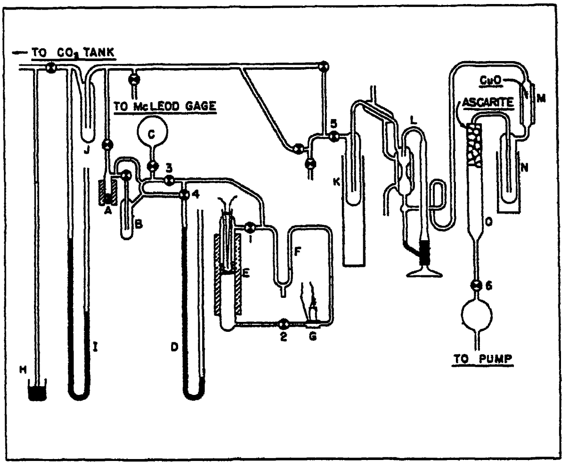

FIG. 1.—Apparatus for the study of the reaction between charcoal and $^{14}CO_2$.

---

[1] Zweibel, Miller and Turkevich, *J. Amer. Chem. Soc.*, 1948, 71, 376.

helium for various reaction vessel temperatures. By making appropriate measurements one was able to determine the specific activity either of the carbon dioxide or of the carbon monoxide. The experimental study revealed two sets of phenomena. At relatively low temperature of 500° C there was no change of either pressure or radioactivity with time. This was interpreted to indicate that there is no exchange between the carbon dioxide in the gas phase and either the carbon on the surface or any adsorbed oxygen-carbon compound present on the surface. Condensation of the carbon dioxide showed several per cent non-condensable gas whose specific gravity was never less than that of the original carbon dioxide. This suggests the reaction

$$CO_2 + \text{charcoal} = CO + \text{oxygenated charcoal}$$

with the carbon dioxide molecules approaching the surface, depositing their oxygen on the surface and the product CO molecules containing the same carbon atom that was originally present in the reactant CO_2 molecules. This point of view has been suggested recently on the basis of kinetic and theoretical considerations by Gadsby and co-workers.[2] At higher temperatures of 735-848° C, over 95 % of the carbon dioxide was converted into carbon monoxide within at most four minutes from the start of the reaction, with no increase in pressure nor change in the specific radioactivity. A full analysis of the kinetics will appear in a forthcoming publication.[3] Suffice it to indicate that the changes in pressure correlate satisfactorily with the changes in the specific radioactivity. The mechanism that is proposed consists of a very rapid reduction of the carbon dioxide to a radioactive carbon monoxide with the formation of an oxygenated surface, followed by a slow decomposition of the latter to give the second molecule of carbon dioxide, which is now non-radioactive.

An Example of the Use of ^3H.—Another study of the use of radioactive tracers in heterogeneous reaction was carried out by Smith and Turkevich[4] on the correlaion of the double bond migration in the butene-1 + butene-2 system with the exchange of tritium from the catalyst to these hydrocarbon molecules. The detection of tritium is a bit troublesome because of the low energy of the 0·0145 MEV β-ray of this tracer nucleus. One is forced to introduce the tritium compound with argon into a counter and essentially make a count for each point of the rate curve. The results of Smith and Turkevich established that the catalysts for the migration of the double bond are also materials which readily exchange their hydrogen with the butene hydrogen, and that the rates of the two processes are comparable. Furthermore, on the basis of these experiments the catalyst was formulated as a configuration of atoms (in a molecule or on a surface of a solid) which contains a hydrogen donor and a hydrogen acceptor separated by about 3·5 Å. Examples of substances which satisfy these criteria are H_2SO_4, H_3PO_4, aluminium silicate, copper pyrophosphate and many metal catalysts partially loaded with hydrogen. Such a "hydrogen switch" mechanism, whereby the catalyst gives one hydrogen to the substrate while it abstracts another, may be applicable to alkylation, polymerization, and cracking of hydrocarbons. Verification of such a mechanism must, however, await the development of a technique of identifying the distribution of deuterium atoms within and among complex hydrocarbon molecules.

An Example of the Use of ^2H.—At present Schissler, Irsa and Turkevich are studying the interaction of ethylene and deuterium on a nickel wire using an apparatus and technique similar to that of Twigg and Rideal.[5] Whereas the previous workers determined the extent of addition from the pressure drop and the extent of exchange from the thermal conductivity analysis of the hydrogen gas, we have analyzed the hydrocarbons in the General Electric Company mass spectrometer of the Brookhaven National Laboratory. To facilitate the interpretation of the mass spectra of the resulting deutero compounds, the analysis was made on the original ethylene and ethane portion and also on an ethane portion obtained by removing the ethylene from the former by treatment with bromine vapour followed by distillation. The mass spectra of the deutero ethylenes was obtained by difference. In order to translate these mass spectra from the positive ion currents of the various masses corresponding to the various deuterated ethanes (ethylenes) and their decomposition products on electron impact, one must know the mass spectra of the pure isotopic compounds C_2D_6, C_2D_5H, . . . C_2H_6 (C_2D_4, C_2D_3H, . . . C_2H_4). Since such mass spectra are known only for one deuterated ethane C_2H_5D, a set of patterns for various isotopic ethanes and ethylenes was calculated from the patterns of the protium compounds assuming that the ease of removal of a hydrogen and a deuterium are the same and that the variations in the pattern of the deuterium substituted compounds are governed solely by probability considerations. It should be pointed out that the calculated pattern agrees with the pattern observed for C_2H_5D in all masses but mass 29, where the calculated ion current is less than the experimentally observed one. This mass, however, is notoriously sensitive to impurities of higher hydrocarbons in the sample and the experimental value may be high for that reason. Further assurance of the validity of such model patterns is the fact that, by successively subtracting the model patterns of the C_2D_6, . . . C_2H_6 (C_2D_4 . . . C_2H_4), a small residue is left for the ion current in the mass 29-24 region. Finally, the validity of the results obtained

---

[2] Gadsby, Long, Sleightholm and Sykes, *Proc. Roy. Soc. A*, 1948, **193**, 357.

[3] Bonner and Turkevich, *J. Amer. Chem. Soc.* (forthcoming publication).

[4] Turkevich and Smith, *J. Chem. Physics*, 1948, **16**, 466.

[5] Twigg and Rideal, *Proc. Roy. Soc. A*, 1939, **171**, 55.

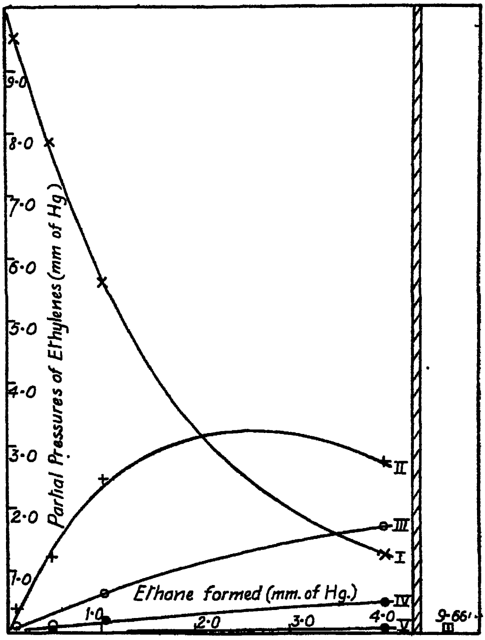

FIG. 2.—Behaviour of ethylenes during the course of reaction between ethylene and deuterium: (I) C_2H_4—× (II) C_2H_3D—+ (III) $C_2H_2D_2$—○ (IV) C_2HD_3—● (V) C_2D_4—⊗. Values at end of the reaction for all isotopic ethylene molecules □.

by such a treatment of the mass spectra of the product is strengthened by the material balance on the isotopic species. Thus, in a typical case, 39·6 mm. hydrogen atoms as ethylene and 37·7 mm. deuterium atoms as deuterium gas were introduced into the reaction vessel. The product gas of hydrogen, deuterium, the various deuterated ethylenes and ethanes gave on mass spectrographic analysis and resolution of the data, 38·6 mm. hydrogen atoms and 38·8 mm. deuterium atoms.

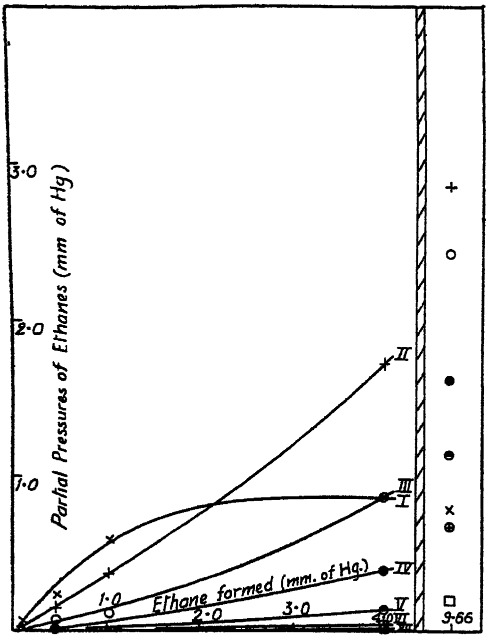

FIG. 3.—The formation of ethanes during the course of the reaction between ethylene and deuterium.
(I) C_2H_6—×
(II) C_2H_5D—+
(III) $C_2H_4D_2$—○
(IV) $C_2H_3D_3$—●
(V) $C_2H_2D_4$—◒
(VI) C_2HD_5—⊕
(VII) C_2D_6—□.

The results obtained for the interaction of ethylene with two volumes of deuterium on a nickel wire at 90° C are presented in Fig. 2 and 3. It is seen that the exchange reaction proceeds more rapidly than the addition reaction, that the concentration of light ethylene decreases exponentially, while that of the substituted ethylenes goes through a maximum before it finally reaches zero. The surprising result is the discovery of completely light ethane from the reaction of ethylene and deuterium. The possibility of the light hydrogen coming from residues left on the catalyst by previous runs is minimized by the pre-treatment of the catalyst overnight with deuterium at 300° C, and by the excellent material balances obtained in each run on the hydrogen and the deuterium. These results suggest that the ethylene hydrogenation is effected by the hydrogen that was previously on another ethylene molecule, and only indirectly by the hydrogen molecule. This point is being further investigated and the mechanism formulation is withheld until the kinetic investigations, which are being vigorously pursued, are completed.

We wish to express our appreciation to Dr. Richard Dodson of the Brookhaven National Laboratory for his interest in these problems. Work presented has been carried out in part under the auspices of the U.S. Atomic Energy Commission.

Chemistry Department,
Brookhaven National Laboratory,
Upton,
Long Island,
New York, U.S.A.

Chemistry Department,
Princeton University,
Princeton,
New Jersey,
U.S.A.

GENERAL DISCUSSION

Mr. J. A. Allen (*Bristol*) said : It is customary in practice to distinguish between chemisorption and physical adsorption in the first layer of an adsorbed gas by measurements of heat of adsorption. In recent work we have found interesting effects on the electrical conductivity of evaporated copper films arising from the adsorption of various gases at −183° C ; these are relevant to this Discussion since they appear to provide a useful alternative method of distinguishing between the two types of adsorption.

The films were deposited on a glass substrate at −183° C, annealed at 100° C and then cooled to −183° C, being maintained during this cycle under a pressure of 7×10^{-8} mm. Hg. In this way it was possible to prepare reproducible clean films which were free of spontaneous resistance changes, which possessed reversible resistance-temperature behaviour below 100° C and which had positive temperature coefficients. Films of a nominal thickness of 400 Å (calculated from the estimated amount of copper in the film, assuming a density of 8·92 g. cm.$^{-3}$) which had a nominal resistivity at −183° C of about 13 times that of bulk copper were generally used.

It was found that the admission of oxygen, carbon monoxide, and nitric oxide to such films at −183° C caused an immediate increase in resistance which rose to a limiting value in a few minutes. Nitrogen and hydrogen had no measurable effect while ethylene produced a small initial increase followed by a gradual rise. The magnitude of these effects are shown in Fig. 1, where R and R' are respectively the resistances of the film at −183° C before and after the gas was admitted.

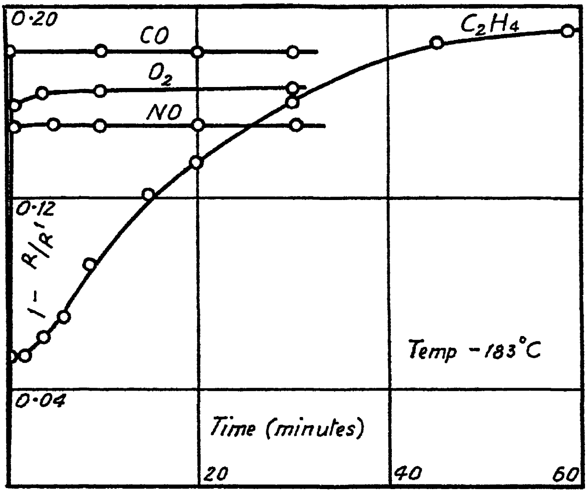

Fig. 1.

The limiting value for the resistance change was reached if the pressure of the gas was $> 10^{-3}$ mm. Hg ; a subsequent reduction in pressure to 10^{-6} mm. Hg did not appreciably affect the increase in resistance. Further, the admission of hydrogen after oxygen, carbon monoxide or ethylene did not affect the increases in resistance which had already taken place and the presence of nitrogen or hydrogen before oxygen or carbon monoxide were admitted only slightly decreased the rate at which the increases in resistance took place. The presence of argon at a pressure of 10^{-5} mm. Hg before the ethylene was admitted prevented the slow rise in resistance shown by the second part of the ethylene curve.

Although it is difficult to account for the magnitude of the resistance changes observed, the gases which cause marked increases in resistance are those which would be expected to be chemisorbed, this involving definite band formation with the metal. Nitrogen, hydrogen and argon which do not cause any increase in resistance are only physically adsorbed on copper at −183° C. A full account of this work together with the reasons which lead to this conclusion will be published elsewhere, but it seems worthwhile to emphasize the differences in behaviour between ethylene and hydrogen which may be useful in formulating the mechanism of the hydrogenation of ethylene.

Mr. A. S. Porter (*Imperial College, London*) (*partly communicated*): The need for accurate corrections for thermomolecular flow in adsorption work at low pressures is not always recognized. Neglect of these precautions, when an adsorbent is at a temperature different from that of the pressure gauge may lead to significant errors in calculating (*a*) the equilibrium pressure over an adsorbent; and (*b*) the amount of gas remaining in the gas phase and, therefore, of the amount adsorbed.

Consider a tube of diameter d cm. connecting two parts of a system at absolute temperatures T_1 and T_2, where the pressures of a gas at equilibrium are respectively p_1 and p_2. Knudsen [1] has shown that, in general, $p_1 \neq p_2$, unless λ, the mean free path of the gas molecules, is negligibly small compared with d. Except when $10 > d/\lambda > 1$, the relationships between p_1 and p_2 are given by eqn. (1) [2] and (3) [1] below.

When $d/\lambda > 10$,

$$\frac{dp}{dT} = \frac{0{\cdot}00139 \cdot \dfrac{1 + C/273}{1 + C/T} \dfrac{\eta_0}{\sqrt{\rho_0}} \cdot k_1}{\dfrac{d}{2} + 32{\cdot}07 \cdot \dfrac{1 + C/T}{1 + C/273} \dfrac{\sqrt{\rho_0}}{\eta_0}\left(\dfrac{d}{2}\right)^2 \dfrac{p}{T} k_2} \quad . \quad . \quad (1)$$

where C is Sutherland's constant, η_0 and ρ_0 are respectively the viscosity and density of the gas at 0° C and 1 μ_0 bar pressure, k_1 and k_2 are constants, and p is measured in μ bars.

Eqn. (1) may be integrated, neglecting as did Knudsen, the variation of the term $(1 + C/T)$ with temperature to give

$$\frac{m - 1}{m + 1} \log \left[\frac{\dfrac{m + 1}{a} \cdot T_1 + p_1}{\dfrac{m + 1}{a} \cdot T_2 + p_2}\right] + \log \left[\frac{\dfrac{m - 1}{a} \cdot T_1 - p_1}{\dfrac{m - 1}{a} \cdot T_2 - p_2}\right] = 0, \qquad (2)$$

where $m = (1 + 0{\cdot}178\, k_1 k_2)^{\frac{1}{2}}$,

and $a = 43040 \dfrac{\sqrt{\rho_0}}{\eta_0} d k_2 \dfrac{(1 + C/T)'}{1 + C/273}$.

Here $(1 + C/T)'$ is the mean value of $1 + C/T$ over the temperature range T_1 to T_2; and p_1 and p_2 are in mm. Hg.

When $d/\lambda < 1$,

$$\frac{dp}{p} = \frac{3k}{8} \cdot \frac{1}{1 + d/\lambda} \cdot \frac{dT}{T}, \quad . \quad . \quad . \quad . \quad (3)$$

where k varies only very slowly with pressure and may be equated to 4/3 over this range.

Integration of eqn. (3) gives p_1/p_2 explicitly as

$$\frac{p_1}{p_2} = p_2\left[\frac{b + (b^2 + 2bT_1/p_2 + T_1T_2/p_2^2)^{\frac{1}{2}}}{2bp_2 + T_2}\right], \qquad (4)$$

where $b = \dfrac{d273}{\lambda_0 760}$, λ_0 = the mean free path of the gas molecules at N.T.P., and p_1 and p_2 are again in mm. Hg.

---

[1] Knudsen, *Ann. Physik*, 1910, **31**, 205. [2] Knudsen, *ibid.*, 1910, **33**, 1435.

When $d/\lambda \ll 1$ integration of eqn. (3) gives

$$p_1/p_2 = (T_1/T_2)^{\frac{1}{2}} \quad . \quad . \quad . \quad . \quad (5)$$

Fig. 2 shows the application of these equations to hydrogen, where $d = 1{\cdot}18$ cm., $T_1 = 78°$ K and $T_2 = 298°$ K.

It is reasonable to assume that eqn. (4) becomes progressively less accurate as d/λ increases in the range $10 > d/\lambda > 1$, and the dotted curve, linking the two calculated curves, is drawn on this assumption. The experimental points show that eqn. (2) and (4) and the above assumption are satisfactory for practical purposes. It may be noted that Dushman's suggestion [3] to use eqn. (5) when $d/\lambda = 0{\cdot}1$ introduces an error of approx. 8 % with the values of T_1 and T_2 used here.

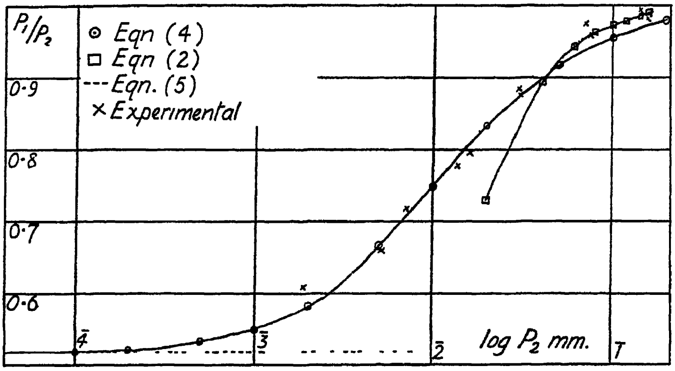

FIG. 2.—Thermomolecular flow of hydrogen in 1·18 cm. diameter tube, where $T_1 = 78$K and $T_2 = 298$K.

The effect of thermomolecular flow on (*a*) above is apparent from the graph, but the significance for (*b*) depends on the ratio of the quantity of gas adsorbed to that remaining in the gas phase. This is illustrated by reference to Allen and Mitchell's results at − 183° C.

Neglecting, for the present, the breakable gas seal, their results may be re-calculated as follows. Mr. Allen gave the final pressure as 10^{-2} mm.; presumably this is the pressure in the bulb, calculated by eqn. (5) from a Pirani gauge reading of $1{\cdot}80 \times 10^{-2}$ mm. For oxygen ($\lambda_0 = 10^{-5}$ cm.), eqn. (4) would give the pressure in the bulb as $1{\cdot}57 \times 10^{-2}$ mm. when $T_1 = 90°$ K, $T_2 = 300°$ K and d, from their diagram, is 1 cm.

Calculated in this manner, column 3 of their Table I would read 0·3, 0·5, 0·7, 1·0, 1·6, 7·3, 9·9, 9·2, 14·2, 21·4, ($\times 10^{15}$ molecules/cm.^{2}) in place of their values of 1·1, 1·3, 1·5, 1·8, 2·4, 8·1, 10·7, 10·0, 15·0, 22·2 ($\times 10^{15}$ molecules/cm.^{2}).

While their ingenious use of the narrow gas seal undoubtedly reduces the errors due to the use of eqn. (5), it cannot be regarded as entirely satisfactory, owing to its short length (1-1·5 cm., from the diagram) and the fact that only one end is attached to the outer glass tube. Both these facts make it unlikely that the upper end of the narrow tube is near to room temperature, which is necessary if it is to be effective. Experimental calibrations might overcome the difficulty, but the precise level of the liquid oxygen bath, and the point of breakage of the seal would then be highly critical.

It is evident that the significance of thermomolecular flow must be assessed experimentally, or by detailed calculation, for any particular case. The above considerations show the desirability of using tubing of uniform diameter throughout a temperature gradient, so that the problem is amenable to accurate calculation. While the initial calculations are laborious, the graphical presentation shown in Fig. 2 permits the necessary corrections to be read off rapidly and accurately.

---

[3] Dushman, *Scientific Foundations of Vacuum Technique* (Wiley, New York, 1949), p. 65.

Mr. J. A. Allen and Dr. J. W. Mitchell (*Bristol*) (*communicated*): With regard to Mr. Porter's criticism of our use of the simple Knudsen correction for the thermomolecular flow, we did in fact carry out calibration experiments with blank bulbs. These experiments showed that the simple correction was strictly applicable with our apparatus for oxygen at temperatures down to − 78° C. At − 183° C deviations from the simple correction value were observed and the results given at this temperature may be too large by $0{\cdot}3 \times 10^{15}$ molecules per cm.^{2} for pressures in the neighbourhood of 10^{-2} mm. Hg. The method used for the calibration did not allow one to distinguish between the error associated with the Knudsen correction itself and the increase in the amount of oxygen adsorbed on the glass surface which might occur in the temperature range between − 78° C and − 183° C. Similar calibration measurements carried out with hydrogen at these pressures showed that the possible error at − 183° C was not greater than $0{\cdot}1 \times 10^{15}$ molecules per cm.^{2} which suggests that there may be an increased adsorption of oxygen on a glass surface when the temperature is reduced from − 78° C to − 183° C.

It may be pointed out that even if the results at − 183° C are too large by $0{\cdot}3 \times 10^{15}$ molecules per cm.^{2}, the interpretation is not seriously affected because this value is of the same order as the spread of the results between different experiments made under the same initial conditions. We should, in conclusion, like to thank Mr. Porter for his valuable contribution to the discussion on the paper.

Dr. B. M. W. Trapnell (*Royal Institution, London*) said: Mr. Allen and Dr. Mitchell have suggested that no oxidation of their copper films takes place between − 183° C and about room temperatures. Their main evidence for this is that the quantity of gas taken up at "equilibrium" does not vary much in this range, and that this quantity corresponds to that expected for a chemisorbed monolayer on (111) faces, assuming a film roughness factor of unity.

Now one would expect the chemisorption of CO, H_2 and N_2 to be nearly complete at − 183° C and at small pressures, and therefore the ratio of CO, H_2, N_2 and O_2 uptakes to be 2/1/1/1. Allen and Mitchell actually find about 2/1/1/4. This leaves us with two alternatives. The first is that 4 oxide layers are formed at these low temperatures, and that the film roughness factor is less than one and about 1/4, which is only understandable for a continuous surface if it is partly covered with initial contamination. The second is that CO, H_2 and N_2 only have one-quarter their expected covering power, which is hardly reasonable.

It is better to conclude that low-temperature oxidation is taking place, and that Allen and Mitchell have only obtained a partially clean surface. This conclusion is supported by the work of Brunauer and Emmett, who found that 7 or 8 oxide layers are formed on iron with great rapidity at liquid-air temperatures, by the work of Beeck, Smith and Wheeler, who found similar phenomena, with nickel, and by my own work on tungsten, where again some low-temperature oxidation takes place.

Mr. J. A. Allen and Dr. J. W. Mitchell (*Bristol*) (*communicated*): We have stated that copper films do not oxidize below 240° K and not below room temperature as has been quoted by Dr. Trapnell. In our opinion, based on measurements of resistance changes accompanying adsorption on thin films, nitrogen and hydrogen are physically adsorbed on copper at low temperatures, and at the pressures used, the formation of complete physically adsorbed layers is unlikely. The number of molecules of oxygen and carbon monoxide taken up per cm.^{2} below 240° K is approximately the same for both gases as is shown in Fig. 3

in which the number of molecules taken up per cm.^{2} is plotted against the temperature.

Trapnell has assumed, without justification, that oxygen is chemisorbed as atoms and that one atom of oxygen and one molecule of carbon monoxide can each occupy one site on the surface. He has also argued that the surfaces of our copper films are initially contaminated to the extent of at least three quarters of their area. We do not accept these arguments for the following reasons. (i) Work in this laboratory over a period of years has established a technique whereby beads of copper on tungsten filaments can be thoroughly outgassed. This has been checked by very sensitive contact potential measurements and the technique used in outgassing the beads used for the present work has been proved to be entirely satisfactory. (ii) Reproducible results are unlikely to be obtained if contaminated films are used for the measurements. (iii) The technique used for depositing the films ensures beyond all reasonable doubt that, provided the beads are thoroughly outgassed, the free surfaces of the films will be uncontaminated.

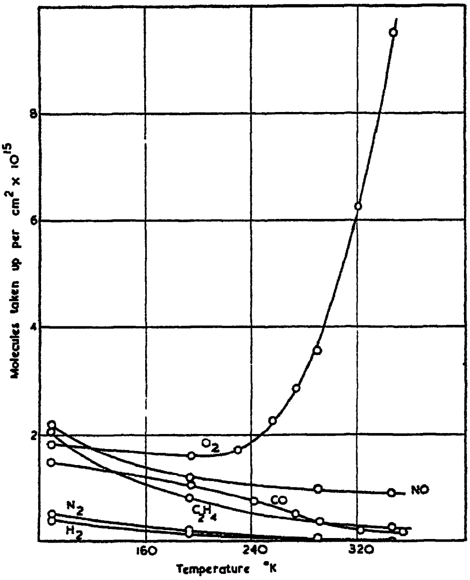

FIG. 3.

As far as we are aware, there is no evidence whatever to support the contention that oxygen is dissociated on copper below 240° K. If this were the case, it seems that oxidation should certainly proceed, the oxide film growing very rapidly to approximately 20 Å in thickness. Our own work with aluminium has shown that, with this metal, oxidation does proceed in this manner even at − 183° C and the comparison of the behaviour of copper with that of aluminium leaves little doubt that an oxide layer is not formed on copper below 240° K. Fig. 3 shows that this is the critical temperature above which oxidation proceeds.

It is suggested, and this may be supported by theoretical arguments, that oxidation of copper does not proceed below 240° K because the oxygen molecules are not dissociated on copper below that temperature. The equality between the number of molecules of oxygen and of carbon monoxide adsorbed below that temperature is most simply accounted for by assuming that one molecule of oxygen and one molecule of carbon monoxide occupy the same number of adsorption sites on the surface.

Mr. P. F. Tiley (*Bristol*) said: With reference to the adsorption of oxygen on metals, I wish to mention some results obtained recently at Bristol on the uptake of oxygen by reduced copper at 20° C. Successive admissions of oxygen were made to a sample of copper powder reduced with hydrogen at 150° C and then evacuated for 16 hr. at 190° C. For each admission the integral heats of adsorption were measured over a period of 12 min. in the calorimeter previously described.[4]

The first two admissions gave a heat value of 108 kcal./mole, falling on the third admission to 83 kcal., and remaining constant (± 3 kcal.) at this value until the 8th admission, when it dropped in two further admissions to 56 kcal. These figures should be compared with the heat of formation of Cu_2O = 81·6 kcal./mole of O_2[5] and heat of adsorption of O_2 on Cu_2O = 55 kcal./mole of O_2.[4]

For the first 7 admissions the rate of uptake of oxygen was very rapid, and appeared to be controlled only by the rate of diffusion of the gas into the calorimeter, but at the 8th admission the rate showed a marked decrease. The total amount of oxygen taken up over the first 8 admissions corresponded to a thickness of cuprous oxide of approx. 15 Å.

The results largely confirm the work of Allen and Mitchell and, in addition, suggest the rapid formation at room temperature of a normal Cu_2O phase. It is felt that the initial high values of > 100 kcal./mole (which cannot be accepted without reservation until the work has been repeated) are relevant to the observations of Prof. Taylor on the posioning of active metal catalysts by small traces of oxygen.

I should also like to draw attention to the fact that the heat of adsorption of oxygen on tungsten of 140 kcal.[6] is very close to the heat of formation of WO_3, which is approx. 130 kcal./mole of O_2.[7] It is open to question whether the observed phenomena on the uptake of oxygen by a clean tungsten surface may not be interpreted in terms of the formation of a thin oxide film due to the rapid mutual penetration of the surface metal atoms and oxygen, followed by adsorption of oxygen on this oxide.

Dr. J. S. Anderson (*Harwell*) said: The results mentioned by Mr. Tiley (that the initial heat of reaction of oxygen with a copper film is greater than corresponds to the formation of Cu_2O) suggest that we must always bear in mind that to get significant thermochemical measurements we must *start from a properly defined state* and *finish up with a properly defined state* thermodynamically. Neither condition is entirely fulfilled in reactions occurring on evaporated films. Until measurements have been made, for example, of the heat of solution of such films, their content of stored energy is quite uncertain. The formation of highly mobile films, when condensation takes place at low temperatures, shows that a considerable degree of metastability may be involved.

On metals such as copper or iron, the nature of the oxide formed is quite undefined. Thus ferrous oxide is thermodynamically unstable below about 600° C, and even within its existence range is not stable with the composition FeO: the wüstite phase has a range of composition from about $FeO_{1\cdot 08}$ to $FeO_{1\cdot 15}$. Dr. Beeck has referred to the formation of oxide films about four layers deep by reaction of oxygen with evaporated films at low temperatures. The composition of such films (if essentially FeO) could be inferred from the cell dimensions, as determinable by electron diffraction measurements, for example. It would be desirable for this sort of analysis to be done before attempting to draw too many theoretical conclusions from calorimetric and other data. Cuprous oxide is likewise a phase of potentially variable composition, and the composition of the surface oxide on a copper film may or may not be $Cu_2O_{1\cdot 000}$.

[4] Garner, Gray and Stone, this Discussion.

[5] Randall, Nielsen and West, *Ind. Eng. Chem.*, 1931, **23**, 388.

[6] Roberts, *Proc. Roy. Soc. A*, 1935, **152**, 473.

[7] Moore and Parr, *J. Amer. Chem. Soc.*, 1924, **46**, 2656; *Int. Crit. Tables*, **5**, 192.

Both the heat of formation and the diffusion coefficient involved in the formation of "polymolecular" oxide films would be sensitive to the composition.

Dr. D. D. Eley (*Bristol*) (*communicated*) : The observations in the paper of Allen and Mitchell (and also Beeck, *et al.*[8] on the stabilization of copper films by chemisorbed hydrogen prompt me to mention the results of some approximate calculations.[9] It is well known that evaporated films show a degree of mobility of atoms at low temperatures even, e.g. Appleyard,[10] Picard and Duffenbach.[11] To a first approximation, we might treat the film as made up of pure liquid drops with a surface tension of *ca.* 1000 dynes/cm. The surface tension will, of course, be the driving force behind aggregation and if a chemisorbed gas tends to lower the surface tension, it will tend to prevent sintering of the film. For hydrogen on tungsten, we know the heat of adsorption of hydrogen from θ (surface covered) = 0 to 1. We may accurately enough calculate the entropy of adsorption for any gas pressure. Thus, we obtain the result that in the presence of 10^{-6} mm. pressure of H_2 gas the surface tension of a W film is lowered 580 dynes/cm, which may well suffice for the purpose of stabilization.

Mr. P. R. Rowland (*Guy's Hospital, London*) said : With reference to the evaporated copper films of Dr. Allen and Dr. Mitchell I would like to ask them if they consider that there may be faces other than (111) present in films sintered at room temperature ? Stranski and Mahl [12] have carried out some calculations which indicate that in the equilibrium crystal forms of face centred cubic metals the faces which predominate are (111) and (001) if we take into account interactions between nearest neighbours only. (If interactions between more distant neighbours are included, the calculations indicate that more vicinal faces will also appear.) Dr. Trapnell has suggested that some molecules may cover more than one adsorption site each. If we consider cases where the effective radius of each adsorbed particle is greater than that of the metal atoms the number of sites covered per adsorbed particle depends on the geometry of the face concerned.[13]

Mr. J. A. Allen and Dr. J. W. Mitchell (*Bristol*) (*communicated*) : We have no evidence as to which crystallographic planes are exposed in our evaporated copper films. The (111) face was used for calculating the number of adsorption sites simply because it is the face of minimum free energy for the close-packed lattice ; the value deduced gives the order of magnitude of the maximum number of adsorption sites on a plane copper surface.

Prof. J. H. de Boer (*Geleen and Delft*) said : Dr. Mitchell has given a most excellent review of the various possibilities of obtaining semi-conductors. May I add two more systems ? There is, in the first place, the substance Fe_3O_4 where the presence of ferrous and ferric ions in equivalent lattice positions causes an excellent semi-conductivity. Secondly, I would like to draw attention to the fact that very thin films of metals, obtained by sublimation *in vacuo*, do not conduct electricity in a purely metallic way. The temperature coefficient of the conductivity is abnormal and it is often found that the thin film behaves formally as a semi-conductor. It was on such very thin molybdenum films that about 12 years ago Dr. H. H. Kraak and I could demonstrate the van der Waals' adsorption of oxygen at low temperatures and chemisorption at higher temperatures. The chemisorption resulted in a large decrease of conductivity. It demonstrated that thin films of metals which are properly annealed can serve as models for studying chemisorption in a similar way as the semi-conductors which are under discussion.

---

[8] Beeck, Smith and Wheeler, *Proc. Roy. Soc. A*, 1940, **177**, 62.

[9] Eley, *Nature*, 1946, **158**, 449.

[10] Appleyard, *Proc. Physic. Soc.*, 1937, **49**, 118.

[11] Picard and Duffenbach, *J. Appl. Physics*, 1943, **14**, 29.

[12] Stranski and Mahl, *Z. physik. Chem. B*, 1942, **51**, 257, 319.

[13] Stranski and Suhrmann, *Ann. Physik*, 1947, **4**, 169.

Dr. D. D. Eley (*Bristol*) said : Dr. de Boer has suggested that very thin metal films are semi-conductors, but I wonder if this may not be misleading. Is it not a question of electrons having to pass from one isolated crystallite to another, across gaps or along the glass ? This jumping process will be activated, and profoundly influenced by adsorbed gases. The effects described by Twigg [14] on silver deposited on glass wool are probably of this type, and possibly also the effects of gases on the conductivity of films as described earlier in this Discussion by Allen and Mitchell.

Prof. J. H. De Boer (*Geleen and Delft*) (*communicated*) : The view expressed by Dr. Eley is often found in literature, but does not, in my opinion, explain the behaviour of well-sintered thin metallic films. I would like to draw his attention to our work published in 1936 and 1937.[15] Gases, when physically adsorbed, give a slight increase of conductivity, when chemisorbed a larger decrease of conductivity may be found, provided the films have been carefully heated to a higher temperature previously. Films of metals like silver on glass show, especially in the presence of oxygen, disturbing (re)crystallization phenomena.

Dr. T. J. Gray (*Bristol*) said : In catalysis it is the interaction of gases with the surface region of the solid which is of major significance. In the course of catalytic processes, defects are created and destroyed. It follows, therefore, that in developing a technique for a study of catalysis by measurements of semi-conductivity those systems should be selected for which there is the optimum change in conductivity during the adsorption and desorption of gases commensurate with stability. At working temperatures for most oxide catalysts the surface zones are of greater significance than the bulk solid both for catalysis and conducivity so that the use of " stabilized " semi-conductors of the TiO_2 varieties would appear to be excluded as insensitive for the required measurements.

To be satisfactory the system selected must show reproducible and reversible changes of semi-conductivity during the adsorption and desorption of various gases. Long-term stability is essential and the various activation energies determined from the kinetic and conductivity relationships must be reproducible between samples although the absolute activity of the samples may vary considerably. These conditions have been found to hold with the copper and manganese oxide systems but with zinc oxide the kinetic study shows some variation with history.

Considering the postulated model for the adsorption of oxygen we have

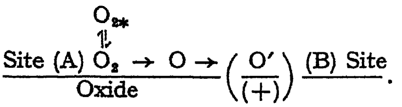

$$\frac{\text{Site (A) }\begin{array}{c}O_{2*}\\ \Updownarrow\\ O_2\end{array} \rightarrow O \rightarrow \left(\frac{O'}{(+)}\right)\text{ (B) Site}}{\text{Oxide}}.$$

Oxygen is initially adsorbed at site A, dissociates and diffuses as atoms over the surfaces. At site B oxygen atoms interact with the surface giving rise to defects which modify the semi-conductivity. The temperature coefficient of conductivity leads to the activation energy for the formation of a current carrier in the process (B). The activation energy derived from the rate of change of conductivity during oxygen adsorption at varying temperatures and pressures leads to the overall activation energy embracing adsorption, dissociation, diffusion and formation of current carrier. The rate of uptake of oxygen gives the activation energy for the initial adsorption process at site A either separately or including the dissociation process. The very large increase in rate of change of conductivity by adsorbing atomic oxygen has indicated the relative significance of this stage while the non-equivalence of the two oxygen atoms from each molecule suggests that one enters into solution in the surface region without affecting conductivity.

---

[14] Twigg, *Trans. Faraday Soc.*, 1946, **42**, 657.

[15] *Rec. trav. chim.*, 1936, **55**, 941, and 1937, **56**, 1103.

Apart from the question of the part played by defects in the catalytic process, it is clear that semi-conductivity measurements afford a satisfactory method of studying the kinetics of catalytic processes.

Dr. A. F. H. Ward (*Manchester*) (*communicated*) : In connection with the measurement of heat of adsorption with small amounts of materials, it may be useful to draw attention to the microcalorimeter which I constructed for this purpose.[16] This functioned as an adiabatic calorimeter, not by varying the temperature of an adiabatic shield, but by removing a quantity of heat from the calorimeter vessel equal to the heat of adsorption. The removal of heat was effected by passing a small current through a series of thermocouples, with one set of junctions in the calorimeter, and producing a cooling by the Peltier effect. This current was adjusted in such a way that the temperature of the calorimeter remained constant, as indicated by another series of thermocouples. A heat evolution of 0·0005 cal. could be detected and heat could be extracted at rates up to about 0·2 cal./min. These figures could be made greater or less by suitable modifications to the electrical circuits.

Dr. B. M. W. Trapnell (*Royal Institution, London*) said : Chemisorption of ethylene takes place with dissociation of hydrogen and formation of a complex MC_2H_2. Deuteration of ethylene, which must proceed through deuteration of the acetylenic complex, will therefore only yield $C_2H_2D_2$ and C_2D_4 unless intermolecular exchanges between complexes take place in the adsorbed layer. Now Turkevich, Bonner, Schissler and Irsa assume that deuteration of ethylene is governed solely by probability considerations, and that mono-, di-, tri- and tetra-substituted bodies are all possible products. The analysis of data on this basis may well give misleading conclusions.

---

[16] Ward, *Proc. Camb. Phil. Soc.*, 1930, **26**, 278.

AUTHOR INDEX*

Allen, J. A., 309, 357, 360, 363.
Anderson, J. S., 238, 305, 362.
Baldock, G. R., 27.
Barrer, R. M., 88, 206.
Beeck, O., 93, **118, 159,** 193, **314.**
Bevan, J. M., 238.
Blekkingh, J. J. A., 200.
Boer, J. H. de, 93, 206, 208, 363, 364.
Bonner, Francis, 352.
Bradley, R. S , 94.
Bremner, J. G M , 79, 92
Bruijn, H. de, 69, 95, 300.
Chapman, P. R., 258.
Colburn, C. B., 39.
Cole, W. A., 314.
Coulson, C. A., 27.
Couper, A., 172.
Denbigh, K. G., 83
Dixon, J. K., 290, 305.
Dowden, D. A., 184, 203, 204, 206, 208, 210, 296, 305
Eggleton, A. E. J., 92, 195
Eley, D. D., 34, 99, 172, 191, 199, 205, 302, 363, 364.
Eucken, A., 128.
Evans, Alwyn G., 302.
Evans, U. R , 296.
Everett, D. H., 86.
Eyring, Henry, 39.
Garner, W. E., 194, **211, 246,** 298.
Given, P. H., 301.
Goodeve, Charles, 192.
Gray, T. J., 246, 250, 331, 364.
Griffith, R. H., 258, 299.
Guinier, A., 344.
Halsey, Jr., J. E., 54, 88.
Hillier, James, 348.
Huang, K., 18.
Hubbell, Harry H., 348.
Hüttig, G. F., 215.
Irsa, Peter, 352.
Johnson, Marvin, F. L., 303.
Kemball, C., 94.
Kropa, E. L., 290.
Laidler, Keith J., 47, 90.
Lindars, P. R., 258.
Los, J. M., 321.
Luft, N. W., 306.
Lyon, Lorraine, 222.
Maxted, E. B., 135.
May, D. R., 290.
Melik, John S., 303.
Mignolet, J. C. P., 105, 326.
Miller, A. R., 57, 80, 87.
Milliken, Jr., T. H., 279.
Mills, G. A., 279.
Mitchell, J. W., 307, 309, 360, 363.
Moon, K. L., 135.
Morrison, J. A., 321.
Oblad, A. J., 279, 302.
Overgage, E., 135.
Porter, A. S , 203, 358.
Reynolds, P. W., 184.
Rideal, Eric K., 96, 114.
Ries, Jr., Herman E , 303.
Ritchie, A. W., 159.
Rowland, P R , 196, 209, 363.
Saunders, K. W., 290.
Savage, S. D., 250.
Schissler, Donald, 352.
Schroyer, F. K., 337.
Schuit, G. C. A., 205, 299.
Schwab, G.-M., 79, 88, 89, 91, **166,** 198, 205, 207, 298.
Selwood, P. W., 222, 306, **337.**
Steiner, H., 264.
Stone, F. S., 194, **246, 254.**
Sykes, K. W., 82.
Tamele, M. W., 270.
Taylor, H. S., 9.
Thomas, N., 80, 82.
Tiley, P. F., 201, 202, **254,** 362.
Tompkins, F. C., 85, 92, 201, 202, 203.
Trapnell, B. M. W., 114, 191, 193, 360, 365.
Turkevich, John, 348, 352.
Twigg, G. H., 89, 90, **152.**
Ubbelohde, A. R., 203, 204.
Uri, N., 207.
Ward, A. F. H., 95. 365.
Weiss, J., 302.
Wheeler, A., 314.
Wicke, E., 199.
Winter, E. R. S., 231, 300.
Wright, P. A., 194.
Wyllie, G., 18, 82, 91.
Young, D. M., 84, 85.
Zawadzki, J., 140.
Zwietering, P., 196.
Zwolinski, Bruno J., 39.

---

* The references in heavy type indicate papers submitted for discussion.

DISCUSSIONS OF THE FARADAY SOCIETY

No. 9, 1950

SPECTROSCOPY AND MOLECULAR STRUCTURE

AND

OPTICAL METHODS OF INVESTIGATING CELL STRUCTURE

THE FARADAY SOCIETY
Agents for the Society's Publications
The Aberdeen University Press Ltd.
6 Upper Kirkgate
Aberdeen

The Faraday Society reserves the copyright of all Communications published in the "Discussions"

PUBLISHED . . APRIL 1951

PRINTED IN GREAT BRITAIN AT
THE UNIVERSITY PRESS
ABERDEEN

A GENERAL DISCUSSION

ON

SPECTROSCOPY AND MOLECULAR STRUCTURE AND OPTICAL METHODS OF INVESTIGATING CELL STRUCTURE

25TH–28TH SEPTEMBER, 1950

A GENERAL DISCUSSION on Spectroscopy and Molecular Structure and Optical Methods of Investigating Cell Structure was held in the Department of Zoology, The University of Cambridge (by kind permission of Prof. James Gray), on the 25th, 26th, 27th and 28th of September. The President, Sir John Lennard-Jones took the Chair at the opening sessions, and later it was taken by Dr. H. W. Thompson and Prof. J. T. Randall. Over 250 members and visitors attended.

Among the distinguished overseas members and guests welcomed by the President were the following :—

Prof. Gladys Anslow (U.S.A.), Prof. C. J. Bakker (Holland), Prof. and Mrs. L. Brewer (U.S.A.), Dr. and Mrs. Brolin (Sweden), Mr. and Mrs. R. D. Brown (Australia), Dr. Emma Carr (U.S.A.), Dr. N. Chako (Holland), Dr. Andrée Cheutin (France), Prof. M. Colonna (Italy), Prof. Barry Commoner (U.S.A.), Dr. E. D. Cook (U.S.A.), Dr. J. Duchesne (Belgium), Prof. and Mrs. B. Edlen (Sweden), Dr. M. Errera (Belgium), Dr. James and Prof. Hertha Sponer Franck (U.S.A.), Dr. A. Gatterer (Italy), Dr. V. E. Gonsalves (Holland), Dr. and Mrs. R. C. Gore (U.S.A.), Prof. and Mrs. E. Havinga (Holland), Dr. J. H. de Heer (Holland), Dr. H. Herzberg (Canada), Prof. D. F. Hornig (U.S.A.), Miss M. Elaine Hungerman (U.S.A.), Prof. H. Hyden (Sweden), Dr. S. Iversen (Denmark), Prof. P. Jacquinot (France), Prof. F. A. Jenkins (U.S.A.), Mr. A. L. Jones (Australia), Dr. Marie-Louise Josien (France), Dr. H. Kaiser (Germany), Dr. and Mrs. M. Kasha (U.S.A.), Prof. and Mrs. A. Kastler (France), Prof. J. A. A. Ketelaar (Holland), Mr. P. F. A. Klinkenberg (Holland), Dr. C. Konigsberger (Holland), Mr. A. L. V. Laforgue (France), Dr. C. La Lau (Holland), Dr. J. Lecomte (France), Prof. and Mrs. J. E. Mack (U.S.A.), Prof. A. Mangini (Italy), Dr. and Mrs. J. P. Mathieu (France), Prof. R. Mecke (Germany), Dr. W. F. Meggers (U.S.A.), Dr. G. Milazzo (Italy), Prof. H. H. Nielsen (U.S.A.), Prof. J. Rud Nielsen (U.S.A.), Mr. R. J. F. Nivard (Holland), Prof. and Mrs. L. J. Oosterhoff (Holland), Prof. R. Passerini (Italy), Prof. M. Pestemer (Germany), Dr. Lucy Pickett (U.S.A.), Dr. E. K. Plyler (U.S.A.), Dr. and Mrs. B. Pullman (France), Prof. and Mrs. D. H. Rank (U.S.A.), Prof. M. Rolla (Italy), Dr. G. Salomon (Holland), Dr. M. Schon (Germany), Dr. A. Schors (Holland), Prof. H. Schuler (Germany), Dr. G. Semerano (Italy), Dr. W. J. W. Serfontein (Holland), Dr. B. W. and Dr. Charlotte Moore Sitterly (U.S.A.), Dr. Eleanor Slifer (U.S.A.), Dr. D. C. Smith (U.S.A.), Dr. U. Stille (Germany), Prof. P. Swings (Germany), Prof. F. J. Taboury (France), Dr. O. H. Theimer (Austria), Dr. Bo. Thorell (Sweden), Dr. B. Vodar (France), Mr. R. A. Vroom (Holland), Dr. K. Wieland (Switzerland), and Mr. D. Williams (U.S.A.).

CONTENTS

A. Spectroscopy and Molecular Structure

I. Electronic Spectra—

PAGE

Introductory Paper: Significant Progress and Present Problems. By C. A. Coulson 1

The Low Excited States of Simple Aromatic Hydrocarbons. By D. P. Craig 5

Characterization of Electronic Transitions in Complex Molecules. By Michael Kasha 14

Discussion of the Lowest Singlet Transition in Naphthalene as a Forbidden Transition $A_{1g}-A_{1g}$ and Remarks on the Higher Singlet Levels. By H. Sponer and (the late) Gertrud P. Nordheim 19

Applications of the Electronic Spectra of Pyridine Homologues to Quantitative Analysis and to the Measurement of Dissociation Constants. By E. F. G. Herington 26

The Ultra-violet Absorption Spectra of Fluorinated Toluenes. By W. T. Cave and H. W. Thompson 35

Natural Hypsochromic Shifts. By Mme. Alberte Pullman and Bernard Pullman 46

The Absorption Spectra of some Substituted Benzenes and Naphthalenes in the Vacuum Ultra-violet. By V. J. Hammond, W. C. Price, J. P. Teegan and A. D. Walsh 53

The Absorption Spectroscopy of Substances of Short Life. By George Porter 60

General Discussion.—Dr. A. Kastler, Dr. D. P. Craig and Prof. H. Sponer, Dr. A. Burawoy, Dr. M. Kasha, Prof. J. Franck, Prof. R. Mecke, Mr. A. R. Burgess, Prof. H. Sponer, Dr. H. W. Thompson, Prof. J. Rud Nielsen, Dr. R. N. Haszeldine, Dr. Lucy W. Pickett, Dr. G. Herzberg, Dr. D. A. Ramsay, Dr. R. F. Barrow, Mr. S. Leach, Prof. P. Goldfinger, Dr. G. Porter, Dr. S. Robin, Dr. B. Vodar . 69

II. Vibrational and Rotational Spectra—

Introductory Paper. By H. W. Thompson 82

A Study of the Low Frequency Fundamental Bands in the Spectrum of AsH_3. By Harald H. Nielsen 85

Infra-red Spectrum and Structure of the HNCO Molecule. By G. Herzberg and C. Reid 92

Infra-red Absorption Spectra of Twelve Substituted Benzene Derivatives from 15 to 40 Microns. By Earle K. Plyler . 100

Determination of Molecular Structure with Microwave Spectroscopy. By E. Bright Wilson, Jr. 108

Infra-red Spectra of Crystals at Low Temperatures. By D. F. Hornig 115

PAGE

Infra-red Adsorption Spectra of Metallic Acetyl-Acetonates. By Jean Lecomte 125

The Infra-red Absorption Spectra of Boron-Nitrogen Compounds. By W. C. Price, R. D. B. Fraser, T. S. Robinson and H. C. Longuet-Higgins 131

Infra-red Spectra of Organic Thiophosphates. By R. C. Gore 138

Some Infra-red Spectroscopic Studies of Rotational Isomerism. By J. K. Brown and N. Sheppard 144

Internal Rotation in Zinc Dimethyl and Mercury Dimethyl. By D. R. J. Boyd, H. W. Thompson and R. L. Williams 154

Infra-red Spectra of Hydroxylic Compounds. By R. Mecke . 161

Infra-red and Raman Spectra of 1 : 3 : 5-Trifluorobenzene. By J. Rud Nielsen, Ching-Yu Liang and D. C. Smith . 177

Vibrational Spectra of Carbon and Silicon Tetramethyl and their Monodeutero Derivatives. By D. H. Rank, B. D. Saksena and E. R. Shull 187

The Raman Spectra of Metallic Nitrates and the Structure of Concentrated Solutions of Electrolytes. By Jean-Paul Mathieu and Mackenzie Lounsbury 196

GENERAL DISCUSSION.—Prof. R. Mecke, Prof. G. B. B. M. Sutherland, Dr. G. Herzberg, Dr. H. W. Thompson, Prof. C. A. Coulson, Prof. D. F. Hornig, Dr. G. L. Coté, Dr. A. Kastler, Dr. D. W. E. Axford, Dr. N. Sheppard, Mr. T. A. Kletz, Prof. J. A. A. Ketelaar, Dr. Mansel Davies, Dr. P. Torkington, Prof. A. R. Ubbelohde, Dr. J. Lecomte, Prof. M. Pestemer, Dr. J. Romand, Dr. B. Vodar, Prof. J. Rud Nielsen, Dr. N. Sheppard, Dr. Delia Simpson, Prof. D. H. Rank, Dr. Orville Thomas, Dr. K. M. Guggenheimer, Dr. D. C. Smith 207

III. Vibrational Spectra of Complex Molecules—

The Infra-red Spectra of Complex Molecules. By H. W. Thompson, D. L. Nicholson and L. N. Short 222

The Infra-red Spectrum of Ethylene Polymers. By L. H. Cross, R. B. Richards and H. A. Willis 235

Evidence of Chain Folding in Polypeptides and Proteins. By A. Elliott and E. J. Ambrose 246

Infra-red and X-ray Studies of Chitin. By S. E. Darmon and K. M. Rudall 251

The Interpretation of the Vibrational Spectra of the *n*-Paraffins. By J. K. Brown, N. Sheppard and Miss D. M. Simpson. . 261

Some Problems in the Interpretation of the Infra-red Spectra of Large Molecules. By G. B. B. M. Sutherland . . 274

The Application of Polarized Infra-red Radiation to Problems in Molecular Structure—

I. Polyisoprenes. By G. B. B. M. Sutherland and A. Vallance Jones 281

Infra-red Analysis of Rubber Derivatives. By G. Salomon, A. Chr. van der Schee, J. A. A. Ketelaar and B. J. van Eyk 291

PAGE

Polymer Types and Specific Absorptions in the Ultra-violet by Hydrogen-bridged Amides and Alcohols with Application to the Protein Structure Problem. By Gladys A. Anslow 299

General Discussion.—Dr. P. Torkington, Prof. G. B. B. M. Sutherland, Dr. H. Lenormant, Dr. G. J. Minkoff, Mr. H. A. Willis, Dr. N. Sheppard, Dr. J. G. Reynolds, Mr. L. H. Cross, Dr. D. C. McKean, Dr. A. Elliott, Mr. E. J. Ambrose, Dr. Mansel Davies, Dr. S. E. Darmon, Dr. P. Holliday, Dr. H. W. Thompson, Prof. R. Mecke, Dr. Delia Simpson, Prof. J. A. A. Ketelaar, Dr. G. Salomon, Dr. E. R. Holiday, Prof. G. A. Anslow 319

IV. Appendix—Studies of the Carboxyl Group—

Part I.—The Geometrical Structure. By Mansel Davies and Orville Thomas 335

Part II.—The Potential Function of the Formate Ion and the Formic Acid Molecule. By Orville Thomas . . . 339

B. Optical Methods of Investigating Cell Structure

I. Microscopical Apparatus—Instrument Design and Technique—

Introductory Paper : Optical Methods in Cytology. By J. T. Randall 353

A Reflecting Microscope of 1·3 Numerical Aperture. By K. P. Norris and M. H. F. Wilkins. 360

Some Aspects of Microspectrography. By M. H. F. Wilkins . 363

Aspects of Ultra-violet and Infra-red Microspectrography with the Burch Reflecting Microscope. By R. Barer . . 369

Infra-red Microspectrometry with a 0·8 N.A. Reflecting Microscope. By R. D. B. Fraser 378

General Discussion.—Dr. R. Barer, Dr. K. W. Keohane, Dr. M. H. F. Wilkins, Mr. E. W. Taylor, Dr. T. A. Kletz, Mr. W. E. Seeds, Prof. B. Commoner, Mr. H. G. Davies, Dr. R. D. B. Fraser 383

II. Application of Micro- and Macro-Spectrography—

Studies with a Reflecting Microscope : Microspectroscopy of Living and Fixed Cells. By Robert C. Mellors . . 398

The Ultra-violet Absorption Spectra of the Aromatic Amino Acids in Proteins and Related Compounds. By G. H. Beaven, E. R. Holiday and E. M. Jope 406

Ultra-violet Microspectrographic Studies of Nucleoproteins and Crystals of Biological Interest. By W. E. Seeds and M. H. F. Wilkins 417

Observations of Proteins in Polarized Ultra-violet Light. By M. F. Perutz, M. Jope and R. Barer 423

Some Comparison between X-ray and Ultra-violet Absorption in Different Tissue and Cell Structures. By Arne Engström 427

PAGE

Self-recording Microspectrography and its Applications on Problems regarding the Endocellular Formation of Haemoglobin. By Bo Thorell 432

Microspectrographic Studies on the Yellow Pigment in Nerve Cells. By Holger Hydén and Bo Lindström 436

Ultra-violet Microspectrography of Living Tissue Culture Cells—Part I.—Radiation Measurements. By H. G. Davies . . 442

Ultra-violet Absorption Spectra of Structures in Surviving Cells. By Barry Commoner 449

Ultra-violet Microspectrography of Living Tissue Culture Cells—Part II.—Microspectrographic Studies of Living Cells and Ultra-violet-Irradiated Chick Fibroblasts. By P. M. B. Walker and H. G. Davies 461

Components of Normal and Abnormal Liver Cells Studied by Ultra-violet Microscopy and by Differential Centrifugation. By Hubert R. Catchpole and Isidore Gersh 471

The Ultra-violet Absorption of Living Cells. By J. R. G. Bradfield 481

General Discussion.—Dr. R. Barer, Dr. E. Schauenstein, Dr. G. H. Beaven, Dr. E. R. Holiday, Prof. B. Commoner, Dr. I. MacArthur, Mr. P. M. B. Walker, Dr. E. M. F. Roe, Dr. B. Thorell, Dr. D. F. Cole, Dr. H. R. Catchpole, Dr. I. Gersh, Dr. J. R. G. Bradfield 491

HETEROGENEOUS CATALYSIS

ERRATA

Faraday Soc. Discussions, No. 8, 1950.

P. 38, l. 9 : $E(\text{Ta} = \text{N})$ *should be* 89·3,

making $Q_{\text{calc.}} = -74{\cdot}4$ kcal /mole⁻¹

for the process, $H_2 + 2\text{Ta} \equiv \text{N} \rightarrow 2\text{Ta} = \text{N} - \text{H}$.

The observed value chemisorption of hydrogen onto a nitrogen film on tantalum is 27 kcal./mole^{-1}, and so the conclusion is now that the model above cannot describe the process.

P. 183, Table III, l. 1 : $\Delta E_{\text{ads.}}$ *For* $W^- \ldots H^+$

should be 8·70 *not* 10·99 eV.

A. SPECTROSCOPY AND MOLECULAR STRUCTURE

I. ELECTRONIC SPECTRA

INTRODUCTORY PAPER

SIGNIFICANT PROGRESS AND PRESENT PROBLEMS

By C. A. Coulson

Received 10*th October*, 1950

The Discussions of the Faraday Society have a habit of marking a turning-point in their subject. It is a long time now since the Society last discussed electronic spectra ; but the moment is very opportune for doing so, and I think we shall look back on the group of papers presented at this session as marking one more of those turning-points of which I have just spoken.

Problems in electronic spectra roughly divide themselves into matters of characterization, or classification, of the transition involved, and the business of calculation, by which confirmation of the characterization is obtained and new predictions are made, or a deeper understanding is achieved of the factors which operate to decide either the magnitude of the energy jump, or its intensity. All these matters receive attention in the series of papers that follow.

We shall see these in perspective if, for a moment, we reflect on the manner in which, between 20 and 25 years ago, a similar attack was being made on the relatively simple task of understanding electronic transitions in diatomic molecules. In those days there was relatively little theoretical guidance, though people like our President Sir John Lennard-Jones, and Hund, Herzberg and Hückel had begun those wave-mechanical studies that were to confirm almost all the details of the picture largely developed semi-empirically by Mulliken. There were three chief tools in the making of this picture :

(*a*) the united-atom viewpoint, in which the energy levels of the molecule are traced back to those of the larger single atom that would result from a coalescing of the two nuclei ;

(*b*) a classification of individual electron orbitals into σ and π, corresponding respectively to complete symmetry around the molecular axis, and to the existence of a plane of zero charge density, which passes through the axis and with respect to which the wave-function is antisymmetric ;

(*c*) use of the isoelectronic principle, in which pairs of related molecules, such as CO and N_2, which share the same number of valence electrons and presumably have related spectral transitions, are studied together, and compared.

The guiding principle behind all this was that the characterization of molecular energy levels and transitions was similar in essence to that of atomic levels : i.e., that we can assign orbits, and energies, to each separate electron, and discuss transitions of any single electron from one such orbit to another—transitions in which the other electrons are not supposed to change their wave functions to any significant degree. All this could be substantiated by qualitative computations, but the intractable character of the numerical work was such that no really detailed *ab initio* calculations could be made except perhaps for molecular hydrogen H_2.

Now the papers in the present Discussion are almost all concerned, not with diatomic molecules, but with relatively large systems like naphthalene. With the exception of that interesting account by Porter who shows that a flash technique enables the same sort of information to be acquired with regard to free radicals and other short-lived substances as was needed for the more normal simple molecules studied since 1925, all the contributions involve molecules with closed rings and, moreover, with conjugation, so that many of the valence electrons cannot even be treated as if they belonged to one bond, with a local behaviour similar to that obtaining in diatomic molecules, but must be treated as if they belonged to the whole molecule. Particularly is this true of the familiar π-electrons of organic chemistry. All this means that the problem of electronic spectra appears quite different now from formerly. But the interesting thing is this : all three of those chief ideas that I described for diatomic molecules are now in use for these large molecules also. They have changed in the process of adaptation, but I do not believe we shall properly appreciate the papers in this section of the Discussion unless we recognize them in their new guise. This I must now explain.

But first two words of warning. In the 1930's we were so bemused by the theory of resonance that attempts were made (and indeed still are made in some quarters) to apply it in an uncritical way to an explanation of electronic transitions. You will often find it stated, for example, that " the more resonance there is, the longer is the wavelength of absorption ". Thus, " in amino naphthalene there is more resonance than in naphthalene : therefore the absorption moves towards the red ". This is plain nonsense, and, as the Pullmans show,* it is often not even in accord with the facts. There is fortunately very little of such stuff in this Discussion : its unforgiveable sin is that it forgets that electronic spectra arise from a transition from one level to another. Only by an analysis of both levels can any satisfactory inferences be drawn.

The second matter is that there is, in this set of papers, practically no sign of any conflict between rival theories of approximation, whether molecular-orbital, valence-bond, or any other, such as we should have had as recently as only two or three years ago. This is a healthy sign. It does not mean that all the methods are in any nice happy state of mutual agreement. But it does mean that we now recognize the very severe limitations that are inescapable in any attempt at a thoroughgoing calculation of molecular spectra. It is an interesting stage at which we have now arrived, that we regard our calculations as being indicative and corroborative, rather than as settling the issues in dispute.

Now for the three principles of which I spoke earlier. First there is the united-atom viewpoint. For a molecule like benzene, or pyridine, this is obviously no use except in a discussion of Rydberg levels, in which the one excited electron moves in an orbit so far outside the greater part of the molecule that the precise location of the net positive charge around which it may be regarded as moving, is not enormously significant. This point of view is well utilized in the paper by Teegan, Walsh, Hammond and Price, though, as they say, there is a great deal more to be done before even these—conceptually the simplest of all molecular transitions—are fully understood.

The second principle was the division into σ and π electron orbits. This " goes over " into a discussion of the symmetry of the molecule, which, as the powerful methods of group theory show with a quite astonishing economy of effort, separates the orbits of individual electrons and the complete electronic wave function for the molecule as a whole, into classes. These classes are quite clear-cut and distinct : they arise solely on account of the particular symmetry of each molecule. When we speak of the characterization of a transition, as, e.g., the familiar

---

* This Discussion.

$A_{1g} \rightarrow E_{1u}$ transition in benzene, we mean, in the first place, the description in terms of symmetry class of the initial and final states of the molecule : and in the second place we often mean an attempt to interpret this transition as the change of one electron in an orbit of given symmetry type to an orbit of a different symmetry type, so that, for example, we can associate a given band with a particular direction in the molecule, and show that only light polarized in this direction will be absorbed, or emitted, in the transition responsible for this band. Criteria of this kind are likely to be particularly important, as later papers in this Discussion show, for understanding the behaviour and structure of many biologically important molecules. In this kind of purely qualitative analysis it is absolutely essential to invoke the aid of theory, to show which transitions are allowed, and which forbidden.

Thirdly, there is the isoelectronic principle. This has reappeared, after a period of eclipse, in two quite different forms. In the first, we discuss a homologous series of molecules, such as benzene, naphthalene, anthracene and other 'acenes, finding in the variation from member to member evidence of the nature of the transitions. This is well-exemplified in the work of Craig and Kasha in this discussion. But it also takes the form of an enquiry into what happens to a given transition when we change one part of the molecule as e.g. by a new substitution, or an old substitution at a new position in the molecule, or by a replacement of a carbon atom in the aromatic nucleus by a nitrogen (cf. benzene and pyridine). This is illustrated in the paper by Herington on different homologues of substituted pyridines, and by Cave and Thompson on fluorinated toluenes. It is also shown in the interplay between electronic and vibrational motion, where, on account of the occurrence of certain vibrations of particular symmetry, the shape of the molecule alters in such a way as to permit otherwise forbidden transitions. This type of argument, originally due to Ingold, is applied with much success to the study of naphthalene by Sponer and Nordheim. The opening-up of this field is now being greatly accelerated by working in glassy solutions at very low temperature. This technique, so ably developed by Kasha and his collaborators, and others, has already provided us with large numbers of new bands, and shown us that some bands which we thought were characteristic of a single transition, are in fact superpositions of two, or even three, separate bands.

I think that now you will see why I regard this Meeting as signalling a most important stage in understanding electronic spectra. There are three particular applications in which it seems to me that real progress has now been made. Thus :

(*a*) we do really know a little about what Rydberg series mean : and how the quantum defect is related to the type of atomic transition to which the series applies. We know a little about the way in which bulky substituents will affect these series, and destroy fine structure, by providing an electron cloud with which the excited electron collides.

(*b*) We do really begin to be able to characterize the valence-shell, or $N \rightarrow V$, transitions. No longer is it true that the benzene molecule is the only one for which we are reasonably certain that we can classify the long-wavelength absorption spectra. This, which is the result of a good deal of work by many people, is a solid achievement which will undoubtedly open up this whole field enormously. It certainly shows the enormous importance of a proper study of the intensities of these, and other, transitions. A greater emphasis on transition probabilities is likely to be a feature of future work in this field.

(*c*) We do really begin to understand the extremely interesting ways —of a different order of magnitude from atomic spectra—in which technically forbidden transitions occur. In fact many of the most characteristic features of molecular spectra arise just from these transitions.

Here, the study of singlet-triplet spectra, and particularly the agreement between calculated and observed intensities, is beginning to be quite impressive.

This does not mean that everything is clear—far from it. Indeed, there are three really serious problems which, although much studied, have at present received no satisfactory answer. In the first place there stands the fundamental concept on which the whole study was built—the concept of a transition in which one electron changes its orbit. This worked well for atoms and for diatomic molecules. But there is a growing sense that it is less valid with large molecules. What is described technically as configuration interaction appears to be quite a lot more important with π-electron systems than we had originally supposed. If this simple and pictorial interpretation has to be abandoned, in whole or in part, it is most essential that we should find an alternative simple picture. For without some easily-visualized model, we shall almost certainly miss the really decisive measurements and calculations.

The second aspect that deserves a fuller study is the way in which we may describe a Rydberg level. For anything like a satisfactory interpretation, it is clearly insufficient to say that these levels are similar to those of an otherwise free electron moving round an effective positive charge of approximately unity at some mean centre of position. For if at the moment of excitation the electron was around nucleus A, then the effective positive charge is at A, and the Rydberg orbit should have A as its centre. Such a situation would not remain for long. Very soon, just as in the migration of F-centres and other singularities in an infinite alkali-halide crystal, the net positive charge and the Rydberg orbit would have moved to be around atoms B, C . . . . If we knew how to introduce this concept adequately into our wave-mechanical analysis, it would not be long before we could deal effectively with the large amount of experimental evidence and observation now available.

The last problem that I should mention is that of the internal conversion of energy within an excited molecule. At present we seem to be without any clear understanding of the mechanism of those radiationless transitions which take place, sometimes very easily, after the absorption of energy. Here, quite evidently, we require a much more detailed study of the interplay between electronic and vibrational motion in cases where the latter energy may be a much larger fraction of a conventional bond energy than is usually found in diatomic molecules. In this sort of study the use of intensities, particularly absolute intensities of transition, is likely to play a dominant role.

Work is being done along these, and other, lines and will doubtless soon yield its successes. What is important just now is that we know what questions to ask! That in itself is a measure of our progress.

It is tempting to say more about what has been done in the batch of papers now under discussion. But I hope at least that I have made clear the background against which you must judge them. I must leave the detailed explaining to the authors themselves.

King's College,
Strand, London, W.C.2.

THE LOW EXCITED STATES OF SIMPLE AROMATIC HYDROCARBONS

By D. P. Craig

Received 18th July, 1950

Lack of experimental knowledge of the polarization of spectral band systems on the one hand, and disagreements between theoretical predictions on the other, have allowed no spectral assignment in the aromatic series to be securely held except that of singlet $A_{1g} - B_{2u}$ for the 2600 Å band system of benzene.

This position has recently become clearer. On the experimental side a key assignment in naphthalene is strongly, even if not conclusively, indicated by Kasha and Nauman's finding that the lowest transition is extremely weak, comparable with the symmetry forbidden system in benzene. And on the theoretical side the major disagreements between molecular-orbital (MO) and valence-bond (VB) calculations are resolved if in the former, used with non-empirical energy terms, configurations are allowed to interact, and if in the latter some polar structures are added to the familiar non-polar ones.

In the simplest cases of benzene and cyclobutadiene the effect of configuration interaction is greatly to diminish the importance of polar structures from the large value associated with conventional MO wave functions. This brings the state wave functions, as well as the sequence of their energies, much nearer to those of VB theory.

The general support given to the VB theory by its agreement in simple cases with a non-empirical theory allows some confidence in its use for more complex molecules. In 'acenes, polar structures being excluded, low-lying A_g and B_{3u} states ought to be calculable without serious error. Low-lying B_{1g} and B_{2u} states will only be so calculable when polar structures are included. The assignments in 'acene spectra which these considerations support are set out and discussed.

Comparisons between theory and experiment in the ultra-violet spectroscopy of aromatic molecules are severely limited because in very few cases is it possible to assert definitely that the experimental band system is that one to which the calculations refer. Indeed there is only a single assignment, that of singlet $A_{1g} - B_{2u}$ for the 2600 Å benzene band, which stands firmly on an experimental basis,[1, 2] although there are others to be mentioned supported by rather convincing but not yet conclusive evidence. We may for example identify a second benzene band system, the intense system at 1750 Å, as $A_{1g} - E_{1u}$ on the ground that this is the only allowed transition within the π-electron shell starting from an A_{1g} state. These two assignments in benzene, together with an assignment in naphthalene to be detailed later, form the more precise part of the experimental basis for theories of π-electron states and no theory which fails to account for them, at least approximately, can be satisfactory. The numerous wavelength and intensity measurements of band systems of unknown assignment do not allow critical tests of such theories although they may give them some support if these two quantities can be correctly calculated.

Two theoretical methods, one empirical and one non-empirical, appear at present to deal satisfactorily with the three assigned band systems already mentioned. The intention of this paper is to discuss these two, and some aspects of the relation between them, and in the course of this to indicate the position and prospects from the theoretical point of view.

---

[1] Sponer, Nordheim, Teller and Sklar, *J. Chem. Physics*, 1939, 7, 207.

[2] Ingold *et al.*, *J. Chem. Soc.*, 1948, 406, *et seq.*

A general problem which prompts detailed study of cases such as those discussed here is that of justifying simple ways for dealing with molecules too complex for direct non-empirical calculations. Broadly, it will be concluded that the agreement in simple cases between these two methods is enough to give considerable support to the empirical one in calculations of certain of the energy levels in complex molecules.

1. Benzene.—The two theoretical methods whose performance is to be discussed are the empirical valence-bond (VB) [3, 4] method and the non-empirical method of interacting molecular-orbital configurations.[5, 6] An empirical method is one in which the results for a series of related molecules are expressed in terms of energy parameters. These are given values by equating calculated and experimental values in one or more band systems which are not themselves to be the subject of the theoretical study. The common practice has been to use the 2600 Å benzene transition in this way and so to calculate the energies of other band systems in aromatic molecules relative to it. In non-empirical methods the terms appearing in the energy calculations are derived mathematically, the only experimental quantity taken for granted being the C—C internuclear distance. Simplifying assumptions underlie both methods, but this fact needs no detailed repetition here being set out in the references already cited.

In the non-empirical method the starting-point is a set of one-electron molecular orbitals formed by combining atomic orbitals situated at the carbon atoms. Molecular wave functions are formed by assigning the six electrons to these molecular orbitals and making the whole antisymmetric to electron interchange. No molecular orbital may appear more than twice in such a wave function but with this restriction it is still possible to place the electrons in 141 different ways, each of which is an electron *configuration*. The wave functions describing actual molecular states are linear combinations of configuration wave functions with coefficients chosen to minimize the energy.[6] The implied variation problem is expressed in a secular equation whose roots are the approximate energy eigenvalues. The results are shown in the third column of Table I.

TABLE I.—THE LOW-LYING STATES OF BENZENE

State	Expt. Energy (eV)[9]	Calc. (eV) (non-empirical)[6, 7]	Calc. (eV) (emp. VB)[8]
$^1A_{1g}$	0	0	0
$^1B_{2u}$	4·7	2·0	(4·7)
$^1E_{2g}$	6·2		6·6
$^1B_{1u}$	—	4·5	7·9
$^1E_{1u}$	7·1	6·3	7·9

A comparison with the experimental values shows adequate agreement on two essential points. Firstly, the lowest excited singlet state is correctly found to be B_{2u}. Secondly, an E_{1u} state is found in the expected energy region and the calculated [7] intensity of transitions leading to it ($f = 0·81$) agrees tolerably well with the experimental ($f = 0·69$).[9] Agreement of this general sort is as much as may be looked for in the non-empirical method, because three- and four-centre integrals, even if included, are somewhat inaccurate, and also because the calculated energies come out

[3] Huckel, *Z. Physik*, 1930, **70**, 204.
[4] Sklar, *J. Chem. Physics*, 1937, **5**, 669.
[5] Goeppert-Mayer and Sklar, *ibid.*, 1938, **6**, 645.
[6] Craig, *Proc. Roy. Soc. A*, 1950, **200**, 474.
[7] Bevan and Craig (to be published).
[8] Craig, *Proc. Roy. Soc. A*, 1950, **200**, 401.
[9] Klevens and Platt, *J. Chem. Physics*, 1949, **17**, 470.

as differences between much larger numbers. In the calculated levels of Table I there are two which fall between the B_{2u} and E_{1u} already referred to. The lower of these is an E_{2g} state and this suggests that the band system at 2000 Å is to be assigned $A_{1g} - E_{2g}$. This assignment is assumed in Table I but it is not yet supported by experimental evidence.

The right-hand column of Table I gives values calculated by the empirical VB method, based on the 5 nonpolar structures and 24 of the polar structures. The bracketed value for B_{2u} is assumed in the course of the calculation and hence affords no test of the theory. An E_{1u} state is found in the correct energy region and the calculated intensity for transitions leading to it is $f = 0{\cdot}22$ (expt. 0·69). The small calculated value is due to the neglect of polar structures with charges on remote atoms, which contribute very strongly to the transition moment even though energetically not so important. Using this method as a guide to the assignment of the band system at 2000 Å we again conclude that it is $A_{1g} - E_{2g}$.

It is unlikely that band systems in the far ultra-violet beyond 1750 Å are to be understood as transitions between π-electron states, and the present discussion therefore embraces only three band systems. As has been explained two of these are assigned independently of detailed theoretical considerations as $A_{1g} - B_{2u}$ and $A_{1g} - E_{1u}$ and the third system, at 2000 Å, is assigned as $A_{1g} - E_{2g}$ from two independent theoretical methods.

In the triplet series there is qualitative agreement between the empirical and non-empirical methods that the lowest and first excited triplet states are $^3B_{1u}$ and $^3E_{1u}$. These will not, however, be discussed in detail because the states have not yet been finally identified experimentally.

2. Configuration Interaction and the Role of Structures.—The purpose of the next few paragraphs is to compare the two methods and to demonstrate that the agreement between their results reflects a strong similarity, which is not at once obvious, in the character of the wave functions used to describe molecular states.

VB structures may be classified into nonpolar and polar structures. Nonpolar structures assign one π-electron to each atomic $2p$ orbital; they alone are used in the VB method in its simplest form. Polar structures have doubly occupied and unoccupied orbitals as illustrated below for cyclobutadiene, and a refinement to the VB method is to include some of these in the description of molecular states. In highly symmetrical molecules this classification is associated with a distinction of symmetry. Thus in benzene the familiar five nonpolar structures are capable of being combined to give molecular wave functions of only three out of the possible six different symmetry types, viz., A_{1g}, B_{2u} and E_{2g}. The others, A_{2g}, B_{1u} and E_{1u}, can therefore be represented in VB theory only by combinations of polar structures. This distinction is one of energy as well as of symmetry since the assumptions of the method make the states admitting nonpolar structures come out to be more stable than the others. This simply means that within the framework of VB theory it is energetically very unfavourable to place two π-electrons on the one atomic centre, as required in a polar structure. In MO theory the formally analogous distinction is between symmetries which do and do not arise in a chosen configuration, and it is easily verified that the symmetries which group together naturally in this scheme are not the same as those in the VB theory. However, when the MO configurations are allowed to interact

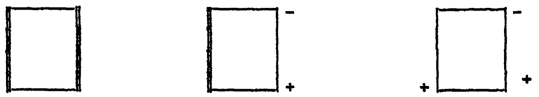

Nonpolar structure. Polar structure (singly charged) Polar structure (doubly charged)

FIG. 1.

and so to effect energetically favourable changes in the composition of the wave functions, we at once notice that it is the states with symmetries compatible with nonpolar structures which are the most reduced in energy and which, finally, become lowest of all. This suggests that the predominance of nonpolar structures taken for granted in the empirical theory is supported by the non-empirical one.

Two aspects of this situation may be illustrated in benzene and cyclobutadiene both of which allow the necessary clear distinction between the symmetry types with respect to nonpolar structures. The first aspect is, that, of the states which arise in a chosen configuration, those for which nonpolar structures may be written are the most changed by configuration interaction, and the second is that, after configuration interaction has been allowed for, states of these symmetries are the lowest of their multiplicity. Table II illustrates the first point.

TABLE II.—ENERGY CHANGES (IN eV) IN CONFIGURATIONAL INTERACTION

	States Compatible with Nonpolar Structures	Others
(*a*) Benzene.[7]		
$^{1}A_{1g}$	4·4	—
* $^{1}B_{2u}$	6·1	—
** $^{1}E_{2g}$	5·9	—
* $^{1}E_{1u}$	—	4·9
* $^{1}B_{1u}$	—	4·1
** $^{1}A_{2g}$	—	~1
† $^{3}B_{1u}$	1·2	—
† $^{3}E_{1u}$	1·1	—
† $^{3}B_{2u}$	—	0·1
(*b*) Cyclobutadiene.[10]		
* $^{1}A_{1g}$	3·3	—
* $^{1}B_{2g}$	2·4	—
* $^{1}B_{1g}$	—	0·1
* $^{3}A_{2g}$	1·6	—
† $^{3}E_{u}$	4·0	—
† $^{1}E_{u}$	—	2·8

Results for the triplet states of benzene are based on configurations within a 10 eV range only as in ref. (6). Otherwise all the important configurations are used.

States similarly marked in Table II by stars or daggers occur in the same MO configuration. Those admitting nonpolar arrangements of the electrons are more, and usually much more, depressed in energy than the others and this must surely be due to the more complete separation of the electrons that such arrangements allow. This interpretation also fits the differences in Table II between singlet and triplet states. A triplet state implies two electrons with parallel spins and these two can never be found on the same atomic centre. Thus the separation of electrons is already partly achieved by the *spin* symmetry even in an MO wave function, and the further effect possible by configuration interaction is less than in singlet states. Specifically, a given triplet is less depressed than the corresponding singlet. Thus $^{3}B_{1u} < {}^{1}B_{2u}$, $^{3}B_{2u} < {}^{1}B_{1u}$, $^{3}A_{2g} < {}^{1}A_{1g}$. In two cases, E_{1u} of benzene and E_{u} of cyclobutadiene, this effect and that connected with structure type are in opposition and no definite interpretation is possible.

---

*† States similarly marked by stars or daggers arise in the same configuration.

The second point, that after configuration interaction is allowed for in the non-empirical theory the lowest states are those compatible with nonpolar structures, is illustrated for benzene in Table I. It will be noticed that the three lowest states are of this type. In cyclobutadiene, Table III, the four lowest states are those for which nonpolar structures may be written.

TABLE III.—The States of Cyclobutadiene in the Non-empirical Theory [10]

* $^1B_{2g}$	0 eV	^1E_u	10·8 eV
* $^3A_{2g}$	0·7	$^3B_{2g}$	11·4
* $^1A_{1g}$	2·3	* $^5B_{2g}$	11·8
* ^3E_u	3·6	$^1A_{2g}$	14·9
$^1B_{1g}$	5·7	$^3A_{1g}$	15·3

For the next stage of the comparison a more precise statement is needed of the relationship between the wave functions used in the two theories. It is the case, as Longuet-Higgins [11] first pointed out, that a complete set of antisymmetric LCAO molecular orbital configuration wave functions as used in the non-empirical theory, and a complete set of VB structures properly mathematically expressed, are equivalent bases for representing molecular states. This means that a wave function expressed in one basis may be transformed into the other provided only that both are simply built up from the same set of atomic orbitals, as they are in practical cases. The fundamental elements in the one basis are MO configuration wave functions with proper space and spin symmetry and in the other are antisymmetric combinations of atomic orbital products conventionally represented as valence-bonded structures. In both cases it is practicable in small molecules to work with complete sets of the fundamental elements, and if energies were calculated in the same way in each, the results would be identical; but for calculations in large molecules it is convenient in both theories to work only with a very few such elements. Thus in the one case the aim is to use a single configuration in *molecular* orbitals and in the other to use a single configuration in *atomic* orbitals. The energetic circumstance that the lowest MO configuration is closed (all orbitals, or all but one, doubly filled) but the lowest atomic orbital one is multiple degenerate, makes the difference that the first contributes a single element to its basis while the second contributes a number, viz., all the structures of a given polar character. But the restriction is the same, in an exact sense, in both cases. A comparison of the wave functions under the restriction is, very nearly, a comparison between those of the simple MO theory and the nonpolar VB theory, and this is familiar ground. It is well known that there is a striking difference in the importance these theories associate with accumulations of charge about a single centre. Now it is already clear, from the improved agreement between the results of the calculations, that abandoning single configurations greatly diminishes this difference, and this may be illustrated more directly by examining the wave function for a particular state. We choose for this the lowest state of cyclobutadiene which belongs to the B_{2g} representation.

The starting point in the non-empirical theory is the set of four LCAO molecular orbitals, written as follows: a, b, c and d are atomic $2p$ wave functions and the σ's are normalizing coefficients:

$$\begin{aligned}\phi_0 &= 1/\sigma_0(a + b + c + d),\\ \phi_{\pm 1} &= 1/\sigma_1(a \pm ib - c \mp id),\\ \phi_2 &= 1/\sigma_2(a - b + c - d).\end{aligned}$$

---

[10] Craig, *Proc. Roy. Soc.* (in press).

* Only the lowest state of each symmetry type is shown. States marked with a star are compatible with nonpolar structures.

[11] Longuet-Higgins, *Proc. Physic. Soc.*, 1948, **60**, 270.

In conventional MO theory we should represent the lowest state as having two π-electrons in ϕ_0 and the remaining two in ϕ_1 or ϕ_{-1}. This configuration is denoted by $(\phi_0)^2$ $(\phi_{\pm1})^2$. But two other configurations $(\phi_0)(\phi_1)(\phi_{-1})(\phi_2)$ and $(\phi_{\pm1})^2(\phi_2)^2$ also admit $^1B_{2g}$ symmetry and the essence of the configuration interaction procedure is to represent the actual state as a *mixture* of all three. The starting points in the empirical theory are the structures compatible with $^1B_{2g}$ symmetry. Examples of the three types are shown in Fig. 1 and the complete set may be found by rotating and reflecting until the possibilities are used up. Two nonpolar, 8 singly-charged polar and 4 doubly-charged polar structures make the complete set. By a straightforward expansion [11a] the configuration wave functions of the first basis can be expressed in terms of the structures of the second, with the results shown in Table IV.

The upper numbers in Table IV are the coefficients with which the structures enter the configuration wave functions. The total contributions by structures of the various types are best measured by their " weights " which are found from the squares of these coefficients, due account being taken of the nonorthogonality of the nonpolar structures. These weights normalized to 100 %, are the bracketed numbers in Table IV. We see

TABLE IV.—COEFFICIENTS OF STRUCTURES IN B_{2g} CONFIGURATIONS OF CYCLOBUTADIENE

Configuration	Non-polar Structures	Singly-charged Polar Structures	Doubly-Charged Polar Structures
$(\phi_0)^2(\phi_{\pm1})^2$	$4\sqrt{2}$ (37·5 %)	4 (50 %)	$2\sqrt{2}$ (12·5 %)
$(\phi_0)(\phi_1)(\phi_{-1})(\phi_2)$	$-8/\sqrt{3}$ (25 %)	0 —	$12/\sqrt{3}$ (75 %)
$(\phi_{\pm1})^2(\phi_2)^2$	$-4\sqrt{2}$ (37·5 %)	4 (50 %)	$-2\sqrt{2}$ (12·5 %)
Energy-minimized mixture of configurations . .	88 %	11 %	1%

that in the simple MO theory, where the first configuration alone is taken to be the state, the wave function is 37·5 % nonpolar while in the simple VB theory it is 100 % nonpolar. Now it is necessary to know how the configurations are combined in the non-empirical theory to give the state of lowest energy. If the first configuration has the coefficient unity it is found that the second must have $-$ 0·329 and the third $-$ 0·145 ; and referring to Table IV this means that to get the actual state the first configuration has to be modified by subtracting from it small fractions of the second and third. The effect of this will clearly be to increase the weight of nonpolar structures at the expense of polar ones. An actual calculation, in which the normalizing coefficients σ must enter as well as the coefficients of Table IV, shows that in the state wave function the weight of nonpolar structures has been increased to 88 %, singly-charged polar structures have been reduced to 11 % and doubly-charged polar structures have been almost entirely eliminated. The non-empirical wave function is thus seen to be dominated by nonpolar structures, and this fact supports the assumption underlying the empirical method. It is tempting therefore to say that the assumption brings the latter method close to physical reality.

This line of argument may be taken one stage further. With properly chosen coefficients the configurations may be combined to eliminate all

[11a] Wheland, *Proc. Roy. Soc. A*, 1938, 164, 464.

polar structures, making the wave function wholly nonpolar. This wave function though formally expressed in MO terms, is the wave function for the two Kekulé structures of cyclobutadiene, and so it is the same, except trivially,* as the simple VB wave function. The energy of the wave function with coefficients so chosen can be calculated. It proves to be 0·9 eV less stable than the energy-minimized wave function but 1·5 eV more stable than the lowest MO configuration wave function. In other words, the nonpolar wave function is considerably more stable than any single configuration wave function and 0·9 eV less stable than the best wave function that can be formed from atomic *2p* orbitals.

The conclusions from this section are that, in benzene, the non-empirical and VB methods are substantially in agreement for the low states. This agreement depends strongly on the inclusion of configuration interaction in the non-empirical method, and somewhat less strongly on the inclusion in the empirical method of some polar structures. The fact that in both methods the low states of benzene, and also of cyclobutadiene, are just those for which nonpolar structures may be written reflects that nonpolar structures play the dominating part, and suggests that the VB theory in its simple form is likely to be correct in at least the lowest states of more complex molecules.

3. Naphthalene.—In naphthalene there is no assignment so well founded experimentally as either of those referred to in benzene at the beginning of this paper. But a very good indication toward one assignment exists in the discovery by Kasha and Nauman [12] that the weak naphthalene band system at 3200 Å records a distinct electronic transition, and that its upper state is so long-lived as to indicate strongly that the transition is symmetry forbidden. Since the ground state is A_g the upper state can be A_g or B_{1g} if this indication is correct, but beyond this the experimental material does not yet go.

Granted this, the theoretical calculations allow a clear choice between the two possibilities and so allow an assignment to be made.

The numerical work in theoretical calculations increases manyfold in going from benzene to naphthalene and the calculations so far reported use only a very small part of the basis of configuration wave functions, or structures, as the case may be. A non-empirical calculation by Miss Jacobs [13] shows that the lowest *forbidden* transition is $A_g - A_g$ but does not make this the lowest of all the transitions in the approximation to which the calculation is taken. It is necessary therefore to assume the forbidden character in order to deduce the assignment from this calculation. The VB theory,[14, 15] however, even without polar structures, does find the first excited state to be ${}^1A_g$ and so directly favours the same assignment without a similar assumption; the lowest B_{1g} state is 4 eV in energy above this first excited A_g state. Some considerable weight thus attaches to the assignment ${}^1A_g - {}^1A_g$ for the 3200 Å naphthalene band system.

In the remaining ultra-violet systems of naphthalene at 2900 Å and 2200 Å a key experimental fact is wanting. This is the polarization of the transitions, i.e. the direction of the active electric vector relative to the molecular axes. The twofold symmetry (Table V) of the 'acenes admits two allowed transitions, $A_g - B_{2u}$ (transverse polarization) and $A_g - B_{3u}$ (longitudinal polarization). It is no longer possible to appeal to agreement between the theories to assign the shorter wavelength band systems to one or other of these allowed transitions because agreement is lacking at the stage to which the calculations have been taken. We shall therefore simply mention the results in the two theories and leave some more general considerations which allow a tentative choice between them to the next section. According to the VB theory including some polar structures the 2900 Å band system is to be assigned $A_g - B_{3u}$, polarized in the direction of the longer molecular axis. The intense band at 2200 Å is $A_g - B_{2u}$ and polarized along the shorter axis. In the configuration interaction calculation however the intense band is expected to be longitudinally polarized while for the 2900 Å system the calculations do not allow a clear assignment to be made.

---

* The only difference is that the overlap integral is neglected in the VB theory.

[12] Kasha and Nauman, *J. Chem. Physics*, 1949, **17**, 516.

[13] Jacobs, *Proc. Physic. Soc.*, 1949, **62**, 710.

[14] Blumenfeld, *J. Physic. Chem. Soc. Russ.*, 1947, **21**, 529.

[15] Craig, *Proc. Int. Congr. Chem.* (London, 1948).

TABLE V.—SYMMETRY GROUP D_2

	E	C_2^z	C_2^y	C_2^x
A_1	1	1	1	1
B_1	1	1	−1	−1
B_2	1	−1	1	−1
B_3	1	−1	−1	1

The z axis is perpendicular to the molecular plane. The x axis is in the direction of the longer molecular extension.

4. Polynuclear Hydrocarbons.—In neither anthracene nor phenanthrene is there experimental evidence leading to spectral assignments; nor have non-empirical calculations of any kind been reported. Even empirical calculations, to be manageable, have to be restricted to small sets of basic structures. Here the uncertainty mentioned earlier whether the calculations refer to the same transitions as the experimental band systems with which they are compared arises in its typical form. This doubt admitted, there are two features of the comparison between experiment and theory which must be mentioned. In the spectrum of phenanthrene [16, 17] and other angular hydrocarbons there is a very weak band system at long wavelengths (3400 Å in phenanthrene) which may plausibly be associated with a VB calculated transition $A_1 - A_1$ of the symmetry group C_{2v}. Also, in these larger molecules, VB calculations of a quite simple sort [18] give an apparently consistent account of the wavelengths of absorption at the long wavelength end of the spectrum and this, on the one hand, supports the claim of the VB theory to be correct in its description of these states and, on the other, indicates the assignment $A_g - B_{3u}$ for the long wavelength allowed transitions.

A surer indication, however, of which states in polynuclear hydrocarbons are likely to be low-lying may be found by relating them through their symmetry to the states of benzene discussed in § 2. The symmetry relations between the assigned transitions in benzene and those of the higher homologues may be found as follows. The group D_{2h} to which the 'acenes belong (and equally group C_{2v} for phenanthrene) are subgroups of the benzene D_{6h}. An irreducible representation of the latter is also a representation of the former, though in general a reducible one. The following relations exist between D_{2h} and D_{6h}:

D_{6h} Representation	Corresponding D_{2h} Representation
A_{1g}	A_g
B_{2u}	B_{3u}
E_{2g}	A_g and B_{1g}
B_{1u}	B_{2u}
E_{1u}	B_{2u} and B_{3u}

---

[16] Craig, *Nature*, 1946, 158, 235.

[17] Sponer and Nordheim, *ONR Contract N6ori*-107, *T.O.*1 (1st June, 1948).

[18] Förster, *Z. physik. Chem. B*, 1938, 41, 287.

The states of benzene may now be labelled according to the representations of D_{2h}. In effect this is as if benzene were the natural first member of the 'acene series. The upward sequence of energy levels now reads (i) A_g, ground, (ii) B_{3u} (from B_{2u} of D_{6h}), (iii) A_g and B_{1g} (degenerate, from E_{2g}), (iv) B_{2u} and B_{3u} (degenerate, from E_{1u}). To carry the argument on demands an appeal to the physical similarity between benzene and the 'acenes. But it must appear at the least very likely that in the 'acenes the lowest B_{3u} state (deriving from the first excited state of benzene) will fall below the lowest B_{2u} (deriving from the third excited state). It is thus likely that the first allowed band systems in 'acenes are to be assigned $A_g - B_{3u}$, polarized longitudinally. This conclusion agrees with, but is derived independently of, that from actual VB calculations mentioned earlier in this section.

The degeneracies noted above arising from the sixfold symmetry of benzene are split if the hexagon is distorted. This could be done by bringing to single bond distance two atoms *para* to one another making an imaginary molecule which physically as well as by its symmetry is the precursor of the 'acene series. The effect of the splitting is to make the A_g component of (iii), which arises from the E_{2g} state of benzene, more stable than the B_{1g} component. But the B_{3u} level (ii), which is nondegenerate even in the regular hexagon, is less affected. Thus the low excited states in the distorted model are A_g and B_{3u}. In actual 'acenes, by analogy, these two symmetries but not B_{1g} or B_{2u} are expected as low-lying states. These considerations, supported by the VB calculations already referred to, suggest the following assignments for the lower transitions in some 'acenes.

Molecule	Experimental Absorption[9] (cm.$^{-1}$)	Proposed Assignment
Naphthalene (see §3)	32000 34600 45400	A_g—A_g A_g—B_{3u} A_g—B_{2u}
Anthracene	26400 39000	A_g—B_{3u} A_g—B_{2u}
Naphthacene	21100 36700	A_g—B_{3u} A_g—B_{2u}
Pentacene	17100 24000 32300	A_g—B_{3u} A_g—A_g A_g—B_{2u}

The $A_g - A_g$ band systems in anthracene and naphthacene are presumably hidden by the more intense $A_g - B_{3u}$ systems, as suggested by Sponer and Nordheim.[17]

This paper may well conclude with a comment on the practical question that arises in energy level calculations by empirical methods. The work of § 2 and § 3 may be taken as general support for the physical basis of the VB method in excited states. But the method cannot be equally reliable for all states even though in polynuclear hydrocarbons all are compatible with nonpolar structures. It is relevant that although all three A_{1g}, B_{2u} and E_{2g} of benzene are compatible with nonpolar structures, the most stable, Kekulé structures, appear only in the first two and it is found that these two alone can be calculated reasonably accurately when polar structures are neglected in the VB method. Likewise in 'acenes the two corresponding symmetries A_g and B_{3u} alone may be constructed from Kekulé structures and we must expect that only states of these two symmetries will be at all reliable calculable by the VB theory in its purely nonpolar form. Just as for E_{2g} and E_{1u} of benzene so for B_{1g} and B_{1u} of 'acenes it will be essential to include polar structures.

The writer acknowledges the award by the University of London of a Turner and Newall Research Fellowship tenable at University College.

The Sir William Ramsay and
Ralph Forster Laboratories,
University College,
London.

CHARACTERIZATION OF ELECTRONIC TRANSITIONS IN COMPLEX MOLECULES

BY MICHAEL KASHA[*][†]

Received 3rd July, 1950

A summary is given of the types of conclusions which may be drawn from a study of the emission properties of complex molecules under optical excitation in suitable systems. The types of radiationless transitions in complex molecules are discussed, and a resultant spectroscopic criterion stated : *The emitting level of a given multiplicity is the lowest excited level of that multiplicity.* Intercombinations in complex molecules are described, and their importance is shown to arise from the high probability of the excitation of triplet states—a conclusion which runs counter to the trend of spectroscopic thought of a few years ago. An atomic number criterion is stated (after McClure) which permits the *identification of intercombinations by a study of intensity of the transition with heavy atom substitutions in a complex molecule.* Finally, a listing of empirical criteria is made which permits a distinction between pure π-electron transitions ($\pi \rightarrow \pi^*$) and transitions involving excitation of non-bonding N, O, and S atom electrons to anti-bonding π molecular orbitals ($n \rightarrow \pi^*$). The most definitive of these criteria is the *disappearance of $n \rightarrow \pi^*$ transitions in acid media.* An unusual enhancement of the spin-orbit coupling process for $n \rightarrow \pi^*$ transitions is reported and a possible interpretation is given.

Much useful information concerning the electronic states of complex molecules can be gained from a study of the emission properties of such molecules under optical excitation. In particular cases it may be necessary to study the molecule in rigid glass solutions at the temperature of liquid nitrogen in order to observe its light emission properties. However, since there is hardly a case in which light emission can not be observed with a moderate quantum efficiency, the method of emission spectroscopy can be applied almost universally. The information derived from such studies forms an essential supplement to that obtained from absorption spectra in the vacuum ultra-violet, high resolution spectra of vapours, and absorption spectra of solutions. In a series of forthcoming publications by the writer a detailed study of emission spectroscopy of complex molecules is reported.[1] The present paper summarizes the type of information revealed by such investigations.

Radiationless Transitions in Complex Molecules.—Two basic types of radiationless transitions are observed in most complex molecules. These are merely defined here, a full discussion and references being given elsewhere.[1b, 1c]

---

[*] U.S. Atomic Energy Commission Research Fellow.

[†] Present address : Department of Chemistry, The University, Manchester, England.

[1] *Emission Spectroscopy of Complex Molecules*, M. Kasha, to be published soon.
(*a*) Relations between Lifetime and Quantum Yield.
(*b*) Internal Conversion of Electronic Energy.
(*c*) Intersystem Crossing of Potential Surfaces.

INTERNAL CONVERSION may be defined as the rapid radiationless combination of excited electronic states of like multiplicity (combination in the spectroscopic sense of undergoing transition between). In general, internal conversion to the ground state does not occur with a high probability, although in certain types of molecules the latter process is significant and diminishes the total intrinsic quantum yield of luminescence.[1f] The phenomenon of internal conversion is manifested by the appearance of a unique luminescence, regardless of which state of a given multiplicity is excited. It yields a most useful spectroscopic criterion : *The emitting electronic level of a given multiplicity is the lowest excited level of that multiplicity.*

An important recent application of this criterion is the re-assignment by Shull [2] of Sklar's lowest calculated triplet level of benzene to the emitting triplet level; Sklar arbitrarily has assigned the observed triplet level to one of the higher calculated levels.

INTERSYSTEM CROSSING is the spin-orbit-coupling-dependent internal conversion. In most cases this is the radiationless transition from the lowest excited singlet level to the lowest triplet level of the molecule. Analogous to *radiative* transitions involving π-electrons (e.g. in aromatic hydrocarbon molecules), a prohibition factor of about 10^6 distinguishes inter-system crossing from internal conversion. Moreover, since spin-orbit coupling forces are involved, the introduction of heavy [1e] (i.e. high atomic number) and paramagnetic [3] atoms into the molecule will strongly increase the probability of the transition, as will strong external electric and magnetic fields. Despite the large prohibition factor, however, inter-system crossing is a rather probable process in most molecules. In fact, although usually observed only very weakly as a direct absorption from the ground (assumed singlet) state, the lowest triplet state is readily excited to emission (under conditions of low quenching, viz., rigid glass solutions). Thus, the lowest triplet state has been located in several hundred complex molecules through a study of their phosphorescence spectra.[4, 5]

The facile excitation of the lowest triplet state (by light absorption to the lowest excited singlet state) is really a consequence of the very high rate of internal conversion (e.g. between singlet states). The following analysis of the rates involved may help to make this clear.

A molecule is excited optically to its nth excited singlet state, S^n. Under steady excitation a spectrum is photographed in search for the spontaneous $S^n \rightarrow \_\_$ emission (this has not been observed thus far in the cases studied). The ratio of the rate constant (reciprocal "lifetime") for the spontaneous $S^n \rightarrow \_\_$ luminescence to the rate constant for the radiationless $S^n \rightarrow S'$ internal conversion is given by the intensity ratio

$$\frac{k_L}{k_{IC}} = \frac{I_{S^n \rightarrow}}{I_{S' \rightarrow S}} < 10^{-4},$$

since the intensity of the fluorescence $S' \rightarrow S$ indicates the number of internal conversions. Numerous observations of this sort have placed the upper limit at the value indicated.

Thus, the internal conversion process takes place at least 10^4 times as fast as the spontaneous $S^n \rightarrow \_\_$ emission. The intrinsic lifetime of the latter can be calculated from the integrated absorption of the band corresponding to the $S^n \leftarrow S$ absorption: we shall assume this to be

(*d*) π- and n-electron Transitions in N-heterocyclics (with C. Reid).
(*e*) n-Electron Transitions in Molecules Containing $- Y = X:$ Groups.
(*f*) Internal Conversion to the Ground State.
(*g*) Summation of the Quantum Yield.

[2] Shull, *J. Chem. Physics*, 1949, **17**, 295.

[3] Yuster and Weissman, *ibid.*, 1949, **17**, 1182.

[4] Lewis and Kasha, *J. Amer. Chem. Soc.*, 1944, **66**, 2100.

[5] Nauman, *Thesis* (University of California, Berkeley, 1947).

10^{-9} sec., a value commonly found for intense u.-v. absorptions. Then the reciprocal rate of the internal conversion process is

$$1/k_{IC} < 10^{-4} \,.\, 1/k_L < 10^{-13} \text{ sec.}$$

The natural limit on the rate of internal conversion may well be the time of a vibrational period; shorter estimates are actually obtained from spectroscopic data in some cases. As a consequence of the very high rate it is to be expected that "internally converting levels" will be somewhat broadened in a band width relative to the band width of the "fluorescing level" with a natural lifetime of 10^{-7} to 10^{-9} sec. In other words, the lowest absorption band of a given multiplicity manifold will be better vibrationally resolved than the higher energy bands of the same manifold (e.g. singlet-singlet transitions).

For intersystem crossing we apply an arbitrary prohibition factor of 10^6, giving an intersystem crossing reciprocal rate

$$1/k_{IS} < 10^6 \,.\, 1/k_{IC} < 10^{-7} \text{ sec.}$$

The probability of intersystem crossing in a molecule is measured by the *intersystem crossing ratio* χ, which is defined as the ratio of quantum yields of phosphorescence to fluorescence under steady simultaneous excitation [1c]

$$\chi = \frac{\Phi_P}{\Phi_F} = \frac{k_{IS}}{k_F} \simeq \frac{10^7}{10^8} = 0{\cdot}1.$$

A fluorescence lifetime of 10^{-8} sec. is arbitrarily assumed here for illustration. The actual observed values of χ are of the order of magnitude of 1 for molecules with π-electron energy levels,[1c] indicating that the general assumptions made in the rate analyses are approximately correct.

Intercombinations in Complex Molecules.—Having observed the long-lived luminescence corresponding to the triplet-singlet emission of the molecule, we can locate the converse singlet-triplet absorption band with confidence. (If there are two luminescences, the long-lived one is naturally identifiable as the intercombination process. However, if only a single luminescence is observed, even under conditions of minimum quenching, the criteria to be described below must be applied.)

The intensity (integrated absorption) of the converse absorption band may be calculated from the measured lifetime of the luminescence by the well-known expression [6, 7]

$$\int \epsilon\, d\nu = \frac{}{8\pi c\nu^2 n^2} \cdot \frac{g_u}{g_l} \cdot \frac{1}{\tau_L}.$$

From the integrated absorption and an assumed band width for the type of transition in question, the peak molar absorption coefficient can be estimated. Using the latter and the frequency of the 0, 0-band of the phosphorescence emission spectrum, the singlet-triplet absorption can be found.[7] Since this is usually about 10^6 times weaker than the normal singlet-singlet transitions, rather long optical paths must be used, or else concentrated solutions or even the pure liquid (or solid) substance must be studied. Under these conditions absorption of light by an impurity easily could be misinterpreted as a forbidden electronic transition, were it not for the double check of correspondence with the 0, 0-band of the emission spectrum, and with the integrated absorption intensity calculated from the mean lifetime of the emission process.

To identify spectroscopically the long-lived luminescence and converse absorption bands as intercombinations, use is made of the characteristics of the spin-orbit coupling process. As is known from the theory of

---

[6] Ladenburg, *Verh. dtsh. physik. Ges.*, 1914, **16**, 769; *Z. Physik*, 1921, **4**, 451. Tolman, *Physic. Rev.*, 1924, **23**, 693. Perrin, *J. Physique Rad.*, 1926, **7**, 90; *Ann. physique*, 1929, **12**, 169.

[7] Cf. Lewis and Kasha, *J. Amer. Chem. Soc.*, 1945, **67**, 994.

atomic spectra, the probability of spin-orbit coupling increases rapidly with increasing atomic number of the atom. This principle has not been applied generally in molecular spectroscopy, although it is well known that, e.g. in the halogen series of molecules, the probability of the singlet-triplet transition in the visible region increases greatly in intensity in the order Cl_2, Br_2, I_2.

McClure[8] made the valuable extension of this principle to heavy-atom substituted complex molecules, showing that like the (radiationless) intersystem crossing process,[1c] the radiative intercombination process likewise increases rapidly in probability with increasing atomic number of the substituent. Thus, the rate constant for phosphorescence $k_p = 1/\tau_p$ as well as the oscillator strength f (or the integrated absorption, $\int \epsilon d\nu$) increase rapidly with increasing atomic number. This is shown clearly in Fig. 1, which is a plot of McClure's data for the monohalo-benzenes and naphthalenes. The solid line indicates the probability of the triplet-singlet emission process measured as the phosphorescence lifetime. The dotted lines show how one of the singlet-singlet transitions behaves for the same series of halo-derivatives. (The increase in f for bromobenzene and especially iodobenzene is probably due to the approach of the non-bonding halogen transition to the benzene 2600 Å absorption; the dotted line is arbitrarily drawn downward to suggest the correction required.) Obviously the atomic number is the wrong parameter against which to plot the probability of singlet-singlet transitions: some other property of the halogen substituent would give a more rational dependence.[9] The atomic number effect is particularly valuable for the identification of intercombinations because the frequency of the transition changes only

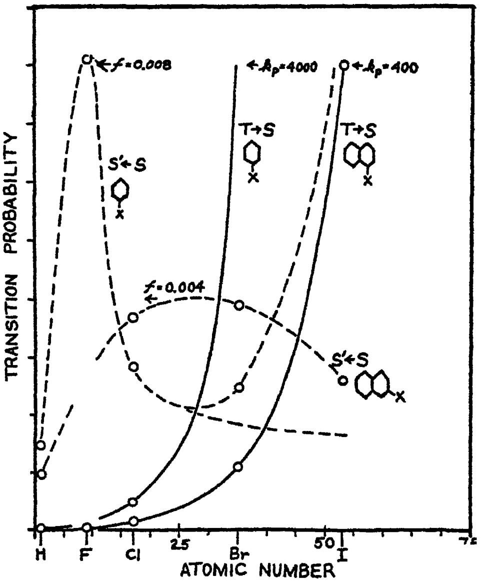

FIG. 1.—The effect of atomic number on intercombinations in the spectra of substituted complex molecules.

---

[8] McClure, *J. Chem. Physics*, 1949, 17, 905.

[9] Matsen (*Symposium on Molecular Structure and Spectroscopy*, Ohio State University, Columbus, Ohio, 13th June, 1950) has presented a molecular orbital treatment of the problem which explains the anomalous f-values of the 2600 Å transition of the halo-benzenes in terms of an inductive effect.

slightly while the intensity changes by a large factor (e.g. the factor is 1000 for the lowest singlet-triplet of the mono-iodonaphthalenes compared with naphthalene).

Armed with this increased knowledge on the nature of intercombinations in complex molecules, great progress in this branch of molecular spectroscopy may be anticipated.

$\pi \rightarrow \pi^*$ and $n \rightarrow \pi^*$ Transitions.—A study of the emission spectral properties of the *N*-heterocyclics, which the writer has carried out together with Dr. C. Reid,[14] has indicated the optical similarities of some of these molecules to such molecules as carbonyl, nitro, and nitroso compounds. In, e.g., the carbonyl compounds, the lowest singlet-singlet transition has been characterized tentatively as a transition corresponding to the excitation of a (nearly) non-bonding (oxygen) electron to an anti-bonding π molecular orbital.[10] We have obtained definite physical evidence for this interpretation and have found analogous transitions (involving the non-bonding nitrogen electrons) in various *N*-heterocyclics (e.g. pyridine, pyrazine, phenazine). For convenience we designate non-bonding electrons as *n*-electrons, and the corresponding transitions as $n \rightarrow \pi^*$ transitions. These transitions are characterized by remarkably different properties in comparison with $\pi \rightarrow \pi^*$ transitions as shown, e.g., by the spectra of the aromatic hydrocarbons. A summary of distinguishing empirical criteria is offered.

VIBRATIONAL BAND WIDTH (VAPOUR SPECTRUM).—$\pi \rightarrow \pi^*$ transitions: moderately broad, owing to unresolved rotational structure. $n \rightarrow \pi^*$ transitions: "atomic" in sharpness, a fact commented upon by numerous observers. This seems to be due to the weakness of the *P* and *R* rotational branches, the strong *Q* branch predominating.

VIBRATIONAL BAND WIDTH (SOLUTIONS).—$\pi \rightarrow \pi^*$ transitions: vibrational fine structure preserved (e.g. the 2600 Å band of benzene). $n \rightarrow \pi^*$ transitions: very blurred, usually only slight vibrational structure remains, even in hydrocarbon solvents. This is all the more striking in view of the sharpness of the vapour absorption lines. Probably it is a characteristic of the non-bonding orbitals which leads to an unusual perturbation in solutions. In hydroxylic and other solvents, vibrational structure is completely blurred. Complex formation, probably involving hydrogen bonding in most cases, occurs and changes the non-bonding character of the orbitals.

ACIDIC SOLVENTS.—$\pi \rightarrow \pi^*$ transitions: the transition is preserved, although some blurring of fine structure occurs; usually there is little change in intensity. $n \rightarrow \pi^*$ transitions: the transition "disappears" (moves to very high energies). Addition of a proton to the non-bonding pair of the hetero-atom greatly increases the binding energy of the "lone pair". This behaviour offers the clearest proof of the excitation of non-bonding electrons in such molecules.

VIBRATIONAL ENVELOPE.—$\pi \rightarrow \pi^*$ transitions: complex vibrational envelope, many normal vibrations excited. $n \rightarrow \pi^*$ transitions: usually a unique $\nu_{\text{vib.}}$ excited; this can probably be explained in terms of the localized character of the non-bonding electron orbital.

RATIO OF TRANSITION PROBABILITIES, P_{11}/P_{31} (singlet-singlet against singlet-triplet).—$\pi \rightarrow \pi^*$ transitions: the oscillator strength ratio $f_{11}/f_{31} \simeq 10^6$ for the radiative process. For the radiationless process $\Phi_p/\Phi_F \simeq 1$, which implies an equal probability of transition to the lowest triplet (and consequent triplet-singlet emission) and of spontanteous singlet-singlet emission.

For $n \rightarrow \pi^*$ transitions $f_{11}/f_{31} \simeq 10^4$, and $\Phi_p/\Phi_F > 1000$. Here is evidence for a striking increase in the probability of the spin-orbit coupling process in such transitions. The increase by a factor 100 to 1000 is much more than can be accounted for by an increase in atomic number in going from C to N to O. It is to be noted that the Φ_P/Φ_F property here means that fluorescence is scarcely to be observed in these molecules (some *N*-heterocyclics, all carbonyl, thiocarbonyl, nitro, nitroso, azo compounds) : the " forbidden " conversion to the triplet state is essentially complete.

---

[10] Mulliken, *J. Chem. Physics*, 1935, **3**, 564. McMurry and Mulliken, *Proc. Nat. Acad. Sci.*, 1940, **26**, 312. McMurry, *J. Chem. Physics*, 1941, **9**, 231 and 241.

A possible interpretation of the greatly enhanced spin-orbit coupling for $n \rightarrow \pi^*$ transitions is that *sp*-hybridization which is present or can be plausibly introduced into non-bonding orbitals brings the optical electron much closer to the nucleus than in the case of an electron in a π-orbital ; the spin-orbit coupling process occurs near the electric field of the nucleus of an atom. There are difficulties in this interpretation,[1d] which, however, must be resolved by theoretical computations.

Department of Physics,
University of Chicago.

DISCUSSION OF THE LOWEST SINGLET TRANSITION IN NAPHTHALENE AS A FORBIDDEN TRANSITION $A_{1g} - A_{1g}$ AND REMARKS ON THE HIGHER SINGLET LEVELS *

BY H. SPONER AND (THE LATE) GERTRUD P. NORDHEIM

Received 18th July, 1950

The absorption system of naphthalene at 3200-2900 Å is interpreted as ${}^1A_{1g}-{}^1A_{1g}$ transition. The infra-red active vibration of 568 cm.$^{-1}$ is tentatively suggested as vibration that makes the forbidden transition allowed in second order. In making this analysis, experimental data on absorption and fluorescence in the different states of aggregation of naphthalene and new results obtained for heavy naphthalene were used. The 0—0 band of the next higher absorption system at 2900-2500 Å is located at 35910 cm.$^{-1}$ and of the third absorption system at about 45100 cm.$^{-1}$, both for the vapour. A brief comparison with theoretical results is given.

The near ultra-violet absorption of naphthalene has been studied in the vapour phase,[1, 2] in liquid [2, 3] and in rigid glass solutions,[4] and in the solid state [5] (crystal at 20° K). The spectrum consists of two absorption regions lying fairly close together. The long wave part ranging from about 3200-2900 Å shows in the vapour sharp narrow bands, whereas the bands from 2900-2500 Å are broad and diffuse. Moreover, the pattern in which the bands appear is different in the two regions. The measurements in liquid solution give an average extinction coefficient ϵ of 200-300 for the first region and of 5000-6000 for the second region. Furthermore, at 2200 Å a very strong and broad band with little indication of structure was observed [2, 6] with $\epsilon \sim 100{,}000$. The absorption spectrum of the solid

---

[*] This research was supported by the Office of Naval Research.

[1] Henri and de Laszlo, *Proc. Roy. Soc. A*, 1924, **105**, 662.

[2] de Laszlo, *Z. physik. Chem.*, 1925. **118**, 369.

[3] For example, Morton and de Gouveia, *J. Chem. Soc.*, 1934, 911 ; Mayneord and Roe, *Proc. Roy. Soc. A*, 1935, **152**, 299.

[4] Kasha and Nauman, *J. Chem. Physics*, 1949, **17**, 516.

[5] Prikhotjko, *J. Physics, U.S.S.R.*, 1944, **8**, 257.

[6] Klevens and Platt, *J. Chem. Physics*, 1949, **17**, 479.

contains discrete relatively sharp bands, but looks different from the vapour spectrum whether obtained with natural or with polarized light.

Fluorescence of naphthalene has been studied mostly in liquid and solid solutions.[4, 7] It consists of a number of bands in the region 3000-3650 Å. Fluorescence of the vapour was excited[8] by irradiation with wavelengths below 3000 Å showing narrow bands between 3000 and 3340 Å superimposed on a continuous background. Fluorescence and absorption bands coincide in the overlapping region. The fluorescence of crystalline naphthalene[9] (at 20° K) consists of a complicated spectrum of many, mostly narrow, bands. From studies of the fluorescence lifetime of naphthalene in rigid glass solution Kasha and Nauman[4, 9a] concluded that the weak long wavelength absorption is a forbidden transition.

Calculations of the electronic terms of naphthalene have been carried out with the bond orbital method taking into account valence structures with no or one "long" bond.[10] With this approximation one obtains as the first two excited singlet states a B_{3u} and a B_{2u} level. Transitions from the symmetrical ground state to the B_{3u} state are allowed with the transition moment in the long molecular axis (x axis), and to the B_{2u} state with the moment in the short (y axis). Earlier more complete calculations by Blumenfeld,[11] taking all 42 canonical structures into account, give for the first excited level a symmetric one, $^1A_{1g}$. The transition from the ground state to this level is forbidden. Blumenfeld obtains as next excited levels a $^1B_{3u}$ and a $^1B_{2u}$ term. Craig[12] also using the valence bond method, has likewise predicted an A_{1g} as lowest excited singlet level, followed by a $^1B_{3u}$, $^1B_{1g}$, $^1B_{2u}$ term, in that order.

Platt's[13] one-dimensional free electron picture leads to the same order of the allowed levels as the bond orbital method, whereas calculations with the standard molecular orbital method (German,[14] Coulson,[15] Davydov[16]) and a slightly modified molecular orbital method (Simpson[17]) reverse this order. In this approach the symmetric level should lie at higher excitation energy. In the most recent treatment of the energy states of naphthalene by Jacobs[18] an antisymmetriced molecular orbital calculation was carried out, taking into account the interaction between the different configurations formed by the molecular orbitals. In this approach a B_{3u} and a B_{2u} are obtained as lowest singlet levels with a very small separation between them. The first excited $^1A_{1g}$ state appears 1·4 eV above the B_{3u} state. Oscillator strengths were calculated for the first three allowed transitions and compared with experimental values omitting the first weak absorption at 3200-2900 Å. The agreement is rather good.

Analysis of the Lowest Electronic Singlet Transition in Naphthalene at 3200-2900 Å.—(*a*) OCCURRENCE OF 0—1 and 1—0 BANDS.—Considering the weakness and structure of the first absorption in naphthalene, and the lifetime of the fluorescence, this system can be explained best as a transition forbidden by symmetry. Possibilities of interpreting the low intensity by cancellation of positive and negative terms of the same order

[7] Compare P. Pringsheim, *Fluorescence and Phosphorescence* (Interscience Publishers, New York, 1949), 408.

[8] Pringsheim, *Ann. Acad. Warsaw*, 1938, **5**, 29.

[9] Obreimov and Shabaldas, *J. Physics U.S.S.R.*, 1943, **7**, 168.

[9a] Remarks of M. Kasha at O.N.R. Spectroscopy Conference, Jan., 1948.

[10] Sponer and Nordheim, *ONR Contract N6ori*-107, *T.O.* 1 (Annual Report, June, 1948).

[11] Blumenfeld, *J. Physic. Chem. U.S.S.R.*, 1947, **21**, 529.

[12] Craig, *Proc. XIth Int. Congr. Chem.* (*Lond.*) (July, 1947).

[13] Platt, *J. Chem. Physics*, 1949, **17**, 484.

[14] German, *J. Physics U.S.S.R.*, 1944, **8**, 276.

[15] Coulson, *Proc. Physic. Soc.*, 1948, **60**, 257.

[16] Davydov, *J. Expt. Theor. Physics U.S.S.R.*, 1947, **17**, 1106.

[17] Simpson, *J. Chem. Physics*, 1948, **16**, 1124.

[18] Jacobs, *Proc. Physic. Soc. A*, 1949, **62**, 710.

in the transition moment integral have also been mentioned.[10, 17] If the long wavelength system arises from a transition forbidden by symmetry, it is obvious that absorption and fluorescence bands should show the same characteristic difference as the near ultra-violet transition in benzene, i.e. a strong o-1 band and a weak 1-o band in absorption and a weak o-1 and a strong 1-o band in fluorescence. Experimental data on absorption and on fluorescence in the different states of aggregation were consulted and the interpretation chosen is presented in Table I. There is no doubt that the narrow band group at 3080·1-3081·3 Å in the vapour represents the o-1 transition. It is very strong in absorption and weak in fluorescence. The band at 3080·4 Å or 32454 cm.$^{-1}$ is taken as main band. Likewise, the band at 3172·4-3173·4 Å occurs strongly in fluorescence and weakly in absorption and is here considered as 1-o transition. Already Pringsheim[8] noticed these intensity ratios which would be in agreement with a forbidden transition. 31513 cm.$^{-1}$ is taken as main band of the 1-o transition. The intensity ratio of the two bands as taken from absorption plates obtained by Cooper[19] is 1/20. From spectrogram No. 169 in the catalogue of ultra-violet spectrograms a ratio of about 1 to 30 may be estimated for the solution.[20] These ratios will be used later in the evaluation of the o—o band. As seen in Table I the band positions in the solution are shifted to the red by about 310 cm.$^{-1}$ as compared to the vapour. For rigid glass solutions Kasha and Nauman's values have been used.

TABLE I.—o—1, 1—o AND o—o BANDS OF LONG WAVELENGTH SYSTEM OF NAPHTHALENE

Bands	Vapour abs., ref. 1 fluor., ref. 8	Liqu. Solution (hexane) abs., ref. 1, 20 fluor., ref. 7	Rigid Glass abs., ref. 4 fluor., ref. 4	Crystal abs., ref. 5 fluor., ref. 9
o—1	32454 cm.$^{-1}$	32145 cm.$^{-1}$	32104 cm.$^{-1}$	—
1—o	31513 cm.$^{-1}$	31173 cm.$^{-1}$	31144 cm.$^{-1}$	31062 cm.$^{-1}$?
Separation	941 cm.$^{-1}$	972 cm.$^{-1}$	960 cm.$^{-1}$	—
O—O	(32080 cm.$^{-1}$)	(31757 cm.$^{-1}$?)	31680 cm.$^{-1}$	(31062 cm.$^{-1}$?)

The corresponding assignments in the crystal spectra are much more difficult to achieve. These spectra are extremely complex and not too well understood. Four different electronic transitions were assumed in the absorption analysis[5] and three were used for the explanation of the fluorescence spectrum.[9] The absorption spectra were taken with natural light and with polarized light where the polarization vector was either parallel to the *a* or *b* axis[21] of the crystal. In the long wavelength part there are bands which appear weakly or not at all in one case and strongly in the other, but above 33400 cm.$^{-1}$ the spectrum is strong only when the polarizato the *a* or *b* axis[21] of the crystal. In the long wavelength part there are bands which appear weakly or not at all in one case and strongly in the other, but above 33400 the spectrum is strong only when the polarization vector is parallel to the *a* axis and it is practically missing for the other position of the Nicol. In spite of the excitation by polarized light as means of differentiation, we found it not possible to obtain a satisfactory analysis. It was expected that, if the analysis presented here is valid for the vapour and solutions, it would also, at least in its main features, apply to the solid. However, the characteristic features may become obscured because interaction with crystal forces (the molecules are arranged in skew packing [21]) may cause the breakdown of the selection rule. It will also lead to splitting of the energy levels [22] and the spectrum will look more complicated than that in the vapour phase. For naphthalene, the fluorescence spectrum is less complex than the absorption spectrum. Obreimov and Shabaldas stated that the fluorescence spectrum has a sharp beginning with a line at 31062 cm.$^{-1}$ and they succeeded in interpreting all stronger lines with the use of known Raman frequencies belonging to totally symmetric vibrations. Small frequencies up to about 100 cm.$^{-1}$ were identified with lattice vibrations found in the Raman effect of naphthalene crystals.[23]

---

[19] Cooper, *Master Thesis* (Duke Univ., 1948).

[20] *American Petroleum Institute Research Project* 44 at the National Bureau of Standards. *Catalogue of Ultra-violet Spectrograms*, Serial No. 169, Naphthalene liqu. sol.).

From the previous discussion it would seem logical to assign the narrow band at 31062 cm.$^{-1}$ to the 1—0 transition in the crystal spectrum. However, the situation becomes confused when considering the absorption spectrum. The groups in the spectrum do not stand out as clearly as in the fluorescence spectrum and the overlapping of the second absorption region is adding to the complexity of the spectrum. A new analysis by Prikotjke [24] was not available to the authors except a very brief abstract in *Chem. Abstr.* in which no mention is made of any figures. Interpreting the band 31062 as 0—0 band would account for the appearance of this band in fluorescence and absorption but it does not lead to a satisfactory analysis of the spectrum. It would also give a very large red shift as compared to the vapour and solution spectra. Work on the spectrum of the crystal is being continued.

(*b*) FIXATION of 0—0 BAND.—The separation between the 0—1 and 1—0 bands in the different states of aggregation are also included in Table I. This separation represents the sum of the vibrational frequencies in the lower and upper electronic state that makes the forbidden transition allowed. Assuming that it is a transition A_{1g}-A_{1g}, it is clear that excitation of a β_{3u} vibration will produce a transition moment in the long molecular axis and a β_{2u} vibration a moment in the short axis. A moment perpendicular to the molecular plane (along the z axis) could be produced by excitation of a β_{1u} vibration. Fixation of the 0—0 band is not easy. The three types of vibration which can produce the necessary moment are Raman inactive. Infra-red measurements are known in the literature [25] only above 600 cm.$^{-1}$. It seems more likely that the separation 941 cm.$^{-1}$ would involve a vibration below that value. Dr. E. K. Plyler and Miss Mary A. Lamb have very kindly taken the infra-red spectrum of naphthalene in solution from 4000 to 360 wave numbers at the National Bureau of Standards. Their absorption curves show four frequencies in the critical region : 618 (m), 568 (w), 476 (vs), 361 (w).* Of these, as far as numerical values are concerned, 568 and 476 seem most plausible. If a 50 % drop of the frequency in the upper state can be assumed, then the 618 is also eligible. Using these values with the separation 941 cm.$^{-1}$ in the gas (although they have been obtained from solution data), this would give an upper state frequency of 323, or 373 or 465 cm.$^{-1}$ respectively, and correspondingly, would place the 0—0 band at 32131, or 32081 or 31989 cm.$^{-1}$ Although faint and narrow bands have been measured by de Laszlo in all three places, this has not much significance. Cooper, who studied the absorption in dependence of pressure and not of temperature, did not observe a band in any of these positions. The solution spectrum obtained by de Laszlo shows a peak at 31757 cm.$^{-1}$ which divides the distance of 970 into 584 + 388 cm.$^{-1}$, but a similar peak has not been obtained by other authors (for example, ref. 20). The interpretation of the 31757 cm.$^{-1}$ peak as 0—0 band must be considered as uncertain, particularly in view of its intensity. Examining the data obtained in rigid glass solution, it is seen at once that the 0—0 band does occur weakly in absorption and in fluorescence. Interaction with the glass medium causes a breakdown of the selection rule. Unfortunately, the measurements are accurate to only ± 30 cm.$^{-1}$. Actually, the two 0—0 bands deviate by about 100 cm.$^{-1}$ from each other. In the absorption curve the distance from the 0—0 band to the next very strong band is 367 cm.$^{-1}$, and the corresponding distance in the fluorescence curve is 482 cm.$^{-1}$. In Table I the values for the 0—1 and 1—0 bands (rigid glass) are the wave numbers of the strongest bands in the spectra and are more reliable than the weak 0—0 peaks. With this in mind and assuming that the ratio of the distance 367 and 482 has some real significance, the position of the 0—0 peak is estimated at about 31680 cm.$^{-1}$ which is the averaged value reported in Kasha and Nauman's paper.

---

[21] Robertson, *Proc. Roy. Soc. A*, 1933, **142**, 674 ; Abrahams, Robertson and White, *Acta Cryst.*, 1949, **2**, 238.

[22] Davydov, *J. Expt. Theor. Physics, U.S.S.R.*, 1948, **18**, 210.

[23] Gross and Vuks, *J. Physique Rad.*, 1936, **4**, 113 ; *Nature*, 1929, **124**, 692.

[24] Prikhotjko, *Nat. Acad. Sci. U.S.S.R., Ser. Phys.*, 1948, **12**, 499, reviewed in *Chem. Abstr.*, 1950, **44**, 433.

[25] For example, Lambert and Lecomte, *Ann. Physique*, 1933, **18**, 329 ; Barnes, Gore, Liddell and Williams, *Infra-red Spectroscopy* (Reinhold, New York, 1944), p. 56.

* *m* = medium, vs = very strong, w = weak.

No additional information can be obtained from the spectra of crystalline naphthalene as was indicated before.

(*c*) SUPPORT OF THE ANALYSIS AND DETERMINATION OF THE INTERACTING VIBRATION FROM THE SPECTRUM OF HEAVY NAPHTHALENE.—Although the preceding analysis (intensities, numerical relations, Boltzmann factor from intensity ratio of 0—1 and 1—0 bands) points to a vibration in the neighbourhood of 600 cm.$^{-1}$ rather than to the strong 476 cm.$^{-1}$ as interacting vibration, the latter cannot be definitely excluded because of the only roughly known positions of absorption and fluorescence peaks in liquid and solid solutions. To facilitate the assignment, a sample of completely deuterated naphthalene was prepared by L. Corrsin * in this laboratory and the ultra-violet absorption spectrum was taken by C. D. Cooper. The first noticeable feature was the greater diffuseness of the spectrum as compared to that of light naphthalene. There was probably a small percentage of not completely deuterated compound in the sample which would produce close lying bands and somewhat obliterate details. However, the edges on the ultra-violet side of the bands would correspond to the completely deuterated substance. It was found that the 0—1 band in heavy naphthalene is shifted by only about 100 cm.$^{-1}$ to the violet as compared to ordinary naphthalene while the corresponding shift in benzene is 180 cm.$^{-1}$. (The shift in mono-deuterobenzene is 31 cm.$^{-1}$). The shift to the violet results from zero point vibrations. The separation between the 0—1 and 1—0 bands is about 910 cm.$^{-1}$ in heavy naphthalene as compared to 941 in the light compound. The infra-red frequencies were taken from curves obtained again by Dr. E. K. Plyler and Miss Mary A. Lamb at the National Bureau of Standards using our samples in solution. In the region pertinent to our dicussion these vibrational frequencies were observed : 594 (m), 566 (vw), 541 (w), 422 (vw), 403 (s), 328 (w). It seems reasonable to assume the following correspondences between light and heavy naphthalene vibrations :
unlikely that the vibration will have a much larger frequency in the excited

Light	*Heavy*
618 (m)	594 (m)
568 (w)	541 (w)
476 (vs)	403 (s)
361 (w)	328 (w)

The separation of 910 cm.$^{-1}$ rules out the participation of the 403 vibration in the mechanism of making the A_{1g}-A_{1g} transition allowed because it is electronic state. For 594 and 541, the ratio of the vibrational frequencies in the two states would be about the same for both naphthalenes. Measurements in rigid glass solution agree better with using the 568 than the 618 cm.$^{-1}$ vibration, but the wide limits of accuracy in these spectra do not entirely exclude the higher value.

---

* A paper by L. Corrsin is in the course of preparation.

A consideration of the symmetrics of these vibrations may permit a further selection. The question to which symmetry class the interacting vibration belongs is identical with the question in which direction the "forbidden" transition is polarized. Firstly, it is expected and assumed that this vibration is a carbon vibration. It is furthermore assumed that the vibrational transition moment will be in the molecular plane and more specifically, in the long axis (x) since the next allowed transition (A_{1g}-B_{3u}) should be polarized in the x direction. This makes the interacting vibration one of type β_{3u}. Either vibration (618 or 568) could belong to this type. From intensity arguments the 618 seems a better choice.* The large drop of almost 50 % in wave number in the upper electronic state would have to be explained. Although a drop of this magnitude was assumed to occur in benzene [26] for the β_{2g} carbon vibration, it is surprising for the β_{3u} mode. Therefore, until further support in favour of the 618 vibration has been found, the 568 vibration is used here tentatively as the interacting vibration. While this refers to the strong part of the long wavelength system, it is quite possible that weak bands which do not fit in this scheme result from a vibrational moment in the short axis (y) and involve a β_{2u} vibration.

In Table II there are collected the main vibrational frequencies occurring in the spectrum produced through interaction of a β_{3u} vibration. All are interpreted as carbon vibrations.

Remarks on the Higher Electronic Singlet Levels—As mentioned in the introduction, a second absorption region occurs in naphthalene at 2900-2500 Å. The beginning of this absorption (0—0 band) was given in Kasha and Nauman's paper as 33736 cm.$^{-1}$. This value was taken from Prikhotjko's absorption measurements in the crystal. Klevens and Platt place the onset of the second absorption in solution at about 35,000 cm.$^{-1}$. From a careful study of our own plates we have chosen the strong broad vapour band at 35910 cm.$^{-1}$ as 0—0 band [19] of a second absorption system. It seems impossible to correlate this value with the 33736 in the solid because of the too large shift. In looking for a possible lower transition we had noticed on our plates a rather strong group of bands located at 34060-33940 cm.$^{-1}$ with the bands spaced about 40 cm.$^{-1}$ apart. They look different from the other naphthalene bands, H group of Henri and de Laszlo appearing strongly in the vapour and in solution. A corresponding group in heavy naphthalene is missing. Dr. Corrsin suggested the group might be due to an impurity which was removed with the sulphonation in the preparation of heavy naphthalene. After refluxing the ordinary naphthalene with sodium, the peculiar band group had disappeared.† The spectra look now more uniform, and it has been possible to extend the analysis ‡ of the ${}^1A_{1g}$-${}^1A_{1g}$ system a little further toward shorter waves, and of the second stronger system to longer waves from the 0—0 band 35910 cm.$^{-1}$. The second system is considered to be the predicted ${}^1A_{1g}$-${}^1B_{3u}$ transition. Although measurements in the spectrum of heavy naphthalene have not been completed, it may be mentioned here that a preliminary calculation indicates a shift of about

---

* Tentative assignments of the infra-red active vibrations of the two naphthalenes will be published by L. Corrsin soon.

[26] Garforth, Ingold and Poole, *J. Chem. Soc.*, 1948, 491.

† Naphthalene which had been sublimed and recrystallized several times still gave a positive test for sulphur before refluxing with sodium. Dr. Corrsin's suspicion that the impurity might be benzothiophene was recently verified spectroscopically by C. D. Cooper.

‡ These results will be published with C. D. Cooper elsewhere.

130 cm.$^{-1}$ of the 0—0 band in the second system of heavy naphthalene as compared to light naphthalene.

The principal vibrational frequencies found in the transition A_{1g}-B_{3u} are included in Table II. Except for 930, they are considered as belonging to carbon vibrations.

Coming back to the absorption spectrum of the crystal, photograph 4*a*, Plate I in Prikhotjko's paper suggests from the intensity distribution of bands that the region 33445-36000 cm.$^{-1}$ may consist of two different transitions. It is tentatively suggested here that the state B_{3u} splits in the crystal into two states, one covering a spectral transition from about 33440-34500, and the other from about 34500 to above 36000 cm.$^{-1}$.

The third absorption region of naphthalene occurs at 2220 Å-2000 Å (45000-50000 cm.$^{-1}$). It is more than 10 times stronger than the second. Structure in this system was obtained in the vapour on u.-v. sensitized plates. It agrees with the general contours of the spectrum of the liquid[6] in this region but shows in addition a few fainter bands on the long wave side which are lost in the sharp rise of the absorption curve in the liquid.

TABLE II.—VIBRATIONAL FREQUENCIES (CM.$^{-1}$) OCCURRING IN THE FIRST TWO SINGLET SYSTEMS OF NAPHTHALENE.

LONG WAVELENGTH SYSTEM A_{1g}-A_{1g}

Ground State	Excited State	Raman	Infra-red	Symmetry of Vibration
510	474	512	—	α_{1g}
(568)	(373)	—	568	β_{3u}
766	701	762	—	α_{1g}
1022	997	1022	—	α_{1g}

520	480	512	—	α_{1g}
—	710	762	—	α_{1g}
930	—	940	—	α_{1g} ?
1030	980	1022	—	α_{1g}
—	1390	1380	—	α_{1g}

Although work on this system is still in progress, a value of 45100 cm.$^{-1}$ may be suggested as possible location of the 0—0 transition.

Comparison with Theory.—The occurrence of a forbidden transition $^1A_{1g}$-$^1A_{1g}$ as lowest electronic transition in the naphthalene molecule is in agreement with calculations based on the valence bond method.[11, 12] The tentative position of the 0—0 band (Table I) is at 3116 Å (32080 cm.$^{-1}$), while Blumenfeld calculated 3193 Å and Craig's value is 2830 Å. The good agreement with Blumenfeld's value is probably fortuitous. The analysis presented here is also consistent with results obtained from Platt's free electron model. The location of the 0—0 band fits well on his curve for the ^1L_b transition in polyacenes.[6]

Both the valence bond and molecular orbital method agree on a B_{3u} level as upper state of the first allowed transition. From these predictions and not from the analysis, the 35910 band was identified with the 0—0 transition of the system $^1A_{1g}$-$^1B_{3u}$. A distinction between a B_{2u} and B_{3u} level from the spectrum is difficult as essentially the same vibrational structure may be expected in the two transitions. The close agreement of the position of our $^1B_{3u}$ level (2784 Å) with Blumenfeld's calculated position is again more or less fortuitous. Craig's calculations place it somewhat lower at 2665 Å. There seems, however, to be disagreement with the latest results obtained with the molecular orbital method. Calculations of Jacobs would place the B_{3u} level at about 3420 Å, that is, in the neighbourhood of the forbidden absorption system. These calculations further predict a B_{2u} level very close to the B_{3u} state. Transitions to these levels from the ground state would give overlapping spectra. Careful search was made for a second system between the long wave forbidden spectrum and the allowed system starting at 35910 cm.[1] This seemed important in view of the appearance of the crystal spectrum in that region, as was discussed before. Now it is true that there are a number of unexplained bands in the critical region of both transitions, but almost all the stronger bands (or rather groups of narrow bands) were found to fit into one of the two systems. There are also a very few fainter bands which look different from the other naphthalene bands in either system and which, remembering the fate of the *H* group (notation of Henri and de Laszlo), might still belong to an impurity. Taking all this into account, the existence of another system in the transition region between the two identified systems cannot be excluded until all the bands have been accounted for, but this existence is not considered very probable. The third, very intense transition is polarized in the long axis as was shown in previous experimental [27] and theoretical research.[18]

The authors would like to express their indebtedness to Dr. E. K. Plyler and Miss Mary A. Lamb of the National Bureau of Standards for taking the infra-red spectra of light and heavy naphthalene in solution.

Department of Physics,
Duke University,
Durham, North Carolina.

[27] Jones, *Chem. Rev.*, 1947, 41, 353.

APPLICATIONS OF THE ELECTRONIC SPECTRA OF PYRIDINE HOMOLOGUES TO QUANTITATIVE ANALYSIS AND TO THE MEASUREMENT OF DISSOCIATION CONSTANTS

BY E. F. G. HERINGTON

Received 27th June, 1950

The difficulty of preparing pure samples of pyridine bases is indicated. The absorption spectra of highly purified samples of pyridine, α-, β-, and γ-picoline and 2 : 6-lutidine obtained under different conditions are discussed from the point of view of chemical analysis. The spectra of the vapours over a wide range of pressures at 20° C using cells of length 14·5 cm , 61·2 cm. and 153 cm. are compared. Special attention has been paid to the effect of small amounts of impurities. The spectra of solutions of these bases in 0·1 N sulphuric acid, 0·1 N sodium hydroxide and cyclohexane are recorded. A method for the analysis of a mixture of β-picoline, γ-picoline and 2 : 6-lutidine based on the differences in absorption coefficient of acid and alkaline solutions is described. The dissociation constants of these bases have been determined from the spectra of buffered solutions.

Compounds of the pyridine series are particularly difficult to prepare in a state of purity, partly because there are no convenient synthetic methods, partly because certain members have boiling points near others and partly because they are difficult to free from water. The modern technique of fractional distillation will readily separate α-picoline and pyridine from a mixture of bases which was impossible when much of the earlier work on the spectra was undertaken (e.g. see Herrman [1]), but certain homologues such as β-picoline (b.p. 144·0° C), γ-picoline (b.p. 145·3° C) and 2 : 6-lutidine (b.p. 144·0° C) have boiling points which are so little different that even now special methods have to be used in their separation.[2] Extensive fractional distillation fails to remove hydrocarbon impurities from pyridine and α-picoline so that chemical treatment is a necessary step in the purification of these bases.[3]

In view of the difficulty of preparing pure samples, it is not surprising that Herrman [1] thought that the bands at 2789·4, 2832·4 and 2876·7 Å obtained by him in the vapour spectra of α-picoline were due to the presence of pyridine in his sample although Purvis [4] at an earlier date had commented upon the large number of near coincidences in the wavelengths of bands in pyridine and α-picoline. The present work shows that some of these bands do occur in the spectra of pure α-picoline. A more recent example of the difficulty of obtaining pure samples of these bases is afforded by the investigation of the Raman spectra by Herz, Kahovec and Kohlrausch [5] who showed that their β-picoline sample contained 2 : 6-lutidine even after extensive treatment. Sponer *et al.*[6, 7] have suggested that the ultra-violet spectra of α-picoline and pyridine vapour should be compared in order to establish whether a band at 33824 cm.$^{-1}$ observed bv them and by Henri and Angenot [8] in pyridine was due to a small quantity of α-picoline.

Highly purified samples of these bases have been prepared at the Chemical Research Laboratory in connection with other work, and in view of the uncertainties concerning published spectra it was decided to record the absorption of these authenticated specimens. Interest at the Chemical Research Laboratory centred on the possibility of devising spectroscopic methods for the analysis of mixtures and no vibrational assignments have been attempted.

The ultra-violet absorption spectra of pyridine in the vapour and in solutions have frequently been described, e.g. vapour spectra by Henri *et al.*[8] and by Sponer *et al.*[6, 7]; heptane solution by Spiers and Wibaut;[9] aqueous solution by Marchlewski and Wyrobek [10] and by Hughes, Jellinek and Ambrose.[11] The spectra of α-picoline in the vapour has been reported by Purvis [4] and by Herman,[1] and in solution by Purvis [4] and by Baker and Baly.[12] The vapour spectra of 2 : 6-lutidine was described by Purvis [4] and that of β-picoline by Herrman,[1] but in view of the spectra reported here it appears probable that his β-picoline specimen was composed largely of 2 : 6-lutidine. A note by Sponer and Rush [13] on the near ultra-violet spectra of α-, β- and γ-picoline appeared when our preliminary work on the spectra had been carried out.

Experimental

General.—The purities of the samples of bases used were established by a freezing point technique [14] and the following values found: pyridine 99·85 ±

[1] Herrman, *Z. Wiss. Photogr.*, 1919, **18**, 253.

[2] Coulson and Jones, *J. Soc. Chem. Ind.*, 1946, **65**, 169.

[3] *Report Chem. Res. Board* (1948), 33.

[4] Purvis, *J. Chem. Soc.*, 1910, **97**, 692.

[5] Herz, Kahovec and Kohlrausch, *Z. physik. Chem. B*, 1943, **53**, 124.

[6] Sponer, *Rev. Mod. Physics*, 1944, **16**, 224.

[7] Sponer and Stücklen, *J. Chem. Physics*, 1946, **14**, 101.

[8] Henri and Angenot, *J. Chim. Phys.*, 1936, **33**, 641.

[9] Spiers and Wibaut, *Rec. trav. chim.*, 1937, **56**, 573.

[10] Marchlewski and Wyrobek, *Bull. Acad. Polanaise*, 1929, *A* 93; 1934, *A* 22.

[11] Hughes, Jellinek and Ambrose, *J. Physic. Chem.*, 1949, **53**, 410.

[12] Baker and Baly, *J. Chem. Soc.*, 1907, **91**, 1122.

[13] Sponer and Rush, *J. Chem. Physics*, 1949, **17**, 587.

[14] Herington and Handley, *J. Chem. Soc.*, 1950, 199.

0·07 %, α-picoline 99·89 ± 0·06 %, β-picoline 99·97 ± 0·02 %, γ-picoline 99·75 ± 0·13 %, 2 : 6-lutidine 99·93 ± 0·04 %. The water content was less than 0·02 % by volume. Sensitive colour reactions[15] gave results consistent with the freezing point determinations, thus, for example, the γ-picoline contents of the β-picoline and 2 : 6-lutidine samples were shown to be less than 0·1 % by volume.

The vapour spectra were obtained by means of a Zeiss quartz spectrometer, slit width 0·01 mm., reciprocal dispersion 7·4 Å per mm. in the wavelength range 2400-3000 Å, using Ilford Selochrome 30° backed plates. The light source was a high tension, 2500-V hydrogen lamp consuming 1 kW and exposure times varied from 4 to 16 min. The vapour absorption cells of lengths 14·5 cm., 61·2 cm. and 153 cm. were of Pyrex glass with quartz windows and carried a side tube containing the liquid. The cells were evacuated with a mercury diffusion pump backed by a rotary oil pump. The pressure of the vapour of the base in the cell was varied by immersing the liquids in the side tube in suitable baths. The temperature of the vapour in the light path was that of the room. The wavelengths of the absorption bands were measured on photographic enlargements of the spectra using an iron arc as standard[16] and employing the Hartman formula for interpolation. The wavelengths in air recorded in the tables are expressed in International angstrom and are believed to be correct to at least 0·5 Å. The letters given in the tables following the wavelengths designate the appearance of various types of band : thus, *a*, strong band with sharp edge on violet side ; *b*, strong band most intense in centre ; *c*, weak narrow band with sharp edges ; *d*, diffuse band ; *e*, centre of very broad band ; *f*, violet edge of very broad band.

Some of the solution spectra were measured on a Beckman quartz spectrophotometer and others on a Unicam quartz spectrophotometer. The 0·1 N sulphuric acid used as solvent had a transmission of 95 % at 2450 Å compared with conductivity water while the value for the 0·1 N sodium hydroxide solution was 97·2 %. The cyclohexane which was used as a solvent was purified by acid treatment followed by percolation through silica gel[17] and had a transmission of 90 % at 2450 Å compared with conductivity water. The appropriate solvent was employed in the blank cell in every instance.

Vapour Spectra.—PYRIDINE.—Henri and Angenot[8] who studied the spectra of this material over a wide range of temperatures and pressures recorded 255 bands. Such a wide range of conditions were not examined here and it was not expected that so many bands would be observed, but nevertheless 109 bands were measured and agreement found with those recorded by Henri in most cases. The only bands recorded by the French workers which were not observed although it was anticipated that these bands would be found from the recorded intensities and from the respective resolving powers of the spectrometers were bands at 2925·5, 2932·2, 2923·0, 2900·0, 2886·3, 2833·1 and 2750·8 Å. *o*-Xylene has been separated from some impure samples of pyridine but it was shown that these bands which we have failed to detect could not have been due to the presence of this hydrocarbon in the pyridine used by other workers. The only bands found in this work which were additional to those recorded by Henri and Angenot were weak and diffuse bands at 2497, 2487, 2466, 2447 and 2427 Å. Plate I is a photograph of the spectra. The absence of diffuse bands of the type shown by α-picoline (Plate II) should be noted. These pyridine spectra exhibited a band at 33824 cm.$^{-1}$ (2955·6 Å) which was not due to the presence of picoline (see below). This is the band which Sponer and Stücklen[7] experienced difficulty in assigning notably because Kline and Turkevich[18] had reported a mediumly strong band in the infra-red at 936 cm.$^{-1}$ (mean 941 cm.$^{-1}$). Measurements of the infra-red spectra of a sample of pure pyridine carried out at the Chemical Research Laboratory failed to reveal the presence of a mediumly strong band at 941 cm.$^{-1}$.

α-PICOLINE.—The spectra of this base shows fewer bands than pyridine (Plate II). The 34 bands which were observed are listed in Table I. Comparison of the wavelengths of these bands with those recorded by Henri[8] for pyridine shows a large number of near coincidences. The general intensity of

---

[15] Herington (in preparation).

[16] *Iron Charts* (Adam Hilger Ltd.), 3rd edn.

[17] Maclean, Jencks and Acree, *J. Res. Nat. Bur. Stand.*, 1945, **34**, 271.

[18] Kline and Turkevich, *J. Chem. Physics*, 1944, **12**, 300.

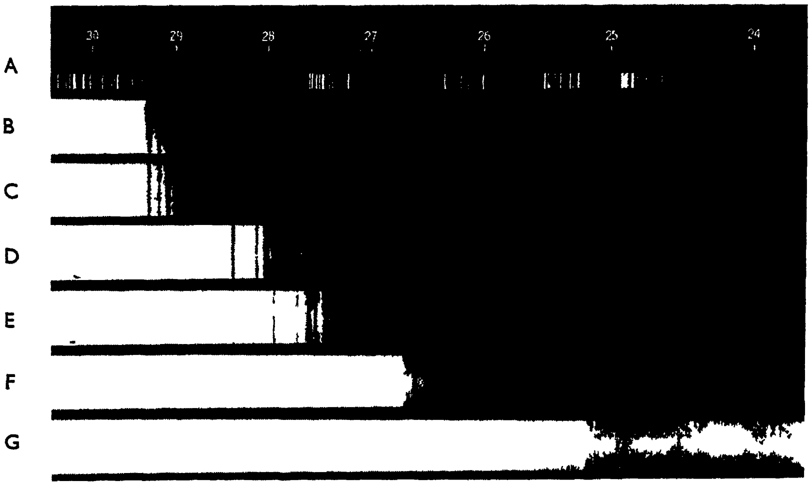

PLATE I.—Vapour spectra of pyridine at 19° C.

A Iron arc. B 153 cm. cell, liquid at 19° C. C 61 cm. cell, liquid at 19° C. D 14·5 cm. cell, liquid at 14° C. E 14·5 cm. cell, liquid at 0° C. F 14·5 cm. cell, liquid at −15° C. G 14·5 cm. cell, liquid at −30° C.

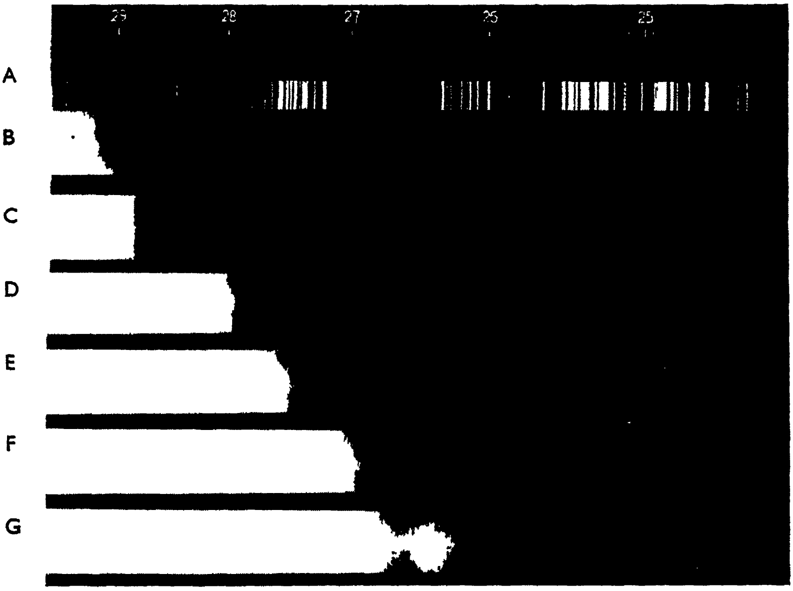

PLATE II.—Vapour spectra of α-picoline at 20° C.

A Iron arc. B 153 cm. cell, liquid at 20° C. C 61 cm. cell, liquid at 20° C. D 14·5 cm. cell, liquid at 18° C. E 14·5 cm. cell, liquid at 0° C. F 14·5 cm. cell, liquid at −17° C. G 14·5 cm. cell, liquid at −22° C.

[*To face page* 28

Plate III—Vapour spectra of β picoline at 19° C
A 153 cm cell liquid at 19° C B 61 cm cell, liquid at 19° C C 61 cm cell, liquid at 0° C D 61 cm cell liquid at −15° C E 61 cm cell, liquid at −30° C F 61 cm cell liquid at −45° C G Iron arc

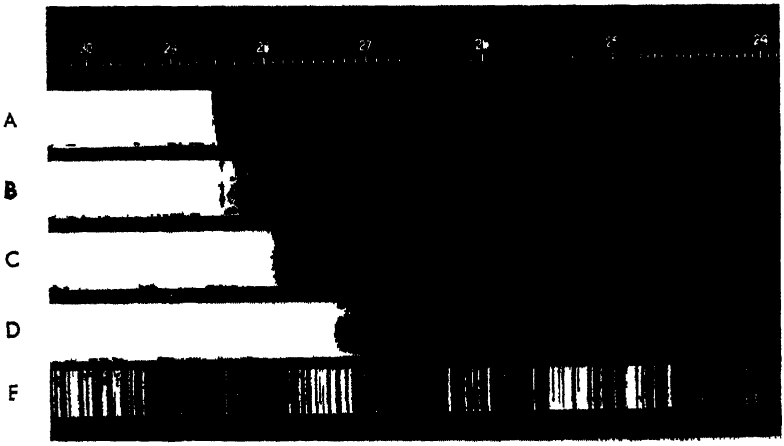

Plate IV—Vapour spectra of γ-picoline at 19° C
A 153 cm cell, liquid at 19° C B 61 cm cell, liquid at 19° C C 61 cm cell liquid at 0° C D 61 cm cell, liquid at −15° C E Iron arc

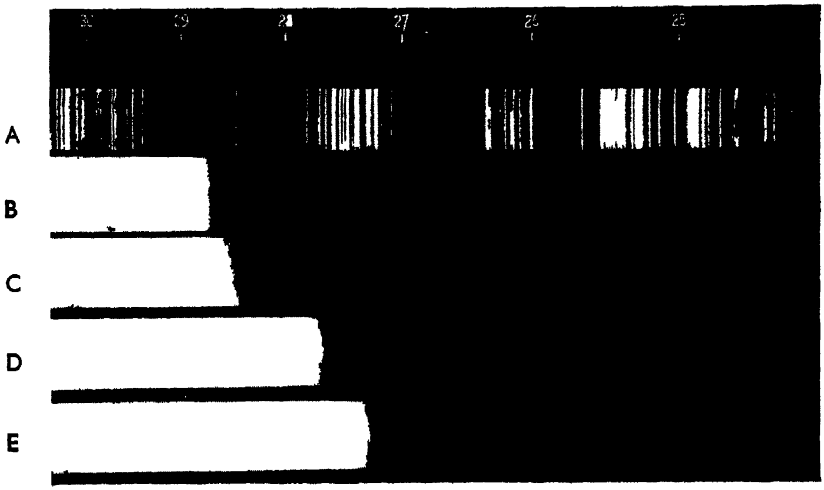

PLATE V—Vapour spectra of 2 6-lutidine at 19° C

A Iron arc B 153 cm cell liquid at 19° C C 61 cm cell liquid at 19° C
D 14 5 cm cell liquid at 15 C E 14 5 cm cell, liquid at – 5° C

the α-picoline spectra is less than that of pyridine. The diffuse bands in the region 2663·3-2516·6 Å are particularly striking.

β-PICOLINE.—Except for the note by Sponer and Rush[13] the absorption spectra of β-picoline vapour has not been studied within recent times.

TABLE I.—WAVELENGTHS OF ABSORPTION BANDS IN α-PICOLINE VAPOUR

Å	Å	Å	Å	Å
2928·8 *c*	2875·9 *b*	2850·0 *c*	2806·9 *c*	2663·3 *e*
2921·3 *c*	2869·7 *b*	2847·6 *c*	2803·8 *c*	2655·3 *f*
2914·7 *c*	2866·1 *c*	2844·1 *c*	2795·9 *c*	2601·6 *e*
2905·1 *c*	2862·1 *d*	2839·7 *c*	2789·0 *b*	2585·1 *f*
2898·7 *c*	2861·3 *d*	2836·4 *c*	2783·5 *c*	2535·3 *e*
2891·7 *c*	2858·8 *d*	2823·3 *b*	2775·5 *d*	2516·6 *f*
2887·9 *c*	2856·0 *d*	2826-2882 *d*	2747·2 *d*	2465·4 *d*
2879-2875·9 *d*	2853·8 *c*	2816·5 *b*	2736·9 *c*	—

Plate III shows the spectra and the wavelengths of 50 bands recorded in Table II. The tendency for bands to occur in small groups gives to this spectra its characteristic appearance. The bands become more diffuse towards shorter wavelengths but wide diffuse bands of the type shown by α-picoline or by 2 : 6-lutidine are absent.

TABLE II.—WAVELENGTHS OF ABSORPTION BANDS IN β-PICOLINE VAPOUR

Å	Å	Å	Å	Å
2938·2 *c*	2880·8 *b*	2833·0 *c*	2759·1 *c*	2635·5 *d*
2934·4 *c*	2872·9 *a*	2828·3 *c*	2755·1 *c*	2618·1 *d*
2925·6 *c*	2867·0 *c*	2823·0 *c*	2750·7 *c*	2606·8 *d*
2922·6 *c*	2859·6 *a*	2816·8 *b*	2746·1 *c*	2594·9 *d*
2918·5 *c*	2856·8 *b*	2813·3 *a*	2742·4 *d*	2579·9 *d*
2912·5 *c*	2853·5 *c*	2809·1 *c*	2723·8 *d*	2450-2550 *d*
2904·5 *c*	2851·1 *c*	2795·2 *d*	2707·8 *d*	—
2896·8 *c*	2848·1 *c*	2784·2 *c*	2687·7 *d*	—
2892·3 *c*	2845·2 *c*	2779·2 *c*	2674·1 *d*	—
2888·9 *c*	2840·1 *a*	2775·3 *c*	2662·7 *d*	—
2884·5 *b*	2837·1 *b*	2762·7 *c*	2648·8 *d*	—

γ-PICOLINE.—The absorption bands in the spectra of this base (see Plate IV) are displaced towards shorter wavelengths compared with those in α- and β-picoline and are much more diffuse particularly below 2800 Å although wide diffuse bands of the type which appear in α-picoline and 2 : 6-lutidine are absent. Table III gives the wavelengths of 25 bands measured.

TABLE III.—WAVELENGTHS OF ABSORPTION BANDS IN γ-PICOLINE VAPOUR

Å	Å	Å	Å	Å
2884·1 *d*	2830·4 *d*	2792·3 *d*	2748·0 *d*	2643 *d*
2864·4 *c*	2826·8 *d*	2783·3 *d*	2727·5 *d*	2615 *d*
2851·2 *c*	2823·3 *a*	2777·5 *d*	2720·6 *d*	2591 *d*
2841·9 *a*	2813·3 *d*	2768·4 *d*	2713·6 *d*	2570 *d*
2834·6 *c*	2805·9 *d*	2755·8 *d*	2694·2 *d*	2548 *d*

2 : 6-LUTIDINE.—The spectra of this material exhibits very few bands, see Plate V.

The wavelengths of the bands measured were: 2866·7 *c*, 2824·9 *c*, 2693·2 *f*, 2702·8 *e*, 2651·8 *d*, 2627·2 *d*, range 2500-2620 Å weak diffuse bands.

General Comparison of the Vapour Spectra.—Pyridine exhibits the largest number of bands, and successive substitution of methyl groups in the α-positions causes a progressive suppression of fine bands and an enhancement of diffuse bands. Amongst the mono-methyl substituted bases, the β- and γ-homologues exhibit most fine bands and of the five bases studied only α-picoline and 2 : 6-lutidine exhibit broad diffuse bands.

Vapour Spectra of Binary Mixtures of the Bases.—Experiments were carried out with the object of establishing the smallest percentage of one base that can be detected in the presence of another by means of the spectra of the vapours. Pyridine could be detected in α-picoline down to a concentration of 3 % by the appearance of a band at 2788·5 Å using the 14·5 cm. cell with the liquid in the side arm at room temperature. β-Picoline or 2 : 6-lutidine in γ-picoline could be detected down to a concentration of 5 % by a change in the position of the " cut off " using the 14·5 cm. cell and liquid at room temperature although no β-picoline or 2 : 6-lutidine bands could be detected. The presence of 50 % of 2 : 6-lutidine by volume in β- and γ-picoline does not produce any marked change in the spectra of the picolines so that clearly the vapour spectra do not provide a convenient means for the detection of small amounts of these bases in the presence of homologues.

Absorption Spectra of Solutions.—Fig. 1, 2 and 3 show the molar extinction ε plotted against wavelength expressed in Å for solutions of these bases in 0·1 N sulphuric acid, 0·1 N sodium hydroxide and cyclohexane respectively. Certain relationships can easily be seen from these figures. Thus the molar extinction coefficient of these bases in acid solution is approximately twice that in alkaline solution and is least in the hydrocarbon solvent. Hartley[19] long ago commented on the sharper spectra of an aqueous solution of pyridine hydrochloride compared with pyridine, while Purvis[20] reported that acid caused a marked persistence in the spectrum of pyridine and α-picoline. The sequence of the main peaks arranged in the order of decreasing wavelength is approximately 2 : 6-lutidine, α-picoline, β-picoline, pyridine and γ-picoline in all the three solvents, and the magnitudes of the maximum extinction coefficients follow the same order. All the spectra studied except 2 : 6-lutidine show the greatest amount of fine structure in 0·1 N sodium hydroxide solution while the lutidine exhibits most structure in cyclohexane. The shift in the position of the main peak to longer wavelengths on substitution in the ring in the sequence, pyridine, α-picoline, 2 : 6-lutidine, is similar to that shown by the series benzene, toluene, dimethyl benzenes, but γ-picoline is an exception as it does not exhibit a shift compared with pyridine.

Estimation of β-, γ-picoline and 2:6-lutidine in Mixtures.—A method for estimating pyridine based on the measurement of the absorption spectra of acid solutions has been described by Hofmann[21] and by Le Rosen and Wiley.[22] Study of Fig. 1 reveals that 2 : 6-lutidine can readily be estimated in a β-picoline fraction by measuring the absorption at 2800 Å of an acid solution. The values of the differences in extinction coefficient (g./l.) in 0·1 N acid and 0·1 N alkali solutions for these bases are plotted in Fig. 4. A very simple method of analysis of the β-picoline fraction which takes advantage of the occurrence of isobestic points has been developed based on the data in Fig. 4. Thus if measurements of the absorption are made at 2416 Å the difference between the extinction coefficients of acid and alkaline solutions so found is independent of the β-picoline concentration while at 2780 Å it is independent of the γ-picoline concentration. As this technique of analysis which employs the difference between the absorption of the unknown in acid and alkaline media does not appear to have been very widely used, a short account of the procedure as applied to mixtures of the three bases β-, γ-picoline, and 2 : 6-lutidine will be given.

Analyses can be made rapidly by this spectroscopic method and to take full advantage of the speed of this method it was decided to carry out measurements on a volume basis. To obtain the necessary calibration points 0·1 ml. of each pure base was made up to 100 ml. with distilled water and each of these solutions were further diluted by taking 1 ml. of the appropriate dilute solution and diluting to 100 ml. with 0·1 N sulphuric acid. The alkaline solutions were prepared similarly except that 2 ml. of the dilute aqueous solution were made up to 100 ml.

---

[19] Hartley, *J. Chem. Soc.*, 1885, **47**, 685.
[20] Purvis, *ibid.*, 1909, **95**, 294.
[21] Hofmann, *Arch. Hyg. Bakt.*, 1942, **128**, 169.
[22] Le Rosen and Wiley, *Anal. Chem.*, 1949, **21**, 1175.

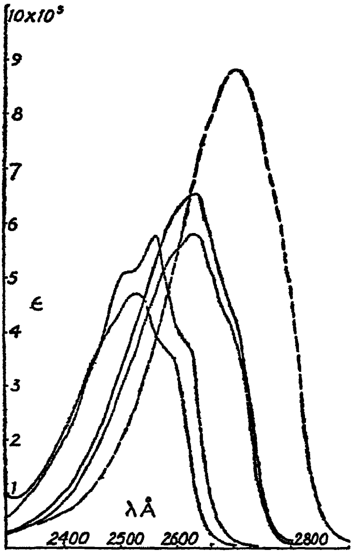

FIG. 1.—Solution spectra, solvent 0·1 N sulphuric acid.

Pyridine- - - - - - - - - -
α-Picoline——————,
β-Picoline. . . . . ,
γ-Picoline—. .—. .—. .—
2 : 6-Lutidine— — — —

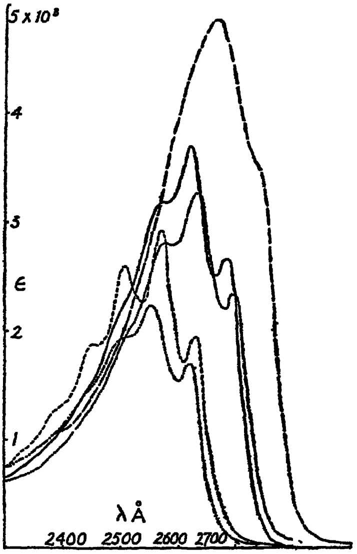

FIG. 2.—Solution spectra, solvent 0·1 N sodium hydroxide.

Pyridine- - - - - - - -
α-Picoline——————,
β-Picoline. . . . . ,
γ-Picoline—. .—. .—. .—
2 : 6-Lutidine— — — —

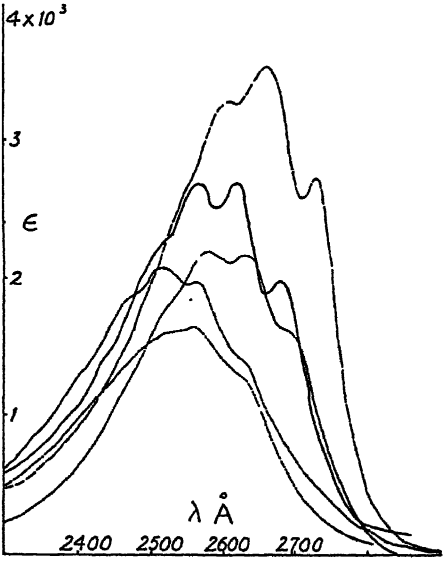

FIG. 3.—Solution spectra, solvent cyclohexane.

Pyridine- - - - - - - - - - -
α-Picoline——————,
β-Picoline. . . . . ,
γ-Picoline—. .—. .—. .—
2 : 6-Lutidine— — — —

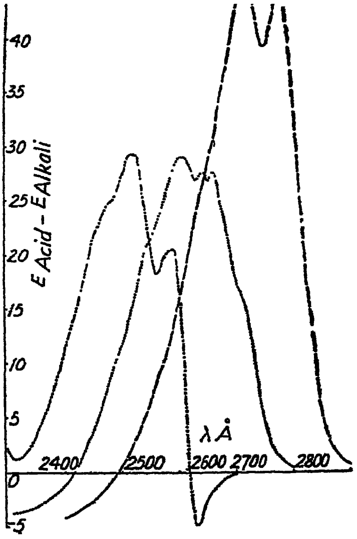

FIG. 4.

β-Picoline. . . . .
γ-Picoline—. .—. .—. .—
2 : 6-Lutidine— — — —

with 0·1 N sodium hydroxide. The absorptions were then measured at 2416, 2646 and 2780 Å and the observed optical densities were multiplied by the factors 100 and 50 for the acid and alkaline solutions respectively to calculate the extinction coefficients equivalent to a base concentration of 1 ml./l. of solution. The differences between these extinction coefficients for acid and alkaline solutions so obtained are recorded in Table IV. To minimize errors it is desirable to carry out this calibration with each spectrometer employing the same volumetric apparatus that is to be used for the estimation of the unknown.

TABLE IV.—WAVELENGTHS AND THE DIFFERENCES BETWEEN THE EXTINCTION COEFFICIENTS (CONC. 1 ml./l.) IN ACID AND ALKALINE SOLUTIONS

Å	β-picoline	γ-picoline	2 : 6-lutidine
2416	0	14·2	−2·8
2646	25·55	−2·2	27·9
2780	0·55	0	40·0

In a typical analysis the unknown mixture was diluted to a concentration equivalent to 0·01 ml. of base per litre in the acid and alkaline solutions and the optical densities measured and the results shown in Table V obtained.

TABLE V

Å	Optical Density Acid Soln.	Optical Density Acid Soln.	Difference in Extinction Coefficient (1 ml./l.)
2416	0·140	0·103	3·7
2646	0·412	0·241	17·1
2780	0·162	0·027	13·5

The concentration of the three bases in the unknown sample were calculated by successive approximation. Let x, y and z be the volume fractions of β-picoline, γ-picoline and 2 : 6-lutidine respectively and let x_1, y_1, z_1 and x_2, y_2, z_2 be the first and second approximations to these quantitives. The first approximation to the 2 : 6-lutidine concentration z_1 is given by 13·5/40·0 since at 2780 Å, the γ-picoline has a zero difference value and the β-picoline difference is so small (0·55) that it can be ignored to a first approximation, hence $z_1 = 0{\cdot}3375$. At 2416 Å, β-picoline has a zero difference so that eqn. (1) applies

$$3{\cdot}7 = 14{\cdot}2\,y_1 - 2{\cdot}8\,z_1, \text{ hence } y_1 = 14{\cdot}2\,y_1 - 2{\cdot}8 \times 0{\cdot}3375 = 0{\cdot}3274 \qquad (1)$$

At 2646 Å, eqn. (2) applies

$$\begin{aligned} 17{\cdot}1 &= 25{\cdot}55\,x_1 + 27{\cdot}9\,z_1 - 2{\cdot}2\,y_1 \\ &= 25{\cdot}55\,x_1 + 27{\cdot}9 \times 0{\cdot}3375 - 2{\cdot}2 \times 0{\cdot}3274, \qquad . \quad . \quad (2) \end{aligned}$$

hence $x_1 = 0{\cdot}3287$.

Using this value of x_1 the second approximation to the 2 : 6-lutidine concentration z_2 is calculated by the equation

$$13{\cdot}5 = 40{\cdot}0\,z_2 + 0{\cdot}55\,x_1 = 40{\cdot}0\,z_2 + 0{\cdot}55 \times 0{\cdot}3287,$$

hence $z_2 = 0{\cdot}334$.

By substituting z_2 in eqn. (1) in the place of z_1 the second approximation to the γ-picoline concentration, y_2, is found to be 0·327. Substituting $z_2 = 0{\cdot}334$, $y_2 = 0{\cdot}327$ in the place of z_1 and y_1 in eqn. (2) yields $x_2 = 0{\cdot}333$. There is no necessity to carry the approximations further and these values are accepted as the final analysis. Table VI gives the results obtained in the analysis of various synthetic mixtures by this method.

The solutions where one component is in large excess were chosen to serve as a fairly exacting test of the method, and as can be seen the results for these solutions appear to be as accurate as for the other mixtures. The wavelengths

2416, 2646, 2780 Å were selected as being most suitable for mixtures containing approximately equal proportions of each base but other wavelengths may with advantage be used if certain components are in excess. Thus while the wavelength 2780 Å is probably always the best choice for the estimation of 2 : 6-lutidine yet 2620 Å may be more suitable for the estimation of β-picoline when 2 : 6-lutidine is in excess, while a wavelength of 2491 Å may be the most suitable for the determination of γ-picoline under these conditions.

TABLE VI.—ANALYSIS OF β-, γ-PICOLINE, 2 : 6-LUTIDINE MIXTURES. ALL PERCENTAGES ARE BY VOLUME

Synthetic Mixtures (%)			Analytical Results (%)			Differences (%)		
β-picoline	γ-picoline	2 : 6-Lutidine	β-picoline	γ-picoline	2 : 6-Lutidine	β-picoline	γ-picoline	2 : 6-Lutidine
33·3	33·3	33·3	33·3	32·7	33·4	0·0	−0·6	+0·1
60·0	20·0	20·0	59·1	18·2	21·1	−0·9	−1·8	+1·1
20·0	60·0	20·0	19·0	59·3	20·4	−1·0	−0·7	+0·4
20·0	20·0	60·0	18·7	19·4	60·8	−1·3	−0·6	+0·8
90·0	10·0	—	90·1	7·7	—	+0·1	−2·3	—
10·0	90·0	—	9·6	88·7	—	−0·4	−1·3	—
90·0	—	10·0	91·3	—	10·3	+1·3	—	+0·3
10·0	—	90·0	8·3	—	89·9	−1·7	—	−0·1

Pyridine and α-picoline will interfere with the determination of β- and γ-picoline by this method and these bases should be removed by fractional distillation before carrying out an analysis of the β-picoline fraction.

Dissociation Constants from the Absorption Spectra.—Table VII taken from a recent paper by Brown and Barbaras [23] shows some of the values which have been reported for the dissociation constants of these bases.

TABLE VII

Base	$K_B \times 10^9$	Ref.
Pyridine . .	2·24	24
	2·4	25
	3·0	26
α-Picoline . .	10·5	24
	45	25
	32	26
β-Picoline . .	11	26
γ-Picoline . .	11	26

The dissociation constants have now been redetermined by studying the change of absorption spectra with pH.* The appropriate expression for the calculation of the logarithm of the thermodynamic dissociation constant K_B from absorption measurements is

$$\log_{10} K_B = \text{pH} + \log_{10} K_W + \log_{10} \frac{\epsilon_2 - \epsilon_3}{\epsilon_1 - \epsilon_2} + \log \gamma_{B^+}$$

where ϵ_1, ϵ_2, and ϵ_3 are the extinction coefficients for the base in acid, buffered and alkaline solution respectively, K_W is the ionic product of water and γ_{B^+} is the activity coefficient of the base ion. The value of log $\gamma_B{}^+$ was calculated from the approximate Debye–Hückel expression.

---

[23] Brown and Barbaras, *J. Amer. Chem. Soc.*, 1947, **69**, 1137.

[24] Barron, *J. Biol. Chem.*, 1937, **121**, 313.

[25] Goldschmidt and Salcher, *Z. physik. Chem.*, 1899, **29**, 114.

[26] Constram and White, *Amer. Chem. J.*, 1903, **29**, 46.

* See Flexser, Hammett and Dingwall [27] also Hughes, Jellinek and Ambrose [11] who obtained a value of $1{\cdot}32 \times 10^{-9}$ for pyridine at 20 ± 2° C.

[27] Flexser, Hammett and Dingwall, *J. Amer. Chem. Soc.*, 1935, **57**, 2103.

$$\log_{10} \gamma_B{}^- = - \frac{Az^2\sqrt{I}}{1 + \sqrt{I}},$$

where I is the ionic strength, z the valency and A has the following values for water, 0·500 at 15° C, 0·509 at 25° C and 0·514 at 30° C.

Solutions were made up by volume and the pH of the solution buffered with a sodium acetate + acetic acid mixture (approximately 0·01 M) was measured with a glass-saturated calomel electrode. The pH meter was standardized with M/20 potassium hydrogen phthalate and sodium borate buffers. The temperature of the buffered solution was determined directly after measuring the extinction coefficient and the appropriate values of A and $\log_{10} K_W$ (see Harned and Owen [28]) were used in the calculation. In order to obtain the highest accuracy the pH was chosen so that the value of $(\epsilon_2 - \epsilon_3)/(\epsilon_1 - \epsilon_2)$ was near unity.

The results are given in Table VIII. Substitution of methyl groups in this series clearly increases the dissociation constant.

TABLE VIII.—THERMODYNAMIC DISSOCIATION CONSTANTS OF SOME PYRIDINE HOMOLOGUES

Base	Wave-length Å	Temp. of Soln. °C	$\frac{\epsilon_2 - \epsilon_3}{\epsilon_1 - \epsilon_2}$	pH	I	$K_B \times 10^9$	Mean Thermo-dynamic Constant $K_B \times 10^9$
Pyridine .	2506	25·5	1·074	5·16	0·010	1·44	1·44
	2558	25·3	1·065	5·16	0·010	1·43	
	2609	25·3	1·077	5·16	0·010	1·45	
α-Picoline	2600	25·2	1·378	5·84	0·013	8·65	8·77
	2650	25·2	1·406	5·84	0·013	8·83	
	2710	25·2	1·407	5·84	0·013	8·83	
β-Picoline	2547	24·6	1·005	5·72	0·0125	4·58	4·54
	2610	24·6	0·985	5·72	0·0125	4·49	
	2660	24·6	1·000	5·72	0·0125	4·56	
γ-Picoline	2485	24·3	1·726	5·86	0·013	10·59	10·62
	2519	24·3	1·710	5·86	0·013	10·50	
	2589	24·3	1·753	5·86	0·013	10·76	
2 : 6-Lutidine	2646	26·7	3·207	6·06	0·014	37·3	38·4
	2720	26·7	3·330	6·06	0·014	38·8	
	2780	26·7	3·356	6·06	0·014	39·1	

I wish to thank Dr. E. A. Coulson, J. B. Ditcham, E. C. Holt, A. Sleven for supplying the pure base samples; R. Handley and A. J. Cook for the estimations of the purity by freezing point determinations and J. L. Hales for the determinations of the water contents. Mr. R. Handley carried out much of the preliminary investigations on the vapour spectra while W. Kynaston made the recorded measurements.

The work described has been carried out as part of the research programme of the Chemical Research Laboratory and this paper is published by permission of the Director, Chemical Research Laboratory, Teddington, Middlesex.

Chemical Research Laboratory,
Teddington,
Middlesex.

---

[28] Harned and Owen, *The Physical Chemistry of Electrolytic Solutions* (Reinhold Publishing Corporation, New York, 1943), p. 485.

THE ULTRA-VIOLET ABSORPTION SPECTRA OF FLUORINATED TOLUENES

By W. T. Cave and H. W. Thompson

Received 30*th June,* 1950

The absorption spectra of some fluorinated toluenes in the vapour phase have been measured in the near ultra-violet. Benzotrifluoride, *m*- and *p*-fluorobenzotrifluoride, *o*-, *m*- and *p*-fluorotoluenes have been studied. A vibrational analysis has been made in each case, and although this is incomplete, important deductions about the values of molecular vibration frequencies have been made. The latter have been correlated with values obtained from the Raman spectra. The most intense progression for each molecule appears to involve a frequency interval which is characteristic of the structural type, and this might be useful for diagnostic purposes with the *o*-, *m*- and *p*-isomers.

Several workers have recently measured the ultra-violet absorption spectra of polyatomic molecules using high resolution, and the theory of the electronic and vibrational transitions permitted with these molecules has become more systematized (Sponer and Teller [1]). One class of molecules of particular interest is the substituted benzenes. Following earlier detailed analysis of the spectrum of benzene in the middle ultra-violet, Sponer and Wollman [2] have measured chlorobenzene, and Wollman [3] has studied fluorobenzene. Recently, Sponer, Hall and Stallcup [4] have given results for 1 : 3 : 5-trichlorobenzene and 1 : 3 : 5-trimethylbenzene, and Sponer [5] has discussed the electronic transitions involved with the tri-substituted benzenes. The spectrum of toluene was studied by Masaki,[6] by Ginsburg, Robertson and Matson [7] and by Savard,[8] who also examined the isomers of cresol.

Following work in this laboratory on the infra-red spectra of some fluorinated toluenes (Thompson and Temple [9]), we have now analyzed the ultra-violet band systems of some of these substances. Although a complete interpretation of all the bands in the spectra cannot be suggested, several useful results have emerged. The present paper includes results for benzotrifluoride, *m*- and *p*-fluoro benzotrifluoride, *o*-, *m*- and *p*-fluorotoluenes, all measured in the vapour phase.

Experimental

The spectra were first measured under low dispersion using a Hilger E 315 spectrograph giving about 10 Å/mm. at 2600 Å, and then with higher dispersion using a large quartz Lithow spectrometer giving about 3 Å/mm. at this wavelength. The absorption cell was a cylindrical quartz tube 1 metre in length, to which a side arm was attached for connection to the sample and to a pumping system. The source of continuous radiation was a hydrogen discharge tube. Owing to the large variation of extinction coefficient with wavelength it was necessary to take many exposures for each substance using a series of pressures.

---

[1] Sponer and Teller, *Rev. Mod. Physics*, 1941, **13**, 75.
[2] Sponer and Wollman, *J. Chem. Physics*, 1941, **9**, 816.
[3] Wollman, *ibid.*, 1946, **14**, 123.
[4] Sponer, Hall and Stallcup, *V. Henri Mem. Vol.* (Liège, 1948), p. 211.
[5] Sponer, *Chem. Rev.*, 1947, **41**, 281.
[6] Masaki, *Bull. Chem. Soc. Jap.*, 1936, **11**, 346.
[7] Matson, Ginsburg and Robertson, *J. Chem. Physics*, 1945, **13**, 309.
[8] Savard, *Ann. Chim.*, 1929, **11**, 287.
[9] Thompson and Temple, *J. Chem. Soc.*, 1948, 1432.

The latter varied from 0·1 mm to 20 mm. An iron arc was superposed for wavelength calibration, and most of the bands were measured from two or more plates taken at different pressures.

The compounds were supplied by Imperial Chemical Industries Ltd. (General Chemicals Division), and were re-distilled before use. The boiling points were as follows: benzotrifluoride 102·5° C, *p*-fluorobenzotrifluoride 105° C, *m*-fluorobenzotrifluoride, 100·5° C, *p*-fluorotoluene 116·5° C, *m*-fluorotoluene 115·5° C, *o*-fluorotoluene 114·5° C. Freedom from small traces of the corresponding isomers was established, where relevant, by the infra-red spectrum.

Benzotrifluoride.[*]—The system of bands extends from about 2700 Å to 2400 Å. Most of the bands degrade to the red, i.e., have a sharp edge on the higher frequency side; others are broader and more diffuse. For uniformity the centre of each band has been measured. At the lowest pressures used there were still strong absorption bands, the lowest frequency of which was 37822 cm.$^{-1}$.

The positions of the bands are given in Table I, and part of the spectrum is shown in Plate I. In Fig. 1 the arrangement of bands is depicted in order to clarify the interpretations given, but although the significant variations of intensity are brought out in this diagram; the intensities shown are not meant to be quantitative.

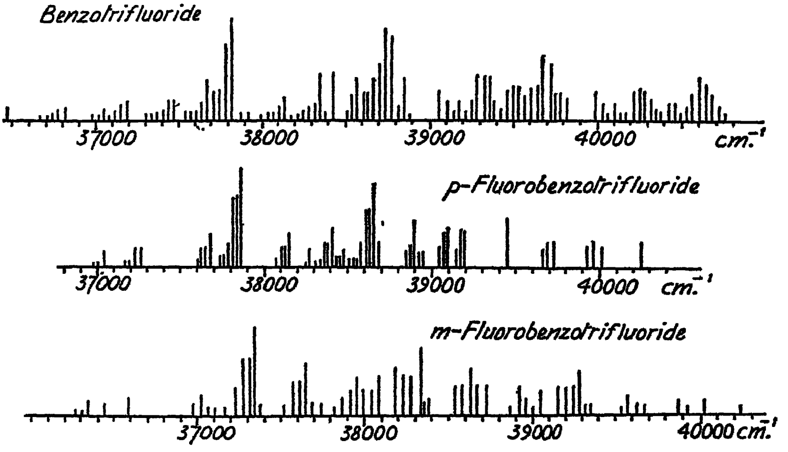

FIG. 1.

The molecule can be regarded to a first approximation as belonging to the symmetry group C_{2v}, and the electronic transition will be A_1-B_1, with a transition moment in the plane of the ring and perpendicular to the C—(CF$_3$) bond. It represents an "allowed" transition, and the o—o band can be confidently fixed at 37822 cm.$^{-1}$. Table I gives an interpretation of most of the bands in terms of vibrational levels in the upper (ω') and lower (ω'') states. A satisfactory explanation of nearly all the bands, which is plausibly consistent with the intensities, is obtained using the following values:

ω'	315,	539,	598,	750,	927,	961,	1035 cm.$^{-1}$
ω''	142,	337,	623,	660,	767,	1006 cm.$^{-1}$.	

Values found by Pendl and Radinger[10] for the Raman intervals are 139 (7), 339 (5), 396 (1/2), 618 (3), 656 (1/2), 771 (8), 839 (0), 1005 (2), 1027 (4).

There is, therefore, close agreement between the strong Raman intervals and the values of ω'' obtained from the ultra-violet spectrum. We might expect these strong Raman intervals to be associated with the symmetrical vibrations, although no measurements of the depolarization factors have been made. The appearances of the bands suggest that 337 (ω'') may correspond to 315 (ω'),

---

[*] During this Discussion we learnt that this substance had recently been examined by Sponer and Lowe (*J. Opt. Sci.*, 1949, **39**, 840). Our results agree closely with those given there.

[10] Pendl and Radinger, 1939.

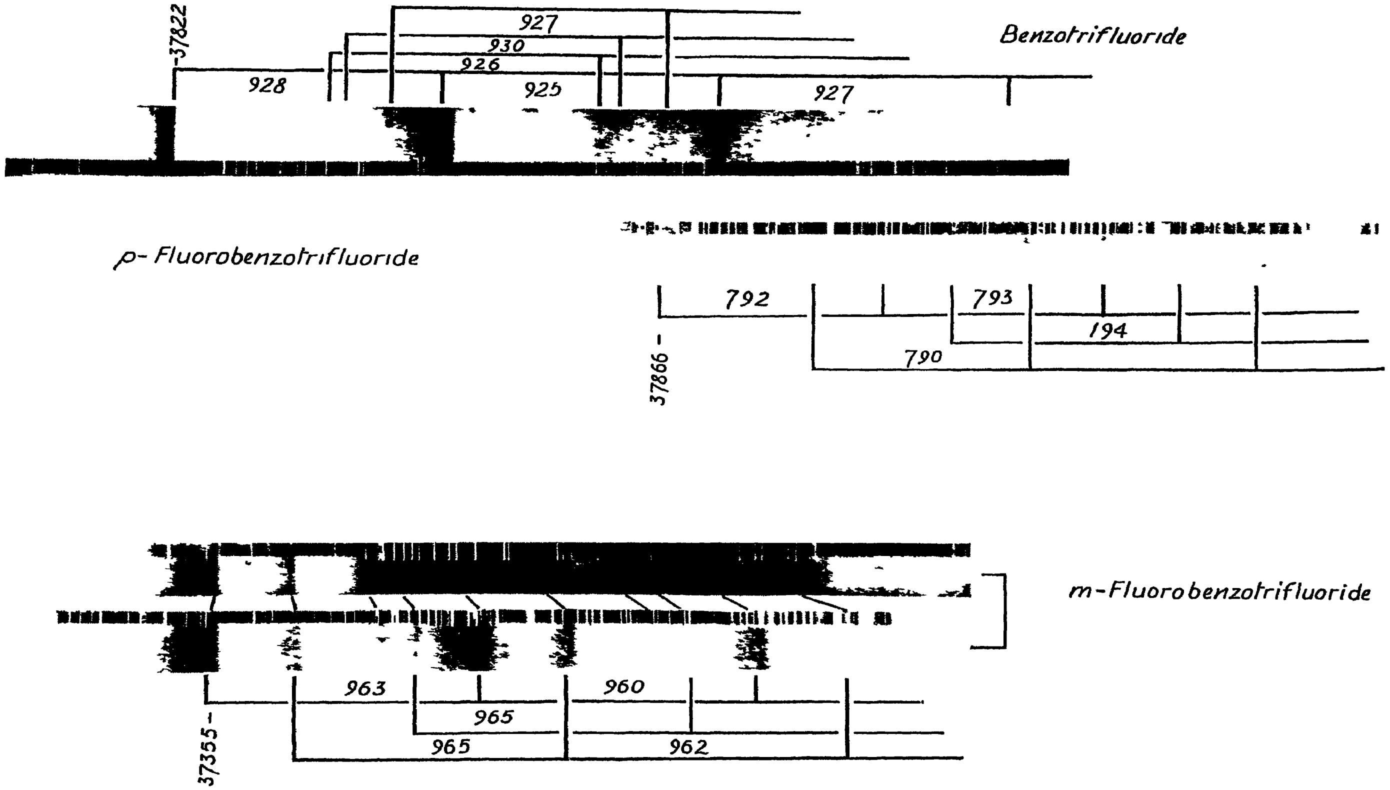

PLATE I.

[To face page 26

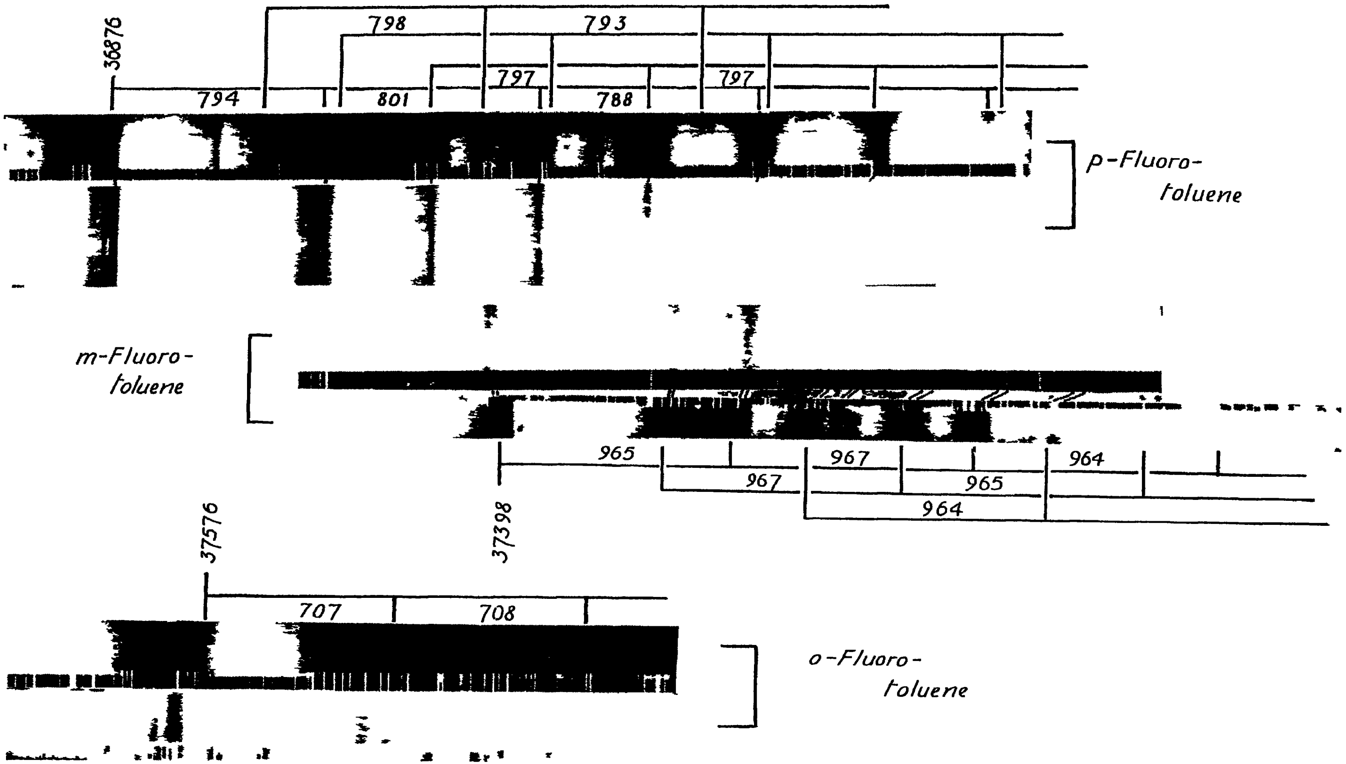
36876
798
793
794
801
797
788
797
p-Fluoro-toluene
m-Fluoro-toluene
965
967
967
965
964
964
37398
37576
707
708
o-Fluoro-toluene

PLATE II

and 1006 (ω'') to 927 (ω'). This last value of 927 cm $^{-1}$ is the strongest recurring interval in the excited electronic state and leads to a well-marked progression and this vibration involves a symmetrical breathing mode of the carbon ring skeleton It is also likely that the three ground state frequencies 623, 660 and 767 cm $^{-1}$ correspond to 539, 598, and 750 cm.$^{-1}$ in the upper electronic level

TABLE I —BENZOTRIFLUORIDE

ν(cm $^{-1}$)	Interpretation	ν(cm.$^{-1}$)	Interpretation
36487	*e*−1006−337	750	*e*+927
670	*e*−1006−142	782	*e*+960
706	*e*−1006−75−36	818	*e*+1035−36
741	*e*−1006−75	858	*e*+1035
778	*e*−1006−36	38892	—
816	*e*−1006	39067	*e*+927+315
36980	*e*−767−75	102	*e*+1035+315−75
37020	*e*−767−36	139	*e*+1035+315−36
055	*e*−767	175	*e*+1035+315 *e*+750+598 *e*+927+539−75−36
092	*e*−623−75−36	211	*e*+927+539−75
126	*e*−660−36 *e*−623−75	250	*e*+927+539−36
162	*e*−623−36 *e*−660)	287	*e*+927+539
199	*e*−623	39319	*e*+960+539
305	*e*−337−142−36	350	*e*+927+598
340	*e*−337−142	389	*e*+960+598
375	*e*−337−75−36	424	*e*+927+750−75
413	*e*−337−75	463	*e*+960+750−75 *e*+927+750−36
447	*e*−337−36	500	*e*+927+750
485	*e*−337	535	*e*+960+750
540	*e*−(2×142)	569	*e*+927+960−142
571	*e*−142−75−36	604	*e*+(2×927)−75) *e*+(2×960)−142
605	*e*−142−75	640	*e*+927+960−75 *e*+(2×927)−36
644	*e*−142−36	675	*e*+(2×927)
680	*e*−142	712	*e*+927+960
711	*e*−75−36	746	*e*+(2×960)
745	*e*−75	783	*e*+927+1035
782	*e*−36	819	*e*+960+1035
37822	*e*	39996	*e*+(2×927)+315
37867	—	40031	—
904	—	065	*e*+(2×927)+539−142
37998	*e*+315−142	101	*e*+(2×927)+539−75−36
38030	*e*+315−75−36	139	*e*+(2×927)+539−75
064	*e*+315−75	176	*e*+(2×927)+539−36
101	*e*+315−36	212	*e*+(2×927)+539
137	*e*+315	246	*e*+927+960+539
185	*e*+539−142−36	280	*e*+(2×927)+598 *e*+(2×960)+539
218	*e*+539−142	316	*e*+960+927+598
251	*e*+539−75−36	355	*e*+(2×927)+750−75
286	*e*+539−75	389	*e*+(2×927)+750−36
323	*e*+539−36	426	*e*+(2×927)+750
361	*e*+539	462	*e*+927+960+750
385	*e*+598−36	499	—
420	*e*+598	533	*e*+(3×927)−75
502	*e*+750−75	568	*e*+(3×927)−36
536	*e*+750−36	602	*e*+(3×927)
573	*e*+750	638	*e*+(2×927)+960
611	*e*+927−142	672	*e*+927+(2×960)
644	*e*+960−142 *e*+927−75−36	708	*e*+(3×960)
676	*e*+960−75−36 *e*+927−75	40744	—
711	*e*+927−36 *e*+960−75		

The small differences 36 cm.$^{-1}$ and 75 cm.$^{-1}$ are less easy to explain. They may arise from $v \rightarrow v$ transitions, but both on grounds of relative intensity and also from a consideration of the frequency scheme as a whole this does not seem satisfactory. They always arise in the interpretation of bands lying just to the longer wavelength side of the main transitions, as if to correspond to low vibration frequencies in the ground state. This matter might be further elucidated by studying the effect of temperature on the relative intensities of the bands. The calculated positions of the bands given in Table I usually agree with the measured values within a few cm.$^{-1}$, which is as close as might be expected in view of the diffuse nature of many bands.

***p*-Fluorobenzotrifluoride.**—The band system extends from about 2700 Å to 2400 Å. At longer wavelengths the bands clearly degrade to the red, but below 2600 Å they become diffuse, making it difficult to fix their positions very precisely. The measured positions are given in Table II, and the spectrum is depicted in Plate I and Fig. 1. As with benzotrifluoride, the symmetry class must be approximately C_{2v}, leading to an " allowed " transition A_1—B_1. The O—O band lies at 37866 cm.$^{-1}$, and although in this case some bands cannot be interpreted unambiguously, several definite vibrational intervals can be seen Plausible values which give a good fit for the important bands are :

TABLE II.—*p*-FLUOROBENZOTRIFLUORIDE

ν(cm.$^{-1}$)	Interpretation	ν(cm.$^{-1}$)	Interpretation
36890	$e-837-50$	449	—
37003	$e-837-25$	38475	—
029	$e-837$	508	—
173	$e-642-50$	532	—
199	$e-642-25$	552	—
224	$e-642$	583	$e+792-75$
270	$e-596$	609	$e+792-50$
608	$e-185-75$	633	$e+792-25$
631	$e-185-50$	658	$e+792$
657	$e-185-25$	693	$e+538+283$
681	$e-185$	852	—
746	—	876	—
768	—	896	$e+1030$
791	$e-75$	917	—
816	$e-50$	38939	$e+(2\times538)$
841	$e-25$	39051	—
37866	e	076	—
		097	$e+1231$
38068	$e+283-75$	148	—
104	$e+283-50$	172	$e+1030+283$
126	$e+283-25$	194	$e+792+538$
149	$e+283$	451	$e+(2\times792)$
261	—	659	—
282	$e+416$	690	$e+1030+792$
310	—	729	$\left\{\begin{array}{l}(e+(2\times792)+283),\\(e+792+(2\times538)\end{array}\right.$
331	$e+538-75$	925	$e+(2\times1030)$
358	$e+538-50$	39967	$e+792+1030+283$
381	$e+538-25$	40003	$e+(2\times792)+538$
404	$e+538$	247	$e+(3\times792)$
424	—		

ω' 283, 416, 538, 792, 1030, 1231 cm.$^{-1}$.
ω'' 185, 596, 642, 837 cm.$^{-1}$.

The marked progression is associated with the interval 792 in the excited electronic state. Raman data are not available for comparison with these results.

With this compound, too, there are satellite bands lying 25, 50 and 75 cm.$^{-1}$ to the lower frequency side of the main bands. These may arise from $v \rightarrow v$ transitions, but this interpretation seems improbable.

There is a close parallelism between the spectra of *p*-fluorobenzotrifluoride and *p*-cresol, measured by Savard[8] A fresh analysis of Savard's results suggests that for *p*-cresol, frequencies in the excited state are 419, 808 and 1187 cm.$^{-1}$ and probably also 210 and 1268 cm.$^{-1}$.

***m*-Fluorobenzotrifluoride.** — The band system extends from about 2750 Å to 2480 Å. It is shown in Plate I, and diagrammatically in Fig. 1, and the positions of the bands are given in Table III. At the longer wavelengths the bands degrade to the red, but at higher frequencies they become diffuse. The strong band at 37355 cm.$^{-1}$ is taken as the 0—0 transition.

The most striking progression in the excited state is associated with a vibration interval of 963 cm.$^{-1}$, and another prominent interval is 298 cm.$^{-1}$. Satisfactory explanation of the main bands can be achieved by assuming the following values :

$$\omega' \quad 298,\ 730,\ 843,\ 963 \text{ cm.}^{-1}.$$
$$\omega'' \quad 326,\ 756,\ 911,\ 1009 \text{ cm.}^{-1}.$$

At the shorter wavelength side of the main bands of the leading progression there occur two bands lying about 40 and 80 cm.$^{-1}$ from the main band. Here again, an interpretation in terms of $v \rightarrow v$ transitions, though possible, does not seem to agree with the observed intensities. Another interval of about 125 cm.$^{-1}$ may be a frequency in the ground state, though this may be the combination (40 + 80).

TABLE III.—FLUOROBENZOTRIFLUORIDE

ν(cm.$^{-1}$)	Interpretation	ν(cm.$^{-1}$)	Interpretation
36270	$e-1009-80$	237	$e+963-80$
307	$e-1009-40$	38279	$e+963-40$
346	$e-1009$	318	$e+963$
444	$e-911$	350	—
599	$e-756$	388	$e+963+730-(2\times326)$
36989	$e-326-40$	535	$e+963+298-80$
37029	$e-326$	574	$e+963+298-40$
067	$e-(2\times125)-40$	618	$e+963+298$
103	$e-(2\times125)$	668	—
176	—	718	$e+963+730-326$
230	$e-125$	878	$e+963+(2\times298)-40$
277	$e-80$	915	$e+963+(2\times298)$
314	$e-40$	38964	$e+963+730-80$
37355	e	39005	$e+963+730-40$
37380	—	046	$e+963+730$
518	—	163	$e+963+843$
577	$e+298-80$	203	$e+(2\times963)-80$
615	$e+298-40$	240	$e+(2\times963)-40$
653	$e+298$	278	$e+(2\times963)$
699	—	312	$(e+963+730+398-40)$
749	—	347	$(e+963+730+298)$
824	$e+(2\times298)-125$	544	$(e+(2\times963)+298-40)$
877	$e+(2\times298)-80$	580	$(e+(2\times963)+298)$
916	$e+(2\times298)-40$	627	—
37952	$e+(2\times298)$	680	$(e+(2\times963)+730-326)$
38000	$e+730-80$	874	$(e+(2\times963)+(2\times298))$
046	$e+730-40$	39928	—
085	$e+730$	40014	$e+(2\times963)+730$
198	$e+843$	242	$e+(3\times963)$

Raman data for comparison with the above are not available. However, a re-examination of Savard's results with *m*-cresol reveals similarity, and the latter suggests excited state intervals of 423, 693, 963, and 1199 cm.$^{-1}$.

***p*-Fluorotoluene.** — With this substance the variation in the absorption coefficient with wavelength is at times so rapid that many exposures at different pressures were required to obtain the full details of the spectrum, and using the higher pressures which are necessary to develop some of the weaker bands, the more intense bands become so broad as to produce serious overlapping which obscures other features.

The band system extends from 2800 Å to 2400 Å, and most bands appear to degrade to the red. It is shown in Plate II and depicted in Fig. 2, although it must be emphasized again that the intensities shown are not quantitative. Many of the bands occur in pairs, having the appearance of doublets, but the relative intensity of the component of such a pair is variable, and the doublet appearance may be accidental.

The symmetry class is C_{2v}, and the allowed transition gives a 0—0 band at 36876 cm.$^{-1}$. The positions of the observed bands are given in Table IV from which a few very weak bands have been omitted. The analysis is complicated in this case, not only by the larger number of bands, but also because of an ambiguity in the allocation of frequencies. Thus $(398 + 794) \approx 1194$, which might mean that the strong interval 1194 is not associated with a fundamental vibrational interval. However, it is certain that the most prominent progressions are associated with a vibration frequency in the excited state of 794 cm.$^{-1}$, and consideration of the intensities and combinations suggests that 1194 cm.$^{-1}$ is another strong frequency in the upper state. A good interpretation of all except a few weak bands has been obtained with the following values:

ω' 185, 398, 584, 794, 843, 1014, 1194, 1229
ω'' 217, 311, 337, 453, 641, 825, 844, 1156.

The Raman spectrum was measured by Kohlrausch[11] and by Paulsen[12] and the following intervals found:

311 (0), 342 (8), 455 (7), 501 (½) 642 (4), 698 (1), 728 (1)
824 (7), 843 (9), 995 (0), 1158 (3), 1213 (6*b*) 1294 (1), 1380 (3

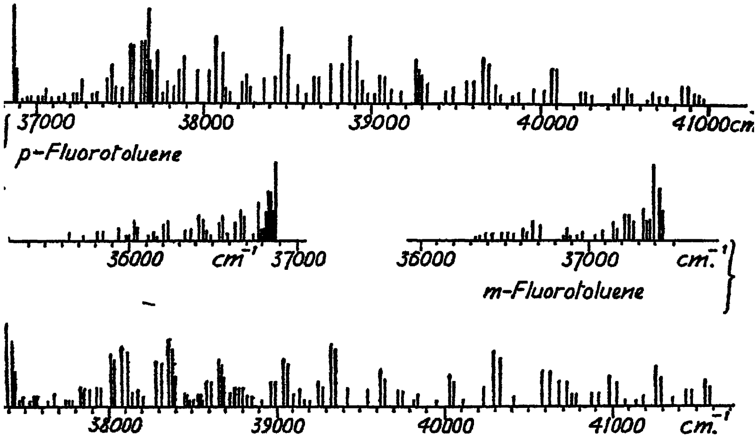

FIG. 2.

All the frequencies for the ground state (ω'') suggested by the present results agree with strong Raman intervals, except that there is no Raman interval corresponding to 217 and the Raman interval 311 is given as weak. As with the other compounds discussed above, there are groups of bands on the longer wavelength side of some of the main bands which cannot be explained convincingly. In the Table given, intervals of 40 and 96 cm.$^{-1}$ are used in this connection. These bands may be associated with $v \rightarrow v$ transitions, but there are at times peculiar splitting phenomena and the intensities are irregular.

There is a marked parallelism between the spectra of *p*-fluorotoluene and *p*-cresol. As stated above, a re-examination of Savard's data for the molecule gives the following frequencies in the excited state: 210, 419, 808, 1187 and 1268 cm.$^{-1}$.

***m*-Fluorotoluene.**—Part of the spectrum is shown in Plate II, and Fig. 2 depicts it diagrammatically. The band system lies between 2750 and 2400 Å. It differs from those discussed above in that most of the strong bands occur in pairs about 20-30 cm.$^{-1}$ apart, and with the longer wavelength component slightly the more intense. Also, at about 70 cm.$^{-1}$ to the lower frequency side

[11] Kohlrausch, *Sitzber Akad. Wien.*, 1933, **142**, 650.
[12] Paulsen, *ibid.*, 1938, **147**, 395.

TABLE IV.—*p*-FLUOROTOLUENE

ν(cm.$^{-1}$)	Interpretation
35636	
720	$e-1156$
810	$e-844-217$
844	$e-825-217$
940	$e-844-96$
35989 36000	$e-844-40$
032	$e-844$
051	$e-825$
109	$(e-453-311)$
140	$e-641-96$
103	
205	$(e-453-217)$, $(e-(2\times 337))$
235	$e-641$
333	$e-453-96$
377	$e-453-40$
423	$e-453$
450	$e-(2\times 217)$
468	$e-311-96$
497	$e-337-40$
539	$e-337$
565	$e-311$
595	
623	$e-217-40$
659	$e-217$
688	$e-(2\times 96)$
751	
780	$e-96$
797	
809	
821	
831 843	$e-40$
852	
36876	e
36888	
911	
938	
36966	$e+185-96$
37004	$e+584-453$
048	
061	$e+185$
097	
132	
175	$e+398-96$
218 231	$e+398-40$
274	$e+398$
334	$e+794-337$
358	$(e+584-96)$, $(e+794-311)$
425	$(e+584-40)$
460	$(e+584)$, $(e+398+185)$
480	
510	$e+843-217$
576 587	$e+794-96$
629 645	$e+794-40$
670 677 691	$e+794$ $e+(2\times 398)$

TABLE IV.—(*continued*)

ν(cm.$^{-1}$)	Interpretation
719	$e+843$
754	$e+1194-311$
793	$(e+1229-311)$, $(e+1014-96)$
821	$(e+584+398-40)$
850	$(e+1014-40)$, $(e+1194-217)$
890	$e+1014$
37973	$(e+1194-96)$, $(e+1014+398-311)$
38034	$(e+1194-40)$
070	$(e+1194)$, $(e+794+398)$
105	$(e+1229)$
123	$(e+(2\times 794)-357)$, $(e+843+398)$
159	$(e+(2\times 794)-311)$
222	$(e+794+584-40)$
258	$(e+794+584)$, $(e+1194+185)$
287	$(e+1014+398)$
372	$(e+(2\times 794)-96)$
425	$(e+(2\times 794)-40)$
471	$(e+(2\times 794))$, $(e+794+(2\times 398))$, $(e+1194+398)$
503	$(e+1229+398)$
564	$(e+(2\times 843))$
617	
654	$(e+1194+584)$
686	$(e+793+1014)$, $(e+1229+585)$, $(e+1014+(2\times 398))$
771	$(e+794+1194-96)$
820	$(e+794+1194-40)$
867	$(e+794+1194)$, $(e+(2\times 794)+398)$, $(e+1194+(2\times 398))$
905	$(e+794+1229)$, $(e+(2\times 1014))$, $(e+1229+(2\times 398))$
946	$(e+1229+843)$
38983	
39017	
040	
051	$(e+(2\times 794)\times 584)$
081	$(e+1194+1014)$
116	$(e+1229+1014)$
184	
259	$(e+(2\times 794))$, $(e+(2\times 1194))$
280	$(e+1229+(2\times 584))$
298	$(e+1194+1229)$, $(e+1229+(3\times 398))$
328	$(e+(2\times 1229))$
448	$(e+794+1194+584)$
39487	$(e+794+1229+584)$
569	
604	
664	$(e+(2\times 794)+1194)$, $(e+(2\times 1194)+398)$
697	$(e+(2\times 794)+1229)$
728	
758	$(e+1194+(2\times 843))$
834	
875	$(e+794+1194+1014)$
39965	
40019	
061	$(e+(4\times 794))$, $(e+(2\times 1194)+794)$
096	$(e+1194+(2\times 1014))$, $(e+(3\times 794)+843)$
244	$(e+(4\times 843))$
274	$(e+(3\times 794)+1014)$
309	
443	$(e+(3\times 794)+1194)$
478	$(e+(3\times 794)+1229)$
522	$(e+(2\times 1229)+1194)$
543	
642	
676	$(e+(2\times 794)+1194+1014)$

TABLE IV.—(*continued*)

ν(cm.$^{-1}$)	Interpretation
712	$(e+(2\times 794)+1229+1014)$
756	$(e+794+1229+1014+843)$
852	$(e+(5\times 794))$, $(e+(2\times 1194)+(2\times 794))$
892	$(e+(4\times 794)+843)$
923	
947	
40985	
41024	
061	$(e+(4\times 794)+1014)$
147	
197	
236	$(e+(4\times 794)+1194)$
41290	$(e+(4\times 794)+1229)$
319	
459	
494	
633	$(e+(6\times 794))$
41672	

of each main pair, there is another similar pair of somewhat lower intensity. The significance of this interval of 70 cm.$^{-1}$ is not clear, since it does not apparently produce other similar bands at 2 × 70 cm.$^{-1}$ below the main bands, certainly not of the intensity which might be expected from consideration of the Boltzmann factor. In Table V the bands have been grouped in pairs where relevant, the first member being underlined and taken as the main band location. The 0—0 band lies at 37398 cm.$^{-1}$.

The strongest interval is 965, which produces marked progressions, and represents an excited state frequency. A similar strong interval is 684 cm.$^{-1}$, and other less certain values for fundamental frequencies in the excited electronic state are 1262, 282, 457 cm.$^{-1}$. The last of these values is in some doubt, but helps to explain several combinations.

From the bands to the longer wavelength side of 37398 cm.$^{-1}$, values of

TABLE V.—FLUOROTOLUENE

ν(cm.$^{-1}$)	Interpretation
36334	
359	$e-(2\times 520)$
395, 423	$e-3003$
486, 517	$e-726-184$
552	
606, 631	$(e-726-70)$, $(e-(3\times 253))$ $(e-520-253)$ $(e-520-184-70)$
672, 703	$e-726$
752	? $(e-(3\times 184))$
878	$e-520$
889	$(e-(2\times 253))$ $(e-(2\times 184)-(2\times 70))$
925	
36964	$(e-253-184)$
37033	$(e-(2\times 184))$
37087	$(e-311)$
145, 176	$(e-184-70)$ $(e-253)$
214, 243	$(e-184)$
273	
37325, 346, 368	$e-70$
37398, 418, 431	e

TABLE V—(*continued*)

ν(cm.$^{-1}$)	Interpretation
486, 494	$(e+694—520—70)$
535	
558, 573	$(e+684-520)$
631	$(e+965-726)$
680	$(e+282)$
751, 763, 792	$(e+684-253-70)$
828	$(e+684-253)$
855, 892	$(e+965-(2\times253))$, $(e+457)$
924, 955	$(e+965-253-184)$
38010, 032	$(e+684-70)$
38082, 108	$(e+684)$, $(e+965-253)$
140	
179, 208	$(e+965-184)$
295, 318	$(e+965-70)$
363, 381, 393	$(e+965)$, $(e+684+282)$
462, 475	
495, 510	
529, 541	
555	
595, 613	$(e+1261-70)$
659, 677, 685	$(e+1261)$
734, 752	
783, 800	
828, 858	$(e+(2\times965)-(2\times253))$
913	
981, 998	$(e+965+684-70)$
39049, 071	$(e+965+684)$
104, 141	$(e+965+1261-520)$
172, 201	
263, 284	$(e+(2\times965)-70)$
39330, 358	$(e+(2\times965))$
420	
554	$(e+965+1261-70)$
623, 650	$(e+965+1261)$
718, 747	$(e+965+(2\times684))$
821, 846	$(e+(2\times965)+684-184)$
39968	
40014, 041	$(e+(2\times965)+684)$
106	$(e+(3\times965)-184)$
234	$(e+(3\times965)-70)$?
294, 327	$(e+(3\times965))$
406	
589, 618	$(e+(2\times965)+1261)$
688, 713	$(e+(2\times965)+(2\times684))$
	$(e+(3\times965)+457-70)$
751, 780	$(e+3\times965)+457)$
40877, 910	$(e+965+(2\times1262))$
	$(e+(3\times965)+684-70)$
40979, 1008	$(e+(3\times965)+684)$
41081	$(e+(4\times965)-184)$
41149	$(e+(2\times965)+(2\times684)+457)$
41193	$(e+(4\times965)-70)$
41263, 291	$(e+(4\times965))$
41365	$(e+(3\times965)+1262-184)$
41437, 471	$(e+(3\times965)+684+457)$
41551, 582	$(e\quad 3\times965)+126$

520, 726 and 1003 cm.$^{-1}$ are obtained for ground state frequencies, and other likely values are 311, 184 and 253 cm.$^{-1}$. The Raman spectrum measured by Kohlrausch[11] gave the following intervals: 209 (4), 243 (8), 298 (2), 444 (00), 512 (4), 527 (6), 552 (2), 728 (10), 775 (½), 852 (00), 1003 (12), 1078 (3), 1152 (1*b*), 1254 (3), 1266 (5), 1379 (3). The strongest Raman intervals 243, 728, 1003 are therefore matched by the values found at 253, 520, 726, 1003 cm.$^{-1}$.

As already stated, a fresh analysis of the results of Savard for *m*-cresol gave as excited state frequencies 423, 693, 963, and 1199, which are closely parallel to those just given for *m*-fluorotoluene.

***o*-Fluorotoluene.**—Part of the spectrum is shown in Plate II. Bands are found between 2750 and 2500 Å, but the arrangement is much more complicated than with the other isomers. There is a marked similarity in the grouping of bands with that shown by Savard in the spectrum of *o*-cresol. It has been impossible to obtain a convincing analysis of the band system, but several points may be noted. There is some ambiguity about the choice of the o—o transition. It almost certainly occurs at 37576 cm.$^{-1}$, but just to the lower frequency side of this position there are several intense bands and a broad strong absorption region occurs 60-100 cm.$^{-1}$ below 37576 cm.$^{-1}$ which might be associated with the o—o transition. This broad absorption occurs similarly at 38200 cm.$^{-1}$ just below the band at 38283 cm.$^{-1}$, but at higher frequencies it appears to split, and the broad nature may in fact arise from overlapping bands. Whatever the exact position of the o—o transition may be, it is certain that the most marked interval leading to a progression is 707 cm.$^{-1}$, a vibration frequency in the excited state. Three members of this progression lie at 37576, 38283, and 38991 cm.$^{-1}$. Another marked interval is 924 cm.$^{-1}$, and a third may be 1230 cm.$^{-1}$. Combinations of these three intervals, corresponding to excited state vibrations, serve to explain many of the observed bands. From the bands at the lower frequency side of the o—o transition, prominent intervals 274 and 749 cm.$^{-1}$ can be derived, which correspond to strong Raman frequencies (Kohlrausch) of 274 and 747.

Discussion

Along the series *o*-, *m*-, *p*- for cresols or fluorotoluenes, the position of the o—o transition moves towards lower frequencies. With *p*-fluorobenzotrifluoride, however, this regularity breaks down, and the alteration in electronic structure which must lead to this is a matter worth further theoretical consideration. Moreover, there are also some striking variations in the absorption coefficients, which have been given elsewhere (Thompson and Miller [13]).

TABLE VI

Benzene	—	923	—	—	—
Phenol	783	—	935	—	—
Toluene	—	—	932	—	964
Benzotrifluoride	—	—	927	—	960
Chlorobenzene	—	—	931	—	965
Flurobenzene	—	—	915	—	966
p-Cresol	—	—	—	808	—
p-Fluorotoluene	—	—	—	794	—
p-Fluorobenzotrifluoride	—	—	—	792	—
m-Cresol	—	—	—	—	963
m-Fluorotoluene	—	—	—	—	965
m-Fluorobenzotrifluoride	—	—	—	—	963
o-Cresol	—	—	—	704	—
o-Fluorotoluene	—	—	—	707	—

Another interesting feature is noticed by comparison of the values of the most marked interval found in the progressions. Table VI gives the values for the above and related molecules. The values for chlorobenzene and fluorobenzene have been taken from the work of Sponer and

---

[13] Thompson and Miller, *J. Chem. Physics*, 1949 **17**, 845.

Wollmann [2] and Wollman,[3] and those of toluene and phenol from Ginsberg, Robertson and Matson.[14] The excited state frequency 923 for benzene is associated with a totally symmetrical carbon ring vibration. Removal of the hexagonal symmetry causes this vibration to split into a set, of which several components have been detected in the spectra of some of the compounds given in Table VI. It seems significant, however, that the value of the strongest interval is characteristic of the type of substitution in the aromatic ring. Thus the *p*-disubstituted benzenes have an interval close to 800 cm.$^{-1}$; *m*-disubstituted compounds near 965 cm.$^{-1}$, and *o*-disubstituted derivatives near 705 cm.$^{-1}$. Monosubstituted benzenes usually show more than one very marked progression interval, but examination of all the data shows that the interval near 925 cm.$^{-1}$ is dominant. Indeed, the interval found near 965 cm.$^{-1}$ is variable in intensity. Its entire absence from the spectrum of phenol, where a lower frequency (783 cm.$^{-1}$) appears is anomalous.

This regularity in the value of the interval in the main progressions may provide a useful diagnostic criterion for the structural type, and suggests an interesting problem for theoretical consideration by the methods of analytical dynamics, similar to that discussed by Bell, Thompson and Vago,[15] for other characteristic vibrations of substituted aromatic compounds.

We are grateful to the Rhodes Trustees for a scholarship to one of us (W. T. C.).

The Physical Chemistry Laboratory,
Oxford.

---

[14] Ginsburg, Robertson and Matson, *J. Chem , Physics*, 1946, **14**, 511.
[15] Bell, Thompson and Vago, *Proc. Roy. Soc. A*, 1948, **192**, 498.

NATURAL HYPSOCHROMIC SHIFTS

BY MME. ALBERTE PULLMAN AND BERNARD PULLMAN

Received 12th October, 1950

The name of ***natural*** hypsochromic shifts is being given to hypsochromic shifts of the longest wavelength of absorption which are being produced by electronic factors alone and are thus independent of steric interference with coplanarity. These natural hypsochromic shifts may be brought about in the same way as the natural bathochromic ones by appropriately choosing the basic molecular skeleton. They may be produced by increasing the size of a conjugated system, by alkylation, by dehydrogenation of a partially saturated system, by replacement of a double bond by a triple one and by internal strain. Numerous examples are quoted and it is shown that simple molecular orbital calculations account satisfactorily for the observed facts.

The name of ***natural*** hypsochromic shift is here given to hypsochromic shifts of the longest wavelength of absorption which are brought about by electronic factors alone and the existence of which are thus completely independent of steric factors. In fact it is generally admitted that, in the absence of steric interference with coplanarity, electronic interaction which follow, say, the increase in size of a conjugated system, alkyl substitution of such a system, dehydrogenation of a partially saturated system, etc., always bring about a bathochromic displacement of the longest wavelength of absorption. It is the aim of this communication to show briefly that this conception is erroneous, to point out different cases of natural hypsochromic shifts and to show at the same time that simple molecular orbital calculations, carried out with the usual approximation of the linear combination of atomic orbitals, are able to account very well for the existence of this phenomenon. It has recently been shown by different people, some of whom are present here, that these approximations are insufficient in more detailed studies.[1] Nevertheless, they seem to account for the *major features* of the spectra of conjugated compounds [2] and it is interesting to note that they account for the existence of natural hypsochromic shifts as well as they do for the existence of the more usual bathochromic ones. This is undoubtedly a pleasant state of affairs as it is rather difficult as yet to carry out more complete calculations for large organic molecules. The point to note is that though the importance of these calculations must not be overestimated, neither should they be underestimated. No details of these calculations are given here; they may be found in the references quoted. The transition energies are expressed in terms of the exchange integral γ in calculations in which the overlap integral has been included, and also in terms of the exchange integral β in calculations in which it has been neglected. American authors usually use these parameters in the reverse sense.

We shall now consider the principal ways in which natural hypsochromic shifts may be brought about.

Increase in Size of a Conjugated System.—(*a*) FULVALENES. The fact that the fulvalenes (I), (II) and (III) belong to a hypothetical group of compounds which have not been prepared does not diminish their theoretical importance. The energy of the $N \rightarrow V_1$ transition in these three molecules [3] is respectively $0{\cdot}296\gamma$, $0{\cdot}357\gamma$ and $0{\cdot}395\gamma$. Its increase with the lengthening of the central chain of conjugated double bonds indicates that there should be a parallel progressive hypsochromic shift of their longest wavelength of absorption. The same thing should happen in the corresponding series of heptafulvalenes (IV), (V) and (VI) for which the $N \rightarrow V_1$ transition is equal respectively[4] to $0{\cdot}263\gamma$, $0{\cdot}300\gamma$, $0{\cdot}325\gamma$. These results are significant as they show that the series of diphenylpolyenes, represented by (VII), which exhibits a bathochromic shift of its longest

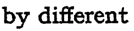

(I)

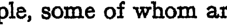

(II)

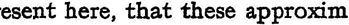

(III)

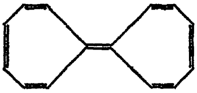

(IV)

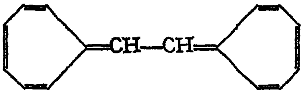

(V)

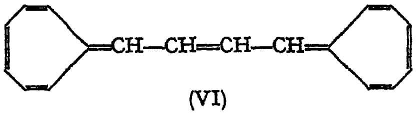

(VI)

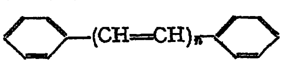

(VII)

---

[1] See e.g. Sponer and Nordheim, *ONR Contract N6ori-107, T.O.I. Report*; Craig, *J. Chem. Physics*, 1949, **17**, 1358; *Proc. Roy. Soc. A*, 1950, **200**, 474; Jacobs, *Proc. Physic. Soc.*, 1949, **62**, 710; Coulson and Longuet-Higgins, *Phil. Mag.*, 1949, **40**, 1172.

[2] See e.g. Klevens and Platt, *J. Chem. Physics*, 1949, **17**, 470; Platt, *J. Chem. Physics*, 1949, **17**, 484; Platt, *ONR Contract N6ori-20, T.O. IX Report*. See also Pullman and Pullman, *J. Chim. Phys.*, 1949, **46**, 212.

[3] Pullman and Berthier, *Compt. rend.*, 1949, **229**, 717.

[4] Mayot and Pullman (in preparation).

wavelength of absorption with the lengthening of the conjugated chain of double bonds, should not be considered, as it generally is, as a typical example of a general rule.

Though the fulvalenes (I), (II) and (III) are unknown, yet their benzenoid homologues, dibiphenylene ethylene (VIII), dibiphenylene butadiene (IX) and dibiphenylene hexatriene (X) are known. Calculations show[5] that, contrary to what happens in the hypothetical compounds (I), (II) and (III), the $N \rightarrow V_1$ transition energy decreases steadily in the series (VIII), (IX), (X) (viz. 0·620γ, 0·515γ and 0·410γ). These compounds should thus show a bathochromic shift of λ_{max} with the lengthening of the chain. In reality we observe a hypsochromic shift on going from (VIII) (λ_{max}, 460 mμ) to (IX) (λ_{max}, 446 mμ) and a bathochromic one on passing from (IX) to (X) (λ_{max}, 555 mμ). It may thus be concluded that the hypsochromic shift is *not* in this case a natural one but is due to steric factors. Owing to the low bond order of its central double bond (0·673 in a hypothetical planar molecule) and to steric repulsion between the positions facing each other on the two sides of this bond, the molecule of dibiphenylene ethylene is partially twisted round the central linkage. This diminishes its $N \rightarrow V_1$ transition energy and makes it absorb at longer wavelength that it otherwise would. Actually it may be concluded from these and other data (dipole moment, diamagnetic susceptibility, reduction potential) that the angle between the two halves of the molecule is[5] approximately 60°.

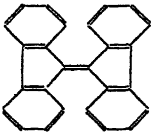
(VIII)

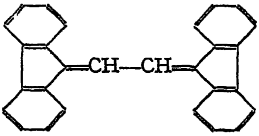

(IX)

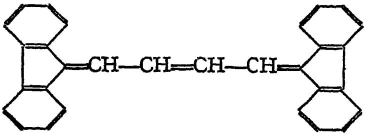

(X)

(*b*) FULVENES.—Though fulvene (XI), benzofulvene (XII) and dibenzofulvene (XIII) are isomers respectively of benzene, naphthalene and anthracene, it is well known that, contrary to what happens in this last group of molecules, there is a steady hypsochromic shift of their λ_{max} with increasing size of the molecule. This is in complete agreement with theory from which one evaluates the $N \rightarrow V_1$ transition as equal to 0·860γ in (XI), 0·881γ in (XII), and 1·081γ in (XIII).[6] Recently the spectra of these compounds have been accurately measured[7] and some more detailed theoretical studies carried out.[8]

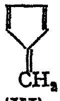

(XI)

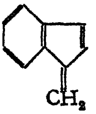

(XII)

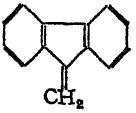

(XIII)

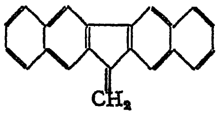

(XIV)

An interesting point concerns the dinaphthofulvene (XIV). Calculations show that this compound, which as yet has not been prepared, should show a bathochromic shift with respect to (XIII). This probably represents a general case: in all the series of molecules mentioned here, the natural hypsochromic shift should probably be limited to the first three or four members of the series and should be replaced afterwards by a bathochromic one. The reason for this lies generally in a crossing-over of molecular orbitals.[9] The preparation and experimental investigation of (XIV) is being undertaken.

---

[5] Bergmann, Berthier, Pullman and Pullman, *Bull. Soc. Chim.* (in press).
[6] Pullman, Pullman and Rumpf, *Bull. Soc. Chim.*, 1948, **15**, 757.
[7] Bergmann and Hirschberg, *Bull. Soc. Chim.* (in press).
[8] Pullman, Berthier and Pullman, *Bull. Soc. Chim.* (in press).

A parallel natural hypsochromic shift should also occur in the series of the hypothetical heptafulvenes (XV), (XVI), and (XVII),[4] the $N \rightarrow V_1$ transition energy being equal to $0{\cdot}661\gamma$ in (XV) and to $0{\cdot}862\gamma$ in (XVII).

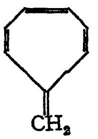

(XV)

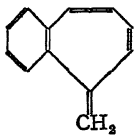

(XVI)

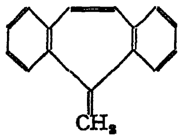

(XVII)

(*c*) QUINODIMETHANES.—In agreement with experiment, which shows a continuous hypsochromic displacement of the longest wavelength of absorption with increasing size of the resonating system in the series of tetraphenyl derivatives of *p*-benzoquinodimethane (XVIII) (orange), *p*-naphthoquinodimethane (XIX) (yellow) and *p*-anthraquinodimethane (XX) (colourless), the calculations show a parallel gradual increase of the $N \rightarrow V_1$ transition energy: this is equal to $0{\cdot}626\gamma$ in (XVIII), to $0{\cdot}726\gamma$ in (XIX) and to $0{\cdot}860\gamma$ in (XX).[10]

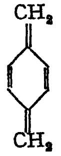

(XVIII)

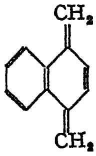

(XIX)

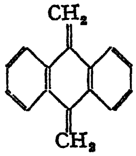

(XX)

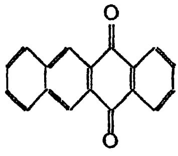

(XXI)

A similar development of colour is observed in the series of the corresponding quinones: the yellow colour of *p*-benzoquinone fades away when we pass to the *p*-naphtho- and *p*-anthraquinones. No exact calculations of energy levels have as yet been carried out for these compounds in which the longest absorption band is due to an $N \rightarrow A$ transition. An interesting point is that, in conformity with the observation made in connection with the hypothetical dinaphthofulvene, the hypsochromic shift seems to be limited to the quinones quoted, and is being replaced from naphthacenequinone (XXI) upwards by a steady deepening of the visible colour.

(*d*) BENZOAZULENES.—It has recently been shown by Plattner and co-workers,[11] that while the 1 : 2-benzazulene (XXII) shows the " normal " bathochromic shift of the longest wavelength of absorption with respect to azulene itself, the 5 : 6-isomer (XXIII) shows on the contrary an " unusual " hypsochromic shift.

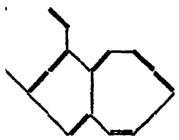

(XXII)

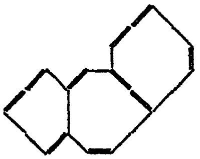

(XXIII)

This evidently is another case of a natural hypsochromic shift and calculations are being carried out in order to verify this assumption.

---

[9] Details will be given in a paper on naphthofulvenes, in preparation.

[10] Pullman, Berthier and Pullman, *Bull. Soc. Chim.*, 1949, **15**, 450.

[11] Plattner, Fürst and Keller, *Helv. chim. Acta*, 1949, **32**, 2464.

Alkylation.—Methyl substitution which is considered as leading always, in the absence of steric factors, to a bathochromic displacement of λ_{max} may in fact give rise as well to natural hypsochromic shifts. An example of this is given by some methylated derivatives of azulene (XXIV).[12]

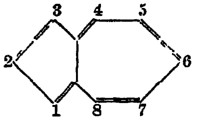

(XXIV)

While the 1- and 5-methylated derivatives show the usual bathochromic shift, the 2-, 4- and 6-methylated compounds manifest a hypsochromic shift. Calculations confirm the assumption that these are *natural* hypsochromic shifts: the $N \rightarrow V_1$ transition energy which is equal to 0·804 β in azulene itself, to 0·755β in the 1-methyl derivative and to 0·789β in the 5-methyl derivative is equal to 0·814β in the 2-methyl derivative, to 0·816β in the 4-methyl derivative and to 0·823β in the 6-methyl derivative.

The methylazulenes are the only known examples of natural hypsochromic shifts brought about by alkylation. Nevertheless it can be predicted that similar shifts should occur in compounds (XXV), XXVI), (XXVII). Experiments are being carried out in order to verify this prediction.

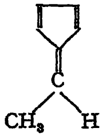

(XXV)

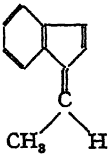

(XXVI)

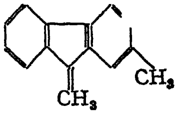

(XXVII)

It may be shown that, as a general rule, natural hypsochromic shifts can only occur, by alkylation, in conjugated compounds containing an odd membered ring. One could thus not expect these to occur in the usual benzenoid molecules. The only thing that may sometimes be observed in this last group of compounds is *the absence* of the expected bathochromic shift. The 1′-methyl-1 : 2-benzanthracene (XXVIII) seems

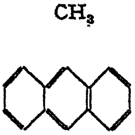

(XXVIII)

to be an example of such a case. This compound absorbs exactly at the same wavelength as the parent unsubstituted hydrocarbon.[13] It may be thought that this absence of the usual bathochromic shift is due to steric interference with the nearby *meso* position but in fact calculations show that the $N \rightarrow V_1$ transition energy of (XXVIII) has exactly the same value (0·916γ) as that of the parent 1 : 2-benzanthracene.[14] A normal bathochromic shift is predicted by calculation for all the remaining methyl derivatives of this compound. (XXVIII) thus represents a particular case of a *natural absence* of a bathochromic shift.

---

[12] For details see Pullman, Mayot and Berthier, *J. Chem. Physics*, 1950, **18**, 257.

[13] Jones, *Chem. Rev.*, 1943, **32**, 1.

[14] Pullman, Berthier and Pullman, *Acta Cancer.* (in press).

Dehydrogenation.—Partial hydrogenation of an unsaturated system generally leads to a hypsochromic displacement of the longest wavelength of absorption while the reverse is true for the dehydrogenation of a partially saturated system. That this is not always the case has recently been pointed out by Longuet-Higgins, Rector and Platt;[15] thus while tetrahydroporphyrine (XXIX) absorbs somewhere near 8000 Å, porphyrine itself (XXX) absorbs only up to 6300 Å. This is thus a special case of a *natural* hypsochromic shift produced by increasing the dimensions of a resonating system through dehydrogenation. The assumption is verified by explicit calculations which give the values of 0·380γ and 0·391γ for the $N \rightarrow V_1$ transition energy of (XXIX) and XXX) respectively.

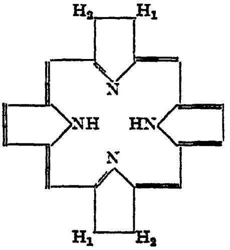

(XXIX)

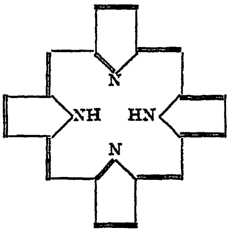

(XXX)

Replacement of a Double Bond by a Triple One.—Though the replacement of a double bond by a triple one increases the number of available mobile electrons the comparison of compounds such as styrene (XXXI) (λ_{max}, 282 mμ) and phenylacetylene (XXXII) (λ_{max}, 278 mμ) or stilbene (XXXIII) (λ_{max}, 295 mμ) and tolane (XXXIV) (λ_{max}, 279 mμ)

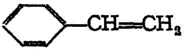

(XXXI)

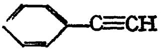

(XXXII)

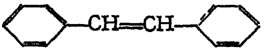

(XXXIII)

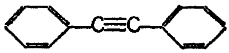

(XXXIV)

shows that it is generally accompanied by a hypsochromic shift of the longest wavelength of absorption. In (XXXII) and (XXXIV) only one of the two pairs of the π electrons of the triple bond conjugates in fact with the benzene nuclei. The hypsochromic shift observed has nevertheless to be considered as a *natural* one as it is due to electronic factors alone, namely to the greater localization of the π electrons of triple bond in comparison with the π electrons of a double bond. This conception which has recently been stressed by Moffitt and Coulson[16] and by Walsh[17] is substantiated by the values of the ionization and reduction potentials of similar ethylenic and acetylenic compounds.[18] Explicit calculations verify the natural character of the hypsochromic shift referred to as they indicate the following values for the $N \rightarrow V_1$ transition energy:[19] 1·589γ in (XXXI), 1·870γ in (XXXII), 1·237γ in (XXXIII) and 1·540γ in (XXXIV).

Internal Strain—There is a continuous hypsochromic displacement of the longest wavelength of absorption in the series cyclopropane

---

[15] Longuet-Higgins, Rector and Platt, *ONR Contract N6ori-20, T.O. IX. Report.*

[16] Moffitt and Coulson, *Phil. Mag.*, 1947, **38**, 634.

[17] Walsh, *Ann. Reports*, 1947, **44**, 32; *Quart. Rev.*, 1948, **2**, 73.

[18] Pullman, Berthier and Pullman, *Bull. Soc. Chim.*, 1950, **17**, 591.

[19] Berthier and Pullman, *Compt. rend.*, 1949, **228**, 397.

(XXXV) (λ_{max}, 1950 Å), cyclobutane (XXXVI), cyclopentane (XXXVII), cyclohexane (XXXVIII) (λ_{max}, 1500 Å). As all these compounds, with the exception of (XXXVIII), are planar this hypsochromic shift cannot be considered as due to steric factors in the usual sense associated with this expression but must be regarded as a natural one. In fact it is to be related to the existence of internal strain whose magnitude is decreasing with the increasing size of the molecule. Though no exact calculations of the distribution of molecular orbitals in any of these compounds have as yet been carried out, it has recently been shown [20] that the strain is associated with a bending of the C—C bonds, a deformation of the hybridization ratio at the C atoms and an appreciable electronic delocalization. These phenomena being the most pronounced in the most strained cycloparaffins it is possible to understand qualitatively the origin of this hypsochromic shift.

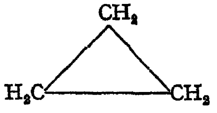
(XXXV)

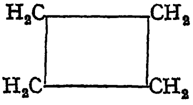
(XXXVI)

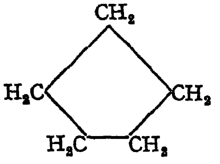
(XXXVII)

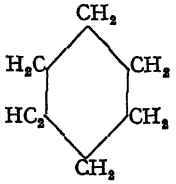
(XXXVIII)

Conclusion.—After this short review it seems to be clear that natural hypsochromic shifts have to be regarded as occurring, at least potentially, as frequently as the natural bathochromic ones. In fact, natural hypsochromic shifts can be produced just in the same way as natural bathochromic ones with an appropriate choice of the basic molecular skeleton. The examples of odd, five- or seven-membered rings show that the properties of the more usual six-membered rings are exceptional and should not be used as a basis for too wide a generalization. It may be noted that even in the group of compounds composed of six-membered rings there is a pronounced difference in the spectroscopic behaviour of the molecules usually represented by a Kekulé structure and those containing crossed-conjugated double bonds.

Institut du Radium,
11 rue Pierre Curie,
Paris 5e,
France.

---

[20] Coulson and Moffitt, *Phil. Mag.*, 1949, 40, 1; Walsh, *Trans. Faraday Soc.*, 1949, 45, 179.

THE ABSORPTION SPECTRA OF SOME SUBSTITUTED BENZENES AND NAPHTHALENES IN THE VACUUM ULTRA-VIOLET

By V. J. Hammond,* W. C. Price,* J. P. Teegan † and A. D. Walsh †

Received 14*th August*, 1950

Vacuum ultra-violet spectra and ionization potential data are given for the molecules, benzene, toluene, ethyl benzene, *iso*propyl benzene, *o*-, *m*-, *p*-xylenes, phenol, monofluorobenzene, benzotrifluoride, *o*-, *m*-, *p*-monofluorotoluene, *m*-fluorobenzotrifluoride, naphthalene and 2-methyl naphthalene. The effect of the nature and position of the substituting groups is discussed and is compared with the effect of solvents in solution spectra. The 2000 Å absorption region of benzene and its derivatives is interpreted as a Rydberg transition.

In order to understand the spectra of the substituted benzenes in the vacuum ultra-violet it is convenient to begin by describing the main features of the spectrum of benzene itself.[1, 2] The modifications in the spectrum resulting from the substitution can then be related to the nature of the attached groups.

The Spectrum of Benzene.—The far ultra-violet absorption spectrum of benzene falls into four main regions (Fig. 1*a*). The first of these consists of a diffuse region of absorption extending from 2070 to 1900 Å. This is followed by an extremely strong region of continuous absorption having a maximum at about 1790 Å. A third region between about 1650 and 1370 Å contains sharp bands which are Rydberg in type. The main bands form two Rydberg series converging to a limit representing the first ionization potential of benzene

$$(\chi_1^2\chi_{2,3}^4 \rightarrow \chi_1^2\chi_{2,3}^3) \text{ at } 9{\cdot}240 \pm 0{\cdot}005 \text{ V‡.}$$

$$\nu_0^n = 74{,}495 - R/(n - 1{\cdot}03)^2 \quad n = 3, 4, 5. \qquad (1)$$

$$\nu_0^n = 74{,}590 - R/(n - 0{\cdot}45)^5 \quad n = 3, 4, 5. \qquad (2)$$

The short vibrational progressions accompanying the main electronic transitions indicate that the electron comes from a weakly bonding orbital and there is no doubt that it is of a π type. It seems certain that the terms of series (1) are associated with *ns* atomic terms and those of series (2) with *np* terms and the quantum defects have been chosen so as to bring this out. In the original paper by Price and Wood, the $n = 3, 4$ terms of series (1) and the $n = 3$ of series (2) were not included in the series. The reasons for this are now fairly clear. Firstly, the $n = 3$ and $n = 4$ terms of series (1), because of the low value of n, have orbitals which are to a large extent still within the dimensions of the molecule. Secondly, because of their *s* character, these orbitals particularly penetrate the molecular framework. The first reason causes the frequencies to deviate appreciably from the Rydberg formula, which can only hold precisely for orbitals that are sufficiently large for the molecule to be considered as a point. The second causes the bands to become very diffuse as a result of internal collision of the excited electron with other electrons in various bonds of the molecule. Thus the $n = 4$ member

---

* Wheatstone Laboratory, King's College, London W.C.2.

† Chemistry Department, University of Leeds.

[1] Price and Wood, *J. Chem. Physics*, 1935, **3**, 439.

[2] Price and Walsh, *Proc. Roy. Soc. A*, 1947, **191**, 22.

‡ Original value of 9·190 V corrected for new value of electronic charge.

of series (1) is to be associated with a set of diffuse bands in the neighbourhood of 61350 cm.$^{-1}$ (1630 Å) in spite of the fact that the calculated series value is 62056 cm.$^{-1}$. The $n = 3$ member is to be identified with the

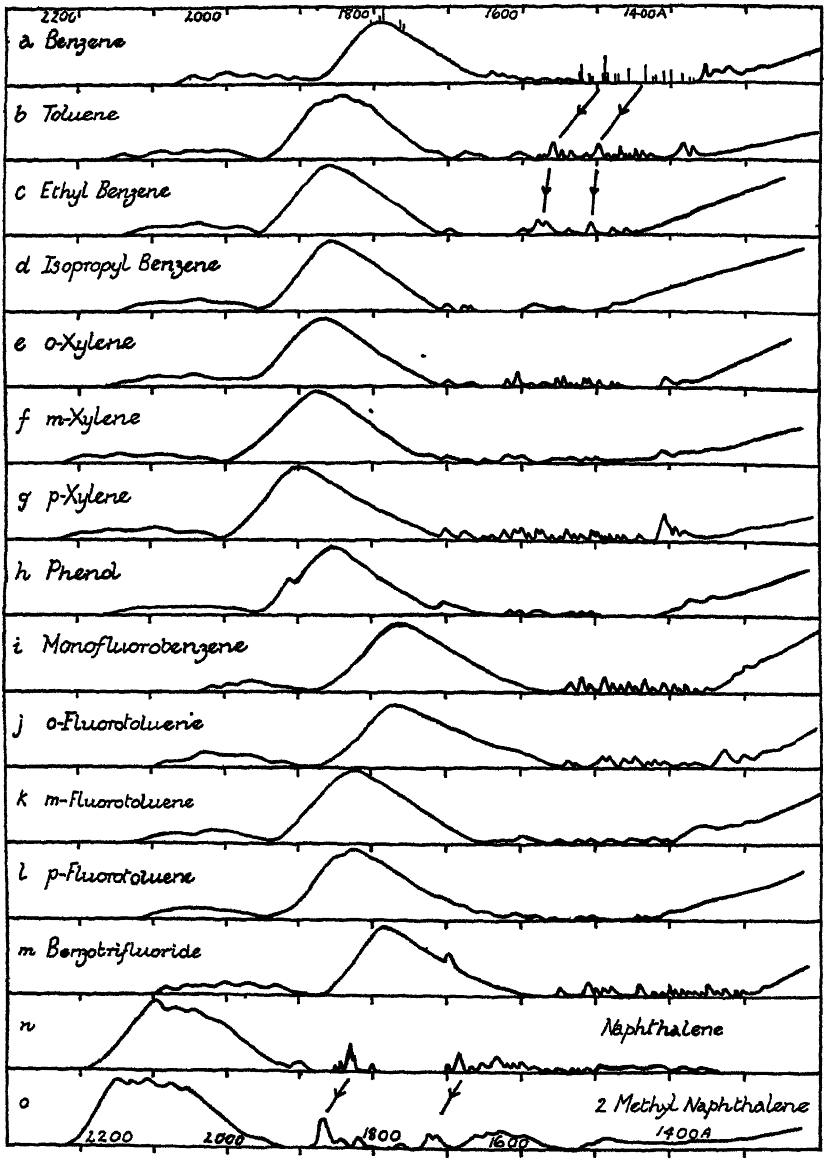

FIG. 1.—Absorption spectra of benzene, naphthalene and derivatives. The ordinates indicate qualitatively the strength of the absorption and are not to be taken quantitatively.

diffuse absorption in the region of 2000 Å (*ca.* 50,000 cm.$^{-1}$ observed, 46210 cm.$^{-1}$ calculated), the deviation from the series being about what might be expected for such a low lying orbital. The intensity of absorption is also about right, judging from the intensity of the higher series members. The $n = 3$ member of series (2) has been identified,[8] beyond any doubt, with a sharp band system near 1790 Å, both by the structure of the band and by its accompanying vibrational pattern. The other interesting facts about series (2) are that its members retain their sharpness even down to the first member and that, apart from the first member, the series is generally weaker and less well developed than series (1). Both these facts are explicable if the excited states are associated with πnp atomic orbitals. Such orbitals will not penetrate the plane of the molecule and be involved in internal electron collision which would cause the bands to become diffuse. Furthermore, since transitions of this type are forbidden in the atomic case, the series will be generally weak, especially for the higher members where conditions are of a more atomic character. The assignment of the 2070-1900 Å absorption to a Rydberg transition is not in disagreement with the theoretical expectations for benzene, since the only allowed transitions within the electron shell is $A_{1g} - E_{1u}$ which is to be identified with intense continuous absorption having a maximum at 1790 Å.

The fourth region of the benzene spectrum lies below 1360 Å. At about 1355 Å a fairly strong band occurs which appears to correspond to the first resonance band leading to the ion $(\chi_1\chi_{2,3}^4)$ and corresponding to an ionization potential of *ca.* 11·7 V. Diffuse absorption from electrons in the basic single CC and CH bonds appears to prevent all but the first two or three Rydberg bands converging to this ionization limit being observed.

Mono-alkyl Benzenes.—The absorption of toluene is illustrated diagrammatically in Fig. 1 *b*. It can be seen that while the spectrum is still very similar to that of benzene it is shifted considerably to longer wavelengths. This shift increases from about 612 cm.$^{-1}$ for the near ultra-violet bands (*ca.* 2600 Å) to about 2250 cm.$^{-1}$ for the 1800 Å maxima and to 3300 cm.$^{-1}$ for the higher Rydberg bands. It is thought to arise largely from polarization or charge transfer effects which particularly develop in the substituent in the excited state. Such effects are naturally greater the nearer the excited state to the ion. The explanation fits with the fact that similar shifts are observed in going from the gaseous phase to solutions in hydrocarbon solvents. For example, bands in the 2600 Å system of benzene are shifted by about 150 cm.$^{-1}$ to long wavelength in going from gas to solution in *iso*-octane, those in the 2000 Å range by about 1000 cm.$^{-1}$ and those in the 1800 Å range by *ca.* 2000 cm.$^{-1}$ (for maxima in solution see ref. (3)). The larger orbitals are clearly much more affected by the solvent molecules. The shifts are attributable to polarization of the solvent. Similar effects for the naphthalenes will be referred to later.

The Rydberg bands of toluene are much less sharp than those of benzene, but a series analogous to the strong series (1) of benzene can be readily picked out and fitted into the Rydberg formula : [2]

$$\nu_0^n = 71{,}130 - R/(n - 0{\cdot}95)^2,\ \text{where } n = 3, 4, 5 \qquad . \quad (3)$$

The corresponding ionization potential is 8·820 ± 0·005 V, which is a reduction of 0·42 V relative to benzene. Deviations from the formula for the $n = 3$ and $n = 4$ members are larger than in benzene because of the more extended structure.

In going from toluene to ethyl benzene there is a further slight shift to long wavelengths, which is, however, much smaller than the shift produced by the primary substitution. The Rydberg bands have increased in diffuseness but it is still possible to establish a correlation with the toluene bands and so to obtain the approximate Rydberg series

$$\nu_0^n = 70{,}750 - R(n - 1{\cdot}10)^2,\ n = 3, 4, 5 \qquad . \quad . \quad (4)$$

which corresponds to an ionization potential of 8·77 ± 0·01 V.

---

[8] Platt and Klevens, *Chem. Rev.*, 1947, 41, 301.

The shifts in going from ethyl benzene to *iso*propyl benzene are still smaller. Although the bands have become increasingly more diffuse, it is still possible to estimate that the ionization potential of *iso*propyl benzene is about 0·01 V less than that of ethyl benzene, i.e. *ca.* 8·76 V. It should be noted that in the near ultra-violet region there is always a *short* wavelength shift on replacing the hydrogens of an attached methyl group by other methyl groups. This has been linked by Matsen, Robertson and Chuoke,[4] with the Baker-Nathan effect and explained in terms of hyperconjugation which would raise the highest occupied ground state π orbital and depress the lowest unoccupied π orbital by an amount greatest for toluene and least for *tert.*-butyl benzene. The difficulty with this explanation is that it does not account for the *long* wavelength shifts of the shorter wavelength bands of *tert.*-butyl (or ethyl or *iso*propyl) benzene relative to toluene. In part these may be due to inductive shifts raising the highest occupied ground state π orbital and increasing from toluene to *tert.*-butyl benzene. We should like, however, to put forward an additional or alternative explanation in terms of the dimensions of the excited orbital. Polarization stabilization of an excited orbital by an alkyl group (regarded as a small piece of dielectric) is clearly most effective when the stabilizing group lies near to or within the excited orbital. A substituted methyl group has its polarized end groups lying far outside the excited orbital of the 2600 Å systems and they are relatively ineffective on this account, the greater stabilization being brought about by hydrogen atoms attached to the α carbon atom. The Baker-Nathan effect could be explained along these lines provided an excited electronic state were involved. A diagram indicating the probable dimensions of the excited orbitals corresponding to the 2600, 2000, 1800 and *ca.* 1600 Å transitions in substituted benzenes is given in Fig. 2. These are drawn at distances 1·2, 2·0, 2·8 and 5·8 Å respectively from the ring carbons, being calculated on the simplified assumption that the average distance of the electron from the ring carbons varies inversely as the term value of the state. It is not difficult to deduce from such a diagram the effects referred to above.

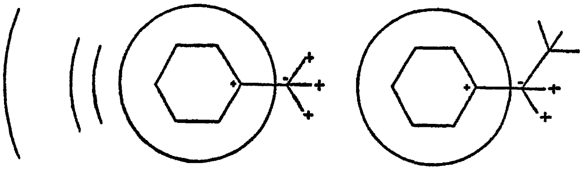

FIG. 2.—Diagram indicating probable dimensions of excited orbitals corresponding to the 2600, 2000, 1790 and 1521 Å transitions in substituted benzenes. Outer circles correspond to shorter wavelength bands.

In the region below 1400 Å the band in benzene at 1355 Å due presumably to the excitation of a χ_1 electron has moved to 1380 Å in toluene. In ethyl and *iso*propyl benzene continuous absorption arising from the alkyl groups appears and tends to blot out all detail at wavelengths shorter than 1400 Å. Long wave shifts of the bands of mono-alkyl benzenes in going from the vapour to the dissolved state are of the same order as those found for benzene.

The Di-alkyl Benzenes.—The substitution of two methyl groups for two hydrogen atoms both attached to the benzene ring produces a further shift in the spectrum towards longer wavelengths, the magnitude of the shift increasing in the order *ortho*, *meta*, *para*. For the 2600 Å systems the shifts relative to toluene are *ca.* 120, 240, 360 cm.$^{-1}$ respectively. The shifts of the maximum of the strong continuum in the 1900 Å region are *ca.* 400, 700, 1200 cm.$^{-1}$ respectively. The Rydberg bands in *o*-xylene, are rather broad and diffuse, but by comparison with the spectrum of toluene a rough Rydberg series could be established:

---

[4] Matsen, Robertson and Chuoke, *Chem. Rev.*, 1947, 41, 273.

$$\nu_0^n = 69{,}200 - R(n - 1{\cdot}08)^2,\ n = 4, 5, 6. \qquad (5)$$

The limit corresponds to an ionization potential of 8·58 ± 0·01 V. In *m*-xylene the Rydberg bands are still fewer and more diffuse. However, it appears from their position relative to those of *o*-xylene that the ionization potential of *m*-xylene is very close to the value for this molecule. For *p*-xylene numerous Rydberg bands were observed. These are somewhat diffuse but a fairly reliable Rydberg series converging to a limit of 8·48 V was established. The appearance of more Rydberg bands is probably to be connected with the greater symmetry of the molecule and it should be pointed out in this connection that in the near ultraviolet *para* derivatives have the sharpest bands and *ortho* derivatives the most diffuse absorption bands. Bands corresponding to the excitation of a χ_1 electron appear in the neighbourhood of 1410 Å for each of the isomers.

The Spectrum of Monofluorobenzene.—The far ultra-violet ab sorption spectrum of monofluorobenzene is very similar to that of benzene itself though the bands are not so sharp as they are in benzene and are shifted slightly to longer wavelengths. The two following series are analogous to the two series observed for benzene.

$$\nu_0^n = 74{,}203 - R/(n - 1{\cdot}05)^2,\ n = 3, 4, 5 \qquad (6)$$

$$\nu_0^n = 74{,}304 - R/(n - 1{\cdot}50)^2,\ n = 3, 4, 5. \qquad (7)$$

Table I shows the agreement between the observed and calculated frequencies. As is usual in molecular Rydberg series, the earlier members deviate somewhat from the formula but the agreement is good for the higher members. The bands are on the average about 300 cm.$^{-1}$ to the low frequency side of the corresponding benzene bands. The limit corresponds to an ionization potential of 9·197 ± 0·005 V. The difference of *ca.* 100 cm.$^{-1}$ between the limits of the two series is equal to the difference between the corresponding limits found for benzene and may represent convergence to slightly different states of the molecular ion. The smallness of the long wave shift of the benzene bands on fluorine substitution as compared with the shift produced for example by chlorine substitution [3] indicates clearly that the high electron affinity of fluorine produces a sufficiently large inductive effect almost to balance the mesomeric effect. Similar conclusions can be reached from infra-red studies.[5] The spectrum

TABLE I.—THE OBSERVED AND CALCULATED FREQUENCIES OF BANDS OF SERIES (6) AND (7)

Series 6			Series 7		
n	$\nu_{\text{obs.}}$ cm.$^{-1}$	$\nu_{\text{calc.}}$ cm.$^{-1}$	n	$\nu_{\text{obs.}}$ cm.$^{-1}$	$\nu_{\text{calc.}}$ cm.$^{-1}$
3	~50,000	45,344	3	~55,560	56,746
4	~61,200	61,593	4	65,314	65,346
5	67,236	67,170	5	~68,870	68,885
6	69,765	69,724	6	70,736	70,676
7	71,107	71,103	7	~71,700	71,707
8	71,940	71,931	8	72,366	72,353
9	72,457	72,467			
10	72,840	72,833			
11	73,075	73,095			

---

[5] Torkington and Thompson, *Trans. Faraday Soc.*, 1945, 41, 237. See also Price, *ibid.*, 1945, 41, 246.

of phenol on the other hand shows considerable long wave shifts of about the same order of magnitude as for monochlorobenzene. The near ultra-violet spectra of these substances show the same relative shifts as observed in the far ultra-violet.

The Spectrum of Benzotrifluoride.—The spectrum of this substance is of special interest because, while the absorptions corresponding to the 2000 Å and 1790 Å regions of benzene are shifted to long wavelengths and occur at practically the same positions as in toluene, the Rydberg bands are shifted to short wavelengths and converge to an ionization potential greater than that of benzene. The series found are

$$\nu_0^n = 78{,}120 - R/(n - 1{\cdot}05)^2,\ n = 3, 4, 5 \quad . \quad . \quad (8)$$

$$\nu_0^n = 78{,}250 - R/(n - 0{\cdot}50)^2,\ n = 3, 4, 5. \quad . \quad . \quad (9)$$

Table II shows the agreement between observed and calculated frequencies. The ionization limit obtained from series (8) is 9·683 ± 0·005 V. That this ionization potential should be greater than that for benzene is in accord with the strong electron attracting power of the CF_3 group known from the strength of trifluoro-acetic acid and dipole moment data. It is also in accord with the absence of complex formation in solutions of iodine in benzotrifluoride. Complexes of iodine and benzene derivatives owe their stability[6, 7] to the donation of electrons from the benzene ring to the iodine molecule and the tendency to such donation will decrease with increasing π^{-1} ionization potential.[8] In benzotrifluoride there is no mesomeric release of electrons as in monofluorobenzene to offset the high inductive pull of the fluorine atoms.

TABLE II.—OBSERVED AND CALCULATED FREQUENCIES FOR THE BENZOTRIFLUORIDE BANDS OF SERIES (8) AND (9)

Series 8			Series 9		
n	$\nu_{\text{obs.}}$ cm.$^{-1}$	$\nu_{\text{calc.}}$ cm.$^{-1}$	n	$\nu_{\text{obs.}}$ cm.$^{-1}$	$\nu_{\text{calc.}}$ cm.$^{-1}$
3	~48,000	49,261	3	~55,250	60,692
4	58,931	65,510	4	66,972	69,292
5	71,040	71,087	5	72,838	72,831
6	73,609	73,641	6	74,640	74,622
7	75,007	75,020	7	75,604	75,653
8	75,838	75,848			
9	Obscured	76,384			
10	76,769	76,750			
11	77,059	77,012			

Whereas in benzotrifluoride the long wave systems are shifted to long wavelengths and the short wave ones to short wavelengths relative to fluorobenzene, the reverse effect happens on a smaller scale in *tert.*-butyl benzene and toluene. The latter effect has already been referred to in discussing the spectra of ethyl benzene and *iso*propyl benzene. This reversal is to be related to the fact that in one case we have an electron-attracting and in the other an electron-releasing substituent.

The Spectra of the *o*-, *m*-, *p*-fluorotoluenes.—The spectra of these substances are given in Fig. 1. The Rydberg bands are too diffuse to enable series to be obtained from them. However, the regions show certain interesting features. While the *meta* and *para* derivatives have their bands shifted to long wavelengths in much the same way as the *m*- and *p*-xylene spectra are moved to the long wavelength side of toluene,

[6] Benesi and Hildebrand, *J. Amer. Chem. Soc.*, 1949, **71**, 2703.
[7] Mulliken, *ibid.*, 1950, **72**, 600.
[8] Chamberlain and Walsh, *Trans. Faraday Soc.*, 1949, **45**, 1032.

the spectrum of the *ortho* derivative is not shifted by nearly as much as might be expected. This we attribute to local action between the fluorine and the methyl group which prevents the latter from releasing negative charge to the ring. A similar effect on a smaller scale must be operative in *o*-xylene. The fields of the adjacent polarized methyl groups tend to depolarize each other and to reduce the charge transfer that might occur if these groups w erewell separated.

The spectrum of *m*-fluorobenzotrifluoride has also been obtained. The Rydberg bands are too diffuse to permit an analysis, but the other regions indicate a slight long wavelength shift relative to benzotrifluoride.

The Spectra of Naphthalene and 2-methyl Naphthalene.—We conclude this series with a discussion of the spectra of naphthalene and 2-methyl naphthalene. The spectra were obtained at pressures of about one-tenth of the vapour pressure of these substances in path lengths of 2 m. They are given in Fig. 1 (*n* and *o*). The main features of the spectra are the very strong absorption systems in the range 2200-2000 Å. Again we should like to call attention to the shifts to long wavelengths in going from vapour to solution and to the way these become larger for the shorter wave bands in much the same way as shifts caused by alkyl substitution. For naphthalene in hydrocarbon solvents the shifts are: for the 3200 Å system *ca.* 310 cm.$^{-1}$,[9] for the 2900-2500 Å system *ca.* 1000 cm.$^{-1}$ (ref. (9) and *A.P.I. Spectrogram* 169) and for the 2200-2000 Å system *ca.* 2250 cm.$^{-1}$. These shifts are clearly due to polarization in the molecules of the solvent when excitation occurs (i.e. to Lorentz-Lorenz forces). This stabilizes the excited state and thus causes the absorption to be at longer wavelengths in solution. There is no doubt that a similar process is operative when substituents are directly attached to the molecule. The fact that the solvent effect is of the same order of magnitude as the substituent effect indicates that the long wave shift produced by alkyl substitution is to be explained as being mainly due to polarization of these groups in the excited state.

The 2200-2000 Å absorption of naphthalene has diffuse structure associated with it. The first diffuse hump, centred at 2108 Å (47,440 cm.$^{-1}$), is relatively much stronger than the diffuse bands accompanying it on the short wavelength side and must thus be regarded as the (O-O) band of the transition, which, in spite of its breadth, does not give rise to much change in bonding. We shall not discuss the diffuse accompanying structure here as our plates have so far been taken with the Lyman continuum which has some undesirable emission lines in this region. It is planned to use the hydrogen continuum for this range in order to obtain more satisfactory details of the band envelope.

To the short wave side of 1900 Å strong sharp bands are obtained which are clearly Rydberg in type. The first set occurs at *ca.* 1830 Å and is followed by a similar weaker set at *ca.* 1780 Å, followed by a set of still weaker bands which are superimposed on a weak continuous absorption (1680-1550 Å; max. *ca.* 1620 Å). The spectrum in the region 1900-1500 Å shows isolated bands getting weaker and closer together as they crowd towards a limit in the region of 1500 Å. The appearance of the spectrum makes it clear that the first ionization potential of naphthalene is not far from 8·1 V. This is confirmed by the electron impact value of 8·3 V.[11] Furthermore, the ionization potential of naphthalene is expected to be appreciably less than that of benzene (9·24 V) and lower even than that of *o*-xylene (8·58 V) because of the additional conjugation. The low ionization potential means that the early Rydberg transitions should fall in the 2500-2000 Å region and their orbitals should lie within the molecular framework. These facts are clearly of considerable importance in considering the origin of the bands in the 2500-2000 Å range.

---

[9] Sponer and Nordheim, this Discussion.

[10] Price, *J. Chem. Physics*, 1936, **4**, 539.

[11] Sugden, Walsh and Price, *Nature*, 1941, **148**, 373.

Below 1500 Å there is a region of weak continuous absorption fading out again about 1450 Å, below which there is no strong absorption down to at least 1100 Å. It is possible that the continua in the regions *ca.* 2100, 1620 and 1485 Å may form a Rydberg series going to a second ionization potential at *ca.* 9·3 V. The ten π electrons in naphthalene fall into five groups each of which should be associated with a different ionization potential. The doublet character of some of the Rydberg bands indicates another possible ionization potential about 400 cm.$^{-1}$ or 0·05 V lower than that at *ca.* 8·1 V.

The spectrum of 2-methyl naphthalene is very similar to that of naphthalene. It suffers the usual long wavelength shift and increase in diffusiveness as a result of methyl substitution. The strong 2200-2000 Å has more diffuse bands superimposed on it. Differences of *ca.* 1000 cm.$^{-1}$, which may correspond to the ring breathing vibration, are observed but the analysis of these together with smaller differences will have to await further experimental work. Observation of shifts relative to the corresponding naphthalene systems indicates ionization potentials of *ca.* 8·0 and 9·2 V.

We wish to acknowledge financial assistance for this work from the U.S. Office of Naval Research (T.O. IX, Contract N6-ori 20 with the University of Chicago), the Royal Society, the Chemical Society and the Institute of Petroleum. One of us (J. P. T.) wishes to thank the Commissioners for the Exhibition of 1851 for the award of an Overseas Scholarship (for Eire).

Wheatstone Laboratory,
King's College, London W.C.2.

Chemistry Department,
University of Leeds.

THE ABSORPTION SPECTROSCOPY OF SUBSTANCES OF SHORT LIFE

BY GEORGE PORTER

Received 17th July, 1950

The experimental methods available for the absorption spectroscopy of free radicals are critically discussed with special reference to flash photolysis and spectroscopy. Some free radical spectra which have been obtained in this way are described and values are given for the dissociation energies and vibration frequencies in the upper and lower states of the ClO, SH and SD radicals.

Most of our knowledge of the molecular structure of free radicals and similar short-lived substances is a result of the interpretation of emission spectra obtained from flames and electrical discharges. About 100 diatomic radicals have now been recognized in this way and many of their molecular constants determined, but there are very many other radicals whose emission spectra have not been observed and about whose structure virtually nothing is known. Chemical methods do not lend themselves readily to high-speed manipulation and other physical methods such as electron diffraction are not at present applicable. The method of absorption spectroscopy is almost alone in its suitability for investigations of this kind and has many advantages ; in particular it can be used to obtain spectra which cannot be observed in emission and it has the great advantage that it makes possible the determination of concentration. Furthermore, as more complex radicals are studied, it will be necessary to use other spectral regions such as the infra-red and far infra-red where absorption techniques become essential.

The difficulties associated with free radical absorption spectroscopy are almost entirely experimental ones and in the first part of this paper a brief account is given of the limitations of the existing methods with particular reference to the flash technique developed by the author. The second part deals with a few of the radical spectra which have been obtained by this method.

Experimental Methods

There are two problems associated with the kinetic absorption spectroscopy of short-lived substances in addition to those encountered with stable molecules. Firstly, the labile molecules must be produced rapidly in high concentration, and secondly, the spectrum must be recorded in a time which is short compared with their average life.

The Preparation of Free Radicals.—The partial pressure of radicals necessary for their observation in a path of 10 cm. varies from 10^{-5} mm. for a radical such as CN with high resolving power to 10 mm. or more under less favourable conditions. In many cases, and especially in the infra-red, a high relative concentration is also necessary if the spectrum is not to be masked by that of the parent molecule. There are four general methods available for free radical preparation and their uses for our purpose are summarized below.

THERMAL DECOMPOSITION.—This is only available when the dissociation of the radical does not occur much more readily than that of the parent molecule. It has not so far been possible to heat a gas rapidly enough to produce radicals instantaneously at high concentrations for kinetic studies and the method is limited to systems in thermodynamic equilibrium which have, however, one great advantage; if the thermochemical constants are known the radical concentration and hence its absorption coefficients can be determined.[1, 2, 3]

CHEMICAL REACTION.—Owing to the fact that diffusion is slow compared with the rate of most radical reactions it is difficult to produce mixing rapid enough to give a long absorption path and except in the special case of flames this method has been unsuccessful.[4] In flames also the reaction zone is narrow and sensitive methods, such as emission line reversal, are usually necessary.[5]

ELECTRICAL DISCHARGE.—By this means accurate synchronization and high percentage decomposition are readily attained and it was, until recently, the only successful method of instantaneous preparation.[6] Its main disadvantages are that it is limited to the low pressures, less than about 1 mm., at which the discharge can be passed, and the fact that the violence of the method results in the production of almost every possible molecular species making the interpretation of the kinetics a matter of great difficulty, except in the very simplest systems.

PHOTOCHEMICAL DISSOCIATION.—This method has many advantages; the system is relatively simple and well understood, a wide range of conditions may be used and almost all radicals can be produced photochemically. With ordinary light sources, however, the concentration of radicals which can be obtained is so low that it has been impossible to detect them by means of their absorption spectra. The use of high intensity flash sources has completely overcome this difficulty and partial pressures of atoms and radicals of the order of cm. Hg have been produced, making this the most powerful of all methods of preparation.[7]

The Rapid Recording of Absorption Spectra.—If the kinetics of the radical disappearance are to be studied the exposure time must be only a fraction of the radical lifetime which may mean 10^{-4} sec. or less. With continuous sources such as the hydrogen lamp the exposure time required is several seconds at least but three methods of high speed recording are available.

---

[1] Bonhoeffer and Reichardt, *Z. physic. Chem.*, 1928, **139**, 75.
[2] Oldenberg, *J. Chem. Physics*, 1938, **6**, 439.
[3] White, *ibid.*, 1940, **8**, 439.
[4] Geib and Harteck, *Trans. Faraday Soc.*, 1934, **30**, 139.
[5] Kondratjew and Ziskin, *Acta Physicochim.*, 1937, **6**, 307.
[6] Oldenberg, *J. Chem. Physics*, 1934, **2**, 713.
[7] Porter, *Proc. Roy. Soc. A*, 1950, **200**, 284.

Electronic Methods.—The response time of radiation detectors such as the photocell may be as low as 10^{-8} sec. but for high speed scanning a limit is set by the statistical fluctuations in the photocurrent. The relative fluctuations F_r are given by

$$F_r = 1/(nt)^{\frac{1}{2}},$$

where n = no. of electrons/sec. from the cathode ≃ no. of photons/sec. and t = time interval resolved. For example, if the rate of scanning were 1000 Å/m. sec. and the s/n ratio were 50, the high output current of 100 μA from the 1P. 28 photomultiplier would only give a resolution of 1 Å. Only if resolution or scanning speed can be sacrificed is this method suitable with present sources, and similar considerations apply to infra-red detectors.

Photographic Integration.—If ordinary light sources are used the intensity may be increased by repeating the process many times, 60,000 such exposures being used by Oldenberg for each spectrum.[8] Maeder and Miescher have used a spinning mirror arrangement so that the decay of the radical is recorded at the same time.[9] Such methods are satisfactory if the interval between exposures is short but in flash photolysis the time required for lamp cooling, and for refilling and cleaning the reaction vessel owing to the high decomposition, makes a large number of exposures impracticable.

Flash Spectrography.—The very high energy which can be dissipated in a single flash, the short duration and easy synchronization coupled with the fact that it gives a very good continuous spectrum makes the high-pressure rare gas filled flash-tube ideal for this purpose. A single flash from a 70 μF condenser at 4000 V across a 15 cm. tube, lasting 5×10^{-5} sec. gives a sufficient exposure on the plate of a Littrow (Hilger E.1) spectrograph down as far as the quartz absorption limit.[7]

Experimental Limitations of the Method of Flash Photolysis.—The construction and properties of flash tubes for photochemical and spectroscopic purposes have been described previously[7] and the present limitations of the method will now be given.

Energy Dissipation.—Energies of 10,000 J per flash have been dissipated in a 1 m. long tube, corresponding to a useful output of 2×10^{21} quanta in the quartz ultra-violet region. At the higher energies occasional refilling is necessary, for example, about every 100 flashes at 5000 J, and it has been found useful to have a separate pumping system for this purpose. It has also been found that xenon filling is the least troublesome in this respect. In most photochemical systems the pressure of intermediates produced by these energies is of the order of several mm. Hg.

Flash Duration.—It has become clear that the flash time of 1 msec. is longer than the lifetime of some of the radicals studied and it will be necessary to use the following methods of reducing its duration.

(*a*) Decrease of Capacity.—This reduces the duration of the flash without decreasing the intensity but the total output is thereby reduced.

(*b*) Increase of Voltage.—Up to the highest voltage used (8000 V) the energy dissipation of the tube does not appear to vary if CV^2 is kept constant by reducing the capacity, and as there is no consequent reduction in output this is the most useful method.

(*c*) Decrease of Tube Resistance.—This may be accomplished by increasing the diameter or decreasing the length of the tube, the latter being approximately proportional to flash duration. It has been found that the maximum energy dissipation of the lamp is also proportional to its length and again the total output must be reduced, but the output/unit length remains unchanged and, if the length of the reaction vessel can be reduced proportionately, the *percentage* decomposition is also unchanged.

The Determination of Radical Concentrations.—The approximate estimation of the lifetime of a radical by noting the disappearance of its absorption spectrum presents no difficulty and yields much interesting qualitative information about its chemical reactions, but there are many important data, such as rate constants and absorption coefficients, which cannot be obtained without a knowledge of absolute concentrations. At present such information is limited to the few radicals which can be obtained in thermodynamic equilibrium and it is important therefore that the relative simplicity of the photochemical system makes possible, in many cases, the estimation of radical concentration indirectly from the decrease in the absorption of the parent molecule

[8] Oldenberg, *J. Chem. Physics*, 1935, **3**, 266.

[9] Maeder and Miescher, *Helv. physic. Acta*, 1942, **15**, 511; 1943, **16**, 503.

and subsequently the appearance of the absorption by the stable products. A complication is introduced by the changing temperature, which is unavoidable in systems containing intermediate products at high concentrations, but the effect of temperature on the absorption spectrum of stable molecules can be determined and suitable corrections applied.

The flash technique was designed primarily for the study of the kinetics of radical reactions but much information is also obtained from the interpretation of the spectra themselves, and two such spectra, of the radicals ClO and SH, will now be considered.

The ClO Radical

A preliminary report and photograph of the spectrum attributed to this radical have been given elsewhere.[7] It appears whenever chlorine is photolyzed in the presence of oxygen and has a half-life of a few milliseconds. The simple vibrational structure strongly suggests a diatomic molecule and, under the circumstances, the only possibility is the ClO radical whose occurrence in chemical reactions has frequently been postulated. Very little is known about the diatomic compounds of Group 6 of the periodic table with Group 7 and the interpretation of this spectrum is therefore of some interest.

VIBRATIONAL STRUCTURE.—The main feature of the spectrum is a series of bands with fairly sharp heads degraded to the red which is clearly a $v'' = 0$ progression and the measurements of these heads with intensities on a scale of 10 are given in Table I. Most of the measurements are accurate to better than 10 cm.$^{-1}$ except for a few bands around $v' = 18$ where the overlapping rotational structure makes the heads difficult to locate.

TABLE I.—$v'' = 0$ PROGRESSION OF ClO

v'	Int.	λ Å	ν cm.$^{-1}$	v'	Int.	λ Å	ν cm.$^{-1}$
4	1	3034·5	32945	14	7	2729·4	36627
5	2	2993·0	33402	15	7	2711·1	36874
6	3	2954·3	33839	16	6	2695·0	37095
7	5	2918·0	34261	17	5	2682·5	37267
8	5	2884·0	34664	18	5	2671·2	37425
9	6	2851·8	35056	19	5	2661·0	37569
10	8	2822·4	35421	20	5	2652·5	37689
11	8	2796·0	35755	21	3	2645·8	37784
12	10	2771·6	36070	22	2	2640·6	37859
13	8	2749·5	36360	23	2	2636·3	37920

An assignment of vibrational quantum numbers in the upper state is not possible on this information alone but a band system attributed to ClO has been obtained in emission from flames containing chlorine or methyl chloride by Pannetier and Gaydon[10] and assuming their interpretation to be correct we may proceed as follows. The average value of the second difference of the wave numbers of the $v' =$ constant progressions in the emission bands is 15 cm.$^{-1}$ and the corresponding value for the upper state, calculated from the absorption spectrum, is 22 cm.$^{-1}$. Starting with the last observed bands of the $v'' = 0$ and $v' = 0$ progressions the positions of further bands heads can be estimated, assuming linear convergence, to give the following values :

	Absorption, $v = 0$ progression cm.$^{-1}$		*Emission, $v' = 0$ progression* cm.$^{-1}$
Obs.	32945	Obs.	27598
Calc.	32466 31965 31442 30897	Calc.	28406 29227 30067 30920

The value for the last observed emission band has been adjusted slightly and the progression starts in effect from the previous band head which is probably the more accurate measurement. It will be seen that there is a coincidence within the accuracy of the extrapolations between the last two figures given and a continuation in this way as far as the observed bands of the other system shows no other coincidence within 100 cm.$^{-1}$. The vibrational quantum numbers obtained in this way are given in Table I and the interpretation is supported by intensity considerations and the close agreement between the values for ω_e' obtained from the two spectra. The value of x in the Table of Pannetier and Gaydon is seen to be 4.

---

[10] Pannetier and Gaydon, *Nature*, 1948, **161**, 242.

These data lead to the following values for the constants of the two states with a probable error in ω_e of 3 %. Account has been taken of a small cubic term in v' in the estimation of ω_e'.

Ground state. $\omega_e'' = 868$ cm.$^{-1}$ $x_e''\omega_e'' = 7{\cdot}5$ cm.$^{-1}$.
Upper state $\omega_e' = 557$ cm.$^{-1}$ $x_e'\omega_e' = 11$ cm.$^{-1}$.
$\nu_e = 31{,}077$ cm.$^{-1}$.

FURTHER DETAILS OF BAND STRUCTURE.—Owing to the extended rotational structure the chlorine isotope effect is difficult to observe, the weaker isotope system being obscured by the stronger, and it has not been possible to confirm the above assignment of quantum numbers in this way.

In addition to the bands already discussed a second progression appears at about one-quarter of the intensity, the heads showing a fairly constant separation to higher frequencies from those of the main system. The bands appear to belong to a second multiplet component, the whole forming a doublet system and over the nine measured heads in Table II the doublet splitting decreases from 200 cm.$^{-1}$ to about 185 cm.$^{-1}$.

TABLE II.—SECOND SYSTEM OF ClO

v'	λ Å	ν cm.$^{-1}$	v'	λ Å	ν cm.$^{-1}$
5	2975·0	33603	10	2807·0	35615
6	2937·6	34032	11	2781·4	35943
7	2902·0	34449	12	2758·0	36248
8	2866·7	34874	13	2735·3	36548
9	2835·7	35255	—	—	—

A full analysis of the rotational structure has not yet been carried out, the resolution being rather too low. The P and R branches appear to be the most prominent feature of the bands and the structure suggests a $^2\Pi - {}^2\Pi$ or $^2\Delta - {}^2\Delta$ transition with near case (a) coupling. The former is supported by theoretical considerations which predict a $^2\Pi$ ground state for ClO.[11]

Determination of the Dissociation Energy.—The bands of the main system are observed almost to the convergence limit and a very good extrapolation can be made, the $\Delta\nu - v$ plot showing slight positive curvature. The value of the dissociation energy to products in the upper state obtained in this way is 37,930 cm.$^{-1}$ or 108·4 kcal./mole, ± about 0·1 %.

To obtain the dissociation energy to unexcited products the only low-lying levels of the atoms to be considered, ignoring multiplet splitting, are the ^2P ground state of chlorine and the ^3P ground and the ^1D and ^1S excited states of oxygen, the latter lying 15,868 and 33,793 cm.$^{-1}$ above the ground state. These lead to three possible values for D_0'' and the lower one is immediately eliminated by the fact that vibrational levels of the ground state are observed which lie above it. The upper one is confirmed by a linear extrapolation of the constants for the ground state which gives a value for D_0'' of 24,680 cm.$^{-1}$. It is clear therefore that the oxygen atom is liberated from the upper level in the ^1D state and the following values for the dissociation energies can now be given unambiguously.

Ground state. Dissociates to Cl ^2P and O ^3P.
$D_0'' = 22{,}062$ cm.$^{-1}$ $= 63{\cdot}04$ kcal./mole ± 0·2 %.

Upper state. Dissociates to Cl ^2P and O ^1D.
$D_0' = 7{,}010$ cm.$^{-1}$ $= 20{\cdot}0$ kcal./mole ± 1 %.

---

[11] Perring (private discussion).

These values assume dissociation to the lowest atomic multiplet levels in each case as the actual levels are unknown. If the atoms are liberated in higher multiplet levels the value of D_0'' would need slight adjustment but the value of D_0' is unchanged. The normal dissociation energy of ClO to chlorine $^2P_{1\frac{1}{2}}$ and oxygen $^3P_2$ depends only on the multiplet level of the Cl atom liberated from the upper state, being the ground state value given above if Cl $^2P_{1\frac{1}{2}}$ is liberated and 881 cm.$^{-1}$ less if the product is Cl $^3P_{\frac{1}{2}}$.

Discussion.—The only existing information about the dissociation energy of ClO is obtained from the spectrum of the ClO_2 molecule.[12] The predissociation at 3750 Å, corresponding to an upper limit of 76 kcal./mole, is not inconsistent with the above value but much lower energies have been suggested from interpretations of the extrapolated convergence limit.

The only existing information about the dissociation energy of ClO is obtained from the spectrum of the ClO_2 molecule.[12] The predissociation at 3750 Å, corresponding to an upper limit of 76 kcal./mole, is not inconsistent with the above value but much lower energies have been suggested from interpretations of the extrapolated convergence limit. The postulated dissociation to normal ClO and O(^1D) now seems quite probable, and although there is some doubt about the heat of formation of ClO_2 it can hardly be high enough to account for this discrepancy. The explanation probably lies in the potential energy surface involved in the dissociation of polyatomic molecules which may lead to products with excess vibrational energy.

It is interesting to compare the bond energy of ClO with the average bond energy in the other chlorine oxides calculated from the heats of dissociation as follows: [13]

Cl_2O	Cl_2O_7	ClO_3	ClO_2	ClO
47·0	50·3	55·6	59·5	63·0 kcal./mole.

The influence of the odd electron in strengthening the bond is clear and the last four molecules form a group of inorganic free radicals showing increasing chemical reactivity as the odd electron becomes localized.

The formation of ClO by the reaction of Cl atoms with O_2 suggests that a radical Cl—O—O· takes part as an intermediate, no trace of other chlorine oxides such as ClO_2 being found in the spectra. Subsequent reactions are then probably

$$\text{Cl—O—O} + \text{Cl} = (\text{Cl}_2\text{O}_2 =)\ 2\text{ClO},$$

and at higher temperatures,

$$\text{Cl—O—O} + \text{Cl}_2 = (\text{Cl}_2\text{O}_2 + \text{Cl} =)\ 2\text{ClO} + \text{Cl}.$$

Similar experiments with bromine indicate that the bromine atom does not react with O_2.

The SH and SD Radicals

The SH radical is the only diatomic hydride of the first two periods whose vibrational constants are completely unknown and one of the few common hydrides for which not even an approximate value of the dissociation energy is available. Its spectrum does not appear readily and only one band, the 0—0 band of the $^2\Sigma - {}^2\Pi$ transition, has ever been observed.[14] It is well known that hydrogen sulphide can be decomposed photochemically into its elements, and although other mechanisms have been proposed [15] it is probable that the primary decomposition is to H and SH.[16] For this reason the flash photolysis of H_2S was studied as a probable source of the SH radical.

---

[12] Finkelnberg and Schumacher, *Z. physic. Chem.* (Bod. Fest.), 1931, 704.

[13] Goodeve and Marsh, *J. Chem. Soc.*, 1939, 1332.

[14] Lewis and White, *Physic. Rev.*, 1939, **55**, 894. Gaydon and Whittingham, *Proc. Roy. Soc. A*, 1947, **189**, 313.

[15] Goodeve and Stein, *Trans. Faraday Soc.*, 1931, **27**, 393.

[16] Herzberg, *ibid.*, 1931, **27**, 402.

Hydrogen sulphide was prepared from ferric sulphide and sulphuric acid and also by the action of water on an intimate mixture of calcium sulphide and phosphorous pentoxide. It was dried over $CaCl_2$ and P_2O_5 and fractionally distilled *in vacuo*. At pressures of 40 mm. of H_2S one flash produced a partial pressure of 9 mm. H_2, sulphur being deposited on the wall, and there was no overall pressure change. Spectra were taken of the products on a Littrow (Hilger E.I.) spectrograph at increasing time intervals, after the flash. Immediately after the flash the absorption spectrum showed, in addition to the continuum of H_2S and the $^3\Sigma - {}^3\Sigma$ system of S_2, the 0—0 band of SH at 3236·6 Å identical with that described by Lewis and White,[14] another similar band at 3060 Å, and a diffuse band system between 3168 and 3797 Å.

TABLE III.—SH 1—0 BAND

ν (cm.$^{-1}$)	Int.	Branch (J)
32664·8	8	R_1 head
32634·4	6	$Q_1(1\frac{1}{2})$
32618·4	8	$Q_1(2\frac{1}{2})$. $P_1(1\frac{1}{2})$
32601·0	5	$Q_1(3\frac{1}{2})$
32587·9	3	$P_1(2\frac{1}{2})$
32580·2	4	$Q_1(4\frac{1}{2})$
32555·7	6	$Q_1(5\frac{1}{2})$. $P_1(3\frac{1}{2})$
32528·1	2	$Q_1(6\frac{1}{2})$
32518·4	2	$P_1(4\frac{1}{2})$
32498·1	2	$Q_1(7\frac{1}{2})$
32480·0	2	$P_1(5\frac{1}{2})$
32498·1	2	$Q_1(8\frac{1}{2})$
32469·6	1	$Q_1(9\frac{1}{2})$
32267·5	3	Q_2 head

SD 0—0 BAND			SD 1—0 BAND		
ν (cm.$^{-1}$)	Int.	Branch (J)	ν (cm.$^{-1}$)	Int.	Branch (J)
30977·4	10	R_1 head	32294·0	10	R_1 head
30959·6	3	$Q_1(1\frac{1}{2})$	32277·0	4	$Q_1(1\frac{1}{2})$
30951·9	3	$Q_1(2\frac{1}{2})$	32269·2	5	$Q_1(2\frac{1}{2})$
30943·6	3	$Q_1(3\frac{1}{2})$	32260·7	3	$Q_1(3\frac{1}{2})$
30934·4	5	$Q_1(4\frac{1}{2})$	32251·1	4	$Q_1(4\frac{1}{2})$
30923·6	2	$Q_1(5\frac{1}{2})$	32238·8	8	$Q_1(5\frac{1}{2})$
30912·1	2	$Q_1(6\frac{1}{2})$	32224·3	5	$Q_1(6\frac{1}{2})$
30899·6	3	$Q_1(7\frac{1}{2})$	32211·4	5	$Q_1(7\frac{1}{2})$
30594·3	5	Q_2 head	32195·4	5	$Q_1(8\frac{1}{2})$
			32174·8	5	$Q_1(9\frac{1}{2})$
			32154·4	4	$Q_1(10\frac{1}{2})$
			31907·1	3	Q_2 head

THE 3060 Å BAND.—The rotational lines of this band appeared with greater intensity than those the 0—0 band, the relative intensity of the two bands always being the same, and both bands had a half-life of about 1 msec. The resolving power of the spectrograph in this region was 1·5 cm.$^{-1}$ which was not sufficient to separate the satelite $^QP_{21}$ and $^RQ_{21}$ branches from the main Q_1 and R_1 branches nor in some cases the main branch lines from each other. For this reason some of the lines were very broad and the line measurements which are given in Table III are the observed maxima with the probable quantum number assignment for the main branch lines. It is found that, apart from the different spacing owing to the higher value of $B'' - B'$, this band is identical in structure with the

3236·6 Å band and it is fairly certain that it is the 1—0 band of the same system. This was confirmed by comparing the SH spectrum with the spectrum of the SD radical obtained from D_2S when it was found that there was a small isotope shift to shorter wavelengths with SD for the 3236·6 Å band and a greater one to longer wavelengths for the 3060 Å band, the order of magnitude leaving no doubt as to the correctness of the above interpretation. The measurements of the strongest lines of the 0—0 and 1—0 bands of SD are given in Table III.

There are two unusual features about the appearance of the 1—0 band of SH ; firstly, it has a greater intensity than the 0—0 band though a careful search for further bands of the progression shows that they are absent and secondly, Lewis and White observed the weaker 0—0 band only. Both these anomalies, as well as the difficulty experienced in obtaining the bands in emission, would be explained if there were a potential energy curve leading to a lower dissociation limit which crossed the ${}^2\Sigma$ curve at about the second vibrational level. In this case the 1—0 band might appear stronger at low resolution owing to the broadening of the lines even if the transition were of lower probability, whilst higher transitions might be completely diffuse.

VIBRATIONAL CONSTANTS AND DISSOCIATION ENERGY.—Apart from the upper limit of 93 kcal./mole set by the above-mentioned predissociation these constants cannot be obtained from the spectrum of SH alone as at least three vibrational bands are necessary for their derivation. By using the different zero point energy of the isotopic molecule, however, another relationship is introduced which makes the calculation possible. If we assume the same force constant for the two molecules it can be shown that

$$\Delta^2\nu = (\nu_{1-0} - \nu^i_{1-0}) - (\nu_{0-0} - \nu^i_{0-0}) = \omega_e'(1 - \rho) - 2x_e'\omega_e'(1 - \rho^2)$$

where $\rho = \sqrt{\mu/\mu^i}$, ν_{1-0} is the wave number of the 1—0 band, etc. and the superscript i refers to the SD molecule. We also have

$$\Delta\nu'_{1-0} = \nu_{1-0} - \nu_{0-0} = \omega_e' - 2x_e'\omega_e'$$

and therefore if the separations of the bands are known the values of ω_e' and $x_e'\omega_e'$ can be obtained. The values $\Delta^2\nu = 471$ cm.$^{-1}$ and $\Delta\nu'_{1-0} = 1787$ cm.$^{-1}$ are obtained from the origins of the ${}^2\Sigma - {}^2\Pi_{3/2}$ sub-bands estimated from the Q_1 branches, and substitution in the above equations gives for the ${}^2\Sigma$ state,

$$\omega_e' = 1950 \text{ cm.}^{-1} \quad \text{and} \quad x_e'\omega_e' = 81 \text{ cm.}^{-1}.$$

A linear extrapolation of these values gives the upper state dissociation energy $D_0' = 10{,}800$ cm.$^{-1}$ and in deriving a value for the normal dissociation energy two analogies with the ${}^2\Sigma$ state of OH, which might be expected to be very similar, will be made. The first is that the products in the upper state are $H({}^2S)$ and $S({}^1D)$ and this is fairly safe as the only alternative of $S({}^1S)$ would give a very low value for the normal dissociation energy.

The second analogy is that the linear extrapolation comes about 25 % too high and the final value obtained in this way will be assumed to have a possible error of 20 %. Applying this correction, subtracting the energy of promotion of S from the ${}^3P$ to the ${}^1D$ state and adding ν_{0-0} we get, for the normal dissociation energy, $D_0'' = 29{,}700$ cm.$^{-1}$ = 84·9 kcal./mole with an error probably less than 5 %.

From the relation

$$\nu_{v-0} - \nu^i_{v-0} = \omega_e'(v' + \tfrac{1}{2})(1 - \rho) - x_e'\omega_e'(v' + \tfrac{1}{2})^2(1 - \rho^2)$$
$$- [\tfrac{1}{2}\omega_e''(1 - \rho) - \tfrac{1}{4}x_e''\omega_e''(1 - \rho^2)]$$

the quantity in square brackets is found to be 369·5 cm.$^{-1}$ and to find the value of ω_e'' a rough estimate of $x_e''\omega_e''$ may be made from the value of D_0'' + 10 % (as in OH) the term in $x_e''\omega_e''$ being small. Using the value $x_e''\omega_e'' = 52$ cm.$^{-1}$ obtained in this way we get $\omega_e'' = 2670$ cm.$^{-1}$. The corresponding values of the vibrational constants of the SD radical are $\omega_e' = 1400$ cm.$^{-1}$ and $\omega_e'' = 1910$ cm.$^{-1}$.

THE DIFFUSE BAND SYSTEM.—These bands form a regularly spaced system showing no fine structure, most of them being degraded to the red with fairly sharp heads, the measurements of which are given in Table IV. They appear and disappear with the SH bands and in all the spectra taken, using pressures of H_2S between 1 cm. and 10 cm. Hg their intensity was proportional to that of the SH bands. That they are not bands of sulphur is shown by the fact that they do not appear along with the S_2 bands in the photolysis of CS_2 or S_2Cl_2 and also that they show a shift when D_2S is used in place of H_2S. At first sight they might be another system of SH, their simple vibrational structure suggesting a diatomic molecule, but this is not supported by the isotope shift which occurs to shorter wavelengths with deuterium and is roughly the same, about 50 cm.$^{-1}$ throughout the system.

TABLE IV.—DIFFUSE BAND SYSTEM

λ Å	Int.	ν cm.$^{-1}$	λ Å	Int.	ν cm.$^{-1}$
3168·0	3	31557	3443·9	10	29028
3195·6	4	31284	2479·5	9	28732
3222·1	4	31027	3519·5	8	28405
3249·7	6	30764	3562·5	6	28062
3278·5	8	30493	3604·4	6	27736
3308·0	8	30222	3647·8	6	27406
3340·0	9	29932	3696·5	4	27045
3373·5	10	29634	3745·6	3	26691
3407·0	10	29343	3796·5	1	26332

These facts suggest that the system is that of a molecule, probably polyatomic, containing S and H atoms only. Of these the most likely are the HS_2 radical and the H_2S_2 molecule, the latter compound being quite stable but without a recorded spectrum. One might expect the spectrum of hydrogen persulphide to be entirely continuous by analogy with hydrogen peroxide and it also seems likely that some of it would survive the reaction and be detected in the products but it cannot be entirely ruled out on these grounds. The vibration frequency of something over 350 cm.$^{-1}$ is a reasonable value for the frequency of the —S—S— bond in either molecule, and the only other information which can be obtained from the spectrum is the dissociation energy which a fairly good linear extrapolation gives as 35,600 cm.$^{-1}$ or 102 kcal./mole. The energy of the —S—S— bond in S_8 is 52 kcal.[17] and if it is this bond which is broken dissociation of HS_2 to SH ($^2\Pi$) and S(^{1}S) gives fair agreement whereas dissociation of H_2S_2 to two SH radicals would not give this value unless there were another state of SH much lower than the $^2\Sigma$ state. Pending an investigation of the spectrum of H_2S_2 it seems more likely that the bands are those of the HS_2 radical which could be formed by the union of H atoms with the S_2 molecule.

Other Diatomic Hydrides of Group 6.—The absorption bands of the $^2\Sigma - {}^2\Pi$ systems of OH and OD have been obtained very strongly by the reaction of H or D atoms, prepared by photolysing a small amount of Cl_2 or Br_2, in the presence of H_2 or D_2, with oxygen. The first three bands of the $v'' = 0$ progression appeared at high intensity and this seems to be the first report of the OD bands in absorption. A very complex system of lines, which is the same in both cases and therefore attributable to oxygen alone, appears from 3000 Å to shorter wavelengths but no diffuse band system similar to that obtained with H_2S is present.

---

[17] Siskin and Dyatkina, *Structure of Molecules* (Butterworth, 1950), p. 255.

Attempts have been made to obtain the spectrum of the SeH radical in the photochemical decomposition of H_2Se but the only spectrum recorded on the plate was that of Se_2 despite the fact that the amount of decomposition was considerably greater than with H_2S. The absence of the spectrum of SeH may be explained if the predissociation occurs below the first vibrational level in this case, or if the SeH radical is chemically less stable, the latter explanation being probable in view of the decrease in stability from OH to SH, the former being observed for as long as 1/10th sec. after the flash.

The author wishes to thank Prof. R. G. W. Norrish for many helpful discussions and suggestions in connection with this work.

The University,
Cambridge.

GENERAL DISCUSSION

Dr. A. Kastler (*Paris*) said : Regarding the polarization of fluorescence of aromatic molecules in monocrystals Dr. H. Benel made in 1940 in Bordeaux University under my direction, an investigation of the polarization of the fluorescence of naphthalene crystals containing anthracene as impurity.* The edges of the crystals used were cut parallel to the three axes of principal indices of refraction. This blue fluorescence was due to absorption and emission of anthracene molecules imbedded in the crystal. From the polarization ratios measured for different crystal orientations it was concluded that the light vector of the fluorescence radiation is directed mainly parallel to the short axis of the anthracene molecules if it is supposed that the anthracene molecules have their axes parallel to the corresponding axes of the naphthalene molecules.

On account of its theoretical interest an analogous investigation on fluorescence of pure naphthalene crystals was taken up at my request by Dr. Svend Brodersen (Copenhagen) in Paris in June, 1950. The crystal at room temperature was illuminated by a hydrogen arc and the fluorescence bands were analyzed by a spectrograph and identified with the known fluorescence bands of naphthalene in the crystal state in the 3100 to 3600 Å region. From the polarization of these bands as a function of various crystal orientations it can be inferred that the light vector of this fluorescence radiation is directed mainly parallel to the short axis of the emitting naphthalene molecules. A closer investigation of the spectral distribution of the fluorescence light seems to show that the electronic transition moment lies along the short axis of the molecules, whereas the small amounts of light polarized along the long axis is due to some vibrations.

This is a preliminary report ; further work will be continued.

Dr. D. P. Craig (*London*) and **Prof. H. Sponer** (*Durham, N. Carolina* (*communicated*) : If we assume that the sequence of electronic states of napththalene is as given in the valence-bond theory, then a polarization of fluorescence emission in the region 3200 Å parallel to the shorter in-plane molecular direction indicates that the intensity borrowing is predominantly from the intense band system at 2220-2000 Å instead of the weaker system at about 2750 Å. This is not in conflict with the Herzberg-Teller rule for the relative intensity of forbidden and allowed band systems, which shows that the perturbation of the 3200 Å transition by the remote 2200 Å system is of the same order as that due to the nearer, but weaker, 2750 Å system. Vibrations belonging to the β_{2u} species would provide the active origins in a forbidden band system with this polarization.

---

* Benel, *Thesis* (Bordeaux, 1940). A short summary of this thesis has been published in *Compt. rend.*, 1940, **211**, 595.

Dr. A. Burawoy (*Manchester*) said: I should like to comment (*a*) on the empirical criteria which allow a distinction between the two types of absorption bands mentioned by Dr. Kasha and (*b*) on the interpretation of the electronic transition responsible for the low intensity absorption bands.

In a series of papers published between 1930 and 1932 [1] an almost complete empirical classification of the electronic spectra of organic molecules appearing above 2000 Å and of their rules has been given. It was shown that there are only two types of electronic transitions in this spectral region. (i) Absorption bands generally of a comparatively high intensity ($\epsilon > 5000$) which are always connected with the presence of systems indicated in (I),

$$\text{(I)}\quad \mathrm{A\,.\,[CH:CH]_{\mathit{n}}\,.\,CH:B}$$

$$(\mathrm{A} = \mathrm{R,\ Hlg,\ OR,\ SR,\ NR_2,\ O^-,\ S^-,\ NR^-};$$

$$\mathrm{B} = (\mathrm{CR_2,\ NR,\ O,\ S,\ \overset{+}{N}R_2,\ \overset{+}{O}R,\ \overset{+}{S}R})$$

i.e. so-called conjugated systems (*K*-bands). These are the absorption bands attributed by Mulliken [2] to transitions of the $N \rightarrow V$ type. The slightly weaker long-wave bands appearing in the spectra of benzene and many of its derivatives are probably of the same type, but "forbidden" by the often small transition moment. (ii) Absorption bands of low intensity ($\epsilon < 2000$) which are due to electronic transitions originating in all multiple linkages such as N═O, NO═O, N═N, C═C, C═N, C═O, C═S (*R*-bands).

These absorption bands are not only distinguished by their different intensity, but they also obey different and characteristic optical rules. One such distinguishing feature discussed in considerable detail is the effect of the addition of a proton mentioned by Dr. Kasha.

Whereas the *K*-bands are generally displaced to longer wavelengths, all low intensity (*R*-) bands disappear. This has been illustrated, e.g. by the spectra of the blue thiobenzophenone in ether (λ, 6200 Å and 3150 Å; ϵ, 70 and 17000) and its orange salt formed in concentrated sulphuric acid (no *R*-band; λ, 3840 Å; ϵ, 25000).

Another possibly more important or useful criterion is the effect of solvents on the position of these absorption bands. The *K*-bands are displaced to longer, all *R*-bands to shorter wavelengths approximately with the increasing dielectric constant of the solvent. Thus, *pp'*-diethoxythiobenzophenone absorbs in hexane at 5960 Å and 3440 Å (ϵ, 366 and 34300, respectively) and in alcohol at 5790 Å and 3535 Å (ϵ, 382 and 30900, respectively).

The effect of substituents, i.e. of modifications in the molecular structure, is also very different and most characteristic. Thus, the introduction of a OH or NH_2 group on the end of a conjugated system displaces the corresponding *K*-band to longer, but the *R*-band always to shorter wavelengths (cf. e.g. the spectra of thiobenzophenone and *pp'*-diethoxythiobenzophenone above).

The above-mentioned and other distinguishing features can be reduced to a simple general rule. The *K*-bands are displaced to *longer* wavelengths as the polarity of the absorbing conjugated system increases. The *R*-bands are displaced to *shorter* wavelengths with the increasing polarity of the multiple linkage involved. This, of course, is only one, although important, factor influencing the position of the absorption bands.

It has also been shown that in contrast to the well-known shift of the

---

[1] Burawoy, *Ber.*, 1930, **63**, 3155; 1931, **64**, 464, 1635; 1932, **65**, 941. For a summary, cf. also *J. Chem. Soc.*, 1939, 1177; *Photochemistry in Relation to Textiles* (1949), p. 32.

[2] Cf. McMurry and Mulliken, *Proc. Nat. Acad. Sci.*, 1940, **26**, 312.

K-bands to longer wavelengths with the increasing length of the conjugated system, the *R*-bands remain almost unchanged. This has been illustrated by a comparison of the corresponding bands in the spectra of azobenzene $C_6H_5—N{=}N—C_6H_5$ (λ, 4480 Å and 3130 Å; ϵ, 425 and 20000 respectively) and benzene-azo-diphenyl $C_6H_5—C_6H_4—N{=}N—C_6H_5$ (λ, 4500 Å and 3345 Å; ϵ, 900 and 30000, respectively).[3] Similarly, in contrast to the *K*-band, the *R*-band in citral and other α,β-unsaturated aldehydes and ketones $R—CH{=}CH—CH{=}O$ is not displaced to longer wavelengths in citrylideneacetaldehyde and related compounds

$$R—CH{=}CH—CH{=}CH—CH{=}O.^4$$

It should be added that the low intensity bands of all multiple linkages must be attributed to the same type of electronic transition, since as far as investigated they all obey the same characteristic optical rules.

The nature of this electronic transition has also been fully discussed. It was shown that these bands obey optical rules similar to those observed for the absorption (colour) of free radicals such as the triarylmethyls. For this and other reasons, it was concluded that the *R*-bands involve a biradical (triplet) state of the double bond. The two possibilities (triplet-triplet and singlet-triplet transition) were discussed and the former preferred. However, in the light of our increased knowledge, the singlet-triplet transition may after all be the correct one. This interpretation of the low-intensity bands has been in recent years taken up by Lewis and his collaborators [5] and by Carr [6] for the very weak bands of ethylene and its homologues.

A different view has been expressed by McMurry and Mulliken [2, 7] who have attributed the low-intensity bands characteristic for the $C{=}O$ and $C{=}S$ groups to an electronic transition arising in the non-bonding (unshared) electrons of the O and S atoms. Qualitatively, such an interpretation is the simplest possible one and had been carefully considered by myself. It was rejected because it is unable to account for numerous observations. May I briefly enumerate some of the difficulties of this interpretation.

(i) Ethylene and its homologues also show such weak absorption bands, although no unshared electrons are available.

(ii) The similar behaviour of these bands and those of certain free radicals cannot be explained, since the given interpretation is not applicable to free radicals.

(iii) According to McMurry and Mulliken their interpretation of the carbonyl (*R*)-band should require a shift to longer wavelengths as the number of conjugated groups increases. They erroneously claimed that this is observed and represents proof for the suggested transition. However, in contrast to the *K*-bands the position of the *R*-bands remains almost unchanged with the increasing length of the conjugated system (cf. above).

(iv) Dr. Kasha believes that the disappearance of these bands on addition of a proton to the non-bonding pair of an oxygen or other atom offers a clear proof of the excitation of the non-bonding electrons, since the binding energy of the lone pair would considerably increase. However, the addition of the proton does also increase the binding energy of the bonding electrons of the double bond and thus does not allow a decision between these two possibilities.

Again, the effect of the proton addition is only one particular instance of the general rule that the *R*-bands are shifted to shorter wavelengths as the polarity of the double bond increases. Substitution by an amino group or a change to a solvent of higher dielectric constant cause also a shift to shorter wavelengths. However, in these cases the increased negative charge at the O or other atom will *reduce* the binding energy of the unshared electrons. Similarly, introduction of nitro and carbonyl groups, e.g. in *p*-nitrobenzaldehyde, *p*-nitroazobenzene and glyoxal, will be responsible for an increased binding energy of the non-bonding electrons at the O and N atoms, but the *R*-bands are displaced to longer wavelengths. The suggested transition is, undoubtedly, incompatible with these facts, if Dr. Kasha's argument is accepted.

---

[3] Burawoy, *J. Chem. Soc.*, 1937, 1865.

[4] Burawoy, *ibid.*, 1941, 20.

[5] Lewis and Kasha, *J. Amer. Chem. Soc.*, 1945, **67**, 994; Kasha, *Chem. Rev.*, 1947, **41**, 401.

[6] Carr, *J. Chem. Physics*, 1939, **7**, 631.

[7] McMurry, *ibid.*, 1941, **9**, 231, 241; *Trans. Faraday Soc.*, 1934, **30**, 93.

For the reasons given, it is most unlikely that the low-intensity (*R*-) bands are due to electronic transitions arising in non-bonding (unshared) electrons. They should involve a biradical state or triplet state involving the bonding electrons, which view is at least in agreement with all known observations including the comparatively low energies of these transitions.

Thus, there should also be little justification to assume that the phosphorescence state and the excited state obtained in absorption are different *electronic* states, particularly, since they would possess at least in the investigated thioketones and nitroso compounds[5] almost equal stability. This would be a remarkable coincidence.†

There is also no need to introduce an almost quantitative radiationless spin-orbit-coupling-dependent internal conversion from the excited singlet state to a triplet state, the quantitative occurrence of which one should have great difficulty to explain.

Dr. M. Kasha (*Chicago*) said : I am glad that Dr. Burawoy made a comprehensive summary of his researches in their relation to the work by Reid and myself on *N*-heterocyclic spectra. This gives me an opportunity to correct any unintended impressions that we feel we are in any way pioneers in the interpretation of non-bonding electron transitions, or in the use of acidic solvents in absorption spectral studies. The comments in the third section of my paper apply strictly only to the *N*-heterocyclic spectra, although in a general way most of the statements should be valid for other $n \rightarrow \pi^*$ transitions. We recognize the work done by Dr. Burawoy, and found his work on azo compounds especially helpful as a guide in our work.

However, it is easy to show that Dr. Burawoy is wrong in trying to give a uniform interpretation to the " weak " bands of azo compounds, carbonyl compounds, possibly our $n \rightarrow \pi^*$ bands in *N*-heterocyclics, the well-known shoulder on the long-λ side of the ethylene absorption band, as well as certain free radical spectra.

Firstly, it is of utmost importance to specify the absolute absorption intensity of such bands. Thus, although all of the above may be considered as " weak " bands, among themselves they differ in intensity by a factor of over 1000 or more. Secondly, singlet-triplet absorption bands may be rigorously identified by the behaviour of their intensity as a function of atomic number of substituted atoms (see my paper and especially Fig. 1). Most of the bands discussed by Dr. Burawoy do not satisfy this behaviour ; certainly the bands we identify as singlet-singlet $n \rightarrow \pi^*$ bands in the *N*-heterocyclics show no sensitivity to atomic number. For small molecules like ethylene, in which halogen substitution greatly perturbs the π-electron system, the energy of the transitions is so greatly affected as to make the study of atomic number effect uncertain. However, of all the cases cited by Dr. Burawoy, the ethylene " hump " referred to may be the only example of a singlet-triplet transition.

The work on singlet-triplet absorption bands done at California by the late Prof. G. N. Lewis and myself (see footnotes 4 and 7)* always made use of the indispensible correlation with emission spectra mentioned in the present paper. I believe that Dr. Burawoy's spectral studies do not touch on singlet-triplet transitions (for which the absorption coefficients have the very low values of from 0·0001 to about 0·1 or 1), nor do they involve triplet states.

---

* My paper, this Discussion.

† The remarks refer only to the weak absorption bands.

Dr. A. Burawoy (*Manchester*) (*communicated*): Dr. Kasha's two arguments cannot be accepted. Firstly, his claim that the extinction coefficient for singlet-triplet transitions should be smaller than unity is already contradicted by the singlet-triplet transitions of the Cl_2, Br_2 and I_2 molecules referred to in his original communication. They are not only responsible for weak absorption bands of much higher intensity (ϵ, 90, 160 and 740 respectively),[8] but as pointed out in 1930 also show the very characteristic solvent effect of all weak (R—) bands arising from highly localized electronic transitions in double bonds. Arbitrarily chosen intensity limits are, of course, no criteria for any particular type of electronic transition.

Secondly, it is misleading to state that most of the weak bands discussed by me do not satisfy the rigorous criterion for singlet-triplet absorption bands requiring increasing intensities with the atomic number of substituted atoms such as the halogen atoms.[8] Actually, no relevant determinations are reported in the literature with exception of a few data for halogen substituted carbonyl compounds, and in this case contrary to Dr. Kasha's claim a considerable increase of the intensity in the order of substituents H < Cl < Br < I is, indeed, observed and thus should apparently represent strong additional evidence for the singlet-triplet character of the weak carbonyl band.

The intensity of the weak carbonyl band is known to increase in the series $H—CH_2CH=O$ (ϵ, 14) Cl— (31), Br— (83) and according to unpublished determinations in hexane with E. Spinner in the series $H—CH_2CPh=O$ (ϵ, 44), Cl— (81), Br— (140), I— (350).

Prof. J. Franck (*University of Chicago*) said: In his interesting and very condensed outline of the content of seven papers, Dr. Kasha has reported on radiating as well as on radiationless transitions in complex molecules. In respect to the latter he makes use of the hypothesis that the transitions are caused by internal conversion; i.e. a radiationless conversion of electronic excitation energy of a molecule into oscillation energy of its atomic constituents. I, too, favour this point of view and have said so on different occasions, for instance in attempts to explain certain features of photosynthesis. I am, therefore, interested to find out whether Dr. Kasha's new observations rule out all possibility that the radiationless transitions from singlet to triplet state may be brought about by other processes. This is the reason why I would welcome additional information about some points relevant in this respect.

(i) Have any direct experiments been made by Dr. Kasha which indicate that the radiationless transitions occur from the non-oscillating singlet state to the triplet state? Or does the transition rather occur from the oscillating state during the period in which oscillation energy given to the molecule by the excitation process is dissipated by the contact with the molecules of the cold solvent? If the former is the case, the ratio of fluorescence yield to phosphorescence yield will be independent of the frequency of the existing light down to the limit of the 0,0 singlet-triplet transition. In the latter case the ratio should rise steeply with declining frequency in the neighbourhood of 0,0 transition. Such a change should, according to my opinion, in many cases be observable if internal conversion is responsible for the radiationless transition.

(ii) Have experiments been made on the dependence of the ratio fluorescence yield to phosphorescence yield upon the concentration of the complex molecules in solid solution? If the ratio stays constant down to very small concentrations this would again speak strongly in favour of transitions caused by internal factors in the complex molecule, whereas a rise of the ratio in the region of low concentrations could be regarded as an indication that intramolecular processes, for instance, sensitized fluorescence, may play a role.

---

[8] Cf. Rabinowitch and Wood, *Trans. Faraday Soc.*, 1936, **32**, 540.

(iii) Finally, I would appreciate clarification of a theoretical problem which, though of minor importance in Dr. Kasha's paper, might be of general interest. The question is as follows : is it justified, as is done by the author in one of his derivations, to assume that the transition probability calculated from the integrated absorption of the whole band of the singlet-triplet intercombination is the same as the one calculated from the observed lifetime of the non-oscillating triplet state ? May it not be that by the removal of oscillation energy the admixture of singlet quality to the triplet state may be considerably lowered ? In that case the non-oscillating triplet state may possess a longer lifetime than the same triplet state containing as much oscillation energy as is transferred to the molecule, together with the electronic excitation by the process of light absorption.

In a discussion with H. Sponer about a week after the meeting the present writer has been informed that Nordheim, Sponer and Teller[9] have already published the same conclusion as was the basis of question (iii), namely, that the probability of a forbidden transition may easily be enlarged by the presence of oscillation energy because the borrowing of intensity from a nearly allowed transition may be increased by the oscillations.

Dr. M. Kasha (*Chicago*) said : In reply to Prof. Franck, the dependence of the ratio $\chi = \phi_P/\phi_F$ on the frequency of excitation was studied. However, because the band-width of the exciting light was of the order of 100 to 200 Å only a limited statement may be made : the ratio χ was found to be *independent* of exciting frequency from a few thousand cm.$^{-1}$ above the zero-point level of the lowest excited singlet state to frequencies corresponding to the fifth singlet electronic state above the ground state. From this it was concluded that the radiationless transition to the lowest triplet state takes place at or within 1000 to 2000 cm.$^{-1}$ of the zero-point vibrational level of the lowest excited singlet state.

The dependence of the ratio χ was not studied specifically for its variation with concentration of the solute. Most of the experiments were done at solute concentrations of 0·001 M or less. It was determined (McClure) that the triplet-singlet decay constants were independent of concentration in this range for most cases. It was also found that fluorescence quenching was absent in the rigid glass. Therefore, it was assumed that at the high viscosities of the rigid glass solution, all collision-dependent processes were inhibited, and that, in this regard, χ was independent of concentration.

Regarding Prof. Franck's point that the intersystem crossing process possibly may be an intermolecular process rather than an internal conversion, there are also numerous experimental data of another kind against this possibility. Thus, in many cases the singlet-singlet *emission* is in a completely different (higher) frequency range from the singlet-triplet *absorption,* so that the assumed condition for a resonance transfer of electronic energy is absent.

Concerning the correspondence of decay constant (as a measure of emission transition probability) and integrated absorption (as a measure of absorption transition probability) in the circumstance that the singlet-triplet absorption is overlapped in part by the lowest singlet-singlet absorption band, in general the question does not come under consideration. Thus, most lowest singlet-triplet separations in complex molecules are sufficiently great so that there is no overlapping of singlet-triplet absorption by singlet-singlet absorption.

Moreover, the mixing of singlet and triplet states is not dependent on the mode of excitation, but on the relationship of the perturbing singlet

[9] *J. Chem. Physics,* 1940, 8, 456.

and the emitting triplet electronic states. Thus, a decay constant of a certain magnitude indicates that the triplet state has a certain amount of singlet character, so that absorption to the former state from the singlet ground state, or emission from that state to the ground state would correspond to the same degree of spin-orbital coupling.

Prof. Franck has indicated that the above answer is not a satisfactory one. In the light of a further discussion with him I should like to add these comments. Aside from the electronic aspect of the problem which is considered above, there is a further point on vibrational-electronic coupling. Not only are there involved oscillations of the triplet state as pointed out by Prof. Franck, but in the emission process, ground state oscillations are excited analogously. The transition probability for both absorption and emission is given by the summation of the transition moment integrals over the vibrational-electronic wave functions. In absorption the wave functions are mainly for the zero-point vibrational level of the ground state and all of the permitted vibronic wave functions of the *excited* state; in emission the wave function for the zero-point vibrational level of the excited state and all of the permitted vibronic wave functions of the *ground* state are involved. Clearly these summations are not the same, and a degree of approximation will be involved in relating the resultant transition probabilities. However, for small configurational changes upon excitation, as may be anticipated for excitation of low electronic levels of multi-bonded nuclei, the relationships may be expected to be quite good. Since these are not calculable, experiment must be used as a guide. Data are now accumulating, and for the half-dozen cases for which reasonably good data are now available, correlations within a factor of 1 to 2 are obtained. Since the lifetimes of, e.g. phosphorescence of molecules range over a factor of 10^6, the correlation is a practicable and useful one.

Prof. R. Mecke (*Freiburg i. Br.*) said: As to the statement by Kasha that in hydroxylic and other solvents vibrational structure is completely blurred, I will refer to my paper (§ II, Fig. 8 and Table III). Here we found phenol to be a hydroxylic compound which is a very sensitive reagent in testing, by the broadening of the OH bands in the infra-red, the effect of solvents on hydrogen bonding. Pure hydrocarbons and halogen derivatives show only a small effect. Aromatic compounds (benzene) broaden the OH band appreciably on account of the π-electrons. Solvents containing oxygen, expecially compounds with carbonyl groups, will almost completely blurr the OH band, so that it is scarcely detectable.

Dr. M. Kasha (*Chicago*) said: The transition probability of absorption bands involving the nitrogen non-bonding electrons ($n \rightarrow \pi^*$) was the same for pyridine in both hydrocarbon and hydroxylic solvents (including water).

Mr. A. R. Burgess (*I.C.I., Welwyn Garden City*) (*contributed*): It is interesting to try to interpret some photochemical reactions in terms of Dr. Kasha's paper. It seems that an $n \rightarrow \pi^*$ excitation results in chemical reactivity developing at the atom carrying the lone pair. Thus, if benzophenone is irradiated in alcohol solution, tetrabenzpinacol is formed in 80 to 90 % yield (even in the presence of oxygen). This may be interpreted in the following scheme,

$$(C_6H_5)_2C{=}O \;.\;.\;.\; HOC_2H_5 + h\nu \rightarrow (C_6H_5)_2\dot{C}{-}OH + \dot{O}C_2H_5 \qquad (1)$$

$$2(C_6H_5)_2COH \rightarrow [(C_6H_5)_2COH]_2 \qquad (2)$$

$$2C_2H_5O \rightarrow C_2H_5OH + CH_3CHO \qquad (3)$$

In Kasha's nomenclature, the excitation of the benzophenone is of the type $n \rightarrow \pi^*$. The molecule changes, by intersystem crossing, from a singlet state to the lowest triplet (or "free radical") state, which is presumably responsible for the dehydrogenation of the solvent. This would resemble the direct attack of oxygen on hydrocarbons,

$$RH + O_2 \rightarrow R\cdot + HO_2^{\cdot} \qquad (4)$$

Many other reactions of aromatic carbonyl compounds listed by Schönberg [10] can be explained using the same initial step.

The dehydrogenating action of an excited carbonyl may show up in the aliphatic series. A simple explanation of Norrish's Type II non-radical decomposition of ketones [11] was advanced by Rice and Teller [12] which fits in with this idea.

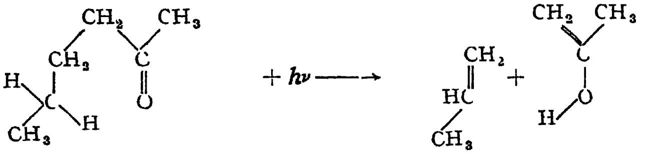
(5)

Recently Blaisdell [13] has shown that photo-excited azobenzene can also dehydrogenate a solvent; again this would seem to involve an $n \rightarrow \pi^*$ transition.

Under the conditions which benzophenone gives 80-90 % yield of the pinacol, we have found that 2-hydroxybenzophenone is quite stable. Its u.-v. absorption is unaltered and evaporation of the solution gives a product of unchanged melting point. This must be due to the intramolecular satisfaction of the dehydrogenating tendency of the excited lone pair. Presumably the hydrogen atom moves to a more central position between the two oxygenation atoms, but it is doubtful if the tautomer is ever formed.

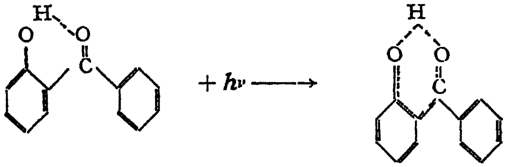
(6)

It is interesting that a large number of 2-hydroxybenzophenones [14] and salicylic compounds [15] have been patented as light stabilizers for plastics. In these laboratories we have concluded that light stabilizers probably function by absorbing powerfully the damaging u.-v. radiation so protecting the light sensitive groups in the substrate. However, the electronic energy gained by the absorber must be lost rapidly (8) before sensitization (9 and 10) can take place:

$$A + h\nu \rightarrow A^* \quad . \quad . \quad . \quad . \quad . \quad (7)$$

$$A^* \rightarrow A + kT \quad . \quad . \quad . \quad . \quad (8)$$

$$A^* + O_2 \rightarrow \text{radicals} \quad . \quad . \quad . \quad . \quad (9)$$

$$A^* + \text{substrate} \rightarrow A + \text{substrate}^* \quad . \quad . \quad . \quad (10)$$

According to Kasha we must in general equate A^* to the lowest triplet state. Either this must be too inactive to undergo reactions (9) and (10) or must itself undergo rapid conversion to the ground singlet state. It will be interesting to see Dr. Kasha's full comments on such conversions. Does he think that this could be brought about by the coupling of the nuclear motion of the H atom with the electronic changes in such hydrogen-bonded molecules?

Prof. H. Sponer (*Durham, N.C.*) (*communicated*): I should like to mention that the research on the picoline spectra by J. H. Rush and myself was finished last year but the results are still unpublished. Since our main objective was a study of the spectra, we made an effort to observe and measure as many bands as possible, that is about 75 bands in α-picoline, about 120 in β-picoline and 65 bands in γ-picoline. An analysis of the spectra has been given. In all three cases did we observe two different systems, one consisting of relatively sharp bands and another consisting of diffuse bands. The diffuseness is least in β-picoline and largest in γ-picoline. In this substance a third system may be present. The solution spectra of the three picolines in *iso*-octane, as taken by Harold P. Stephenson in our laboratory, show the same appearance as those in cyclohexane presented by Dr. Herington, and our curves in alcohol solutions resemble those in sodium hydroxide solutions reported on here.

---

[10] Schönberg and Mustafa, *Chem. Rev.*, 1947, 181.
[11] See Waters, *Chemistry of Free Radicals* (Oxford, 1946).
[12] Rice and Teller, *J. Chem. Physics*, 1938, **6**, 489.
[13] Blaisdell, *Photochemistry in Relation to Textiles* (S.D.C., 1949).
[14] U.S. Pat. 2,364,027; U.S. Pat. 2,434,496.
[15] Brit. Pat. 545, 326.

Prof. H. Sponer (*Durham, N.C.*) said: As was pointed out in the paper by Dr. Cave and Thompson the appearance of the absorption spectra of *o*-, *m*-, *p*-disubstituted benzenes is of interest in connection with structural problems. These spectra show indeed some marked differences. In the cases which were studied in our laboratory, namely the dichlorobenzenes [16] and the xylenes recently by C. D. Cooper, we found that the *para* spectra exhibit the valence vibration of the substituents against the ring carbon atoms in a strong band comparable in intensity to the main totally symmetric carbon vibrations, while the corresponding substituent vibration in the *ortho* and *meta* derivative gives rise to a band of much smaller intensity or it may even be absent. The *para* spectrum usually looks less complex than the other two. This may be connected with the fact that the higher symmetry of the *para* derivative will impose more selection rules than the other lower symmetries do. For two like substituents the *para* spectrum is notably stronger than the other two spectra which has been explained theoretically by Sklar. If, however, the substituents have different directing powers as in the fluorobenzotrifluorides the *para* spectrum may have the least intensity of the three.[17] It would be interesting to determine the *f*-values of the spectra reported by Cave and Thompson.

The appearance of the individual groups in the spectra of di-substituted benzenes is also different for the different isomers. This structure, usually attributed to v—v transitions, has in no case been explained quite satisfactorily. The possibility of overlapping of v—v transitions resulting from various vibrations and of similar transitions involving different vibrations in the upper and lower states will contribute to the complexity.

In connection with the irregularity in the shifts of the 0,0 bands in the fluorobenzotrifluoride series it may be mentioned that Beck [18] has observed that in the series of the di-hydroxybenzenes the usual shift towards lower frequencies along *o*-, *m*-, *p*-substitution is here replaced by the order *m*-, *o*-, *p*-substitution.

The question of which of the fluorinated toluenes shows the sharpest bands seems interesting. We have reasoned from plates taken at low pressures that the *ortho* bands are sharpest in the cases we have studied although the bands of *m*-dichlorobenzene are almost equally sharp. The *p*-dichlorobenzene bands look slightly diffuse. In the xylene series the *m*-compound has the most diffuse bands.

In conclusion, I should like to add that I am pleased to see that the assignments of the benzotrifluoride bands given in the presented paper are practically identical with those discussed by Lowe and myself.[19]

Dr. H. W. Thompson (*Oxford*) said: I am sorry that we had missed the recent work of Sponer and Lowe on benzotrifluoride, but it is very pleasing now to find that our separate vibrational analyses agree so well. As regards the sharpness of the bands found with substituted aromatics, we have had the impression that with ortho derivatives the bands are less sharp than with the *para* compounds, but this may be illusory and may even vary from case to case.

---

[16] *Rev. Mod. Physics*, 1942, **14**, 224.

[17] Sklar, *J. Chem. Physics*, 1942, **10**, 135.

[18] *J. Chem. Physics*, 1950, **18**, 1135.

[19] *J. Opt. Soc. Amer.*, 1949, **39**, 840.

I should like to ask Prof. Sponer about her views on the close groups of bands near those main bands forming the main progressions. We have explained these as $v - v$ transitions, but the intensity relationships are not very satisfactorily explained. This peculiar feature seems to occur with many of the substituted benzenes.

Prof. J. Rud Nielsen (*Oklahoma University, U.S.A.*) said : It may be of interest to point out that the ω'' values given for benzotrifluoride and *m*-fluorobenzotrifluoride agree within a few cm.$^{-1}$ with Raman frequencies recently observed at the University of Oklahoma by Hudson. For *p*-fluorotoluene all but the lowest ω'' value obtained agree with observed Raman frequencies.

Dr. R. N. Haszeldine (*Cambridge*) (*communicated*) : The ultra-violet absorption spectra of the fluoro- and chloro-benzotrifluorides in solution in petroleum ether and in alcohol have been examined. The results for the fluoro-benzotrifluorides are in general agreement with those of Miller and Thompson, with the exception of the values of extinction coefficient. With *m*-fluorobenzotrifluoride there is the expected shift to the red of the intense band of longest wavelength relative to the corresponding band in benzotrifluoride. With the chlorobenzotrifluorides, both *o*- and *m*-chlorobenzotrifluoride have the long wavelength band at approximately 8 mμ further into the red than benzotrifluoride, whereas with *p*-chlorobenzotrifluoride the long wavelength band almost coincides with that of benzotrifluoride itself. There is, however, an inflection at 4mμ furthe into the red than benzotrifluoride. The extinction coefficients for the long wavelength absorption maxima are also anomalous for benzotrifluoride and the *o*-, *m*- and *p*-chlorobenzotrifluorides and are in the approximate ratios 1 : 2 : 1·5 : 0·5, whereas in the series toluene, *o*-, *m*-, *p*-fluorotoluenes, the approximate ratios are 1 : 3 : 2 : 4. The unusual electronic interaction between the trifluoromethyl group and the *para* halogen atom is thus still apparent although reduced for the chlorobenzotrifluorides.

Dr. A. Burawoy (*Manchester University*) (*communicated*) : The evidence advanced for the various suggested assignments of the absorption bands of benzene at about 1800 Å and 2000 Å to certain electronic transitions is, on the whole, rather inconclusive.[20] Based on theoretical considerations and an analysis of the vibrational structure and intensity of the bands, it always involves the consideration of the spectrum of benzene alone.

Attention may, therefore, be called to another empirical approach to this problem which is based on the comparison of the spectrum of benzene with the spectra of its derivatives and leads to a more convincing assignment of the two benzene bands under discussion. This may be illustrated with the help of a few examples which could be easily multiplied [21] :

X	$X—CH=CH—CH=CH_2$[22]			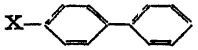			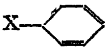		
	Solv.	λ Å	ε	Solv.	λ (Å)	ε	Solv.	λ (Å)	ε
H—	C_6H_{14}	2170	21000	EtOH	2470	19500	C_7H_{16}	2030	6900[24]
H_2N—	,,	2810	24000*	,,	2790	20000	EtOH	2340	11500
O=CMe—	EtOH	2630	27000**	,,	2810	29000	,,	2400	13000
C_6H_5—	,,	2800	28000	C_6H_{14}	2760	35000[23]	,,	2470	19500

* Et_2N— ** O=CH—.

---

[20] Cf. Craig, this Discussion.

[21] My determinations, if not otherwise stated.

[22] Cf. Braude, *Ann. Reports*, 1945, 105.

[23] Gillam and Hey, *J. Chem. Soc.*, 1939, 1170.

[24] Platt and Klevens. *Chem Rev*

The spectra of butadiene and diphenyl show strong long-wave bands at about 2170 Å and 2470 Å.† Substitution of these substances and of benzene by groups such as NH_2, $CCH_3{=}O$ and C_6H_5 is responsible for a shift of these bands as well as of the benzene band system at 2000 Å to longer wavelengths in a similar order, the displacement being also accompanied by similar increases of the intensity. The above groups were arbitrarily chosen because they are of a very different type and responsible for comparatively big effects.

This is convincing evidence that, independent of any interpretation, these absorption bands are of the same type (*K*-bands). Since the strong long-wave absorption bands of conjugated hydrocarbons such as butadiene and diphenyl (and of their derivatives) correspond in Mulliken's terminology to allowed electronic transitions of the *NV* type, the benzene band at 2000 Å should also correspond to the only quantum-mechanically allowed transition of this type with the upper level of symmetry E_{1u}. The comparatively high intensity (ϵ, about 6900) is also better accounted for than by the assumption of any forbidden transition.

Dr. Walsh [25] has already pointed out that it is the benzene band at 2000 Å which fits well in a graph relating the first ionization potential with the frequency of the allowed *NV* transitions for ethylene and its conjugated derivatives, but in the present paper this band is attributed to a Rydberg transition.

Having assigned the upper level E_{1u} to the band at 2000 Å, it is necessary to reconsider the origin of the 1800 Å band. The only alternative is its identification as a Rydberg transition. The authors of this paper have given convincing evidence that this band at least partly represents a Rydberg transition. It may be suggested that the whole absorption band originates in this transition.

Its greater intensity as compared with the higher members of the corresponding Rydberg series is not surprising since the lowest member should have a much higher intensity. The fact that the 1800 Å band is to a much lesser degree influenced by substituents as compared with the 2000 Å band (already recognized by Dr. Walsh [26] and supported by the apparent absence of such bands in more complicated organic molecules at least above about 2300 Å) is in good agreement with this assignment since it indicates an increased localization of the electronic transition.

In the course of their fundamental investigations of the spectra of olefines, Carr and Stücklen [27] have called attention to the similarity of the benzene bands under discussion with those observed in the spectra of ethylene and its homologues. The latter also possess a strong band system at 1650 to 1750 Å and a weaker one (mainly) at longer wavelengths. Substitution of ethylene by alkyl groups leads to an increasing separation of the two band systems indicating a slightly greater influence on the weaker band system.

Carr and collaborators identified the strong system with an *NV* transition and the weaker one with a Rydberg transition. These assignments appear to be generally accepted. This necessitated the assumption that substitution by a vinyl group, e.g. in butadiene, would displace the strong band system at shorter wavelengths of ethylene to about 2100 Å (this band definitely corresponding to an *NV* transition), whereas the weaker band system would be only slightly changed. This is in contradiction to the effect of alkyl groups and, particularly, to the observation that in styrene the weaker 2000 Å band of benzene is much more strongly displaced to longer wavelengths than the intense 1800 Å band.[26]

---

† The " benzene " band of the B_{2u} type to be expected in the spectrum of diphenyl approximately at λ, 2700 Å and ϵ, 500 is not observed, being obscured by this band of much higher intensity.

[25] Walsh, *Ann. Report*, 1947, 39 ; cf. also Mulliken, *J. Chem. Physics*, 1939, **7**, 20, 353 ; Price and Walsh, *Proc. Roy. Soc. A*, 1947, **191**, 22.

[26] Walsh, *Proc. Roy. Soc. A*, 1947, **191**, 32.

[27] Carr and Stücklen, *J. Chem. Physics*, 1936, **4**, 760 ; 1938, **6**, 55 ; 1939, **7**, 631.

These facts indicate that the assignments of these band systems in olefines should be reversed. The 1800 Å benzene band should correspond to the strong bands observed at about 1650 Å in ethylene and 1750 Å in ethylene homologues, butadiene and hexatriene which should also be Rydberg transitions. Its high intensity is accounted for by the presence of three ethylene groups.

Dr. Lucy W. Pickett (*Mt. Holyoke Coll.*) (*communicated*) : Some recent experimental results on the intensity of the absorption of benzene vapour in the vacuum ultra-violet which were obtained at Mount Holyoke College perimental results on the intensity of the absorption of benzene vapour in the vacuum ultraviolet which were obtained at Mount Holyoke College under ONR sponsorship may be of interest in connection with the above papers, one of which attributes the benzene band at 2000 Å to an $A_{1g}-E_{2g}$ transition and the other to the first member of a Rydberg series. The measurements show that this band system has a maximum height $\epsilon=6600$ and an oscillation strength of 0·12. The first band of the group is lower than the others ($\epsilon = 5000$) but not sufficiently so to indicate a transition from a higher vibrational level of the ground state. It seems reasonable to suppose, as was suggested earlier,[28] that a Rydberg transition is superimposed on a forbidden $N \rightarrow V$ transition and that the diffuse appearance of the bands may be partially explained by such superposition.

Dr. G. Herzberg and **Dr. D. A. Ramsay** (*Ottawa*) (*communicated*) : Experiments similar to those reported by Dr. Porter have been in progress at the National Research Council in Ottawa for some time. The starting point of these experiments was the observation of the 4050 Å group of cometary spectra in laboratory sources by one of us [29] and its tentative identification as due to CH_2. An attempt was made to obtain these bands in absorption in ketene that was photochemically decomposed by a mercury lamp. When this proved unsuccessful an apparatus using the flash technique first described by Porter and Norrish was set up. In order to check the efficiency of our set-up we have repeated some of the earlier experiments of Porter on CS and ClO and, in addition, not knowing of Porter's recent work on HS, we have carried out independent work on it.

Our absorption spectra were taken in the second order of a 21-ft. grating giving a dispersion of 1·25 Å/mm. which is considerably larger than the dispersion used by Porter. It was for this reason that with ClO we were able to detect a distinct diffuseness of the rotational lines of the absorption bands of low v' while those of high v' are quite sharp. This diffuseness at low v' is undoubtedly due to a predissociation of the upper electronic state of the ClO bands. The predissociation limit is below the energy of the upper levels of the first observed absorption bands. One is therefore necessarily led to the conclusion that at the convergence limit of the absorption bands dissociation takes place into a normal (^2P) Cl atom and an O atom in the ^1D state. The same conclusion was already drawn by Porter but on the basis of an extrapolation of the vibrational levels of the ground state which is somewhat uncertain. Depending on whether the Cl atom at the convergence is in the $^2P_{3/2}$ or $^2P_{1/2}$ level one obtains for D_0° (ClO) 22141 or 21260 cm.$^{-1}$.

The 0,0 band of HS was obtained in photochemically decomposed H_2S under the same high dispersion as the ClO bands. The satellite branches are well separated from the main branches. The 1,0 band is rather weak at high resolution but stronger at low resolution confirming the suggestion of Porter concerning this point.

In none of our experiments was the diffuse band system given by

---

[28] Carr and Stücklen, *J. Chem. Physics*, 1939, **7**, 631.

[29] Herzberg, *Astrophys J.*, 1942, **96**, 314.

Porter observed. In one experiment, however, when H_2S was photolyzed in the presence of oxygen, the S_2O_2 bands[30] near 3000 Å were obtained.

Dr. R. F. Barrow (*Oxford*) (*communicated*): We have recently obtained the absorption spectra of some relatively long-lived species by using an electrodeless discharge in a large bulb (10 l.). At suitable pressures the luminous discharge may be confined to a region near to the walls of the bulb, leaving the region along the axis of the bulb dark. The absorption spectra of radicals formed presumably near the walls and diffusing into the centre may then be observed. In this way, Mr. R. K. Laird has photographed bands of the $A^2\Pi - X^1\Sigma$ system of CS, the 1, 0 and 0, 0 bands of the $^2\Sigma - X^2\Pi$ system of NS and a progression of CF_2 bands,[31] identical with some of those observed in emission by Venkateswarlu.[32] Qualitative experiments suggest that the life-times are all of the order of a few seconds. CF_2 appears to be one of the first polyatomic radicals to be identified in absorption, and it is worth remarking that its life-time under these conditions seems to be longer than that of CF which has not so far been detected in absorption.

Mr. S. Leach (*Paris*) said: In a recent investigation of the emission of H_2S using a Schüler-type discharge tube, I found the 0,0 band of SH at 3236·6 Å but no trace of any other SH bands. With D_2S the 0,0, 0,1 and 0,2 emission bands of SD were obtained. Work is at present proceeding on an analysis of these bands. In addition to well-known S_2 bands of the $^3\Sigma \rightarrow {}^3\Sigma$ transition there appear about 30 bands between 3100 Å and 4200 Å which show no isotopic displacement and are presumably due to sulphur although they do not fall into any known transition of S_2. No indication was found in emission of the diffuse band system 3168-3797 Å obtained by Porter in absorption.

Prof. P. Goldfinger (*Universite Libre de Bruxelles*) (*communicated*): I should like to ask Dr. Porter whether the following point has been considered. The new value of the dissociation energy of the SH radical of about 85 kcal. permits us to calculate the energy of removal of the first H atom of H_2S if the dissociation energy of S_2 is known: 4·4 eV is the usually accepted value. However, Goldfinger, Jeunehomme and Rosen[33] have given arguments for a lower value of 3·3 eV and Herzberg and Mundie[34] for 3·6 eV. These three values yield for the energy required for the removal of the first H of H_2S, 88, 79 or 75 kcal. Is there any direct evidence about the magnitude of this energy? This could decide, even if it were only an upper limit, the value of D_{S_2}. Or could a comparison with H_2, for which the figures are well known (about 115 and 102 kcal.) help to answer the question about H_2S?

Dr. G. Porter (*Cambridge*) (*communicated*): Like Dr. Herzberg and Dr. Ramsay we have made several attempts to obtain the spectrum of methylene in absorption, some of these experiments being mentioned at a previous Discussion of the Society,[35] and in fact the flash technique was originally developed for this purpose. All attempts have been unsuccessful despite the fact that a partial pressure of methylene of several mm. Hg was probably present in some cases; it is possible that the higher resolution of the apparatus mentioned by Herzberg and Ramsay will be of assistance in this problem. The long life of CF_2 reported by Dr. Barrow is interesting in this connection, we have been unsuccessful in attempts to find the spectrum of CCl_2 in the photochemical decomposition of CCl_4, both alone and sensitized by Cl_2, and it seems improbable that it has a comparable stability. Incidentally CF_2 and CS should not, by the usual definition, be described as free radicals as both have singlet ground states.

---

[30] Vallance-Jones, *J. Chem. Physics* (in press).

[31] Laird, Andrews and Barrow, *Trans. Faraday Soc.*, 1950, **46**, 803.

[32] *Physic. Rev.*, 1950, **16**, 676.

[33] Goldfinger, Jeunehomme and Rosen, *Nature*, 1936, **138**, 205.

[34] Herzberg and Mundie, *J. Chem. Physics*, 1940, **8**, 263.

[35] Norrish and Porter, *Faraday Soc. Discussions*, 1947, **2**, 97.

The diffuse band spectrum obtained in the photolysis of H_2S appeared quite strongly as is shown in Plate I which is taken through 4-cm. H_2S, 1 msec. after the beginning of the flash, the total decomposition being about 25 %. It may have been missed by the other workers owing to the relative weakness of diffuse spectra at high resolution. Owing to this diffuseness the isotope shift is difficult to detect and it will be useful to have measurements of the band system mentioned by Leach, which occurs in the same region, to see whether there are any coincidences.

In reply to the question of Prof. Goldfinger, the only direct evidence about the energy of removal of the first H atom from H_2S is the low frequency limit of continuous absorption at 37,000 cm.$^{-1}$ which is of no assistance in deciding between the three suggested values for $D(S_2)$. All the known data show a close resemblance between the H_2O and H_2S molecules and the OH and SH radicals and although analogies of this kind are somewhat uncertain one would not expect the energy of removal of the first H atom from H_2S to be less than that of the second in view of the great difference in H_2O. If this argument is accepted we are led to $D(S_2) = 4{\cdot}4$ eV rather than the lower values.

Dr. S. Robin and **Dr. B. Vodar** (*Paris*) (*communicated*) : We would like to quote a few results concerned with the solvent effect upon the displacement of the electronic absorption bands. This effect was studied with compressed gases as solvents.[36] The solubility of phenanthrene in compressed N_2, A, or H_2 is sufficient for permitting the study of the strongest ultra-violet bands. Spectra were obtained as a function of pressure up to 1200 atm. Thus it was possible to obtain the displacement of the absorption bands as a function of the solvent density for various solvents H_2, N_2 and A. At equal density the shifts are smaller for H_2 than N_2 or A. For all three solvents the shifts in wave numbers, for bands at about 2450 and 2850 Å, are not far from a linear function of the solvent density ; they are certainly not a quadratic function of this density, as they should be according to the " statistical " theory.[37] However, this theory was developed for the shifts of atomic lines and is not easily applicable to phenanthrene, but some preliminary results found for the sodium resonance line with argon as the compressing gas show that the quadratic shift is certainly not observed up to 1200 atm. This points to the fact that the solvent effects at high densities may perhaps be described only by taking into account the potential energy curves for the solvent and solute.

Finally we want to emphasize that various compressed gases can be used as solvents in the Schumann region where ordinary solvents are not transparent. We recently obtained the absorption spectrum of phenanthrene in argon up to 900 atm. between 2300 and 1500 Å.

[36] Robin, *Compt. rend.*, 1950, **230**, 1757.

[37] Foley, *Physic. Rev.*, 1946, **69**, 616.

II. VIBRATIONAL AND ROTATIONAL SPECTRA

INTRODUCTORY PAPER

By H. W. Thompson

The remarkable development during the past ten years of technical equipment for measuring infra-red and Raman spectra has given a far-reaching stimulus to the application of such measurements in physics

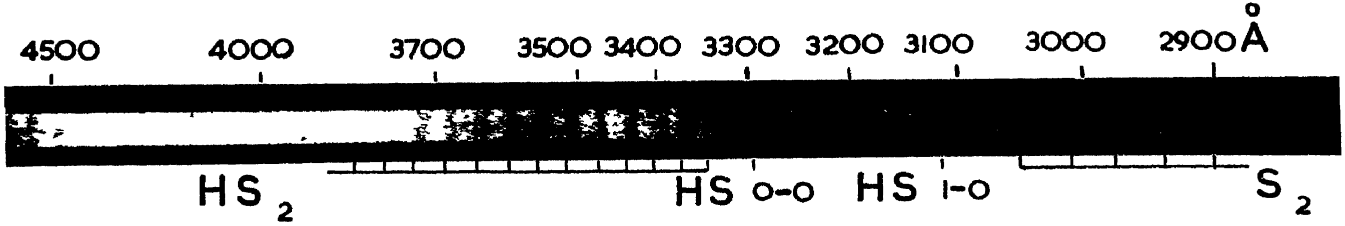

PLATE I.—Spectrum of the products of photolysis of H_2S taken 1 msec. after the flash, showing the diffuse band system attributed provisionally to HS_2.

[*To face page* 82

and chemistry. It would have been impossible within the compass of a Discussion of this kind to deal effectively with all aspects of the field, and therefore we shall not—other than incidentally—deal with the variety of current experimental problems which interest many of those present. I may perhaps say, however, that the underlying basis of the technical advances has been primarily concerned with better methods of detection and measurement of small amounts of radiation, whether in the infra-red, visible or ultra-violet. Moreover, apart from enhanced sensitivity, the speed of measurement and general reliability of the results has been so greatly improved that infra-red work has passed from being a delicate capricious child into a sturdy respected adult.

The effects of these experimental achievements have been twofold, namely (1) to provide greater freedom in choosing the kind of apparatus suitable for different kinds of problem, and (2) to allow us, because of the increased detector sensitivity, to introduce ancillary equipment appropriate to certain problems which by its very nature may involve a loss in the detectable energy. Thus, on the one hand quick scanning of the infra-red spectrum using the oscillograph can now be applied to the study of flames and rapid reactions, robust recording spectrometers of moderate speed and good resolving power are available for routine industrial work, or infra-red apparatus without a dispersing element can be applied to analytical determinations. On the other hand, spectra can be measured at low temperatures, or with polarized radiation, and crystals or fibres may be measured if a reflecting microscope is harnessed to a suitable spectrometer.

At the time of the last Discussion on this subject held by this Society five years ago, the sharp impact of the new technique upon essentially chemical problems had just become felt. It had been possible to measure rapidly the vibrational spectra of a large number of fairly complex compounds, thus revealing the significance of the new tool in chemical analysis and structural diagnosis. Since that time, an immense volume of work has been carried out which has restored a balanced application in both physics and chemistry, and points to many useful applications in biochemistry. It may be pertinent to note that whereas most of the earlier work had the primary aim of measuring frequencies as accurately as possible, i.e. the positions of lines and bands, more recently we have been at least equally concerned with the intensities of absorption.

The kind of information which we can obtain is determined primarily by the kind of molecule which is to be examined. With very small molecules, usually in the vapour state, analysis of the rotational structure of vibration bands may lead to knowledge of the molecular geometry, and to the assignment of frequencies to normal modes. Closer examination of some of these bands using the higher resolving power now available promises to give further information about vibrational-rotational energy interactions, and the energy levels of polyatomic molecules, about the anharmonic character of vibrations, and to lead to a deeper understanding of molecular dynamics in general. In some of these cases, special phenomena such as internal rotation of molecular groups or the inversion of pyramidal structures like ammonia can be explored. The intensities of absorption of infra-red rotation lines or bands, or of Raman lines, are also of great interest, since with smaller molecules where some sort of normal co-ordinate treatment can be made it may be possible to correlate the intensities with the ionic properties or polarizabilities of bonds. Results show, however, that in many such simple cases, the standard absorption laws break down, and the question arises whether any general absorption law can be formulated. Measurements on pressure broadening, in this connection, can lead to information about processes of energy transfer during molecular collisions. From a more practical standpoint, the understanding of such absorption laws for simple gases is vital in such fields as meteorology, where atmospheric gases are to be determined.

With molecules of intermediate size, too, we may in some cases hope to derive an essentially complete assignment of frequencies, and the main features of the molecular structure both as regards geometry and internal field of force. The use of isotopes, especially deuterium, has often extended such theoretical analysis. Even when the vibrational analysis is incomplete, the spectra can be used empirically for analysis and sometimes for diagnosis. More recently, attention has been directed to the study of spectra under different conditions, e.g. in different states of aggregation and particularly at low temperatures. The selection rules permitting appearance of vibration bands with a free molecule of given symmetry may be completely changed if the molecule is placed in a crystal lattice and surrounded by a field of essentially different symmetry. Bands usually sharpen at lower temperatures and hence it may arise that a degenerate mode of the free molecule may be split up in the crystal, and the nature of such splitting may conversely indicate the symmetry properties of the crystal. Alternatively, the occurrence of phase changes in the solid state may be accompanied by spectral changes. Also, when rotational isomerism can arise, the influence of temperature upon the intensities of bands may reveal much about this phenomenon.

With highly complex molecules, such as polymers, peptides, carbohydrates, or resins, our approach must be somewhat different. A complete vibrational analysis is impossible here, but the spectra of different molecular skeletons usually show sufficiently characteristic differences as to make empirical differentiation and analysis possible. More important, however, is the fact that certain atomic groupings retain in different molecules essentially constant vibration frequencies, so that key bands can be adopted for diagnosis. Tables of such correlations have now been drawn up and have been valuable not only in working out the structure of new compounds of biological interest, but also for detecting unsuspected groups in synthetic polymers and condensates. A recent extension of this work has come from the use of polarized infra-red radiation, which enables us to determine in some measure the relative orientation of special groups in an ordered or crystalline structure, or to estimate chain branching or chain folding, and thus elucidate further the relationship between molecular structure and physical properties.

Several other points deserve special mention. For instance, there is good cause to think that hydrogen bridge formation is of fundamental importance in controlling the properties of many kinds of compound, and infra-red spectroscopy is well suited to its investigation. Yet we cannot at present maintain that this phenomenon is at all well understood, and there is still room for more work on the subject. Again, the development of the region of mm. and cm. waves and the enormous resolving power which can be obtained there has already given data about the rotational spectra of simple molecules from which bond lengths and molecular geometry can be determined with high precision, far exceeding that possible by other infra-red methods. These measurements, providing as they do other information about nuclear spin moments, internal torsion and so on, are of supreme value, but it must be realized that infra-red measurements on the higher vibrational levels are still required for a complete knowledge of the molecular dynamics.

The later part of this Discussion will deal with the reflecting microscope. This instrument, which in the infra-red has obvious advantages over a refracting instrument, was used several years ago for studying very small quantities of material and for fibres, and its great promise for work with crystals, particularly using polarized radiation, has still to be exploited. The possibility of using it for work with biological cells and tissues involves certain limitations, but that will emerge in our subsequent discussion.

This, then, provides an outline of the topics which will be considered at this Discussion. We shall first deal with the smaller molecules, problems of geometric structure, frequency assignment, and molecular dynamics. We shall then deal with complex molecules, many of which are of interest in relation to the biology of the living cell which is to follow. Some questions which may well be in our minds throughout are: (1) what can we learn further about the dynamics and force fields in the simpler molecules, (2) how far can we safely use the correlation of frequencies with groupings in diagnostic work, and (3) how can we extend our knowledge by the use of special additional techniques such as low temperature spectroscopy, polarized radiation or the reflecting microscope.

A STUDY OF THE LOW FREQUENCY FUNDAMENTAL BANDS IN THE SPECTRUM OF AsH_3

BY HARALD H. NIELSEN

Received 10*th July*, 1950

An analysis of the two low frequency fundamental bands ν_3 and ν_4 in AsH_3 is attempted and conclusions drawn in a previous paper [1] are thereby tested.

The two high frequency fundamental bands in the infra-red spectrum of AsH_3 and AsD_3 (ν_1 and ν_2 in Dennison's notation) have been studied and an analysis of their structure has been reported upon in an earlier article.[1] This analysis permitted certain conclusions to be drawn concerning the dimensions of the molecule and concerning the force constants. We shall attempt in this article to report on an analysis of the two low frequency fundamental bands (ν_3 and ν_4 in Denison's notation) in AsH_3 and thereby test the conclusions drawn in the earlier paper.

The experimental details are the same as those discussed in the earlier communication. The measurements were made using an absorption cell 24 cm. long fitted with windows of NaCl and filled with gas to a pressure of about 30 mm. Hg. The spectrograph used has been described elsewhere [2] and was equipped with a replica grating made by Wood with 3600 lines per inch concentrating the radiant energy of 7·0 μ in first order. The data was recorded with slits equivalent to a frequency interval of about 0·25 cm.$^{-1}$. The data, redrawn from the records, are shown as the upper curve of Fig. 3. Table I gives the positions of the lines in the high frequency branch of the higher frequency band and the low frequency branch of the lower frequency band. The lines in the region between the bands form a pattern too complicated for analysis and their frequency positions are not given here.

The frequency ν_4 is a perpendicular band. It arises from a transition from the normal vibration state to the two-fold degenerate state characterized by the quantum numbers $V_4 = 1$ and $l_4 = \pm 1$, V_4 being the total vibration quantum number and l_4 being the quantum number of angular momentum associated with $V_4 = 1$. Each rotation level is, moreover, two-fold degenerate corresponding to the plus and minus values of the rotation quantum number K. Hence every rotation-vibration energy level would be four-fold degenerate in K and l_4 except for the fact that the degeneracy is partly removed by a Coriolis interaction between rotation and the two components of the vibration ν_4. Each of these component

[1] McConaghie and Nielsen, *Physic Rev.*, 1949, **75**, 604.
[2] Bell, Noble and Nielsen, *Rev. Sci. Instr.*, 1947, **18**, 48.

states remains, nevertheless, two-fold degenerate. The frequency ν_3 is a parallel band and arises from a transition from the normal vibration state to a state characterized by the vibration quantum number $V_3 = 1$. This state is non-degenerate. The frequencies ν_3 and ν_4 are nearly coincident in the AsH_3 molecule and here, unlike in the instance of ν_1 and ν_2, a rather strong Coriolis coupling between them is to be expected. The net Coriolis interaction between the frequencies ν_3 and the two components of ν_4 is, therefore, similar to that which occurs in molecules like CH_4 where three-fold degenerate vibrations exist. Coriolis interactions in symmetric molecules of the nature here described have been discussed by Nielsen[8] where it was shown that the energy matrix breaks down into steps, a separate step for each value of J. Each substep, corresponding to a given J value, is found to consist of $3(2J + 1)$ rows and columns and will factorize into further substeps. Since $|K| < J$ there will always be two identical steps with a single element each, two identical steps each with two rows and columns and the rest will have three rows and columns each. The form of the determinant for the general substep is found to be

TABLE I.—TABLE OF LINE FREQUENCIES IN THE BANDS ν_3 AND ν_4 IN AsH_3*

Line No.	Frequencies in cm.$^{-1}$	Line No.	Frequencies in cm.$^{-1}$	Line No.	Frequencies in cm.$^{-1}$
−19	857·5	14	1022·5	47	1077·9
−18	857·8	15	1023·5	48	1078·7
−17	860·0	16	1024·7	49	1079·9
−16	861·7	17	1025·7	50	1080·8
−15	864·5	18	1027·1	51	1084·0
−14	866·3	19	1027·9	52	1086·2
−13	868·0	20	1028·5	53	1088·0
−12	875·1	21	1030·4	54	1089·1
−11	875·8	22	1032·4	55	1090·0
−10	876·7	23	1035·0	56	1090·8
− 9	879·3	24	1037·0	57	1093·8
− 8	883·6	25	1037·6	58	1094·7
− 7	887·6	26	1038·9	59	1096·1
− 6	889·2	27	1040·8	60	1097·3
− 5	891·8	28	1044·7	61	1098·3
− 4	893·5	29	1045·7	62	1099·2
− 3	899·5	30	1047·4	63	1100·5
− 2	904·4	31	1049·0	64	1104·8
− 1	906·9	32	1050·6	65	1105·8
		33	1054·1	66	1106·8
1	1005·4	34	1054·9	67	1107·9
2	1005·9	35	1056·1	68	1108·7
3	1007·2	36	1058·1	69	1110·2
4	1008·9	37	1059·7	70	1114·3
5	1010·0	38	1061·0	71	1115·7
6	1010·8	39	1064·0	72	1116·7
7	1011·7	40	1065·6	73	1118·4
8	1013·1	41	1067·2	74	1119·3
9	1014·6	42	1068·3	75	1120·5
10	1016·3	43	1069·9	76	1125·5
11	1018·5	44	1071·5	77	—
12	1020·3	45	1076·4	78	—
13	1021·6	46	1077·2	79	—
				80	1129·6

* The data given here are from the dissertation, *A Study of Some Bands of* AsH_3, AsD_3, PH_3, presented in 1948 by Virginia Marie McConaghie for the degree of Doctor of Philosophy at the Ohio State University, Columbus, Ohio.

---

[8] Nielsen, *Physic. Rev.*, 1945, **68**, 181.

$$\begin{array}{c|c|c|c|}
 & K+1 & K & K-1 \\
\hline
K+1 & -K-1-\epsilon & \left[\frac{J(J+1)-K(K+1)}{2}\right]^{\frac{1}{2}}a & 0 \\
\hline
K & \left[\frac{J(J+1)-K(K+1)}{2}\right]^{\frac{1}{2}}a & -\delta-\epsilon & -\left[\frac{J(J+1)-K(K-1)}{2}\right]^{\frac{1}{2}}a \\
\hline
K-1 & 0 & -\left[\frac{J(J+1)-K(K-1)}{2}\right]^{\frac{1}{2}}a & K-1-\epsilon \\
\hline
\end{array} = 0,^{1}$$

where

$$-\epsilon = [(R_0 - R_2 - 3R_3) + K^2(R_2 + 6R_3) + K^4 R_3 - E/hc]/2(\zeta Z_e - R_2 - 2R_3)$$

and $\quad \delta = -\Delta/2(\zeta Z_e - R_2 - 2R_3)$

with $\quad \Delta = (R_0 - R_0' - R_2 - 3R_3) + K^2(R_2 - R_2' + 6R_3)$.

The R_t in the above are those defined in an earlier paper,[4] the primed and unprimed values referring to ν_3 and ν_1 respectively. a in (1) is defined to be

$$\xi_{34}[(\omega_3 + \omega_1)/(\omega_3\omega_4)]^{\frac{1}{2}} B_e/2(\zeta Z_e - R_2 - 2R_3),$$

where $$B_e = h/8\pi^2 I_{xx}^{(e)} c$$

and ξ_{34} is the Coriolis coupling factor between ω_3 and ω_4. There will be an odd number of substeps with three rows and columns each and these will be identical in pairs except for the step where $K = 0$ which is unique. The substep where $K = 0$ may be factorized to give the roots $\epsilon = -1$ and

$$\epsilon = -[(1 + \delta)/2] \pm \{[(1 - \delta)/2]^2 + J(J + 1)a^2\}^{\frac{1}{2}},$$

the latter two roots degenerating to $\epsilon = -\delta$ and $\epsilon = -1$ when $J = 0$. It is interesting to note that the residual two-fold degeneracy of the rotation-vibration levels of the state ν_4 referred to earlier is thus removed by the perturbation for the states, where $K = l_4 = +1$ and $K = l_4 = -1$. This is a case of l-type doubling entirely like that discussed by Nielsen[5] except that here the perturbing frequencies are close enough to each other to produce resonance. The effect is, therefore, of first-order significance. The determinant (1) leads to the well-known Coriolis splitting, discussed by various authors,[6] in spherically symmetric molecules where $I_{xx}^{(e)} = I_{zz}^{(e)}$ $\omega_3 = \omega_4$ and also $\zeta_1 = \xi_{34}$.

Application of the Theory to the Observed Bands.—An analysis of the observed bands from which the constants of the molecule might be determined in the usual manner does not seem to be a practicable procedure here because of the extreme overlapping of the high frequency side of ν_3 with the low frequency side of ν_4 which prevents effective application of the combination principles. Moreover, if the energy levels were identified each value would have to be identified with some value ϵ *before* evaluation of the molecular constants could be carried out. Theoretically, the evaluation of ϵ depends in general on the solution for the roots of a cubic equation. Since this is, at best, a difficult task we have chosen to proceed in the following somewhat different manner.

We have anticipated, from previous knowledge concerning such interactions, that their effect will also here be essentially to alter the effective moments of inertia in the excited states. We shall here assume that the deviations of the moments of inertia in these excited states from the values obtained for them in the normal state due to other causes than the Coriolis interaction is negligible. We shall take Δ to be simply $\nu_4 - \nu_3$ and set it equal to 100 cm.$^{-1}$ which is approximately the distance between band centres. It is necessary further to draw some conclusions concerning ξ_{34}. This quantity has been expressed theoretically by Shaffer [7] who gives for it the following relation

---

[4] Nielsen, *Physic. Rev.*, 1941, **60**, 794.

[5] Nielsen, *ibid.*, 1950, **77**, 130.

[6] Johnson and Dennison, *ibid.*, 1935, 48, 868; Jahn, *Proc. Roy. Soc. A*, 1938, **168**, 469.

$$\xi_{34} = \delta[\beta(1 - b^2)^{\frac{1}{2}} - \alpha b/\sqrt{2}],$$

where

$$b^2 = (1 - I_{zz}^{(e)}/2I_{xx}^{(e)})$$

and α, β and δ are constants of a transformation to normal co-ordinates and may be evaluated from a knowledge of the normal frequencies. We have evaluated ξ_{34} to be about 0·54. A verification of this value may be had in the following manner. The coefficient of δ in the relation for ξ_{34} is found to be 0·86. It was concluded in our earlier work on ν_1 and ν_2 that the Coriolis coupling coefficient ξ_{12} must be very close to zero. One may obtain an independent value of 0·87 for $[\beta(1 - b^2)^{\frac{1}{2}} - \alpha b/\sqrt{2}]$ if ξ_{12}, given by Shaffer [5] to be

$$\xi_{12} = \nu[\alpha(1 - b^2)^{\frac{1}{2}} + \beta b/\sqrt{2}],$$

is set equal to zero so that

$$\alpha = - \beta b/\sqrt{2}\,(1 - b^2)^{\frac{1}{2}},$$

remembering that

$$\alpha^2 + \beta^2 = 1.$$

The degenerate Coriolis coupling factor ζ_4 may be determined from the relation

$$\zeta_2 + \zeta_4 = (I_{zz}^{(e)}/2I_{xx}^{(e)}) - 1,$$

ζ_2 having been found in the earlier work to be $\zeta_2 = - 9{\cdot}0602$. The value obtained is $\zeta_4 = - 0{\cdot}432$. When the above quantities are substituted into (1) the energies for various values of J and K may be obtained by solving for the roots ϵ. This has been done here up through the value of $J = 10$.

The selection rules governing the transitions must be known before predictions concerning the spectrum may be made. The frequency ν_4 is a perpendicular vibration where the selection rules are $\Delta J = \pm 1, 0$; $\Delta K = \pm 1$ and the frequency ν_3 is a parallel vibration where the selection rules are $\Delta J = \pm 1, 0$; $\Delta K = 0$. The Coriolis interaction links these two vibrations so that in both instances both types of transitions are permitted. It becomes a prohibitive task, however, to calculate the degree to which the mixing of the wave function of the two frequencies takes place, but in any event, it seems unlikely that it need be taken into account in computing the intensities since only when the rotational energies are large compared to the difference $\nu_3 - \nu_4$ will the effect be significant. This would be true only for large values of J and K. It has, therefore, been assumed that for transitions to the higher frequency component of the resonating doublet $(\nu_4 : \nu_3)$, (Dennison's notation) the selection rules are those for a perpendicular vibration and for transitions to the lower frequency component of the resonating doublet $(\nu_3 : \nu_4)$, the selection rules are those for a parallel band.

It is not possible to set down explicitly the energies of the molecule in the excited state because the energies depend upon the roots of a cubic equation. Neither, therefore, can the frequency positions of the lines be set down explicitly. A study of the roots of (1) for various values of J and K allows one to state, however, that the interval between the highest frequency components of the groups of lines in the high frequency branch of the band $(\nu_4 : \nu_3)$ (i.e. $J \rightarrow J + 1$; $K = J - 1 \rightarrow K = J$) is very nearly equal to $\Delta\nu = (21 - \zeta_4)C$. Similarly, one may show that the intervals between the lowest frequency components of the groups of lines in the low frequency branch of the band $\nu_3 : \nu_4$ (i.e. $J \rightarrow J - 1$; $K = 0 \rightarrow K = 0$) increase with J from $\Delta\nu = 2B$ to $\Delta\nu = 2(1 - 4\xi_{34})B$. The principal effect of the interaction on the energy levels is to produce characteristic convergences in the bands. Since bands in which Coriolis resonance interactions of the nature here described occur have not, to the author's knowledge, been studied before Fig. 1 and 2 are inserted. Fig. 1(*a*) shows the Q branches of a perpendicular band ($\Delta J = 0$, $\Delta K = \pm 1$) for a molecule like AsH_3 where the interaction is set equal to zero. Fig. 1(*b*) shows the effect of the perturbation in the case of AsH_3 on each of the Q branches. It is of interest to note how the first ^RQ branch is split into two parts because of the removal of the degeneracy of $K = l = \pm 1$, one part where the components diverge toward higher frequencies and another part where all the components fall together. Fig. 2(*a*) shows the appearance of the ^RR lines associated with $J = 7$, K taking the values $K = 0$ to $K = 6$ for a molecule like AsH_3 when the Coriolis resonance interaction is set equal

---

[7] Shaffer, *J. Chem. Physics*, 1941, 9, 607.

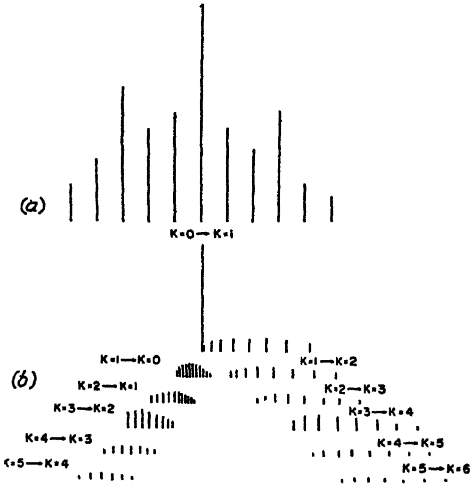

FIG. 1.—Structure of ^PQ and ^RQ branches in a symmetric molecule where Coriolis resonance does not exist and where Coriolis resonance does exit.

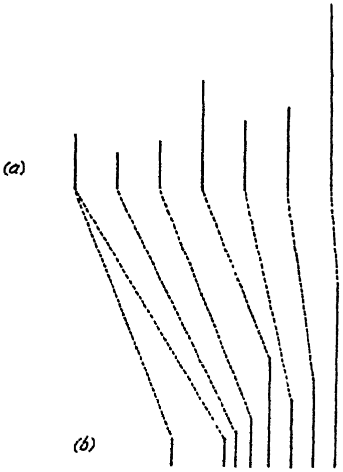

FIG. 2.—^RR lines in a symmetric molecule where Coriolis resonance does not exist and where resonance does exist.

to zero. Fig. 2(*b*) shows the effect of the perturbation on these same lines for the AsH_3 molecule. The lines in the high frequency branch of $(\nu_4 : \nu_3)$ predicted from the energy levels computed from (1) using the constants stated earlier with C' set equal to 3·628 cm.$^{-1}$ are shown below the experimental curve in Fig. 3(*b*). The intensities have been computed on the basis that the mixing of the wave functions may be neglected for the J values involved in the transitions involved here. It is further assumed that the two parts of the first ^RR branch have the same intensity. It is seen that the agreement between experiment and theory is good, particularly among the ^RR lines.

The frequency ν_3 in XY_3 molecules may be regarded essentially as one where the pyramid is deformed symmetrically, i.e. alternately flattened and made more pointed. It is, moreover, evident that in such molecules two positions of equilibrium will exist for the X atom, one at a distance h_0 above and another at a distance h_0 below the Y_3 triangle. The double minimum of the potential energy function associated with the vibration has a result that the vibration levels occur in pairs, one symmetric and the other antisymmetric with respect to a reflection at the origin. In the instance of the NH_3 molecule, which may be regarded as the prototype of all XY_3 molecules, the doubling is approximately 1 cm.$^{-1}$ in the lowest state, but in the first excited state the doubling is about 35 cm.$^{-1}$. The frequency ν_3 is therefore a double parallel band with two Q branches and in which two sets of P and R lines can be identified. The reader is referred to the work of Sheng, Barker and Dennison [8] for a complete discussion of this band.

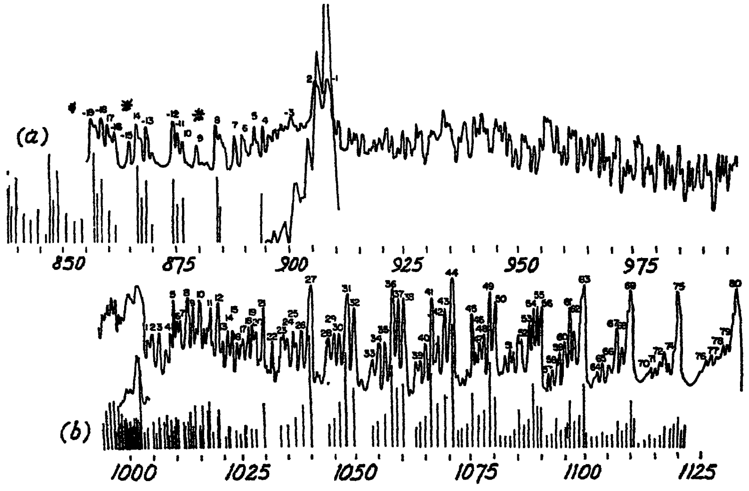

FIG. 3.—The frequencies ν_3 and ν_4 in the infra-red spectrum of AsH_3.

The Q branch in the band ν_3 in the spectrum of PH_3 was observed by Fung and Barker [9] to be double in nature, the separation being about 2·4 cm.$^{-1}$. This was interpreted by them and subsequently by Sutherland, Lee and Wu [10] to mean that the doubling in the normal state is negligible and in the first excited state is equal to about 2·4 cm.$^{-1}$. Sutherland, Lee and Wu have argued convincingly that the doubling in the AsH_3 molecule must be a great deal smaller than in the PH_3 molecule. It is, therefore, surprising to observe that the Q branch in the band ν_3 (i.e. $(\nu_3 : \nu_4)$) also has a doubling of about 2·5 cm.$^{-1}$. Nevertheless, an attempt was first made to interpret the region $(\nu_3 : \nu_4)$ in the spectrum of AsH_3 on the basis that it was a double parallel band, as with NH_3, with band centres separated about 2·5 cm.$^{-1}$. One encounters the immediate difficulty that two sets of *P* lines are not observed; in fact, if one superimposes two parallel bands separated by 2·5 cm.$^{-1}$ plotted from the energies for the component $(\nu_3 : \nu_4)$ as determined from (1) one obtains entirely too many lines. On the other hand, if it is assumed that the doubling in the first excited state is also negligible, i.e. 0·1 cm.$^{-1}$ or less, the band which one would observe would be a single parallel band. Such a band, predicted from the energies given by (1), will be seen in Fig. 3(*c*). Again the intensities are those for the unperturbed molecule. It will be seen that this band predicted theoretically accounts for all the lines observed except four or five. Those nearest the centre of the band may almost certainly be ascribed to transitions higher than $J = 10$ contributing to the *Q* branch. No immediate explanation is available for the two lines farther from the centre and marked with asterisks, although they might perhaps be ascribed to lines in the extremity of the low frequency branch of $(\nu_4 : \nu_3)$. It is also just conceivable that they might be two of the most intense lines in a transition from the first excited vibration state to the second.

---

[8] Sheng, Barker and Dennison, *Physic. Rev.*, 1941, **60**, 786.
[9] Fung and Barker, *ibid.*, 1934, **45**, 238.
[10] Sutherland, Lee and Wu, *Trans. Faraday Soc.*, 1939, **35**, 1373.

It is suggested, therefore, that the doubling of the *Q* branch in $(\nu_3 : \nu_4)$ in the spectrum of AsH_3 is only an apparent one which is due to the nature of the convergence of the *Q* branch caused by the perturbation we have considered. The lines for transitions up through $J = 10$ contributing to the *Q* branch were plotted as triangles, the base of which is about equal to twice the effective slit width and the result integrated. The result of this is shown in Fig. 3(*c*) although the individual lines are not indicated. It is suggested that the reason the two principal components appear equally intense experimentally is due to the fact that the gas sample used was sufficient to produce complete absorption at these points.

It is, of course, of interest to inquire what the inversion doubling is in PH_3. While this spectrum will be discussed elsewhere the reader is referred to the bands $(\nu_3 : \nu_4)$ and $(\nu_4 : \nu_3)$ [11] which are extremely similar to the corresponding bands in AsH_3. It will be seen that the *P* branch of $(\nu_3 : \nu_4)$ plotted in 3(*c*) is almost an exact reproduction of $(\nu_3 : \nu_4)$ as observed in the PH_3 spectrum. This suggests further that even in PH_3 the doubling is only an apparent one and that the doubling in both the lower and first excited states may be regarded as negligible.

A knowledge of the altitude h_0 of the AsH_3 pyramid will permit an estimate of the splittings of the vibration levels of ν_3 to be made if certain assumptions concerning the potential barrier restricting the passage of the As atom through the H_3 plane can be made. This problem has been studied by Dennison and Uhlenbeck [12] who have adopted a potential function which may be expressed in the following manner:

$$2V/h\nu_3 = (x - x_0)^2 \text{ from } x = (x_0 - \alpha) \text{ to } x = +\infty;$$
$$2V/h\nu_3 = (x + x_0)^2 \text{ from } x = (\alpha - x_0) \text{ to } x = -\infty$$
and $$2V/h\nu_3 = \alpha^2 \text{ from } x = (x_0 - \alpha) \text{ to } x = (\alpha - x_0).$$

They have derived the following relations for the splittings in the normal and first excited vibrational states.

$$(\Delta\nu_0/\nu_3) = (2\alpha/\pi^{\frac{1}{2}}) \exp[-\alpha^2 - 2(x_0 - \alpha)(\alpha^3 - 1)^{\frac{1}{2}}] \quad . \quad . \quad . \quad (2)$$
$$(\Delta\nu_1/\nu_3) = [(4\alpha^3 - 4\alpha)/\pi^{\frac{1}{2}}] \exp[-\alpha^2 - 2(x_0 - x)(\alpha^2 - 3)^{\frac{1}{2}}] \quad . \quad . \quad (3)$$
where $$h_0 = (h/4\pi^2\mu\nu_3)^{\frac{1}{2}}x_0 \text{ and } \mu = 3mM/(3m + M),$$

h being Planck's constant.

The assumption we shall make here is that the height of the potential barrier *V* remains the same for AsH_3 as for the NH_3 molecule where the splittings are well known. The potential barrier in the case of NH_3 may be computed from the relations (3) to be about 1770 cm.$^{-1}$. Using the above assumption we obtain then for α and x_0 in the instance of AsH_3 these values, $\alpha = 1{\cdot}943$ and $x_0 = 8{\cdot}212$. Substituting these values into (3) a value $\Delta\nu_1 = 0{\cdot}004$ cm.$^{-1}$ is obtained. While the above approximation is admittedly rough and the splittings of the vibration levels calculated in this manner can not be expected to be of great accuracy they should, nevertheless, be of the right order of magnitude. As may be seen, the value obtained for $\Delta\nu_1$ is far too small to be observed spectroscopically, thus tending to confirm our earlier conclusion concerning the splitting of the levels in the frequency ν_3 in AsH_3.

---

[11] McConaghie and Nielsen, *Proc. Nat. Acad.*, 1948, **34**, 456.
[12] Dennison and Uhlenbeck, *Physic. Rev.*, 1932, **41**, 313.

The author wishes to make grateful acknowledgment to the Research Corporation, New York City, for a grant-in-aid which faciliated the accomplishment of this work.

Mendenhall Laboratory of Physics,
The Ohio State University,
Columbus, Ohio.

INFRA-RED SPECTRUM AND STRUCTURE OF THE HNCO MOLECULE

BY G. HERZBERG AND C. REID

Received 12th June, 1950

The infra-red spectrum of cyanic acid vapour from 400 to 14,000 cm.$^{-1}$ has been studied with medium and, above 8000 cm.$^{-1}$, with high dispersion. Comparison of the spectrum with that of related molecules shows that free cyanic acid in the vapour phase consists only of HNCO molecules (isocyanic acid). The structure of the observed bands shows conclusively that the NCO group in HNCO is very nearly linear and that the H atom is off that line. All six fundamentals of HNCO have been found and have been confirmed by the observation of a considerable number of overtone and combination bands. A brief discussion of the spectra of liquid and solid HNCO is included.

A. Introduction

The structure of "cyanic acid" has been the subject of several investigations but up to this time has remained in some doubt. This doubt applies both to its chemical constitution and to its geometrical structure. With regard to the former the weight of evidence seems to be in favour of the keto form, that is, of the structure H—N═C═O (isocyanic acid) rather than H—O—C≡N. The chemical properties of the esters of cyanic acid suggest strongly the keto-form. The study of the ultra-violet absorption spectrum by Woo and Lin [1] has revealed diffuse absorption bands in the region 2570-2250 Å very similar to those in various amines and thus suggesting the presence of an NH bond. According to Goubeau [2] the Raman spectrum of liquid cyanic acid shows it to have the keto form since the strongest frequency is 1307 cm.$^{-1}$ similar to the isosteric CO_2. The keto form is also supported by early calculations of Heitler and Rumer [3] on the basis of an extension of the original Heitler-London valence theory.

[1] Woo and Lin, *J. Chem. Physics*, 1935, **3**, 544.
[2] Goubeau, *Ber.*, 1935, **68**, 912.
[3] Heitler and Rumer, *Göttinger Nachr.*, 1930, 277.

On the other hand, more recently, Werner and Gray [4] have concluded on the basis of the two solid polymers formed from liquid cyanic acid that the liquid is a mixture of the keto and enol forms. Moreover, according to Goubeau [2] some salts show Raman lines characteristic of the keto form (e.g. AgNCO) while others show lines characteristic of the enol form (e.g. KOCN).

The geometrical structure of HNCO has been discussed by Herzberg and Verleger.[5] They found in the photographic infra-red, with an absorbing path of 4 m., a single irregular band at 9700 cm.$^{-1}$ which suggested that the molecule was far from being a symmetric top and therefore that the N—C—O group was not linear. However, the electron diffraction data of Eyster, Gillette and Brockway [6] point rather strongly to a linear or nearly linear structure of the NCO group both in HNCO and CH_3NCO. This conclusion is further supported by the similarity of the infra-red spectra of CH_3NCO and CH_3N_3 found by Eyster and Gillette.[7]

The present investigation represents an attempt to settle more definitely the question of the chemical and geometrical structure of cyanic acid by means of a detailed study of its infra-red spectrum in the vapour phase. A brief re-investigation of the Raman spectrum of the liquid is included. Up until now no investigation of the infra-red spectrum of this substance seems to have been made except for the above-mentioned observation of one photographic infra-red band by Herzberg and Verleger.

B. Experimental

Cyanic acid was prepared by the thermal depolymerization of cyanuric acid. The general technique employed was similar to that described by Linhard,[8] but the following modifications were found necessary to ensure good yields.

(*a*) Preliminary heating *in vacuo* to 200° C was found necessary to remove water. Failure to observe this precaution led to the formation of some ammonia during the depolymerization.

(*b*) The depolymerization was carried out *in vacuo*, and because of the tendency for cyanuric acid to sublime without depolymerization it was found necessary to volatilize it slowly at a rather low temperature (450° C) and pass the gas stream through a hotter tube furnace (700° C).

(*c*) The bulk of the HNCO was collected in a trap kept at − 80° C, and the CO_2 which is formed in appreciable quantities during the reaction, passed on to a second guard trap cooled by liquid nitrogen. This reduced considerably the fractionation time necessary to obtain a pure product.

The material prepared in this way and further purified in the manner described by Linhard (oxidation of any HCN formed by Ag_2O, final drying by P_2O_5 and distillation from a bath at − 30° C) had a vapour pressure which agreed well with the values given by Linhard. It was considered better than 99·5 % pure.

The infra-red spectrum of the vapour was examined in the region 450-8000 cm.$^{-1}$ by means of a Perkin-Elmer Model 12B Infra-red Spectrometer using 10 cm. and 100 cm. absorption cells, and LiF, NaCl and KBr prisms. In addition the infra-red spectrum of the solid at − 190° C was recorded with the same instrument using a layer of about 0·1 mm. thickness. The photographic infra-red spectrum of the vapour was investigated with a 21 ft. grating spectrograph in a 5 m. glass absorption tube in which an absorbing path of up to 500 m. was obtained by multiple reflections according to the technique of White [9] as modified by Bernstein and Herzberg.[10] An upper limit to the vapour pressure which could be used was set by the fact that above 14 cm. spontaneous polymerization is liable to occur. (If the vapour was only in contact with glass, occasionally pressures above 20 cm. were attained before polymerization but in the presence of metal surfaces polymerization was always induced at lower pressures.)

---

[4] Werner and Gray, *Sci. Proc. Roy. Dublin Soc.*, 1947, **24**, 209.

[5] Herzberg and Verleger, *Physik. Z.*, 1936, **37**, 444.

[6] Eyster, Gillette and Brockway, *J. Amer. Chem. Soc.*, 1940, **62**, 3236.

[7] Eyster and Gillette, *J. Chem. Physics*, 1940, **8**, 369.

[8] Linhard, *Z. anorg. Chem.*, 1938, **236**, 200.

[9] White, *J. Opt. Soc. Amer.*, 1942, **32**, 285.

[10] Bernstein and Herzberg, *J. Chem. Physics*, 1948, **16**, 30.

The Raman spectrum of liquid cyanic acid at − 40° C was photographed for us by Dr. D. Andrychuk using a Toronto-type mercury lamp and a Zeiss spectrograph of dispersion 40 Å/mm.

TABLE I.—OBSERVED INFRA-RED ABSORPTION BANDS OF HNCO VAPOUR

ν_{vac} (obs.) (cm.$^{-1}$)	Band Type [a]	Intensity	Assignment	ν(calc.) [b]
572	irr. c.	8300	ν_5 (a')	—
(670)	irr. $\perp$?	16000	ν_6 (a'')	—
797	res. hybrid	31000	ν_4 (a')	—
1134	unres. c.	270	$2\nu_5$ (A')	1144
1236	irr. c.	44	$\nu_5+\nu_6$ (A'')	1240
1327	unres. p.	580	ν_3 (a')	—
1371 (?)	p.[c]	150	$\nu_4+\nu_5$ (A')	1369
1480	p. (+H_2O)	44	$\nu_4+\nu_6$ (A'')	1467
1592	p. (+H_2O)	44	$2\nu_4$ (A')	1594
1802	p. (+H_2O)	35	$2\nu_5+\nu_6$ (A'') ?	1814
1895	‖ *PR*	150	$\nu_3+\nu_5$ (A')	1899
1980	p.	100	$\nu_3+\nu_6$ (A'')	1997
2018	p.	300		
2060	p.	500		
2116	p.	1000	$\nu_3+\nu_4$ (A')	2124
2145	p.	4000		
2168	p.	4000		
2202	p.	7000	[d]	—
2274	‖ *PR*	100000	ν_2 (a')	—
2594	irr. c.	80	$\nu_3+\nu_5+\nu_6$ (A'')	2596
2650-2800	several p.	20	unassigned [e]	—
2865	‖ *PR* ?	120	$\nu_2+\nu_5$ (A')	2846
2951	irr. c.	240	$\nu_2+\nu_6$ (A'')	2944
3063	unres. hybrid	500	$\nu_2+\nu_4$ (A')	3071
3531	res. hybrid	24000	ν_1 (a')	—
4091	irr. c.	460	$\nu_1+\nu_5$ (A')	4103
4206	irr. c.	550	$\nu_1+\nu_6$ (A'')	4201
4349	irr. c.	1300	$\nu_1+\nu_4$ (A')	4328
4530	p.	160	$2\nu_2$ (A')	4548
4864	‖ *PR*	290	$\nu_1+\nu_3$ (A')	4858
5790	unres. hybrid	140	$\nu_1+\nu_2$ (A')	5805
6913	p. unres. hybrid	680	$2\nu_1$ (A')	6912·7
7428	p.	12	$2\nu_1+\nu_5$ (A')	7485
7538	p	10	$2\nu_1+\nu_6$ (A'')	7583
7692	p.	50	$2\nu_1+\nu_4$ (A')	7710
8250	res. hybrid [f]	(10)	$2\nu_1+\nu_3$ (A')	8240
9162·9	res. hybrid	(5)	$2\nu_1+\nu_2$ (A')	9187
10145·1	res. hybrid	(15)	$3\nu_1$ (A')	—
10525	res. ‖	(1)	$2\nu_1+\nu_2+\nu_3$ (A')	10514
10790	res. $\perp$	(1)	$3\nu_1+\nu_6$ (A'')	10815
10988	res. hybrid [f]	(1)	$3\nu_1+\nu_4$ (A')	10942
13217·2	res. hybrid	(2)	$4\nu_1$ (A')	13228·2

[a] irr. = irregular band.
unres. = unresolved band.
res. = resolved band.
c. = band for which the centre is given in column 1.
= wave number refers to a peak.
‖ *PR* = parallel band with *P* and *R* maximum; the minimum between the two maxima is given in such cases.
(+H_2O) = overlapped by H_2O bands.

[b] Harmonic oscillator approximation except for $\nu_1\nu_1$ for which the formula on p. 3B is used.

[c] This peak may belong to the band ν_3 at 1327.

[d] Probably one of the ^PQ peaks of the $\perp$ component of ν_2.

[e] Probably *Q* branches of adjacent bands.

[f] Not analyzed, rough band centre.

C. Observed Spectra

The infra-red absorption spectrum of HNCO as derived from recordings with the Perkin-Elmer spectrometer is shown in Fig. 1 which covers the region

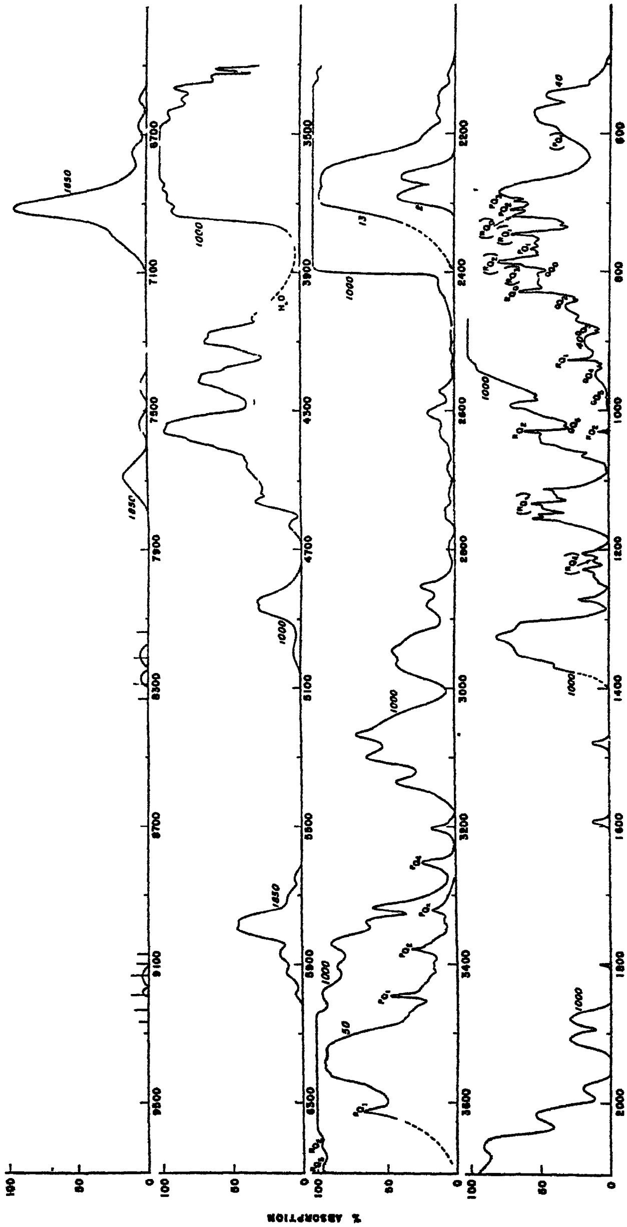

FIG. 1.—Infra-red absorption spectrum of HNCO.

The two bottom strips are plotted on twice the wave number scale as the two top strips. The product of pressure and path (in cm. × cm.) is indicated by italic numbers written on the curves.

400 to 8000 cm.$^{-1}$. The top curve refers to an absorbing path of 100 cm. at a pressure of 10 cm. below 5300 cm.$^{-1}$ and of 18·5 cm. above that wave number. In the regions of strong bands additional curves for lower pressures or path lengths

are given (compare the italic numbers near the curves which give the product of pressure and path in cm. × cm.). The centres of the observed bands are listed in Table I. The band at 2274 cm.$^{-1}$ is by far the strongest band. Taking its intensity as 100,000 (and assuming Beer's law) approximate intensities of the other bands are listed in the fourth column of Table I.

Table I includes seven bands found in the photographic infra-red. Of these the one at 10,145 cm.$^{-1}$ is the strongest. Two of the photographic infra-red bands are included in Fig. 1. Their contours, unlike those of the ordinary infra-red bands, are not drawn to scale. It is to be noted that the band at 9700 cm.$^{-1}$ found by Herzberg and Verleger[5] is not among the bands found here with much longer paths. Comparison of the old plates with new photographs of the photographic infra-red spectrum of NH_3 prove conclusively that the 9700 cm.$^{-1}$ band is really the $3\nu_1$ band of NH_3 which must have been present as an impurity. This result removes the only argument mentioned above against the linear structure of the NCO group. Moreover, the photographic infra-red bands that have been observed and definitely assigned to HNCO show clearly very widely spaced sub-bands as would be expected for a molecule with one very small moment of inertia. This wide rotational structure is partially resolved even in the ordinary infra-red (see Fig. 1). These observations establish the presence of one very small moment of inertia for the HNCO molecule and therefore the *nearly linear structure of the* NCO *group.*

The wide structure of the bands causes the absorption spectrum in the region of the low frequency fundamentals (400-1000 cm.$^{-1}$) to appear rather complex. It was hoped that by studying the spectrum of the solid at − 190° C the spectrum would be simplified and the band centres could be determined more precisely. Even though this did not turn out to be the case the band centres observed in the solid are given in Table II along with the newly determined Raman frequencies of the liquid at − 40° C and the corresponding infra-red values for the vapour.

TABLE II.—SPECTRUM OF LIQUID AND SOLID HNCO

Assignment	Raman Spectrum of Liquid HNCO		Infra-red Spectrum of Solid HNCO	Infra-red Spectrum of HNCO Vapour
	Present Authors	Goubeau		
$\nu_5+\nu_6$	—	1204	—	1236
ν_3	1318	1307	1326	1327
$\nu_4+\nu_5$	—	—	1377	1371
$\nu_4+\nu_6$	—	—	1460	1480
ν_2	—	—	2246	2274
ν_1	3410	3320	3133	3531

D. Vibrational Analysis

The rotational structure of the absorption bands of HNCO will be discussed in more detail in a separate paper by one of us. From the presence of several sub-bands in each infra-red band it follows immediately that not all four atoms can be on one straight line but rather that the molceule is approximately a symmetric top. The moments of inertia of this top in the lowest vibrational level were found to be

$$I_A = 0{\cdot}9153_7 \times 10^{-40}, \quad I_B = 75{\cdot}90_7 \times 10^{-40}, \quad I_C = 76{\cdot}82_4 \times 10^{-40} \text{ g.cm.}^2.$$

The fact that I_A is appreciably smaller than even the moment of inertia of free NH (which is 1·714 × 10^{-40}) shows conclusively that the three heavy atoms N—C—O must lie at least approximately in one straight line with the H atom off that line at an angle much different from 90°. All four atoms are most probably in one plane.[11] The structure is entirely similar to that of the iso-electronic N_3H established by Eyster.[12]

The point group to which such a molecule belongs is C_s; there is only one element of symmetry, the plane of the molecule. Consequently there are two species of normal vibrations and eigenfunctions designated A' and A'' which are respectively symmetric and antisymmetric with respect to the plane of symmetry. It is readily seen [13] that five of the six normal vibrations of HNCO belong to species A' and only one to species A''. The former are designated ν_1, ν_2, ν_3, ν_4, ν_5 in order of decreasing frequency, and the latter ν_6. In Fig. 2 these normal vibrations are represented schematically.

---

[11] It would be difficult to prove this point rigorously from the spectrum.

[12] Eyster, *J. Chem. Physics*, 1940, 8, 135.

Since the figure axis of the nearly symmetric top lies in the plane of the molecule (at a small angle to the N—C—O line) the antisymmetric vibration ν_6 (a'') and any overtone and combination bands of species A'' will give rise to perpendicular bands consisting of a series of sub-bands of spacing $2(A-B)$. On the other hand for the symmetric vibrations the change of the dipole moment occurs in a direction which is in general not at right-angles to nor in line with the figure axis. Therefore the corresponding bands are in general hybrid bands consisting of both a perpendicular and a parallel contribution. The ratio of these two contributions varies for different vibrations.

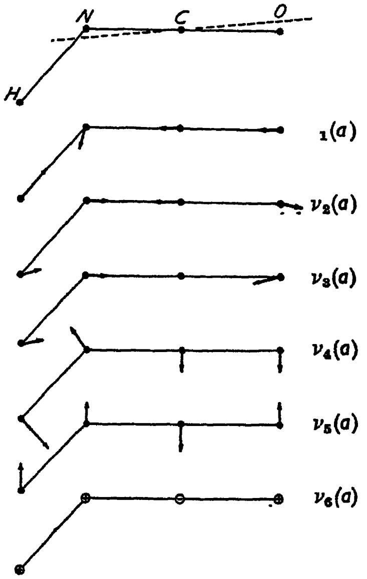

FIG. 2.—Normal vibrations of HNCO.

The vector diagrams are qualitative. The geometrical dimensions are drawn according to the results of the rotational analysis.

With these considerations in mind most of the fundamentals are readily identified. The strong band at 3531 cm.$^{-1}$ is a clear example of a hybrid band; the strong double maximum at the centre corresponds to the ∥ component; the side maxima are Q branches of the sub-bands of the ⊥ component. This band must be identified with the N—H vibration ν_1. The very strong band at 2274 cm.$^{-1}$ shows almost only ∥ structure and fits the assignment ν_2. The magnitude of this frequency is similar to that of the antisymmetric stretching vibration ν_3 of CO_2 into which HNCO would go over if one could combine the H and N nuclei. The predominant ∥ character of this band is in agreement with the fact that the NCO group gives the main contribution to the change of dipole moment for this vibration as in CO_2. The vibration ν_3 of HNCO is expected to have about the same frequency as the symmetric vibration (ν_1) of CO_2. It must be identified with the strong Raman band 1318 cm.$^{-1}$ of HNCO. The corresponding infra-red band at 1327 cm.$^{-1}$ is comparatively weak corresponding to the fact that ν_1 of CO_2 is infra-red inactive. Even though this band corresponds to an N—C—O stretching vibration it has pronounced hybrid

[13] See, for example, Herzberg, *Molecular Spectra and Molecular Structure, II : Infra-red and Raman Spectra of Polyatomic Molecules* (New York, 1945).

character because the dipole moment change in the N—C—O group is very small (compare CO_2) and the motion of the H atom gives the main contribution.

Two strong perpendicular or hybrid bands are superimposed in the region 650-1000 cm.$^{-1}$. On the basis of the rotational levels of the ground state of HNCO known from the photographic infra-red spectrum an analysis of the coarse rotational structure of one of these bands has been possible and the band centre has been located at 798 cm.$^{-1}$ This band has clearly a || and a ⊥ component. The Q branches of the sub-bands are indicated in Fig. 1. It seems certain that this band is due to the N—H bending vibration ν_4. The peaks at 786, 760, 746, 732, 720 and 683 cm.$^{-1}$ are not accounted for in this way. They must be ascribed to a second band whose centre we assume to be at 670 cm.$^{-1}$ (see below).

A third strong band occurs near 572 cm.$^{-1}$ whose insufficiently resolved structure suggests a hybrid band with predominating || component. It appears natural to interpret the two bands 670 and 572 cm.$^{-1}$ as due to the two HN—C—O bending fundamentals ν_5 and ν_6 (see Fig. 2), that is, corresponding to the CO_2 fundamental $\nu_2 = 667$ cm.$^{-1}$. Since ν_6 is a pure perpendicular band it cannot be identified with the band at 572 cm.$^{-1}$. Thus we are led to the assignment $\nu_5 = 572$, $\nu_6 = 670$ cm.$^{-1}$. The structure of the 670 cm.$^{-1}$ band is not sufficiently clear to show conclusively that it has no || component. The spacing of the observed peaks is rather less than one would expect for a ⊥ band. However, in view of the proximity of ν_6 to ν_4 a strong Coriolis interaction may be expected similar to that discussed by Nielsen[14] for H_2CO. Evidence for this is the anomalously large divergence of the Q branches of ν_4 toward higher wave numbers. With this in mind a provisional assignment of the peaks not belonging to ν_4 has been made in such a way that they diverge to lower wave numbers (see the designations in parentheses in the botton strip of Fig. 1). It is assumed that the $^PQ_1$ peak is superimposed on the 572 cm.$^{-1}$ band and ^PQ branches at longer wavelengths lie beyond the region accessible to us. That is why the zero line (670 cm.$^{-1}$) is placed to the long-wavelength side of the prominent peaks mentioned above. It must be admitted that this point in the vibrational analysis is not entirely satisfactory and needs further study with higher resolution. The fundamentals are printed in bold-face type in Table I.

In addition to the fundamentals a considerable number of overtone and combination bands has been found (see Fig. 1). The assignments are readily obtained and are given in Table I. The series of hybrid bands ν_1, $2\nu_1$, $3\nu_1$, $4\nu_1$ extending into the visible region is particularly noteworthy. It can be represented by the formula

$$\nu_{v_1} = 3605{\cdot}6\, v_1 - 74{\cdot}65\, v_1^2,$$

which has been derived from the two most accurately measured bands, ν_1 and $3\nu_1$.

The three vibrations ν_4, ν_6, ν_5 occur in combination with each of the other fundamentals ν_1, ν_2, ν_3 as well as with $2\nu_1$, forming fairly characteristic groups of three bands. Their structure is similar to that of the group of fundamentals ν_4, ν_6, ν_5 but not as well resolved. The || components seem to be more prominent. However, $\nu_1+\nu_6$, $\nu_2+\nu_6$, $\nu_3+\nu_6$ should be pure ⊥ bands just like ν_6. A way out of this difficulty seems to be to assume that again the Coriolis interaction between $\nu_1+\nu_6$ and $\nu_1+\nu_4$ (and similarly for the other pairs) complicates the rotational structure. An alternative would be to assume that the group of lines near 700 cm.$^{-1}$ is due to $2\nu_6$ (A') which, like ν_4 and ν_5, would be a hybrid band. Its strength could be accounted for by Fermi resonance with ν_4 which would occur in a similar way in all the combination bands mentioned. This assumption would place ν_6 at 350 cm.$^{-1}$, a value that appears rather too low but perhaps not impossibly so. Our equipment did not allow a recording of the absorption spectrum near 350 cm.$^{-1}$.

E. Discussion

As mentioned in the Introduction there has been some uncertainty with regard to the constitution of HNCO although the arguments in favour of the isocyanate structure are rather strong. In presenting the vibrational analysis of its spectrum we have tacitly assumed that the HNCO structure is the correct one. A number of additional arguments confirm this assumption.

---

[14] Nielsen, *J. Chem. Physics*, 1937, **5**, 818. Ebers and Nielsen, *ibid.*, 1937, **5**, 822.

The fact that the large number of infra-red bands can be readily accounted for in terms of six fundamentals is strong evidence that only one type of molecule exists in the vapour and not a tautomeric mixture of two forms, confirming Goubeau's conclusion from the Raman spectrum of the liquid.[15] This rules out the existence of a keto-enol equilibrium as assumed by Werner and Gray.[4]

That the form actually occurring is HNCO and not HOCN is confirmed by a comparison with certain other molecules. Table III gives the frequencies and estimated intensities of the stretching vibrations of HNCO, CO_2, HN_3, N_2O, HNCS and OCS. As mentioned before there is a considerable similarity between HNCO and CO_2. If the structure of cyanic acid were HOCN it would be expected to be similar to FCN. While the spectrum of this molecule has not been investigated it is clear that in the series of isoelectronic molecules $O{=}C{=}O$, $O{=}N{\equiv}N$, $F{-}C{\equiv}N$ the asymmetry increases. In CO_2 one of the stretching vibrations is so symmetrical that it does not occur in the infra-red, in N_2O both stretching vibrations are very strong in the infra-red. The fact that in cyanic acid the lower stretching vibration is quite weak in the infra-red shows that the molecule is nearly symmetric, that is, similar to CO_2 and not to FCN ; in other words, the molecule has the structure HNCO. It may be noted that in N_3H which corresponds to N_2O both N—N—N stretching vibrations are about equally strong in the infra-red.

The HNCO structure is further confirmed by the fact that thiocyanic acid has one very similar frequency. The 3531 cm.$^{-1}$ frequency of cyanic acid by itself might have been equally well accounted for as an NH or an OH frequency ; but in thiocyanic acid the frequency 3536 cm.$^{-1}$ can only be an NH frequency. The close agreement of the two frequencies in HNCS and HNCO makes it certain that also in HNCO the observed frequency (3531 cm.$^{-1}$) is due to an NH vibration and that the molecule is HNCO rather than HOCN.

TABLE III.—STRETCHING VIBRATIONS OF RELATED MOLECULES

$HN{=}C{=}O$	$O{=}C{=}O$	$HN{=}N{\equiv}N$	$O{=}N{\equiv}N$	$HN{=}C{=}S$	$O{=}C{=}S$
3531 *s*	—	3335·6 *m*	—	3536 *s*	—
2274 *vs*	2349·3 *vs*	2140·4 *s*	2223·5 *vs*	1963 *vs*	2050·5 *vs*
1327 *w*	$\left\{\begin{matrix}1388{\cdot}3\\1285{\cdot}5\end{matrix}\right.$ *R*	1269·0 *s*	1285·0 *vs*	995 *s*	859·2 *vs*

The large deviation of the NH frequency in HNCO and HNCS from that in N_3H is noteworthy. It emphasizes the need for caution in drawing conclusions from the agreement or non-agreement of normal frequencies in polyatomic molecules.

The large shift of the NH frequency in going from the vapour to the liquid (see Table II) is due to hydrogen bonding. An even larger shift occurs for example for the OH frequency in CH_3OH (see [13]). The vapour-liquid shift of the frequency ν_3 is very much smaller than that of ν_1. There appears to be an additional large shift of ν_1 in going from the liquid to the solid indicating stronger hydrogen bonding.

We are greatly indebted to Dr. D. Andrychuk for a photograph of the Raman spectrum of liquid cyanic acid.

National Research Council,
Division of Physics,
Ottawa, Canada.

---

[15] The infra-red spectrum allows one to ascertain that there cannot be more than 0·5 % of a tautomer while the Raman spectrum had placed this limit at 5 %.

INFRA-RED ABSORPTION SPECTRA OF TWELVE SUBSTITUTED BENZENE DERIVATIVES FROM 15 TO 40 MICRONS

By Earle K. Plyler

Received, 29th June, 1950

The infra-red spectra of benzene and twelve benzene derivatives have been measured in the liquid state in the region from 14 to 38 μ in order to observe the location of the bands and to compare the experimental values with those that have been theoretically predicted. The substituted benzenes included were the mono-substituted halogen benzenes, toluene, ethylbenzene, the three dimethylbenzene isomers, and the three trimethylbenzene isomers, all of which were highly purified samples.

Assignments of the observed bands of benzene are discussed, and a table is given listing the observed bands and their classifications for the singly and doubly substituted benzenes. A list is also given of the observed bands of the trimethylbenzene isomers, and their classifications are discussed.

A brief discussion of the experimental method used in the long wavelength measurements with the thallium bromide-iodide prism is included.

For certain types of measurements in the infra-red region a prism spectrometer is better suited than a grating spectrometer. At present nearly all testing and analysis is carried out with a sodium chloride prism, whereas the potassium bromide and thallium bromide-iodide prisms have been employed somewhat sparingly for such work. Since 1946 prisms of thallium bromide-iodide have been grown and its use has extended the spectral region to 40 μ. This crystal is usually grown with 58 % thallium iodide and 42 % thallium bromide. A certain amount of difficulty has been experienced in the growth of high quality pure crystals, and consequently some prisms contain regions of different indices that cause a blurring of the image and lead to poor resolution. The crystal is so soft that it has been necessary to devise special methods for polishing. These methods have been perfected to the point that surfaces which are flat to within three fringes of green light for over 95 % of each of the prism faces can be obtained. Usually there can be observed a large number of very fine scratches which are insignificant in the long wavelengths unless they produce scattered reflections. The prism is held in position by sealing it to the prism table. If the prism is clamped to the table with the pressure at the top, deformation may result. Over a period of two years no appreciable change in the index of refraction of the prism has been observed.

Some prisms have been tested that introduce a large amount of stray radiant energy, and in some cases this has been found to originate in the body of the prism. Two prisms of good quality have been obtained and a partial separation of the water absorption lines at 357·5 and 359 cm.$^{-1}$ has been accomplished. A Golay cell and a Perkin-Elmer thermocouple have been used for detectors. The instrument is calibrated by the use of the water absorption lines as measured by Randall, Dennison, Ginsburg, and Weber.[1] In order to reduce the water absorption when spectral measurements are being taken, drying agents are placed under the cover of the spectrometer.

Many substances have been measured from 14 to 40 μ, and as a class the substituted benzenes show the most intense absorption bands in this region.

[1] Randall, Dennison, Ginsburg and Weber, *Physic. Rev.*, 1937, 52, 160.

Experimental Results

Samples of chlorobenzene, bromobenzene and fluorobenzene were obtained from Dr. D. R. Stull of Dow Chemical Company and were purified in their laboratories. The iodobenzene was obtained from Eastman Kodak Company and was redistilled at this Bureau. All remaining compounds were obtained from Dr. F. D. Rossini of the Chemistry Division of this Bureau, where they were purified under his direction in connection with the American Petroleum Institute Project No. 6.

Since most of these materials have been previously studied in the region from 2 to 15 μ using a sodium chloride prism, and some [2] have been measured to 22 μ, this paper is concerned only with frequencies less than 650 cm.$^{-1}$.

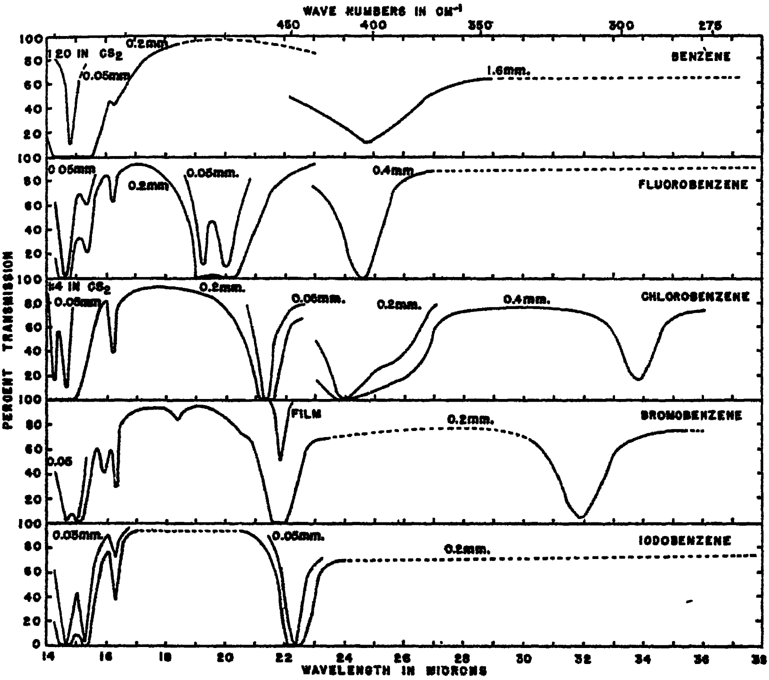

FIG. 1.—The infra-red absorption spectra of benzene, fluorobenzene, chlorobenzene, bromobenzene, and iodobenzene from 14 to 38 μ. The observations for the insert curve marked " film " in bromobenzene were made on a thin layer of the liquid between two potassium bromide windows.

In Fig. 1 are shown the spectra of benzene, fluorobenzene, chlorobenzene, bromobenzene, and iodobenzene from 14 to 38 μ. A cell of 1·6 mm. in thickness is necessary to observe the weak benzene band at 403 cm.$^{-1}$. This band is also observed in the Raman spectrum for liquid benzene. The halogen substituted benzenes all contain a very intense band in the region between 450 and 525 cm.$^{-1}$, which is not present in the spectrum of benzene. Also the band at about 608 cm.$^{-1}$ is considerably stronger in the substituted benzenes. At lower frequencies there are other bands which are characteristic of the particular compound. The dotted portions of the curves represent regions where only general absorption and no bands of appreciable strength were observed even when fairly thick cells were used.

The spectra of toluene, ethylbenzene, 1 : 2-dimethylbenzene, 1 : 3-dimethylbenzene, and 1 : 4-dimethylbenzene from 14 to 40 μ are shown in Fig. 2. The band that occurs at 465 cm.$^{-1}$ in toluene is of high intensity. The other compounds have one or two intense bands and other bands of lower intensity. In order to observe the bands in the region from 24 to 40 μ in these compounds, cell thicknesses of the order of 0·4 to 1·6 mm. were necessary. The 1 : 2-dimethylbenzene band at 38 μ, however, is sufficiently intense that it shows considerable absorption when a 0·2 mm. cell was used.

---

[2] *Catalog of infra-red absorption spectrograms* (American Petroleum Institute Research Project 6 at the National Bureau of Standards).

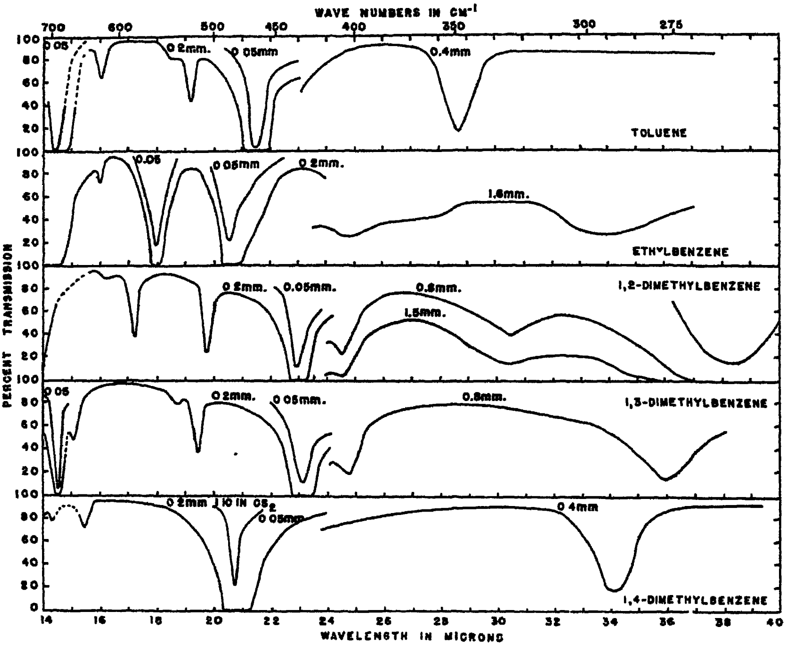

FIG. 2.—The infra-red absorption spectra from 14 to 40 μ of toluene, ethylbenzene, 1 : 2-dimethylbenzene, 1 : 3-dimethylbenzene, and 1 : 4-dimethylbenzene.

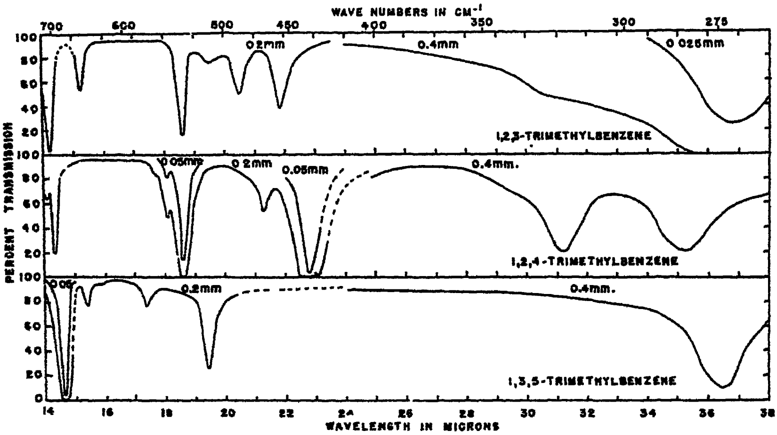

FIG. 3.—The infra-red absorption spectra of 1 : 2 : 3-trimethylbenzene, 1 : 2 : 4-trimethylbenzene, 1 : 3 : 5-trimethylbenzene from 14 to 38 μ.

In Fig. 3 are shown the infra-red spectra of 1 : 2 : 3-trimethylbenzene, 1 : 2 : 4-trimethylbenzene, and 1 : 3 : 5-trimethylbenzene from 14 to 38 μ. The 1 : 2 : 3- and 1 : 2 : 4-isomers are characterized by several bands in this region, the latter by the two strong bands at 18·7 and 22·9 μ. A strong band was observed at $38\ \mu$ for 1 : 2 : 3-trimethylbenzene as it was for 1 : 2-dimethylbenzene. There is noted a marked similarity between the spectra for 1 : 3 : 5-trimethylbenzene and 1 : 4-dimethylbenzene. The spectra of these two compounds include only a few bands most of which are not very intense in this region.

A group of substituted benzenes which includes toluene, chlorobenzene, bromobenzene, and iodobenzene has been investigated by Barchewitz and Parodi [3] and has been compared by them with the Raman spectral data obtained by Kohlrausch. Most of the intense bands found in this investigation for these four compounds were also observed by Barchewitz and Parodi. These authors, however, listed additional bands in each compound that were not observed in this study although the cell thicknesses used here were even greater than the ones used in their investigation. These extra bands may have been produced by impurities. For example, the bands listed at about 360 cm.$^{-1}$ for chlorobenzene, bromobenzene, and iodobenzene were not observed in the present study.

Discussion

A number of workers [4, 5, 6, 7, 8] have considered the normal vibrations of benzene. In the work of Pitzer and Scott [9] the problem has been reconsidered leading to a characterization of the modes of vibration and an assignment of frequencies. Fig. 4 illustrates the motion of those modes that are of particular importance in discussing the frequencies of benzene and its derivatives that are considered in the present paper. For example, 6*a* and 6*b* represent a doubly degenerate motion of the carbon skeleton which gives rise to the band at 610 cm.$^{-1}$ in benzene. The position of this weak band was not precisely determined. When one or more substitutions are made for the hydrogens in benzene, thereby reducing the molecular symmetry, the motions will be somewhat altered, and the frequencies will be shifted and split, but may still be characterized by the same numbering system. Since the vibrations 6*a* and 6*b* at 610 cm.$^{-1}$ involve principally carbon motions the shifts will not be great. The same may be said for the other low-frequency skeletal vibrations, 16*a* and 16*b*, which occur in benzene at 403 cm.$^{-1}$ The other bands which could be

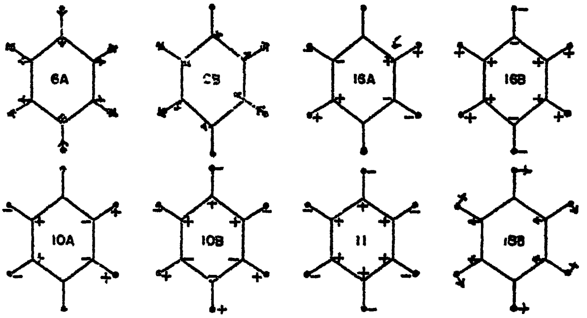

FIG. 4.—Eight of the normal modes of vibration according to Pitzer and Scott [9] of the benzene molecule which would be expected to give rise to bands in the region from 150 to 650 cm.$^{-1}$ for the substituted benzenes; + and − refer to motions above and below the plane of the ring.

---

[3] Barchewitz and Parodi, *J. Physique Rad.*, 1939, **10**, 143.

[4] Wilson, *Physic. Rev.*, 1934, **45**, 706.

[5] Langseth and Lord, *Danske Vidensk Selskab. Math.-Fys. Medd.*, 1938, **16**, 1.

[6] Angus, Bailey, Hale, Ingold, Leckie, Raisin, Thompson, and Wilson, *J. Chem. Soc.*, 1936, 912.

[7] Bailey, Hale, Ingold and Thompson, *ibid.*, 1936, 931.

[8] Herzberg, *Infra-red and Raman Spectra of Polyatomic Molecules* (D. van Nostrand Co., Inc., New York, N.Y., 3, 1947), p. 347.

[9] Pitzer and Scott, *J. Amer. Chem. Soc.*, 1943, **65**, 803.

expected in the long wavelength region are out-of-plane bending vibrations of the substituents altering the benzene ring, as illustrated by 10*a*, 10*b* and 11, and in-plane bending vibrations, as illustrated by 18b.

The molecular symmetry requires certain selection rules, which limit the number of active bands in the infra-red spectrum, and which reduce or eliminate the coincidences between the infra-red and the Raman frequencies. When thick cells are used, these "forbidden" bands may appear, and in addition difference bands and a few combination and overtone bands may be observed. For example, the 403 cm.$^{-1}$ band in benzene (16*a* and 16*b*) is of low intensity, a 1·6 mm. layer of benzene transmitting about 20 % of the radiation. From the selection rules this band should not be active in the infra-red spectrum, and its presence indicates that the symmetry of the molecule has been altered by the liquid state. Another forbidden band, 6_{ab}, was observed with low intensity at 610 cm.$^{-1}$ which is in good agreement with the value found in the Raman spectrum. Since the observations were made on the material in the liquid state, this Raman band is also found in the infra-red. In the mono-substituted benzenes, all 4 frequencies, 6*a*, 6*b*, 16*a* and 16*b* become infra-red active. When the spectra of the mono-substituted halogens are observed, an intense band appears in each spectrum with a wave number between 400 and 525 cm.$^{-1}$ depending on the halogen involved. As the position of this band is only slightly affected by the particular halogen, it must not involve primarily the motion of the halogen. The bands with wave numbers between 400 and 525 cm.$^{-1}$ and at about 620 cm.$^{-1}$ are classified as 6*a* and 6*b* vibrations respectively. The spectrum of fluorobenzene has two additional bands at 405 and 499 cm.$^{-1}$. These bands are classified as the in-plane 18*b* and the out-of-plane 16*b* vibrations. In chlorobenzene the two corresponding bands occur at 297 and 415 cm.$^{-1}$, and the bromobenzene spectrum shows one of the bending vibrations with a wave number of 314 cm.$^{-1}$ which is assigned to the classification of 16*b*. In bromobenzene no intense bands were observed between 330 and 425 cm.$^{-1}$. When cells of 1 mm. in thickness were used, some general absorption was observed in this region.

The spectrum of toluene has been classified by Pitzer and Scott.[9] They assign the intense band at 465 cm.$^{-1}$ to type 16*b* and the band at 347 cm.$^{-1}$ to the bending vibration 18*b*. The small band at 521 cm.$^{-1}$ is attributed to 6*a*. This is in good agreement with the regular shift in frequency of this band with mass of the substituent in the halo-benzenes, if the CH_3 group may be considered as a unit of mass slightly less than fluorine. It is also confirmed by the strong appearance of this frequency difference in the ultra-violet spectrum [10] as would be expected for a vibration of symmetry, A_1. The different relative intensity of 6*a* in fluorobenzene and toluene is undoubtedly associated with the differing polarities of electron structures of the substituents.

The ethylbenzene spectrum consists of two strong bands at 486 and 556 cm.$^{-1}$, and Taylor and Pitzer [11] have made assignments of the general type as given in Table I. However, their assignments include a band at 452 cm.$^{-1}$ which is assigned to 16*b* and shows up as a very weak band on the side of the intense band at 486 cm.$^{-1}$ when observed in the infra-red spectrum. In addition to the bands listed by Taylor and Pitzer the infra-red spectrum contains the band of high intensity at 556 cm.$^{-1}$ which is not classified by them. There are no other bands of appreciable intensity except the two mentioned in the spectrum although a weak band is found in the region of 365 cm.$^{-1}$ which is classified as the C—C bending vibration in the ethyl group and there is a region of general absorption at 295 cm.$^{-1}$ which has been assigned to the vibration 18*b*. There is more uncertainty as to the classification of the spectrum of ethylbenzene than of the mono-substituted halogenated benzenes.

---

[10] Ginsburg, Robertson and Matsen, *J. Chem. Physics*, 1946, 14, 511.

[11] Taylor and Pitzer, *J. Res. Nat. Bur. Stand.*, 1947, 38, 1.

Assignments have been made by Pitzer and Scott for the three dimethylbenzene isomers considered here. Most of the observed bands coincide in frequency with Raman bands, and hence may also be assigned to the vibrations numbered according to Pitzer and Scott. This has been done in Table I. It will be noted, however, that the intensity relations are in many cases not satisfactory, since the strongest band in the infra-red spectrum, for each of the three molecules, is assigned to an inactive mode.

TABLE I.—CLASSIFICATION OF THE BANDS OF MONO- AND DI-SUBSTITUTED BENZENES

Type	(cm.$^{-1}$)	Int.	Type	(cm.$^{-1}$)	Int.
FLUOROBENZENE					
B_1 (6*b*)	615	*m*	B_1 (18*b*)	405	*s*
A_1 (6*a*)	519	*w*	B_2 (11)	240*	*m*
B_2 (16*b*)	499	*s*	—	—	—
CHLOROBENZENE					
B_1 (6*b*)	616	*w*	B_1 (18*b*)	297	*w*
A_1 (6*a*)	467	*s*	B_2 (11)	200*	—
B_2 (16*b*)	415	*s*	—	—	—
BROMOBENZENE					
B_1 (6*b*)	615	*w*	B_1 (18*b*)	260*	—
A_1 (6*a*)	458	*vs*	B_2 (11)	180*	—
B_2 (16*b*)	314	*m*	—	—	—
IODOBENZENE					
B_1 (6*b*)	613	*w*	B_1 (18*b*)	220*	—
A_1 (6*a*)	448	*s*	B_2 (11)	160*	—
B_2 (16*b*)	270*	—	—	—	—
TOLUENE					
B_1 (6*b*)	623	*w*	B_1 (18*b*)	347	*m*
A_1 (6*a*)	521	*w*	B_2 (11)	214*	—
B_2 (16*b*)	465	*s*	—	—	—
ETHYLBENZENE					
A'' (6*b*)	622	*vw*	A'' (16*a*)	404	*vw*
A' (6*a*)	486	*s*	A'' (18*b*)	295	*vw*
A' (16*b*)	455	*w*	A' (11)	154†	—
1 : 2-DIMETHYLBENZENE					
B_2 (11)	619	*vw*	A_2 (16*a*)	436	*s*
A_1 (6*a*)	581	*w*	B_1 (18*a*)	328	*vw*
B_1 (6*b*)	505	*w*	A_2 (10*b*)	260	*m*
1 : 3-DIMETHYLBENZENE					
A_1 (6*a*)	535	*vw*	A_2 (16*a*)	404	*w*
B_1 (6*b*)	515	*w*	A_2 (10*a*)	278	*w*
B_2 (16*b*)	432	*s*	B_2 (11)	200†	—
1 : 4-DIMETHYLBENZENE					
B_{3g} (6*b*)	645	*w*	B_{2g} (10*b*)	292	*w*
A_{1g} (6*a*)	483	*vs*	B_{3u} (11)	170*	—

* Raman value. † Value of Pitzer and Scott.[9]

In view of the new infra-red data now available in the long wavelength region, it may be worthwhile to consider a revision of the assignments of the bands as given by Pitzer and Scott. There are several ways in which the stronger bands may be assigned to allow vibrations in the expected frequency range, but it seems unprofitable to attempt this without more detailed calculations.

Of the three trimethylbenzene isomers measured only 1 : 3 : 5-trimethylbenzene has been classified by Pitzer and Scott. Although the bands at 275 and 576 cm.$^{-1}$ are not supposed to be active in the infra-red they agree well with Raman values assigned to vibrations of type 10 and 12 respectively. The band at 515 cm.$^{-1}$ has the same value as that assigned to the vibration of type 6 by Pitzer and Scott. A weak band was also observed at 649 cm.$^{-1}$ which may be a difference band. The spectra of the 1 : 2 : 3- and 1 : 2 : 4-trimethylbenzenes show more relatively intense bands in this region than were observed in 1 : 3 : 5-trimethylbenzene. Since the 1 : 3 : 5-isomer is the most symmetrical of the trimethylbenzenes, it is expected to have fewer active bands. The three bands that have been assigned, however, do show up in most cases in the other two isomers with slight shifts in their positions. The small wave number band at about 275 cm.$^{-1}$ of type 10 is reasonably intense in all three trimethylbenzenes. A list of the observed bands is given in Table II.

TABLE II.—OBSERVED BANDS IN TRIMETHYLBENZENES

ν (cm.$^{-1}$)	Int.	ν (cm.$^{-1}$)	Int.
	1 : 2 : 3-TRIMETHYLBENZENE		
657	*w*	487	*w*
538	*m*	458	*w*
513	*vw*	272	*s*
	1 : 2 : 4-TRIMETHYLBENZENE		
568	*vw*	439	*s*
554	*w*	322	*w*
539	*s*	284	*w*
470	*w*	—	—
	1 : 3 : 5-TRIMETHYLBENZENE		
649	*vw*	515	*m*
634	*vvw*	275	*w*
576	*vw*	—	—

On account of the many bands with small wave numbers which are present in the spectra of the benzene derivatives measured here, it would be expected that difference and combination bands would have sufficient intensity to be observed in the region studied. Some difference bands have been observed in the spectra of these benzene derivatives. It was often necessary to use cells of the order of 1·0 mm. in thickness to observe these bands since they are relatively weak. In toluene a band was found at 539 cm.$^{-1}$ and is assigned as the difference between the bands at 890 and 347 cm.$^{-1}$. The 385 cm.$^{-1}$ band of chlorobenzene is attributed to the difference between the bands at 682 and 297 cm.$^{-1}$. The difference between the bands at 735 and 180 cm.$^{-1}$ of bromobenzene accounts for the weak band at 545 cm.$^{-1}$ and the low intensity band at 493 cm.$^{-1}$ corresponds fairly well with the difference between the bands at 667 and 180 cm.$^{-1}$. In the spectrum of 1 : 2-dimethylbenzene the 406 cm.$^{-1}$ band checks closely with the difference between the bands at 733 and 328 cm.$^{-1}$

Certain weak bands observed from 15 to 38 μ in the spectra of dimethylbenzenes correspond well in wave number with those predicted values of combinations of the assigned fundamentals. In the spectrum of 1 : 2-dimethylbenzene the combination of the two fundamentals 18*b* (180 cm.$^{-1}$) and 16*b* (148 cm.$^{-1}$), which are Raman values listed by Pitzer and Scott, may give rise to a very weak band that was observed at 328 cm.$^{-1}$. The first overtone of the 18*b* vibration should occur near 360 cm.$^{-1}$ where a very weak band was observed. A combination of the fundamentals, 10*b* (260 cm.$^{-1}$) and 16*b* (148 cm.$^{-1}$) checks closely with a weak band at 406 cm.$^{-1}$. The first overtone of the vibration of type 11 (200 cm.$^{-1}$) in the spectrum of 1 : 3-dimethylbenzene should occur near 400 cm.$^{-1}$, but is probably overlapped by the band of low intensity assigned to the type 16*a* vibration at 404 cm.$^{-1}$. In the spectrum of 1 : 4-dimethylbenzene the combination of the fundamental vibrations 10*b* (292 cm.$^{-1}$) and 11 (170 cm.$^{-1}$) should give rise to a band at 462 cm.$^{-1}$ which was not observed in the infra-red spectrum because of the presence of the strong band assigned to the type 6*a* vibration at this same wave number. There should be many other difference and combination bands in the spectra of the various benzene derivatives. However, when cell thicknesses of 2 or 3 mm. are employed, usually a general absorption is observed and it is difficult to locate definitely bands of low intensity.

When the spectra of the mono-halogen substituted benzenes, toluene, and the dimethylbenzene isomers obtained here were compared with the Raman spectra given in *Ramanspektren* by Kohlrausch,[13] it was seen that many of the bands observed in the infra-red had corresponding Raman values. With the exception of the strong bands at 465 cm.$^{-1}$ in toluene and 432 cm.$^{-1}$ in 1 : 3-dimethylbenzene all bands of high intensity in the infra-red spectra were also observed in the Raman spectra. There were, however, a number of weak bands observed in the infra-red that did not appear in the Raman, and also there were considerably more bands listed in the Raman than in the infra-red spectra. As would be expected, a comparison of the intensities of the Raman and infra-red bands showed rather widespread variation. The Raman spectrum of 1 : 3 : 5-trimethylbenzene as given by Kohlrausch does not contain any bands between 600 and 800 cm.$^{-1}$. In the infra-red spectrum two bands of low intensity are observed at 634 and 649 cm.$^{-1}$.

To complete the work on the classification of the benzene derivatives, it would be desirable to have the vapour spectrum of each of the compounds to check the classifications of the bands observed in the liquid state. In this study measurements have been made on the vapours of chlorobenzene, toluene, 1 : 2-dimethylbenzene, and ethylbenzene in the region beyond 15 μ. Because of the relatively low vapour pressures and the cell lengths used, only the more intense bands could be observed. There were indications of several bands in each of the compounds, but most of them were too weak to determine the band shapes with sufficient clearness for use in the analysis of the band spectra. In chlorobenzene the band with the wave number 297 cm.$^{-1}$ was observed in the vapour state and also several of the small wave number bands of the other materials could be detected but not accurately measured. These observations were made to ascertain whether or not these bands were present in the spectrum of the vapour. A band with P, Q and R branches was observed in the toluene vapour spectrum that was also present in the liquid spectrum at 465 cm.$^{-1}$. The most intense band of the ethylbenzene vapour containing P, Q and R branches was observed at 556 cm.$^{-1}$. This band is also intense in the liquid state, but appears of low intensity at 553 cm.$^{-1}$ in the Raman spectrum.

Except for certain bands of the ethylbenzene spectrum the assignments of all the observed bands of the mono-substituted benzenes are in good agreement with the calculated values. Before a comparison of the spectra of the trimethylbenzenes can be made, further theoretical classifications should be made. Improvement in the experimental results can be made by observing these spectra of the vapours in long cells so that the band shapes can be determined.

---

[13] Kohlrausch, *Ramanspektren* (Akademische Verlagsgesellschaft Becker and Erler Kam. Ges., Leipzig, 1, 1943).

The author is indebted to Dr. R. L. Hudson of the University of Oklahoma for a list of his assignments of the fluorobenzene spectrum, and to Dr. R. L. Arnett of this Bureau for his suggestions pertaining to the assignments of the dimethylbenzenes.

Radiometry Section,
National Bureau of Standards,
Washington, D.C.

DETERMINATION OF MOLECULAR STRUCTURE WITH MICROWAVE SPECTROSCOPY

BY E. BRIGHT WILSON, JR.

Received 17th July 1950

The characteristics and limitations of microwave spectroscopy as a tool for the determination of the structure of simple molecules in the vapour state are discussed. The great advantages are the tremendous frequency resolving power and great precision. The applications of the method to the measurement of moments of inertia, interatomic distances, dipole moments, barriers hindering internal torsion, magnetic moments, and valence information from hyperfine structure are outlined.

The region of the electromagnetic spectrum in which the wavelength ranges from a few millimetres to a few centimeters has become of considerable importance, particularly for the study of rotational energy levels in simple molecules in the gas phase. This new field of microwave spectroscopy has now had time to demonstrate that it is as powerful and useful as its early enthusiasts claimed. In four years this method has become one of the principal tools for the study of molecular structure, nuclear spins and dipole moments. It also provides information about nuclear quadrupole moments, molecular and nuclear magnetic moments, valence, centrifugal distortion, barriers hindering internal torsion, and the exchange of rotational energy on collision. It is the purpose of this report to summarize the present status of microwave spectroscopy as a research tool for the study of molecular structure, including some discussion of its limitations. Only the application to gases at low pressures will be considered. Earlier work has been reviewed by Gordy.[1]

General Characteristics.—The key to the uniqueness of this technique is its enormous frequency resolving power. Spectral lines as close as 140 k./sec. (4×10^{-6} cm.$^{-1}$) have been clearly separated,[2, 3] which is to be compared with perhaps 0·1 cm.$^{-1}$ for the best infra-red spectrographs. Actually, the limitation on resolving power is not set, as yet, by the apparatus but by the line widths. At the present time there is no very practical prospect for decreasing line widths further by more than a factor of perhaps three because of the limit set by Doppler broadening. The great resolution makes possible the observation of a whole new class of effects, such as the Stark effect, Zeeman effect, *K*-splitting due to centrifugal distortion, isotope effect, change of moment of inertia with vibrational state, and nuclear quadrupole hyperfine splitting.

---

[1] Gordy, *Rev. Mod. Physics*, 1948, **20**, 668.

[2] Townes, Holder and Merritt, *Physic Rev.*, 1948, **74**, 1113.

[3] Geschwind, Minden and Townes, *ibid.*, 1950, **78**, 174.

Related to the high resolving power is the considerable accuracy and ease with which frequencies can be measured. Incidentally, this is one branch of spectroscopy in which time and not distance is the fundamental unit of measurement. Frequencies can be measured to a few hundredths of a megacycle without great trouble. At 25,000 megacycles (which is the centre of the most popular region) this is an accuracy of nearly one part in a million. Naturally the spacing of fine structure lines cannot be determined with as great percentage accuracy as that. Furthermore, it is not easy to get spectral lines sufficiently narrow to take full advantage of this precision. Also it must be remembered that Planck's constant is involved in applications of the data, and is not known to any such accuracy.

Microwave spectroscopy has limitations, some of which may ultimately be overcome. Its use is essentially confined to molecules having a permanent dipole moment. (An exception is O_2.) This is a severe restriction and rules out many interesting molecules. Electron diffraction does not suffer from this disability. Furthermore, the molecules must possess sufficient vapour pressure (about 0·01 mm. Hg) at reasonable temperatures. The molecule must not have too small a moment of inertia (e.g. HCl) or its pure rotation spectra will be at too high a frequency. It must not be too large or it will have too weak a spectrum. Finally, the analysis can prove to be very troublesome, if not impossible, in unfavourable cases.

Molecular Structure.—From the chemist's viewpoint, the main usefulness of microwave spectroscopy is as a tool for the determination of the structure of small, polar molecules in the vapour phase. Within this limited range, it is unmatched by any other technique in precision, power and certainty. The method employed is the same as in the infra-red, i.e. from the spectral frequencies which are observed, moments of inertia are calculated. From the moments of inertia of several isotopic species, interatomic distances and angles are deduced. This process is dependent upon several critical steps. Firstly, it is necessary to make a correct assignment of quantum numbers to the observed lines. Secondly, it is required that quantum-mechanical formulas be available which represent the energy levels sufficiently accurately, provided that suitable molecular dimensions are inserted. Thirdly, the assumption that the interatomic distances are the same for the several isotopic species must be valid.

How well are these conditions met in practice ? The assignment of the correct quantum numbers is simple enough for uncomplicated linear molecules and is usually easy for symmetrical-rotor types, such as CH_3F. The reason for this fortunate state is that the spectral lines for these types exhibit a simple pattern so that an approximate knowledge of the structure and dimensions enables a preliminary calculation of expected frequencies to be made which normally suffices to identify unambiguously any observed lines. With asymmetric rotors (three unequal moments of inertia) such as water or ethylene oxide, the situation can be quite different. The frequencies do not fall into any simple pattern and can be very sensitive to the trial values of the molecular parameters. When such molecules are nearly symmetric (by accident), as with vinyl chloride, analysis is not difficult.

The Stark effect provides the most powerful tool for identifying transitions in these difficult cases, but is not always applicable. The number, spacing, and relative intensities of the components into which a line is split by an electric field normally give sufficient information. However, not all lines can be resolved into separate components with existing equipment, so that an element of chance enters here. If a spectral line with sufficiently low quantum numbers falls within an observable frequency region, its Stark effect can usually be resolved and its quantum numbers determined. Recently a difficult case, CH_2CFCl, has been analyzed [4] by using the hyperfine structure patterns as indicators of the quantum numbers.

Other potential sources of information exist but they have mostly not yet been fully developed and applied. It is almost a necessity that they should be if the full value of the method for structural woik is to be realized.

The next limitation is the extent to which adequate quantum-mechnical formulas have been derived. Again, for linear and symmetrical-top molecules, the situation is quite good. The first approximation, the rigid rotor model, is usually adequate and correction terms for centrifugal distortion are available if needed. Various complications such as nuclear quadrupole coupling, Stark effect, Zeeman effect, K-splitting, etc. can usually be handled. For asymmetric rotors the situation is fairly good, but not ideal. Even for the rigid model, the calculations can be quite troublesome, and the corrections for non-rigidity are difficult indeed. The Stark effect and some cases of quadrupole coupling can be treated but not with ease.

As chemists realize, most molecules are not even approximately rigid, but usually contain one or more links about which torsional motions can occur. Sometimes these molecules can be approximately handled by considering them as equivalent to mixtures of separate species, one for each of the several equilibrium orientations. If the only torsional motion is that of a methyl group, more rigorous treatments are possible. In general, not many molecules with these complications have been studied as yet with microwaves, but as the subject advances, more of them will be encountered and there will be need for more advanced theoretical considerations.

Finally, the question of the invariance of interatomic distances under isotopic substitution requires attention. Fortunately, this assumption can be tested by internal methods. In many cases, OCS for example, there are available more isotopic species than are needed to establish the molecular structure. Consequently, several checks are available. In general, it would appear that distances determined in this way are consistent to within 0·01 Å and usually better. This is not necessarily true when the isotopic atom is near the centre of mass of the molecule, but such cases are obviously unfavourable and should be avoided.

The reason why perfect consistency is not achieved is presumably the non-rigidity of real molecules. Because molecules are vibrating even in their lowest quantum states, only a special kind of weighted average interatomic distance enters the equations. In principle the more accurate model, consisting of point masses (the atoms), connected by forces, has been treated by quantum mechanics, but insufficient information is available about these forces.

Attempts have been made to correct for the vibration of the atoms but they have so far not been completely successful. One method requires measurements for molecules in each of the one-quantum states of vibrational excitation, so that linear extrapolations to the hypothetical equilibrium state can be made. This has been done for a few diatomic molecules such as BrF[5] and FCl[6] but cannot usually be accomplished for polyatomic molecules with presently available sensitivities.

The high resolving power and senstitivity makes it possible to study many isotopic species in the natural mixture, without artificial enrichment. Thus molecules containing one C^{13}, S^{34}, N^{15}, or O^{18} are often observable as well as the easier cases involving B, Cl, Br, etc.

Table I lists a few of the molecules for which partial or complete structural information has been published during the present year. An especially interesting example is provided by bromdiborane, shown in

---

[4] Bragg, Madison and Sharbaugh, *Physic Rev.*, 1950, **77**, 148.

[5] Smith, Tidwell and Williams, *ibid.*, 1950, **77**, 421.

[6] Gilbert and Roberts, *ibid.*, 1950, **77**, 742.

Fig. 1. Here there was some question at first as to whether the Br atom was located in the " bridge " between the borons or at the end, as shown. This was easily answered by the boron isotope effect. In the first structure the two borons would be symmetrically located so that there should be three species: B^{10}—B^{10}, B^{10}—B^{11} and B^{11}—B^{11}, since the B^{11}—B^{10} would be the same as B^{10}—B^{11}. In the structure found, however, the two borons are not equivalent so that four species should occur. Actually there are eight found, because of the two bromine isotopes. This molecule is also of interest because it provides confirmation of the hydrogen bridge and some dimensions for it. The spectral analysis shows clearly that the molecule is not planar, the bridge hydrogens being above and below the plane of the other atoms. This demonstrates one advantage of the microwave technique as compared with electron diffraction : it can locate hydrogen atoms.

TABLE I.—SOME MOLECULES FOR WHICH STRUCTURAL INFORMATION HAS RECENTLY BEEN PUBLISHED

CO[7]	$HCCCN$[9]	SiF_3Br[11]	PCl_3[15]
FCl[6]	SiH_3F[10, 11]	CF_3Br[13, 14]	SiF_3CH_3[11]
BrF[5]	SiF_3Cl[11]	CF_3I[13]	BH_3CO[16]
HCN[8]	$CHCl_3$[12]	CF_3CN[13]	B_2H_5Br[17]
—	—	—	C_2H_4O[18]

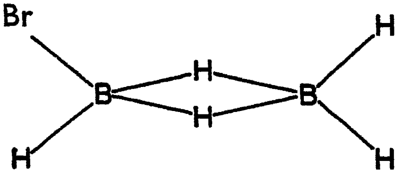

FIG. 1.—The structure of bromdiborane as determined by microwave spectroscopy. One bridge hydrogen is above the plane of the rest of the molecule, the other is below this plane. The H—H distance is 2·0 ± 0·2 Å.

Determination of Dipole Moments.—The extent of the splitting of spectral lines in the presence of an electric field is determined in part by the magnitude of the electric dipole moment of the molecule. If the quantum numbers for the transition and the magnitude of the electric field are known, measurements of the Stark pattern can be used to determine the dipole moment. When the conditions are not too unfavourable, accuracies of about 1 % or better can be achieved.

One advantage of this method is that it gives a vapour-phase value, uncomplicated by solvent interaction or serious deviations from the ideal gas law (because of the low pressure used). Of course, it is not applicable if the vapour pressure available is less than perhaps a hundredth of a millimeter. Because of the low pressures and volumes used, very little material is required of the order of micrograms.

Since the isotopic species often show in the spectra without artificial enrichment, the effect of isotopic substitution can easily be studied. In one case,[19] at least, (OCS) no measurable differences were found. However, differences (about 1 %) were found between the dipole moment for the ground vibrational state and the first excited state for the bending mode of OCS. Because of the effect of the vibration on the effective moments of inertia, molecules in different vibrational states undergoing the same rotational transition will exhibit slightly different frequencies. Therefore the Stark effect and thus the dipole moment can be determined separately for these vibrational states. Table II shows some dipole moments determined by the microwave method.

---

[7] Gilliam, Johnson and Gordy, *Physic Rev.*, 1950, **78**, 140.
[8] Simmons, Anderson and Gordy, *ibid.*, 1950, **77**, 77.
[9] Westenberg and Wilson, *J. Amer. Chem. Soc.*, 1950, **72**, 199.
[10] Sharbaugh, Thomas and Pritchard, *Physic. Rev.*, 1950, **78**, 64.
[11] Sheridan and Gordy, *ibid.*, 1950, **77**, 719.
[12] Unterberger, Trambarulo and Smith, *J. Chem. Physics*, 1950, **18**, 565.
[13] Sheridan and Gordy, *Physic. Rev.*, 1950, **77**, 292.
[14] Sharbaugh, Pritchard and Madison, *ibid.*, 1950, **77**, 302.
[15] Kislink and Townes, *ibid.*, 1950, **78**, 347.
[16] Gordy, Ring and Burg, *ibid.*, 1950, **78**, 512.
[17] Cornwell, *J. Chem. Physics*, 1950, **18**, 1118.
[18] Cunningham, Boyd, Gwinn and LeVan, *J. Chem. Physics*, 1949, **17**, 211.

TABLE II.—Some Dipole Moment Values from Microwave Spectroscopy in D

OCS	0·709[19]	N_2O	0·166[20]
AsF_3	2·82[20]	ClCN	2·80[20]
CH_3I	1·65[20]	HCCCl	0·44[21]
CH_3Cl	1·87[20]	HCCCN	3·6[9]
CH_3Br	1·80[20]	BrF	1·29[5]
CH_3CF_3	2·32[20]	SiH_3F	1·27[10]
PF_3	1·03[20]	POF_3	1·74[22]
—	—	BH_3CO	1·80[23]

Internal Torsional Motions.—Recent work[24] has focused attention on the inadequacy of the thermodynamic methods for determining the potential barriers which hinder free internal rotation about single bonds. Microwave spectroscopy provides two methods for attacking this problem in special cases. The first method sometimes applies when the torsional motions are spectroscopically active, as with methyl alcohol. Transitions between different states of torsional motion are of too high frequency to appear directly in the microwave region, but in CH_3OH, at least, transitions between components of torsional levels have been observed, with and without overall rotational changes as well. These components arise from the quantum-mechanical tunnelling phenomena associated with the existence of several (here three) equivalent equilibrium positions. Although the calculations are difficult, the interpretation appears to be sure and results in the estimation of a barrier height of 932 cal. on the basis of a sinusoidal potential energy function.[25]

The second method is more general, involves simpler calculations, but at present is less precise experimentally. It is based on the fact that molecules in excited vibrational, or torsional, states have effective moments of inertia slightly different from those in the ground state so that a rotational transition due to such excited molecules appears as a weaker, displaced satellite to the main line from molecules which are not vibrating. The ratio of the satellite intensity to the main line intensity is a measure of the population ratio for the excited and ground states. From the Boltzmann law, one then calculates the energy of the excited state relative to the ground state. This procedure needs correction if the excited state is split up into components, or has a different spin statistical weight, or displays a different dipole moment. By measuring the effect of a temperature change on the intensities, an alternative set of data can be obtained with certain advantages. So far only a few molecules have been treated in this way, notably CF_3CH_3[26] and CH_3CHO,[27] which gave barriers of about 1500 cal. and 2600 cal. respectively. More work needs to be done in improving the technique of intensity measurements, but there can be little doubt that valuable data will be obtained with this new method.

---

[19] Shulman and Townes, *Physic. Rev.*, 1950, **78**, 500.
[20] Shulman, Dailey and Townes, *ibid.*, 1950, **78**, 145.
[21] Westenberg, Goldstein and Wilson, *J. Chem. Physics*, 1949, **17**, 1319.
[22] Senatore, *Physic. Rev.*, 1950, **78**, 293.
[23] Strandberg, Pearsall and Weiss, *J. Chem. Physics*, 1949, **17**, 429.
[24] Blade and Kimball, *ibid.*, 1950, **18**, 630.
[25] Burkhard and Dennison, see Halford, *ibid.*, 1950, **18**, 361.
[26] Dailey, Mindon and Shulman, *Physic. Rev.*, 1949, **75**, 1319.
[27] Baird (to be published).

The quantity directly obtained is not the height of the barrier but the energy of the first (and sometimes the second and third) excited torsional states above the ground state. Conversion of this information into a barrier height requires an assumption regarding the shape of the barrier. This same difficulty arises with the thermodynamic methods, which actually yield a weighted average of the positions of the torsional levels, with the low lying levels much the most heavily weighted. For the practical purpose of making thermodynamic predictions, the positions of the first few levels will often suffice, but for comparison with any eventual quantum-mechanical theory, a knowledge of barrier shape and height would be desirable.

Magnetic Effects.—Molecules may possess magnetic moments from several sources. Thus many nuclei have spin magnetic moments. A polar molecule which is rotating should have a small magnetic moment due to the rotation of its positive and negative charges. Finally, paramagnetic molecules will show very much larger moments due to unpaired electrons or orbital electronic effects.

With fields of several thousand gauss, Zeeman effects in NH_3,[28] H_2O,[32] HDO,[32] N_2O,[29] CH_3Cl,[28] CH_3I,[31] and OCS[30] have been resolved and interpreted. Nuclear magnetic moments (in one case[31] for an artificially produced radio-active isotope I^{129}) have been the principle product of these studies, but molecular moments arising from rotation have been obtained for a few light molecules. For heavier (and therefore more slowly rotating) species, they are at present too small to observe. The nuclear moments will influence the spectra only when they are coupled to the molecular rotation, usually by electric quadrupole interaction.

Odd molecules such as NO and NO_2 have Zeeman effects which can be resolved at very much lower magnetic fields. Thus the splitting in NO_2 can be observed[33] with the aid of a few gauss from a one layer solenoid wound around the wave-guide absorption cell. The effect of even the earth's magnetic field can be detected. Similar large effects in paramagnetic O_2 have been made the basis for a Zeeman-effect modulation spectrograph[34] analogous to the Stark-effect type of apparatus. Magnetic resonance spectra—transitions between the Zeeman components—have been studied with NO[35] in strong fields.

The analysis[33] of the NO_2 spectrum was aided by the Zeeman pattern. The spectrum is complicated by the various internal coupling energies, such as those between electron spin and nuclear spin magnetic moments, electron spin and molecular rotation magnetic moments, nuclear electrical quadrupole moment and molecular electron distribution, etc. The unravelling of these is in progress.

Perhaps the main point of such studies is that free radicals with unpaired electrons should show similar phenomena. So far no spectra due to gaseous free radicals have been announced, but several groups are working in this field and success should ultimately be achieved in spite of the formidable difficulties.

Nuclear Quadrupole Effects and Chemical Valence.—One of the richest sources of interest and information is the hyperfine structure exhibited by many pure rotation lines due to the coupling of nuclear spin and molecular rotation. This arises from the interaction of the electrical quadrupole moment possessed by many nuclei and the gradient of the electric field

[28] Jen, *Physic. Rev.*, 1948, **74**, 1396.

[29] Jen, *ibid.*, 1949, **76**, 1494

[30] Jen, *ibid.*, 1950, **78**, 339.

[31] Gordy and Gilliam, *ibid.*, 1949, **76**, 443.

[32] Jen, *ibid.*, 1949, **76**, 471.

[33] McAfee, *ibid.*, 1950, **78**, 340.

[34] Burkhalter, Anderson, Smith and Gordy, *ibid.*, 1950, **77**, 152.

[35] Beringer and Castle, *ibid.*, 1950, **78**, 581.

due to the electrons and other nuclei in the molecule. First discovered in ammonia,[36] this effect has now been observed and analysed in a large number of molecules.

In the first place, the number of components in the hyperfine structure components, and their spacings and relative intensities, have provided one of the most important methods of determining the nuclear spin angular momenta of atomic nuclei. Several spins previously accepted have been found to be incorrect and new values determined with considerable certainty, examples [2, 16] being Cl^{35}, Cl^{37} and B^{10}.

The chemist is mainly interested in the application of this phenomenon to structure and valence. The importance for these fields arises from the argument [37] that the gradient of the electrical field at the quadrupolar nucleus arises mainly from the valence electrons associated with the given atom. The nucleus thus provides a sensitive measuring instrument, located in the heart of the molecule, for giving information about certain aspects of the electron distribution.

The electrons in closed shells about the nucleus should not contribute much to the field gradient because closed shells are spherically symmetrical, except for small distortions caused by other atoms. Electrons on other atoms are too far away to affect the situation greatly because of the rapid diminution with distance. This leaves the valence electrons as the principal contributors. Even these should be unimportant if in *s* orbitals because of the spherical symmetry of these, or if in *d* or higher orbitals because of their low penetrating power. Consequently, the hyperfine splitting is ascribed mainly to the amount of *p*-orbital character of the valence electrons.

This theory provides an explanation for the striking differences in quadrupole splitting between NaCl and CH_3Cl, for example. In the former, the structure is essentially ionic so the Cl nucleus is surrounded by closed spherical shells. In the latter, the bond is primarily covalent with some hybridization and the hyperfine spacing is very much greater than for NaCl. This idea has been applied to interpret the data for a number of molecules in terms of valency theories.

An interesting further application [38] of these ideas has been made to CH_2CHCl and CH_2CFCl. These are asymmetric rotors and their hyperfine structure is correspondingly more complicated. The analysis has been carried out, however, and shows that the electron distribution around the C—Cl bond is not cylindrically symmetrical, but is distorted in a way which can be explained by assuming 4 or 5% double-bond character due to conjugation with the carbon-carbon double bond, an idea originally put forward by Pauling to explain the shortening of the C—Cl bond in vinyl chloride.

Department of Chemistry,
Harvard University.
12 *Oxford Street,*
Cambridge 38,
Mass., U.S.A.

---

[36] Good, *Physic Rev.*, 1946, 70, 213.
[37] Townes and Dailey, *J. Chem. Physics*, 1949, 17, 782.
[38] Goldstein and Bragg, *Physic. Rev.*, 1950, 78, 347.

INFRA-RED SPECTRA OF CRYSTALS AT LOW TEMPERATURES

By D. F. Hornig

Received 17*th July*, 1950

Examination of available data, some previously unpublished, shows many of the features expected in low temperature spectra. These include line widths which are frequently less than 10 cm.$^{-1}$, a multiplicity of lines due to the coupling of molecular motions and apparently rigorous selection rules which may be determined from the symmetry of a unit cell. The relative magnitudes of equilibrium and coupling terms in the crystal field are compared. The spectroscopic data are found to be inconsistent with the X-ray structure of crystalline CO_2. A structure for crystalline HCN, not hitherto determined, is obtained which satisfies the infra-red data, possibly uniquely. Combination bands between internal modes and lattice torsions have been observed as well as the torsional fundamentals (NH_3, ND_3). Large changes in intensity occur on crystallization but insufficient data are available to draw quantitative conclusions.

The useful characteristics of low temperature vibrational spectra, both infra-red and Raman, have resulted in their application to a number of problems in recent years, although the total number of molecules investigated is still small. The paucity of work has been due both to experimental problems and to the difficulties encountered in the theoretical interpretation of the spectra obtained. Considerable progress has been made recently in both respects.

The chief advantages of low temperature spectra are obtained only in crystals, but the spectra of molecules in crystals are useful in a number of types of interrelated problems: (1) the study of the interaction forces between molecules at close distances of approach and the effect of the field of neighbouring molecules on the internal potential function, the electrical charge distribution, etc., of the molecule in question; (2) the structure of crystals, particularly those containing hydrogen atoms which are not amenable to complete X-ray determinations; (3) the study of the hydrogen bond under known conditions of geometry; (4) the study of the structure of molecular species, e.g. complex ions, which exist only in crystals; molecular complexes which are stable only at low temperatures in crystals also fall into this category; (5) the study of molecules whose spectra in the gas phase are inadequate for a complete vibrational analysis and (6) the identification and analysis of complicated molecules. The latter two types of studies may be aided because of the characteristically sharp line spectra at low temperatures which make possible the observation of many more transitions, because of changes in symmetry from the gas phase coupled with strict selection rules for fundamental vibrations and because of the polarization properties of crystals.

The number of simple molecules whose infra-red spectra have been reported in the crystalline state is small and includes N_2O_4,[1] HCl,[2, 3] DCl,[3] HBr,[4] HI,[4] CO_2,[5] C_2H_6,[6] HCN,[7] BF_3,[8] CH_4,[9] NH_3,[10] ND_3,[10] H_2S,[11]

---

[1] Sutherland, *Proc. Roy. Soc. A*, 1933, **141**, 342.

[2] Hettner, *Z. Physik*, 1934, **89**, 234.

[3] Lee, Sutherland and Wu, *Proc. Roy. Soc. A*, 1940, **176**, 493.

[4] Zunino, *Z. Physik*, 1936, **100**, 335. [5] Dahlke, *ibid.*, 1936, **102**, 360.

[6] Avery and Ellis, *J. Chem. Physics*, 1942, **10**, 10.

[7] Hoffman and Hornig, *ibid.*, 1949, **17**, 1163.

[8] Hoffman, *Dissertation* (Brown University, 1949).

[9] Holden, Taylor and Johnston, *J. Chem. Physics*, 1949, **17**, 1356.

[10] Hornig and Reding, *Physic. Rev.*, 1950, **78**, 348.

[11] Lohman and Hornig, *ibid.*, 1950, **79**, 235.

C_2H_2 and C_2H_4.[12] The latter two were studied only in the near infra-red region. More complex hydrocarbons have been investigated at low temperatures by several authors [6, 13–16] and the effect of state of aggregation on these spectra has recently received attention.[14–16] The low temperature spectrum of benzene has been used to aid in determining the fundamental vibrational frequencies of the molecule.[17–19] The spectra of ammonium halides have been studied in some detail over a wide temperature range in order to determine their structure and to ascertain the nature of the λ-point transitions.[20–22] A number of substances have been examined by Walsh and Willis [23] who conclude, in conflict with other investigators,[6, 15, 19] that there is little temperature effect on line widths. King, McMahon and Hainer have developed techniques suitable for work at liquid helium temperatures [24] and have applied them to polymers [25] and to cholesterol.[26] No work with polarized radiation at low temperatures has been reported but polarization effects have seemingly appeared in several of the investigations.[7, 19] Rank has applied the low temperature infra-red spectra of crystals to the problem of rotational isomerism in hydrocarbons.[15]

However, at the present time there appears to have been no quantitative interpretation of the effect of the crystalline field and of temperature on the spectra, their frequencies, line widths and intensities and it may be necessary to acquire considerably more empirical data on simple systems before significant progress is made.

First Order Theory.—The theory of the vibrational spectra * of crystals takes a very simple form if (*a*) the crystal is harmonic (i.e. only squared terms appear in the potential energy function) and (*b*) only linear terms need be included when the dipole moment or the polarizability are expanded as functions of the normal co-ordinates. Under these circumstances it has been shown that the observed spectrum should consist of extremely sharp lines and should arise only from those fundamental vibrations in which equivalent atoms in every unit cell move in phase.[27]

If the crystal has symmetry elements other than the lattice translations, some of these vibrations may be inactive in either the Raman or infra-red spectrum ; the selection rules may be determined from a knowledge of the symmetry elements contained in a single unit cell, i.e. from the unit cell group which consists of the group of symmetry elements of the unit cell when lattice translation is considered an identity operation.[28, 29] Since this group is simply isomorphous with the crystallographic point group, the same selection rules are obtained if the crystallographic point group is used. This type of classification has been widely applied to the

---

[12] Rodnikova, *J. Physics (U.S.S.R.)*, 1946, **10**, 236.

[13] Avery and Morrison, *J. Appl. Physics*, 1947, **18**, 960.

[14] Richards and Thompson, *Proc. Roy. Soc. A*, 1948, **195**, 1.

[15] Axford and Rank, *J. Chem. Physics*, 1949, **17**, 430 ; *ibid.*, 1950, **18**, 51.

[16] Halford and Carpenter, *J. Chem. Physics*, 1947, **15**, 99.

[17] Leberknight, *Physic. Rev.*, 1933, **43**, 967.

[18] Halford and Schaeffer, *J. Chem. Physics*, 1946, **14**, 141.

[19] Mair and Hornig, *ibid.*, 1949, **17**, 1236.

[20] Pohlman, *Z. Physik*, 1932, **79**, 394.

[21] Bovey and Sutherland, *J. Chem. Physics*, 1949, **17**, 843.

[22] Wagner and Hornig, *ibid.*, 1950, **18**, 296 ; *ibid.*, 1950, **18**, 305.

[23] Walsh and Willis, *ibid.*, 1950, **18**, 552.

[24] McMahon, Hainer and King, *J. Opt. Soc. Amer.*, 1949, **39**, 786.

[25] King, Hainer and McMahon, *J. Appl. Physics*, 1949, **20**, 559.

[26] Hainer, King and McMahon, *Physic. Rev.*, 1949, **75**, 1320.

* We mean here the infra-red or Raman spectrum observed experimentally rather than the complete frequency spectrum.

[27] See, for example, Born and Goeppert-Meyer, *Geiger-Scheel Handbuch der Physik* (Julius Springer, Berlin, 1933), 2nd edn., Chap. 4.

[28] Bhagavantam and Venkatarayudu, *Proc. Indian Acad. Sci. A*, 1939, **9**, 224.

[29] Hornig, *J. Chem. Physics*, 1948, **16**, 1063.

Raman spectra of crystals [30, 31] but it does not seem to have been applied to the infra-red spectra of simple molecules or ions in crystals.

The selection rules for any group may be obtained from its sub-groups and a knowledge of the coefficients connecting the irreducible representations of the sub-groups with those of the group.[29] In the unit cell group such sub-groups are the site groups which describe the point symmetry of the crystal about the site in question. However, the concept is not uniquely one of the crystal. For example, the selection rules for benzene can be obtained by using the fact that each C—H group is on a site of symmetry C_{2v} together with the abstract relation between the groups C_{2v} and D_{6h}. When, as in benzene, the motions of the groups are closely coupled, there is no simple relation between the physical frequencies of a C—H group, five of which are zero frequency rotations and translations, and the frequencies of the benzene molecules which arise when they are coupled. Consequently, the concept is of little utility in this case. Correspondingly, the concept has only a slight value in classifying the lattice vibrations arising from the translational and rotational motions of the molecules as a whole which are strongly coupled together.

However, for crystals containing molecules or complex ions in which the internal motion is only slightly affected by the crystalline field the situation is quite different. In such cases the complete harmonic potential function may be written in the form

$$V = V_L + \sum_j (V_j{}^0 + V_j') + \sum_j \sum_k V''_{jk} + V'''_{Lj}, \qquad . \qquad . \quad (1)$$

where V_L, the lattice potential, includes the terms involving the centre of gravity and orientation terms of the molecules, $V_j{}^0$ is the potential energy function of the free molecule and V_j', V''_{jk} and V'''_{Lj} are perturbations. The first describes the change in $V_j{}^0$ due to the equilibrium field of the crystal, the second, the interaction between the displacement co-ordinates of the j^{th} and k^{th} molecules and the third, the interaction between internal and lattice motions.

Since the kinetic energy may simply be summed over the molecules [29] the vibrational problem can be separated into that of the *free molecules* and of the lattice vibrations if the perturbations are ignored. The zero-order normal co-ordinates can then be classified by the symmetry of the free molecule.

If the terms V_j' are included, the problem is still separable but all of the frequencies are shifted. Since the term V_j' has the *site symmetry* of the j^{th} molecule, which is usually lower than that of the free molecule, it may also split degeneracies and change the selection rules. In this approximation the vibrations may all be classified under the *site groups*. If all of the molecules of a given kind in the crystal are symmetrically equivalent, each non-degenerate vibration of the free molecule yields one slightly shifted vibration in the crystal; but if molecules of a given kind fall into several symmetrically non-equivalent sets, one frequency might be observed for each set.

It should be noted that even if the remaining terms are negligible and the site-symmetry is adequate for calculating the frequencies, it is not adequate to determine the polarization properties of the normal vibrations. This is true because even if all sites are symmetrically equivalent they may be variously oriented in space.

Even if the remaining terms are important and couple the motions of the molecules, the site approximation is of some utility in setting up suitable symmetry co-ordinates for the unit cell and in determining the selection rules, the latter because it breaks the problem down into a series of smaller problems since each molecular motion may be discussed separately, using

---

[30] Bhagavantam, *Proc. Indian Acad. Sci. A*, 1941, **13**, 543.

[31] Couture, *Ann. Physique*, 1947, **2**, 5, ser. 12.

the abstract relation between site and unit cell groups. This will be illustrated later. Furthermore, it has been shown quite generally[29] that (1) no vibration may be active in the crystal if it is forbidden by the site approximation, (2) every vibration which is active under the site group will give rise to at least one active component in the crystal and (3) any vibration which is degenerate under the site group remains so in the crystal.

The terms V''_{jk} couple the vibrations of all of the molecules. If they are small their effect can be computed by first order perturbation theory, in which case only the coupling between equivalent modes of vibration of the various molecules need be considered, except in rare cases of accidental coincidences of frequency. If there are N molecules of a given kind in a unit cell, the zero order problem yields N-fold degenerate solutions for each non-degenerate normal vibration of the free molecule. These coupling terms resolve this degeneracy. Although it has not yet been done, the problem of calculating these terms is a tractable one since even if there is no simplification introduced by symmetry the resulting secular determinant is only of order N. Explicitly, if a zero order normal co-ordinate of the j^{th} molecule is $Q_j{}^0$, the coupling terms for this vibration in a single unit cell are

$$\begin{aligned} 2V_j{}' &= fQ_j{}^{02}, \\ V''_{jk} &= f_{jk}Q_j{}^0Q_k{}^0, \end{aligned} \qquad \ldots \quad (2)$$

and the secular equation is

$$\begin{vmatrix} \lambda_0 + f - \lambda & f_{12} & \ldots f_{1N} \\ f_{21} & \lambda_0 + f - \lambda & \ldots f_{2N} \\ \vdots & \vdots & \\ f_{N1} & f_{N2} & \lambda_0 + f - \lambda \end{vmatrix} = 0,$$

where $\lambda_0 = 4\pi^2\nu_0{}^2$ and ν_0 is the zero order frequency. The sum of the roots and hence the mean position of all of the coupled components depends only on the diagonal force constants f and hence on $V_j{}'$. The maximum number of resulting components is equal to N, the number of molecules of a given kind in the unit cell. The evaluation of these intermolecular force constants can contribute the same sort of information to the knowledge of the detailed inter-molecular field as the valence force constants have contributed to the understanding of the internal field.

The remaining harmonic terms V_{Lj} may be expected to be negligible in their effect on the internal vibrational frequencies, even in second order perturbation theory, in most cases, because of the great frequency separation of the lattice vibrations and the internal vibrations.

The changes in the spectrum when a substance is crystallized are frequently used empirically to draw conclusions regarding the state of the molecule in the crystal, even when data regarding the crystal structure are not available. For example, the disappearance of lines is used to conclude that certain rotational isomers which exist in the liquid do not exist in the crystal.[15] Such conclusions must be drawn with caution since lines may equally well disappear because of the operation of selection rules in the crystal which do not exist in the liquid. An example of this type is benzene[18] in which the fundamental ν_{10} shows strong absorption in the liquid and none at all in the crystal; the same behaviour is shown by four combination bands, at least one of which is intense in the liquid. On the other hand, the appearance of new components in the crystal has been used to argue that more complicated molecular species (such as dimers) exist in the crystal whereas in most cases they arise from the coupling of the motions of the molecules with varying phases. As will be seen in the next section, the splitting due to coupling may be quite considerable.

Comparison of First Order Theory with Experiment.—It is immediately apparent that the simple model of the preceding paragraph is not completely adequate since, for example, combinations and overtones appear and in this approximation they are not allowed. Furthermore, there is abundant evidence that although sharp the line widths are temperature dependent, contrary to the harmonic picture, and considerably wider than would be expected if only radiation damping limited their width. Nevertheless, the picture of the preceding paragraph applies exceedingly well to the fundamental vibrations.

In simple molecules whose gas spectra are known, it is possible to compare the effect of the equilibrium field (V_i') and coupling (V_{jk}'') terms. The available data are collected in Table I. The numbering of the vibrational modes is that of Herzberg, except for benzene where the numbering of Wilson [32] is used. The gas frequencies are all taken from Herzberg [33] and the crystalline frequencies from the sources noted. The line widths are at best approximate and are measured at half the maximum absorption

TABLE I.—SOME CHARACTERISTICS OF INFRA-RED SPECTRA OF SIMPLE MOLECULES AT LIQUID NITROGEN TEMPERATURE

Molecule	Mode of Vibration	Frequency (cm.$^{-1}$)		Line Width (cm.$^{-1}$)	Frequency Shift (cm.$^{-1}$)	Maximum Splitting (cm.$^{-1}$)
		Gas	Crystal			
HCl^{34}	ν_1	2886	2617*	—		
			2704	32	−196	131
			2748	25		
HBr^{34}	ν_1	2559		—		
			2404	30	− 162	34
			2438	24		
HCN^{8}	ν_1	2089	2097	7	+8	—
	ν_2	712	828	—		
			838	19	+121	10
	ν_3	3312	3132	32	−180	—
H_2S^{35}	ν_1	2610	2523	7		
			2532	6	−114 ?	21
	ν_3	2684 ?	2544	8		
	ν_2	1290 ?	1171	6	−112 ?	15
			1186	6		
D_2S^{35}	ν_1	1892	1834	4		
			1844	3	−101 ?	22
	ν_3	1999 ?	1856	6		
	ν_2	934 ?	846	2	−82 ?	11
			857	4		
NH_3^{36}	ν_1	3336	3223	—	−113	—
	ν_2	932	1060	27	+110	—
		968				
	ν_3	3414 ?	3378	17	−36 ?	—
	ν_4	1627	1646	20	+19	—
ND_3^{36}	ν_1	2419	2318	18	−101	—
	ν_2	749	815	9	+66	—
	ν_3	2555	2500	19	−55	—
	ν_4	1191	1196	20	+5	—
$NH_4^+(Cl)^{22}$	ν_3	—	3126	35	—	—
	ν_4	—	1403	7	—	—
$NH_4^+(Br)^{22}$	ν_3	—	3124	52	—	—
	ν_4	—	1408	8	—	25
			1433	8	—	

---

[32] Wilson, *Physic. Rev.*, 1934, **45**, 706.

[33] Herzberg, *Infra-red and Raman Spectra of Polyatomic Molecules* (D. Van Nostrand Company, Inc., New York, 1945).

[34] W. E. Osberg (unpublished data). [35] F. P. Reding (unpublished data).

[36] Reding and Hornig (submitted to *J. Chem. Physics*).

* Shoulder.

TABLE I.—(*cont.*)

Molecule	Mode of Vibration	Frequency (cm.$^{-1}$)		Line Width (cm.$^{-1}$)	Frequency Shift (cm.$^{-1}$)	Maximum Splitting (cm.$^{-1}$)
		Gas	Crystal			
$NH_4 . BF_4$[37]	$\nu_3 NH_4$	—	3335	55	—	—
	$\nu_4 NH_4$	—	1425	15	—	—
	$\nu_4 BF_4$	—	518	9	—	—
			530	6	—	
$ND_4^+(Cl)$[22]	ν_3	—	2336	32	—	—
	ν_4	—	1067	8	—	—
$ND_4^-(Br)$[22]	ν_3	—	2332	40	—	—
	ν_4	—	1067	8	—	20
			1087	8	—	
$(Na)BH_4^-$[37]	ν_3	—	2298	35	—	—
	ν_4	—	1121	20	—	—
BF_3[8]	ν_1	888	879	8	−9	—
	ν_2	691	632	24	−59	—
		720	622	22	−57	—
	ν_3	1446	1406	16	−40	—
		1497	1465*	—	−32	—
	ν_4	481	479	10	−2	—
CO_2[5]	ν_2	667	642	10		
			656	12	−10	30
			672*	—		
	ν_3	2349	2276*	—	−67	12
			2288	35		
Benzene[19]	ν_{11}	671	687	20	16	—
	ν_{12}	1010	1010	6	0	—
	ν_{14}	—	1312	3	—	—
	ν_{15}	—	1147	10	—	—
	ν_7	970	975	7	+11	12
			987	5		
	ν_{18}	1037	1035	9	−2	—
	ν_{19}	1485	1478	5	−7	—

coefficient. If there are several components, the mean of all reported components is used to compute the frequency shift. The maximum shift is the difference between the extreme components. In BF_4^- the doubling is due to the two boron isotopes and isotopic doubling probably contributes to the width of ν_4 in BH_4^-. The width of $\nu_3^{NH_4}$ in NH_4BF_4 is probably due to failure to resolve a number of components since the crystal is of low symmetry and has four molecules per unit cell. Similarly, ν_3 of NH_4^+ in NH_4Br may actually consist of two superimposed lines. Finally, the splitting of ν_{17} in benzene has been ascribed to the removal of a degeneracy by Mair and Hornig[19] but it is possible that it is actually due to coupling.

It is apparent from Table I that the largest frequency shifts occur in hydrogen-bonded substances although ν_2 of BF_3 is displaced by 8 %; ν_{11} of benzene, ν_3 of CO_2 and ν_3 of BF_3 are each displaced by about 2·5 %. Line widths at − 195° C are approximately 35 cm.$^{-1}$ for hydrogen stretching vibrations in the strongly hydrogen-bonded substances (hydrogen halides, ammonium halides and HCN) and considerably less in NH_3 and H_2S. Many of the line widths approach the resolution of the measurements. In this connection it should be noted that at 80° K, Hainer, King and McMahon[26] found the line widths in cholesterol crystals to be of the order of 2 cm.$^{-1}$ and they resolved ten peaks between 798 cm.$^{-1}$ and 844 cm.$^{-1}$. There is no doubt that very sharp lines may be obtained at low temperatures; in cases where this has been denied[23] it is probable that individual lines were not resolved, either instrumentally, because of scattering or because the substance was not genuinely crystalline.

---

[37] Walnut, *Dissertation* (Brown University, 1950).

As to the relative effects of V_j' and V_{jk}'', Table I indicates that both shifts and coupling must be taken into account but that, at least in polar substances, the effect of the former may be several times greater than the latter. The general correlation between a gas frequency and a set of crystalline frequencies is obvious in all cases. The only substances in the Table whose crystalline frequencies have been analyzed in any detail are benzene, the ammonium halides, NH_3 and ND_3, and no discrepancies with either the X-ray structures or the theory have emerged.

In low temperature NH_4Cl and ND_4Cl the ion symmetry is tetrahedral and there is but one molecule per unit cell so that the triply degenerate vibrations should have but one component, as was found.[22] In low temperature NH_4Br and ND_4Br the ion symmetry is V_d and ν_4 should be split into two components; they are given in Table I. Further, because there are two molecules per unit cell each vibration should be doubled but the second component should be observed only in the Raman spectrum. The close coincidence of Raman [38] and infra-red spectra indicate that the coupling is negligible, as might be expected because the heavy Br^- ions isolate each NH_4^+ ion.

The benzene spectrum was classified by Mair and Hornig purely on the basis of site symmetry. Recently Hainer and King [39] have reported four new lines between 680 cm.$^{-1}$ and 1171 cm.$^{-1}$ in the spectrum at 4° K; three of them are spaced only 4 cm.$^{-1}$ from lines previously observed. Since the space group of benzene is V_h^{15} with four molecules per unit cell, each non-degenerate vibration should yield four components, three of them infra-red active. This is sufficient to account for all of the new components but further study is needed to discriminate the equilibrium splitting and the coupling effects. It is interesting to note, incidentally, that a comparison of the frequency shifts between gaseous and crystalline NH_3 and ND_3 suggests that the frequency ν_3 of NH_3, which has not been positively established in the gas phase, is not 3414 cm.$^{-1}$, as given by Herzberg,[33] but 3450 cm.$^{-1}$ as suggested by Sutherland.[40] Similarly, the crystalline spectra of H_2S supports the frequency 2625 cm.$^{-1}$ for ν_3 and 1179 cm.$^{-1}$ for ν_2 which have been proposed recently [41] rather than the values in Table I.

The Structure of Solid CO_2.—Enough published data are available to compare the spectrum and X-ray structure of solid CO_2. According to the X-ray data the space group is T_h^6 with four molecules per unit cell.[42, 43] The molecules all lie on sites of symmetry $C_{3i}(\equiv S_6)$. This site symmetry alone is sufficient to establish that the exclusion rule between infra-red and Raman spectra should hold, as indeed it does. Comparison of the character tables of groups C_{3i} and T_h shows that, in addition, the totally symmetric vibration ν_1 (species A_g of C_{3i}) should give rise to two components, species A_g and F_g, of T_h. They may both be Raman active. In fact, this vibration is split by Fermi resonance with $2\nu_2$, just as in the gas, so that only the A_g component has been identified.[44] Similarly, the antisymmetric stretching vibration, ν_3 (species A_u), should give rise to two components, species A_u and F_u, of T_h and only the latter should be infra-red active. However, two active components were observed by Dahlke.[5] Finally, the bending vibration, ν_2 (species E_u of C_{3i}), should yield three components, one of species E_u and two of species F_u. Only the latter pair should be active but three components were observed.

At the moment these conflicts cannot be reconciled. The appearance

[38] Krishnan, *Proc. Indian Acad. Sci. A*, 1948, **27**, 321.

[39] Hainer and King, *Physic. Rev.*, 1949, **76**, 473.

[40] Sutherland, *ibid.*, 1939, **56**, 836.

[41] King, *J. Chem. Physics*, 1947, **15**, 85; Hainer and King, *ibid.*, 1947, **15**, 89.

[42] de Smedt and Keesom, *Proc. K. Akad. Wetensch.*, 1924, **27**, 839.

[43] Mark and Pohland, *Z. Krist.*, 1925, **61**, 293.

[44] McLennan and Smith, *Can. J. Res.*, 1932, **7**, 551.

of more than the predicted number of active components suggests that the symmetry is lower than found in the X-ray investigations. On the other hand, the difficulty may lie in the interpretation of the spectroscopic observations. It is interesting that the observed number of infra-red components is exactly equal to the total predicted number, active and inactive. A variety of qualitative explanations might be offered but it is clear that CO_2 deserves further study.

The Structure of Crystalline HCN.—The structure of crystalline HCN has not been reported by X-ray investigators. It is possible, however, to reach some fairly definite conclusions on the basis of the low temperature infra-red spectrum. The salient facts about the spectrum which must be explained are (1) that although HCN is one of the most perturbed molecules listed in Table I the stretching frequencies have but one component, in contrast to the hydrogen halides, and (2) that the bending frequency has two components which are polarized, as shown by the fact that only one appears in thin non-scattering films, but both appear in thick films and that the ratio of their intensities is variable.[7]

The first fact implies either that there is but one molecule per unit cell or that, if there are more, the remaining coupling components must be inactive because of symmetry. This conclusion is strengthened by the extreme sharpness of the $C{\equiv}N$ stretching vibration, ν_1 (only 7 cm.$^{-1}$).

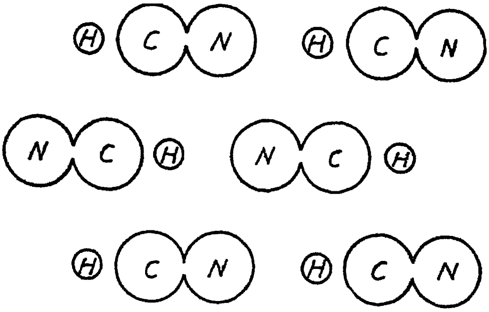

FIG. 1.—Single layer of HCN crystal.

If a structure with only one molecule per unit cell is assumed, the molecule must lie on an axis of symmetry no higher than C_2 to explain the second fact. No reasonable structure of this sort can be found.

If there are several molecules per unit cell the number cannot exceed four, the maximum number in which a non-degenerate vibration can couple to yield but one active component. This can occur by coupling to yield an active triply degenerate component plus an inactive totally symmetric mode in a cubic group, or by coupling to yield a doubly degenerate vibration and two inactive vibrations in a tetragonal group. Cubic groups are ruled out by the polarization and a tetragonal (or hexagonal) structure is possible only if the axis of the molecule is perpendicular to the symmetry axis.

It does not seem possible to construct a tetragonal crystal with only two molecules per unit cell which will meet these specifications. Neither does it seem possible to construct a hexagonal crystal with molecules perpendicular to the 3-fold axis. However, it is possible to construct a tetragonal crystal with four molecules per unit cell which satisfies all requirements. It is a layer structure in which each layer consists of antiparallel chains of HCN and alternate layers are rotated by 90°. A characteristic layer is shown in Fig. 1. This structure has symmetry C_{4h}^2. It is readily ascertained that the unit cell contains two four-fold screw axes, two C_2 axes, two planes of symmetry (containing the HCN molecules), and eight centres of symmetry (four in each plane, midway between chains of HCN molecules and at the point of intersection of the screw and C_2 axes with the plane). In this structure the HCN molecules occupy points of symmetry C_{1h}. Comparison of the character tables for C_{1h} and C_{4h} shows that each vibration of species A' in C_{1h} (both stretches and one component of the bend) gives rise to one component each of species A_g, B_g and E_u in C_{4h}. The first two may only be Raman active but the latter may only be infra-red active. It is polarized perpendicular to the S_4 axis. Similarly, the component of bend parallel to the tetragonal axis is of species A'' in C_{1h} and the four molecules may couple to give components A_u, B_u and E_g. Species A_u is active in the infra-red spectrum, E_g in the Raman and B_u in neither; the A_u component is polarized parallel to the S_4 axis. These conclusions could readily be checked from the Raman spectrum since mutual exclusion is expected.

No other structure which is compatible with the observed spectrum could be found. Nevertheless, these conclusions should be taken with caution until Raman and X-ray data are available. It is interesting to note that if the distance between layers is nearly the same as the distance between chains in a single layer, as one would expect, this structure would yield a nearly cubic crystal.

Complicating Features.—If the first order approximations are not valid and higher order terms must be included in the expansions, the spectra will be complicated by overtone and combination bands, not only of the internal modes but also between lattice and internal vibrations. Furthermore, there are essentially no selection rules for overtone and combination bands since, as was pointed out by Born and coworkers [45, 46] and recently in elegant form by Winston and Halford,[47] the only rigorous selection rule is that the combining states must have the same wave-number vector in the crystal. Since every internal vibration gives rise to coupled modes with essentially all wave-number vectors this amounts, in general, to removing all restrictions on overtones and combinations. Overtone bands may then have a line width equal to twice the width of the frequency distribution of the branch arising from the coupling of a given internal mode of vibration, and a combination band may have a width equal to the algebraic sum of the widths of the distributions of the combining branches. Frequency distribution functions have not been calculated for any complex crystals but an idea of their width may be obtained by noticing that the splitting due to coupling within a single unit cell constitutes an extremum, so that the width of the distributions may safely be taken to be of the order of magnitude of the splittings tabulated in Table I. The widths allowed by the general theory may be as great as a hundred wave numbers in this case.

Empirically, however, such line widths are not observed in ordered crystalline substances. With overtones and combinations of internal vibrations in such molecules as benzene, HCN, the ammonium halides and NH_3 they are only slightly, if at all, greater than the widths of fundamentals. Moreover, the general theory predicts that selection rules vanish, not only for combinations, but effectively also for fundamentals (i.e. coupling components of internal fundamentals) since at any temperature but absolute zero fundamental transitions may originate in excited lattice states whose symmetry, in general, may include all of the irreducible representations of the unit cell group, i.e. they may be of the form $\nu_I + \nu_L - \nu_L$, where ν_I is the internal frequency and ν_L is the lattice frequency. The fundamental might also appear as an allowed combination with very low-lying lattice vibrations so that it would not be recognized as a combination. These phenomena have not yet been observed, however; in all of the cases which have been examined to date, the selection rules for combination bands can be obtained from the unit cell group

---

[45] Born and Blackman, *Z. Physik*, 1933, **82**, 551.
[46] Born and Bradburn, *Proc. Roy. Soc. A*, 1947, **188**, 161.
[47] Winston and Halford, *J. Chem. Physics*, 1949, **17**, 607.

and no violations of selection rules have been observed for fundamental vibrations.

Combinations with Lattice Vibrations.—Combinations between internal and lattice vibrations have been observed in a number of cases. Mair and Hornig [19] observed three lines in the spectrum of benzene at − 170° C which could only be interpreted as combinations of ν_{11} with torsional vibrations of the benzene molecule in the lattice having frequencies 82, 98 and 128 cm.$^{-1}$. Such vibrations have been observed as fundamentals in the Raman spectrum of crystalline benzene at liquid N_2 temperature [48] with the frequencies 81, 101 and 124 cm.$^{-1}$.

In the ammonium halides [22] it was found that the line which occurs in both the infra-red and Raman spectra at 1790 cm.$^{-1}$ in NH_4Cl, 1718 cm.$^{-1}$ in NH_4Br and 1685 cm.$^{-1}$ in NH_4I can only be a combination between the triply degenerate bending vibration ν_4 of the NH_4^+ ion which has a frequency of about 1400 cm.$^{-1}$ in all three cases and torsional vibrations in the lattice with frequencies 390 cm.$^{-1}$, 315 cm.$^{-1}$ and 285 cm.$^{-1}$.

The NH_3 and ND_3 crystals show regions of absorption extending from 1350 to 1650 cm.$^{-1}$ and 1050 to 1200 cm.$^{-1}$, respectively, which must be combinations of the parallel bending vibration ν_2 at 1060 cm.$^{-1}$ and 815 cm.$^{-1}$ with lattice torsions. In this case this conclusion was confirmed directly by the observation of strong absorption maxima in NH_3 at 527 cm.$^{-1}$ and at 362 cm.$^{-1}$ which must be the corresponding fundamentals. Similar maxima were observed in ND_3 at 406 cm.$^{-1}$ and at approximately 250 cm.$^{-1}$.

Such torsional frequencies offer one of the easiest routes to the direct calculation of intermolecular potentials. They are also important because for crystals composed of polar molecules they must be the chief source of the atomic polarization term in the dielectric constant, both because they are the lowest lying frequencies and because the line strength may be very great. In NH_3 the line at 362 cm.$^{-1}$ is the most intense, by far, in the entire spectrum. These torsional frequencies (termed " librations " by some authors) have also been observed as broad combination bands in HCl, HBr and H_2S and as a fundamental in HCl.

Up to the present time no definitely established combinations of internal modes with translational lattice vibrations have been observed although the absorption at 3223 cm.$^{-1}$ in NH_4Cl and 3195 cm.$^{-1}$ in NH_4Br has been attributed [22] to the combination of the totally symmetric vibration of the NH_4^+ ion at 3048 and 3037 cm.$^{-1}$ with the lattice frequencies in the vicinity of the Reststrahlen frequency. It seems quite certain that combinations with torsional frequencies are of much more common occurrence.

Intensities.—All of the preceding discussion has been in terms of vibration frequencies. In these terms the effect of the crystal may be considered a small perturbation of the molecules, except for the introduction of a new effect, the lattice vibrations. However, in the case of intensities enough data has been accumulated to indicate that major changes may take place on crystallization. For example, the relative intensities of the vibrational fundamentals in HCN [7] and in NH_3 [36] change tremendously. Moreover, it has been reported for both the ammonium halides and benzene that the integrated intensity of the fundamental vibrations decreases by about 30 % in going from room to liquid nitrogen temperatures.[22] The available data are so slight, however, that no conclusions can yet be drawn except that significant effects occur and that both theoretical and experimental studies of intensities are needed.

Metcalf Chemical Laboratories,
Brown University,
Providence, Rhode Island.

---

[48] Sirkar, *Indian J. Physics*, 1936, **10**, 189.

INFRA-RED ADSORPTION SPECTRA OF METALLIC ACETYL-ACETONATES

By Jean Lecomte

Received (in French) 20th July, 1950

The absorption spectra of seven metallic acetyl-acetonates have been obtained from the powders in the region 525-1750 cm.$^{-1}$. These experimental results are interpreted in terms of the vibrations of the carbon chain and the CH_2 or CH_3 groups, and taking account of the keto-enol isomerism. The changes caused in the spectra by the presence of the metal are stressed. From the infra-red spectra it is deduced that the acetyl-acetonates behave as complexes and that a cyclic formula is most probable.

The work * was commenced in 1939.[1] but it did not give any clear interpretation of the spectra of the three metallic acetyl-acetonates studied, and we have since repeated this work and increased the number of substances studied to seven, using instruments built by Perkin-Elmer and Beckman in the region 700-1750 cm.$^{-1}$ (cf. spectrograph of weak dispersion used during 1939 and 1940). We have extended the range between 525 and 700 cm.$^{-1}$ by using a prism of sylvine in the spectrograph. The spectra were easily obtained with dry powder using either the technique previously employed at the Sorbonne,[2] or by moistening the powder with Nujol. We have also examined the spectra of freshly distilled acetyl-acetone. Four metal acetyl-acetonates were studied in the same way as Morgan [3] with acetyl-acetone between 400 and 3000 cm.$^{-1}$, mainly with the object of investigating the characteristic bands of the metal-oxygen bands. In the interpretation of our measurements we use these results in the same way as those obtained for the Raman effect by Kohlrausch and his collaborators[4] on the important series of substances showing keto-enol isomerism.

Experimental Results

Our results are summarized in Fig. 1 in which the positions of the absorption bands are indicated by lines, the height of which is proportional to the intensity. This Figure also includes Morgan's results. On the whole we find the same behaviour as that found by Morgan, but our results for ferric acetyl-acetonate do not agree with his. (This is the only acetyl-acetonate which is common to both sets of results.) We consider that this difference is due to the fact that the preparations did not lead to the same product in both cases.

From Morgan's results for the region 400 to 525 cm.$^{-1}$ and from our results for the region 525 to 1750 cm.$^{-1}$, the main regions of absorption for all the acetyl-acetonates are found in the same position, whatever the metal, and have mean wave numbers as follows :

410 450 and 470 512 and 530 760 to 824 930 1020
∓ 2 3 4 5 6
1185 and 1266 1310 to 1368 1400 1450 1520 1560 cm.$^{-1}$.
7 8 9 10 11 12

---

* Carried out in collaboration with M. René Freymann, Professeur à la Faculté des Sciences de Rennes. and with M. Clement Duval, Maître de Recherches au Centre National de la Recherche Scientifique

[1] Lecomte and Freymann, *Compt. rend.*, 1939, **208**, 1401.

[2] Lecomte, *Cahiers physique*, 1943, **17**, 1.

[3] Morgan, *U.S. Atomic Commission*, 1949 ; AECD, 12659, 16.

[4] Kohlrausch and Pongratz, *Ber.*, 1934, **67**, 976, 1465 ; Kahovec and Kohlrausch, *Ber.*, 1940, **73**, 1304 ; Kohlrausch and Pongratz, *Sitz. Akad. Wiss. Wien.*, 1937, **146**, 226 ; *Monatsh.*, 1937, **70**, 226.

A certain number of well-defined absorption maxima also exist between 600 and 700 cm.$^{-1}$ to which we refer later.

Interpretation of Results.—An interpretation of the vibration spectra of metallic acetyl-acetonates does not seem to have been previously attempted and an approach has only been made to certain parts of this difficult problem. For the sake of clarity we use a semi-empirical method in considering in turn: (i) the bands due to skeletal carbon atoms (and also the hydrogen atoms), but not of the metal, nor of the keto-enol isomerism; (ii) the bands due to keto-enol isomerism; (iii) the bands due to the presence of metal.

When we consider the problem of the whole system it appears too difficult to solve by methods at present available, using the number of relatively important vibrating masses, and also the influence exerted by the metal on the spectra about which so little is known, for compounds such as acetyl-acetonates. Although the method appears to be somewhat indirect and is open to criticism, we shall, where possible, consider the problem to be one analogous to that of a carbon chain of the acetyl-acetone type, with which in fact we are left after removal of the metal. Then we investigate how the metal interferes, and consider possible new structures. We assume that although the final structure may be cyclic, we apply conclusions obtained from the consideration of a non-cyclic type. In effect, the cyclic form is necessary to explain our results, but such a specialized cyclic structure need not be considered as a whole, as we do for aromatic and cyclohexanol nuclei (at least for the modes of vibration of the carbon chain). On examining the cyclic structure in its several parts, the constitution of which need only be known to a first approximation, we are able to obtain interpretations which are clearer than those obtained from the study of the problem as a whole.

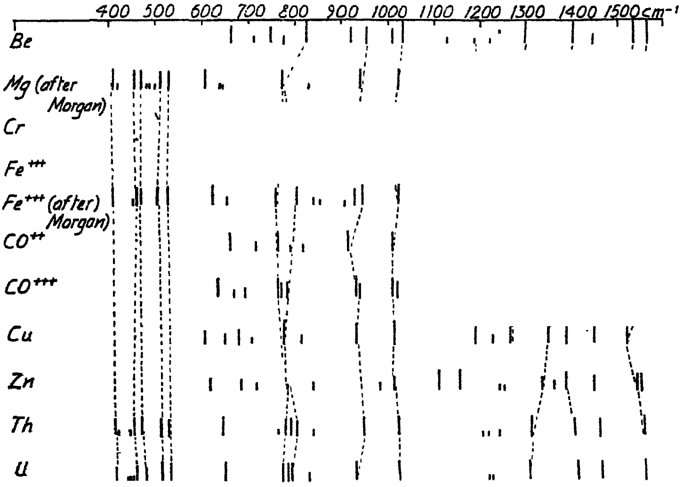

FIG. 1.

Discussion

I.—Bands Due to Skeletal Carbon Atoms or CH_2 or CH_3 Groups.—(*a*) To simplify the problem we consider the carbon chain of acetyl-acetone in the keto form in which the groups CH_2 and CH_3 appear as single entities (it may be noted that if the ion is in the enolic form, with the groups CH, CH_3 and OH considered as points, the result is the same). With the molecular model for seven masses similarly constituted the number of fundamental vibrations is 15. It is interesting to note that modes of vibration are obtained which, as a first approximation, are applicable to the acetyl-acetonates.

We note that it is possible to consider the carbon skeleton of acetyl-acetone as formed by the combination of two molecules of acetone connected by a common CH_2 group, thus :

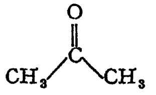

acetone

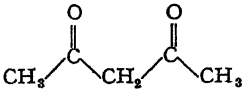

acetyl-acetone.

The modes of vibration of a molecular model are then obtained in the form of a coupled double Y structure sometime in-phase and sometime out-of-phase, i.e. the six well-known modes of vibration for acetone considered as a model in the form of a Y structure with the CH_3 groups as points. This leads to 12 modes of vibration to which must be added 3 others obtained by appropriate coupling of one translation and two rotations which do not give absorption bands for the free acetone molecule. One thus gets the scheme shown in Fig. 2. Two of these modes of vibration are inactive in absorption. The symmetry of the scheme conforms to that found for a molecular model of symmetry C_{2v} with one mass vibrating on the binary axis and three symmetrical masses on both sides of the axis.

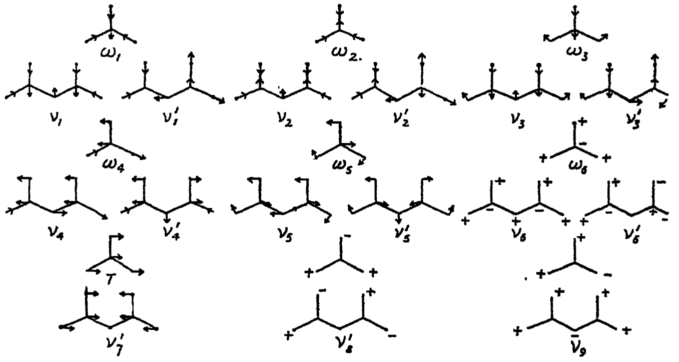

FIG. 2.

Our procedure gives a ready interpretation of the absorption maxima of metallic acetyl-acetonates as being due to the skeletal carbon atoms. In effect, the coupling of a single vibration of acetone, sometime in phase sometime out-of-phase, produces two vibrations of acetyl-acetonates the wave numbers of which have a small separation and which also approach the vibrations of acetone by which they are caused. The maxima included in the regions 1, 2, 3, 4 and 7 can be compared with the following vibrations of acetone.

ω_6	ω_3	ω_5	ω_1	ω_4
390 (D)	489 (P)	527 (D)	787 (P)	1225 (D) cm.$^{-1}$.

The letters D and P indicate polarized or depolarized Raman lines.

We consider further the vibration ω_2. It will be difficult to claim a better agreement between the calculations and the spectra of the acetyl-acetonates. It may be noted in passing that region 1 only gives a single band for these latter substances because coupling in-phase and out-of-phase of the ω_6 vibration of acetone leads only to an active vibration in the infra-red for the simplified model considered here.

(*b*) If we now take into account the characteristic vibrations of the CH_2 and CH_3 groups, we find a new series of bands which can also be compared with those of acetone. We have previously given [5] an analysis of the vibrational spectra of the latter substance. But here we must note that the coupling in-phase and out-of-phase of two molecules of acetone will probably not produce large differences between the wave numbers with the result that the bands will be considered as single ones for the acetyl-acetonates as is confirmed by experiment. The agreement found with the older measurements on acetone is given as follows :

Acetone . .	(907 918)	1070	1060	(1298 1346)	(1429 1444) cm.$^{-1}$
	Ra IR	IR	Ra	IR Ra	IR Ra
Acetyl acetonates	920-930	1005-1025	?	1310-1368	1447-1460 cm.$^{-1}$

II.—Bonds due to Keto-enol Isomerism.—The question of the keto-enol isomerism is more complicated than the preceding one because the molecular structure is not exactly known and because, at least in the enolic form, the position of the bands usually attributed to C═C and C═O undergo important variations.

Our measurements lead to the conclusions that metallic acetyl-acetonates, exist solely in the enolic form and that a cyclic formula of the Sidgwick type best represents the experimental results.

We will now give a brief review of the wave numbers attributable to the vibrations of the CO bond. These results then help in the interpretation of the metallic acetyl-acetonate spectra and allow a choice between the possible enolic structures.

(*a*) We recall the well-known result that the normal values of the characteristic bands of the C═O group, for example those of the aldehydes and the aliphatic acetones, as with the esters of formic acid, occur at about 1718 cm.$^{-1}$. The introduction of halogen atoms increases these wave numbers appreciably. Numerous examples of the reduction of the frequency are known in other work, for example, in aldehydes and aromatic acetones, and recently Jones has given evidence showing that in the sterols the CO band could be characterized by bands varying between quite wide limits.

It is also noteworthy that in measurements made at the Sorbonne on almost a thousand salts of organic acids [6] which ionize giving the carboxyl group, a resonance was found to occur between the bonds of the carbon atom and each of the two oxygen atoms. One can no longer speak of a double or single bond, but one may write it in the form 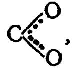 $\mathrm{C}\genfrac{}{}{0pt}{}{\cdot\cdot\,\mathrm{O}}{\cdot\cdot\,\mathrm{O}}$, a grouping in which the symmetrical and anti-symmetrical vibrations are at 1300 to 1400 and at about 1550 cm.$^{-1}$. An analogous phenomenon seems to occur in substituted amides when resonance tends to reduce the bonding force between carbon and oxygen and to increase that between the bonding force between carbon and oxygen and to increase that between carbon and the NH$_2$ group. We therefore write the formula

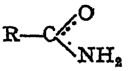

$\mathrm{R{-}C}\genfrac{}{}{0pt}{}{\cdot\cdot\,\mathrm{O}}{\cdot\cdot\,\mathrm{NH_2}}$

unsubstituted amide

and

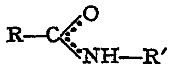

$\mathrm{R{-}C}\genfrac{}{}{0pt}{}{\cdot\cdot\,\mathrm{O}}{\cdot\cdot\,\mathrm{NH{-}R'}}$

mono-substituted amide

One can consequently determine from the vibration spectra whether a CO group exists in a perturbed or unperturbed state, from the positions of the characteristic bands between 1300 and 1750 cm.$^{-1}$.

(*b*) The above conclusions can be applied to the metallic acetyl-acetonates. The complete absence of a band in the region 1700 to 1750 cm.$^{-1}$ shows that we are not dealing with a formula derived from the ketonic form or acetyl-acetone.

---

[5] Lecomte, *J. Physique*, 1945, **6**, 127.

[6] Lecomte, *Rev. Optique*, 1949, **28**, 353 ; Duval, Lecomte and Mme. Douvillé, *Ann. Physique*, 1942, **17**, 5 ; Mme. Douvillé, Duval and Lecomte, *Bull. Soc. chim.*, 1942, **9**, 548.

$$CH_3\,CO\,CH_2\,CO\,CH_3.$$

The changes which we find in the characteristic frequencies of the CO groupings favour the enolic form. The latter becomes more probable if one considers the number of bands which occur in the region 1300 to 1600 cm.$^{-1}$. We attribute two of these to the CH_2 or CH_3 groups (see above), so that there remain three bands characteristic of the enolic form. These latter are clearly interpreted in terms of an enolic form, two absorption bands arising from the ω_2 vibration of acetone (affected by the necessary perturbations), and another ν_7', from a translation mode of the acetone molecule, but with the C=C bond perturbed.

One can then think of the strong bands between 1550 and 1562 cm.$^{-1}$ on the one hand and between 1310 and 1403 cm.$^{-1}$ on the other, as caused by the two CO groups. Inasmuch as one can consider separately the bonds between atoms without taking account of the rest of the molecule, the first would represent a CO group with an attractive force reduced relatively to a "double" bond; the second represents a "single" bond of increased strength. In a paper on the esters of aliphatic organic acids we have shown that this latter occurs in the region 1200 cm.$^{-1}$.[7] (when we are concerned with a simple non-perturbed bond). The variations of the bonds between carbon and oxygen, which we have considered, apparently tend to reduce the separation between the two wave numbers previously indicated. In its turn the maximum found between 1500 and 1534 cm.$^{-1}$ would represent a perturbed C=C bond.

We show that it is equally possible to choose for the perturbed vibration of C=C bond the intense band between 1550 and 1562 cm.$^{-1}$ and for the perturbed C=O vibration, the band which exists between 1503 and 1534 cm.$^{-1}$. We nevertheless think that the first alternative which we have given above is the more correct by reason of the results of the Raman spectra of zinc and aluminium complexes of acetyl-acetone, of methyl or ethyl malonate (measured by Kohlrausch *et al.*). The study of analogous compounds in the infra-red is in progress.

(*c*) Until now we have proceeded to the identification making use of the maxima of the absorption spectra of various modes of vibration without making a precise statement about the structure of the enolic form and we were satisfied to indicate the changes in the normal characteristic absorption bands of the different groupings caused by the presence of the metal. The problem has been to indicate the nature of the vibrations rather than to apply them to a known formula of the molecule. This latter, however, will now be attempted. Kohlrausch, in particular from a study of Raman spectra, has been interested in this question, and in the case of acetyl-acetone has indicated the possibility of four enolic forms, two mono-enolic and two di-enolic. We shall only reproduce the first two.

$$CH_3 - C(OH) = CH - CO - CH_3,$$
$$CH_2 = C(OH) - CH_2\,CO - CH_3,$$

and Kohlrausch shows that neither of these is satisfactory.

Limiting ourselves to the infra-red spectra, we observe that these formulae indicate the existence of an OH group and that we will have to find corresponding bands (fundamental and harmonics) in the near infra-red which, however, are not found. Alternatively, the spectra would have to be similar to those of the tertiary alcohols, but they actually show few analogies to these. Also, in the region 10 to 12 μ one should find evidence of a "double bond" in the linear molecule, but the bonds of the acetyl acetonates do not correspond to what one would expect.

For these reasons, and others which have been given by other authors, a cyclic formula seems the most likely. With acetyl acetone the internal cyclic formula explains perfectly why no OH bands exist (see the analogous classical cases of salicylaldehyde or of methyl salicylate).

---

[7] Lecomte, *J. Physique*, 1942, 3, 193.

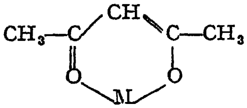

With acetyl acetonates we have stressed that the introduction of a metallic atom into the molecule leads to important changes in the positions of the bands representing the C═O or C═C (perturbed) bonds. If the metal is bonded to only one of the oxygen atoms the vibrations of the two atoms is not markedly disturbed. We have shown, moreover, an analogy between the acetyl-acetonates and the metallic salts of organic acids in which we are concerned with the valency vibrations of CO. In a number of different papers we have shown that even with monovalent metals in the salts the metal is bonded to two oxygen atoms in the ionized carboxyl groups. We show below that it is not possible to consider the acetyl-acetonates as salts, but that the cyclic formula of Sidgwick is quite satisfactory.

III.—Characteristic Bands of the Metal.—In the large number of salts of organic and inorganic acids which have been studied at the Sorbonne, characteristic bands of the metal are not found. The latter appear then as " transparent " in the region extending from the visible to less than 500 cm.$^{-1}$ (except for certain rare earth metals which show bands of an electronic nature in the near infra-red). At most, one finds a few little understood variations in the position of maximum absorption.

It is not possible with the few measurements available in the infra-red to confirm the nature of the bonds between the metal and the oxygen atoms according to the structure which we have indicated. It is, however, certain that the metallic acetyl-acetonates do not behave as salts but as complexes and in the same way we can forecast other physical properties.

At first the set of bands between 1310 and 1405 cm.$^{-1}$ and which we have attributed to a CO vibration, were clearly displaced to the lower frequencies according to the increase in weight of metal. We have never found a similar result for salts.

The important point is that between 600 and 700 cm.$^{-1}$, there are well-defined bands the number and position of which vary with the metal. The wave numbers which have been found are :

Be	661 (F) cm.$^{-1}$.
Mg (after Morgan)	608 (F), 621, 639, 642.
Cr	596 (F), 606 (m), 650 (F), 671 (F).
Fe^{+++}	660 (F).
Fe (after Morgan)	626 (F) 655.
Co^{++}	666 (F).
Co^{+++}	634 (F), 669 (aF), 694 (F)
Cu	607 (F), 648 (F), 677 (aF).
Zn	622 (m), 677 (m).
Th (after Morgan)	644 (F).
U (after Morgan)	619, 626, 651 (F).

If the metal only plays an inactive role as in the salts we shall not have to consider it when listing the vibrations. We have shown that all the vibrations which were expected have been identified with sets of bands which are found when one passes from one acetyl-acetonate to another. To explain subsidiary absorption maxima between 600 and 700 cm.$^{-1}$, one must suppose that several molecular forms exist which have common bands except in this region. This theory appears unlikely.

These difficulties are not present if one considers a ring in which the metal is included. The list of vibrations shows that three are known, besides that of the molecular forms in which the metal is not included. In agreement with Morgan this argument leads to the possibility of the bands in question being due to the metal-oxygen bonds. Unfortunately, we have been unable to show the precise nature of these bonds so one cannot state that they do not resemble those present in a salt. All that can be stated is that the region 600-700 cm.$^{-1}$ corresponds to a relatively feeble elastic force for these vibrations.

We have attempted to explain the variation in the position of Me—O bonds, but have not reached any conclusive result. It may only be noted that for the heavy metals, e.g. Th and U, the bands occur in the same region as for light metals, e.g. Be. To a certain extent the atomic radius divided by the valency of the metal helps in the elucidation of this fact.

It is not possible at present to explain why the number of bands is variable between 600 and 700 cm.$^{-1}$ as one passes from one metal to another. One would expect that associated with the metal one ring exists for monovalent metals, two rings for bivalent metals, etc. Unfortunately, as indicated for example by Co^{++} and Co^{+++}, the number of bands is not in accord with the valency.

Conclusions.—In this work we have tried to contribute to the knowledge of infra-red absorption spectra and to the analyses of the results obtained. In elucidating the difficult problem of the structure of the metallic acetyl-acetonates, we have accurately listed and identified the vibrations of the carbon chain obtained with a structure which seems to be cyclic (probably a single enolic form) and shown that complexes are involved. Unfortunately a number of points remain unsettled, amongst the most important being the manner in which the metal is bonded to the rest of the molecule.

We hope to return to this question in other work dealing with other metallo-organic compounds which behave similarly to these complexes.

This work was carried out in the Laboratoire des Recherches physiques, Sorbonne, under the direction of Monsieur le Professeur Cabannes to whom we wish to express our sincere appreciation for the interest which he has taken and for facilities placed at our disposal. Our appreciation is due also to our colleagues M. René Freymann and M. Clément Duval who have allowed us access to unpublished work. Thanks are also due to M. Fauvarque and Mlle. Morandat for measuring and analyzing the spectra.

Laboratoire de Reserche physiques,
Sorbonne,
Paris.

THE INFRA-RED ABSORPTION SPECTRA OF BORON-NITROGEN COMPOUNDS *

BY W. C. PRICE, R. D. B. FRASER, T. S. ROBINSON AND H. C. LONGUET-HIGGINS

Received 27th July, 1950

The infra-red spectra of borazole, *N*-trimethyl borazole, aminodimethylborine and trimethylamine-borine are described and interpreted. Analogies are drawn between the spectra of these compounds and those of benzene, mesityl-

---

* Part of this work was done at the University of Chicago under U.S. Office of Naval Research, N6-ori-20.

ene, *iso*butene and *neo*pentane respectively, with which they are isoelectronic. The resolution employed enabled a satisfactory analysis to be made of the spectrum of borazole throughout the range from 7000-400 cm.$^{-1}$.

The extremely high intensities of the bands indicate the high polarities of the structures and correlations are made with the strengths of the bands and the corresponding modes of vibration. Certain bands, which can be associated with simple vibrational modes, indicate how the bonds to the hydrogen atoms from boron, nitrogen and carbon atoms change with the nature of the BN bond.

The compounds borazole ($B_3N_3H_6$), *N*-trimethylborazole(*NN'N''*-$Me_3N_3B_3H_3$), aminodimethyl-borine (Me_2NBH_2) and trimethylamine-borine (Me_3NBH_3) are of great interest not only from the point of view of the chemistry of boron but also because they present structural problems which are amenable to spectroscopic attack. The molecules have much more strongly polar structures than those of more common substances because of the formation of a co-ordinated bond between the donor nitrogen and the boron atom, the BN bond tending to become similar to its isoelectronic CC counterpart. Amongst the various spectroscopic effects to which this gives rise the most striking is the unusually high intensity of certain of the infra-red absorption bands. A consideration of band intensities and corresponding modes of vibration gives some idea of where the high polarities are located in the molecule. In what follows a short discussion of the spectra of each compound will be given. While the analysis for borazole is fairly complete, that for the other substances is only partial because of the large number of fundamental modes which these substances have and also because it was only possible to record the strongest bands with our experimental arrangement on account of their relatively low vapour pressures.

Borazole.—Borazole is isoelectronic with benzene, a substance which it resembles in many ways. Chemical evidence,[1,2] electron diffraction [3] and spectroscopic studies [4] support a regular hexagonal structure similar to that of benzene, the carbon atoms of the ring being alternately replaced by boron and nitrogen atoms respectively. The hydrogen atoms do not, of course, form a regular hexagon because of the different lengths of the NH and BH bonds. The Raman and infra-red spectra of borazole were obtained by Crawford and Edsall [4] who, assuming the molecule to have D_{3h} symmetry, were able to make a satisfactory assignment of most of the fundamental frequencies. The resolving power of their infra-red spectrometer was, however, very poor compared with that of modern instruments, its limitations being clearly stated in their paper. The spectra we have obtained, which were recorded on a modern high resolution prism spectrometer (Perkin-Elmer 12B, with LiF, NaCl, KBr prisms) bring out many important features which they were unable to observe especially in the short wavelength region. The slit widths previously used (e.g. 250 cm.$^{-1}$ at 3000 cm.$^{-1}$) resulted in observed absorption intensities on narrow bands roughly 50 times less than those reported here and in some cases led to completely misleading values of relative intensities. Work on the higher frequency overtones was impossible in the earlier work and the structure of band envelopes and the isotope effects were not resolved.

The spectrum of borazole is given in Fig. 1. Many of the bands are so intense that a few tenths of a mm. pressure in a path length of 10 cm. is all that is needed for their observation. The theoretical expectations for a model of D_{3h} symmetry are contained in Tables I and II. These are followed by Tables III and IV of assignments of the bands observed.

---

[1] Stock, *Hydrides of Boron and Silicon* (Oxford University Press, 1933).

[2] Bell and Emeleus, *Quart. Rev.*, 1948, **2**, 132.

[3] Bauer, *J. Amer. Chem. Soc.*, 1938, **60**, 524.

[4] Crawford and Edsall, *J. Chem. Physics*, 1939, **7**, 223.

TABLE I.—SELECTION RULES FOR FUNDAMENTALS OF BORAZOLE (D_{3h} MODEL)

Species	Activity	Number
A_1'	R(p)	4
A_1''	Inactive	0
A_2'	Inactive	3
A_2''	I	3
E'	R(d) and I	7
E''	R	3

Species marked $'$ give rise to in-plane modes, and those marked $''$ to out-of-plane modes. R denotes Raman activity (p polarized, d depolarized), and I infra-red activity. The I fundamentals of species E' will have marked PQR band structures.

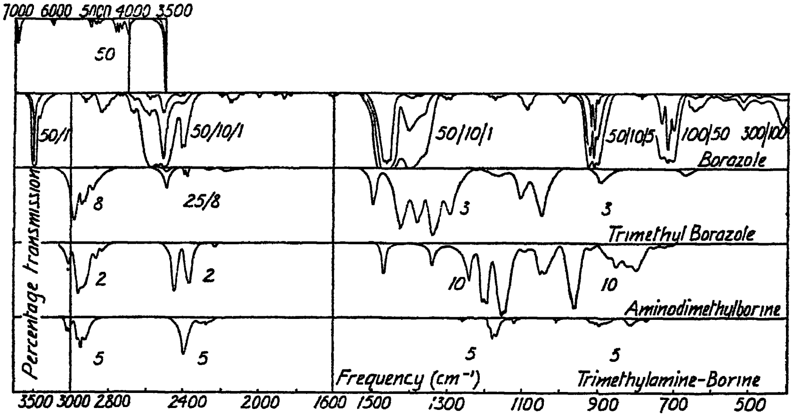

FIG 1.—The infra-red spectra of borazole, N-trimethyl borazole, aminodimethylborine and trimethylamine-borine in the range of 7000-400 cm.$^{-1}$ All spectra taken in the vapour phase with a cell length of 10 cm., pressures are shown in millimetres of mercury.

SELECTION RULES FOR COMBINATION BANDS.—As there are no fundamentals of species A_1'', this species is omitted in the following multiplication table:

TABLE II.—SELECTION RULES FOR COMBINATION BANDS OF BORAZOLE (D_{3h} MODEL)

	A_1'	A_2'	A_2''	E'	E''
A_1'	A_1'	—	—	—	—
A_2'	A_2'	A_1'	—	—	—
A_2''	A_2''	A_1''	A_1'	—	—
E'	E'	E'	E''	$A_1'+A_2'+E'$	—
E''	E''	E''	E'	$A_1''+A_2''+E''$	$A_1'+A_2'+E'$

Combinations having the species A_2'' or E' are allowed in the infra-red. Hence the allowed combinations are:

$$A_1' \,.\, A_2'' = A_2'', \qquad A_1' \,.\, E' = E', \qquad A_2' \,.\, E' = E' \qquad A_2'' \,.\, E'' = E',$$
$$E' \,.\, E' = E'(+A_1'+A_2'), \quad E' \,.\, E'' = A_2''(+A_1''+E''), \quad E'' \,.\, E'' = E'(+A_1'+A_2')$$

The combinations of species E' will have PQR contours, like the corresponding fundamentals.

ASSIGNMENT OF FUNDAMENTALS.—The following assignment is essentially that of Crawford and Edsall. Our data have been taken for the range above 500 cm.$^{-1}$ in the infra-red and their data for the Raman bands.

TABLE III.—ASSIGNMENTS OF FUNDAMENTAL FREQUENCIES OF BORAZOLE FREQUENCIES IN CM.$^{-1}$

Species	Infra-red	Raman
A_1'	—	851 (6p)
	—	938 (7p)
	—	2535 (9p, vb)
	—	3450 (10p)
E'	519 (i)	519 (3d)
	718 (5, *PQR*)	708 (1)
	918 (15, i, *PQR*)	—
	1465 (100, *PQR*)	1465 (1)
	1605 (0·1, *PQR*)	—
	2530 (30)	— (h)
	3490 (100)	— (h)
(Calculated values are available, but these are not too reliable.)		
E'' . .	—	288 (2b)
	—	798 (2)
	—	1070 (5d)
A_2''	415 (3, C. and E.)	—
	649 (2, *PQR*)	—
	1088 (1·5, *PQR*)	—

PQR indicates branches observed; i = band shows strong isotope effect; b = broad; vb = very broad; figures in brackets in infra-rep column are rough relative values of extinctions of maxima, in Raman column figures are C. and E.'s estimates of intensity; h = hidden by A_1' fundamentals.

The 3490 cm.$^{-1}$ band is clearly an NH stretching mode. Its value is appreciably greater than the value of *ca.* 3350 cm.$^{-1}$ for amines or 3337 cm.$^{-1}$ in ammonia. This is probably mainly due to the positive nature of the nitrogen atoms though possibly a small portion results from the aromatic nature of the bond in the same way that aromatic CH has a slightly higher frequency than alkyl CH. The intensity of this band is extraordinarily high, the extinction being about a hundred times as great as that of the corresponding band in ammonia. Its overtone at 6880 cm.$^{-1}$ is also very strong, appearing with 50 % absorption at 100 mm. pressure in a path length of 10 cm. Bands of this intensity are only observed with very strongly polar compounds.

The next strong band at 2530 cm.$^{-1}$ is the BH stretching mode. It is single as required and not double as for terminal BH_2 in diborane or aluminium borohydride,[5] or in Me_2NBH_2 (reported here). Its frequency is close to the value which from the analysis of these compounds we associate with a single (2 electron) BH bond. Its intensity though not quite as great as that of the NH band is still very high and about equal to the corresponding bands in aluminium borohydride where the binding is considerably ionic in character. The 1465 cm.$^{-1}$ frequency is a ring vibration (B, N deformation in which the differently charged atoms move relative to one another). In view of the positive charges on the nitrogen and the negative ones on the boron it is not surprising that this is the strongest band in the spectrum. The band 918 cm.$^{-1}$ is an NH, BH in-plane bending mode as also is the band at 718 cm.$^{-1}$. The numerous other bands represent weak fundamentals and combination bands. For example, the 649 cm.$^{-1}$ fundamental is an out-of-plane bending mode in which the B_3N_3 hexagon moves against the H_6 hexagon. This may be expected to be relatively weak because of the compensation of the positive charges on the nitrogen atoms by the negative ones on the boron atoms and also that of the positive hydrogens attached to the nitrogen atoms by the negative hydrogens attached to the boron atoms. The weakness of the 519 and 1605 bands is to be attributed to the fact that the corresponding modes in benzene are only Raman active while those of the 415 and 1088 are inactive.[4] All the combination bands which would be expected to appear are found and the spectrum is generally in very good agreement with the D_{3h} model for borazole.

---

[5] Price, *J. Chem. Physics*, 1949, 17, 1044.

TABLE IV.—ASSIGNMENT OF COMBINATION BANDS

Frequency	Intensity	Assignment	Symmetry
567	(0·02)	288+288=576	$E'(+A_1'+A_2')$
789	(0·1, *PQR*)	1088−288=800	"
986	(0·5)	718+288=1006	$A_2''(+A_1''+E'')$
1175	(0·2 *PQR*)	918+288=1206	"
1310	(0·2 *PQR*)	—	—
1360	(1·0)	1070+288=1358	$E'(+A_1'+A_2')$
1410	(20)	718+718=1436	$E'(+A_1'+A_2')$
	and/or	519+918=1436	"
1835	(0·1)	918+938=1856	E'
1865	(0·2)	1070+798=1868	$E'(+A_1'+A_2')$
2000	(0·15)	1088+918=2006	E'
2144	(0·4, *PQR*)	1070+1070=2140	$E'(+A_1'+A_2')$
2158	(0·4, *PQR*)	1070+1088=2158	E'
2197	(0·1, *PQR*)	1465+718=2183	$E'(+A_1'+A_2')$
2400	(5)	1465+938=2403	E'
2408	(5)	1605+798=2403	$A_2''(+A_1''+E'')$
2493	(10)	—	—
2522	(20?)	1605+918=2523	$E'(+A_1'+A_2')$
	or	1465+1070=2535	$A_2'(+A_1'+E'')$
2592	(15)	1465+851+288=2604	$A_2''(+A_1''+E'')$
2668	(3 *PQR*)	1070+1605=2675	"
2734	(0·01)	3450−718=2732	E'
2743	(0·01)	2490−718	$E'(+A_1'+E'')$
2801 2810 2830	(8)	2530+288=2818	$A_2''(+A_1''+E'')$
2931	(0·5, *PQR*)	1465+1465=2930	$E_1(+A_1'+A_2')$
3985	(0·6)	2530+1465=3995	"
4135	(0·3)	2530+1605=4135	"
	or	3450+718=4168	
4274	(0·4)	3490+798=4288	$A_2''(+A_1''+E'')$
4305	(0·5)	3450+918=4368	E'
4765	(0·2)	—	—
4850	(0·3)	3490+1465=4955	$E'(+A_1'+A_2')$
4965	(0·4)	2530+2530=5060	"
	or	2530+2535=5065	E'
6000	(0·3)	3490+2530=6020	E'
6880	(1·0)	3490+3490=6980	$E'(+A_1'+A_2')$
	or	3450+3490=6940	E'

BAND ENVELOPES.—The contours of many of the bands are of a simple *P*, *Q*, *R* type, the separation of the *P*, *R* maxima being about 27·5 cm.$^{-1}$ and corresponding to a moment of inertia about an axis in the plane of the molecule. Similar contours are obtained for benzene in the vapour phase where the separation is 28 cm.$^{-1}$ [6] and also for 1 : 3 : 5-trifluorobenzene (separation 15 cm.$^{-1}$).[7] The band at 649 cm.$^{-1}$ presumably corresponds to the benzene parallel band at 671 cm.$^{-1}$, and, like the latter band, has a strong *Q* branch. The analogous band in trifluorobenzene, at 871 cm.$^{-1}$, has a similar contour.

Bands which correspond to modes in which the boron atoms move appreciably against the nitrogen or hydrogen atoms should show the isotope effect. With a B^{10}/B^{11} ratio of 1/4, the relative abundances of the four molecules $B_3{}^{11}N_3H_6$, $B^{10}B_2{}^{11}N_3H_6$, $B_2{}^{10}B^{11}N_3H_6$ and $B_3{}^{10}N_3H_6$ are in the ratios 50 : 40 : 10 : 1. The 918 cm.$^{-1}$ (900-935) band appears to show the isotope effect though the band structure is complicated by the presence of the *P* and *R* as well as the *Q* branches of the isotopic bands. The *Q* branch of the $B_3{}^{11}N_3H_6$ molecule, appears at 918·5 cm.$^{-1}$. A slightly weaker *Q* branch at 928·4 cm.$^{-1}$ may be attributed to the $B^{10}B_2{}^{11}N_3H_6$ molecule. The *Q* branches of the molecules containing $B^{11}B_2{}^{10}$ and $B_3{}^{10}$ are apparently too weak to show above the *P* and *R* branches of the two more abundant molecules. The isotopic separation is about what is expected for this vibration.[4] An alternative explanation of the structure of this band is to attribute it to splitting arising from Fermi resonance with the combination band $519(E') + 415(A_2'') = 934(E')$. This seems equally probable to the explanation in terms of the isotope effect. Many of the combination bands show structure which might be interpreted as an isotope effect but the situation is usually complicated by the presence of a number of allowed combinations occurring in the same range.

N-TRIMETHYL BORAZOLE.—In spite of the fact that this material has a vapour pressure of only 12 mm. at 25° C, the absorption is so strong that it was possible to obtain a large number of bands with a 10 cm. cell. For the stronger bands pressures of only 1 mm. were required in this cell length (Fig. 1). Starting at the high frequency end we have the bands of the CH_3 group in the 3000-2800 cm.$^{-1}$ range appearing at moderate strength, *ca.* 50 % absorption at pressures of 8 mm. These are followed by a band at 2485 cm.$^{-1}$ which is clearly the BH stretching mode. This is very much weaker than the corresponding band in borazole, equivalent pressures of 25 mm. in a 10 cm. path being required for a peak absorption of 50 %. The great reduction in intensity relative to the same mode in borazole is probably to be connected with polarization effects in the surrounding methyl groups.

The region 1500-1200 cm.$^{-1}$ contains a number of bands of which those at 1498 and 1383 cm.$^{-1}$ correspond to CH_2 and CH_3 deformation vibrations respectively which normally occur around 1450 and 1375 cm.$^{-1}$ in hydrocarbons. The increase may arise from the proximity of the intermediate hydrogen atoms (in liquid mesitylene * the values are 1443 and 1377 cm.$^{-1}$. Other strong bands at 1425, 1342 and 1294 cm.$^{-1}$ are probably ring vibrations analogous to the 1465 cm.$^{-1}$ band of borazole. The bands corresponding to in-plane deformation modes of the BH bonds (918 and 718 in borazole) are expected to move to higher frequencies due to larger repulsions from the methyl groups as in the alkyl benzenes and are thus probably to be associated with the bands at 1107·5 and 1056·2 cm.$^{-1}$ in trimethyl borazole. The 894 ·4 cm.$^{-1}$ frequency is no doubt an out-of-plane vibration similar to the 835 cm.$^{-1}$ band in mesitylene. The 672 cm.$^{-1}$ band is also probably analogous to that at 687 cm.$^{-1}$ in mesitylene. The following is a list of the frequencies of the observed bands, their intensities are best judged from the spectrum in Fig. 1 :

4600, 4350, 2989, 2938, 2885, 2495, 2397, 2386, 2275, 2160, 1498, 1425, 1383, 1342, 1294, 1163, 1107, 1056, 894, 672.

---

[6] Bailey, Hale, Ingold and Thompson, *J. Chem. Soc.*, 1936, 931.

[7] Nielsen, Ching-Yu Liang and Smith, this Discussion.

* See *A.P.I. Spectrogram* 1104.

AMINODIMETHYLBORINE (Me_2NBH_2).—This compound again has strong absorption bands and some of its main features can be interpreted fairly simply. In the 3009-2800 region we have the absorption characteristic of the methyl groups. Compared with the corresponding bands in *iso*-butene † they are shifted slightly to lower frequencies and are intensified by a factor of about 10. It appears likely that these facts are consistent with the withdrawal of some negative charge from the methyl groups. The absorption in the 2400 cm.$^{-1}$ region is quite characteristic of the terminal BH_2 group. It consists of two strong bands at 2447 and 2369 cm.$^{-1}$ These are clearly analogous to the band pairs in diborane at 2614 and 2522 cm.$^{-1}$ or in aluminium borohydride [8] at 2559 and 2493 cm.$^{-1}$. The strength of these bands is much greater than that of the 2495 cm.$^{-1}$ band in trimethylborazole and is of the same order as that of the corresponding bands in aluminium borohydride and borazole. Bands at 1467 and 1340 cm.$^{-1}$ are associated with the usual CH_2 and CH_3 vibrations. Of the remaining bands correlations with other borohydride spectra [5] indicate that the strong band at 1156 cm.$^{-1}$ is the in-plane deformation vibration of the BH_2 group and that at 964 cm.$^{-1}$ corresponds to the out-of-plane mode (1175 and 974 in B_2H_6 and 1114 and 978 in $Al(BH_4)_3$ respectively). The absence of Raman data prevents further speculation on the nature of the other bands. One of the remaining strong bands should be associated with a valence vibration of the BN bond. Judging from the force constants calculated for borazole by Crawford and Edsall [4] this is probably to be indentified with the 1193·5 cm.$^{-1}$ band.

The following is a list of the frequencies of the bands observed for this substance: 4300, 4180, 3013, 2962, 2932, 2861, 2813, 2447, 2369, 2225, 1467, 1340, 1240, 1209·6, 1193·5, 1156, 1148, 1054, 1046, 966·5, 961, 853, 795. The intensities are best judged by reference to the spectrum given in Fig. 1.

TRIMETHLYAMINE-BORINE (Me_3NBH_3).—Because of the low vapour pressure of this substance, which is a crystalline solid, it was only possible to bring out a few of the strongest bands with a heated cell. The CH stretching bands in the 2900 cm.$^{-1}$ range warrant no comment. The BH stretching band occurs at 2390 cm.$^{-1}$ which is to be compared with the value 2440 cm.$^{-1}$ found for the corresponding band in the somewhat related compound [9] borine carbonyl H_3BCO. The band at 1178-1169 cm.$^{-1}$ is by comparison with the spectra of the other borohydrides (ref. (5), Table III). a deformation mode of the BH_3 group. In borine carbonyl this vibration has a frequency of 1091 cm.$^{-1}$, in the latter spectrum this is interpreted as a BH_3 rocking mode. The higher value in trimethylamine-borine is no doubt due to repulsion from the methyl groups. A further band at 818 cm.$^{-1}$ has a counterpart in borine carbonyl at 809 cm.$^{-1}$. As in the latter spectrum this is interpreted as a BH_3 rocking mode. The frequencies of the bands observed in this spectrum (Fig. 1) are 3055, 3030, 3010, 2965, 2945, 2930, 2390, 2278, 1260, 1178, 1169, 1120, 1010, 905·5, 894, 873, 818 and 773 cm.$^{-1}$.

In conclusion we should like to acknowldge our indebtedness to Prof. H. I. Schlesinger's Group at the University of Chicago for the preparation of the substances investigated and to Prof. R. S. Mulliken for exciting our interest in the problems of their structures. Financial assistance for the work was supplied by the U.S. Office of Naval Research, the Department of Scientific and Industrial Research and the Medical Research Council.

King's College,
London, W.C. 2.

Manchester University.

---

† *A.P.I. Spectrograms* 378 and 912.

[8] Price, *J. Chem. Physics*, 1948, 16, 894.

[9] Cowan, *ibid.*, 1950, 18 (in press).

INFRA-RED SPECTRA OF ORGANIC THIOPHOSPHATES

By R. C. Gore

Received 21st August, 1950

In connection with some Company research, it became of interest to investigate the infra-red absorption of over one hundred organic thiophosphates and related molecules. The regions of particular interest were those of the characteristic infra-red absorption for the P → O, the P → S, and the C—S—P linkages which could furnish spectroscopic evidence for the presence of those groups in molecules of doubtful structure It was thought probable that the P → O and P → S linkages would exhibit sufficiently characteristic absorption to be recognizable but that the C—S—P linkage might prove to be less characteristic.

The Absorption Frequencies of P → O and P → S.—In order to understand the nature of these co-ordinated covalent bonds, it is, perhaps, worth while to review what has been learned about them in simpler molecules such as P_4O_{10} and $P_4O_6S_4$. Electron diffraction studies[1,2] of P_4O_{10} and $P_4O_6S_4$ indicate that the structures belong to the tetrahedral point group T_d with the following geometry:

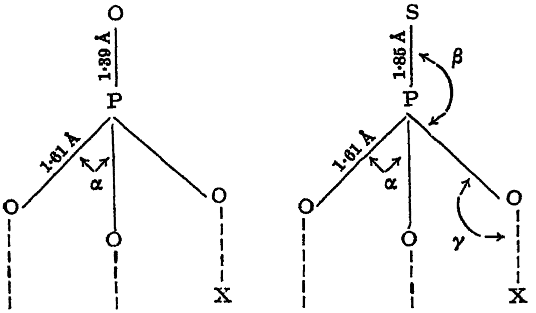

$\alpha = 101{\cdot}5°$
$\beta = 116{\cdot}5°$
$\gamma = 123{\cdot}5°$

The P—O and P—S distances of 1·61 Å and 1·85 Å are both less than the usual covalent single bond distances of 1·76 Å and 2·14 Å as reported by Pauling and Higgins for these pairs of atoms. The co-ordinated covalent P→O and P→S distances in various other compounds closely related to these molecules are shown to be the following:

Compound	P→O	Compound	P→S
	Å		Å
P_4O_{10}	1·39	$P_4O_6S_4$	1·85
$POCl_3$	1·58	$PSCl_3$	1·94
$POFCl_2$	1·54	PSF_3	1·85
POF_2Cl	1·55	Covalent	2·14
POF_3	1·56		
Covalent	1·76		

These distances indicate that the P→O and P→S bond types in the molecules containing three oxygen atoms attached to the phosphorus atom are of an unusual class. The usual C═O distance is 1·1 to 1·3 Å.

---

[1] Stosick, *J. Amer. Chem. Soc.*, 1939, **61**, 1130

[2] Hampson and Stosick, *ibid.*, 1938, **60**, 1814.

The O—P—O valence angle α of 101·50 is close to the X—P—Y angle found in the following compounds:

Compound	X—P—Y *angle*
PCl_3	101°
PBr_3	100°
$PFCl_2$	102°
$P(CH_3)_3$	100°

The increase of this angle from 99° in P_4O_6 to 101·5° in P_4O_{10} and $P_4O_6S_4$ indicates that the increased co-ordination of the phosphorus atom from 3 to 4 tends to make the valence angles approach the tetrahedral value of 109° 28′ as is found in the trivalent PO_4 ion. As the number of oxygen or sulphur atoms around the phosphorus is increased from 3 to 4 the hybrid band orbitals formed by the linear combination of the spherically symmetrical *s* and the cubically symmetrical *p* orbitals tend to have less of the *p* orbital character and to approach the hybrids having the maximum bond-forming power or the usual sp^3 tetrahedral orbitals.

Empirical Rules for Relating Internuclear Distances and Force Constants.—In order to estimate the spectral region in which the P→O and P→S absorption might occur it is necessary to obtain some idea of the value of the force constant between the atom pairs. With such knowledge it is possible to calculate the spectral region in which the absorption should occur using the equation for the simple harmonic oscillator:

$$v(\text{cm.}^{-1}) = 1307\sqrt{k/\mu},$$

where ν is the frequency in cm.$^{-1}$,
μ is the reduced mass of atom pair, and
k is the force constant $\times 10^{-5}$ in dynes/cm.

There are, among others in the literature, two approximate rules for expressing the relationship between internuclear distances and the force constants. The earlier of these, Badger's rule,[3] gives an obviously high value for the P→O force constant while for the P→S link a value of $3{\cdot}03 \times 10_5$ dynes/cm. is of the right order of magnitude. A more recent expression, Gordy's rule, is [4]

$$k = 1{\cdot}67\, N\left(\frac{\chi_A \chi_B}{d^2}\right)^{\frac{3}{4}} + 0{\cdot}30,$$

where k is the force constant $\times 10^{-5}$ dynes/cm.,
N is the order of bond (effective number of covalent or ionic bonds acting between the two atoms considered),

χ_A, χ_B is the electronegativity of atoms A and B $\begin{cases} P = 2{\cdot}1 \\ S = 2{\cdot}53 \text{ and} \\ O = 3{\cdot}45 \end{cases}$

d is the internuclear distance in Å.

The application of this rule gives the following values of the force constants using a bond order of 2, a P—O distance of 1·39 Å, and a P—S distance of 1·85 Å:

$$k_{P \rightarrow O} = 9{\cdot}30 \times 10^5 \text{ dynes/cm.},$$
$$k_{P \rightarrow S} = 5{\cdot}24 \times 10^5 \text{ dynes/cm.}$$

Using these values in the equation for the harmonic oscillator the following frequencies are obtained:

$$v_{P \rightarrow O} = 1221 \text{ cm.}^{-1},$$
$$v_{P \rightarrow S} = 725 \text{ cm.}^{-1}.$$

---

[3] Badger, *J. Chem. Physics*, 1934, **2**, 128; 1935, **3**, 710.

[4] Gordy, *ibid.*, 1946, **14**, 305.

Using an internuclear distance of 1·58 A for P—O the Gordy rule force constant is $7{\cdot}65 \times 10^5$ dynes/cm. with a stretching vibration at 1112 cm.$^{-1}$. The vibrational frequencies appear to be :

Using Badger's Rule Force Constants—	Gordy's Rule Force Constants—
$\nu_{P\rightarrow O}$ obviously too high.	$\nu_{P\rightarrow O,\,1{\cdot}58\,Å} = 1112$ cm.$^{-1}$.
$\nu_{P\rightarrow S} = 574$ cm.$^{-1}$.	$\nu_{P\rightarrow O,\,1{\cdot}39\,Å} = 1221$ cm.$^{-1}$.
	$\nu_{P\rightarrow S} = 752$ cm.$^{-1}$.

From these values it appears as if the stretching frequency for the P→O linkage could occur in the region 1100-1300 cm.$^{-1}$ and for the P→S link in the region 550-750 cm.$^{-1}$. It should be emphasized, however, that when the mass of the involved atoms is large as compared with the force constant the position of the absorption frequencies may not be as characteristic as with lighter atoms. The effect of the other structure of the molecule may be readily reflected in shifts in the position and changes in the character of the absorption frequencies.

A check through the literature reveals that up until 1950 practically no phosphorus bearing molecules had been studied in the infra-red region. Thompson and Meyrick[5] report that the P=O stretching vibration absorption occurs between 1250 and 1260 cm.$^{-1}$. Raman studies[6, 7, 8] have been made on $POCl_3$ and $PSCl_3$, however, in which the frequency associated with the parallel stretching of the P—O or P—S bond occurs at 1292 and 748 cm.$^{-1}$, respectively.

Accordingly then, with the aid of the approximate relations between internuclear distances and force constants and Raman studies on simple molecules, it was thought to be worth while to attempt to determine experimentally the position of the P→O and P→S absorption studying the regions 1100-1300 cm.$^{-1}$ and 550-750 cm.$^{-1}$ in particular for the respective groups.

Experimental

Most of the infra-red spectra have been obtained on a Perkin-Elmer spectrometer equipped with NaCl or KBr prisms and strip chart recording. Solid samples have been prepared by mulling with white mineral oil in order to reduce interfacial scattering. Liquid samples were usually observed in cells of approximately 0·01 mm. thickness similar to those described by Colthup.[9] Most of the spectra shown in the Figures were made from the instrument recordings by a careful measurement of the absorption frequencies and a visual estimation of the percentage transmission at those frequencies.

The samples of the various organic materials were made by many workers in the Research Division of the Stamford Research Laboratories. Most of them are thought to be of reasonable purity and identity from their other physical and chemical properties. It is to be expected, however, that a number of the samples are mixtures of molecules and isomers if for no other reason than the complexity of the preparation and purification problems found with this class of compounds.

Results

The infra-red spectra of a number of molecules containing the P→O and P→S links are shown in Fig. 1, 2 and 3. The spectra of $P_2O_5(P_4O_{10})$ and $P_2S_5(P_4S_{10})$ shown in Curves 1 and 2, Fig. 1, are those obtained from these molecules in the solid phase. Interfacial light scattering has made it necessary to reduce the sample thickness to such an extent that the absorption bands are rather weak. P_2O_5 has an absorption band near 1280 cm.$^{-1}$ which is absent in P_2S_5 and can be assigned to the P → O linkage inasmuch as it lies within the calculated range (shown by cross-hatching in the Figures). The absorption

---

[5] Meyrick and Thompson, *J. Chem. Soc.*, 1950, 225.

[6] Wu, *Vibrational Spectra and Structure of Polyatomic Molecules* (Peking, 1939), p. 243.

[7] Kohlrausch, *Raman Spektren* (Edwards Bros., Ann Arbor, 1943), p. 142.

[8] Herzberg, *Infra-red and Raman Spectra* (Van Nostrand, New York, 1945), p. 314.

[9] Colthup, *Rev. Sci. Instr.*, 1947, **18**, 64.

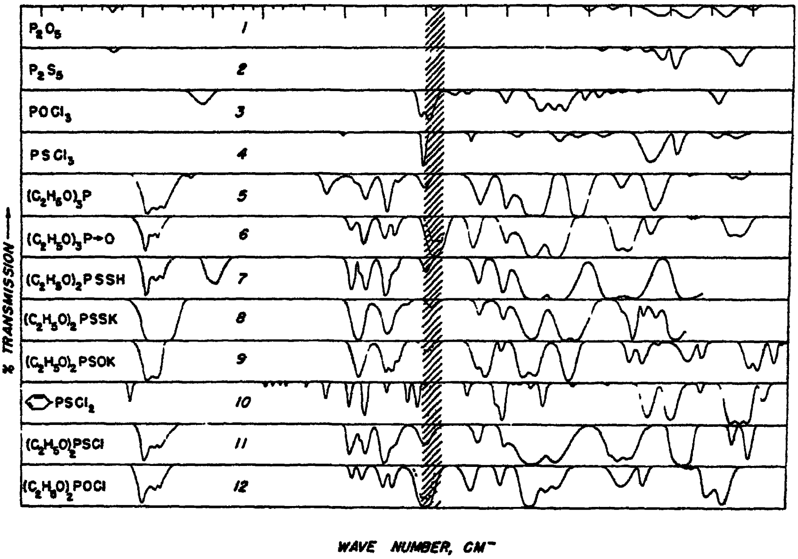

FIG. 1.

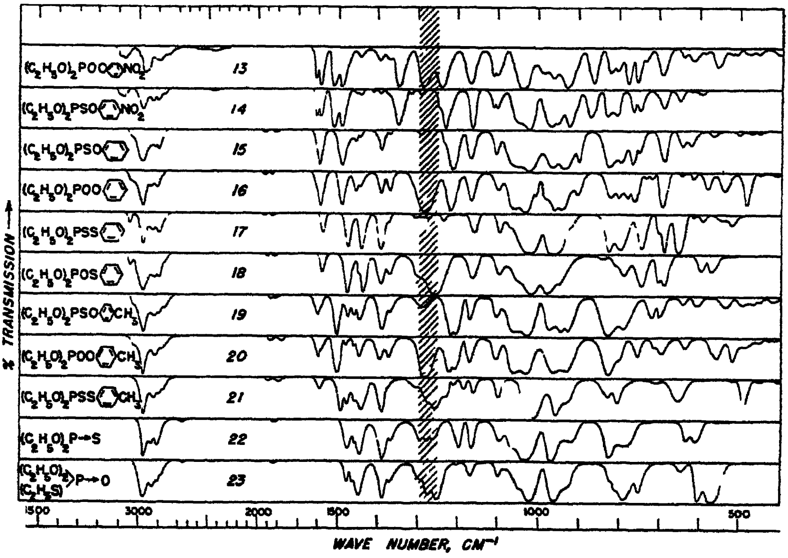

FIG 2.

near 530 cm. or near 690 cm.$^{-1}$ in P_2S_5 may be caused by the similar vibration in this molecule.

In the comparison of $POCl_3$ and $PSCl_3$, Curves 3 and 4, using the literature values for the Raman lines at 1292 and 748 cm.$^{-1}$ as guides, it can be seen that the $POCl_3$ molecule absorbs strongly near 1290 cm.$^{-1}$ while the $PSCl_3$ does not.

The latter molecule absorbs strongly near 750 cm.$^{-1}$ while the former has no absorption. In this pair then it appears probable that the P→O link absorbs near 1290 cm.$^{-1}$ and the P→S near 750 cm.$^{-1}$.

The spectra of triethyl phosphite and triethyl phosphate are shown in Curves 5 and 6. There is little chance to miss the strong absorption band near 1275 cm.$^{-1}$ which, on the basis of the accumulating evidence, may be assigned to the P→O stretching vibration. On thinning the preparation of the phosphate the 1275 cm.$^{-1}$ band is resolvable into the doublet shown by the dotted line with absorption maxima at 1265 and 1277 cm.$^{-1}$. Inasmuch as there appears to be evidence in the Raman literature indicative of an absorption band near 1290 cm.$^{-1}$ associated with the ethoxyl radical, this doublet may be caused by the presence of both the C_2H_5O and P→O groups in the molecule.

The spectra of the diethyl dithiophosphoric acid and its potassium salt are shown in Curves 7 and 8 of Fig. 1. In Curve 7, the spectrum of the free acid, the mercapto group stretching vibration absorbs near 2500 cm.$^{-1}$, the ethoxyl group near 1295 cm.$^{-1}$ and the intense absorption near 650 cm.$^{-1}$ may be the P→S stretching vibration. When the hydrogen atom is replaced by a potassium the 2500 cm.$^{-1}$ S—H band disappears and there are slight shifts in the ethoxyl and P→S bands.

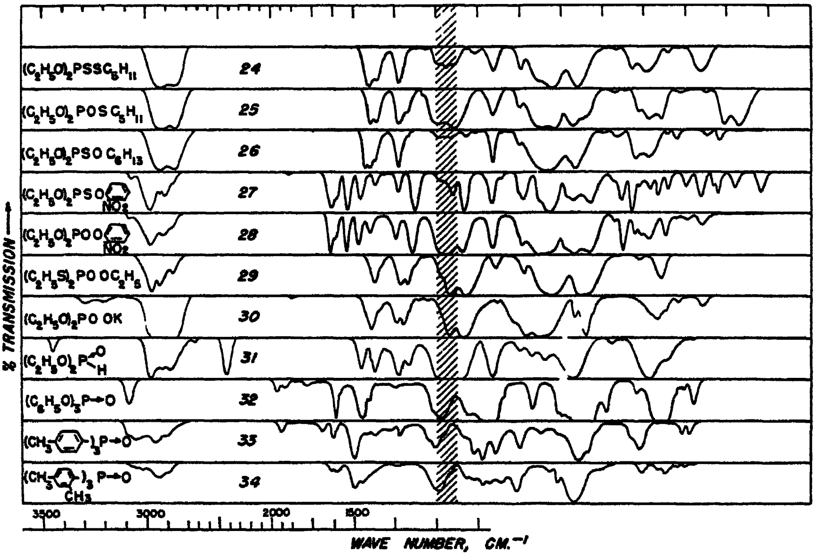

FIG. 3.

The spectrum of the potassium salt of the diethyl monothiophosphoric acid, Curve 9, exhibits several interesting features. The solid phase run, indicated by the solid line, shows no evidence of the P→O stretching vibration near 1300 cm.$^{-1}$. When this material is dissolved in water and observed, absorption near 1290 cm.$^{-1}$ is found, shown in the broken line of Curve 9. This absence of possible P→O absorption in the solid phase spectrum with its appearance in the solution (ionized) spectrum is indication of the potassium atom being attached to the oxygen. This interpretation is in keeping with electronegativities of these atoms as reported by Pauling,[10] S = 2·5, O = 3·5. Absorption bands are also found near 650 cm.$^{-1}$ which may be attributed to the P→S stretching vibration.

Curve 10, Fig. 1, of phenyl phosphorus thiodichloride exhibits no absorption between 1250 and 1300 cm.$^{-1}$ as is to be expected. There are absorption bands below 700 cm.$^{-1}$ sufficiently strong to be associated with the P→S link.

The spectra of diethyl chlorothiophosphate and diethyl chlorophosphate, Curves 11 and 12, Fig. 1, substantiate the assignment to the P→O linkage of strong absorption between 1250 and 1300 cm.$^{-1}$. In the thio compound the 1290 cm.$^{-1}$ absorption may be associated with the ethoxyl radical. In the phosphate the strong 1290 cm.$^{-1}$ band may be resolved into a doublet (in CCl_4 solution) as indicated by the broken line. This permits the assumption that the doublet is caused by the ethoxyl and P→O linkages.

---

[10] Pauling, *Nature of the Chemical Bond* (Cornell, 1939), p. 64.

The spectra of the oxygen analogue of parathion and parathion itself (O, O-diethyl O-*p*-nitrophenyl thiophosphate) are shown in Curves 13 and 14 of Fig. 2. Observing the cross-hatched region it is easily seen that the oxygen analogue exhibits intense absorption near 1290 cm.$^{-1}$ which is absent in parathion. The parathion does show slight absorption near 1290 cm.$^{-1}$ which may be attributed to the ethoxyl radical. This band may be obscured in the oxygen analogue by the intense P→O absorption. The equally intense band between 1200 and 1250 cm.$^{-1}$, evident in both spectra, appears to be associated with a P—O-phenyl linkage. Both molecules exhibit weaker bands below 700 cm.$^{-1}$ where the P→S link may be expected to occur.

The spectra numbered 15, 16, 17 and 18 of Fig. 2 are those of a series of diethyl phenyl phosphates with from none to two sulphur atoms. It appears that intense absorption between 1250 and 1300 cm.$^{-1}$ occurs only when a P → O linkage is present such as occurs in Curves 16 and 18. The S-phenyl compound (Curve 17) does not exhibit the intense band between 1200 and 1250 cm.$^{-1}$ which has been mentioned in connection with the P—O-phenyl grouping. Again no intense bands attributable to the P→S linkage are found below 700 cm.$^{-1}$ although Curve 17 has an intense band near 650 cm.$^{-1}$.

Curves 19, 20 and 21, Fig. 2, are the spectra of a similar series of diethyl, *p*-tolyl phosphates. Again the P→O link appears to absorb between 1250 and 1300 cm.$^{-1}$ while no clearly defined P→S absorption is evident. The disulphide, Curve 21, shows some absorption with multiplet character in the region which is probably not all caused by ethoxyl but could be the result of oxygen bearing impurities. This molecule also exhibits a rather intense band near 650 cm.$^{-1}$ as do many other disulphides.

The spectrum of the triethyl thiophosphate, Curve 22, shows several minor bands between 1250 and 1300 cm.$^{-1}$ perhaps attributable to the ethoxy radical and impurities, as well as a fairly intense doublet between 600 and 650 cm.$^{-1}$ which could be absorption by the P→S link. The S-ethyl isomer, Curve 23, again shows strong 1255 cm.$^{-1}$, P→O absorption.

Curves 24, 25 and 26, Fig. 3, are obtained from thiophosphates containing no phenyl ring. Only in Curve 25, which has the P→O link in the molecule is found intense absorption in the marked region. It should also be noted that these aliphatic molecules show no intense band between 1200 and 1250 cm.$^{-1}$ which has been suggested as being caused by the P—O-phenyl grouping.

The spectra of the *ortho*-nitro isomer of parathion and its oxygen analogue are shown in Curves 27 and 28 with the usual results. Again an intense band, slightly higher in frequency than in the *para*-isomers but below 1250 cm.$^{-1}$ may be associated with the P—O-phenyl structure.

Conclusions.—A preponderance of evidence indicates that the P→O linkage absorbs strongly in the region 1250-1300 cm.$^{-1}$. The P→S link appears, in general, to be a weak and poorly characterized absorber in the infra-red spectral region.

The author wishes to express his appreciation to the members of the infra-red spectroscopy group both past and present for obtaining many of the spectra shown here. He also wishes to thank the members of the Research Division of these Laboratories for preparing the samples and to the Directors of the Stamford Research Laboratories for permission to publish the results.

Stamford Research Laboratories,
American Cyanamid Company,
Stamford, Connecticut.

SOME INFRA-RED SPECTROSCOPIC STUDIES OF ROTATIONAL ISOMERISM

BY J. K. BROWN AND N. SHEPPARD

Received 20th July, 1950

Infra-red spectra in the crystalline state are reported for 1 : 2-dibromoethane, 1 : 4-dibromobutane, *n*-propyl bromide, and *n*-butyl bromide between 1500 and 700 cm.$^{-1}$; also for *n*-butyl, *n*-hexyl and *n*-octyl alcohol from 1200 to 850 cm.$^{-1}$. All these spectra showed considerable simplification when compared with the corresponding spectra of the liquids. The complexity of the liquid state spectra is caused by the presence of several rotational isomeric configurations, only one of which is allowed in the solid state. The solid state spectra are completely analyzed for 1 : 2-dibromoethane and 1 : 4-dibromobutane, and are shown to be consistent with the presence of a single configuration in the solid state for *n*-propyl and *n*-butyl bromide. Strong absorptions between 1070 and 880 cm.$^{-1}$ in the spectra of the alcohols in the crystalline state are interpreted as being mainly caused by the skeletal stretching modes of the planar zig-zag chain.

The investigation of the spectra in the crystalline state of molecules which exhibit rotational isomerism will probably be of general use in the analysis of their spectra. Some advantages and limitations of this method are discussed.

The purpose of this paper is to give a general account of the results recently obtained in a study of the liquid and solid state infra-red spectra of substances exhibiting rotational isomerism. In the past little progress has been made in the interpretation of the spectra of these and similar substances mainly because of the complexity caused by the existence of several forms.

Whenever a molecule contains an internal single bond about which restricted rotation can occur, various relative orientations of the groups or atoms attached to opposite ends of the bond are possible. The number and relative concentrations of the different stable rotational isomers represented by the orientations will depend respectively on the number of minima in the potential energy curve associated with rotation about the bond, and on Boltzmann factors involving the energy differences between these minima. If, as in ethane, the molecule is sufficiently symmetrical about the internal single linkage the different (staggered) configurations allowed will be indistinguishable, and the infra-red and Raman spectra will show approximately the expected number of fundamentals for a single molecular species. If, on the other hand, the configurations have different symmetries, as in 1 : 2-dichloroethane and *n*-butane, spectroscopically distinguishable rotational isomers will be present, each of which will contribute its own set of fundamentals. The large number of Raman lines associated with 1 : 2-dichloroethane in the liquid state initially led Kohlrausch [1] to postulate the existence of two such isomeric forms. The presence of more than one internal single bond in a molecule can give a corresponding increase in the number of rotational isomers.

Although the various stable configurations will normally be present in both the gaseous and liquid states, it often happens that a single isomer occurs in the crystalline solid state, and accordingly a simplification results from careful freezing of the material. Mizushima and his co-workers [2] were the first to show this effect in a study of the Raman spectra of the

---

[1] Kohlrausch, *Z. physik. Chem. B*, 1932, 18, 61.

[2] Mizushima, Morino and Noziri, *Sci. Papers Inst. Phys. Chem. Res. Tokyo*, 1936, 29, 63 and 188.

1 : 2-dihalogen ethanes in the liquid and solid states, and more recently marked spectral simplifications of the same type have been obtained on freezing the straight chain paraffins.[3, 4, 5, 6] Both X-ray [7] and spectroscopic data show that, in the crystalline state, these molecules take up a planar zig-zag configuration.

The energy differences between the isomers can be obtained from measurements of the temperature dependence of the intensity of groups of Raman lines or infra-red bands associated with the several configurations. Langseth and Bernstein [8] first employed this method using photographic Raman techniques, and, more recently, Rank has used a photoelectric Raman spectrograph to obtain more accurate results.[9, 10] Similar measurements on infra-red bands in the vapour phase have been made by Mizushima [11] and Bernstein.[12, 13]

This short account of recent work shows that spectroscopic methods can contribute very extensively to the qualitative and quantitative understanding of rotational isomerism. It is equally true that an understanding of rotational isomerism can contribute much to the interpretation of the spectra of molecules showing this phenomenon. The application of infrared and Raman spectroscopy to the solution of the problems of molecular structure has recently become much more general by reason of the recognition of group frequencies arising from the vibrations of small units in large molecules. In order to extend this method it is becoming increasingly necessary to obtain fairly complete spectral analyses of small and medium-sized molecules containing the appropriate groupings. Although it has not always been clearly recognized in the past, the failure to make such analyses of molecules containing internal C—C linkages is due in many cases to the additional complexity arising from rotational isomerism, and thus until experimental methods are available for distinguishing between the frequencies of one isomer and of another little advance can be made. Some progress is possible in this direction from a determination of the temperature dependence of absorption lines as outlined above,[8] but in practice the overlapping of bands is such that only the strongest absorptions can be attributed to the different isomers in this fashion. An alternative and easier method is the study of the solid state spectrum with a view to its complete interpretation in terms of the fundamental frequencies of the one rotational isomer in the crystalline lattice.

If only two isomers are expected to be in reasonable concentration, then an assignment of the fundamentals of one, the solid state form, may enable a corresponding assignment of the other to be made by a comparison of the solid and liquid spectra. Alternatively, in more complex cases the force fields determined by an analysis of the one spectrum may be sufficiently complete to enable approximate calculations to be made of the frequencies of the others, so that they may be identified in the infra-red and Raman spectra.

The method of analysis using solid state data has already been used for the partial interpretation of the spectra of 1 : 2-dichloroethane [2] and *n*-butane,[6, 9] but we feel that it has much wider applications than has previously been realized, especially to the spectra of medium-sized molecules. Consequently a programme of infra-red experimental work has been carried

---

[3] Rank, Sheppard and Szasz, *J. Chem. Physics*, 1949, **17**, 83.

[4] Sheppard and Szasz, *J. Chem. Physics*, 1949, **17**, 86.

[5] Mizushima and Simanouti, *J. Amer. Chem. Soc.*, 1949, **71**, 1320.

[6] Axford and Rank, *J. Chem. Physics*, 1949, **17**, 430 and 1950, **18**, 51.

[7] Müller, *Proc. Roy. Soc. A*, 1928, **120**, 437.

[8] Langseth and Bernstein, *J. Chem. Physics*, 1941, **8**, 410.

[9] Szasz, Sheppard and Rank, *ibid.*, 1948, **16**, 704.

[10] Rank, Kagarise and Axford, *J. Chem. Physics*, 1949, **17**, 1354.

[11] Mizushima, Morino, Watanabe, Simanouti and Yamaguchi, *ibid.*, 1949, **17**, 591.

[12] Bernstein, *ibid.*, 1949, **17**, 258.

[13] Bernstein, *ibid.*, 1950, **18**, 897.

out on selected series of molecules, all of which contain an unbranched carbon-carbon chain. On the one hand, a series of fairly simple molecules have been chosen, such as the *n*-propyl and *n*-butyl halides, and the first members of the α,ω-dibromoparaffins, for which it should be possible to make fairly complete analyses of the spectra. On the other hand, series of long chain molecules were chosen, such as the *n*-paraffins and straight chain alcohols. It was hoped to identify in their spectra the skeletal stretching frequencies in the region 1400-700 cm.$^{-1}$, and to separate them from the CH_2 and CH_3 deformation modes which also occur in the same frequency range.

In all cases, after suitable cooling techniques had been devised, a considerable simplification of the spectra was observed on crystallization, and typical results are presented and discussed below for each type of compound studied. More detailed experimental and theoretical studies will shortly be published elsewhere. The detailed interpretation of the spectra of the straight chain paraffins in the solid state is given in another paper in this Discussion.

Experimental

The infra-red spectra were taken in the frequency range 1500-700 cm.$^{-1}$ using a Perkin-Elmer 12B spectrometer, with an auxiliary system of mirrors before the entrance slit to provide a suitable focus for the low temperature cell. This cell was of the simple transmission type and was designed by Dr. A. Vallance Jones. It will be fully described elsewhere. Liquid oxygen was used for cooling and the cold, dry gas produced by its evaporation was directed in front of the cell windows to minimize frosting. The rate of cooling could be varied at will over a wide range of temperatures by means of a heating coil wound round a copper rod supporting the cell, and the temperature was measured using a copper-constantan thermocouple in contact with the thin cell windows.

The liquid under examination was placed between two silver chloride plates separated by a silver foil spacer. The plates were held in a mount coated with silver to prevent contamination. Silver chloride was used in preference to rock salt on account of its mechanical stability to rapid temperature variation, although it had the disadvantage of higher reflection losses. Owing to the softness of the plates it is not possible to quote accurate values for the thickness of samples.

The procedure followed was that of first recording the spectrum of the liquid at room temperature (or at low temperatures for the volatile propyl halides) and then cooling down to the freezing point and allowing the material to freeze. The alkyl halides and lower freezing point alcohols when subjected to this treatment gave glasses, which were recognized by their high transmission and by the similarity of their spectra to that of the liquid. On allowing the glass to warm up from liquid air temperatures a visible transition to the crystalline form took place, and a marked modification of the spectrum was observed. The spectra obtained for *n*-butyl bromide at various stages of this sequence are shown in Fig. 1. They will be discussed further below. It is probable that the cooling of the glass favoured the formation of a few crystalline nuclei which increased in number as the temperature was lowered. On warming, the relaxation time of the molecules was sufficiently reduced to allow the rapid crystallization of the mass of material, seeded by these nuclei. When crystals were obtained in this manner a number of absorption bands, presumably those of the non-planar isomers in the amorphous material, were greatly reduced in intensity, only small residues remaining. A further reduction took place on re-cooling the solid down to the temperature of liquid oxygen. These temperature dependent residues are marked with small arrows in the figures to distinguish them from weak bands of the crystalline isomer. The methylene halides and *n*-paraffins did not give glasses but crystallized at the freezing point. In these cases many of the strong bands of the liquid completely disappeared on crystallization.

Owing to the large amount of radiation scattered by the crystalline solid the intensities of the absorption bands could only be estimated. It was assumed that the percentage absorption could be measured from the flat portion of the recorder trace in the vicinity of each band. Hence it is important to note that the intensities of the low temperature solid bands are of relative significance only, and cannot be compared quantitatively with those of the liquid spectra. In a few cases small variations in the relative intensities of bands of the solid forms were noted from different runs. This effect appeared to depend on the thickness of the sample. A possible cause is that the crystalline material was preferentially orientated, and in doubtful cases further studies are planned using polarized radiation.

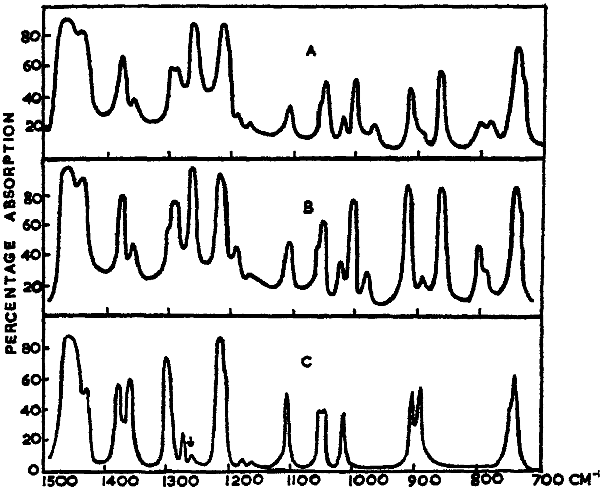

FIG. 1.—The infra-red spectrum of *n*-butyl bromide (*a*) in the liquid state, (*b*) as a glass, and (*c*) in the crystalline state. Approximate thickness : 0·05 mm.

Materials.—ALKYL HALIDES.—These were obtained from two sources, viz. B.D.H. Ltd. and L. Light & Co., the latter claiming a purity of 95-99 %. They distilled at the following temperature :

n-propyl bromide 71° C ; *n*-butyl bromide 101·5° C.

1 : 2-DIBROMOETHANE, B.D.H. Ltd. and Judex Chemicals; distilled at 131·5° C.

1 : 4-DIBROMOBUTANE, B.D.H. Ltd. and L. Light & Co. ; distilled at 110° C under 60 mm. Hg.

ALCOHOLS

n-Butyl Alcohol : B.D.H. Ltd. ; b.p. 117·5° C.
n-Hexyl Alcohol : L. Light & Co. and Messrs. Boake-Roberts ; b.p. 157° C.
n-Octyl Alcohol : Messrs. Boake-Roberts ; b.p. 195° C.

All samples were fractionated twice, the middle fraction only being used. The compounds obtained from more than one source gave identical spectra, both as liquids and as solids. The spectra are shown in Fig. 1 to 5, and the absorption frequencies are given below.

n-BUTYL BROMIDE

LIQUID : 742 (s), 779 (m), 797 (m), 864 (s), *ca.* 890 (w), 912 (m), 969 (m), 998 (m), 1017 (m), 1051 (m), 1105 (m), *ca.* 1165 (w), 1188 (w), 1216 (s), 1262 (s), 1290 (s), 1298 (s), 1355 (w), 1373 (s), *ca.* 1430 (s), *ca.* 1460 (s).

SOLID : 742 (s), *ca.* 750 (m), 894 (m), 905 (m), 1017 (m), 1051 (m), 1056 (m), 1107 (m), 1158 (w), 1173 (w), 1215 (s), 1275 (w), 1299 (s), 1360 (m), 1376 (m), 1433 (m), *ca.* 1465 (s).

n-PROPYL BROMIDE

LIQUID : 740 (m), 777 (s), 839 (s), 884 (s), 892 (s), 1030 (m), 1040 (m), 1084 (m), 1103 (m), 1146 (w), *ca.* 1175 (w), 1201 (m), 1228 (s), 1286 (s), 1326 (m), 1340 (w), 1378 (s), 1435 (s), *ca.* 1465 (s).

SOLID : 739 (s), 850 (m), *ca.* 884 (m), 894 (s), 1025 (m), 1040 (s), 1103 (m), 1146 (m), 1175 (w), 1222 (s), *ca.* 1246 (w), 1326 (s), 1374 (s), 1435 (m), *ca.* 1465 (s).

1 : 2-DIBROMOETHANE

LIQUID : 750 (m), *ca.* 775 (m), 834 (s), 894 (m), 1018 (w), 1090 (m), *ca.* 1105 (m), 1192 (s), 1248 (s), 1278 (m), 1430 (s).

SOLID : 745 (m), 776 (m), 1095 (m), 1192 (m), 1435 (m).

1 : 4-DIBROMOBUTANE

LIQUID : 742 (s), 759 (s), 800 (m), 846 (w), 868 (m), 914 (m), 967 (m), 1008 (m), 1040 (w), 1061 (w), 1103 (w), 1146 (w), 1170 (m), 1195 (m), *ca.* 1230 (s), *ca.* 1265 (s), 1435 (s).

SOLID : 752 (m), 759 (m), 869 (m), 1008 (s), 1096 (w), 1171 (m), 1258 (s), *ca.* 1295 (s), 1310 (m), 1433 (m), 1440 (m).

ALCOHOLS : *n*-BUTYL ALCOHOL

LIQUID : 878 (w), 901 (m), 951 (s), 989 (s), 1008 (s), 1030 (s), *ca.* 1040 (s), *ca.* 1070 (s), 1115 (s).

SOLID : 894 (m), 903 (m), 996 (s), 1041 (s), 1067 (s), 1162 (m).

n-HEXYL ALCOHOL

LIQUID : 889 (m), 920 (s), 962 (w), 1017 (s), *ca.* 1060 (s), 1121 (s).

SOLID : 884 (m), 891 (m), 994 (s), 1019 (s), 1029 (s), 1040 (s), 1057 (s), 1065 (s), 1159 (m).

n-OCTYL ALCOHOL

LIQUID : 889 (m), 955 (m), 990 (s), *ca.* 1060 (s), *ca.* 1075 (s), 1122 (m).

SOLID : 886 (m), 948 (m), 989 (m), 998 (s), 1040 (s), 1056 (s), *ca.* 1066 (m), 1071 (s), 1162 (m).

(s = strong ; m = medium ; w = weak)

Discussion

1 : 2-Dibromoethane.—The infra-red spectrum of the *trans* form of this molecule in the solid state is shown in Fig. 2*b*. Many extra absorption bands occur in the spectrum of the liquid (Fig. 2*a*) which are caused by the vibrations of the *gauche* form. Similar spectra have recently been obtained by Mizushima [11] and his co-workers, and our results are in fair agreement with this earlier work and with that of Cheng and Lecomte [14] on the liquid spectrum only. A few medium or weak absorptions not observed by the above authors have been detected in the present work.

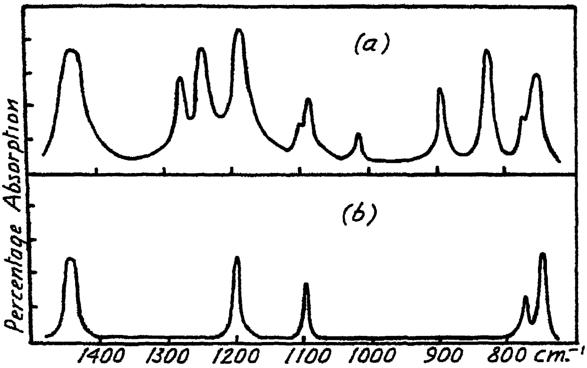

FIG. 2.—The infra-red spectrum of 1 : 2 -dibromoethane in (*a*) the liquid, and (*b*) the crystalline state. Approximate thickness : 0·06 mm.

The infra-red spectrum in the solid state, when taken in conjunction with the earlier Raman work,[11] completes the vibrational spectra in the region 1500-700 cm.$^{-1}$, and thus it is now possible to make a complete assignment for the *trans* form between these limits. This C_{2h} isomer of

---

[14] Cheng and Lecomte, *J. Physique Rad.*, 1935, **6**, 477.

1 : 2-dibromoethane will have 18 fundamentals, and because the molecule has a centre of symmetry, 9 of these will be infra-red active and 9 Raman active vibrations. The infra-red modes comprise 4 of symmetry A_u and 5 of symmetry B_u. The Raman active modes are made up of 6 of type A_g and 3 of type B_g. In the frequency range 1500-700 cm.$^{-1}$ only 4 infra-red active fundamentals are expected (A_u CH_2 twisting and rocking modes, and B_u CH_2 bending and wagging vibrations) and this is in good agreement with the observation of 4 strong infra-red absorptions. The weaker neighbour of the 745 cm.$^{-1}$ absorption observed by us at 776 cm.$^{-1}$ will be referred to below.

In the Raman spectrum 5 fundamentals are predicted and found.[2, 11] These include four CH_2 deformation modes, 2 of type A_g and two B_g, and the single A_g C—C stretching mode. Of the remaining 9 vibrations 4 are C—H stretching modes, occurring near 3000 cm.$^{-1}$, and 5 are C—Br stretching and skeletal bending vibrations having frequencies below 700 cm.$^{-1}$.

Table I gives a summary of the observed frequencies and the interpretation now suggested. The polarization of the Raman lines is taken from the liquid spectrum of Kohlrausch and Wittek.[15] The infra-red active modes are assigned in a straightforward manner by reference to a recent analysis of the infra-red and Raman spectra of ethyl bromide,[16] in which the bending, wagging, and rocking vibrations of a CH_2 group in similar surroundings were reliably identified as strong absorptions at 1440, 1255, and 770 cm.$^{-1}$ respectively. The CH_2 twisting mode could not be identified with certainty in ethyl bromide, but in 1 : 2-dibromoethane it must correspond to the remaining absorption at 1095 cm.$^{-1}$. The CH_2 bending and wagging modes can similarly be picked out from the 5 Raman lines using the accepted frequency ranges for these vibrations. The polarization of the 934 cm.$^{-1}$ line shows it to be the remaining A_g C—C stretching vibration as suggested by Wu.[17] The assignment of the frequency at 1438 cm.$^{-1}$ to an A_g fundamental, despite its apparently depolarized nature, is in agreement with the well-known observation that these modes usually have highly depolarized lines. Furthermore, if this were not done there would be too few polarized lines. The remaining Raman lines corresponding to CH_2 twisting and rocking modes are assigned in the same manner as that used for their infra-red analogues. The infra-red band at 776 cm.$^{-1}$, which has not so far been assigned, is probably a combination frequency involving one or more of the lower frequency fundamentals which have not yet been observed in the infra-red spectrum.

TABLE I.—THE ASSIGNMENT OF THE INFRA-RED AND RAMAN SPECTRA OF *trans*- 1 : 2-DIBROMOETHANE IN THE REGION 1500-700 cm.$^{-1}$

Type of Vibration	A_g (R.p)	A_u (I.R.)	B_g (R.dp)	B_u (I.R.)
CH_2 bending . .	1438 (3) dp	—	—	1435 (m)
CH_2 wagging . .	1250 (8) p	—	—	1192 (s)
CH_2 twisting . .	—	1095 (m)	1157 (1) ?	—
CH_2 rocking . .	—	745 (m)	1056 (5) dp	—
C—C stretching .	934 (1) p	—	—	—

R = Raman ; I.R. = infra-red ; p = polarized ; dp = depolarized
s = strong ; m = medium

---

[15] Kohlrausch and Wittek, *Z. physik. Chem. B*, 1940, **47**, 55.

[16] Sheppard, *J. Chem. Physics*, 1949, **17**, 79.

[17] Wu, *Vibration Spectra and Structure of Polyatomic Molecules* (Pekin, 1939), pp. 306-312.

The above assignment is in partial accord with the earlier work of Kohlrausch and Wittek,[16] Wu,[17] and Odan, Mizushima, and Morino,[18] particularly with respect to the Raman frequencies, for which the solid state data have been previously available. However, it is thought to be a marked improvement on earlier assignments of the infra-red frequencies as spectra of the crystalline state were not available until recently.

1 : 4-Dibromobutane (tetramethylene dibromide).—The infra-red spectra of this substance in the liquid and solid states are shown in Fig. 3*a* and 3*b*. Once again the spectrum of the crystalline solid is much simpler than that of the liquid, showing that there is more than one rotational isomer present in the latter phase.

It seems likely that the planar zig-zag form exists in the solid state, as for 1 : 2-dibromoethane and the *n*-paraffins. The overall symmetry is again C_{2h}, and the existence of a centre of symmetry makes the Raman and infra-red active fundamentals mutually exclusive. On the basis of such a model only 9 infra-red active modes would be expected between 1500 and 700 cm.$^{-1}$, viz. 2 each of CH_2 bending, wagging, twisting and rocking vibrations, and a single B_u C—C stretching mode. This prediction is in excellent agreement with the observed spectrum, there being 10 infra-red absorption of medium strength or greater at 1440 (m), 1433 (m), 1310 (m), 1258 (s), 1171 (m), 1096 (m), 1008 (s), 869 (m), 759 (m), and 752 (m) cm.$^{-1}$. For any other model many more strong absorptions would be expected.

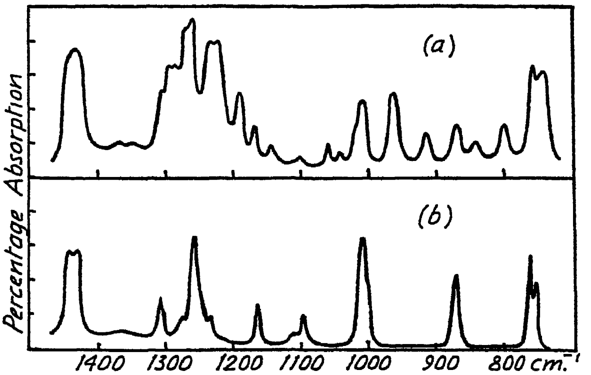

FIG. 3.—The infra-red spectrum of 1 : 4-dibromobutane in (*a*) the liquid, and (*b*) the crystalline state. Approximate thickness : 0·06 mm.

In order to assign the observed absorptions to the fundamentals it should be noted that four pairs of CH_2 modes are to be expected, probably not far removed from the corresponding single modes of 1 : 2-dibromoethane at 1435, 1191, 1095 and 745 cm.$^{-1}$. Accordingly 8 of the fundamentals can be identified with confidence as follows : CH_2 bending, 1440 and 1433 cm.$^{-1}$; CH_2 wagging, 1310 and 1258 cm.$^{-1}$; CH_2 twisting, 1171 and 1095 cm.$^{-1}$; CH_2 rocking, 869 and 759 cm.$^{-1}$. The single C—C stretching mode almost certainly corresponds to the strong infra-red absorption at 1008 cm.$^{-1}$. The only absorption of medium strength which has not been assigned is that at 752 cm.$^{-1}$. It seems to correspond to the similar extra absorption found in the infra-red spectrum of 1 : 2-dibromoethane. Unfortunately the Raman spectrum of 1 : 4-dibromobutane in the solid state does not appear to be available between 1500 and 700 cm.$^{-1}$.

---

[18] Odan, Mizushima and Morino, *Sci. Papers Inst. Phys. Chem. Res. Tokyo*, 1944, **42**, 27.

***n*-Propyl Bromide and *n*-Butyl Bromide.**—The experimental results for these molecules are shown in Fig. 1 and 4, and once again show the simplification of spectra to be expected in the crystalline state when several rotational isomers are present in the liquid. Detailed assignments of these spectra will be given in later publications with the help of similar experimental data obtained for the chlorides and iodides. For the present the discussion will be confined to a few points of a general nature.

These molecules are of a similar atomicity to 1: 4-dibromobutane, but it is seen that the solid state spectra are considerably more complicated than that of the dihalide. This results from the absence of a centre of symmetry and the correspondingly less strict selection rules. The virtual impossibility of analyzing the liquid state spectra is very apparent for these molecules. If each solid state spectrum corresponds to the presence of a single configuration there should be an approximate correlation of the number of observed frequencies of moderate strength with the expected number of fundamentals. *n*-Propyl bromide would be expected to have 5 methyl deformation frequencies, 8 CH_2 deformation modes, and 2 C—C skeletal stretching modes in the range 1500-700 cm.$^{-1}$. The two unsymmetrical internal deformation modes of the methyl group will lie very close to the absorption caused by the two CH_2 bending modes near 1450 cm.$^{-1}$, and hence only 11 fundamentals are to be expected below 1400 cm.$^{-1}$. Eleven absorptions are observed experimentally of medium strength or greater in this region. Similar arguments lead us to expect *n*-butyl bromide to have 15 fundamentals between 1400 and 700 cm.$^{-1}$, compared with 12 observed of medium strength or greater. It can, therefore, be confidently assumed that the solid state spectra correspond to a single configuration in each case.

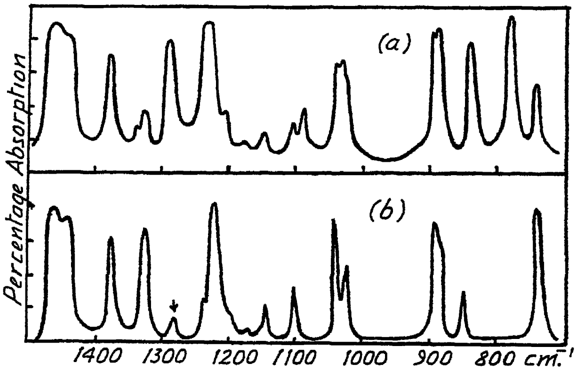

FIG. 4.—The infra-red spectrum of *n*-propyl bromide in (*a*) the liquid at — 60°C and (*b*) the crystalline state. Approximate thickness : 0·05 mm.

The spectrum of the glassy form of *n*-butyl bromide is shown in Fig. 1 together with those for the liquid and crystalline solid. There is a strong resemblance between the glass and liquid spectrum, showing that several different rotational isomers are present in the glassy form. Relative changes in intensity in the spectrum of glass when compared with the liquid spectrum can be attributed to changes in the isomeric composition of the liquid between room temperature and the onset of super cooling. The reduced width of some of the absorption bands in the glass as compared with the liquid is a simple temperature effect.

Some Straight Chain Alcohols—A necessary preliminary to the analysis of the vibrational spectra of long chain molecules such as the *n*-paraffins, alcohols, amines, etc., is the isolation of the planar zig-zag configuration in the crystalline lattice. A programme of work with this as its aim has been initiated by a study of the infra-red spectra of a series of alcohols and paraffins in the solid-state. Some points of interest will be mentioned here relating to the spectra of the alcohols.

Once the infra-red or Raman spectra of the planar zig-zag forms have been obtained the first task is to distinguish between the skeletal stretching and hydrogen deformation modes occurring in the region 1500-700 cm.$^{-1}$. The infra-red spectra of the smaller straight chain paraffins published recently by Axford and Rank[6] do not contain a set of absorptions which can obviously be picked out as skeletal stretching modes. This is not very surprising as they are expected to be generally weak in view of the almost non-polar nature of the C—C linkages. It was felt, however, that the corresponding skeletal modes of the alcohols might be of much greater intensity, as all the stretching vibration must involve some degree of motion of the highly polar C—O linkage. A highly polar linkage usually gives rise to intense infra-red absorptions, and the presence of a series of strong bands between 1070 and 880 cm.$^{-1}$ in the crystalline alcohols confirms the above hypothesis. These can clearly be assigned to skeletal modes and the limiting frequencies can be compared with the limits 1145 and 890 cm.$^{-1}$ found for the skeletals in the *n*-paraffins.[19]

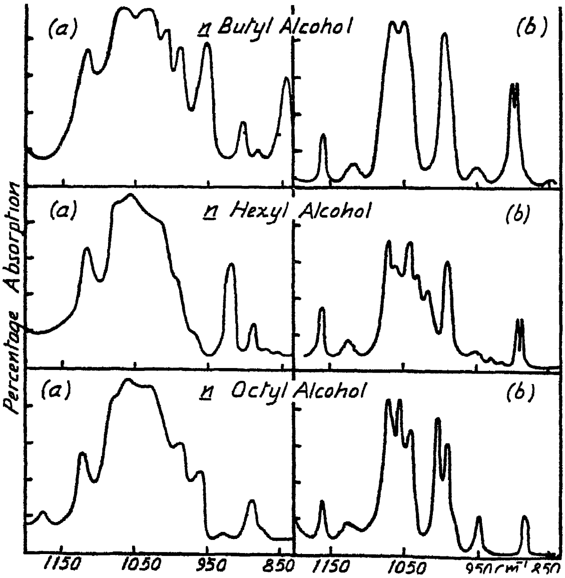

FIG. 5.—The infra-red spectra of *n*-butyl, *n*-hexyl and *n*-octyl alcohol in (*a*) the liquid and (*b*) the crystalline state. Approximate thickness : 0·02 mm.

Fig. 5 shows the spectra of *n*-butyl, *n*-hexyl and *n*-octyl alcohol in the liquid and solid states over the region 1200-850 cm.$^{-1}$. In the spectra of the liquids a very strong broad absorption centred about 1060 cm.$^{-1}$ has been known for some years as the C—O stretching frequency. Its broadness results from a superposition of the strongest skeletal stretching modes of the different isomers present in the liquid state. In the solid state it is replaced by a series of much sharper absorption bands, corresponding to the various skeletal frequencies of the planar zig-zag isomer. The three molecules whose spectra are shown in Fig. 5 should have respectively 4, 6 and 8 skeletal stretching modes, compared with 5, 8 and 8 absorptions stronger than 20 % occurring between 1070 and 880 cm.$^{-1}$ in the solid state spectra. This is fair agreement when account is taken of two methyl wagging modes which are also expected to give absorptions in this region.[19]

---

[19] Brown, Sheppard and Simpson, this Discussion.

The spectrum of *n*-hexyl alcohol in the solid state contains more weak bands than those of the other alcohols. Very slow cooling over the freezing point and subsequently down to liquid air temperature did not eliminate these, neither did the technique of forming a glass and allowing it to change to the crystalline solid. These residuals are most probably due to the persistence of small amounts of amorphous material, and hence of other planar isomers. The amount of such material remaining is thought to be not more than a few per cent.

Conclusion.—The above discussion shows how a comparatively simple technique can be used to reduce the complexity of the spectra of medium size polyatomic molecules which exhibit rotational isomerism. At the same time this method provides in many cases the simplest method of detecting rotational isomerism in the liquid, and also makes possible the interpretation of the spectra of at least one of the isomeric forms. The examples of molecules with unbranched paraffin chains that have been discussed above have shown how in these cases the simplified experimental data can be used to make reliable assignments for skeletal stretching frequencies and CH_2 deformation modes, fundamentals which have been difficult to distinguish in the past.

It is important to realize, however, that this method has its limitations. On the experimental side it has not always proved to be easy to obtain the solid state material in the crystalline state, and it has been demonstrated that the spectrum of the glass is little different from that of the liquid and hence useless for the present purposes. This, however, is not a fundamental limitation and can probably be overcome with careful technique in many cases. Our experiments so far suggest that the greatest difficulties of this sort may be met with substances of a polar nature of low freezing point, and hydrogen bonding may be another relevant factor as shown by the experimental difficulties experienced in obtaining consistent spectra of the alcohols in the crystalline state. Furthermore, with non-isotropic crystals a high degree of orientation in the thin films necessary for infra-red work may arise and give apparently slightly different spectra with different experimental techniques. Effects of this sort can probably best be investigated with the help of polarized radiation.

On the theoretical side, one limitation of the technique is that in many cases only the interpretation of the spectra of the single isomer that exists in the solid state can be achieved, although this in itself is a considerable advance. However, in order to achieve this, in many cases the Raman spectra in the crystalline state also will be needed, so that complete assignments can be made for complex molecules and for those which have a centre of symmetry. Raman technique would seem to lag behind that of infra-red spectroscopy for the detection of weak lines in the solid state spectra. Finally, the change in environment of a molecule in the crystalline state as compared with that in the liquid may give rise to frequency and intensity variation of the different fundamentals which will cause difficulties in interpretation. For molecules of low symmetry these effects will probably be small except when hydrogen bonding is operative. A further possible cause of complexity in crystalline spectra will be the presence of more than one molecule in the unit cell; under such conditions some of the molecular fundamentals may split into several components.

The existence of isomerism arising from restricted rotation about single linkages is not confined to the C—C linkage, and hence this method of analysis may be of equal use in the investigation of the spectra of molecules with internal single linkages containing atoms such as nitrogen, oxygen, phosphorus and sulphur.

The authors are indebted to Dr. Delia M. Simpson for helpful discussions and criticism. One of us (J.K.B.) is grateful to the D.S.I.R. for a maintenance grant, and the other (N.S) to the Royal Commissioners for the Exhibition of 1851 for a Senior Studentship.

Department of Colloid Science,
Free School Lane,
Cambridge.

INTERNAL ROTATION IN ZINC DIMETHYL AND MERCURY DIMETHYL

BY D. R. J. BOYD, H. W. THOMPSON AND R. L. WILLIAMS

Received 30*th June*, 1950

Vibrational absorption bands near 3 μ have been measured for zinc dimethyl and mercury dimethyl using high dispersion. Analysis of the perpendicular bands suggests that the results are explained well by the assumption of essentially free internal rotation of the methyl group in these molecules.

The infra-red and Raman spectra of zinc dimethyl and mercury dimethyl are of interest not only as a means of determining the vibration frequencies of these molecules, but also in connection with the question of the free or restricted rotation of the methyl groups about the metal-carbon bond. The Raman spectra have been measured by Venkateswaran,[1] by Pai,[2] and by Feher, Kolb and Leverenz.[3] The infra-red spectra were also studied using low dispersion by Thompson, Linnett and Wagstaffe [4] and more recently by Gutowsky.[5] The vibrational analysis of these spectra, together with the polarization measurements in the Raman effect, agree with the supposition of a linear C—metal—C skeleton, and suggest that the methyl groups are either in the eclipsed configuration, or are free to rotate. These two alternatives correspond to the point groups D_{3h} and D'_{3h}, which cannot be distinguished from the spectra alone. On other grounds, the staggered structure of the two methyl groups might be regarded as more probable than the eclipsed form, and the evidence is therefore inclined to the hypothesis of free internal rotation.

The rotational fine structure of the perpendicular-type infra-red bands should be markedly different according to whether there is free rotation or not. Nielsen [6] considered the problem theoretically for the case where there is no vibrational-rotational interaction, and Howard [7] extended the treatment to allow for such interaction. Howard applied his results to ethane and concluded that internal rotation does not occur.

We have measured some appropriate vibration bands of ethane, dimethyl zinc, dimethyl mercury and dimethyl acetylene to compare the fine structure in each case. There is independent evidence that free rotation of the methyl groups occurs in dimethyl acetylene. Our results show that with zinc dimethyl and mercury dimethyl the rotational fine structure of certain perpendicular bands is strongly suggestive of completely

[1] Venkateswaran, *Ind. J. Physics*, 1930, **5**, 145.
[2] Pai, *Proc. Roy. Soc. A*, 1935, **149**, 29.
[3] Feher, Kolb and Leverenz, *Z. Naturforsch.*, 1947, **2a**, 454.
[4] Thompson, Linnett and Wagstaffe, *Trans. Faraday Soc.*, 1940, **36**, 797.
[5] Gutowsky, *J. Chem. Physics*, 1949, **17**, 128.
[6] Nielsen, *Physic. Rev.*, 1932, **40**, 455.
[7] Howard, *J. Chem. Physics*, 1937, **5**, 451.

free rotation. A full analysis will not be possible until our measurements have been completed on the bands at longer wavelengths, but preliminary consideration of certain bands of dimethyl acetylene supports this conclusion.

Experimental

The metal alkyls were purified by repeated fractionation *in vacuo*, all traces of methane and ethane being removed, the final products having the correct vapour pressures, and showing no spurious infra-red bands. The Pyrex absorption cell was 10 cm. in length and the rock salt end plates were fixed to its flanged ends by means of Silicone grease or hard vacuum grease. A series of measurements were made with pressures 10-40 mm. The grating spectrometer has been described elsewhere,[8] the region investigated here being 3-4 μ, where the fundamental C—H stretching vibration bands are observed. The grating had 7200 lines per inch, and the detector was a lead telluride cell, used in the manner described previously.

Results and Discussion

The spectrum of zinc dimethyl is shown in Fig. 1, and Table I gives the frequencies of the main lines and the "mean" centres of related groups of lines. One perpendicular band and two parallel bands are seen between 2800-3100 cm.$^{-1}$. The fine structure of the parallel bands is not resolved and with these molecules, which have a large value of the ratio I_B/I_A, the central Q branch has low intensity. However, the centres of these bands appear to be near 2914 cm.$^{-1}$ and 2841 cm.$^{-1}$. The origin of the perpendicular band also cannot be fixed, but lies close to 2960 cm.$^{-1}$.

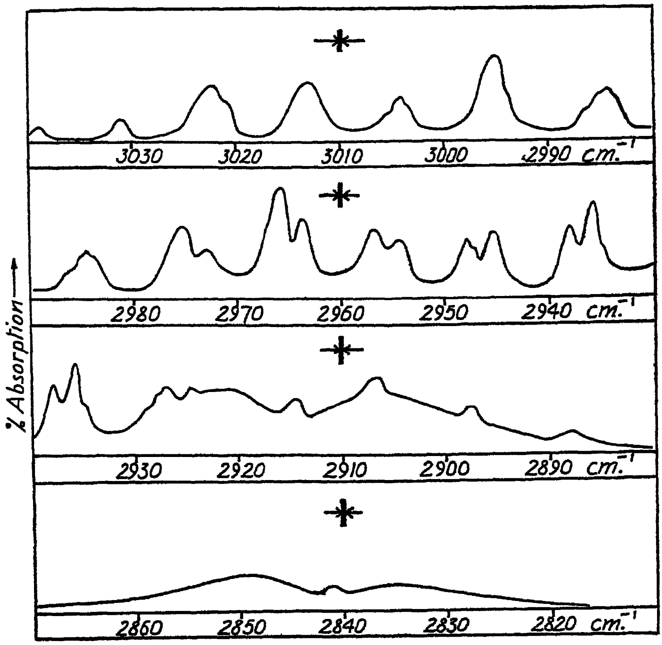

FIG. 1.—Zinc dimethyl. Path length 10 cm, pressure 20 mm.

The symmetry types and vibrational species for the point groups D_{3h} and D'_{3h} are given in Table II. The perpendicular band at 2960 cm.$^{-1}$

---

[8] Miller and Thompson, *Proc. Roy. Soc. A*, 1950, 200, 1.

must belong to the E' class, and can be assigned to ν_8. This band corresponds to the Raman interval 2948 cm.$^{-1}$. The only C—H stretching vibration which will give a parallel type fundamental is ν_5, and this is assigned to 2914 cm.$^{-1}$. The weaker parallel band at 2841 cm.$^{-1}$ may be assigned to the combination $(\nu_{13} + \nu_9)$, which will be expected near 2828 cm.$^{-1}$, if the assignment of Gutowsky for the fundamentals is used.

TABLE I.—ZINC DIMETHYL

Perpendicular Band

Position of Line ν_{vac} (cm.$^{-1}$)	" Centre "	Interval $\Delta\nu$
3039·0	—	—
3031·1	—	7·9
3022·5	—	8·6
3013·2	—	9·3
3004·3	—	8·9
2995·0	—	9·3
2984·6	—	10·4
2975·4	2974·2	10·4
2973·1		
2965·8	2964·7	9·5
2963·7		
2956·8	2955·6	9·1
2954·4		
2947·7	2946·5	9·1
2945·3		
2938·0	2936·9	9·6
2935·9		
2927·3	2925·9	11·0
2924·6		
. . . . . .	. . . .	. . . .
2906·4	—	8·9
2897·5	—	9·5
2888·0	—	—

Parallel Bands

Centre (cm.$^{-1}$)	Max P branch	Max R branch	$\Delta\nu$
2914·0	2906·5	2921·5	15·0
2841·0	2835·0	2849·6	14·6

Since the parallel bands were not resolved, we cannot determine the rotational constant $B = h/8\pi^2cI_B$, and thence the value of I_B, the moment of inertia about an axis perpendicular to the C—Zn—C direction. If we assume plausible molecular dimensions, namely,

$$r_{\mathrm{Zn—C}} = 2·05 \text{ Å}, \quad r_{\mathrm{C—H}} = 1·09 \text{ Å},$$

with tetrahedral methyl groups, $I_B = 221 \times 10^{-40}$ g. cm.^{2}, and the line spacing in the P and R branches will be about 0·24 cm.$^{-1}$. Using the formula of Gerhard and Dennison [9] for the separation of intensity maxima in the P and R branches, namely,

$$= \frac{S(\beta)}{\pi}\sqrt{\frac{kT}{I_B}},$$

---

[9] Gerhard and Dennison, *Physic. Rev.*, 1933, 43, 193.

an appropriate value for $\Delta\nu$ at 22° C is 15·1 cm.$^{-1}$. The values found for the two bands are 15·0 cm.$^{-1}$ and 14·6 cm.$^{-1}$ respectively, in satisfactory agreement.

The perpendicular band is more interesting. If there is a high barrier to internal rotation, the fine structure should resemble closely that found in the corresponding band of ethane. The latter has been measured by Smith,[10] and we have also recorded it for comparison using our own spectrometer. In fact, the band of zinc dimethyl shows little resemblance to it, for whereas the Q branches for ethane are sharp and spaced by 3-4 cm.$^{-1}$, those of zinc dimethyl are very broad and have a spacing of about 9 cm.$^{-1}$.

Howard has shown that in free internal rotation, where two degenerate frequencies of different symmetry classes are themselves accidentally degenerate, the spacing of the Q lines in the perpendicular bands should be $[4A(1 - \zeta) - 2B]$ rather than $[2A(1 - \zeta) - 2B]$ for a rigid symmetrical top. Also, where there is free rotation, the Q lines will themselves have a fine structure of spacing $[2B]$. The positions of the centres of the Q lines will be given by

Type	Number of Vibrations	Activity in		Form
		Raman	Infra-red	
A_1'	3	Yes	No	ν_1 CH$_3$ valency ν_2 CH$_3$ deformation ν_3 C—Zn—C valency
A_1''	1	No	No	ν_4 Torsional
A_2''	3	No	Yes	ν_5 CH$_3$ valency ν_6 CH$_3$ deformation ν_7 C—Zn—C valency
E'	4	Yes	Yes	ν_8 CH$_3$ valency ν_9 CH$_3$ deformation ν_{10} CH$_3$ rocking ν_{11} C—Zn—C deformation
E''	3	Yes	No	ν_{12} CH$_3$ valency ν_{13} CH$_3$ deformation ν_{14} CH$_3$ rocking

$$\nu = \nu_0 - [2A\zeta - B] \pm [4A(K \pm K')(1 - \zeta) - 2BK],$$

where K' is the quantum number for internal free rotation. If the number of quanta excited in the vibration is odd, as in the present case, $K' = \pm 1, \pm 3, \pm 5, \ldots$ for even K, and $0, \pm 2, \pm 4 \ldots$ for odd K. Now, since the spacing $2B$ of the P and R lines in the parallel bands is not resolved, we should not expect the fine structure of the Q lines in the perpendicular bands to be resolved either, but the broad lines of zinc dimethyl, compared with those of ethane would be explained.

At the low frequency side of the perpendicular band, the Q lines show a definite splitting into two or more components. The reason for this is not yet clear, but it is possible that the submaxima may arise from intensity accumulations in the sub-structure. The mean spacing of the "centres" of the groups of lines is 9·43 cm.$^{-1}$. Using the value of A

---

[10] Smith, *J. Chem. Physics*, 1949, 17, 139.

obtained for ethane by Smith, namely 2·588 cm.$^{-1}$, and the estimated value for B of 0·12 cm.$^{-1}$, we find that assuming free rotation the Coriolis coupling factor ζ is 0·066. If a fixed configuration is assumed, ζ would be $-0·88$. Both these values for ζ are possible in principle, but strong reasons exist for regarding the second value as inadmissible. As a rule, ζ for fundamental bands of C—H stretching vibrations is small and positive, which would be expected, since the light hydrogen atoms move almost in a straight line and contribute little angular momentum of vibration to the total angular momentum. For the corresponding methane band $\zeta = 0·05$, and from other measurements, which we shall shortly publish on allene, methyl acetylene, methyl cyanide and methyl isocyanide, the values are also very small. In the corresponding bands of methyl halides,[11] ζ varies between 0·05 and 0·1. It therefore seems that the first smaller value may be the correct one, and we must assume that the internal rotation is essentially free.

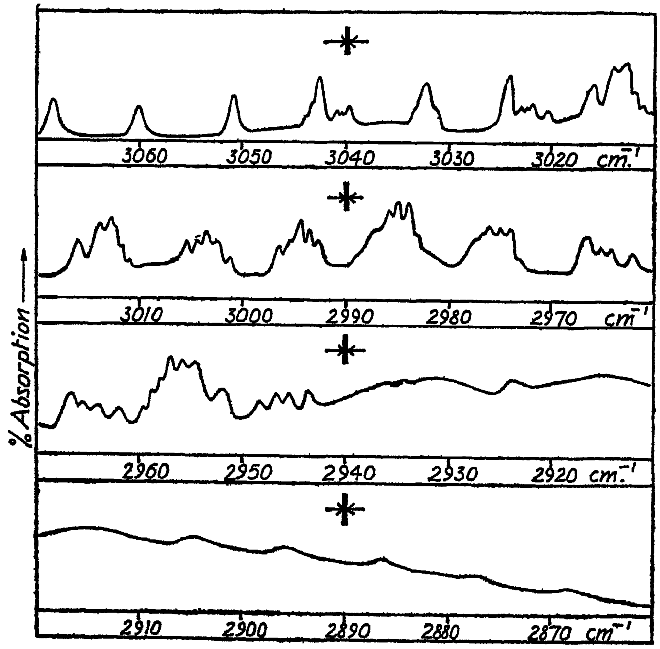

FIG. 2.—Mercury dimethyl. Path length 10 cm., pressure 40 mm.

This question may be further clarified by an analysis of the other perpendicular bands at longer wavelengths, and by application of the Teller summation rule for the values of ζ found. These bands are now being measured.

The results with mercury dimethyl are very similar to the above. The measurements of the Raman spectrum, and infra-red spectrum under low dispersion, are again best fitted with the assumption of point group D_{3h} or D'_{3h} with either eclipsed or freely rotating methyl groups. The bands now measured are shown in Fig. 2, and the position of lines are given in Table III. In this case, the Q lines on the low frequency side of the perpendicular band are more markedly split than those of zinc dimethyl, and the lines on the higher frequency side of the band are sharper than with the latter substance.

---

[11] Herzberg, *Infra-red and Raman Spectra* (van Nostrand, 1945).

TABLE III—MERCURY DIMETHYL

Perpendicular Band

Position of Lines ν_{vac} (cm.$^{-1}$)	"Centre"	Interval $\Delta\nu$
3068·4	3068·4	—
3060·1	3060·1	8·3
3050·9	3050·9	9·2
3043·6	3041·6	9·3
3043·2		
3042·5		
3040·9		
3040·3		
3039·7		
3032·1	3032·1	9·5
3024·0	3022·9	9·2
3022·9		
3021·9		
3020·4		
3015·7	3013·1	9·8
3013·7		
3012·5		
3011·6		
3011·0		
3010·2		
3005·3	3003·5	9·6
3004·4		
3003·5		
3002·4		
3001·3		
2996·5	2994·0	9·5
2995·3		
2994·4		
2993·5		
2992·6		
2987·3	2984·8	9·2
2985·7		
2984·8		
2983·8		
2977·2	2975·3	9·5
2976·0		
2974·9		
2974·0		
2966·4	2965·8	9·5
2965·3		
2964·0		
2961·9		
2959·6	2956·5	9·3
2958·7		
2957·8		
2957·0		
2955·6		
2954·5		
2952·0		
2948·1	2946·5	10·0
2946·7		
2945·5		
2943·5		
. . . . .	. . . .	. . . .
2904·5	2904·5	—
2895·6	2895·6	8·9
2886·3	2886·3	9·3
2877·2	2877·2	9·1
2868·4	2868·4	8·8

Parallel Bands

Centre (cm.$^{-1}$)	Max P branch	Max R branch	$\Delta\nu$
2924·0	2914·5	2930·5	16·0
2834·0	2826·0	2841·5	15·5

The centre of the perpendicular band cannot be located with certainty, but is probably close to 2980 cm.$^{-1}$. This frequency must be assigned to the E' class methyl group stretching vibration. Gutowsky, on the basis of low dispersion measurements and Raman spectra of the liquid, gave a rather lower value for this vibration frequency, but our results make the higher one more likely. The parallel bands lie near 2924 cm.$^{-1}$ and 2834 cm.$^{-1}$, the former being assigned to ν_5 (Gutowsky gave 2880 cm.$^{-1}$) and the latter probably to $(2\nu_{14} + \nu_{13})$, which from the assignment of Gutowsky would be expected near 2843 cm.$^{-1}$.

The parallel bands of mercury dimethyl could not be resolved. Assuming for the molecular dimensions

$$r_{\mathrm{Hg-C}} = 2{\cdot}23 \text{ Å}, \; r_{\mathrm{C-H}} = 1{\cdot}09 \text{ Å},$$

and tetrahedral methyl groups, $I_B = 269 \times 10^{-40}$ g. cm.^{2}. This would give a mean line spacing in the P and R branches of 0·21 cm.$^{-1}$, and 13·1 cm.$^{-1}$ between the intensity maxima of these maxima if I_A is assumed to be equal to the corresponding value in ethane. The spacing observed between the maxima is 15 to 16 cm.$^{-1}$, but owing to overlap with lines of the perpendicular band these values are not very convincing.

If the "centres" of the group of Q lines in the perpendicular band are taken, the mean spacing is 9·3 cm.$^{-1}$. Using the same argument as for zinc dimethyl, the assumption of free internal rotation leads to a Coriolis factor ζ of 0·08, but for a fixed configuration ζ is $-$ 0·84, and the former value is much more likely. The complex nature of the Q lines in this case, and the sharper nature of these lines at higher frequencies, cannot at present be explained. Here, too, measurement of the other perpendicular bands at longer wavelengths may clarify the position. These refinements do not, however, affect the main conclusion that the internal rotation must be essentially free.

It is interesting to consider the corresponding infra-red bands of dimethyl acetylene, since in this case the comparison of experimental and calculated thermodynamic properties[12] suggest a zero barrier to internal rotation of the methyl groups. Our measurement on the perpendicular bands of this molecule are incomplete, but low dispersion measurements have already shown that in the perpendicular band near 7 μ there is a spacing of Q lines of about 13 to 15 cm.$^{-1}$. The Coriolis coupling factor of an analogous C—H deformation band in ethane has been found by Smith to be $-$ 0·33, and a value close to this applies in corresponding bands of related molecules. If this value is taken, with moments of inertia $I_A \approx 11$, $I_B \approx 100 \times 10^{-40}$ g. cm.^{2}, the spacing of Q lines calculated for free rotation, namely $[4A(1 - \zeta) - 2B]$, is about 13·5 cm.$^{-1}$, whereas a fixed configuration would give about half this value. It therefore seems certain that theory is in good agreement in this case where the internal rotation has been established independently, and the conclusions with regard to the metal alkyls are thereby strengthened.

We are grateful to the Hydrocarbon Research Group of the Institute of Petroleum, and to the Government Grant Committee of the Royal Society for financial assistance. We also express our thanks to the Telecommunications Research Establishment for the photoconductive cells.

The Physical Chemistry Laboratory,
Oxford.

---

[12] Osborne, Garner and Yost, *J. Amer. Chem. Soc.*, 1941, 63, 3492; *J. Chem. Physics*, 1940, 8, 131. Crawford and Rice, *ibid.*, 1939, 7, 437.

INFRA-RED SPECTRA OF HYDROXYLIC COMPOUNDS

By R. Mecke

Received 8th August, 1950

This is a short report of the work done during the last few years on infra-red intensity measurements in my laboratory. The following problems were investigated :

(i) the nature of the hydrogen bond and comparison with thermal and dielectric measurements ; [1,2,3,4]

(ii) the influence of solvents on compounds with hydrogen bonds and the effect of the proton-attracting power of these solvents ; [5]

(iii) infra-red absorption measurement for the determination of the dipole moments (bond moments) of different XH bonds and the changes brought about by inter- and intramolecular action with other molecules.[6]

I. Hydrogen Bond and Mass-action Law.—Quantitative measurements of association can be obtained by two different, independent methods :

(i) by thermal investigations, especially using the classical methods for the determination of molecular weights in solutions ; [7]

(ii) by infra-red absorption measurements of characteristic frequency bands (e.g. the OH band) and % deviations from Beer's absorption law :

$$\log (I_0/I) = \epsilon cd$$

In the first, we observe as the directly measured quantity the *mean molecular weight* $\overline{M}$ of a mixture of the polymers conveniently given as a ratio f in units of the (known) formula weight M_1 :

$$f = \overline{M}/M_1.$$

In the second, only a *partial weight* is measured, usually the fraction of non-associated monomers.

Unfortunately the range of the directly measured molecular weight is often limited at certain temperatures (melting point, boiling point of the solvent). The method of infra-red measurements is free from this disadvantage. It depends on the appearance of *two* OH *bands* in solutions

---

[1] General report : Mecke, *Z. Elektrochem.*, 1948, **52**, 269. Infra-red measurements : Mecke and Kempter, *Naturwiss.*, 1939, **27**, 583 ; *Z. physik. Chem. B*, **46**, 1940, 229. Mecke and Kreuzer, *ibid.*, 1941, **49**, 309. Hoffmann, *ibid.*, 1943, **53**, 179. Mecke and Nückel, *Naturwiss.*, 1943, **31**, 248. Mecke, *Z. Elektrochem.*, 1944, **50**, 57. Kreuzer, *Z. physik. Chem.*, *B*, 1943, **53**, 213.

[2] Thermal measurements : Mecke, *Z. Elektrochem.*, 1948, **52**, 107.

[3] Dielectric measurements : Mecke and Schupp, *Z. Elektrochem.*, 1948, **51**, 40 ; 1948, **52**, 54. Schupp, *ibid.*, 1949, **53**, 12. Mecke, Reuter and Schupp, *Z. Naturforsch.*, 1949, **4a**, 182. Mecke and Reuter, *Naturwiss.*, 1949, **36**, 251. Mecke and Reuter, *Z. Naturforsch.*, 1949, **4a**, 368.

[4] Measurements of conductivity : Mecke and Zeininger, *Z. Elektrochem.*, 1948, **52**, 49. Mecke and Zeininger, *ibid.*, 1950, **54**, 174.

[5] Lüttke and Mecke, *ibid.*, 1949, **53**, 241.

[6] Mecke and Timm, *Z. Physik*, 1935, **98**, 363. Mecke, *Z. physik. Chem. B*, 1936, **33**, 156 ; *Z. Physik*, 1937, **107**, 595. Kempter and Mecke, *Z. Naturforsch.*, 1947, **2a**, 549. Mecke, *Z. Elektrochem.*, 1950, **54**, 38.

[7] Hoyer, *ibid.*, 1943, **49**, 134. Davies, *Ann. Reports*, 1946, **43**, 4.

[8] Fox and Martin, *Trans. Faraday Soc.*, 1940, **36**, 897.

at sufficient molar concentrations.[8] Those bands are observed as fundamentals as well as overtones. Fig. 1 shows an example, the second overtone for phenol in CCl_4. The intensity of the first (sharp) band ($\nu = 10330$ cm.$^{-1}$) increases with decreasing concentration and increasing temperature while the second band, which is much broader and displaced to shorter frequencies ($\nu \sim 10140$ cm.$^{-1}$), decreases. To-day one assumes that only the free vibrating OH group of the non-associated or monomeric molecules contributes to the "*sharp* OH *band*", while the "*association band*" is attributed to hydroxyl groups bonded in polymeric molecules. Assuming Beer's law to be valid, the fraction α of monomeric molecules in the solution is given by the quotient of the extinction coefficients, ϵ_c (at concentration c) and ϵ_∞ (at infinite dilution),

i.e. $$\alpha = \epsilon_c/\epsilon_\infty.$$

Hence the question arose as to what extent those two methods (i) and (ii) could be brought to comparable agreement and furthermore, what conclusions concerning the mechanism of association could be drawn when agreement was found.

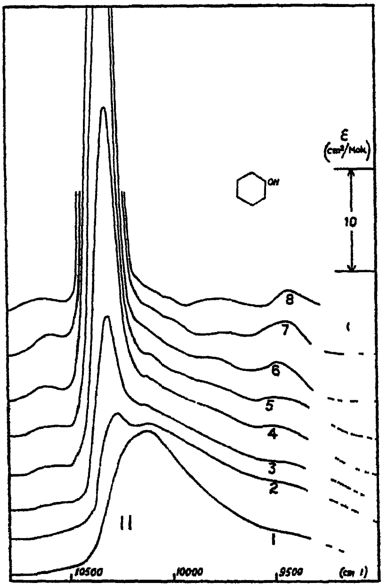

FIG. 1.—Change in the intensity (molar extinction coefficient ε) of the "sharp" OH band and the "diffuse" association band with variation of concentration (Phenol in CCl_4.)

Phenol in CCl_4 20° C

1. Phenol, pure. 2. 5·0 mole/l.
3. 2·5 mole/l. 4. 1·0 mole/l.
5. 0·5 mole/l. 6. 0·25 mole/l.
7. 0·1 mole/l. 8. 0·05 mole/l.

An objection might be made that the intensity of the sharp OH band of alcohols and phenols does not give the actual number of monomeric molecules because of accidental overlapping of different bands or because the simultaneous measurement of part of the association band cannot be entirely avoided. This objection we were able to refute by careful examination of several absorption bands obtained from a large number of substances. Fig. 2 shows measurements of α using the fundamental and overtones of phenol, all of which show satisfactory agreement within the limits of error.

If we assume that the association is governed by the law of mass action,[2] it follows from the Duhem-Margules relation that the following differential equation always exists between the fraction α of the monomer and the mean molecular weight $\overline{M}$:

$$d \ln (1 - x + M_1 x/\overline{M}) = x \, d \ln \alpha, \quad . \quad . \quad . \quad (1)$$

where x = mole fraction.

In any case, however, the integration of this equation allows the conversion of measured α values to $\overline{M}$ values and vice versa.*

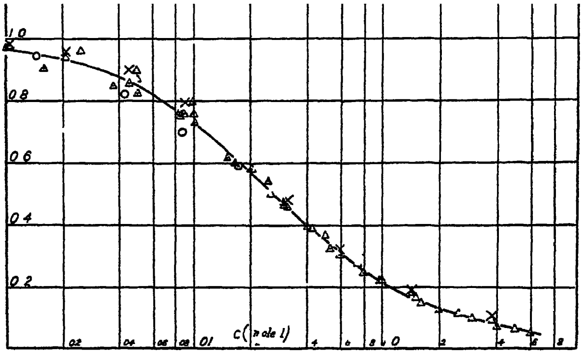

FIG. 2.—Fraction α of monomeric phenol obtained from the extinction coefficients of the fundamental, first and second overtone of the " sharp " hydroxyl band.

$$\alpha = \frac{\epsilon_c}{\epsilon_\infty} = f(c) \quad 20^\circ \text{ C.}$$

1 ν_{OH} ⊙ Fox and Martin. 2 ν_{OH} × Oswald.

3 ν_{OH} △ Hoffman, Kempter, Kreuzer, Lüttke, Oswald, Wulf and Jones.

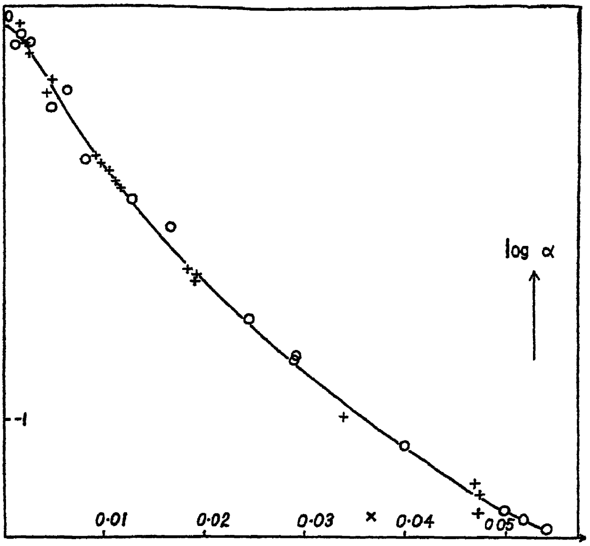

FIG. 3.—Fraction α of the monomer CH_3OH (solvent CCl_4) determined spectroscopically (+) and by measurements of the partial vapour pressure (o) at room temperature (t = 20° C, x = mole fraction).

Methanol + CCl_4. + Infra-red extinction. ○ Vapour pressure.

As an example, for the system $CH_3OH + CCl_4$ we compared the spectroscopically measured α values with those which we have obtained from measurement of vapour pressure by a new method.[2] The agreement is quite good up to remarkably high concentrations (x = 0·2) (Fig. 3).

---

* The real mole fraction is $x/(1 - x + M_1x/\overline{M})$. In dilute solutions it is possible to replace the mole fraction by the mole concentration (mole/l.).

Having thus decided that spectroscopic measurements will give reliable molecular weights we can now enquire into the nature of the association mechanism.

We consider the two limiting cases :

(i) *dimeric* association leading to *double molecules* (monocarboxylic acids),

(ii) *polymeric* association leading to *chain molecules* (alcohols, phenols).

Some relations which can be anticipated to exist between the measurable quantities, α, f and c are shown in Table I. Thorough investigations carried out on this subject but which cannot be reported in detail have led to the result that alcohols and phenols mainly associate to polymeric molecules, but with the limitation that there are practically no dimeric molecules with alcohols.[9] Here the association begins with trimeric molecules which we suppose to have a cyclic structure. As is well known, similar behaviour has been observed in the polymerization of formaldehyde and acetaldehyde to trimeric trioxan and paraldehyde or to tetrameric metaldehyde. Since higher polymers ordinarily have chain structures the question arises, whether or not the band of the end OH group may be observed in the infra-red when the group is not affected by intermolecular hydrogen bonding. In phenol we ascribe to the end OH group [8, 11] an intermediate band that we observed between the sharp OH band of the monomeric molecules and the broad association band (Fig. 4). Concentration and intensity measurements of the dipole moment also point to this assignment, but the investigations are not as yet complete. For alcohols we have been unable as yet to confirm the presence of an intermediate band, possibly due to the small resolving power and to the overlapping of a CH band.

TABLE I.—ASSOCIATION AND MASS ACTION LAW

α = fraction of monomers.

$f = \bar{M}/M_1$ degree of association (mean molecular weight).

$c \sim x/(1 - x + x/f)$ = concentration ($\sim$ real mole fraction)

$$d \ln (1 - x + x/f) = x\int d \ln \alpha \text{ (Duhem-Margules' equation).}$$

Dimeric association leads to molecular rings. 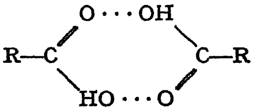 (e.g. mono-carboxylic acids)	Polymeric association leads to molecular chains. 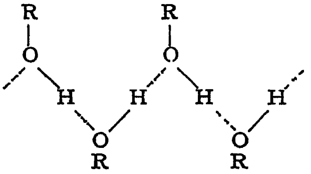 (e.g. alcohols, phenols)
(a) $1 - \alpha = 2k\alpha^2 c$ (b) $f(f - 1) = kc(2 - f)^2$ (c) $\alpha f = 2 - f$	$1 - \sqrt{\alpha} = k\alpha c$ $f(f - 1) = kc$ $\alpha f^2 = 1$

If we have a system in which chain association mainly takes place, we can calculate the mean association energy $\overline{W}$ from the dependence of the extinction ϵc on temperature :

---

[9] Hoffmann, *Z. physik. Chem. B*, 1943, 53, 179.

$$\overline{W} = RT^2\left[\frac{d \ln (\epsilon c)}{dT}\right]_{f} \quad . \quad . \quad . \quad . \quad . \quad (2)$$

In order to carry out this calculation we plot the extinction values ϵc logarithmically against the mean molecular weight $\overline{M}$ and $f \simeq 1/\sqrt{\alpha}$ and

TABLE II.—MEAN ASSOCIATION ENERGY $\overline{W}$ AND DEGREE OF ASSOCIATION f OF ALCOHOLS AND PHENOLS FROM INFRA-RED MEASUREMENTS

Substance		Solvent	$\overline{W}$ kcal./mole	f at $c = 1$ mole/l.
Methanol	$H_3C . OH$	CCl_4	4·72	3·05
„	„	C_6H_6	3·67	—
tert.-Butanol	$(H_3C)_3 . C . OH$	CCl_4	(5·3)	2·0
Benzylalcohol	$C_6H_5 . H_2C . OH$	CCl_4	4·60	2·50
„	„	C_6H_6	4·38	—
Phenol	$C_6H_5 . OH$	CCl_4	4·35	2·30
„	„	C_6H_6	3·55	1·20
„	„	$C_6H_5 . Cl$	3·48	1·50
p-Chlorophenol	$Cl . C_6H_4 . OH$	CCl_4	3·72	1·90
o-Cresol	$H_3C . C_6H_4 . OH$	CCl_4	3·8	1·7
p-Cresol	$H_3C . C_6H_4 . OH$	CCl_4	4·4	2·3

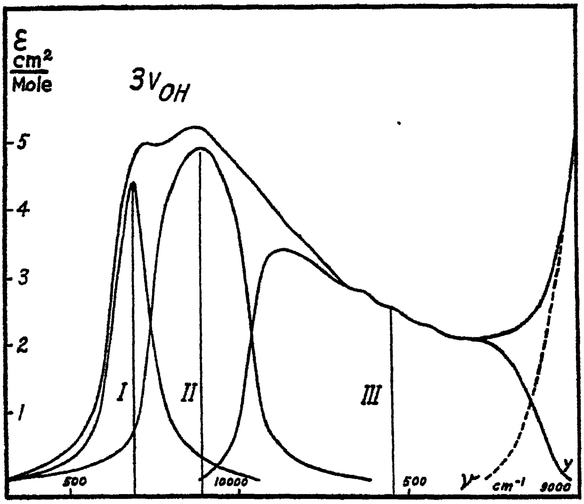

FIG. 4.—The different OH bands of associated phenol. I, monomer ; II, OH end-groups of polymers ; III, OH groups associated by hydrogen bonding.

Phenol in CCl_4. $c = 6{\cdot}16$ mole/l.

determine the association energy from distances between the curves at $f =$ const. (Fig. 5). This method leads to quite exact values, practically independent of the concentration, but dependent on the structure of the compound under investigation and especially on the solvent used (Table II).

The results for the methanol-CCl_4 system have also been compared with values obtained from calorimetric measurements, in this case using the heat of solution, and good agreement was found.[2] The observed heat of solution is proportional to the association energy $\overline{W}$ when plotted as a function of reciprocal mean molecular weight (Fig. 6):

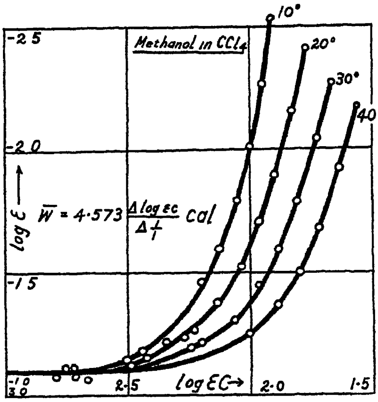

FIG. 5.—Determination of the energy of association $\overline{W}$ from the extinction curves: log ϵc at different temperatures (methanol in CCl_4).

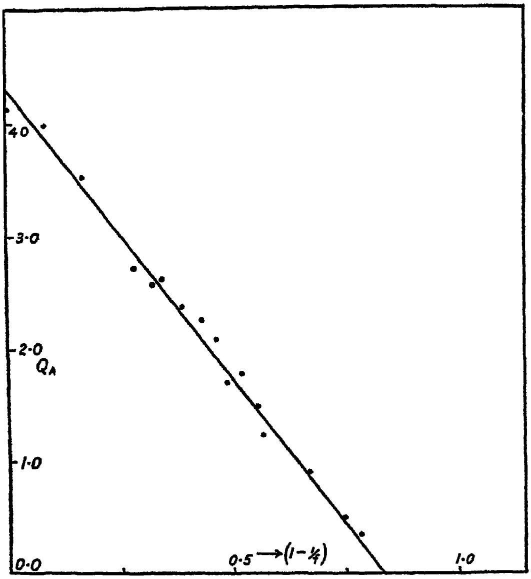

FIG. 6.—Relation between heat of solution Q and mean association energy

$$Q_s = Q_\infty - \overline{W}(1 - 1/f).$$

(methanol in CCl_4: $\overline{W} = 5{\cdot}15$ kcal./mole, $Q_\infty = 4{\cdot}34$ kcal./mole).

$$Q_s = Q_\infty - \overline{W}(1 - 1/f).$$

Finally, Fig. 7 shows the influence of chemical structure and the nature of the solvent on the mean molecular weight. It shows that primary alcohols are more associated than phenols, and in the same sense, *p*-chlorophenol is less associated. This latter fact is to be explained by the mesomeric effect of the Cl atom.

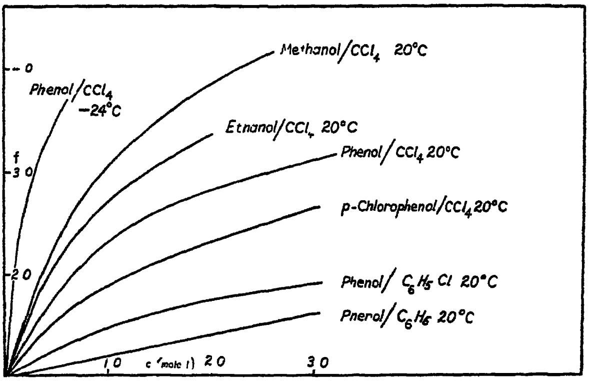

FIG. 7.—Degree of association $f = \overline{M}/M_1$ of different phenols and alcohols determined spectroscopically, as a function of concentration: $f(f - 1) \sim kc$.

II. Influence of Solvent on Association.—The OH bands show, as already mentioned, very strong interaction with other molecules having proton-attracting power. Naturally there is a strong influence exerted by these compounds when these compounds are used as solvents on the OH group which can be detected spectroscopically. Thus, as many authors have already stated,[5, 9, 12] frequency, absorption area and form of a band as well as the dipole moment of the molecule depends on the nature of the solvent. For lack of time and space we exclude the dipole moment from our considerations here. The investigation of the OH bond of phenol in infra-red absorption directly leads to conclusions concerning all specific interactions. We restrict ourselves to our own investigations on phenol in 18 different solvents.[5] Comparable measurements of other authors [9, 12] unfortunately do not contain intensity results. The changes of frequency which they observed, however, show the same trend as our own. Hence we believe the results to have general validity. We state as a rule that changing from "indifferent" solvents (e.g. CCl$_4$, C$_6$H$_{12}$) to solvents which are supposed to possess a stronger interaction by reason of other (e.g. thermal) measurements, a broadening of the band combined with decreasing intensity in addition to a change to smaller frequency is always observed (Fig. 8).

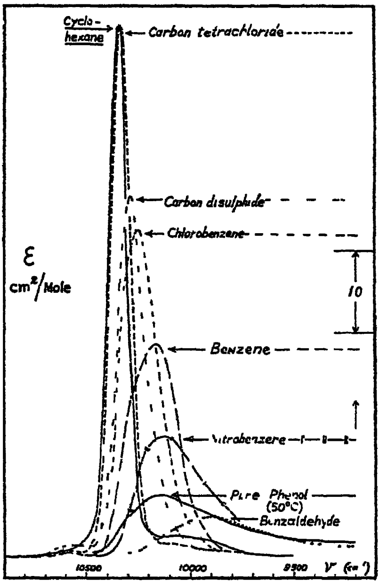

FIG. 8.—Phenol in different solvents (c = 0·05 mole/l. 20° C). Changes of intensity and shifts of frequency with increasing proton-attracting power of the solvent.

These three related effects show that the equilibrium nuclear distance *increases* on account of *inter*molecular interaction and thereby a different potential curve, a decrease in the OH dipole moment and weaker absorption follows. With phenols, comparison with dipole moment measurements was possible[8] since the CH moments are small (0·3) and moreover, because they compensate themselves to such an extent that the total moment of the molecule is mainly localized in the OH group. Variations of these moments run parallel with infra-red observations. Because of space we shall not expand on this very interesting comparison. It has lead, however, to a confirmation of Onsager's theory of orientation polarization.[15]

TABLE III.—Frequency ν, Max. Absorption Coefficient ε, Integrated Absorption $I = \int \varepsilon d\nu$ and Half Width of the 2 OH Overtone of Phenol in Different Solvents

(c = 0·05 mole/l., t = 20° C)

Solvent		Diel. Const.	Frequency ν (cm.$^{-1}$)	Max. Absorption Coefficient ε cm.^{2}/mole	Integrated Absorption cm./mole	Half-Width cm.$^{-1}$
Cyclohexane	C_6H_{12}	2·02	10 340	64·5	8·0	100
Cyclohexene I	C_6H_{10}	2·22	10 340	18·5	5·6	230
,, II		—	9 950	7·0	—	—
Carbon tetrachloride	CCl_4	2·24	10 330	64·0	8·2	110
Tetrachloro-ethylene	C_2Cl_4	2·29	10 325	63·5	7·7	120
Trichlor-ethylene	C_2HCl_3	3·43	10 305	53·0	7·5	120
Chloroform	$CHCl_3$	4·82	10 295	49·0	7·7	155
Carbon disulfide	CS_2	2·64	10 285	43·5	8·2	160
Pentachloro-ethane	C_2HCl_5	3·82	10 285	54·5	7·7	160
Chlorobenzene	C_6H_5Cl	5·69	10 250	40·0	9·3	210
Benzene I	C_6H_6	2·28	10 175	27·0	7·8	270
,, II		—	10 330	10	—	—
Toluene I	$C_6H_5CH_3$	2·34	10 140	25·2	9·0	340
II		—	10 330	10	—	—
Nitromethane	CH_3NO_2	39·4	10 160	11·0	4·5	370
Anisol	$C_6H_5 . O . CH_3$	4·37	10 130	11·6	6·2	430
Nitrobenzene	$C_6H_5 . NO_2$	33·7	10 120	14·0	5·5	370
Benzaldehyde	C_6H_5CHO	18·0	$\sim$9 920	5·0	2·8	540
Acetophenone	$C_6H_5 . CO . CH_3$	18·0	$\sim$9 870	4·0	2·6	650
Diethylether	$(C_2H_5)O$	4·33	$\sim$9 700	4·0	2·7	700
Acetone	$CH_3 . CO . CH_3$	21·5	$\sim$9 600	5·0	3·1	750

Table III shows our experimental results, which will not be discussed in detail; we merely point out some peculiarities concerning the operation of intermolecular interaction. These may perhaps be called "*association isomerism*". In some solvents (benzene, toluene, cyclohexene) a remarkable partial splitting of the OH band into two components is observed, e.g. in the second overtone, *ca.* 150-300 cm.$^{-1}$. This effect can be explained if it is remembered that molecules of the solvent may be situated in two different positions relative to the OH bond and that they can remain in both positions for some time. Benzene (Fig. 10) for instance, can have its molecular plane parallel (CH groups) or vertical (π electrons) to the OH group. In toluene we have in addition the CH_3 group; in cyclohexene

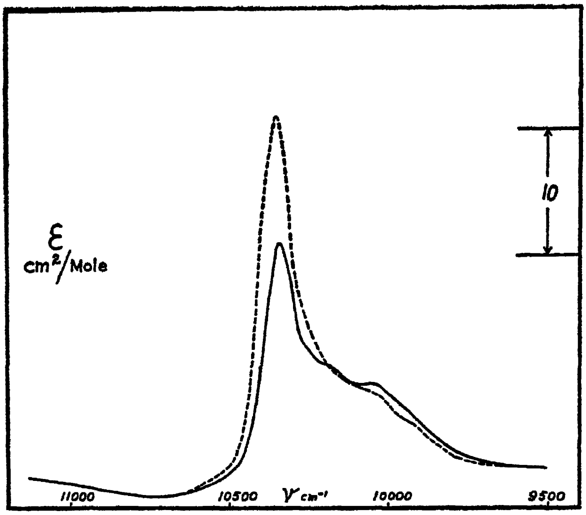

FIG. 9.—Phenol in cyclohexene (C_6H_{10}): two OH bands according to the two "association isomers" of an "aliphatic" and "olefinic" association.
(c = 0·05 mole/l.; 20° C: ———; 40° C: - - - -).

(Fig. 9), besides the interaction with the aliphatic CH_2 group, another interaction with the double bond (π electrons) is observed by reason of this frequency splitting. Since in all these directions the polarizability of the molecule is very different, the interaction energy will have different values for different orientations. This not only affects the nuclear distance and force constant of the bond (frequency position) but also the OH dipole

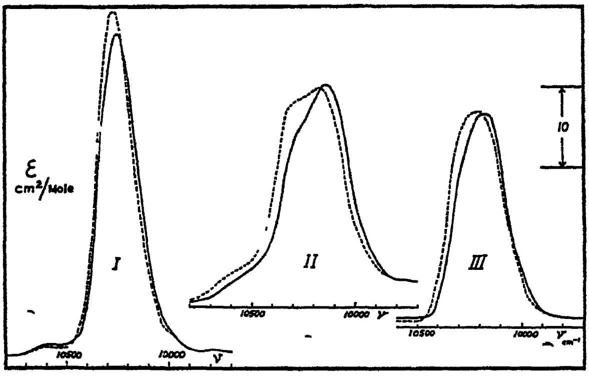

FIG. 10.—Phenol in three solvents with different proton polarization power: I, Chlorobenzene; II, Toluene; III, Benzene.
(c = 0·05 mole/l.; 20° C: ———; 50°: - - - - -).

moment and its variation during vibration (intensity). In this case changes in frequencies to smaller values always means a decrease of intensity. Since both states are relatively stationary, the equilibrium changes in the direction of the weaker bounded form if the temperature is increased because the coupling is less. This has in fact been observed. Particularly remarkable is the effect if π electrons of a double bond, which are acting as proton acceptors, are present. Hence phenol with its reactive OH groups is a very sensitive reagent in testing for the presence of such attrative effects caused by π-electrons or hydrogen bonds.

III. Dipole Moment and Chemical Bond.—As yet, infra-red investigations have been mainly restricted to the determination of frequency position, to fine structure investigations on gases and especially to the evaluation of the normal vibrations of a molecule and their relations to chemical constitution. Apart from analytical investigations the *intensity* problem has been almost neglected, until quite recently.[10] We became particularly interested in the question of how the intensity of an absorption band is related to the nature of the bond and to the chemical constitution and we succeeded in obtaining some interesting results.[6, 11, 13] Apart from the possibility of determining experimentally the so-called "bond moment" of a CH or OH bond, valuable information about the nature of the hydrogen bond can be obtained.

Looking at a series of overtone bands of CH and OH valency vibrations we see that the intensity ratio of neighbouring bonds is in order of magnitude of 1 to 10. Following the series up to $v = 5$—and that is experimentally quite possible—an intensity ratio of 1/100,000 has to be measured. By using different spectrometers, changing the cell length and concentration after a careful examination of the validity of Beer's law, we were able to overcome those experimental difficulties, and we already have a considerable amount of data. Fig. 11 shows the specific area absorption $\frac{1}{n_{\mathrm{CH}}}\int \epsilon d\nu$ per bond of the third overtone band ($4\,\nu_{\mathrm{CH}}$) of 71 different CH bonds which we have so far investigated. Plotting $\frac{1}{n_{\mathrm{CH}}}\int \epsilon d\nu$ as a function of frequency a very close relation between band *intensity*, band *position* and the *type of chemical bond* is found. The different vibrating groups are situated in this figure in small squares (with the exception of a few special cases) and thus we are able to identify them. Furthermore, we are able to make certain conclusions concerning constitutional conditions from deviations in the diagram. As these intensity investigations have received little attention as yet, we shall discuss them in some detail.

The total absorption

$$A = \frac{1}{n_{\mathrm{CH}}}\int \epsilon d\nu$$

where n_{CH} is the number of CH bonds, is related to the so-called transition moment μ_{ov} by the equation,

$$\mu_{ov}^2 = \frac{3hcf_iF_{ov}}{8\pi^3N\nu_{ov}}\,\frac{1}{n_{\mathrm{CH}}}\int \epsilon d\nu. \qquad . \quad . \quad . \quad . \quad (3)$$

$$\mu_{ov} = 0{\cdot}00198 \times 10^{-18}\sqrt{(f_iF_{ov}A/\nu_{ov})}$$

---

[10] Bartholomé, *Z. physik. Chem. B*, 1933, **23**, 131. Bell, Thompson and Vago, *Proc. Roy. Soc. A*, 1948, **192**, 498. Cole and Thompson, *Trans. Faraday Soc.*, 1950, **46**, 103. Richards and Burton, *ibid.*, 1949, **45**, 874. Wilson and Wells, *J. Chem. Physics*, 1946, **14**, 578. Thorndike, Wells and Wilson, *ibid.*, 1947, **15**, 157. Thorndike, *ibid.*, 1947, **15**, 868. Rollefson and Havers, *Physic. Rev.*, 1940, **58**, 710. Vergnoux, *Thesis* (Paris, 1945). Francis, *J. Chem. Physics*, 1950, **18**, 861.

[11] Oswald, *Diss.* (Freiburg i. Br., 1950), to be published.

[12] Davies, *J. Chem. Physics*, 1940, **8**, 577. Tuomikoski, *Suomen Kemistilehti B*, 1948, **21**, 59; 1950, **23**, 44. Freymann, *Compt. Rend.*, 1931, **193**, 928; *Ann. phys.*, 1933, **20**, 10, 242. Hartwell, Richards and Thompson, *J. Chem Soc.*, 1948, 1440.

[13] Lippert, *Diss.* (Freiburg i. Br., 1950), to be published.

where h, c, N are the well-known natural constants. f_i is of the so-called "internal field" factor. Concerning its magnitude there is still some doubt. Following Debye's theory [14] it follows that,

$$n\left(\frac{3}{n^2+2}\right)^2 \sim 0{\cdot}80$$

(n = refractive index). We prefer, however, the value calculated from Onsager's theory,[15]

$$n\left(\frac{2n^2+1}{3n^2}\right)^2 \sim 1{\cdot}00.$$

F_{0v} is a reduction factor transforming the above-mentioned large differences of absorption areas into ones of comparable magnitudes. It follows from wave-mechanical calculations of the normalized eigenfunctions of the vibration. In the case where the potential energy is describable by Morse's function,[16]

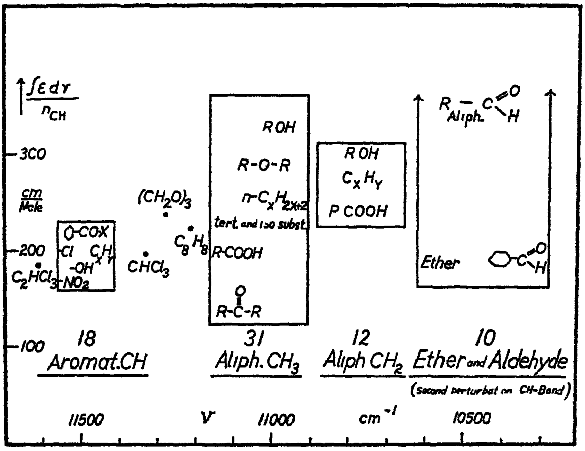

FIG. 11.—Mean specific integrated absorption $A_{04} = \frac{1}{n_{CH}}\int \epsilon d\nu$ (cm./mole) of 71 hydrocarbons as a function of frequency (third CH overtone, $4\nu_{CH}$).

$$E_{pot} = -D_0 + D_0(1-y)^2\,; \quad y = e^{-a(r-r_0)}\,; \quad a^2D_0 = 2\pi^2\nu_0^2\mu, \quad . \quad (4)$$

the series of overtone bands is given by the well-known equation :

$$\nu_{0v} = \nu_0 v[1 - x(v+1)]\,; \quad k = 1/x \quad . \quad . \quad . \quad (5)$$

whence it may be calculated that

$$F_{0v} = \binom{k}{v}\left(\frac{k}{k-1}\right)\left(\frac{k-v}{k-2v-1}\right) \sim \frac{k^v}{v\,!} \quad . \quad . \quad . \quad (6)$$

The transition moment is an expression for the mean change of the dipole moment caused by the vibration of the bond. Fig. 12 shows the change of the transition moment for a given change of the dipole moment in the different overtone bands. Assuming the unknown variation of the dipole moment to be a power series of the nuclear distance $z = a(r - r_0)$ then

$$\mu(z) = \mu_0 z + \mu_0' + \frac{1}{2\,!}\mu'' z^2 \ldots, \quad . \quad . \quad . \quad (7)$$

---

[14] Debye, *Hand. Radiologie*, 1933, **6**, 69.

[15] Onsager, *J. Amer. Chem. Soc.*, 1936, **58**, 1486.

[16] Morse, *Physic. Rev.*, 1929, **34**, 57. Bourgin, *ibid.*, 1927, **29**, 794; 1928, **32**, 237. Dunham, *ibid.*, 1929, **34**, 438.

where $\mu^{(n)} = (\partial^n \mu / \partial z^n)_{z=0}$, we obtain by further wave-mechanical calculations the transition moments from the partial derivatives $\mu^{(n)}$:

$$\left.\begin{aligned}
-\mu_{01} &= \frac{1}{1!}\,\mu' \\
\mu_{02} &= \frac{1}{2!}\,(\mu'' - \mu') \\
-\mu_{03} &= \frac{1}{3!}\,(\mu''' - 3\,\mu'' + 2\,\mu') \\
\mu_{04} &= \frac{1}{4!}\,(\mu^{(4)} - 6\,\mu''' + 11\,\mu'' - 6\,\mu') \\
-\mu_{05} &= \frac{1}{5!}\,(\mu^{(5)} - 10\,\mu^{(4)} + 35\,\mu''' - 50\,\mu'' + 24\,\mu') \\
\mu_{06} &= \frac{1}{6!}\,(\mu^{(6)} - 15\,\mu^{(5)} + 85\,\mu^{(4)} - 225\,\mu''' + 274\,\mu' - 120\,\mu')
\end{aligned}\right\} \quad (8)$$

These equations are easily solved, and the derivatives $\mu^{(n)}$ determined, and thus we should be able to construct experimentally the dipole curve from measured μ_{0v} values. This method, however, is not very accurate. On the other hand details of certain molecular models are as yet lacking.

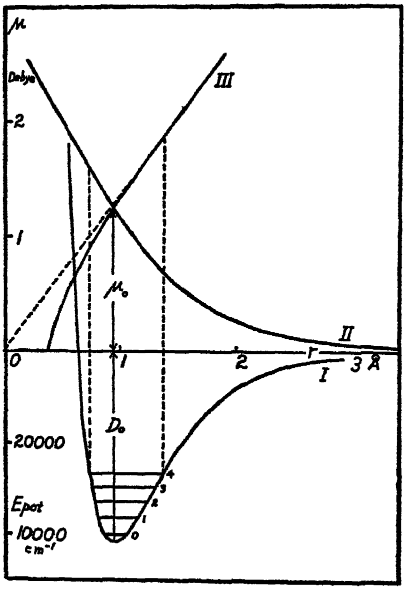

FIG. 12. — Dipole moment and potential function of a single bond :

I : Morse-function :

$$E_{pot} = -D_0 + D_0(1 - y)^2$$
$$y = \exp\,(-a(r - r_0)).$$

$$\text{II}: \ \mu = \mu_0\left(\frac{r + r_m}{r_0 + r_m}\right)^2 . y.$$

$$\text{III}: \ \mu = \epsilon r - \epsilon\alpha/r^2.$$

The vertical, dotted lines show the total change of the dipole moment caused by the vibration of the third overtone 4ν.

We tentatively make therefore the following simple assumptions. The effective charge of the dipole moment of the bond is ϵ, and the effective dipole length $d = r + r_m$, i.e. we consider the charge concentrated on one side at the vibrating hydrogen atom and on the other side in the interior of the rest of the molecule at a distance r_m from that atom which is binding the hydrogen atom (viz. C and O). Hence we assume that the dipole length does not coincide generally with the nuclear distance r_0. The total moment of the bond consists of the polar part

$$\epsilon d = \epsilon(r + r_m),$$

and of a inductive part caused by the internal field of the bond ϵ/d^2 and the difference of polarizability $\Delta\bar{\alpha}$:

$$\mu = \epsilon d - \frac{\Delta\bar{\alpha}\epsilon}{d^2}. \qquad . \quad . \quad . \quad . \quad . \quad (9)$$

Ordinarily the effective change ϵ as well as the polarizability $\Delta\bar{\alpha}$ of the atoms is assumed to be constant during the vibration. If this were so, we obtain in Table IV the transition moments mentioned in § I (see also Fig. 12, curve III). This assumption of constant ϵ and $\Delta\alpha$ is, however, wrong. The effective charge of a homopolar bond decreases with increasing nuclear distance from wave mechanics according to an exponential law:

TABLE IV

$\mu = \epsilon_0\left[r - \frac{\bar{\alpha}}{r^2}\right]$ $\mu_0 = \epsilon_0 r_0\left[1 - \frac{\bar{\alpha}}{r_0^3}\right]$	$\mu = \mu_0\left[\frac{r + r_m}{r_0 + r_m}\right]^2 \cdot y$ $y = e^{-a(r - r_0)}$; $z_0 = a(r_0 + r_m)$	Observed Phenol
$\mu_{00} = \mu_0$	$\mu_{00} = \mu_0$	(1·07)
$\mu_{01} = \epsilon_0/a[1 + 2\,\bar{\alpha}/r_0^3]$	$\mu_{01} = \mu_0[1 - 2/z_0]$	0·73
$\mu_{02} = \epsilon_0/2a[1 + 5\,\bar{\alpha}r/_0^3]$	$\mu_{02} = \mu_0[1 - 3/z_0 + 1/z_0^2]$	0·48
$\mu_{03} = \epsilon_0{}'3a[1+19{}'2\,\bar{\alpha}/r_0^3]$	$\mu_{03} = \mu_0[1 - 11/3\,z_0 + 2/z_0^2]$	0·34
$\mu_{04} = \epsilon_0{}'4a[1 + 16\,\bar{\alpha}/r_0^3]$	$\mu_{04} = \mu_0[1 - 25/6\,z_0 + 35/12\,z_0^2]$	0·29
$\mu_{05} = \epsilon_0\,5a[1 + 25\,\bar{\alpha}/r_0^3]$	$\mu_{05} = \mu_0[1 - 137/30\,z_0 + 15/4\,z_0^2)$	—
$\mu_{06} = \epsilon_0\,6a[1 + 38\,\bar{\alpha}/r_0^3]$	$\mu_{06} = \mu_0[1 - 49/10\,z_0 + 208/45\,z_0^2)$	—
I	II	III

Moments of transition μ_{0v}.

I. Constant effective charge ϵ_0 and constant polarization $\bar{\alpha}$; $z_0 = ar_0 = 2$.
II. Variable effective charge $\epsilon = \epsilon_0 y$, polarization $\alpha = \alpha_0(r/r_0)^4$.
III. Observed values for phenol in CCl_4, $Z_0 \sim 4{\cdot}6$.

$$\epsilon = \epsilon_0 e^{-a(r-r_0)} \quad . \quad . \quad . \quad . \quad . \quad (10)$$

Furthermore, if we assume the difference of polarizability to increase as r^4—and there are theoretical arguments for this assumption—we obtain the following results:

(i) From the electric bond energy of a dipole of this type we immediately get Morse's potential function.[16]

$$E_{\text{pot}} = -D_0 + \frac{e^2(\bar{\alpha}_1 + \bar{\alpha}_2)}{2r_0^4}(1 - y)^2. \quad . \quad . \quad . \quad (11)$$

As an empirical function it correctly gives the observed series of eigenvalues but had no theoretical foundation at all up till now.

(ii) Furthermore, we likewise obtain a relation which Morse [16] had proposed empirically ($\nu_0 r^3$ rule) and which has successfully been used to estimate nuclear distances from frequencies. Again, in this case there was no theoretical explanation. Now we find:

$$\nu_0 r_0^3\sqrt{\bar{m}} = 3500\sqrt{\bar{P}\left(\frac{\nu_0 x}{4B_0}\right)}, \quad . \quad . \quad . \quad . \quad (12)$$

where ν_0 is measured in cm.$^{-1}$, r_0 in 10^{-8} cm., $\bar{P}$ as mean atom refraction of both vibrating atoms in cm.^{3} and $\bar{m}$ is the reduced mass of the bond, B_0 is the constant of rotation, $B_0 = h/8\pi^2 cI$, the ratio $\nu_0 x/4B_0 \sim 1$ being nearly constant.

(iii) For the curve of the dipole moment of our bond we get a function of the type z^2e^{-z}, where $z = a(r + r_m)$. Hence the dipole moment vanishes for $z = 0$ (the case of joined nuclei $r_H = -r_m$), it reaches a

TABLE V.—EXPERIMENTAL

Type of Compound	Molecule and Structure	ν_0 cm.$^{-1}$	r_0[e] Å	k	D_0 kcal./mole bond
Strong polar XH *bonds*					
OH *and* ClH *Bonds*					
Water[g]	H_2O	3850	0·956	55	151
Methyl alcohol[g]	CH_3OH	3813	0·92	44·3	121
Phenol[g]	C_6H_5OH	3780	0·96	44·5	102
Hydrogen chloride[g]	HCl	2990	1·28	56	120
Unsaturated CH *Bonds*					
Hyperaromatic					
Furanal[h]	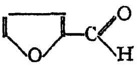	3197	1·07	52·4	120
Aromatic and Related					
Benzene[f]	C_6H_6	3180	1·08[b]	50·5	115
Toluene[f]	$C_6H_5CH_3$	3166	1·08	51	115
Phenol[g]	C_6H_5OH	3170	1·08	56·6	124
Dibenzyl ether[h]	$(C_6H_5)_2O$	3200	1·07	46·4	106
p-Dibromobenzene[f]	$C_6H_4Br_2$	3201	1·09[b]	50	114
Pyridine[h]	C_5H_5N	3205	1·07	49·3	113
Olefinic					
Cyclo-octatetrene[g]	C_8H_8	3128	1·07[c]	48·8	109
Saturated CH *Bonds*					
Ketones, Aldehydes (*normal mode*), *Acids*					
Acetone[h]	$(CH_3)_2CO$	3110	1·09	47·8	106
Acetaldehyde[h]	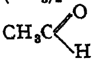 $CH_3C\genfrac{}{}{0pt}{}{O}{H}$	3104	1·09	48·5	108
Acetic acid[h]	CH_3COOH	3120	1·08	48·8	109
Ethers					
Diethyl ether[h]	$(CH_3HCH)_2O$	3093	1·06	52·4	116
Diethyl ether[h] (vapour)	$(CH_3HCH)_2O$	3070	1·06	50·6	111
Tetrahydrofuran[h]	C_4H_8O	3117	1·08	43·9	98
1 : 4-Dimethyltetrahydrofuran[h]	$(CH_3)_2C_4H_6O$	3117	1·08	43·9	98
Trioxan[h]	$(HCHO)_3$	3108	1·06[d]	57·6	128
Paraldehyde[h]	$(CH_3CHO)_3$	3140	1·08	44·9	96
Alcohols					
Methyl alcohol[g]	CH_3OH	3085	1·09[c]	43	94
Hydrocarbons					
Cyclohexane[h]	C_6H_{12}	3045	1·10	46·8	102
Hexamethylethane[h]	$(CH_3)_6C_2$	3134	1·08	40·7	91
Toluene[f]	$CH_3C_6H_5$	3070	1·09[c]	46·5	102
Ethers, perturbed mode					
Diethylether[h]	$(CH_3HCH)_2O$	2958	1·06	47·7	101
Diethylether[h] (vapour)	$(CH_3HCH)_2O$	2930	1·06	53·3	111
Trioxan[h]	$(HCHO)_3$	2998	1·06[d]	38·0	81
Paraldehyde[h]	$(CH_3CHO)_3$	3093	1·06	40·7	90
Aldehydes, perturbed mode					
Furanol[h]	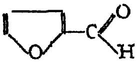	2865	1·08	47·7	98
Acetaldehyde[h]	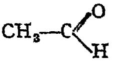 $CH_3{-}C\genfrac{}{}{0pt}{}{O}{H}$	2921	1·08	41·2	86
Polyhalogen compounds					
Non-aromatic CH *Bonds*					
Chloroform[f]	$CHCl_3$	3146	1·11	50	112
Trichloroethylene[f]	C_2HCl_3	3200	1·08	53·5	122
Hexachloro-cyclohexane[h]	$C_6H_6Cl_6$	3117	1·08	47·8	107

[a] Extrapolated values.

[b] D'Ans-Lax, *Taschenbuch, für Chemiker und Physiker* (Berlin, 1943).

[c] Herzberg, *Polyatomic Molecules* (New York, 1947), gives the values $r_0 = 1{\cdot}093$ for C—CH$_3$, $r_0 = 1{\cdot}07$ for C$=$CH$_2$ from infra-red measurements.

[d] Carpenter (*J. Amer. Chem. Soc.*, 1936, **58**, 1274) gives the value $r_0 = 1{\cdot}06$ for paraldehyde (from electron diffraction) and metaldehyde (from X-ray scattering).

TRANSITION MOMENTS

ar_0	$\frac{P_1+P_2}{2}$ cm³/mole bond	$\pm\mu_{01}$ D	$\pm\mu_{02}$ D	$\pm\mu_{03}$ D	$\pm\mu_{04}$ D	$\pm\mu_{05}$ D	$\pm\mu_{06}$ D	$\pm\mu_0$ D
1·90	0·99	1·2	0·45	0·21	0·16	—	—	1·52[a]
2·02	0·67	—	0·45	0·30	0·23	—	—	1·2
2·10	0·88	0·89	0·58	0·41	0·35	—	—	1·3
2·23	2·40	0·47	0·24	—	—	—	—	1·03
1·98	1·22	—	0·24	0·24	0·23	—	—	0·26
2·01	1·22	--	0·20	0·26	0·24	0·23	0·22	0·29
2·01	1·20	—	23	28	26	24	23	25
1·93	1·21	0·21	24	28	26	25	—	23
2·11	1·24	—	—	29	24	—	—	46
2·02	1·31	—	23	24	23	—	—	23
2·03	1·24	—	24	28	24	—	—	43
2·02	1·14	—	26	29	25	20	(11)	42
2·08	1·26	-	15	20	18	—	—	27
2·06	1·26	—	—	21	18	—	—	30
2·04	1·18	—	—	23	23	—	—	23
1·93	1·02	—	18	30	25	—	—	46
1·95	1·01	—	14	23	21	—	—	30
2·15	1·20	—	16	26	21	16	—	42
2·15	1·20	—	15	24	15	11	—	43
1·84	1·00	—	24	36	35	40	—	32
2·14	1·21	—	19	18	17	—	—	22
2·00	1·22	—	20	46	43	36	—	(60)
2·09	1·28	—	18	30	27	22	19	43
2·25	1·23	—	12	19	16	—	—	29
2·07	1·21	—	12	15	13	10	—	23
1·70	0·93	—	17	27	22	—	—	47
1·70	0·93	—	17	28	25	—	—	36
2·23	0·99	—	16	18	13	11	—	36
2·20	1·01	—	18	22	17	—	—	40
1·98	0·87	—	22	32	32	—	—	29
2·15	0·92	—	(13)	33	27	—	—	(50)
2·07	1·44	—	37	32	24	18	—	52
1·98	1·24	—	30	27	27	26	—	30
2·13	1·18	—	21	20	—	—	—	(24)

[a] Unless otherwise mentioned, calculated from values of related molecules by Morse's equation $r_0^3\nu_0 = \text{const.}$

[f] Mecke and Kempter, *Z. Naturforsch.*, 1947, 2*a*, 549.

[g] Oswald, *Diss.* (Freiburg, 1950).

[h] Lippert, *Diss.* (Freiburg, 1950).

maximum at $z = 2$ and approaches asymptotically the value 0 again for $z = \infty$. Furthermore, the derivatives are

$$\mu^{(n)} = \mu_0[(z_0 - n)^2 - n]/z_0^2. \qquad (13)$$

A thorough discussion of the data obtained so far now shows us that the transition moment calculated according to this formula (12, case II) shows very good agreement with the results obtained. For phenol one obtains $z_0 = 4{\cdot}6$ (i.e. an effective length of the dipole, $d_0 = 2{\cdot}3\, r_0$).* The dipole moment of the OH band using this value is 1·1 D. This means that the effective charge, calculated as a dipole moment $\mu = \epsilon d$, would be $\epsilon \sim 0{\cdot}1e$. But it is better, however, to assume here an induced moment and then from $\bar{\alpha} = \mu_0 d_0^2/e$ one obtains a mean polarizability of

$$\bar{\alpha} \sim 1{\cdot}1 \times 10^{-24}\ \text{cm}^3.$$

Further results are given in Table V and Fig. 13.

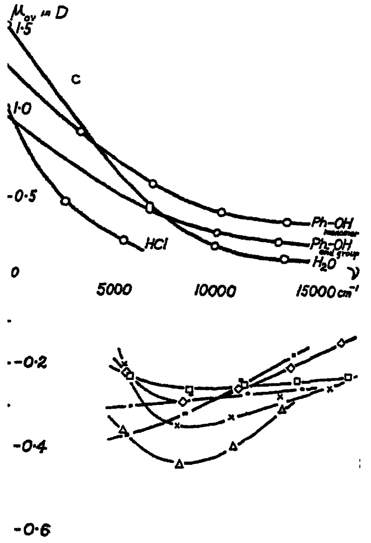

FIG. 13.—Reduced transition moments of CH and OH bands.

□ Benzene and derivatives.
● Trichloroethylene.
◇ Cyclo-octatetraene.
■ Chloroform.
× Cyclohexane.
△ Toluene (CH_3).

From these facts we conclude that:

(i) The function z^2e^{-z} has the character we expect for the variation of the dipole moment of a covalent band with nuclear distance.

(ii) In all cases investigated † the effective length of the vibrating dipole seems to be greater than the nuclear distance at its equilibrium position ($r > r_0$) and

(iii) therefore the moment μ_0 at the equilibrium position is on the falling branch of the dipole curve ($z_0 > 2$) and, furthermore, in that part which is convex to the r axis ($z_0 > 3{\cdot}41$).

If we now observe a decrease of the vibration frequency on account of interaction together with an increase of the bond length, these result from the fact that the binding moment is lowered and, because of this,

---

* The contribution of the induced moment is $\mu_i = \mu_0\ (r_0/d_0)^2$, of the polar moment,

$$\mu_p = \mu_0[1 - (r_0/d_0)^2].$$

† As regards the CH band there is a possible second solution of $z_0 \sim 1{\cdot}7$ ($d = 0{\cdot}85\, r_0$). The question will be settled as soon as the fundamental band at 3μ is remeasured.

the intensity of the absorption band also. As regards the sign of the dipole moment, absorption measurements alone can never give any information. But for the hydroxyl bond we can without hesitation assume the hydrogen atom is positively charged. For the CH bond there are some indications that a change of sign has taken place, i.e. that the hydrogen carries the negative charge.

Physikalisch-chemisches Institut der Universität,
Freiburg i. Br.

INFRA-RED AND RAMAN SPECTRA OF 1:3:5-TRIFLUOROBENZENE *

By J. Rud Nielsen, Ching-yu Liang and D. C. Smith

Received 10*th July*, 1950

The infra-red spectrum of 1 : 3 : 5-trifluorobenzene in the gaseous and liquid states has been investigated between 2 and 22·5 μ by means of a prism spectrometer of high resolution. The Raman spectrum of the liquid has been studied with a three-prism glass spectrograph of linear dispersion 15 Å/mm. at 4358 Å. The 17 fundamental vibration frequencies that are active in infra-red absorption or in the Raman effect have been assigned and tentative values given for two of the three inactive fundamentals. The observed spectra have been interpreted in detail.

An attempt to determine the fundamental vibration frequencies for a number of fluorinated aromatics has recently been made by R. L. Hudson.[1] Because of the low molecular symmetry of these compounds the assignments were incomplete and in part uncertain. A short time ago a sample of 1 : 3 : 5-trifluorobenzene became available, and an investigation of its vibration spectra was undertaken in the hope that a complete assignment of fundamentals could be made for this compound and data obtained that could be used to check and extend Hudson's assignments.

No previous spectroscopic study has been made of 1 : 3 : 5-trifluorobenzene. However, the work of Dadieu, Kohlrausch and Pongratz on the corresponding chlorobenzene and mesitylene,[2] the mechanical model data of Murray, Dietz and Andrews,[3] the work of Langseth and Lord on deuterated benzenes,[4] and especially the detailed study made by Ingold *et al.* of 1 : 3 : 5-trideuterobenzene,[5] have provided some guidance in the present work.

Experimental

The sample of 1 : 3 : 5-trifluorobenzene (b.p. 75·5° C) was prepared and purified by G. C. Finger, F. H. Reed and J. L. Finnerty of the Illinois Geological

---

* This work has been supported by the U.S. Office of Naval Research under Contract N7onr-398, T.O.I.

[1] *Naval Research Laboratory Report 3567* (" Spectroscopic Properties of Fluorocarbons and Fluorinated Hydrocarbons "), Washington, D.C., 1949.

[2] Dadieu, Kohlrausch and Pongratz, *Akad. Wiss. Wien, Ber.*, 1932, **141**, 747 ; *Monatsh.*, 1932, **60**, 426. Kohlrausch and Pongratz, *Akad. Wiss. Wien, Ber.*, 1934, **143**, 358 ; *Monatsh.*, 1934, **64**, 374. Kohlrausch, *Physik. Z.*, 1936, **37**, 58.

[3] Murray, Dietz and Andrews, *J. Chem. Physics*, 1935, **3**, 180.

[4] Langseth and Lord, *Kgl. Danske Vid. Selsk., Math.-fys. Medd.*, 1938, **16**, 6.

[5] Bailey, Ingold, Poole and Wilson, *J. Chem. Soc.*, 1946, **149**, 222. Bailey, Hale, Herzfeld, Ingold, Leckie and Poole, *ibid.*, 1946, **149**, 255.

Survey.[b] No information was available about its purity However, the spectra showed no trace of any of the other fluorinated aromatics for which spectral data have been obtained [1]

The infra-red spectrum of the compound, in both the gaseous and the liquid state, was measured over the range from 2 to 22·5 μ by means of a prism spectrometer of high resolution [6] The Raman spectrum of the liquid was photographed with a high-speed three-prism glass spectrograph, briefly described elsewhere,[7] of linear dispersion 15 Å/mm at 4358 Å. The irradiation apparatus [8] employed two high-current low-pressure mercury lamps with internally water-cooled electrode ends of the kind developed by Welsh and Crawford at the University of Toronto [9] Polarization measurements were made with an apparatus similar to that described by Crawford and Horwitz [10]

Results

The infra-red absorption spectrum of gaseous 1 : 3 5-trifluorobenzene is shown in Fig 1. The cell length was 10 cm The pressure in mm Hg is shown for each percentage transmittance curve Fig 2 shows the infra-red spectrum

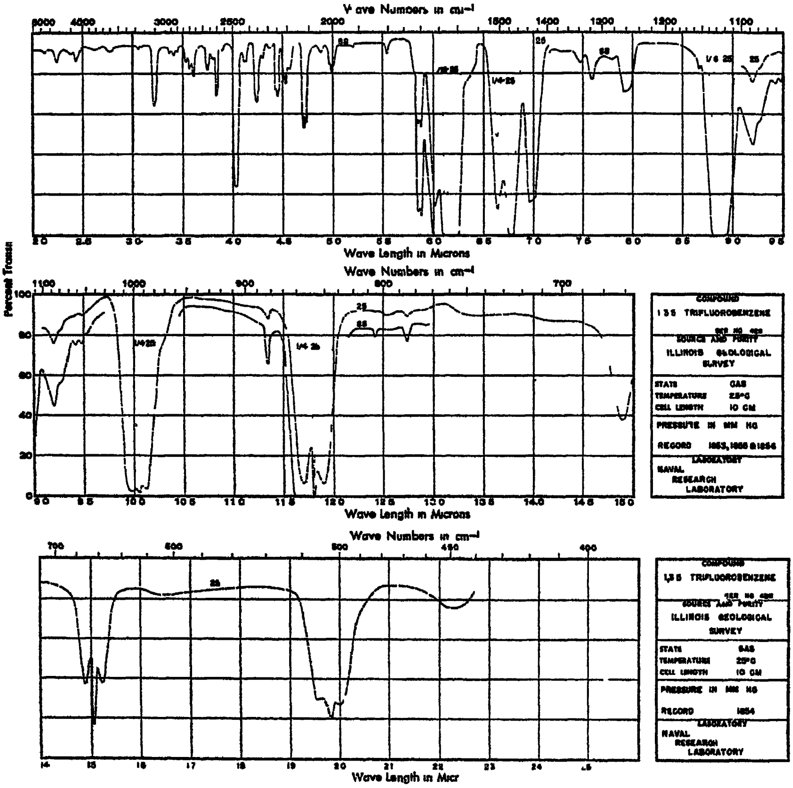

FIG. 1.—Infra-red spectrum of gaseous 1 . 3 : 5-trifluorobenzene.

---

* Reported at the meeting of the *American Chemical Society* held at Philadelphia, 10th to 13th April, 1950.

[6] Nielsen, Crawford and Smith, *J. Opt. Soc Amer.*, 1947, **37**, 296.

[7] Smith, Nielsen and Claassen, *J. Chem. Physics*, 1950, **18**, 326.

[8] Nielsen, Claassen and Smith, *ibid.*, 1950, **18**, 485.

[9] See Rank, Sheppard and Szasz, *J. Opt. Soc. Amer.*, 1948, **16**, 698.

[10] Crawford and Horwitz, *J. Chem. Physics*, 1947, **15**, 882.

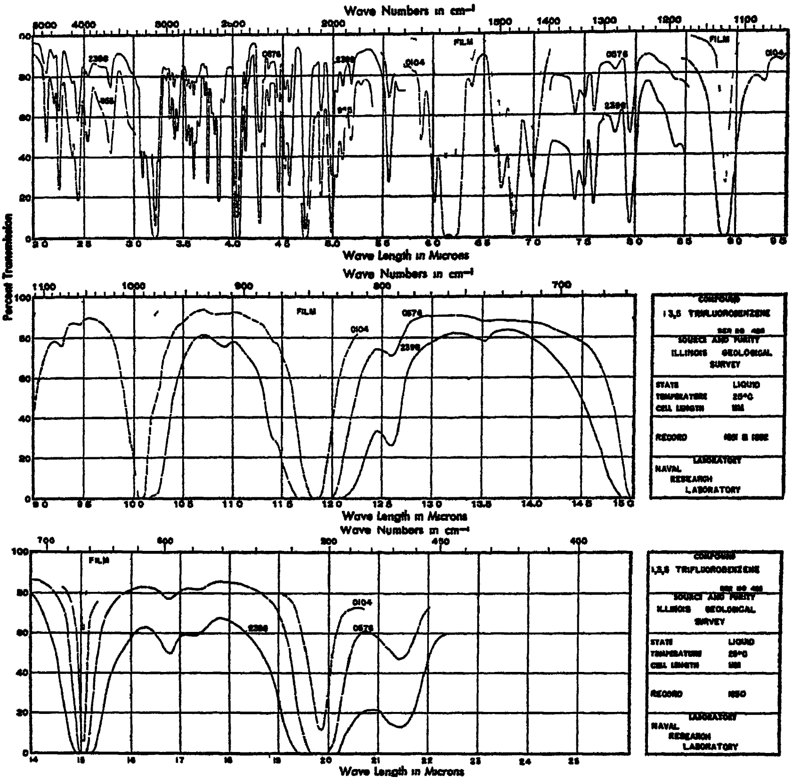

FIG 2 —Infra-red spectrum of liquid 1 : 3 : 5-trifluorobenzene.

TABLE I —INFRA-RED SPECTRUM OF 1 : 3 : 5-TRIFLUOROBENZENE

Gas		Liquid		Interpretation
Wave Number cm⁻¹	Description	Wave Number cm⁻¹	Description	
448	vw	—	—	—
—	—	467	w	214+253=467 (E')
500 505 511	s s s	— 504 —	— s —	E' fundamental
—	—	575	vvw	253+326=579 ($A_1''+A_2''+E''$)
605	vvwd	595	vw	E'' fundamental ; 845−253=592 (E')
657 664 671	s	665	s	A_2'' fundamental
—	—	741	vvw	993−253=740 ($A_1''+A_2''+E''$) , 253+503=756($A_1''+A_2''+E''$)
785	vvw	794	vw	214+578=792 (A_2'')
805	vvw	—	—	214+595=809 (E')
840 847 855	vs	845	vs	A_2'' fundamental

TABLE I—*contd.*

Gas		Liquid		Interpretation
Wave Number cm $^{-1}$	Description	Wave Number cm $^{-1}$	Description	
882	*vw*	875	*vvw*	$1471-595=876\ (A_1''+A_2''+E'')$
—	—	916	*vvw*	$253+665=918\ (E')$, $326+595=921\ (A_1''+A_2''+E'')$
989 995 1001	*vs*	993	*vs*	E' fundamental
1055	*vw*	—	—	—
—	—	1058	*vvvw*	—
1062	*vw*	—	—	—
1087	*w*	1078	*vw*	$503+578=1081\ (E')$
1122 1131	*vs*	1124	*vs*	E' fundamental
1155	*vvw*	—	—	—
—	—	1192	*vvw*	$2\times 595=1190\ (A_1'+E')$
—	—	1215	*vvvw*	$1471-253=1218\ (A_1''+\mathrm{A}_2''+E'')$; $214+1010=1224\ (A_2'')$
1264	*vw*	1258	*m*	$595+665=1260\ (E')$
1284	*vvw*	1282	*vvw*	$1610-326=1286\ (A_1'+A_2'+E')$
1318	*vw*	1316	*m*	$326+993=1319\ (A_1'+A_2'+E')$
1337	*vvw*	1333	*vw*	$326+1010=1336\ (E')$
—	—	1350	*w*	A_1' fundamental
1437	*s*	1431	*m*	$595+845=1440\ (E')$; $578+845=1423\ (A_2'')$; $253+1191=1444\ (A_1'+A_2'+E')$
1473	*vs*	1471	*s*	E' fundamental
1506	*s*	1497	*m*	$503+993=1496\ (A_1'+A_2'+E')$
—	—	1508	*w*	$503+1010=1513\ (E')$; $326+1191=1517\ (A_1''+A_2''+E'')$
—	—	1565	*vw*	$214+1350=1564\ (A_2'')$; $578+993=1571\ (E')$
1618	*vs*	1610	*vs*	E' fundamental ;
1631	*vvs*	1631	*vs*	$[326+1300=1626\ (E')]$,
1637	*vs*	—	—	$503+1123=1626\ (A_1'+A_2'+E')$
1664	*vw*	1661	*m*	$326+1350=1676\ (E')$; $665+1010=1675\ (A_2'')$
1701	*m*	1701	*w*	$578+1123=1701\ (E')$,
1709	*m*	—	—	$503+1191=1694\ (A_1''+A_2''+E'')$
1720	*vvvw*	—	—	$253+1471=1724\ (A_1''+A_2''+E'')$
1802	*vvw*	1799	*vw*	$326+1471=1797\ (A_1'+A_2'+E')$
—	—	1894	*vvw*	$253+1631=1884\ (A_1''+A_2''+E'')$
1923	*vvvw*	1931	*vvw*	$326+1610=1936\ (A_1'+A_2'+E')$
—	—	1961	*vvw*	$326+1631=1957\ (A_1'+A_2'+E')$
—	—	1984	*vvw*	$2\times 993=1986\ (A_1'+E')$
1996	*vvw*	—	—	—
2004	*vw*	2004	*vw*	$993+1010=2003\ (E')$
2012	*vvw*	—	—	$665+1350=2015\ (A_2'')$
2049	*vvw*	2049	*vvw*	$578+1471=2049\ (E')$
—	—	2070	*vvvw*	$595+1471=2066\ (A_1''+A_2''+E'')$
2114	*w*	2114	*w*	$993+1123=2116\ (A_1'+A_2'+E')$
2123	*w*	—	—	—
2188	*vw*	2188	*vw*	$578+1610=2188\ (E')$; $993+1191=2184\ (A_1''+A_2''+E'')$; $845+1350=2195\ (A_2'')$
2208	*vw*	2208	*vw*	$578+1631=2209\ (\mathrm{E}')$; $595+1610=2205\ (A_1''+A_2''+E'')$
2247	*vw*	2242	*vw*	$2\times 1123=2246\ (A'+E')$
2294	*vvvw*	2294	*vvvw*	$[993+1300=2293\ (E')]$

TABLE I—*contd.*

Gas		Liquid		Interpretation
Wave Number cm.$^{-1}$	Description	Wave Number cm.$^{-1}$	Description	
2326	*vvvw*	2315	*vvvw*	$326+1010=2326\ (E')$
2353	*vw*	2342	*w*	$993+1350=2343\ (E')$
2421	*vvw*	2421	*vvvw*	$[1123+1300=2423\ (E')]$
2427	*vvw*	—	—	—
2481	*m*	2469	*w*	$326+1350=2472\ (E')$; $993+1471=2464\ (A_1'+A_2'+E')$
2564	*vvvw*	2558	*vvvw*	—
2604	*vw*	2591	*vw*	$1123+1471=2594\ (A_1'+A'_2+E')$
2625	*vvvw*	2618	*vvw*	$1010+1610=2620\ (E')$; $993+1631=2624\ (A_1'+A_2'+E')$
2639	*vvvw*	2639	*vvvw*	$1010+1631=2641\ (E')$
2667	*vvw*	2667	*vw*	$1191+1471=2662\ (A_1''+A_2''+E'')$
—	—	2688	*vvvw*	$578+1123=2701\ (E')$?
—	—	2732	*vvvw*	$1123+1610=2733\ (A_1'+A_2'+E')$
	—	2755	*vvvw*	$1123+1631=2754\ (A_1'+A_2'+E')$
2770	*vw*	2770	*vw*	$[1471+1300=2771\ (E')]$
2801	*vvw*	2801	*vvw*	$1191+1610=2801\ (A_1''+A_2''+E'')$
2833	*vvvw*	2825	*vvw*	$1350+1471=2821\ (E')$; $1191+1631=2822\ (A_1''+A_2''+E'')$
2899	*vvvw*	2907	*vvw*	$[1610+1300=2910\ (E')]$
2924	*vvvw*	2933	*vvw*	$2\times1471=2942\ (A_1'+E')$
2967	*vvvw*	2967	*vvw*	$1350+1610=2960\ (E')$; $1350+1631=2981\ (E')$
—	—	3003	*vvw*	$[1471+1540=3011\ (E')]$
3115	*vw*	3106	*m*	E' fundamental
—	—	3205	*vvvw*	$2\times1610=3220\ (A_1'+E')$
3236	*vvvw*	3236	*vw*	$1610+1631=3241\ (A_1'+A_2'+E'$
3268	*vvvw*	3257	*vvvw*	$2\times1631=3262\ (A_1'+E')$
3610	*vvvw*	3610	*vvvw*	$503+3111=3614\ (A_1'+A_2'+E')$
3802	*vvvw*	—	—	—
—	—	3937	*vvvw*	$845+3092=3937\ (A_2'')$, $845+3071=3916\ (A_2'')$
4115	*vvvw*	4098	*vw*	$993+3111=4104\ (A_1'+A_2'+E')$; $1010+3111=4121\ (E')$
4202	*vvvw*	4184	*vvvw*	$1123+3071=4194\ (E')$; $1123+3092=4215\ (E')$
4464	*vvw*	4444	*vw*	$1350+3111=4461\ (E')$
—	—	4545	*vvw*	$1471+3071=4542\ (E')$; $1471+3092=4563\ (E')$
4539	*vvvw*	4717	*vvw*	$1631+3092=4723\ (E')$; $1631+3071=4702\ (E')$

TABLE II.—RAMAN SPECTRUM OF 1 : 3 : 5-TRIFLUOROBENZENE (LIQUID)

Wave Number cm.$^{-1}$	Description	Exciting Hg Lines	Deplorization Ratio	Interpretation
253·4	*vs d*	$\underline{e}$, *k*, *i*	0·85	E'' fundamental
326·0	*w*	$\underline{e}$, *k*	0·87	E' fundamental
465	*vw*	*e*	—	$214+253=467\ (E')$
502·3	*s*	*e*, *k*, *i*	0·85	E' fundamental
577·6	*vs sh*	$\underline{e}$, *f*, *k*, *i*, *d*	0·04	A_1' fundamental
594·6	*s*	$\underline{e}$, *k*, *i*, *d*	0·83	E'' fundamental
652	*vvw*	*e*	—	$2\times326=652\ (A_1'+E')$
666	*vvw*	*e*	—	A_2'' fundamental

TABLE II—*contd.*

Wave Number cm.$^{-1}$	Description	Exciting Hg Lines	Deplorization Ratio	Interpretation
806	*vvw d*	*e, k*	—	214+595=809 (E')
829	*vw d*	*e, k*	—	253+578=831 (E'') ; 326+503=829 ($A_1'+A_2'+E'$)
847	*vw d*	*e, k, i*	*p* ?	253+595=848 ($A_1'+A_2'+E'$)
993	*m*	*e, k, d*	~ 0·7	E' fundamental
1010·0	*vs sh*	*e, f, g, k, i, l, d*	0·02	A_1' fundamental
1053	*vvw*	*e, k*	—	214+845=1059 (A_1')
1079	*vvw*	*e, k*	—	503+578=1081 (E')
1121·8	*s*	*e, k, i, l*	0·85	E' fundamental
1191	*w*	*e*	*p* ?	E'' fundamental ; 2×595=1190 ($A_1'+E'$)
1247	*vvvw*	*e*	—	253+993=1246 ($A_1''+A_2''+E''$)
1336	*vw*	*k*	—	214+1123=1336 (E'') ; 326+1010=1336 (E') ; 2×665=1330 (A_1')
1350	*s*	*e, k, i, l*	0·04	A_1' fundamental
1441	*vvw*	*e*	—	595+845=1440 (E') ; 253+1191=1444 ($A_1'+A_2'+E'$) ; 326+1123=1449 ($A_1'+A_2'+E'$)
1471	*vw*	*e*	~0·7	E' fundamental
1609	*m*	*e*	0·89	E' fundamental ; [326+1300=1626 (E')] ; 503+1123=1626 ($A_1'+A_2'+E'$)
1631	*m*	*e*	0·82	
1662	*vw*	*e*	~0·5	665+993=1658 (E'')
1696	*vvw*	*e*	—	2×845=1690 (A_1') ; 503+1191=1694 ($A_1''+A_2''+E''$)
1833	*vvw*	*e*	—	845+993=1838 (E'')
1854	*vvw*	*e*	—	503+1350=1853 (E') ; 665+1191=1856 (E')
1867	*vvw*	*e*	—	253+1610=1863 ($A_1''+A_2''+E''$)
1924	*vvw*	*e*	—	578+1350=1928 (A_1')
1941	*vvvw*	*e*	—	595+1350=1945 (E'')
1962	*vvvw*	*e*	—	845+1123=1968 (E'')
1981	*vvvw*	*e*	—	2×993=1986 ($A_1'+E'$)
2096	*vvvw*	*e*	—	—
2115	*vvvw*	*e*	—	993+1123=2116 ($A_1'+A_2'+E'$)
2137	*vvvw*	*e*	—	665+1471=2136 (E'') ; 1010+1123=2133 (E')
2308	*vvvw*	*e*	—	845+1471=2316 (E'') ; 1123+1191=2314 ($A_1''+A_2''+E''$)
2347	*vvvw*	*e*	—	993+1350=2343 (E')
2389	*vw*	*e, k*	—	2×1191=2382 ($A_1'+E'$)
2500	*vw*	*k*	—	[1191+1300=2491 (E'')]
2528	*vw*	*k*	—	[993+1540=2533 (E')]
2628	*vw sh*	*k*	—	[2×1300=2600 (A_1')] ; 993+1631=2624 ($A_1'+A_2'+E'$)
2664	*vvw*	*k*	—	1191+1471=2662 ($A_1''+A_2''+E''$)
2704	*vw sh*	*k*	—	2×1350=2700 (A_1') ; 578+1123=2701 (E')
3071	*m*	*e, k, i, q*	0·2	A_1' fundamental ; [2×1540=3080 (A_1')] ; 1610+1471=3081 ($A_1'+A_2'+E'$) ?
3092	*m*	*e, k, i, q*	0·3	
3111	*s*	*e, i, q, o, p*	0·4*	E' fundamental
3213	*vvw*	*e*	—	2×1610=3220 ($A_1'+E'$)
3232	*vvw*	*e*	—	1610+1631=3241 ($A_1'+A_2'+E'$)
3256	*vvvw*	*e*	—	2×1631=3262 ($A_1'+E'$)
3620	*vw sh*	*e*	—	503+3111=3614 ($A_1'+A_2'+E'$)

* This low value may be caused by overlapping with the polarized bands at 3071 and 3093 cm.$^{-1}$ and with the Rayleigh scattered mercury line at 5045·82 Å.

of the liquid. The number adjacent to each curve indicates the cell thickness in mm. The wave numbers of the observed absorption maxima are listed in the first and third columns of Table I. In the second and fourth columns the relative intensities are indicated by means of the following abbreviations: *vs* very strong, *s* strong, *m* medium, *w* weak, *vw* very weak, etc.

The observed Raman shifts for liquid 1 : 3 : 5-trifluorobenzene are listed in the first column of Table II. In the second column, under the heading "Description", the relative intensities are indicated; for some bands exceptional sharpness or diffuseness are indicated by *sh* or *d* respectively. The exciting mercury lines are given, in Kohlrausch's letter symbols,[11] in the third column. Underlining indicates that an anti-Stokes as well as a Stokes shift has been observed. In the fourth column are listed the depolarization ratios obtained for the stronger Raman bands.

Discussion

Assignment of Fundamentals.—The molecule of 1:3:5-trifluorobenzene undoubtedly has the symmetry D_{3h}. The normal vibrations therefore divide themselves into symmetry species in the following manner: $4A_1' + 3A_2' + 3A_2'' + 7E' + 3E''$. The vibrations of species A_1', E' and E'' are Raman-active, those of species A_1' giving rise to polarized and the others to depolarized Raman bands. The vibrations of species A_2'' and E' are infra-red active, the former giving rise to parallel and the latter to perpendicular bands. Since the molecule is a plane symmetrical top, the separation between the maxima of the rotational branches for the perpendicular infra-red bands should be approximately two-thirds of the corresponding separation for the parallel bands.[12] The three vibrations of species A_2' are inactive as well in infra-red absorption as in the Raman effect.

SPECIES A_1'.—The intense polarized Raman bands at 577·6, 1010·0 and 1350 cm.$^{-1}$ certainly represent totally symmetrical fundamentals. The first may be characterized roughly as a "breathing vibration", the second as a trigonal deformation of the aromatic ring, and the third as a C—F stretching mode. The fourth A_1' fundamental, a symmetrical C—H stretching, should lie somewhat above 3000 cm.$^{-1}$. Three Raman bands with measured depolarization ratio below 6/7 have been observed in this region, at 3071, 3092 and 3111 cm.$^{-1}$. The first two are certainly polarized. The low value obtained for the depolarization ratio of the third is probably caused by overlapping with the polarized bands and with the Rayleigh-scattered mercury line at 5045·8 Å. Thus, the conclusion seems inescapable that the bands at 3071 and 3092 cm.$^{-1}$ represent the remaining A_1' fundamental coupled with an overtone or a combination band of the same species. The identity of the latter will be discussed below. Since the band at 3092 is more intense than that at 3071 cm.$^{-1}$, it undoubtedly lies closer to the unperturbed value of the A_1' fundamental.

SPECIES E''.—The lowest E'' fundamental must be represented either by the very strong Raman band at 253·4 cm.$^{-1}$ or by the weak band at 326·0 cm.$^{-1}$, both of which are depolarized. A consideration of combination bands favours the former assignment which is tentatively adopted. It is hoped to check this assignment by observation of 326 cm.$^{-1}$ with KRS-5 prism. The strong depolarized Raman band at 594·6 cm.$^{-1}$ must be the intermediate E'' fundamental. The very weak infra-red absorption band occurring at this place in the liquid may result from a weakening of the selection rules by intermolecular forces or may be interpreted as a difference band, $845 - 253 = 592$ (E').

Some difficulty was experienced in assigning the highest E'' fundamental. The Raman band at 829 cm.$^{-1}$, which has no counterpart in the infra-red, can readily be interpreted as a combination band. Other possibilities were similarly eliminated, and it was finally concluded that, unless the E'' fundamental is masked by one of the strong bands at 993,

---

[11] Kohlrausch, *Der Smekal-Raman-Effekt* (Julius Springer, Berlin, 1931).

[12] Gerhard and Dennison, *Physic. Rev.*, 1933, 43, 197.

1010 or 1123 cm.$^{-1}$, it must be represented by the weak Raman band at 1191 cm.$^{-1}$ of uncertain polarization. This is a higher value than expected, and the band could be interpreted as an overtone, 2×595 $(A_1' + E')$. On the other hand, the assumption that 1191 cm.$^{-1}$ is an E'' fundamental leads to satisfactory interpretations of the very weak Raman bands at 2389 and 2664 cm.$^{-1}$ and of the infra-red bands at 2667 and 1801 cm.$^{-1}$, as well as to alternative interpretations of other bands. This assignment is therefore adopted tentatively. It is hoped to check it by normal co-ordinate analysis.

The vibrations of this species are at right angles to the plane of the molecule. The lowest E'' fundamental may roughly be designated as a ring deformation, the intermediate as a C—F wagging, and the highest as a C—H wagging mode.

SPECIES E'.—These planar vibrations are active in both spectra. If the Raman band at 253 cm.$^{-1}$ has been correctly assigned as the lowest E'' fundamental, the weak depolarized Raman band at 326·0 cm.$^{-1}$ must be the lowest fundamental of species E'. It may be characterised as a planar ring deformation.* The strong depolarized Raman band at 502·3 cm.$^{-1}$, and the strong infra-red band observed at 504 cm.$^{-1}$ (in the liquid state), evidently also represent an E' fundamental. It may be roughly characterized as an unsymmetrical C—F bending in the plane of the molecule. The medium Raman band and very strong infra-red band at 993 cm.$^{-1}$ must also be a fundamental of species E'. The rather low depolarization ratio observed is undoubtedly caused by the proximity to the very strong polarized Raman band at 1010 cm.$^{-1}$, and perhaps also by overlapping with the overtone 2×503 $(A_1' + E')$.

The very strong infra-red band at 1124 cm.$^{-1}$ and the strong depolarized Raman band observed at 1121·8 cm.$^{-1}$ certainly represent an E' fundamental. The contour of the infra-red band in the spectrum of the gas is abnormal and indicates failure to observe the zero branch. The infra-red and Raman bands at 1471 cm.$^{-1}$ must also be assigned as an E' fundamental. Its low intensity in the Raman effect is in accord with the finding that Raman bands associated with vibrations involving largely C—F stretching are usually very weak.[1] The rather low value observed for the depolarization ratio may result from partial overlapping with 3071 cm.$^{-1}$ excited by the mercury line 4077·7 Å, as well as from the high experimental error in measuring the polarization of so weak Raman bands.

The doublet occurring at 1610 and 1631 cm.$^{-1}$ in both spectra of liquid 1 : 3 : 5-trifluorobenzene must also be ascribed to an E' fundamental. The doubling probably results from Fermi coupling, either with a binary E' level involving an A_2' fundamental or with

$$503 + 1123 = 1626\ (A_1' + A_2' + E').$$

The remaining E' fundamental, which may be characterized as an unsymmetrical C—H stretching mode, must be represented by the strong Raman band at 3111 cm.$^{-1}$ and the medium infra-red band observed at 3106 cm.$^{-1}$. The low value found for the depolarization ratio is rather puzzling. It is undoubtedly caused in part by overlapping with the polarized bands at 3092 and 3071 cm.$^{-1}$, but overlapping with a combination band, perhaps

$$1471 + 1631 = 3102\ (A_1' + A_2' + E'),$$

may be a contributing factor.

* *Note added in Proof.*—Using a spectrometer with KRS-5 prism we have recently verified the occurrence of the frequency 326 cm.$^{-1}$ with considerable intensity in infra-red absorption. Thus, there can be no doubt about its assignment as an E' fundamental. However, contrary to what is stated above, it is possible that the corresponding motion is predominantly CF bending and that the next higher fundamental, 503 cm.$^{-1}$ may be characterized as largely a ring deformation. A similar remark applies to the two lowest fundamentals of species E''.

SPECIES A_2''.—The intense infra-red bands at 665 and 845 cm.$^{-1}$ must be interpreted as A_2'' fundamentals. The separation between the maxima of the rotational branches of these bands for gaseous 1 : 3 : 5-trifluorobenzene is about 1·4 times the average separation for the three E' fundamentals for which it can be estimated, in fair agreement with the theory of Gerhard and Dennison.[12] The appearance of a very faint Raman band at 666 cm.$^{-1}$ probably results from a disturbance of the molecular symmetry and weakening of the selection rules in the liquid state. The very weak Raman band at 847 cm.$^{-1}$ can readily be interpreted as a binary combination,

$$253 + 595 = 848 \ (A_1' + A_2' + E').$$

These fundamentals may be characterized roughly as a trigonal deformation of the aromatic ring at right-angles to its plane and a trigonal wagging of the hydrogen atoms. The remaining A_2'' fundamental must involve a corresponding motion of the fluorine atoms and must be so low as to lie outside the range covered by the infra-red measurements. Attempts to determine it from combination bands have led to the value 214 cm.$^{-1}$. This value rests primarily upon the interpretation of the weak infra-red and Raman frequency at 466 cm.$^{-1}$, for which no other reasonable interpretation could be found, as the sum (species E') of the lowest A_2'' and E'' fundamentals. It is useful in interpreting four other infra-red bands and two additional Raman bands, but is, of course, neither as certain nor as accurate as the directly observed fundamentals. The frequencies assigned for the 17 active fundamentals are listed in Table III.

SPECIES A_2' (INACTIVE).—The three fundamentals of this species can be determined only from overtone and combination bands. Consideration of the work on 1 : 3 : 5-trideuterobenzene [5] and mechanical model data [3] led to the expectation that two of the A_2' fundamentals should lie between 1000 and 1400 cm.$^{-1}$ and the third in the region from 400 to 600 cm.$^{-1}$. The motions associated with the two highest A_2' fundamentals may be characterized as mixtures of planar trigonal ring deformation and C—H bending and the third as largely C—F bending.

If it is assumed that the apparent doubling of the highest A_1' fundamental, at 3071 and 3092 cm.$^{-1}$, is caused by Fermi coupling with a totally symmetrical binary level, the latter must be the overtone of the highest A_2' fundamental and have a value of about 1540 cm.$^{-1}$. This seems rather high. On the other hand, this assignment permits the interpretation of the Raman band at 2528 cm.$^{-1}$ as $993 + 1540 = 2533$ (E') and the infra-red band at 3003 cm.$^{-1}$ as $1471 + 1540 = 3011$ (E') and leads to alternative interpretations of three other Raman and two infra-red bands. If this assignment is rejected, no equally plausible explanation of the doubling of the highest A_1' fundamental appears possible. The assignment is therefore tentatively adopted.

It seems reasonable that one of the faint Raman bands in the region from 2300 to 2700 cm.$^{-1}$ should be an overtone of an A_2' fundamental. The exploration of this possibility points to a value near 1300 cm.$^{-1}$. In addition to explaining the very weak sharp Raman band at 2628 cm.$^{-1}$ as the overtone (species A_1'), this assignment leads to satisfactory interpretations of the infra-red bands at 2294, 2421, 2770 and 2907 cm.$^{-1}$ and the Raman band at 2500 cm.$^{-1}$. Moreover, it offers the possibility of explaining the doubling of the E' fundamental at 1610 and 1631 cm.$^{-1}$ as resulting from Fermi coupling with $326 + 1300 = 1626$ (E'). This assignment is therefore tentatively adopted. The value 1300 cm.$^{-1}$ is about what was expected for the highest A_2' fundamental. However, it does not seem impossible that it may actually be the intermediate inactive frequency.*

* *Note added in Proof.*—It has not yet been possible to identify any of the corresponding fundamentals in the four other fluorinated benzenes investigated. However, in support of the high frequencies assigned to two A_2' fundamentals

The attempts to determine the lowest A_2' fundamental have been less successful. Although several of the values considered, in particular 490 and 625 cm.$^{-1}$, have provided alternative interpretations of infra-red and Raman bands, none has been useful in explaining bands not already interpreted. Although it is possible that a renewed study of the spectra of other fluorobenzenes, now in progress, may provide valuable clues, it appears that the final determination of the inactive fundamentals must await the completion of a normal co-ordinate analysis or additional spectral data.

Interpretation of the Spectra.—On the basis of the 17 active fundamentals listed in Table III it has been possible to interpret all but seven of the 74 infra-red absorption maxima observed for liquid 1 : 3 : 5-trifluorobenzene and all but two of the 51 observed Raman shifts. The interpretations are given in the third columns of Tables I and II. When the tentative assignments for the two A_2' fundamentals are also used, all but the extremely weak Raman band at 2096 cm.$^{-1}$ and the faint infra-red bands at 1058 and 2558 cm.$^{-1}$ are interpreted. These can be accounted for, in more than one way, as ternary combination bands, e.g.,

TABLE III.—ACTIVE FUNDAMENTAL VIBRATION FREQUENCIES FOR 1 : 3 : 5-TRIFLUOROBENZENE

Symmetry Species	Infra-red (gas)		Infra-red (liquid)		Raman (liquid)	
	Wave Number cm.$^{-1}$	Intensity	Wave Number cm.$^{-1}$	Intensity	Wave Number cm.$^{-1}$	Intensity
A_1'	—	—	—	—	577·6	*vs*
A_1'	—	—	—	—	1010·0	*vs*
A_1'	—	—	1350	*w*	1350	*s*
A_1'	—	—	—	—	3071 3092	*m*
A_1''	—	—	214^*	—	—	—
A_2''	664	*s*	665	*s*	666	*vvw*
A_2''	847	*vs*	845	*vs*	—	—
E'	—	—	—	—	326·0	*w*
E'	505	*s*	504	*s*	502·3	*s*
E'	995	*vs*	993	*vs*	993	*m*
E'	1122 1131	*vs*	1124	*vs*	1121·8	*s*
E'	1473	*vs*	1471	*s*	1471	*vw*
E'	1618 1631	*vs*	1610 1631	*vs*	1609 1631	*m*
E'	3115	*vw*	3106	*m*	3111	*s*
E''	—	—	—	—	253·4	*vs*
E''	—	—	595	*vw*	594·6	*s*
E''	—	—	—	—	1191	*w*

* Determined from combination bands.

$$214 + 253 + 595 = 1059\ (A_1'' + A_2'' + E'')$$

and

$$2 \times 993 + 578 = 2564\ (A' + E').$$

---

the following findings may be pointed out. (*a*) The frequency corresponding to one component of the E_{2g} ring deformation, 1596 cm.$^{-1}$, in benzene increases with increasing fluorination to 1643 cm.$^{-1}$ in 1 : 2 : 4 : 5-tetrafluorobenzene; (*b*) one component corresponding to the E_{1u} CH bending, 1485 cm.$^{-1}$, in benzene appears to increase in frequency with increasing fluorination to 1534 cm.$^{-1}$ in 1 : 2 : 4 : 5-tetrafluorobenzene.

The interpretation involving the A_2' fundamentals have been enclosed in brackets in Tables I and II.

Since the unperturbed frequencies for the highest A_1' fundamental and the E' fundamental at 1610 and 1631 cm.$^{-1}$ are uncertain, the observed frequencies have been used in interpreting the spectra. As a result several ternary combinations occur in the Tables concealed as binary combinations. Apart from these, ternary combinations have not been invoked, although it is quite possible that some of the observed bands, in particular the four infra-red bands interpreted as difference bands, may actually be ternary sum bands.

With a few exceptions, the agreement between calculated and observed wave numbers is very close. For several bands more than one interpretation is possible. However, not all of the alternatives have been included in the Tables.

There are 125 infra-red-active binary sum and overtone bands, 21 of which involve the three A_2' fundamentals. The total number of Raman-active binary bands is 177, of which 36 involve the inactive fundamentals. Thus, it appears that about half of the infra-red-active binary bands have been observed and somewhat over one-fifth of the Raman-active. Because of the rather numerous cases of coincidence or overlapping a considerably greater number of binary combination bands has actually been accounted for.

The writers wish to acknowledge their indebtedness to Dr. G. C. Finger for the gift of the sample and to Mr. Morris Alpert for help with infra-red measurements.

Department of Physics,
University of Oklahoma,
Norman, Oklahoma.

Naval Research Laboratory
Washington, D.C.

VIBRATIONAL SPECTRA OF CARBON AND SILICON TETRAMETHYL AND THEIR MONODEUTERO DERIVATIVES *

BY D. H. RANK, B. D. SAKSENA AND E. R. SHULL

Received 26th June, 1950

Infra-red spectra in the region 3 μ to 15 μ and Raman spectra, along with the polarizations and intensities, have been obtained for carbon and silicon tetramethyl and their monodeuterium derivatives. The infra-red spectra have been obtained in the gas phase and the Raman spectra in the liquid phase.

Assignments of the vibrational frequencies occurring in the spectra of these molecules have been made as completely as the experimental data allow. The argument for the assignment of 922 cm.$^{-1}$ to n_4 of the skeletal framework vibrations of tetramethylmethane appears to be quite strong as the result of the new experimental data. It seems necessary to assign 1250 cm.$^{-1}$, the other alternative frequency for the n_4 assignment, to ν (CH) for a large number of reasons. The behaviour of the totally symmetric vibrations of these molecules casts grave doubts upon the correctness of making force constant calculations treating the methyl group as a single atom in dealing with molecules of this type.

Tetramethylmethane, because of its symmetrical structure, should furnish a key to the analysis of the vibrational spectra of the paraffin hydrocarbons. The Raman spectrum of tetramethylmethane was first obtained by Kohlrausch and Barnes.[1] These authors were aware of the fact that the spectrum they observed was both incomplete and contained spurious lines. Kohlrausch and Barnes propounded the so-called sum rule based on purely empirical grounds to correlate the framework vibrations of the paraffin hydrocarbons. The sum rule is $\overline{\omega}^2 = \frac{1}{S}\sum \omega_i^2$, where $\sum \omega_i^2$ is the sum of the squares of the framework frequencies (vibrations which are doubly or triply degenerate enter into the sum twice or thrice respectively). S is the number of C—C links minus one for normal or branched paraffins and identically equal to the number of C—C links for cyclic hydrocarbons. On the basis of the sum rule, Kohlrausch and Barnes were able to make as assignment of the framework vibrations of tetramethylmethane predicting the existence of a triply degenerate frequency at approximately 400 cm.$^{-1}$.

---

* This research was carried out on Contract N6onr-269, Task V of the Office of Naval Research.

Unfortunately, the sum rule has never been justified theoretically. It must be stated, however, that no theoretical reasoning has been applied to the analysis of the spectra of small hydrocarbons which shows without doubt that the sum rule is invalid.

Rank[2] obtained the Raman spectrum of a good sample of tetramethylmethane and found the missing framework frequency to be in almost the exact position predicted by the sum rule of Kohlrausch and Barnes. The framework frequencies n_1, n_2, n_3 and n_4 according to this assignment are 335, 415, 732 and 921 cm.$^{-1}$ respectively. n_2 and n_4 are triply degenerate, n_1 doubly degenerate, and n_3 is a single frequency. Kohlrausch and Koppl[3] have made central force field calculations to support the above-mentioned frequency assignments. However, the C—C force constant obtained by these authors, namely, $2{\cdot}03 \times 10^5$ dynes/cm. seems to be much too low to be in accord with our modern ideas of the value of the C—C force constant.

Rank and Bordner[4] obtained the Raman spectra of a number of *neo*pentyl derivatives. Among these was the spectrum of a 50-50 mixture of *neo*pentane and *neo*pentane-d_1. Unfortunately, the spectrum of this mixture did not yield much information other than to demonstrate that new lines appeared, both due to isotope effects and the breakdown of the symmetry of the molecule. The last mentioned authors also obtained the spectrum of silicon tetramethyl which supported the assignment given by Rank[2] since it was possible to show that the 1250 and 1450 cm.$^{-1}$ frequencies remained practically invariant in passing from tetramethylmethane to tetramethylsilicon.

Theoretical treatment has been given to the framework vibrations of the tetramethylmethane molecule by Wall and Eddy,[5] Silver,[6, 7] Pitzer and Kilpatrick,[8] Young, Koehler and McKinney,[9] Rasmussen,[10] and most recently, Simpson and Sutherland.[11] The first three of the above authors and the last authors favour an assignment of $n_4 \sim 1250$ cm.$^{-1}$. Young, Koehler and McKinney, and Rasmussen support the original assignment of $n_4 \sim 921$ cm.$^{-1}$ with more or less indifferent success. It must be stated that all of the calculations with the exception of those of Simpson and Sutherland are based fundamentally on the measurements of Rank.[2] Simpson and Sutherland, however, have made use of empirical correlations

---

[1] Kohlrausch and Barnes, *Anal. Fis. Quim.*, 1932, **30**, 733.
[2] Rank, *J. Chem. Physics*, 1933, **1**, 572.
[3] Kohlrausch and Köppl, *Z. physik. Chem. B*, 1934, **26**, 209.
[4] Rank and Bordner, *J. Chem. Physics*, 1935, **3**, 248.
[5] Wall and Eddy, *ibid.*, 1938, **6**, 107.
[6] Silver, *ibid.*, 1939, **7**, 113.
[7] Silver, *ibid.*, 1940, **8**, 919.
[8] Pitzer and Kilpatrick, *Chem. Rev.*, 1946, **39**, 435.
[9] Young, Koehler and McKinney, *J. Amer. Chem. Soc.*, 1947, **69**, 1410.
[10] Rasmussen, *J. Chem. Physics*, 1948, **16**, 712.
[11] Simpson and Sutherland, *Proc. Roy. Soc. A*, 1949, **199**, 169.

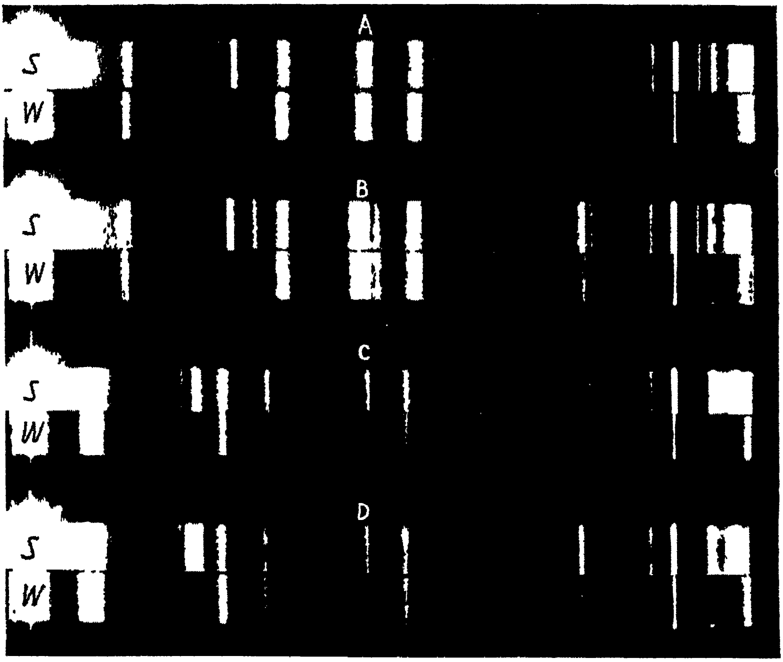

FIG. 1.—Reproductions of polarization plates of the Raman spectra of carbon and silicon tetramethyl and their monodeuterium derivatives.

A, Tetramethylmethane ; B, Tetramethylmethane-d_1 ; C, Silicon tetramethyl ; D, Silicon tetramethyl-d_1.

W and S refer to " weak " and ' strong " components. Lines which are depolarized appear with equal intensity in W and S spectrograms. Polarized lines appear with less intensity in the W spectrograms than in the strong spectrograms.

[*To face page* 189

from the spectra of hydrocarbons containing the *neo*pentyl group. Most of the infra-red spectra which Simpson and Sutherland have used in making their correlations were obtained by Sutherland and Thompson and their co-workers and as yet are largely unpublished. The Raman spectra made use of by Simpson and Sutherland are largely those obtained in this laboratory during the war for analytical purposes (Fenske *et al.*[12]).

During the last several years it has become more and more obvious that the correct analysis of the vibration spectra of even relatively simple polyatomic molecules cannot be accomplished unless the most complete possible experimental data are available. The complexity of the molecular dynamics and the necessary crude approximations which must be made make it seem quite doubtful as to the virtue of trusting such calculations to fill in gaps in assignments except as a last resort when all experimental possibilities have been exhausted.

It is absolutely necessary to have both complete infra-red and Raman spectra along with the polarizations and qualitative intensities if analysis is to be attempted. Whenever feasible deuterium derivatives can, and probably must, be used to settle unequivocally certain theoretical points in the analysis of hydrocarbon spectra.

Experimental

We have prepared tetramethylmethane-d_1 and tetramethylsilicon-d_1 approximately 99 % pure by means of the familiar Grignard reaction. Strong Raman spectra have been obtained for tetramethylmethane and tetramethylsilicon and their monodeuterium derivatives. The polarizations of all of the Raman lines have been obtained making use of a photographic method based on the method of polarized incident light described by Douglas and Rank.[13] The intensities of the Raman lines have been measured with the photoelectric spectrograph described by Rank and Wiegand.[14] We have obtained the infra-red spectra of these molecules in the gas phase by means of a Perkin and Elmer spectrometer Model 12C equipped with a rock salt prism.

The results of our experimental investigation of these spectra along with the assignment of the frequencies are given in Table I. In Fig. 1 reproductions of the polarization plates for the Raman spectra of the molecules mentioned above are shown. Lines which have the same intensities in the spectrograms marked W as in those marked S are depolarized. Lines which are weaker in the W reproductions than in the S reproductions are polarized lines. Fig. 2 and 3 show reproductions of the infra-red transmission curves obtained for these molecules in the rock salt region, i.e. 3 μ to 15 μ.

It is believed that the frequency measurements in the Raman spectra are in almost all cases accurate to ± 2 cm.$^{-1}$ or better. The infra-red frequencies vary somewhat in accuracy throughout the spectrum and are probably not as accurate as the Raman frequencies. In addition, small shifts in the neighbourhood of the experimental errors occur between the two spectra, i.e. infra-red gas, Raman liquid. In our assignment Table I, we have given the observed Raman frequency when coincidences were available. For infra-red bands the position of the *Q* branch has been taken for the frequency. In the case of $n_4 \sim \nu_2(e)$ for *neo*pentane-d_1 the *Q* branch occurs at 925 cm.$^{-1}$ and the corresponding Raman line was measured to be 922 cm.$^{-1}$.

Discussion

A complete treatment of the *neo*pentane molecule shows that we should expect to find 19 vibrational modes. Fourteen of these modes should make their appearance in the combined Raman and infra-red spectrum. There should be three vibrations of the type A_1, one of type A_2, four of type *e*, four of type f_1, and seven of type f_2. Vibrations of type A_1 are totally symmetric and appear only in the Raman effect as polarized lines. Vibra-

---

[12] Fenske, Braun, Wiegand, Quiggle, McCormick and Rank, *Ind. Eng. Chem.* (*Anal.*), 1947, **19**, 700.

[13] Douglas and Rank, *J. Opt. Soc. Amer.*, 1948, **38**, 281.

[14] Rank and Wiegand, *ibid.*, 1946, **36**, 325.

TABLE I.—SUMMARY OF EXPERIMENTAL DATA OBTAINED ON INFRA-RED AND RAMAN SPECTRA OF CARBON AND SILICON TETRAMETHYL AND THEIR MONODEUTERIUM DERIVATIVES ALONG WITH FREQUENCY ASSIGNMENTS

Frequencies are given in cm.$^{-1}$ under columns marked Obs. R refers to appearance in Raman spectrum and I to appearance in infra-red. The numbers in the columns marked R refer to relative intensities of lines obtained by integration of intensities under intensity against wavelength curves. In columns marked I, *w*, *m* or *s* refers to intensity of observed infra-red bands, i.e. weak, medium or strong. The observed polarizations are in accord with the class to which the Raman lines have been assigned in all cases. In the case of combination frequencies where no definite assignments have been made observed polarizations are indicated by P or D in the columns marked R.

Freq. No.	$C(CH_3)_4$					$Si(CH_3)_4$			$Si(CH_3)_3CH_2D$				$C(CH_3)_3CH_2D$		
	Species	Char.	Obs.		ν	Obs.		ν	Species	Obs.		ν	Obs.		ν
			R	I		R	I			R	I		R	I	
1	$\nu_1 f_2$	Skel.	4	—	415	46	—	245	ν_1 (*e*)	59	—	242	8	—	409
2	—	—	—	—	—	—	—	—	ν_1 (*a*)	—	—	—	—	—	—
3	$\nu_2 f_2$	Skel.	40	*w*	921	33	*vs*	694	ν_2 (*e*)	25	*vs*	690	40	*w*	922
4	—	—	—	—	—	—	—	—	ν_2 (*a*)	30	?	609	6	—	815
5	$\nu_3 f_2$	γ (CH)	60	*s*	1249	8	*s*	1250	ν_3 (*e*)	3	*s*	1248	40	*s*	1251
6	—	—	—	—	—	—	—	—	ν_3 (*a*)	—	—	—	—	*w*	919
7	$\nu_4 f_2$	δ (CH)	—	*s*	1376	—	*m*	1285	ν_4 (*e*)	—	*m*	1285	—	*s*	1376
8	—	—	—	—	—	—	—	—	ν_4 (*a*)	—	—	—	—	—	—
9	$\nu_5 f_2$	δ (CH)	—	*s*	1475	—	*s*	1430	ν_5 (*e*)	—	*sb*	1415	—	*s*	1476
10	—	—	—	—	—	—	—	—	ν_5 (*a*)	—	—	—	—	—	—
11	$\nu_6 f_2$	—	—	—	—	—	—	—	ν_6 (*e*)	—	—	—	—	—	—
12	—	—	—	—	—	—	—	—	ν_6 (*a*)	—	—	—	—	—	—
13	$\nu_7 f_2$	ν(CH)	88	*s*	2955	88	*s*	2957	ν_7 (*e*)	93	*s*	2955	100	*s*	2955
14	—	—	—	—	—	—	—	—	ν_7 (*a*)	10	*s*	2189	10	*s*	2176
15	$\nu_1 A_1$	Skel.	25	—	733	40	—	593	ν' (*a*)	45	—	570	35	—	720
16	$\nu_2 A_1$	—	—	—	—	8	—	1263	ν_2' (*a*)	2	—	1259	—	—	—
17	$\nu_3 A_1$	—	100	—	2909	100	—	2900	$\nu^1{}_3'$(*a*)	60	—	2898	90	—	2908
18	$\nu_1 e$	Skel.	22	—	335	80	—	199	ν_1 (*e*)	100	—	197	28	—	331
19	$\nu_2 e$	γ (CH)	1	—	1146	—	—	—	ν_2 (*e*)	—	—	—	—	—	—
20	$\nu_3 e$	δ (CH)	55	—	1451	40	—	1418	ν_3 (*e*)	18	—	1416	55	—	1449
21	$\nu_4 e$	ν (CH)	88	—	2955	88	—	2957	ν_4 (*e*)	93	—	2955	100	—	2955
—	f_1	—	IN	—	—	IN	—	—	(*e*)	—	—	—	39	*m*	1217
—	f_1	—	IN	—	—	IN	—	—	(*e*)	—	—	—	17	*s*	1298
			COMBINATION FREQUENCIES												
			P 8	—	2715	—	—	—	—	P 43	—	2915	P 4	—	2716
			P 50	—	2868	—	—	—	4+18→		*w*	780	P 5	—	2779
			P 55	—	2896	D 33	*s*	862	←3+18→	D 14	*s*	855	P 50	—	2865
			—	—	—	—	—	—	4+15→	P 2	*s*	1164	P 43	—	2879
			—	—	—	—	—	—	—	—	—	—	P 80	—	2933

tions of type A_2 are antisymmetric, of e doubly degenerate, and of f_1 triply degenerate. Vibrations of type A_1 are active only in the Raman effect. Vibrations of type f_1 and A_2 are inactive in both the infra-red and Raman spectrum while those of class f_2 are active in both spectra. The vibrations of class e are active only in the Raman effect.

The complete theoretical calculations of the modes of vibration of the *neo*pentane molecule are very complex and have never been seriously attempted. The various force constant calculations referred to previously in this paper have all concerned themselves chiefly with the treatment of the methyl group as a single atom. These calculations fundamentally follow the classical approach of Rosenthal [15], [16], [17] on tetrahedral XY_4 type molecules with certain variations and simplifications. The chief point of contention in the *neo*pentane spectrum is the location of n_4 of the skeletal vibrations, (i.e. 921 cm.$^{-1}$ or 1250 cm.$^{-1}$ which assignment is of great fundamental importance in further progress in analysis of the spectra of hydrocarbons).

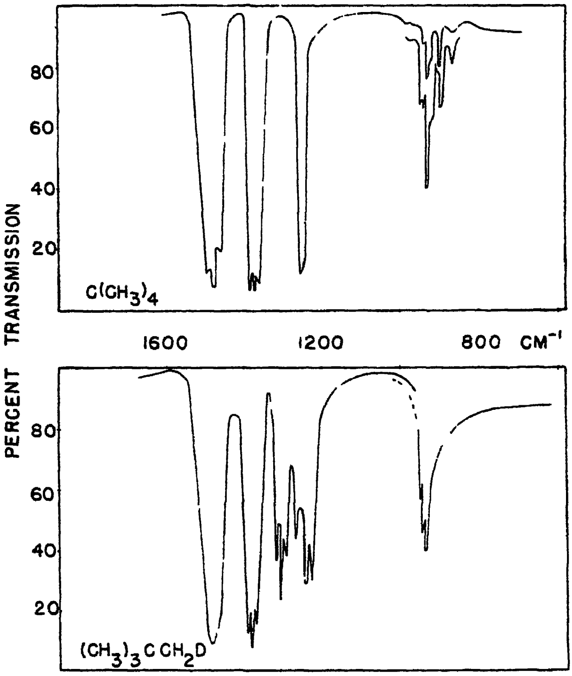

FIG. 2.—Infra-red transmission curves for tetramethylmethane and tetramethylmethane-d_1.

Curves were obtained in the gaseous phase by admitting the vapour into the case of the spectrometer. The amount of absorption was controlled by varying the partial pressure of the gas to show the structure of the various bands.

Before proceeding with a detailed discussion of the observed spectra it is necessary to discuss the modifications to be expected upon introduction of a deuterium atom into the *neo*pentane molecule. Upon introduction of a deuterium atom essentially we shall pass over into the XY_3Z type molecule and it is now possible to have only (e) and (a) type vibrations. The mall perturbation produced by the single D atom can hardly be expected, however, to produce observable splittings for all the vibrations. Furthermore, it can be expected that the vibrations in the monodeuteride which have arisen from f_1 and A_2 classes of vibrations of the group T_d are now theoretically active and may appear in the spectrum experimentally to a limited extent. Thirdly, certain line frequency shifts will occur in passing from the hydrocarbon to the deuteride. Unfortunately, these shifts are not calculable from the familiar Redlich-Teller rule which would be applicable only to a totally deuterium substituted molecule.

---

[15] Rosenthal, *Physic. Rev.*, 1934, **45**, 538.
[16] Rosenthal, *ibid.*, 1934, **46**, 730.
[17] Rosenthal, *ibid.*, 1935, **47**, 235.

We shall first consider the analysis of the spectrum of $Si(CH_3)_4$ since in many respects there are many features of this spectrum that allow

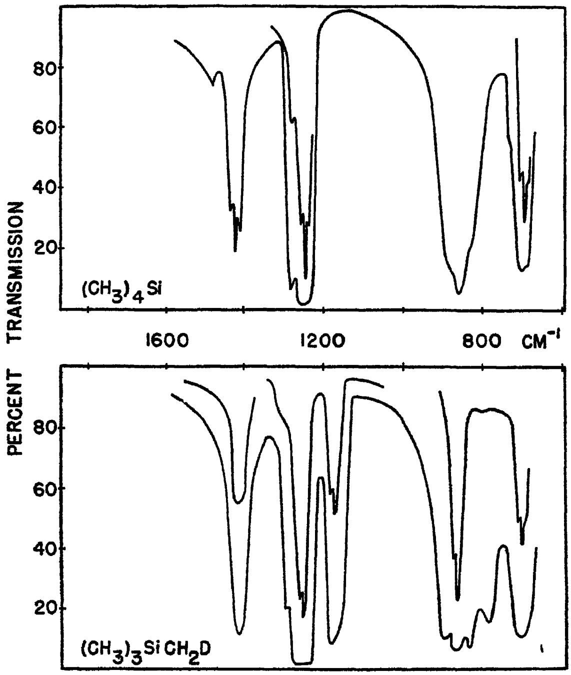

FIG. 3.—Infra-red transmission curves for silicon tetramethyl and silicon tetramethyl-d_1.

Curves were obtained in the gaseous phase by admitting the vapour into the case of the spectrometer. The amount of absorption was controlled by varying the partial pressure of the gas to show the structure of the various bands.

unambiguous conclusions to be drawn, particularly when the monodeutero derivative is considered. The spectrum of $Si(CH_3)_4$ breaks up into two distinct regions, i.e. frequencies under 700 cm.$^{-1}$ and frequencies over 1200 cm.$^{-1}$. (The depolarized line of $Si(CH_3)_4$ observed at 863 cm.$^{-1}$ and 855 cm.$^{-1}$ in the monodeutero compound is obviously the combination tone arising from the strong frequencies $\nu_1(e) + \nu_2(f_2)$.) It is obvious that these vibrations under 700 cm.$^{-1}$ must be assigned to the skeletal modes.

Observations of the $Si(CH_3)_4$ spectrum show that the Raman lines under 700 cm.$^{-1}$ have very great intensity and the intensity of the infra-red bands at 863 cm.$^{-1}$ and 694 cm.$^{-1}$ are probably the most intense bands in the spectrum. This situation is exactly what one would expect since the introduction of the silicon atom into the skeletal framework will give rise to unequal charges on the framework atoms and thus produce a very effective vibrating dipole. Thus, it is at once apparent that the assignment of the skeletal modes must follow the scheme given in Table I. Passing on to $Si(CH_3)_3CH_2D$ the assignment of the skeletal frequencies is again immediately obvious. In this molecule, $\nu_2(f_2)$ of $Si(CH_3)_4 \rightarrow \nu_2(e)$ and $\nu_2(a)$ which splitting produces the strong polarized Raman line at 609 cm.$^{-1}$. There are indications that a strong infra-red frequency corresponding to this vibration makes its appearance since a region of absorption is beginning at the end of the rock salt region which absorption does not occur in $Si(CH_3)_4$.

The vibrations of Type A_1 are completely accounted for in $Si(CH_3)_4$ since resolution of the broad band at approximately 1264 cm.$^{-1}$ was easily achieved on our present plates showing the strongly polarized line at 1263 cm.$^{-1}$ and a more diffused depolarized line at 1250 cm.$^{-1}$. The medium intensity polarized line which appears in the spectrum of the monodeuteride at 1164 cm.$^{-1}$ is very probably the combination tone arising from the very strong frequencies $\nu_2(a) + \nu_1(a)$. The remaining assignments of the frequencies of this molecule as far as observations permit is perfectly straight-forward and nearly unambiguous.

The assignment of the frequencies in $Si(CH_3)_4$ and its monodeuterium derivative, plus certain physical conditions which must be satisfied by experimental observations, make the assignment of the frequencies of $C(CH_3)_4$ and its monodeuterium derivative feasible without the help of any force constant calculations with their attendant approximations and uncertainties.

From the arrangement of the charges on the carbon atoms of the *neo*pentane framework it is to be expected that the lines in the Raman spectrum due to framework vibrations, with the exception of the totally symmetric vibration, should be relatively much weaker than the corresponding frequencies in $Si(CH_3)_4$. Particularly in the infra-red absorption spectrum any bands due to framework vibrations will be especially weak since the equality of charge presupposes a rather ineffective vibrating dipole. It is well known and generally accepted that framework vibrations are almost nonexistent in the infra-red absorption spectrum of normal paraffins. Simpson and Sutherland [11] have given reasons why a more effective vibrating dipole may be present in branched hydrocarbons than in straight paraffins. However, the incontrovertible fact exists that the 925 cm.$^{-1}$ infra-red absorption band of *neo*pentane is relatively much weaker than the 694 cm.$^{-1}$ band in $Si(CH_3)_4$. On the other hand, the bands at 1250 cm.$^{-1}$ which are present in both molecules are also very strong in both infra-red spectra. Furthermore, the 1250 cm.$^{-1}$ and 1450 cm.$^{-1}$ frequencies are practically invariant in the spectra of silicon and carbontetramethyl.

On the basis of the relative ineffectiveness of the vibrating dipole alone, i.e. very weak infra-red absorption band, it is practically certain that the framework vibration n_4, $(\nu_3 f_2)$ must be assigned to the 921 cm.$^{-1}$ frequency. However, there is supporting evidence to this assignment since a polarized line at 815 cm.$^{-1}$ appears in the Raman spectrum of *neo*pentane-d_1 which is strictly analogous to the behaviour of $Si(CH_3)_4$ even to the extent that $\nu_2(a)/\nu_2(e)$ is a constant for the two molecules to nearly one part in a thousand.

On the other hand, it seems necessary to assign 1250 cm.$^{-1}$ to ν(CH) for a number of reasons :

(i) strength in infra-red absorption band ;

(ii) invariance of frequency passing from $Si(CH_3)_4$ to $C(CH_3)_4$;

(iii) hydrogen isotope effect observed by the appearance of a band at 919 cm.$^{-1}$ superimposed on the *P* branch of the 925 cm.$^{-1}$ infra-red absorption band in the spectrum of monodeutero *neo*pentane.

In support of (iii), there are numerous empirical observations that frequently the ratio of the frequency of the CD to the CH stretching frequency is exactly the same as the CD to CH bending frequency.*

If we assume the ratio of isotopic stretching and bending frequencies to be constant, a frequency should appear at 920·5 cm.$^{-1}$ in the spectrum of *neo*pentane-d_1 if our assignment of ν(CH) in *neo*pentane is correct. We have observed an infra-red band at 919 cm.$^{-1}$ in excellent agreement with predictions. The corresponding Raman line would, of course, be completely obscured by the 921 cm.$^{-1}$ framework frequency which is relatively much stronger in the Raman effect than its analogous infra-red band. The calculated position for the analogous band in silicon tetramethyl-d_1 is 926 cm.$^{-1}$ and it is obscured in the infra-red by the tremendously strong and broad combination band with its centre at 855 cm.$^{-1}$. A search was made for the calculated 926 cm.$^{-1}$ band in the Raman spectrum tetramethyl silicon-d_1. However, if this line exists it is certainly less than 1/200 the intensity of the strongest line in the spectrum of this molecule.

We have been forced to assign the depolarized Raman lines at 1217 and 1298 cm.$^{-1}$ in *neo*pentane-d_1 to (*e*) vibrations arising from the forbidden f_1 classes in *neo*pentane. The 1217 cm.$^{-1}$ band has a companion peak at 1224 cm.$^{-1}$ in the infra-red spectrum, the origin of which is somewhat obscure. It is to be noted that nearly all infra-red bands observed in all the spectra reported in this paper showed *PQR* structure with more or less prominence, except the bands above 1500 cm.$^{-1}$ for which our resolving power was inadequate. The observation of a single type of infra-red band is completely in accord with theoretical predictions since only one class of vibrations is active in the infra-red. The exceptions to this *PQR* structure were the 919 cm.$^{-1}$, 1217 cm.$^{-1}$ and 1224 cm.$^{-1}$ bands in the spectrum *neo*pentane-d_1 where the overlapping bands made determination of $\parallel$ or $\perp$ character impossible.

Advisability of Treating Methyl Group as a Single Atom.—Various calculations on the framework vibrations of tetramethylmethane have been made. All calculations essentially treat the methyl group as a single atom. Uniformly the calculations agree on the assignment of n_1, n_2 and n_3. There is, however, wide disagreement on the assignment of n_4, some authors choosing $n_4 = 921$ cm.$^{-1}$ and others choosing 1250 cm.$^{-1}$. In any event, the results of the calculations uniformly lead to results which fit the experimentally determined frequencies so badly that it is hard to see how any of the calculations made up to the present time are capable of deciding the assignment of n_4. As a further example of the futility of treating the methyl group as a single atom, let us examine the experimental data on the totally symmetrical vibration of these molecules which certainly should be the simplest possible case to consider.

---

* Wood and Rank [18] noted that this situation applied strictly in the spectrum of heavy chloroform. These authors were able to calculate the isotope effect for the hydrogen bending frequency exactly in a simple fashion considering suitably chosen diatomic oscillators by assuming that the hydrogen or deuterium atom had an effective mass larger by a small constant amount than the true mass of the hydrogen or deuterium atom. The constant was determined from the ratio of C—D to C—H stretching frequency and then the C—D bending frequency was calculated exactly. This crude idea has been made use of by Silver [6] where the tetramethylmethane molecule is treated as a 5 atom tetrahedral molecule each methyl group being considered as a single atom. Silver makes use of an effective mass of the methyl group which is somewhat greater than the true mass in carrying out his calculations. The most recent work on the tetramethyl type molecules by Sheline and Pitzer [19] and Sheline [20] has considered in considerable detail the introduction of an effective mass for the methyl group somewhat larger than the true mass in making force constant calculations.

[18] Wood and Rank, *ibid.*, 1935, **48**, 63.

[19] Sheline and Pitzer, *J. Chem. Physics*, 1950, **18**, 595.

[20] Sheline, *ibid.*, 1950, **18**, 602.

In addition to the spectra reported in this paper we have obtained corresponding spectra for the monochloro and monobromo derivatives of *neo*pentane and the monochloro derivative of silicon tetramethyl. The analyses of these spectra will be published elsewhere. The values obtained for the totally symmetric frequencies are given in Table II.

A well-known formula (see Herzberg [21]) allows the calculations of the totally symmetric frequency in a symmetrically substituted isotopic molecule of the tetrahedral XY_4 type. It is generally supposed that in the case of a symmetrical isotopic substitution the expression for the frequency becomes

$$\nu_i = \frac{1}{4}\nu\sqrt{\frac{\Sigma M}{\Sigma M_i}}, \quad . \quad . \quad . \quad . \quad . \quad (1)$$

where ν_i is the isotopic frequency. ΣM is the sum of the masses of the Y atoms and ΣM_i the sum of the isotopic Y masses. This formula has been shown to hold with high precision for CCl_4 by Langseth [22] and Rank and Van Horn.[23] Making use of this formula considering the CH_3 group as a single atom the values tabulated in Table II ν-ν_i(calc.) were obtained. The observed values for the isotopic *neo*pentanes are grating measurements and are believed to be accurate to about a tenth of a wave number. From the above observation it is immediately obvious that any calculation assuming the methyl group to behave as a single atom will not represent the facts correctly.

TABLE II.—TOTALLY SYMMETRIC FREQUENCIES FOR SOME PENTA-ATOMIC TYPE MOLECULES

Totally symmetric frequencies are given in Table II in cm.$^{-1}$ in column marked Obs. The calculated values of the isotope shift according to eqn. (2) are given in column marked ν-ν_i (calc.) while the observed values are given in column marked ν-ν_i (obs.).

Molecule	Obs.	ν-ν_i (obs.)	ν-ν_i (calc.)
$C(CH_3)_4$	732	13·7	5·8
$C(CH_3)_3CH_2D$	720		
$C(CH_3)_3CH_2Cl$	721	—	—
$C(CH_3)_3CH_2Br$	657	—	—
$Si(CH_3)_4$	593	23	4·7
$Si(CH_3)_3CH_2D$	570		
$Si(CH_3)_3CH_2Cl$	582	—	—

The strange behaviour of the totally symmetric frequencies of the halides of tetramethylmethane and tetramethyl silicon finds plausible explanation from electron diffraction work of Bauer.[24] The C—CH_3 distance was found to be 1·54 Å ± ·03 Å. The C—CH_2Cl distance was found to be 1·58 Å ± ·04 Å for *neo*pentyl chloride. The implications of the electron diffraction evidence and their effect on the spectrum are obvious. The increase in the force constant of the stretched C—CH_2Cl bond nullifies the mass effect of the heavy chlorine atom in the monochloro derivative of carbon tetramethyl. In the bromide, apparently the mass is great enough presumably to again take control of the situation.

---

[21] Herzberg, *Infra-red and Raman Spectra* (D. van Nostrand Co., Inc., New York, 1945), p. 233.

[22] Langseth, *Z. Physik.*, 1931, **72**, 350.

[23] Rank and Van Horn, *J. Opt. Soc. Amer.*, 1946, **36**, 239.

[24] Hastings and Bauer, *J. Chem. Physics*, 1950, **18**, 13.

The results obtained by Bauer for the chloride of silicon tetramethyl show no distortion of the tetrahedron. Thus, it does not seem possible to explain the even larger discrepancy between calculated and observed values for the totally symmetric frequency on the basis of the C—C bond being under tension for the silicon molecule.

The experimental facts mentioned in this paper seem to present a firm argument against the assignment of the 1250 cm.$^{-1}$ frequency rather to n_4 in the spectrum of *neo*pentane.

The authors are indebted to Mr. P. R. Yoder, Jr., for the preparation of the figures and to Mr. R. E. Kagarise for making the intensity measurements of the Raman lines.

Spectroscopy Laboratory,
Pennsylvania State College,
State College, Pennsylvania.

THE RAMAN SPECTRA OF METALLIC NITRATES AND THE STRUCTURE OF CONCENTRATED SOLUTIONS OF ELECTROLYTES

BY JEAN-PAUL MATHIEU AND MACKENZIE LOUNSBURY

Received 3rd July, 1950

A comprehensive study of the Raman spectra of solutions of metallic nitrates at various concentrations shows that the NO_3^- ions experience some deformation as the concentration increases and that in concentrated solutions of most of them an equilibrium takes place between two forms of NO_3^-. The facts can be interpreted by assuming that the saturated solutions have a structure very similar to that of the hydrated crystals which are deposited from them.

It has long been known that the formation of ions by electrolytic dissociation can be detected by the study of the Raman spectrum in solutions of acids such as HNO_3[1] and H_2SO_4.[2] In these cases, there is a rearrangement of the molecular structure, in agreement with the views put forth by Hantzsch. As the concentration of the solutions increases, the molecular form, which is that of the pure substance, becomes more abundant than the dissociated form.

Quite different is the case where the electrolyte is a typically strong one, e.g. a neutral crystalline salt dissolved in an ionizing solvent. Certain authors have attempted, by means of the Raman effect, to investigate the presence of undissociated molecules, and of intermediate ions such as $CaNO_3^+$, for polyvalent electrolytes. But the idea of the molecule is then without meaning, because the pure state of strong electrolytes is the ionic crystal. If one admits that the form of the pure substance becomes increasingly abundant in these solutions as the concentration increases, then one would expect to find in concentrated solution, a structure analogous to that of the ionic crystal, or at least fragments of such a structure. In the Raman spectrum, lines analogous to those arising from the " external " vibrations of the crystal would appear. Now, a phenomenon of this kind has never been observed. On the other hand, when the ions are complex, i.e. composed of several atoms (so that they possess characteristic vibrational frequencies), these frequencies must be alterable by the changes with concentration in the electric field created by the charges of the other ions and of the dipoles of the ionizing solvent.

---

[1] Rao, *Proc. Roy. Soc. A*, 1930, **127**, 279.
[2] Woodward and Horner, *ibid.*, 1934, **144**, 129.

Experimental and Results

We have studied systematically the influence of concentration on the Raman spectra of solutions of metallic nitrates. The complex ion NO_3^- has a plane structure in the form of a centred equilateral triangle, and possesses four fundamental modes of vibration (Fig. 1). Only the totally symmetrical vibration $\Delta\nu_1$, and the doubly degenerate vibrations $\Delta\nu_3$ and $\Delta\nu_4$ are active in the Raman effect.

The Raman spectrograms were obtained using a Cojan spectrograph with a numerical aperture of $F/1{\cdot}9$, and a dispersion of about 30 Å per mm. Measurements were made of the frequency ($\Delta\nu$ in cm.$^{-1}$) of the lines, of their relative intensity I, and their depolarization factor ρ by photographic photometry.

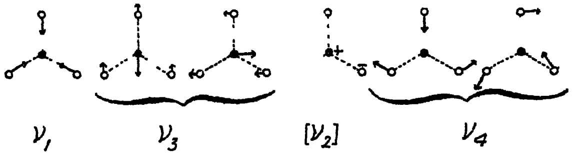

FIG. 1.

Tables I and X summarize the results of these measurements. The following abbreviations have been used:

P, polarized line ($0 < \rho < 6/7$);
D, depolarized line ($\rho = 6/7$);
s, strong intensity;
m, medium intensity;
w, feeble intensity;
b, broad line;
n, narrow line;
N, normality of the solution studied.

Unless otherwise stated, the temperature was 40° C.

Analysis of Results.—The preceding results (and many others which do not appear in the Tables) may be analyzed in the following manner.

(i) Only for concentrations of normal or less does the Raman spectrum contain no more than three lines corresponding to the three active fundamental frequencies. The polarization of the lines is in accord with the theory. The frequency $\Delta\nu_3$ always appears as a broad, diffuse band. Several of these results are presented in Table II.

To the above facts, valid for all nitrates in aqueous solution, may be added another which has been observed by various authors :[3, 4, 5, 6] the frequency $\Delta\nu_1$ of the totally symmetrical line tends towards the value $1048{\cdot}0 \pm 0{\cdot}2$ cm.$^{-1}$ as the concentration decreases. Thus, in dilute solution, the spectrum of the nitrate ion agrees with the form of a centred equilateral triangle. This structure appears as a limiting case, corresponding to the ion surrounded in an isotropic manner by the water molecules of the solution.

(ii) In every case, the first effect of increasing the concentration is to cause a splitting of the band $\Delta\nu_3$ into two others. The band of lower frequency is polarized ($\rho \sim 0{\cdot}6$ to $0{\cdot}7$); the other is depolarized. Results for several cases are presented in Table III.

The splitting of the band $\Delta\nu_3$ when the concentration increases may be interpreted by a cessation of the degeneracy of the fundamental vibration to which it corresponds. One finds, as one should, a polarized band and a depolarized band, which excludes the hypothesis of a Fermi resonance between the frequency $\Delta\nu_3$ and the first harmonic of $\Delta\nu_4$. This modification of the

[3] Gerlach, *Ann. Physik*, 1930, **5**, 196.
[4] Grassmann, *Z. Physik*, 1932, **77**, 616.
[5] Grassmann, *ibid.*, 1933, **82**, 765.
[6] Theimer, *Acta Physica Austriaca*, 1948, **1**, 384.

spectrum reveals a lowering of the symmetry of the nitrate ion. It is probable that this phenomenon is due to the deformation of the electronic envelope of the ion by its surroundings. The ionic atmosphere is no longer isotropic when the concentration is increased: a cation can draw nearer to a particular nitrate ion than to the other anions and thus form an association by pairs. Although Bjerrum considered only Coulomb forces in the formation of ion pairs, the forces of induction and of dispersion are not excluded from playing a part in the interaction of ions when they come very close together.

TABLE I

(*a*) LiNO$_3$

N = 1	718 (wDn)	1047 (sPn)	—	1392 (mDb)	—
3·2	721 (wDn)	1050 (sPn)	1362 (w)	1438 (mb)	—

(*b*) Be(NO$_3$)$_2$

N = 6·4	720 (wD)	1051 (sP)	1342 (wP)	1420 (wD)	—

(*c*) Cd(NO$_3$)$_2$

N = 7·1	715 (wD)	739 (wD)	1051 (sP)	1308 (mP)	1418 (mD)

(*d*) Ca(NO$_3$)$_2$

N = 2·2	717 (mD)	740 (wD)	1050 (sP)	—	1378 (mD)
4·4	716 (mD)	741 (wD)	1051 (sP)	1350 (mD)	1430 (mD)
7·6	717 (mD)	744 (mD)	1050 (sP)	1358	1428
10·8	716 (mD)	741 (mD)	1051 (sP)	1353	1428
12·6	717 (mD)	744 (mD)	1049 (sP)	1358	1428
16	716 (mD)	746 (mD)	1050 (sP)	1358 (mD)	1428 (mD)

(*e*) Cu(NO$_3$)$_2$

N = 1·2	717 (D)	—	—	1048 (sP)	—	1378 (mDb)	—
5·4	716 (mD)	—	—	1050 (sP)	1344 (mb)	1406 (mDb)	—
7·9	718 (mD)	756 (wP)	1024 (w)	1049 (sP)	1328 (mPb)	1414 (mDb)	1478 (wb)
9·9	719 (wD)	756 (wP)	1024 (wP)	1050 (sP)	1313 (mPb)	1412 (mDb)	1478 (mDb)
11·5	718 (mD)	759 (wP)	1024 (wP)	1050 (sP)	1313 (mPb)	1413 (mDb)	1478 (mDb)
14	719 (mD)	757 (mP)	1024 (mP*)	1048 (sP)	1315 (mPb)	1405 (mDb)	1481 (mDb)

(*f*) Ce(NO$_3$)$_3$

N = 3·5	714 (wD)	741 (wD)	1048 (sP)	1380 (wD)	—
Sat. soln.	714 (wD)	741 (mD)	1047 (sP, double)	1348 (wP)	1463 (mD)

(*g*) Th(NO$_3$)$_4$

N = 1·3	714 (mD)	749 (wD)	—	1048 (sP)	—	1360 (mD)	1528 (wPb)
3·5	714 (mD)	750 (wD)	—	1051 (sP)	—	1368 (mD)	1528 (mPb)
6·3	715 (mD)	751 (wD)	1034 (w)	1051 (sP)	1318 (wD)	1408 (wD)	1538 (mPb)
10	713 (wD)	750 (mD)	1034 (m)	1050 (sP)	1323 (wD)	1408 (wD)	1538 (double)
14·3	715 (wD)	751 (mD)	1034 (sP)	1050 (sP)	1323 (vw)	—	1540 (double)
16·3	716 (wD)	751 (mD)	1034 (sP)	1050 (mP)	1317 (vw)	—	1500 1543 (mP)

* Values deduced from the decomposition of the photometric curve (cf. Fig. 4).

TABLE II

Cation	Li	Na	Ba	La	Cu
N . .	1·0	1·7	0·6	1·5	1·2
$\Delta\nu_1$.	1047	1048	1047	1050	1048 (ρ = 0·25)
$\Delta\nu_4$.	718	714	720	720	717 (ρ = 0·86)
$\Delta\nu_3$.	1392	1380	1370	1383	1378 (ρ = 0·83)

One may ask why there is not a similar splitting of the doubly degenerate vibration $\Delta\nu_4$. This does not occur because this vibration should approach that of a pure deformation. Now, the study of crystals [7] as well as the theoretical calculations [8] shows that vibrations of deformation are always much less sensitive to variations in the symmetry of the local field of force than are the vibrations of valency.

Thus the Raman effect brings its contribution to the study of a much debated question, that of changes in the polarizability of ions in solution. Measurements of refraction,[9] of absorption [10, 11] and of rotatory power [12] have been directed towards this question. In particular, Böttcher, from a detailed study of the internal electric field in fluid dielectrics, has attempted recently to draw the conclusion that the polarizability of ions and of simple molecules is not influenced by their surroundings.[13] Although calculations based on the numerical data of refraction show that the *mean* polarizability of the nitrate ion in fact does remain constant in solutions of alkaline nitrates,[14] our results scarcely permit us to think that the same is true of all the terms of the tensor of polarizability and for the derived tensor. The study of the Rayleigh radiation from solutions of NaNO$_3$ [15] gives similar indications.

TABLE III

Cation	Na	Li	Be	Sr	Zn	Cu	Al
N . .	7·6	3·2	6·4	3·8	6·9	4·6	3·9
$\Delta\nu_3$.	1357 1410	1362 1438	1342 1420	1353 1423	1340 1408	1347 1418	1315 1410

(iii) Above a certain concentration, which depends on the nature of the cation, more profound modifications appear in the spectra of the nitrates of certain polyvalent cations.

TABLE IV

Cation	Ca	Cu	Ce	La	Th	
N . . .	10·8	13·0	Sat.	8·8	14·3	
$\Delta\nu_3'$ . .	1428	1481	1463	1461	1500	1543
ρ . . .	0·83	0·93	*D*	0·82	*D* ?	0·55

(*a*) One or two new bands, as broad as the bands $\Delta\nu_3$, appear at frequencies $\Delta\nu_3'$, which are a little higher than $\Delta\nu_3$ (Fig. 2 and 3) as shown in Tables I and IV.

(*b*) There appears a new line, of frequency $\Delta\nu_4'$ a little higher than $\Delta\nu_4$ (see Table V), which several authors have already observed.[4, 16] Its frequency depends on the cation, but not on the concentration. On this point, our measurements for Ca(NO$_3$)$_2$ agree with those of Grassmann [4] and of Nisi,[17] but not of Bauer.[16] We have not found the frequency claimed by Ollano and Frongia [18] for Ba, Mg and Al.

[7] Couture, *Ann. Physique*, 1947, **2**, 94.

[8] Bauer and Magat, *J. Physique*, 1938, **9**, 319.

[9] Fajans, *Trans. Faraday Soc.*, 1927, **23**, 357.

[10] von Halban and Eisenbrand, *Z. physik. Chem.*, 1928, **132**, 401.

[11] Kortüm, *Das Optische Verhalten geloster Elektrolyte* (Enke, Stuttgart, 1936).

[12] Darmois, *Progrès récents dans l'étude de la structure des solutions électrolytiques* (A.S.I. No. 785) (Hermann, Paris, 1939).

[13] Böttcher, *Physica*, 1942, **9**, 937.

[14] Böttcher, *Rec. Trav. Chim.*, 1946, **65**, 14.

[15] Mathieu and Lelong, *Compt. rend.*, 1943, **216**, 800.

[16] Bauer, Magat and Silveira, *ibid.*, 1933, **197**, 313.

[17] Nisi, *Proc. Phys. Math. Soc. Japan*, 1933, **15**, 114.

[18] Ollano and Frongia, *Nuova Cimento*, 1933, **10**, 306.

(c) The line $\Delta\nu_1$ broadens and its apparent half-width in some cases reaches 20 to 30 cm.$^{-1}$. This phenomenon is very probably due, in all cases, to the appearance of a polarized line of frequency $\Delta\nu_1'$ close to $\Delta\nu_1$, because we have been able to prove the existence of a new line, $\Delta\nu_1' = 1024$ cm.$^{-1}$, in the spectrum of copper nitrate (cf. Fig. 4 and 7) and $\Delta\nu_1' = 1034$ cm.$^{-1}$ in the spectrum of thorium nitrate (cf. Fig. 8).

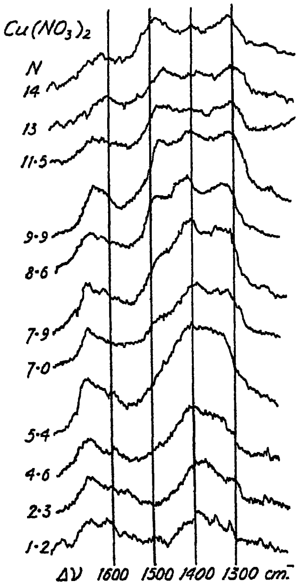

FIG. 2.

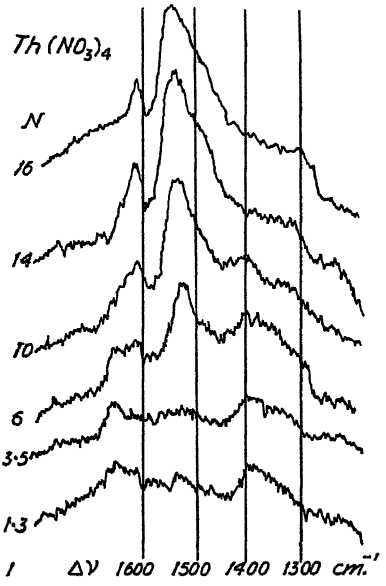

FIG. 3.

The modifications of the spectrum indicated in the preceding section cannot be explained by the hypothesis of a cessation of the degeneracy of the vibrations of the nitrate ion for the following reasons: the simple frequency $\Delta\nu_1$ would never under any conditions split into two; the lines $\Delta\nu_4$ and $\Delta\nu_4'$ are almost always both depolarized; the number of lines in the region of $\Delta\nu_3$ exceeds two (always three, sometimes four).

TABLE V

Cation	Ca	Sr	Cd	Cu	Ce	La	Th
N . .	16·1	5·6	7·1	13·0	3·6	5·7	16·3
$\Delta\nu_4$ . .	716(*D*)	718(*D*)	715(*D*)	718(*D*)	714(*D*)	715(*D*)	716(*D*)
$\Delta\nu_4'$ . .	746(*D*)	735(*D*)	739(*D*)	755(*P*)	741(*D*)	743(*D*)	751(*D*)

In addition, the measurements of the relative intensity of the lines as a function of concentration do not agree with such an hypothesis. The intensity of the bands $\Delta\nu_1'$, $\Delta\nu_3'$ and $\Delta\nu_4'$ increases relatively much more quickly as a function of the concentration than does that of the bands $\Delta\nu_1$, $\Delta\nu_3$ and $\Delta\nu_4$. This phenomenon occurs simultaneously for the three frequencies. Fig. 2 and 3 show this for Cu and Th in the region $\Delta\nu_3$; Fig. 5 and 6 do likewise for Ca and Th in the region $\Delta\nu_4$ (see later). When the line $\Delta\nu_1'$ is not clearly separated from the line $\Delta\nu_1$, its appearance and its increase in intensity cause a displacement of the centre of gravity of the two lines, which varies continuously with the concentration. This renders doubtful the conclusions which have been drawn[6] from variations in the frequency of $\Delta\nu_1$.

Existence of Two States of the Nitrate Ion.—The preceding facts suggest that, in concentrated solutions of certain nitrates, at least two states of the nitrate ion exist. The passage from one state to the other is discontinuous, as is shown by the constancy of the frequency of the lines, particularly $\Delta\nu_4$ and $\Delta\nu_4'$. (The diffuse bands $\Delta\nu_3$ do not lend themselves so well to a precise measurement.) A progressive variation of the dynamic parameters, due to an increasing deformation of the nitrate ion, would involve a continuous modification of the frequency of the lines.*

Let us suppose then, that the intensities I and I' of the lines $\Delta\nu_4$ and $\Delta\nu_4'$ are proportional respectively to the numbers n and n' of the two forms of the nitrate ion, as expressed by

$$\sigma = I'/I = n'/n.$$

Fig. 5 and 6 show the variation of the ratio $\sigma = I'/I$ as a function of the concentration. The relationship is linear, which gives

$$n/n' = Kn_0, \quad . \quad . \quad . \quad (1)$$

where $$n_0 = n + n'. \quad . \quad . \quad . \quad (2)$$

We have investigated the influence of various factors on the proportions n and n' of the two forms of the nitrate ion.

(i) The addition of an electrolyte having one ion (either cation or anion) in common with the considered nitrate increases the ratio σ just as a simple increase in concentration does. This result (see Table VI) agrees with that of Bauer [16] and of Grassmann.[4]

(ii) The addition of neutral salts (i.e. without a common ion) likewise increases the ratio σ, but less than in the preceding case. Some results are given in Table VII.

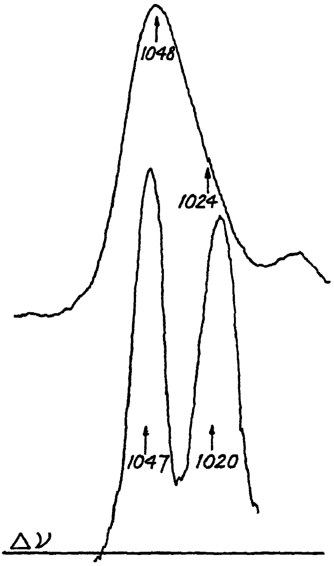

Fig. 4.

Upper curve : solution.
Lower curve : crystal.

(iii) A rise in temperature increases the ratio σ as does the addition of salts, as indicated in Table VIII.

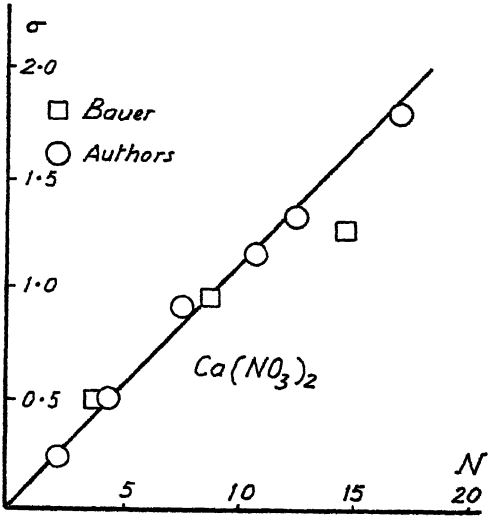

Fig. 5.

---

* Let us recall that the hypothesis of two forms of the nitrate ion has been made in order to explain the absorption spectrum.[10]

TABLE VI

N	7·00 A —	7·00 A 1·34 B	8·34 A —	6·35 A 2·42 C	8·77 A —	5·10 A 4·56 D	9·66 A —
σ	0	0·3	0·3	0·37	0·32	0·35	0·35

(A = $Cu(NO_3)_2$, B = $RbNO_3$, C = $CuSiF_6$, D = $Cu(ClO_3)_2$.)

N	4·40 E —	4·40 E 7·08 F	11·48 E —
σ	0·49	1·1	1·2

(E = $Ca(NO_3)_2$, F = HNO_3.)

TABLE VII

N	4·40 E —	4·40 E 2·55 G	4·40 E 2·55 H	6·95 E —	6·34 K —	6·34 K 3·64 H	9·98 K —
σ	0·56	0·67	0·82	1·04	1·0	1·2	1·6

(E = $Ca(NO_3)_2$, G = CsCl, H = LiCl, K = $Th(NO_3)_4$.)

TABLE VIII

Solution .	N				
$Ca(NO_3)_2$.	4·40	T° C σ	40 0·49	70 0·56	— —
$Th(NO_3)_4$.	6·3	T° C σ	43 0·96	65 1·12	95 1·27

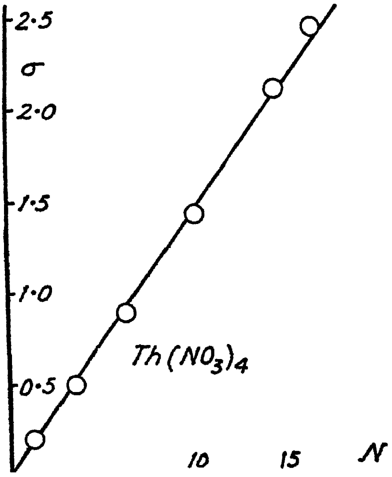

FIG. 6.

These last results show that the energy U necessary to form the second state (n') of the nitrate ion from the first (n) is positive. Applying these results to those expressed by relations (1) and (2), one may write:

$$n/n' = n_0 e^{-U/kT} \quad (U > 0). \quad . \quad . \quad . \quad . \qquad (3)$$

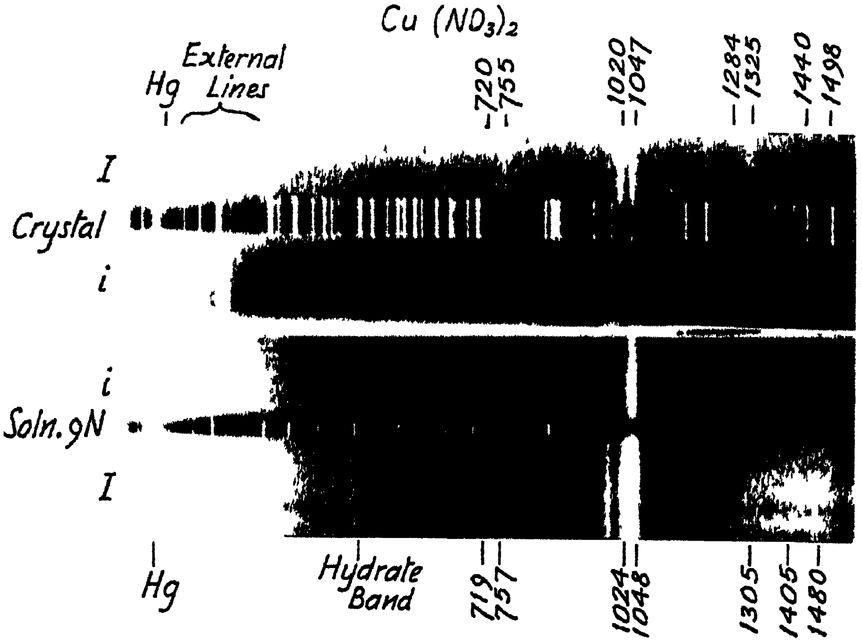

FIG. 7.

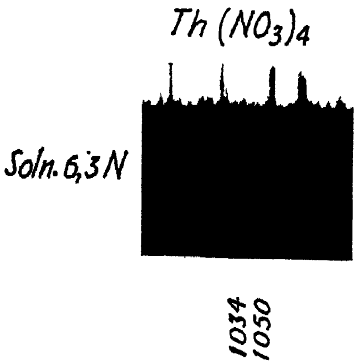

FIG. 8.

[*To face page* 203

Discussion

Nature of the Two States of the Nitrate Ion.—(i) The experimental results do not agree with the hypothesis of an electrolytic dissociation following Ostwald's law. This law leads, at a given temperature, to the relation

$$\frac{1-\alpha}{\alpha^2} = An_0,$$

where $\alpha = n/n_0$ and $1 - \alpha = n'/n_0$; whereas relations (1) and (2) give the following:

$$\frac{1-\alpha}{\alpha} = Kn_0. \quad . \quad . \quad . \quad . \quad . \quad (4)$$

Similarly, the influence of neutral salts does not occur in the direction predicted by the theory of dissociation. On this point our experiments confirm the conclusions of Bauer.[16]

(ii) It could be admitted that, in concentrated solution, some cation-anion associations are formed which are closer than those whose existence Bjerrum has supposed, in that they would be formed without interposition of water molecules. They would differ, however, from undissociated molecules or from ionic molecules in that their formation would involve only electrostatic forces, account being taken of the polarization of the ions. Let us suppose that the frequencies $\Delta\nu'$ (740, 1030, 1500 cm.$^{-1}$) are characteristic of these associations and the frequencies $\Delta\nu$ (715, 1050, 1400 cm.$^{-1}$) characteristic of the non-associated nitrate ions. If the associated form possesses only three frequencies, then it must retain to a high degree the ternary symmetry. This condition is satisfied if the cation M is placed on the axis of the nitrate ion and not in its plane. If the valence force system is used to calculate the nitrate frequencies, the direction, $\Delta\nu \rightarrow \Delta\nu'$, of the variation in frequencies can be explained by admitting a decrease in the force constant f of the valence bond and an increase in the deformation force constant d. But the previous hypothesis leads on the contrary to a decrease in f. The frequency $\Delta\nu_1$ is expressed as follows:

$$\Delta\nu_1 = \sqrt{f/m},$$

where m = mass of an oxygen atom. Placed in the non-uniform field H of the cation M, each of these atoms, of negative charge e, is subjected to a force of attraction proportional to its elongation s with a coefficient equal to $e\mathrm{d}H/\mathrm{d}s$ and the frequency $\Delta\nu_1$ undergoes a change:

$$\Delta\nu_1' - \Delta\nu_1 = -\frac{e}{2m\Delta\nu_1}\cdot\frac{\mathrm{d}H}{\mathrm{d}s}.$$

As $\mathrm{d}H/\mathrm{d}s > 0$ and $e < 0$, the frequency must increase. Thus it is evident that the elementary electrostatic considerations cannot account for the observed facts.

On the other hand, the hypothesis of a cation-anion association by contact does not easily explain the specific differences in the action of each cation. One would expect, for example, the electrostatic effects to increase with the polarizing power of the cation, as measured by the ratio q/r of its charge to its radius.

Now the order of increasing values of q/r in no way corresponds to that of the appearance of the second state of the nitrate ion in the solutions of these cations at comparable equivalent concentrations. In particular, the cations Al and Be with great polarizing power, produce no important modifications of the nitrate spectrum. Neither can one understand by the hypothesis of association by contact, why the line $\Delta\nu_4'$, for example, is in most cases depolarized, but in other cases polarized as it is in the nitrate solutions of copper and of mercury.

(iii) Several authors [3, 4, 17] have already compared the spectra of nitrate solutions to those of crystallized nitrates. The comparison has rested solely on the line $\Delta\nu_1$ and usually for the powdered crystals. On this subject, Gerlach has stated two facts. (*a*) In dilute solution, the frequency $\Delta\nu_1$ tends towards the value which it has in the crystallized nitrates of large cations. (*b*) With the introduction of water of crystallization into a nitrate, the frequency $\Delta\nu_1$ approaches the value which it has in dilute solutions.

We have extended this comparison to much more complete spectra, obtained from single crystals. In general, there is no strict relationship between the spectra of the saturated solutions and those of the anhydrous nitrates, as shown in Table IX. For each cation, the first column gives the frequencies observed in the concentrated solution, the second in the anhydrous crystal. On the contrary, the spectra of nitrate solutions and of the hydrated nitrate crystals, which grow in them at ordinary temperatures, are quite analogous. Rousset and his co-workers [19] have already made a similar observation with copper sulphate. The analogy may be drawn from the results presented in Table X.

Consideration of the results given in Table X suggests that, as the concentration of the solutions increases, the disposition of the nitrate ions tends towards that which is characteristic of the hydrated crystals which are deposited from the saturated solutions.

TABLE IX

Li		Na		K		Rb		Ca		Sr		Ba		Pb	
(20)	(3)		(20)	(19)	(20)	(17)	(17)		(3)		(21)		(21)		(21)
720	—	717	728	730	713	—	—	—	—	718	715	—	703	—	704
—	—	—	—	—	—	—	—	—	—	735	736	721	731	717	730
1051	1086	1050	1070	1049	1048	1048	1056	1050	1064	1050	1055	1047	1048	1044	1049
—	—	1357	—	—	1340	—	—	—	—	—	—	1323	—	—	1327
1357	—	1410	1390	1357	1354	—	—	—	—	1353	1369	—	1356	—	—
—	—	—	—	—	—	—	—	—	—	—	1403	—	1387	1390	1395
—	—	—	—	—	—	—	—	—	—	1423	1423	1462	1412	—	—

The Quasi-crystalline Structure of Concentrated Solutions.—Let us try to make more precise the preceding idea.

(i) By X-ray diffraction, Prins [22, 23] and then Beck [24] have detected some regularities in the arrangement of ions in aqueous solutions of electrolytes. Prins obtained the most definite results with thorium nitrate. These may be interpreted by assuming that the Th ions, surrounded by the other constituents of the solution, form close packings, whose distribution is statistically regular and homogeneous. These experiments give information on the distribution of heavy cations. Ours, based on the diffusion of light by anions, complete them and allow more precise conclusions. If the interpretation which we propose is accurate, then the structure given as possible by Prins must be replaced by that of the hydrated crystal.

---

[19] Rousset, Lochet and Magne, *Compt. rend.*, 1947, **224**, 270.

[20] Magat, *Tables annuelles de constantes—Effet Raman* (Hermann, Paris, 1937).

[21] Couture and Mathieu, *Ann. Physique*, 1948, **3**, 521.

[22] Prins, *J. Chem. Physics*, 1395, **3**, 72.

[23] Prins and Fonteyne, *Physica*, 1935, **2**, 570.

[24] Beck, *Physik Z.*, 1939, **40**, 479.

(ii) The specific action of the various cations may be probably accounted for by the differences between the crystal structures of the salts which we have studied. It is likely that none of them are isomorphous. Unfortunately, the crystal data on the hydrated nitrates are yet incomplete and the structure of none of them is known.

At least their Raman spectra provide some information. The existence of two lines of the same type in the neighbourhood of the symmetrical frequency $\Delta\nu_1$ in the spectra of the nitrates of aluminium, copper and cerium allows the conclusion, for example, that the crystal lattice contains at least two families of nitrate ions, whose surroundings do not possess the same symmetry. These structural details are found in the saturated solutions, certainly for the copper salt and probably for that of cerium. On the other hand, the line $\Delta\nu_1$ which is still present, though feeble, in the concentrated solutions of $Th(NO_3)_4$, has disappeared in the spectrum of the crystal.

TABLE X

Lithium Nitrate, $LiNO_3 . 3H_2O$									
7 N soln. . .	720	—	—	1051	—	1357	—	1422	—
Crystal . .	717	—	—	1054	—	1332	—	1416	—
Fused crystal .	722	—	—	1055	—	1370	—	1440	—
Calcium Nitrate, $Ca(NO_3)_2 . 4H_2O$									
16 N soln. .	716	746	—	1050	—	1358	—	1428	—
Crystal . .	721	746	—	1052	—	1354	—	1424	—
Zinc Nitrate, $Zn(NO_3)_2 . 6H_2O$									
7 N soln. . .	719	—	—	1050	—	1340	—	1408	—
Crystal . .	710 to 720 (double ?)			1053	—	1350	—	1370	—
Copper Nitrate, $Cu(NO_3)_2 . 9H_2O$									
13 N and 14 N soln. . .	719	757	1024	1048	—	1315	1405	—	1480
Crystal . .	720	755	1020	1047	1284	1325	1381	1440	1498
Aluminium Nitrate, $Al(NO_3)_3 . 9H_2O$									
4 N soln. . .	719	—	—	1050	—	1315	—	1410	—
Crystal . .	730	—	1046	1057	—	1321	1388	1434	—
Fused crystal .	721	—	—	1050	—	1323	—	1435	—
Cerous Nitrate, $Ce(NO_3)_3 . 6H_2O$									
Sat. soln. . .	714	741	1047 (double)		—	1348	—	1468	—
Crystal . .	716	738	1044	1054	—	1353	—	1444	—
Thorium Nitrate, $Th(NO_3)_4 . 4H_2O$									
16 N soln. .	(716)	751	1034	(1050)	—	(1370)	—	1500	1543
Crystal . .	714	748	1036	—	—	—	—	1487	1542
Zinc Neodymium Nitrate, $Zn_3Nd_2(NO_3)_{12} . 24 H_2O$ *									
2·5 N soln. .	716	746	—	1048	—	—	—	—	—
Crystal . .	719	749	1041	1045	—	—	—	—	—

* In this case, the selective absorption of the Nd^{+++} ions does not permit the determination of the frequency of the bands situated in the region 1300-1400 $cm.^{-1}$ for the solution.

Naturally, the regular surroundings which we assume for the nitrate ions has a statistical character; there are important instantaneous fluctuations about the mean distribution of the ions and molecules. This explains the fact that the Raman lines always have a much greater width for the solutions than for the crystals (Fig. 4). In particular, the width of the high frequency bands in the copper nitrate solutions (cf. Fig. 2) can mask the splitting into lines which one observes in the crystal.

(iii) Prins [22] emphasizes that his conception of the state of solutions is quite opposed to that which envisages microscopic nitrate crystals dispersed in a disordered medium.[26] From our experiments, it is not possible to draw such definite conclusions: where quantitative measurements are available, it is found that the ratio of the intensities of the lines is not always the same in the crystal as in the saturated solutions. For instance, the ratio σ has the following values *:

$Ca(NO_3)_2$: Solution (16N) 1·8 ; Crystal (16·1N) 2·2.
$Th(NO_3)_4$: Solution (16·3N) 2·5 ; Crystal (20N) $\sim$ 5.

It is hardly possible to tell whether such differences are due to the influence of the fluctuations in the liquid state or to the superposition of the spectrum characteristic of the crystal on that of the solution.

(iv) In addition to the lines characteristic of the complex ions or molecules, there appear in the diffusion spectra of ionic or molecular crystals, "external" lines corresponding to oscillations of the lattice, in the course of which the ions or molecules execute translational or rotatonal vibrations.[25, 27] The spectra of hydrated nitrates are rich in such lines,[28] whose frequency varies from 40 to 200 cm.$^{-1}$ (13 lines for aluminium nitrate, 12 for the double nitrate of zinc and neodymium), see also Fig. 7. These external lines are not found in the spectra of any of the solutions. Doubtless the reason is that because these vibrations bring forces or couples of interionic or intermolecular attraction into play, their frequencies are sensitive to fluctuations in density; and as these lines are numerous, their increase in width is sufficient to obscure them in a continuous spectrum.

Interpretation of the Influence of the Various Factors.—(i) The effect of the elevation of temperature on the Raman spectrum of the solutions studied shows that the modification of the nitrate ions by the increase in concentration is accompanied by an absorption of energy ΔU. The change in heat content

$$\Delta H = \Delta U - T\Delta S$$

may be calculated from the data of Table VIII, by means of the van't Hoff equation:

$$\Delta H = \frac{R}{J} \cdot \frac{T_1 T_2}{T_2 - T_1} \cdot (\log_e K_1 - \log_e K_2)$$

where $K = n'/n = I'/I.$
For $Th(NO_3)_4$, $\Delta H = -1200$ cal./mole.

In principle, one might attempt to evaluate ΔH theoretically for a given solution from the difference between the heat content of the quasi-crystalline state and of the disordered state. But certain of the necessary data, such as the lattice energy and the heat of fusion are unknown; others, such as the mutual potential energy of the ions in solution, are difficult to calculate correctly; only the energies and entropies can be estimated.[29] Theimer,[6] who has attempted some calculations of this type in the hypothesis of an incomplete dissociation, recognizes that they are too uncertain to justify their use.

---

* These values are only approximate, because they refer to a single crystal in a given orientation and may vary with the orientation.

[25] Mathieu, *Spectres de vibration* (Hermann, Paris, 1945).

[26] Stewart, *J. Chem. Physics*, 1934, **2**, 147.

[27] Rousset, *La diffusion de la lumière* (Gauthier-Villars, Paris, 1947).

[28] Mathieu, *Compt. rend.*, 1949, **229**, 1068.

[29] Bernal and Fowler, *J. Chem. Physics*, 1933, **1**, 515.

(ii) The action of electrolytes having an ion in common with the nitrate studied (Table VI) may be interpreted as that of an increase in concentration. As for the influence of foreign electrolytes (Table VII), which is contrary to the hypothesis of an incomplete dissociation,[16] it acts in an indirect manner, and one can think that it favours the approach of a nitrate ion to a cation by dehydrating them. We have observed, in fact, that this influence is stronger for LiCl (small cation, strongly hydrated) than for CsCl (voluminous cation, weakly hydrated).

Laboratoire des Recherches Physiques,
Sorbonne,
Paris.

GENERAL DISCUSSION

Prof. R. Mecke (*Freiburg i. Br.*) said : I should like to ask Prof. H. H. Nielsen whether any tertiary derivatives of arsine ($AsR_1R_2R_3$) are known which show optical activity ? This would settle the question of a high potential barrier for AsH_3. As is well known, no simple tertiary derivatives of NH_3 showing optical activity can be found on account of the inversion of the ammonia molecule.

Prof. G. B. M. Sutherland (*Michigan*) said : Prof. Nielsen's paper is extremely important in connection with the problem of determining the height of the potential barrier hindering the inversion of the arsine molecule, which is in turn related to the feasibility of obtaining optically active derivatives of arsine. Without the complete analysis which Prof. Nielsen has made of the fine structure of certain key bands in phosphine and arsine, it was natural to assume that these contained two Q branches the separation of which might be used to give information on the inversion potential in both these molecules. Now that it has been shown that only one of these Q branches is real in each case and that the other arises from an accidental conglomeration of rotation lines, some other method of attack on the problem of the inversion potential must be sought.

In this connection, I should like to report some preliminary results obtained by Mr. C. C. Costain and myself in an attempt to derive the height of the inversion barrier from deformation force constants. If one assumes that the molecule inverts by gradually increasing the amplitude of the symmetrical deformation frequency, then the force constant derived from this frequency can be used to plot a parabolic potential of the form $V = k(r)^2$ on either side of the planar configuration. If this is done for ammonia, the calculated barrier differs only by 2 % from that derived from the inversion splittings by the Manning[1] potential function, viz. 2070 cm.$^{-1}$. This remarkably close agreement encouraged us to make similar calculations for phosphine and arsine. The corresponding barrier heights come out to be close to 6000 cm.$^{-1}$ and 17000 cm.$^{-1}$ respectively. If these results are now used to predict the splittings which should be observed in the various vibrational levels of the symmetrical deformation frequency in each molecule, it appears that in phosphine the fundamental should have a splitting of $4\cdot7 \times 10^{-6}$ cm.$^{-1}$ and in arsine of 6×10^{-22} cm.$^{-1}$. It is therefore not surprising that Prof. Nielsen finds no sign of inversion splitting in the fine structure of these bands. However, the inversion splitting increases very rapidly as one goes to higher vibrational levels (i.e. comes nearer the top of the potential barrier) and for the 5th vibrational level of the deformation frequency in phosphine the splitting is computed to be about 33 cm.$^{-1}$. It would seem worth while to examine some of the higher overtones of this frequency with a very long absorption path in order to get confirmation of this method of attack.

Dr. G. Herzberg (*Ottawa*) said : In view of the high precision of the data obtained from microwave spectra it appears of interest to compare these data with those obtained from photographic infra-red spectra in cases where both have been studied. In the photographic infra-red the high dispersion of large diffraction gratings can be used and the data obtained have, in a few cases, an accuracy up to 1 in 10,000. The following Table gives the rotational constants B_0 as determined from infra-red and microwave spectra as well as the differences between these two quantities. The data given have all been transformed to the same units to facilitate the comparison. It must be remembered that the microwave spectrum gives usually only $2B_0 - 4D_0$. In several cases the photographic infra-red spectrum does give D_0 separately and in these cases the microwave values have been corrected accordingly. It is seen from the Table that the agreement is most satisfactory and well within the accuracy assumed for the infra-red values. For HCN there are two B_0 values in the literature obtained from photographic infra-red spectra, but only one of these [3] agrees exactly with the microwave value.

---

[1] Manning, *J. Chem. Physics*, 1935, 3, 136.

The excellent agreement between infra-red and microwave values gives one confidence in the accuracy of the infra-red values even for symmetrical molecules which cannot be investigated by microwave spectroscopy. For non-symmetrical molecules the microwave spectrum in general does not lead to a value of B_e corresponding to the equilibrium position while the infra-red spectrum does yield such values.

TABLE I.—ROTATIONAL CONSTANTS B_0 DETERMINED FROM INFRA-RED AND MICROWAVE SPECTRA

Compound	Infra-red (I.)	Microwave (M.)	I. - M.
CO	$1·9226_5$	$1·922624_5$*	$-0·0000_{25}$
ICl	0·11389 †	0·1138940	$-0·00000_4$
HCN	$1·4789_0$ 1·4779	1·47896*	$-0·0000_6$ $-0·0010_6$
N_2O	$0·4191_{25}$	$0·419034_{09}$*	$+0·0000_{91}$
CHF_3	$0·3451_6$	$0·345218_7$*	$-0·0000_{59}$
CH_3CCH	0·2848	$0·2850_1$	$-0·0002_1$
HNCO	$0·36664_5$	$0·3666_4$	$-0·0001_9$
	cm.$^{-1}$	cm.$^{-1}$	cm.$^{-1}$

* Corrected with D_0 from infra-red.
† From electronic absorption bands.

It should be remarked that the microwave values given in the Table are based on the value $c = 2·99776 \times 10^{10}$ cm./sec. for the velocity of light. If the value $2·99796 \times 10^{10}$ cm./sec. recently suggested is used a slightly worse agreement of infra-red and microwave values is obtained.

Dr. H. W. Thompson (*Oxford*) (*partly communicated*): In my introductory remarks I gave the impression that rotational constants of simpler molecules determined from microwave measurements were more exact than those derivable from vibration-rotational bands in the infra-red. As Prof. Herzberg now points out, this may be a somewhat pessimistic view. It is quite true that from measurements on overtone and combination bands in the photographic infra-red region, the higher accuracy of wavelengths measurement should enable us to get more accurate values of B_0, the rotational constant in the ground state, but measurements on the fundamental vibration bands may be less exact. In the course of a re-examination of the band of nitrous oxide at 4·5 μ, using the very high resolution obtainable with a grating spectrometer and lead telluride detector, Mr. Williams and I found a value for B_0 rather higher than that suggested by microwave measurements. The question is whether B_0

---

[3] Herzberg and Spinks, *Proc. Roy. Soc. A*, 1935, **147**, 434.

can be determined to the fourth decimal place in cm.$^{-1}$. Perhaps the discrepancy is caused by insufficiently accurate wavelength calibration.

We have now re-examined our data on nitrous oxide and other molecules with most interesting conclusions. If as wavelength standards in the region of 4·5 μ we use the values for rotational lines of carbon monoxide calculated by Herzberg from his exhaustive study of the overtones and combinations, we then obtain a value for B_0 of nitrous oxide in perfect agreement with microwave work. It seems definite therefore that some of the standards previously laid down by other workers, such as the lines of carbon dioxide and carbon monoxide, are unsatisfactory. This is borne out too by our results with other molecules, and complete details of this work will shortly be published elsewhere.

Dr. H. W. Thompson (*Oxford*) said : Could Prof. Plyler give us any further details about the optical properties of the new caesium bromide crystals, such as its dispersion characteristics ?

Prof. C. A. Coulson (*King's College, London*) said : Prof. E. Bright Wilson has quite properly pointed out in his paper the interesting way in which nuclear quadrupole effects may be used to throw light on certain aspects of chemical valence. We must, however, be careful not to claim more in this field than can be justified. Thus the quadrupole coupling coefficient measures the lack of spherical symmetry in the distribution of valence electrons around a particular atom (e.g. Cl in CH_3Cl). In this molecule we cannot therefore infer anything about the degree of $s-p$ hybridization in the C—Cl bond, as is sometimes incorrectly supposed, but only about the total asymmetry, including all the bonds from this atom and all the non-bonding electrons also. Indeed, it is not difficult to show that, in general, it is only when there are one or more pairs of non-bonding electrons that we shall be able to make any inferences from quadrupole coupling measurements : and even then they tell us nothing directly about the hybridization in the bond, or bonds, but only about any possible change in the sum total of all s, p, . . . electrons around the atom.

Prof. D. F. Hornig (*Brown University, Rhode Island*) (*communicated*): Since writing that section of my paper on the structure of the HCN crystal I have been informed by Prof. W. Lipscomb that preliminary X-ray studies of this crystal show the structure described there to be incorrect. According to the X-ray determination the structure below −100° C is orthorhombic with two molecules per unit cell, consisting of parallel chains of HCN molecules, each of which lies on a C_2 axis. This structure is consistent with the reasoning presented in my paper but had been excluded because it was considered physically unreasonable for the four chains adjacent to any given chain to be situated at different distances.

Dr. G. L. Coté and **Dr. H. W. Thompson** (*Oxford*) (*communicated*) : In connection with the work of Hornig, we may mention that we have recently measured the spectra of the borofluorides of sodium, potassium and ammonium, and of the bifluorides of potassium and ammonium, between room temperature and that of liquid air. From the effect of temperature on some of the bands we have been able to observe splitting of degenerate modes in the crystal state and also to identify certain modes. With ammonium borofluoride we appear to have split a frequency of the ammonium ion quoted by Hornig as being single, and in the case of potassium bifluoride our results provide further evidence that the bifluoride ion is symmetrical. Details will be given shortly elsewhere.

Dr. A. Kastler (*Paris*) said : Dr. Hornig has shown that, in the infrared spectra of crystals, combinations between internal and lattice vibrations have been observed from which the frequencies of the lattice vibrations can be deduced. As he points out, the knowledge of the torsional frequencies of the ions and molecules in the lattice enables us to calculate the intermolecular forces acting in the crystal. The investigations of the low frequency lines in the Raman spectra of crystals give direct information on torsional frequencies[3] and two interesting attempts have been made recently to deduce lattice forces from these results: a detailed investigation of the low frequency Raman spectra of aromatic crystals and their interpretation led Dr. Fruhling[4] to the conclusion that in the benzene crystal the value of the force constants between hydrogen atoms of neighbouring molecules is of the order of 4 × 10^2 dyne cm.$^{-1}$. For an inorganic crystal Giulotto and Olivelli[5] were able to show that the interpretation of the low frequency Raman lines of calcite leads to force constants of the order of 4 × 10^4 dyne cm.$^{-1}$ for the forces acting between the Ca ions and the O atoms of the CO_3 ions in the crystal. It is interesting to compare these intermolecular force constants with the constants of intramolecular bond-forces which are known to be of the order of 10^5 to 10^6 dyne cm.$^{-1}$. The macromechanical properties of crystals (their hardness) are related to the intermolecular forces, and it is a well-known fact that organic crystals, where these forces are small, are of low hardness. Benzene crystals can be cut with a knife.

Dr. D. W. E. Axford (*Maidenhead*) and **Dr. N. Sheppard** (*Cambridge*) (*communicated*): Prof. Hornig has pointed out in his paper that frequencies observed in the infra-red and Raman spectra of a rigid molecule in the liquid state may disappear on transition to the solid state because of the operation of more strict selection rules in the crystal lattice. Because of this possibility, he suggests that caution must be exercised in deducing the existence of rotational isomers in the liquid state from the observation that the solid state spectrum of a molecule has fewer frequencies than exist in the liquid.

This is a valuable comment, but in case it should be interpreted too generally as reducing the significance of such evidence for rotational isomerism in specific cases, it is perhaps worth while to consider the probable extent to which such changes in selection rules could modify the spectra.

Since in the crystalline lattice a molecule is in a less symmetrical environment than in the isolated (gaseous) state, it follows that any fundamental internal vibrational mode allowed in the gaseous state will also be allowed in the crystalline state, and in the liquid state also. The only fundamental frequencies that can occur in the liquid state spectrum but not in that of the crystalline solid are hence those which are present in the liquid state because of violation of the selection rules for the isolated molecule by the intermolecular forces. The frequency ν_{10} of benzene is of this type. As usually for covalent compounds the selection rules are only slightly perturbed in the liquid state, it follows that in the majority of cases only a few medium or weak frequencies in the spectrum of a rigid molecule will behave in this manner on solidification. When, as in most cases for which evidence for rotational isomerism is claimed, a considerable number of strong frequencies disappear on solidification, there can be little doubt about the reality of the effect.

As has been pointed out already,[6] care has to be taken to ensure that the solid state spectrum is that of the substance in the crystalline as opposed to the vitreous state. This can generally be detected by visual observation and by the fact that the transmitted intensity for a glass is usually much higher than for a polycrystalline mass due to the greater scattering in the latter case. There may, however, in any individual case, be some doubt as to whether the substance has actually crystallized and in such cases it is obviously desirable to supplement the infra-red evidence with other experimental data. Accordingly in such cases, where the probability or otherwise of the occurrence of rotational isomerism cannot be inferred from the behaviour of related compounds, definite conclusions as to its existence should be drawn only after considering, in addition, (*a*) variations with temperature of the relative intensities of line pairs in the liquid state in the Raman effect or the infra-red spectrum, (*b*) the feasibility of explaining the spectrum in terms of one species, and (*c*) the agreement between experimental and calculated thermodynamic functions.

---

[3] Kastler and Rousset, *Physic. Rev.*, 1947, **71**, 455.

[4] Fruhling, *Thesis* (1950); *Ann. Physique* (in press). A short summary is given in *J. Chem. Physics*, 1950, **18**, 1119.

[5] Giullotto and Olivelli, *J. Chem. Physics*, 1948, **16**, 555; *Rendiconti Istituto Lombardo di Scienze*, 1949, **82**, fasc. 1.

[6] Brown and Sheppard, this Discussion.

Mr. T. A. Kletz (*I.C.I. Billingham*) said : We have examined the infra-red spectra of a number of alkylphenols in the liquid and crystalline states and in dilute solution in carbon tetrachloride using a lithium fluoride prism. The difference in wave-number between the sharp monomeric hydroxyl band obtained in dilute solution and the broad association band obtained in the condensed states is a measure of the strength of the hydrogen bonds formed. The results show that, as pointed out by Herzberg and Reid for HNCO, the hydrogen bonding is stronger in the crystal than in the liquid. Some typical results are :

	Wave no. difference (*cm.*$^{-1}$) *between dilute solution and*	
	Liquid	*Solid*
4-Ethylphenol	290	410
Phenol	270	400
3 : 5-Dimethylphenol	250	373
4-Methylphenol	237	367
2 : 3-Dimethylphenol	190	310
2 : 4-Di-*tert.*-butylphenol	70	100

Owing to the disordered nature of the liquid state the molecules cannot be all arranged in positions in which hydrogen bonding is a maximum, but it is quite possible for this to occur in the ordered arrangement of the crystal lattice ; this may account for the shift of the hydroxyl band on crystallization. In the spectrum of the crystal the hydroxyl band is sharper than in the spectrum of the liquid but still much broader than in the spectrum of the dilute solution.

The broad shape of the hydroxyl band in the spectrum of the liquid is usually attributed to the molecules being involved in hydrogen bonding to different extents, the shape of the band giving the distribution of the molecules forming hydrogen bonds of different strengths.[7] This explanation is unlikely to apply to the crystal as it is to be expected that the hydrogen bonds will then be equivalent. Is it possible that the broad hydroxyl band obtained in the spectrum of the crystal is due to variable changes in the vibration energy of the crystal lattices (*Reststrahlen* frequency) accompanying the change in the vibration energy of the O—H bond, the O—H bond being broadened while the C—H bonds are not because the coupling between the molecules in the crystal lattice takes place through the O—H group ?

Prof. J. A. A. Ketelaar (*Amsterdam*) said : The fact that broad bands due to hydrogen bonding do exist in crystals even at low temperatures is very clearly illustrated by the infra-red absorption of KH_2PO_4. In this case an extremely broad band without fine structure is observed setting in at $1{\cdot}5\mu$ with a maximum at $3{\cdot}56\mu$. However, at liquid-air temperature, and thus far below the Curie point of this ferro-electric substance, and also with dielectrical saturation (1 kV/cm.), no change in this band can be observed. The true nature of this extreme broadening in an ordered crystal is unexplained. Perhaps coupling with a continuous spectrum of low frequency, elastic, vibrations might be taken into consideration or it might be a highly anharmonic vibration due to a peculiar potential function.

---

[7] Fox and Martin, *Proc. Roy. Soc. A*, 1937, **162**, 419 ; Sutherland, *Trans. Faraday Soc.*, 1940, **36**, 889.

Dr. Mansel Davies (*Aberystwyth*) (*communicated*): As Prof. Ketelaar indicated, the width of the "associated" ν(O—H) band in hydroxylic compounds is a striking feature which probably arises from the combination of a number of low frequency (including deformation) vibrations with the stretching mode. This was one of the suggestions advanced by Badger and Bauer[8] which has been strongly supported by later evidence.[9] It does not appear to be generally appreciated that, in agreement with this interpretation, the width of the band is usually greater the stronger the hydrogen bond (giving higher deformation frequencies), whilst deuterium substitution markedly reduces its width.[10] Furthermore, a marked increase in the integrated intensity occurs on association: a number of factors are involved here, including the flatter potential minimum in the $U(r)$ curve when the hydrogen bonding occurs (giving increased amplitudes of vibration) and the increased polarity accompanying this change.

Dr. P. Torkington (*B. Rayon Res. Assoc.*) (*communicated*): In connection with the association band due to hydrogen bonding, which has come under discussion, the following approach seems more successful in relating the hydrogen bond to molecular orbital theory (a step surely considered necessary by now), than others proposed hitherto. In the hydrogen-bonded system X—H . . . Y, $r_{H.Y}$ has such value that the normal van der Waals' force across it would be one of repulsion. For this to become attraction, it is necessary that the X—H bonding electrons should be localized more between X and H than in a normal covalent bond, leaving the proton more exposed and partially attracted to the electron shell of Y. It might be noted that it is common to read of the localization of bonding electrons *between* bonded atoms; the accurate fact is that the bonding orbitals *enclose* the bonded atoms—over-localization between them would lead to a weaker bond, the interatomic distance being increased, effectively to avoid too high an internuclear electron density. This change in type of bond orbital can apparently only occur when unshared electron pairs are available on both X and Y. The function of the pair on X will be obscure for the present, but the pair on Y, in this interpretation, presumably makes the electron shell sufficiently proton-attracting (note the concept of mobile orientable electronegativity), to bring about the transition of orbital type to give over-localization of bonding electrons between X and H. The association band can be accounted for fairly readily by the above theory. Displacement of the proton from a given equilibrium position towards Y will lead to a weaker bond X—H of lower frequency, the attractive force across H . . . Y being simultaneously increased. After a certain limit has been reached, further displacement towards Y will result in sudden increase in energy of the system due to too high a contribution required from the ionic structure involving X^-, but clearly the total energy of the system can in principle remain unchanged for displacements of the proton within certain limits, by balancing of the energies of the X—H and H . . . Y bonds on the slope of the energy surface arising from increasing ionic structure involving X^-. The function of the unshared pair on X should now be clear. The limits for the position of the proton determine the maximum and minimum X—H frequencies. This orbital theory of the hydrogen bond can thus be accommodated with the concept of a flat potential minimum for the proton. It should be noted that a proper combination of both the molecular orbital and resonance theories, as described briefly above, is necessary for a satisfactory description of the hydrogen bond.

In conclusion, it does not appear to have been pointed out that in the system X—H . . . Y the hydrogen bond H . . . Y will not be cylindrically symmetrical unless the system is linear. Where hydrogen-bonding determines crystal structure to any extent stereochemical considerations nearly always preclude linear systems. At any rate, there will in general be an intrinsic potential barrier hindering rotation about hydrogen bonds, which is probably not present where ordinary van der Waals' forces operate. In view of the importance of hydrogen bonding in cell structure the new aspect has been briefly described here ; it is hoped to publish details in due course.

---

[8] *J. Chem. Physics*, 1937, **5**, 839.

[9] Davies and Sutherland, *J. Chem. Physics*, 1938, **6**, 762. Davies, *ibid.*, 1940, **8**, 586.

[10] E.g. Wall and Claussen, *J. Amer. Chem. Soc.*, 1939, **61**, 2812.

Prof. R. Mecke (*Freiburg i. Br.*) said : The considerable broadening of the OH— stretching bands in the solid state is quite understandable if one remembers that the hydrogen atom (proton) is vibrating between two oxygen atoms both of which have considerable proton-attracting power. This will certainly cause some damping effect resulting in broad bands. We observe similar effects in the case of internal hydrogen bindings (chelation). As will be shown [11] we observed in chelation two different classes of internal hydrogen binding ; in the one case the hydrogen binding gives rise to a displacement of the frequency still with a quite narrow band, so that the *cis*- and *trans*-position of the OH band is detectable ; In the other case, which contains substituents like NO_2, CHO, COOR, COR in the *ortho*-position, the band is totally blurred in a very broad absorption region and therefore hardly recognizable. We suppose that this is the " real " hydrogen-bond, the proton vibrating between the two oxygen atoms in a mesomeric manner.

Prof. A. R. Ubbelohde (*Belfast*) said : In condensed phases it may frequently happen that the molecular attraction termed hydrogen bonding is a co-operative effect. The large frequency shift in going from liquid to solid HNCO can hardly be interpreted if only the attraction between pairs of molecules are considered. Solids containing hydrogen bonds tend to have anomalously small volume changes on melting, owing to the partial collapse of " open structures " on liquefaction.[12] But melting does involve some breakdown of the co-operative effects in the solid.

Although much of the attraction in hydrogen bonds must be purely electrostatic, there is reason to believe that particularly in the case of short hydrogen bonds (2·5-2·6 Å) some resonance contribution is present.[13] This resonance may also involve three-dimensional effects in the crystal lattice, i.e. the possibility of co-operative resonance contributing to the crystal lattice energy must be considered.

The broadening of the absorption band associated with certain types of hydrogen bonds in crystals is paralleled by the anomalously large thermal expansion in the direction of such bonds in the crystals, and by the anomalous isotope effect (expansion of the lattice on substituting D for H[12, 13]).

Prof. J. A. A. Ketelaar (*Amsterdam*) said : The further decrease of the OH frequency in going from the liquid to the solid state is, at least for the most important part, due to the fact that in the solid state the mean distance of the molecules bridged by the hydrogen is smaller and thus the interaction larger.

Dr. J. Lecomte (*Paris*) said : Dr. Freymann, at the Sorbonne, was able, by absorption in the near infra-red of aqueous solutions of nitric acid, to follow the variations in the constitution of this acid, and to show the association between the molecules of pure nitric acid, or between the molecules of nitric acid and the molecules of water, and to measure the dissociation of the acid in ions.

Prof. M. Pestemer (*Leverkusen/a. Rhein*) said : There is a possibility of showing the presence of hydrogen bonds by measuring the ultraviolet absorption, if groups, the vibrations of which are coupled with the

[11] Cf. Ubbelohde, *J. Chim. Phys.*, 1949, **46**, 429, and earlier ref.

[12] Cf. Robertson and Ubbelohde, *Proc. Roy. Soc. A*, 1938, **167**, 136.

[13] Cf. Ubbelohde, *J. Chim. Phys.*, 1949, **46**, 429, and earlier ref.

electronic transition, become fixed in their position in the molecule. Merkel and Wiegand [14] have demonstrated that in this case there is a vibrational fine-structure in the absorption bands, because the superposition of the vibrations is determined in its direction. However, in the case of a superposition of vibrations of freely movable and rotating groups, which orientate on the molecule more or less accidentally, the fine-structure disappears. This effect can be clearly observed in the measurements of Morton and Earlam [15] with derivatives of the anthraquinones

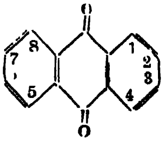

The OH groups of the mono- and di-oxy-derivatives in the positions 1, 4, 5, 8 are able to form hydrogen bonds with the quinone oxygen atoms and show vibrational fine structure. If the hydrogen bond is rendered impossible by methylation, the fine structure disappears. Likewise the oxy-derivatives with OH groups in the positions 2, 3, 6, 7, where no hydrogen bond is possible on account of the too large distance to the oxy-groups, do not show a fine structure.

Dr. J. Romand and Dr. B. Vodar (*Paris*) (*communicated*): To the various methods suitable for the study of the hydrogen bond we can add ultra-violet absorption spectroscopy. An example is the study of the hydrogen fluoride gas which is known as a strongly associated substance. This study is now in progress and we have already some preliminary results. As the results are only interesting in relation to those obtained for the other hydrogen halides, which are not strongly associated, we will give here a brief survey of the whole work related to HCl, HBr, HI and HF in the Schumann region.

Our normal work in the far ultra-violet region is done by spectrographic method [16] with a grating spectrograph. We use an hydrogen discharge lamp for the light source, a set of wire screens for the plate calibration and an optical system made of fluorite or lithium fluoride, the transparency of which makes possible measurements down to 1350 Å.

In the spectra of the gaseous hydrogen chloride, bromide and iodide we have observed the narrow bands of the *B*, *C*, *D*, *E* groups (first described by Price [17]) but we have particularly studied the continuous band *A*. This latter shifts towards the long wavelengths when we pass from Cl to Br and I (the λ of the maximum being 1535 Å for HCl, 1785 Å for HBr and 2150 Å for HI). The agreement with the previous results of the near ultra-violet works is very good and the whole curve is accurate enough to be compared with theoretical calculations. These calculations were made principally by the reflection method and also by the complete integration method.[18] Both methods are able to reproduce the experimental curves of HCl and HBr when the maximum and another point of the curve are given. For HI this is only possible when we take into account the two states $^2P_{1/2}$ $^2P_{3/2}$ of iodine (which are widely separate). This shows that the agreement of the calculations is not so bad in spite of the fact that we have to neglect various factors, such as the variation of the electronic matrix.

---

[14] Merkel and Wiegand, *Natwiss.*, 1947, 34, 122.
[15] Morton and Earlam, *J. Chem. Soc.*, 1941, 159.
[16] Romand, *Ann. Physique*, 1949, 4, 529.
[17] Price, *Proc. Roy. Soc. A*, 1938, 167, 216.
[18] Kohei Siga and Plumley, *Physic. Rev.*, 1935, 48, 105.

Hydrogen fluoride was studied down to 1500 Å in silver or stainless steel cells with aluminium oxide windows and Teflon gaskets. We first found that the bands in the near ultra-violet previously described, and attributed to the associated molecule, disappear when the gas is sufficiently pure. The pure gas having a 500 mm. path length, under 500 mm. Hg pressure and at room temperature is transparent down to 1650 Å, where a continuous absorption band starts. We were not able to obtain the maximum of this absorption. In the region studied, the intensity of the absorption strongly increases when the gas is heated to 100° C where, as is well known, the vapour density becomes normal. This clearly shows the effect of association on the absorption spectrum. For this temperature effect our data are so far only of a preliminary character, but it is probable that the knowledge of the temperature variation of the absorption coefficient would make possible the calculation of the degree of association for a given temperature. The fact that there are no discrete bands in the whole spectrum down to 1500 Å is a good reason to think that there are no or very few cyclic H_6F_6 molecules in the associated vapour. This confirms the conclusions obtained from other measurements, such as dielectric constants. Even at a temperature above 100° C, where the HF vapour should not be associated, the continuous absorption at 1500 Å is weak. From this we can expect that the maximum is somewhere far in the ultra-violet at a wavelength which would be shorter than the wavelength computed by analogy from the HCl, HBr, HI series; this shows how different the electronic structure is in comparison with the other hydrogen halides.

Prof. J. Rud Nielsen (*Oklahoma University, U.S.A.*) said: The very high intensity of the infra-red band of borazole associated with NH-stretching of species E' is paralleled by the high intensity of the corresponding stretching mode in 1 : 3 : 5-trifluorobenzene. We have also observed the overtone of this band, although apparently with considerably lower intensity than that of the corresponding borazole band. Our observations did not extend to high enough wave numbers to reveal the overtone of the E' CH stretching mode.

The difference between calculated and observed frequencies of some of the combination bands listed in Table IV of the paper by Price, Fraser, Robinson and Longuet-Higgins seems rather high. I wonder if Dr. Price has any explanation of this fact.

Prof. R. Mecke (*Freiburg i. Br.*) (*communicated*): For comparison with our investigations concerning the CH and OH bond I am interested in the values of the maximal extinction coefficients ϵ_{max}, and of the absorption areas $\int \epsilon d\nu$ of the BH and NH stretching vibration bands and their overtones of borazole.

Prof. J. Rud Nielsen (*Oklahoma University, U.S.A.*) said: As indicated in our paper, we realize that the value 1191 cm.$^{-1}$ assigned to the highest E'' fundamental of 1 : 3 : 5-trifluorobenzene is considerably higher than what one should expect. Mr. Liang is at present carrying out a normal co-ordinate treatment of the out-of-plane vibrations largely for the purpose of checking this assignment.

The observation of the frequency 275 cm.$^{-1}$ in the infra-red spectrum of 1 : 3 : 5-trimethylbenzene shows that this belongs to species E' rather than to E'' as assumed by Pitzer and Scott. This frequency, and the E' fundamental at 515 cm.$^{-1}$, undoubtedly correspond to the E' fundamentals occurring at 326 and 503 cm.$^{-1}$ in 1 : 3 : 5-trifluorobenzene.

Dr. J. Lecomte (*Paris*) said: I remember that sixteen years ago, I published with Dr. H. C. Cheng, a paper on the infra-red adsorption of 1 : 2-dihalogen derivatives of ethane. It was possible, in the liquid state, to recognize in the spectrum, the bands belonging to the *trans* form, with the use of selection rules. The symmetrical vibrations of symmetrical 1 : 2-derivatives give only Raman lines, and the asymmetrical vibrations produce only infra-red absorption bands. Instead, with asymmetrical 1 : 2-dihalogen derivatives, all the vibrations are allowed in the two phenomena.

Dr. N. Sheppard, Dr. Delia Simpson (*Cambridge*), **and Prof. Sutherland** (*Michigan, U.S.A.*) (*communicated*) : The paper by Prof. Rank and his colleagues is an important contribution to the study of the vibration spectra of the hydrocarbons. Since, however, certain of the conclusions therein are diametrically opposed to those reached by us [19] from earlier data, we should like to make the following comments based on the remarks made by Prof. Sutherland and Dr. Sheppard at the Discussion.

We agree entirely with Prof. Rank and his co-workers in concluding that there is a great need at the present stage in investigating hydrocarbon spectra for better experimental data on the simpler molecules, more especially those containing isotopic atoms. We do not consider, however, that the new facts presented by these authors are sufficient to settle finally the assignment of the 1249 and 921 cm.$^{-1}$ frequencies in *neo*pentane, nor to justify their condemnation of the simplifying device of treating CH_3 groups as point masses in making approximate calculations of the skeletal frequencies of branched hydrocarbons.

The correct interpretation of the spectrum of *neo*pentane is of vital importance in the discussion of the spectra of the larger paraffins. The point at issue is the assignment of the 1249 and 921 cm.$^{-1}$ frequencies. Prof. Rank and his colleagues allot them respectively to a CH_3 wagging mode and to a skeletal vibration of the same symmetry class F_2. We had formerly given the reverse interpretation.[19] We shall, in the following discussion, consider in turn the arguments used by Prof. Rank and his co-workers.

I. POSITIVE ARGUMENTS FOR THE ASSIGNMENT OF RANK, SAKSENA AND SHULL.—(i) 921 *cm.*$^{-1}$ *as a skeletal vibration.*—(*a*) We consider that the argument based on intensity considerations to be inconclusive. Too little is known as yet about the factors which influence the absolute intensities of vibration frequencies especially in the infra-red. It may, however, be noted that in the infra-red spectra of the *n*-paraffins (this Discussion) some of the bands assigned to skeletal vibrations appear with a strength comparable to those arising from CH deformation modes.

(*b*) The argument based on the isotopic splitting of the 921 cm.$^{-1}$ frequency to give a new polarized component at 815 cm.$^{-1}$ is open to criticism, since it implies a splitting of more than 100 cm.$^{-1}$ in a skeletal frequency, arising from the substitution of one D atom in place of a H atom in one of the CH_3 groups in the molecule. There is no theoretical justification for expecting the splitting to be much greater than 10 cm.$^{-1}$. Some years ago one of us [20] made some calculations comparing the skeletal frequencies of the molecules $C(CH_3)_4$, $[T_d]$ and $C(CH_3)_3 . CH_2D$. These employed a simple valency force field with CH_3, CH_2D as point masses and the same force constants as those used in our previous work.[19b] As a first approximation the configuration of monodeutero-*neo*pentane was assumed to be C_{3v}, thus partially taking into account the reduction of symmetry in this molecule. The results are shown in Table I where the calculated shifts are compared with those actually observed. It would be presumptuous to claim any great accuracy for these calculations, but we do think that they suggest that the splitting of the skeletal frequencies of *neo*pentane produced by the isotopic substitution $CH_3 \rightarrow CH_2D$ is much smaller than from 921 to 815 cm.$^{-1}$ as now proposed. Furthermore, there is some experimental evidence against the argument, since in propane the substitution of one D atom in one of the CH_3 groups gives rise to an analogous shift from 923 to 834 cm.$^{-1}$ in a band which certainly cannot be due to a skeletal frequency.[21]

---

[19] (*a*) Sheppard, *J. Chem. Physics*, 1948, **16**, 690. (*b*) Simpson and Sutherland, *Proc. Roy. Soc. A*, 1949, **199**, 169.

[20] Simpson, unpublished work.

(*c*) An analogy is drawn between the splitting on deuteration of the 921 cm.$^{-1}$ frequency in *neo*pentane and of the 694 cm.$^{-1}$ frequency of tetramethyl silane. It is claimed that since the ratio of the frequencies of the two components in the two monodeuterated compounds is identical [viz. 922/815 for $C(CH_3)_3 . CH_2D$ and 690/609 for $Si\ (CH_3)_3 . CH_2D$], the parent frequencies in the undeuterated molecules must be assigned to the same type of vibration. We suggest that this numerical agreement may be fortuitous, so that the resultant conclusion is not necessarily valid. Examination of the theoretical treatment of the vibrations of the X_4Y and X_3YZ molecules using a simple valency force field,[22] shows that the corresponding theoretical ratio depends not only on the ratio of the masses of the isotopically substituted groups, viz. X/Z, but also on the mass of the central atom Y and the ratio of the stretching to the deformation force constants. Hence we should not expect identical ratios for the two molecules $C(CH_3)_3 . CH_2D$ and $Si(CH_3)_3 . CH_2D$.

(ii) 1250 *cm.*$^{-1}$ *as a* CH_3 *vibration.*—(*a*) For a discussion of the intensity argument, see I (i) (*a*).

(*b*) The second argument is based on the appearance of a frequency at 1250 cm.$^{-1}$ in the Raman and infra-red spectra of both *neo*pentane and tetramethyl silane. Since in the silicon compound Prof. Rank and his co-workers have unequivocally demonstrated that all the skeletal frequencies lie below 700 cm.$^{-1}$, they conclude that the 1250 cm.$^{-1}$ frequency must be associated with a CH_3 wagging vibration, and therefore assume that the apparently analogous frequency in *neo*pentane cannot be attributed to a skeletal mode. We should like to suggest an alternative assignment of the infra-red spectrum of tetramethyl silane which, if our interpetation is correct, shows that the frequencies numerically coincident at 1250 cm.$^{-1}$ in *neo*pentane and tetramethyl silane are to be attributed to two different types of vibration.

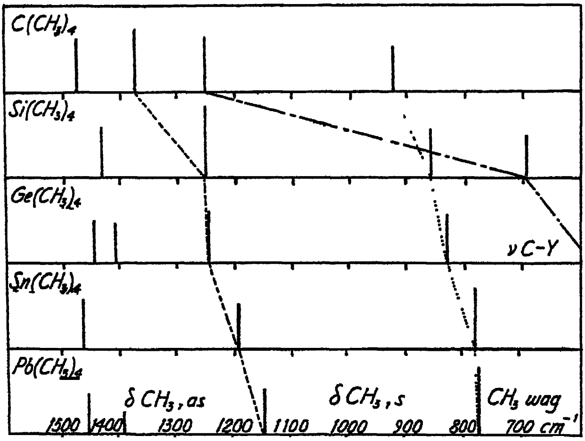

FIG. 1.—The prominent bands in the infra-red absorption spectra of $Y(CH_3)_4$ molecules between 1500 and 500 cm.$^{-1}$.

Fig. 1 shows in a schematic fashion the position of all the strong absorption bands in the series of molecules *neo*pentane to lead tetramethyl[23] between 1500 and 600 cm.$^{-1}$. In *neo*pentane the well-known F_2 symmetrical deformation mode of the methyl groups occurs near 1375 cm.$^{-1}$; this shifts to lower frequencies when the methyl group is attached to a heavier atom. In our opinion this mode undoubtedly follows the correlation indicated by a dashed line in the figure, connecting the strong absorption bands[24] between 1376 and 1147 cm.$^{-1}$. Prof. Rank and his co-workers have identified the polarized Raman line at 1263 cm.$^{-1}$ in the spectrum of tetramethyl silane as the A_1 CH_3 symmetrical deformation vibration; this falls quite near the corresponding F_2 infra-red frequency now put at 1250 cm.$^{-1}$. In the infra-red spectrum of tetramethyl silane the same authors have shown that the F_2 carbon–silicon skeletal vibration gives an intense band at 695 cm.$^{-1}$, and they suggest that an equally intense absorption at 862 cm.$^{-1}$ (which has a strong Raman counterpart) is to be attributed to a combination band. We consider that this last assignment is improbable. If, as suggested in Fig. 1, the 862 cm.$^{-1}$ frequency corresponds to the CH_3 wagging mode (the remaining allowed F_2 fundamental), then it falls naturally in line as a member of a series of strong absorption bands (shown by the dotted line) which gradually shift to lower frequencies on passing to the tetramethyl compounds of the heavier elements.[24]

---

[21] McMurry, Thornton and Condon, *J. Chem. Physics*, 1949, **17**, 918. Friedman and Turkevich, *ibid.*, 1949, **17**, 1072.

[22] Kohlrausch, *Smekal-Raman-Effekt, Ergängzungsband* (Julius Springer, 1938), p. 72.

The weak shoulder at 1285 cm.$^{-1}$ in the infra-red spectrum of tetramethyl silane, which was considered by Prof. Rank and his co-workers to be a fundamental, can be interpreted as an allowed combination band of the two skeletal stretching modes.

(*c*) Prof. Rank and his colleagues consider that in passing from *neo*pentane to monodeutero-*neo*pentane the 1249 cm.$^{-1}$ frequency in the symmetrical molecule gives an isotopic splitting to an E frequency at 1251 cm.$^{-1}$ and an A_1 frequency at 919 cm.$^{-1}$. However, the corresponding splitting in the silicon compounds is not observed. If the interpretations of these authors are accepted, there seems no good reason for its non-appearance. Furthermore, we consider that the empirical rule that the ratio of the frequencies of the CH and CD stretching modes is the same as for the bending vibrations requires theoretical justification before it is safe to conclude that it is applicable to H/D substitution in all types of molecules.

II. Positive Arguments for the Assignment of Sheppard, Simpson and Sutherland.—One point of difference remains for discussion. In the infra-red spectrum of monodeutero-*neo*pentane Prof. Rank and his co-workers observed a band of moderate strength at 1224 cm.$^{-1}$ for which they were unable to offer any interpretation. In Table I we have suggested that the 1224 cm.$^{-1}$ band is the A_1 component of the F_2 skeletal vibration which appears at 1249 cm.$^{-1}$ in *neo*pentane, the E component being at 1251 cm.$^{-1}$. The polarized Raman line corresponding to the 1224 cm.$^{-1}$ band would be obscured by the intense depolarized lines at 1217 and 1251 cm.$^{-1}$. This possible assignment, as Table I shows, gives a reasonable isotopic shift of the same order as that observed for the other frequencies.

To sum up, we should like again to draw attention to the arguments for our assignment of the *neo*pentane spectrum previously published;[1] in particular we emphasize that by choosing reasonable values of the force constants with a simple valency force field, it is possible to reproduce the skeletal frequencies of *neo*pentane to within 4 %, which is all that can be expected for this treatment (see Table I). We consider that I (i)(*b*), dealing with the isotopic shift of the skeletal frequencies and I (ii)(*b*) on the series of absorption bands of the molecules $Y(CH_3)_4$ answer the criticisms of Prof. Rank and his co-workers, and provide some further evidence in favour of our original assignment, which we still prefer on the data available. However, in agreement with Prof. Rank, we do not think that it will be possible to decide finally between the alternative assignments, until the experimental data for the completely deuterated *neo*pentane $C(CD_3)_4$ are available, when it will be possible to apply the Redlich-Teller product rule with confidence.

---

[23] Kettering and Sleator, *Physics*, 1933, 4, 39. Young, Koehler and McKinney, *J. Amer. Chem. Soc.*, 1947, 69, 1410. Sheline and Pitzer, *J. Chem. Physics*, 1950, 18, 595.

[24] Sheppard, unpublished work.

Prof. D. H. Rank (*Pennsylvania State College, U.S.A.*) (*communicated*): I wish to reply to Dr. Sheppard, Dr. Simpson and Prof. Sutherland in answer to their criticisms of our interpretation of the spectra presented in our paper.

I agree that the totally deuterated *neo*pentane is necessary for a completely unambiguous solution of this assignment problem. We are now engaged in the preparation of this molecule which will require a great deal of time and effort.

TABLE I.—OBSERVED AND CALCULATED FREQUENCIES OF *neo*PENTANE AND MONODEUTERO-*neo*PENTANE

Observed Frequencies cm.$^{-1}$ (Rank, Saksena and Shull)			Calculated Frequencies cm.$^{-1}$ (Simpson)	
$C(CH_3)_4$	$C(CH_3)_3 . CH_2D$	Isotopic Shift	Isotopic Shift	$C(CH_3)_4$ *
A_1 n_1 733	A_1 ν_1 720	− 13	−6·3	724 n_1
E n_2 335	E ν_4 331	− 4	−1·0	346 n_2
F_2 n_4 415	A_1 ν_5 ?	?	−3·9	398 n_4
	E ν_6 409	− 6	−4·0	
F_2 n_3 921 (R,S and S)	E ν_2 922	+ 1		
	A_1 ν_3 815	−106		
F_2 n_3 1249 (S, S and S)	E ν_2 1251	+ 2	0	1258 n_3
	A_1 ν_3 1224	− 25	−7·6	
			Notation and force constants, ref. 1(*b*)	

I agree that infra-red intensity considerations are not completely conclusive since we cannot quantitatively calculate the absolute intensities. However, the 921 cm.$^{-1}$ band of *neo*pentane differs by between one and two orders of magnitude in intensity from the 694 cm.$^{-1}$ band of silicon tetramethyl which we have assigned as its analogous vibration. We have recently obtained the 415 cm.$^{-1}$ infra-red absorption band of *neo*pentane in the KBr region which verifies our assignment of this band completely. This band has an intensity comparable to the 921 cm.$^{-1}$ band which further supports our thesis.

With regard to the appearance of strong polarized lines at 815 cm.$^{-1}$ and 609 cm.$^{-1}$ in the spectrum of *neo*pentane-d_1 and tetramethylsilicon-d_1. It is perfectly true that the empirical observation of exact ratios of these lines with the assigned parent line may be a fortuitous but nevertheless an existing fact. Furthermore, there are certainly very limited possibilities for the origin of these strong lines which appear in strict analogy in the spectrum of the monodeutero derivatives of both carbon and silicon tetramethyl. Objection has been raised that our assignment of these frequencies to $V_2(a)$ produces isotopic splittings which are too large for framework vibrations. I must point out that in tetramethylmethane our assignment of the 815 cm.$^{-1}$ frequency seems to be unique since I know of no cases of deuterium isotope effects in molecular spectra where V_H/V_H is less than 0·7 and usually hydrogen isotope effects yield a frequency ratio considerably larger than this value in spectra of polyatomic molecules. If this frequency was split from the 1250 cm.$^{-1}$ frequency $V_H/V_H \sim 0{\cdot}65$ and in silicon tetramethyl-d_1 the situation is incomparably worse.

Objection has been raised to our assignment of the 862 cm.$^{-1}$ strong band (Raman and infra-red) in the spectrum of silicon tetramethyl to a combination band. I wish to point out that intensities of combinations and harmonics are not always weak compared to fundamentals. As an example in the Raman spectrum of liquid methane it is well known that two harmonics appear which are much stronger than their fundamentals. The broad character of the 862 cm.$^{-1}$ Raman band is striking on the original plates in comparison with other depolarized lines. This diffuse character has been observed many times when lines known to be combinations or harmonics have been photographed in other spectra.

The situation in the infra-red spectrum of tetramethylmethane-d_1 is somewhat complicated in the 1200 cm.$^{-1}$ region. Since all bands free of overlapping show *P, Q, R* structure it is certain that the bands at 1218, 1224 and 1253 cm.$^{-1}$ respectively consist of overlapped structure. We have assigned the 1218 cm.$^{-1}$ band to one of the f_1 vibrations since it is in coincidence with a Raman line. The 1298 cm.$^{-1}$ band which shows beautiful *P, Q, R* structure and is in coincidence with a Raman line we have also assigned to an f_1 vibration. The absorption peak at 1251 cm.$^{-1}$ is also in coincidence with a Raman line and has been assigned to $V_3(e)$. The band at 1224 cm.$^{-1}$ which appears to be strong might easily be due to a superposition of an *R* and *P* branch from 1217 cm.$^{-1}$ and 1251 cm.$^{-1}$, i.e. the intensity of the *R* branch of the 1217 cm.$^{-1}$ band modified by the proximity of the 1251 cm.$^{-1}$ band. Since the structural situation in the spectrum here is quite complex and certainly not completely resolved, there does not seem to be any good reason for assigning 1224 cm.$^{-1}$ to a molecular frequency.

With regard to observation of (*a*) type frequencies in the infra-red absorption spectrum we have not been able to find any of these in tetramethylmethane-d_1, which we can assign to skeletal frequencies, even when the one metre path has been used. However, with tetramethylsilicon-d_1 an (*a*) type skeletal vibration, i.e. 570 cm.$^{-1}$ makes a strong appearance with a 10 cm. path. This observation seems to bear out our contention of the tremendous difference of the intensities of the skeletal modes in infra-red absorption for the carbon and silicon tetramethyls.

Dr. Simpson's calculations of isotope effects for the skeletal vibrations of *neo*pentane-d_1 are interesting. She obtains 6·3 cm.$^{-1}$ for the totally symmetrical vibration. This is compared with the value of 5·8 cm.$^{-1}$ calculated from a cruder approximation in our paper. However, it is apparent that the splittings obtained with both methods of calculation are sensibly the same. However, I must point out that either result is in error by more than 100 % for *neo*pentane and by nearly 500 % for tetramethylsilicon. It is quite certain that the expressions used up to the present time in calculating these isotope effects do not adequately satisfy the observed experimental data.

The reassignment of the medium intensity infra-red band at 1285 cm.$^{-1}$ in the spectrum of silicontetramethyl to a combination band, i.e. 593 cm.$^{-1}$ + 694 cm.$^{-1}$ seems to be untenable. This band appears in the spectrum of silicon tetramethyl-d_1 with very similar characteristics and at 1285 cm.$^{-1}$ (unshifted). If the reassignment were correct this band should appear at 1260 cm.$^{-1}$ which is not in accord with observations.

Dr. Orville Thomas (*Aberystwyth*) (*communicated*) : The electron diffraction results quoted by Rank, Saksena and Shull indicate a greater C—C bond length in the group —C—CH$_2$Cl than in —C—CH$_3$. Contrary to their suggestion, it would be unlikely then for an increase in force constant to occur in the chlorinated derivative of *neo*pentane. For a given pair of atoms it is difficult to see how the equilibrium force constant can do anything but decrease on increasing the bond length.

TABLE I

$$\text{(I)}\ k = 2{\cdot}738 \times 10^5\,(z_1z_2)^{\frac{1}{2}}\,r^{-2.46}\ \text{dynes/cm.}$$
$$\text{(II)}\ k = 2{\cdot}490 \times 10^5\,(z_1z_2)^{\frac{1}{2}}\,r^{-1.81}\ \text{,,}$$
$$\text{(II}_s\text{)}\ k = 3{\cdot}178 \times 10^5\,(z_1z_2)^{\frac{1}{2}}\,r^{-2.06}\ \text{,,}$$

	r_e	$\omega_{\text{obs.}}$	$\omega_{\text{pred.}}$	% diff.	$z_1 z_2$	Series	$k_{\text{pred.}}$	$k_{\text{emp.}}$	Bond
CH_3I .	2·14	533	531	−0·4	4×7	I	2·23	2·23	C—I
CH_3Br .	1·93	610	620	1·6	4×7	I	2·85	2·85	C—Br
CD_3Br .	—	577	575	−0·3	4×7	I			
CH_3Cl .	1·786	732	754	3·0	4×7	I	3·47	3·35	C—Cl
CD_3Cl .	—	701	708	1·0	4×7	I			
CH_3F .	1·42	1049	1116	5·5	4×7	I	6·09	5·96	C—F
CH_3OH .	1·428	1034	1088	5·8	4×6	I	5·64	—	C—O
CH_3SH .	1·81	707	716	1·3	4×6	I	3·12	3·00	C—S
CH_3NH_2	1·469	1037	1021	−1·5	4×5	I	4·67	4·86	C—N
CH_3NO_2.	1·48	918	913	−0·5	4×5	I	5·55	—	C—N
CH_3CH_3.	1·55	993	986	−0·7	4×4	II	4·45	4·50	C—C
$ZnCl_2$.	2·13	278	275	−1·1	2×7	I	1·59	1·6	Zn—Cl
$ZnBr_2$.	2·25	173	173	0·0	2×7	I	1·39	1·4	Zn—Br
$CdCl_2$.	2·23	237	236	0·4	2×7	I	1·42	1·2	Cd—Cl
$CdBr_2$.	2·30	160	161	0·6	2×7	I	1·20	1·2	Cd—Br
CdI_2 .	2·56	119	117	1·7	2×7	I	1·02	1·05	Cd—I
$HgCl_2$.	2·23	330	323	−1·5	2×7	II	2·13	2·3	Hg—Cl
$HgBr_2$.	2·38	205	202	−1·5	2×7	II	1·89	1·9	Hg—Br
HgI_2 .	2·55	142	147	3·5	2×7	II	1·66	1·5	Hg—I
BF_3 .	1·29	888	869	−2·1	3×7	II_s	8·52	8·83	B—F
BCl_3 .	1·73	471	449	−4·7	3×7	II	4·16	4·63	B—Cl
BBr_3 .	1·87	279	277	0·7	3×7	II	3·61	3·66	B—Br
CF_4 .	1·34	908	908	—	4×7	II_s	9·17	9·14	C—F
SiF_4 .	1·54	800	779	−2·6	4×7	II_s	6·81	7·16	Si—F
CCl_4 .	1·76	458	475	3·7	4×7	II	4·66	4·38	C—Cl
$SiCl_4$.	2·00	424	423	−0·2	4×7	II	3·68	3·71	Si—Cl
$TiCl_4$.	2·21	386	386	—	4×7	II	3·06	3·07	Ti—Cl
$GeCl_4$.	2·08	396	407	2·8	4×7	II	3·42	3·27	Ge—Cl
$SnCl_4$.	2·30	367	371	1·1	4×7	II	2·85	2·80	Sn—Cl
CBr_4 .	1·94	267	289	7·6	4×7	II	3·89	3·36	C—Br
$SiBr_4$.	2·19	249	259	4·0	4×7	II	3·12	2·92	Si—Br
$GeBr_4$.	2·32	234	245	4·5	4×7	II	2·80	2·58	Ge—Br
$SnBr_4$.	2·44	220	234	6·4	4×7	II	2·55	2·28	Sn—Br
$C(CH_3)_4$.	1·54	731	714	−2·3	4×4	II	4·45	4·50	C—C
$Si(CH_3)_4$.	1·93	598	580	−3·0	4×4	II	2·97		C—Si
$Sn(CH_3)_4$	2·18	506	518	2·3	4×4	II	2·37		C—Sn
$Pb(CH_3)_4$	2·29	460	496	7·8	4×4	II	2·17		C—Pb
SF_6 .	1·58	790	788	0·3	6×7	II	6·95		S—F
SeF_6 .	1·67	755	732	2·4	6×7	II	6·28		Se—F
TeF_6 .	1·82	701	692	1·3	6×7	II	5·36		Tl—F
UF_6 .	2·0	656	635	3·2	6×7	II	4·51		U—F

Dr. K. M. Guggenheimer (*Glasgow*) said: With respect to the discussion of the tetramethyl compounds, I should like to mention that a few years ago[25] I published two empirical formulae which relate force constants of diatomic molecules with the number of the outer electrons and the bond length :

$$\left.\begin{array}{l}\text{(I)}\ k = 2{\cdot}738 \times 10^5\,(z_1z_2)^{\frac{1}{2}}\,.\,r_e^{-2.46}\\ \text{(II)}\ k = 2{\cdot}490 \times 10^5\,(z_1z_2)^{\frac{1}{2}}\,.\,r_e^{-1.84}\end{array}\right\}\ \text{dynes/cm.}\ (r_e\ \text{in Å}).$$

---

[25] Guggenheimer, *Proc. Physic Soc.*, 1946, **58**, 456.

Series (I) contains molecules with weak or zero polarity, and Series (II) strongly polar molecules like NaCl.

In a forthcoming paper it will be shown that these formulae can be applied also to polyatomic molecules. The Table gives some of the numerical material. The first group contains some compounds where the methyl group is treated as a unit of molecular weight 15. Then follow some symmetrical molecules where in the valency force system, in contradistinction to the central force system, the " breathing " vibration leads immediately to the value of the stretching force constant. It can be seen from the Table that results obtained in Series (I) or (II) are valid for these molecules within a few per cent. Thus, forces between atoms not linked by chemical bonds, contribute only slightly to the value of the force constant.

The list of XY_4 molecules contains also the tetramethyl compounds of C, Si, Sn and Pb. This supports the usual interpretation of the given vibration frequencies as symmetrical " breathing " vibrations.

Dr. D. C. Smith (*U.S. Naval Research Laboratory, Washington, D.C.*) said: With regard to the paper by Dr. Gore, it appears worthwhile to call attention to two points concerning the characteristic PO stretching frequency. Firstly, since this frequency occurs at 1176 cm.$^{-1}$ in $(CH_3)_3PO$ and at 1395 cm.$^{-1}$ in F_3PO,[1] the spectral interval for this vibration extends from about 1175 to 1400 cm.$^{-1}$, rather than from 1250 to 1300 cm.$^{-1}$. Secondly, the exact position within this interval appears to depend upon the electronegativity of the three other substituents on the phosphorus atom. In studying the infra-red spectra of a variety of compounds containing the PO linkage, Mr. Daasch has found that the frequency occurs roughly in the intervals 1175-1200 cm.$^{-1}$ (no electronegative substituents), 1200-1250 cm.$^{-1}$, 1250-1275 cm.$^{-1}$, and 1275-1350 cm.$^{-1}$, as the number of electronegative substituents increases, respectively, from 0 to 3. Knowledge of this dependency increases considerably the usefulness of the characteristic PO frequency for structure determination.

Prof. J. A. A. Ketelaar (*Amsterdam*) said: The infra-red absorption spectra of parathion (diethyl *p*-nitrophenylthiophosphate) and its dimethyl analogue do show characteristic differences, especially the presence of a sharp band at 1160 cm.$^{-1}$ in the former and several differentiations in the 800-1000 cm.$^{-1}$ region which allows identification of a commercial product as the latter compound.

Dr. H. W. Thompson (*Oxford*) said: It may be noted that the intrinsic intensity of the characteristic P=O stretching vibration is high, which may be valuable in work with compounds of biological interest.

III. VIBRATIONAL SPECTRA OF COMPLEX MOLECULES

THE INFRA-RED SPECTRA OF COMPLEX MOLECULES

H. W. Thompson, D. L. Nicholson and L. N. Short

Received 18*th July*, 1950

Infra-red spectroscopy is applied to complex molecules for analysis and structural problems. Characteristic frequencies of groups sometimes facilitate their identification. Examples are given from recent work on polymers, cellulose and related compounds, carbohydrates, amides, urethanes, amino acids, peptides and derivatives of pyrimidine.

For our present purpose, complex molecules fall into one of two classes, (1) polymers or condensates in which there is some sort of recurring nuclear skeleton and (2) complicated organic structures of intermediate molecular weight such as occur in substances of biological interest. The former class includes the hydrocarbon polymers, rubbers, polypeptides, celluloses and resins; examples in the second group are simpler carbohydrate materials, derivatives of pyrimidine, nucleic acids and other compounds involving heterocyclic rings.

Hitherto, infra-red spectroscopy has been applied here with two main objects, namely (1) for qualitative or quantitative analysis and (2) for elucidating structural problems. It is, moreover, not merely the question of determining the molecular formula of a particular compound, but often of correlating structural features with physical properties or with chemical reactivity. The ease with which infra-red spectra can now be measured between 2-25 μ has enabled us to record data for a very large number of compounds, and we now have to consider how far the vibrational spectra alone can answer the vital questions. With polymers, grouping of characteristic frequencies sometimes simplifies the spectrum, but in many cases the complex array of bands, with consequential ambiguity of frequency assignment, puts a definite limit upon possible interpretations.

Attempts can be made to extend the spectral data by means of auxiliary techniques, such as the deuteration of key groups like OH or NH, the study of spectral changes with change of temperature, the use of polarized infra-red radiation with orientated polymers or crystalline materials, or the application of the reflecting microscope in conjunction with an infra-red spectrometer so that small crystals, fibres or even biological cells can be measured. Each of these methods has proved useful in individual cases, but there seem at present to be both experimental and theoretical difficulties and sometimes, as for example with the pyrimidines or sugars, further data obtained from X-ray analysis or other methods may be needed before the spectral results can be fully explained. Another difficulty with many of these complex molecules is insolubility in organic solvents, since infra-red measurements in solutions in water or deuterium oxide are far from satisfactory.

In this paper we shall mention a few illustrative examples from recent work carried out in this laboratory, some of which is being described in detail elsewhere.

The principles of infra-red analysis are well known. The question is whether with complex molecules the spectra will contain so many bands that in a mixture severe overlapping will preclude resolution. This often occurs, and the difficulty is accentuated when the qualitative composition of the mixture is uncertain. On the other hand, rather complex mixtures can sometimes be analyzed, particularly when one or more components have a strong band lying clear of those of the remainder. Fig. 1 gives part of the spectra of some amino acids. Although the bands are drawn as lines which do not indicate their breadth, it is seen that differentiation and analysis of simple mixtures can be carried out. We would emphasize here that the infra-red spectrum provides an excellent and quick method for identifying amino acids which have been separated from a complex mixture by chromatrography or similar means, as well as giving a check on the efficiency of the separation. Other typical spectral differences between complex stereoisomers are given below. Since with all except the simplest molecules we cannot yet predict the full vibrational spectrum of a nuclear skeleton, it is impossible to know *a priori* whether a given analysis will be feasible, and this must be discovered by trial. Most workers have used the region 6-14 μ for this purpose, but we may mention that in our experience distinguishing features are often to be found in the range 15-25 μ.

Another aspect of analytical work with polymers and condensates is the determination of their content of some special group, e.g. acyl groups in cellulose esters, or alkylene groups in hydrocarbon polymers. This is possible in favourable circumstances, but it may be necessary to assume that the group extinction coefficients remain unchanged in both the molecules studied and those used for setting up the calibration, and if high sensitivity is required these extinction coefficients must be high. These two conditions do not always apply.

Infra-red spectral diagnosis is based upon the existence of characteristic vibration frequencies for linkages and groups. Examples are now legion,

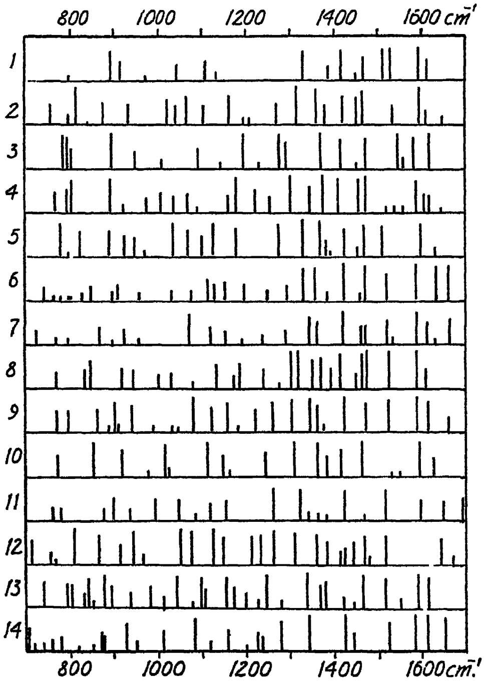

FIG. 1.

(1) DL-Glycine.
(2) DL-α Amino-*n*-butyric acid.
(3) DL-α Amino-*iso*butyric acid.
(4) DL-α Amino α methyl-*n*-butyric acid
(5) DL-Valine.
(6) DL-Norleucine.
(7) DL-α Amino-*n*-caproic acid.
(8) L-Leucine.
(9) DL-α Amino-*n*-caprylic acid.
(10) DL-Alanine.
(11) DL-Aspartic acid.
(12) DL-Glutamic acid.
(13) L-Tyrosine.
(14) DL-Methionine.

and reference tables have been published.[1] It is evident, however, that any such frequency can be modified by factors such as local electronic influences of neighbouring groups, conjugation, ring strain, or the formation of hydrogen bridges, and in any case a strictly localized oscillation in part of the molecule represents an idealized extreme. In complex molecules all these factors may play a part in modifying the correlation rules, and thus lead to ambiguities in structural problems, particularly when the factors operating in a given case are unpredictable. There is probably little hope of constructing the complete molecular formula from the vibrational spectrum alone, and at best we may try to establish a few main groupings to decide between alternative formulae which have been suggested by chemical methods. This is illustrated by the work on penicillin.[2]

---

[1] Barnes, Gore, Liddel and Williams, *Ind. Eng. Chem.* (*Anal.*), 1943, **15**, 659. Thompson, *J. Chem. Soc.*, 1948, 328. Williams, *Rev. Sci. Instr.*, 1948, **19**, 135; Colthup, *J. Opt. Soc. Amer.*, 1950, **40**, 397.

Some small variation occurs in the stretching vibration frequencies of C—H bonds according to their type, e.g. alkyl groups (2800-3000 cm.$^{-1}$), alkylene groups (2900-3000), alkyne (3200-3300) or aromatic ring CH (3000-3100). Deformations of C—H bonds in substituted olefines give rise to characteristic differences at 10-11 μ. A few alkyl groups have sets of frequencies which, in simple hydrocarbons at least, may enable us to identify them, e.g. $—C(CH_3)_3$, $—CH(CH_3)_2$, $—(CH_2)_4—$. Other "hydrogen" vibrations are P—H (~ 2400), and S—H (~ 2500), but the intrinsic intensity of some of these bands are low.

Some useful "double bond" frequencies are: sulphoxide (~ 1050), sulphone (~ 1150 and ~ 1325), —P=O(1260-1280), nitroso —N=O, (1350-1400), N=O in nitrite (~ 1650), nitro group (~ 1550 and ~ 1350), $>C{=}S$ (1300-1400), $\rightarrow P{=}S$ (600-750), and we have recently found a band due to the $>S{=}N$ group near 1000 cm.$^{-1}$. The C=C bond in open chains gives rise to bands at 1640-1680 cm.$^{-1}$ according to the attached groups, and these vary in intrinsic intensity and are affected by conjugation. The C=N bond in open chains or in rings (oxazoles, oxazolones) usually gives rise to a band near 1650 cm.$^{-1}$, but this is more variable.

With compounds of biochemical interest, the most important links spectroscopically are probably O—H, C=O, and N—H, and combinations of them such as —CO—NH—. The free hydroxyl group has a stretching frequency near 3600 cm.$^{-1}$ which is lowered by bonding to 3000 cm.$^{-1}$ or less. Bending of this link usually gives rise to a band at 1000-1200 cm.$^{-1}$, but assignment is often difficult in complex cases. Although small differences have been found for primary, secondary and tertiary alcohol groups, it is doubtful whether they can be used convincingly for diagnosis. Deuteration is sometimes useful in making an assignment.

The free NH_2 group in primary amines usually gives a pair of bands near 3300 and 3400 cm.$^{-1}$, secondary amines having a single band in the range 3100-3500 cm.$^{-1}$ according to the type of attached groups. The imino group in C=NH has a band at 3300-3400 cm.$^{-1}$. Bending vibrations of the N—H link are not easily fixed, but usually lie in the region 1500-1600 cm.$^{-1}$. Hydrogen bridge formation lowers the stretching frequencies and raises the bending frequencies. Again, deuteration sometimes aids assignment. When the N—H link is part of a charged group, as in NH_3^+ or NH_4^+, the frequencies are affected as discussed below.

The C=O group stretching vibration frequency lies between about 1600-1800 cm.$^{-1}$ according to structural type, ring strain, conjugation or state of aggregation. Its value in ketones, esters, COO^-, COOH, anhydrides, some ring systems, and other classes is as a rule sufficiently characteristic for establishing the type in simple cases.[3] It is discussed in more detail later.

The spectra of several classes of polymer have already been described elsewhere, and the measurements have been extended by other workers.[4] More detailed structural work on these compounds requires special methods such as the use of polarized infra-red radiation, before and after special physical treatment. An example of current interest is the polyester from ethylene glycol and terephthalic acid (Terylene). From measurements using polarized radiation with films before and after orientation, it appears that this molecule may not have the planar structure suggested by Astbury and Brown,[5] since certain vibration bands show dichroic behaviour inconsistent with this. A similar example of the use of polarized radiation was that of mycophenolic acid crystals,[6] where the existence of two hydroxyl groups, one free and the other bonded, was revealed by rotation of a crystal in the polarized incident beam. The great importance of hydrogen bridge formation was previously emphasized in connexion with phenolic resins,[7] and this is further illustrated by measurements on cellulose derivatives and simple carbohydrates.[8]

---

[2] Thompson, Brattain, Randall and Rasmussen, *The Chemistry of Penicillin* (Princeton, 1949). chap. 13.

[3] Hartwell, Richards and Thompson, *J. Chem. Soc.*, 1948, 1436. Rasmussen, Tunnicliff and Brattain, *J. Amer. Chem. Soc.*, 1949, **71**, 1068.

[4] Thompson and Torkington, *Proc. Roy. Soc. A*, 1945, **184**, 21; *Trans. Faraday Soc.*, 1945, **41**, 246. Thompson, *J. Chem. Soc.*, 1947, 289. Richards and Thompson, *ibid.*, 1949, 124. Elliott, Ambrose and Temple, *J. Chem. Physics*, 1948, **16**, 877. Ambrose, Elliott and Temple, *Proc. Roy. Soc.*, *A*, 1949, **199**, 183.

Fig. 2 shows the spectra of cellulose, a sample of "hydrocellulose," cellulose acetate and ether, and sodium alginate. Cellulose itself has intense absorption due to the hydroxyl group near 3450 cm.$^{-1}$, and to hydroxyl and ether linkages near 1050 cm.$^{-1}$. Partial degradation by acid hydrolysis produces hydrocellulose which shows spectral changes in these regions, and also in the range 15-20 μ. The alteration in bands due to bridged hydroxyl groups are of special interest.

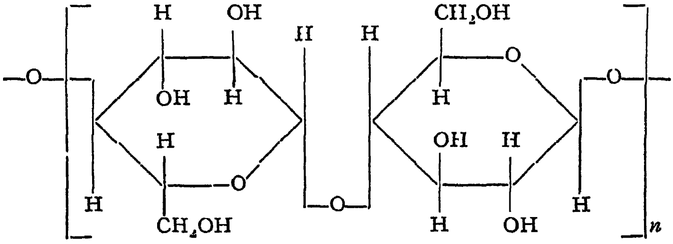

Cellulose.

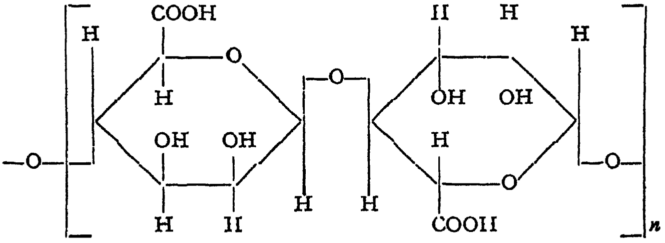

Alginic acid.

Sodium alginate also shows differences of this kind. It may be noted that alginic acid is a polymannuronic acid with 1 : 4 linkages, but there are marked spectral differences between sodium alginate and either mannose or galacturonic acid. Samples of cellulose which had been treated with periodic and chlorous acid have also been measured, and again show alterations in the bands due to bridged hydroxyl groups as well as a small change near 975 cm.$^{-1}$. These results agree broadly with those of Rowen, Hunt and Plyler,[9] but emphasize the value of work with a prism of lithium fluoride to bring out the differences near 3 μ.

The simpler carbohydrates also show important spectral differences. Fig. 3 and 4 show some examples, measured as powders in paraffin or

---

[5] Astbury and Brown, *Nature*, 1946, **158**, 871.
[6] Barer, Cole and Thompson, *Nature*, 1949, **163**, 198.
[7] Richards and Thompson, *J. Chem. Soc.*, 1947, 1260.
[8] Unpublished work by I. F. Trotter and A. F. Eggleston.
[9] Rowen, Hunt and Plyler, *J. Res. Nat. Bur. Stand.*, 1947, **39**, 133.

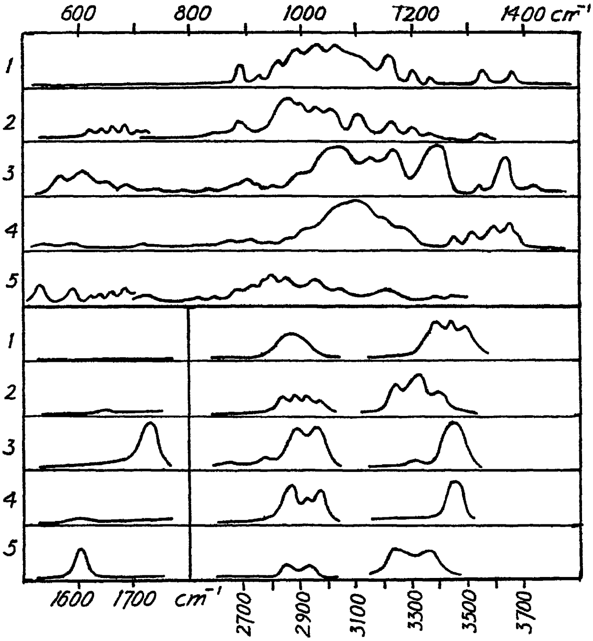

FIG. 2.—Celluloses.

(1) Cellulose. (2) Hydrocellulose. (3) Cellulose acetate.
(4) Cellulose ether. (5) Sodium alginate.

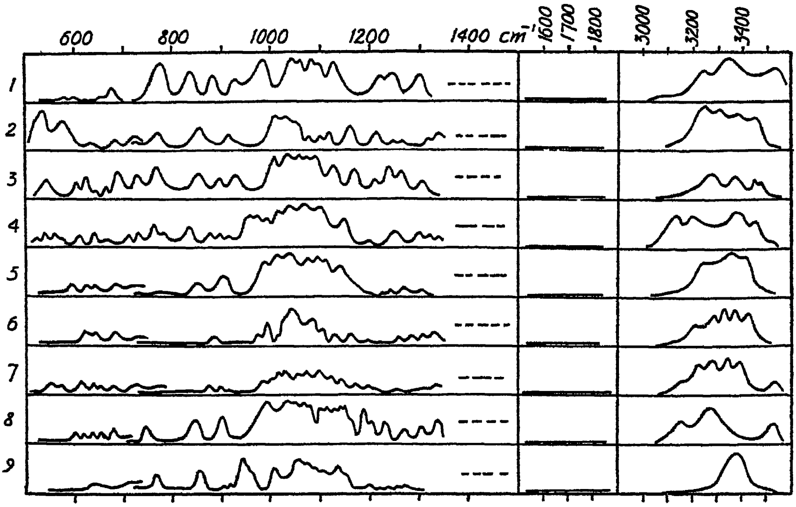

FIG. 3.—Carbohydrates.

(1) Arabinose. (2) Glucose. (3) Mannose.
(4) Galactose. (5) Maltose. (6) Cellobiose.
(7) Lactose. (8) α-Methyl glucose. (9) 2 : 3 : 6 Trimethyl glucose.

perfluorokerosene. The spectra are so complex that analysis of mixtures would in many cases be impossible, but the spectra show none the less their characteristic nature. Perhaps the most important feature is the range 3200-3800 cm.$^{-1}$. These bands are almost certainly associated with stretching vibrations of O—H linkages, differing in strength due to variation in the hydrogen bridges. On grounds of intensity and for other reasons they are unlikely to be due to overtones or combinations. Further, the fully acetylated derivatives have no absorption in this region, e.g. the octa-acetates of cellobiose, maltose and lactose, penta-acetyl glucose, hexa-acetyl difructosan. Similarly 2 : 3 : 6-trimethyl glucose has only one broad hydroxyl band, and there is an appreciable difference between diacetone glucose and monacetone glucose. The oxide ring structure is borne out by strong absorption near 1000 cm.$^{-1}$, to some extent paralleled by bands in the spectra of tetrahydropyran, tetrahydrofuran and their derivatives. Overlying this ether ring absorption, there are bands due to OH groups, which are removed or affected by acetylation, but the region 950-1150 cm.$^{-1}$ is usually highly complex. Marked differences occur between the spectra of sugar isomers such as glucose and mannose, or compounds differing only slightly, such as dulcitol and mucic acid.

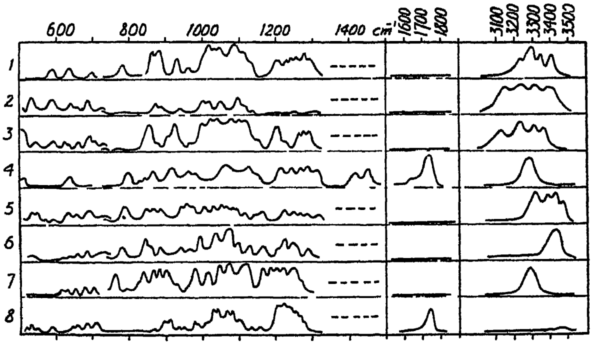

FIG. 4.—Carbohydrates.

(1) Mannitol.
(2) Sorbitol.
(3) Dulcitol.
(4) Mucic acid.
(5) Monoacetone glucose.
(6) Diacetone glucose.
(7) Diacetone fructose.
(8) Penta-acetyl glucose.

Some measurements with deuterated sugars have also given interesting results, but work with polarized radiation and small crystals in the reflecting microscope as described by Barer, Cole and Thompson,[10] seem particularly promising Here it was found that the different bands near 3 μ in a polyhydroxylic carbohydrate corresponding to different bridged hydroxyl groups behave differently in polarized radiation. Although the relationships are obviously complicated, this may provide a striking new way for differentiating and locating different OH groups in the solid. This matter is now being examined in greater detail. Some similar measurements with polarized radiation on sucrose and pentaerythritol were described by Ellis and Bath,[11] working in the region 1-2·5 μ.

The group —CO—NH— is vitally important in many compounds of biological interest. It occurs in amides, ureas, urethanes, peptides, and may form part of the ring structure in cyclic compounds such as some derivatives of pyrimidine. The group may have a ketonic form (I) or enolic form (III), but in the two cases respectively resonance stabilization may occur with a dipolar form (II) or (IV).

---

[10] Barer, Cole and Thompson, *J. Chem. Soc.*, 1947, 1260.

[11] Ellis and Bath, *J. Chem. Physics*, 1938, **6**, 221 ; 1939, **7**, 862 ; *J. Amer. Chem. Soc.*, 1940, **62**, 2859 ; *Physic. Rev.*, 1939, **55**, 1098 ; *J. Physic. Chem.*, 1941, **45**, 204.

—CO—NH

(I)

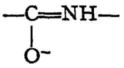

$-\mathrm{C}(\mathrm{O}^-){=}\mathrm{NH}-$

(II)

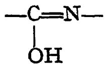

$-\mathrm{C}(\mathrm{OH}){=}\mathrm{N}-$

(III)

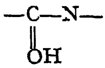

$-\mathrm{C}(\mathrm{{=}OH})-\mathrm{N}-$

(IV)

In addition, the linkages may be affected by hydrogen bonding of the type —C=O . . . H—N—. Spectroscopically, the significant consideration is the stretching and bending vibration frequencies of carbon-oxygen, carbon-nitrogen, N—H and O—H bonds, and in order to elucidate questions of hydrogen bonding, measurements on both solids and solutions are desirable. Detailed work on simple amides has shown [12] that the ketonic form (I) modified by resonance with (II) exists, with hydrogen bridges —C=O . . . H—N— being formed in the solid state. Mean values of the vibration frequencies are given in Table I, small variations occurring in different cases and with the particular nature of the solvent.

TABLE I

	Solid	Solution	Solid	Solution	Solid	Solution
R . CONH$_2$.	1655	1690	1630	1620	3200, 3350	3400, 3520
R. CONHR$_{alk}$	1640	1680	1560	1530	3270	3430
R . CONHR$_{ar}$	1660/80	—	1530/70	—	—	—
R . CONR$_1$R$_2$.	1650	1650	—	—	—	—

These general conclusions seem to apply also to other related compounds. Table II gives the positions of bands near 6 μ for some urethanes and anilides.

TABLE II

	Solid or Liquid		Solution (dioxane)		Solution (chloroform)	
	(i)	(ii)	(i)	(ii)	(i)	(ii)
H . CO . HNϕ . .	1560	1680	1549	1712	1534	1699
H . CON(C$_2$H$_5$)ϕ .	—	1682	—	1684	—	1674
CH$_3$CO . N(CH$_3$)ϕ .	—	1666	—	1673	—	1652
NH$_2$. CO . OR .	1613	1690	1614	1740	1585	1728
R . NH . CO . O(C$_2$H$_5$)	1540	7000	1540	1740	1530	1735
R$_1$R$_2$N . CO . O(C$_2$H$_5$)	—	1710	—	1710	—	1690

ϕ = phenyl.

Urethane is usually represented by formula (A), but like an amide might enolize (C), either of these forms being stabilized by resonance with the dipolar forms (B) or (D) respectively.

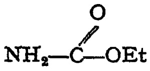

$\mathrm{NH_2{-}C({=}O){-}OEt}$

(A)

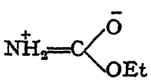

$\mathrm{\overset{+}{N}H_2{=}C(\bar{O}){-}OEt}$

(B)

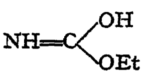

$\mathrm{NH{=}C(OH){-}OEt}$

(C)

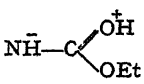

$\mathrm{N\bar{H}{-}C({=}\overset{+}{O}H){-}OEt}$

(D)

The band (ii) at 1710 cm.^{1} in the solid *N*-, *N*-, disubstituted urethanes and that between 1660-1680 cm.$^{-1}$ in the *N*-alkylanilides must be assigned to a carbonyl group stretching mode. It is natural to assign the bands (ii) in the simple or *N*-monosubstituted urethanes in the same way. If, however, enolization occurred, this band might be assigned to a C=N stretching mode. As with the amides previously, the spectra of *N*-substituted urethanes are against this. For example, with the strongly electrophilic NO_2 group, the dipolar form (B) should be relatively less stable and the C=O frequency should rise. With an enolic form (C), the dipolar form (D) would be more stable and the C=N group frequency would fall. The band concerned does in fact rise to 1740 cm.$^{-1}$. The other band (i) is consistently assigned to a N—H deformation, and the displacements in solvents are also as expected if hydrogen bridges are being broken. Measurements at 3 μ agree with this.

---

[12] Richards and Thompson, *J. Chem. Soc.*, 1947, 1248.

The spectra of some alkyl, aryl and acyl substituted ureas have also been measured. Urea is usually regarded as having a ketonic structure (1), but possible dipolar forms are (2) and (3). The enolic form (4) can form an internal salt (2) or (5), (2) being the more likely. There is other

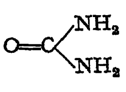
(1)

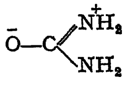
(2)

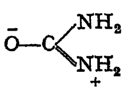
(3)

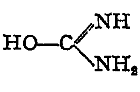
(4)

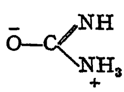
(5)

evidence for a structure in which (2) plays a prominent part. The band near 1660 cm.$^{-1}$ found in solid tetrasubstituted ureas (e.g. tetraphenyl, diethyl-diphenyl) must be due to ν_{CO}, and a similar band in the mono- and di-substituted compounds (e.g. benzyl, diphenyl, dimethyl) can be assigned similarly. With *N*-electrophilic substituents this value rises, due to a smaller participation of the dipolar form (2). The vibrations due to NH at 6 μ and 3 μ are complex. Here too, as with amides and urethanes, some shifts on passing to solution can be explained in terms of hydrogen bonding, but when strongly electrophilic *N*-substituents are present, e.g. —NO_2 or CH_3CO—, these shifts are minimized, which suggests that in some of these cases, even with solids, association is small. Since the dipolar form (2) in such cases is much suppressed, less powerful bonding might be expected.

We may comment briefly on the spectra of amino acids, some of which were given in Fig. 1. These compounds have the zwitterion structure NH_3^+ . . . COO^-. The strong band at 1590/1600 cm.$^{-1}$ is due to a stretching vibration of the ionized carboxyl group. The other mode of this type probably lies near 1400 cm.$^{-1}$, as suggested by Edsall from Raman measurements,[13] but the region 1300-1550 cm.$^{-1}$ is very complex and contains vibrations of CH_3, CH_2 and NH groups which are not easily disentangled, even by means of deuteration. The sodium salt of phenyl glycine has the strong band at 1590 cm.$^{-1}$, but in glycine ester hydrochloride and betaine hydrochloride which contain respectively a carbethoxy and normal carboxyl group, the ν_{CO} band is at 1745 cm.$^{-1}$ and 1730 cm.$^{-1}$. The electrically charged nature of the NH_3 groups is also confirmed by the spectra. As already explained, the stretching vibration frequencies of N—H links in amines, imines and amides (unassociated) are usually between 3200-3450 cm.$^{-1}$. None of the simple unsubstituted amino acids has a band above 3200 cm.$^{-1}$, ν_{NH} lying around 3000-3200 cm.$^{-1}$. Glycine ester hydrochloride also has the band near 3100 cm.$^{-1}$, but the sodium salt of phenyl glycine in which the amino group is not similarly charged, has a band near 3370 cm.$^{-1}$ more like that of an amine.

Acetylation of the amino group in amino acids might be expected to destroy the zwitterion structure, and the spectra confirm this. The position of the C=O band of the carboxyl group in acyl and aryl derivatives of glycine or alanine, acetyl glutamic acid, etc., cannot always be definitely fixed, but in many cases at least it must be much above 1600 cm.$^{-1}$. Also, after acylation bands appear above 3200 cm.$^{-1}$ due to the NH vibrations. Both points indicate that the ionic structure has been eliminated.

---

[13] Edsall and Scheinberg, *J. Chem. Physics*, 1940, **8**, 520; *J. Amer. Chem. Soc.*, 1943, **65**, 1767. Edsall, Otvos and Rich, *ibid.*, 1950, **72**, 474.

Another feature of the simple α-amino acids is a weak but definite band near 2100 cm.$^{-1}$. This band is absent from spectra of the *N*-acylated derivatives, and does not appear with phenyl glycine sodium salt, nor with *p*-amino phenyl acetic acid. It may therefore be attributed to a charged NH_3 group in the zwitterion, and may be a valuable criterion since it lies in a relatively clear part of the spectrum.

Spectral measurements on polypeptide materials have already been described by other workers,[14] and our results with a large number of such compounds agree with their main conclusions. As a rule, we find bands near 1640 cm.$^{-1}$ and 3280 cm.$^{-1}$ due to ν_{CO} and ν_{NH} (bonded) of the —CO . NH— group, and another near 1550 cm.$^{-1}$ due to δ_{NH}. Apart from vibrations of CH links near 2950 cm.$^{-1}$ and 1470 cm.$^{-1}$, the rest of the spectrum (500-1400 cm.$^{-1}$) depends upon the amino acid skeleton, and this region may possibly be used in some simple cases to identify the amino acid residues in a complex polypeptide or protein. Many of the substances also have a weak band near 3050 cm.$^{-1}$, whch must be due to NH groups since it disappears when the polyamide is fully methylated or methoxylated. Whatever the origin of this band, it is certain that different kinds of hydrogen bridge formations may occur simultaneously in some polypeptides. Here too, as suggested with the carbohydrate materials, work with polarized radiation should be most informative, as has already been shown.[15]

On the other hand, before a complete interpretation can be reached, the spectra of simpler peptides and related compounds must be understood. Fig. 5 shows spectra of a series of polyglycines, measured as powders in paraffin or perfluorokerosene. In glycine, as already explained, we find bands at 1600 cm.$^{-1}$ and 3160 cm.$^{-1}$ corresponding to COO^- and NH_3^+ groups, confirming the zwitterion structure suggested by X-ray work.[16] Diglycine has a peculiarly complex set of bands between 1200-1700 cm.$^{-1}$, differing from any of the higher members of this series. After deuteration, the bands at 1630, 1575, 1540 and 1240 cm.$^{-1}$ disappeared, suggesting that they are due to NH linkages. The bands at 1608, 1655 and 1670 cm.$^{-1}$ might be associated with different kinds of C=O group, e.g. 1655 cm.$^{-1}$ with —CONH— and 1608 with COO^-. The higher polyglycines have bands near 1440, 1540, 1640, and 1680 cm.$^{-1}$. Those at 1540 and 1640 cm.$^{-1}$ are due to the —CONH— group, and that at 1440 cm.$^{-1}$ probably to CH_2 groups. The band near 1680 cm.$^{-1}$ might be attributed to non-ionized COOH groups, increasing in strength as the chain lengthens and the zwitterion structure is diminished, and indeed another band near 1400 cm.$^{-1}$ attributable to the COO^- group disappears as that near 1680 cm.$^{-1}$ appears. If this interpretation were correct, we might have a useful method for determining end groups, but the bands due to NH_2 groups at the other end of the molecule are less obvious, and that at 1680 cm.$^{-1}$ is rather stronger than might be expected. In the 3 μ region, diglycine is again abnormal; the higher members have bands near 3080 and 3300 cm.$^{-1}$, except that the former is strangely absent with pentaglycine.

A similar series of polyglycine ester hydrochlorides is shown in Fig. 5. In the higher members there are bands at 1550 (δ_{NH}) and 1640 (ν_{CO}) of the peptide group and 1740 (ν_{CO}) of the ester. The bands near 3 μ due to NH vibrations are less easily assigned, but the dimer is again abnormal.

---

[14] Astbury, Dalgleish, Darmon and Sutherland, *Nature*, 1948, **162**, 596. Darmon and Sutherland, *J. Amer. Chem. Soc.*, 1947, **69**, 2074. Ambrose, Elliott and Temple, *Nature*, 1949, **163**, 567.

[15] Elliott, Ambrose and Temple, *Nature*, 1949, **163**, 859.

[16] Albrecht and Corey, *J. Amer. Chem. Soc.*, 1939, **61**, 1087. Levy and Corey, *ibid.*, 1941, **63**, 2095.

Fig. 6 shows spectra of some simple peptides. These formed from two simple amino acids (2-, 3-, 4-, 5-) have strong bands near 3250 cm.$^{-1}$ and 3070 cm.$^{-1}$. The former must be due to ν_{NH} of the CONH group, and the latter to a charged amino group, i.e. some dipolar character remains. In the region 1400-1700 cm.$^{-1}$ these four simple peptides again differ from the polyamides and the CO and NH groups must be affected by ionisation or hydrogen bonding. With the acetylated compounds (6-, 7-, 8-, 9-, 10-) which have no residual NH_2 and COOH groups, the spectra near 3 μ and 6 μ are much more like those of a polyamide.

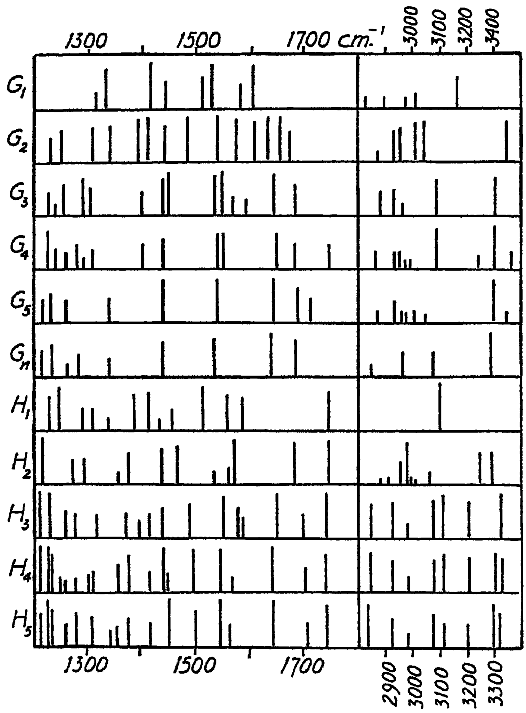

FIG. 5.

G_1—G_n. Glycine, di-, tri-, tetra-, penta- and poly-glycine.
H_1—H_5. Ditto, ester hydrochlorides.

Derivatives of pyrimidine and purine are important in connexion with the biochemistry of nucleic acids. We have measured the vibrational spectra of about 80 of these compounds between 2-20 μ as solids in paraffin or perfluorokerosene. More detailed results will be given elsewhere, but a few points may be mentioned. Spectra are shown in Fig. 7 and 8, showing rather better resolution than that obtained by Blout and Fields [17] for a few of these compounds. The spectra are highly characteristic with no obvious regularities, but closer inspection reveals features connected with the tautomerism which can occur in some of the compounds and which may be fundamental in metabolic processes.

Pyrimidine itself shows some similarities with benzene and pyridine as regards the strong bands. The chloro- and ethoxy-derivatives (Fig. 7, (2)-(6)) all have a strong band around 1550 cm.$^{-1}$, probably due to a C=N ring vibration. In the other substituted pyrimidines and particularly those in which tautomerism is possible, this band is displaced. This might occur because the enolic form (—N═C(OH)—) ketonizes to

---

[17] Blout and Fields, *ibid.*, 1950, **72**, 479.

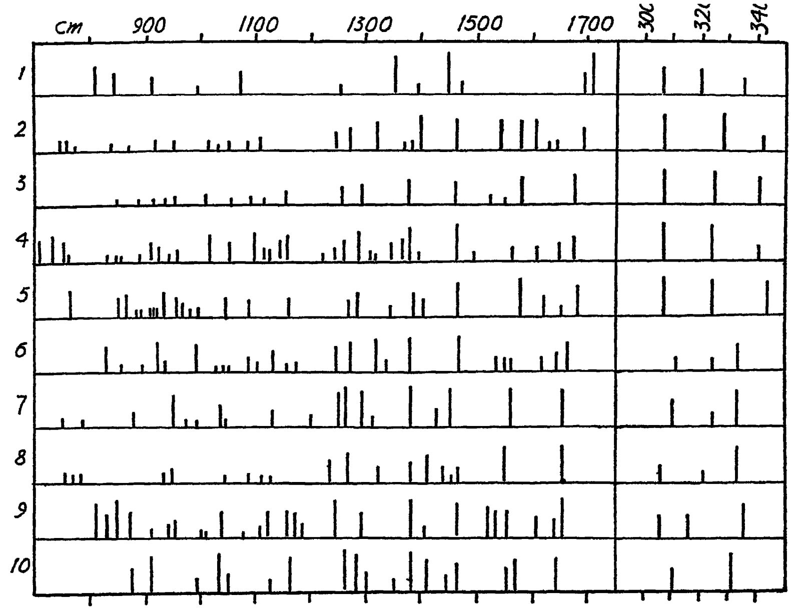

FIG. 6.—Peptides.

(1) Diketopiperazine. (2) *l*-Leucyl-α-phenyl alanine.
(3) 4-(1-valyl) 1-ornithine. (4) 1-Ornithyl-1-leucine.
(5) 1-Prolyl-valine. (6) Diglycyl ethylene diamine.
(7) Acetyl diglycyl ethylene diamine. (8) Dichloroacetyl ethylene diamine.
(9) Acetyl tyrosyl methylamide. (10) Acetyl glycine methylamide.

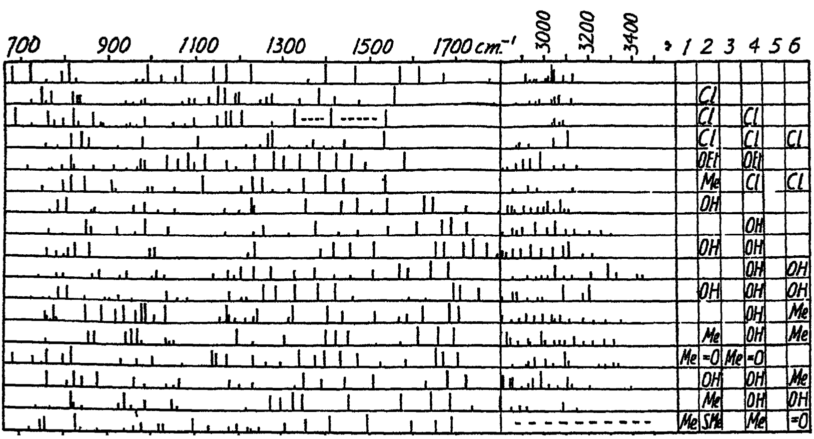

FIG. 7.—Pyrimidines: chloro, ethoxy, and hydroxy derivatives.

(—NH—CO—), with variable degrees of participation of the dipolar form (—NH⁺═CO⁻—) according to the other substituents present. It may also be recalled that the ring vibrations of substituted benzenes at 1500-1600 cm.$^{-1}$ are much dependent as regards position and intensity upon the substituent groups.

The hydroxy derivatives (Fig. 7) show new bands between 1620-1750 cm.$^{-1}$ which strengthen the idea of a ketonic form modified by the dipolar structure. The bands often occur in pairs. Thus 2-hydroxy pyrimidine has a "pair" at 1625-1645 cm.$^{-1}$, the 4-hydroxy derivative a pair at 1670-1685, and the 2 : 4-dihydroxy compound two pairs at 1650-1670 and 1715-1735 cm.$^{-1}$. In this region the 4-hydroxy-6-methyl and 4-hydroxy-2 : 6-dimethyl derivatives resemble 4-hydroxypyrimidine fairly closely. 2-hydroxy, 4-hydroxy and 2 : 4-dihydroxypyrimidine (uracil) have no bands above 3200 cm.$^{-1}$. This may mean that if the NH is present at all, it is present as NH$^+$, although there is little difference between chloropyrimidines and the hydroxy derivatives in this region. Piperidine and pyrrole and the amino-pyrimidines have bands near 3300 cm.$^{-1}$, but with diketopiperazine the main bands lie $<$ 3200 cm.$^{-1}$.

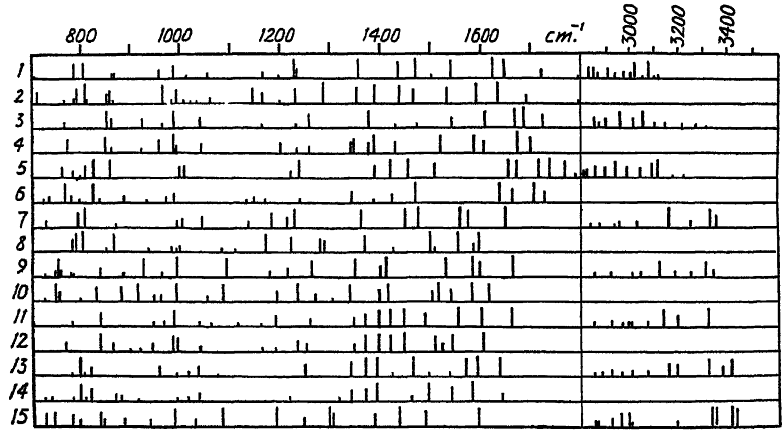

FIG. 8.—Pyrimidines.

(1) 2-OH. (2) 2-OH deuterated. (3) 4-OH.
(4) 4-OH deuterated. (5) 2 : 4-di-OH. (6) 2 : 4-di-OH deuterated.
(7) 2-NH$_2$. (8) 2-NH$_2$ deuterated. (9) 4-NH$_2$-6-Cl.
(10) 4-NH$_2$-6-Cl deuterated. (11) 4-NH$_2$-2 : 6-dimethyl.
(12) 4-NH$_2$-2 : 6-dimethyl, deuterated. (13) 4 : 6-dimethyl-2-NH$_2$.
(14) 4 : 6-dimethyl-2-NH$_2$ deuterated. (15) 2-methyl-4 : 6-dimethoxy 5-NH$_2$.

In 4 : 6 dihydroxypyrimidine, where only one ketonic group is likely to arise, only one pair of bands at 1640-1680 cm.$^{-1}$ appears, with bands near 3300 cm.$^{-1}$. The 4-hydroxy-6-methyl and 2-methyl-4 : 6-dihydroxy compounds are similar at 1650-1700 cm.$^{-1}$ but have no bands $>$ 3200 cm.$^{-1}$. 2 : 4 : 6-trihydroxypyrimidine surprisingly has only one pair near 1700 cm.$^{-1}$, but two strong bands near 3100 and 3200 cm.$^{-1}$. The 1 : 3-dimethyl uracil, which must contain two ketonic groups also has only one pair near 1650 cm.$^{-1}$. In an attempt to sort out the bands at 1620-1750 cm.$^{-1}$ several of the compounds were deuterated. As seen from Fig. 8 (1)-(6), the pairs of bands are not much affected, and not as expected if they were due to NH vibrations.

To summarize, it seems that although no detailed analysis can be given, many of the results are best explained in terms of the ketonic structure with a variable participation of the dipolar form. Variation in hydrogen bonding will also affect the situation, and the type and position of substituent groups will be important.

One final point arises with the amino-substituted derivatives (Fig. 8 (7)-(15)). These usually show a strong band near 1650 cm.$^{-1}$ which is removed by deuteration (Fig. 8 (8) (10) (12) (14)) and must be due to an NH mode of some kind. In 2-methyl-4 : 6-dimethoxy-5-amino pyrimidine (Fig. 8 (15)) which is incapable of tautomerism the band at 1650 cm.$^{-1}$ is absent. We could argue from this that in the previous amino derivatives tautomerism had occurred, leaving an imino group responsible for the 1650 band, and also for those near 3300 cm.$^{-1}$. A closer correlation of these results with structures determined from X-ray work [18] might be helpful, and the dichroic behaviour of some of the bands might assist in their correlation.

One of us (L.N.S.) is indebted to the Australian National University for the award of a scholarship.

The Physical Chemistry Laboratory,
Oxford.

[18] Clews and Cochran, *Acta Cryst.*, 1948, **1**, 4 ; 1949, **2**, 46.

THE INFRA-RED SPECTRUM OF ETHYLENE POLYMERS

BY L. H. CROSS, R. B. RICHARDS AND H. A. WILLIS

Received 19*th July*, 1950

Infra-red methods have been devised for the determination in ethylene polymers of methyl group concentration, the type and amount of unsaturation, and the nature and quantity of oxygen containing groups. These determinations are important in considerations of the physical properties, polymerization mechanism and sensitivity to chemical attack of the polymers.

A strong correlation between the extent of chain branching and the degree of crystallinity has been established for higher molecular weight polymers. Unsaturation determinations on a series of fractions covering a wide range of molecular weights show that the total number of double bonds per molecule is of the order of 0·3 to 0·4 both for original polymer and for the fractions. Whilst the $RR'C{=}CH_2$ type of unsaturation is most common in direct polymers of ethylene, the $RCH{=}CH_2$ type is prominent in low molecular weight pyrolyzed polythenes and in photo-oxidized polyethylenes. The oxygen containing groups found by infra-red methods in natural or oxidized polyethylene are mainly ketonic or aldehydic, though some hydroxyl exists.

The wide range of products which can be made by the polymerization of ethylene includes liquids, greases, soft and hard waxes and thermoplastics varying in melting point by as much as 25° C as well as in hardness, softness and tensile strength. To some extent these variations in physical properties can be attributed to changes in average molecular weight and, to a minor extent, in molecular weight distribution, but major differences in physical properties are observed at constant molecular weight and are due to variations in the degree of crystallinity and, in turn, to the variations in the degree to which the molecules have a branched chain structure. The most powerful tool for the determination of the degree of chain branching in ethylene polymers is the infra-red spectrum.[1]

Many ethylene polymers, including normal commercial samples, differ from a simple high molecular weight straight-chain paraffin also in being to some extent unsaturated. The total extent of the unsaturation is known from measurements of iodine number, bromine number and hydrogenation number, but the infra-red spectrum is able to show the extent to which the unsaturation occurs in the various types of olefinic bond such as $R.CH:CH_2$, $R.CH:CH.R'$ or $R R'C:CH_2$. The double bonds in ethylene polymers are normally present to the extent of, as a maximum, only one per molecule and have little effect on physical properties, but may be, of course, a centre of sensitivity to chemical attack in, for example, oxidative deterioration. The extent of the various types of double bond is also of importance in connection with studies of the mechanism of ethylene polymerization, and measurement of the concentration of the various types by the infra-red method has been used in a recently published study [2] of the mechanism of the thermal degradation of ethylene polymers.

---

[1] (*a*) Thompson and Torkington, *Trans. Faraday Soc.*, 1945, **41**, 246 ; (*b*) Downing, quoted by Bryant, *J. Polymer Sci.*, 1947, **2**, 547.

The infra-red spectrum may also be used to detect and estimate quantitatively oxygen-containing groups in ethylene polymers which may occur as a result of an oxygen-containing catalyst or of impurities such as carbon monoxide in the ethylene. They also arise as a result of thermal or photo oxidation. The groups which can be most readily identified and estimated are carbonyl and hydroxyl; unfortunately the peroxide group, which may occur as a result of oxidation is not readily detected by the infra-red spectrum.

Determination of Chain Branching.—In the examination of the infra-red spectrum of polyethylene in the 3 μ region, Fox and Martin [3] observed that the strength of the band at 3·2 μ indicated that there was an unexpectedly high proportion of the methyl groups in the polymer molecule, and hence the molecule had a branched-chain structure. This is confirmed by examination of the spectrum at around 7·3 μ and 11·3 μ where there are also bands which are caused by methyl but not by methylene groups and which can, in principle, be used for the determination of the number of branches in the polymer chain. Considerable caution must, however, be used in obtaining quantitative figures for methyl group contents in ethylene polymers.

The band at 7·3 μ (1378 cm.$^{-1}$) has been used by Thompson [1] to estimate methyl groups. An examination of the extinction coefficient of this band in a number of straight and branched chain paraffins shows that there is a linear relation between the extinction coefficient $K = \frac{1}{d}\log\frac{I_0}{I})$ at 1378 cm.$^{-1}$ and the ratio of the number of methyl groups to the total number of carbon atoms in the molecule ($[CH_3]/[C]$). This is shown in Fig. 1A, based on the spectra from the Naval Research Laboratory given in *American Petroleum Institute Collected Infra-red Spectra*. The following relation is obtained from this graph:

$$[CH_3]/[C] = 1{\cdot}35 \times 10^{-3} K_{1378}.$$

Extinction coefficients depend to some extent on instrument and technique, and for the Grubb-Parsons instrument used for most of the work on chain branching, the coefficient in the above expression has been found to be $1{\cdot}9 \times 10^{-3}$. When, however, one comes to use this band for the determination of the methyl group concentration in a typical sample of an ethylene polymer, two important points arise. The first is that the 1378 cm.$^{-1}$ band lies close to and overlaps a doublet at 1367 and 1355 cm.$^{-1}$ which appears to be characteristic of methylene groups, and considerable care in graphical resolution is necessary, particularly in polyethylene samples where the amount of branching is small. The second point is that the intensity of the 1378 cm.$^{-1}$ band has a different value for solid polyethylene at ordinary temperatures than that for the same polyethylene above its melting point. For a normal sample the intensity in the solid is about twice that in the liquid. The expression derived above from the low molecular weight paraffins applies only to liquid polyethylenes and consequently the intensity of the 1378 cm.$^{-1}$ band must be measured in the molten state. Unfortunately the intensity of the 1367 and 1355 cm.$^{-1}$ doublet is much greater in the molten state than it is in the solid, and in many polyethylene samples in the molten state the 1378 cm.$^{-1}$ band is only a shoulder on the side of the methylene doublet. Some examples of the spectrum in the 1350 to 1400 cm.$^{-1}$ region for ethylene polymers of varying methyl contents are shown in Fig. 2. Nevertheless, provided these points are borne in mind, the 1378 cm.$^{-1}$ band can be used as a measure of the methyl group content and hence the extent of chain branching in ethylene polymers. A sample of commercial polyethylene (Alkathene 20) is found to have one methyl group for every 25-35 carbon atoms.

---

[2] Oakes and Richards, *J. Chem. Soc.*, 1949, 2929.

[3] Fox and Martin, *Proc. Roy. Soc. A*, 1940, **175**, 208.

Another band which may be used in the determination of chain branching lies at 11·2 μ or 891 cm.$^{-1}$. This band, although only one-tenth of the intensity, is in some ways more satisfactory than the 1378 cm.$^{-1}$ band as in high molecular weight paraffins it lies well away from other bands and no resolution from near neighbours is required. Fig. 1B, also based on the data from the Naval Research Laboratory given in *A.P.I. Collected Spectra*, shows the linear relation between the extinction coefficient of this band and the methyl content of the hydrocarbon :

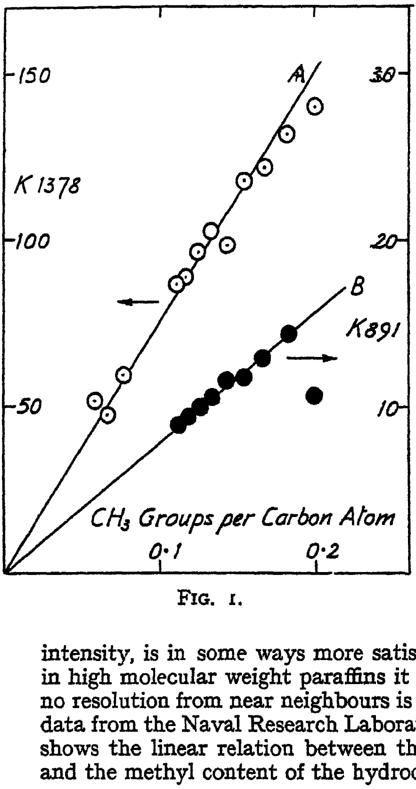

FIG. 1.

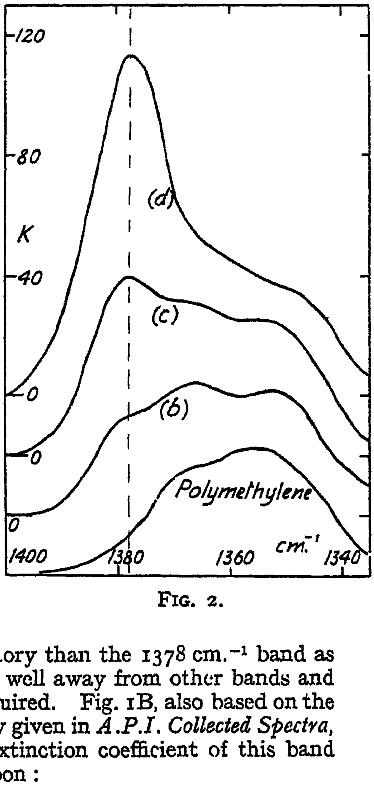

FIG. 2.

$$[\mathrm{CH_3}]/[\mathrm{C}] = 1{\cdot}25 \times 10^{-2}\, K_{891}.$$

For the Grubb-Parsons spectrometer, as used in this work, the coefficient is $2{\cdot}0 \times 10^{-2}$. Here again, however, attention must be paid to the effect of phase changes on the intensity of this band. For example, in straight-chain paraffins such as hexatriacontane there is something like a six-fold increase in intensity in passing from the liquid to the solid state, and although the change in ethylene polymers is less marked than this, there may be a 2- or 3-fold variation. Here again, therefore, the intensity of this band must be measured in the molten state if the expression above is to be used for methyl content determination. There is, however, a second cause of error. It is that there is a band characteristic of one of the types of double bonds which are found in polythene which has an almost identical wave number value (888 cm.$^{-1}$) and cannot be separated from the methyl group band (891 cm.$^{-1}$). In a sample of polyethylene of molecular weight about 15,000 (e.g. Alkathene 20) the contribution of the double bond to the band at 891 cm.$^{-1}$ may be as much as one-third of the total intensity, and in low molecular weight polythenes, where the double bond concentration is greater, the bulk of the absorption of 885-895 cm.$^{-1}$ is due to unsaturation. This is shown by the fact that hydrogenation or bromination reduces the intensity of this band and moves the peak slightly in the direction of increasing wave number, and the absorption at this wave length only gives a true measure of methyl group content if the measurement is done on a polymer sample after all unsaturation has been removed by, for example, hydrogenation. When these precautions have been taken the methyl group content determination on a sample of Alkathene 20 from this band is also about one methyl group in 25-35 carbon atoms.

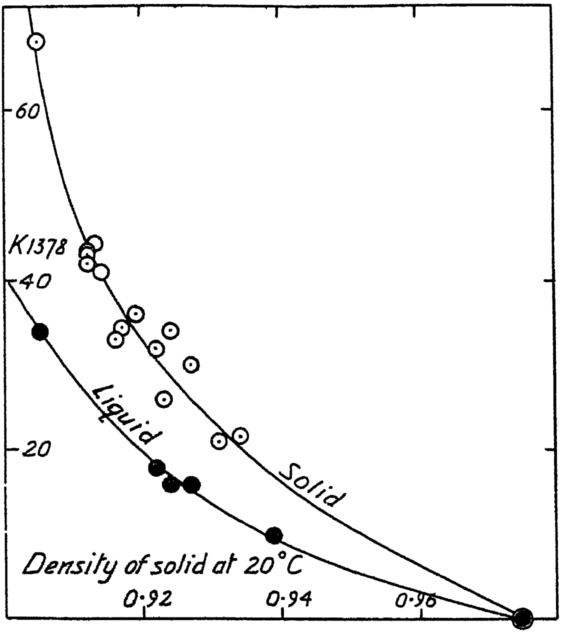

FIG. 3.—Density of solid at 20° C.

The methyl group concentration determined in either of these ways varies from as much as one in every 15 carbon atoms to as little as one in 200 carbon atoms, and in the higher molecular weight polymers there is a clear cut correlation between the degree of chain branching, as measured by infra-red spectrum, and the degree of crystallinity, as measured by the density, the X-ray absorption, or the intensity of certain infra-red bands which have shown to be characteristic of methylene groups in crystalline or amorphous regions only (Fig. 3). The effect of crystallinity and phase changes on the infra-red spectrum of long-chain paraffins and ethylene polymers is described in a forthcoming paper.

Determination of Unsaturation.—Olefinic double bonds lead to absorption in the infra-red at wave lengths of about 3·3 μ, 5·6 μ, 6·1 μ and

[4] Thompson, *J. Chem. Soc.*, 1948, 328.

[5] Anderson and Seyfried, *Anal. Chem.*, 1948, **20**, 998.

10-14 μ.[4, 5] For quantitative estimation the last region is most convenient for here each separate type of double bond gives a well-defined intense band at frequencies so far apart that resolution one from the other is simple. The frequencies corresponding to the different types of double bond are listed in Table I.

TABLE I.—INFRA-RED BANDS FOR OLEFINIC UNSATURATION

Double Bond Type	Wave Number cm.$^{-1}$	Molar Extinction Coefficients *
R . CH=CH$_2$	990	—
	908	121·0
R . CH=CH . R′ (*trans*. only) . .	964	85·4
RR′C=CH$_2$	888	103·4
RR′C=CHR″	835	34·6
R . CH=CH . R′ (*cis* ?) . . .	705	21·0

* Molar extinction coefficient $\epsilon = \frac{M}{Cd} \log \frac{I_0}{I}$,
where M = mol. wt. of absorbing group (i.e. 24 for C=C),
C is concentration of the group in g./l.,
d is cell thickness in cm.

Table II also gives average values for the molar extinction coefficients corresponding to each of these bands, based on the extensive work of Anderson and Seyfried [5] on a large number of low molecular weight liquid olefines. If one could be assured that these molar extinction coefficients were valid for solid or semi-solid high molecular weight materials, it would be simple to measure quantitatively the proportion of any type of double bond in polythene. There is, however, a serious complication, account of which must be taken before the infra-red spectrum can be used quantitatively. It is that, as has been shown in the previous section, saturated hydrocarbons also absorb at *ca.* 890 cm.$^{-1}$ and that in a normal polyethylene of molecular weight around 15,000 the greater part of the absorption here is due to methyl groups, rather than to the group RR′C : CH$_2$. The absorption spectra of saturated aliphatic hydrocarbons also show a band at 964 cm.$^{-1}$; this is almost exactly superimposed on the band corresponding to R . CH=CH . R′. If, therefore, the proportion of these two types of double bonds in polythene is to be measured, a correction must be applied for a proportion of the absorption at these frequencies due to the

TABLE II.—ABSORPTION AT 885-895 cm.$^{-1}$ AFTER REMOVAL OF UNSATURATION

Sample	1	2
Molecular Weight	1400	12,000
	$\frac{1}{d} \log \frac{I_0}{I}$ at 885-895 cm.$^{-1}$	
Original sample	33·0	6·6
After bromination, i.e. due to methyl .	5·0	4·7
Difference, i.e. due to RR′C=CH$_2$.	28·0	1·9
After hydrogenation, i.e. due to methyl.	5·0	4·6
Difference, i.e. due to RR′C=CH$_2$.	28·0	2·0

saturated portions of the polymer chain. In low molecular weight ethylene polymers the bulk of absorption at 885-895 cm.$^{-1}$ is due to unsaturation, but in high molecular weight materials the bulk is due to chain branching and great care must be taken in separating the contributions caused by the two types of structure. The extent of the separate contributions in high and low molecular weight polythenes is shown in Table II, in which values of $\frac{1}{d} \log \frac{I_0}{I}$ (d in cm.) of two samples of ethylene polymers before and after removal of double bonds by hydrogenation or bromination, are listed.

Absorption at 964 cm.$^{-1}$ remaining after removal of unsaturation is generally small and only in high molecular weight samples is serious error introduced by neglecting this in a determination of R . CH : CH . R′ groups from the infra-red spectrum.

The three types of unsaturation found in ethylene polymers are R . CH : CH_2, R . CH : CH . R′ (*trans*) and RR′C : CH_2. The last is generally the most common in direct polymers of ethylene, whereas the vinyl group is most common in low molecular weight pyrolyzed polythenes. The group RR′C : CHR″ has so far been found only in two polymer samples, and then only in an amount corresponding to less than 10 % of the whole. The band near 700 cm.$^{-1}$ corresponding to *cis*-R.CH:CH.R′ has not yet been detected in an ethylene polymer sample. It is unfortunate that there is not a definite band for the tetra-alkyl ethylene group RR′C : C R″R‴. Anderson and Seyfried in their work on petroleum derivatives used the difference between the total unsaturation measured by bromine absorption and the sum of the values for the R . CH : CH_2, R . CH : CH . R′ (*cis*- and *trans*-) RR′C=CHR″ and RR′C : CH_2 groups as a measure of the proportion of RR′C=CR″R‴. Fig. 4 shows a plot of the sum of the percentages of the various types of double bonds (calculated from the infra-red spectra with the aid of the coefficients given in Table II) against the iodine number for a number of samples of ethylene polymers ranging from a solid of molecular weight about 15,000 to greases of molecular weight as low as 480 and liquid pyrolysis products of molecular weight as low as 220. The broken line is the total double bond concentration calculated from the iodine number. The samples, in addition to covering a wide range of iodine numbers, molecular weight and physical forms (solids, pastes, greases and liquids), also varied considerably in the proportions of the types of double bonds ; they include polymers in which the bulk of the unsaturation is of the type RR′C : CH_2 and samples made by pyrolysis in which the bulk occurs as vinyl groups. It is seen that in Fig. 4 the points representing the sum of the percentage concentrations of C=C calculations for the infra-red lie close to the line representing the C=C concentration calculated from the iodine number, but since we cannot assume that the coefficients based on Anderson and Seyfried's work on liquids are valid for solid or semi-solid polymers the presence or absence of the RR′C=CR″R‴ group is still an open question.

As an example of the use of infra-red absorption in the study of unsaturation we may quote the results on a sample of Alkathene 70 and on a series of fractions of number average molecular weight from 1250 to *ca.* 35,000 made from the sample. In all, 53 fractions were produced ; the spectra of six have been examined and the values of $\frac{1}{d} \log \frac{I_0}{I}$ for the bands at 908, 964 and 888 cm.$^{-1}$ have been measured. When these values are plotted against the reciprocal of the number average molecular weight of the fractions it is found that whereas for the 908 cm.$^{-1}$ band the points lie reasonably close to straight lines through the origin (as would be found if the number of R . CH : CH_2 groups per molecule were constant), the points for the 888 cm.$^{-1}$ band are better represented by a line with an intercept (corresponding to infinitely high molecular weight) of about 3·0 for $\frac{1}{d} \log \frac{I_0}{I}$.

It is suggested that this corresponds to the degree of branching in the polymer chain, and, if this is constant for the various fractions, the difference between the total value of $\frac{1}{d}\log\frac{I_0}{I}$ and 3·0 is a measure of RR′C : CH$_2$ unsaturation. The points for the 964 cm.$^{-1}$ band are best represented by a line with a small intercept of about 0·4. Taking account of these intercepts, values are calculated for the concentration of C=C in the original polymer and in the fractions, and by combining this result with the molecular weights, for the average number of double bonds per molecule.

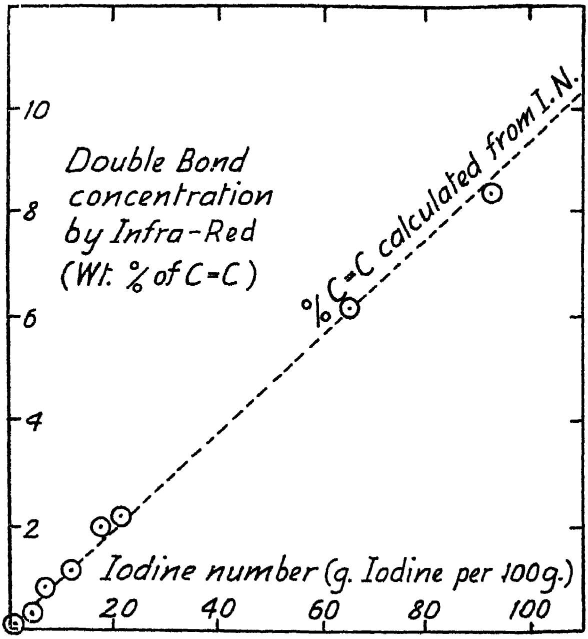

FIG. 4.—Relation between sum of concentration of R . CH=CH$_2$, RCH=CHR′ and RR′C=CH$_2$ double bonds and iodine number

It is seen that the RR′C : CH$_2$ group is the most frequent and that the total number of double bonds per molecule is of the order of 0·3-0·4 for all samples. The figures for the high molecular weight fractions and indeed for all polymers of molecular weight above *ca.* 10,000 are of course very approximate as they depend so much on the value assigned to the contribution to absorption at 888 and 964 cm.$^{-1}$ due to non-olefinic groups. In other ethylene polymers which have been examined the total double bond concentration is usually within the range 0·3 to 1·0.

Presence of Oxygen containing Groups in Polyethylenes.—In the infra-red spectra of some samples of polyethylene, weak absorption bands are found at 1720 wave numbers and 3600 wave numbers. Absorption bands in these positions are not found in the spectra of paraffins and olefins, and the presence of some other structure is indicated. Since small amounts of free or combined oxygen may be present in the gases used or the catalyst, we have attributed these absorption bands to the presence of carbonyl and hydroxyl groups respectively. This assignment is borne out by the fact that the intensities of these absorption bands vary considerably between different samples.

The frequency of the carbonyl group absorption band (1720 wave numbers) indicates aldehydic or ketonic groups, but since some long chain aliphatic carboxylic acids have absorption bands in their spectra at 1715 wave numbers, an absorption band due to the carboxyl group might not be resolved if it were present, and the possibility that some of the absorption at 1720 wave numbers is due to the carboxyl group must be considered. However, if carboxyl groups were present, a further band near 1200 wave numbers should occur, due to the C—O vibration within the carboxyl group. Since we have not detected a band in this region which varies in intensity in different samples, the conclusion is that at least the major portion of the absorption at 1720 wave numbers is due to aldehydic or ketonic groups.

From the point of view of the estimation of the oxygen content of polyethylenes by means of the absorption band at 1720 wave numbers, possible interference from the presence of the carboxyl group is an important factor, since the molar extinction coefficient for the carboxyl group at 1715 wave numbers is about twice that of the ketonic or aldehydic carbonyl group at 1720 wave numbers. To neglect possible interference by the carboxyl group band would therefore involve the possibility of considerable error in oxygen determination.

TABLE III.—DOUBLE BOND CONCENTRATIONS IN POLYTHENE FRACTIONS

Sample	Mol. wt. (Number average)	Wt. % of C=C			Total	Double Bonds per Molecule
		$R.CH{=}CH_2$	*trans*-$R.CH{=}CH.R'$	$RR'C:CH_2$		
Fraction 1 .	1250	0·120	0·095	0·400	0·615	0·32
Fraction 2 .	2300	0·059	0·080	0·169	0·308	0·30
Fraction 3 .	4500	0·042	0·040	0·110	0·192	0·36
Fraction 4 .	7700	0·014	0·022	0·099	0·135	0·43
Original Polymer .	11000	0·019	0·012	0·047	0·078	0·36
Fraction 5 .	15500	0·011	0·011	0·020	0·042	*ca.* 0·3
Fraction 6 .	35000	0·007	0·004	0·011	0·022	*ca.* 0·3

The absorption band at 3360 wave numbers in some samples indicates the presence of fully associated hydroxyl groups of an alcoholic nature. Absorption in this position also occurs when the polyethylene sample contains a small quantity of water, but if this is removed by vacuum-drying there is often residual weak absorption in this position. In no case have we observed an absorption band at 3600 wave numbers, which would indicate the presence of free hydroxyl groups. However, the molar extinction coefficient of the band at 3360 wave numbers, due to the associated hydroxyl group, is greater than that due to the free hydroxyl group at 3600 wave numbers, and it is therefore possible that a relatively small concentration of free hydroxyl groups might not be detected, in view of comparatively intense absorption of polythene in this region.

Although the spectra of some peroxides and hydroperoxides have been examined, there does not appear to be an absorption band, comparable in intensity with the carbonyl and hydroxyl group absorption bands, which is characteristic of the peroxide or hydro-peroxide group, and the infra-red spectrum cannot therefore be used to detect these groups. This is particularly unfortunate in oxidation studies, when the initial peroxide content might be expected to be an important factor in determining the rate of oxidation.

We have no evidence of the presence of other oxygen containing groups which could be readily detected, such as the ether linkage, in either natural or oxidized polyethylene samples.

The Study of Heat and Photo Oxidation of Polyethylene.—The spectrum of a sample of Alkathene 20, before and after heat oxidation for 80 hr. at 105° C is reproduced in Fig. 5A and 5B. The most prominent difference in the spectrum is at 1720 wave numbers, where the very weak absorption band occurring in the original sample has increased markedly in intensity. This difference is attributed to the uptake of oxygen as carbonyl groups.

The evidence is that here also the absorption is almost entirely due to aldehydic or ketonic carbonyl groups. The only additional absorption band which might be attributed to the C—O vibration of a carboxyl group is the weak band which appears at 1170 wave numbers in oxidized samples. The presence of a small concentration of carboxyl groups in a sample of very heavily oxidized polythene was established by boiling a heat oxidized film in dilute sodium hydroxide solution. The spectrum of the film after this treatment showed an absorption band at 1550 wave numbers (Fig. 6). Absorption in this position is characteristic of the presence of a metallic salt of a carboxylic acid, and it was therefore presumed that the sample contained some carboxyl groups although these could not be quantitatively estimated owing to the difficulty of ensuring complete conversion of the carboxylic acid to the salt. This sample, however, was so heavily oxidized that, as can be seen from Fig. 6, the carbonyl group absorption band was much too intense to measure, and a similar experiment performed with a less oxidized film, in which it was hoped to measure the intensity of the absorption band at 1720 wave numbers before and after this treatment, produced neither a measurable absorption band at 1550 wave numbers nor a measurable decrease in the intensity of the 1720 wave number absorption band. It was concluded from this evidence that the contribution of carboxyl groups to the absorption band at 1720 wave numbers was negligible.

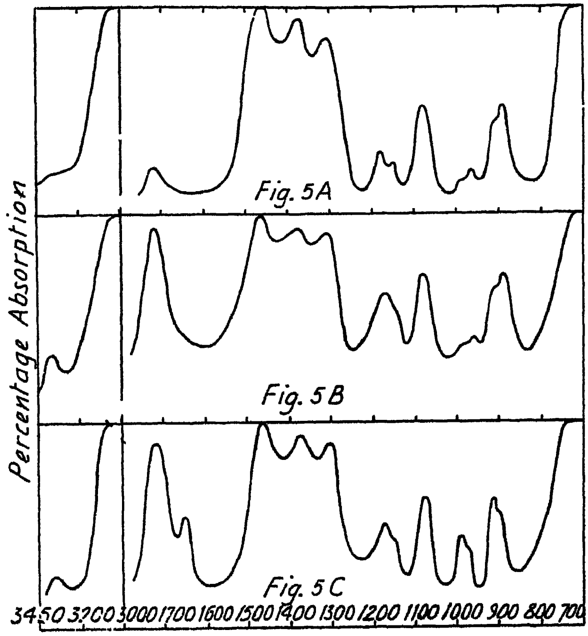

FIG. 5A.—Alkathene, grade 20.
FIG. 5B.—Alkathene, grade 20. Heat oxidized.
FIG. 5C.—Alkathene, grade 20. Photo oxidized.

The other major spectral difference is the greatly increased intensity of the hydroxyl group absorption band at 3360 wave numbers. Even in heavily oxidized samples, containing an appreciable concentration of hydroxyl groups, there was no indication of the presence of an absorption band at 3600 wave numbers due to the free hydroxyl group.

Another effect of oxidation, which was noted by Thompson and Torkington [8] in their examination of heat-oxidized rubber, is a general increase in the intensity of absorption in the region of 800-1700 wave numbers. This effect is partially due to optical scattering by the solid film, since the transmission of an oxidized film increases considerably on melting, but this does not appear to be the complete explanation.

Minor spectral differences occur in the region of 900-1000 wave numbers, which are due to small differences in unsaturation on oxidation, but there does not appear to be a marked difference in any of the three types of unsaturated groups found in polyethylene on heat oxidation.

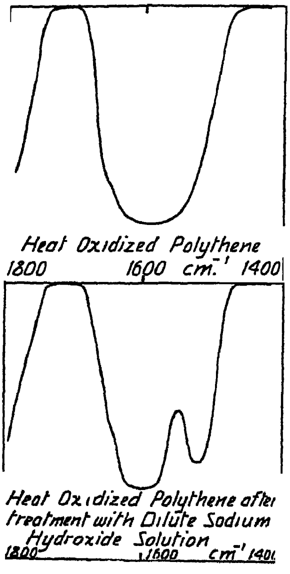

FIG. 6.

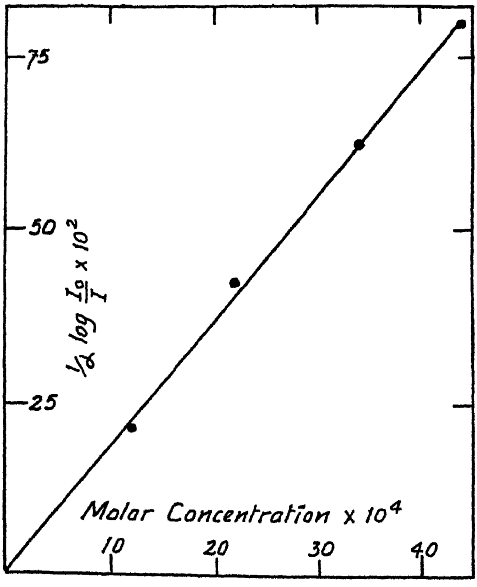

FIG. 7.—Determination of the molar extinction coefficient of di-*n*-butyl ketone at 1720 cm.$^{-1}$.

The effect of photo-oxidation has also been studied. The infra-red spectrum of Alkathene 20 after photo-oxidation is given in Fig. 5c. All the effects noted on heat oxidation are apparent in photo-oxidation. There are, in addition, certain other well-defined differences. An absorption at 1645 wave numbers, which is sometimes found as a very weak band in the spectra of thick samples of natural polyethylenes appears as a moderately intense absorption after photo-oxidation. The absorption bands at 909 and 990 wave numbers also increase markedly in intensity.

All these differences may be attributed to a considerable increase in unsaturation of the type $RCH{=}CH_2$; the absorption bands at 909 and 990 wave numbers being the frequencies associated with the deformation of the C—H linkages about the double bond; the absorption at 1645 is the corresponding C=C stretching frequency. The difference at 909 and 990 wave numbers are comparatively more marked, since the molar extinction coefficients for these absorption bands are much greater than that of the 1645 wave number absorption band.

It may be said, therefore, that the major qualitative differences observed in the infra-red spectra of samples of oxidized polyethylenes may be correlated with the formation of carbonyl and hydroxyl groups ; while in heat oxidation there are no well marked differences in unsaturation there is, in photo-oxidation, a considerable increase in unsaturation of the type $RCH{=}CH_2$.

The Quantitative Determination of Oxygen containing Groups.—The estimation of the oxygen present as carbonyl groups is of particular interest, since this accounts for the major proportion of the combined oxygen which can be detected both in normal polyethylenes and in oxidized samples.

The molar extinction coefficient for the absorption band at 1720 wave numbers has been determined on a number of simple aldehydes and ketones. A calibration curve produced from measurements taken on solutions of di-*n*-butyl ketone in cyclohexane is reproduced in Fig. 7 : from the slope of this graph the molar extinction coefficient, as determined on the D209 spectrometer (used as a single beam instrument with dried air-path) is 188. Other comparable ketones and aldehydes give values within 20 % of this figure.

The carbonyl concentration in a sample is found by measuring the value of $\frac{1}{d} \log \frac{I_0}{I}$ (d = thickness of sample in cm.) at 1720 wave numbers dividing by the molar extinction coefficient, and calculating from molar concentration to grams per cent. The accuracy attainable may be exemplified by a comparison between chemical determinations and infra-red results obtained on two ethylene-carbon monoxide interpolymers which were measured in chloroform solution.

TABLE IV.—CARBONYL CONTENT OF ETHYLENE-CARBON MONOXIDE INTERPOLYMERS

	Sample 1		Sample 2	
	Chemical	Infra-Red	Chemical	Infra-Red
Carbon	75·7 %		82·1 %	
Hydrogen	11·2 %		12·8 %	
Carbonyl (by difference)	22·9 %	26 %	9·0 %	10·1 %

In the measurement of I_0, it is necessary to apply a correction for general absorption or scattering, otherwise appreciable error may be introduced especially with highly oxidized samples.

The magnitude of the correction is determined by measuring the transmission of the required sample, and that of a similar sample containing no carbonyl groups, at some frequency near 1720 wave numbers at which no specific absorption occurs in either sample. The ratio of the transmissions at this frequency gives a measure of the relative scattering of the two samples. It is assumed that the relative scattering is the same at 1720 wave numbers, which is justified if the comparison position is sufficiently near this frequency. The transmission of the comparison sample at 1720 wave numbers is now measured, and from the determined scattering ratio the transmission I_0 of the required sample at 1720 wave numbers may be calculated. I is then measured directly, and the oxygen content as carbonyl groups may be calculated.

The concentration of hydroxyl groups in a sample is found in a similar way, using a molar extinction coefficient calculated from measurements on simple alcohols. This molar extinction coefficient is found to be approximately 54 for the D209 spectrometer.

Imperial Chemical Industries Research Departments,
Alkali Division, Northwich,
Plastics Division, Welwyn Garden City.

EVIDENCE OF CHAIN FOLDING IN POLYPEPTIDES AND PROTEINS

By A. Elliott and E. J. Ambrose

Received 5th July, 1950

Observations of the infra-red spectrum of proteins and polypeptides in the overtone region, using polarized radiation, have shown that a band at approximately 4840 cm.$^{-1}$ can be used to distinguish between extended and folded configurations, even in the presence of liquid water. These observations are used to interpret some observations on single haemoglobin crystals, from which it appears that the N--H bonds have a preferential orientation along the *a* crystallographic axis. The results are consistent with previously published work by Perutz. Some observations on orientation phenomena in a synthetic polypeptide solution are described.

It has been shown in earlier communications from this laboratory that synthetic polypeptides can be obtained in folded as well as in extended forms; evidence for this is found from infra-red spectra obtained with polarized radiation [1, 2, 3] and from X-ray fibre diagrams.[4] The solvent used in the preparations of films or fibres plays an important part in deciding which form is obtained.[5]

The problem of the physical structure of proteins, both in solution and in the solid form, can be greatly simplified by studying polypeptides with inert side chains, so that the properties of the polypeptide chain itself are not masked by the presence of ionogenic groups, as in proteins. A further simplification is made by using a polypeptide which is soluble in relatively inert solvents. The first part of this paper deals with observations, optical and spectroscopic, using such a material. In the second section, we describe observations with single crystals of haemoglobin, using polarized infra-red radiation. The interpretation of these observations is assisted by some of the experiments described in the first section.

Experimental and Results

Infra-red Spectrum of Poly-γ-benzyl-L-glutamate.—Observations made on oriented films of some synthetic polypeptides with polarized infra-red radiation have shown that they are in a folded configuration. These effects are especially marked in a poly-γ-benzyl-L-glutamate

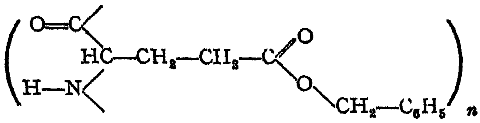

of chain length of about 300 units which has been prepared in this laboratory.[6] It is readily soluble in A.R. chloroform but dissolves very slowly in chloroform from which alcohol has been removed.

Oriented films of this polymer show infra-red dichroism of the N—H stretching frequency at 3305 cm.$^{-1}$ in which the optical density with the electric vector of the plane polarized radiation parallel to the chain axes is as much as 14 times

---

[1] Ambrose and Hanby, *Nature*, 1949, **163**, 483.
[2] Elliott and Ambrose, *ibid.*, 1950, **165**, 921.
[3] Ambrose and Elliott (submitted for publication).
[4] Bamford, Hanby and Happey, *Nature*, 1949, **164**, 138.
[5] *Idem*, *ibid.*, 1949, **164**, 751.
[6] Hanby, Waley and Watson, *J. Chem. Soc.* (in press).

as great as that when the vector is perpendicular to the chain axis. Observations made with dilute solutions of the polymer in chloroform and in carbon tetrachloride show that there are no N—H groups in the polymer which cannot be satisfied by hydrogen bonding within the molecule.[2, 3]

The polymer also shows infra-red dichroism in other parts of the spectrum. There is an absorption band at approximately 4825 cm.$^{-1}$ in the overtone region. A band at approximately the same wave number in Nylon has been identified by Glatt and Ellis [7] as a combination band of the N—H deformation and stretching modes. A number of thin oriented films of poly-γ-benzyl-L-glutamate were superimposed to provide sufficient thickness for observations in the overtone region. The band at 4825 cm.$^{-1}$ was found to show strong perpendicular dichroism (strongest absorption with *E*-vector perpendicular to the chain axis). This band is therefore of opposite character to the N—H stretching band at 3505 cm.$^{-1}$ but of the same character as the N—H deformation band at 1550 cm.$^{-1}$.[3] Observations of α-keratin (porcupine quill) show that it gives the same kind of dichroism in the bands at 4840 cm.$^{-1}$, 3305 and 1550 cm.$^{-1}$ as are observed in the poly-γ-benzyl-*L*-glutamate. Fig. (1) shows the 4840 cm.$^{-1}$ band in α-keratin. The perpendicular dichroism is, however, much less than can be obtained in the synthetic polymer.

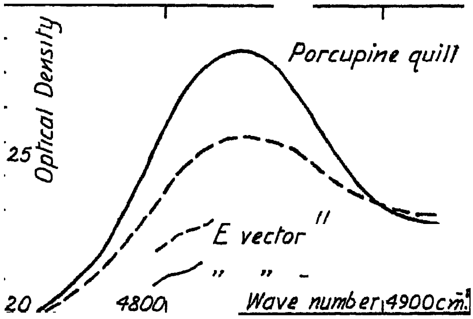

FIG. 1.

In silk (a β or extended form of polypeptide chain) the dichroism of the bands at 1535 cm.$^{-1}$, 3301 cm.$^{-1}$ and 4810 cm.$^{-1}$ are all of opposite character to those observed in the folded polypeptide and in α-keratin. The combination band at 4840 cm.$^{-1}$ does therefore provide a means of distinguishing between α and β forms in oriented specimens which are too thick for observation in the fundamental region of the spectrum. In addition, unlike the fundamental N—H and C═O stretching modes, this frequency does not coincide with that of a liquid water absorption band. It therefore provides a method of investigating protein crystals which contain a high precentage of water and are of considerable thickness.

Orientation Phenomena in a Synthetic Polypeptide Solution.—The synthetic poly-γ-benzyl-L-glutamate appears from the infra-red data to be completely in the folded form.[2, 3] It shows certain unusual properties in solution which appear to be characteristic of the α-folded polypeptide chains.

If a film is cast from a homogeneous chloroform (A.R.) solution, the film is translucent, not clear, and appears bright when examined between crossed nicols, unlike most polymer films, which at normal incidence appear black under the same conditions. If the film is examined with high power in the polarizing microscope, local orientation is shown by the pattern produced (Fig. 2(*f*)). Small regions of the film behave like a film or fibre of oriented material, but the direction of orientation varies from place to place in the film. In general, this variation is not random, as shown by the curious pattern produced (the irregularity in the centre shows the effect of a foreign body, in all probability). This orientation arises spontaneously.

It is evident that the polymer becomes oriented either before or during the drying process, and photographs of a drying solution show both these effects. These photographs were obtained by putting a drop of the polymer solution between two microscope slides slightly separated by thin glass rods. This again [illegible] geneous, but at a suitable concentration (very roughly about 15 % by weight) spherulites begin to appear in great numbers. These grow to a considerable size (compare with scale) and eventually coalesce. The material at this stage shows strong flow birefringence, and the currents caused by evaporation of the solvent produce large areas of almost uniform orientation. Further drying produces a solid phase, whose boundary is marked AA in Fig. 2(*b*). This boundary is extremely sharp, and is doubtless the same as the " middle boundary" which Hartley[8] has described in the penetration of cellulose acetate by chloroform and other swelling agents and solvents and which is the subject of further work by Robinson.[9] The solid film shows a large number of lines approximately normal to the drying edge.

---

[7] Glatt and Ellis, *J. Chem. Physics*, 1948, 16, 551.

The above observations suggested a technique for making thin, highly oriented films for polarized infra-red spectroscopy, and for X-ray diffraction work. A drop of solution (concentration about 25 % by weight) is placed on a glass plate and stroked out by a razor blade. The blade has previously been honed slightly for a length of about 2 cm. in the middle, so that it rests on the ends, leaving a suitable gap between glass and blade through which the solution is extruded. This method gives the highest infra-red dichroism we have observed in polymers; the X-ray photographs are also extremely good. More important, perhaps, than the orientation is the high crystallinity; the amount of amorphous material appears to be very low.

The orientation is, in fact, capable of improvement, as is shown by Fig. 2(*c*), 2(*d*) and 2(*e*) of an oriented, fairly thick film prepared as described above. The direction of chain orientation is that of the edge of the film. Fig. 2(*d*) gives the position of the film with respect to the nicols for the best black field; 2(*c*) and 2(*e*) show the effect of small rotation of the film from this position. Although the movement of the film makes it difficult to identify structure, 2(*c*) and 2(*e*) are actually complementary, what is dark in one picture being light in the other. It appears that there is a considerable " spread " around the direction of orientation; it is possible that this spread is caused by shrinkage on drying. With very thin films, the effect is not so marked.

The effects produced by drying a solution in dioxan are similar to those described above. In this case, however, striations somewhat similar to those shown in Fig. 2(*c*)-2(*e*) have been observed in the gel; it is not known whether these are only to be seen when dioxan is used, and it may be connected with the slower rate of drying from dioxan.

As we have shown elsewhere,[2] poly-γ-benzyl-L-glutamate film cast from chloroform is almost completely in the folded α-polypeptide form. It is not certain that the orienting properties of the polymer are specifically due to the side chains, for both poly-L-glutamic acid and poly-γ-methyl-L-glutamate give similar high orientation when cast from *m*-cresol (they are not soluble in inert solvents). We consider that the properties of the folded polypeptide chain itself are responsible for the easy orientation, and this appears the more probable when one considers how many highly oriented (at least as far as the crystallites are concerned) protein structures occur in nature. For example, with wool keratin it has been shown[10] that orientation of the keratin molecules occurs in a gentle constriction of the cell wall at the roots of the hair. The actual rate of flow is extremely small and the effects are in some ways analogous to those observed in the poly-γ-benzyl-L-glutamate. The formation of disulphide linkages occurs at a later stage.

From models, it is easily seen that the polypeptide chain, folded in the way suggested by Ambrose and Hanby,[1] is nearly rigid in the plane of the paper, but is more flexible when bent *out* of the plane. The side chains do not interfere with this bending, as far as individual molecules are concerned. It is possible that the ease of orientation is connected with the limited flexibility and with the absence of *inter*-molecular hydrogen bonds.

It may also be pointed out that, though most polymers show orientation effects on drying out from solution, these effects are generally far smaller than those we have described above, and are usually caused by shrinkage during drying. We believe that the orientation of poly-γ-benzyl-L-glutamate is not produced in this way, but arises from a process akin to crystallization in the solution.

---

[8] Hartley, *Trans. Faraday Soc.*, 1949, **45**, 820.

[9] Robinson (in course of publication).

[10] Mercer, *J. Textile Inst.*, 1949, **40**, 1640.

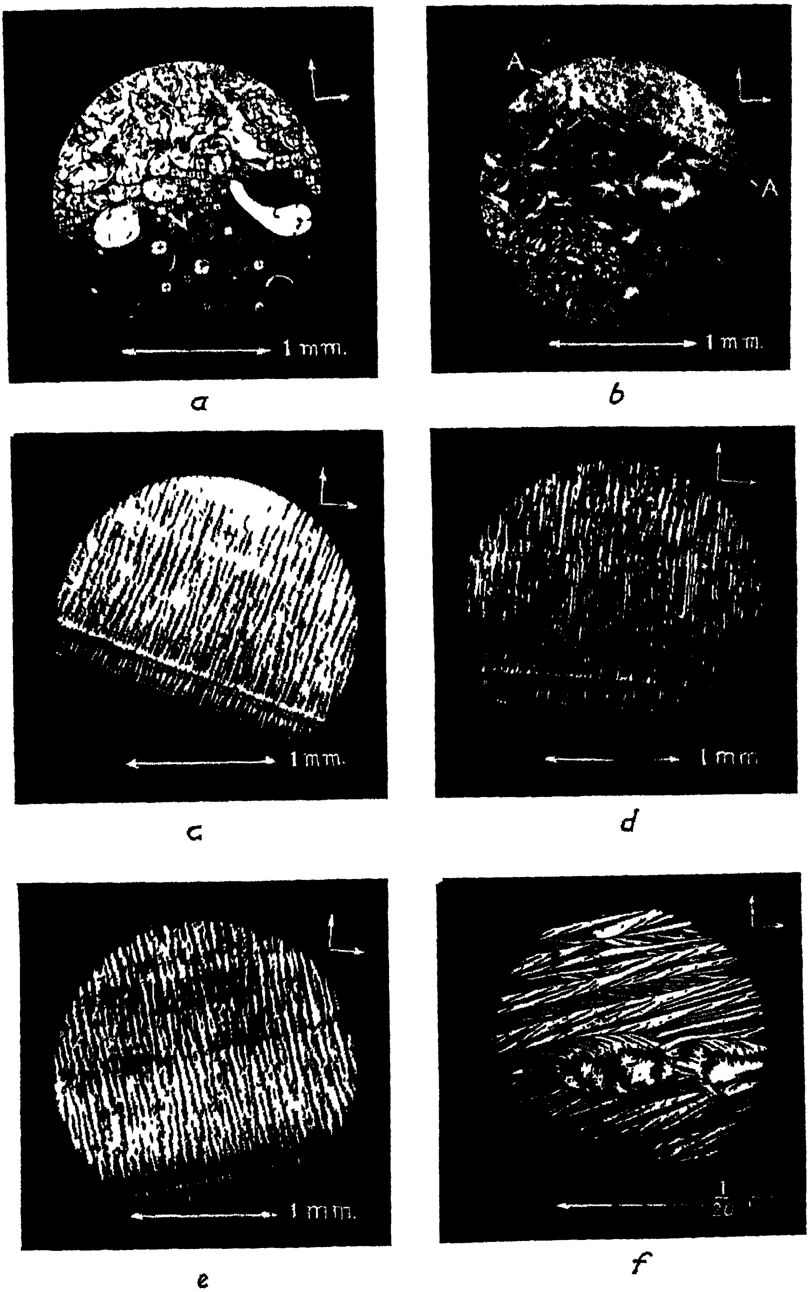

Fig. 2.

(*a*), (*b*)—Solution of poly-γ-benzyl-L-glutamate in chloroform, photographed between crossed nicols, showing spherulites.

(*c*)-(*f*)—Solid film of poly-γ-benzyl-L-glutamate, between crossed nicols.

[*To face page* 248

Orientation of the N—H Group in Crystals of Horse Methaemoglobin.—Horse methaemoglobin can be crystallized from salt-free solution in monoclinic plates, with a thickness of a few 1/10 mm., and length and breadth about 1-2 mm. They contain, when fully swollen, about 52 % water.[11] These large crystals are much too thick to allow observation of the fundamental N—H or C=O bands, as absorption is very high. The band in the overtone region (4840 cm.$^{-1}$) referred to above makes observation of an N—H mode possible, however.

The dichroism of horse methaemoglobin is of more than ordinary interest because of the very extensive X-ray investigation which Perutz and his collaborators have carried out on this material.[12] We were fortunate in obtaining some large salt-free crystals through the kindness of Dr. Crick, who was able to grow very suitable crystals for us.

EXPERIMENTAL AND RESULTS.—It is necessary, in order to get the highest molecular order, that the crystals of haemoglobin should not be allowed to dry out [11] and we therefore mounted the specimens in cells made from microscope cover glass, with the crystal surrounded by a layer of liquid paraffin; in one instance the cell was filled with the mother liquor from which the crystals were grown. The cell was mounted on the rocking stage of a reflecting microscope set up in front of the spectrometer. The basic design for the elements of this microscope (which are spherical) was provided by Mr. Bracey of the British Scientific Instrument Research Association. A five-fold magnified image of the specimen was projected on the slit of a lithium fluoride spectrometer, and a rocking mechanism moved the specimen so that the crystal was alternately in and out of the radiation beam.

In order to reduce the possible harmful effects of radiation on the haemoglobin crystal, an infra-red filter (kindly provided by the Admiralty) was interposed to cut out the visible spectrum. The *a* and *b* crystallographic axes of horse methaemoglobin, which are mutually at right-angles, are in the plane of the plate-like crystal, and *b* is the direction of the diad axis.[13] If the dichroism is measured with the radiation incident normally on the face parallel to the *a* and *b* axes, then from symmetry considerations it follows that the *E* vector directions for maximum and minimum absorption dichroism in this aspect of the crystal will therefore be obtained from such measurements. Fig. 3(*a*) shows one set from a number of measurements made with different crystals. The relatively weak N—H combination band is superposed on a rising background of absorption from water or from other modes within the protein molecule. In order to show the dichroism, the background absorption has been subtracted in Fig. 3(*b*). Although the interpolation of the background is to some extent arbitrary, it is quite impossible to do this in such a way as to remove the dichroism, still less to change its character.

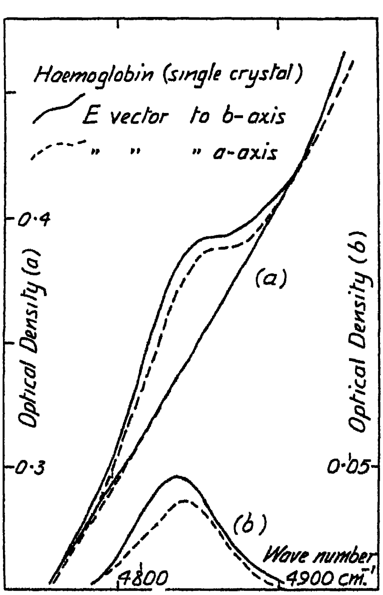

FIG. 3.

Because the effect is small, we have been at some trouble, in the case of haemoglobin, to make quite sure that it is real. In addition to multiplicity of measurements we have, for instance, made observations of the dichroism first with the *b* axis parallel to the spectrometer slit, then with the crystal rotated in its own plane to bring the *a* axis parallel to the slit. Such a measurement would reveal any instrumental asymmetry; none was found. The dichroic ratio, for light incident normally on the face parallel to *a* and *b*, is probably between 1·2 and 1·3, the *a* axis being the direction of least absorption.

---

[11] Perutz, *Trans. Faraday Soc.*, 1946, **42B**, 187.

[12] A summarizing article by Perutz appears in *Research*, 1949, 252.

[13] Perutz, *Nature*, 1939, **143**, 731.

The dichroic ratio is apparently unaltered if the crystal is rotated about the *a* axis from the position of normal incidence to one in which the radiation is incident on the plate face at about 60°. To do this the crystal was placed, in paraffin, between the hypotenuse faces of two small glass prisms, a technique we have described elsewhere.[14]

These observations suggest that, in any crystal aspect, the *a* axis is the direction of least absorption, the direction for maximum absorption being any direction at right-angles to *a*. This was further examined by sending the radiation beam as far as possible along the *a* axis and observing any dichroism which might be present. In practice, one has to be content with the *a* axis inclined at about 30° to the radiation direction. In this position, no dichroism could be detected with certainty. This means that there was no indication that the direction of the dipole moment for the N—H combination band has any preferred direction other than perpendicular to the *a* axis. With such low dichroism as we have observed with the radiation normal to the *ab* face, a moderate amount of planar orientation might, however, escape detection.

It was found that prolonged exposure to radiation, even when the crystal was surrounded by liquid paraffin, reduced the water content, as revealed by the strength of the liquid water absorption band at 5113 cm.$^{-1}$. This was accompanied by a reduction in dichroic ratio. In one instance, when the water content was reduced from 0·82 g. per gram protein (wet crystal) to 0·42 g. per gram protein (as measured by the absorption), the dichroic ratio was 1·14. Haemoglobin crystals freshly immersed in paraffin were found to have the same dichroic ratio as a crystal which was immersed in mother liquor.

Discussion

Perutz's X-ray investigation[12] has led him to suggest that haemoglobin contains folded polypeptide chains whose directions are parallel to the *a* axis. Because the total length of the molecule is much greater than the *a* dimension of the unit cell, the chains must again be folded (secondary folding) many times. The details of these secondary folds are not known, nor is the nature of the primary fold understood. The dimensions of certain important vectors in the Patterson projection of haemoglobin are, however, very suggestive of X-ray spacings found in fibrous proteins, for instance α keratin, and Perutz has suggested that the primary haemoglobin fold could perhaps be the same as that of α keratin.

Our observations are quite compatible with Perutz's suggestions, since we have found the dichroism of haemoglobin to be of the same character as that of α keratin with the fibre axis in the direction of the *a* axis of haemoglobin. Quite apart from the question whether the primary fold is the same in haemoglobin and α keratin, it may be concluded that the peptide N—H groups in haemoglobin have a preferred direction along the *a* axis.

The dichroism observed in haemoglobin, which is very low, is of the same order as that in α keratin. The cause of the low dichroism may, however, be very different in the two cases. For instance, there must be a large fraction of unoriented material in the keratin of porcupine quill, for an X-ray photograph shows a strong amorphous ring, in addition to the well-oriented arcs characteristic of the α keratin. The effect of this unoriented material will be to lower the measured dichroic ratio. In the haemoglobin crystal we have a water content of 52 %. It is possible that there are water molecules in the neighbourhood of the C=O . . . H—N hydrogen bond ; if so they may be expected to exert an influence on the dipole moment of the N—H modes and the low observed dichroism may be partly due to this effect. In addition, secondary folding must lower the dichroism by reason of the change in direction of the polypeptide chains. The infra-red evidence is not inconsistent with an arrangement in which the chains are tilted with respect to the diad axis. Such a structure does not, however, seem to be consistent with results obtained from the Patterson projection. It is not possible to say more than that the N—H bonds are directed more along than across the *a* axis; the exact direction cannot be determined from our observations.

---

[14] Ambrose, Elliott and Temple, *Proc. Roy. Soc. A*, 1949, 199, 183.

Courtaulds Ltd., Research Laboratory,
Lower Cookham Road,
Maidenhead,
Berkshire.

INFRA-RED AND X-RAY STUDIES OF CHITIN

By S. E. Darmon and K. M. Rudall

Received 7th July, 1950

The absorption spectra of chitin, chitosan, chitin nitrate and wood cellulose have been recorded in the region 3600 cm.$^{-1}$ to 750 cm.$^{-1}$, using polarized radiation. A preliminary interpretation of the spectra, in conjunction with the X-ray data, has increased our knowledge of the detailed structure of chitin. The principal feature is hydrogen bonding between CO . NH groups of adjacent amino-acetyl side-chains, to form linked piles of chitin chains within the crystalline regions. But consistent with the particular symmetry, this type of linkage seems to occur between only some of the amino-acetyl groups (presumably half of them). The remaining acetyl groups are bonded differently and the evidence points to a linkage of the type CO . . . HO. As a result of the progressive deacetylation which occurs during chitosan formation, the principal inter-chain bonding is of the type OH . . . OH, as in cellulose. The results of these investigations form a basis for an understanding of the role of *N*-acetylhexosamines in the inter-chain bonding of polysaccharides.

A most important outcome of X-ray diffraction studies of natural high polymers has been the determination of the repeating unit along the length of the chain-molecule. The interpretation of other axial spacings, particularly those referring to inter-chain separations, is comparatively little advanced. The properties in these directions are, nevertheless, of first importance in determining the physical and chemical behaviour of the material in the aggregate. The present work, which combines infra-red and X-ray studies of some common polysaccharides of biological interest, throws considerable light on the nature of inter-chain bonding.

By the use of polarized infra-red radiation we have observed the general directions of certain intramolecular bonds. An exact determination of bond directions by this technique is only possible with perfectly crystalline material, and with imperfectly oriented natural polymers it is only possible to assess the relative orientation of specific bonds with reference to the axis of the specimen. Nevertheless it is of the greatest interest to know simply whether a particular bond or group is more nearly parallel or perpendicular to the molecular chains, and this can be found from a purely qualitative study of the polarized infra-red spectra. Such qualitative information, especially when combined with X-ray diffraction data, has proved during the present investigations to be of considerable value in a more complete determination of the structure of various polysaccharides.

The polysaccharide chitin has engaged our main attention. Chitin is widely distributed in invertebrates, chiefly as protective cuticles, and is best known as a major constituent of the exoskeleton or cuticle of Arthropods. In plants it replaces cellulose as the cell-wall material in some fungi and it is present, with cellulose, in the walls of certain algal cells. Chitin, which is polyacetylglucosamine, is ideal as a starting point for the investigation of the role of amino-sugars in polysaccharide structure. *N*-acetyl hexosamines are prominent constituents of many important polysaccharides such as hyaluronic acid, chondroitin and mucoitin sulphates, specific pneumonococcus polysaccharides, blood group *A* substance and ovomucoid. In our present studies the active group with which we are specially concerned is the quasi-peptide linkage, --NH . CO —, arising from the *N*-acetylation of glucosamine, but in common with polysaccharides generally, chitin also contains hydroxyl groups. Thus in the interchain linkages of chitin we can investigate group interactions of a kind that might be expected to occur between polysaccharides and proteins.

The space-group derived from X-ray analysis of chitin implies two different types of inter-chain bonding. It is thus of particular interest to seek a verification of this from the infra-red spectra and to follow changes in the two types of bonding during the formation of derivatives. Furthermore, certain derivatives of chitin show well-defined changes in molecular chain-separations, which are such as to allow or exclude particular types of bonding.

In the present article we shall give an account of our preliminary infra-red studies of chitin, chitosan and chitin nitrate in relation to existing X-ray data. Although these investigations are but a starting point in the detailed structural analysis of polysaccharides, they have revealed more clearly than was known hitherto the spatial arrangement in chitin itself and have thrown some light on the formation of chitosan and of chitin nitrate.

Experimental

Preparation of Specimens.—The soft cuticles of insect larvae such as puss moth, privet hawk moth and blowfly larvae have, when purified, provided us with conveniently thin membranes for infra-red absorption studies. A considerable degree of molecular orientation can be obtained if fresh cuticles are stretched and held stretched during purification. They were purified in 5 % KOH solution at 100° C for two days and thoroughly washed for 1 to 2 days.[1] Sheets of lobster tendon were also used and purified in a similar manner.

Chitosan sheets were made from the above types of specimen, while chitin nitrates were prepared from purified chitin obtained from the puparia of *Sarcophaga falculata*.

Chemical Considerations.—(*a*) CHITIN.—There is wide agreement that chitin is a poly-condensation product of *N*-acetyl glucosamine.[2] Naturally-occurring chitin can be considerably purified by treatment in dilute caustic potash at 100° C. The main test of purity is the nitrogen content, which should be 6·89 %, but this theoretical value is rarely obtained. With insect cuticles the type of purification we have used results in nitrogen contents corresponding to about 93 % pure chitin. Purified lobster tendon chitin has shown a nearer approach to the theoretical nitrogen content.

(*b*) CHITOSAN.—Various methods have been used by different workers to produce chitosan :—

(1) Heating in fused caustic potash at 170° to 180° C. for 30 min.[3]
(2) Heating at 160° C for 30 min. in potash solution saturated at room temperature (histological test).[4]
(3) Heating in 50 % caustic soda solution for 35 to 40 hr. at 100° C.[3].

There is disagreement as to the extent of the deacetylation that occurs. Earlier studies were brought to a head by Löwy's detailed work.[4] Using the fused potash treatment (1), he obtained a 70 % yield of chitosan sulphate and from analysis of this crystalline product concluded that his chitosan consisted of monoacetyldiglucosamine. By contrast the more recent study by Meyer and Wehrli[2] using method (3) indicated that chitosan was polyglucosamine as judged by the nitrogen value and the very low acetyl content. Clark and Smith[5] claimed that methods (1) and (3) gave chitosans of the same X-ray structure and the same chemical analysis. While giving no quantitative data on the acetyl present they state that the nitrogen content of their chitosans suggests only one nitrogen atom per chitobiose residue. Meyer and Wehrli's result, indicating that chitosan is polyglucosamine, seems at first sight to be the most reasonable; but X-ray studies are in favour of two different kinds of acetyl groups, suggesting a reasonable basis for the structure of chitosan as found by Löwy. In support of Löwy it must be stated that his work was most detailed and repeated on many preparations.

---

[1] Fraenkel and Rudall, *Proc. Roy. Soc. B*, 1940, **129**, 1.
[2] Meyer and Wehrli, *Helv. chim. Acta*, 1937, **20**, 353.
[3] Löwy, *Biochem. Z.*, 1910, **23**, 47.
[4] Campbell, *Ann. Ent. Soc. Amer.*, 1929, **22**, 401.

In our experiments we desired to follow the process of chitosan formation (see also ref. (5)). The method we found convenient was to treat samples of chitin in a solution of caustic soda (68 g. NaOH/100 ml. water) at 100° C for times which ranged from 30 min. to over 60 hr. All preparations were subsequently very thoroughly washed in water. Using this procedure we obtained substantial changes in the X-ray and infra-red spectra after 2 to 3 hr. treatment.

(*c*) CHITIN NITRATE.—The maximum nitration observed by Shorigan and Hait[6] corresponds to about 1·5 nitrate groups per acetylglycosamine residue, compared with 2 groups for completion. We have studied only the nitrate fraction which is insoluble in formic acid. Purified blowfly puparia were dissolved in fuming nitric acid for periods of 45 min. and 90 min. and were filtered through glass wool. The solution was precipitated in water and thoroughly washed. The precipitate was extracted in changes of formic acid for two days and dried giving a very brittle material. Conveniently thin films were made by pressing re-wetted precipitate between plates of silver chloride and drying. Several such preparations were examined. Nitration is so important a procedure in the analysis of oriented polysaccharides by infra-red means that we suggest the usefulness of attempting complete nitration in the solid state using nitrogen pentoxide.[7]

(*d*) CELLULOSE.—Sections of wood cellulose as used here were chosen because of the desirability of having uniform sheets of oriented material of considerable dimensions. The purification procedure was designed to remove practically all the lignin, and to reduce the xylan and polyuronide fractions. At the same time it was necessary to maintain the oriented structure intact. The infra-red spectra show the absence of carbonyl and carboxyl groups.

Infra-red and X-ray.—A Beckman I.R. 2 spectrophotometer was used, with a rocksalt prism for the region 2000 to 700 cm.$^{-1}$ and a lithium fluoride prism, for greater dispersion, above 2000 cm.$^{-1}$. The energy traces were recorded on a Brown Electronik Recorder. The pre-collimator optics of the spectrometer had been modified so as to include a focus of small area, at which specimens could be mounted. With this arrangement, an area of specimen 2·0 × 0·3 cm. was the maximum required, and this could be conveniently obtained from our materials.

The polarizer, which is of the transmission type, is constructed of silver chloride plates, 0·025 cm. thick. Six such plates are mounted in a Perspex frame, at an angle of approximately 26° to the incident beam, thus permitting maximum reflection of the unwanted component. The degree of polarization obtained, as measured by crossing two such identical polarizers, is better than 95 %. The position of the specimen was kept constant during the experiment, only the polarizer being rotated. The specimens used were mainly coherent films, for which the correction for scattered radiation was negligible.

Wide-angle diffraction patterns were obtained using Cu$K\alpha$ radiation. The specimens were dried at room humidity and were in the form of variously oriented films or as naturally oriented fibres.

Results

Infra-red.—The absorption spectra of chitin, chitosan, chitin nitrate and wood cellulose are plotted in Fig. 1 for the regions 3600 cm.$^{-1}$ to 2600 cm.$^{-1}$ and 1750 cm.$^{-1}$ to 750 cm.$^{-1}$. No perceptible absorption maxima occur

[5] Clark and Smith, *J. Physic. Chem.*, 1936, **40**, 863.

[6] Shorigan and Hait, *Ber.*, 1934, **67**, 1712.

[7] Caesar and Goldfrank, *J. Amer. Chem. Soc.*, 1946, **68**, 372.

between 2600 cm.$^{-1}$ and 1750 cm.$^{-1}$ with the thickness of specimens used. In Fig. 2 the spectrum of chitin is compared in the regions 3600 cm.$^{-1}$ to 2600 cm.$^{-1}$ and 1750 cm.$^{-1}$ to 1550 cm.$^{-1}$ with the spectra of specimens which have been treated with NaOH for 2, 3 and 17 hr. under the conditions specified in the section on chemical considerations for chitosan formation. The chitin, chitosan and cellulose spectra are plotted with the electric vector vibrating respectively parallel and perpendicular to the chain-axes. The degrees of orientation and the thicknesses of the chitin and chitosan specimens are comparable but not identical, and we have facilitated comparison by plotting optical density instead of percentage absorption. Unpolarized radiation was used for the nitrated specimens, as these are difficult to orient.

X-rays.—(*a*) CHITIN.—The structure derived for chitin by Meyer and Pankow[8] gives a lattice of space group $P2_12 2_1$, with *a* 9·3, *b* 10·4 and *c* 19·2 Å. We are able to add that there is confirmation of the space group $P2_12 2_1$ in preference to $P222_1$. Blowfly larval cuticles and puparia show a well-defined double orientation with {00*l*} planes lying nearly parallel to the surface. The best resolved and oriented of these diffraction patterns show absence of the 100 reflection. Of special interest to our present work is the distance of 4·65 Å between chitin chains along the *a* axis, a figure which is closely similar to the separation of *β*-protein chains in the direction of the backbone linkage.

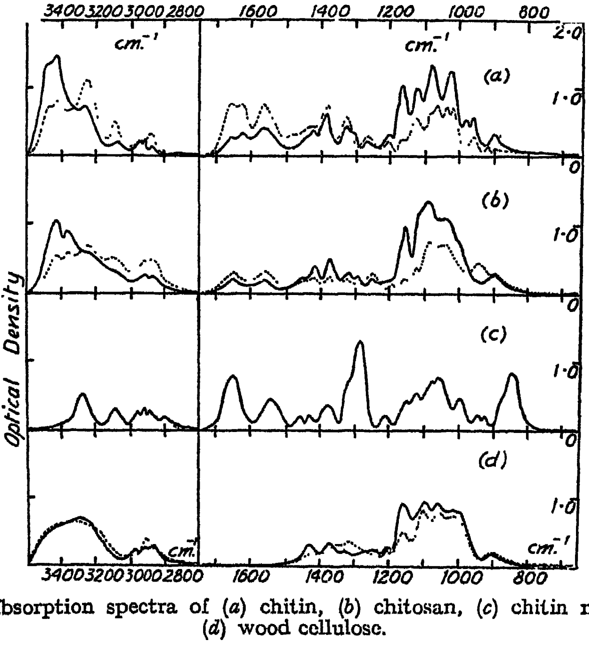

FIG. 1.—Absorption spectra of (*a*) chitin, (*b*) chitosan, (*c*) chitin nitrate and (*d*) wood cellulose.

—— Electric vector parallel to axis of orientation.
- - - - Electric vector perpendicular to axis of orientation.

In stretched cuticles the molecular chains are well oriented parallel to the direction of stretching. The chains are *very* highly oriented in lobster tendons. Stretched insect cuticles were used in obtaining the spectra of Fig. 2(*b*) and (*c*), while lobster tendons gave the spectra of Fig. 1(*a*) and (*b*) and Fig. 2(*a*) and (*d*). The degree of main-chain orientation is about the same in chitosan as in the chitin from which it is prepared.

(*b*) CHITOSAN.—The available X-ray data for chitosan indicate an orthorhombic lattice probably showing the same symmetry as that of chitin. The principal differences are the *a* and *c* axis periods of 8·9 Å and 17·0 Å respectively; that is, the separation of chains along the *c* axis should be 8·5 Å, which is only a little greater than the 8·35 Å found in cellulose. If the structure corresponds to polyglucosamine the density should be 1·37, which is rather a low figure as polysaccharides bonded by hydroxyls usually have densities of 1·5 to 1·6 or more.

---

[8] Meyer and Pankow, *Helv. chim. Acta*, 1935, **18**, 589.

(*c*) CHITIN NITRATE.—A principal reason for studying chitin nitrate followed from Clark and Smith's observation that the chain separation was about 11·5 Å.

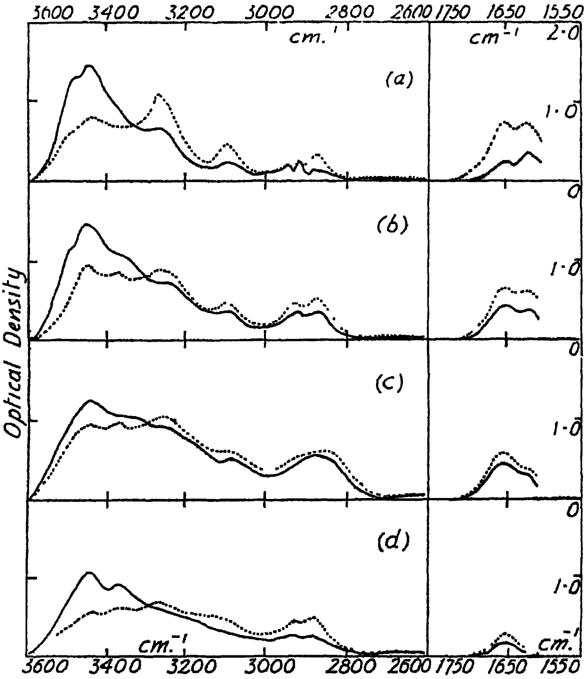

FIG. 2.—Progressive chitosan formation. (*a*) chitin, (*b*) 2 hr. treatment with NaOH, (*c*) 3-hr. treatment and (*d*) 17-hr. treatment.
—— Electric vector parallel to axis of orientation.
- - - - Electric vector perpendicular to axis of orientation.

This gave the possibility of full bonding of CO . . . HN groups according to Fig. 3.

The types of diffraction patterns of the nitrate which we have obtained agree in general with those of Clark and Smith.[5] We find the *c* axis reflection is nearer

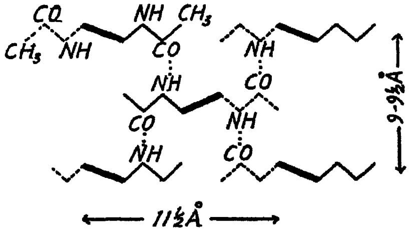

FIG. 3.

to 11·7 Å. Most characteristic is the high secondary orientation in thin films, i.e. both the *c* axis and the fibre axis lie in the plane of the film. The *c* axis reflection is also very sharp and intense and shows a well-defined second order at 5·86 Å. The periodicity in the *a* direction, which is oriented approximately perpendicular to the film surface, is subject to much variation. This depends chiefly on the degree of extraction of the crude nitrate in formic acid. Well-defined reflections do occur in the insoluble fraction after prolonged extraction and measured periodicities are 4·6 Å and 4·96 Å. Very little success was obtained when attempting to make fibres of chitin nitrate.

(*d*) CELLULOSE.—The purified wood sections gave the pattern of native cellulose. The degree of orientation of the main-chains corresponded to a spiral making an angle of about 10° with the long axis of the specimen.

Discussion

Infra-red.—(*a*) CHITIN. A number of bands in the region 3600 cm.$^{-1}$ to 1300 cm.$^{-1}$ of the spectrum of chitin may be immediately assigned to certain molecular groups which are presumed on chemical evidence to exist in chitin. The most prominent of these are the bands at 3265 cm.$^{-1}$ 3100 cm.$^{-1}$, 1656 cm.$^{-1}$ and 1560 cm.$^{-1}$, which are frequencies characteristic of the CO . NH linkage occurring in amides, polyamides and fibrous proteins[9, 10] The values of these frequencies show that the CO . NH groups participate in inter-group hydrogen bonding, of the type CO . . . HN, and further that the strengths of these hydrogen bonds in chitin are comparable with those in polyamides and proteins. The extinction coefficients of all these bands are higher when the beam is plane-polarized so that the electric vector vibrates perpendicular to the fibre axis of the specimen. Not only do the NH stretching bands (3265 cm.$^{-1}$, 3100 cm.$^{-1}$) and the CO stretching band (1656 cm.$^{-1}$) exhibit " perpendicular dichroism " * but so does the NH deformation band at 1560 cm.$^{-1}$. This band has been shown to arise from the deformation of the NH bond *in the plane* of the CO . NH group,[11] and it is thus apparent that the plane of the CO . NH group, as well as the CO and NH bonds themselves, is roughly perpendicular to the chain axis.

A number of strong bands occur in the region 1250 cm.$^{-1}$ to 950 cm.$^{-1}$ These frequencies and their high intensities suggest that the bands originate mainly in C—O (single bond) linkages, such as the C—O—C and C—OH groups in sugar rings, and the glucosidic linkage, C—O—C. A closely similar set of intense bands occurs in wood cellulose (Fig. 1(*d*)) and, in fact, this general pattern of absorption is present in all the spectra of Fig. 1. Without a detailed analysis it is not possible to determine the resultant direction of dipole moment change in particular vibrational modes of the glucose ring, but one would predict C—OH stretching frequencies with perpendicular dichroism, and a C—O—C (glusosidic bridge) frequency with high parallel dichroism in this region. Fig. 1(*a*) shows that although most of the absorption in this region has parallel dichroism there are two maxima (1060 cm.$^{-1}$ and 1014 cm.$^{-1}$) with definite perpendicular dichroism.

The foregoing infra-red evidence has shown the existence in chitin of parallel chains with structural units similar to those in cellulose, but of especial importance is the observation that lateral hydrogen bridges, comparable in strength with those of fibrous proteins, are established between the CH_3CO . NH groups of neighbouring chitin chains.

A feature of great structural interest is the intense doublet absorption with maxima at 3485 cm.$^{-1}$ and 3445 cm.$^{-1}$. The two bands together show strong parallel dichroism but they overlap to such an extent that it is difficult to disentangle their separate dichroisms. The 3485 cm.$^{-1}$ frequency is unlikely to be an NH vibration, since the NH stretching frequency of simple amides [10] has not been found to occur higher than

---

[9] Astbury, Dalgliesh, Darmon and Sutherland, *Nature*, 1948, **162**, 596.

[10] Darmon and Sutherland, *ibid.*, 1949, **164**, 440.

* We have used the term " parallel dichroism " to describe greater absorption when the electric vector vibrates parallel to the axis of orientation than when it vibrates in a perpendicular direction. " Perpendicular dichroism " is the converse of this.

[11] Elliott, Ambrose and Temple, *J. Chem. Physics*, 1948, **16**, 877.

about 3445 cm.$^{-1}$, which is the "unbonded" position of the vibration. It must therefore be an OH vibration, since OH vibrations occur as high as 3640 cm.$^{-1}$, the unbonded position for alcohols.[12] The 3445 cm.$^{-1}$ band may be either an OH or an NH vibration, although its coincidence with the known unbonded position of NH (amide) vibrations suggests that it is a free NH vibration. The 3485 cm.$^{-1}$ frequency suggests that the OH group is probably weakly hydrogen-bonded, occurring as it does well below 3600 cm.$^{-1}$, but the OH . . . OH bond so formed is not comparable in strength with those in liquid alcohols and cellulose, where the absorption band has a much lower frequency and greater width.

The spectrum of chitin nitrate in Fig. 1 has no maxima at 3485 cm.$^{-1}$ or 3445 cm.$^{-1}$ but some of our specimens, which are presumably less completely nitrated, do show slight residual peaks at these frequencies. One interpretation is that both these bands represent OH vibrations which are lost on substitution but structural changes resulting from nitration could cause the loss of any free NH (amide) groups which exist in chitin itself. The assignment of the 3485 cm.$^{-1}$ band to a weakly bonded OH vibration is consistent with the spectrum of chitosan and the series of spectra depicting the intermediate stages of chitosan formation (Fig. 2). Among other changes, the 3485 cm.$^{-1}$ peak weakens and finally disappears; concurrently, there is a marked increase of absorption between 3300 cm.$^{-1}$ and 3000 cm.$^{-1}$, corresponding closely to the bonded OH absorption of cellulose.

The remaining band of structural interest we shall discuss is the 1625 cm.$^{-1}$ band of chitin which is, however, absent in chitosan and chitin nitrate. This band is most reasonably interpreted as being a second carbonyl frequency arising, like the 1656 cm.$^{-1}$ band, from the acetyl groups, but whereas the 1656 cm.$^{-1}$ CO frequency corresponds closely to those found in amides, polyamides and proteins, the 1625 cm.$^{-1}$ band is significantly lower. The only other cases in which we have found so low a peptide carbonyl frequency are the acylated amino-acids,

$$R . CO . NH . CHR . COOH$$

(R is CH_3 or H). For example, acetyl and formyl leucines show their CONH carbonyl frequencies within the range 1628 cm.$^{-1}$ to 1605 cm.$^{-1}$, and in acetyl glycine this frequency is as low as 1588 cm.$^{-1}$. It is significant to the interpetation of this low CO frequency that the acylated amino-acids and chitin have a common structural feature, namely hydroxyl groups which are potentially capable of forming hydrogen bonds to the carbonyl oxygen of the CO . NH group. It is possible, therefore, that the low CO frequency of chitin may arise from a NH . CO . . . HO system.

The carbonyl band in chitosan and chitin nitrate is at the usual position, near 1650 cm.$^{-1}$. Fully nitrated chitin has no hydroxyl groups for participation in CO . . . HO bonding and the nitrate spectrum of Fig. 1 is consistent with the formation solely of CO . . . HN bonds. Fig. 2 shows a progressive decrease in intensity of the 1625 cm.$^{-1}$ band as chitosan formation proceeds, but the 1656 cm.$^{-1}$ band vanishes less quickly and some absorption remains here when the 1625 cm.$^{-1}$ band is imperceptible. This spectral evidence suggests that it is those acetyl groups which are bonded to hydroxyl groups, that are most easily removed. Prolonged treatment with NaOH weakens the 1656 cm.$^{-1}$ band also, so that deacetylation is not apparently arrested when only half the acetyl groups have been removed.

On purely spectroscopic grounds, the postulate of CO . . . HO bridges is at present a tentative one, necessitated by an unusual carbonyl frequency and proposed on the evidence of a similar frequency in other hydroxylic peptide structures. However, the presence of such a bond satisfies very well the X-ray data, as regards both the symmetry of the chains and the inter-chain separations.

[12] Errera and Mollet, *Nature*, 1936, 138, 882.

Assuming that CO . . . HO bridges do exist in chitin, it follows that there are an equivalent number of non-hydrogen bonded NH groups. This would readily account for the band at 3445 cm.$^{-1}$ which was tentatively interpreted as a free amide NH vibration. However, it is not easy to find an absorption maximum which could be attributed to the OH stretching vibration of the CO . . . HO system. If the absorption is a broad band of low intensity, as is the OH absorption of cellulose, it may be obscured by the more intense NH bands in this region, especially as there is only one contributing OH group per biose unit. Furthermore, thicker specimens of chitin show weak absorption between 2750 cm.$^{-1}$ and 2600 cm.$^{-1}$, which does not appear to be present in the nitrate spectrum. Whether this is OH absorption or overtone absorption must remain undecided at present.

(*b*) CHITOSAN.—The high frequency spectrum of chitosan shows very broad OH absorption, which resembles that of cellulose. It is thus apparent that strong hydrogen bridges between hydroxyl groups are the principal inter-chain linkages. During chitosan formation (Fig. 2), there is progressive weakening of the 1625 cm.$^{-1}$ carbonyl band and of the amide NH frequencies at 3265 cm.$^{-1}$ and 3100 cm.$^{-1}$, due to increasing deacetylation. A new peak appears progressively at 3365 cm.$^{-1}$, and this together with the 3445 cm.$^{-1}$ absorption in chitosan may well constitute the stretching vibrations of the NH_2 groups which would result from deacetylation.

(*c*) CHITIN NITRATE.—The absence of free NH vibrations points to the existence of complete hydrogen bonding between all the CO . NH groups of chitin nitrate. Intense bands originating in the nitrate groups occur at 1284 cm.$^{-1}$ and 845 cm.$^{-1}$. These absorptions confirm spectroscopically that nitration has actually occurred and they may subsequently prove useful in assessing the degree of nitration.

Correlation of X-ray and Infra-red Results.—(*a*) CHITIN.—The infra-red spectrum of chitin shows hydrogen bonding between the amino-acetyl side-chains, and we can use this information in trying to fix the positions of neighbouring main-chains in the lattice. If we view the chitobiose residue in projection along the length of the chitin chain we obtain the units of Fig. 3. The dotted side-chain —NH . CO . CH_3 indicates that it is in a lower plane, i.e. attached to the next sugar ring below. The arrangement of chains in Fig. 3 gives maximum bonding of C=O . . . HN— groups.

In an orthorhombic structure this would give a period in the side-chain direction of about 11½ Å and between the planes of sugar rings a period of 9 to 9½ Å. This cannot be the lattice of typical arthropod chitin where the density is much higher and the *c* axis period is 2 × 9·6 Å. In Fig. 5 we show a structure with the appropriate symmetry[8] and allow for the presence of CO . . . HN bonds between amino-acetyl groups. In this, however, the period along the *c* axis is again too large, being approximately 23 Å. The group of chains A in Fig. 5 are related by two-fold screw axes and can therefore have CO . . . HN bonding between trans-type side-chains, while the group of chains B are related by two-fold rotation axes and thus cannot have *trans*-type bonding. Bonding between chains of this latter symmetry is possible if they adopt the *cis*-configuration as in Fig. 4.

This arrangement would not, however, reduce the *c* axis period to 19·2 Å. It thus seems impossible to reconcile CO . . . HN bonding of both the A and B chains with the lattice dimensions, and as evidence points towards the existence of a pile of bonded chains, as at A, we are obliged to maintain this structural feature and move the piles towards one another along the *c* axis until the period is reduced to 19·2 Å. This results in the arrangement of Fig. 6.

Between the chains A there would be full bonding of CO . . . HN groups. Attached to side-chains of the type B there would be non-hydrogen-bonded NH groups, and this agrees with the infra-red spectra which give evidence for free —NH groups at 3445 cm.$^{-1}$.

The behaviour of the carbonyl groups in side-chains B must now be considered. The probable apposition of chitin chains in a layer such as C, Fig. 6, is given diagrammatically in Fig. 7, the relative position of the two chains being adjusted to allow the bulky CH_3 groups to occupy positions of minimum density. This is achieved by displacing chain II downward by one-sixth of the *b* axis period, a displacement which, as was pointed out by Meyer and Pankow, would give intensity to the 031 reflection. This degree of displacement is also near to that which would bring the linked piles of side-chains A′, A″ on to (031) planes. The difference of bonding, and hence of configuration, between the side-chains A and B would explain the small departure from perfect halving of the *b* axis period.

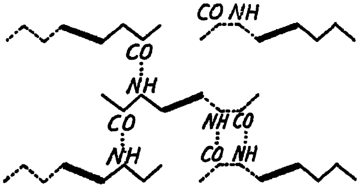

FIG. 4.

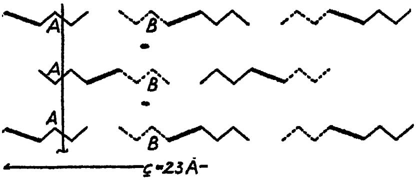

FIG. 5.

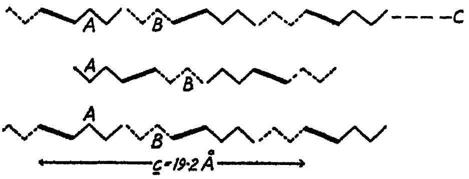

FIG. 6.

From Fig. 7 there are two main possibilities of bonding involving the carbonyl groups of chains B, viz. a cross-linking between carbonyl II and hydroxyl I or an intramolecular linking of carbonyl II and hydroxyl II. There is also the possibility of OH . . . OH bonding between hydroxyls I and II, but if C=O . . . HO bonding occurs, the hydroxyl bonding is eliminated. Thus with regard to the apposition and the distance between chains I and II, bonds of the C=O . . . HO type are justifiable. Furthermore, the infra-red evidence shows the absence of OH . . . OH and requires just such a bond as CO . . . HO.

The orientation of free OH and NH vibrations parallel to the main-chain axis, and the orientation of the C=O vibration of C=O . . . HO at right-angles to this axis need not be discussed at present. There seems no obvious reason why these orientations should not be obtained while keeping to the main features of Fig. 7.

(*b*) Chitosan.—Infra-red studies of the earlier stages of chitosan formation show a rapid loss of absorption corresponding to the proposed $C=O \ldots HO$ bond, while the carbonyl absorption of the $C=O \ldots HN$ linkage remains relatively intact. Parallel with the loss of $C=O \ldots HO$ there is increase of $OH \ldots OH$ bonding. This seems to correspond very well to removal of the acetyl groups II from Fig. 7, allowing nearer approach of chains I and II and formation of $OH \ldots OH$ bonds between hydroxyls I and II.

Löwy's contention that there is a structure corresponding to monoacetyldiglucosamine has support from the infra-red data, which demonstrate two kinds of $C=O$ groups, one of which is more readily removed. And from the symmetry of the chains in the chitin lattice, as deduced from X-ray studies, there is also evidence for two differently arranged types of acetyl groups. The considerably advanced chitosan preparation (17 hr. in 40 % NaOH solution at 100° C) does, however, show great reduction of the normal $CO \ldots HN$ linkages, which is probably due to extensive deacetylation of the more stably linked acetyl groups. We can regard this as evidence that the structure is proceeding towards polyglucosamine.

(*c*) Chitin Nitrate.—The considerable separation of the chains in the *c* axis direction is apparently due to incorporation of nitrate groups. In the infra-red spectra absorption due to weakly bonded OH has been lost as well as absorption corresponding to $C=O \ldots HO$. These changes would follow naturally from the substitution of hydroxyl groups. But because of the increased chain separation we have the possibility of full bonding between all the amino-acetyl side-chains. The evidence that this does occur rests upon the absence of absorption due to free NH groups. We are not as yet able to establish that there is relative intensification of the NH bands at 3265 cm.$^{-1}$ and 3100 cm.$^{-1}$, and the $C=O$ band at 1656 cm.$^{-1}$.

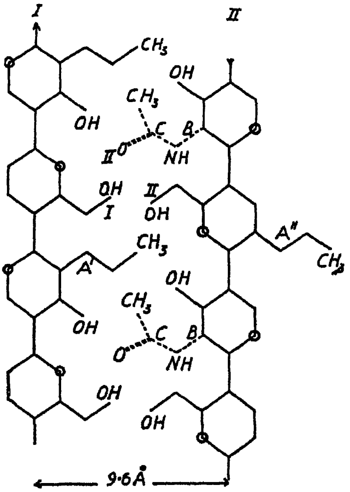

Fig. 7.

We are indebted to Prof. W. T. Astbury for his interest and criticism. One of us (S. E. D.) is indebted to Imperial Chemical Industries Ltd. for a Fellowship during the tenure of which this work was carried out.

Note added in Proof.—In a private communication from Prof. Richards we have learned of other infra-red studies of chitin and chitosan.[13] For chitin Richards observed bands at 1660 and 1630 cm.$^{-1}$ which must correspond to the two carbonyl frequencies we have observed at 1656 and 1625 cm.$^{-1}$. We regard his chitosan spectrum in the $6\ \mu$ region as approximating more closely to polyglucosamine than our most advanced chitosan spectrum (Fig. 2*d*). The strong absorption at 1600 cm.$^{-1}$ we would interpret as an NH deformation frequency resulting from free NH_2 groups, and the very weak absorption at 1700 cm.$^{-1}$ as arising from residual non-bonded carbonyl groups.

Department of Biomolecular Structure,
The University,
Leeds.

---

[13] See Richards, *The Integument of Arthropods* (University of Minnesota Press, Minneapolis) (in press).

THE INTERPRETATION OF THE VIBRATIONAL SPECTRA OF THE *n*-PARAFFINS

By J. K. Brown, N. Sheppard, and Miss D. M. Simpson

Received 31*st July*, 1950

Infra-red spectra in the crystalline state from 1500 to 700 cm.$^{-1}$ are presented for the even numbered paraffins from *n*-octane to *n*-tetradecane, and also for *n*-nonane. Detailed consideration is given to the assignment of the collected infra-red and Raman spectra of the planar *trans* isomer of *n*-butane, and partial interpretations are attempted of the less complete experimental data available for the planar zig-zag isomers of the other even-numbered paraffins to *n*-tetradecane. The skeletal stretching modes are shown to occur between 1150 and 880 cm.$^{-1}$ for the paraffins with more than six carbon atoms, and five series of such frequencies which run through the spectra of the different hydrocarbons have been picked out and identified. Series of CH_2 wagging and twisting modes occur between 1350 and 1150 cm.$^{-1}$; CH_2 rocking modes, which originate near 700 cm.$^{-1}$ in the infra-red spectra of the smaller molecules, give rise to series of absorptions spreading to 1000 cm.$^{-1}$ in the spectra of the larger molecules. The in-plane methyl wagging modes are found near 1060 cm.$^{-1}$. The present position with respect to the theoretical estimation of the skeletal frequencies is discussed. Such calculations are found to be of considerable help in the partial analysis of the spectra, but inadequate for the accurate calculation of all the skeletal frequencies. The infra-red and Raman spectra of polythene are discussed.

The interpretation of the vibrational spectra of the *n*-paraffins would seem to provide a profitable field of investigation for the experimentalist in search of a series of related molecules, since in principle the carbon skeleton of a molecule of the type $CH_3(CH_2)_{n-2}\,CH_3$ approximates to a regular zig-zag chain of equal masses capable of a straightforward theoretical treatment. The *n*-paraffins are available in a pure state and their vibrational spectra have been studied extensively, but contrary to expectation these spectra have proved to be exceptionally difficult to analyze.

The conventional formulae of these molecules suggest that the dominant form should be the planar zig-zag configuration, but the work of Kohlrausch and Köppl [1] on the Raman spectra of the liquids has indicated clearly that this is not so. They concluded from the experimental evidence that more than one rotational isomer of each molecule was present. Systematic accounts of the formulation of the configurations of all possible isomers have been given by Pitzer,[2] and by Simanouti and Mizushima.[3] In the gaseous and liquid states the planar zig-zag form of the *n*-paraffins is the most stable; the stability of the other isomers, which are formed by one or more rotations about different carbon-carbon bonds away from the planar configuration, decreases with the number of rotations. Since each isomer has its own set of vibrational frequencies, and as the number of possible isomers increases with the chain length, the complexity of the spectra of the long chain molecules makes their analysis impossible. It is therefore necessary to seek methods which will overcome this difficulty, and the most direct appears to be an investigation of the spectra of the *n*-paraffins in the solid state.

X-ray data by Müller [4] show that these hydrocarbons assume the planar zig-zag form in the crystalline lattice. This method of spectroscopic analysis therefore eliminates all the other possible configurations. Such a procedure has experimental difficulties, but once they are surmounted the resulting spectra are drastically simplified and their interpretation becomes reasonably possible. Data on the Raman spectra of the solids have been previously published by Rank, Sheppard and Szasz,[5, 6] and by Mizushima and Simanouti.[7] Between them these papers cover the molecules n-butane to n-decane, and also n-dodecane and n-hexadecane. Axford and Rank[8, 9] have investigated the corresponding infra-red spectra from n-butane to n-heptane. The purpose of this paper is to present further infra-red work on the solid state spectra of the n-paraffins including the series of molecules containing an even number of carbon atoms from n-octane to n-tetradecane (Fig. 1). Using the combined infra-red and

---

[1] Kohlrausch and Köppl, *Z. physik. Chem. B*, 1934, **26**, 209.

[2] Pitzer, *J. Chem. Physics*, 1940, **8**, 711.

[3] Simanouti and Mizushima, *Sci. Papers Inst. Phys. Chem. Res. Tokyo*, 1943, **40**, 467.

[4] Müller, *Proc. Roy. Soc. A*, 1928, **120**, 437.

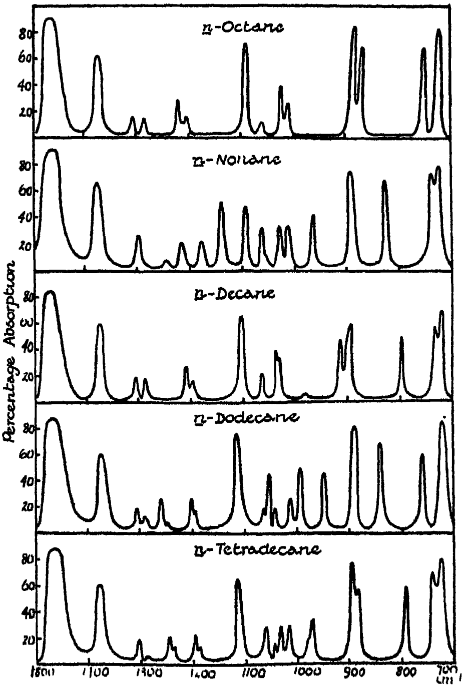

FIG. 1.—The infra-red spectra between 1500 and 700 cm.$^{-1}$ of some n-paraffins in the crystalline state.

Raman data, an attempt will also be made to analyze the spectra of these molecules in the region 1350 to 700 cm.$^{-1}$ where reasonably complete results are available. The solid state spectrum of n-nonane is also presented in Fig. 1. Although detailed interpretations of the spectra of the odd-numbered hydrocarbons will not be attempted here, the experimental data are of use for identifying series of skeletal frequencies.

Experimental

The experimental and spectroscopic techniques used in obtaining the spectra in the liquid and solid states were mainly as described in an earlier paper.[10]

---

[5] Rank, Sheppard and Szasz, *J. Chem. Physics*, 1949, **17**, 83.
[6] Sheppard and Szasz, *ibid.*, 1949, **17**, 86.
[7] Mizushima and Simanouti, *J. Amer. Chem. Soc.*, 1949, **71**, 1320.
[8] Axford and Rank, *J. Chem. Physics*, 1949, **17**, 430.
[9] Axford and Rank, *ibid.*, 1950 **18**, 51.
[10] Brown and Sheppard, this Discussion.

The cells used for containing the liquids were, however, of rocksalt rather than silver chloride. The solids were cooled to 20 or 30° C below their freezing points before taking their spectra. A constant thickness of 0·2 mm. of material was used throughout. Crystallization occurred in every case at the freezing point and no glasses were formed. The scattering of radiation by the substances in the solid state was particularly bad for these materials because of the thickness of the samples. Accordingly intensities measured in the spectra of the solid materials are approximate only.

Data related to the source and purity of the hydrocarbons studied are listed below :

n-Octane : Anglo-Iranian Oil Co. Ltd. ; 99·98 mole % purity.
n-Nonane : Anglo-Iranian Oil Co. Ltd. ; 99·8 mole % purity.
n-Decane : Pennsylvania State College ; b.p. 174·15° C.
n-Dodecane : Elsner ; n_D^{20} 1·4219 (literature, n_D^{20} 1·42188).
n-Tetradecane : Anglo-Iranian ; $>$99·9 mole-% purity.

The principal absorption frequencies are listed below :

n-OCTANE.

Liquid. 722 (s), *ca.* 751 (s), *ca.* 765 (s), *ca.* 794 (m), *ca.* 844 (m), *ca.* 878 (s), 889 (m), *ca*, 896, 915 (m), *ca.* 967 (m), *ca.* 1005, *ca.* 1036, *ca.* 1078, 1136 (m), 1200 (m), 1225 (m), 1270 (m), 1301 (s), 1341 (s), *ca.* 1353 (s), 1378 (s), *ca.* 1465 (s).

Solid. 722 (s), 748 (s), 864 (s), 881 (s), 1008 (m), 1020 (m), 1058 (w), 1088 (s), 1205 (w), 1218 (m), 1286 (w), 1303 (w), 1378 (m), *ca.* 1465 (s).

n-NONANE.

Liquid. 721 (s), *ca.* 752 (s), *ca.* 776 (m), *ca.* 830 (m), *ca.* 844 (m), *ca.* 874 (m), 889 (s), *ca.* 927 (m), *ca.* 968 (m), *ca.* 986 (m), *ca.* 1043 (m), 1063 (m), *ca.* 1086 (m), *ca.* 1137 (m), *ca.* 1189 (m), 1217 (m), 1258 (m), 1303 (s), 1341 (s), 1355 (s), 1378 (s), *ca.* 1470 (s).

Solid. 721 (s), 736 (s), 826 (s), 889 (s), 962 (m), 1012 (m), 1029 (m), 1049 (w), 1063 (m), 1094 (m), 1138 (m), 1178 (m), 1215 (m), 1243 (w), 1298 (w), 1376 (s), *ca.* 1465 (s).

n-DECANE.

Liquid. 721 (s), *ca.* 769 (s), *ca.* 815 (m), *ca.* 846 (m), *ca.* 893 (m), *ca.* 921 (m), *ca.* 971 (m), *ca.* 995 (m), *ca.* 1008 (m), *ca.* 1026 (m), *ca.* 1076 (m), *ca.* 1091 (m), 1135 (m), *ca.* 1187 (m), *ca.* 1210 (m), 1247 (m), *ca.* 1278 (m), 1303 (s), 1342 (s), *ca.* 1355 (s), 1378 (s), *ca.* 1465 (s).

Solid. 720 (s), 730 (s), 795 (m), 890 (s), 912 (m), 980 ? (w), 1032 (m), 1037 (m), 1062 (w), 1103 (s), 1195 (w), 1208 (m), 1283 (w), 1303 (w), 1378 (s), *ca.* 1465 (s).

n-DODECANE.

Liquid. 721 (s), *ca.* 770 (m), *ca.* 806 (m), *ca.* 847 (m), *ca.* 887 (s), *ca.* 960 (m). *ca.* 1015 (m), 1075 (m), 1098 (m), 1135 (m), *ca.* 1179 (m), *ca.* 1197 (m), *ca*, 1232 (m), *ca.* 1262 (m), 1303 (s), 1342 (s), 1355 (s), 1377 (s), *ca.* 1465 (s).

Solid. 722 (s), 760 (s), 839 (s), 887 (s), 945 (m), 993 (m), 1010 (m), 1038 (w), 1052 (m), 1062 (w), 1112 (s), 1191 (w), 1201 (m), *ca.* 1248 (w), 1262 (m), *ca.* 1288 (w), 1303 (w), 1378 (m), *ca.* 1465 (s).

n-TETRADECANE.

Liquid. 721 (s), *ca.* 803 (m), *ca.* 841 (m), *ca.* 888 (m), *ca.* 934 (m), *ca.* 961 (m), *ca.* 980 (m), *ca.* 1075 (m), *ca.* 1102 (m), 1133 (m), *ca.* 1170 (m), *ca.* 1250 (m), *ca.* 1272 (m), *ca.* 1304 (s), 1341 (s), 1355 (s), 1378 (s), *ca.* 1465 (s).

Solid. 722 (s), 742 (s), 795 (s), 881 (m), 891 (s), 970 (m), *ca.* 978 (m), 1012 (m), 1031 (m), 1040 (w), 1060 (m), 1114 (m), 1187 (w), 1197 (m), *ca.* 1236 (w), 1248 (m), *ca.* 1286 (w), 1305 (w), 1376 (m), *ca.* 1465 (s).

Interpretation of the Spectra

Introduction.—Although the *trans* zig-zag forms of the *n*-paraffins are simple in structure, yet the analysis of their spectra presents certain difficulties. For convenience of interpretation, the vibrations of these molecules may be divided into two types, those involving mainly the hydrogen atoms, and those concerned with the movements of the nuclear framework when the CH_3, CH_2 groups may be considered as mass units. The assignments of certain of the frequencies of the first class are well established, viz. the CH stretching frequencies in the region 3000 to 2800 cm.$^{-1}$, the internal hydrogen deformation frequencies of the methyl group near 1450 and 1380 cm.$^{-1}$, and the symmetrical deformation frequency of the CH_2 group near 1450 cm.$^{-1}$. In the region 1350 to 700 cm.$^{-1}$ much overlapping occurs since the stretching vibrations of the carbon skeleton, the remaining deformation frequencies of the CH_2 groups and the four methyl wagging modes all occur in this range of frequencies. Some progress has already been made in the sorting out of these different types of vibrations, but the picture is by no means complete.

Some conclusions about the range of the skeletal vibrations of the *n*-paraffins have already been obtained from the Raman data on the solid state.[6, 7] The lower limit of these vibrations seems to be defined unequivocally by the pronounced polarized line near 890 cm.$^{-1}$ which is observed in the spectra of all of these molecules. It has been suggested[6] that the upper limiting skeletal frequency must correspond to one or the other of the two series of Raman lines found near 1145 and 1060 cm.$^{-1}$. Following Kohlrausch,[1] most authors have assumed the 1060 cm.$^{-1}$ frequency to be the highest skeletal vibration and that at 1145 cm.$^{-1}$ the in-plane CH_3 wagging mode. Recent work on the branched paraffins[11, 12, 13] has shown, however, that skeletal modes may well occur at frequencies greater than 1100 cm.$^{-1}$. Hence the assignment of these two frequencies must be re-examined.

Each CH_2 group has wagging, rocking, and twisting frequencies.[13] Empirical evidence derived from measurements with polarized radiation[14] and from the spectrum of a completely deuterated *n*-paraffin,[15] shows clearly that the 720 cm.$^{-1}$ absorption band found in all the *n*-paraffins is associated with CH_2 rocking modes. The Raman line about 1300 cm.$^{-1}$ which is always present, is also associated with the vibrations of the CH_2 groups, although whether it arises from twisting or wagging modes has been the subject of some discussion.[13, 16]

Less certain is the identification of the CH_3 wagging modes. In ethane[17] they appear at 1155 and 821 cm.$^{-1}$; in the branched paraffins some authors have suggested that they may be as high as 1250 cm.$^{-1}$,[16] while others[11, 12] prefer to locate them at lower frequencies, < 1100 cm.$^{-1}$. Perhaps the most probable frequency range for these vibrations in the *n*-paraffins is roughly 1200 to 800 cm.$^{-1}$.

The deformation frequencies of the carbon skeleton, and the torsion frequencies of the framework and terminal methyl groups occur together at frequencies below 600 cm.$^{-1}$. Few experimental data are available for the solid materials in this range, and the spectra will not be considered in detail. The collected empirical evidence is summarized in Table I.

***trans*-*n*-Butane.**—This molecule, the first of the series of *n*-paraffins with multiple CH_2 groups, can exist in two different rotational configurations. The *trans* isomer, the only form present in the solid state, is of symmetry C_{2h} and because of its centre of symmetry fairly strict selection rules operate. The distinct frequencies of the *gauche* isomer (C_2) may be picked out from the spectra of the liquid or vapour, which show the lines of both isomers.

[11] Pitzer and Kilpatrick, *Chem. Rev.*, 1946, **39**, 435.

[12] Simpson and Sutherland, *Proc. Roy. Soc. A*, 1949, **199**, 169.

[13] Sheppard, *J. Chem. Physics*, 1948, **16**, 690.

[14] Vallance-Jones and Sutherland, *Nature*, 1947, **160**, 567.

[15] Sheppard and Sutherland, *Nature*, 1947, **159**, 739.

[16] Rasmussen, *J. Chem. Physics*, 1948, **16**, 712.

[17] Herzberg, *Infra-red and Raman Spectra of Polyatomic Molecules* (Van Nostrand, New York, 1945), pp. 342-346.

A number of authors [16, 18, 19, 20] have already proposed assignments for *n*-butane based on measurements of the spectra in the liquid or vapour state. Since the experimental data did not allow them to distinguish unambiguously the frequencies of either isomer, none of these is entirely correct. More recently Szasz, Sheppard and Rank [21] used Raman data observed over a range of temperature to make a new assignment for both configurations, and this was modified by Axford and Rank [8, 9] with the help of the infra-red spectrum of the solid. The present discussion is based on this earlier work, but suggests some important changes. In this paper only the *trans* isomer will be considered; Table I summarizes the types of vibration, selection rules, and expected frequency ranges together with the assignment now proposed for this form. The numbering of the frequencies is uniform with the previous work.[21] There is little doubt that the frequencies higher than 1370 cm.$^{-1}$ were adequately dealt with in the previous treatments.

TABLE I.—THE ASSIGNMENT OF THE FUNDAMENTAL VIBRATIONS OF *trans-n*-BUTANE BELOW 1500 CM.$^{-1}$

Description	A_g (R. p)	A_u (I. R.)	B_g (R. dp)	B_u (I. R)	Expected Frequency Range (cm.$^{-1}$)
CH_2 bending	$\nu_1=1455$	—	—	$\nu_{30}=1461$	*ca.* 1450
CH_3 asymm. deformation	$\nu_5=(1455)$	$\nu_{14}=(1461)$	$\nu_{22}=(1455)$	$\nu_{31}=(1461)$	*ca.* 1450
CH_3 symm. deformation	$\nu_6=1370$	—	—	$\nu_{32}=1382$	*ca.* 1380
CH_2 wagging	$\nu_7=1304$	—	—	$\nu_{33}=1350$	1200-1350
CH_2 twisting	—	$\nu_{15}=1299$	$\nu_{23}=?$	—	1100-1350
C—C stretching	$\left\{\begin{matrix}\nu_8=1148\\ \nu_9=835\end{matrix}\right\}$	—	—	$\nu_{34}=965$	800-1200
CH_3 wagging	$\nu_{10}=1058$	$\nu_{16}=951$	$\nu_{24}=956$	$\nu_{35}=984$	800-1200
CH_2 rocking	—	$\nu_{17}=732$	$\nu_{25}=?$	—	700-1050
Skeletal deformation	$\nu_{11}=432$	—	—	$\nu_{36}=?$	<600
Skeletal torsion	—	$\nu_{18}=?$	—	—	
Methyl torsion	—	$\nu_{19}=?$	$\nu_{26}=?$	—	

R.=Raman; I.R.=infra-red; p=polarized; dp=depolarized.

For the *trans* isomer within the region 1370-700 cm.$^{-1}$ six infra-red active modes are expected, three being of the A_u and three of the B_u type. The former should give rise to contours in the gaseous state similar to those of a planar molecule with the change of electric moment along the greatest axis of inertia, i.e. a sharp and pronounced *Q* branch with coarse rotational fine structure on either side. The B_u bands on the other hand would be expected to have rather indeterminate shapes. Six regions of absorption are observed in the solid state spectrum,[8] at 1350 (w), 1299 (m), 984 (w), 965 (s), 951 (s) and 732 cm.$^{-1}$ (s). Gates [22] has made high resolution studies in the gaseous state of all but the 984 cm.$^{-1}$ band. He also investigated bands which must be attributed to the *gauche* isomer, because of their absence in the solid state spectrum.

The band at 732 cm.$^{-1}$ is certainly the CH_2 rocking mode as suggested by Axford and Rank.[8] In the gaseous curves it shows the correct contour

---

[18] Eliashevich and Stepanov, *Compt. rend. U.R.S.S.*, 1941, **32**, 481.

[19] Stepanov, *Acta Physicochim.*, 1947, **22**, 238.

[20] Kassel, *J. Chem. Physics*, 1935, **3**, 326.

[21] Szasz, Sheppard and Rank, *ibid.*, 1948, **16**, 704.

[22] Gates, *ibid.*, 1949, **17**, 393.

for an A_u band and occurs in the expected frequency range. The gaseous absorption at 951 cm.$^{-1}$ also has a strong Q branch and coarse structure on the low frequency side, although it is badly overlaid by the 965 cm.$^{-1}$ band at higher frequencies. Accordingly it is assigned to the out-of-plane A_u methyl wagging frequency. The 965 cm.$^{-1}$ absorption, which certainly does not have the same type of contour, must be a B_u band and is very probably the asymmetrical skeletal stretching mode which should be strong in the infra-red spectrum. The weak 984 cm.$^{-1}$ absorption which is apparent in the solid state spectrum must then be the B_u in-plane CH_3 wagging frequency, although it is just possible that it might be an overtone or combination band.

The contours in the gaseous state are not very helpful in deciding which of the bands at 1350 and 1299 cm.$^{-1}$ corresponds to the A_u CH_2 twisting mode, and which to the B_u CH_2 wagging mode. Both have fairly prominent Q branches and coarse fine structure, but in neither case is the Q branch as pronounced as would be expected for an A_u band. Since it is probable that this region contains absorption from similar vibrations of the *gauche* isomer, overlapping may explain the anomalous contours. In Table I the absorption at 1350 cm.$^{-1}$ is attributed to the CH_2 wagging mode and that at 1299 cm.$^{-1}$ to the twisting vibration, but this assignment must be considered tentative until further experimental evidence becomes available.

In the region 1370-700 cm.$^{-1}$ seven fundamentals are allowed in the Raman spectrum; four of these should be polarized (A_g), and the remaining three depolarized lines, (B_g). The spectrum of solid n-butane [5, 6] shows lines at 1304, 1148, 1058 and 835 cm.$^{-1}$ all of which are polarized in the liquid and must therefore be A_g in type; a fifth depolarized line at 956 cm.$^{-1}$ found in the liquid may also, on account of its temperature variation,[21] be attributed to a B_g vibration of the *trans* isomer. Experimental difficulties have so far precluded measurements of polarization in the solid state. Of the A_g frequencies there is little doubt in the assignment of the 835 cm.$^{-1}$ line to the lowest skeletal stretching vibration, and the 1304 cm.$^{-1}$ line falls in the region expected for the CH_2 wagging mode. Thus the frequencies at 1058 and 1148 cm.$^{-1}$ must correspond to the remaining modes, the higher skeletal stretching and methyl in-plane wagging vibrations. Szasz, Sheppard and Rank [21] attributed the 1148 cm.$^{-1}$ line to the A_g methyl wagging mode because the 1134 cm.$^{-1}$ band in the infra-red could be considered its B_u counterpart. The more recent work of Axford and Rank [8] has shown that this latter band disappears in the infra-red spectrum of the solid, so that this argument is invalidated. As has already been discussed, the B_u methyl wagging mode is now considered to appear at 984 cm.$^{-1}$; it would therefore seem more likely that the corresponding A_g vibration should be at 1058 cm.$^{-1}$, thus reversing the former assignment and putting the skeletal vibration at 1148 cm.$^{-1}$. This reasoning is admittedly not conclusive, but if the assignment of n-butane is considered in relation to those of the whole series of n-paraffins, then as will be shown later, the evidence for this interpretation is very strong.

The single observed B_g frequency in the spectrum of *trans* n-butane at 956 cm.$^{-1}$ is almost certainly the out-of-plane methyl wagging mode, the A_u frequency of this type appearing at 951 cm.$^{-1}$ in the infra-red spectrum. The two remaining B_g frequencies corresponding to the CH_2 twisting and rocking modes are missing. It is probable that the twisting mode lies near 1250 cm.$^{-1}$, but it is difficult to predict the frequency of the rocking mode since these vibrations spread over a range of frequencies in the higher n-paraffins. Further experimental work is necessary for their exact identification.

The spectroscopic data below 700 cm.$^{-1}$ are less complete in that only the Raman spectrum has been obtained in the solid state.[6] As methyl torsion modes seem usually to be weak in both infra-red and Raman spectra, the single line at 432 cm.$^{-1}$ in the solid state Raman spectrum must be the A_g skeletal deformation mode, since it is polarized in the liquid. The infra-red spectrum in the gaseous state between 700 and 400 cm.$^{-1}$ is available,[23] and it has been studied between 400 and 170 cm.$^{-1}$ by Gates.[22] Two weak absorption bands were found at 444 and 215 cm.$^{-1}$. However, their definite assignment to the *trans* isomer must also await further work in the solid state.

The Planar Isomers of *n*-Hexane to *n*-Tetradecane.—It is not feasible at this stage to give an account of the complete assignments for each of the planar zig-zag isomers of the molecules *n*-hexane to *n*-tetradecane. However, series of related frequencies in the spectra of the even-numbered paraffins will be discussed in detail. The data on the spectra of the odd-numbered molecules will be used only to confirm the assignments of some of the skeletal series in the even-numbered molecules, but it is hoped to treat their spectra in more detail at a later date.

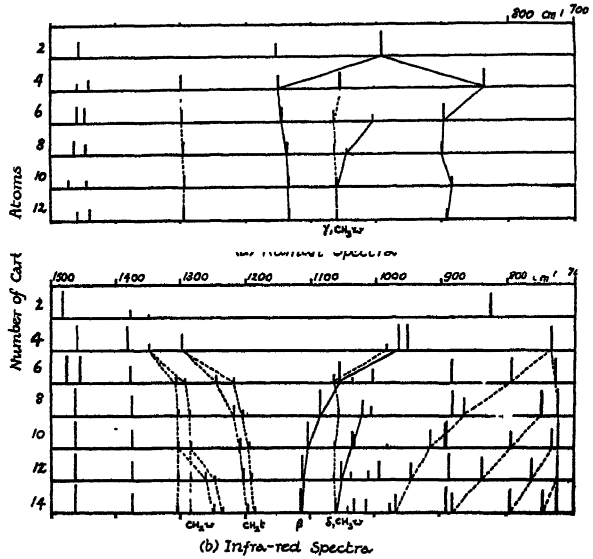

FIG. 2.—(*a*) The Raman spectra of the planar isomers of the even-numbered paraffins. (*b*) The infra-red spectra of the same molecules.
—— skeletal modes. - - - - - CH deformation modes.

Fig. 2(*a*) and 2(*b*) are line diagrams showing separately the Raman and infra-red frequencies in the solid state for the even-numbered *n*-paraffins. Fig. 3 is a similar line diagram for the molecules with odd numbers of carbon atoms. The series of lines which can be picked out and attributed to the different modes of vibration are indicated. The following discussion is a summary of the reasoning on which these assignments are based. From the detailed assignments of *trans* *n*-butane it may be expected that for molecules with an even number of carbon atoms the Raman lines of symmetry B_g corresponding to methyl wagging, CH_2 rocking, and CH_2 twisting modes will be weak or unobservable. It is clear at the outset that the number of Raman lines observed is very much smaller than the number actually allowed.

(1) THE REGION 1350-1500 cm.$^{-1}$.—The deformation modes of the CH_3 and CH_2 groups occur within this frequency range. The CH_3 symmetrical deformation vibrations give a single infra-red absorption near 1380 cm.$^{-1}$

---

[23] *Amer. Petroleum Inst. Res. Project* 44; Catalogue of Infra-red Spectra, No. 61, contributed by Shell Oil Co. Inc., Houston, Texas.

The CH_3 unsymmetrical internal deformation and the CH_2 bending modes occur in both the Raman and infra-red spectra at frequencies between 1450 and 1470 cm.$^{-1}$, the Raman lines being depolarized.

(2) THE VIBRATIONS OF THE CH_2 GROUPS IN THE REGION 700-1350 cm.$^{-1}$. (i) CH_2 ROCKING MODES.—The number of allowed frequencies of this type for the molecule C_nH_{2n+2} with an even number of carbon atoms is $(n - 2)/2$ for modes of symmetry A_u and $(n - 2)/2$ for symmetry B_g. These vibrations are expected to originate near 720 cm.$^{-1}$ for molecules with only a few CH_2 groups, and to be prominent in the infra-red spectra. Without difficulty all the infra-red active A_u bands may be picked out as progressions starting near 720 cm.$^{-1}$ which extend in a regular manner to high frequencies as the chain length increases (Fig. 2*b*). None of the Raman lines that are allowed to appear are observed. The normal co-ordinate calculations for the *n*-paraffins by Stepanov [19] using a reasonably complete force field indicate the range as 700 to 1000 cm.$^{-1}$ in good agreement with that actually found.

(ii) THE CH_2 WAGGING AND TWISTING MODES.—For the even-numbered paraffins $(n - 2)/2$ CH_2 wagging modes of each of the symmetry types

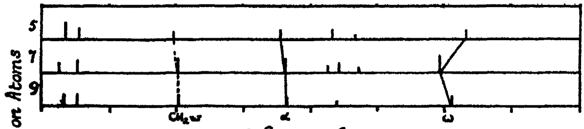

(a) Raman Spectra

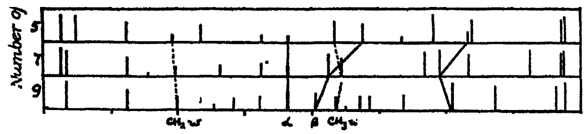

(b) Infra-Red Spectra

FIG. 3.—(*a*) The Raman spectra of the planar isomers of the odd-numbered paraffins. (*b*) The infra-red spectra of the same molecules.

A_g and B_u are expected; the same number of A_u and B_g twisting modes are also allowed in the infra-red and Raman spectra respectively. The assignment of *n*-butane suggests that the wagging mode occurs at higher frequencies than the twisting mode. This is also confirmed by the calculations of Stepanov.[19]

In the infra-red spectra of these molecules groups of bands may be distinguished. One group always has a doublet structure and shifts down as the chain length increases approaching a limiting value at $n = 14$ of *ca.* 1190 cm.$^{-1}$. This doublet has been assigned to the A_u CH_2 twisting vibrations. No Raman lines corresponding to the B_g CH_2 twisting modes are found. The other group of infra-red bands which has a more complex structure seems to settle down as the chain length increases to a pattern of two absorptions, one near 1300 cm.$^{-1}$ and the other near 1240 cm.$^{-1}$. These have been assigned to the B_u CH_2 wagging vibrations. The corresponding A_g CH_2 wagging vibration shows as the single Raman line near 1300 cm.$^{-1}$, and presumably most of the vibrations occur near this frequency. These lines are usually considerably depolarized in the spectra of the liquids,[24] but there is no doubt of the polarized nature of the first line of this series in the spectrum of *n*-butane.

(3) THE REGION 850-1150 cm.$^{-1}$.—The most difficult part of the spectrum to analyze is the region 850-1150 cm.$^{-1}$ where the four methyl wagging frequencies and the $(n - 1)$ skeletal stretching frequencies occur together. For a molecule having several CH_2 groups separating the

---

[24] Herz, Kahovec and Wagner, *Monatsh.*, 1945, 76, 100.

terminal methyls, it is plausible to suggest that the methyl wagging modes will occur in two pairs, one corresponding to the in-plane and one to the out-of-plane vibrations. One member of each pair will always be allowed in the Raman spectrum and the other in the infra-red spectrum, so that accidental coincidences of these infra-red and Raman frequencies are probable even for the even-numbered paraffins.

The clue to the assignment of the skeletal stretching modes was provided by a consideration of the simplest possible theoretical treatment. As has been shown by a number of authors [25-28] the skeletal vibrations of a zig-zag chain of n equal masses are approximately obtained by applying the Born-Karmann periodicity condition, $x = \pi l/n$. Here l has integral values from 1 to $(n - 1)$. The frequencies ν may then be calculated using the formula :

$$\nu = \frac{1}{2\pi}\sqrt{\frac{2f}{m}(1 \pm \cos\theta \cos x)}, \quad . \quad . \quad . \quad (1)$$

where f is the stretching force constant, m the mass of the repeating unit (CH_2 group), and θ the angle between the bonds, taken as the tetrahedral angle.

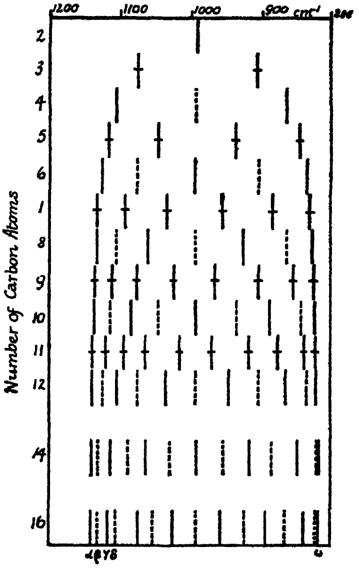

FIG. 4.—The distribution of skeletal frequencies for planar zig-zag paraffins, calculated with a stretching force constant of $4{\cdot}0 \times 10^5$ dynes/cm. and a zero deformation force constant.

———Raman active ;
- - - - - Infra-red active ;
+ Infra-red and Raman active.

The characteristic pattern produced [29] is shown in Fig. 4. The $(n - 1)$ frequencies of the molecule C_nH_{2n+2} split out from the single frequency of ethane to give a distribution roughly parabolic in shape. For even values of n the vibrations counting from the lower limit are alternately allowed in the Raman (polarized) and infra-red spectrum ; for n odd all may appear in both spectra, the Raman lines being alternately polarized and depolarized.

It might be thought that such a drastically simplified model would not be very helpful in assigning the skeletal vibrations, and might even be misleading. That this is not so will be apparent from the following discussion. The lower limiting frequency (ω in Fig. 4), which is allowed as a

---

[25] Bartholomé and Teller, *Z. Physik. Chem. B*, 1932, **19**, 366.
[26] Stepanov, *J. Phys. Chem. Russ.*, 1940, **14**, 474.
[27] Parodi, *J. Physique Rad.*, 1941, **2**, 58.
[28] Kellner, *Trans. Faraday Soc.*, 1945, **41**, 217.
[29] Kohlrausch, *Ramanspektren* (Becker and Erler, Leipzig, 1943), p. 206.

polarized line in the Raman spectra of odd- and even-numbered paraffins, has already been identified near 900 cm.$^{-1}$ by Simanouti and Mizushima,[7] and by Sheppard and Szasz.[6] The upper limiting frequency α was put near 1060 cm.$^{-1}$ in the first place by Kohlrausch [1] and since then by many other workers. This implies that one methyl wagging frequency must be put at about 1140 cm.$^{-1}$. As has already been suggested in the discussion on *n*-butane, this assignment should be reversed. The selection rules are such that the highest skeletal mode is forbidden in the infra-red spectrum of those molecules with an even number of carbon atoms, although it can appear as a Raman line for all molecules. On the other hand, as already indicated, there may be accidental infra-red and Raman coincidences for the methyl wagging modes even when the molecule has a centre of symmetry. In all the *n*-paraffins Raman lines are observed near 1140 and 1060 cm.$^{-1}$,[6, 7] but infra-red counterparts to the former are found only for those molecules with an odd number of carbon atoms in agreement with the selection rules for the highest skeletal frequency. Furthermore, as expected for the methyl modes, infra-red absorption is observed near 1060 cm.$^{-1}$ for all the molecules that have so far been investigated. This leaves little doubt about the assignment of these two sets of frequencies. The prominence of the frequencies near 1060 cm.$^{-1}$ in the Raman spectrum, and the polarization of the *n*-butane line of this series,[21] suggest that they are the in-plane methyl wagging vibrations.

Having thus established the frequencies of the limiting (α and ω) skeletal stretching vibrations, the next task is to identify as far as possible the remaining skeletal modes. Guidance is once more provided by the simple theoretical treatment. The second series of skeletal modes β is always active in the infra-red for both odd- and even-numbered molecules. Starting from the band at 965 cm.$^{-1}$ in *n*-butane, it is easy to pick out a prominent infra-red band which shifts to higher frequencies as the chain length increases. The third series γ is always Raman active. It originates at the 1007 cm.$^{-1}$ Raman line of *n*-hexane and may be recognized as far as *n*-decane. The fourth δ which is again always infra-red active starts from the infra-red band at 1020 cm.$^{-1}$ in *n*-octane. No lines are found corresponding to the fifth or subsequent Raman active series except for ω as already discussed. Evidently as the chain length increases they have become too weak to be observed.

The regular pattern found in the infra-red spectra in the range 1150-1050 cm.$^{-1}$ for the even-numbered paraffins is not apparent between 1050 and 850 cm.$^{-1}$. In order to interpret this observation, the theoretical treatment was considered in more detail. One obvious fault in the predictions of the simple theory is that the range of values expected for the stretching mode is too great (1150 to 820 cm.$^{-1}$ as compared with 1150 to 890 cm.$^{-1}$ found by experiment). Clearly a discussion employing only a stretching force constant is too approximate, and at least a simple valency force field with both stretching and deformation force constants must be used. Such a treatment was given by Kirkwood [30] and modified by Pitzer.[31] Their equations are:

$$\nu \text{ stretching} = \frac{1}{2\pi}\sqrt{\frac{2f}{m}\left(\frac{a+b}{2}\right)^{\frac{1}{2}}} \quad . \quad . \quad . \quad (2)$$

and

$$\nu \text{ deformation} = \frac{1}{2\pi}\sqrt{\frac{2f}{m}\left(\frac{a-b}{2}\right)^{\frac{1}{2}}} \quad . \quad . \quad . \quad (3)$$

where a and b are functions of θ and x which have been defined earlier, and of ϵ which is the ratio of the deformation force constant, d to f. A similar treatment has also been given by Barriol and Chapelle.[32] The upper limit ($x = \pi$), identical with that derived from eqn. (1), is independent of ϵ. Since this is known to be 1140 cm.$^{-1}$, it fixes the value of f as $4{\cdot}05 \times 10^5$ dynes/cm. The curves of frequency against phase angle for this value of f and various values of ϵ are shown in Fig. 5. All these curves are nearly coincident for $\pi/2 < x < \pi$, and hence it is at once apparent why the simplest possible treatment (with $\epsilon = 0$) was adequate for the identification of the skeletal series in the range 1050-1150 cm.$^{-1}$. As the lower limiting frequency is dependent upon ϵ, the best value for this quantity is obtained, on this approximation, by substituting the known value of 890 cm.$^{-1}$ in eqn. (2) and solving for ϵ with $x = 0$. The value so derived is 0·031, corresponding to

---

[30] Kirkwood, *J. Chem. Physics*, 1939, **7**, 506.

[31] Pitzer, *ibid.*, 1940, **8**, 711.

[32] Barriol and Chapelle, *J. Physique Rad.*, 1947, **8**, 8.

$$d = 0{\cdot}127 \times 10^5 \text{ dynes/cm.}$$

The curve of frequency against phase angle for this value of ϵ is drawn in with a dashed line in Fig. 5, and if this more refined theory is adequate it should be possible to predict fairly accurately with the help of this curve the skeletal frequencies for the different hydrocarbons, and hence to analyze the experimental data between 1050 and 890 cm.$^{-1}$. In order to test whether this is so, reference was first made to the infra-red experimental data on *n*-hexane and *n*-octane. For each of these molecules all the expected skeletal modes have been identified with one exception. The two remaining infra-red absorptions in each spectrum in this region have to be assigned to this skeletal mode and to the A_u out-of-plane wagging mode. For *n*-hexane the two absorption bands at 1006 and 884 cm.$^{-1}$ have to be compared with the value of the expected skeletal frequency near 920 cm.$^{-1}$; in *n*-octane the observed frequencies are at 1008 and 881 cm.$^{-1}$ and the predicted value of the skeletal vibration is near 900 cm.$^{-1}$.

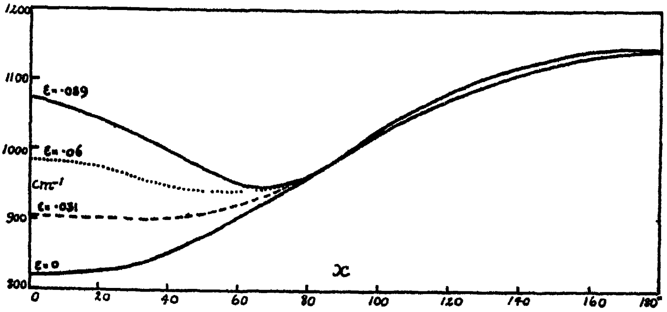

FIG. 5.—Curves showing the skeletal stretching frequencies as a function of phase angle x, for different values of ϵ, the ratio of the deformation force constant to the stretching constant.

At first sight it would seem more likely that the lower observed frequency, which has counterparts in the spectra of the longer chain paraffins near 890 cm.$^{-1}$, should be correlated with the calculated skeletal frequency. If this were correct, a series of infra-red absorptions near 1030 cm.$^{-1}$ in the longer chain paraffins would continue the series of methyl wagging modes, and a reasonable assignment could be made for the remaining skeletal frequencies of the even-numbered paraffins with the help of the frequency-phase angle curve. However, the details of this assignment have not been elaborated here because of some doubt concerning the key attribution of the lower frequency in *n*-hexane and *n*-octane to the skeletal mode. Thus if the other methyl wagging mode does lie near 1030 cm.$^{-1}$ it would be expected to show up near this position in the infra-red spectra of the odd-numbered paraffins, and this is not consistently the case. Furthermore, the acceptance of the low frequency absorption as the skeletal mode in *n*-hexane and *n*-octane implies that in the longer chain paraffins several frequencies crowd very closely together at 890 cm.$^{-1}$. and there appears to be little experimental evidence for this. Finally, the recently obtained solid state infra-red spectra of the *n*-propyl and *n*-butyl halides would seem to indicate the presence of a methyl wagging mode near 890 cm.$^{-1}$. In view of these difficulties no further discussion of the skeletal vibrations will be made at present although it should be noted that about the right number of infra-red absorptions between 890 and 1150 cm.$^{-1}$ are to be found for future assignment to the skeletal modes. It is hoped to distinguish between the two alternative possibilities with the help of further experimental and theoretical work, in the course of which the data on the odd-numbered paraffins will be given detailed consideration.

Polythene.—Polythene is of interest in the present context because it represents an infinite paraffin chain with the (—CH_2—CH_2—) repeating unit. Kellner [33] was the first to interpret the infra-red spectrum of polythene from this point of view and, as will be seen below, her conclusions are in essential agreement with those of the present work. Simanouti and Mizushima [34, 35] made a similar attempt to assign the infra-red spectrum, and also suggested values for the Raman active frequencies by analogy with the series of frequencies found in the Raman spectra of the long chain crystalline paraffins. As the foregoing analysis of the infra-red spectra of the long chain paraffins provides more evidence for the assignment of the frequencies of an infinitely long chain, and as frequencies attributable to the methyl groups in polythene have been included in previous assignments, it seemed desirable to present a more up-to-date picture. The present conclusions are presented in Table II in which the symmetry nomenclature used by Simanouti and Mizushima [35] has been reproduced, and descriptions of the types of normal co-ordinate added. The previous assignment by the Japanese authors is also shown together with that of Kellner [33] for the infra-red frequencies.

There seems little doubt about the correctness of the infra-red assignments when account is taken of the experimental data of Fox and Martin,[36] and Thompson and Torkington.[37] The latter authors also showed clearly that the 1375 cm.$^{-1}$ absorption attributed by Simanouti and Mizushima [35] to the B_{1u} CH_2 wagging mode is in fact a methyl frequency. The assignments given in Table II for the infra-red frequencies are also in agreement with the data of Elliott, Ambrose and Temple,[38] and of Vallance Jones and Sutherland,[14] who used polarized radiation. The Raman active CH_2 stretching modes and the CH_2 bending vibrations have been assigned in agreement with the earlier work of Simanouti and Mizushima, with the exception that the Raman frequencies found in the spectrum of *n*-hexadecane at 2963 and 2878 cm.$^{-1}$ are assumed to be methyl frequencies (Fox and Martin [36] give values of *ca.* 2960 and 2870 cm.$^{-1}$ for the analogous modes of methyl groups in the infra-red). The assignment of the CH_2 wagging mode to 1295 cm.$^{-1}$ takes account of another of the Raman series which persists in the spectra of the long chain hydrocarbons, and is in line with our previous conclusions for such molecules.

It has been shown in the discussion of the spectra of the even-numbered paraffins that the Raman line at 1135 cm.$^{-1}$ is the upper limiting skeletal stretching frequency. Its symmetry properties in the spectra of the odd and even paraffins shows that it corresponds to the B_{1g} C—C stretching mode of polythene. The Raman line near 1060 cm.$^{-1}$ has been shown in the present work to be caused partially by a methyl wagging mode and partly by the third highest frequency skeletal stretching mode, and hence is not the A_{1g} C—C stretching frequency. This latter vibration should, like the other allowed skeletal, correspond to a mode of motion of a finite chain in which there is a node at the centre of each C—C linkage. The 1135 cm.$^{-1}$ frequency corresponds to such a vibration in which all the displacements of the neighbouring carbon atoms are in opposite directions, and parallel to the chain direction. The A_{1g} vibration will be similar except that the displacements will be perpendicular to the chain length. In terms of a short chain this will correspond to one of the limiting "deformation" modes of the skeleton, although for a very long chain this vibration will be controlled mainly by the C—C stretching force constant and will hence have a fairly high frequency, as shown by the calculations of Kellner[33] and Simanouti and Mizushima.[35] However, it cannot be identified in the Raman spectra of the *n*-paraffins so far observed, as the remaining two series near 890 cm.$^{-1}$ and at lower frequencies are undoubtedly the other limiting stretching and deformation modes of the skeleton with a single node at the centre of the chain. This has been clearly stated by Mizushima and Simanouti.[7]

---

[33] Kellner, *Nature*, 1949, **163**, 877.
[34] Simanouti, *J. Chem. Physics*, 1949, **17**, 734.
[35] Simanouti and Mizushima, *ibid.*, 1949, **17**, 1102.
[36] Fox and Martin, *Proc. Roy. Soc. A*, 1940, **175**, 208
[37] Thompson and Torkington, *ibid.*, 1945, **184**, 3.
[38] Elliott, Ambrose and Temple, *J. Chem. Physics*, 1948, **16**, 877.

TABLE II.—A PARTIAL ASSIGNMENT OF THE FUNDAMENTAL FREQUENCIES OF POLYTHENE

Symmetry	Description	Selection Rules	Kellner[33]	Simanouti and Mizushima[35]	This Work
A_{1g}	C—C stretch	R.	—	1135	?
	CH_2 bend			1471	1471
	CH_2 stretch		—	2846 2878	2846
A_{2g}	CH_2 twist	R.	—	?	?
B_{1g}	C—C stretch	R.	—	1058	1135
	CH_2 wag			1442	1295
B_{2g}	CH_2 rock	R.		1295	?
	CH_2 stretch		—	2934 2963	2934
A_{1u}	CH_2 bend	I.R.	1460	1475	1462
	CH_2 stretch		2925	2853	2853
A_{2u}	CH_2 twist	—	—	—	—
B_{1u}	CH_2 wag	I.R.	1310	1375	1309
B_{2u}	CH_2 rock	IR.	725	728	721
	CH_2 stretch		2960	2926	2925

R.=Raman active; I.R.=infra-red active.

Conclusion.—In conclusion it is appropriate to give some general comments on the theoretical treatments of the vibrations of the *n*-paraffins. From the earlier discussion it is clear that the calculations made using a simple valency force field, while they provide a very good guide to the interpretation of the observed spectra, are inadequate for exact numerical agreement between calculated and observed stretching frequencies. Simanouti and Mizushima[3, 7] have used a Urey-Bradley field, involving forces between next to nearest carbon atoms, to discuss the limiting skeletal and deformation frequencies with $x = 0$. They have obtained excellent numerical agreement between calculated and observed frequencies by a suitable choice of force constants. Similarly they have given calculations for an infinitely long chain (polythene).[35] It may be that similar calculations for all the skeletal vibrations of the smaller molecules would give better agreement with experiment.

Stepanov [10] has used a much more complex force field: he has given sufficient information for the calculation in principle of both the skeletal and CH vibrations of any long chain hydrocarbon, although these calculations have only been carried out as far as *trans* *n*-pentane. His force constants are obtained from a detailed discussion of the paraffins from methane to butane and, as might be expected, are not identical with these employed by the Japanese authors. Whereas the calculations so far carried out are undoubtedly of considerable value, it is felt that it is unlikely that these extremely detailed and time-consuming calculations with a complex force field will add a proportionate amount to the understanding of the spectra of the higher members of the series. In the present paper very considerable success in the interpretation of the spectra of these related molecules has been achieved by the empirical correlation of series of frequencies. It seems that this approach, used in conjunction with approximate calculations of the skeletal frequencies, will prove adequate to enable an interpretation to be made in due course of most of the experimental data on the planar configurations of these molecules. Further work on the detection of weak Raman lines and on the infra-red spectra of higher odd-numbered paraffins would undoubtedly be a help in attaining this end.

One of us (N.S.) is very grateful to the Royal Commissioners for the Exhibition of 1851 for a Senior Studentship. Another (J.K.B.) is indebted to the Department of Scientific and Industrial Research for a maintenance grant. We should also like to thank the Anglo-Iranian Oil Co. Ltd. for some of the pure hydrocarbons studied, and the Hydrocarbon Research Group of the Institute of Petroleum for financial assistance.

Departments of Colloid Science and Physical Chemistry,
Free School Lane,
Cambridge.

SOME PROBLEMS IN THE INTERPRETATION OF THE INFRA-RED SPECTRA OF LARGE MOLECULES

BY G. B. B. M. SUTHERLAND

Received 3rd July, 1950

The principles governing the infra-red method of investigating the structure of large molecules are reviewed. It is emphasized that the method will continue to lack preciseness until the various factors affecting the constancy of characteristic group frequencies have been more fully investigated. Attention is drawn to the uncertainties in the detection of OH and NH bonds under certain conditions because of insufficient knowledge of the characteristic deformation frequencies of these groups.

During the past ten years or so infra-red spectroscopy has changed from a branch of molecular physics dealing with the structural features of the smaller, and generally inorganic, molecules to a subject of considerable interest to the organic chemist and the biochemist, and of growing interest to the biologist. The reason is, of course, that it is now possible because of advances in experimental and theoretical methods to deal with large molecules including synthetic and natural polymers. However, these advances have been made at a sacrifice in the preciseness of the information which can be delivered by the spectroscopist to the interested party. Whereas it is possible to give a complete analysis of the spectrum of the ammonia molecule, from which the bond lengths and angles can be deduced with an accuracy of 1 part in 1000 and the height of the potential barrier inhibiting inversion is known to within a few per cent, the most that can be stated at present about a large organic molecule or polymer is that it does or does not contain certain chemical groups, and even this statement has frequently to be hedged about with qualifications. Nevertheless, such information can be of vital importance especially if the qualifications can be made precise, as it is often possible to deal with these qualifications by using evidence from chemical or other sources. The purpose of this paper is to review briefly the infra-red methods now being used to identify groups or portions of the structure of large molecules, so that the causes of the lack of precision may be more clearly realized and if possible used eventually to yield still more information about the structure of such molecules. Since this is a very large theme, it will be necessary to restrict attention to a few selected problems, and in view of the scope of these discussions, examples will generally be taken from the biochemical and biological field. Certain current views of biological activity are based on the shapes of the active molecules; it is, therefore, particularly important that any method of determining molecular structure should be critically reviewed to see what contribution it can be expected to make towards the evaluation of such theories.

The general principles which govern the correlation of the vibrational spectra of large molecules with their structural features can be stated quite simply:

(1) Every distinct configuration of atoms to form a molecule will have a unique vibration spectrum which will depend on the masses of the constituent atoms and on the nature of the forces which maintain the atoms in that configuration and are brought into play when the atoms are displaced from their equilibrium positions.

(2) The most important part of the vibration spectrum (viz. the fundamental frequencies) is readily observable since it is generally associated with a change of the permanent electric moment and of the polarizability of the molecule, the former being the cause of infra-red absorption and the latter of Raman scattering.

(3) Although each fundamental frequency involves motion to some extent of all the atoms in a molecule, many of the fundamental frequencies in a complex molecule have been shown to be separable and determined to a high degree of approximation by the vibration characteristics of isolated groups in the molecule. Such frequencies may be used to establish the presence or absence of the corresponding groups in polyatomic molecules by observations on their infra-red and Raman spectra.

The preceding considerations apply ideally to molecules in the gaseous state at moderate pressures, where intermolecular forces are negligible compared with the intramolecular forces which control the vibrations. However, in practice the majority of observations on large molecules in the infra-red (and virtually all observations on such Raman spectra) have to be carried out with the molecules in the liquid or solid state or in a solvent. The effects of intermolecular forces on the characteristic vibrations of key groups cannot then be neglected. It is obvious that the changes occurring in the spectrum of any particular molecule as the conditions vary from gaseous, through dilute solution, to the liquid and finally to the solid state must be thoroughly understood before reliable statements can be made regarding the constancy of group frequencies from one type of molecule to another.

The initial proposition in this discussion was that for each type of molecule free from interaction, there exists a set of frequencies which is unique. In the language of the quantum theory, each molecule can be described by a unique set of energy levels (including statistical weights arising from degeneracy and overlapping) and the transitions which occur between these in the excitation of infra-red and Raman spectra enable us to establish the energy level scheme. This throws the whole emphasis on the determination of the *magnitudes* (i.e. absolute values) of the characteristic frequencies, and spectroscopic work on large molecules has in fact been almost exclusively concentrated on the *positions* of the infra-red bands characterizing chemical groups. In small polyatomic molecules with a few symmetry elements, the transitions allowed between energy levels are sharply conditioned by these symmetry properties and frequently the configuration can be established beyond question by such selection rules. Although the majority of polyatomic molecules have no symmetry elements and thus cannot be tackled *in toto* in this way, the vibrations of separable portions may still be analyzed as those of slightly perturbed simpler molecules. Thus the *relative and absolute intensities* of absorption bands are just as important as their positions, in correlating spectrum with structure in a complex polyatomic molecule. Moreover, the intensity of an absorption band, being dependent on the change of electric moment associated with a vibration, can give very valuable information on the charge distribution in a chemical group, and this property may also be used for diagnostic structural work. Finally, when the compound under investigation is in the crystalline state or at least has some degree of regular orientation of the individual molecules, the use of polarized infra-red radiation can frequently give information on the orientation of the characteristic groups with respect to the macroscopic features of the specimen. Such information, especially when combined with results from X-ray diffraction spectra and a knowledge of allowable interatomic distances, should serve to fix a structure unequivocally or at least to differentiate between certain proposed models. Although the X-ray method of determining the structure of a molecule in the crystalline state is in general superior to the infra-red method, the fact that only infra-red methods can decide whether the structure alters in going from the crystalline to the liquid or dissolved state is of vital importance to the organic chemist who seldom deals with reactions in the solid state.

For good empirical and theoretical reasons which need not be repeated here, the fundamental frequencies of any polyatomic molecule may be classified in the following manner :

(*a*) Frequencies involving the motions of hydrogen atoms mainly along the bonds connecting them to other atoms. These will be referred to as *hydrogenic stretching frequencies* and are found to range between 3800 cm.$^{-1}$ and 2100 cm.$^{-1}$ in going from OH to SiH.

(*b*) Frequencies involving the motions of hydrogen atoms mainly perpendicular to the bonds connecting them to other atoms. These will be referred to as *hydrogenic deformation frequencies* and are found to range from 1650 cm.$^{-1}$ down to the order of 200 cm.$^{-1}$ in going from OH in water to that motion of the OH in methyl alcohol [1] where the OH executes a restricted rotation about the CO axis.

(*c*) Frequencies involving mainly the stretching and contraction of double and triple bonds between atoms in the first row of the periodic table. These will be referred to as *multiple bond frequencies* and are found to range between about 2000 cm.$^{-1}$ (e.g. $C\equiv C$ and $C\equiv N$) to about 1600 cm.$^{-1}$ (e.g. $C=C$ and $C=O$ in certain environments).

---

[1] Koehler and Dennison, *Physic. Rev.*, 1940, **57**, 1006.

(*d*) Frequencies which involve comparable motions of more than two and sometimes of all of the non-hydrogenic atoms, the hydrogens being essentially carried with the atoms to which they are attached. These will be referred to as *skeletal frequencies.* It is frequently possible to divide this class into *skeletal stretching frequencies* involving mainly changes in bond lengths with very little distortion of band angles and *skeletal deformation frequencies* for which the opposite is true, but this distinction is not always possible either empirically or theoretically.

The frequencies in the first three classes have been separable because they are virtually independent of the rest of the molecule and are now extensively used for structural diagnosis. Occasionally it is possible to use those of the fourth class when vibrations of parts of the non-hydrogenic skeleton of the molecule interact very little with the motions of the rest of the molecule.

The majority of these group frequencies have been established by empirical methods, i.e. running the spectra of a series of molecules having the particular group as an invariant. Although in a few cases theoretical justifications are being developed, there are many cases where unexplained anomalies occur. Such anomalies form one of the most important problems in this section of infra-red spectroscopy. Until their causes are clearly understood, structural information on large molecules obtained by infra-red methods will be open to question. Moreover, it is often in those molecules where the chemist and biochemist needs help most urgently (i.e. where a group occurs in an unfamiliar environment) that the spectroscopist is least sure of his ground. Limitation of space unfortunately prohibits the discussion of more than a few of these cases in this paper. An endeavour has been made to choose examples which are likely to recur in many structures and are of particular interest in biological applications. These will be dealt with following the classification given in the preceding paragraph.

Hydrogenic Stretching Frequencies.—This class contains the fewest deviations, the presence or absence of certain infra-red bands in sharply defined positions between 3800 cm.$^{-1}$ and 2100 cm.$^{-1}$ being a reliable indication of the presence or absence of OH, NH, CH, SH, PH and SiH groups in a molecule. The most important anomaly here has long been recognized as a shift of the characteristic bond to longer wavelengths caused by hydrogen bonding. This makes it difficult to differentiate between OH and NH in certain cases when hydrogen bonding occurs. This difficulty would be resolved if the positions of the OH and NH deformation frequencies were well established and recognizable under various conditions. Unfortunately this is not the case, as will be seen from the next section. Overlapping of some of the well-recognized OH and NH frequencies involved in hydrogen bonding is shown as follows :

—O—H . . . O—	3500–3200 cm.$^{-1}$
—O—H . . . O═C—	3330–2830 cm.$^{-1}$
—N—H . . . O═C—	3320–3240 cm.$^{-1}$
—N—H . . . N	3300–3150 cm.$^{-1}$.

Small shifts in SH frequencies attributed to the same cause have also been detected and although CH stretching frequencies have been assumed free from such effects, it may be added that an internal hydrogen bond between a CH$_2$ group and a C═O group in certain cyclic ketones has recently also been observed,[3] although this particular shift has been detected on the first overtone of the CH fundamental frequency near 5700 cm.$^{-1}$.

Because of the success of the hydrogen bond theory in explaining the displacement of hydrogenic frequencies in so many cases, there is a tendency

---

[2] Gordy, *J. Amer. Chem. Soc.*, 1940, **62**, 497.

[3] Prelog, *J. Chem. Soc.*, 1950, 420, and unpublished work by author.

to attribute all such shifts to hydrogen bonding. It seems quite possible, however, that in the solid phase some of these shifts may be due to an interaction between hydrogenic frequencies in neighbouring molecules oriented in a particular way through the restrictions imposed by a particular crystalline lattice. Such an effect was recently observed for CH deformation frequencies in *n*-paraffins and polythene (cf. succeeding section). It would also be expected in the stretching frequencies, and still more recently evidence has come to hand [4] that this effect is present in the CH stretching frequencies of polythene.

This effect may possibly be of importance in the study of proteins and polypeptides where two NH stretching frequencies are found near 3280 cm.$^{-1}$ and 3060 cm.$^{-1}$. These were originally interpreted as due to two different types of hydrogen bond [5] and while this may still turn out to be the case, it is quite possible that this particular splitting arises from a frequency interaction between identical NH bonds in certain crystalline phases although the exact mechanism cannot be the same as in the hydrocarbons. In support of this hypothesis there is the observation that these two bands exhibit similar polarization properties,[6] but more important is the fact that the lower frequency component is very much diminished in intensity in Nylon when the temperature is raised.

It is also to be realized that shifts in hydrogenic stretching frequencies and modifications in their intensities can arise from variation in the intra-molecular field caused by changes in charge distribution on the bond. Such changes may arise from substitution of strongly electronegative or electropositive atoms or groups in various parts of the molecule or from changes in the bond type due to charges in hybridization. Such effects were first noticed in the force constant of the CH bond in going from methane to acetylene [7] and have since been investigated in some detail in a variety of hydrogenic frequencies through calculations of the force constant.[8] Further work is required here, however, before changes in frequency can be unambiguously associated with changes in bond nature. There is some evidence that the changes in CH deformation frequencies shown to arise from this cause in ethylenic compounds are paralleled by corresponding changes in the CH stretching frequencies.[9] In general the changes so far attributed to effects of this kind in hydrogenic stretching frequencies are so much smaller than those produced by intermolecular forces that they are unlikely to cause mistakes in identifying a bond in a complex molecule. Such effects, however, are likely to be important in giving more specific information about the exact nature of an identified bond.

Hydrogenic Deformation Frequencies.—Here the situation is not nearly so satisfactory and this is understandable. The forces controlling the deformation of hydrogen atoms are only about one-tenth of those controlling the stretching motions, hence deformation vibrations are much more sensitive to intra- and inter-molecular interactions. The deformation motion has two degrees of freedom and the restoring forces for the resulting various types of deformation motion are found to vary by a factor of at least two and sometimes much more. This accounts for the much greater fractional variation in these frequencies. Thus CH stretching frequencies only vary between 3300 cm.$^{-1}$ and 2800 cm.$^{-1}$, whereas CH deformation frequencies vary from about 1500 cm.$^{-1}$ to 600 cm.$^{-1}$. Moreover, the range of the spectrum covered by such deformation frequencies is exactly the same as that for the majority of skeletal frequencies by which they can therefore be obscured and from which they are sometimes rather hard to differentiate. We shall confine our attention to

[4] Private communication from Dr. G. W. King.
[5] Darmon and Sutherland, *Nature*, 1949, **164**, 440.
[6] Ambrose, Elliott and Temple, *ibid.*, 1949, **163**, 854.
[7] Sutherland and Dennison, *Proc. Roy. Soc. A*, 1935, **148**, 250.
[8] Linnett, *Trans. Faraday Soc.*, 1945, **41**, 223.
[9] Unpublished work by D'Hont with the author.

certain difficulties in the assignment of CH, OH and NH deformation frequencies.

(*a*) CH DEFORMATION FREQUENCIES.—These have been extensively studied especially in the hydrocarbons, and detailed assignments to specific normal modes are well established in most cases by careful comparison with detailed analyses of simpler molecules, by polarization observations [10] and by theoretical calculation. There are cases, however, where assignments are still open to question [11] or where anomalies appear, e.g. fine structure.

For instance, in solid *n*-paraffins the CH_2 deformation frequencies at 1460 cm.$^{-1}$ and 720 cm.$^{-1}$ are double below the transition point but single from the transition point to the melting point and in the liquid state.[12] This has been shown to arise from an interaction between the CH_2 deformation frequencies in neighbouring hydrocarbon chains.[13] A phenomenon of this type is likely to occur not infrequently among polyatomic molecules in crystalline or highly oriented states. Since much future work will be done with oriented molecules in order to utilize the greater analytical power of polarized infra-red radiation, the detection and proof of such phenomena become matters of considerable importance in the correct assignment and interpretation of hydrogen deformation frequencies.

In certain cases small shifts occur in the positions of well-established characteristic CH deformation frequencies. It is essential that the reasons for these shifts and their maximum permissible variations be clearly established. Otherwise the presence of a band fairly close to the mean position of a key frequency cannot be accepted as a proof of the presence of the corresponding group in the molecule. The principal cause of such shifts seems to be a change in the charge distribution on the carbon caused by the presence of strongly electronegative atoms attached to the same on a neighbouring carbon atom.[14, 15] Shifts as much as 100 cm.$^{-1}$ can occur in this manner in alkene groups. It is interesting to consider whether such effects can occur in the branching of hydrocarbon chains. Thus there is a well-established empirical result that the CH_2 rocking frequency at 725 cm.$^{-1}$ in long chain *n*-paraffins is modified to 740 cm.$^{-1}$ and further to 770 cm.$^{-1}$ when the number of CH_2 group in the chain drops to two and one respectively.[16] It is important to understand the reason for such a shift which can be important in locating a small side chain near the end of a long chain, e.g. structure of phthiocerane.[17] One possibility is that the charge distribution on a CH_2 group depends on the number of adjacent CH_2 groups.

(*b*) OH DEFORMATION FREQUENCIES.—In spite of their importance in structural analysis, very little systematic work has been done on OH deformation frequencies and no such simple rules exist as for the CH frequencies. In water this frequency lies near 1660 cm.$^{-1}$ but no other molecule with an OH group has exhibited a band higher than 1450 cm.$^{-1}$ which could possibly be attributed to OH deformation. It might be thought that the OH deformation frequencies in polyatomic molecules might best be approached through the complete analysis of the methyl alcohol spectrum. While this has indeed shown that one of the motions is a severely hindered rotation of the OH bond about the CO axis giving rise to an absorption [18] in the gaseous phase extending from 700 cm.$^{-1}$ to

---

[10] Sutherland and Vallance Jones, *Nature*, 1947, **160**, 567.

[11] Simpson and Sutherland, *Proc. Roy. Soc. A*, 1949, **199**, 169.

[12] Stein and Sutherland, to be published shortly.

[13] Montroll and Stein, to be published shortly.

[14] Sheppard and Sutherland, *Proc. Roy. Soc. A*, 1949, **196**, 195.

[15] Torkington, *J. Chem. Physics*, 1949, **17**, 1277.

[16] Fellgett, Harris, Simpson, Sutherland, Thomspon, Whiffen and Willis, *Inst. Petroleum Report No. XI* (Infra-red Spectra of Hydrocarbons), 1946.

[17] Stenhagen, Sheppard, Sutherland and Walsh, *Nature*), 1947, **160**, 580.

[18] Burkhard, *Ph.D. Thesis* (Universtiy of Michigan, 1949.

50 cm.$^{-1}$, there is disagreement in the literature about the assignment of the other OH deformation frequency in which the H atom moves in the COH plane and mainly perpendicular to the OH bond. Some authors [19, 20] favour a value of 1109 cm.$^{-1}$ while others [21, 22] consider 1340 cm.$^{-1}$ as the true value. In an attempt to resolve this difficulty, new studies [23] were made on the spectra of some of the simpler aliphatic alcohols in the vapour and liquid state to see which bands moved to shorter wavelengths in such a transition (cf. the well-known effect of hydrogen bonding on deformation frequencies). While this work indicates that the primary alcohols have an OH deformation frequency near 1350 cm.$^{-1}$ in the liquid state, there is another frequency near 1100 cm.$^{-1}$ which also moves to lower values in going from liquid to vapour. A similar effect has been noted in phenol [24] where the corresponding frequencies are at 1350 cm.$^{-1}$ and 1200 cm.$^{-1}$ and deuteration shows that both these frequencies must arise from deformation motions of hydrogen atoms. The complexity of the changes in the spectra of the alcohols between 1450 cm.$^{-1}$ and 600 cm.$^{-1}$ in the transition from the vapour, through dilute solution to the liquid state indicates that much more experimental work on hydroxylic (and the corresponding OD) compounds must be carried out before the spectroscopist can make reliable assignments of OH deformation frequencies. In view of the impossibility of distinguishing OH from NH stretching frequencies in many instances, this is an urgent requirement. Two of the current classifications [25, 26] of characteristic frequencies put the OH deformation frequency as lying between about 1050 cm.$^{-1}$ and 1080 cm.$^{-1}$ but in neither case is any justification given for the assignment, which is certainly wrong in many cases.

NH Deformation Frequencies.—Here the situation is also very unsatisfactory. There is general agreement [25, 26, 27] that in simple amines the internal deformation frequency of the NH_2 group occurs in the range 1590 cm. to 1650 cm.$^{-1}$, but no convincing assignments are available for the external deformation motions of the NH_2 group. Furthermore, in monosubstituted amines there is still disagreement on the NH deformation frequency. From work done in connection with the penicillin problem in various laboratories,[28] it is established that all non-cyclic monosubstituted amides have a strong band near 1550 cm.$^{-1}$, but there is still disagreement [26, 27, 28, 29] on whether this should be assigned to an NH deformation or to a C—N frequency. It is not possible to summarize the detailed arguments here but two new pieces of evidence in favour of the former interpretation may be mentioned.

Examination [30] of the spectrum of acetyl glycine containing 32 % of N^{15} showed no decrease in the intensity of this band and a negligible shift in the position (~ 2 cm.$^{-1}$). If the 1550 cm.$^{-1}$ had been due to a C—N frequency (with the necessary high force constant) a much greater isotopic shift would have been anticipated. Furthermore, the acetyl glycine enriched with N^{15} showed a reduction in intensity of a band near 996 cm.$^{-1}$ and the appearance of a subsidiary maximum near 986 cm.$^{-1}$.

[19] Borden and Barker, *J. Chem. Physics*, 1938, **6**, 553.

[20] Davies, *ibid.*, 1948, **16**, 267.

[21] Noether, *ibid.*, 1942, **10**, 693.

[22] Herzberg, *Infra-red and Raman Spectra* (Van Nostrand, New York, 1945), p. 334.

[23] Ramsay and Sutherland, to be published shortly.

[24] Williams, Hofstadter and Herman, *J. Chem. Physics*, 1939, **7**, 802.

[25] Barnes, Gore, Stafford and Williams, *Anal. Chem.*, 1948, **20**, 402.

[26] Thompson, *J. Chem. Soc.*, 1948, 328.

[27] Randall, Fowler, Fuson and Dangl, *Infra-red Determination of Organic Structures* (Van Nostrand, New York, 1945).

[28] Clarke, Johnson and Robinson, *Chemistry of Penicillin* (Princeton University Press, Princeton, N.J., 1949), Chap. 13.

[29] Richards and Thompson, *J. Chem. Soc.*, 1947, 1248.

[30] Darmon and Sutherland, to be published shortly.

This is what might be expected for a C—N (single bond) frequency in this neighbourhood. The second fact is that the spectrum of Nylon in which about 38 % of the NH amide groups have the hydrogen replaced with *iso*butyl groups shows a marked decrease in the intensity of the 1550 cm.$^{-1}$ band relative to the C═O band at 1650 cm.$^{-1}$. It must be remembered, however, that the effects of deuteration on the spectrum of a —CO—NH— group are very complex [28, 30] and it seems probable that effects similar to those mentioned in the case of OH deformation frequencies also occur in the amides in the liquid and solid state.

Unfortunately limitation of space does not permit the discussion of problems connected with multiple bond and skeletal frequencies. The former will be much more important than the latter in biological work and considerable success [31] has already been achieved in locating C═O groups in steroids through small changes in the position and intensity of the C═O band according to the situation of the C═O group in the steroid skeleton.

The main conclusion from this brief discussion is that much more work is required on the spectroscopic effects of the following factors in modifying group frequencies in large molecules :

(i) Intermolecular forces (including hydrogen bonding) encountered in solution, in the liquid state and in solids, both amorphous and crystalline.

(ii) Weak intramolecular forces such as occur in internal hydrogen bonding and in restricted rotation about a single bond.

(iii) Changes of charge distribution in characteristic groups caused by the presence of strongly electronegative or electropositive groups in certain positions relative to the group under consideration.

(iv) Changes in group force constants due to changes in bond hybridization, arising from different environments of a particular group in different molecules.

The effects of all these factors on the *intensities* as well as on the *positions* of characteristic frequencies must be studied. Finally the need for more theoretical work on the determination of the force constants governing the frequencies of characteristic groups must be stressed. In the last analysis it is the force constants and not the frequencies which are the fundamental physical constants of groups of atoms in large molecules.

Physics Laboratory,
University of Michigan,
Ann Arbor,
Michigan, U.S.A.

---

[31] Jones, Williams, Whalen and Dobriner, *J. Amer. Chem. Soc.*, 1948, **70**, 2024.

THE APPLICATION OF POLARIZED INFRA-RED RADIATION TO PROBLEMS IN MOLECULAR STRUCTURE

I. POLYISOPRENES

BY G. B. B. M. SUTHERLAND AND A. VALLANCE JONES

Received 3rd July, 1950

The infra-red spectra of rubber and of both forms of gutta-percha have been investigated between 5 and 15 μ under various conditions. When rubber and gutta-percha are each in the amorphous state, their infra-red spectra are closely similar although not identical ; in the crystalline state, marked differences occur between the spectra of these three forms of polyisoprene. Using polarized radiation, the dichroic ratios of bands which can be assigned with certainty are in general qualitative agreement with the crystalline structures proposed by Bunn. The spectrum of rubber crystallized by freezing has been examined at low temperatures and it is shown that apparent intensity changes occur in certain absorption bands on crystallization. The importance of this effect in using infra-red methods to estimate the degree of crystallinity produced in rubber by stretching is emphasized. Assignments of a few of the main bands are discussed but no attempt is made to give a complete interpretation of the spectra.

Polarized infra-red radiation has been used to investigate the molecular structures of crystalline compounds for over 30 years, but the early work was almost entirely confined to ions of inorganic materials such as nitrates, sulphates and carbonates.[1] Within the past few years there has been a revival of interest in the field [2] because the interpretation of the infra-red spectra of organic molecules has now reached a stage where many of the intense bands can be assigned unequivocally to separable modes of vibration of small key groups in such large molecules. It thus becomes possible to deduce the orientation of these key groups in a crystalline or partially oriented solid with respect to the crystalline axes or to the direction of orientation as defined by other physical means. Once the orientation of these key groups has been fixed it should often be possible (using the knowledge of internuclear distances and bond angles derived by other physical methods and chemical evidence) to arrive at a unique model for the molecule or polymer of which the solid is composed. Most of the characteristic frequencies of key groups which form the basis of this method have been derived from observations in simpler molecules in the liquid or gaseous state; the effects of solidification and of crystallization on these characteristic frequencies have not been very fully investigated. It is well known, for instance, that certain absorption bands are altered in intensity and position by the transition from the liquid to the solid state and in many cases new absorption bands appear close to the position of the original one. Until such changes are understood the method of polarized infra-red radiation has serious drawbacks. In this paper we shall describe some investigations made in this general field, in which particular attention has been paid to such effects on the spectra of polymers. The polymers are particularly interesting subjects for study since in many respects they may be regarded as mixtures of liquids (amorphous part) and solids (crystalline part).

The polymers discussed in this paper are the various forms of polyisoprene, viz., rubber and α- and β-gutta-percha.

Experimental

The spectrometer used was a Perkin-Elmer Model 12-B, with a rocksalt prism. The output from the thermocouple detector was amplified by a General Motors breaker type amplifier and recorded by a Brown recorder. A selenium transmission polarizer was kindly put at our disposal by Dr. A. Elliott; it has been described by him elsewhere.[3] The polarizer was mounted directly in front of the entrance slit of the spectrometer. Most of the polymer samples were examined as thin films which were of sufficient area to be mounted immediately in front of the polarizer, with the direction of orientation either parallel or perpendicular to the entrance slit of the spectrometer.

The spectra at high temperatures were obtained by the use of a heated cell of the type described by Richards and Thompson.[4] The low temperature spectra were obtained using a cell (to be described elsewhere) which is similar to that described by Ubbelohde and Woodward.[5] In this case, and also when the area of the sample was limited, it was arranged that the sample could be placed at a subsidiary focus of the source. Since it is then essential that the sample can be replaced very accurately at the subsidiary focus, the heated cell, the low temperature cell and the minimum area sample holder were all fixed to kinematically mounted sliding carriages[6] on which they could be moved in or out of the path of the beam for the measurement of percentage transmission.

---

[1] Schaefer and Matossi, *Das Ultrarote Spektrum* (Julius Springer, Berlin, 1930), 1st edn., p. 329.

[2] Gore, *Ind. Eng. Chem.* (*Anal.*), 1950, **22**, 7.

[3] Elliott, Ambrose and Temple, *J. Opt. Soc. Amer.*, 1948, **38**, 212.

[4] Richards and Thompson, *Trans. Faraday Soc.*, 1945, **41**, 183.

It has been found essential in order to detect small changes in polarization properties of bands to follow a regular routine in observing and checking the intensities of bands. The following was our procedure. Firstly, the incident energy was recorded with the electric vector parallel to the slit. The sample was then placed in position and a duplicate set of absorptions superposed on the same length of recorder paper. Without disturbing the sample the polarizer was then rotated until the electric vector of the polarized radiation was perpendicular to the slit. A second absorption run was then recorded in duplicate. The sample was then removed and a second incident energy run recorded. From these records the percentage absorption may be plotted as a function of frequency and the polarization effects revealed. The results obtained by the above method were checked at the absorption maxima of important bands by making measurements at fixed frequency settings of the spectrometer.

Results

Spectra of Polyisoprenes.—Polyisoprene occurs naturally as rubber and gutta-percha ; the differences between the two forms are attributed to *cis-trans* isomerism about the carbon-carbon double bond. X-ray investigations by Bunn[7] are generally accepted as showing that rubber has the *cis* and gutta-percha the *trans* configuration. Gutta-percha may exist in two different forms at room temperature; the naturally occurring form is known as the α-form, but on heating above 65° C and cooling rapidly the β form is produced. Thus, above 65° C only one form exists and is known by X-ray methods to be amorphous. The difference between the α- and β-forms arises from different crystalline structures, the former having a repeat distance of 8·7 Å and the latter a repeat distance of 4·7 Å. At room temperature rubber is amorphous but crystallinity may be produced by cooling to about − 20° C.

The infra-red spectra of rubber and of the α- and β-forms of gutta-percha when examined at room temperature show certain features in common but also show very marked differences (Fig. 1A and 6).* The differences between the α- and β-forms must be attributed to the differences in crystalline structure ; the differences between the spectrum of rubber and either gutta-percha may be due partly to the effects of crystallinity and partly to the effects of *cis-trans* isomerism. In order to separate out these effects the spectrum of gutta-percha was investigated in a heated cell at 73° C. This spectrum, given in Fig. 1B, shows that the main differences (especially those in the region of 700-800 cm.$^{-1}$) are due to crystallinity and that the spectra of *cis* and *trans* polyisoprene when both are in the amorphous form are closely similar. Whether the remaining differences which are presumably due to *cis-trans* isomerism can be shown on spectroscopic grounds to arise from this effect is not yet certain although some suggestive correlations have been pointed out by Saunders and Smith[8] between the spectra of simpler *cis* and *trans* analogues of the polyisoprene series and the corresponding bands in rubber and gutta-percha near 1640 cm.$^{-1}$ and 890 cm.$^{-1}$.

We may now consider the spectra of the crystalline forms of *cis* and *trans* polyisoprene, starting with that of rubber, in which crystallinity has been produced by stretching. The spectrum of a lightly vulcanized latex is given in Fig. 2, the two curves corresponding to the electric vector parallel and perpendicular to the direction of stretching. It will be observed that although nearly every band shows dichroism the effects are most marked for the bands at 1665 cm.$^{-1}$, 1365 cm.$^{-1}$, 1130 cm.$^{-1}$ and 840 cm.$^{-1}$. The assignments of two of these bands (1665 cm.$^{-1}$ and 840 cm.$^{-1}$) are well known from work in simpler hydrocarbons[9] but the 1365 cm.$^{-1}$ and the 1130 cm.$^{-1}$ frequencies which have the greatest dichroic ratios are not so well established.

---

[5] Ubbelohde and Woodward, *Proc. Roy. Soc. A*, 1947, **188**, 358.

[6] Strong, *Modern Physical Laboratory Practice* (Blackie and Son, London, 1938), 1st edn., Fig. 17, p. 587.

[7] Bunn, *Proc. Roy. Soc. A*, 1942, **180**, 40.

* We are very much indebted to Dr. A. J. Harding, who obtained the spectra of α- and β-gutta-percha, for permission to include Fig. 6.

[8] Saunders and Smith, *J. Appl. Physics*, 1949, **20**, 953.

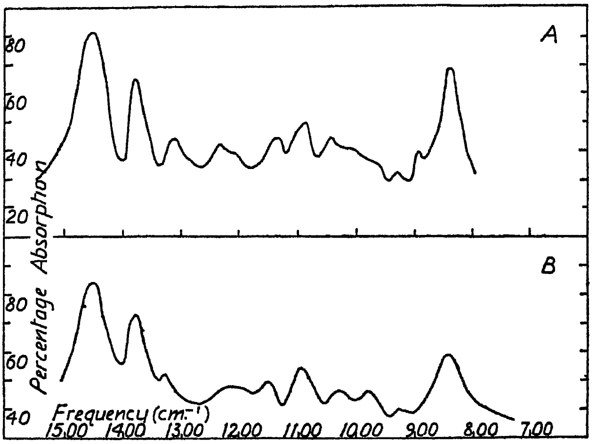

FIG. 1.

A. The infra-red spectrum of natural rubber.
B. The infra-red spectrum of gutta-percha at 73° C.

The 1665 cm.$^{-1}$ band due to the stretching of the C=C bond has greater intensity for the parallel than for the perpendicular polarization in agreement with the generally accepted idea that the crystallites are aligned with the polyisoprene chains parallel to the direction of stretching. At first sight it seems surprising that the effect is so small but this point is dealt with in a later paragraph.

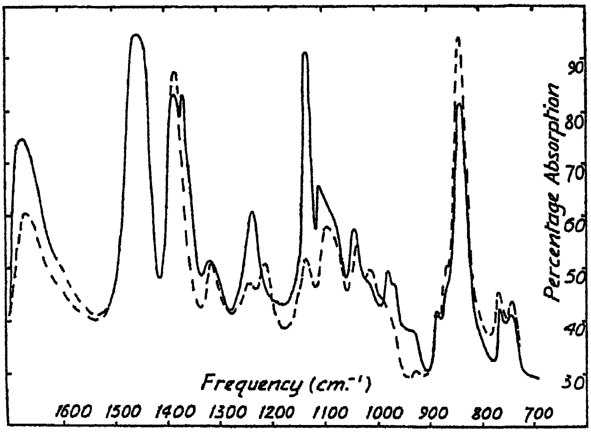

FIG. 2.—Infra-red spectrum of vulcanized latex, stretched 650 %, obtained with polarized radiation.

Electric vector parallel to direction of stretch.
– – – – Electric vector perpendicular to direction of stretch.

In the region of 1370 cm.$^{-1}$ it will be observed that there are two bands, one at 1375 cm.$^{-1}$ showing a weak perpendicular polarization, the other at 1365 cm.$^{-1}$

[9] Thompson and Torkington, *Trans. Faraday Soc.*, 1945, 41, 255; Sheppard and Sutherland, *Proc. Roy. Soc. A*, 1949, **196**, 195.

showing a strong parallel polarization. The 1375 cm.$^{-1}$ band is well known to be associated with the symmetrical internal deformation mode of the methyl group and thus shows the correct polarization properties. Since the change of electric moment is perpendicular to the axis of stretching the polarization effect here would be expected to be lower than in a parallel frequency such as that at 1665 cm.$^{-1}$ since the crystallites are presumably randomly oriented about the orientation direction. The 1365 cm.$^{-1}$ band which shows strong parallel polarization is assigned to the in-plane deformation mode of the C—H group which would be expected to have such properties. This assignment disagrees with that of Saunders and Smith [8] who attribute this band to a CH_2 deformation (wag), placing the CH deformation at 1285 cm.$^{-1}$ where an extremely weak band has been detected by them which shows no marked polarization properties. Our assignment is based on the expectation that the CH in-plane frequency would show a more pronounced parallel polarization character than a CH_2 wagging frequency which must have some perpendicular character. Moreover, the corresponding CH_2 band in polythene might be expected to have very similar intensity and polarization properties. There is, however, no intense band with parallel polarization properties in stretched polythene.[10]

The band at 1130 cm.$^{-1}$ which has such strong parallel polarization cannot be assigned with certainty. It could be an in-plane deformation motion of the methyl group but has been assigned by Saunders and Smith to a wagging motion of the CH_2 groups. Further evidence is required to differentiate these assignments. Finally, the 840 cm.$^{-1}$ frequency is well known to be a CH out-of-plane frequency [9] and shows the correct perpendicular polarization properties. An interesting phenomenon was noticed in connection with this band. It was found that if the specimen of rubber which was stretched was at least three times as wide as it was long (in the direction of stretching) then no dichroism was observed. However, Gehman and Field [11] have suggested that in such a case double orientation occurs which would put the CH bonds very nearly in the plane of the sheet. If such were the case then the perpendicular polarization would be almost destroyed. The observation that this was so while the perpendicular polarization of the methyl frequency at 1375 cm.$^{-1}$ was unaltered gives independent confirmation of the double orientation. No further discussion will be given here of the assignment of bands which in any case we think would be premature; instead, we shall discuss the effects of crystallinity on the spectra of polyisoprenes.

Effects of Crystallinity.—(*a*) RUBBER.—It is important to separate out effects due to crystallinity from those due to orientation both of amorphous and crystalline material which are present in the spectrum of stretched rubber. We therefore examined the spectrum of rubber in which crystallization had been produced by cooling. It was found that if unstretched latex is cooled rapidly to −140° C no appreciable changes occur in the spectrum. The bands near 1370 cm.$^{-1}$, 1100 cm.$^{-1}$ and 840 cm.$^{-1}$, to which particular attention was paid are shown in Fig. 3. If, however, the unstretched latex is cooled to −20° C held at this temperature for 4¾ hr. to give considerable crystallization and then cooled to −140° C for examination, a small shift occurs towards higher frequency for the band at 840 cm.$^{-1}$ coupled with a small increase in intensity (Fig. 3) while the band at 1130 cm.$^{-1}$ also appears to increase somewhat in intensity. There are, therefore, two effects produced by random crystallization on the spectrum of rubber taken at a temperature of −140° C, viz. a small shift in one band and small apparent increase in intensity in at least two other bands. In order to separate out the effect of temperature change from that due to crystallization the spectrum of stretched latex was observed after rapid cooling to −140° C. This is given in Fig. 4. Here there is a marked increase in intensity in most of the bands, in particular, in those at 1130 cm.$^{-1}$ and 840 cm.$^{-1}$ which showed an apparent increase in intensity in the unstretched latex. It might appear that the intensity change was entirely due to the effect of temperature on the spectra of the crystallites. However, Saunders and Smith have examined the spectrum of unstretched latex cooled to −25° C and held

[10] Elliott, Ambrose and Temple, *J. Chem. Physics*, 1948, **16**, 877.

[11] Gehman and Field, *J. Appl. Physics*, 1939, **10**, 564.

at that temperature. Their curve shows that the 1130 cm.$^{-1}$ band increases in intensity when crystallization occurs while the band at 840 cm.$^{-1}$ increases in frequency and in intensity. It is interesting to note that

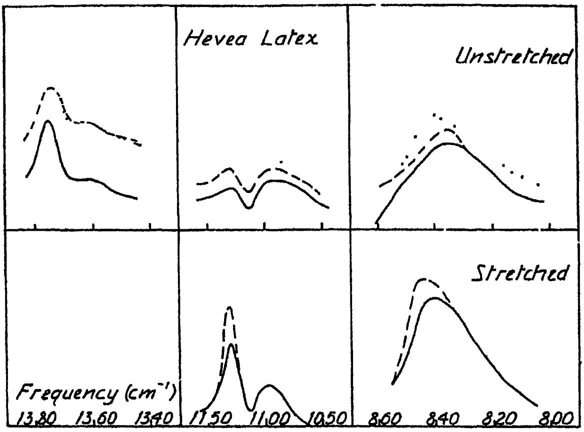

FIG. 3.—Infra-red spectra of stretched and unstretched latex.

——— Room temperature.
- - - - Rapid cooling to − 140° C.
. . . . Crystallized at −20°, observed at −140° C.

Saunders and Smith observed no change in the 1665 cm.$^{-1}$ band on crystallization. We did not examine this band at low temperature. We may conclude, therefore that in going from the amorphous to the crystalline state absorption bands in rubber may show (i) no change in intensity or position (1665 cm.$^{-1}$), (ii) a change in intensity but not in position (1130 cm.$^{-1}$) or (iii) a change in intensity and in position (840 cm.$^{-1}$).

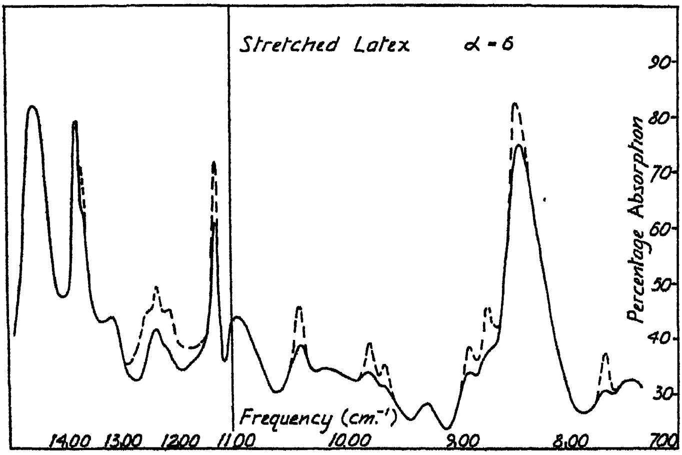

FIG. 4.—Infra-red spectrum of stretched vulcanized latex; 400 % extension.

——— Room temperature.
- - - - −140° C.

These conclusions have an important bearing on the interpretation of the infra-red spectra (polarized and unpolarized) of stretched rubber.

For instance, Williams and Dale,[12] who first observed the shift in the 840 cm.$^{-1}$ band on stretching, have concluded that this indicates a change in the C—C bond length produced by stretching. This effect is now seen to be due to crystallization which occurs either on stretching or cooling. Moreover, their assignment of this band to a C—C skeletal frequency is no longer defensible in view of the polarization results mentioned earlier in this paper, especially those in connection with double orientation. One other observation made in the course of this work may be quoted in this connection. Using polarized radiation, the behaviour of the 840 cm.$^{-1}$ band was studied for various degrees of stretching. It was found that with the electric vector perpendicular to the direction of stretching a sharp change took place in the frequency, from 835 cm.$^{-1}$ to 840 cm.$^{-1}$ at an extension ratio of about 3·5. For the parallel case the change was much slower. Now the X-ray evidence indicates that crystallization becomes very much enhanced near an extension ratio of 3·5. There would seem to be evidence from the polarization observations of Fig. 5 that there are two separate bands near 840 cm.$^{-1}$, one due to the amorphous form and one due to the crystalline form of rubber and that the relative intensities of these might be used to provide a measure of crystallinity in rubber.

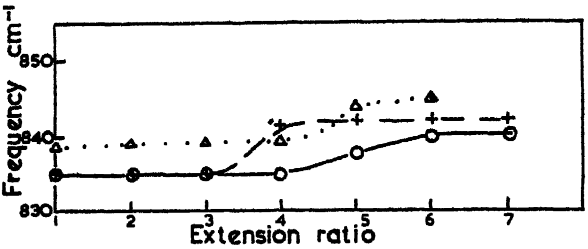

FIG. 5.—Frequency of maximum of band near 840 cm.$^{-1}$ in infra-red spectrum of rubber.

△ Williams and Dale.

O——Present work, electric vector parallel to elongation; + electric vector perpendicular to elongation.

The degree of crystallinity in rubber produced by stretching has been investigated by X-ray methods, but different workers have arrived at different conclusions. Field [13] estimated that the crystallinity might be as high as 80 % in rubber stretched to the highest elongations, while Goppel [14] concluded that the figure was nearer 40 %. The use of polarization studies in infra-red spectroscopy offers an independent way of studying the phenomenon. However, the dichroic ratio differs very greatly from one band to another and the effects of crystallinity just discussed must be taken into account. Thus, if one chooses the band at 1130 cm.$^{-1}$ the dichroic ratio would at first sight indicate a very high degree of crystallinity. However, the band was one which shows a considerable increase in intensity on crystallization and consequently all the high dichroic ratio indicates is that on stretching the crystallites become almost perfectly oriented. On the other hand the 1665 cm.$^{-1}$ band shows no increase in intensity due to crystallization and so the dichroic ratio here must give a much truer estimate of the degree of orientation and therefore indirectly of crystallinity in stretched rubber. A detailed investigation of the relation between dichroic ratio and extension

[12] Williams and Dale, *Appl. Sci. Res.*, 1944, **15**, 585.

[13] Field, *ibid.*, 1941, **12**, 23.

[14] Goppel, *ibid.*, 1947, **1**, 3.

ratio and how it may be interpreted in terms of the degree of crystallinity has been made but cannot be given here because of limitations of space. The result of this investigation is that the lower value of crystallinity found by Goppel is confirmed.

One further consequence of the effect of crystallinity on the apparent intensity of an absorption band arises when dichroic ratios are used to differentiate between alternative models. Thus, from the low value of the dichroic ratio for the 1665 cm.$^{-1}$ band in rubber Saunders and Smith have suggested that the Bunn structure for rubber may have to be modified since on this model the C═C bonds do not make an angle of more than 20° with the fibre axis. The apparent low value of this dichroic ratio when compared with that found for the 1130 cm.$^{-1}$ band may well be due to the fact that the former bands show no increase in intensity on

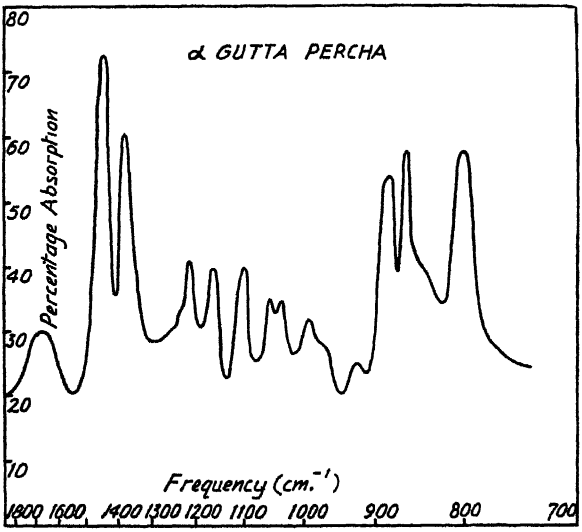

FIG. 6a.—Infra-red spectrum of α-gutta-percha.

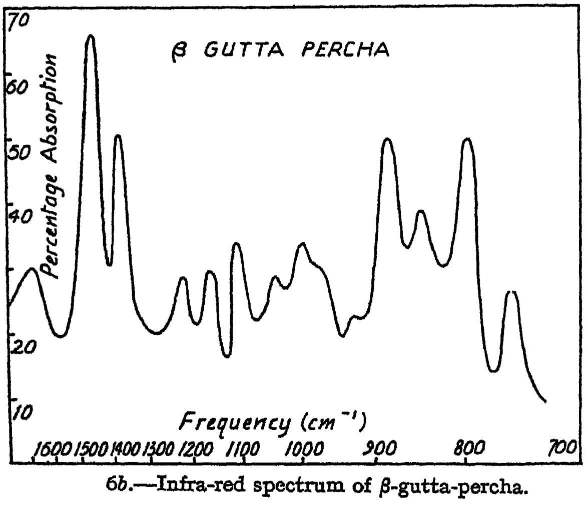

6b.—Infra-red spectrum of β-gutta-percha.

crystallization whereas the latter does. Consequently the high dichroic ratio of the 1130 cm.$^{-1}$ band compared to the 1665 cm.$^{-1}$ band must be due in large part to the increased intensity arising from crystallinity. Such effects must be carefully considered before valid deductions can be made on such structural questions. It should also be noted that the 1665 cm.$^{-1}$ band may contain a contribution from the overtone of the 840 cm.$^{-1}$ band which would also affect the dichroism.

(*b*) GUTTA-PERCHA.—The spectra of the α and β forms of gutta-percha observed at room temperature with unpolarized radiation are given in Fig. 6 and agree in essential features with those reported by Saunders and Smith. The principal differences between these spectra and the spectrum of amorphous gutta-percha observed at 73° C occur in the region of 700-900 cm.$^{-1}$. These differences must be due to crystallization and are much more pronounced than the corresponding effects in rubber. Thus new bands appear at 800 cm.$^{-1}$, 870 cm.$^{-1}$ and 890 cm.$^{-1}$ in the α form and at 750 cm.$^{-1}$, 800 cm.$^{-1}$ and 890 cm.$^{-1}$ in the β form. There may be a small shift of the 840 cm.$^{-1}$ band of the amorphous form towards higher frequencies in crystallization to either the α- or the β-form which would correspond to the behaviour of this band in rubber. The gradual disappearance of these new bands arising from the β-crystalline form as the gutta-percha is heated to 71° C is shown in Fig. 7, and the appearance of the α bands is also given as the same specimen was cooled very slowly to 54° C. Clearly these bands could be used to estimate the relative crystallinity of a sample of gutta-percha at various temperatures.

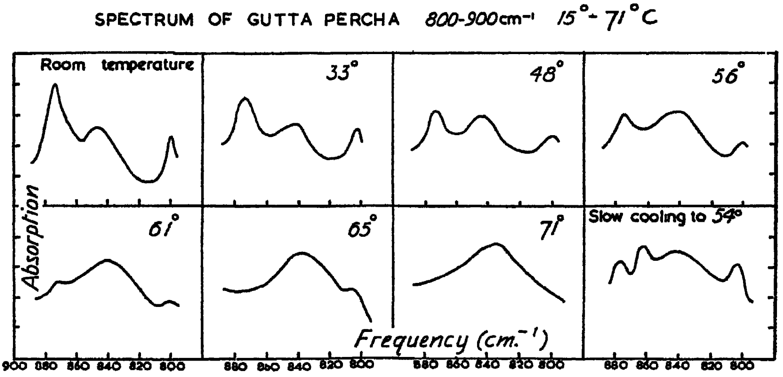

FIG. 7.—Spectrum of gutta-percha 800-900 cm.$^{-1}$, 15° C-71° C.

The dichroism in a film of cold-drawn β gutta-percha is shown in Fig. 8. The results are in general agreement with those of Saunders and Smith except that the perpendicular polarization of the CH_2 frequency at 1460 cm.$^{-1}$ is much more pronounced in our curve. It may be remarked that this band would be expected to show more marked dichroism in gutta-percha than in rubber on the basis of Bunn's models, and that no dichroism has yet been observed for this band in rubber. Furthermore, the 1665 cm.$^{-1}$ (arising from the C=C frequency) should show a smaller dichroic effect in gutta-percha than in rubber according to the Bunn structures. This effect was first observed by Saunders and Smith and has been confirmed by us although the spectra are not reproduced here.

The interpretation of the appearance of extra bands between 700 cm.$^{-1}$ and 900 cm.$^{-1}$ in gutta-percha or crystallization remains obscure. The explanation must come from a closer study of the relation between absorption spectra and crystallinity. A few remarks may be made on the tentative assignments given for these bands by Saunders and Smith. These authors have assigned the 840 cm.$^{-1}$ band in α and β gutta-percha to a C—C skeletal stretching frequency although in rubber their assignment of the 845 cm.$^{-1}$ band is the same as ours, viz. to the CH out of plane deformation frequency. In gutta-percha, they assume that the latter mode of vibration has moved to 800 cm.$^{-1}$. No supporting evidence is given for these assignments and we feel there is some evidence against them. The 840 cm.$^{-1}$ band in rubber shifts somewhat to higher frequencies on crystallization; a similar effect was found by us in the 840 cm.$^{-1}$ band in gutta-percha. This indicates that this band has the same origin in the two spectra, whereas the assignment of Saunders and Smith and of Williams and Dale would imply that in amorphous gutta-percha the 840 cm.$^{-1}$ band is entirely due to a C—C skeletal mode. It would seem strange that the spectra of amorphous rubber and gutta-percha which are so similar should have different interpretations for this intense band. On the other hand, Saunders and Smith, and Williams and Dale assign the bands at 860 cm.$^{-1}$ and 880 cm.$^{-1}$ to CH_3 deformation modes.

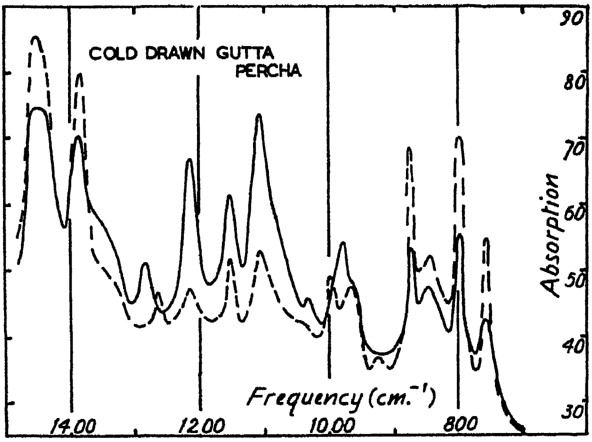

FIG. 8.—Infra-red spectrum of cold-drawn β-gutta-percha; polarized radiation.
——— Electric vector parallel to elongation.
– – – – Electric vector perpendicular to elongation.

This seems reasonable, but the failure of these bands to appear in crystalline rubber is still unexplained. The possibility that interaction effects may occur between some of the hydrogenic deformation frequencies analogous to these found in polythene and hydrocarbons by Stein and Sutherland [15] should not be overlooked.

We wish to acknowledge the loan of the Perkin-Elmer Spectrometer used in these investigations from Aero Research Limited. This work was carried out during the tenure of an 1851 Exhibition Scholarship by A. V. J. We are indebted to Dr. L. R. G. Treolar of the British Rubber Producers' Research Association for certain of the samples used. We would acknowledge the benefit of valuable discussions with Dr. N. Sheppard and Dr. R. S. Stein. We are grateful to Dr. D. C. Smith for communicating some of his results to us before publication.

Physics Department,
University of Michigan,
Ann Arbor, Michigan, U.S.A.

---

[15] Stein and Sutherland (to be published).

INFRA-RED ANALYSIS OF RUBBER DERIVATIVES *

By G. Salomon,† A. Chr. van der Schee,‡ J. A. A. Ketelaar § and B. J. van Eyk ||

Received 24th July, 1950

Changes in the intensity of the double bond frequencies (6·0 μ, 10·3 μ, 11 μ, 11·9 μ) and the CH_3 bending vibration occurring during the chlorination of natural rubber and the formation of various rubber derivatives have been studied. From the weakening of the original 11·9 μ band and the appearance of a strong band at 11·2-10·9 μ it is concluded that a double bond shift in rubber occurs readily under the conditions of polar reactions :

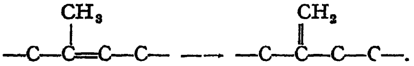

$$-C-\overset{\displaystyle CH_3}{\overset{|}{C}}=C-C- \longrightarrow -C-\overset{\displaystyle CH_2}{\overset{\|}{C}}-C-C-.$$

The significance of vinylic groups for the ageing properties of rubber derivatives is pointed out.

The intensity of the 6·0 μ C=C stretching frequency cannot be used as a relative measure of unsaturation, as it depends on many other factors. It is, however, remarkable that chlorinated rubber with 70 % Cl has still a measurable absorption at 6 μ.

The relative intensity of the 7·25 μ CH_3 bending vibration has been estimated from the k_{CH_3}/k_{CH_2} ratio. Controlled addition of HCl or Cl_2 to the double bonds of rubber leads to an increased intensity at 7·25 μ, while it is reduced in technical chlorinated rubber, of similar chlorine content.

This paper is a continuation of our studies on rubber derivatives, which were surveyed in a previous communication.[1] The scientific purpose of those studies is to elucidate the correlation between structure and mechanical properties of polymers derived from natural and synthetic rubber,[2] while the technological aim is to produce plastics from rubber.[3]

Identification of halide structures in rubber derivatives has been achieved by kinetic analysis with organic bases.[4] The nature of certain double bonds can be established kinetically using perbenzoic acid as a reagent [5] and additional information on double bond structure can be gained from the course of reaction with ICl [6] and finally with HCl.[7] These methods are, however, useless in the study of unsaturation of halogenated polymers as the double bonds in many olefinic halides are not reactive at all with these reagents. We decided therefore to explore the possibilities of infra-red analysis as an analytical tool. Evidence for the

---

* Communication No. 132 of the Rubber Foundation, Delft, The Netherlands.

† At present Adviser to the National Council of Industrial Research and to the Rubber Foundation.

‡ Rubber Foundation, Delft.

§ University of Amsterdam.

|| University of Amsterdam. Present address : Medical Faculty of the University of Indonesia, Surabaja.

[1] Salomon, *Faraday Soc. Discussion*, 1947, **2**, 361.

[2] Salomon, *Schweizer Archiv*, 1950 (in press).

[3] Salomon, van Amerongen, van Veersen, Schuur and de Decker, A.C.S. Cleveland Meeting, Oct. 1950 (preprint).

[4] Salomon, Koningsberger and Ultée, *Proc. 2nd Rubber Tech. Conf.* (London 1948), p. 106.

[5] Kolthoff, Lee and Mairs, *J. Polymer Sci.*, 1947, **2**, 220.

[6] Lee, Kolthoff and Mairs, *ibid.*, 1948, **3**, 66.

[7] Salomon, unpublished results.

migration of double bonds in thermally degraded rubber, in chlorinated rubber and in vulcanized rubber has been previously reported briefly by Sheppard and Sutherland.[8]

In addition to the double bond problem it was hoped to gain some semi-quantitative information on the remaining number of unchanged methyl groups in certain rubber derivatives.

Experimental

The spectrometer used was a single-beam instrument with Wadsworth-mirror, rock salt prism and photographic registration. A Globar was used as a source of radiation. Spectra were measured between $5 \cdot 7$-$14\ \mu$.

Methods applied for preparing chlorinated rubber,[9] hydrochlorinated rubber[10] and cyclized rubber[11] have been extensively discussed elsewhere. Chlorinated rubbers of low chlorine content were fractionated sharply and analyzed immediately after preparation when the amount of oxidation, deduced from the intensity of the $C{=}O$ bond, was still small. Details of the preparation of rubber-silver salt complexes will be published later. Films were prepared from chloroform solutions on glass or rock salt plates, the former being measured as a free film on a metal frame. The thickness *d* of the films, measured with a micrometer, varied between 30 to 150×10^{-4} cm.

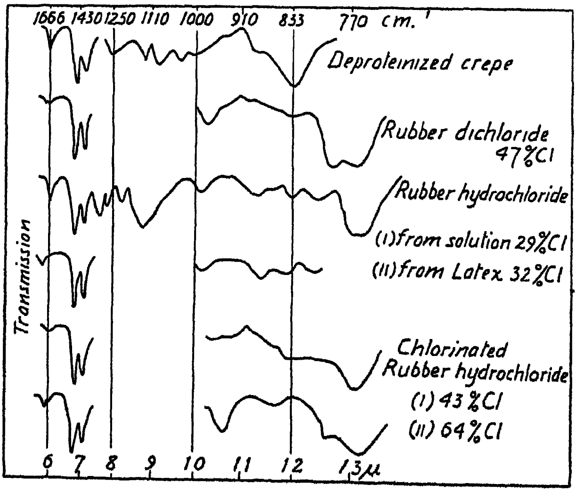

FIG. 1.—Spectra of rubber, rubber chlorides and rubber hydrochlorides.

The curves of the transmission *T* and the extinction coefficient *k*, where $k = (1/d) \log 1/T$, as a function of wavelength were derived in the ordinary way from the curves of transmitted and incident energy and the energy transmitted through the blank NaCl plate, the scattering being very low. As the intensity of a characteristic bond we took the difference of the maximal value of absorption and its value at the lowest neighbouring minimum.

Some representative spectra of rubber and rubber derivatives are reproduced in Fig. 1, 2 and 3. The extinction coefficients derived from these Figures are summarized in Table I and II and Fig. 4 and 5. Most of the points given in Fig. 4 and 5 were measured on two different films from the same product. Data for rubber refer to three different samples, and those for rubber hydrochlorides and rubber chlorides to 2-5 samples prepared independently.

---

[8] Sheppard and Sutherland, ref. (1), p. 374; *J. Chem. Soc.*, 1947, 1699.

[9] (*a*) van Amerongen, Koningsberger and Salomon, *J. Polymer Sci.* (in press). (*b*) van Amerongen and Koningsberger, *ibid.* (in press). (*c*) van Amerongen, *ibid.* (in press).

[10] van Veersen, *Proc. 2nd Rubber Tech. Conf.* (London, 1948), p. 87.

[11] van Veersen, *J. Polymer Sci.* (in press).

These results are discussed in the order of increasing complexity of the chemical problem.

Results

The Double Bond Frequencies in Rubber and Rubber Derivatives.—RUBBER.—The intensity of the 6·0 μ C=C stretching frequency is nearly the same for a number of samples but it changes as the rubber becomes oxidized. The intensity of the 11·9 μ band is much stronger and typical of the RRC=CHR group. A weak band at 11·2 μ, typical of a vinyl group has been observed already by previous workers,[12] who assigned its occurrence tentatively to end groups in the rubber chain (III). In our view the vinyl group would be also

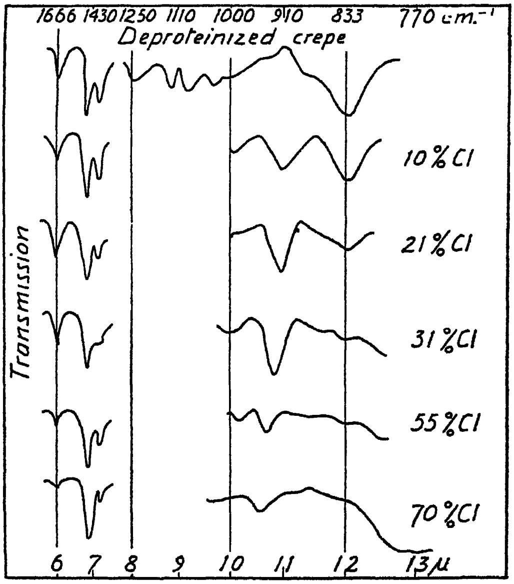

FIG. 2.—Changes in the spectrum of rubber during the course of chlorination.

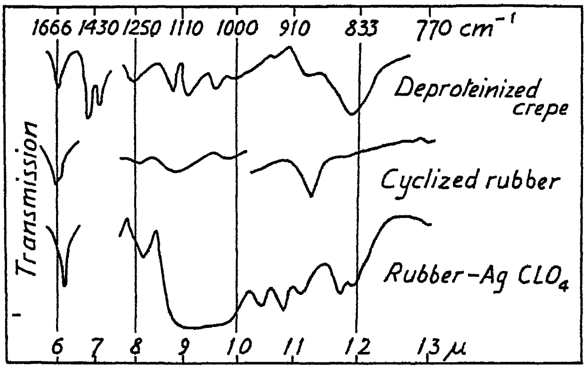

FIG. 3.—Spectra of rubber and some rubber derivatives.

---

[12] Dinsmore and Smith, *Anal. Chem.*, 1948, **20**, 11.

consistent with the structure (II), which could occur in small or larger quantities *within* the chain.

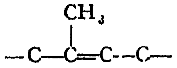

$-C-\overset{CH_3}{\overset{|}{C}}=C-C-$

(I) 11·9 μ

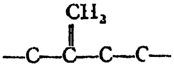

$-C-\overset{CH_2}{\overset{\|}{C}}-C-C-$

(II) 11·2 μ

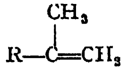

$R-\overset{CH_3}{\overset{|}{C}}=CH_2$

(III) 11·2 μ.

This band at 11·2 μ shifts on chlorination to shorter wavelength and is finally found at 10·6 μ at a chlorine content of 70 %. We shall call this band in rubber and its derivatives the 11 μ band.

Finally, there is a weak band at 10·3 μ which has been identified in other polymers [13] and in many other substances with the *trans* configuration of the double bond. It has been observed by us as well as by others [8] in some samples of rubber as a very weak band which is stronger in certain derivatives (see Fig. 1 and 2) and in ebonite.[8]

TABLE I.—DOUBLE BOND AND METHYL GROUP INTENSITIES OF RUBBER, RUBBER HYDROCHLORIDE, RUBBER DICHLORIDE AND CHLORINATED RUBBER HYDROCHLORIDE

Polymer	% Cl	Relative % of Double Bonds	$k_{6\,\mu}$	$k_{10.3\,\mu}$	$k_{10.8\,\mu}$	$k_{11.2\,\mu}$	$k_{11.9\,\mu}$	k_{CH_3/CH_2}
HYDROCHLORINATION OF RUBBER								
Natural rubber from latex	0	100	55	0-20	0-10	30	160	0·45
Rubber—HCl from solution	29	20	30	30	0	50	50	0·75
Rubber—HCl from latex	32	10	0-8	20	0	40	40	0·75
ADDITION OF CHLORINE TO THE DOUBLE BOND								
Natural rubber from latex	0	100	55	0-20	0-10	30	160	0·45
Rubber dichloride from solution	38	42	20	40	15	0	20	0·70
,, ,,	44	25	5	30	45	0	15	0·70
,, ,,	47	15	15	45	15	0	25	0·70
SUBSTITUTION OF HYDROGEN BY CHLORINE IN RUBBER HYDROCHLORIDE								
Rubber—HCl from solution	29	20	30	30	0	50	50	0·75
Chlorinated rubber—HCl	43	?	10	15	15	0	0-10	0·65
,, ,,	56	?	0-5	15	35	0	0	0·70
,, ,,	64	?	0-5	15	50	0	0	0·75

RUBBER HYDROCHLORIDES.—The addition of HCl to rubber in solution and in latex occurs with great ease. It is difficult to saturate all double bonds although the theoretical figure has been approached in some experiments starting from latex.[10] The products prepared from solution are saturated to 80 % but the intensity of the 6 μ band does not differ essentially from that of the original rubber (see Table I and Fig. 1).

Those substances made from latex are saturated to 90 % and show no absorption at 6 μ, while the presence of residual unsaturation is indicated by a weakened 11·9 μ band. This indicates that small changes in the structure can cause great differences in the 6·0 μ intensity.

RUBBER CHLORIDES.—The addition of chlorine to the double bond can be achieved with SO_2Cl_2 and a source of radicals.[9b]

---

[13] Hampton, *Anal. Chem.*, 1949, **21**, 921.

Substitution leading to the formation of allyl chlorides occurs, however, as a side reaction. The amount of allylic groups can be estimated from the reaction with aniline. Nothing was known about the possible shift of double

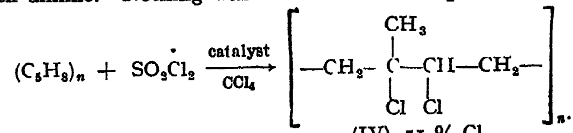

$$(C_5H_8)_n + SO_2Cl_2 \xrightarrow[CCl_4]{catalyst} \left[-CH_2-\underset{Cl}{\overset{CH_3}{C}}-\underset{Cl}{CH}-CH_2- \right]_n.$$

(IV) 51 % Cl

bonds in the course of the reaction with radicals. Infra-red analysis (Table I and Fig. 1) confirms the existence of residual double bonds, some of which must be of the original structure (11·9 μ band), while a somewhat irregular increase of the 10·3 μ and 10·8 μ intensities indicates the presence of isomerized and migrated double bonds.

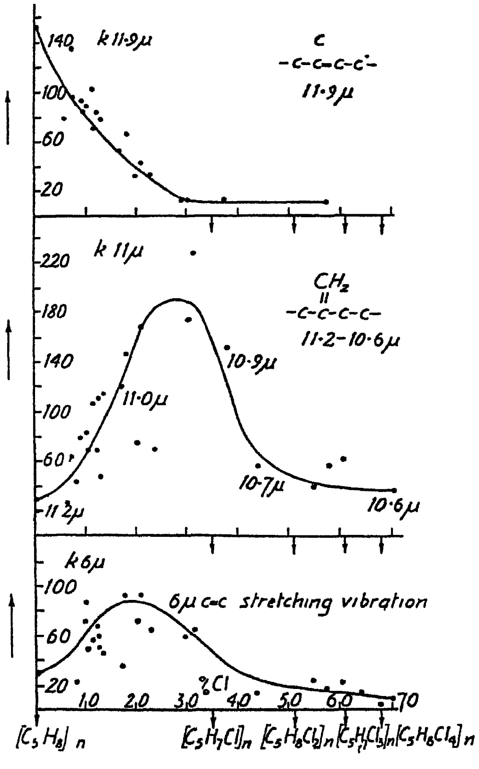

FIG. 4.—Influence of the degree of chlorination on the double bond intensities in chlorinated rubber.

CHLORINATED RUBBER HYDROCHLORIDES.—A product similar to this rubber-dichloride is obtained from the reaction of rubber hydrochloride with chlorine activated by light. The substitution leads first to the transformation of the tertiary chloride into a dichloride at a chlorine content of about 50 % and can be continued to 70 % chlorine content. The chemical evidence therefore points to the structures (IV), (V) and (VI).

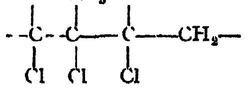

$$--\underset{Cl}{\overset{H}{C}}--\underset{Cl}{\overset{CH_3}{C}}-\underset{Cl}{\overset{H}{C}}-CH_2-$$

(V) 61 % Cl

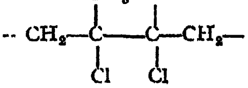

$$--CH_2-\underset{Cl}{\overset{CH_3}{C}}-\underset{Cl}{\overset{Cl}{C}}-CH_2-$$

(VI)

Nothing is definitely known about the formation of new double bonds or of C—Cl_2 groups in the course of this smooth chlorination reaction. Stability is, however, considerably higher than that of the corresponding chlorinated rubbers with 50-60 % chlorine. The absence of the 11·9 μ band excludes the occurrence of the original double bond, but the increase in intensity of the 11 μ band is consistent with a possible formation of small quantities of allylic groups (Table I and Fig. 1).

CHLORINATED RUBBER.—It is known from extensive studies in this field that the interaction of chlorine and rubber in solution as well as in latex first leads to the formation of allylic chlorides, which are gradually transformed into polychlorides. The latter process can occur either by addition of chlorine to the double bond of the allylic chloride or by continuous substitution leading to polychlorinated olefins. The vigorous beginning of the reaction makes the production of a homogeneous derivative difficult and the following results refer therefore always to fractionated chlorinated rubber obtained by gradual precipitation.

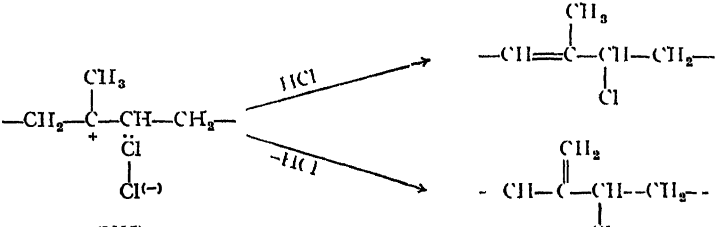

(VII) (VIIIa) (VIIIb)

Chemical evidence makes an ionic mechanism probable.[9a] The hypothetical intermediate (VII) can lead to two different types of allylic chlorides, (VIIIa) and (VIIIb). A decision between (VIIIa) and (VIIIb) could be made by infra-red analysis. The double bond absorption of (VIIIa) should be found near the original 11·9 μ band, that of (VIIIb) near the 11·2 μ band. Fig. 2 and 4 allow one to draw the following conclusions.

(i) The original 11·9 μ band shows a weakening in intensity already in the first phase of the chlorination; it practically disappears when one atom of chlorine has been substituted in each isoprene unit. This makes formula (VIIIa) improbable.

(ii) The weak 11 μ band of rubber shifts to shorter wavelength in the derivative. The intensity of this 11 μ band becomes of the same order as that of the original strong 11·9 μ band at the chlorination phase of $(C_5H_7Cl)_n$. This result is consistent with formula (VIIIb).

The shift of the original 11·2 μ band to 10·9 μ on chlorination has been observed by us also in the following two reference compounds (IX) and (X).

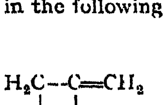

$\underset{Cl}{H_2C}-\underset{Cl}{C}=CH_2$

Maximum at 11·05 μ.
(IX)

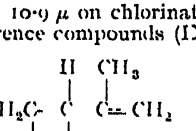

$\underset{Cl}{H_2C}-\overset{H}{\underset{Cl}{C}}-\overset{CH_3}{C}=CH_2$

Maximum at 10·85 μ.
(X)

Moreover, Barnard *et al.*[14] found a similar change on introduction of a chlorine atom.

This shift of the original 11·2 μ band to higher frequencies is continued on further chlorination of the rubber. The points at 50-70 % chlorine content in Fig. 4 refer actually to absorption maximum at 10·7 μ. The observed intensity of this band decreases with the introduction of two or three chlorine atoms until it has reached the original low value. It is, however, not of zero intensity, indicating that some double bonds are left even in highly chlorinated rubber.

(iii) The intensity of the 6·0 μ band increases with increasing chlorine content up to 30 % Cl. This increase might be due to a shift of the double bond resulting in the formation of vinyl groups as derived from the behaviour of the 11 μ band. But it should be borne in mind that the attachment, especially of polar groups, to a bond may also greatly change the intensity of the characteristic absorption band due to a change in the effective dipole moment associated with the oscillation. However, the fact that the 6·0 μ band is persistent even in highly chlorinated rubbers proves the occurrence of residual double bonds, and so confirms the conclusions drawn from the behaviour of the 11 μ band.

---

[14] Barnard, Bateman, Harding, Koch and Sutherland, *J. Chem. Soc.*, 1950, 915.

(iv) Support for the assumption of formula (VIII*b*) is also obtained from changes in the 7·25 μ CH_3 band. At 30-40 % Cl content the original sharp methyl band is disfigured into almost a shoulder, by an additional absorption in the transparent region between the absorption bands at 7·25 μ and 6·85 μ (see Fig. 2). This might indicate the absorption due to the ethylenic CH-deformation frequency at 7·1 μ. Actually the CH_3 intensity cannot be measured in these fractions of the chlorination product; it reappears with a reduced intensity in chlorinated rubber containing 40-70 % Cl (see Fig. 5B).

CYCLIZED RUBBER.—Cyclization is a polar polymerization reaction catalyzed by Lewis acids. The first phase must be a polarization of double bonds, which does not differ in principle from that of the assumed intermediate structure (VII) in chlorination. An analogous double bond shift could therefore be expected. An increase in intensity at the 11 μ band, together with a decrease at the 11·9 μ, has already been observed by Sears.[15]

We have measured four samples of cyclized rubber prepared from latex[11] with an approximate loss of 50, 70 and 80 % of the original unsaturation and have found in all samples a strong band at 11·2 μ and only a weak 11·9 μ band (see Fig. 3). The chemical evidence points also to two types of double bonds, which differ measurably in their ease of reaction with HCl.[11]

TABLE II.—INTENSITIES OF THE DOUBLE BOND IN RUBBER AND RUBBER–SILVER SALT COMPLEXES

Polymer	Position in μ and Intensities of the Bands			
Natural rubber . .	6·00 m.	10·30 v.w.	11·25 w.	11·9 v.s.
Complex with 19·8 % $AgNO_3$ (*a*) . .	6·11 s.	10·25 w.	11·14 s.	11·9 v.s.
Complex with 41·3 % $AgClO_4$ (*b*) . .	6·14 v.s.	10·38 s.	10·9 v.s. 11·14 s.	11·9 w.

v.s., very strong; s, strong; m, medium; w, weak; v.w, very weak.

(*a*) 0·1 mole $AgNO_3$/1 mole C_5H_8. A broad band in the region between 6·9-7·9 μ is due to the nitrate group.

(*b*) 0·23 mole $AgClO_4$/1 mole C_5H_8. A broad band in the region between 8·8-9·9 μ is due to the perchlorate group.

COMPLEX COMPOUNDS WITH SILVER SALTS.—Chemical evidence led us to the assumption that the dissociation of crystalline complexes between silver nitrate or perchlorate and rubber was completely reversible. Some preliminary measurements of the spectra (see Table II and Fig. 3) indicate, however, a decrease of intensity of the 11·9 μ band, whereas the 11 μ and 10·3 μ region increase both markedly in intensity. This suggests the occurrence of *cis-trans* isomerization and of a double bond shift. Moreover, the 6·0 μ C=C stretching vibration band is shifted to 6·1-6·2 μ and becomes much stronger, indicating a weakening of the C=C bond due to the formation of π complexes. A study of the rubber regenerated from the complex is under way.

INTENSITY OF THE CH_3 DEFORMATION FREQUENCY AT 7·25 μ. In this section the term relative intensity of the CH_3 band refers to the ratio

$$k_{CH_3}/k_{CH_2} = k_{7.25\mu}/k_{6.85\mu}.$$

Measurements on a number of paraffinic reference compounds as well as data from literature make clear that this relative intensity is not independent of the rest of the molecule. Introduction of 2 or 3 neighbouring chlorine atoms leads generally to a reduction of the CH_3 intensity. A decrease in intensity on chlorination is therefore not a direct measure of a reduced number of CH_3 groups. Unfortunately our reference data are not sufficiently extensive to discuss fully the changes in relative intensity observed on HCl or Cl_2 addition

[15] Sears, *J. Appl. Physics*, 1941, **12**, 35.

to the double bond of rubber. It is seen from Fig. 5A that these reactions cause not a decrease but a marked increase in the k_{CH_3}/k_{CH_2} intensity, which remains apparently unchanged on further chlorination of the hydrochloride. We do not yet know the influence of double bonds and the difference between —CHCl—CHCl— and —CH_2—CCl_2— groups in relation to the 7·25 μ band which effects may partly compensate each other. A comparison of Fig. 5A, and 5B reveals immediately that an essential difference exists between the controlled addition and substitution reactions (5A) and the complicated reaction products of direct chlorination (5B). The points in Fig. 5B refer to the same fractions as those in Fig. 4. It has already been mentioned that the original 7·25 μ band disappears in chlorinated rubber with 30-40 % Cl content. Only a few of the other fractions indicate a stronger relative intensity, most of them are unchanged or show a decrease. The ratio 0·4 for the highly chlorinated products in Fig. 5B should be compared with the ratio 0·7 obtained for products with similar chlorine content in Fig. 5A. The loss of methyl groups on direct chlorination is tentatively suggested from these data. Methyl groups could disappear either by chlorine addition at the intermediate (VIII*b*) or by direct chlorination leading to the primary R—CH_2Cl group. A search for the corresponding C—Cl frequency is now being made.

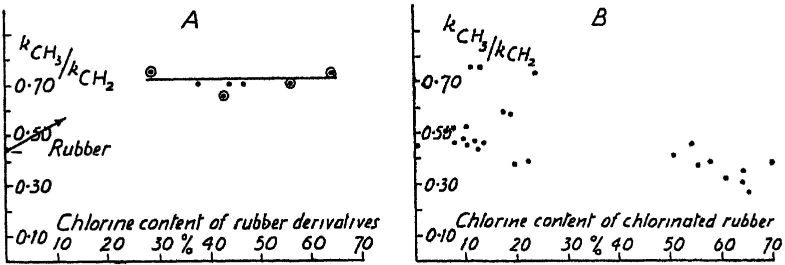

Chlorides with known structure

Chlorinated rubbers

FIG. 5.—Relative intensities $k_{CH_3}/_{CH_2}$ of the methyl groups in chlorine containing rubber derivatives.

●, Rubber dichlorides ;
○ Rubber hydrochlorides and chlorinated rubber hydrochlorides.

Discussion

Our data suggest that the intermediate formation of the vinyl configuration $—C—\overset{\overset{CH_2}{\|}}{C}—C—$ by a shift of the original double bond occurs not only in the course of chlorination reactions, but also in other reactions of rubber with acceptor molecules. The vinyl group in turn leads to a relative increase in the intensity of the 6·0 μ C=C stretching vibration, so that the latter becomes useless for even a rough estimate of double bond concentration in a polyisoprene derivative. The curious observation, that a hydrochloride with 20 % of the original double bond number shows still a moderate 6 μ absorption while one with 10 % double bonds [10] has no 6 μ band, indicates that small differences can cause significant changes in the 6·0 μ intensity. The 6·0 μ frequency is, however, very useful for the qualitative indication of residual double bonds. We have shown that chlorinated rubber with 65-70 % Cl content still contains some double bonds, while the unsaturation of fully sulphurized ebonite has been previously mentioned by Sheppard and Sutherland.[8]

The discovery of vinyl-groups in rubber derivatives explains immediately many observations made by the first-named author and his colleagues in past years. It is well known that the strong cross-linking tendency of polybutadienes is due to the presence of 15-20 % vinyl groups

$_2$, which are more apt to polymerize than "internal" double bonds. A significant difference between natural rubber and all its derivatives is, that the latter cross-link on the slightest provocation like synthetic rubbers. This has been found with partly chlorinated rubber, cyclized rubber, isorubber, partly hydrochlorinated rubber and even with the silver salt complexes. Our infra-red data suggest double bond shifts as the probable cause of these disturbing side reactions.

Our data as well as those of previous authors [12] are consistent with the assumption of 1-5 % vinyl groups in rubber. Chemical evidence on the structure of rubber does not exclude such small quantities of vinyl groups. Vulcanization is partly a polar reaction just as is chlorination, and thus might lead to an increase of the originally small number of vinyl groups. In one case at least this supposition is supported by experimental evidence ; the vulcanization of rubber with S_2Cl_2 is accompanied by the formation of a strong 11·2 μ band according to Thompson.[16] This method of cross-linking rubber differs, however, chemically from the technical vulcanization with sulphur.

No positive indication of similar changes on reaction either with sulphur alone or with a mercaptobenzothiazol-type accelerated mix can be deduced from published data.[12, 17, 18] This, however, does not exclude double bond shifts and isomerization, especially under other conditions of technical vulcanization.[8] The occurrence of vinyl groups in raw rubber and intermediate double bond shifts deserve closer study, in view of their importance in relation to the tendency of rubber to form cross-links during vulcanization.

The results of our attempts to measure the methyl groups are rather disappointing. It is obvious that the relative intensity of the CH_3 bending deformation can be increased as well as decreased by a combination of addition and substitution reactions. Therefore not more than a rough qualitative picture has been obtained.

Summing up, our impressions gained from these exploratory experiments are that infra-red analysis is a useful but delicate tool in polymer chemistry. The discovery of intermediate processes by qualitative observation of new frequencies can stimulate the work of technologists, but any attempt to draw semi-quantitative conclusions from intensity measurements must be preceded by a detailed knowledge of the chemistry involved.

We wish to thank Miss E. van Brussel for technical assistance and the Rubber Foundation for permission of publication.

Rubber Foundation, Delft.

Department of Inorganic Chemistry,
the University of Amsterdam.

[16] Thompson, *Trans. Faraday Soc.*, 1945, **41**, 275.
[17] Sheppard and Sutherland, *Trans. Faraday Soc.*, 1945, **41**, 277.
[18] Saunders and Smith, *J. Appl. Physics*, 1949, **20**, 953.

POLYMER TYPES AND SPECIFIC ABSORPTIONS IN THE ULTRA-VIOLET BY HYDROGEN-BRIDGED AMIDES AND ALCOHOLS WITH APPLICATION TO THE PROTEIN STRUCTURE PROBLEM

By Gladys A. Anslow

Received 17th July, 1950

The objective of these investigations was to locate and to attempt the identification of the origins of the absorption continua, which appear in the ultra-violet spectra of hydrogen-bridged molecules, correlating these with information from

other types of physical measurements; to explore the nature of the excitation process and to establish equations giving the minimum frequency of the respective continua; and finally to correlate the findings with the spectra of proteins. The principal absorptions below 250 mμ in amides and alcohols prove to be of electronic-vibrational origin, the onset frequencies and respective types depending on the dimer or polymer type of associated molecule. Polymeric alcohols appear to be associated through ionic OH^+ bonds. Weak ground state dissociation of OH $\cdots$ O with onset near 35,000 cm.$^{-1}$ seems to be characteristic of bound water. CH $\cdots$ N and CH $\cdots$ O association effects are discussed. Applications are made to the spectra of the proteins, zein and gelatin.

Since molecular association through hydrogen bridges produces the well-known frequency shifts in the stretching and bending vibration bands in infra-red absorption spectra, it seems probable that the effects of association also appear in ultra-violet absorption spectra. In the latter region electronic-vibrational excitation of hydrogen-bridged bonds must occur at higher energies than in unassociated molecules, the excess energy being expended in vibrational excitation of the bridge, at times resulting in its rupture. It has previously been suggested that the " end " absorption, which sets in near 220-200 mμ in carboxylic acids,[1] has such an origin.[2] The wave number ν of the long wavelength edge of this absorption in fatty and amino acids has been shown [3] to be linear with the inverse square root of the reduced mass μ of the bridged units, obeying an equation,* which may be written

$$h\nu = h\nu_{00}(\mathrm{OH}) + h\nu_v(\mathrm{OH} \cdots \mathrm{O}), \quad . \quad . \quad . \quad . \quad (1)$$

where ν_{00} is 32,400 cm.$^{-1}$, the frequency of the transition $v' = 0 \rightarrow v'' = 0$ in the strong OH band [4] near 306 mμ, and $h\nu_v(\mathrm{OH} \cdots \mathrm{O})$ is the dissociation energy of the bridged bond in the excited state.

Since the spectra of the alcohols [5, 6] and of the fatty acids [1, 2, 6] in this region have similar character and the amides exhibit continua at slightly higher wavelengths, an extensive investigation of the ultra-violet spectra of the alcohols and of the acid amides has been conducted to locate their absorption continua, to observe the differences in the character of OH $\cdots$ O and NH ... O absorption, and to test the validity of eqn. (1). It is believed that such information may prove a valuable complement to infra-red data in the discussion of the structure of large molecules.

The Polymer Types of Amides and Alcohols.—In solutions a portion of the molecules which are subject to hydrogen bridging will be in the unassociated state and others associated, the relative amounts depending on the molar concentrations and the polarity of the solvent; consequently the spectra studied may contain bands characteristic of monomers as well as of the various polymers. The latter may occur as linear polymers, dimers, trimers or higher multiple polymers.

Amide association must be dimeric or trimeric. An X-ray analysis of acetamide crystals [7] indicates trimeric association with each oxygen bridged to one of the hydrogens of two neighbouring molecules and the methyl groups tied closely by van der Waals' forces. It is probable that such formation occurs in the crystals of other amides. Although by analogy with the behaviour of carboxylic acids, amides might be expected to polymerize as dimers and to fuse, as suggested by Copley,[8] layer to layer through weaker NH $\cdots$ O bonds, an attempt to build the model shows that the bond angles would be distorted, resulting in considerable strain. If, however, the dimers are associated through water, the strain disappears.

---

[1] Ley and Arends, *Z. physik. Chem. B*, 1929, **4**, 234; 1932, **17**, 177.

[2] Anslow, *Physic. Rev.*, 1942, **61**, 546.

[3] Anslow and Foster, *J. Biol. Chem.*, 1932, **47**, 37.

* In the earlier paper ν_{00} was erroneously identified as an atomic rather than a molecular excitation frequency.

[4] Dieke and Blue, *Physic. Rev.*, 1935, **47**, 261; Tanake and Koana, *Proc. Physic. Math. Soc. Jap.*, 1934, **16**, 365.

[5] Schiebe, *Z. physik. Chem. B*, 1929, **5**, 355.

[6] Platt, Rusoff and Klevens, *J. Chem. Physics*, 1943, **11**, 535.

[7] Senti and Harker, *J. Amer. Chem. Soc.*, 1940, **62**, 2008.

X-ray studies have shown that cyclic amides, such as glycine anhydride,[9] are dimerically associated, forming long chains tied by van der Waals' forces or CH $\cdots$ O bridges to form crystalline layers. A diffraction study of urea crystals [10] indicates two hydrogens to each carbonyl oxygen and two other hydrogens associated with it through van der Waals' forces. In solutions this weak association is broken leaving two " free " amides per molecule. These crystalline types are reflected in the infra-red spectra of solid specimens.[11, 12]

Crystallographic measurements [13] show that alcohols associate as long linear polymers. Dielectric constant measurements [14] indicate that primary alcohols form longer polymers than secondary and tertiary alcohols. In the latter steric hindrance may prevent linear polymerization, resulting in the formation of open dimers or of closed trimers, as determined by the configuration of the R groups. Consequently two families of association bands may be expected to appear in the isomeric alcohols.

The Photo-Dissociation Process.—Whereas before ultra-violet irradiation the bridged group consists of a covalent bond, which is partially ionic in character as a result of the bridge, and of a bridge of greater ionic character, after electronic excitation, the ionic character of the bond is greatly increased. The theories of the nature of the hydrogen bond in the lower state have been ably discussed by Davies.[15] In the excited state OH $\cdots$ O groups must exist as O : H : O configurations with the bridge energy considerably increased and the bond and the bridge equivalent in character. In the N : H : O configuration the vibrational energy of the bond must be less than that of the bridge. The minimum photon energy required to dissociate the group must be equivalent to the sum of the bond and bridge energies plus the resonance energy in the lower state.

Following the method used in the dissociation theory of diatomic molecules it can be shown that for polyatomic molecules, the dissociation energy is

$$D_s = \omega_s^2/(-4x_{ss})\left\{1 + 2x_{ss}g_s/\omega_s + 2/\omega_s \sum_{s'} x_{ss'}\ (v_{s'}+g_{s'}/2)\right\}, \quad . \quad (2)$$

an equation derived from Nielsen's [16] expression for the vibrational-rotational energy of polyatomic molecules, where v_s and $v_{s'}$ are vibrational quantum numbers, g_s and $g_{s'}$, the orders of degeneracy of the normal vibration frequencies, ω_s and $\omega_{s'}$, of the s and s' modes of normal vibration, respectively, and x_{ss} and $x_{ss'}$ are anharmonicity constants. To the first approximation

$$D_0 = \omega_s^2/(-4x_{ss}), \quad . \quad . \quad . \quad . \quad . \quad (3)$$

as for diatomic molecules. Since the force constants depend on the electronic configuration, $D_0 \propto \mu^{-\frac{1}{2}}$, approximately.

It must be emphasized that in general this dissociation occurs in the excited state ; but occasionally, when the steric configuration of the larger molecules results in considerable perturbation of the energy levels, the transition probability for dissociation in the ground may be finite. In

[8] Copley, Zellhoefer and Marvel, *J. Amer. Chem. Soc.*, 1938, **60**, 1598.

[9] Corey, *ibid.*, 1948, **60**, 1598.

[10] Wycoff and Corey, *Z. Krist.*, 1939, **89**, 4629.

[11] Kellner, *Proc. Roy. Soc. A*, 1940, **176**, 448 ; 1941, **177**, 456.

[12] Bushwell, Downing and Rodebush, *J. Amer. Chem. Soc.*, 1939, **43**, 219.

[13] Zachariasen, *J. Chem. Physics.*, 1933, **1**, 515 ; Harvey, *ibid.*, 1938, **6**, 111 ; Pierce and Marmella, *J. Amer. Chem. Soc.*, 1939, **60**, 779.

[14] Kumler, *J. Amer. Chem. Soc.*, 1935, **57**, 600.

[15] Davies, *Ann. Reports*, 1947, **43**, 5.

[16] Nielsen, *Physic. Rev.*, 1941, **60**, 794.

both states r_e exceeds the corresponding value in unassociated molecules, the upper state being displaced upwards on the potential energy diagram by an energy equal to that of the bridge.

Experimental

The ultra-violet spectra were obtained with a Beckman quartz spectrophotometer employing silica cells and permitting monochromatic measurements to 220 mμ and with a Lyman vacuum spectrograph * together with an Allen type [17] hydrogen lamp with the filament turned at right-angles from the position described in the original paper.† The intensity of this source, when the lamp was flushed out daily with hydrogen, proved extremely constant during operation. Cells of less than 0·3 mm. thickness were formed by surface tension according to the method employed by Schiebe [5] and by Platt, Rusoff and Klevens [6] by slowly dripping the liquid between the parallel quartz windows of the lamp and the spectrograph.

Spectrograms were read on a photoelectric densitometer and approximate extinction coefficients calculated from comparisons of the photographic densities of the spectrograms formed by beams transmitted through the solvent and the solution for various time intervals. For infra-red correlations a Perkin-Elmer type 12C single-beam infra-red spectrophotometer with calcium fluoride prism and cells was employed. The pH of the amide solutions was measured with a Leeds and Northrup Universal pH potentiometer assembly.

The chemicals employed were with only a few exceptions White Label grade Eastman Kodak Company products. All amides were recrystallized to a constant melting point from appropriate solvents. The spectra of most amides were studied as solutions in redistilled water and alcohol; some were studied as ether or chloroform solutions and a few as dried crystalline depositions from methanol on quartz plates. The alcohols were redistilled to constant boiling point, usually through three distillations, discarding all but the middle portion in each distillation. Spectra of the final distillates were taken promptly, a few being repeated after an eight-week period. The alcohol spectra reported are of *iso*-octane ‡ solutions. In the vacuum region pure liquids were employed as well as *iso*-octane solutions. The purity of the distillates was tested chemically by the bromine water reaction and spectroscopically through a study of their infra-red spectra, comparisons being made with standard spectra.[18] Neither the typical C═C band group in the 2000-1800 cm.$^{-1}$ region nor the strong single band at 1600 cm.$^{-1}$ could be detected. Since the infra-red spectrum is a sensitive method for detection of components it is believed that the redistilled alcohols are essentially free of unsaturated impurities and that specific absorption in the ultra-violet region is characteristic of the alcohols and not of impurities.

In addition to the amides and alcohols, thin films of Nylon § formed from hexamethylene adipamide and hexamethylene sebacamide and alcohol-water solutions of Nylon 6B crystals were examined, also water solutions of gelatin at various pH values before and after irradiation, and solutions of protein zein in 80 and 95 % EtOH+H_2O solutions. The 95 % EtOH zein solutions were denatured by the high alcohol content, the resulting mucilaginous mass filtered, and the density of filtered liquid determined to estimate the % concentration.

Since in the preliminary studies [19] it was observed that the character of the spectrum of a given amide solution appeared to be a function of its age and the temperature, exhibiting two types as shown graphically for acetamide and propionamide in Fig. 1, water solutions were studied before and after the following heat treatment. The solutions were heated for one, two or three hours on a steam bath, then divided into two portions, one of which was cooled slowly to room temperature, thus permitting normal polymerization, while the other was quenched by immediate immersion into an ice and salt bath. Almost invariably the slowly cooled sample yielded the *B* type of absorption curve, while the rapidly cooled sample yielded the type *A* curve. The latter type proved to be very stable, resisting heat treatment attempts to convert its form to type *B*. Since during heating the crystalline state must have been destroyed, it is probable that the quenched samples consist mainly of monomers and dimers.

---

* Loaned by Harvard University to Smith College through the courtesy of Prof. Theodore W. Lyman.

[17] Allen, *J. Opt. Soc. Amer.*, 1941, **31**, 268.

† Suggestion given privately by John Loofbourow.

‡ Spectroscopic grade *iso*-octane from the Phillips Petroleum Company.

[18] *Amer. Petroleum Res. Proj.* 44 (Nat. Bur. Stand., Washington), Charts 425-437; 745-758.

§ The Nylons were furnished by the du Pont de Nemours Experimental Station. The gelatin and zein were Harris Laboratories products. The zein was certified as of very high purity.

[19] Anslow and Shea, *Physic. Rev.*, 1949, **75**, 1318.

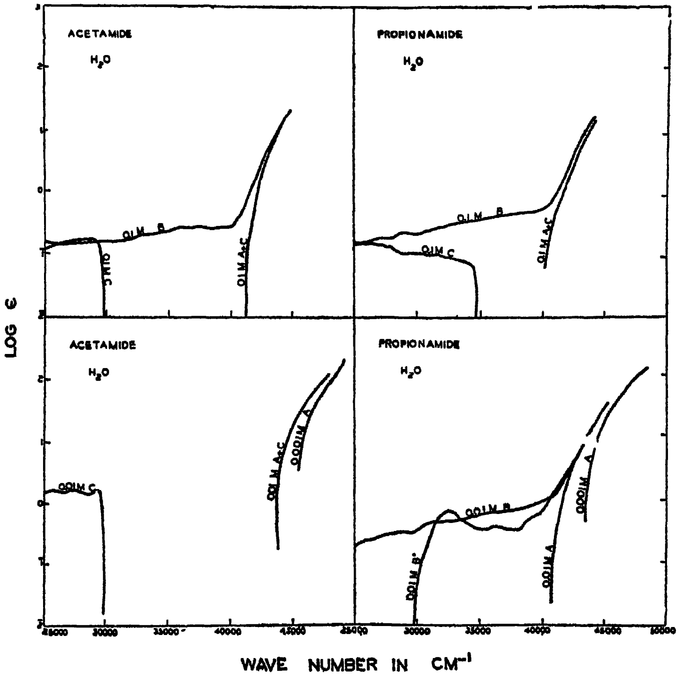

FIG. 1.—Log $E = \log_{10}$ absorptivity.

The significance of the various spectra obtained will be discussed with such polymer type considerations in mind.

Results and Discussion

The Amides and Related Substances.—Solutions of linear amides, Fig. 1-4, exhibit three definite types or spectra, all types being yielded by fresh solutions, as well as definite types by the heat treated specimens, as follows :

TYPE *A*, in which sudden onset appears at the higher frequency with log $\epsilon_{max}{}^2$. These appear to result from dimer association. If the frequency of onset for a particular concentration is plotted, Fig. 5, upperline, against the inverse square root of the reduced mass $\mu^{-\frac{1}{2}}$, the linear relation of eqn. (1) is obtained where $\nu_{00} = 29{,}750$ cm.$^{-1}$; * this is ν_{00} (NH) of the 336 mμ band system.[20] The reduced mass is calculated from the masses of the two units adjacent to the bridge in which the photon energy is absorbed. If it is assumed that in most cases the amide is associated through the solvent and the mass of the solvent included in the calculation, excellent agreement is obtained. In some samples, indicated on the graph, conformity is obtained by assuming direct association. The frequency of onset decreases with increase in concentration, probably resulting from the lowering of the bond energy consequent to inter-association of dimers at the higher concentration.

---

* The accuracy of results for ν_{00} permits only four significant figures, with uncertainty in the last digit.

[20] Fowler and Gregory, *Phil. Trans. A*, 1919, **218**, 251 ; Funke, *Z. Physik*, 1935, **96**, 787.

TYPE *B*, already ascribed to trimeric association shows general weak absorption in the 400-250 mμ region, followed by a gradual onset of stronger absorption at frequencies slightly less than in type *A*. This lower frequency would be expected from trimers, for which the reduced mass is 4/3 that of dimers, causing $D'_0(\mathrm{NH}\cdots\mathrm{O})$ in trimers to be about 15 % less than the dimer value. The general absorption frequently shows specific effects, which may result from the electronic excitation of free NH in the vicinity of 29,750 cm.$^{-1}$, particularly obvious in the spectrum of urea, Fig. 4, or of free NH_2 and C=O, and also of C=N and O—H, if the amides resonate as proposed by Pauling.[21] In the weaker solutions the NH absorption is evident. If vibrational dissociation occurs in the ground state a weak continuum is expected to start near 32,800 cm.$^{-1}$, corresponding to $D_0''(\mathrm{NH}) = 3{\cdot}77$ eV.[22] At higher frequencies onsets consequent to the dissociation of the bridge of $\mathrm{NH}\cdots\mathrm{O}$ in the excited state may be observed. Many of these effects overlap.

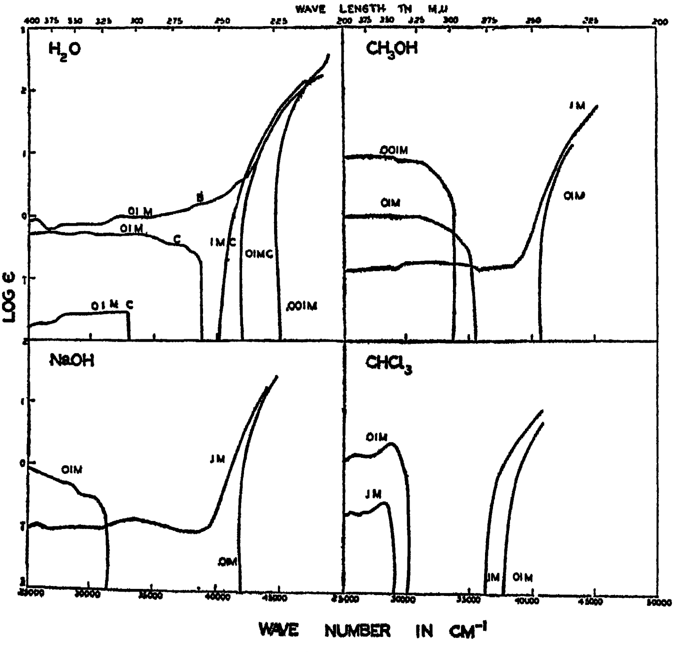

FIG. 2.

TYPE *C*, a duplicate of type *B* between 25,000-30,000 cm.$^{-1}$ and of type *A* at beyond 40,000 cm.$^{-1}$, with an intervening region in which negative density readings were obtained on the Beckman instrument. This indicates fluorescent effects, probably resulting from the formation of strongly associated molecules after the excitation by energies exceeding the electronic excitation energy of a free amide or methyl group at

[21] Pauling and Sherman, *J. Chem. Physics*, 1933, **1**, 606.
[22] Glockler, *ibid.*, 1948, **16**, 602.

29,750 cm.$^{-1}$ and 31,800 cm.$^{-1}$, respectively, or after the rupture of a bridge. The energy required to effect the latter is

$$E_{\text{bridge rupture}} = h\nu_{00} + D_0'(\text{H} \cdots \text{O}). \quad . \quad . \quad . \quad (4)$$

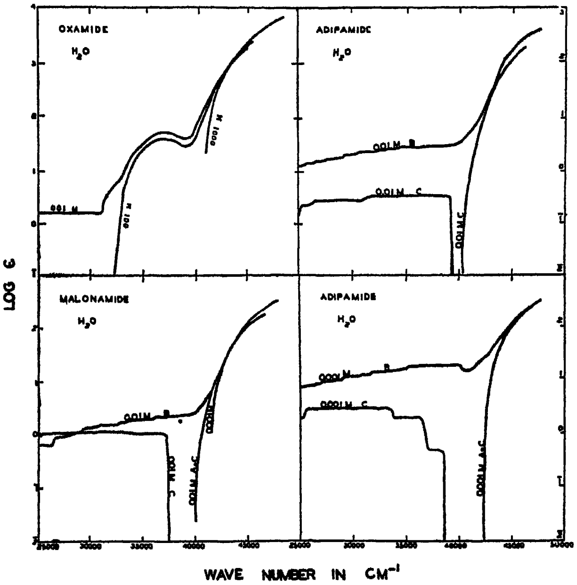

FIG. 3.

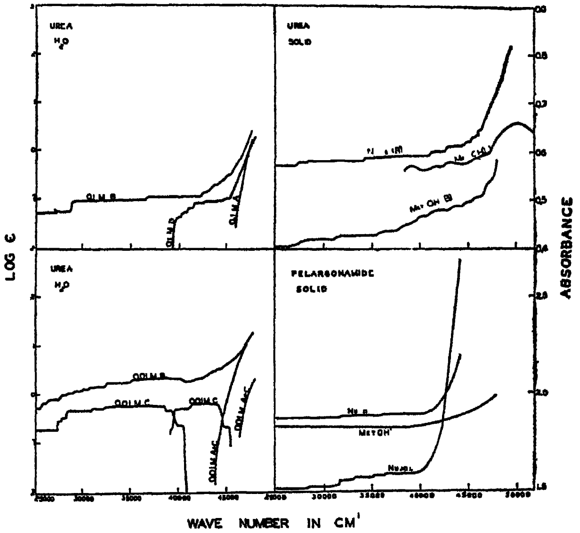

FIG. 4.

When the frequencies of the observed onsets of the discontinuities, which are suspected to result from bridge rupture in various solutions, are plotted against $\mu^{-\frac{1}{2}}$ the lower line in Fig. 5 is obtained.

TYPE *D* exhibited by 0·1 M urea, Fig. 4. The absorption beginning at 39,000 cm.$^{-1}$ occurs at the frequency given by eqn. (4). This absorption band has structure with frequency differences similar to those in the 0·01 M sample of urea with centre near 29,750 cm.$^{-1}$. The frequency differences compare approximately with the stretching and bending vibration infra-red frequencies of urea.[11] Those at 29,750 cm.$^{-1}$ may be ascribed to the excitation of unassociated NH in the dilute solution and those at 39,000 cm.$^{-1}$ to the same effect accompanied by bridge rupture. The structure was clearest in freshly prepared samples. These showed onset frequencies near 43,800 cm.$^{-1}$ indicating dimer association through water. A sample which had been dried for several weeks was transparent to 45,900 cm.$^{-1}$, the frequency for the direct association onset.

CRYSTALLINE SPECIMENS of urea and pelargonamide, Fig. 4, render type B spectra exhibiting similar " free " NH structure. Infra-red spectra of the urea sample indicated that while ageing after drying in a vacuum desiccator, the crystals became more associated. This ageing effect may explain the difference found in the ultra-violet spectra of solutions made from aged crystals.[23]

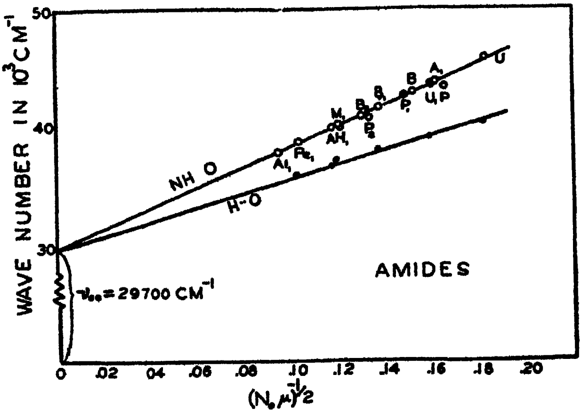

FIG. 5.—Symbols on upper line indicate: U—urea, A—acetamide, P—propionamide, B—butyramide, M—malonamide, A—adipamide, H—hydantoin, Pe—pelargonamide, Al—allantoin. Without subscript association is direct; with subscript 1, through water; without subscript or with subscript 2, through solvent.

The solvent effect on the location of the onset of the disassociation continua was tested for H_2O, MetOH, NaOH and $CHCl_3$ solutions of butyramide, Fig. 2. Realizing that the reduced mass of units associated through the solvent affects the onset frequencies, reduced mass values have been calculated and onset frequencies estimated from the slope of the NH · · · O line in Fig. 1. These and the observed onset frequencies are listed in Table I.

It is obvious that the very slight shifts in the onset frequencies in H_2O, MetOH and NaOH result from the utilization of the solvent in the association process. The $CHCl_3$ absorption does not fit these results. It will be correlated later in the paper with suggested CH · · · N association.

All samples were measured for their hydrogen ion concentration. Irradiation had only a slight effect upon the pH, certainly not more than the results of standing. Heating the samples markedly increased the pH. No observable shift in the onset frequency for *D'*(NH · · · O) resulted either from irradiation or from heating. The specific absorption ν_{00}(NH) was effected.

---

[23] Shea and Anslow, *Bull. Amer. Physic. Soc.*, April, 1950, 43.

The spectrum of Nylon 6, Fig. 6, in a very dilute alcohol water solution was[24] of type *A*, indicating the dimer, i.e. the *cis*-configuration, type of association at this low concentration. For the films of hexamethylene-adipamide and hexamethylene-sebacamide type *B* spectrum, which is typical of *trans*-configurations, was obtained, the cold-rolled sample showing some specific absorption. In the infra-red spectra the *trans* 3280 cm.$^{-1}$, but not the *cis* 3160 cm.$^{-1}$ vibration frequency, is observed[26] for Nylon films, agreeing with this interpretation of the ultra-violet absorption.

TABLE I.—Effect of Solvent on Frequency of Onset of Dissociation Continua

Solvent	$\mu^{-\frac{1}{2}}$	ν_{00}(NH) + ν_s(NH · · · O)	
		Calc.	Obs.
H_2O^a	0·152	42900 cm.$^{-1}$	42920 cm.$^{-1}$
H_2O^b	0·138	41700 ,,	41700 ,,
CH_3OH^{cb}	0·130	41020 ,,	41000 ,,
$NaOH^d$	0·139	41830 ,,	42000 ,,

a. Association directly between molecules of the solvent.
b. Association through the solvent.
c. Association to solvent.
d. Association through OH of NaOH.

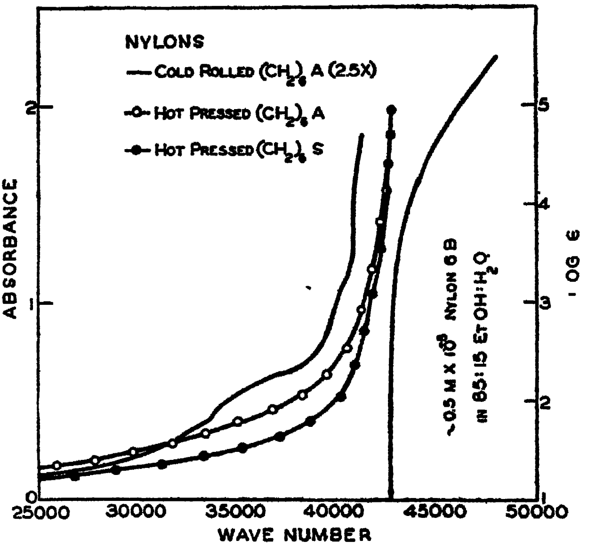

Fig. 6.

---

[24] Anslow, *J. Opt. Soc. Amer.*, 1950, 40, 262.
[25] Thompson and Torkington, *J. Chem. Soc.*, 1947, 1248.
[26] Darmon and Sutherland, *Nature*, 1949, 164, 440.

Cyclic amides give the spectra shown in Fig. 7 and 8. The ultra-violet spectrum of glycine anhydride, the long chain dimer associated polymer with two free CH_2 groups in each molecule, shows structure in the region in which the electronic vibrational bands of CH are expected. The dimer character of the association is indicated by the yield of type *A* spectra at 0·01 and 0·001 M concentrations.

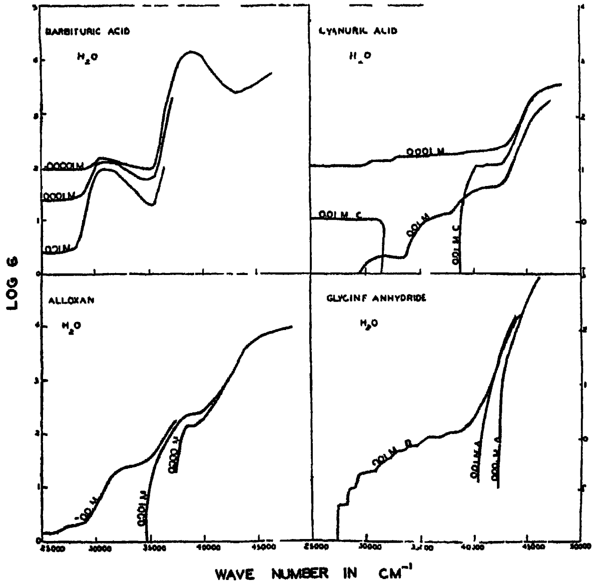

Fig. 7.

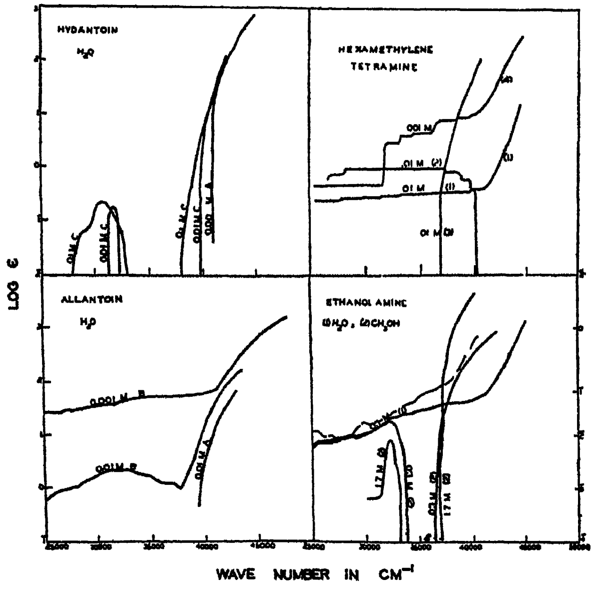

Fig. 8.—(1) in H_2O ; (2) in CH_3OH ; (3) in $CHCl_3$; (4) in ether.

The other cyclic amides, barbituric acid, cyanuric acid and alloxan for stable hydrates, the first two being dihydrates and the latter a tetrahydrate in water solutions. The spectra of barbituric acid and alloxan show no evidence of NH and NH $\cdots$ O bridges but have absorptions starting near 35,000 cm.$^{-1}$, which is the frequency of D_0'(OH)[27] 4·4 eV and 43,800 cm.$^{-1}$, the dissociation energy for OH $\cdots$ O in the excited state. This spectroscopic evidence and a positive ferric test led Shea [28] to postulate an enolic form for barbituric acid at alkaline pH, associated through the enol hydroxyls, and with bound water chelated between the carbonyl and two nitrogen atoms on the opposite end of the molecules. In this structure there are two " free " OH groups, but no NH bond. It is suggested that the 35,000 cm.$^{-1}$ absorption arises from D'(OH $\cdots$ O) in the bound water and the 43,800 cm.$^{-1}$ absorption from excited state dissociation of the inter-associated enolic groups. The band with maximum near 31,800 cm.$^{-1}$ probably results more from electronic excitation of CH_2 than from the twice associated C=O. At acid pH, i.e. in the keto form, the 35,000 cm.$^{-1}$ band decreases in intensity, as remarked by Loofbourow and Stimson,[29] who suggested the origin as C=N and C=C groups in the tautomeric structure—but unless these are conjugated the absorption should occur at considerably higher frequencies.

Similar structures are proposed for cyanuric acid and alloxan, Fig. 7, to explain the absorption near 35,000 cm.$^{-1}$. This appears to be characteristic of molecules containing water of hydration. Since cyanuric acid also shows D_0''(NH $\cdots$ O) absorption, one of its stable forms may be the glycine anhydride type of dimer. Both cyanuric acid and alloxan exhibit weak absorption in the region of C=O electronic excitation. The spectra of hydantoin and allantoin, Fig. 8, are of interest, since both exhibit the 31,800 cm.$^{-1}$ ν_{00}(CH) band; in addition to type A absorption and types A and B NH $\cdots$ O excitation for hydantoin and allantoin, respectively, appear.

The Alcohols.—The spectra of *iso*-octane dilutions of isomeric forms of propyl, butyl, amyl, hexyl and óctyl alcohol are shown in Fig. 8-13. The lower frequency portions are Beckman spectrophotometer curves and the higher frequency portions to 53,000 cm.$^{-1}$ Lyman vacuum spectrograph results, a region also studied by Platt *et al.*[6] Spectra of pure liquid specimens, except of strongly absorbing secondary hexyl alcohols, were obtained in the higher frequency range. Comparison of the spectra in the latter range revealed that corresponding absorptions start more than 4000 cm.$^{-1}$ earlier in the normal alcohols than in their isomers. Consequently, two families are identified.[30]

THE A FAMILY is the predominating absorption in the normal primary alcohols and hence is characteristic of long linear polymers. It also appears in *tert.*-butyl, a trimeric structure,[31] and in other isomers in which steric hindrance does not interfere with the formation of polymers. There are two members of the family, a fairly weak A_1, difficult to identify in the heavier alcohols since it coincides with other absorptions, and a strong A_2 component. Their onsets are indicated by arrows placed on the respective diagrams at the frequency where the curve starts to rise. The identification of the onset frequency is not nearly as precise as for the dimer form of the amides, since absorption starts in gradually. It should be noted that the behaviour of *n*-octyl alcohol is anomalous, since its spectrum falls in the B family. Its isomer, methyl *n*-hexyl alcohol, shows strong A as well as B absorption.

THE B FAMILY appears in the spectra of those isomers in which steric

[27] Gaydon, *Dissociation Energies and Spectra of Diatomic Molecules* (John Wiley Sons, Inc., New York, 1937), p. 190.

[28] Shea, *M.A. Thesis* (Smith College, Northampton, Mass., 1950), p. 106.

[29] Loofbourow and Stimson, *J. Chem. Soc.*, 1940, 1275.

[30] Anslow and Hsieh, *Physic. Rev.*, 1950, **77**, 423.

[31] Hoffmann, *Z. physik. Chem. B*, 1943, **53**, 185.

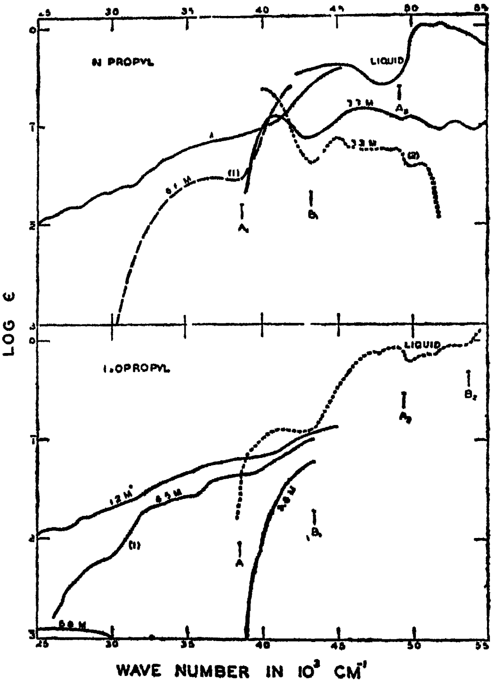

FIG. 9.—In all the alcohol studies *iso*-octane solutions are recorded except: liquids and (1)—MeOH solution. Primed marking = solution at least 8 weeks old. (2) = spectrum taken immediately after distillation

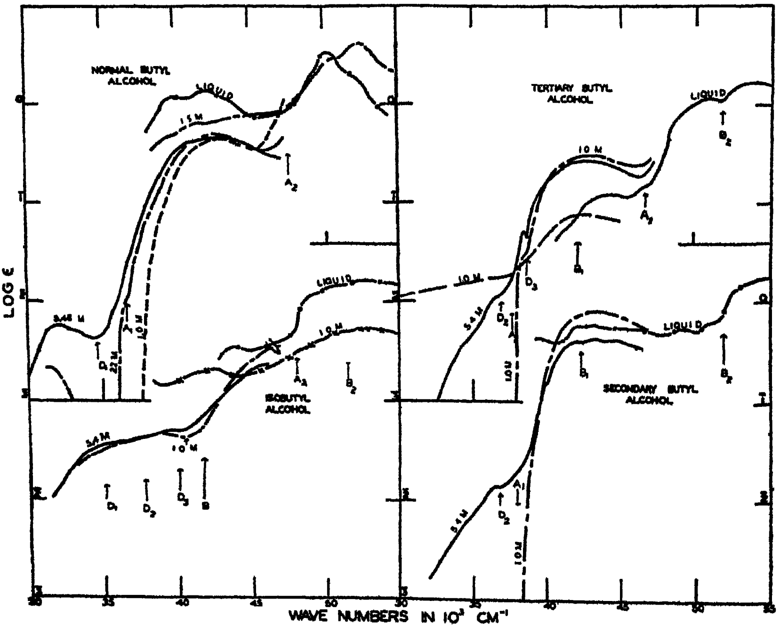

FIG. 10.

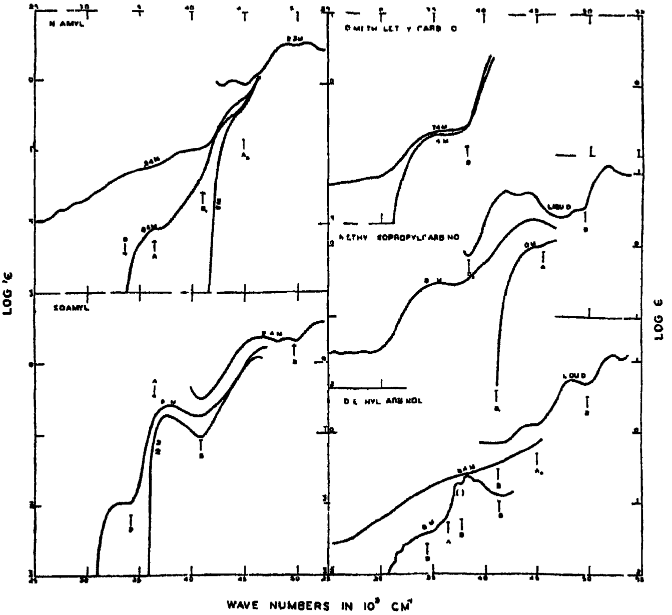
N AMYL
ISOAMYL
LOG ε
LOG ε
LIQUID
A
B
A₁
B₁
WAVE NUMBERS IN 10³ CM⁻¹
25
30
35
40
45
50
55

FIG. 11.

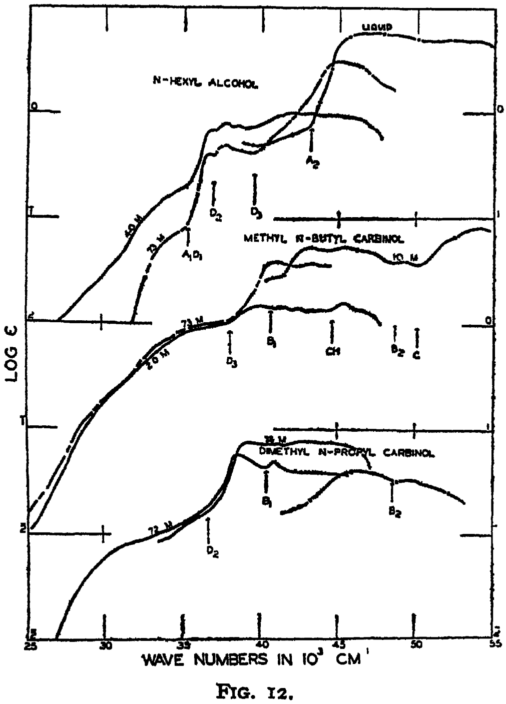
LIQUID
N-HEXYL ALCOHOL
4.0 M
7.3 M
A₂
D₂
D₃
A₁D₁
METHYL N-BUTYL CARBINOL
1.0 M
7.3 M
2.0 M
D₃
B₁
CH
B₂
C
DIMETHYL N-PROPYL CARBINOL
3.5 M
7.3 M
B₁
B₂
D₂
LOG ε
0
1
2
WAVE NUMBERS IN 10³ CM⁻¹
25
30
35
40
45
50
55

FIG. 12.

hindrance prevents association beyond the open dimer stage. Again there are two components, but with B_0 normally stronger than A_1 and B_2 not as prominent as the A_2 of its related normal alcohol.

The frequency of onset of each obeys eqn. (1), as illustrated by the graphs in Fig. 14. Consequently, the origin is an electronic transition leading to vibrational dissociation. It is of considerable significance that in the A family ν_{00} is approximately 28,000 cm.$^{-1}$, the wave number of the 0—0 band of OH+, whereas that of the B family is approximately 32,400 cm.$^{-1}$, the 0—0 transition of normal OH. Thus, it is revealed that in linear polymers and in trimers, such as *tert.*-butyl alcohol, the hydroxyl bonds are ionic, the covalent character being maintained in the other isomers. An important consequence is that it requires less energy for the A family than for the B family to reach the excited state in which dissociation occurs.

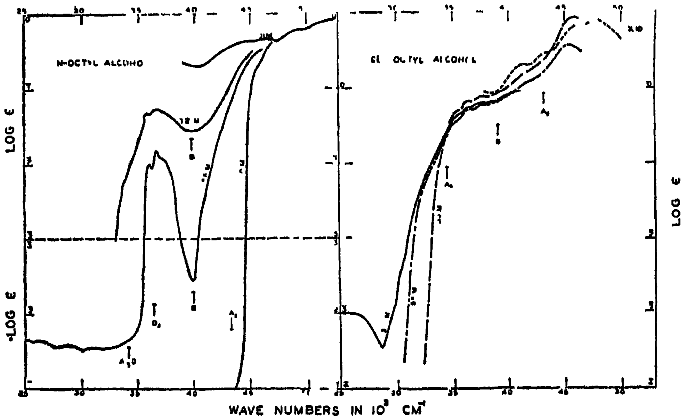

FIG. 13.

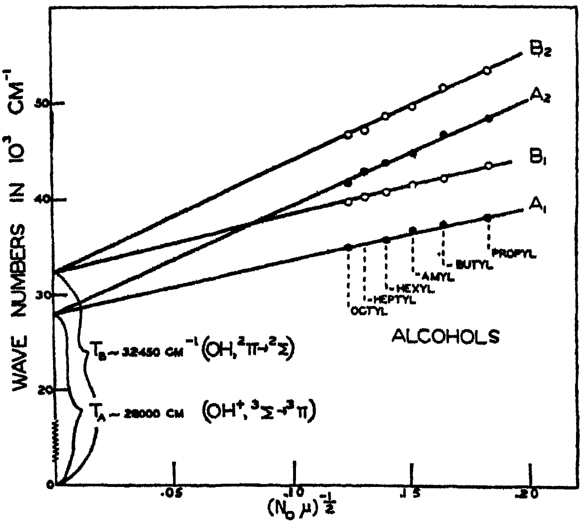

FIG. 14.

The A_1, B_1 and the A_2, B_2 lines in Fig. 14 are respectively parallel; consequently the vibrational dissociation energy of the two families is the same. The slope of the lower line, representing dissociation of the bridge, is approximately half the slope of the upper line, which represents dissociation of the bond and the bridge or alternatively of two bridges in family A. From the respective slopes, these energies expressed in wave numbers are calculated as functions of the reduced masses of the respective associated molecules.

$$D_0(\mathrm{H}\cdots\mathrm{O}) = 0{\cdot}577(N\mu)^{-\frac{1}{2}} \times 10^5;\ D_0(\mathrm{OH}\cdots\mathrm{O}) = 1{\cdot}145(N\mu)^{-\frac{1}{2}} \times 10^5. \quad (4)$$

Thus, approximately at least,

$$D_0(\mathrm{OH}) = D_0(\mathrm{H}\cdots\mathrm{O}). \quad . \quad . \quad . \quad . \quad (5)$$

These are in accord with the first approximation value of D_0 given in eqn. (4), variations indicated by eqn. (2) being expected.

Similar calculations from the slope of lines in the amide graph, Fig. 5, give

$$D_0(\mathrm{N}\cdots\mathrm{HO}) = 0{\cdot}867\ (N\mu)^{-\frac{1}{2}} \times 10^5, \quad . \quad . \quad (6)$$

and consequently

$$D_0(\mathrm{NH}) = D_0(\mathrm{H}\cdots\mathrm{N}) = 0{\cdot}290\ (N\mu)^{-\frac{1}{2}} \times 10^5. \quad . \quad (7)$$

From eqn. (4) and (5) the positions of the respective onsets in other alcohols may be calculated. For example, the A_1 and B_1 absorption onsets predicted for ethyl alcohol are at 235 and 241 mμ respectively. Both of these appear on spectrograms taken in this laboratory, the latter being recorded by Klevens and Platt.[32] The A_2 and B_2 onsets are predicted at 176 and 164 mμ, where the alcohol is known to absorb.

From eqn. (4), D_0(OH) for water vapour may be calculated. This in wave numbers is 18,760 cm.$^{-1}$, or 2·33 eV, approximately, close to the 2·4 eV value estimated by Gaydon.[27] Moreover, absorptions of unassociated OH should appear in the spectra of all open OH dimers and polymers. Calculations for the alcohols predict excited state dissociations at 51,160, and 50,920 and 50,860 cm.$^{-1}$ in the spectra of ethyl, methyl and propyl alcohol, respectively, and at slightly lower wave numbers for the heavier alcohols. This absorption in ethyl and methyl alcohol is well known; it appear in the spectra of Fig. 8-13 and also in those published by Klebens *et al.*[32]

GROUND STATE DISSOCIATION.—The 34,000-37,000 cm.$^{-1}$ region in most of the alcohol spectra show various weak specific absorptions. At first these were suspected as indicating impurities. Further distillations did not eliminate the structure; attempts to correlate the maxima with published spectra of saturated molecules failed. Absorption in this region had been recorded by Henri [33] and others. Finally, the hypothesis that these originate in the alcohols was accepted. Since the onsets are at lower frequencies than would be anticipated for the structure in the $\nu_{0,1}$ (OH) transition, the theory is advanced that they result from ground state dissociation of associated and unassociated hydroxyls. This point of view is supported by the existence of the strong 35,000 cm.$^{-1}$ onset in the spectra of barbituric acid and other cyclic amides containing water of hydration; that absorption has been ascribed to $D_0(\mathrm{OH}\cdots\mathrm{O})$ of the bound water.

Three distinct absorptions are identified, the frequencies vary slightly in the different isomers, apparently decreasing with the complexity of the R group. The spectra of the isomers which exhibit the A type of electronic excitation absorption exhibit definite onsets near 35,000 cm.$^{-1}$, those showing the B type contain a 37,400 cm.$^{-1}$ onset. In many a 36,800 cm.$^{-1}$

[32] Klevens and Platt, *J. Amer. Chem. Soc.*, 1947, **69**, 3055.

[33] Henri and Bielecki, *Compt. rend.*, 1931, **156**, 1322.

also appears. The results of a correlation of these locations with the infra-red 3 μ spectra of the respective isomers in *iso*-octane solutions at different concentrations are given in Table II. The infra-red spectra are similar to those of other observers.[34, 35, 36]

Assignment of the D_1, D_2 and D_3 absorptions to monomer, dimer and polymer dissociations is still tentative; they may well be in this order. Yet it is probable that the magnitude of ω_e is so much lowered by polymer association that the consequent dissociation energy is less than that of the monomer. Evidence for this possibility includes the appearance of the D_1 absorption in the spectra of the polymeric alcohols of the *A* family, its absence in the dimeric alcohols, the *B* family, and its appearance in the spectra of hydrated cyclic amides. The D_2 component is narrow and is strong in the samples which clearly showed monomer components in their infra-red spectra. The D_3 component correlates with the *B* family absorption. Thus, the present evidence forces the assignments of D_2 to the monomer, D_3 to the dimer, and D_1 to the polymer and trimer

TABLE II.—CORRELATION OF 3μ INFRA-RED SPECTRA WITH ULTRA-VIOLET SPECTRA OF ALCOHOL ISOMERS

Isomer	Resolution of I.-r. Components		U-v Components			
			350-380 × 10² cm.⁻¹			*A* or *B*
	Monomer	Associated	D_1	D_2	D_3	
n-Propyl . .	Absent	Unresolved	—	—	—	*A*
*iso*Propyl . .	Weak	Unresolved	355	—	—	*A* and *B*
n-Butyl . . .	Absent	Unresolved	$\underline{352}$	—	—	*A*
sec.-Butyl . .	Weak	Mainly dimer	—	368	380	*B*
tert.-Butyl . .	Strong	*d* and $\underline{t}$	$\underline{348}$	$\underline{368}$	374	*A* and *B*
*iso*Butyl . . .	Weak	Unresolved	—	365	—	?
n-Amyl . . .	Absent	Unresolved	$\underline{340}$	—	—	*A*
Methyl *iso*propyl carbinol . .	Absent	$\underline{\text{Dimer}}$	—	—	$\underline{375}$	*B*
Diethyl carbinol .	Weak	Unresolved	352	—	377	*A* and *B*
Dimethyl ethyl carbinol . .	Weak	*d* and *t*	—	—	$\underline{375}$	*B*
*iso*Amyl . . .	Absent	Unresolved	340	—	—	?
n-Hexyl . . .	Present	$\underline{d}$ and *t*	352	368	—	*A* and *B*
Methyl *n*-butyl carbinol . .	Weak	Dimer	—	—	378	*B*
Dimethyl *n*-propyl carbinol . .	$\underline{\text{Strong}}$	*d* and *t*	—	$\underline{368}$	374	*B*
n-Octyl . . .	$\underline{\text{Strong}}$	Dimer	—	$\underline{363}$	370	*B*
Methyl *n*-hexyl carbinol . .	Present	Unresolved	348	?	?	*A* and *B*

Note.—In the tabulation for the associated components of the I.-r. OH bands, *d* and *t* are used to represent dimers and trimers (or polymers) respectively, in so far as they are resolved. Components which are very strong are underlined.

---

[34] Badger and Bauer, *J. Chem. Physics*, 1936, **7**, 618.
[35] Fox and Martin, *Proc. Roy. Soc.*, *A*, 1937, **162**, 419.
[36] Gordy and Stanford, *J. Amer. Chem. Soc.*, 1940, **62**, 1247.

associations. This assignment gives 104 kcal./mole, 4·56 eV, as the dissociation energy, D_0''(OH), to be compared with the 107 kcal./mole value obtained by Fox and Martin[35] from the infra-red data of butyl alcohol, and the 4·35 eV value[37] obtained from the ultra-violet spectra of water vapour.

NH ··· N, OH ··· N, CH ··· N and CH ··· O Absorptions.—Gordy's[38] infra-red investigations of solutions of the amines indicate complex associations through NH ··· N and OH ··· N bonds. To establish these the ultra-violet spectra of ethanolamine and hexamethylene tetramine in water, methanol, ether and chloroform solvents were studied and are shown in Fig. 8. The methanol solution of ethanolamine proved to be of type *A* and the others of type *B*. The predicted and observed values for NH ··· N and OH ··· N absorptions are given in Table III. Also included is a suggested assignment for CH ··· N absorption with association between the solute and chloroform.

The data indicate that in methanol solutions ethanolamine is intra-associated through NH ··· N bridges. This would result if polymers are formed between monomers at right-angles to each other. Probably the 37,000 cm.$^{-1}$ absorption results from the transition ν_{00}(OH) + (H ··· N). In water solutions the hydroxyl groups appear to be associated through the solvent. OH ··· N association in hexamethylene tetramine through the solvent appears as a type *B* spectrum in water solution, with a predicted association frequency of 41,200 cm.$^{-1}$.

TABLE III.—ABSORPTION ONSETS IN ETHANOLAMINE

Bond	Solvent	$\mu^{-\frac{1}{2}}$	ν_{00} cm.$^{-1}$	ν_v(H ··· N) cm.$^{-1}$	$\nu_{00} + \nu$(H ··· Y)		$\nu_{00} + \nu$(XH ··· Y)	
					Calc. cm.$^{-1}$	Obs. cm.$^{-1}$	Calc. cm.$^{-1}$	Obs. cm.$^{-1}$
NH ··· N	CH_3OH	0·183ν	29800	3740	33500	33800	37280	37000
OH ··· N	CH_3OH	0·218ν' ν	32400	4500	36900	37000	41500	—
OH ··· O	H_2O	0·159ν	32400	9250	41650	41000	50900	—
CH ··· N	$CHCl_3$	0·151ν	31800	4360	35860	—	?	38000

Note.—*a, b, c* are the types defined in Table I. ν_v (H ··· N) was calculated from eqn. (7).

If the CH ··· N assignment for the absorption in ethanolamine is tenable, other absorptions in chloroform may lie between the solvent and the solute. To test this assumption a frequency against reduced mass graph has been plotted for the onsets of ethanolamine, hexamethylene tetramine and butyramide in $CHCl_3$. Since the ordinate, line (2), Fig. 15, is approximately 31,800 cm.$^{-1}$, the $2\pi \rightarrow 2\Sigma$ CH transition,[39] it is believed that the CH ··· N association exists. If in ether the solvent forms CH ··· N bridges between two hexamethylene molecules, the onset at 36,200 cm.$^{-1}$ is predicted for CH ··· N.

CH ··· O absorption must be very strong in the alcohols. If values of (H ··· N) and (H ··· O) are calculated from eqn. (4) and (7) for specific values of $\mu^{-\frac{1}{2}}$ and their difference added to the slope of the CH ··· N line in Fig. 15, a predicted CH ··· O line, (3), with electronic origin at 31,800 cm.$^{-1}$ is obtained. When this is correlated with the reduced masses of the alcohols studied it is obvious that some of the absorption onsets near 40,000 cm.$^{-1}$ must have CH ··· O onsets. Similar absorption with electronic centres at 23,170 and 25,710 cm.$^{-1}$ would give rise to the common absorption onsets in the alcohols near 31,000 cm.$^{-1}$ identified in spectra of butyl, amyl, hexyl and octyl alcohols, as recorded in the line of Fig. 15. These absorptions frequently disappear in dilute solutions.

---

[37] Herzberg, *Spectra of Diatomic Molecules* (D. Van Nostrand Co. Inc., New York, 2nd edn., 1950), p. 560.

[38] Gordy, *J. Amer. Chem. Soc.*, 1938, **60**, 605.

[39] Gero, *Z. Physik*, 1941, **118**, 27.

APPLICATION TO PROTEIN SPECTRA. The preceding results are applied in the analysis of the spectra of two proteins, with emphasis on the characteristic protein band at 280 mμ and on the continuum which appears near 240 mμ, the region of excited state NH···O and OH···O continua. Previous studies[10] established that the 280 mμ absorption is not entirely the resultant of tryptophane and tyrosine excitations, for it appears in gelatin which lacks these acids. In the previous study this was ascribed to the protein skeleton, in particular to the peptide linkage, but since this band does not appear in linear amides, it must have an origin other than the peptide.

In this application the spectra of zein and gelatin are compared, selected because of the differences in their amino acid constituents.[41] Zein is poor in basic arginine, histidine and lysine, but rich in glutamic acid and leucine. Gelatin is rich in these basic constituents, which through participation in inter-associations between the protein units of the large molecule render the dimer (*A*) type of NH···O continua. These will not appear in the zein spectrum, except for a weak arginine component. If the protein skeleton is a polypeptide, the polymer (*B*) type of NH···O continua should be recognized with onsets in the 37,500-42,000 cm.$^{-1}$ region.

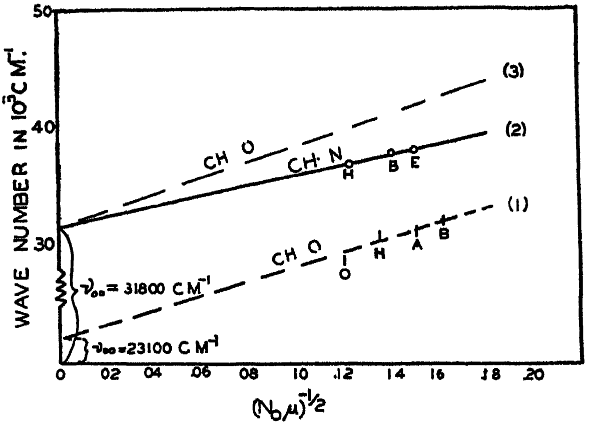

FIG. 15.—Line (1): B—butyl; A—amyl; H—hexyl; O—octyl alcohols. Line (2): E—ethanolamine; B—butyramide; H—hexamethylene tetramine.

The high percentage of glutamic acid and other acid residues in zein, must produce OH···O continua of the dimer type, resulting from inter-associations. Also, if the protein skeleton is similar to the Wrinch cyclol pattern,[42] strong OH···O or OH$^+$···O continua of the trimer type should be recognized.

Spectra of zein at various concentrations are reproduced in Fig. 16. Successive dilutions were studied until changes in spectral type indicated the loss of inter-associations, permitting the spectrum to register more

---

[40] Anslow and Nassar, *J. Opt. Chem. Soc.*, 1938, **60**, 605.

[41] Cohn and Edsall, *Proteins, Amino Acids and Peptides* (Reinhold Publishing Corp., New York, 1943), p. 258.

[42] Wrinch, *Proc. Roy. Soc. A*, 1937, **160**, 59; *Trans. Faraday Soc.*, 1937, **33**, 1368; *Phil. Mag.*, 1941, **31**, 177 and other papers.

clearly the associations of the fabric itself. To determine the specific origins, keys have been added in light lines on the diagram, to indicate predicted onset frequencies, the solid lines representing the more abundant residues which may be active in the particular absorption. These frequencies are calculated for various pairs of the amino acid residues involved.

At the 0·1 % concentration very little difference appears between the 80 % and 95 % alcohol solutions. In both a sharp onset near 34,200 cm.$^{-1}$ is specific. But at 0·03 % concentration spectral changes are registered. The 80 % alcohol solution is transparent to 34,500 cm.$^{-1}$ CH···O associations must have been ruptured through dilution. The spectrum of the 95 % solution indicates the rupture of CH···N bands, with CH···O (ν_{00} = 21,300 cm.$^{-1}$) absorption setting in after 30,000 cm.$^{-1}$.

Particularly striking is the well in the lower concentration spectra between 36,000 and 41,000 cm.$^{-1}$, beyond which the CH···O (ν_{00} = 31,800 cm.$^{-1}$) continua are initiated. It is clearly the effect of broken inter-associations between the protein units of the synthesized molecule, consequent to dilution. A spectrum taken of the same sample, with a dry ice blanket around the cell container, yielded spectrum (3) which shows the inter-associations unbroken. In a search for its source a very dilute, 0·003 % concentration, 95 % solution, probably undergoing denaturation. was run through and proved to be unstable at 34,200 and 36,800 cm.$^{-1}$, the polymer and monomer ground level dissociation onsets. Thus, the origin of the absent absorption seems to be the D_1 polymer band, resulting either from direct inter-association between acid residues or more probably from the bound water. In the absence of this band the tyrosine and phenyl alanine electronic band structures appear.

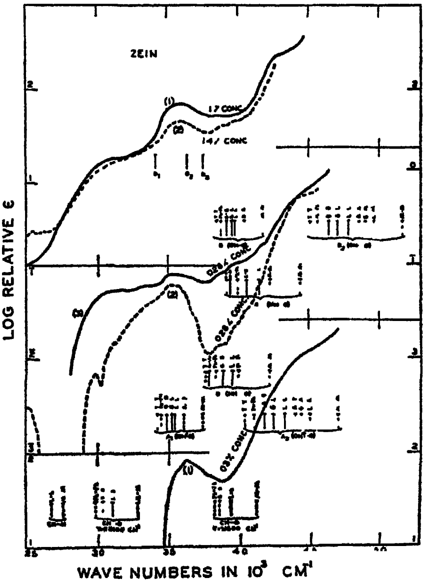

FIG. 16.—(1) Spectra of 80 % EtOH–H_2O solutions.

(2) and (3) spectra of 95 % EtOH–H_2O solutions.

In the zein spectrum no polymer (B) type of NH···O excitation can be located, but the correlation for the A_2 (OH^+···O) origin is surprising. This implies a fabric with ionic OH trimers as a principal building block. The B_2 (OH···O), absorption seems to start near 45,000 cm.$^{-1}$.

Finally, the gelatin results appear in Fig. 17. Considerable A type NH···O absorption seated in the basic residue appears to level out the 38,000 cm.$^{-1}$ region. In alkaline solutions both the specific absorption and the continuum are shifted more than 2000 cm.$^{-1}$. Such a large shift is not characteristic of NH···O absorption, but is typical of CH···N continua in carboxylic acids.[43] Also recorded are the effects of dilution and irradiation, both of which weaken CH···N associations and lead to the ν_{00}(CH) structure in this protein spectrum.

---

[43] Anslow, Foster and Klingler, *J. Biol. Chem.*, 1933, **103**, 81-92.

Summary.—Comparative studies of the ultra-violet spectra of hydrogen-bridged amides and alcohols appear to have established the existence of:

(*a*) NH···O, OH···O and OH⁺···O electronic excitation continua with vibrational dissociation in the upper state, their locations and character being distinctive of the polymer type. Equations for the frequency of onset, i.e. approximate of corresponding dissociation energies, have been established. Some absorptions appear to indicate bridge rupture, but the strongest absorption results from dissociation of the bond as well.

(*b*) OH···N, NH···N, CH···N and CH···O absorptions have been recognized.

(*c*) Ground state dissociation of alcohols and of bound water in amides has been identified. The monomer, dimer, and polymer components are discussed.

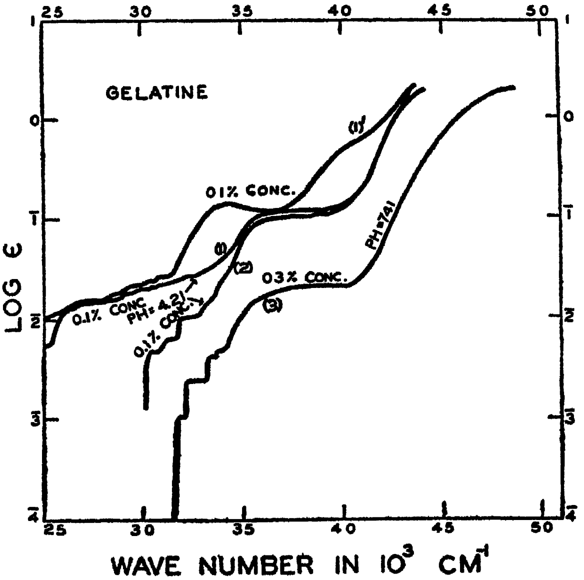

FIG. 17.—(1) Solution near isoelectric point.
(2) Same solution irradiated 3 hours with 280 mμ source;
(1)′ Solution in 0·1 N NaOH.
(3) Effect of dilution.

(*d*) These absorptions have been identified in the protein spectra, The 280 mμ absorption may be ground level disociation of the OH···O. polymer. The strongest component of the 240 mμ continuum appears to be an OH⁺···O excited state dissociation. CH···N and CH···O components of the general absorptions appear.

The author acknowledges with deep appreciation the considerable contributions made to these studies by Hsi-teh Hsieh and Ruth C. Shea, and the assistance of Joan Mencher Frosch, Ann Fairley Schabas and Helen Hagelbarger. The investigations were supported by the Office of Naval Research, U.S. Navy, and the Research Corporation.

Department of Physics,
Smith College,
Northampton, Massachusetts, U.S.A.

GENERAL DISCUSSION

Dr. P. Torkington (*B. Rayon Res. Assoc.*) (*communicated*): It seems to be implied in the paper of Thompson, Nicholson and Short that the evidence for the O—H bending frequency having a value in the range 1000 to 1200 cm.$^{-1}$ comes from the observation that substitution in the sugars leads to the disappearance of bands in this region and the appearance of new ones. Surely in the system C—O—R, (R = alkyl (or any other substituent, even deuterium according to Dr. Shull)), the interactions between C—O and O—R stretching would lead to a fundamentally different type of absorption than in C—OH. The bands which disappear when sugars are substituted would be thought to be C—O stretching modes. Comparison of the spectra of the allyl halides with allyl alcohol (which spectra were studied by Dr. Thompson and myself some years ago), suggests that δ_{OH} here had a frequency of 1300 or 1340 cm.$^{-1}$.

The bands in diglycine mentioned as being anomalous seem most likely to be due to perturbed C═O stretching and N—H bending, in the cyclic structure, stabilized by hydrogen bonding, which would seem the most probable configuration. (Diglycine would presumably precede diketopiperazine; the latter is formed along with polyglycine when glycine is heated in a sealed tube. This confirms the cyclic structure for diglycine).

Prof. G. B. B. M. Sutherland (*Michigan*) said: In connection with the spectra of the amino acids reported by Thompson, Nicholson and Short, Dr. S. E. Darmon and myself have a large collection of spectra of amino acids obtained at Cambridge during the past few years which we hope to publish in the near future. It is clear from these spectra that not only are the various amino acids easily distinguishable from one another spectroscopically but that in the solid state, the infra-red spectrum of either of the optically active forms (D or L) differs from that of the racemate (DL), a fact first noticed for cystine by Wright.[1] This distinction is most important if infra-red methods are being used for the analysis of mixtures of amino acids, e.g. in the estimation of the ratio of leucine to *iso*leucine in protein hydrolysates.[2]

In connection with the spectra of the sugars, I might mention Dr. D. A. Ramsay and I have a collection of such spectra which will be published shortly with a discussion of their interpretation. The reason for mentioning them now is that we have some indication that it may be possible from infra-red observations to say whether a glucoside is in the D or L configuration. The D and L forms give distinctly different spectra in all cases but for the glucosides the D forms contain certain bands which are consistently absent from the L forms. It would be interesting to know whether any other workers with the sugars have found evidence of a similar empirical correlation.

Dr. H. Lenormant (*Paris*) (*communicated*): In the papers of Thompson, Nicholson and Short, on the one hand, and Sutherland on the other hand, an interpretation of the 1560 cm.$^{-1}$ band is given, which requires some comments. This interpretation in which this band is identified with a δ(N—H) is based on various arguments of unequal value; this we have discussed in a previous paper.[3] The most important of these is the behaviour of this bond when the spectrum is obtained with polarized infra-red radiations.

There are, however, important objections to this interpretation:

(i) δ(N—H) is usually very weak in secondary amines and so are $\delta(N—H_2)$ or $\delta(N—H_2)^+$, while the 1560 cm.$^{-1}$ bond of monosubstituted amides is generally strong.

---

[1] Wright, *J. Biol. Chem.*, 1937, **120**, 641.
[2] Darmon, Sutherland and Tristam, *Biochem. J.*, 1948, **42**, 508.
[3] Lenormant, *Thesis* (1949).

(ii) If the band observed is really δ(N—H), it is abnormal in that this bond is missing in cyclopeptides and lactames.[4]

(iii) The vibration at the origin of the 1560 cm.$^{-1}$ absorption is inactive in the Raman spectrum, but there is no reason to suppose that this is the case for a δ(N—H) vibration.

(iv) The deuteration of monosubstituted NH grouping effects a relatively weak frequency variation (1560 cm.$^{-1}$ to 1480 cm.$^{-1}$) whereas one could reasonably expect a much lower frequency (about 1190 cm.$^{-1}$) if δ(N—D) is concerned.

In fact, the problem seems to be very complex, the study of a great number of amides, peptides and polyamides, showing that the intensity ratio of 1560 cm.$^{-1}$ and 1650 cm.$^{-1}$ bands is variable. For instance for *N*-ethyl benzamide, the 1560 cm.$^{-1}$ band has a high intensity while the 1650 cm.$^{-1}$ band is weak. It is possible to vary the relative intensity of these bands: alkalinity increases the 1650 band and this is particularly evident with cyclopeptides. Under usual conditions these compounds do not show bands in that region but after being placed in N/10 NaOH a strong absorption appears at about 1560 cm.$^{-1}$. Simultaneously the normal band is much reduced in intensity. A similar phenomenon is seen with bivalent metals.[4, 5] We have suggested that the 1560 cm.$^{-1}$ band is due to a second molecular form. A first form would be responsible for the 1650 cm.$^{-1}$ band, the second one being very likely in a much more accentuated mesomeric state. The 1560 cm.$^{-1}$ frequency is possibly due to a vibration affecting all angular groupings of the type $\widehat{OCN}$. The assumption of two forms is in agreement with the existence of two bonds in the 3300 cm.$^{-1}$ region, a fact which has been pointed out by many authors.

Prof. G. B. B. M. Sutherland (*Michigan*) said: The paper of Cross, Richards and Willis is of considerable interest in connection with the assignment of the internal CH$_3$ deformation frequencies in hydrocarbons since it contains independent evidence through careful quantitative work that there is a CH$_3$ deformation frequency at 890 cm.$^{-1}$. I should like to ask the authors whether they had any evidence other than that mentioned in their paper for that assignment.

Secondly, their observation that whenever an OH stretching frequency was picked up, this was always in a position which indicated that the OH group was hydrogen bonded reminds me of a similar (unpublished) observation made by Dr. A. J. Harding and myself in the infra-red spectra of oxidized rubber. This must mean that the oxygen molecule is incorporated into the hydrocarbon chain in each case in such a way that a hydrogen bond is formed between each of the two oxygen atoms. I should be interested to know whether they have any views on the configuration giving rise to this internal hydrogen bond.

Dr. G. J. Minkoff (*Imperial College, London*) said: Cross, Richards and Willis report that they were unable to observe any intense lines characteristic of the peroxide groups in those peroxides whose absorption spectra they have studied; we have received similar information from some other workers. We think it may therefore be of interest to consider the results being obtained in a study of the infra-red absorption of organic peroxides now in progress at Imperial College (during the course of our studies of combustion). So far, we have been concerned with the following molecules: CH_3O_2H, $C_2H_5O_2H$, *tert.*-BuO$_2$H ; $(C_2H_5)_2O_2$, *tert.*-Bu$_2$O$_2$;
$CH_3CO \,.\, O_2H$, $C_2H_5CO \,.\, O_2H$, $C_3H_7CO \,.\, O_2H$; $(CH_3CO\,.)_2O_2$,
$(C_{11}H_{23}CO\,.)_2O_2$; $C_2H_4(OH)O_2H$, $(C_2H_4(OH))_2O_2$, $(CH_2(OH))_2O_2$;
several more remain to be prepared. In general, a line of weak to moderate intensity has been observed at 830-890 cm.$^{-1}$. Now, it is known with

---

[4] Lenormant, *Bull. Soc. Chim.*, 1948, **15**, 33.

[5] Lenormant and Chouteau, *J. Physiologie*, 1949, **41**, 203A

certainty[6] that in the infra-red and Raman spectra of H_2O_2 and D_2O_2, a weak line at 877 cm.$^{-1}$ is characteristic of the O—O stretching frequency. Nevertheless, we cannot proceed immediately to ascribe the 830-890 cm.$^{-1}$ lines of the organic peroxides to this vibration, since a number of lines exist in this region of the spectra of several molecules. For example, Cross, Richards and Willis[7] show that at 880-890 cm.$^{-1}$ there appear frequencies associated both with $CH_3\cdot$ and with unsaturation in polythenes. It has also been shown[8] that the line at *ca.* 840 cm.$^{-1}$ is a C—H out-of-plane frequency. Sheppard, too, reports[9] that lines characteristic of the wagging CH_3 appear at 880 cm.$^{-1}$ in *iso*propyl halides and mercaptan, and at 810 cm.$^{-1}$ in the corresponding *tert.*-butyl compounds. We have attempted to support our tentative assignment by comparing the spectra of the molecules R . OO . R′ with those of the corresponding molecules R . O . R′; however, this method is not entirely sound, as is shown, for example, by the observation[10] that in *tert.*-Bu_2O_2, Sheppard's line at 810 cm.$^{-1}$ disappears, and the nearest lines are now at *ca.* 750 and 880 cm.$^{-1}$. A better method is probably to compare the spectra of R . OO . R′ with those of R . SS . R′, employing the data of Thompson[11] and of Sheppard;[12] so far, this has been done only with the diethyl compounds, with results apparently supporting our assignment.

To sum up, we would (provisionally) suggest that the O—O group has a characteristic frequency in the region 830-890 cm.$^{-1}$; that it is not strong; and that in large molecules, it may be hidden by, or confused with, several skeletal frequencies of comparable intensities. Furthermore, we should stress that owing to the great difficulties, first of purifying the peroxides, and then of keeping them from decomposing to some extent, little reliance can be placed, in general, on the spectra of the smaller peroxides unless these have been freshly prepared and purified.

Mr. H. A. Willis (*Welwyn*) said: In reply to Dr. Sutherland, our assignment of the absorption band at approximately 890 cm.$^{-1}$ in the infra-red spectra of hydrocarbons and polythene to the methyl group is based on intensity measurements. In Fig. 1 of our paper we have plotted the extinction coefficient of this absorption band, as measured on a series of pure hydrocarbons, against methyl group content and it is seen that the relationship is approximately linear, as is the case with the 1378 cm.$^{-1}$ absorption band.

In reply to Dr. Sutherland's second question, concerning the presence of associated hydroxyl groups in oxidized polythene, we would suggest that this is due to the fact that the carbon atom adjacent to a carbonyl group may be a centre of attack by oxygen, with the result that hydroxyl groups would be formed adjacent to carbonyl groups:

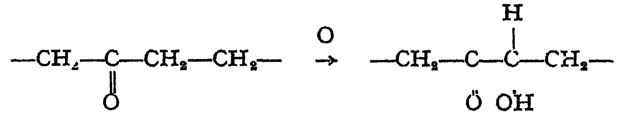

$$—CH_2—\underset{\underset{O}{\|}}{C}—CH_2—CH_2— \xrightarrow{O} —CH_2—\underset{\underset{O}{\|}}{C}—\overset{\overset{H}{|}}{\underset{OH}{C}}—CH_2—$$

The hydroxyl groups, although in very small concentration, would thus always be associated with adjacent carbonyl groups.

---

[6] Taylor, *J. Chem. Physics*, 1950, **18**, 898. Giguere, *J. Chem. Physics*, 1950, **18**, 88. Bailey and Gordon, *Trans. Faraday Soc.*, 1938, **34**, 1133. Simon and Feher, *Z. Elektrochem.*, 1935, **41**, 291.

[7] Cross, Richards and Willis, this Discussion. Williams and Dale, *J. Appl. Physics*, 1944, **15**, 585.

[8] Williams, *Rev. Sci. Instr.*, 1948, **19**, 143. Sheppard and Sutherland, *Proc. Roy. Soc. A*, 1949, **196**, 195.

[9] Sheppard, *Trans. Faraday Soc.*, 1950, **46**, 527, 533.

[10] Raley, Rust and Vaughan, *J. Amer. Chem. Soc.*, 1948, **70**, 1337. Ahles (private communication).

[11] Trotter and Thompson, *J. Chem. Soc.*, 1946, 481.

[12] Sheppard, *Trans. Faraday Soc.*, 1950, **46**, 429.

In reply to Dr. Minkoff's remarks on a characteristic frequency between 800 and 900 cm.$^{-1}$ for the peroxide or hydroperoxide group we have never detected an additional absorption band in this region in oxidized polythene. It would be interesting if Dr. Minkoff could give us an approximate value for the molar extinction coefficient for the band due to the peroxide group, which would give us some indication of the minimum concentration of peroxide which could be detected.

Dr. N. Sheppard (*Cambridge*) said: The question raised by Cross, Richards and Willis with reference to the possibility of detecting peroxide and hydroperoxide groups by infra-red spectroscopic methods is one of great practical importance. Many applications could be made in oxidation studies of any correlations that proved to be of use for identifying these groups. From the theoretical point of view, however, it seems unlikely that such correlations will be easy to find at least for the disubstituted peroxides of the type R—O—O—R′ where R and R′ are hydrocarbon groupings. For example, the relatively symmetrical surroundings of the O—O linkage are such that the vibration of the O—O linkage itself will not be associated with a very great change in dipole moment and accordingly the corresponding frequency will be expected to be weak in the infra-red. Furthermore, since the oxygen atoms are of similar masses to the neighbouring skeletal carbon atoms, and since the O—O linkage probably has a force constant of similar magnitude to those of the neighbouring C—O and C—C linkages, it would not be expected that the O—O linkage would have a very characteristic frequency. Instead, the vibrations of this bond will contribute one more to the several skeletal frequencies of the molecule, which are very sensitive to the overall structure.

The example of the hydroperoxide group is to some extent a different case as the O—O linkage has in this case a more unsymmetrical substitution pattern and also the 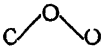 $C\overset{O}{\wedge}O$ group is an end group of the molecule. The fact that the O—O stretching vibration will contribute to the skeletal modes of the overall molecule will once again make any " characteristic " frequency somewhat variable in position. However, if as has been done for the alcohols,[13] separate correlations are made for a sufficient number of different types of hydrocarbon substituents of the O—O linkage (primary, secondary, tertiary alkyl groups, aromatic groups, etc.) it might be possible to draw up working correlation rules, although this will involve the investigation of the spectra of a wide range of pure compounds. In connection with this expectation and the results reported by Dr. Minkoff in this discussion it is of interest to note that Whitcomb, Moorhead, and Sharp[14] of the Kansas State College have also investigated the spectra of a limited number of pure hydroperoxides and find a consistent absorption band between 11·5 and 12·1 μ. The same authors also found frequencies characteristic of the OH linkage in hydroperoxides near 2·95 and 7·3 μ, but since alcohols and other hydroxy compounds have absorption bands near these positions[15] they are likely to be of less use for the identification of the OOH group. It should be noted, however, in agreement with the comments by Cross, Richards and Willis, that the extinction coefficients of the *ca.* 12 μ absorption bands are considerably less than those found with skeletal O—H and C=O stretching modes, and the degree of usefulness of the correlation for the investigation of oxidation studies will be correspondingly less.

Dr. J. G. Reynolds (*Thornton Res., Chester*) said: M. Cross's determination of unsaturation is interesting to people like myself who are engaged on similar analyses. Using a Grubb Parsons S3 instrument, my molar extinction coefficients are 150 for $RCH{=}CH_2$ at 908 cm.$^{-1}$, 130 for *trans* $RCH{=}CHR'$ at 964 cm.$^{-1}$ and 168 for $RR'C{=}CH_2$ at 888 cm.$^{-1}$. The calibration standards used are *n*-octene, *n*-decene, *n*-dodecene, and *n*-pentadecene for analyses in the C_8—C_{18} range. These figures are considerably higher than the author's which move me to ask:

---

[13] Lecomte, in *Traité de Chimie Organique* by Grignard and Baud (Masson, Paris, 1936, 2, 143).

[14] S. E. Whitcomb, A. D. Moorhead and D. B. Sharp, data presented at the *Symposium on Molecular Structure and Spectroscopy* (Ohio State University, U.S.A.), June 1950.

[15] Sutherland, this Discussion.

(*a*) Were the coefficients quoted obtained by the author on high molecular weight olefins or are they those of Anderson and Seyfried ?

(*b*) If the former, what calibration standards were used ?

(*c*) If the latter, is he justified in using such coefficients for high molecular weight olefin samples ?

Another point which I should like Mr. Cross to clear up is whether he considered the possibility of the bands at 1720 cm.$^{-1}$ being due to esters, especially as the presence of carboxylic acids has been considered and there is no evidence for free hydroxyl groups. Inspection of some ester and ketone spectra[16] does not show any characteristic bands by which esters and ketones might be easily differentiated.

Mr. L. N. Cross (*I.C.I. Alkali Div., Nantwich*) (*communicated*): In reply to Dr. Reynolds our paper admits that the molar extinction coefficients, based on the work of Anderson and Seyfried, may not be valid for high molecular weight materials, particularly when these are solid, and we have emphasized in the work on methyl group concentration that molar coefficients are not necessarily transferable from instrument to instrument. However, we obtained an apparent correspondence between total unsaturation as measured chemically and by infra-red for a wide range of polymers in which the relative proportions of the different types of double bonds varied considerably. We appreciated that this agreement might be somewhat fortuitous and indicated in the paper the possibility that some $RR' = CR''R'''$ groups might also be present.

The possibility that 1720 cm.$^{-1}$ band arises from esters has been considered. Unfortunately no C—O absorptions are found and these might be expected to be strong if esters are present.

Dr. D. C. McKean (*Oxford*) (*communicated*) : In connection with the oxidation discovered in samples of polyethylene by Cross, Richards and Willis, I should like to mention that a recent infra-red study of the series of nine *n*-octadecynes, seems to reveal the occurrence of two types of oxidation product. One may be an α-acetylenic ketone and the other an α-diketone, monoketone or aldehyde, or a mixture of these.

In certain of the samples supplied, strong absorption bands were found at 1720 cm.$^{-1}$ and 1680 cm.$^{-1}$, the latter being usually but not always stronger than the former. Associated with these two bands there were two weaker ones near 3440 cm.$^{-1}$ and 1170 cm.$^{-1}$. The intensities of the bands at 3440, 1170 cm.$^{-1}$ usually ran parallel to that of the band at 1680 cm.$^{-1}$ but not to that at 1720 cm.$^{-1}$.

Another feature of the spectra was the appearance in those compounds with the $C{\equiv}C$ band in the 3, 4, 5, 6, 7 and 8 positions of a moderately strong band near 2223 cm.$^{-1}$, the intensity of which was paralleled by that of the band at 1680 cm.$^{-1}$, but not by that of the band at 1720 cm.$^{-1}$ The band near 2223 cm.$^{-1}$ could only have been due to a $C{\equiv}C$ stretching vibration. However, a strong band in this region was not found in the repurified, unoxidized samples, except with 1-octadecyne. Presumably this arises because it is only with 1-octadecyne that the $C{\equiv}C$ group is sufficiently unsymmetrical ($HC{\equiv}C\,.\,R$) to give rise to a significant change of dipole moment during stretching. Thus the origin of the band at 2223 cm.$^{-1}$ in the oxidized samples must have been due to some acetylenic chain in which the $C{\equiv}C$ lies in an unsymmetrical environment, such as

---

[16] *J. Chem. Soc.*, 1945, 640.

R—C≡C—CO—R′. Conjugation of this kind would lead to the lowering of the carbonyl group frequency observed near 1680 cm.$^{-1}$.

This conclusion is confirmed by Raman data on 6-dodecyne, with which Murray and Cleveland[17] isolated an oxidation product and identified it as 6-dodecyne-5-one. The latter has an intense Raman displacement at about 1680 cm.$^{-1}$.

The band at 1720 cm.$^{-1}$ mentioned above can be ascribed to an aldehyde, ketone or α-diketone, for no conjugation occurs between contiguous carbonyl groups. It is therefore impossible to decide whether the oxidation sequence usually suggested for acetylenes is occurring, namely :

R—C≡C—R′ → (peroxides) → R . CO . CO . R′ → aldehydes, acids.

The peroxide first formed can react to form an α-diketone, or by interaction with a molecule of octadecyne to form an acetylenic ketone. In the latter case, the alcohol R . C≡C—CH(OH)R′ might be an intermediate, and in that case the bands seen near 1170 cm.$^{-1}$ and 3440 cm.$^{-1}$ might be interpreted as being due respectively to bending and stretching vibrations of the hydroxyl group. The alternative is to ascribe them to the presence of a carboxylic acid.

Prof. G. B. B. M. Sutherland (*Michigan*) said: I should like to ask Dr. Elliott and Dr. Ambrose in connection with their statement that "there are no N—H groups in the polymer which cannot be satisfied by hydrogen bonding within the molecule" what the essential evidence is, since some of it is unpublished. If this evidence comes solely from work in solution it would seem rather dangerous to draw conclusions about hydrogen bonding in the solid state from observations on spectra with the polymer in the liquid state.

Dr. A. Elliott and **Mr. E. J. Ambrose** (*Maidenhead*) (*communicated*): In reply to Prof. Sutherland, we have measured the infra-red spectrum of a dilute solution in chloroform of poly-γ-benzyl-L-glutamate, the synthetic polypeptide described in our paper which shows the unusual self-orienting properties. There is no indication of an absorption band at 3450 cm.$^{-1}$ which would correspond to unbonded N—H groups. But a solution of poly-carbo-benzoxy-*dl*-lysine, which has N—H and C═O groups both in the main chain and side chains, shows the unbonded N—H bond at 3450 cm.$^{-1}$ indicating that the polypeptide chains are effectively isolated from each other under the experimental conditions.[18] These results show that the synthetic polypeptide can exist quite stably in a form in which all the peptide N—H, C═O hydrogen bonds are satisfied within the chain while in solution. Although it would be possible that there was a change over into a different kind of fold when the solution was concentrated and a solid film of polymer prepared, the very high dichroic ratios obtained in these films appear to exclude any folded structure in which all the NH . . . OC hydrogen bonds do not lie almost parallel to the chain axis. Bamford, Hanby and Happey[19] have produced strong evidence that all the hydrogen bonds in the folded form are formed within the chain in the solid state by experiments on the solubility of films of the α and β forms of the copolymer of DL-phenylalanine and DL-leucine.

Dr. A. Elliott (*Courtaulds, Maidenhead*) said : The weak band appearing at about 3060 cm.$^{-1}$ in proteins, polypeptides, Nylons, etc., is probably another manifestation of multiple peaks which we have found in the spectra of simple substances containing an N—H . . . O═C hydrogen bond. For instance, a single crystal of diketopiperazine has no less than five peaks in the neighbourhood of the N—H stretching frequency. These peaks all show the same extremely high dichroism in polarized radiation, and we have no doubt that they are all N—H modes. Some kind of interaction between molecular modes and crystal lattice modes seems to be indicated here, and this may also be the explanation of the broad O—H band in, for instance, crystals of carboxylic acids. The weak N—H band in polypeptides shows a considerable amount of structure, which is different in extended and in folded forms of the same polypeptide, and this strongly suggests a common origin for the phenomena referred to above.

---

[17] *J. Amer. Chem. Soc.*, 1941, **63**, 1363.

[18] Elliott and Ambrose, *Nature*, 1950, **165**, 921.

[19] *Nature*, 1950, **166**, 829.

Dr. Mansel Davies (*Aberystwyth*) said: Relevant to the discussion of interactions in polyamides and related structures are some results recently obtained at Aberystwyth by Mr. H. E. Hallam. Very briefly, studies of acetamide in $CHCl_3$ show it to associate principally (though not quite exclusively) in a monomer ⇌ trimer equilibrium :

$$\Delta H = - 3{\cdot}3 \text{ kcal./mole trimer.}$$

This conforms to indications from the crystal structure,[20] and qualitative evidence for the liquid showing n to be about 3·0. In acetone at the boiling point, however, the results conform to a monomer ⇌ dimer equilibrium. Perhaps the immediate significance of these results is that it is dangerous to discuss amide interactions by analogy with the carboxylic acids, as there are qualitative as well as quantitative differences between them. For acetic acid in $CHCl_3$ the hydrogen bond energy is at least twice that in the amide. The smaller value in the latter may be important for its reversible rupture in systems of biological interest.

Spectroscopically, acetamide shows (mostly in $CHCl_3$) monomer ν(N—H) frequencies at 3538 and 3420 cm.$^{-1}$, the associated molecules providing absorptions centred at 3510, 3350, 3185 cm.$^{-1}$. The carbonyl absorption ($\sim$ 1700 cm.$^{-1}$) is clearly resolved into monomeric and associated components separated by about 20 cm.$^{-1}$ (depending on the solvent), the individual peaks showing the expected changes with concentration and temperature. The band at 1600 cm.$^{-1}$ $\left(\delta\mathrm{N}\begin{matrix}\diagup\mathrm{H}\\ \diagdown\mathrm{H}\end{matrix}\right)$ certainly arises from the associated molecules. There is little change in 1380 cm.$^{-1}$ (νC—N), and 1120 cm.$^{-1}$ (δC—N(?)) : the other features observed, including the broad band at 700 cm.$^{-1}$, will be discussed in a fuller account.

Dr. S. E. Darmon (*Leeds University*) said : It is evident from the spectra of cyclic and non-cyclic amides which Prof. Sutherland and I have examined that there are more than one absorption maximum near 3μ associated with the hydrogen-bonded NH stretching frequency. Non-cyclic amides have a main peak near 3280 cm.$^{-1}$ and cyclic amides near 3175 cm.$^{-1}$. In both types there is usually a weaker band near 3060 cm.$^{-1}$, the relative intensity of which is very variable. Whilst it is fairly certain that the 3175 cm.$^{-1}$ and 3280 cm.$^{-1}$ bands are to be associated with the *cis* and *trans* forms respectively of the hydrogen-bonded NH group in CONH, our previous interpretations [21, 22] of the 3060 cm.$^{-1}$ band are open to considerable doubt. In the more recent publication [22] we assigned the band to NH bonds in the *cis* configuration only, but later work, at Leeds and Michigan and by Ambrose and his co-workers,[23] has indicated that other factors are operative. I cannot suggest a precise interpretation of the 3060 cm.$^{-1}$ band but would agree with Prof. Sutherland (later paper in this section) that it may conceivably arise from some kind of interaction effect. With regard to Dr. Thomspon's remark about the narrowness of this band, we find that although in some spectra the 3060 cm.$^{-1}$ band is quite narrow, this is by no means always the case.

Dr. P. Holliday (*Courtaulds Ltd., Coventry*) said : A film of Nylon 66 about 5 microns in thickness has been heated in a cell of the Richards

[20] Senti and Harker, *J. Amer. Chem. Soc.*, 1940, **62**, 2008.

[21] Astbury, Dalgliesh, Darmon and Sutherland, *Nature*, 1948, **162**, 596.

[22] Darmon and Sutherland, *ibid.*, 1949, **164**, 440.

[23] Elliott and Ambrose, *ibid*, 1950, **165**, 921.

and Thompson type [24] and its absorption spectrum in the 2-5 μ region measured at intervals of about 50° up to 312° C. Fig. 1 shows the changes in absorption intensity for the CH_2 stretching bands, the " 3300 " $cm.^{-1}$ bonded NH band and the 3050 $cm.^{-1}$ band of doubtful assignment. The 3300 $cm.^{-1}$ band undergoes a frequency shift at the same time which roughly parallels the fall in its intensity, as shown in Fig. 2. From the diagrams it is evident that the changes in intensity and frequency of the 3300 $cm.^{-1}$ band are gradual at first, becoming more marked as the temperature rises, although no break is observed as the melting point of Nylon (255° C) is exceeded. These changes can be simply explained on the basis of thermal agitation giving increased hydrogen bond distances, a hypothesis confirmed by an observation of the 1540 $cm.^{-1}$ NH deformation and 1640 $cm.^{-1}$ C=O stretching modes, which simultaneously increase their separation by 25-35 $cm.^{-1}$. The 3050 $cm.^{-1}$ band behaves differently, however, in that it undergoes no frequency shift and its intensity falls rapidly in a linear fashion until it finally disappears at about 312° C. These results indicate that the 3050 $cm.^{-1}$ band cannot be due to any ordinary bonded NH vibration, since, having a lower frequency than the 3300 $cm.^{-1}$ band, the bonding would presumably be stronger and less easily broken up, whereas in fact the 3050 $cm.^{-1}$ band is the first to weaken. The band reappears when the specimen is cooled.

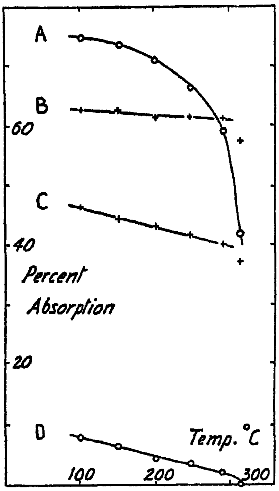

FIG. 1—Effect of temperature on the intensity of Nylon 66 bands in the 2-5 μ region.

A. " 3300 " $cm.^{-1}$ bonded NH band;
B. 2935 $cm.^{-1}$ antisymmetrical CH_2 band;
C. 2865 $cm.^{-1}$ symmetrical CH_2 band;
D. 3050 cm^{-1} band.

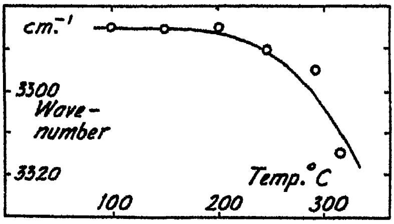

FIG. 2.—Effect of temperature on the frequency of the " 3300 " $cm.^{-1}$ band of Nylon 66.

A grid of filaments [25] of Nylon 6 has been examined with a selenium transmission polarizer.[26] Both the 3300 $cm.^{-1}$ and 3050 $cm.^{-1}$ bands are of the perpendicular type, but it appears that the dichroic ratio of the latter is the greater. This implies that the vibrations giving rise to absorption at 3050 cm.$^{-1}$ must be better oriented than the ordinary bonded NH groups, and cannot therefore be vibrations of single molecules, but must be vibrations associated with regular aggregates of molecules in the form of crystallites which are highly oriented along the fibre axis.

---

[24] Richards and Thompson, *Trans. Faraday Soc.*, 1945, **41**, 183.
[25] Holliday, *Nature*, 1949, **163**, 602.
[26] Elliott and Ambrose, *J Opt. Soc Amer.*, 1948, **38**, 212.

It may be mentioned that the 3300 cm.$^{-1}$ band is not simple: all the polyamides we have measured have shown a weak shoulder at about 3200 cm.$^{-1}$. We have verified that this is not due to water by means of measurements using a dried cell and specimens mounted in a stream of hot dry nitrogen. The shoulder probably represents bonded NH groups in the amorphous region, where a closer approach of C=O and NH groups is possible for interlocking molecules.

Dr. H. W. Thompson (*Oxford*) said: In connection with work on polypeptides and polyamides, I should like to raise the question of the interpretation of the band found near 3050 cm.$^{-1}$. This band is usually weak, and since complete methylation of the NH groups removes it, must be due to a vibration of this group. It remains puzzling, since there is always a strong bonded NH band at higher frequencies, and I should like to hear the views of others present about this band.

Prof. R. Mecke (*Freiburg i. Br.*) said: Concerning the splitting of CH-stretching vibrations, which has been often observed, I should like to remark that this fact is difficult to explain. For instance, cyclohexane shows frequency splitting in its ground state as well as in its overtone bands. The splitting of the CH bands is especially large if the molecule contains (mainly) oxygen, e.g. ethers. The long-wave component vanishes almost completely if HCl or HBr is added to the solvent, perhaps by formation of an oxonium salt $(R_2OH)^+Cl^-$, while the other band remains unchanged in its frequency and intensity. Freyman [27] first observed these facts. Recently [28] we started to investigate this subject but as yet we have no reasonable explanation. The solution of this problem of this frequency splitting is an urgent one because the assignment of frequencies is made difficult by this splitting.

Dr. P. Torkington (*B. Rayon Res. Assoc.*) (*communicated*): It seems to me that the interpretation of hydrocarbon spectra will only be finally satisfactory when the methyl rocking frequencies can be identified with certainty; not enough is yet known about the effect of adjacent groups on these modes for this to be done. The relative difficulty in assigning them would appear to be related to their potential degeneracy—such terms as in-plane and out-of-plane methyl rocking must be very approximate where there is any degree of internal rotation of the methyl group. The actual form of a particular methyl rocking mode and its vibration frequency will presumably be mutually dependent, except in systems CH_3—X of symmetry C_{3v}, where all possible motions compounded of two mutually-perpendicular deformations have the same frequency. In dimethylacetylene, the methyl rocking frequencies are probably independent of the relative orientation of the two methyl groups, but the intensity must surely depend on this factor. We may conclude that both frequency and intensity in methyl bending modes are in general related to the orientation of the methyl group, and hence to adjacent groups causing steric hindrance. It would seem more likely that the above order was correct, rather than that steric hindrance led directly to increased frequencies due to repulsion forces; though if it is finally proved that van der Waals' forces do contribute to any extent to the bending force constants, then the possibility of a direct effect must be considered. In poly*iso*butene the lowest methyl rocking mode would appear to be at about 1160 cm.$^{-1}$; most recent evidence suggests that the strong band at about 1230 cm.$^{-1}$ is also due to some C—H bending mode, possibly methyl. This might suggest that restriction of rotation of a methyl group was associated with more difficulty in rocking.

---

[27] Freymann, *Ann. Physique*, 1933, **20**, 42; *Compt. rend.*, 1937, **205**, 859.

[28] *Z. physik. Chem.* (to be published).

[29] Zeininger (to be published). Lippert, *Diss.* (Freiburg, 1950).

Prof. R. Mecke (*Freiburg i. Br.*) said: I call attention to an early paper of mine in which I tried to assign the fundamental frequencies of normal hydrocarbon compounds using the same formulae (2). I found that these fundamentals lie on two different curves with the limiting frequency $\nu_0 = (1/2\pi)\sqrt{f/m} = 802$ and 824 cm.$^{-1}$ just if the compound contains an even or an odd number of carbon atoms giving rise to a "staggering" of the characteristic frequencies in the spectra of *n*-paraffins.

Dr. N. Sheppard and **Dr. Delia Simpson** (*Cambridge*) (*communicated*): In reply to Prof. Mecke we would like to say that we were aware of his earlier paper and regret that we omitted to include it in the list of references relevant to our formula (1). With regard to the experimental limiting Raman frequencies of 802 and 824 cm.$^{-1}$ for *n*-paraffins with an even and odd number of carbon atoms respectively we think that the more recent evidence from spectra in the solid state (ref. (5), (6) and (7) of our paper) shows clearly that these correspond to non-planar isomers. For the planar isomers, with which we are concerned, we find (*a*) no such frequency alternation for the lowest skeletal frequency and (*b*) that it is possible to calculate these frequencies with one value of f for both odd and even paraffins with six or more atoms.

Prof. R. Mecke (*Freiburg i. Br.*) (*communicated*): I agree with Prof. Sutherland in demanding more work on large molecules and the collection of the obtained results in a way most suitable for practical requirements. With respect to the latter, I refer to the figure of my paper, showing an absorption frequency diagram of a large number of third overtone CH stretching bands. Diagrams of that kind may be constructed for all kinds of bands. They make possible an interpretation of spectroscopical measurements on large molecules with respect to their constitution by comparison only.

Furthermore, from all diagrams that we have compiled till now, it is seen that intensity measurements are indispensable, or at least of great importance, for constitution determinations in many cases. Sometimes the influence of substitution and of branching is not recognizable in the frequency position but in the amount of absorption. For instance, the absorption area of the bands of a methyl group in the 2nd and 3rd overtone of the CH stretching vibration is about 25 % smaller in branched than in normal molecules, although they are situated at almost the same frequency position. Another example is the intensity of the characteristic bands of ethers, the intensity of which is two or three times less than that of the CH band of the aldehyde group CHO although they are again in nearly the same frequency position.

Dr. P. Torkington (*B. Rayon Res. Assoc.*) said: Regarding the difference in solid structure of otherwise identical materials synthesized naturally in different environments, I would like to make the following suggestion. The rate of a natural synthesis would possibly determine to a considerable extent the structure type of resulting solid material. Generalizing in order to clarify the argument (not to state a hypothesis), in the instance quoted substance found in organisms occurring in surface plants could reasonably be expected to have a more open structure if the reactions giving rise to it proceeded more rapidly than in organisms where a lower concentration of exciting energy from radiation led to less available thermal energy for molecular distortions during synthesis. The more open structure would be associated with absorbed water—possibly trapped (interstitial type) water. If this sort of determinism were valid, then it might be possible to relate degree of order in a given region of a specimen of, say, cellulose, with the energy available during formation of this region. On this view, a possible analogy for the pair crystalline-amorphous in cellulose would be winter-summer growth rings in trees.

Prof. J. A. A. Ketelaar (*Amsterdam*) said: It is interesting to note that though the differences between the spectra of rubber and of gutta-percha at 73° C are small, the latter shows a distinct band at about 970 cm.$^{-1}$. Now in the *cis-trans* isomers of unsaturated fatty acids, e.g. oleic and elaidic acid, the latter isomers are characterized by a band at about 965 cm.$^{-1}$. This would thus indicate that gutta-percha has a *trans*-form or at least predominatingly so. The intensity of this band was found independent of the chain length in the higher fatty acids and this band could be used for a quantitative determination in mixtures of methyl esters of *trans*-forms in mixtures containing also *cis*-isomers and the saturated acids

The solid triglycerol-esters show also a more complicated behaviour which is absent in the liquid form

Dr. G. Salomon (*Delft*) said: The great similarity of the spectra of amorphous rubber and gutta-percha is a rather serious blow to the rubber chemist. It was hoped that the relative amount of *cis*- and *trans*-groups in both polymers could be estimated from infra-red data. It must be kept in mind that there is not the slightest experimental evidence for an *exclusive trans*-structure of gutta-percha. Quite to the contrary, we know from (unpublished) chemical evidence that the gutta-percha hydrocarbon has a much more complicated structure. Is there any possibility left to estimate the *cis-trans* ratio with some accuracy from infra-red data ? Why is it that the polybutadienes give such a distinct difference in *cis-trans* and the polyisoprenes do not ?

At the 1947 Labile Molecule Discussion, Dr. Sheppard and Dr. Sutherland made a discussion remark [30] in connection with our paper which gave us guidance in the work reported to-day The authors suggested also at that time that the irregularities in the neoprene chain might be due to *cis-trans* isomers as indicated by infra-red analysis In view of the fact that Mochel and Hall[31] do not consider this possibility in their recent paper I should be glad to learn more about the experience of Dr. Sheppard with this particular polymer.

Prof. G. B B M. Sutherland (*Michigan*) said: In reply to Dr Salomon's questions, it is true that the differences between the spectra of rubber and gutta-percha are small, when both are in the amorphous form, but the distinction is there and could be used, although not with the same quantitative accuracy as in the polybutadienes. It is not surprising that the *cis-trans* isomerism causes a smaller change in the spectra of the polyisoprenes than it does in the polybutadienes. The main differences in the latter case arise from vibrations of the hydrogen atoms at right angles to the plane of the molecule and these vibrations have been shown to be very sensitive to the position and nature of the non-hydrogenic atoms directly attached to the double bond. In the case of the polyisoprenes, the environment of the lone CH group is not markedly different in the *cis*- and *trans* forms since it has been shown that whether the substituent is a single methyl group or an alkyl chain, the non-planar hydrogen deformation frequencies change very little, if at all, in the polybutadienes.

Dr. N. Sheppard (*Cambridge*) (*communicated*) : I would like to reply to the point made by Dr. Salomon with respect to *cis-trans* isomerism in neoprene. The two possible configurations around the double bond consistent with 1 : 4 polymerization are in this case

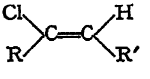

and

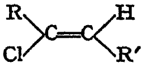

where R and R′ are long chain hydrocarbon groupings. As for the case of polyisoprene these are both trisubstituted double bonds, but on the one hand the chlorine atoms is a neighbouring double-bond substituent to the C—H linkage whereas on the other hand the hydrocarbon group is in this position. It accordingly seemed reasonable that the out-of-plane deformation mode of the CH bond might give rise to absorption at slightly different wavelengths in these two cases. In view of the fact that we found two strong absorptions at 12·1 and 12·7 μ in the infra-red spectrum of neoprene[32] (in contrast to the single absorption near 12 μ in the spectrum of natural rubber) Prof. Sutherland and I tentatively suggested[33] that a possible explanation of this was that the two absorptions in neoprene might correspond to the out-of-plane CH vibration frequencies of the *cis* and *trans* type double bonds. The more recent work by Mochel and Hall[34] on polychloroprene and polybromoprene has shown that these absorption bands both show predominantly perpendicular polarization in stretched neoprene, and that they are associated with the hydrocarbon part of the molecule in agreement with our original assignment. However, these authors also made the observation that the 12·7 μ absorption band is enhanced in intensity with increased crystallinity of the material, and in view of the complexity of the spectroscopic phenomena associated with the crystallization of gutta-percha and rubber as demonstrated by Prof. Sutherland and Dr. Vallance Jones. it would be injudicious to regard the above assignment as other than a possible one.

---

[30] *Labile Molecule Discussion*, 1947, p. 374.

[31] *J. Amer. Chem. Soc.*, 1949, 71, 4086.

Dr. P. Torkington (*B. Rayon Res. Assoc.*) said : I suggest that there is an alternative, somewhat simpler, interpretation of the spectroscopic data presented by Dr. Salomon as evidence for double bond migration during chlorination of rubber, as follows. In the spectra of simple chlorinated paraffins there are absorption bands in the region 800 to 1000 cm.$^{-1}$ which in some cases coincide with accepted key frequencies of C—H bending vibrations in unsaturated systems. Thus :

(*a*) 1 : 3-dichloropropane ; 863, 963 cm.$^{-1}$.
(*b*) 1 : 2-dichloropropane ; 906, 913 cm.$^{-1}$ (doublet).
(*c*) 2 : 3-dichlorobutane ; 952, 962, 977 cm.$^{-1}$ (triplet).
(*d*) 1 : 2 : 3-trichloropropane ; 873, 911, 930, 995 cm.$^{-1}$

These spectra have been published ;[35] the compounds were studied with a view to identifying structures in polyvinylchloride, which has fairly strong absorption in the region 900 to 1000 cm.$^{-1}$. It would seem that C—H bending modes were responsible, the chlorine atoms having the same effect on intensity as unsaturation. In the light of the above, it would seem unlikely that the absorption maxima in chlorinated rubber and in the compounds designated (IX) and (X) by Dr. Salomon should be identified with unsaturated systems, unless the key compounds (*a*) to (*d*) above had either undergone isomerization, ((*b*) and (*d*) were prepared from propylene and allyl chloride respectively, by addition of chlorine), or had lost HCl as in the characteristic decomposition of D.D.T. type chloro-hydrocarbons. These explanations seem rather unlikely, unless such changes can occur in these compounds on distillation and have remained unreported. Also, compound (*b*) has no band at 990 cm.$^{-1}$, to correspond to the absorption at 910 cm.$^{-1}$, if this is due to a vinyl group. Furthermore, with regard to the actual magnitudes of the frequencies stated by Dr. Salomon to be due to CH_2 bending modes in the compounds (IX) and (X), all the available evidence suggests that the presence of a C—Cl bond adjacent to C═C lowers the frequency of non-planar CH_2 bending from its value in the corresponding hydrocarbon. Values of the frequency in cm.$^{-1}$ are : in *iso*butene, 890 ; in vinylidene chloride, 872.[35, 36] The value 895 in vinyl chloride should of course be compared with 910 in propylene, not the 890 of *iso*butene. The raising of the vinyl CH_2 bending to 928 in allyl chloride is due to the saturated CH_2 group preventing conjugation of the chlorine atom with the C═C bond [37] (compare the opposing orienting effects in aromatic substitution of —Cl when (*a*) directly attached to an aromatic nucleus, (*b*) bonded to a carbon which is in turn attached to the aromatic nucleus, as in $\phi CHCl_2$.[38]

---

[32] Sheppard, *Thesis* (Cambridge University, 1947).
[33] Sheppard and Sutherland, *Faraday Soc. Discussion*, 1947, **2**, 374.
[34] Mochel and Hall, *J. Amer. Chem. Soc.*, 1949, **71**, 408.
[35] Thompson and Torkington, *Proc. Roy. Soc. A*, 1945, **184**, 21
[36] Thompson and Torkington, *J. Chem. Soc.*, 1944, 303.

Dr. G. Salomon (*Delft*) (*communicated*): Dr. Torkington's critical remarks must be rejected for the following reasons:

The preponderance of allylic chloride groups in rubbers with 35 % Cl and in certain cases even up to 50 % Cl has been proved by several independent kinetical methods within an accuracy of 3-5 %. We have used infra-red analysis only to distinguish between the *position* of the double bond in structure (VIII*a*) and VIII*b*)). The absence of paraffinic chloride groups in these polymers, now suggested by Dr. Torkington, has been proved kinetically.

Using another way of synthesis the structures (IV), (V) and (VI) with vicinal chloride groups have been prepared from rubber. These polymers contain some chemical active residual double bonds, to which correspond a *weak* 11 μ band; there are no new *strong* bands in the 11 μ region to support Dr. Torkington's contentions. The chlorinated polythenes studied by Thompson and Torkington [39] show also no typical 11 μ band although they are chemically related to the structures suggested by Dr. Torkington.

From the available evidence [40] it is seen that a decrease *as well as an increase* of the C—H wagging vibration can be produced by an adjacent C—Cl group.

Dr. P. Torkington (*B. Rayon Res. Assoc.*) (*communicated*): The chlorinated polythenes (halothenes) studied by Dr. Thompson and myself certainly showed no single typical 11μ band, but in the compounds of higher chlorine content there was continuous absorption over 100 wave numbers or so in this region. So single band would be expected with random substitution. The halothenes were *certainly* only very slightly unsaturated. It is difficult to avoid the conclusion that C—H deformation modes in chlorinated paraffinic systems do contribute to the absorption in the region of 11μ. I do not believe that it is justifiable to state that one can prove the absence of chlorinated paraffinic groups in chlorinated rubbers kinetically.

Dr. N. Sheppard (*Cambridge*) said: With reference to the paper on the infra-red analysis of rubber derivatives by Salomon, van der Schee, Ketelaar and van Eyk, I would like to report some similar unpublished infra-red studies of chlorinated rubber made by Prof. Sutherland and myself a few years ago. We studied chlorinated rubber films containing 8 and 36 % of combined chlorine and obtained spectra almost identical with those shown in Fig. 2 of Dr. Salomon's paper for similar percentages of chlorine. In agreement with these authors we also concluded from the appearance of a new absorption band at *ca.* 11 μ and the decrease of the 11·9 μ absorption that double bond shifts had occurred from the type $R_1(CH_3)C{=}CH{-}R_2$ found in natural rubber to the type $R'R''C{=}CH_2$ (R_1, R_2, R', R'', etc.,are alkyl groupings) with a chlorine atom at an allylic position with respect to the double bond. This latter feature explains the shift of the absorption from the usual position of 11·2 μ for molecules with purely hydrocarbon constituents R′ and R″.[41] As pointed out by Salomon *et al.*, the change in type of the double bonds also explains th initial increase in intensity of the absorption band at 6 μ caused by th

---

[37] Torkington, *Nature*, 1949, **163**, 96; *Proc. Roy. Soc.* (in press).

[38] It might be noted that the infra-red spectrum of allyl chloride shows that the orienting effect of chlorine in $\phi CHCl_2$ (where all positions are about equally reactive) is due to real electronic disturbance by the $-CHCl_2$ group, not to any intermediate formation of ϕCHO in the substitution reactions.

[39] Thompson and Torkington, *Trans. Faraday Soc.*, 1945, **41**, 246.

[40] Rasmussen, *Progress in the Chemistry of Organic Natural Products* (Springer-Verlag, Wien, 1948), p. 353.

[41] Sheppard and Sutherland, *Proc. Roy. Soc. A.*, 1949, **196**, 195.

$C{=}C$ stretching frequency, and we have been able to confirm this further by detecting a slight expected shift of this absorption band to longer wavelengths in the spectrum of the sample with 36 % combined chlorine.

As mentioned by Dr. Salomon and his co-workers, we have previously obtained infra-red evidence of double bond migrations occurring during the chemical reaction of rubber with sulphur (vulcanization).[42] In answer to a suggestion by them, however, we would like to emphasize that in this case we found no changes in the spectrum which could be associated with the production of $C{=}CH_2$ groups during vulcanization. An increase of absorption was observed at 10·4 μ corresponding to new $R_1{-}CH{=}CH{-}R_2$ type double bonds, but none was observed near 11·2 μ as would be expected if $R_1R_2C{=}CH_2$ groups were formed. These conclusions apply also to the reaction with sulphur carried to the ebonite stage, and to vulcanization using accelerators of the mercaptobenzothiazol type.

Finally the possibility, originally suggested by Dinsmore and Smith,[43] that the weak 11·2 μ absorption band in the spectrum of natural rubber may indicate the presence of $R_1R_2C{=}CH_2$ groups in the pure material is of great interest to the rubber chemist whether such groups are associated with the ends of the chain [43] or, as suggested by Salomon and his co-workers, whether they correspond to such groupings along the length of the chain. We are of the opinion, however, that considerable caution should be exercised in making this assignment. The absorption band is not a strong one and hence might easily be caused by a $C{-}C$ skeletal stretching mode or by a methyl wagging mode of the

$$—CH_2—C(CH_3){=}CH—CH_2—$$

repeating unit, particularly as many straight chain paraffins have absorption bands close to this wavelength.[44, 45] It has been suggested [43] that the weak absorption at 6·1 μ in rubber might also be the $C{=}C$ stretching frequency of the $C{=}CH_2$ group, but on the other hand this could be as easily assigned to an overtone of the strong 12 μ absorption band in rubber which is also associated with the C C part of the molecule. The correlation of the 11·2 μ absorption in natural rubber with $C{=}CH_2$ groups, although suggestive, is hence not altogether certain, and independent evidence seems desirable before it can be finally accepted.

Dr. Mansel Davies (*Aberystwyth*) (*communicated*) : The last paragraph of the experimental section of Prof. Anslow's paper suggests that various (including remarkable metastable) association equilibria occur with acetamide in aqueous solution. It so happens that the freezing-point depressions for aqueous acetamide solutions are amongst the most accurate in the literature.[46] An analysis of these shows that up to 3M there is certainly less than 2 % deviation from ideal (monomeric) solutions : i.e. the mean degree of association for a 20 % (by weight) solution is less than 1·02 at − 3° C. Our own data confirm and extend this conclusion.

As the changes observed by Prof. Anslow are not due to association factors in the case of acetamide, has she considered the other possibile changes (including hydrolysis) on heating the solutions ?

Dr. E. R. Holiday (*Spectrographic Res. Unit, London Hospital*) (*communicated*) : The experimental findings by which Dr. Anslow justifies her theoretical arguments may perhaps be conveniently divided into two groups, viz. spectral absorption measurements at wavelengths (*a*) longer and (*b*) shorter than what she terms the onset. Confining attention to the first group one is compelled to question the validity of absorption measurements when calculation shows that the solutions measured had optical densities (absorbance) values in the region of 0·01, i.e. 98 % transmission. Such measurements seem to form an unsatisfactory basis for theoretical deductions about chemical structure unless very stringent proofs of chemical purity and control of optical conditions are provided. We have found that distillation of *n*-butyl alcohol over potash through an efficient column yields successive fractions showing progressively decreasing absorption of the type described by Dr. Anslow in Fig. 10 until a product is obtained having an absorption at 250 mμ one six-hundredth of that of the sample she used. The negative optical densities obtained by Dr. Anslow at the foot of the onset must certainly be due to fluorescence and provide a phenomenon of great interest. In view of the importance of the theoretical propositions made by Dr. Anslow in this paper and elsewhere it would be a pity if the cogency of her arguments were weakened by her laying emphasis on effects which are possibly of doubtful validity.

---

[42] Sheppard and Sutherland, *J. Chem. Soc.*, 1947, 1699.

[43] Dinsmore and Smith, *Ind. Eng. Chem.* (*Anal.*), 1948, **20**, 11.

[44] Cross, Richards and Willis, this Discussion.

[45] Brown, Sheppard and Simpson, this Discussion.

[46] Chadwell and Politi, *J. Amer. Chem. Soc.*, 1938, **60**, 1291.

Prof. J. A. A. Ketelaar (*Amsterdam*) said: At many points the results of Prof. Anslow are completely at variance with well-established conceptions. Thus the irreversible dissociation of amides and urea on heating and subsequent cooling is contrary to what has been found for association through hydrogen bonds. Chemical decomposition may have perhaps played a role.

However, most of the abnormal behaviour is restricted to the region of very small extinctions (log $E < 0$, most curves extending to log $E = -2$, and lower than -3). It is a well-known fact that in spectral regions at these low specific extinctions minor impurities may play a predominant role. Thus different samples of ethanol which are considered to be pure do show quite considerable differences in absorption at shorter wavelengths, probably due to slight amounts of aldehydes. Absolute ethanol when made by the CaO process contains even more absorbent material and when made by azeotropic distillation contain traces of benzene. "Pure" butanol was shown to absorb much less after treatment with Raney nickel.[47] In fact many of the spectra of alcohols reproduced, show a band at about 2800-3000 Å which could be very well assigned to aldehydes, etc. The fluorescence observed in some cases also indicates impurities.

The theoretical interpretation, where the electronic transitions observed in the free radicals are identified with those of the bound groups, seems doubtful. The assumed dependence of the vibrational frequence of the total masses of the attached groups is contrary to what is found in numerous complex molecules, where about constant characteristic frequencies are obtained irrespective of the attached masses.

Prof. G. A. Anslow (*Smith Coll., Northampton, Mass.*) (*communicated*): Discussions of the results reported in this paper with members of the Conference suggest that additional details concerning the observations may be important. Criticisms were directed at the interpretation of the weak specific absorptions reported in the 33000-38000 cm.$^{-1}$ region. It was suggested that:—

(1) The amides cannot be associated at 0·1 M and 0·01 M, since chemical evidence indicates that aqueous solutions, particularly of acetamide, are mainly monomeric below 5 M, and that the absorption registered may result from hydrolyzed products consequent to heat treatment.

(2) This absorption may originate in the C=N chromophore of enolic forms of the amides, and similarly for the proteins in the C=N chromophore of enolic polypeptide chains, as suggested by Schauenstein.[48]

(3) The alcohols, even after successive fractional distillations, may contain slight impurities, such as the aldehydes or peroxides.

---

[47] Beale, Harris and Roe, *J. Chem. Soc.*, 1950, 1397.

[48] Schaustein, *Monatsh.*, 1949, **80**, 820, 843. Shaustein and Treiber, *J. Polymer Sci.*, 1950, **5**, 145.

For the consideration of these points of view it may be significant that :—

(1) Molecular weight determinations taken of various amide specimens in an attempt to detect photolytic dissociation, indicated, for example in acetamide, not more than 2-3 % polymerization, and no measurable change after irradiation. This small degree of polymerization was interpreted by the investigators as responsible for (*a*) the low magnitude of the absorptivity E; (*b*) the presence of the solvent as an intermediate molecule in the associated molecules, as described in the discussion of Type A amide spectra and Fig. 5; (*c*) the persistence of the dimer Type A and C spectra. Since these spectral types were characteristic of the non-heat treated solutions as well as of quenched samples, it seems improbable that hydrolyzed material is responsible for the main features of these spectra. Some of the irregularities exhibited in the C types, particularly in those of urea may have this origin.

(2) Enolic forms of the amides may absorb not only through C=N excitation, but also through the excitation of the OH . . . N groups. Rupture of the H . . . N bridge without the OH bond dissociation should result from energy absorption with wave-numbers 36000-37000 cm.$^{-1}$. Most type B amide spectra show weak maxima and type A exhibit fluorescence in this region. Possibly the latter results from the formation of enolic dimers consequent to the photolytic rupture of the H . . . O bridge of the normal ketonic forms. The specific absorption which appears in the spectra of alkaline solutions of the proteins, Fig. 17, may have a similar origin.

(3) Since aldehydes have relatively low boiling points, it seems unlikely that thrice-distilled high-grade alcohols can retain sufficient amounts to produce even the weak absorption observed. Nor can the absorption maxima be checked with the published spectra of aldehydes. Moreover, the absorptions onsets occur at wave-numbers which depend on the reduced mass of the respective associated alcohol, and not on the mass of an impurity. Recently portions of approximately 1 M solutions, used for the published graphs, now aged for 20-30 weeks, were run through the Beckman spectrophotometer after redistillation. The specific absorptions were practically identical with those given by the freshly prepared solution showing no changes indicating decreased impurities. Non-redistilled portions exhibited, in most cases, stronger absorption in the 25000-35000 cm.$^{-1}$ region and less definitely in the 40000 cm.$^{-1}$ region similar to the results reported in the M^1 curves of Fig. 9, 10 and 11. (Note the differences between the M and M^1 results for *tert.*-butyl, *n*-amyl- and *tert.*-amyl alcohols.) In addition similarly located specific absorptions appear in the spectra of fresh solutions of higher concentration. Most of the additional absorption is probably Tyndall scattering from molecular aggregate of increased volume. Possibly these form through CH . . . O association either between adjacent polymers or between the solute and the solvent, an association which may have caused the onsets in the 31000 cm.$^{-1}$ region which are most apparent in the spectra of the freshly prepared weak solutions.

Finally, in comparing the published spectra, in the 25000-47000 cm.$^{-1}$ region which were obtained with the Beckman photo-electric spectrophotometer, with those obtained in spectrograms, it must be realized that the use of the Beckman monochromator permits an analysis of the unirradiated solution step by step, whereas photographic methods simultaneously record the specific absorptions of the photolysis products and fluorescence, as well as the specific absorption of the initial solution. Consequently the Beckman instrument reveals weak specific absorptions, which are obscure in the usual spectrogram. On the other hand, it does not separate fluorescent radiation resulting from photolysis products. Ideally the beam which has passed through the sample at the exit slot of the monochromator should be analyzed by a second monochromator before falling on the photo-electric cell.

IV. APPENDIX *

STUDIES OF THE CARBOXYL GROUP

PART I.—THE GEOMETRICAL STRUCTURE

By Mansel Davies and Orville Thomas

Received 9*th October*, 1950

The various quantitative data on the geometrical structure of the carboxyl group are discussed and marked discrepancies are indicated. A structure is proposed which is in much better accord with the range of results available than is the case for previous models.

Despite its apparent simplicity and very frequent study by a variety of methods, there remains considerable uncertainty in the literature on the bond lengths in the carboxyl group. This is principally expressed in the wide range of values for the C—O ("single") bond length. The immediately relevant data come from X-ray diffraction analysis of crystalline acids and electron diffraction and vibrational spectra in the gaseous state.

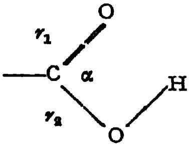

Fig. 1.—Molecular parameters in the carboxyl group.

X-Ray Data.—A reference [1] to the more detailed (Fourier) evaluations of X-ray results may be summarized by quoting the ranges of the individual "best" values :

$$r_1 = 1{\cdot}20 - 1{\cdot}28\ \text{Å},\ r_2 = 1{\cdot}25 - 1{\cdot}31\ \text{Å},\ \alpha = 122°\text{-}126°.$$

Whilst the limits $\pm$ 0·04 Å are about double those given by individual X-ray workers, a consideration of one of the most careful X-ray studies [2] shows that the overall accuracy in bond lengths is often significantly less than is allowed. Accepting Brill, Hermann and Peters' data for the oxalic acid dihydrate crystal parameters ($a = 6{\cdot}12$, $b = 3{\cdot}60$, $c = 12{\cdot}03$, $\beta = 106{\cdot}2°$) and their own estimated errors in the atomic co-ordinates in terms of these parameters ($\Delta x = 0{\cdot}0025$; $\Delta y = 0{\cdot}0040$; $\Delta z = 0{\cdot}0010$), we have calculated the limiting configurations of the carboxyl group which are in accord with their X-ray results. These are :

$$r_1 = 1{\cdot}23_6\ \text{Å},\ r_2 = 1{\cdot}30_8\ \text{Å},\ \alpha = 126°\ 0' ;$$
$$r_1 = 1{\cdot}18_4\ \text{Å},\ r_2 = 1{\cdot}25_3\ \text{Å},\ \alpha = 128°\ 42'.$$

---

* Papers accepted for publication but not issued as preprints.

[1] (*a*) Hendricks, *Z. Krist.*, 1935, **91**, 48. (*b*) Robertson and Woodward, *J. Chem. Soc.*, 1936, 1817. (*c*) Verweele and McGillavry, *Nature*, 1938, **142**, 161. (*d*) Dunitz and Robertson, *J. Chem. Soc.*, 1947, 142. (*e*) Morrison and Robertson, *J. Chem. Soc.*, 1949, 980. (*f*) Morrison and Robertson, *J. Chem. Soc.*, 1949, 987. (*g*) McGillvary, *Rec. trav. chim.*, 1941, **60**, 605. (*h*) Morrison and Robertson, *J. Chem. Soc.*, 1949, 993. (*i*) Morrison and Robertson, *J. Chem. Soc.*, 1949, 1001.

[2] Brill, Hermann and Peters, *Ann. Physik.*, 1942, **42**, 357.

Thus, it would not appear unreasonable to put limits ± 0·03 Å to the bond lengths available in this one instance. It need only be emphasized that the data of Brill, Hermann and Peters used here are of an accuracy much greater than that of most X-ray work.

A point which must also be borne in mind is the possibility of special features arising in any one crystal structure which might give the carboxyl group there " abnormal " parameters. Thus the occurrence of several special resonance structures has been discussed for oxalic acid dihydrate itself,[3] but the X-ray data referred to include such presumably normal members as succinic, adipic and sebacic acids. However, one general feature will be the changes arising on the transition vapour ⇆ solid. Even with the distinctive carboxyl group interactions occurring in these cases it initially seemed unlikely that the bond lengths would alter by more than 0·04 Å.[4]

Again, a small change in the bond-angle α of not more than 3° in going from vapour to solid is a possibility; as the maximum work involved in this deformation would be 300 cal./mole it cannot be ruled out for that reason. Similarly, about 700 cal. per mole are involved in stretching the C—O bond 0·04 Å.

Electron Diffraction Data.—Recent electron diffraction results[5] are interpreted to give for monomeric formic acid molecules:

$$r_1 = 1{\cdot}24\ \text{Å}\ ,\ r_2 = 1{\cdot}42\ \text{Å},\ \alpha = 117°.$$

Except for the angle, which is uniquely low here, the figures for acetic acid are identical, with α as 122° to 138°. The C—O bond length is far outside the permissible X-ray values.

Molecular Spectra.—Some of the most important spectroscopic evidence for the structure of the carboxyl group comes from an analysis of the rotational fine structure of the harmonic bands of the O—H stretching frequency in formic acid:[6, 7, 8] further, and indeed more precise, rotational constants are available for H . COOH and its deuterated derivatives from fundamental bands.[9]

Both the spectroscopic[7, 9] and the dipole moment[10] data indicate that the formic acid molecule is planar. Thus the three principal moments of inertia are related by $I_1 = I_2 + I_3$, and I_3 will be much smaller than the other two. In units of 10^{-40} g.cm.^{2} Van Zant Williams' values are $I_1 = 86{\cdot}3_8 \pm 0{\cdot}9$; $I_2 = 75{\cdot}2_7 \pm 0{\cdot}7$; $I_3 = 11{\cdot}1_1 \pm 0{\cdot}1$: the possible uncertainties indicated are based on the (extreme) assumption of errors of 1 % in the experimental rotational constants. (The apparent difference between the I values of Bauer and Badger,[7] and of Thompson[8] from those of Van Zant Williams[9] is almost entirely due to changes in the accepted value of h: we have used $h = 6{\cdot}626 \times 10^{-27}$ erg sec.)

Assuming values $r_{CH} = 1{\cdot}08$ Å, $r_{OH} = 0{\cdot}97$ Å, and $\angle$COH = 107°, from the above values and his own data for the rotational constant $(\gamma'' - \delta)$ for the deuterated derivatives of formic acid, Van Zant Williams deduced $r_1 = 1{\cdot}22_5 \pm 0{\cdot}02$ Å, $r_2 = 1{\cdot}41 \pm 0{\cdot}02$ Å, $\alpha = 125° \pm 1°$, as providing an adequate representation for the four molecules

H . COOH, H . COOD, D . COOH, D . COOD

involved.

This result of the interpretation of a considerable amount of quantitative spectroscopic data approximates to the electron diffraction values[5] but is clearly incompatible with the large body of X-ray results. In arriving at his model, however, Van Zant Williams considered only the possible ranges r_1 = 1·22 to 1·23 Å, r_2 = 1·38 to 1·43 Å; his solution can best be regarded as one possible form which fits the spectroscopic data.

---

[3] Robertson and Ubbelohde, *Proc. Roy. Soc. A*, 1939, **170**, 222; *Proc. Roy. Soc. A*, 1939, **170**, 241.

[4] Davies and Sutherland, *J. Chem. Physics*, 1938, **6**, 755.

[5] Karle and Brockway, *J. Amer. Chem. Soc.*, 1944, **66**, 574.

[6] Herzberg and Verleger, *Physik. Z.*, 1936, **12**, 444.

[7] Bauer and Badger, *J. Chem. Physics*, 1937, **5**, 852.

[8] Thompson, *J. Chem. Physics*, 1939, **7**, 453.

[9] Van Zant Williams, *J. Chem. Physics*, 1947, **15**, 232, 243.

[10] Coop, Davidson and Sutton, *J. Chem. Physics*, 1938, **6**, 905.

Accordingly, a systematic calculation of the moments of inertia for a much wider range of models was made. Hirschfelder's neat determinantal form [11] of evaluation reduces in this case (with his notation) to $I_1 = C$; and I_2 and I_3 as the roots of

$$I^2 - CI + (AB - D^2) = 0.$$

The values quoted above for r_{CH} and r_{OH} are well supported by reference to related molecules and are unlikely to be in error by more than 0·01 Å. Fortunately the moments of inertia are not sensitive to these values. Similarly, the ∠COH can be varied 3° or more, without appreciably affecting the result. Values of 107° to 110° have been used for it. On the other hand, with any of the suggested bond distances the ∠OCO is determined as near 126° (± 1°) for best agreement with the moments of inertia. Some of the results approximating to the spectra requirements are reproduced in Table I.

TABLE I

Model	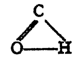 γ°	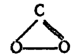 α°	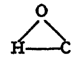 δ°	r_1 Å	r_2 Å	I_1	I_2	I_3
						× 10^{40} g. cm.^{2}		
1	122	125	107	1·24	1·29	78·5	67·6	10·9
2	122	125	107	1·24	1·32	81·0	70·1	10·9
12	135	122	107	1·24	1·32	84·2	74·8	9·4
4	120	126	107	1·27	1·33	84·7	74·0	10·7
11	120	130	107	1·27	1·32	85·1	75·1	10·0
13	120	126	108	1·27	1·35	85·3	74·3	11·0
14	118	125·5	108	1·27	1·35	85·1	73·9	11·2
16	117·5	126	108	1·27	1·35	85·3	74·3	11·0
17	118	126	110	1·27	1·35	85·5	74·4	11·1
V.Z.W.	122	125	107	1·23	1·41	86·4	75·3	11·1
Expt.	—	—	—	—	—	$86{\cdot}3_8$	$75{\cdot}2_7$	$11{\cdot}1_1$

The essential difference between our own and Van Zant Williams's calculations is that we have used the X-ray data as a basis for our models rather than the electron diffraction results. Retaining the geometrical features of model 17, the rotational constants were calculated for the deuterated derivatives. These are compared in Table II with the experimental values (δ from Bauer and Badger, and the others from Van Zant Williams) and those calculated by Van Zant Williams for his model.

Both these models thus reproduce the spectral constants to within the probable uncertainty in the latter. The value r_1 = 1·27 Å in model 17 is near the upper limit permissible by X-ray data: omitting the oxalic acids, the mean value of r_1 in seven other carefully measured cases is 1·25 Å. Although limits of ± 0·02 Å are often given with the X-ray figures, this is increased to ± 0·04 Å in some cases (ref. 1, *f* and *h*). Even with the latter uncertainty our value r_2 = 1·35 Å is beyond the X-ray limits, as for the same seven cases the average r_2 = 1·30 Å. If r_2 be reduced in value, compatibility with the spectral data can only be achieved by a corresponding increase in r_1. Furthermore, the characteristic absorptions of the carboxyl group suggest that the two carbon-oxygen bonds differ far more than their approximate equality in much X-ray data would allow.

---

[11] Hirschfelder, *J. Chem. Physics*, 1940, 8, 431.

The model now proposed is seen to be, at least in respect to the carbon-oxygen bond length (r_2), intermediate between the X-ray and electron diffraction values. If an uncertainty of ± 0·04 Å were imposed on the latter (which is not unreasonable as a general assessment) the electron diffraction data would not show any divergence from our model. It must, too, be emphasized that model 17 strictly applies only to formic acid molecules in the gaseous phase and significant though slight (± 0·04 Å) changes in the CO bond lengths may arise from changes in environment.

TABLE II

Molecule	Rotational Constants	Expt. Values cm.$^{-1}$	V. Z. W. Model	Model 17
H . COOH	δ	0·348	0·350	0·352
	γ'' δ	2·172	2·172	2·178
H . COOD			0·338	0·339
	$\gamma'' - \delta$	1·829	1·822	1·819
D . COOH	δ	-	0·343	0·345
	$\gamma'' - \delta$	1·544	1·550	1·549
D . COOD	δ	- -	0·331	0·333
	$\gamma'' - \delta$	1·328	1·339	1·331

It is interesting to compare the bond lengths proposed here for formic acid with the available data on similar links in other molecules. In terms of bond-order (N), Gordy [12] has given for the C—O links the correlation

$$N = \frac{5{\cdot}75}{r^2} - 1{\cdot}85,$$

where r is in Å. This is probably as precise a relation as the available data will allow. On its basis the bond-orders in formic acid are 1·30 and 1·71. These figures certainly serve to emphasize the " abnormality " of the bonds in the carboxyl group, a feature expressed chemically, for instance, in the absence of the typical carbonyl reactions. Any further discussion of the binding in the group is postponed until the potential functions (i.e. force constants) deduced in Part II, have been evaluated.

It may at least be claimed for our proposed dimensions that they represent a closer synthesis of the available physical data than any other single set of bond lengths.

The Edward Davies Chemical Laboratories,
University College of Wales,
Aberystwyth.

---

[12] Gordy, *J. Chem. Physics*, 1947, **15**, 305.

STUDIES OF THE CARBOXYL GROUP

PART II.—THE POTENTIAL FUNCTION OF THE FORMATE ION AND THE FORMIC ACID MOLECULE

By Orville Thomas

Received 9th October, 1950

A complete assignment of the in-plane vibrational frequencies of formic acid and the formate ion is made. Generalized quadratic potential functions for these structures are first evaluated by treating them as three-particle systems. The extreme solutions possible with that simplification are taken to indicate the limiting range of the conventional valence-force constants. Four-particle treatments are carried out using Torkington's [**A**], [**e**] and [**h**] matrices to arrive at the force-constant matrix [**d**]. The significance of the force-constants deduced is discussed. An apparent inconsistency between the carbon-oxygen bond orders as indicated by their lengths and force constants remains.

---

1. Three-Particle Treatment.—As a first approximation the formate ion and the formic acid molecule may be treated as three-particle systems. For the formate ion $m_1 = m_3 = m(\text{O})$; $m_2 = m(\text{CH})$ and $r_1 = r_2$. For formic acid $m_1 = m(\text{O})$; $m_2 = m(\text{CH})$; $m_3 = m(\text{OH})$.

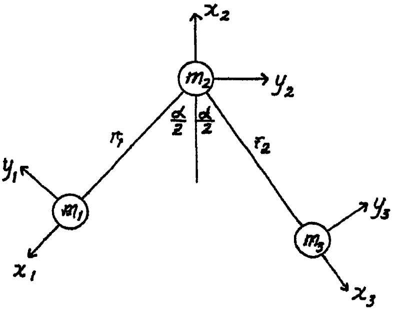

Fig. 1.—Non-linear three-particle system.

(*a*) Frequency Assignment in the Formate Ion.—Lecomte and his collaborators [1, 2] have reported the absorptions between 600 to 1600 cm.$^{-1}$ for a large number of formates. Using the Grubb-Parsons S3 spectrometer with a rock-salt prism, the spectrum of sodium formate melted as a thin film between NaCl plates has been redetermined. Fig. 2 and Table I summarize the observations.

Lecomte found frequencies within certain ranges common to most of the formates: these frequencies and the assignments, in the conventional three-particle notation, as given by Lecomte are :

1500-1600	1280-1350	800-850	745-775.
ν_3	ν_1	ν_2	

In the range above 1200 cm.$^{-1}$ Lecomte's frequencies are admittedly uncertain and the assignment $\nu_1 = 1374$ cm.$^{-1}$, $\nu_2 = 775$ cm.$^{-1}$, $\nu_3 = 1678$ cm.$^{-1}$ is proposed here. No absorption was detected at 800 to 850 cm.$^{-1}$ for Na and K formates and it appears absent from five out of fourteen formates examined by Lecomte, who gives a frequency near 750 cm.$^{-1}$ in all cases. The Raman data [3]

---

[1] Duval, Lecomte and Douville, *Ann. Physique*, 1942, **17**, 5.
[2] Lecomte and Freyman, *Compt. rend.*, 1939, **208**, 1401.
[3] Edsall, *J. Chem. Physics*, 1936, **4**, 1.

show strong lines corresponding to 1374 cm.$^{-1}$ and 772 cm.$^{-1}$. The absence of ν_3 in the Raman is according to expectations.

As Edsall has indicated,[4] the formate ion is closely related both in electronic structure and mass factors to the NO_2 molecule. For the latter [5] ν_1 = 1320 cm.$^{-1}$, ν_2 = 648 cm.$^{-1}$, ν_3 = 1621 cm.$^{-1}$. Further observations on the spectrum of Na and K acetate suggest that the formate frequencies at 1678 and 1374 cm.$^{-1}$ become 1586 and 1418 cm.$^{-1}$ in the acetate: these two pairs of frequencies are split about a common mean value of about 1515 cm.$^{-1}$.

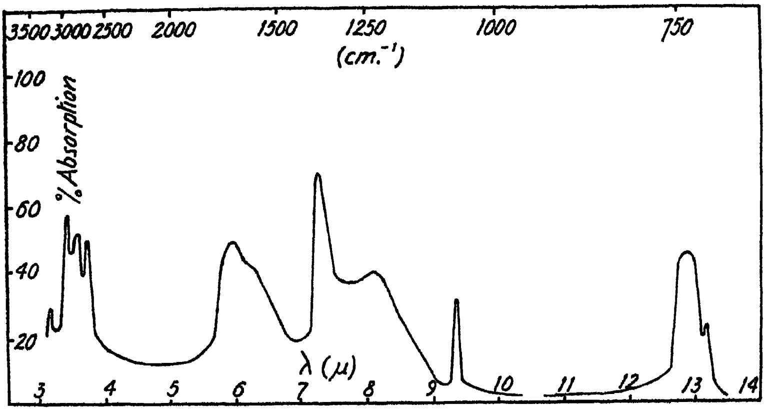

FIG. 2.—Infra-red absorption spectrum of sodium formate.

(*b*) FREQUENCY ASSIGNMENT IN FORMIC ACID.—In this instance, the three fundamental frequencies can be further (approximately) described as

$\nu_1 = \nu(C—O)$, $\nu_2 =$

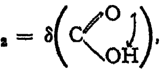

$\nu_2 = \delta\left(C\begin{smallmatrix}\nearrow O\\ \searrow OH\end{smallmatrix}\right)$, $\nu_3 = \nu(C{=}O)$.

The vapour absorption spectrum for H . COOH and its deuterated derivatives has been reported by various authors.[6, 7] The grating-values of Van Zant Williams [7] are used, where they are available, in the following calculations.

TABLE I

Absorptions : cm.$^{-1}$	3176	2938 2816 2602	1678
Remarks . .	Weak but sharp	Triplet	Broad, shoulder at 1605

Absorptions : cm.$^{-1}$	1374	1069	775	760
Remarks . .	Strong	Strong	Strong	Strong subsidiary peak

Considerable certainty attaches to the allocation ν_3 = 1770 cm.$^{-1}$ and only slightly less to ν_2 = 658 cm.$^{-1}$. The latter becomes 678 cm.$^{-1}$ in D. COOH and is to be compared with ν_2 = 648 cm.$^{-1}$ in NO_2.[5] On the basis of a complete assignment of the symmetry type *A′* vibrations in H . COOH (see below), a partial assignment in H . COOD and the Teller-Redlich product rule, a value ν_2 = 560 cm.$^{-1}$ is predicted for H . COOD. As these spectra have not been reported below 650 cm.$^{-1}$, the absence of the corresponding band in H . COOD and

[4] Edsall, *J. Chem. Physics*, 1937, **5**, 514.
[5] Bailey and Cassie, *Nature*, 1933, **131**, 239, 910.
[6] Bonner and Hofstadter, *J. Chem. Physics*, 1938, **6**, 531.
[7] Van Zant Williams, *J. Chem. Physics*, 1947, **15**, 232, 243.

D . COOD can be understood. Furthermore, the Raman spectrum of $CH_3 . COOH$ shows a frequency of 623 cm.$^{-1}$ which becomes 580 cm.$^{-1}$ in $CD_3 . COOD$.[8]

The formic acid molecules all show a strong absorption at 1140 ± 40 cm.$^{-1}$ which, as previously,[6] is taken as ν_1. The choice of this frequency is more fully discussed later: in H . COOH vapour it is found at 1105 cm.$^{-1}$.

The Potential Function.—(*a*) THE FORMATE ION. With the parameters of Fig. 1, suitable symmetry co-ordinates are,

$$\Delta_1 = \Delta r_1 + \Delta r_2, \quad \Delta_2 = r_1 \Delta\alpha, \quad \Delta_3 = \Delta r_1 - \Delta r_2.$$

The generalized valence force potential function (V.F.P.F.) is then

$$2V = d_{11}\Delta_1^2 + d_{22}\Delta_2^2 + 2d_{12}\Delta_1\Delta_2 + d_{33}\Delta_3^2. \quad . \quad . \quad . \quad (1)$$

This may be written in an equivalent form as

$$2V = (d_{11} + d_{33})(\Delta r_1^2 + \Delta r_2^2) + d_{22}r^2\Delta\alpha^2 + 2(d_{11} - d_{33})\Delta r_1 \Delta r_2 + 2d_{12}r\Delta\alpha(\Delta r_1 + \Delta r_2). \quad . \quad (2)$$

The latter may be compared with the usual form of the V.F.P.F., viz.

$$2V = f'(\Delta r_1^2 + \Delta r_2^2) + f''r^2\Delta\alpha^2 + 2f_{13}\Delta r_1 \Delta r_2 + 2f_{12}r\Delta\alpha(\Delta r_1 + \Delta r_2) \quad (3)$$

where $f' = f_{(C—O)}$ and $f'' = f$ 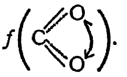.

The constants in eqn. (1.1) are found by using Torkington's results[9] for the secular equation of second degree and from the linear equation,

$$|A_{33}d_{33} - \lambda_3| = 0$$

where A_{33} is the appropriate element of Torkington's **A** matrix. The values obtained are quoted in Table II, the force constants being in units of 10^5 dynes/cm.

TABLE II

Force Constant	Solution				
	I	II	VII (min. d_{22})	VII (min. d_{11})	General
d_{11}	$4\cdot8_{66}$	$6\cdot9_{18}$	$6\cdot3_{60}$	$2\cdot3_{10}$	$6\cdot3_{60}$
d_{33}	$4\cdot5_{22}$	$4\cdot5_{22}$	$4\cdot5_{22}$	$4\cdot5_{22}$	$4\cdot5_{22}$
d_{22}	$1\cdot4_{31}$	$1\cdot2_{63}$	$1\cdot2_{00}$	$3\cdot3_{03}$	$1\cdot2_{00}$
d_{12}	$0\cdot0_{00}$	$1\cdot2_{14}$	$1\cdot0_{34}$	$0\cdot7_{93}$	$0\cdot7_{88}$
f'	9·39	11·4	10·9	6·83	10·9
f''	1·43	1·26	1·20	3·30	1·20
f_{12}	0·00	1·21	1·03	0·79	0·79
f_{13}	0·34	2·40	1·84	—2·21	1·84

The conventional force constant terms obtained by comparison of eqn. (2) and (3) are also shown. Solution I corresponds to the idealized V.F.P.F. with $d_{12} = 0$, a condition which is not generally applicable as it sometimes leads to imaginary values of the other constants. Torkington found that the energy contributions from the two square terms in (1) for the ideal case $d_{12} = 0$ were mutually reciprocal in the two modes: imposing this condition as a necessary feature leads to solution II. Solutions VII are particular limiting versions.

For secular equations of degree higher than two, Torkington[10] achieves a solution for the force constants by equating to zero all elements below the diagonal of his form of the determinantal equation:

$$|\mathbf{dA} - \mathbf{1}| = 0.$$

---

[8] Hibben, *Raman Effect and Its Chemical Applications* (Reinhold, New York, 1939.)

[9] Torkington, *J. Chem. Physics*, 1949, **17**, 357.

[10] Torkington, *J. Chem. Physics*, 1949, **17**, 1026.

For the significance and method of this solution the original paper should be consulted. In practice it is found that acceptable values of the force constants are obtained notwithstanding the somewhat arbitrary method of solution: excellent results are found when the fundamentals are group vibrations involving principally only one co-ordinate. In the present instance with the Cartesian displacement co-ordinates of Fig. 1, the **A** matrix is, with $M = m_2$ ·

$$\begin{bmatrix} 2\mu + 4c^2 & 4sc & 0 \\ 4sc & 2\mu + 4s^2 & 0 \\ 0 & 0 & 2\mu + 4s^2 \end{bmatrix}$$

where $\mu = m_2/m_1, \quad s = \sin(\alpha/2), \quad c = \cos(\alpha/2).$

Taking Zachariassen's X-ray values[11] $r(C—O) = 1{\cdot}27 \pm 0{\cdot}02$Å, $\alpha = 125°$, the elements of the force constant matrix [**d**] given as the general solution in Table II are obtained. It is important to note that this "general" solution does not markedly differ from solution II which is, perhaps, the most physically plausible, whilst it is almost identical with solution VII (min. d_{22}).

(*b*) FORMIC ACID.—As a three-particle system with the notation of Fig. 1 the **A** matrix is

$$\begin{bmatrix} 1 + \mu_1 & \cos\alpha & \sin\alpha\sqrt{\frac{r_1}{r_2}} \\ & 1 + \mu_3 & -\sin\alpha\sqrt{\frac{r_2}{r_1}} \\ \text{Symmetrical} & & \frac{r_2}{r_1}\mu_1 + \frac{r_1}{r_2}\mu_3 + \frac{r_1^2 + r_2^2}{r_1 r_2} - 2\cos\alpha \end{bmatrix}$$

where $\mu_1 = m_2/m_1, \quad \mu_3 = m_2/m_3.$

The molecular dimensions (see Part I) are taken as $r_1 = 1{\cdot}27$ Å, $r_2 = 1{\cdot}34$ Å, $\alpha = 126°$. Using Torkington's general solution[10] the terms of the [**d**] matrix given in Table V are found for the three-particle system.

2. Four-particle Treatment.—Fig. 3(*a*) provides a full representation of the formate ion, whilst the formic acid molecule can be approximated as 3(*a*) with $m_1 = m(H)$, $m_2 = m(O)$, $m_3 = m(C)$, $m_4 = m(OH)$, or as in 3(*b*) with $m_1 = m_3 = m(O)$, $m_2 = m(CH)$, $m_4 = m(H)$. The planar normal modes of 3(*a*), the model first treated are

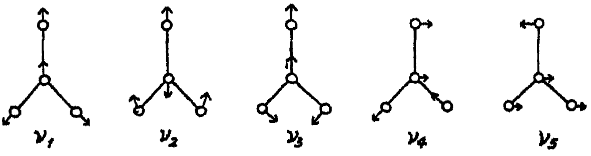

The formate ion is a plane symmetrical XYZ_2 molecule whose point group is C_{2v}. The Class A_1 vibrations are ν_1, ν_2, and ν_3; ν_4 and ν_5 belong to Class B_1. Formic acid has the point group C_s and the five planar vibrations belong to Class A'.

FREQUENCY ASSIGNMENT. (*a*) FORMATE ION.—Values have already been assigned to ν_1, ν_3 and ν_4; ν_2 represents the ν(C—H) frequency and is taken from Table I as 2816 cm.$^{-1}$. In the same Table the alternatives for ν_5, i.e. $\delta C\langle^{H}_{O}$ are the bands at 760 and 1069 cm.$^{-1}$. The $X\overset{\frown}{.}C$—H deformation frequency[12] in other simple molecules having the carbon in sp^3 or sp^2 valence states lies in the range 1000–1100 cm.$^{-1}$. The choice $\nu_5 = 1069$ cm.$^{-1}$ is further supported by Lecomte's finding a band at 1030 ± 40 cm.$^{-1}$ in ten of the fourteen formates that he examined. It is not surprising that the intensity of the fundamental is not great, a circumstance which possibly accounts for its non-appearance in some instances. The sharp subsidiary band at 760 cm.$^{-1}$ may possibly be ν_6, the out-of-plane Class B_2 vibration.

---

[11] Zachariassen, *J. Amer. Chem. Soc.*, 1940, **61**, 1011.

[12] Herzberg, *Molecular Spectra and Molecular Structure*, Vol. 2 (Van Nostrand Co., Inc., N.Y., 1945), Table 51, p. 195.

(*b*) FORMIC ACID.—Formic acid when treated as the four-particle system illustrated in Fig. 3(*b*) has two normal modes associated with the stretching and bending of the OH link. They are $\nu_7 = \nu(\text{O—H})$ and $\nu_8 =$ 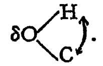 $\delta\text{O}\overset{\text{H}}{\underset{\text{C}}{\langle}}$.

In addition to the data already mentioned [6, 7] which refer to the gaseous state, quantitative observations on the influence of dimerization of the molecules upon the absorption spectrum in solution have been acquired. The position of the monomer ⇌ dimer equilibrium in the moist solvents can be determined from distribution data.[13, 14]

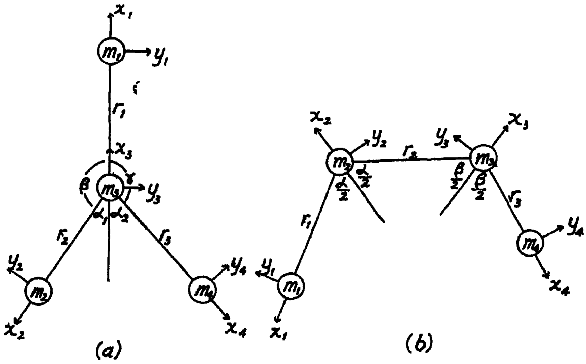

FIG. 3.—The formate ion (*a*) and formic acid (*a*, *b*) as four-particle systems.

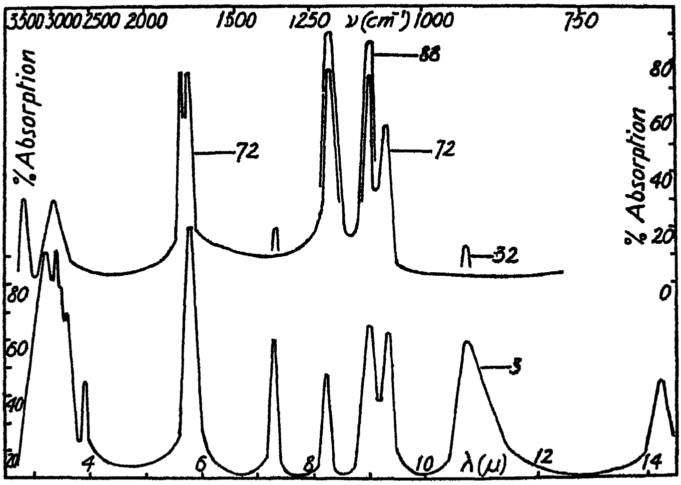

FIG. 4.—Infra-red absorption spectrum of formic acid in CCl_4 and CS_2. The numbers give the percentage monomer present.

Using cells ranging from 0·8 to 40 mm. in thickness and temperatures from 25° to 60° C (read with a thermocouple), an attempt has been made to follow systematically the spectral changes accompanying the association. For the data reproduced, the total number of molecules (H . COOH) in the path length is constant to ± 5 %. Fig. 4 represents the overall picture in CCl_4, apart

---

[13] Seidell, *Solubilities of Organic Compounds* (Van Nostrand Co. Inc., 1941), pp. 27 and 29.

[14] Moelwyn-Hughes, *J. Chem. Soc.*, 1940, 850.

from the region 1100-1200 cm.$^{-1}$ where CS_2 is the solvent. The band-centres are recorded in the following table, where the conditions give the temperature and percentage monomer in the solution.

TABLE III

Condition	ν (cm.$^{-1}$)							
25°: 3 % (CCl_4)	2922	1721	1363	1210	1105	1064	927	700
60°: 72 % (CCl_4)	3505	2930	1761	1732		1064		
25°: 88 % (CS_2)					1208	1103		

Some of the expected changes are immediately recognized in Fig. 4. The broad association (O—H) band around 3000 cm.$^{-1}$ is replaced in dilute solutions by sharp bands at 3505 and 2930 cm.$^{-1}$, these being respectively ν(O—H) and ν(C—H) in the monomer. Similarly, the single intense absorption at 1721 cm.$^{-1}$ is replaced by two components at 1732 and 1761 cm.$^{-1}$ on dilution: of these, that at 1761 cm.$^{-1}$ is the ν(C═O) frequency in the monomer.

The band at 1363 cm.$^{-1}$ which comes up strongly in the associated solution but disappears and has no near neighbours in the monomer spectrum, is almost certainly the δ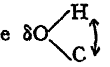

mode in the dimer. It appears as one of the strongest lines in the Raman spectra of the pure carboxylic acids, which state, of course, can safely be taken as almost completely dimeric. This frequency, after ν(O—H), is certainly the one most likely to be markedly influenced by association. Its identity in the monomer is a crucial point. The present evidence suggests, and the correlation with the frequencies in the D-substituted formic acids is taken to confirm, that this frequency is at 1208 cm.$^{-1}$. Fig. 4 shows that the latter is the absorption which decreases most markedly as the 1363 cm.$^{-1}$ band increases. The value 1208 cm.$^{-1}$ for the deformation O—H frequency is sensibly related to those in other molecules. In monomeric methyl alcohol a similar frequency is below 1100 cm.$^{-1}$: in phenol [15] it is near 1170 cm.$^{-1}$. Consideration of the intramolecular interaction in the carboxyl group certainly leads one to anticipate that the corresponding frequency will be higher there than in the simple hydroxylic compounds. The pronounced shift in the frequency on association ($\Delta\nu \sim 155$ cm.$^{-1}$) is significantly greater than for the alcohol or phenol: this conforms to the greater strength of the hydrogen bridge in the dimeric acid. The bands at 1205 cm.$^{-1}$ in H . COOH [7] and 1206 cm.$^{-1}$ in D . COOH [16] appear to be replaced by bands at 972 and 945 cm.$^{-1}$ in H . COOD and D . COOD respectively.[7] These give the values 1·23 and 1·27 for the frequency ratio δOH/δOD in corresponding molecules. In CH_3OH the same factor is 1·19: this degree of concurrence is satisfactory.

The band at 1103 cm.$^{-1}$ is also more prominent in solutions containing a larger proportion of monomer, although the relative increase in peak height is less than for the band at 1208 cm.$^{-1}$. This is not inconsistent with the allocation of this frequency to ν_1, i.e. to the ν(C—O) mode: it is a monomer frequency but is not so intimately connected with the association process as the 1732 and 1208 cm.$^{-1}$ frequencies.

In the formate ion the (C—H) deformation frequency was placed at 1069 cm.$^{-1}$: consistent with this the 1064 cm.$^{-1}$ band in formic acid, which is assigned to the same mode (ν_5), is quite insensitive to the monomer ⟷ dimer change. An interesting feature is the significant change in this frequency between the vapour (1033 cm.$^{-1}$) and solution (CCl_4: 1064 cm.$^{-1}$). Unlike the δ(O—H) vibration which can be regarded as stabilized by intramolecular interaction, the (C—H) group is essentially "unprotected" in H . COOH. Additional constraint on its angular movement will arise in solution from the polar forces which can be represented as

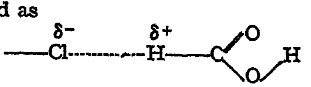

Finally Fig. 4 establishes that the 927 cm.$^{-1}$ band (917 cm.$^{-1}$ in vapour) arises from the associated molecules. It is provisionally allocated to one of the out-of-plane vibrations, e.g. the out-of-plane δ(O—H) vibration in the dimer. The above conclusions are summarized in Table IV.

---

[15] Davies, *J. Chem. Physics*, 1948, 16, 267.
[16] Hermann and Williams, *J. Chem. Physics*, 1940, 8, 447.

TABLE IV

Vapour Phase		Solution in CCl_4 and CS_2		Assignment
Dimer	Monomer	Dimer	Monomer	
ν (cm.$^{-1}$)	ν (cm.$^{-1}$)	ν (cm.$^{-1}$)	ν (cm.$^{-1}$)	
—	3576	—	3505	$\nu_7 = \nu(O—H)$
3080	—	2922	—	—
—	2943	—	2930	$\nu_2 = \nu(C—H)$
2530	—	—	—	—
1740	1770	1732	1761	$\nu_4 = \nu(C{=}O)$
1350	—	1363	—	—
—	1205	—	1208	$\nu_8 =$ 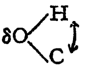
—	1105	—	1103	$\nu_1 = \nu(C—O)$
—	1033	—	1064	$\nu_5 =$ 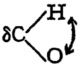
917	—	927	—	—
667	—	700	—	—
—	658	—	—	$\nu_3 =$ 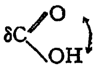

The Potential Function.—(*a*) THE FORMATE ION.—Using the notation of Fig. 3(*a*) the symmetry co-ordinates are :

$$\text{Class } A_1: \ \Delta_1 = \Delta r_1, \quad \Delta_2 = \Delta r_2 + \Delta r_3, \quad \Delta_3 = r_2\Delta\alpha.$$
$$\text{Class } B_1: \ \Delta_4 = \Delta r_2 - \Delta r_3, \quad \Delta_5 = r_1(\Delta\beta - \Delta\gamma).$$

With $c = \cos(\alpha/2)$, $s = \sin(\alpha/2)$, $M = m_3$, $\mu_1 = m_3/m_1 = 11{\cdot}92$, $\mu_2 = m_3/m_2 = 0{\cdot}751$, the [A] matrix becomes :

$$\begin{bmatrix} 1+\mu_1 & -2c & 2s & 0 & 0 \\ & 2(\mu_2+2c^2) & -4cs & 0 & 0 \\ & & 2(\mu_2+2s^2) & 0 & 0 \\ & & & 2(\mu_2+2s^2) & -4s\left(1+c\frac{r_1}{r_2}\right) \\ \text{Symmetrical about the diagonal} & & & & 4\mu_1+2\mu_2\frac{r_1^2}{r_2^2}+4\left(1+c\frac{r_1}{r_2}\right)^2 \end{bmatrix}$$

With the molecular parameters already chosen (see Part I) this is converted to its numerical form and, via the [e] and [h] matrices and the frequency assignments, leads to the [d] matrix for the Class A_1.

$$\begin{bmatrix} 4{\cdot}382 & 0{\cdot}347 & -0{\cdot}108 \\ 0{\cdot}347 & 6{\cdot}360 & 0{\cdot}792 \\ -0{\cdot}108 & 0{\cdot}792 & 1{\cdot}200 \end{bmatrix} \times 10^5 \text{ dynes/cm.}$$

Similarly, for Class B_1 the [d] matrix is,

$$\begin{bmatrix} 4{\cdot}463 & 0{\cdot}168 \\ 0{\cdot}168 & 0{\cdot}157 \end{bmatrix} \times 10^5 \text{ dynes/cm.}$$

Comparison with the terms of the conventional V.F.P.F. leads to the constants for the latter given in Table V.

(*b*) FORMIC ACID.—Treated as the four-particle model of Fig. 3(*a*), the following valence-force co-ordinates may be used:

$$\text{Class } A': \quad \Delta_1 = \Delta r_1, \quad \Delta_2 = \Delta r_2, \quad \Delta_3 = \Delta r_3,$$
$$\Delta_4 = r_1(\Delta\beta - \Delta\gamma), \quad \Delta_5 = r_2\Delta\alpha.$$

These lead to the [**A**] matrix, when $M = m_3$, $c\alpha = \cos\alpha$ and $\mu_i = m_3/m_i$.

$$\begin{bmatrix} 1+\mu_1 & c\beta & c\gamma & s\gamma\frac{r_1}{r_3} \quad s\beta\frac{r_1}{r_2} & s\beta + s\gamma\frac{r_2}{r_3} \\ & 1+\mu_2 & c\alpha & -s\alpha\frac{r_1}{r_3} \quad 2s\beta & s\alpha\frac{r_2}{r_3} \\ & & 1+\mu_4 & s\alpha\frac{r_1}{r_2} + 2s\gamma & -s\alpha \\ & & & \begin{matrix} 4(1+\mu_1) + (1+\mu_2)\left(\frac{r_1}{r_2}\right)^2 \\ + (1+\mu_1)\left(\frac{r_1}{r_3}\right)^2 + 2ca\left(\frac{r_1^2}{r_2 r_3}\right) \\ - 4\left(c\beta\frac{r_1}{r_2} + c\gamma\frac{r_1}{r_3}\right) \end{matrix} & \begin{matrix} -(1+\mu_2)\left(\frac{r_1}{r_2}\right) \\ + (1+\mu_1)\left(\frac{r_1 r_2}{r_3^2}\right) \\ + 2\left(c\beta - c\gamma\frac{r_2}{r_3}\right) \end{matrix} \\ & & & & \begin{matrix} 1+\mu_2 + 2c\alpha\frac{r_2}{r_3} \\ + (1+\mu_4)\left(\frac{r_2}{r_3}\right)^2 \end{matrix} \end{bmatrix}$$

Symmetrical about the diagonal

By Torkington's method this leads, on substitution of the numerical values to the [**d**] matrix

$$\begin{bmatrix} 4{\cdot}778 & 0{\cdot}531 & 0{\cdot}323 & 0{\cdot}000 & -0{\cdot}087 \\ & 14{\cdot}05 & 2{\cdot}287 & 0{\cdot}018 & 0{\cdot}631 \\ & & 6{\cdot}460 & -0{\cdot}165 & 0{\cdot}656 \\ & & & 0{\cdot}148 & 0{\cdot}047 \\ & & & & 0{\cdot}981 \end{bmatrix} \times 10^5 \text{ dynes/cm.}$$

Symmetrical about diagonal

Again, there is no difficulty in identifying the valence force potential constants which are given in Table V.

For the four-particle model of Fig. 3(*b*) the valence-force co-ordinates leading to the [**a**] and [**A**] matrices are:

$$\text{Class } A': \quad \Delta_1 = \Delta r_3, \quad \Delta_2 = \Delta r_1, \quad \Delta_3 = \sqrt{r_2 r_3}\,.\,\Delta\beta;$$
$$\Delta_4 = \Delta r_2, \quad \Delta_5 = \sqrt{r_1 r_2}\,.\,\Delta\alpha.$$

and the [**A**] matrix becomes with $M = m_2$ and $\mu_i = \dfrac{m_2}{m_i}$.

$$\begin{bmatrix} \mu_3+\mu_4 & 0 & -\mu_3 s\beta\sqrt{\frac{r_3}{r_2}} & \mu_3 c\beta & \mu_3 s\beta\sqrt{\frac{r_1}{r_3}} \\ & 1+\mu_1 & s\alpha\sqrt{\frac{r_3}{r_2}} & c\alpha & -s\alpha\sqrt{\frac{r_1}{r_2}} \\ & & \begin{matrix} \frac{r_3}{r_2}(1+\mu_3) - 2\mu_3 c\beta \\ + \frac{r_3}{r_2}(\mu_3+\mu_4) \end{matrix} & -\mu_3 s\beta\sqrt{\frac{r_2}{r_3}} & \begin{matrix} c\alpha\sqrt{\frac{r_3}{r_1}} + \mu_3 c\beta\sqrt{\frac{r_1}{r_3}} \\ - (1+\mu_3)\sqrt{\frac{r_1 r_3}{r_2^2}} \end{matrix} \\ & & & 1+\mu_3 & -s\alpha\sqrt{\frac{r_2}{r_1}} \\ & & & & \begin{matrix} \frac{r_1}{r_2}(1+\mu_3) + \frac{r_2}{r_1}(1+\mu_1) \\ - 2c\alpha \end{matrix} \end{bmatrix}$$

Symmetrical about the diagonal

With the given frequency assignment, the derived [**d**] matrix is :

$$\begin{bmatrix} 7\cdot12 & 0 & 0 & 0\cdot08 & 0 \\ & 14\cdot28 & -0\cdot07 & 2\cdot12 & 0\cdot62 \\ & & 0\cdot58 & 0\cdot35 & 0\cdot13 \\ & & & 6\cdot40 & 0\cdot72 \\ \text{Symmetrical about diagonal} & & & & 1\cdot00 \end{bmatrix} \times 10^5 \text{ dynes/cm.}$$

The valence-force constants are given in Table V.

TABLE V

Force Constant	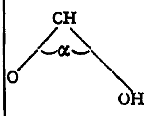	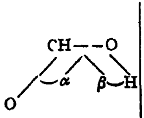	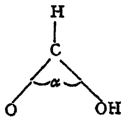	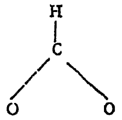
$f(\mathrm{C{=}O})$	$14\cdot0_0$	$14\cdot2_8$	$14\cdot0_5$	—
$f(\mathrm{C}\overset{\cdots}{-}\mathrm{O})$	—	—	—	$10\cdot8_2$
$f(\mathrm{C{-}O})$	$5\cdot0_6$	$6\cdot4_0$	$6\cdot4_6$	—
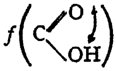	$0\cdot8_8$	$1\cdot0_0$	$0\cdot9_8$	—
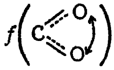	—	—	—	$1\cdot2_0$
$f(\mathrm{C{-}H})$	—	—	$4\cdot7_8$	$4\cdot3_8$
$f(\mathrm{O{-}H})$	—	$7\cdot1_2$	—	—
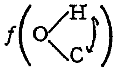	—	$0\cdot5_8$	—	—
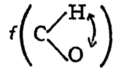	—	—	$0\cdot1_5$	$0\cdot1_6$
$f(\Delta r_{\mathrm{O-H}}\,\Delta r_{\mathrm{C=O}})$	—	$0\cdot0_0$	—	—
$f(\Delta r_{\mathrm{C-H}}\,\Delta r_{\mathrm{C-O}})$	—	—	$0\cdot5_3$	$0\cdot3_5$
$f(\Delta r_{\mathrm{O-H}}\,\Delta r_{\mathrm{C\cdot O}})$	—	—	$0\cdot3_2$	$0\cdot3_5$
$f(\Delta r_{\mathrm{C=O}}\,\Delta r_{\mathrm{C-O}})$	$1\cdot8_1$	$2\cdot1_2$	$2\cdot2_9$	$1\cdot9_0$
$f(\Delta r_{\mathrm{OH}}\,\Delta\alpha)$	—	—	$-0\cdot0_9$	$-0\cdot1_1$
$f(\Delta r_{\mathrm{C=O}}\,\Delta\alpha)$	$0\cdot6_1$	$0\cdot6_2$	$0\cdot6_3$	$0\cdot7_9$
$f(\Delta r_{\mathrm{C-O}}\,\Delta\alpha)$	$0\cdot6_4$	$0\cdot7_2$	$0\cdot6_8$	—
$f(\Delta r_{\mathrm{C-O}}\,\Delta r_{\mathrm{O-H}})$	—	—	$0\cdot0_8$	—
$f(\Delta r_{\mathrm{C-O}}\,\Delta\beta)$	—	$0\cdot3_5$	—	—
$f(\Delta\alpha\,\Delta\beta)$	—	$0\cdot1_3$	—	—

Discussion

It is fully appreciated that the results in Table V represent only one possible set of constants derived from the general quadratic potential function satisfying the frequencies observed in formic acid. These factors, however, are no more arbitrary than the force constants derived by more restricted methods which would be equally difficult of application in unsymmetrical molecules such as formic acid. As Torkington has pointed out, the elements of the [**d**] matrix can be adjusted when it is desirable to fit any well-established value for a force constant and, in particular (what would be very helpful in our present state of ignorance) any theoretical indication of the negligible value for certain of the cross-term constants can be written into the final solution by such adjustment. Apart from Torkington's own findings, the generally significant value of the constants in Table V is obvious: thus the concordant values for *f*(C═O) in three calculations, 14·15 ± 0·15, and the sensible decrease of *f*(C—H) in going from the acid to the ion, conforming to the frequency change 2943 → 2816 cm.$^{-1}$, may be cited in this connection. Accordingly, without pursuing the finer details of the picture, the following aspects of the force constant values deserve attention.

The *f*(O—H) bond-stretching constant is lower than that usually ascribed to this bond (cf. Herzberg,[12] p. 193; 7·66). This can be explained by the lengthening of the O—H bond by intramolecular forces. A comparison with the OH radical and H_2O molecule shows a consistent change in this respect.

	OH	H_2O	H . COOH
r(OH) Å:	0·971	0·958	0·98 [17]
f(OH) in 10^5 dynes/cm. . .	7·12	7·76	7·12

Similarly the change in *f*(C—H) on going from the acid to the ion may be related to a partial change in the state of hybridization of the carbon atom in these two structures.

The values obtained for the carbon-oxygen force constants are of especial interest and a comparison with those in a number of other molecules may be made.

TABLE VI

Molecule	CO	CO_2	C_3O_2	CH_2CO	CO_3''	CH_3OH
Force constant × 10^{-5} dynes/cm.						
Linnett [18]	18·9	15·5	14·2	12·3	—	—
Wu [19]	—	15·9	16·0	12·1	6·2	5·8
r(CO) × 10^8 cm. . . .	1·12	1·15	1·20	1·225	1·33	1·43

Methyl alcohol and formaldehyde correspond to the conventional single and double carbon-oxygen bonds, the values for carbon suboxide and carbon dioxide being taken to indicate appreciable triple-bond character. Although the *f* values of 14·1 and 6·4 found in H . COOH would accordingly suggest values of the bond-order somewhat in excess of 2·0 and 1·0 respectively, the reality of that condition is doubtful. Thus, if Gordy's approximate relation [20] for carbon-oxygen bonds,

$$f = 1{\cdot}67\, N\left(\frac{8{\cdot}8}{r^2}\right)^{\frac{3}{4}} + 0{\cdot}30$$

is solved for *N*, the values are 1·94 and 0·90 respectively. These values differ only insignificantly (and in the unexpected direction) from 2·0 and 1·0, and they are not consistent with the orders suggested solely on the basis of the bond lengths: i.e. 1·71 and 1·30 (see Part I). These inconsistencies may arise from the uncertainty in the " standard " *f*-values and their dependence upon the cross-terms included in the potential function.

---

[17] Davies and Sutherland, *J. Chem. Physics*, 1938, **6**, 755.

[18] Linnett, *Quart. Rev.*, 1947, **1**, 73.

[19] Wu, *Vibrational Spectra and the Structure of Polyatomic Molecules* (Edwards, Michigan, 1946).

[20] Gordy, *J. Chem. Physics*, 1946, **14**, 305.

In the present instance, a reference to the treatment of formic acid as an unsymmetrical three-particle system shows that the expression equated to $4\pi^2 \sum_{i=1}^{3} \lambda_i^2$ (a term fixed by the acceptance of the set of fundamental frequencies) is of the form :

$$f(\mathrm{C{=}O})A + f(\mathrm{C{-}O})B + f\left(\mathrm{C}{<}^{\mathrm{O}}_{\mathrm{OH}}\updownarrow\right)C + \frac{2}{m_3}[f_{12}(c^2 - s^2) + f_{13}(r_2 sc)] - 2f_{23}scr_2\frac{1}{m_3}.$$

A, B and C are positive constants and a consideration of the remaining terms shows that, provided $f_{12} > f_{13}$ as is both generally expected and certainly found in practice, then the inclusion of the cross-terms inevitably increases the values of $f(\mathrm{C{=}O})$, $f(\mathrm{C{-}O})$ and $f\left(\mathrm{C}{<}^{\mathrm{O}}_{\mathrm{OH}}\updownarrow\right)$. Thus the apparently higher values of the bond force constants in the present treatment may arise from the inclusion of a more complete set of cross-terms than was used for the other molecules. In general, there is everything to be said for including these cross-terms in the carboxylic acid where appreciable bond interaction is anticipated.

Resonance with an ionic structure has provided a commonly advocated interpretation of the (classically) unexpected features of the carboxylic group. Thus Pauling[21] based his comments on the possible analogy between the —NO_2 and —COOH groups. If this were significant, then the bond orders and force constants of the carbon-oxygen bonds would tend in the direction of equality. Whilst the bond lengths certainly conform to this behaviour, the force constants do not. It is difficult to see at present which, if either, of these two criteria provides the correct assessment. Mulliken, Riecke and Brown[22] have concluded that there is pronounced hyperconjugation in all carbonyl compounds. If this feature were present in an extended version in the carboxyl group, a structure representable electronically as shown would be a possibility,

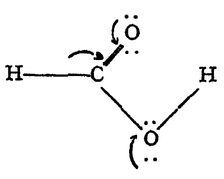

This model would appear to be in sensible agreement with most of the results presented in this study of formic acid: e.g. the (C—H) and (O—H) force constants are on the low side, whilst both carbon-oxygen values may be taken as on the high side of their norms. The bond-length $r(\mathrm{C{=}O}) = 1{\cdot}27$ Å is one of the apparently inconsistent items.

The foregoing discussion has related principally to the bond-stretching force constants. Qualitative deductions at most can be based on the remaining terms of the potential function, if only because of the absence of any accepted set of "normal" values for these factors.

The deformation force constant for the OCO angle is (in units of 10^5 dynes/cm.) near 1·0 in formic acid and increases to 1·2 in the formate ion. This increase is expected from the additional repulsion between the oxygens when they share the ionic charge. The values are both understandably higher than is frequently found for deformation constants. Comparing the C—H and O—H deformation constants, it is seen that the former is notably low and, for an X–H deformation, the latter is perhaps high. These are readily accepted features.

---

[21] Pauling, *The Nature of the Chemical Bond* (Cornell Univ. Press, 1939), pp. 187 *et seq.*

[22] Mulliken, Rieke and Brown, *J. Amer. Chem. Soc.*, 1941, 63, 41.

Of the cross-term constants, much the most significant is $f(\Delta r_{\mathrm{C=O}}\,\Delta r_{\mathrm{C-O}})$: the different solutions give this as 2·0 ± 0·2 × 10^5 dynes/cm. This high value is a measure of the degree of coupling between the electrons forming the two bonds. Its range of values agrees exactly with that found by Torkington [9] in the closely related NO_2 molecule: a value of 1·4 occurs for the same factor in the linear N_2O molecule. Coulson, Duchesne and Manneback [23] have suggested that such cross-terms arise from resonance, atomic interaction, and hybridization effects. All these contributions would be expected to be positive in the present instance, which accounts qualitatively for the large value observed. The same authors indicate that $f(\Delta r\Delta\alpha)$ for non-linear triatomic molecules will be of the same order as $f(\Delta r_1\Delta r_2)$. Values of 0·6 to 0·7 are consistently obtained for the cross-term in question, and it is a satisfactory feature of the results that $f(\Delta r_{\mathrm{C=O}}\,\Delta\alpha)$ and $f(\Delta r_{\mathrm{C-O}}\,\Delta\alpha)$ are sensibly equal: in the formate ion they are reduced to a single factor. The greater value of $f(\Delta r_{\mathrm{C-H}}\,\Delta r_{\mathrm{C=O}})$ than of $f(\Delta r_{\mathrm{C-H}}\,\Delta r_{\mathrm{C-O}})$ may be indicative of hyperconjugation to the double-bond such as is mentioned above. Finally, the zero value of the cross-term $f(\Delta r_{\mathrm{O-H}}\Delta r_{\mathrm{C-O}})$ is entirely reasonable.

The author wishes to express his gratitude to Dr. Mansel Davies for much helpful discussion and encouragement. Acknowledgment is due to the Royal Society Grants Committee for the provision of a calculating machine.

The Edward Davies Chemical Laboratories,
University College of Wales,
Aberystwyth.

[23] Coulson, Duchesne and Manneback, *Contribution a l'etude de la structure Moleculaire* (Liege, 1948).

B. OPTICAL METHODS OF INVESTIGATING CELL STRUCTURE

I. MICROSCOPICAL APPARATUS—INSTRUMENT DESIGN AND TECHNIQUE

INTRODUCTORY PAPER

OPTICAL METHODS IN CYTOLOGY

By J. T. Randall

Received 3rd August, 1950

Cells are for the most part small objects of the order of size of 5 to 50 microns, and the cytologist is concerned with the demonstration and understanding of structural detail within them. The microscope has always, therefore, been a fundamental physical tool in cytology. During the last twenty years or so advances in physics, and a better appreciation of the value of the tools of physics in the understanding of biological problems, have led to a much closer collaboration between workers from the two fields of science. One of the consequences of this is the present Discussion, which is largely concerned with new (and the elaboration of old) optical techniques in the study of biological problems. The proper use of the microscope and the spectrograph, and their union in the field of microspectrography will receive a large share of the available time. The methods, assumptions and associated calculations underlying the work of the Stockholm school in the cytological use of ultra-violet radiation have been the subject of considerable controversy during recent years, and it is proper that these matters should be thoroughly discussed so that the implications of this important pioneer work shall not be any longer misunderstood. I shall return to some aspects of these questions later. But meanwhile I think it important that we should not forget the wider implications of optical methods in cytology. In order that our Discussion shall not become too narrow and distorted I shall take a rather broad view of the field in these opening remarks.

In the first place, the importance of microscopic methods should not blind us to the value of the macroscopic ones of ordinary spectroscopy in the study of cells. Examination of red blood cells or yeast cells * in suspension by such means gives us a great deal of information about the haemoglobin or cytochrome components, as Keilin [1] and others have shown. But it is only rarely that a macroscopic method can give us information relating to components of a cell, unless indeed those components have already been isolated by some chemical or physical means, in which case their cytological identity may well be in doubt. Such approaches are valuable as accessory methods, particularly in the clarification of the biochemical mechanism so closely bound up with structure. Haemoglobin may be studied (*a*) by a macrospectrometric examination of the cells containing it; (*b*) by a microspectrometric study of single cells;[37] the isolated solution,[2] and the crystals [3] prepared from such solutions. For the most part, however, this Discussion will centre on microscopic and microspectrometric methods of studying cells. Nevertheless, it is important to realize that even in such an arbitrarily chosen method as indicated by the title of this Discussion, we are by implication drawing on a very large number of techniques to some extent foreign to our main theme. A successful attack on the study of cells requires a very broad approach combining, wherever possible, a number of methods.

---

* Dhéré [31] in 1906 was the first to show that the ultra-violet absorption of yeast cells at 2600 Å was due to the purine and pyrimidine constituents of the (ribose) nucleic acid.

[1] Keilin and Hartree, *Nature*, 1940, **164**, 254.

[2] *Haemoglobin*, ed. Roughton (Butterworth, London, 1949).

[3] Perutz, *Proc. Roy. Soc. A*, 1949, **195**, 474.

Before the meeting enters into the detailed discussion of more or less precise optical methods for the study of cells it is instructive to survey the larger field very briefly, in order to consider not only what methods are available, but what kind of information the methods are likely to yield, having at least some regard to the techniques and difficulties associated with the various methods.

The growth, differentiation, and architecture of cells depends ultimately on the assembly of molecules into particular structures. Such structures may in themselves contain the enzymes responsible for the chemical dynamics of that or some other part of the cell at any given time. Mitochondria have, for example, been suggested as the seat and origin of ribose nucleic acid.[4] *

At the present time one of the most valuable methods of obtaining evidence about the molecular architecture of the cell is the electron microscope. As a rough figure good electron microscopes are not yet able to resolve neighbouring objects whose distance apart is much less than 30 Å. The electron microscope is at present performing a valuable function in giving detailed information on the micromorphology of cells or their components. Examples of importance are the detailed structure of the nuclear membrane,[5] the myofibrils of vertebrate muscle,[6] the microstructure of spermatozoa,[7] and vaccinia virus.[8] It will be noticed at once that the examples I have given are of two types:

(i) Material consisting of whole, comparatively untreated, cells;
(ii) Cellular components.

Attempts to sub-divide cells by new methods of sectioning are being developed,[9, 10] but are not yet entirely successful.

The electron miscroscope may also be induced to give information on crystalline extracts of secretions or other cellular material, e.g. edestin, insulin, and catalase,[11] thus providing an important link with X-ray crystallography.† More important from our immediate point of view is the indication that the electron microscope may have a considerable future, especially in the study of material of type (i), relating to the cytochemistry and chemical architecture of cells, as distinct from structure unrelated to function. This possibility is being pursued in a number of ways: (*a*) the slow and perhaps painful development of electron stains of a specific nature ‡ (Bell, Danielli and Lamb, unpublished); (*b*) the study of cells specifically treated by solvents or enzymes to remove particular components.

The possibilities and difficulties of improving the resolving power of electron microscopes beyond their present figure have been considered by many, particularly by Gabor,[12] who has shown theoretically that a diffraction pattern of the object obtained by means of a coherent beam of electrons may be reconstructed optically to give detail down to 5 to 10 Å If this scheme should show the success it promises, the possibilities (considered merely from the viewpoint of this Discussion) of adding considerably to the functional information on cells are very important. More recently Scherzer[12a] has discussed the problem from a different standpoint.

---

[4] Ludford and Smiles, *J. Roy. Micro. Soc.*, 1950, **70**, 194.

* As Wilkins [40] points out, a slightly out-of-focus object gives rise to photographs simulating phase-contrast and absorption effects. Great care must therefore always be taken to ensure accurate focusing in ultra-violet work.

[5] Callan and Tomlin, *Proc. Roy. Soc. B*, 1950, **137**, 167.

[6] Draper and Hodge, *Austral. J. Expt. Biol.*, 1949, **27**, 465.

[7] Randall and Friedlaender, *Expt. Cell Res.*, 1950, **1**, 1.

[8] Dawson and MacFarlane, *Nature*, 1948, **161**, 464.

[9] Baker and Pease, *ibid.*, 1949, **163**, 282.

[10] Newman, Borysko and Swerdlow, *Science*, 1949, **110**, 66.

[11] Hall, *J. Amer. Chem. Soc.*, 1949, 71.

† The crystal may not normally grow in a habit best suited to give the information most wanted by the X-ray crystallographers.

‡ Phosphomolybdic and phosphotungstic acids do not appear to be specific.

I have introduced this paper by a consideration of some of the features of electron microscopy in relation to cells for two reasons. Firstly, the electron microscope is essentially an optical instrument and it is, I think, essential at the outset of a discussion such as this to approach our subject in a broad and fundamental way. Secondly, I think that our knowledge of cells will increase more rapidly whenever we are able to bring to bear the techniques of the optical and electron microscopes on the same material.

The application of X-ray diffraction techniques has usually been applied, for example by Astbury[14] and collaborators, and by Bear,[15] to fibrous material such as muscle which forms an organized syncytium, or to intercellular material such as collagen. The study of molecules in solution by X-ray[16] diffraction or optical scattering methods[13] involves, essentially, isolation of the material to be studied and lies outside the scope of the present meeting. The proper assessment, however, of light scattering by cellular components is of the greatest importance in microspectrography of biological material. X-ray absorption methods, both in relation to the microscopic image, and as a cytochemical tool, have been well considered by Engström in his paper at this meeting and elsewhere.[17] The possibility of electron diffraction in the study of biological material and crystals is at present being examined.

Most of the methods so far mentioned lie outside the scope of the normal biological laboratory. We now come to the range of wavelengths more conventionally regarded as optics; but even here our considerations stretch in wavelength from 2000 Å to several microns. Within this range several methods and correspondingly different types of technique and information are involved:

A Visible Microscopy	(1) Good apochromatic instruments. (2) Phase-contrast. (3) Fluorescence microscopy. (4) Polarization microscopy. (5) Interference microscopy.
B Ultra-violet Microscopy	(1) Conventional refracting instruments of quartz or ultra-violet transmitting components (with or without phase). (2) Modifications of (1) to allow observation of living cells and detailed absorption measurements.(with or without phase). (3) Reflecting microscopes for achromatic photography of cells in ultra-violet. (4) Reflecting microscopes combined with u.-v. spectrometers
C Infra-red Microscopy	Reflecting microscope and infra-red spectrometer.

A. Standard microscopical equipment, though by no means always as good as it should be, will remain a valuable adjunct of all cytological work. Two points only of a technical nature will be mentioned here: that the objective surfaces are not always accurately figured may be seen from the interferograms published by the manufacturers; and that immersion liquids and coverslips are in urgent need of standardization.

---

[12] Gabor, *Proc. Roy. Soc. A*, 1949, **197**, 454.
[12a] Scherzer, *J. Appl. Physics*, 1949, **20**, 20.
[13] Oster, in *Progress in Biophysics*, 1 (Butterworth, London, 1950).
[14] See, for example, Rudall in *Progress in Biophysics*, 1.
[15] Bear, *J. Amer. Chem. Soc.*, 1945, **67**.
[16] Riley and Herbert, *Biophysica Acta*, 1950, **4**, 374.
[17] Engström, *Acta Radiologica*, Suppl. **53** (Stockholm, 1946).

In spite of the long-standing inadequacy of the theory of the complex microscopic image, there is still too great a tendency to interpret images beyond the limits indicated by theory. As few physicists, and fewer biologists, have taken the trouble to understand the theory a word of caution is not out of place here.

Phase-contrast microscopy, in spite of the slow realization of its possibilities, has come to stay and is of great value in the study of the medium-scale structure of living cells.[18] It is also proving to have a special value in relation to ultra-violet microscopy. I refer here not to the direct use of phase-contrast in the ultra-violet,[19] but to its use in choosing a suitable field in the visible prior to ultra-violet measurement or photography. The papers by Davies and Walker [20] make further reference to this aspect.

The phase-contrast optical system is as yet primarily a tool for the study of living cells, whereby small objects or structure within a cell differing only slightly in refractive index from their surroundings may be distinguished. The limits to resolution fundamental to all optical instruments apply equally to this.

The method of fluorescence microscopy is receiving little attention in this Discussion,[21] but its possibilities as a cytochemical and structural tool should not be ignored.

The polarizing microscope has long been used in the study of cells and detailed accounts have been given by Frey-Wyssling [22] and Schmidt.[23] By its very nature, the method is particularly valuable in strongly oriented plant or animal material (plant walls or sperm-heads). By this means it is easy to observe birefringence. The determination of the thickness of the observed object is, however, often less easy as it may well lie near the limit of resolution. Fundamental determinations of orientation or concentration of a given cell component, such as nucleic acid in a sperm-head, are not therefore easy and the method is not devoid of deep pitfalls for the unwary. Swann and Mitchison have recently made improvements by means of which path differences as small as a few Ångstroms can be measured.

A further important application of the method has recently been made by Wilkins and others [24] in the study of nucleoprotein crystals of tobacco mosaic virus in the living cell (leaf-hair cells of the tobacco plant). It has not so far proved possible to isolate such crystals from the cell and the direct observation of a specific substance in a living cell is probably unique. A most interesting physical point is that the lamellae of virus rods forming the crystal are about the same thickness as the virus rod is long. The separation between layers is *ca.* 3000 Å. In consequence, optical diffraction effects analogous to Bragg reflexions in X-ray diffraction may be observed in the polarization microscope with this material. Observations on material extracted from cells (e.g. nucleic acid) have frequently been made. This type of application has its repercussions on cytology, but cannot be discussed further here. Dichroism in the ultra-violet and infra-red is briefly discussed later in this paper.

The interference microscope has been proposed at various times over a number of years and is not of course confined to biological material. The method depends on the interference of two light beams that have travelled almost identical path lengths: the difference in path is due entirely to the object under examination. Linnik [25] used two identical microscopes for the purpose. Dyson,[26] by an ingenious device, has succeeded with one.

---

[18] Hughes in *Progress in Biophysics*, 1 (Butterworth, London, 1950).

[19] Ludford and Smiles, (unpublished).

[20] Davies and Walker, this Discussion.

[21] Seeds and Wilkins, this Discussion.

[22] Frey-Wyssling, *Submicroscopic Morphology of Protoplasma and its Derivatives* (Elsevier, 1948).

[23] Schmidt, *Die Doppelbrechung von Karyoplasma, etc.* (Berlin, 1937).

[24] Wilkins, Seeds, Stokes and Oster, *Nature*, 1950, 166, 127.

B. Ultra-violet microscopy has been known for some long time, as the work of Köhler [32] and Barnard [27] shows; it has, as far as the purpose of this Discussion is concerned, two main objects. The first relates in an obvious way to the size of the structural unit involved. The resolving power of an optical instrument is given by $0{\cdot}61\ \lambda/\mu \sin \theta$ where λ is the wavelength, μ the refractive index, and θ the half-aperture of the objective. Given comparable optical quality it should, therefore, be possible to obtain a factor of two on resolving power by this means. No great direct use of this has so far been made; on the one hand the quality of ultra-violet transmitting objectives has not been particularly good; on the other, interest has centred on the use of ultra-violet to distinguish between particular chemical components of cells. This aspect of the subject is so well-known that I shall now refer to certain features which I hope will receive more detailed attention at this meeting.

Since 1936 [28] Caspersson and his collaborators have carried out a great deal of pioneer work in the use of ultra-violet microscopy as a cytological method. This work has depended, as indeed does all quantitative ultra-violet miscroscopy, (i) on the development of suitable microspectrographic equipment and (ii) on the now well-known strong absorption characteristics of the purine and pyrimidine components of the nucleic acids in this region of the spectrum. The much less marked, but still valuable, absorption of the heterocyclic amino acid tryptophane, and the aromatic amino acids phenyl alanine and tyrosine, have also been used to give information about certain proteins. There would seem to be a number of important considerations still to be resolved, or at least re-examined, at this meeting. The Stockholm school has always attempted to be quantitative in its approach, but a great deal of ultra-violet work has been qualitative in the extreme, and correspondingly lacking in value. The time has come to decide whether such work has much real value for the future.

The greater part of the work of Caspersson has been on fixed material. In view of the lack of detailed cytochemical knowledge of the processes of fixation it can legitimately be asked to what extent results on such material may be applied to considerations of the living cell. Until a direct quantitative comparison has been made with the ultra-violet microscope on living and fixed material, we do not know how to assess these results. This comparison alone is no easy task and brings out one fundamental difficulty of which Caspersson has been well aware from the beginning. In early papers [29] he examined the scattering of light by colloidal systems, since it was obvious that for ultra-violet absorption measurements to have any real meaning corrections would have to be made for scattering. The misgivings of some critics of the later work are in part due to lack of knowledge as to how such corrections may properly be made in a given case, and what degree of accuracy may be expected in the final result. The precipitation effects of fixation will depend on whether the precipitate is particulate or homogeneous, and on the refractive index of the surroundings. The application of standard scattering theory is obviously difficult; in experimental work on fixed cells use is frequently made of the scattering observed at wavelengths lying to the long wavelength side of the main peak. Experimentally there is no doubt that the use of fixed material presents much the easier problem. To what artefacts, physical and biological, the processes involved give rise is one of the real problems I hope to see discussed. The questions raised by Wilkins[40] are very relevant in this connection; for it must not be forgotten that the ultimate aim of all this work is to gain new knowledge of the living cell.

---

[25] Linnik, *Compt. rend. U.S.S.R.*, 1933, 21.

[26] Dyson, *Nature*, 1949, **164**, 229.

[27] Barnard and Welch, *Practical Photomicrography*, (Arnold, London, 1925).

[28] Caspersson, *J. Roy. Micro. Soc.*, 1940, **60**, 8.

[29] Caspersson, *Kolloid-Z.*, 1932, **60**, 151; 1933, **65**, 162 and 301.

A further difficulty arises from the effects of the ultra-violet radiation on the living cell. In order to obtain photographs or measurements on living cells considerable dosages have to be used. In recent experiments Davies[20] has shown that 5×10^3 ergs/cm.^{2} are necessary to obtain a photograph of sufficient detail on the most suitable sensitive film. A cell nucleus may occupy a volume of the order of 10^{-10} cm.$^{-3}$. Unless, therefore, the absorption coefficient is very low the dosage of ultra-violet required to give a photograph may be the equivalent of as much as 10^5 roentgens; the equivalent temperature rise is *ca.* 0·2° C. This last figure will, however, be affected by the thermal properties of the surroundings of the cell. Energy absorption of the order of magnitude indicated by these calculations is sufficient to inactivate tobacco necrosis virus.[36] The effects of ultra-violet radiation on cells are serious and careful consideration must always be given to the inferences that may be made under any prevailing experimental conditions. Wyckoff[42] was one of the first to obtain ultra-violet photographs of tissue culture cells.

Significant developments of the last few years have been on items indicated in headings B and C above. The work of Davies and Walker[20] shows the extent to which "conventional" refracting microscopes of high numerical aperture (N.A.) may be linked with monochromators and the photographic method, including microphotometry as a quantitative means of estimating absorption in living cells. The further development of this work should enable a more comprehensive comparison to be made between the results for living and fixed material under well-defined conditions. For the first time (see also Mellors[41]) physical measurements of dosage have been made, and an apparatus built by means of which an ultra-violet cine-film of living cells can be produced and studied.

Such an apparatus has disadvantages which are removed to some extent by the use of the reflecting microscope. The achromatic characteristics of this instrument and its large working-distance are now so well known as to need little further comment. This meeting will be valuable in bringing out the advantages and limitations of (*a*) aspheric objectives[33] as designed by Burch; (*b*) objectives with spherical or quasi-spherical surfaces;[31, 34] (*c*) objectives of type (*b*) combined with refracting components.[34] The work described by Seeds and Wilkins[31] on tobacco mosaic virus material and nucleic acid fibres is a good indication of what can be done in this field with well-designed instruments which also allow for the temperature variation of the specimen.

Further distinctions between designs of ultra-violet apparatus are apparent from the papers in this volume. The value to fundamental biology of ultra-violet microscopy may arise in two different ways: structural (high resolving power) and cytochemical (specific absorption). Instruments of high numerical aperture[34] (say 1 to 1·3) can be used to give highly detailed pictures of cells, and the extent to which this will be exploited during the next few years will depend on the quality of the objectives. Calculations by Caspersson showed that accurate absorption measurements cannot be expected on objects less than 3-4 λ (i.e. *ca.* 1 μ) (where λ is the irradiating wavelength).* On the other hand, resolving power at λ 2600 is *ca.* 0·1 μ. Structural information may therefore extend to much smaller objects than those used to give precise cytochemical data.

---

[30] Caspersson, *Skand. Arch. Phys.*, Supp., 1936, **73**, 8.

[31] Dhéré, *Compt. rend. Soc. Biol.*, 1906, **60**, 34.

[32] Köhler, *Z. Wiss. Mikrosk., etc.*, 1904, **21**, 129.

[33] Barer, this Discussion.

[34] Norris and Wilkins, this Discussion.

* Wilkins,[40] however, thinks it is possible to obtain absorption measurements with an accuracy of *ca.* 10 % on objects 1 to 2 λ in size.

In the conventional ultra-violet microscope a suitable wavelength is selected by means of a monochromator, falls on the specimen, and is ultimately received by a suitable detector. Another method is to allow the whole spectrum of the source to pass through the specimen and achromatic optical system of a reflecting microscope so that an image of the object falls on the slit of the spectrograph (spectroheliograph technique).[37] One photographic plate should then contain all the relevant information on the given object. For some types of object it is convenient and useful to move the photographic plate in its own plane during exposure.[38]

The electron microscope allows us to see objects of molecular size and the assembly of molecules into aggregates and crystals. In optics the directions of maximum and minimum absorption of the electric vector (pleochroism) may be used to give valuable supplementary information about assemblies of molecules or particular groups of molecules. The decisive nature, or otherwise, of such information depends not only on the electric characteristics of the molecules but on their spatial arrangement. In such a comparatively simple case as a purine or pyrimidine crystal the ring systems may not all be crystallographically equivalent. Furthermore, there may be an optimum direction of absorption of the electric vector in the plane of the ring. These considerations are not meant to be comprehensive in any way, but to point to the necessity for great care in the interpretation of such data in all relevant regions of the spectrum. Paracrystalline material, such as oriented layers of tobacco mosaic virus, or fibres of sodium thymonucleate, may be at least, if not more suitable, for such investigations as crystalline material: it is by no means always possible to make a crystal grow in the preferred habit for such optical measurements to be made. Pleochroic measurements are well suited to instruments such as the reflecting microscope which can be used satisfactorily in the ultra-violet, visible, and infra-red regions of the spectrum.

c. Earlier remarks have made it clear that reflecting microscope systems may be used in the infra-red. What precise value this application will have for the future depends on a number of factors as yet unresolved. The presence of water in most biological material is perhaps one of the lesser disadvantages attending application of microspectrography to the infra-red.

The very multiplicity of vibrational absorption peaks makes interpretation difficult and unspecific. One likely field of application lies in the study of a particular material under a variety of conditions. (The example of muscle in different stages of contraction is an obvious one; Elliott and others have recently examined native and denatured insulin [43] and Fraser with a high resolution microspectrometer has begun work on collagen.[44]) On sounder basis is the use of the method on small crystals derived from, or having biochemical importance in relation to, living material. These matters and others relating to them will no doubt receive much discussion.

I have sketched in this Introduction some of the important factors of the wider optical approach to cytology in the hope that the value of the integrated approach, employing different methods, will not be neglected by those working in this field. Whatever else may happen in these discussions, the symposium should at least achieve one important result:

---

[35] Gray, *J. Opt. Soc. Amer.*, 1950, **39**, 719, 723; 1950, **40**, 283.

[36] Lea and Smith, *Parasitology*, 1940, **32**, 405.

[37] Jope, *Haemoglobin* (Butterworth, London, 1949), p. 213.

[38] Holiday, *J. Sci. Instr.*, 1937, **14**, 166.

[39] Thorell, *Acta Med. Scand.*, 1947, Suppl. **200**.

[40] Wilkins, this Discussion.

[41] Mellors, this Discussion.

[42] Wyckoff, Eherling and Ten Louw, *J. Morph.*, 1932, **53**, 189.

[43] Elliott, Ambrose and Robinson, *Nature*, 1950, **166**, 194.

[44] Fraser, this Discussion.

the precise laying down of the principles and limitations of the microspectrographic method as applied to biological material. Let us make that our aim so that the record of the meeting provides a landmark in the history of the subject.

Wheatstone Physics Laboratory,
King's College,
Strand, London, W.C. 2.

A REFLECTING MICROSCOPE OF 1·3 NUMERICAL APERTURE

By K. P. Norris and M. H. F. Wilkins

Received 31*st July*, 1950

The construction and use of a focusing polychromatic ultra-violet microscope objective of 1·3 numerical aperture, formed by adding a fused quartz amici lens to a reflecting objective, is described.

The complete achromatism of the reflecting microscope makes it specially suitable for study of ultra-violet absorption spectra of living cells. With present designs[1, 2, 3] the numerical aperture (N.A.) of a purely reflecting system cannot exceed about 0·7, and, to increase the N.A. to the highest value, *ca.* 1·3 which may be used on living cells, it is necessary to add an immersion lens to the mirror system. A hemispherical normal incidence lens[1] only increases the N.A. by a factor equal to the refractive index of the lens (in our case fused quartz $\mu \simeq 1{\cdot}5$). If, however, a simple amici lens is added to a mirror system of only 0·6 N.A. The resultant aperture is increased to 1·3 by a factor equal to the square of the refractive index. Such an amici lens must, however, be refocused for different wavelengths.

Our reflecting objective with an amici lens has the following characteristics which enable it to satisfy the various requirements of microspectrographic work.

(i) The objective has the highest possible N.A., a negligible central obstruction (19 % of N.A.), and is entirely free from spherical aberration at all wavelengths transmitted. As a result, the light distribution in the image may reproduce as nearly as possible the variation of transmission from point to point in the object.

(ii) The exceptionally high N.A. enables almost all the forward scattered light from the object to be collected, thus reducing errors in absorption measurements.

(iii) Light passing through the objective is twice reflected by front aluminized glass mirrors, and once refracted at a fused quartz-air interface. As a result, transmission of ultra-violet light through the system is exceptionally high and radiation damage to the specimen is made a minimum.

(iv) Although not achromatic, the objective may be changed in focus from one wavelength to another and this motion is exact, rapid and simple in operation.

(v) Three spherical surfaces only are used on the optical parts of the objective and there is, therefore, no difficulty in obtaining these.

---

[1] Burch, *Proc. Physic. Soc.*, 1947, **59**, 41.
[2] Seeds and Wilkins, *Nature*, 1949, **164**, 228.
[3] Norris, Seeds and Wilkins (in preparation).

Experimental

Design of the Mirror System.—The first designs used by us had N.A. 0·5 and 45 % central obstruction.[3] Experimental work using the microscope interferometer [3] showed it was possible, by increasing the ratio of the radii of curvature of the two mirrors, to attain a design with only 19 % central obstruction with exact spherical correction to above 0·6 N.A. The objective is made large (diameter of concave mirror 2½ in.) so that the focal length (1·5 mm.) is not inconveniently small. The field of the objective is not large, but is adequate for microspectrographic work.

Effect of Central Obstruction.—Dall,[4] by careful visual inspection of critical objects through a telescope, has decided that central obstruction up to 20 % has no detectable effect on the image. When the central obstruction is increased above 20 %, contrast in fine absorbing detail is reduced progressively owing to the fact that, in the image of a point, relatively more light is thrown into the diffraction rings than into the central Airy disc. This effect is usually not very obvious until the central obstruction is greater than 35 %.

Amici Lens.—The principle of the amici lens, which is added to the reflecting objective, may be understood by reference to Fig. 1. ABCDE is a sphere of fused quartz of refractive index μ, with centre O and radius r. The dotted spheres have radius μr and r/μ. P and Q, which are two points on these spheres, are then the aplanatic points of the sphere ABCDE. Thus, for an object placed at Q all rays appear to diverge from the point P. If the sphere is cut along the line BE, and BEA is removed, it becomes quite practicable to place an object at Q, and the system will remain aplanatic if the space between Q and the lens is filled with a liquid of the same refractive index as that of the lens.

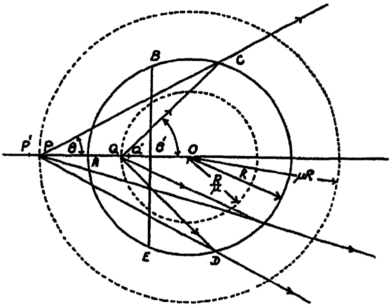

FIG. 1

If sin θ is the N.A. of the objective which is to receive the rays diverging from P, we have $\sin \theta' = \mu \sin \theta$. Furthermore, since the N.A. is defined as $\mu \sin \theta'$, where μ is the refractive index of the material in which the object is immersed, the total numerical aperture of the system is $\mu^2 \sin \theta$. For fused quartz $\mu^2 \simeq 2{\cdot}25$. Thus when an amici lens is added to a mirror system of 0·58 N.A. the resulting objective has an aperture of 1·3.

Refocusing.—We have already seen that the aplanatic points of the sphere are at a distance μr and r/μ from the centre of the lens. When the refractive index changes by $\delta\mu$ the aplanatic points move distances $r\delta\mu$ and $-r\delta\mu/\mu^2$. Let P′ and Q′ be two such points. In practice it is inconvenient to move the large and heavy reflecting objective on a fine adjustment so that it is always in focus on the point P. It was decided to fix the objective and point P, and to move the lens and the stage to maintain the object at the other aplanatic point. In order to do this the lens must move $r\delta\mu$ and the object $r\delta\mu + (r\delta\mu/\mu^2)$.

$$\therefore \frac{\text{movement of lens}}{\text{movement of object}} = \frac{r\delta\mu}{r\delta\mu + (r\delta\mu/\mu^2)} = \frac{1}{1 + (1/\mu^2)}.$$

If the objective is to be used between two wavelengths where the refractive index of quartz is μ_1 and μ_2 then

$$\frac{\text{movement of lens}}{\text{movement of object}} = \frac{1}{1 + (1/\mu_1\mu_2)}.$$

For the range 546 mμ to 238 mμ ratio of movements = 0·687. This is the ratio of distances the lens and object must be moved in order to keep the objective in focus and free from spherical aberration as the wavelength is changed.

The total movements necessary to maintain the objective in focus are proportional to the radius r of the amici lens; the reasons for keeping these small are as follows.

(i) Many of the spectral lines from a mercury arc are either multiple or broad, resulting in chromatic aberration which is proportional to r.

(ii) Since the stage moves more than the lens the movement is restricted by the thickness of immersion oil. Allowing for a thickness of oil of 0·18 mm.

---

[4] Dall, *J. Brit. Ast. Ass.*, 1938, 48, 163.

the radius of the lens must be less than 0·16 in. for the objective to be used over the range 546 to 234 mμ.

(iii) The depth of focus of the objective is only 100 mμ and it is desirable to keep the total movement as small as possible in relation to this. The ease of focusing the objective correctly increases as the total movement decreases. As a result, r was made as small as possible, and along these lines an immersion lens compatible with the use of a 0·18 mm. quartz coverslip was designed.

Immersion Liquid.—Johnson and Martin [5] have described a method of preparing suitable immersion liquids for an ultra-violet monochromatic objective. For our objective these liquids were unsuitable and an investigation [6] resulted in n-hexadecane being used. Although the dispersion is not equal to that of quartz, it is still possible to correct the objective for all wavelengths.

Mechanical System.—The mechanism for moving the lens and stage in the right ratio for adjustment with wavelength consists of a number of links and levers driven by the micrometer screw S (Fig. 2). When the lens is adjusted for use at a particular wavelength the object is then brought into focus by a further fine adjustment screw which rotates the stage about an axis through the centre of the balls A and A′. This motion is independent of the adjustment for change of wavelength. All these motions are rotations about axes through the centres of steel balls in trihedral holes in steel. The motions are kinematic and therefore free from backlash, and, to a first approximation, independent of wear. The micrometer screws for wavelength change and fine adjustment are turned by 9 in. long levers, so that a movement of the end of the lever of 1/4 mm. over a scale moves the stage 100 mμ. When using the microscope, the object is first focused in visible light using the fine adjustment lever; next, ultra-violet light is admitted and the wavelength lever is moved to a previously determined position on the scale. The fine adjustment is then used to give a focusing range through the object. By photographing pin-holes with the levers set in varying positions it is possible to find a position for both levers, such as that the second-order spherical aberration introduced by the immersion liquid is compensated by using the lens at a focus slightly removed from the aplanatic points for that wavelength. In this way the instrument is calibrated in terms of wavelengths.

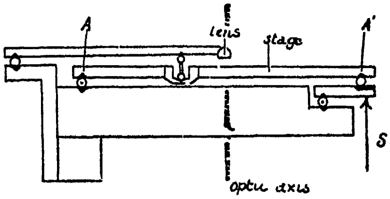

FIG. 2

The preliminary adjustment of the objective in visible light is similar to the adjustment of a dry objective.[3] Firstly, the mirror system is adjusted for coma zero spherical aberration using a pin-hole object without a coverslip. The pin-hole is then covered by a fused quartz coverslip, the amici lens is added, and oil placed between the lens and the slide. By viewing the image of a pin-hole, the large objective may be moved on a fine adjustment fitted to the microscope body until the separation of the lens and the mirror system is such that the image above and below focus has a similar appearance; the complete objective is then free from spherical aberration. The final adjustment consists in centring the amici lens until the centre of the field shows no coma.

General Arrangement of Apparatus.—The condenser used with this objective is a purely reflecting system of 0·81 N.A. and 30 % central obstruction, and the light obstructed in the objective is removed by the obstruction in the condenser. Since the hole in the condenser concave mirror is always larger than the convex mirror it is necessary to interpose stops so that the light which passes into the objective has been focused by the condenser. A fused quartz right-angled prism is used to reflect light from the field stop into the condenser. Interposed between the field stop and the prism is an inclined mirror which reflects light from an alternative phase illumination system into the microscope. This illumination is used for focusing the objective in visible light and for photographing objects under phase contrast.

For work on living material the microscope is enclosed in a Perspex incubator with all the microscope controls outside. Under the base are heaters so that the temperature of the stage may be maintained constant. A kinematic ball-bearing mechanical stage is provided and is driven by a pantograph outside the incubator. This device not only allows the stage to be moved in any direction, but it facilitates searching and returning to a particular object on the slide for further study.

---

[5] Johnson and Martin, *J. Sci. Instr.*, 1928, **5**, 337; 380.

[6] Norris (in preparation).

We wish to thank Prof. J. T. Randall, F.R.S., for advice and encouragement; Dr. C. R. Burch, F.R.S. and Mr. W. E. Seeds for useful suggestions; and Mr. H. E. Gunn and Messrs. R. and J. Beck Limited for making the optical parts.

Wheatstone Physics Laboratory,
and Medical Research Council Biophysics Research Unit,
Kings College,
London.

SOME ASPECTS OF MICROSPECTROGRAPHY

By M. H. F. Wilkins

Received 8th August, 1950

Simple theory is given for errors in microspectrography due to (i) use of very small objects, (ii) refractile and non-refractile objects being slightly out of focus, (iii) aberrations in the microscope objective. Dichroism of nucleic acid is also discussed.

The present paper is a discussion of some aspects of ultra-violet microspectrography to which attention has been drawn by preliminary experimental work in our laboratory. Some of the ideas presented have not been tested experimentally and it may be found necessary to modify some of the conclusions, most of which have been derived by very rough theory, and some of which are probably by no means new.

Minimum Size of Object for Microphotometric Study.—Caspersson[1] has dervied theoretically the minimum width of a strip object, the absorption of which can be measured to 1 to 2 % as 2 to 3 λ for an objective of 1·3 numerical aperture (N.A.), but states that the practical limit for accurate microspectrography is 3 to 4 λ.

The writer thinks that absorption measurements may usefully be made on objects as small as 1 λ and, as much absorbing matter in living cells is in the form of small bodies of about this dimension (*ca.* 0·25 μ), the feasibility of such measurements has biological importance.

An exact diffraction theory of this problem does not appear to be available, but the physical arguments given below should be roughly correct. Caspersson used the Abbe theory and considered the total absorption of energy by a small body. It should be stressed that the results below do not contradict those of Caspersson but merely place the matter in a somewhat different perspective. The Abbe theory undoubtedly holds for very small condenser apertures, but when the condenser has an appreciable N.A. it is well known that diffraction patterns become smaller, roughly in inverse proportion to the sum of the N.A.'s of the condenser and objective. This may be seen as follows. If we apply the Abbe theory to a wavefront proceeding in a direction such that it falls just within the numerical aperture of the objective we find that diffracted light is collected by the objective for angles of diffraction twice as great as for axial illumination. However, because only the diffracted light on one side of the direct light is collected, the contrast in the image is reduced and the image of small opaque regions of the object appears grey and not black, and accurate microphotometry of the image is not possible. For this reason, in the calculations below, the condenser N.A. is taken, as a compromise, at half that of the objective. Also it is desirable to use appreciable condenser N.A. to reduce out of focus phase-contrast effects and to decrease the size of the diffraction patterns. In practice it is found that the resulting diffraction pattern is similar to that produced when an incoherently illuminated object is viewed with an objective of N.A. equal to the mean of the N.A.'s of the condenser and objectives. Using this approach we have calculated the intensity in the centre of the image of an opaque strip. For the unidimensional case the intensity of light at points distant y from the geometrical image of a bright line object is given by $\frac{\sin^2 x}{x^2}$, where $x \quad y\frac{\pi 2 \sin\theta'}{M/\lambda}$ and $\sin\theta'$ is the mean of the N.A.'s of the condenser and objective and M is the magnification.

---

[1] Caspersson, *Skand. Arch. Physiol.*, 1936, **73** Suppl. 8.

(For the circular aperture of objective used in practice, the diffraction fringes are less intense but the pattern is slightly enlarged.) The intensity in the centre of the image of an opaque strip of width a is given by $2\int_{a/2}^{\infty}\frac{\sin^2 x}{x^2}dx$ and because $\int_{0}^{\infty}\frac{\sin^2 x}{\lambda^2}dx \quad \pi$ the ratio of the illumination outside the strip to that in the centre is

$$\frac{1}{\pi}\int_{a/2}^{\infty}\frac{\sin^2 x}{x^2}dx.$$

By graphical integration the results in Table I were obtained for an objective of 1·0 N.A. and condenser 0·5 N.A.

TABLE I

Width of Strip in λ	Intensity of Light in centre of Image of Opaque Strip as % of Background Intensity	Apparent Density measured at Centre of Image when strip is not opaque		
0·9	15	0·243	0·444	0·62
1·3	7	0·272	0·522	0·796
2·6	2	0·292	0·568	0·920
3·9	0·7	0·299	0·592	0·974
∞	0	0·301	0·602	1·0

The optical density measured at the centre of the image for different widths and densities of the strip is also given. In small rod-shaped bodies of thickness about equal to their width the density cannot be high—for 40 % nucleic acid content the density is 0·25 in a thickness of 0·25 μ. Hence, if λ is about 0·25 μ the density may be determined to about 20 %. If the thickness is 0·4 μ the error is about 3 %. The accuracy could be increased somewhat by the use of an objective of 1·3 N.A. All the errors will be roughly doubled if round or square objects are used instead of strips. In infra-red microscopy small objects may be surrounded by an opaque screen thus making possible use of objects of width as small as is compatible with measurement of the transmitted energy.

Effect of high N.A. on Path Length of Light Rays through the Specimen.—Parallelism of light rays and resolving power are incompatible; hence in microphotometry non-parallel light must be used. The degree of divergence of the light rays passing through a specimen is determined by the refractive index of the specimen and the N.A. of the condenser, if large objects are used. With objects of dimensions comparable with the resolving power, or in regions of the specimen close to a rapid change of absorption, diffraction spreads the rays further. If the object consists of a plate of uniform thickness with its plane perpendicular to the axis of the microscope the effect of a uniformly illuminated finite condenser N.A. may be calculated, and corresponds to an increase in effective thickness of the specimen.[2] Objects of spherical symmetry [1] show no such effect and cylindrical rod-shaped objects with their length in the image plane show much less effect than plates. Lack of knowledge of the precise shape of small bodies clearly makes this type of correction of their measured absorption unreliable or impossible.

Effect of Aberrations in the Microscope objective.—When, in a microscope, one relates the intensity distribution in the image to the variation of transmission in the object one generally assumes a perfect objective. It may not be sufficiently realized the extent to which imperfections in the objective modify the image and cause errors in microspectrography. Provided the objective has been adjusted so that no coma or astigmatism is apparent in the centre of the field, we need only consider symmetrical deviations from spherical of the wavefront issuing from the objective. As most microspectrography can be performed using a very small field, off-axis aberrations are normally of little significance and, in general, an objective for microspectrography may obey the sine conditions less closely than an objective intended for normal use (cf. Caspersson [1]).

Let us take a common example of spherical aberration, an objective with a zonal aberration. In a case considered by Conrady [3] the aberration is $\lambda/4$ and the intensity in the centre of the Airy disc is reduced to 73 % of that due to a perfect objective and light energy is increased considerably in the second diffraction ring. Such an objective will give about 10 % intensity in the centre of the image of an opaque strip 2λ wide as compared with 1λ for a perfect objective (see above). It is clear that ability to perform photometric measurements on small objects is seriously limited when errors reaching the Rayleigh limit [4] are present in an objective, although the performance of the objective for visual use and its resolving power are altered little. In fact, for measurements on small objects a perfect objective of half the N.A. would in many ways be preferable to the above objective with zonal aberraton. The intensity of light diffracted out of the Airy disc is, for small errors, proportional roughly to the square of the error on the wavefront. Hence, to achieve about 2 % accuracy on objects $2\ \lambda$ wide the above zonal error should not exceed $\lambda/10$.

A second important case is that of a "cobbled" objective (e.g. Burch [5]) which has been hand-figured. In this case the error on the wavefront may be roughly represented as a sine wave and it can be shown that an extreme difference of phase of $\lambda/5$ gives about 10 % of the light energy diffracted into a region distant from the Airy disc about n times its diameter, where n is the number of cobbles across a diameter of the objective aperture. Hence, if n is 20, 10 % light intensity is diffracted into the central regions of the image of an opaque strip object of width as great as $20\ \lambda$ and 20 % intensity for a round object of diameter $20\ \lambda$. If diffraction is to produce less than 1 % light in the images of opaque objects the cobbling should not be higher than about $\lambda/15$ for the wavelength used.

In general, one may say that small local errors such as zones, cobbling, etc., are particularly objectionable in an objective for microspectrography as they cause light to be diffracted into the images of large opaque objects; slowly varying errors covering large parts of the N.A. affect performance only on objects of a size close to the resolving power of the objective. Clearly an objective should be tested on small opaque objects.

Central, or any other, obstruction also affects performance. 20 % central obstruction of N.A. causes the maximum of the Airy disc to drop 7 %, but most of this energy is diffracted into the first diffraction ring (calculated by K. P. Norris) and thus does not limit accuracy of

[2] Blout, Bird and Grey, *J. Opt. Soc. Amer.*, 1950, **40**, 304.
[3] Conrady, *Mon. Not. R.A.S.*, 1918, **79**, 575.
[4] Rayleigh, *Phil. Mag.*, 1879, **8**, 403.
[5] Burch, *Proc. Physic. Soc.*, 1947, **59**, 41.

photometry except on the smallest objects. Higher central obstruction may be objectionable in some cases.[6]

Effects due to the Object being out of Focus.—(*a*) PHASE CONTRAST EFFECTS.—It is well known that if the condenser of a microscope is stopped down differences of refractive index in the object become visible as differences of intensity in the image. An interpretation of this effect has been given to the writer by Dr. C. R. Burch, F.R.S., and the general nature of the argument is as follows. Let parallel light fall on E, a small object of dimensions comparable with the resolving power of the objective F (Fig. 1).

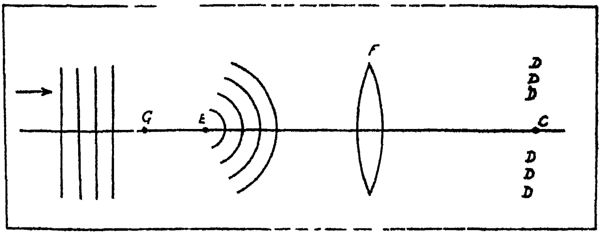

FIG. 1.

Let the plane wavefront falling on E be represented in phase and amplitude by the vector OA (Fig. 2). Vector OB represents this light when retarded (due to E having a refractive index higher than its surroundings) by phase angle θ. ($\theta = 2\pi$ for retardation λ.) But OB = OA + AB; hence the light falling on the object plane may be considered as a uniform plane wave OA plus a wave generated in the region of E of amplitude and phase AB. Because E has a small area, AB is diffracted into a spherical wavefront of uniform amplitude. OA is focused on axis at C in the back focal plane of F, while AB is spread out in diffraction spectra DDD. . . . In the image plane of the microscope, interference between the light from the spectra and the central rays produces even illumination in the field. In the phase microscope[7] OA is accelerated in phase (generally about 90°) to OC which then interferes with AB to produce an image in which the intensity varies in a manner corresponding to the variation of θ. If, however, our microscope is focused not at E but at G, then for rays on axis OA, and OB have the same relative phase but for off axis directions OB lags behind OA. For an angle of diffraction ϕ the phase difference P is approximately $\frac{EG}{2}\sin^2\phi$ (see Fig. 3). The resultant phase ω, consider-

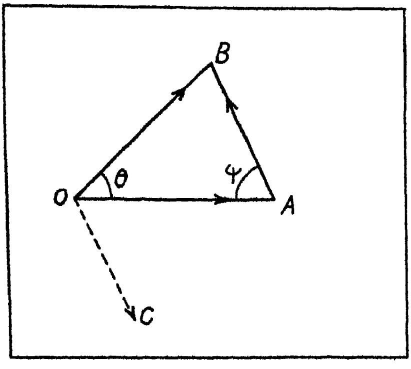

FIG. 2.

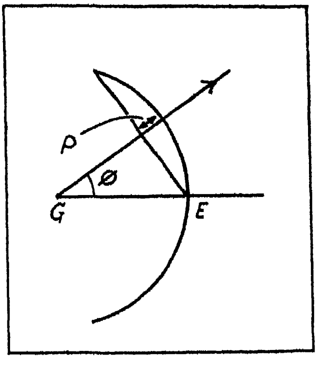

FIG. 3.

---

[6] Dall, *J. Brit. Astr. Ass.*, 1938, 48, 163.

ing all values of ϕ, is given by a circular phase amplitude diagram, and is half the extreme phase. Hence, if the N.A. of the objective is 0·7, $\omega \sim \frac{EG}{8}$. This is also about correct if the N.A. is 1·2 and E is not very small but has diameter equal to λ or the resolving power.

If ψ is equal to ω (Fig. 2) the image of E will be of maximum darkness and appears as if it were viewed with a phase-contrast microscope. The light removed from the image of E is spread in the form of a faint bright halo around E. Reverse effects are obtained if the microscope is focused above E.

Example—If θ is 60° ($\lambda/6$) an almost black image of a small object is obtained if a microscope of N.A. 1·0 is defocused approximately λ, which is about within the depth of focus when the condenser N.A. is not large. An object consisting of 0·3 μ thickness of 50 % nucleic acid gel immersed in water (difference of refractive index about 0·15) will produce such effects in the ultra-violet. The optical density of such a specimen at 2600 Å is only 0·36.

The fraction of N.A. of the objective filled by diffracted light is inversely proportional to the diameter of E. Hence the extent of defocusing necessary to produce a certain change of illumination in the image is proportional to the square of the size of the object, and therefore large objects appear "out of focus" before much phase-contrast effect shows. For rod-shaped objects the diffracted wave is cylindrical; its phase amplitude diagram is the Cornu spiral, and the phase-contrast effects are rather less than for round objects.

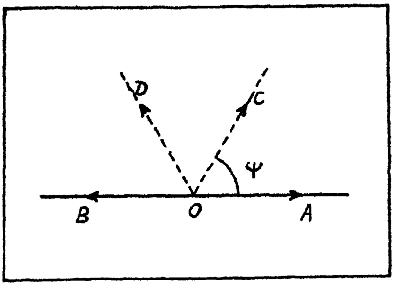

FIG. 4.

(*b*) DEPTH OF FOCUS.—If the image of a small pinhole is viewed out of focus (distance λ for N.A. 0·7) so that the edge of the wavefront is $\lambda/4$ different in phase from the centre, the intensity at the centre of the Airy disc drops about 20 % compared with the in-focus image. (This follows from the phase amplitude diagram of the out-of-focus wavefront which is a quadrant of a circle.) The energy lost from the Airy disc appears[8] in the diffraction rings, and smaller changes of focus may often be appreciable.

(*c*) OUT-OF-FOCUS EFFECTS ON NON-REFRACTILE OBJECTS.—Let OA (Fig. 4) be the light falling on a very small opaque object. When in focus OB is the diffracted wave $|OB| = |OA|$. If, by defocusing, OA is altered in phase $\lambda/6$ to OC then the resultant $OD = OC + OB$ and $|OD| = |OA|$. Hence, the object appears non-absorbing. To produce 50 % change of intensity ω is $\lambda/8$ and the extreme phase difference for the diffracted wave is $\lambda/4$ (cf. above). This effect (which may be used to test objectives) is symmetrical; on both sides of focus a black dot appears as a dark ring with a white centre.

(*d*) OBJECTS WITH REFRACTION AND ABSORPTION.—The effect of combined absorption and refraction is for the amplitude of OB (Fig. 2) to be less than OA. All the information we have about the object is contained in the amplitudes and phases of the diffraction spectra in the back focal plane of the objective. If we cannot decide by focusing what is the true value of θ we cannot find the ampltiude of OB.

(*e*) DEPTH OF FOCUS OF THE PHASE MICROSCOPE.—By making the phase ring have a small transmission[7] the amplitude of the direct light may be made equal to that of the diffracted light even though θ is very small.

---

[7] Martin, *Nature*, 1947, 159, 827.

Hence very small changes of θ may be detected but the depth of focus is not much different from the case in (*c*) above.

(*f*) EFFECT OF FINITE CONDENSER APERTURE.—If the condenser has the same N.A. as the objective, each plane wave from the condenser supplies light to two points in the object plane in different phases and, if the two points are separated at least by a distance equal to the resolving power, every possible phase difference exists. The result is that the object appears to be illuminated incoherently. Hence all phase effects discussed above disappear and the image is obtained by summation of the intensities of the Airy diffraction patterns due to each point in the object. If the condenser N.A. is $1/n$ that of the objective, phase effects appear for objects of dimension smaller than n times the resolving power.

(*g*) CONCLUSIONS TO BE DRAWN FROM THE ABOVE.—It is clear that appreciable errors in absorption measurements may result if the microscope is not focused accurately. These errors become very large if small objects are studied (e.g. mitochondria[8]), the condenser is stopped down, and short wavelengths used. It has sometimes been claimed that "good images" of living material, i.e. images full of clear detail, are obtained with the ultra-violet microscope when the condenser is stopped down; such images are clearly not a measure of absorption. It would be very desirable for more microscopists to state in publications the N.A. of the condenser as well as that of the objective.

It must not be supposed that the presence of peaks on curves of apparent absorption with wavelength signify real absorption, because phase contrast effects will also produce peaks due to dispersion in the region of an absorption band. Absence of haloes round the images of small bodies is a good check of focus, but the best way to avoid errors of this kind is to use a microscope which is either exactly achromatic or may be changed in focus exactly from one wavelength to another. The object is then viewed with a wavelength of light which is not absorbed, and the microscope focused until the image disappears as nearly as possible.[9] Phase contrast gives more exact focus, however.[10] If photographic methods of recording are used, it is easy to guard against spurious effects by inspecting the images at different wavelengths but the objective requires to be free from spherical aberration over the range of wavelengths used.

Effect of Pleochroism on Absorption Measurements.—Ultra-violet dichroism has been searched for by Caspersson [11] in various objects in cells and when present has been used to determine the orientation of nucleic acid molecules. Recently, however, Commoner [12] has given a criticism of the microspectrographic cytochemical work of the Caspersson school (and other workers using similar methods) and has suggested that a large part of this work is invalid because the dichroism of nucleic acid has not been taken into account. As this criticism has received much attention it is desirable to state why the criticism appears unsound.

Dr. Commoner's argument is as follows. If nucleic acid molecules are oriented so that the maximum and minimum optical densities for polarized 2600 Å light are 1·0 and 0, the apparent density, using unpolarized light, will be about 0·3 instead of 0·5 if the nucleic acid were disoriented. With half the above quantity of nucleic acid the densities obtained are almost equal. We have measured the birefringence of 100 % oriented nucleic acid (about 30 % water) and found it to be very high, viz. between 0·05 and 0·10. Therefore the path difference due to birefringence of visible light will be at least 50-100 Å before appreciable error due to dichroism can result. Such a path difference causes an object to appear brightly illuminated when viewed between crossed nicols and occurs only in exceptional biological objects, e.g. the grasshopper sperm head as studied by Caspersson.

---

[8] Ludford and Smiles, *J. Roy. Micro. Soc.*, 1950, **70**, 194.

[9] Seeds and Wilkins, this Discussion.

[10] Davis and Walker, this Discussion.

[11] Caspersson, *Chromosoma*, 1940, **5**, 605.

[12] Commoner, *Science*, 1949, **110**, 31.

It might be argued that systems may occur where the high birefringence of nucleic acid is compensated by birefringence due to large quantities of oriented protein. This is possible, but unlikely, and if one wishes to consider unlikely possibilities it may be worth while, in view of the interest in this matter, to consider one of the many possible pleochroic systems which could give rise to much more complicated phenomena, and would be much more intractable to experimental approach, than the example chosen by Dr. Commoner. Such a possibility is as follows. It may well be that there is considerable dichroism when the electric vector for ultra-violet light lies in different directions in the plane of the asymmetric purine and pyrimidine rings (I am indebted to Prof. C. A. Coulson, F.R.S., for this information). Suppose, in a region of a cell, all the rings are arranged in space so that the direction for greatest absorption of the electric vector is normal to the plane of the slide. In this case the absorption of the specimen may be almost zero for rays normal to the slide (as in the case when the condenser is stopped down) and the absorption may be independent of the direction of polarization of the incident light (and, furthermore, the specimen may appear non-birefringent). Absorption will increase as the condenser aperture is opened and inclined rays pass through the specimen. Analysis of such an absorbing object requires the mineralogist's procedure of passing plane-polarized pencils of light through the specimen in different directions, and it would be necessary to add the universal stage (with tilting motions) to the biologist's already complicated ultra-violet microscope. The writer finds it comforting to think that these complications will not be found necessary, and that there will be little reason to consider pleochroism except in those cases where there is evidence (e.g. obtained from birefringence) of a high degree of molecular orientation in the specimen.

I wish to thank Prof. J. T. Randall, F.R.S., for advice and encouragement, many colleagues, in particular Dr. A. R. Stokes, for much helpful discussion, and Mrs. I. Trott for help with the diagrams and the integration.

Medical Research Council,
Biophysics Research Unit,
King's College, London.

ASPECTS OF ULTRA-VIOLET AND INFRA-RED MICROSPECTROGRAPHY WITH THE BURCH REFLECTING MICROSCOPE

By R. Barer

Received 3rd July, 1950

Some of the difficulties encountered in microspectrography with reflecting microscopes are discussed. The development of objectives achromatic over all the regions of the spectrum enables the technique to be greatly simplified. The object is illuminated by the total radiation emitted by the source and the transmitted radiation is analyzed by means of a suitable spectrometer. In the ultra-violet region photographic recording enables the absorption characteristics of the object to be observed simultaneously at a large number of wavelengths. Present infra-red techniques do not allow simultaneous recording but nevertheless continuous sources of radiation can be used. This feature permits the position of absorption maxima and the presence of spectral fine structure to be determined with accuracy. These techniques can be used with polarized radiation for work on dichroism of oriented structures. The types of problem for which such methods are particularly suitable are indicated. Infra-red microspectrophotometry is limited chiefly by the long wavelengths employed, resulting in low resolution in the microscope, and by the relative insensitivity of present thermal detectors. It is rather doubtful whether the method can ever be applied to living cells. Even with dry cells the present indications are that the differences in infra-red absorption spectra obtained from such complex mixtures of proteins and other substances as occur in biological material are very slight. Technical improvements will be necessary before really useful information can be obtained from such material.

One of the main purposes of this Discussion is to assess the applications, validity, and limitations of microspectrographic methods. In this contribution it is proposed to refer briefly to certain techniques which have been developed during the last few years with the Burch reflecting microscope.[1] The types of problem for which these methods are particularly suitable will be discussed and some of the practical and theoretical limitations will be indicated. More consideration will be devoted to problems of infra-red rather than ultra-violet microspectroscopy, as the former is a much newer technique whose possibilities remain largely unexplored.

The most important single feature of the Burch microscope is its achromatism. This is of course true of any reflecting objective, but the special superiority of the Burch instrument lies in the fact that it uses aspherical, rather than spherical mirrors, which makes possible a greatly improved performance as regards correction of aberrations, increase of numerical aperture and reduction of obstruction ratio. The importance of these factors has been discussed elsewhere and will not be further referred to here.[2]

Ultra-violet Microspectrography.—Spectroscopic eye-pieces have long been used for the observation of the absorption characteristics of microscopic objects in the visible region. Their use depends on the availability of reasonably achromatic objectives. Such objectives have until recently not been readily at our disposal for work in other regions of the spectrum and the somewhat laborious procedure of illuminating the object with monochromatic light at a large number of separate wavelengths has had to be adopted.[3, 4] The purely reflecting objective is with certain minor reservations completely achromatic and can be used over a spectral range limited only by the reflectivity of the mirrors and the existence of suitable radiation detectors. It thus becomes possible to go back to the principle of the spectroscopic eye-piece for microspectrographic work in any region of the spectrum. This method was first employed with the Burch microscope in the ultra-violet region.[5] The principle used was to illuminate the object in the microscope by means of the total radiation emitted by the source, to focus an image on the entrance slit of a quartz spectrograph, and in this way to analyze the radiation transmitted by the object. The chief advantage of dispersing the radiation *after* passage through the object rather than before, is that with photographic recording it is possible to observe the transmission characteristics *simultaneously* at a number of wavelengths.[6] With certain types of material the illumination of the object by a broad and intense band of u.-v. light may seem objectionable but it must be remembered that even in techniques which employ monochromatic illumination, observations must be made at a large number of different wavelengths in order to obtain a spectral transmission curve. The new technique is seen to special advantage when a source such as a hydrogen discharge tube, which emits a continuous spectrum in the u.-v. region, is used. In this way, it is possible to obtain a smooth curve showing the transmission at every wavelength and not merely a series of separate points which have to be joined up. The value of this is that it allows the exact position of absorption maxima to be determined with accuracy and reveals the presence of spectral fine structure where this exists.

---

[1] Burch, *Proc. Physic. Soc.*, 1947, **59**, 41.

[2] Barer, *Trans. London Conference* (Optical Instruments, 1950, in press).

[3] Caspersson, *Skand. Arch. Physiol.*, 1936, **73**, suppl. 8.

[4] Caspersson, *J. Roy. Micro. Soc.*, 1940, **60**, 8.

[5] Barer, Holiday and Jope, *Biochim. Biophys. Acta*, 1950, **6**, 123.

[6] Barer in Bourne, *Cytology and Cell Physiology* (Clarendon Press, Oxford, 1950), 2nd. edn., Chap. 1.

The methods of analysis used in this method of microspectroscopy are in many ways similar to those which have been developed in the absorption spectroscopy of macroscopic samples. A very convenient method of calibrating optical density is to use a rotating logarithmic or stepped sector placed immediately in front of part of the slit. The image of the microscopic object is projected on to the remainder of the slit. With a suitable densitometer it is possible to match the optical density of any area of the image with a known optical density recorded at the same wavelength. It is of course essential that the illumination of the entire slit should be quite uniform, and preliminary tests to ensure this are necessary.

The Holiday logarithmic cam technique[7] is particularly useful for the study of very small image areas.[5] In this case a very short slit is used and the photographic plate of the spectrograph is moved at a logarithmically varying rate. In this way a " silhouette " of the absorption spectrum is obtained. The method, though qualitative, is very sensitive for the detection of spectral fine structure.

The main limitations of the technique, apart from the question of improvement of microscope design, are the lack of an ideal source of light, and the problem of illumination of the spectrograph. As regards the source, various types of mercury arcs are very useful where a number of intense, well-spaced lines are required, as is the case for many purposes, but the only really practical source of a truly continuous ultra-violet spectrum is the hydrogen discharge, the intensity of which is unfortunately low. The tungsten filament lamp is excellent for work in the near u.-v. and visible regions. As regards the spectrograph, there is no point in using an instrument of large aperture when high image magnifications are employed since under these conditions the collimator will not be filled with light. For cytological work the final image on the spectrograph plate should correspond as closely as possible to the image projected on to the entrance slit, i.e. the aberrations of the instrument, particularly astigmatism, should be as low as possible. A spectrograph of low aperture but high dispersion, and unusually well corrected optically, has been designed for this work by Mr. W. Weinstein.

For work on ultra-violet dichroism, the only modification required is to introduce some form of polarizer which is effective in the ultra-violet region. A Glan-Thompson prism cemented with glycerine has proved satisfactory and experiments are also being carried out on new types of polarizing films.[8] Possible errors due to the polarizing action of the spectrograph must be avoided. Some spectrographs show polarization effects to a much greater degree than others,[8, 9] perhaps due to a lack of complete symmetry between the two halves of the Cornu prism, and it is essential to carry out preliminary tests using a continuous spectrum in conjunction with a polarizer. Another puzzling source of error which has been found is the appearance of interference fringes of the Edser-Butler type, the cause of which was traced to reflections at the interface between the two halves of the polarizing prism.

---

[7] Holiday, *J. Sci. Instr.*, 1937, **14**, 166.

[8] Barer, *ibid.*, 1949, **26**, 325.

[9] Ellis and Kaplan, *J. Opt. Soc. Amer.*, 1935, **25**, 357.

What are the problems for which techniques of this type are specially useful ? In the first place, of course, the method is suitable for work on absorption spectrophotometry of very small quantities of material of biological interest, whether in the form of cells, fibres or crystals. For cytological work it can be used for much the same type of problem as has been investigated by Caspersson and others. The increased precision resulting from the use of a continuous spectrum may lead to a clearer understanding of the behaviour of proteins and nucleic acids within the cell, though I am afraid it is even likelier to show a still more complex state of affairs than has hitherto been realized. The investigation of spectral fine structure and small wavelength changes in absorption maxima in biological systems remains to be explored. The fact that the tryptophane absorption band differs slightly in human foetal and adult haemoglobins has already been pointed out,[10] and no doubt other examples will occur.

The optical properties of cells at wavelengths outside the 2500-3000 Å band deserve more attention,—other substances besides proteins and nucleic acids are present in cells ! Even in cases where no selective absorption can be found in a certain spectral region, it may be possible to learn something by the introduction of substances which do show strong absorption in that region. For example, an attempt was made to introduce certain carcinogenic hydrocarbons into cells in order to observe their distribution and metabolic changes, if any.[11] Many of these compounds show a series of absorption bands in the near ultra-violet region which are not likely to be confused with the absorption due to substances normally present in a cell. The analogy between such methods and the use of stains in the visible region will be apparent.

The use of polarized ultra-violet light has been mentioned above. The investigation of ultra-violet dichroism in crystals, fibres, and other oriented structures, over a wide spectral range may be very informative in revealing the orientation of specific constituents such as aromatic amino acids, purine bases, etc. Dr. Perutz will refer to such studies in more detail elsewhere in this Discussion.

Space does not permit more than a very brief reference to certain questions of fundamental importance in ultra-violet microscopy. The whole problem of the validity of ultra-violet absorption measurements on cytological material has been called into question as the result of recent work which has shown that the absorption of living cells may differ considerably from that of fixed material or cells which have undergone irradiation with ultra-violet light.[12, 13, 14] The mechanism of this change is far from clear. It may be related to changes in scattering by the cell,[13] the depolymerization of nucleic acids,[15, 16] or to changes in the state of orientation of cellular constituents.[17, 18] The question of scattering and other non-specific light losses is clearly of great importance. A pioneer attempt was made by Caspersson to calculate the influence and magnitude of some of these effects. Unfortunately the analytical difficulties involved are so formidable that it seems improbable that any full theoretical estimation will ever be possible. To mention only two points : (i) Caspersson's calculations are based on the Abbe theory of the formation of the microscope image and (ii) the Mie theory of scattering as applied to spherical particles only is considered. The Abbe theory is of course only an ap-

[10] Jope, in Roughton and Kendrew, *Haemoglobin* (Butterworth, London, 1949), p. 216.

[11] Barer, Berenblum and Jope, 1948 (unpublished work).

[12] Larionov and Brumberg, *Compt. rend. U.R.S.S.*, 1946, **54**, 267.

[13] Ris and Mirsky, *J. Gen. Physiol.*, 1949, **32**, 489.

[14] Bradfield and Errera, *Nature*, **164**, 532.

[15] Oster and Grimmson, *Arch. Biochem.*, 1949, **24**, 119.

[16] Oster and McLaren, *J. Gen. Physiol.*, 1950, **33**, 220.

[17] Commoner, *Science*, 1949, **110**, 31.

[18] Commoner and Lipkin, *ibid.*, 1949, **110**, 41.

proximation, as Caspersson himself points out, and a full diffraction theory of the microscope has yet to be evolved. Calculations on scattering by anisotropic particles give different results from those based on spherical particles. In biological systems one might expect a mixture of both types, as well as possible orientation effects. The estimation of light losses by reflection and refraction is also not simple. Estimates based on refractive index measurements in the visible region may be inaccurate as it is important to remember that the refractive indices of many substances are anomalous in the neighbourhood of absorption bands. The exact influence of different degrees of refractivity and absorption in different regions of the spectrum is also difficult to judge. The use of precipitant fixatives must certainly affect non-specific light losses as can easily be demonstrated by means of the phase-contrast and interference microscopes. In collaboration with Dr. Crawford,[19] an investigation on the action of various fixatives on living cells has been carried out using such methods of microscopy, and it appears that formalin or osmium tetroxide used under certain conditions produce the least change in the refractive properties of cells in the visible region. Even these substances, however, seem to exert hitherto unsuspected actions on the nuclei of some cells.

Whatever the cause of the observed variations in transmission of cells undergoing irradiation, the effect must clearly be fully investigated. It may be found that ultra-violet microspectrographic methods are incapable of giving accurate results with living material, but this would not necessarily invalidate the results obtained on fixed material. After all, most of our knowledge of cytology and cytochemistry is based on the examination of fixed material and although there may have been some misinterpretations and artefacts, there is no real reason for discarding all the results of such work. The physicist is fortunate in dealing with things which he can usually examine under controlled conditions. The biologist is less fortunate and has to make the best use of the difficult and variable materials provided for him by Nature.

Infra-red Microspectrophotometry.—The ultra-violet absorption spectra of many complex substances of biological interest suffer from the disadvantage that the absorption maxima are often rather broad and poorly defined. Thus, the spectra of two quite different substances may not always be easy to distinguish, particularly if only a narrow spectral range is observed. Despite the theories which have been put forward concerning the role and distribution of ribose-nucleic acid and desoxyribose nucleic acid in the cell, it is important to remember that they cannot at present be distinguished by means of ultra-violet absorption spectroscopy alone. Infra-red absorption spectra are, however, sometimes capable of giving much more precise characterization of organic compounds. The use of purely reflecting objectives has rendered possible the extension of this technique to microscopic specimens. The principle of the method adopted with the Burch microscope is similar to that used for ultra-violet microspectrography.[20] A slightly different mode of approach is necessary, however, due to the lack of direct photographic recording in most of the infra-red region. The usual detectors available are thermocouples, bolometers, and for certain wavelengths, photocells. This makes the simultaneous recording of transmission at a large number of wavelengths extremely difficult or even impossible. The radiation, after passage through an entrance slit, is dispersed by a prism of suitable material such as lithium fluoride or rock salt, and a narrow region of the spectrum is selected by means of an exit slit. The selected band is then focused on to the detector. The analyzing instrument is thus strictly speaking a monochromator, rather than a spectrograph. This has the disadvantage that the specimen is exposed to the entire radiation from the source during the time required to scan the desired range of the spectrum. The consequent heating of the specimen might be undesirable, though this has rarely been found to be serious in practice. The possibility of using an infra-red monochromator *before* the microscope so that the object is illuminated by a narrow band of infra red light should not be overlooked. The image could be focused with visible light and the area whose transmission it is desired to measure could be selected by means of an aperture behind which is placed the thermal detector. This technique would then resemble in many ways that adopted by Caspersson and others in the ultra-violet.

---

[19] Crawford and Barer, 1950 (in course of publication).

[20] Barer, Cole and Thompson, *Nature*, 1949, **163**, 198.

In our first experiments an attempt was made to obtain spectra by projecting a microscope image directly on to the entrance slit of the spectrometer. It was soon found that the energy available was too small to give reasonable readings without the use of very wide slits and, moreover, the aperture of the collimator mirror could not be filled. In order to overcome this, the microscope image was projected on to a screen containing a variable aperture which was used to select the area of the image whose transmission it was desired to measure. The light passing through this preliminary aperture was then condensed down by means of a spherical mirror. This device greatly increased the energy available and improved the illumination of the collimator. The magnification of the primary image at the screen was usually about 150-200 times, the final magnification being about 20-30 times. Although the full magnification of the microscope could not be used with the spectrograph available, it was nevertheless very convenient to be able to observe the image at a reasonably high magnification so as to enable the structure of the object to be studied, and the most suitable portion to be selected. It would of course be possible to use an objective of lower initial magnification, but then this particular advantage would be lost.

If it is desired to use polarized infra-red radiation for studies on dichroism, the simplest method is to allow the bundle of rays which have passed through the image-selecting aperture, to fall at the polarizing angle (19°) on a simple selenium mirror and thence to be reflected on to the condensing mirror. The specimen can then be rotated in order to observe dichroism. Transmission polarizers of the silver chloride [21] or selenium film [22] type could also be used. These are not easy to make of sufficiently large aperture, but have the advantage that they can be rotated without disturbing the specimen.

The sources of light available for infra-red microspectrophotometry are rather limited. Those most commonly used in macroscopic work are the Globar and Nernst filament. There is little to choose between these at wavelengths above 6 μ, but the Nernst filament is used at a higher temperature and emits much more visible light, which renders focusing, examination of the object, and optical alignment much easier. The main disadvantage of the Nernst filament is the high energy output in the near infra-red which may lead to errors due to scattering in the spectrometer. The use of carbon arcs for infra-red work has recently been suggested.[23] Although the energy emission is higher than that of the Nernst filament, the errors due to scattered short-wave radiation would be even more serious.

Let us now consider the special applications of infra-red microspectrophotometry, its limitations, and its possibilities. In the first place, it is clear that this technique has greatly facilitated work on small quantities of material. In principle, with the macroscopic technique, it should be possible to examine specimens which are no larger than necessary to cover the area of the widest entrance slit used. In practice,

[21] Newman and Halford, *Rev. Sci. Instr.*, 1949, **19**, 270.
[22] Elliott, Ambrose and Temple, *J. Opt. Soc. Amer.*, 1949, **38**, 212.
[23] Rupert and Strong, *J. Opt. Soc. Amer.*, 1949, **39**, 1061.

however, mechanical difficulties arise when it is attempted to mount such small quantities of material and in fact the use of a low-power microscope would be a convenience for many samples considerably bigger than the area of the slit. A simple system of this type has been described by Elliott *et al.*[24] and has been particularly useful for work on small fibres.

The specimens can be in the form of crystals, fibres, microscopic droplets or smears of waxy material. There is a special advantage to be gained by the use of the microscope for the examination of crystalline material. In the macroscopic technique it is often difficult or impossible to obtain single crystals large enough to cover the slit of the spectrometer and the material usually has to be examined in the form of a powder composed of micro-crystals. Such a powder gives rise to considerable light losses by scattering, reflection and refraction, and it is usually necessary to mount it in a medium such as liquid paraffin. This reduces scattering, but introduces other difficulties due to the absorption of the mounting medium itself. When a microscope is used, it is often possible to select small single crystals whose transmission can be measured without having to mount them in a liquid. It is of course necessary to select crystals which are reasonably well formed or else scattering may still be serious. In general, non-prismatic flat plates or needles are most suitable if serious reflection and refraction losses are to be avoided. The ability to use small single crystals and fibres is of great value in work on dichroism and should provide a useful auxiliary method in the crystallographic investigation of organic compounds.

What are the possibilities of infra-red microspectrophotometry in cytology? This is a question which further investigation alone can answer, but it is possible at this stage to assess some of the difficulties and limitations. In the first place, can the method be applied to structures of the order of size of single cells? Let us assume the formula $R = 0{\cdot}61\lambda/\text{N.A.}$ (where λ is the wavelength and N.A. the numerical aperture), for the resolving power of a microscope. The present Burch microscope has an N.A. of 0·65 so that the resolving power is roughly equal to the wavelength. Thus, if it is desired to cover the infra-red range up to 15 μ, the smallest object which could be resolved would be 15μ in diameter. On this basis, it might just be possible to examine the average transmission of portions of the nucleus and cytoplasm of at least the larger single cells. If microscopes of N.A. approaching 1·4 were available, the size of the smallest resolvable object would be reduced to about 6 μ. Even then it will be clear that there is no prospect of examining the smaller cellular constituents. Moreover, it is by no means certain that even those limits could be attained. According to Caspersson[3] an accurate quantitative estimate of absorption can only be made on particles of the order of 4λ in diameter. If his analysis is applicable to the infra-red region, then the smallest area which could be measured would be about 60 μ in diameter. This would render work on all but the largest cells somewhat impracticable. It is of course true that smaller areas could be observed if we were content to restrict the wavelength range. At $\lambda = 3\ \mu$ for example, the resolution with N.A. 1·4 would be about 1·3μ and the Caspersson limit would be 12μ. The latter figure is still large relative to cellular dimensions but the former corresponds to the order of size of bacteria. The quantitative validity of spectra obtained from such particles might however be rather doubtful. It should also be pointed out that the construction of infra-red microscopes of N.A. exceeding 1·0 would necessitate the use of a lens component. This could be made in such a way as to avoid the introduction of longitudinal chromatic error, but some restriction of the spectral range would be inevitable. Moreover, an immersion medium of suitable refractive index and dispersive power would have to be used and this might very well exhibit absorption bands in the same region as those of the object. In practice these difficulties may not be too serious and lens components of rock salt or thallium bromo-iodide might be used with immersion media such as liquid paraffin.

---

[24] Elliott, Ambrose and Temple, *J. Sci. Instr.*, 1950, **27**, 21.

The next question which is of considerable interest to the biologist is whether it will ever be possible to apply the method to the study of *living* cells. The difficulties here are formidable. With few exceptions, living cells must be examined in an aqueous medium, and all cells contain water. Water possesses a number of strong absorption bands in the infra-red region, and, indeed, workers in this field know all too well that the effect of even the small amount of water vapour normally present in the atmosphere can be very disturbing. It might conceivably be possible to work with extremely thin films of water and at wavelengths at which the absorption due to such films would not overshadow everything else. Another possibility is to use heavy water, which has a rather different absorption spectrum, provided that it did not affect the structure and viability of the cell. In this way, by the use of two different media it might be possible to derive the absorption spectrum of the object itself. Another factor to be considered is the possible action of the absorbed radiation on the cell. I have carried out preliminary observations on the action of short-wave infra-red radiations on living cells and the results suggest that they do not tolerate this treatment very well. For all these reasons it must be admitted that the prospect of applying the method to living material is extremely remote.

Even if we are content to restrict ourselves to the study of comparatively large areas of fixed cells, is infra-red spectrophotometry likely to yield any useful information from such complex material? The value of ultra-violet microspectrometry of cells rests upon the fact that some cellular constituents are known to be present in such quantities that their absorption at certain wavelengths is likely greatly to overshadow the absorption due to other substances which may be present. The position is rather different in the infra-red region, for the infra-red absorption spectrum gives what is essentially information concerning the presence or absence of certain specific chemical groups such as OH, CH, NH, CO, etc. In a complex molecule such as a protein, many such groups will be present and it may be wondered whether it is possible to distinguish different proteins by their infra-red spectra. This subject is still in its infancy, but the indications are that such differences as exist are relatively small and occur mainly at wavelengths greater than 6μ. These slight differences of band position and intensity are not easy to interpret and much more work on the comparison of spectra obtained from amino acids, polypeptides and proteins will be necessary.[25, 26] If this is the case with single proteins, how much more complicated will be the position in the living cell in which we have a mixture of proteins, lipoids, nucleic acids and other substances? Any observations on the infra-red spectroscopy of cells or tissues will almost certainly be largely empirical until the fundamental data on these classes of substances have been obtained and interpreted.[27, 28] The difficulties of examining such complex material are made even greater by using a microscope, for the amount of energy available is less and there is a consequent loss of spectral resolving power due to having to increase slit widths, and if the amplification of the small signals available is pushed to its limit the noise level and base-line instability may make quantitative measurements of transmission unreliable. If the recognition of different parts of the cell or different types of cells

[25] Dawson and Sutherland, *J. Amer. Chem. Soc.*, 1947, **69**, 2074.
[26] Astbury, Dalgliesh, Darmon and Sutherland, *Nature*, 1948, **162**, 596.
[27] Blout and Mellors, *Science*, 1949, **110**, 137.
[28] Blout and Fields, *ibid.*, 1948, **107**, 252.

is to depend on small differences of frequency and height of absorption bands, some improvement in the performance of infra-red spectrophotometers, particularly in the detecting devices, is highly desirable, and until such improvements have taken place, the full value of the technique as applied to cytological material will not be realized. The fact that the most important differences seem to occur at wavelengths longer than 6μ is particularly unfortunate owing to the low energy emission of most sources at such wavelengths and the lack of sensitive photocell detectors such as are available in the 3μ region. The minimum area which can be studied is also adversely affected by having to work at these wavelengths.

These conclusions may seem to be pessimistic but nevertheless there are a number of ways in which infra-red microspectrophotometry could be applied to cytological material. In the first place, we can attempt to alter the chemical constitution of the cell by various procedures. One method of approach is to extract materials from the cell and to follow the structural and spectroscopic changes which occur. Preliminary work on the extraction of nerve tissue with lipoid solvents has already been reported [20] and comparisons between the spectra from unmyelinated nerves from various species have been made with those from extracted myelinated nerves. The use of other extraction procedures such as those of Bensley,[29] Szent-Gyorgyi,[30] and Pollister and Ris[31] may also be suggested. Other means include digestion with enzymes such as ribonuclease and desoxyribonuclease. Another method of investigation has already been referred to in the discussion on ultra-violet microspectroscopy, namely the introduction of substances with rather specific absorption spectra. The difficulty in the case of infra-red work is to find a substance with sufficient absorption due to groups which do not normally occur in the cell or are only present in very small amounts. Not only must such substances be found, but some method of introducing them into the cell in reasonable concentration will also be necessary. If these conditions can be met, it may be possible to determine the distribution of such substances between the nucleus and cytoplasm and perhaps to follow metabolic changes under various conditions.

Finally, there remains the investigation of biologically important fibres and other oriented structures using polarized infra-red radiation. In favourable cases studies on infra-red dichroism can provide much information concerning the orientation of various chemical groups. Investigations on infra-red dichroism of protein films have already been reported [32] and the comparison of the properties of natural fibres with oriented films of protein extracted from those fibres might prove fruitful.

Conclusions.—The problems involved in microspectroscopic techniques are far from solved. On the instrumental side there is room for improvement in both microscope and spectroscope construction, and particularly in the design of instruments specially adapted for work in this field. More sensitive detectors are badly needed in the infra-red region in order to improve spectral resolution, and in the ultra-violet in order to reduce the irradiation of the specimen. Many theoretical aspects remain obscure, particularly those concerning the importance of non-specific light losses and the possible changes induced by u.-v. radiation on some materials. Despite these difficulties microspectroscopic methods appear to be firmly established, and if due caution is exercised, it is only when attempting to draw highly quantitative conclusions from observations on complex and variable objects whose physical properties are largely unknown, that any serious errors are likely to arise.

[29] Bensley, *Biol. Symp.*, 1943, **10**, 323.
[30] Banga and Szent-Gyorgyi, *Enzymologia*, 1940, **9**, 111.
[31] Pollister and Ris, *Cold Spring Harbor Symp.*, 1947, **12**, 147.
[32] Ambrose, Elliott and Temple, *Nature*, 1949, **163**, 859.

I wish to acknowledge the assistance received as Alan Johnston, Lawrence and Moseley Research Fellow of the Royal Society and also the financial help given by the Nuffield Foundation.

Department of Human Anatomy,
University Museum,
Oxford.

INFRA-RED MICROSPECTROMETRY WITH A 0·8 N.A. REFLECTING MICROSCOPE

By R. D. B. Fraser

Received 11th September, 1950

The numerical aperture (N.A.) of a reflecting objective employed with an infra-red spectrometer determines the minimum size of sample from which spectra may be obtained. High numerical apertures are important both to increase the energy collected from a given sample and to reduce the size of the diffraction pattern of its image. A 0·8 N.A. reflecting objective used in conjunction with a Grubb-Parsons spectrometer is described. Optical refinements have been introduced which (i) ensure the efficient transfer of energy from microscope to spectrometer, and (ii) facilitate the alignment and focusing of the magnified image of the sample in the plane of the slit. Details of the size of the micro-focus at various wavelengths, and examples of the spectral resolution of which the instrument is capable, are given.

Since Barer, Cole and Thompson [1] first used a reflecting microscope for infra-red microspectrometry, various applications to biological problems have been made, both in this country and in America. The particular value of this method lies in the small size of specimens from which spectra may be obtained. With present-day spectrometers and reflecting objectives, the limiting size of specimen is set, not so much by diffraction as by the amount of energy that may be passed through it. This arises because a minimum radiant flux is necessary on the detector to obtain satisfactory spectra. Below this, random fluctuations in detector output constitute an excessively large proportion of the signal. The size of specimen from which this minimum radiant flux may be collected is determined by the numerical aperture of the microscope. It is clear, therefore, that the development of high numerical aperture objectives is of great importance if the specimen size is to be reduced to the limits set by diffraction. Since the smallest dimension of the specimen which may be resolved at wavelength λ and numerical aperture N.A. is given approximately by $\Delta S = 0{\cdot}6\lambda/\text{N.A.}$, it is clear that the numerical aperture has a two-fold importance in determining the smallest objects from which spectra may be obtained.

Reflecting objectives used in conjunction with infra-red spectrometers have been described by various authors; Barer, Cole and Thompson [1] used a 0·65 N.A. Burch microscope with aspherized mirrors, whilst Gore [2] and Blout [3] in America have used the Polaroid-Grey 0·4 N.A. objective with spherical mirrors. In this paper the use of a 0·8 N.A. objective with spherical mirrors, designed by K. P. Norris, [4] is described.

---

[1] Barer, Cole and Thompson, *Nature*, 1949, **163**, 198.
[2] Gore, *Science*, 1949, **110**, 710.
[3] Blout, Bird and Grey, *J. Opt. Soc. Amer.*, 1950, **40**, 304.
[4] Norris, this Discussion.

Experimental and Results

Description of Apparatus.—The radiation from a Nernst glower N, see Fig. 1, is collected by a spherical mirror M_1 and condensed into the plane of a slit and an iris diaphragm S. This provides a convenient system for field limitation. The reflecting condenser, which is identical with the objective, focuses an image of that portion of the source image admitted by the field stop on to the object. The object is mounted over a small aperture on a horizontal focusing stage O, which is provided with two motions at right-angles and a rotation. The energy transmitted by the sample is collected by the objective and emerges as parallel light. This light is collected by a lens L and the object is viewed in the usual manner through an eyepiece. A small mirror M_2 at 45° to the microscope axis is introduced to reflect the energy into the condensing system of the spectrometer. This comprises two spherical mirrors, the first of which M_3 acts as a field mirror, by forming an enlarged image of the small mirror of the objective on the condensing mirror M_4 of the spectrometer.

Exact focusing and orientation of the sample image in the plane of the slit jaws is accomplished by the insertion of a reflecting prism P, immediately behind the entrance slit. An enlarged image of the slit jaws and sample may then be viewed through an eyepiece. The overall magnification is such that the aperture of the spectrometer is just filled. The radiation selected by the monochromator is detected with a Hilger Schwartz thermocouple, the signal is amplified with a General Motors D.C. amplifier, and recorded on a Brown recorder.

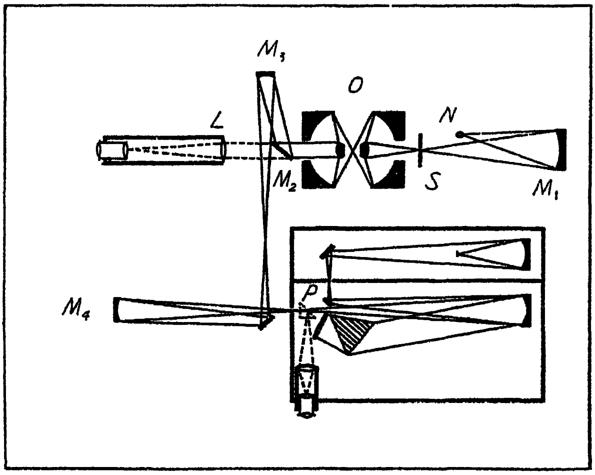

Fig. 1. Optical system used with the 0·8 N.A. reflecting microscope and infra-red spectrometer.

The Reflecting Objective. The functions of a microscope objective when used for infra-red microspectrometry are somewhat different from those in visible or ultra-violet photomicrography. In the system employed in the present instrument, the condenser is used to define the portion of the specimen from which a spectrum is to be obtained, whilst the objective gathers the transmitted radiation and passes it into the spectrometer. With relatively large objects the off-axis aberrations in the condenser and objective are not important, their effect being the introduction of a small amount of "impurity spectrum". Where physical limitation of the field is possible—e.g. when the specimen is suspended over an aperture in metal foil, which acts as a field stop—extreme aberrations result only in a small loss of signal in the detector output. The aberrations are much less with smaller specimens, as the objective is used but a little off-axis. Again, at wavelengths of the order of 10μ the dimensions of the diffraction pattern are greatly increased so that aberrations which might be important at visible and ultra-violet wavelengths are of little consequence.

The 0·8 N.A. reflecting objective described in this paper was constructed from spherical mirrors with a central obstruction of 12 % of area. The maximum field which may be used at the full aperture is of the order of 1 mm. The errors in the wavefront from an axial point in the specimen have been measured, and found to be less than $\lambda/4$ in the wavelength range 2 to 15 μ. This means that the Rayleigh criterion is satisfied for the realization of the full resolving power of the objective. The design of these mirrors was carried out by Norris,[4] and is based on the work of Seeds and Wilkins.[5] The possibility of increasing the N.A. to 1·4, by the inclusion of thallium bromo-iodide hemispheres, is being investigated.

Field Limitation and Field Mirror.—Various systems of field limitation have been described,[1, 2, 3] but that used in this instrument has proved extremely satisfactory. The microscope is mounted on a commercial stand so that the specimen may be viewed by means of an eyepiece in the usual manner. Beneath the condenser a slit and iris diaphragm are mounted in the plane of an image of the source. The condenser then focuses a reduced image of this system in the plane of the specimen. By means of the stage motions, and the regulation of the slit height and width, the desired portion of the specimen is defined. A further refinement which has proved to be of great value is the insertion of a reflecting prism immediately behind the entrance slit of the spectrometer. The slit jaws, and objects imaged in the plane of the slit, may then be viewed through an eyepiece. This permits accurate focusing and alignment of the specimen with the slit jaws.

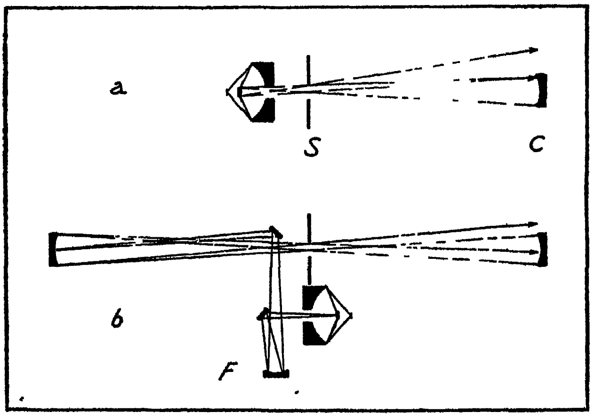

FIG. 2.—(*a*) Shows diagrammatically why the extreme portions of the slit cannot be used when an image is focused directly on to the slit. (*b*) Shows how this is avoided by the inclusion of a field mirror.

The dimensions of conventional reflecting objectives are such that when an image is formed in the plane of the slit at the optimum magnification, the cones of radiation from the ends of the slit S fall partly above and below the collimating mirror C of the spectrometer. This effect is depicted in Fig. 2*a*, and may be remedied by the inclusion of a field mirror F, as shown in Fig. 2*b*. It has been found possible to utilize the full slit height by this method.

Condenser Illumination.—The function of the condenser is to illuminate every point in the object with a cone of radiation sufficient to fill the aperture of the objective. Three convenient systems which satisfy this requirement are :—

(1) Critical illumination, in which the condenser is used to form an image of the source in the plane of the specimen.

(2) " Kohler " illumination, where a mirror surface is imaged in the plane of the specimen. This mirror focuses an image of the source on to the small mirror of the condenser, which must be filled with light.

(3) The condenser may be focused on an image of the source at infinity.

Of these methods (1) provides a convenient sub-focus conjugate with the entrance slit of the spectrometer, whilst (2) gives a uniformly illuminated circular field. Method (3) is convenient where a selenium or silver chloride transmission polarizer is used, as it may be introduced into the parallel beams before the condenser. This eliminates any difficulties arising from image displacement.

---

[5] Seeds and Williams, *Nature*, 1949, 164, 228.

The particular system employed is best chosen in relation to the specific requirements of the problem, and provision for all is made.

Performance.—The possibilities and limitations of infra-red microspectrometry in the investigation of cell structure have been discussed by Barer.[6] The particular aspects where it is most likely to be profitable are in the study of:

(1) Single crystals of pure material extracted from cells, where polarized infra-red measurements are to a certain extent complementary to X-ray diffraction data.

(2) Oriented natural fibres, again in conjunction with X-ray measurements.

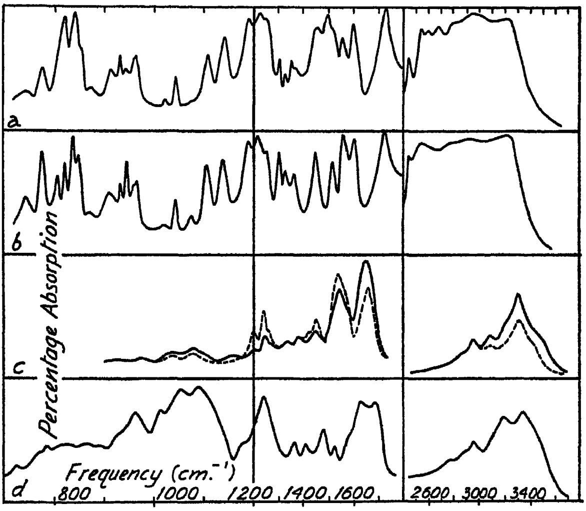

FIG. 3.—Infra-red spectra illustrating the application of microspectrometry to the study of cell structure. (*a*) and (*b*) Tyrosine hydrochloride crystal 0° and 90°. (*c*) Mouse tail collagenic fibre, electric vector parallel (dotted line) and perpendicular (full line) to fibre axis. (*d*) Sample of sodium thymonucleate, estimated weight 2 μg.

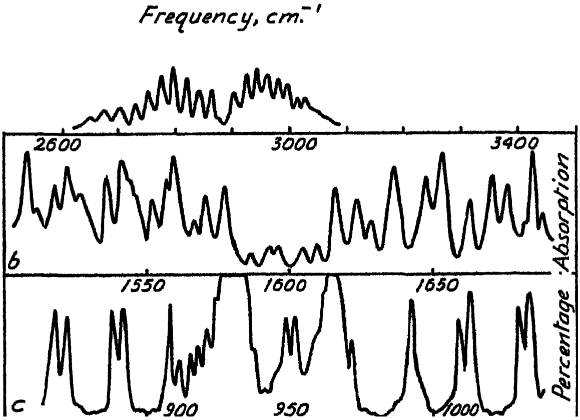

FIG. 4.—Spectra showing the spectral resolution of which the microspectrometer is capable with a rocksalt prism.

(*a*) The rotation structure of the HCl band at 2900 cm.$^{-1}$.
(*b*) Atmospheric water vapour absorption in the range 1500-1700 cm.$^{-1}$.
(*c*) Ammonia in the range 850-1050 cm.$^{-1}$.

---

[6] Barer, this Discussion.

(3) Small quantities of complex compounds of high molecular weight, where spectra may be used as criteria of purity and slight differences in spectra may be correlated with the particular source or method of extraction. Also the prediction of certain atomic groupings present in the molecule may be possible.

In Fig. 3 spectra illustrating these applications are shown. In each case the size of the sample was such that the full slit height could be used. The slit widths were identical with those used in macro work.

The spectral resolution of which the instrument is capable may be judged from the spectra shown in Fig. 4. It will be noticed that this is better than that usually obtained with standard rocksalt prism spectrometers. In particular the resolution in the 3000 cm.$^{-1}$ region is adequate for the study of hydrogen stretching vibrations, without recourse to a lithium fluoride prism.

Discussion

At the present time a considerable amount of information has been collected on the infra-red absortion spectra of organic compounds. From these data a large number of empirical correlations of absorption regions and particular atomic groupings have been made.[7] These correlations have been valuable in a great variety of problems in molecular structure but their application to materials of biological interest has been handicapped by the relatively large amount of material required to obtain a spectrum. With the advent of infra-red microspectrometry it is now possible to obtain spectra from objects of microscopic size. In many published spectra, however, it is apparent that the amount of radiant flux collected from the specimen has been a very small fraction of that normally used to operate the spectrometer. The increased slit widths used to obtain spectra under these conditions have led to a significant decrease in spectral resolution. This is to be avoided if possible, as the value of the information obtained is dependent, in general, on the spectral resolution employed.

Every attempt has been made in this instrument to collect a maximum of radiant flux from the sample and to ensure its efficient transfer from the objective to the spectrometer. About one-third of the usual operating energy is obtained with the full field size. This is adequately compensated by an increase in recording time, so that the spectral resolution is not impaired by increased slit widths. The objective is used at its optimum magnification, which is equal to the ratio of the numerical aperture of the microscope and the equivalent numerical aperture of the spectrometer.[8] At this magnification the aperture of the collimating mirror of the spectrometer is just filled. The objective was designed to cover a field sufficient to utilize the full slit at this magnification. This is only made possible, as explained previously, by the introduction of a field mirror. The calculated dimensions of the microfocus at various wavelengths, neglecting diffraction, are shown in Fig. 5.

These values are obtained with the usual slit widths employed in macro work and a root-mean-square noise level of less than 1 % of full scale recorder deflection. The variation in *a* is due to the decrease in source brightness as wavelength increases, together with changing absorption in the rocksalt prism and windows of the spectrometer.

In practice, where the full slit height may not be used or a polarizer is inserted into the beam, or considerable scatter is present in the sample, the radiant flux on the detector is reduced. This reduction is compensated by one or more of the following expedients : —

(1) Increase in recording time.
(2) Increase in root-mean-square noise level.
(3) Increase of exit slit width, independent of entrance slit width.

Of these, (1) and (2) do not affect the spectral resolution which is obtained. However, where the full resolution of the spectrometer is not

[7] Colthup, *J. Opt. Soc. Amer.*, 1950, 40, 397.

required, e.g. with broad featureless absorption bands, (3) is to be preferred.

The microfocus is particularly valuable where the dichroism of a crystalline material is to be studied; the advantages of working with a single crystal or even a small portion of a crystal are considerable. High numerical aperture objectives have a unique advantage in this respect, as a significant proportion of the electric vector vibrates along the axis of the microscope with the aperture suitably masked. Absorption bands in which the dipole moment change is preferentially oriented along the axis of the microscope mav thus be demonstrated.

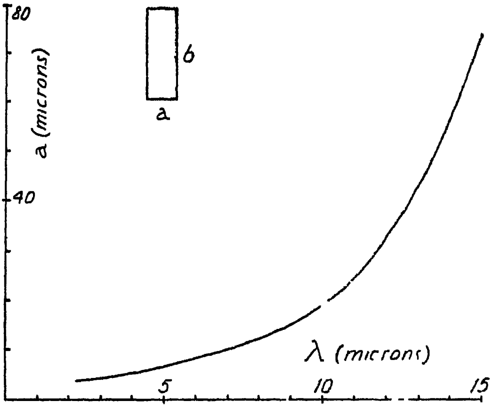

FIG. 5.—The dimensions of the microfocus ($b = 700\ \mu$) with which the spectrometer may be operated without increase in noise or reduction in spectral resolution. Diffraction effects are neglected.

When the performance of the microspectrometer described in this paper is compared with that of other instruments it must be remembered that the Grubb-Parsons spectrometer has an aperture of $f/6{\cdot}7$, and is capable of high spectral resolution by virtue of its large prism. If the instrument were operated at a reduced aperture comparable with other commercial instruments the dimensions of the microfocus could be reduced, as the optimum magnification would be correspondingly increased.

I wish to acknowledge a Medical Research Council Studentship which has enabled me to carry out this work, and to thank Prof. Randall for his encouragement. I am indebted to Mr. K. P. Norris for assistance in the initial adjustment of the objective, Mr. A. H. Benfield for constructional work, and Dr. W. C. Price for his continued advice and encouragement.

Medical Research Council Biophysics Unit,
King's College,
Strand, W.C.2.

GENERAL DISCUSSION

Dr. R. Barer (*Oxford*) said: I welcome the opportunity which this Faraday Society Discussion gives me to put forward the *user's* point of view on the new spherical mirror objectives which have been described by Prof. Randall and his colleagues. No matter how conventional or unconventional may have been the stages which have led to the design of an objective it is very important that a clear statement of its performance should be given. This statement should include (1) calculations of aberrations based either on accurate ray tracing, or if for any reason this is not possible, Gaussian optics, or other accepted methods, (2) practical performance tests. If the results of (1) are satisfactory we may consider (2), but if the preliminary calculations have not been done or indicate that the objective does not satisfy accepted criteria, we cannot always easily judge its performance from practical tests alone. It must be borne in mind that the standard of performance required from an objective intended for accurate absorption measurements is higher than in the case of an objective intended for routine visual or photographic use. However, given the proper facts and figures the user can decide for himself what order of accuracy he may reasonably expect from work carried out with any given objective. In the absence of such facts the true interpretation of results becomes impossible.

My general criticism is that the King's College work on reflecting objectives has been described in such a way as to make it impossible to evaluate at present the performance of these objectives in terms of generally accepted optical standards. Furthermore, there is evidence to suggest that the designers may be unwittingly accepting a standard of performance very much lower than they have themselves stated to be necessary (Wilkins [1]).

In order to elaborate this criticism a few words of explanation concerning reflecting microscope design will be necessary. Spherical mirror objectives are by no means new,[2] but certain facts concerning them have hitherto been accepted by nearly all designers. Burch [3] showed that a well-corrected microscope objective using only spherical mirrors could be made with a field of normal size and N.A. (numerical aperture) approaching 0·5. In this case the mirrors would have to be approximately concentric, so that the design is often referred to as a monocentric pair though it is not in fact strictly monocentric. The great disadvantage of the monocentric pair is that a very high proportion of the N.A. is shadowed out by the small mirror. The actual figures for the obstruction are 45 % of the N.A. or 20 % of the exit pupil area. This central obstruction has a curious effect on the image. It causes a redistribution of energy in the image of a point (the Airy disc) so that the light in the central maximum is reduced, whereas that in the outer rings is increased. The contrast in the image may be affected and the photometric relationships between object and image are disturbed, reducing the accuracy of absorption measurements. It has been pointed out [4] that the effect of central obstruction resembles in a general way that of optical aberrations in that the Airy disc pattern is altered. The question of the maximum permissible central obstruction in a microscope objective has been considered both theoretically and experimentally by several workers [4-7] with good general agreement. It is suggested that the obstruction should not exceed 30 % of aperture (11 % of area) and this value has not as yet been criticized. Thus the monocentric pair is deficient in two respects. The N.A. (0·5) is a little low, and the obstruction (45 %) is undesirably high. Now a spherical mirror objective is not at first sight a very complicated system for the purpose of making calculations. The important variables are the radii of the mirrors, their separation, and the focal length of the combination. Designers who investigated the problem soon found that it was possible either to increase the N.A. or to reduce the obstruction ratio, but only at a very heavy price. The aberrations, particularly coma, increased very rapidly and the useful field of view shrank at an alarming rate. For this reason the majority of designers have not felt it worth while to deviate greatly from the approximately monocentric condition. The King's College group has adopted a different, and in some respects refreshing, approach. Their method seems to have been purely experimental. Mirrors of different radii were adjusted on a microscope-testing interferometer until the interferogram indicated that the spherical aberration was well corrected in the centre of the field. This procedure differs considerably from orthodox optical practice. No preliminary calculations are made in order to assess possible limitations; and attention is concentrated on the elimination of one aberration without regard for the others.

---

[1] Wilkins, this Discussion.

[2] Brumberg, *Nature*, 1943, **152**, 357.

[3] Burch, *Proc. Phyics. Soc.*, 1947, **59**, 41.

[4] Grey, *J. Opt. Soc. Amer.*, 1949, **39**, 723.

[5] Bouwers, *Achievements in Optics* (Elsevier, New York, Amsterdam, 1946).

[6] Dunham, *Special Report No. 2, American Cancer Soc. Grant No. PH 1B*, 1948.

[7] Barer, *Trans. London Conference on Optical Instruments*, 1950 (in press).

In assessing an optical instrument the generally accepted criterion of performance is the Rayleigh limit.[8] This is based on the assertion that the performance is not likely to fall far short of perfection if the maximum optical path difference does not exceed one quarter of a wavelength ($\lambda/4$) (see also my discussion following Wilkins'[1] paper). That this criterion is of course accepted by the King's College workers is evident from the statement of Wilkins[1] in his paper: " It is clear that the ability to perform photometric measurements on small objects is seriously limited when errors reaching the Rayleigh limit are present in an objective, although the performance of the objective for visual use and its resolving power are altered little." It must be pointed out that the Rayleigh limit must be applied to the *total* effect of all aberrations. It is no use having one aberration less than the limit if another exceeds it.

Since the question of coma is of fundamental importance in this discussion it will be as well to quote the words of Conrady[9] (p. 281): " The want of symmetry in the coma image is its worst feature: it causes a point of light to be rendered as a comet-like smudge with a strong concentration of light near the principal ray and a gradual fading away towards the broad tail of the figure. Such a caricature of what should be a small round dot is not only extremely unsightly in ordinary visual observations or in photographs, but also renders exact measurements quite impossible, as it is difficult to decide which part of such an unsymmetrical patch should be regarded as the location of the mean image-point. For that reason coma has been looked upon as the worst of all aberrations from the earliest days of practical optics, and even in the days of pure empiricism its removal to the utmost practicable extent was regarded as imperative. The beginner will be wise if he accepts this result of long experience and declares relentless war against any easily visible residue of coma." Conrady also points out that the Rayleigh limit is particularly severe in the case of coma, but he maintains that for astrophotographic instruments and for photographic lenses used for process work and copying maps we should "' try to keep within the single or at any rate the doubled Rayleigh limit ". The question which must be decided now is whether we are prepared to accept a lower standard in a microscope objective intended for accurate photometric work than in a photographic objective intended for process work. If the answer is no, then we must clearly have some means of estimating how much coma is present. This question has always been investigated by the majority of microscope designers. Burch[10] evidently regarded it as sufficiently important to devote an entire paper to the numerical calculation of the offence against the sine condition (coma). He concluded that an objective composed of one aspheric concave mirror and one spherical convex mirror should be " reasonably coma-free up to 0·65 N.A." Johnson[11] also calculates the offence against the sine condition for his reflecting objectives. He is careful to point out that this exceeds the accepted tolerance and results in a small field. Dyson[12] calculates the coma in his long working-distance objectives in terms of the Rayleigh limit. It is remarkable that he should have adopted so rigorous a test in the case of objectives in which for many purposes considerable departures from optical perfection could perhaps be tolerated. Grey[13] takes care to calculate the aberrations of his designs and to express them in terms of the Rayleigh limit. These few examples will suffice to show what an important role such calculations play in optical designing. It is only by their use that we can hope to obtain a generally accepted and objective standard of performance. The King's College group have not carried out such calculations. Instead, they have proposed a new, experimental and purely arbitrary method of judging when coma becomes excessive. If I understand the test correctly they look at the image of a pin-hole (the familiar star-test) using an intense light source. The asymmetric coma pattern is then observed and the field diameter at which the first bright ring on one side of the pattern appears to the eye to be equal in intensity to the second bright ring on the other side is taken as a measure of the useful field. This might seem to be a difficult test to apply with accuracy as it depends on the ability of the observer to match the intensity of two non-adjacent points of light. The errors and difficulties of such estimates have been dealt with by Wright.[14] I shall only point out that in trying to compare by eye the intensities of two points separated by two very much brighter regions great errors of contrast may arise. Even if different observers agreed in their judgments that would not prove that the test had any absolute value. I freely admit that I have not been able to carry out the test as described, but even if it is 100 % accurate, we may still ask "what does this test mean in terms of the Rayleigh limit or any other accepted criterion ?" There seems to be no immediate answer to this and I believe one could only be given by means of difficult and laborious mathematics. The proposed test may be very much worse than the Rayleigh limit, or may be very much better. In its present form the test is quantitatively meaningless.

---

[8] Rayleigh, *Phil. Mag.*, 1897, 8, 403.

[9] Conrady, *Applied Optics and Optical Design* (Oxford Univ. Press, 1929).

[10] Burch, *Proc. Physic. Soc.*, 1947, 59, 47.

[11] Johnson, *J. Sci. Instr.*, 1949, 26, 148.

Several King's College objectives have been described. One of the earliest had N.A. 0·65, obstruction ratio 35 % of N.A. or 12·5 % of area. The field of this was stated by Mr. Norris to be 150-200 μ in the ultra-violet and it is also said to show slight spherical aberration in the ultra-violet. This objective does not in fact depart very considerably from the monocentric pair and its obstruction ratio is still in excess of the accepted tolerance (30 % of N.A.). We might hardly expect it to show any very gross departure from reasonably good optical correction. I have been able to examine four of these objectives, two of them for a period of some months in my own laboratory. In every case the star test seemed to me to reveal the presence of a good deal more coma than I had been prepared to accept. That is of course a purely subjective opinion. The presence of coma worried me and during a recent visit to the U.S.A. I carried out similar tests on the commercially produced Grey type of reflecting-refracting objective. There was no noticeable coma even at fields in excess of 200 μ. I later asked Mr. Grey if he had done any calculations which would enable him to compute the field of an objective similar to the one described above. He was able to state that in a spherical mirror reflecting objective of N.A. 0·65 and 12·3 % of area obstruction, third and higher order coma would reach the Rayleigh limit at a field diameter of approximately 15 μ. This calculation concerns coma alone and takes no account of spherical aberration (which is stated to be present). On this basis there is a serious discrepancy between the calculated figure of 15 μ and the experimental figure of 150 to 200 μ. It appears in fact that the criterion used by the King's College workers has led them to accept a degree of coma at least ten times in excess of the Rayleigh limit.

---

[12] Dyson, *Proc. Physic. Soc.*, 1949, 62, 565.

[13] Grey, *J. Opt. Soc. Amer.*, 1950, 40, 283.

[14] Wright, *Photometry and The Eye* (London, Hatton Press Ltd., 1949).

I shall refer to two other objectives which have been discussed in public. They are (1) the objective referred to in the paper by Norris and Wilkins,[15] with N.A. 0·6 and central obstruction 19 % of N.A. (just under 4 % of area). The field of this was stated to be 40-50 μ. (2) An objective referred to by Wilkins in the programme of the Seventh International Congress on Cell Biology, Yale, 1950. This was stated to have 0·7 N.A. and central obstruction 5 % of area (about 22 % of N.A.). It will be seen that in both these cases the obstruction ratio has been reduced below the suggested limit of 30 %, a very desirable result. Now, in the first Burch microscope using aspheric mirrors, the N.A. was 0·58 and the obstruction ratio 25 % of N.A. or 6 % of area. Thus these new King's College objectives, using only spherical mirrors, have excelled the performance of an aspheric mirror objective, both as regards N.A. and obstruction ratio. The second Burch microscope has N.A. 0·65 and obstruction ratio 14 % of N.A. or 2 % of area, i.e. its obstruction ratio is better but its N.A. is only intermediate between the two new spherical mirror objectives. Grey has calculated that for a spherical mirror objective of N.A. 0·6 with an obstruction ratio of 9 % of area, third and higher order coma alone would limit the field to less than 10 μ. A reduction of the obstruction ratio below 9 % would still further limit the field and these figures should be compared with those given by the King's College workers. In the case of an objective of N.A. 0·7 and obstruction ratio 10 % of area the u.-v. field is limited by 3rd and higher order coma alone to 8·3 μ. In this case the spherical aberration may not be entirely negligible. There did not seem to be much point in calculating the field for obstruction ratios below 10 %. I think nevertheless that these calculations should be done, for the sake of completeness.

I feel that the evidence I have presented is at least sufficient to cause us to adopt a cautious attitude towards these objectives until further calculations have been made. As was pointed out by Mr. E. W. Taylor in the discussion and is also stressed by Conrady,[9] and is in fact implied in the statement by Wilkins [1] quoted earlier on, it is often very difficult to judge the performance of an objective by its photographic performance, particularly with objects whose structure is unknown. Thus apparently good photographs can often be obtained in the presence of quite severe coma, particularly when high-contrast photographic materials are used. The image no longer bears any definite photometric relationship to the object as much light has been scattered in a haphazard manner over the field. The very real danger exists that biologists who may be unaware of the limitations of these objectives may take full-field photographs and try to interpret them as true absorption records. These objectives should therefore always be referred to as " small-field objectives ".

The preliminary calculations of Grey must clearly be repeated independently and extended if possible. It must not be thought, however, that this case depends on the accuracy of these particular calculations. In a sense they are irrelevant, and if they had never existed microscopists would still have wanted to know about the performance of these objectives in terms of the Rayleigh limit. There is no justification for assuming that it would be safe to use such objectives for quantitative microphotometry *whatever the size of the field* in the absence of this information.

During the discussion it was suggested that the history of science is full of examples of experiment triumphing over theory. That is a perfectly valid defence of an experimental approach provided that there is any reason to believe that the theory is founded on some vague and not generally accepted hypothesis. In the present case our theory is based on (1) the laws of reflection of light, which have been verified up to the limits of experimental accuracy and (2) a generally accepted criterion—

accepted even by the King's College group themselves [15]—based on the diffraction theory of light. This theory has provided a basis for the calculation and design of optical instruments which has been used by the optical industry for many years without being seriously questioned. If, therefore, as the result of a purely experimental approach the King's College group should now, or in the future, arrive at conclusions which conflict with those derived from theory we should have to decide whether their experimental methods are sufficiently accurate or whether nearly all our fundamental optical concepts are ill-founded. If the future attitude of designers is to be " this instrument was made experimentally and we believe that it works until someone proves otherwise ", then much time will be wasted in supplying that proof.

Let us beware lest in our anxiety to elevate biology to the status of a quantitative physical science, we do not at the same time lower physics to the present qualitative level of biology.

My criticisms may be summarized as follows :

(1) Spherical mirror microscopes have been designed, apparently without detailed preliminary calculations. In the absence of such calculations it is impossible to assess the performance of these instruments in terms of generally accepted standards. These standards have even been accepted by the designers themselves.[1]

(2) A new, experimental, and arbitrary criterion has been suggested for estimating coma. The relationship of this criterion to the generally accepted ones is not known.

Dr. K. W. Keohane (*Bristol University*) said : The question of spherical mirrors for reflecting microscope objectives is one which has been fully examined on a theoretical basis. It is an accepted fact that for limited N.A. (less than 0·5) a spherical reflecting objective can be designed to give a performance comparable with that given by a standard refracting objective of equivalent N.A. If, however, it is desired to obtain higher numerical apertures it has always been held by opticians that a departure from spherical surfaces is essential.

Dr. Wilkins' photographs of newt cells certainly appear to be good but here should come a word of warning ; one must not judge the performance of a 0·7 N.A. objective by the study of large objects. Specimens must be chosen that are approaching the limit of resolution of a 0·7 N.A. objective ; thus, a photograph of *Treponema Pallida* or tubercle bacillus would have demonstrated the performance more conclusively. (The width of a spirochaete is about 200 times smaller than the diameter of a newt cell.)

Burch [16] has shown that a reflecting objective can be designed up to 0·65 N.A. using one aspheric and one spherical surface and that if the tolerable offence against the sine condition is set as 1/400 (the Rayleigh-Conrady tolerance), the field is reasonably coma free. Such objectives have a good performance over at least 250 μ, as indeed would be expected. Now, regarding Dr. Wilkins' design, the only aberration that has been taken into account is that of spherical aberration. Conrady [17] quotes permissible tolerance for the aberrations in his standard work. His actual figures are :

(i) permissible spherical aberration is 6 × focal range, and

(ii) permissible coma tolerance is $\dfrac{\pm \frac{1}{2}\lambda}{N \sin U_m}$.

Now the focal range is $\dfrac{\lambda}{N \sin^2 U_m}$ where U_m is the angle that the marginal ray makes with the axis.

---

[15] Norris and Wilkins, this Discussion.

[16] Burch, *Proc. Physic. Soc.*, 1947, 59, 47.

[17] Conrady, *Applied Optics and Optical Design* (1929).

Therefore if $\sin U_m = 0{\cdot}65$ then :

(i) permissible spherical aberration is equal to $\dfrac{6\lambda}{0{\cdot}65^2}$

(ii) permissible coma is equal to $\dfrac{\pm\frac{1}{2}\lambda}{0{\cdot}65}$.

This shows that the degree of latitude one has with coma is about eight times smaller than with spherical aberration. Now, as spherical aberration affects the whole field, it must be removed first in order to obtain good performance on-axis, but coma grows in direct proportion with the angle of the field, and undoubtedly is the most serious aberration for points a small distance off-axis. For larger distances astigmatism is the most troublesome.

My opinion on the subject of bispherical objectives are that Dr. Wilkins was very wise to use an objective designed with spherical surfaces when he found that a Burch type microscope was not immediately available as valuable results may be obtained using them. However, I feel that in this position one has two choices : (*a*) a monocentric bispherical type up to 0·5 N.A. (Burch [18]) which gives a quite large aberration-free field (there is only one drawback to this—as is well known from astronomical experience—planetary detail is lost if large obstruction ratios, which are an inherent property of this type, are used). (*b*) A bi-spherical type similar to Wilkins's design : in this case one must necessarily be restricted to the small aberration-free central field.

Assuming that Dr. Grey's figures are obtained using conventional permissible tolerances then the useful field may quite well be extremely small, but, nevertheless, useful for limited purposes.

The method adopted by Mr. Norris for judging tolerable coma (that the intensity of the second ring on one side of the Airey disc should be equal to the intensity of the first ring on the other side) is not one that we adopt, and I should have thought the estimation difficult unless photometric methods were used. Our practice is to measure the off-axis coma interferometrically and our mirror pairs have negligible coma at distances off-axis before the astigmatism becomes the over-riding error. This is obtained in practice by adjusting the mirrors so that the fifth order coma is optimally " balanced " by negative Seidel coma before final figuring. The criterion of " balancing " is only capable of precise definition when the correct use of the instrument is specified, i.e. it may be different for viewing bright stars or planetary detail, but one would expect such differences to be unimporrant when, as here, the residual coma is very small. So, what we do, is to make the interference fringes " as good as possible ".

The controversy really reduces to : how much coma can be tolerated. In this respect, we in Bristol feel that conventional tolerances should not be lightly disregarded.

On the question of Dr. Barer's on the correct illumination of a microscope : if one is to do accurate absorption measurements, the subject of microscope illumination becomes of the utmost importance. Some idea of the errors that might arise, if an objective is incorrectly fed and a pin-hole object viewed, can be illustrated as follows. A comatic image of a pin-hole can be simulated by such illumination, and, if light is thrown into regions where absorption measurements are being taken then clearly the measurements will not be reliable. Here one must make one proviso —if the measurements are taken at the centre of a homogeneous field then as much light is thrown out of the area as into it from the neighbouring area. If, however, the measurements are taken on an area of a non-homogeneous field, then serious errors would arise. It is thus essential that one uses a well-corrected objective fed properly from a corrected condenser.

[18] Burch, *Proc. Physic. Soc.*, 1947, **59**, 41.

Underfeeding is well known to give rise to peculiar effects apart from decreasing the resolving power of the objective by decreasing its effective numerical aperture. In fact, if one wants to get photographs which appear good one can underfeed the objective and get phase effects which produce hard sharp outlines to the structure that is being examined.

Dr. M. H. F. Wilkins (*King's College, London*) (*communicated*) : Dr. Barer's criticisms of our spherical mirror reflecting objectives can be answered briefly as follows :

(1) MEASUREMENT by interferometer shows that a Beck type objective of 0·60 numerical aperture and 35 % central obstruction of N.A. gives coma error on the wavefront reaching Rayleigh limit $(\lambda/4)$ at the edge of a field of *ca.* 70 μ diameter for visible light and 35 μ diameter for 0·26 μ ultra-violet light. For qualitative work the field is quite useful to twice the above size.

(2) CALCULATION [19-23] confirms that our coma criterion (intensity of first diffraction ring equal to that of second ring on opposite side of Airy disc) is approximately equivalent to the Rayleigh limit.

Our new measurements of aberrations will be published soon. Almost all microspectrographic work may be done with a field diameter of *ca.* 10 μ, and it is a pity that discussion was side-tracked at a Conference where it had been hoped to clear away confusion and to help establish microspectrography as a standard biological technique.

Mr. E. W. Taylor (*York*) said : Dr. R. Barer has pointed out that, for the simple type of reflecting objective under discussion, there are few variables at the disposal of the designer. If the focal length is fixed there remain only the ratio R between the two radii of curvature and their axial separation.

As the system is necessarily achromatic and only the two most important aberrations can be eliminated, the choice must be spherical aberration and coma in that order. The separation must therefore be adjusted to control the former and the ratio R fixed with regard to the latter. This gives rise to an objective with a maximum aperture of about 0·55 N.A. and an obstruction ratio of, say, 22 % by area. Field curvature and astigmatism will be present, but a useful field of view with a radius of 175 microns in the object space may be realized at a focal length of 3 to 4 mm. This is the so-called monocentric construction in which $R = r_1/r_2 = 2{\cdot}63$.

Dr. C. R. Burch, in his well-known design, has strictly adhered to the generally accepted tolerances for coma, and faced the very great technological difficulties of producing an aspheric surface correctly figured to $\lambda/10$ or better. The reward will be an achromatic reflecting objective of the highest optical quality, characterized by increased numerical aperture and a low obstruction ratio.

A less rigorous approach has been made at King's College as here the monocentric form has been abandoned for one which, when corrected for spherical aberration, also permits increased numerical aperture and a lowered obstruction ratio. This is, however, achieved at a price, and the price is an offence against the sine condition. This is the point about which there is some misgiving.

In designing refracting objectives every effort is made to control the length of the comatic flare and a 3-4 mm. objective may be expected to yield good central definition over a field of about 175 μ radius in the object space. The sagittal coma, at any point in the image, should not exceed 0·53 μ if the Rayleigh limit is not to be exceeded.

If this tolerance is exceeded the useful field of view will shrink and

---

[19] Kingslake, *Proc. Physic. Soc.*, 1948, **61**, 147.

[20] Martin, *Mon. Not. R. Astro. Soc.*, 1922, **82**, 310.

[21] Nijboer, in Bouwers' *Achievements in Optics* (Elsevier Pub. Co. Inc., 1946).

[22] Steward, *Phil. Trans. Roy. Soc.*, 1926, **225**, 131.

[23] Lord Rayleigh, *Phil. Mag.*, 1879, **8**, 403.

there will be a reduction in image contrast, since each point in the image will receive some light from neighbouring points. Moreover, on imaging an evenly illuminated object area, a symmetrical redistribution of light depending on the sign and magnitude of the comatic flare will take place in the image—each zone receiving some light from neighbouring zones. Such an objective may, however, give good photographic results as most of the light is concentrated at the head of the comatic flare and a plate of suitable characteristics will be little affected by the stray light present in the oblique image.

The ratio of radii for the monocentric construction is 2·63 and the radius of the useful field, which is not in fact limited by coma, may be taken as 175 μ. If R is between the limits 2·55 and 2·75 the coma will be within tolerance, but at R equals 3·0 the useful field is halved, at R equals 3·5 it shrinks to about one-quarter, and at 5·0 it is reduced to a radius of 22 μ. These figures assume a numerical aperture of 0·55 and as the object of departing from the monocentric form is to increase the numerical aperture, the useful field will be still further reduced.

The conclusion is that it is very desirable when specifying a reflecting objective, in which coma is present beyond the usually accepted limits, to state the radius of the field of view over which the coma does not exceed the permitted tolerance, and this, I think, is the main point which Dr. Barer wishes to make.

Dr. R. Barer (*Oxford*) (*communicated*) : I am glad that Dr. Wilkins has now measured coma (as well as spherical aberration) by an interferometer method. Had this been done before the Discussion three months ago (and particularly before some of these objectives were released commercially), much criticism could have been avoided. Unfortunately the results of the test as applied to the objectives mentioned at the Discussion and in my criticism are not given. Instead, an entirely new objective is mentioned, and the size of field as estimated by the King's College coma criterion is not stated. I shall not at present dispute Dr. Wilkins' statement that calculation shows that the latter criterion is approximately equivalent to the Rayleigh limit. If that is the case, the doubts expressed by Dr. Keohane and myself concerning the practical difficulty of the test seem to be justified. The u.-v. field of the 0·65 N.A. objective was originally given as 150-200 μ. The field of a similar 0·6 N.A. objective is now given as 35 μ. As the field of an objective of higher aperture would be even smaller, it is clear that there is a very considerable discrepancy between these figures.

It will be noted that the 0·65 N.A. objective is no longer considered by the designers to be suitable for critical ultra-violet work, irrespective of the field used. Users of this objective would thus hardly regard the discussion of its performance as a " side-track ". We shall not " help establish microspectrography as a standard biological technique " until we adopt a critical attitude towards our methods and apparatus.

Dr. R. Barer (*Oxford*) said : I do not think there is any great mystery about the estimation of absorption in small objects. Caspersson's theory [24] shows that good accuracy can be obtained from measurements on objects 3 to 4 λ in width. This figure fits in well with other investigations on diffraction phenomena which often show that the equations derived from physical optics approach those derived from geometrical optics at about these dimensions. It is generally agreed that the accuracy of measurement must fall off below this limit. By making certain simplifying assumptions Wilkins has shown that the density of a rod-shaped body 1 λ in width and thickness can be determined with about 20 % error. If the body is round or square the errors are doubled, i.e. to 40 %. It seems doubtful whether such measurements could be called quantitative. The great difficulty in all biological work is that we usually have to deal with bodies which are not regular in size or shape and whose thickness may be unknown. Nearly all theories of microscopy deal with two-dimensional objects, whereas in practice most objects are three-dimensional.

---

[24] Caspersson, *Skand. Arch. Physiol.*, 1936, **73**, Suppl. 8.

There is another cause of inaccuracy to which insufficient attention has been drawn, namely the fundamental limitations of our microscopes. The Rayleigh limit is sometimes referred to as if it were a standard of perfection beyond which it is unnecessary to go.[25] This is by no means the case. Even in a theoretically perfect optical instrument the image of a point is rendered as a central concentration of light surrounded by a series of rings. About 85 % of the light is concentrated in the centre. At the Rayleigh limit, however, only about 68 % is concentrated in the centre, the rest being spread out over the surrounding area. Thus even in an instrument corrected to this degree of accuracy (which is generally agreed to be desirable) our absorption measurements would be by no means devoid of error. In fact, in order that the loss of light from the central condensation *should not exceed* 1 %, we should have to work within *one-quarter of the Rayleigh limit.* I fear that this would impose too great a limitation on the designers and constructors of high-aperture microscope systems. Thus, added to our biological difficulties we have fundamental physical limitations. We must clearly exercise great care lest we overestimate the accuracy of our results.

I am in full agreement with Dr. Wilkins concerning the pitfalls due to out-of-focus effects. Such effects have, of course, been very familiar to biologists for many years and were dealt with by Zernike[26] in his well-known papers on phase-contrast microscopy. The point to emphasize, however, is that such effects are almost inevitable in most cytological material, as our specimens are very rarely homogeneous, even in very thin sections. This is another fact which must limit the accuracy of photometric work, and unfortunately the magnitude of the errors involved must vary from specimen to specimen, and is very difficult to assess.

Another rather paradoxical point concerns the method of illumination used for absorption measurements in microscopy. It is often suggested that a narrow illuminating cone should be used as this avoids disturbing refraction and reflection effects, as well as enabling a greater proportion of the diffracted light to be collected by the objective. On the other hand every practical microscopist, from the days of Nelson, knows that such illumination usually results in a very poor quality image. Ideally one would like to obtain incoherent illumination, i.e. the object should behave like a self-luminous body. This is substantially the case when the illuminating aperture is equal to the objective aperture. In practice most microscopists use anything between a 2/3 and 9/10 illuminating cone, in order to avoid loss of contrast. If the illuminating cone is further reduced the illumination becomes more coherent and unpleasant interference haloes may appear. Out of focus phase-contrast effects also become pronounced. Thus we are apparently faced with the choice of using a narrow illuminating cone with a poor image, or a wide illuminating cone with a good image, but with a danger of introducing refraction effects and possibly not collecting all the diffracted light. It would be useful if these two methods could be compared experimentally. It is possible that for large homogeneous specimens the results would not differ very greatly, but for biological material composed of small heterogeneous areas, considerable differences might be found. It should not be too difficult to measure the absorption of a given object under varying conditions of illumination.

It will be clear from the remarks I have made during the discussion

[25] Hardy and Perrin, *The Principles of Optics* (McGraw Hill, New York, 1932).

[26] Zernike, *Physik. Z.*, 1935, **36**, 848 ; *Physica*, 1942, **9**, 686, 974.

that I am not in entire agreement with those who set great store by very accurate quantitative measurements of u.-v. absorption by biological material. This is mainly because during the last few years I have been very greatly impressed by the difficulties, both physical and biological, which beset this type of work. We must not confuse accuracy of measurement with accuracy of interpretation. I believe it is possible to obtain measurements of transmission which are highly reproducible, but the translation of these into quantitative chemical terms is another matter. For that reason I believe a qualitative or semi-quantitative approach is likely to be more fruitful and certainly less misleading at this stage. The crux of the matter is that it is the *biological* problem which counts. Microspectrographic methods are most valuable when they can be related to functional or physiological variations.

Dr. T. A. Kletz (*I.C.I. Billingham*) said : We also have constructed a reflecting microscope for recording the infra-red spectra of smaller objects than is possible by conventional means. The general arrangement is similar to that described by Mr. Fraser though the spectral resolution we have obtained is not as good as his. For a rock-salt prism his results would be exceptionally good even without a microscope in the optical path.

As the usual difficulty in infra-red spectroscopy is the small amount of energy available our microscope was designed by Mr. C. H. Bosanquet so as to give high radiation transmission (i.e. high N.A. combined with low central obstruction) without too much loss of definition in the final image. The N.A. is 0·866 and 13 % of the light is lost by central obstruction ; the sphere of confusion is 5 microns (i.e. the image at the sample of a point on the slit is 5 microns diameter). This should be compared with the N.A. of 0·40 used by Blout, Bird and Grey[27] and by Gore.[28]

The microscope consists of identical condenser and objective halves. The radii of curvature are 25 cm. for the large mirror and 0·25 cm. for the small one. The microscope is used with a Hilger Industrial (H. 603) spectrometer fitted with a rock-salt prism, used as a recording instrument. The spectrometer is of the Wadsworth type but modified so that the off-axis aberrations of the two spherical mirrors compensate.[29] The output from the Schwarz thermopile is amplified by a Hilger photo-electric amplifier and recorded photographically.

At a magnification of 12 diameters the beam coming from the microscope just fills the aperture of the spectrometer ($f/4{\cdot}8$). In practice it is found convenient to use a magnification of 18 and the beam then has an aperture of $f/7{\cdot}35$. The quantity of radiation entering the spectrometer is thus reduced to $(4{\cdot}8/7{\cdot}25)^2$ or 42·5 % of its normal value. When allowance is made for the radiation lost by central obstruction and by reflection at nine extra mirrors (5 % each time) it is seen that only 23 % of the normal amount of radiation enters the spectrometer. If the amplification is kept the same the slits widths have to be doubled, but it is found possible to double the amplification without increasing the noise level too much and then the slits widths have only to be increased 1·4 times. It would be preferable to use the reflecting microscope with a spectrometer of lower aperture than $f/4{\cdot}8$ but the Hilger Industrial was the only one available.

The length of the slit is 8 mm. and its maximum width 0·5 mm. ; at a magnification of 18, objects as small as 450 $\mu \times 30\ \mu$ can be examined. If it is desired to examine an object only 225 μ long then it is possible to double the magnification to 36 times, thus decreasing the energy entering the spectrometer a further 4 times, or to use only half the length of the slit, thus halving the energy entering the spectrometer. The latter is the better course provided the object is 30 μ wide and, except for fibres, this is usually the case. The slit widths used with the microscope are equivalent to 10 cm.$^{-1}$ at 6 μ and 5 cm.$^{-1}$ at 10 to 13 μ. Many of the materials examined scatter a lot of radiation and the slit widths used have to be increased to compensate for this.

---

[27] *J. Opt. Soc. Amer.*, 1950, **40**, 305.

[28] *Science*, 1949, **110**, 710.

[29] Czerny and Turner, *Z. Physik.*, 1930, **61**, 792.

The image formed by the microscope is transferred to the slit by 2 concave mirrors arranged so that their off-axis aberrations compensate. The spectrum obtained is of a portion of the object selected by the slit. As the image (or strictly the portion of it that passes through the slit) is larger than the small mirror of the microscope, radiation from the small mirror passing through the extremities of the slit diverges widely from that passing through the centre. If the image from the microscope is formed directly on the slit, much of the radiation falls above and below the collimater and is lost; in the present case 37 % would be lost in this way. It is important that the mirrors used to transfer the image on to the slit collect all this diverging radiation and focus it on to the collimator. Similarly, the mirrors used to illuminate the microscope condenser must illuminate it with the correspondingly convergent rays. Stray light can be eliminated by mounting the object on a plate with a small hole in it for the light to pass through, or by focusing an aperture stop in the plane of the small mirror of the condenser.

The reflecting microscope has been used for obtaining the spectra of small crystals, fibres and of small pieces of plant tissue. Many of the spectra that we have obtained for plant tissue are rather similar; highly specialized types are the most likely to produce characteristic spectra: thus the cuticle, the layer of alcohols, long-chain acids, esters, etc., forming the outer layer of a leaf, has a spectrum quite distinct from that of the epidermis immediately beneath it.

Dr. M. H. F. Wilkins (*King's College, London*) (*said*): The method we use to test a microscope objective and, in fact, the whole apparatus for microspectrographic work, is to photograph small opaque objects of a size equal to that of the object, the absorption of which is to be measured. We then measure the amount of light scattered or diffracted into the part of the image which should be black. In this way the errors of the method may be estimated directly.

Recent measurements by K. P. Norris show a Beck 0·65 N.A. objective has almost Rayleigh limit spherical aberration for λ 0·25 μ, and half Rayleigh limit for visible light. As a result it would be advisable for critical ultra-violet work to use a Beck 0·60 N.A. (instead of 0·65 N.A.) objective which has half the above spherical aberration.

Mr. W. E. Seeds (*King's College, London*) (*said*): Experiments are being carried out on 4 : 6-dimethyl-2-hydroxypyrimidene-$2H_2O$ whose structure has been determined by Pitt.[30] The pyrimidene rings are flat and lie with their planes parallel; in these planes the molecules all point in the same direction. When the crystals are grown on a slide the normal habit is such that the pyrimidene planes lie normal to the surface. Preliminary measurements of the ultra-violet absorption and dichroism of these crystals have been made, for light polarized with the electric vector E mainly perpendicular, and parallel to the pseudo diad axis of the crystal. There is a very marked dichroism, the absorption of E parallel being about nine times as great, at the maximum of the absorption curve, as that of E mainly perpendicular. The absorption curves both show fine structure. However, as divergent light is used, the curve of E mainly perpendicular will contain not only the absorption of light polarized with E perpendicular to the diad axis and the plane of the molecule, but also of E perpendicular to the diad axis and parallel to the plane of the molecule. We have now succeeded in growing the crystals such that the plane of the pyrimidene ring lies parallel to the surface, and it is hoped to investigate the dichroism in this plane.

[30] Pitt, *Acta Cryst.*, 1948, 1, 168.

In connection with this work we have been using a low-temperature stage which was designed by Dr. Wilkins and myself. The specimen is mounted on a fragment of coverslip and rests on a small copper disc which is cooled by circulating liquid air through very thin copper tubes soldered to it. The stage and cooling tubes are enclosed in a vacuum chamber and viewed through a fused quartz window, 0·18 mm. thick. Full details will be published elsewhere, but it is of interest to note that temperatures of the order of 90° K are reached in approximately 1½ sec., actual freezing being almost instantaneous. The overall thickness of the apparatus which fits on the stage of the microscope is 5 mm. approximately. With this apparatus it is hoped to accentuate the fine structure of the absorption curve.

As suggested by Prof. C. A. Coulson, the results of this investigation should enable one to decide between alternate possible theories of ultraviolet absorption.

Prof. B. Commoner (*Washington University, Saint Louis*) said: I find it necessary to take exception to certain parts of Dr. Wilkins' paper. He has devoted part of his paper to (i) a presentation of what he purports to be certain points made by me in a recent paper on u.-v. absorption by cellular nucleic acids, (ii) an attempt to show that my criticism, as described by Dr. Wilkins, of certain practices in u.-v. microspectrophotometry is "unsound", and (iii) a statement concerning the practical importance of dichroism in u.-v. analysis of biological objects. I should like to make the following comments concerning these three statements.

(i) Dr. Wilkins' restatement of my criticisms of certain interpretations of u.-v. extinctions is not accurate. He attributes to me the argument that nucleic acid concentrations which give extinctions of 0·5 when unoriented, give extinctions of 0·3 when oriented (examined in unpolarized light), and offers an argument which is supposed to answer this version of my criticisms. I shall discuss his argument below, and at this point assert that nothing resembling Dr. Wilkins' restatement of my position appears in the papers which I have written on the subject. In the interest of accuracy, I should like with your indulgence to summarize the actual content of the arguments offered by me in the papers in question. These are the following:

(*a*) It is the apparent purpose of studies of the u.-v. absorption of cytological objects to determine the amount of specifically absorbing material, usually nucleic acid, present in the structure. The success of the experimental and interpretive procedures used in such studies should therefore be judged by this criterion.

(*b*) In the investigations which I have undertaken to criticize, the relative concentration of nucleic acid is calculated from the extinction of a given thickness of the object at 260 mμ. This calculation is based on the assumption that extinction *is proportional to nucleic acid concentration for all concentrations encountered.* In some studies the absolute nucleic acid content of the object is calculated from the measured extinctions and the specific extinction of nucleic acid in dilute solution. This calculation involves the further assumption that the extinction at 260 mμ per molecule of nucleic acid *is identical in solution and in the complex physical states occurring in biological objects.*

(*c*) These assumptions are not warranted by fact. To my knowledge the assumed linearity between extinction and concentration has never been demonstrated by actual experiment for any biological object other than the fluid vacuoles of plant cells. Furthermore, there are a number of reasons for believing that the relationship between extinction and nucleic acid concentration of biological objects cannot be linear over the range of concentrations encountered. One of these reasons is the effect of nucleic acid dichroism in limiting the maximum extinction given by an absorbing structure. That extinctions of 0·3 occur with unusual frequencies in these investigations fits in with this suggestion.

To my knowledge no alternative explanation of the unanticipated predominance of this particular extinction value has been published. There are, of course, several other grounds on which the assumption of linearity may be questioned. It is a commonplace that the relationship between E and concentration for *dissolved* substances is not linear beyond the most dilute solutions, and indeed few chemists would be willing to forego the practice of actually measuring calibration curves for colorimetric reactions. My chief criticism of the investigations in question is, therefore, that the assumed linearity between extinction at 260 mμ and nucleic acid concentration, while essential to the validation of the conclusions reached, has in fact never been proven, and on the grounds of dichroism as well as for other reasons is open to serious question.

There is a clear disparity between Dr. Wilkins' restatement of my argument on this question and the actual statements which I have made. His version of my criticism restricts the problem to that of a single extinction, 0·5 ; the essence of my position is that the point in question is that of proportionality over a wide range of nucleic acid concentrations.

Dr. Wilkins' restatement of my position is incorrect in another way. He ascribes to me the view that the work of the Caspersson school " is invalid because the dichroism of nucleic acid has not been taken into account ".* This is not my view of the question. The point which I *have* made is this : " The extinctions of intracellular objects at 260 mμ do not necessarily reflect their actual nucleic acid content and (that) considerable caution must be used in interpreting such data ".[31] It is not my position that the quantitative investigations of Caspersson and others *are* invalid, but that with respect to a very critical assumption, *the validity of such studies has yet to be established.* It is essential that this be done, or that the question be otherwise resolved, for in the absence of such validation biologists have no sound basis for judging the significance of the rather sweeping biological conclusions which have been drawn from many u.-v. microspectrophotometric studies.

(ii) Dr. Wilkins argues that the absence of birefringence in visible light in a biological object is evidence that the nucleic acid is not oriented. The fallacy in this argument is shown by Caspersson's report [32] that a nucleic acid film sufficiently oriented to give a dichroic difference in extinction of 0·22 will show birefringence in visible light which is so slight as to lie at the limit of sensitivity of this method. Since this small effect would need to be detected in the presence of a much larger effect of opposite sign rising from protein orientation, it seems obvious that the possibilities of judging the degree of nucleic acid orientation in biological objects from visual estimations of the degree of birefringences are very slight indeed. The use of such a crude and fallible method would certainly jeopardize the precision of microspectrophotometric procedures, the accuracy of which is so carefully protected at other points.

(iii) Finally, Dr. Wilkins finds it " comforting " to think that the effects of nucleic acid dichroism may be neglected except in certain unspecified cases where there is a " high degree " of orientation. He is of course at liberty to ignore the need for determining quantitatively the relation between extinction and the number of molecules scanned. But he does so at his own peril. The " comfort " achieved by ignoring experimental complications is notoriously short-lived.

Dr. M. H. F. Wilkins (*Biophysics Res. Unit, King's College, London*) (*communicated*) : Dr. Commoner's arguments give me no reason to alter my evaluation of his paper on ultra-violet dichroism. He is mistaken about the sensitivity of birefringence measurements ; 5 mμ of path difference (referred to in the reference he quotes) is obvious in any good polarizing microscope, and with refined technique it is possible to detect even 0·03 mμ.[33]

---

* This Discussion.

[31] *Science*, 1949, 110, 31.

[32] *Chromosoma*, 1940, 1, 614.

[33] Swann and Mitchison, *J. Expt. Biol.*, 1950, 27, 226.

Mr. H. G. Davies (*Biophysics Res. Unit, King's College, London*) (*communicated*): It has been shown that under the conditions given in my paper the ultra-violet dosage used in examining living cells photographically is likely to produce some upset to the cells after only a few photographs at a wavelength of 265 mμ. Calculations have been made to determine approximately what reduction in dosage may be expected when cells are examined using a photoelectric technique. Clearly, using this latter method we can study the absorption of one particular cell component without irradiating the rest of the cell. This would be difficult to do photographically. Conversely, to obtain information about the entire cell photoelectrically we should have to use some sort of scanning technique. However, it is proper to compare the relative amounts of energy required photographically and photoelectrically to obtain the optical density of the same area of the cell to the same degree of accuracy. This accuracy is that of recording apparent optical density which itself is subject to the many errors arising out of the nature of the biological material. These latter errors are the same in both cases.

Consider first the photographic film. When all pure calibration errors have been eliminated from the photographic method, errors still arise due to the uneven distribution of the silver grains. These errors can be determined by taking a series of microphotometer traces across an evenly exposed film with microphotometer spots of varying area. It is found, as is to be expected, that percent. mean deviation of galvanometer deflection is inversely proportional to the square root of the area of the microphotometer spot. The use of this method for comparing the relative graininess of films is well known.[34] The error in measuring cell apparent optical density is related to the error in measuring film density by the film gamma. The accuracy of recording the former increases with increasing film gamma. Furthermore, it is to be expected that the error due to graininess in recording the density of any particular area will itself be a function of density,[35] since it is generally stated that film resolving power which partly depends on graininess is a function of film density. Experimental data obtained for Kodak Microfile Panchromatic show that at × 100 magnification the smallest body of apparent optical density 0·3 that can be measured to accuracy of ± 2 % due to errors from this cause is about 0·2 μ^2 in area. These considerations represent the directly useful approach to film resolving power under conditions where turbidity can be neglected, and indicate how the proper magnification on to the film can be chosen.

Photoelectrically the ultimate limit is set by the statistical fluctuations in the number of emitted photoelectrons and accompanying thermionic electrons. The calculations are referred to a caesium antimony surface such as is found in the R.S.A. I.P. 28 photomultiplier, where the quantum efficiency is about 6 % at 265 mμ and the thermionic emission is 10^{-14} Å.*

It may be shown that the signal/noise S_n for a photomultiplier tube and the energy E required for a measurement are given by the expressions:

$$S_n^2 = \frac{i_p^2}{2e\Delta f(i_p + i_t)}, \qquad (1)$$

$$E = \frac{i_p\tau}{\alpha}, \qquad (2)$$

where i_p is the current due to emission of electrons by the photoelectric effect; i_t is the thermionic current; e is the electronic charge and Δf the band width; E is the energy in W sec.; τ is the response time of the system and α is the sensitivity of the photo-cathode in A.W.$^{-1}$ The bandwidth Δf is taken as 2 c./sec. and the corresponding response time of the system 1/4 sec. Calculation using eqn. (1) and (2) shows that in measuring

[34] Dunham, *Proc. VIIIth Int. Phot. Congress* (Dresden, 1931).
[35] van Kreveld, *J. Opt. Soc. Amer.*, 1936, **26**, 170.
* R.C.A. Data Sheet.

the same area as above of density 0·3 to the same degree of accuracy, ± 2 % at a wavelength 265 mμ, only about 1/7 of the energy is required photoelectrically. By suitably cooling the photocathode the thermionic emission can be almost completely eliminated [36] and statistical theory simply shows that the energy E for a measurement is given by

$$E = \frac{S_n{}^2 e}{\alpha}. \quad . \quad . \quad . \quad . \quad . \quad (3)$$

The energy required photoelectrically is then only about 1/30 of that required photographically. This ratio is also approached in the presence of thermionic emission with light sources of high intensity and correspondingly reduced response time. Comparison of this sort, provided the assumptions on which they are made are kept in mind, show the ultimate ratios of sensitivity which can be attained photoelectrically and photographically when account is taken of inherent limitations of a statistical nature and all calibration and such-like errors have been removed from the apparent optical densities recorded.

Dr. R. D. B. Fraser (*King's College, London*) (*communicated*) : The frequencies of the absorption maxima in the spectra of Fig. 5 of my paper are given below :

COLLAGEN FIBRE : 3325 s. perp., 3085 w. perp., 2950 w, (2860), 1655 s. perp., 1550 s. par., 1455 w. par., (1420) par., 1391 w, 1340 w, 1245 m. par., 1203 w. par., 1165 w. perp., 1082 w. perp., 1032 w. perp.

SODIUM THYMONUCLEATE : 3350 s., 3195 s., 2960 m., (2860), 2770 w., 1690 s., 1632, 1530 w., 1482 m., 1412 w., 1358 w., 1243 s., (1180), 1092 s., 1070 s., (1011), 964 m.

(Approximate relative intensity is indicated by s = strong, m = medium and w = weak; brackets refer to shoulders on stronger bands. Perpendicular dichroism refers to a greater absorption with the electric vector vibrating at right angles to the fibre axis.)

It is noteworthy that the NH stretching band in collagen occurs at 3325 cm.$^{-1}$, which is significantly higher than the values observed in α and β-keratins. The spectrum of sodium thymonucleate shows considerably more detail than that published by Blout and Fields [37] and should assist in the assignment of some bands. From the contributions of R. C. Gore and D. C. Smith to the Discussion it seems probable that the band at 1243 cm.$^{-1}$ is to be assigned to the valence vibration of the phosphoryl groups, whilst the region of strong absorption around 1080 cm.$^{-1}$ is to be associated with the C—O—P linkage.

---

[36] Engstrom, *J. Opt. Soc. Amer.*, 1947, **37**, 420.

[37] *J. Biol. Chem.*, 1949, **178**, 335.

II. APPLICATION OF MICRO- AND MACRO-SPECTROGRAHY

STUDIES WITH A REFLECTING MICROSCOPE : MICROSPECTROSCOPY OF LIVING AND FIXED CELLS

BY ROBERT C. MELLORS

Received 18*th July*, 1950

The reflecting microscope is used with a spectrograph to record the ultraviolet absorption and fluorescence emission in cellular areas of 1 μ^2 or less, and to detect in cervical smears optical differences between normal cells and cells which have abnormal features suggestive of but not conclusive for cancer. Quantitative measurements of light absorption are made in uninjured *living* cells of mesenchymal origin in the resting and the dividing states : the corrected extinction at 260 mμ is of the order of 0·3 or less in the nuclei of resting cells and 0·8 in chromosomal material of dividing cells.

A method of secondary fluorescence microphotometry developed for the scanning of cells of a smear and the detection of cellular abnormalities relates the fluorescence intensity and the chromatin content of the nucleus. Two classes of normal epithelial cells of the cervical smear have average relative fluorescence intensities of 1·7 and 2·4, whereas three classes of cells with increasing degrees of morphologic abnormality have relative values of 3·0, 4·1 and 6·2 respectively.

During the last two years the potential usefulness of the reflecting microscope has been investigated in diverse problems of cellular biology and pathology.[1, 2, 3] The present communication describes the methods and the results of some of these investigations. The reflecting microscope is used with a spectrograph to record the ultra-violet absorption or the fluorescence emission in minute portions of cells. In another optical system the microscope is illuminated with a monochromator for the determination of the ultra-violet light absorption of living cells in the resting and the dividing states. A quantitative method for the detection of cellular abnormality in terms of nuclear secondary fluorescence is developed from the point of view of its potential usefulness in scanning and processing diagnostic smears in clinical oncology.

Experimental

Optical Methods.—The reflecting microscope has been used in the following manner for studies in the ultra-violet and visible regions :

(*a*) With an achromatic monochromator (Plate I, A) and either photographic or photoelectric recording, as in (1) microscopy and photomicrography, (2) fluorescence microscopy, (3) colour translating microscopy,[4] (4) polarized light microscopy, and (5) microradiation of living cells, and

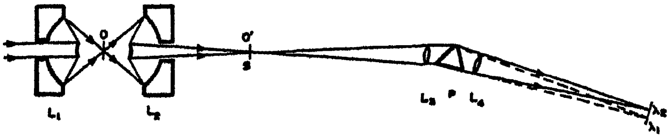

FIG. 1.—Diagram of reflecting microscope and spectrograph.

(*b*) With a quartz spectrograph (Fig. 1 and Plate I, B) and photographic recording, as in (1) absorption spectrography and (2) fluorescence spectrography. Reflecting condenser L$_1$ focuses spectrum of source on object. Reflecting objective L$_2$ images object O on slit S. Images O' are dispersed by prism P and refocused by lens L$_4$ on photographic plate. For fluorescence spectrography suitable filter is inserted near S, or proximal to L$_1$.

Monochromator.—The monochromator (Perkin-Elmer) which has effective aperture numbers of 4·5 and 6·0, respectively, in the axes of slit height and width is achromatic throughout the optical spectrum. Two methods of illuminating the reflecting microscope are illustrated in Fig. 2. In the usual system, (*a*), the prism or the grating of the monochromator is imaged in the plane of the object ; the field of the objective but not the aperture can be filled with light as the slit width is decreased ; and there is no variation of wavelength across the field. In the alternative system, (*b*), the exit slit of the monochromator is imaged in the plane of the object; the dimensions of the field but not of the aperture decrease

---

[1] Mellors, *Amer. J. Med.*, 1948, **5**, 626.
[2] Mellors, Berger and Streim, *Science*, 1950, **111**, 627.
[3] Mellors, Keane and Streim, *Nature*, 1950, **166**, 26.
[4] Brumberg, *Compt. rend. U.R.S.S.*, 1939, **25**, 473.

with the slit width and there is variation of wavelength across the field. System (*a*) is preferred for photomicrography whereas system (*b*) is more useful for micro-absorption measurements of small areas at high spectral resolution.

In the general expression relating the optics of the microscope and the monochromator[5]

$$\frac{f_c}{d_c} = \frac{f_0}{d_0}\,\frac{d}{d_f}(1 + 1/M)$$

f_c/d_c and f_0/d_0 are the aperture numbers of the monochromator collimator and microscope objective respectively, d is the monochromator slit width, and d_f and M are respectively the field of view and the magnification of the microscope objective. If the values $f_c/d_c = 6.0$, $f_0/d_0 = 0.5$, and $d_f = 0.15$ mm are substituted in the equation the slit width l_s is found to be 1.8 mm. At 250 mμ the linear dispersion at the exit slit of the monochromator is 20 mμ per mm

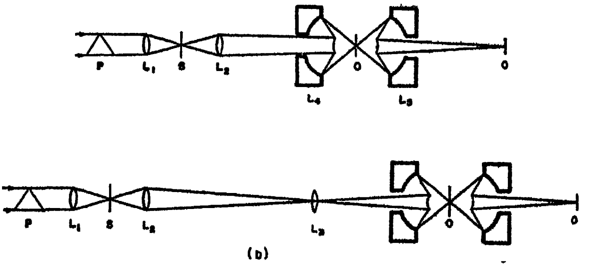

FIG. 2.—Two systems of illumination with a monochromator.

(*a*) The prism or grating P, is imaged in the object plane, O. (*b*) The exit slit, S, is imaged in the object plane O.

so that the required band pass is 36 mμ. In practice the bright lines of the mercury arc (Type AH—4) rather than a continuum are used as the source of radiation.

Reflecting Objectives.—The achromatic objectives are used in identical pairs as objective and condenser which are illuminated by the method of Kohler. Two designs are employed: that of Kavanagh,[6] a two mirror spherical system with numerical aperture 0.56, aperture number 0.7 and magnification 50 times, and that of Grey,[7] a two mirror spherical and refracting system with numerical aperture 0.72, aperture number 0.5 and magnification 53 times.

Spectrograph.—The quartz spectrograph (Hilger) which has as aperture number 11 is used with a reflecting objective of aperture number 0.7. After substitution of these values in the general expression[5]

$$\frac{f_c}{d_c} \div \frac{f_0}{d_0} \approx M + 1,$$

where f_c/d_c and f_0/d_0 are respectively the aperture numbers of the spectrograph collimator and the microscope objective, it is found that the objective magnification M required to fill the aperture of the spectrograph with light should not exceed 15. In actual practice the objective magnification is 50 so that less than the full aperture and resolving power of the spectrograph are utilized. For a source of radiation from 230 to 650 mμ the continuum of the hydrogen arc and the bright lines of the mercury arc are used. The minimum slit width limited by the sensitivity of the recording material and by other considerations is 15 μ which corresponds to a linear dimension of 0·3 μ in the object. The minimum slit height limited by the image dimension which can be analyzed in the recording densitometer is 30 to 50 μ.

Recording Methods.—The most satisfactory photographic emulsions are Kodak 1372, 103-0 UV, and Spectrum Analysis No. 1 for ultra-violet photomicrography, Kodak 103-0 UV and SWR for absorption spectrography, and Kodak Tri X Pan for fluorescence spectrography. The calibration of film or plate is carried out by means of a rotating sector placed near the image plane

---

[5] Loofbourow, *J. Opt. Soc. Amer.*, 1950, **40**, 317.

[6] Kavanagh, personal communication.

[7] Grey, *J. Opt. Soc. Amer.*, 1950, **40**, 283.

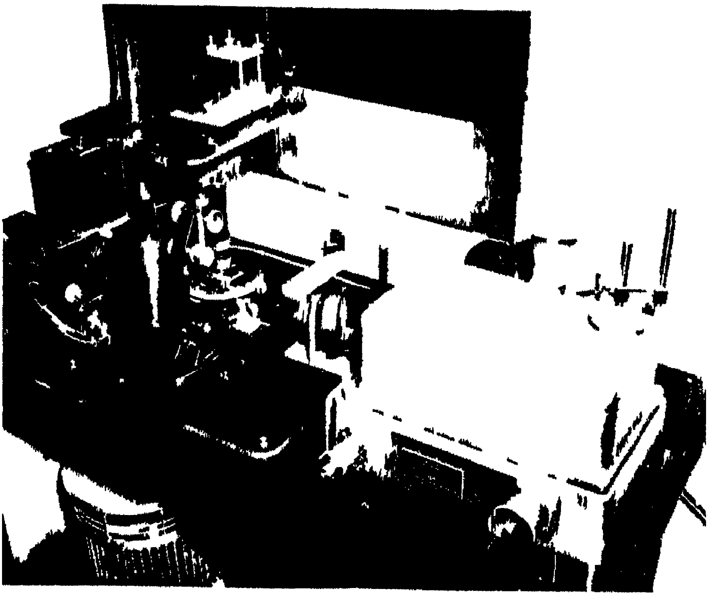

A

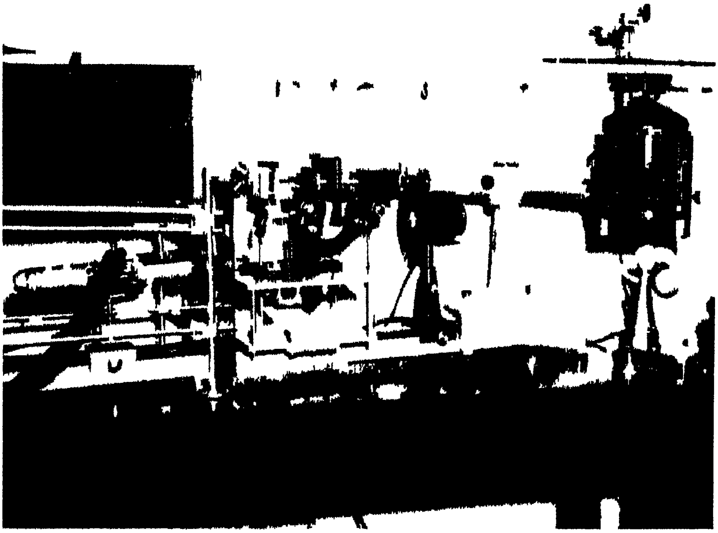

B

PLATE I

(A) Reflecting microscope illuminated with achromatic monochromator

(B) Reflecting microscope illuminated with hydrogen or mercury arc and used with spectrograph

[*To face page* 100

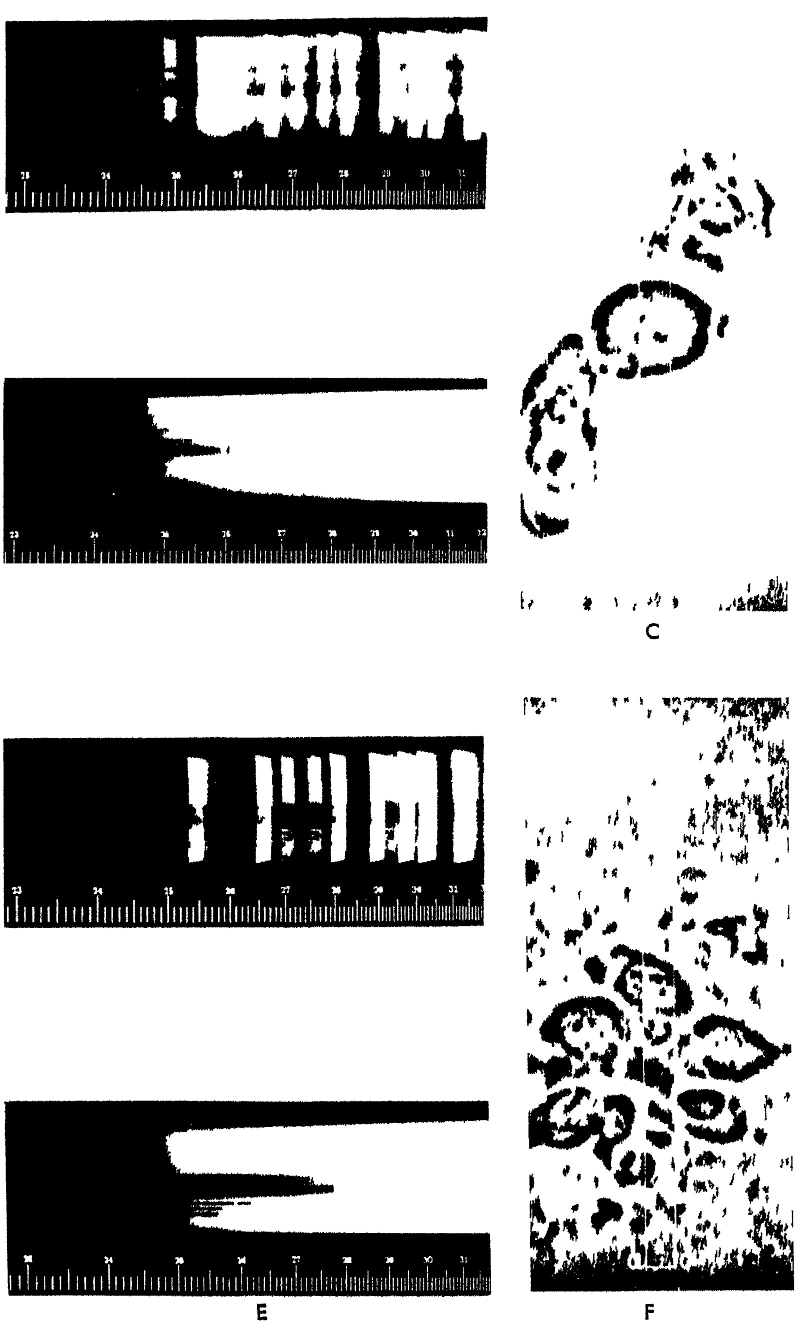

PLATE II.

(A), (B), (D) and (E) are spectromicrographs, respectively, of fields indicated in phase photomicrographs, (C) and (F), by the area *abdc*. Parabasal cell in (C), Class V (malignant) cell in (F). Field magnification in phase photomicrographs, ×600; in astigmatic spectromicrographs, ×600 laterally, ×200 vertically. Cervical smears fixed in formalin-saline.
λ scale = mμ/10.

A sensitive densitometer (Ansco) fitted with an illuminating aperture of 50 μ or less is used with a high-speed recording potentiometer (Leeds and Northrup). A graphic computation [8, 9] is made of the extinction ($E_\lambda = \log_{10} I_0/I$) at various wavelengths, where I_0 is the incident intensity and I is the transmitted intensity of monochromatic light λ. Due to the characteristics of the spectrograph, the images recorded on the plate are 150 times that of the object in width and 50 times in height. A densitometer aperture of 50 μ is therefore equivalent to an area of the object which is approximately 0·3 μ in width and 1 μ in height. Direct photometric measurements of light intensity are made with a photomultiplier tube (RCA 1P28) operating at 100 volts per dynode stage and appropriately standardized with a rotating sector and a thermopile. The colour translating projector was designed and described by Land *et al.*[10]

Biological.—Material chosen for study with reference to particular problems in cellular biology and pathology includes living mammalian cells in tissue culture, protozoa, a variety of cells in smears and tissue sections, and isolated cellular products such as chromosomes, nucleic acids, vitamins and hormones. Tissues are prepared principally as thin ($< 4\mu$), unfixed frozen sections [11] dehydrated by sublimation.[12] Infiltration procedures with water-soluble materials such as the polyethylene glycols remove certain cellular constituents such as steroids. Ultra-thin sections [14] prepared with celloidin-paraffin and cut at 0·1 μ are optically, but not chemically, satisfactory. The mounting media consist of glycerine for fixed cells, a balanced solution of electrolytes and glucose [15] with an air phase for living cells in tissue culture, and a viscous cellulose gel for mobile protozoa. Microscope slides are made of optically polished silica glass (Corning Vycor No. 791), and cover glasses of similar composition are polished to a thickness of 0·184 mm. ± 0·001 mm.

Results

Absorption Spectrography of Cells.—When the reflecting microscope is used with a spectrograph [3, 16] the images of a cell in many wavelengths of light are brought to focus in the plane of the slit, and the light that passes through the slit is dispersed and focused on the photographic plate. Thus, images of the emission lines or of the continuum of the source are formed, and upon these are superimposed the absorption patterns of the cell. Typical results together with phase photomicrographs which serve for morphologic reference are given in Plate II. The portion of the cell through which the incident light passes in order to gain entrance to the slit is a volume bounded by two parallel planes, *ab* and *cd*, and by the upper and the lower surfaces of the cell. In practice the separation of the two planes is 2 μ for the continuous and 6 μ for the bright line spectra. The *spectromicrograph* recorded in this manner has two dimensions: the *spectral* or horizontal dimension which relates the absorption and wavelength for any morphologic component; and the *morphologic* or vertical dimension which indicates the absorption in various morphologic components at a particular wavelength.

In collaboration with Dr. Papanicolaou this analytical method was used to study fixed and unfixed exfoliated cells of the vaginal and the cervical smear with special reference to cellular pathology in the human cervix uteri. A comparison was made between normal squamous and parabasal cells of the cervical mucosa and a class of cells designated by Papanicolaou [17] as *suspicious* or *Class III* and described by him as cells with abnormal features suggestive of, but not conclusive for cancer. The ultra-violet spectro-micrographs of portions of these various cells were recorded, and the extinctions were calculated over the range from 240 to 350 mμ. In nuclear chromatin a principle broad absorption maximum occurred over the region from 250 to 280 mμ. Representative data for the extinction maxima at 260 mμ in the nuclei of cells of the

---

[8] Brode, *Chemical Spectroscopy* (John Wiley and Sons, New York, 1943), 2nd edn., pp. 110, 275.

[9] Pierce and Nachtrieb, *Ind. Eng. Chem.* (*Anal.*), 1941, **13**, 774.

[10] Land *et al.*, *Science*, 1949, **109**, 371.

[11] Linderstrom-Lang, *The Harvey Lectures* (The Williams and Wilkens Co., Baltimore, 1939), p. 214.

[12] Gersh, *Anat. Record*, 1932, **53**, 309.

[13] Carsten, *Arch. Path.*, 1947, **44**, 96.

[14] Pease and Baker, *Proc. Soc. Expt. Biol. Med.*, 1948, **67**, 470.

[15] Gey and Jey, *Amer. J. Cancer*, 1936, **27**, 45.

[16] Barer, Cole and Thompson, *Nature*, 1949, **163**, 198.

[17] Papanicolaou, *Ann. Int. Med.*, 1949, **31**, 661.

three classes are given in Fig. 3. The majority of the observations are made on formalin-saline fixed material. The average values, the arithmetic means of 15 or more determinations, are 0·23, 0·36 and 0·54 respectively for squamous, parabasal, and Class III cells. There is, in addition to the greater magnitude, a broader range of values for the extinction maxima in the Class III cells as compared with the normal cells. While the frequency distribution of nuclear dimensions has a greater range and the average nuclear diameter is also larger in the Class III cells than in the normal cells, there is poor correlation between the nuclear dimensions and the extinction maxima. Thus, the optical path length estimated from the nuclear size is not alone sufficient to account for the differences in the extinctions. There is an increase in the average nuclear chromatin density of the Class III cells.

Ultra-violet Microscopy of Living Cells.– Results reported elsewhere[3] together with the data of Mayer[18] provide an estimate of the amount of ultra-violet radiation which is tolerated by living mammalian cells without injury. The amount, a product of intensity and time expressed as energy per unit area of cell, is of the order of 1 × 10^4 ergs/cm.^{2} at 260 mμ and in excess of 1 × 10^6 ergs/cm.^{2} at 315 mμ. These data when compared with the energy per unit area of photographic emulsion required to produce a satisfactory image indicate the necessity of recording images of *uninjured* living cells at a minimum magnification with emulsions of a maximum ratio of sensitivity to resolution. An estimate is that approximately 18 photographs can be recorded on Kodak 1372 at 260 mμ with a reflecting objective of magnification 53 times and transmission 0·2

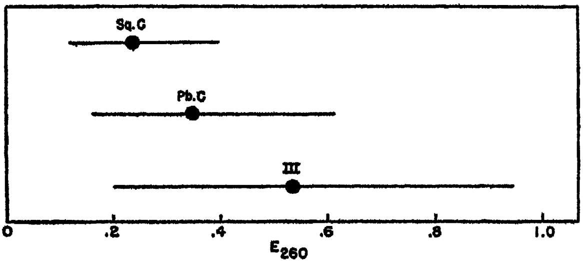

FIG. 3.—Extinction at 260 mμ in nuclei in epithelial cells of cervical smears.

Sq. C = Squamous.
Pb. C = Parabasal.
III = Papanicolaou classification.

● Average value.
— Range of values.

Under conditions which do not produce radiation injury the light adsorption of the nuclear material of *resting* living cells is found to be qualitatively[19, 20] and quantitatively low both in the ultra-violet and the visible regions. The corrected extinction at 260 mμ for which representative average values are given in Fig. 4 varies between 0·12 and 0·33 in the nuclear material of living *resting* (interphase) fibroblasts of the rat, chicken, and mouse, endothelium of the mouse, and sarcoma of the mouse. In the living *dividing* cell at metaphase when the reduplicated chromosomes are condensed the corrected extinction at 260 mμ in chromosomal material is of the order of 0·77. The ultra-violet absorption of cytoplasmic material in the living cell resides in great part in formed elements such as mitochondria which dimensionally are at the limit of resolution 0·2 μ for the objective used. The corrected extinction at 260 mμ for the cytoplasmic ground substance of resting cells of the type under consideration is approximately 0·12 whereas that for formed elements is undoubtedly much greater but not accurately measurable. During cell division the ultra-violet absorption of extrachromosomal material increases so that the corrected extinction at 260 mμ rises to 0·65. The supposition is that some or much of this absorbing material is derived from mitochondria[21] and is dimensionally not resolved.

---

[18] Mayer, *Tabulae Biologicae*, 1939, 19, 65.
[19] Brumberg and Larionow, *Nature*, 1946, 158, 663.
[20] Ris and Mirsky, *J. Gen. Physiol.*, 1949, 32, 489.
[21] Ludford, Smiles and Welch, *J. Roy. Micro. Soc.*, 1948, 68, 1.

The degeneration, death, or chemical fixation of a cell is accompanied by an increased opacity of the nucleus in both the ultra-violet and the visible regions. In the cytoplasm under these conditions the formed elements are either altered or dispersed and then contribute to the ultra-violet absorption of the cytoplasmic ground substance. There are several factors underlying this change in light absorption among which the most significant are an increase in the loss of light by dispersion and refraction [22] and a change in the volume occupied by the absorbing materials.[20]

Secondary Fluorescence Photometry.—Much consideration has been given in the present study to the development of a quantitative physical method for detecting abnormal cells. An ultimate objective is to process diagnostic smears in clinical oncology by an automatic scanning technic. In view of the significance attached to nuclear chromatin in cellular pathology [23, 24] a rational beginning is made with a method that determines the relative contents of nuclear chromatin in cells. Two principles exist: (*a*) the ultra-violet absorption of the cell nucleus as shown by the pioneer work of Caspersson [23] resides principally in the nucleic acids of nuclear chromatin and (*b*) the staining properties of nuclear chromatin have long been known [25] to be due to the affinity of nucleic acids for basic dyes. The potential usefulness of absorption measurements in a scanning technique, however, is limited by the fact that in areas of the smear in which cells overlie each other the total absorption will be related by some positive exponential function to the number of absorbing elements. If recourse is made to a light emission method, such as secondary fluorescence photometry, a more favourable situation occurs: the intensity of the exciting radiation—and thus the intensity of fluorescence—decreases in successive layers of stained cells. The definitive method depends upon the following essential procedures:

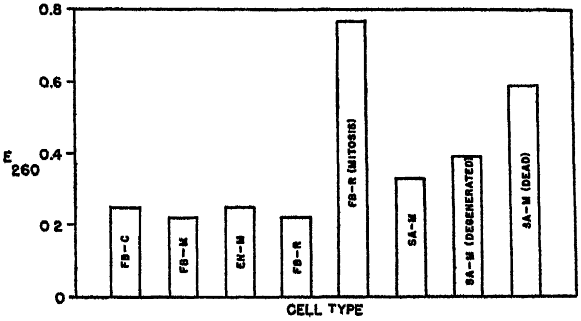

FIG. 4.—Extinction at 260 mμ (corrected for light dispersion) nuclear material of living resting cells unless otherwise indicated.

FB = Fibroblasts. EN = Endothelium. SA = Sarcoma.
C = Chick. M = Mouse. R = Rat.

(*a*) Staining cells under conditions which favour selective combination of basic fluorochrome with nuclear chromatin, such as 1×10^{-3} M berberine sulphate [26] at pH 6·3 [27, 30] (but not at pH 8·0 [28] and with other fluorochromes as described elsewhere [29]);

(*b*) quenching the fluorescence of chromatin derived from tightly packed clusters of inflammatory cells, such as polymorphonuclear leukocytes and histiocytes, by the deposition of opaque pigment in the cytoplasm of these cells at the site of the peroxidase reaction[29] with benzidine; and subsidiary steps which await final and complete evaluation:

---

[22] Caspersson, *J. Roy. Micro. Soc.*, 1940, **60**, 8.

[23] Caspersson and Santesson, *Acta Radiologica*, 1944, **25**, 113.

[24] Papanicolaou, *Diagnosis of Uterine Cancer by the Vaginal Smear* (The Commonwealth Fund, New York, 1943), 1st edn., p. 28.

[25] Michaelis, *Cold Spring Harbor Symposia on Quantitative Biology* (The Biological Laboratory, Cold Spring Harbor, 1947), p. 132.

[26] Haitinger, *Fluoresenz-Mikroskopie* (Akademische Verlagsgesellschaft M. B. H., Leipzig, 1938), 1st edn., p. 93.

[27] Pollister and Leuchtenberger, *Proc. N.A.S.*, 1949, **35**, 111.

[28] Friedman, *Amer. J. Obst. Gyn.*, 1950, **59**, 852.

(*c*) initial binding of the more strongly acidic groups of cellular constituents, such as polymeric organic sulphuric acid, with a non-fluorescent, λ365 mμ transparent, basic blue dye, such as 3×10^{-3} M Methylene Blue at pH 3·2,[30] and

(*d*) binding the free amino groups of cellular proteins with a non-fluorescent, λ365 mμ transparent, acidic blue dye, such as 1×10^{-3} M Fast Green at pH 6·3 in order to quench the fluorescence of dye bound with carboxyl groups.

The physical conditions for secondary fluorescence microphotometry are as follows:

(*a*) an essential control of the intensity of the incident ultra-violet radiation at 365 mμ by varying the slit width of the monochromator or by using neutral density filters;

(*b*) the theoretically ideal condition of achromatic optics for the ultra-violet and the visible spectrum;

(*c*) a photomultiplier tube (RCA 1P28) fitted with apertures so that when object dimensions of 5-70 μ are magnified 82 times by the objective the images fall on a diffusing plate and the change in sensitivity with varying position of illumination on the cathode is minimized;[31]

(*d*) a known relation between the light flux and the photoelectric emission under varying conditions of illumination of the photocell cathode.

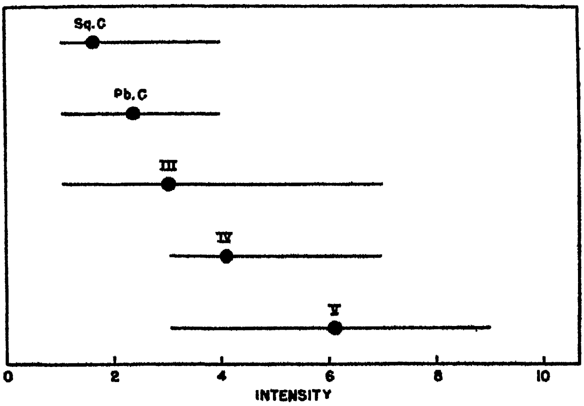

FIG. 5.—Secondary fluorescence intensity. Relative values, in nuclei of epithelial cells of cervical smears.

Sq. C = Squamous.
Pb. C = Parabasal.
III, IV, V = Papanicolaou classification.
● Average value.
— Range of values.

Data for the secondary fluorescence of epithelial cells of the vaginal and the cervical smear are given in Fig. 5 in terms of the relative intensity or brightness of the fluorescence. The physical dimensions are in terms of the maximum radiant flux per unit surface area of the cell. The fluorescence intensity is maximum over an area of the cell that is concentric with the nucleus and which has a diameter of the order of that of the nucleus, namely, about 10 μ. The average values, or the arithmetic means, of 15 to 50 determinations of the relative intensity of nuclear fluorescence are 1·7 and 2·4 respectively for squamous and parabasal cells, and 3·0, 4·1 and 6·2 respectively for abnormal cells of Classes III, IV and V. According to the criteria of Papanicolaou[17] cells of Class III have abnormal features suggestive of, but not conclusive for, cancer, while cells of Class IV are fairly conclusive and cells of Class V are conclusive for cancer. As the morphological appearance of epithelial cells of the cervical smear become more significantly abnormal, the average values for the secondary fluorescence intensity of their nuclei increase. Of course the range of values indicates that there are variations. Less than the average fluorescence intensity is to be expected and does occur in large nuclei which although morphologically malignant do not have a proportionate increase in volume and in chromatin content or in nuclei which, because of degenerative changes, have lost chromatin. The fluorescence intensity is a measure of the chromatin content which is but one of many cytological criteria of malignancy. The significance of the present observations will be known therefore only when the frequency distribution of chromatin content as determined by the binding of basic fluorochrome is studied in a much larger population of normal and abnormal cells. This is conveniently done by means of automatic scanning technique which at the present writing appear to be applicable to the problem.

---

[29] Lillie, *Histopathologic Technic* (The Blakiston Co., Philadelphia, 1948), 1st ed., p. 113.

[30] Dempsey and Singer, *Endocrinology*, 1946, **38**, 270.

[31] Engstrom, *J. Opt. Soc. Amer.*, 1947, **37**, 420.

Fluorescence Spectrography.—The reflecting microscope can be used as illustrated in Fig. 1 for combined fluorescence and absorption spectrography. It is possible by the use of chemical filters [32, 33] together with glass filters to limit the exciting radiations of the mercury arc to band widths of approximately 15 mμ in the ultra-violet region from 245 to 365 mμ. The fluorescence spectrum of fluorochromes, certain biochemical compounds and some cellular material can be photographed in a few or several minutes. The simultaneous recording of the fluorescence and the absorption spectromicrograph of chemical compounds indicates the general relation between the wavelengths of excitation and emission: for example, a simple chromophore such as the carbonyl group absorbs at 280 mμ and emits in the region of 300-400 mμ; a complex chromophore, such as the nitro group absorbs at 370 mμ and emits in the visible region.

Discussion

The theoretical limitations in the use of optical methods for the study of the cell are emphasized by the number of factors [2, 20, 22, 34, 35] that influence the absorption of light in cellular material: the amount, volume of distribution, spatial orientation, photochemical reactivity, and multiplicity of the absorbing materials together with the non-specific loss of light by reflection, dispersion, and diffraction. The complexity of the problem at first thought insoluble is resolved into analyzable components by the development of the reflecting micrscope [36, 37] which permits work in the entire optical spectrum. In the infra-red region [16, 38] the potentialities in terms of chemical resolution are greater while the non-specific optical effects and the structural resolution are less; whereas in the far ultra-violet, the vacuum ultra-violet, and the X-ray region the structural resolution is greater, the possibility of chemical resolution exists, and the photochemical effect may be appreciable. An analysis of Raman spectra provided they can be recorded by the optical system-monochromator, reflecting microscope, and spectrograph, has the greatest theoretical advantage of all in regard to structural and chemical resolution. The exciting radiations are in the ultra-violet region and the frequency differences produced in the Raman spectrum correspond to the frequencies of vibrational and rotational band spectra in the the infra-red region.[8] Thus it appears at this writing that microscopic work in the optical spectrum will prosper as a synthesis is made of information from its component regions.

This work was done in part under a fellowship grant of the American Cancer Society recommended by the Committee on Growth of the National

[32] Bowen, *The Chemical Aspects of Light* (Oxford University Press, Oxford, 1946), 2nd edn., p. 279.

[33] Kasha, *J. Opt. Soc. Amer.*, 1948, 38, 929.

[34] Commoner, *Science*, 1949, 110, 31.

[35] Danielli, in *Cold Spring Harbor Symposia on Quantitative Biology* (The Biological Laboratory, Cold Spring Harbor, 1949), p. 37.

[36] Burch, *Proc. Physic. Soc.*, 1947, 59, 41.

[37] Brumberg and Shevchenko, *Compt. rend. U.R.S.S.*, 1941, 32, 486.

[38] Blout, Bird and Grey, *J. Opt. Soc. Amer.*, 1950, 40, 304.

Research Council. The writer is indebted to Dr. G. N. Papanicolaou without whose collaboration much of the work could not have been undertaken. Thanks are acknowledged to Dr. Virginia Pierce for valuable clinical material and Dr. V. Z. Williams and Mr. A. J. Kavanagh respectively for the use of the monochromator and the reflecting objectives. The author is grateful to Dr. E. H. Land and Dr. E. R. Blout, and Messrs. D. S. Grey and L. V. Foster for the opportunity of obtaining a reflecting microscope of their design.

Sloan-Kettering Institute for Cancer Research,
New York, New York.

THE ULTRA-VIOLET ABSORPTION SPECTRA OF THE AROMATIC AMINO ACIDS IN PROTEINS AND RELATED COMPOUNDS

BY G. H. BEAVEN, E. R. HOLIDAY AND E. M. JOPE

Received 27th July, 1950

Soret[1] suggested in 1883 that the selective absorption of ultra-violet radiation by solutions of proteins was due to the contained aromatic amino acids. It was not, however, until the work of Ward,[2] Smith[3] and Stenström and Reinhardt[4] that this became generally accepted. Subsequently, Holiday[5] devised a quantitative method of estimating tyrosine and tryptophan in proteins based in the supposition that the absorption spectrum of proteins in the region λ 2700 to 3000 Å could be analyzed as a two-component mixture of tyrosine and tryptophan. His results were in fair agreement with those of chemical analysis. Morton and Goodwin[6] criticized this method from the point of view that extraneous absorption interfered with the estimation, and could not be satisfactorily allowed for. Parallel with this work and quite independently, evidence was accumulating that the spectra of these two amino acids were slightly altered by combination in a protein. Lavin and Northrop[7] and Coulter, Stone and Kabat[8] showed that tyrosine and tryptophan exhibit fine structure in their absorption spectra and that the corresponding bands in proteins were all shifted to longer wavelengths by 10 to 30 Å. Bearing also on this was the observation of Crammer and Neuberger,[9] who noted the anomalous pK of tyrosine in insulin and egg albumin. These observations were of interest from two points of view. Firstly, they invalidated one of the assumptions on which the quantitative analytical method of Holiday was based, namely that the absorption of tyrosine and tryptophan is not altered by combination in protein. Further work has, however, shown that if the wavelengths at which the absorption measurements on proteins and the aromatic amino acids are suitably chosen, then the small shift of the spectrum of the protein to longer wavelengths than those of the free amino acids does not vitiate the results of the analysis. It will be shown later that better standard curves may be found than those of simple solutions of tyrosine and tryptophan. The second point of interest in these observations on the fine structure of the spectra of proteins is their bearing on protein structure. Some observations referring to this second point are given in this paper.

THE NON-AROMATIC ABSORPTION OF PROTEINS.—Except for cystine, non-aromatic amino acids are almost completely transparent to wavelengths longer than λ 2,500 Å and would therefore not be expected to interfere with the absorption of the aromatic amino acids in this region. Moreover, there is no *a priori* evidence that the peptide linkage will have any effect in this respect. As will be shown, the peptide linkage has a negligible effect on the ***intensity*** of absorption of its contained amino acids. Nevertheless it has been maintained by some workers that the polypeptide "fabric"[28] has appreciable absorption in this region. We cite the following evidence against this:

---

[1] Soret, *Arch. Sci. Physig. Nat.*, 1883, **10**, 429.
[2] Ward, *Biochem. J.*, 1923, **17**, 898.
[3] Smith, *Proc. Roy. Soc. B*, 1929, **104**, 198.
[4] Stenström and Reinhardt, *J. Biol. Chem.*, 1925, **66**, 919.
[5] Holiday, *Biochem. J.*, 1936, **30**, 1795.
[6] Goodwin and Morton, *ibid.*, 1946, **40**, 628.
[7] Lavin and Northrop, *J. Amer. Chem. Soc.*, 1935, **57**, 874.
[8] Coulter, Stone and Kabat, *J. Gen. Physiol.*, 1936, **19**, 739.
[9] Crammer and Neuberger, *Biochem. J.*, 1943, **37**, 302.

(1) Proteins and polypeptides containing no tyrosine or tryptophan show negligible absorption in the region λ 2650 to 3100 Å.
(2) Proteins containing either tyrosine or tryptophan but not both (insulin tyrosin 12·0 %) or gramicidin (35 % tryptophan) show spectra closely similar to those of simple solutions of the corresponding amino acids.
(3) The results of spectral analysis would not agree so well with those of chemical analysis if there were much extraneous absorption.

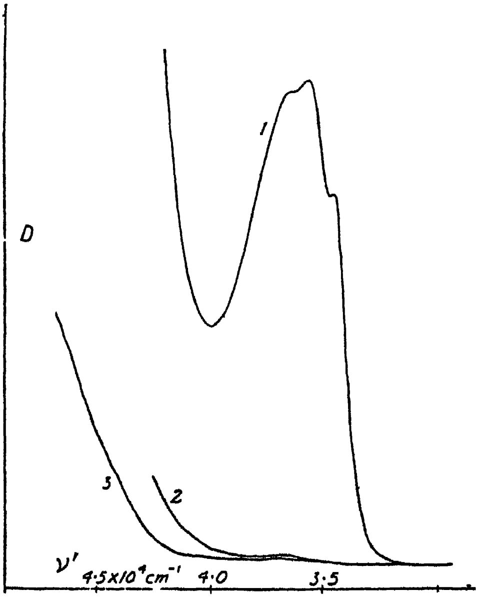

FIG. 1.

1. Lysozyme, 0·05 %. 2. Gelatin, 0·1 %. 3. Clupein, 0·1 %.

These facts are illustrated in Fig. 1 to 3 and Table I. It is therefore concluded that at wavelengths longer than λ 2650 Å the absorption is due to tyrosine and tryptophan. It is, of course, always possible that in any particular protein or protein sample absorption may occur in this region due to a non-amino acid residue, whether present as an integral part of the molecule (e.g. haemoglobin, flavoprotein, etc.) or as an impurity. Light scattering contributes also in varying degree to the net absorption. Such cases require special discussion and lie outside the scope of the present inquiry.

In 1935 Coulter, Stone and Kabat[8] published the results of an investigation of the fine-structure characteristics of the spectra of several proteins and of the aromatic amino acids. They noted close correspondence between the spectral fine structure of the amino acids and those of protein spectra, but found that with proteins the bands were shifted to longer wavelengths by 10-35 Å. These observations have been fully confirmed by subsequent workers. Over a period of years we have, in our laboratory, investigated all new proteins coming into our hands by the moving plate method[10] which was devised specifically for the detection of fine structure in absorption spectra. In the course of this an interesting observation was made by Jope,[11] that a very distinct difference existed in the positions of the fine structure band systems in adult and foetal human haemoglobins, both in solution and in the intact red blood corpuscle.

---

[10] Holiday, *J. Sci. Inst.*, 1937, **14**, 166.

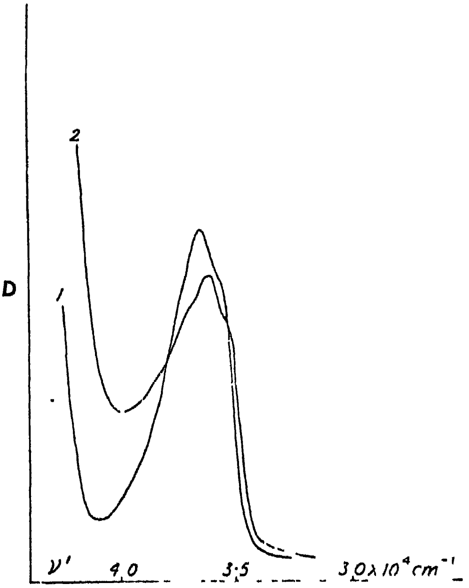

Fig. 2.

1. Tyrosine. 2. Insulin at pH 3.

TABLE I.—Comparison of Estimations of Tyrosine and Tryptophan in Proteins and Poltpeptides by Chemical and Spectrophotometric Methods

	Tyrosine		Tryptophan	
	Chem.	Spectro.	Chem.	Spectro.
Horse Serum Globulin	5·7	6·3	2·8	2·7
Horse Serum Albumin	5·9	6·35	0·8	0·0
Casein	6·1	6·7	1·1	1·15
Gelatin	0·15	0·26	0·0	0·05
Gliadin	3·1	3·4	0·84	0·65
Zein	5·9	6·3	0·17	0·0
Insulin	12·9	12·7	0·0	0·0
Edestin	4·34	4·60	1·63	1·21
β-Lactoglobulin	4·3	4·9	1·9	2·2
Pepsin	8·7-12·0	8·25	2·3	2·43
Tyrocidin	13·0	14·7	16·3	15·8
Gramicidin	0·0	0·0	39·6	39·3

Values are expressed as percent by weight of free amino acid.

This difference is, so far as we know, confined to human haemoglobin. The difference is particularly evident in the region λ 2900 Å where the λ 2880 Å fine structure band of tryptophan (the tryptophan "notch") occurs. In foetal haemoglobin it is shifted to λ 2898 Å (resolved maximum) while in adult it is at λ 2910 Å (unresolved inflection), as shown in Fig. 4. Since then we have studied the change of spectral absorption of human haemoglobin from the third month of foetal life until 6 months after birth (Table II). Although the change is very small and, so far as we have been able to detect, only involves the position of the tryptophan notch, it is quite regular. The positions and relative intensities of all other features of the foetal and adult types of spectra are indistinguishable (Fig. 4). Jope and O'Brien [12] have discussed other differences between the two types of haemoglobin. These include crystallographic and solubility characteristics, while Porter and Sanger [13] have shown that the adult

---

[11] Jope in *Haemoglobin* (Butterworth, London, 1949).

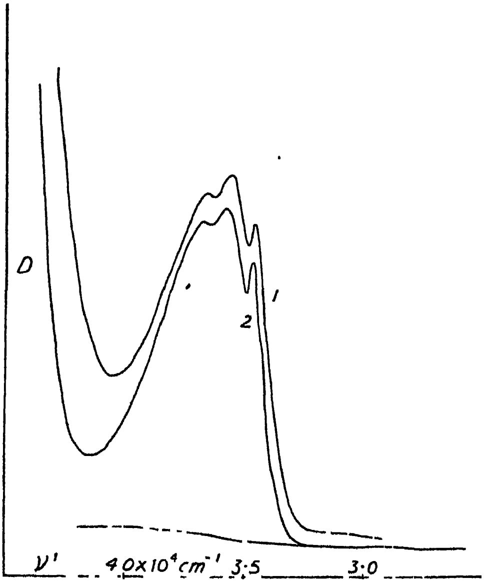

FIG. 3.

1. Gramicidin in ethanol. 2. Tryptophan in ethanol.

TABLE II.—LOCATION OF THE TRYPTOPHAN "NOTCH" IN FOETAL AND ADULT HUMAN HAEMOGLOBIN AT pH 7·0

Description	Position (Å)	Description	Position (Å)
Foetus, 16 weeks .	2898	New born . .	2898
" " .	2898	" . . .	2900
" " .	2898	Baby 2 months .	2904
" " .	2897	Baby 4 months .	2908
" " .	2898	Adult . . .	2909
" 26 weeks .	2898	"	2910
" 8 months .	2897	"	2909
" 9 months .	2897	"	2910
" " .	2897	"	2910
" " .	2899	"	2909
New born . .	2900	"	2908
"	2899		

---

[12] Jope and O'Brien in *Haemoglobin* (Butterworth, London, 1949).
[13] Porter and Sanger, *Biochem. J.*, 1948, **42**, 287.

type contains 5 terminal valyl residues per molecule, whereas the foetal type contains 2·6. Recently Dr. H. Hoch [14] has shown that the electrophoretic mobility of the adult type is slightly greater than that of the foetal type.

All recent work has confirmed the original observations of the shift in the fine structure of the spectra of proteins. Further evidence of the reality of the effect is obtained from the change of spectrum which occurs on enzymic degradation of a protein. Although little reference to the fact is to be found in the literature, the effect is well seen in absorption curves of serum globulin (horse) before and after tryptic digestion.[15] Some time ago we made some preliminary experiments to find at what stage of protein degradation by enzymes the anomalous spectrum of proteins reverted to normal. It was first confirmed that peptic digestion of serum albumin and globulin caused a complete reversion of the spectrum to the normal position (Fig. 5). Then it was shown that with very short digestion periods at high dilutions of enzyme the spectral reversion took place at a very early stage of digestion. In a particular case in which serum albumin was subjected to digestion with pepsin the extent of breakdown was estimated in a parallel ultracentrifugal run. It was found that the spectra reversion was complete at a stage at which the mean sedimentation constant had dropped from $4{\cdot}1 \times 10^{13}$ for the native albumin to $1{\cdot}95 \times 10^{13}$. Although the material at this stage was obviously polydisperse, it can

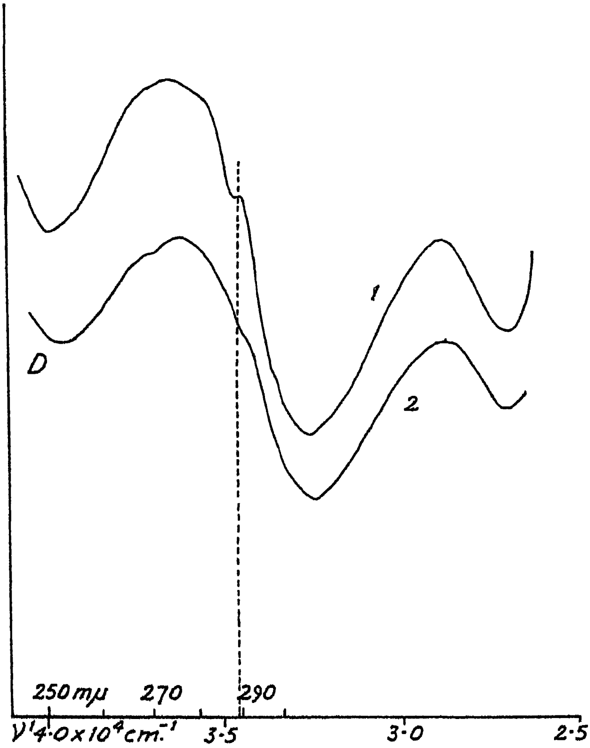

FIG. 4.

1. Foetal haemoglobin. 2. Adult haemoglobin.

---

[14] Hoch, H. (private communication).

[15] Haurowitz and Astrup, *Nature*, 1939, **143**, 118.

be concluded from the lowering of S by 50 % that the mean level of protein breakdown was to a stage of approximately half-molecules. Attempts to bring about this reversion by means other than enzymic digestion failed. Denaturation by saturated urea, boiling, strong alkali or acid, brought about no significant change. On the other hand it can be surmized from the data of Jope, Jope and O'Brien [16] that globin of human red cell haemoglobin shows on denaturation a partial reversion from the anomalous absorption of the native protein.

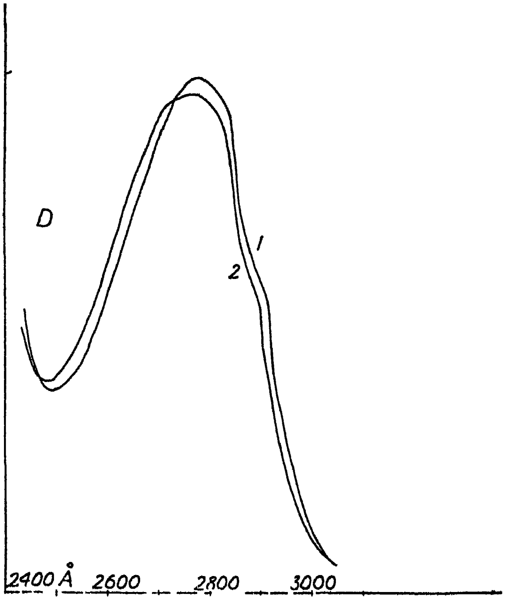

FIG. 5.
Horse serum globulin.
1. Before digestion with pepsin. 2. After digestion with pepsin.

Polymyxin B.- This polypeptide contains only leucine, phenylalamine, threonine and αγ-diamino butyric acids, combined with *ca.* 10 % of a fatty acid.[17] Absorption spectra and moving-plate spectrograms of polymyxin B in the pH range 2 to 8 show a highly developed phenylalanine fine structure. Comparisons between phenylalanine and polymyxin B show that in this polypeptide from which the other two aromatic amino acids are absent, the fine structure is located at exactly the same wavelengths (with a precision of ± 1 Å) as in phenylalinine itself. The absorption of the phenylalanine residue thus appears to be completely unaffected by peptide combination. From the extinction coefficients at the maxima and the corresponding figures for the parent amino acid, polymyxin B has an apparent phenylalanine content of *ca.* 14 % by weight, which may be compared with an estimate by other methods of *ca.* 10 %.

The appreciable absorption above λ 2700 Å, the degree of resolution of the fine structure maxima and the steeply-rising shortwave absorption all indicate that the samples of polymyxin B used exhibit irrelevant absorption (which appears to be increased at low pH) so that a more precise analysis requires some form of base-line correction. Using such a base line extrapolated from the curve above λ 2700 Å gives a corrected figure of 8·9 % by weight.

[16] Jope, Jope and O'Brien, *Nature*, 1949, **164**, 622.
[17] Jones, *Ann. N.Y. Acad. Sci.*, 1949, **51**, 909.

Gramicidin.—This crystalline antibiotic of molecular weight[18] *ca.* 3000 contains only one aromatic amino acid, viz. tryptophan, and its absorption spectrum in ethanol (Fig. 3) is very similar to that of tryptophan in the same solvent, except that the entire curve is shifted 10-15 Å to longer wavelengths. In analyzing gramicidin spectrophotometrically for tryptophan, Edwards[19] took account of this shift by using acetyl tryptophan as reference compound, rather than tryptophan itself; the molar extinction coefficients of the acetyl derivative at the various maxima are significantly lower than the corresponding values for the parent amino acid. For 38 samples of gramicidin Edwards[19] found a mean tryptophan content of 39·3 % (range 38-41 %; standard deviation 1·12) compared with 39·6 % by chemical methods. The excellent agreement obtained indicates the precision obtainable by spectrophotometric methods in a favourable case, and emphasizes the necessity for obtaining accurate wavelength and extinction coefficient data for the aromatic amino acids in peptide combination.

Tyrocidin.—This related antiobiotic[18] is of greater complexity and contains all three aromatic amino acids but no cystine. Its absorption spectrum in neutral and acid methanol clearly shows the tryptophan fine structure band at 2900 Å and the main maximum at 2810 Å. In alkali the whole curve shifts to longer wavelengths to give a typical "alkaline tyrosine" spectrum. Neglecting the small contribution made by phenylalanine to the total absorption, the alkaline curve can be accounted for by 2 moles each of tryptophan and tyrosine per mole of tyrocidin (mol. wt. 2546 (calc.) for a N_{26} molecule), in good agreement with the chemical figures (Table I). The phenylalanine fine structure is clearly visible in moving-plate spectrograms, although the contribution of this constituent (3 moles/mole of tyrocidin) is only about 6 % of the total absorption at the most favourable wavelength.

α-Keratin from Wool.—A sample of α-keratin, prepared by treating native wool fibre with dilute aqueous peracetic acid,[20] has been examined. This reagent destroys all the tryptophan and oxidizes all the cystine of the wool to cysteic acid. The product is soluble in dilute alkalis and in hydrogen bond-breaking solvents, such as urea and lithium bromide solutions and formic acid from which it may be recovered as a pale yellow powder. It gives the typical X-ray diffraction pattern of α-keratin. The absorption spectrum of this material at pH 8 shows a poorly-defined band in the 2800-2900 Å region, which changes to a well-resolved "alkaline tyrosine" band in alkali; the position of the maximum at pH 13 (max. 2915 Å) suggests that ionization of the tyrosine phenolic hydroxyl groups is barely complete at this pH, although the pK of the same group in tyrosine itself is *ca.* 10. Further evidence that the tyrosine residues of the material are involved in some form of structure that is irreversibly broken down at pH 12 to 13 is provided by the fact that the spectrum at pH 8 after exposure to alkali at pH 12 to 13 is not identical with that of the original solution at pH 8, but shows a band of increased intensity and resolution, with some poorly-resolved fine structures on the shortwave side of the maximum. This is more easily seen in a moving-plate spectrogram, and can be identified as due to phenylalanine, shifted about 10 Å to longer wavelengths. The characteristic tryptophan maximum at about 2900 Å is completely absent. The absorption curve at pH 12 to 13 indicates that there is considerable absorption not due to aromatic amino acids, but after applying an approximate base-line correction for this, the calculated tyrosine content (5·5 % by weight) is in fair agreement with the chemical figure (4·8 % by weight). This material provides an example of the Neuberger-Crammer[9] effect in a modified protein, which cannot be regarded as native, but which still retains a high degree of structure, evidently involving the tyrosine hydroxyl groups.

---

[18] Hotchkiss in *Advances in Enzymology* (Interscience, New York), 1946, **4**.

[19] Edwards, *Arch. Biochem.*, 1949, **21**, 103.

[20] Alexander and Earland, *Nature*, 1950, **166**, 396.

Lysozyme.—A recent review by Fromageot [26] discusses the absorption spectrum of this enzyme, which has a molecular weight of *ca.* 14,000. It contains all three aromatic amino acids, together with cysteine. Fromageot and Schnek [27] found that in acid solution its absorption was in good agreement with the additive absorption of 3 moles of tyrosine, 5 moles of tryptophan and 5 of cystine, apart from a longwave shift of *ca.* 20 Å in lysozyme and additional absorption at wavelengths below 2500 Å. In alkali the agreement was also good though the wavelength anomalies were consistently in the opposite direction. The variation of the spectrum with pH indicated that the pK of the tyrosine hydroxyl group ionization was different from the value for free tyrosine. The apparent pK varied linearly with pH from 10·1 at pH 9·5 to 12 at pH 13, behaviour analogous to that of insulin and egg albumen.[9] With lysozyme, however, the effect of alkali at pH 12 on spectrum was completely reversible, as subsequent acidification gave a curve identical with that of the original sample in acid. The curve which we have obtained for lysozyme (Fig. 1) shows in acid a very well-defined tryptophan spectrum with the notch clearly resolved and located at 2911 Å, a long wavelength displacement of 31 Å. The phenylalanine fine structure is just visible on the shortwave side of the band in a moving plate spectrogram. The additive tyrosine and tryptophan and cystine curves of Fromageot and Schnek are in good agreement with chemical figures, though direct application of the two-component method based on the absorption at 2800 Å and 3050 Å shows poorer agreement. As noted above, lysozyme is outstanding for its very low absorption at wavelengths longer than 3200 Å, i.e. outside the absorption bands of the aromatic amino acids proper.

The Spectra of Simple Peptides and Polypeptides.—Having established to our own satisfaction that the spectral shift is a real one, we have made preliminary studies of certain factors which might be responsible for the effect. The effect of simple peptide linkage on the absorption of the aromatic amino acids is the first question that arises. The three aromatic amino acids are β derivatives of alanine and in each case the aromatic chromophore is separated from the peptide carbon by two single bonds. It is generally stated that two single bonds insulate a chromophore from electromeric changes. This is not strictly true. Braude [21] has discussed the effect and shown quite clearly that the chromophore is not insulated although the effect is a minor one. A good example of electromeric effects being transmitted over two single bonds is to be found with phenylalanine where there is a quite significant change in spectrum as between acid and alkali (Table III). The change

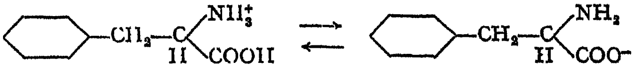

$$\text{C}_6\text{H}_5\text{—CH}_2\text{—}\underset{\text{H}}{\text{C}}\begin{matrix}\text{NH}_3^+\\ \text{COOH}\end{matrix} \rightleftharpoons \text{C}_6\text{H}_5\text{—CH}_2\text{—}\underset{\text{H}}{\text{C}}\begin{matrix}\text{NH}_2\\ \text{COO}^-\end{matrix}$$

has affected the benzene chromophore, although it is insulated by two intervening single bonds from the α carbon atom. This fact makes it appear likely that peptide combination will have some effect on the absorption spectrum of the aromatic amino acids. In fact, with the advance in recent years of the precision of spectrophotometry, evidence has accumulated that this is so. We have ourselves made absorption measurements on several peptides of aromatic amino acids acid and compared their spectra with those of the simple amino acids. Since all the aromatic amino acids show fine structure readily detectable by the moving-plate method, we have assembled the data from our measurements in the form of charts (Fig. 6 and 7), showing the positions of the fine structure bands of the compounds investigated. Unfortunately, we have so far had no phenylalanine peptides available. The present results show that peptide combination has a definite small effect on the absorption spectrum of the aromatic amino acids, which consists in every case of a shift to long wavelength of about 5 to 15 Å.

---

[21] Braude, *J. Chem. Soc.*, 1949, 1902.

The Effect of Change of State on the Absorption Spectra of the Aromatic Amino Acids.- Inspection of Fig. 6 and 7 show that although peptide linkage has a displacing effect on the spectra of the aromatic amino acids, it is not sufficient to account for the displacement found in the spectra of proteins. Some observations we have made indicate that non-valency forces may also bring about spectral shifts, which, added to those due to peptide combination, may be sufficient to account for the displacements found in protein spectra. In those experiments the positions of fine structure bands were determined on thin films and on solutions of the aromatic amino acids in gum arabic, dextrin and gelatin in the liquid and solid state. Some low temperature measurements were also made on the films.

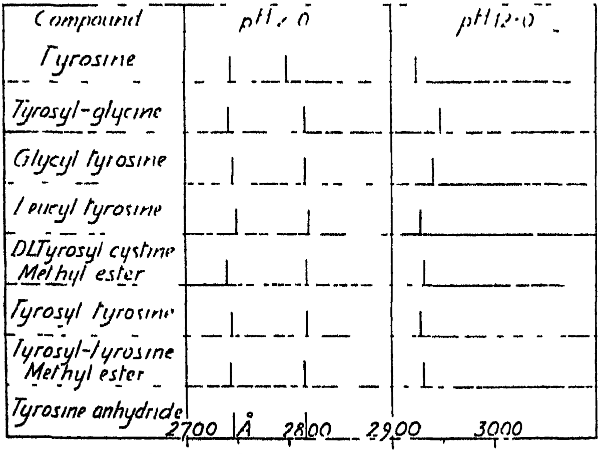

FIG. 6.—Fine structure band positions of tyrosine and some tyrosyl peptides.

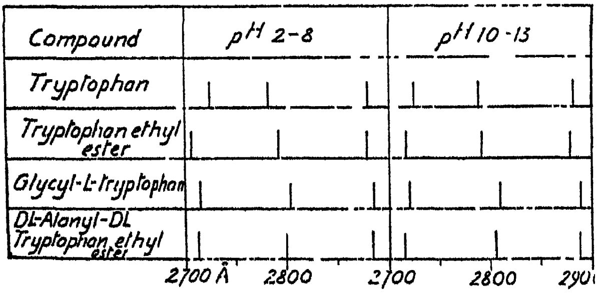

FIG. 7.—Fine structure band positions of tryptophan and some peptides.

Gelatin itself is of particular interest. Since it contains no tryptophan and very little tyrosine it is reasonably transparent in the range λ 2500 to 2700 Å in which phenylalanine absorbs.

Since the content of phenylalanine is high its fine structure bands show up very clearly. It is quite evident from inspection of Table III that there is a displacement of these bands to longer wavelength when passing from liquid to solid state. Again phenylalanine in a gum arabic gel shows band displacement compared with the same solution in liquid form. Tryptophan shows the same type of spectral displacement in gelatine and gum solutions. It was also possible to prepare a thin film of tryptophan by rapid evaporation of a solution on a quartz plate. This also showed a displaced spectrum.

The low temperature spectra were disappointing in that they showed little increase in the resolution of the fine structure bands. There is some evidence that cooling produced a displacement to shorter wavelengths in two cases (tryptophan in gum and phenylalanine in gelatin) but the results are not clear-cut and no deductions are made from these observations.

TABLE III.—POSITION OF FINE STRUCTURE BANDS OF TRYPTOPHAN AND PHENYLALANINE UNDER VARYING CONDITIONS

Compound	Conditions	Band Positions (Å)							
Phenylalanine	Acid solution*	2353	2415	2465	2516	2575	2603†	2634	2671
	Alk. solution*	—	2415	2468	2522	2580	2610	2640	2676
Phenylalanine	In gelatin, liquid solution	—	—	—	2515	2577	—	2635	2672
Phenylalanine	Same solution after gelling	—	—	2473	2528	2588	—	2650	2690
Phenylalanine	In thin film gelatine at − 180°C (approx.)	—	—	2472	2522	2582	2614	2643	2682
Gelatin	Dry sheet	—	—	—	—	2586	2618	2645	2680
Tryptophan	Solution in water†	—	—	—	—	—	2710	2790	2880
,,	In film of gum arabic	—	—	—	—	—	2727	2811	2901
,,	In film at − 190°C	—	—	—	—	—	—	2808	2892
,,	In dextrin film	—	—	—	—	—	2710	2818	2910
,,	In gelatin film	—	—	—	—	—	2737	2822	2911
,,	Dried down on quartz plate	—	—	—	—	—	2717	2813	2906

* Compare McLaren in *Advances in Enzymology*, (Interscience, New York, 1949).
† Very faint.

Effect on the Spectrum of Indoles of Substitution in the Indole Ring.—Following up the work of Gróh[22] and co-workers on the effect of formaldehyde on the absorption spectra of proteins, we made an isolated observation many years ago that formaldehyde displaces the spectrum of skatole 20 to 30 Å to longer wavelenths. Fraenkel-Conrat, Brandon and Olcott[23] showed that the compound formed in this reaction was *N*-methylol-skatole. Edwards[19] recorded the spectrum of this compound and other substituted indoles. The remarkable fact about these results is the small effect on the spectral absorption of substitution in either the 1 (*N*) or 2 positions when the 3 position is already substituted as in skatole. Presumably the same would be found in 1- and 2-substituted tryptophans. The spectrum of 2 : 3-dimethylindole is almost identical with that of skatole except for a slightly higher specific extinction coefficient. Again methylol-skatole resembles closely methylol 2 : 3-dimethylindole except for a higher specific extinction coefficient. In each the methylol substitution has the effect of shifting the position of the long wave fine structure band of skatole 20 to 30 Å towards longer wavelengths. A 1-substituted tryptophan, if it existed in a protein, would account for the observed spectral shift of the tryptophan bands. We can find no evidence in the literature of the existence of such a compound as a product of protein decomposition. We have found only one example of a naturally occurring 1(*N*)-substituted indole, Indigo Green of Benedicenti.[24, 25] On the other hand, it is accepted that humin formed during acid hydrolysis of tryptophan-containing proteins arises from the action of an aldehyde on the indole nucleus of the tryptophan, it being assumed that the aldehyde is formed during the hydrolysis. It is a striking observation of Fraenkel-Conrat [23] that gramicidin gives no humin on acid hydrolysis, whereas formaldehyde-treated gramicidin yields humin copiously.

---

[22] Gróh and Hanák, *Z. physiol. Chem.*, 1930, **190**, 169.
[23] Fraenkel-Conrat Brandon and Olcott, *J. Biol. Chem.*, 1947, **168**, 99.

Our observations bring no new evidence to bear on this point but do raise the question of the possible occurrence of 1(*N*)-substituted tryptophan in native proteins. It seems to us, however, that in foetal and adult human haemoglobins we have a case uniquely suited to the investigation of such a possible combination of tryptophan in a native protein.

Experimental

Two spectrographic methods were employed: (1) The moving plate method [10] modified to give a greater density range, by which the wavelength position of fine structure bands and inflections can be estimated to ± 1 Å in favourable conditions.

(2) An automatic recording ultra-violet spectrophotometer designed and built as a joint enterprise by one of us (E.R.H.) with Mr. G. G. Sutton of the Telecommunications Research Establishment at Malvern. It is hoped to publish in the near future a complete description of the instrument.

Discussion

It seems now established beyond doubt that minor modifications of the spectra of the aromatic amino acids are brought about through linkage into peptide chains and that incorporation into a native protein is responsible for a further change. These changes are recognizable as small shifts to longer wavelengths of 10 to 30 Å, and are most easily detectable by a method which shows up the fine structure of the main absorption band.

Combination in peptide linkage is sufficient to explain only a small part of this anomalous behaviour and, therefore, an effect due to combination in the native form of a protein must be sought. In attempting to explain anomalies of behaviour of specific groups in proteins recourse is had to the following: (i) the influence of hydrogen bonding, (ii) blocking of an active group by combination with another compound, (iii) the influence of the intra-molecular polarizability of the protein molecule on the activity of the group concerned, (iv) the masking of many of the groups in question owing to their being inaccessible to reagent.

Tyrosine has been the subject of most investigation from this point of view. The anomalous pK of tyrosine in proteins has been investigated by Crammer and Neuberger,[9] who favoured H-bonding of the phenolic hydroxyl as an explanation. Philpot and Small [29] showed that only 50 % of the tyrosine in pepsin was available for the reaction with nitrous acid. These findings do not, however, give a lead to an explanation of the effects discussed in this paper. Our experiments on the effect on the spectra produced by change of state adds a fifth possible mechanism for the anomalous behaviour of active groups in proteins. The fact that the spectrum of tryptophan is shifted when the gelatin solution in which it is

---

[24] Benedicenti, *Z. physiol. Chem.*, 1907, **53**, 181.
[25] Rastelli, *Arch. Int. Pharmacodynamie*, 1931, **40**, 482.
[26] Fromageot, *Bull. Soc. Chem. Biol.*, 1948, **30** (Suppl.), 63.
[27] Fromageot and Schnek (unpublished results quoted in (26)).
[28] Anslow, *J. Appl. Phys.*, 1945, **16**, 41.
[29] Philpot and Small, *Biochem. J.*, 1938, **32**, 542.

dissolved solidifies, suggests that mere restriction of vibration by a semi-rigid framework is sufficient to produce these second-order effects on the spectrum. It may possibly be that the causes of anomaly are different in different proteins, for although denaturation had no effect on the spectra of horse serum albumin and globulin, it appears from the work of Jope, Jope and O'Brien[16] that globin on denaturation shows a shift of the tryptophan notch of about 16 Å to shorter wavelengths. The effect, therefore, is obscure and no explanation is forthcoming at the moment. It is an effect which should not be forgotten in the interpretation of spectra of large molecules. There is good evidence that a similar effect is observable in a large molecule such as ribo-nucleic acid, which has been shown by Kunitz[30] to give a spectral shift to shorter wavelengths when acted on by depolymerase. Any attempt to analyze the spectrum of a large molecule in terms of the spectra of its components must be made with the certainty that no anomalous effects are present such as are described in this paper. It appears that the best chance of ensuring this is to break down the molecule, for instance, with an enzyme, preferably specific, to a point where it can be shown that the anomaly is abolished. Furthermore, with a protein, it will be preferable to take as reference compounds peptides of the aromatic amino acids rather than the simple acids. This has been done by Edwards,[19] who used *N*-acetyl-tryptophan as reference compound for estimating tryptophan spectrophotometrically in gramicidin. A tripeptide with the aromatic amino acid in the middle would be the best model. Such compounds are, however, difficult to obtain, and it is still more difficult to make them pure enough for reference. It would, however, be valuable to have even a small pure sample of each for absorption measurement for it might be found that they differed so slightly from the dipeptide (or *N*-acetyl derivatives) that these latter could be used satisfactorily.

We are indebted to Doctors E. P. Abraham, P. Alexander, A. C. Chibnall, T. S. G. Jones, R. A. Keckwick, A. B. Roy, R. L. M. Synge for gifts of samples of proteins and polypeptides, also to Mr. J. St. L. Philpot for the ultracentrifugal measurements quoted in this paper.

Medical Research Council,
Spectrographic Unit,
London Hospital, E.

[30] Kunitz, *J. Biol. Chem.*, 1946, **164**, 563.

ULTRA-VIOLET MICROSPECTROGRAPHIC STUDIES OF NUCLEOPROTEINS AND CRYSTALS OF BIOLOGICAL INTEREST

By W. E. Seeds and M. H. F. Wilkins

Received 28th July, 1950

A method of obtaining ultra-violet absorption curves and dichroic ratios of microscrystals and films using an achromatic reflecting microscope is described. Results for tobacco mosaic virus, nucleic acid, calf thymus nucleoprotein and tyrosine are given.

The purpose of this work, which is in a preliminary stage, is to obtain ultra-violet absorption data which may be combined with X-ray diffraction and infra-red absorption studies on the same material. In this way new information about the molecular architecture of large biological molecules may be obtained. Most of the work is on a truly micro scale but, whenever possible, the standard macro-methods are used, either by themselves or as a check.

Experimental

Methods and Apparatus.- The microspectrographic method used is essentially the spectroheliographic type of method first used by Jope,[1] in which all the radiation consisting of a line spectrum from the ultra-violet source is passed through the specimen and analyzed by a spectrograph. For this purpose a large dispersion, low aperture, anastigmatic spectrograph was computed by Weinstein,[2] though it has been found that in practice a much smaller dispersion instrument would be more effective as the majority of the lines of the mercury spectrum are not sharp. More than half of the twelve lines between 2360 Å and 3000 Å are diffuse or multiple, while there is often a fair amount of continuum superimposed on the spectrum from 2530 Å upwards. In this method an actual image of the specimen at various wavelengths is obtained, and, if the lines are not sharp or have continuum superimposed, the image is confused owing to the superposition of images due to different wavelengths. With certain types of object, e.g. flat plates of uniform thickness, this effect will cause no error, but with many biological objects this is not the case and care must be taken in interpreting the results. For the most part it has been possible to choose objects which conform to the above requirement in the form of crystals, oriented films, etc.

The achromatic microscope used is a reflecting miscroscope of the spherical mirror type,[3, 4] fitted with a rotating focusing stage. The object is illuminated by a 0·29 N.A. (numerical aperture) reflecting condenser using a Köhler type illumination with mirrors, and the object is viewed with a 0·55 N.A., 35 % central obstruction, reflecting objective and a standard × 10 eyepiece. Many objects have to be mounted with a fused quartz coverslip which introduces chromatic aberration into the system. This is corrected by a thin fused quartz convex lens placed above the objective. This lens is computed[4] for a given coverslip thickness and magnification. It is very important that this achromatizing lens is incorporated wherever coverslips are used, as the chromatic defocusing will give rise to very pronounced phase contrast effects[5] which may give large errors in absorption data, especially if the objects are small (e.g. $\sim 3\ \mu$). Directly above the objective is a movable 45° front aluminized mirror (or 90° fused quartz prism) which deflects the image from the eyepiece on to the slit of the spectrograph. A low power refracting objective approximately parfocal with the reflecting objective is used for searching, both objectives being fitted to a standard Leitz type semi-kinematic centring interchanger. Most of the materials studied are dichroic and polarizers are fitted in the miscroscope for orienting the specimen with respect to the the electric vector of the light used, as an aid to viewing and positioning the object, and for measuring the birefringence. The polarizer must be ultra-violet transparent for measurement of dichroic ratios ; while the analyzer, which is used only in the visible, is a sheet of polaroid fitted in the viewing eyepiece. The polarizer, a calcite-quartz double image prism computed by K. P. Norris such that the ordinary ray is not deviated at 2650 Å, is inserted below the condenser. The deviation of the extraordinary ray is sufficiently great for it to be cut off by the condenser stop. It must be stressed that the calcite half of the prism (which is effectively the polarizer) must always be placed towards the object to be studied, as the crystalline quartz prism will rotate the plane of polarization of the light by an amount which varies with the wavelength. (The rotatory power of crystalline quartz at 2500 Å is as large as 143° mm.$^{-1}$, while at 3180 Å it is only 84° mm.$^{-1}$.) The calcite prism ($\sim 20^\circ$ angle) is cut with the optic axis parallel to the edge of the prism. Calcite absorbs appreciably in the far ultra-violet, a 1 cm. slab absorbing 50 % of the radiation at 2500 Å and 95 % at 2300 Å. Using a thin prism the effect is only noticeable below 2480 Å. The microscope is fitted with a rotary mica compensator, and slots are also provided to take either a quartz wedge or a Berek compensator. The microscope and the illuminating system are all mounted on an optical bench which is a rigid extension of the base of the spectrograph. By means of a movable 45° mirror the mercury line source can be replaced by a Thermal Syndicate hydrogen burner.

---

[1] Jope, *Haemoglobin* (Butterworths, London, 1949), p. 213.

[2] Weinstein (private communication).

[3] Seeds and Wilkins, *Nature*, 1949, **164**, 228.

[4] Norris, Seeds and Wilkins, in preparation.

[5] Wilkins, this Discussion.

The spectrograph contains a 60° Cornu quartz prism and the aperture of the collimating lens is approximately $f/20$. Directly in front of the slit is a stepped rotating sector used to calibrate the photographic material. With some biological objects, and when studying high dichroic ratios, it is desirable that the range of the calibrating sector should go up to a density 2. Close to the slit is placed a fused quartz convex lens which images the convex mirror of the microscope objective on to the collimating lens of the spectrograph. A small viewing telescope with a Polaroid analyzer is fitted behind the slit to help exact positioning of the image of the object on the slit of the spectrograph. This device is essential for accurate rapid working of the instrument. The camera of the spectrograph is designed so that the plate holder may be rotated about λ 2450 Å, the line of zero astigmatism. The plate holder is fitted in chrome hardened ball slides to permit an easy smooth motion of the plate for use with the Holiday cam technique.[6] This method of detection is just on the limit of its usefulness with a microspectrographic apparatus, unless faster photographic material becomes available. It is hoped in the next few months to attach an electron multiplier detector, as described by Price,[7] in the focal plane of the spectrograph for use with a stabilized hydrogen lamp. Fig. 1 shows the general arrangement of the microspectrographic apparatus.

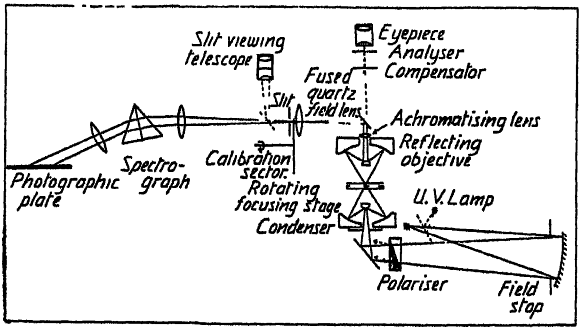

FIG. 1.—Schematic diagram of microspectrographic apparatus.

Essentially the microspectrographic methods employed may be divided into two types. Firstly, a line source is used and a wide slit (viz. 0·5 mm.) giving a photographic record in the form of a series of images, as in the spectroheliograph, at different wavelengths. Secondly, the continuum of the hydrogen arc is used with a narrow slit, the data being detected photographically, or preferably photo-electrically. To date only the photographic method has been used by us with the line source from a mercury arc (an under-run 125-W Osira H.P. mercury arc with the outer glass bulb removed). With this lamp exposure times from 2 sec. to 2 min. will cover all the lines from 2360 Å to 3020 Å. The photographic material used is the Kodak B20 plate which is developed for 4 min. in undiluted D158 stock solution. This development gives a value of γ of about 1·2 ; a higher value of γ of about 1·5 can be obtained using concentrated D.8 developer, but there is a very great tendency to stain the plates, making microphotometry inaccurate. The plates are microphotometered on a non-recording Hilger microphotometer which has been adapted for continuous recording on Bromide paper. The photocell is replaced by an R.C.A. 931A electron multiplier with volts supplied by dry batteries.

Specimens are mounted between a 0·5 mm. fused quartz slide and a 0·18 mm. fused quartz coverslip. Whenever possible a small quantity of n-hexadecane is allowed to run in between the coverslip and slide to minimize the errors due to refraction and scatter. The transmission through 1 cm. of pure n-hexadecane at 2300 Å is greater than 3 % and no appreciable absorption occurs in the thin film of liquid between the slide and the coverslip. The refractive index of

[6] Holiday, *Biochem. J.*, 1936, **30**, 1795.
[7] Price, *I.C.I. Reports*, 1949.

n-hexadecane at 2500 Å is 1.490 which matches fairly well with fused quartz $n = 1.507$, and most of the materials studied have refractive indices between 1.5 and 1.6

Results

Tobacco Mosaic Virus (T.M.V.). Thin films of T.M.V. gel (in which the particles have aggregated end to end) may be oriented by repeated heating between coverslips; well-oriented specimens several millimetres square for absorption measurements are readily obtained[8] Such a specimen was placed close to the spectrograph slit and illuminated by the continuous spectrum of the hydrogen lamp with the electric vector E polarized parallel to and perpendicular to the direction of shear. A Holiday cam plate was taken in each case. The plates show a very pronounced absorption band at 2900 Å for E parallel to, and no such band for E perpendicular to, the direction of shear (Plate I). Comparing these results with those of Butenandt *et al.*[8] [9] it is seen that, according to their absorption curves, the absorption peak at 2900 Å should correspond to the case where E is perpendicular to the shearing direction, and not parallel as shown above. In view of this discrepancy the results were checked on a streaming solution of T.M.V., as used by Butenandt. A 0.5% solution of T.M.V. in distilled water (pH ~ 6.4) was made to oscillate four times per second in a very thin walled fused quartz capillary of 0.5 mm bore in front of the slit of the spectrograph. The oscillating motion was obtained by means of a motor driven cam bearing on a rubber bulb. The average streaming velocity of the liquid in the capillary was about 2 m sec^{-1}. To avoid loss of light due to refraction at the walls of the capillary, two fused quartz coverslips were mounted, one on either side of the capillary, and the space filled with water. A pair of cam plates was taken with the light polarized with E parallel and perpendicular to the direction of streaming. A third plate was taken with the liquid stationary and E perpendicular to the tube. The polarizer was placed directly in front of the capillary with the calcite half of the prism towards the tube. The characteristic tryptophane absorption peak at 2900 Å appears on all these plates (Plate II). The band is most pronounced where E is parallel to the direction of streaming, i.e. parallel to the length of the virus particle rods. The plate for the non-streaming case lies somewhere between the other two

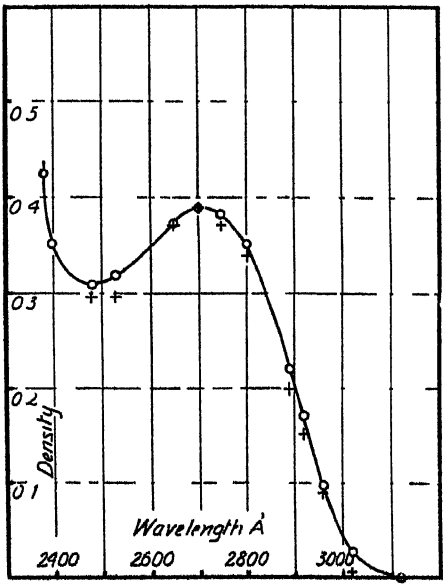

Fig. 2.—Absorption curve of hexagonal crystalline inclusion in leaf hair of T.M.V. infected tobacco plants, with comparison points (+) from absorption curve of oriented T.M.V. film with E perpendicular to shear direction

---

[8] Perutz (private communication)

[9] Butenandt, Friedrich-Fricksa, Hartwig and Scheibe *Z. Physiol. Chem.*, 1942, **274**, 276

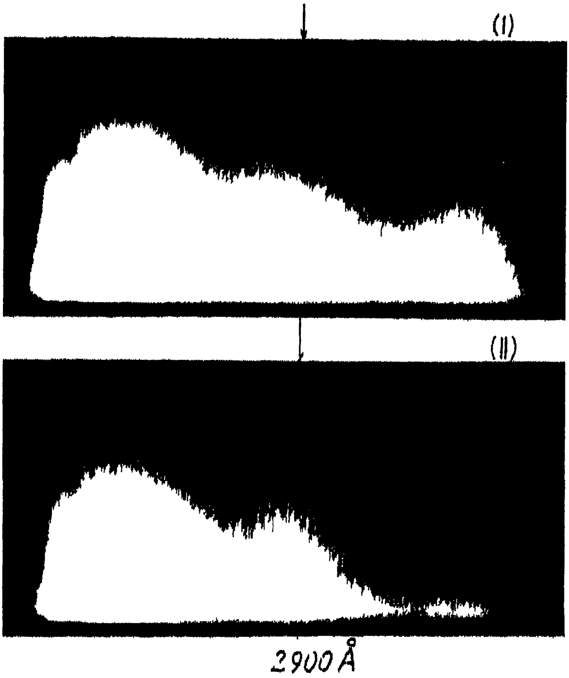

PLATE I. Contact print of camera plate of tobacco mosaic virus oriented film
(i) *E* perpendicular to direction of shear
(ii) *E* parallel to direction of shear

[*To face page* 120

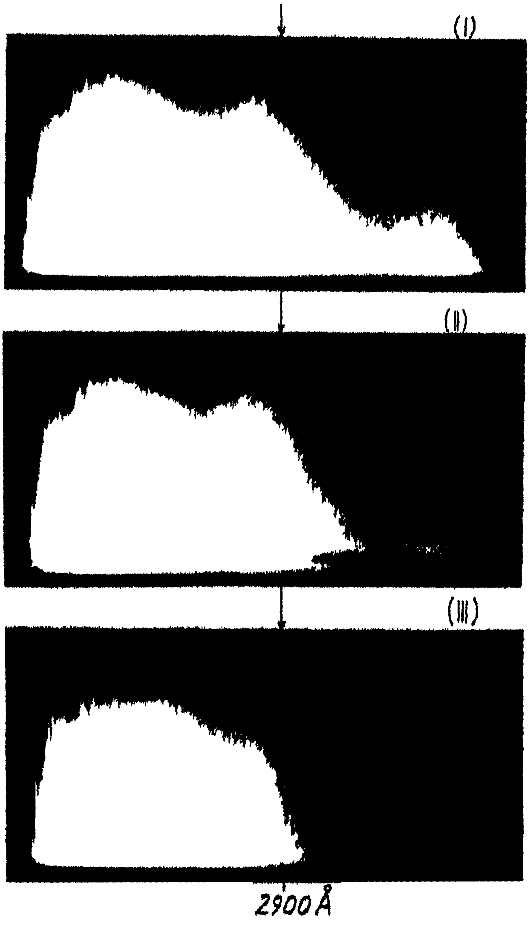

PLATE II. Contact print of sample of tobacco mosaic virus solution

(i) Streaming with *E* perpendicular to direction of streaming
(ii) Non streaming
(iii) Streaming with *E* parallel to direction of streaming

It must be noted that this method of oscillating the liquid in a tube will result only in a partial alignment of the virus particles which accounts for the fact that the plate taken with *E* perpendicular to the rods does not show an absence of the tryptophane peak at 2900 Å The direction of the electric vector has been checked using a pile of 12 fused quartz coverslips as a polarizer Microspectrographic absorption curves of small regions of T M V oriented dry gel confirm that the general shape of the curves published by Butenandt *et al* is correct, but that the curves must as stated above be reversed with respect to the direction of polarization

It is very doubtful if one can interpret the dichroism of T M V as an indication of the direction of the absorbing ring compound within the molecule as suggested by Butenandt In tryptophane the narrow absorption band at 2900 Å might occur only when the vector *E* is perpendicular to the plane of the ring (and not parallel as suggested) or when *E* is in a particular direction in the plane of the indole ring (dichroism for *E* in the plane of the ring) The dichroic ratio at the maximum of the T M V absorption curve is of the same order of magnitude, and of the same sign as would be expected from form dichroism,[10] and might not be due to oriented nucleic acid as suggested This point is being investigated more fully

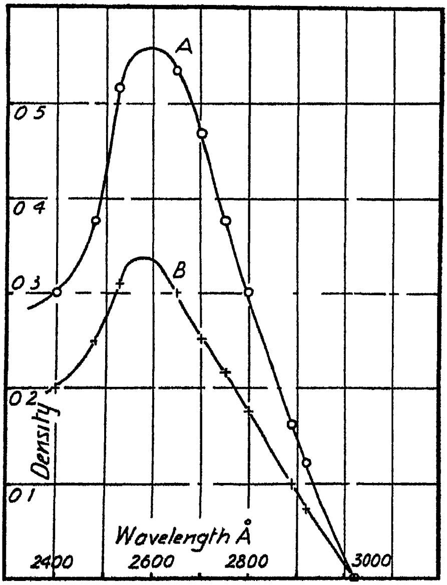

FIG 3 —Absorption curves of oriented film of sodium salt of thymus nucleic acid (A) *E* perpendicular and (B) *E* parallel to direction of shear

Microspectrographic absorption curves of the hexagonal crystals in the leaf hairs of virus infected tobacco plants have the same general shape as the absorption curve of T M V smear for *E* perpendicular to the smear direction (Fig 2) It is difficult to obtain an accurate curve for these crystals as they very often form on or near the nucleus and have more or less varying quantities of cytoplasm or other absorbing matter at the side, or above or below the crystals

Nucleic Acid The highly polymerized sodium salt of thymus nucleic acid when moistened with a small amount of distilled water swells and forms a very viscous transparent mass which can be oriented, either in thin sheets by repeated shearing between coverslips, or may be drawn into thin fibres of a few μ diameter The thin smears are dried in air leaving approximately 30 % water in the film the dry film is then scratched with a sharp scalpel leaving narrow islands of nucleic acid film separated by clear regions The fused quartz coverslip is placed on the preparation and *n*-hexadecane allowed to run in Well-oriented regions of uniform thickness are chosen, using crossed polarizers Microspectrographic absorption curves for these nucleic acid films have been obtained for light polarized perpendicular and parallel to the direction of shear (Fig 3) The results confirmed the work of Caspersson[11] and the maximum dichroic ratio of these specimens is 1 : 1·68 at 2600 Å and is constant throughout the 2600 Å band. The fibres of nucleic acid are usually negatively birefringent and X-ray data[12] shows that they are *ca.* 100% oriented. Unfortunately the fibres are rather thick for ultra-violet absorption spectrography as they are generally at least 3 μ in diameter and being round in section not ideal objects. However useful information can be obtained on the tail of the curve at λ 2800–3000 Å. The fibres will stretch to double their length with permanent set. The resulting fibre is positively birefringent. The positive fibres are readily turned back into negative in the presence of water vapour with resulting diminution in length. The dichroic ratio for both types of fibre is in the same direction, i.e. the maximum absorption occurs for *E* perpendicular to the fibre length but for the positive fibre the ratio at 2600 Å is much lower. Negative fibres give ratios of the order of 1 : 1·75 and a birefringence of 0·11. The change in the dichroic ratio for the transformation from positive fibre to negative in the presence of water vapour has been measured and in all cases the ratio rises from about 1 : 1·05–1·1 to 1 : 1·5–1·7. The transformation was carried out on the microscope stage by supporting the coverslip on small glass fibres and laying small scraps of wet filter paper near the slide.

---

[10] Wiener, *Ambronn-Festschr Kolloid Chem Beih*, 1926, **23**, 189

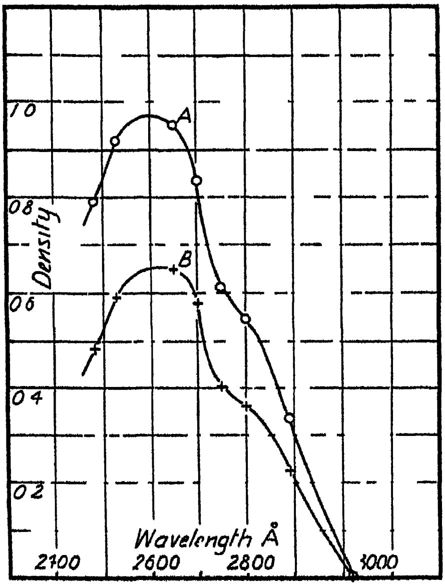

Fig. 4.—Absorption curves of calf thymus nucleoprotein, (A) *E* perpendicular and (B) *E* parallel to direction of shear.

Calf Thymus Nucleoprotein. The nucleoprotein of calf thymus can be made into films and fibres in a manner similar to that used for nucleic acid. The material does not orient as readily as the nucleic acid and fibres tend to be uneven. For this reason absorption curves are not very accurate (Fig. 4). The nucleoprotein is negatively birefringent and dichroic ratios as high as 1 : 1·5 to 1 : 1·6 have been obtained for specimens with a birefringence of 0·014. As for nucleic acid the maximum occurs when the light is polarized with *E* perpendicular to the direction of shear.

Tyrosine.—Some preliminary experiments have been carried out on crystalline tyrosine deposited on the microscope slide from a solution in warm water. The crystals are needle-shaped and are positively birefringent with respect to the length of the needles; the specimens were mounted in the usual way with a fused quartz coverslip and immersed in *n*-hexadecane. The absorption curves were drawn for the light polarized with E parallel and perpendicular to the direction of greatest refractive index The curves (Fig 5) show that the whole absorption peak from 3000 Å to 2500 Å is dichroic, the ratio varying along the curve and being at a maximum about 2800 2900 Å when values of 1 7 or more are obtained It is to be expected that the benzene rings in tyrosine crystals lie with their planes almost parallel

---

[11] Caspersson, *Chromosoma*, 1940, **4**, 605.

[12] Gosling (private communication).

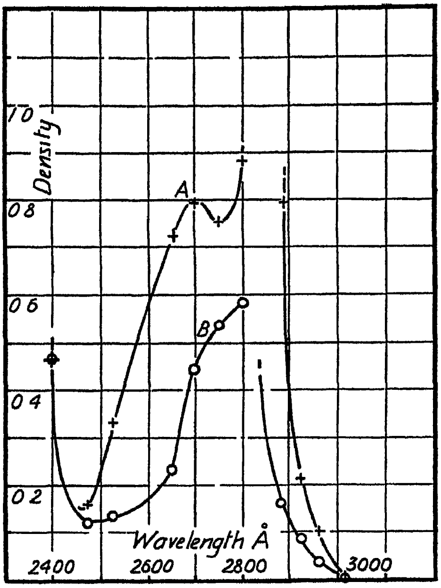

Fig 5 —Absorption of curve of tyrosine (A) E parallel and (B) E perpendicular to direction of greatest refractive index

We wish to thank particularly Miss H Yates for much painstaking microphotometry Prof J T Randall for constant advice and encouragement, Dr R Markham for virus and plante Dr G Oster for suggesting the investigation on tyrosine and T M V Prof R Signer for nucleic acid Dr J A V Butler and Dr Smith for nucleic acid and nucleoprotein, Mrs I Trott for diagrams and Miss F Ticehurst for the plates

Wheatstone Physics Laboratory and
Medical Research Council Biophysics Research Unit
King's College
Strand W C 2

OBSERVATIONS OF PROTEINS IN POLARIZED ULTRA-VIOLET LIGHT

By M F Perutz,[*] M Jope,[†] and R Barer[‡]

Received 21st August, 1950

The absorption spectra in polarized ultra-violet light of single crystals of horse methaemoglobin, of oriented gels of tobacco mosaic virus, and of a number of fibrous proteins of the α keratin type were examined Haemoglobin showed

[*] Cavendish Laboratory, Cambridge
[†] Spectrographic Research Unit, London Hospital
[‡] Department of Human Anatomy, Oxford

marked dichroic effects in the regions of both the Soret band and the tryptophan absorption maximum, indicating preferred orientation of the haem groups, the indol groups of tryptophan and possibly some of the other aromatic amino acid side chains. Tobacco mosaic virus showed the type of dichroism observed by Butenandt *et al.*,[6] except for a reversal of sign. None of the fibrous proteins of the α-keratin type showed any significant dichroic effects.

Crystals of pigments commonly exhibit polarization pleochroism or dichroism. If the pigment molecules contain systems of conjugated double bonds, either of a planar or a linear kind, absorption is usually greatest if the vibration direction of the incident light is parallel to the double bonds and least if the light vibrates at right-angles to them. Studies of the pleochroism of such substances can therefore provide useful information on their molecular structure.

Proteins contain three aromatic groups with pronounced absorption in the ultra-violet : the indol group of tryptophan, the phenolic group of tyrosine and the phenyl group of phenyl alanine.[1-4] It seemed possible that some of or all these groups might show preferred orientation within protein crystals or fibres, thus giving rise to pleochroic effects. Evidence of such preferred orientation would be of great value when the merits of different polypeptide chain models are considered.[5]

U.-v. dichroism had actually been observed in streaming solutions of tobacco mosaic virus by Butenandt *et al.*,[6] who claimed to have found evidence for preferred orientation of tryptophan and nucleotides. Their results have recently been criticized by Wilkins *et al.*[7] who found the dichroism to be of a sign opposite to that described by Butenandt *et al.* and who pointed out that some of the differences between Butenandt's two absorption curves may be due to form dichroism.

The specimens examined here include single crystals of horse methaemoglobin, thin sections of porcupine quill tip and of frog sartorius muscle, stretched films of tropomyosin and fibrinogen and oriented gels of tobacco mosaic virus. Crystalline haemoglobin and tobacco mosaic virus gel were the only substances in which pleochroic effects were observed.

Experimental

PREPARATION OF SPECIMENS.—Owing to the high light absorption of proteins in the ultra-violet, specimen thicknesses had to be of the order of only 3 to 10 μ. Thin plate-like crystals of haemoglobin were prepared by dialyzing a solution of horse methaemoglobin against an unbuffered 2·5 M ammonium sulphate solution. The wet crystals were then mounted between quartz cover-slips. Thin sections of porcupine quill were shaved off the tip of the quill with a razor blade and mounted in glycerine between quartz slides. Frog muscle was fixed in alcohol, dried, impregnated with wax, cut on a microtome and mounted in glycerine between quartz cover-slips. Tropomyosin and fibrinogen films were made by evaporating drops of solution on thin strips of polythene. The drops were dried, remoistened by breathing on them and then stretched by about 500 % by drawing the polythene base. The stretched films contained well-oriented protein as judged by their birefringence and dichroism in the infra-red. Gels of tobacco mosaic virus were made by spinning virus solutions in a Servall angle centrifuge ; the virus particles were oriented by shearing the gel between two quartz cover-slips.

---

[1] Holiday, *Biochem. J.*, 1936, **30**, 1795.

[2] Abderhalden and Haas, *Hoppe-Seyl. Z.*, 1927, **166**, 78.

[3] Abderhalden and Rossner, *ibid.*, 1928, **176**, 249.

[4] Abderhalden and Rossner, *ibid.*, 1929, **178**, 156.

[5] Bragg, Kendrew and Perutz, *Proc. Roy. Soc. A*, 1950 (in press).

[6] Butenandt, Friedrich-Fieska, Hartwig and Scheibe, *Hoppe-Seyl. Z.*, 1942, **274**, 276.

[7] Wilkins, Stokes, Seeds and Oster, *Nature*, 1950, **166**, 127.

OPTICAL TECHNIQUE.—Single crystals of haemoglobin were examined with the aid of the Burch reflecting microscope.[8] Light from a mercury vapour lamp was polarized with a Glan-Thompson prism sealed together with glycerine. The image of the crystal obtained with the reflecting objective of the Burch microscope was focused straight on to the slit of a quartz spectrograph which produced a spectrogram of the crystal and of the background next to it on a photographic plate. The intensity of the background was graded by placing a rotating sector in front of the spectrograph slit. The spectrograms were photometered by comparing the light intensity transmitted through the crystal with that of the graded background for each mercury line. In this way comparable photometer records could be obtained for two mutually perpendicular positions of the polarizer. (For details of the optical arrangement, see Barer, Holiday and Jope.[9])

Sections of porcupine quill tip and frog muscle, and gels of tobacco mosaic virus were examined directly using Holiday's quartz spectrograph which incorporates a logarithmic cam moving-plate device[10] and gives a direct picture of absorption maxima. Thin films of fibrinogen and tropomyosin were examined with the Beckman spectrophotometer. In both cases the Glan-Thompson prism was used as a polarizer.

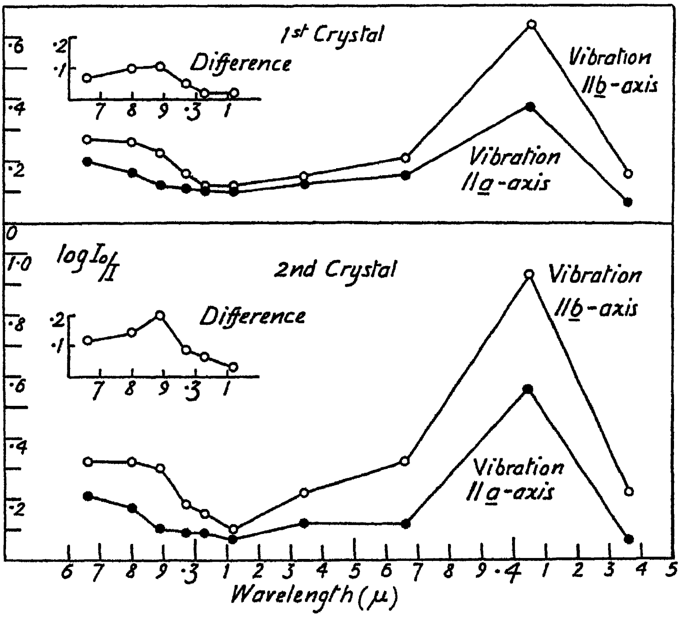

FIG. 1.—Absorption curves of two single crystals of horse methaemoglobin as determined with the Burch reflecting microscope. Electric vectors of the polarized light are parallel to the crystallographic *a*- and *b*-axes. The weights of the crystals were of the order of 10^{-9} g.

Results

Single crystals of horse methaemoglobin about 3 μ thick and 10 μ square were examined with the light incident normal to the plane containing the *a* and *b* axes, where they show strong dichroism in the visible.[11] The absorption curves covering the violet and u.-v. regions of the spectrum are shown in Fig. 1. There is marked dichroism in the Soret band at 0·4 μ, absorption with the electric vector parallel to the *b*-axis being 2·3 times stronger than in the direction at right-angles. At 0·31 μ the two curves move close together. The dichroism rises to another maximum at about 0·29 μ and remains high right down to 0·266 μ, the last mercury line where measurements could be taken. The direction of maximum absorption is always parallel to the *b*-axis.

---

[8] Burch, *Proc. Physic. Soc.*, 1947, **59**, 41 and 47.

[9] Barer, Holiday and Jope, *Biochem. Biophys. Acta*, 1950 (in press).

[10] Holiday, *J. Sci. Instr.*, 1937, **14**, 166.

[11] Perutz, *Nature*, 1939, **143**, 731.

Oriented gels of tobacco mosaic virus showed the type of dichroism first observed by Butenandt *et al.*, except that the polarization directions reported by these authors should be interchanged, as pointed out by Wilkins *et al.*[7] When the electric vector is parallel to the length of the virus particle, the fine structure band of tryptophan at 0·291 μ appears and general absorption below 0·3 μ is high. With the electric vector normal to the particle length the fine structure band of tryptophan is invisible and general absorption below 0·3 μ is low. The amount of dichroism rises to a maximum in the neighbourhood of the absorption peaks both of tryptophan at 0·278 μ and of ribonucleic acid at 0·258 μ. Incidentally, our photographs show the absorption maximum of the tryptophan fine structure band to lie at 0·291 μ, as in most proteins, and not at 0·288 μ as given by Butenandt *et al.* The latter position corresponds to free tryptophan. In none of the other specimens could any significant dichroic effect be detected.

Discussion

The sign of the dichroism of the Soret band is the same as that of the absorption bands of haemoglobin in the visible part of the spectrum. The latter proved to be strong when the electric vector was parallel to the plane of the haem groups; the same condition seems to apply also to the Soret band.

Since the absorption curve of haem shows no maximum on the short-wave side of the Soret band, the dichroic effects in the spectral region below 0·3 μ must be due to preferred orientation of aromatic amino acid side-chains. The relationship between the numbers of each of the aromatic amino acid residues in the haemoglobin molecule, and the position and relative heights of their absorption maxima is shown in Table 1.

TABLE 1

Amino acid residue	No. of residues in horse haemoglobin[12]	Wave length of absorption maximum (μ)	Molecular extinction coefficient at absorption maximum	Extinction coefficient per haemoglobin molecule
Tryptophan .	5	0·278	5300	26,500
Tyrosine . .	11	0·275	1400	15,400
Phenylalanine .	33	0·258	190	63,000

Tyrosine and phenylalanine show little absorption at 0·290 μ; therefore the pronounced dichroic effect in this region can only be due to preferred orientation of the indol rings of tryptophan, which must lie with their flat sides normal to the *a*-axis. Due to the very high absorbing power of the crystals, we were unable to make more than one observation on the short-wave side of the tryptophan maximum; it is difficult to decide, therefore, whether the dichroism is due to tryptophan alone, or whether the other aromatic side chains also show preferred orientation.

Perutz has shown that the *a*-axis corresponds to the direction of the polypeptide chains;[13] hence the flat sides of the aromatic rings appear to be oriented roughly normal to the chain direction; their orientation is the same, in fact, as that of the haem groups. The X-ray data indicate the chain configuration in haemoglobin to be similar to that of the fibrous proteins of the α-keratin type. It was this fact which induced us to search for a dichroic effect in the latter. Its absence appears surprising.

[12] Tristram, *Haemoglobin* (Butterworths, 1949), p. 110.

[13] Perutz, *Proc. Roy. Soc. A*, 1949, **195**, 474.

Interpretation of the dichroic effect of the tryptophan fine structure band in tobacco mosaic virus will have to await a study of the orientation of this band relative to the position of the indol ring in crystalline tryptophan As Wilkins *et al.* have pointed out, a further study of the relative importance of intrinsic and form dichroism will be needed before any definite conclusions regarding the orientation of the nucleosides in the virus particles can be drawn.

The authors wish to thank Dr. K. Bailey, Dr. Roy Markham and Dr. L. E. R. Picken for gifts of specimens, and Dr. E. R. Holiday, Dr. G. H. Beaven and Dr. E. A. Johnston for their hospitality and help in working the Cam spectrograph.

SOME COMPARISON BETWEEN X-RAY AND ULTRA-VIOLET ABSORPTION IN DIFFERENT TISSUE AND CELL STRUCTURES

BY ARNE ENGSTRÖM

Received 31*st July*, 1950

The results from investigation of a number of tissues and cells by an X-ray absorption technique for the determination of mass of cell structures are presented. The variations in density in different structures are compared with the absorption of ultra-violet light. Attention is drawn to errors inherent in the experimental material and influencing the accuracy of the results.

It is important in quantitative cytochemical analysis to have a standard, such as weight or thickness, to which analytical findings can be referred. The principal physical methods used in cytochemistry, absorption measurements with different kinds of radiation, permit the estimation of substances or compounds under analysis but only as grams per unit area or extinction values. Integration over an entire area is necessary to give total amounts. In the latter case an analytical result can be expressed in grams per cell, etc. In order to calculate the percentage of a substance being analyzed the thickness and specific gravity of the cell structure must be known. At present, however, there are no reliable methods for the determination of the thickness and specific gravity of small biological specimens like cells or cell structures. Thus for different reasons there is a great need for a method permitting the quantitative determination of mass or dry weight of cell structures. It is also important that the sample should not be destroyed in the analytical procedure.

This paper is mainly concerned with the results obtained with a recently developed X-ray method for the determination of mass of cell structures. In some cases a comparison has been made between mass as determined by X-rays and the ultra-violet extinctions for different wavelengths in different tissues and cell structures.

Experimental

It was previously shown that by utilizing selected bands in a long wavelength, continuous X-ray spectrum, it is possible to determine the dry weight of single cells and cell structures by absorption measurements. A consideration of the theory of X-ray absorption [1] reveals that the mass of a structure in biological material might be determined with an error of less than 5 % even if there were relatively large variations in the proportions of the constituent elements.

[1] Engström and Lindström, *Nature*, 1949, **163**, 563.

Calculations showed that a great change in carbon, oxygen or nitrogen content (with nitrogen up to 60 %) produces an error of only 5 % in the determination of mass.[2, 3] The same error will occur if other elements such as phosphorus, sulphur, chlorine and calcium are present in very high concentrations; i.e. the concentration of phosphorus would have to be about 5 %, sulphur 14 %, chlorine 17 %, and calcium 9 %. Fig. 1 shows the effect on the accuracy of measurement of different elements superimposed upon a basic carbon, oxygen and nitrogen mixture of the same proportions as a protein. From Fig. 1 and the examples just given it is obvious that only in special instances, e.g., calcified tissues, need a correction for other elements, except hydrogen, be made. The correction for the absorption of hydrogen (less than 10 %) is calculated by means of a formula derived for this purpose.[2] Mass can be determined by the X-ray absorption technique with an overall error under 10 %. Calculations showed that even with thyroid tissue the iodine present does not disturb the determinations of mass.

The X-rays used for determination of mass have wavelengths from 8 Å and longer. Proper wavelength distribution in the X-ray spectrum is obtained by filtering 3000-V continuous X-rays through 9 μ Al. For the experiments thin Lippmann-emulsion on celluloid base (manufactured by Gevaert, Antwerp) was used.

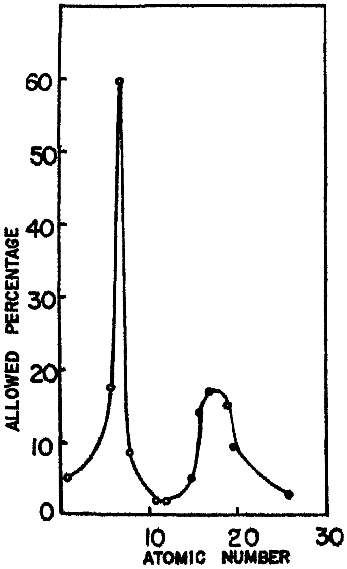

FIG. 1.—The allowed percentage of the common biological elements giving an error of 5 % in mass determination. The diagram is calculated for the wave-length region 8 to 12 Å. (From Engström and Lindström [2])

The resolving power of the X-ray absorption technique is dependent upon the granularity and homogeneity of the fine grained film emulsion used for recording the microradiogram (X-ray absorption image). For qualitative work the resolving power is about 1 μ but it is somewhat less satisfactory for quantitative determinations. The properties of fine-grained film emulsions suitable for microradiography have recently been examined.[4]

A small reference system made up of nitrocellulose foils was printed on the fine-grained film simultaneous with the recording of an X-ray absorption image of a biological specimen. By photomicrography the images of the sample and the reference system were magnified. The absorption of X-rays in different cell structures was determined by photometric measurements on the enlarged image of the sample and reference systems. Details are given elsewhere.[2, 3] In order to minimize the absorption of the soft-X-rays in air the determination of mass must be performed in vacuum.

[2] Engström and Lindström, *Biochem. Physics. Acta,* 1950, 4, 351.

[3] Engström, in *Progr. in Biophysics and Biophys. Chem.,* ed. Randall and Butler (London, 1950).

[4] Engström and Lindström, *Acta Radiol.* (in press).

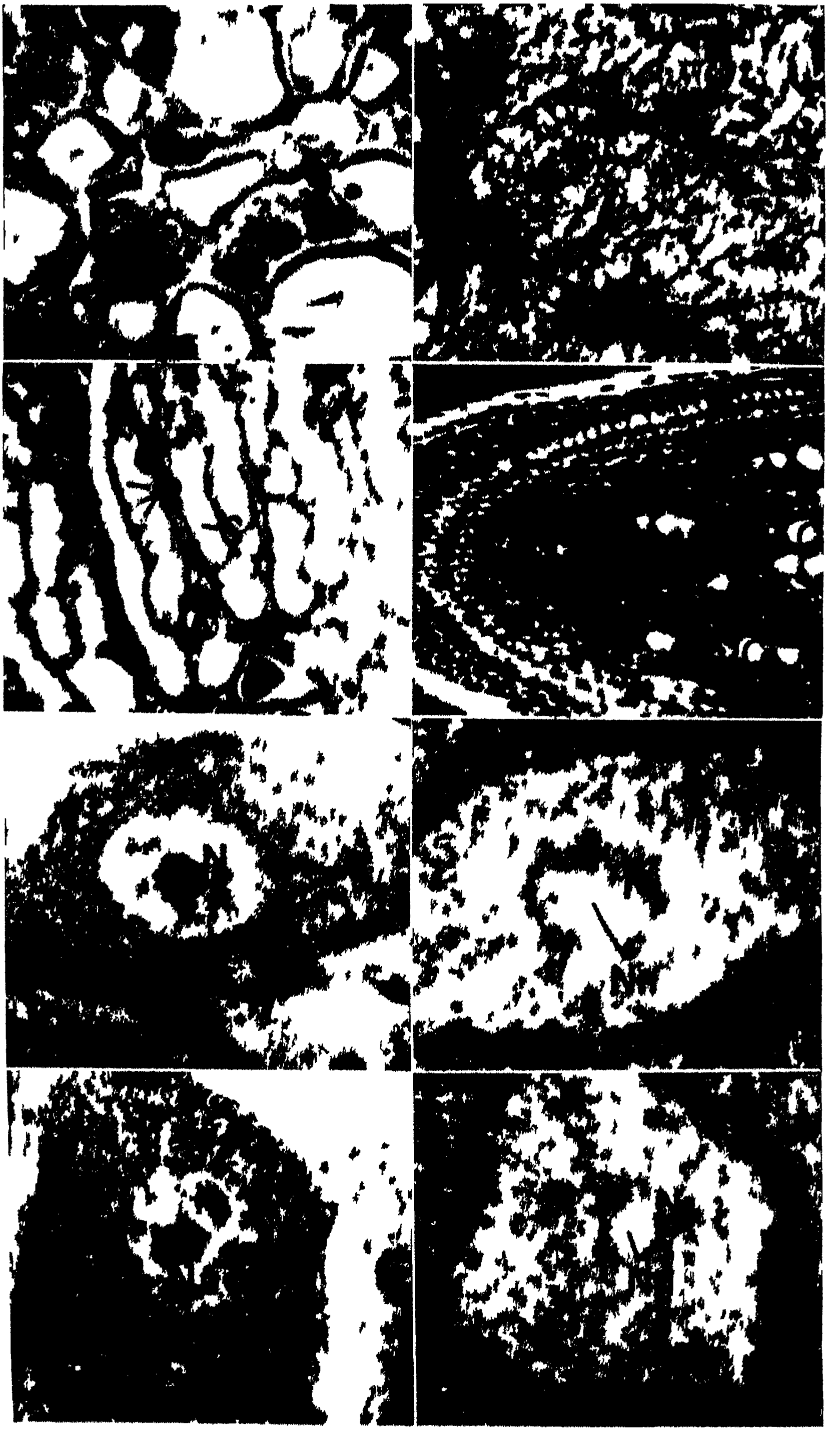

[To face page 429

In some objects which had been "weighed" by X-rays the ultra-violet absorption at different wavelengths was also determined The specimens were photographed at 2570, 2750 and 3100 Å and the ultra-violet extinction was determined by a photographic-photometric technique The ultra-violet determinations were performed by Dr J Nurnberger *

The thickness of the sections was determined by focusing a microscope on the upper and lower surfaces of the specimen An ordinary and a phase contrast microscope were used, the objectives had a numerical aperture (N A) of 1 30 Depending on the focal depth of the objective[5] the error in the determination of thickness was 0 5 to 1 0 μ thus permitting only estimates of thickness Metal shadowing at oblique angles as used in electron microscopy was also tried for determinations of thickness This method worked well on isolated cells but not on sections

Results

In Plate I some photomicrographs of microradiograms are shown All pictures were taken with 3000-V X-rays, filtered through 9 μ Al For the photo-micrography Gevaert high contrast replica plates were used

Plate I (1) shows the X-ray picture of a section of thyroid tissue This illustration shows the great variation in density between different parts of the tissue Fixation and sectioning defects are also well demonstrated in the non homogeneous distribution of mass within the follicles, (2) shows a malignant process in the thyroid gland and also here the great variation in density between cells is clearly observable

Plate I (3) is a photomicrograph of a microradiogram of a section from gastric mucosa The chief cells have the weight of about 0 4 $\times 10^{-12}$ g $/\mu^3$ and the parietal cells only 0 2 $\times 10^{-12}$ g $/\mu^3$ These findings have been discussed elsewhere[6] In connection with the analysis of the gastric mucosa, it was found that the fixative exerted an influence on the cellular substance For example, in formalin a loss of weight was observed, presumably due to the dissolving of some proteineous cell substance

Plate I (4) shows an X-ray picture of a section from the root tip of *Hyacinthus* The accumulation of cellular material in the growth zone can be seen The highly absorbing areas are calcium oxalate crystals However, as pointed out previously, the X-ray method in the modification used here, is not applicable for the determination of the mass of these structures At higher magnification, nuclei and nucleoli can be distinguished and cells in different mitotic stages can be seen

PLATE I

(1) An X-ray picture of a 5 μ thick section of thyroid tissue The white areas are those absorbing X-rays Depending upon the very high gamma values on the plates used for recording the X-ray pictures, differences in thickness and density are much amplified Magnification *ca* ×100

(2) A malign degeneration of the thyroid gland Some cells absorb X-rays strongly indicating a high mass Magnification *ca* ×100

(3) Photomicrograph of a microradiogram of gastric mucosa The chief cells C have higher density than the parietal cells P Magnification *ca* ×100

(4) Enlarged microradiogram of a longitudinal section of root tip from *Hyacinthus* The difference in density in different regions is clearly seen At higher magnification nucleoli and nuclei are distinctly observable C are cacium oxalate crystals having high X-ray density

(5) *a* A nerve cell from cat spinal cord photographed at 2750 Å (*left*)
b The same cell photographed with X-rays Magnification ×1000

(6) *a* Ultra-violet picture (2750 Å) of a nerve cell (*left*)
b X-ray picture of the same cell Magnification ×1000 In Fig (5) and (6) N indicates nucleus and Nn nucleolus In both pictures the close correlation between the distribution of mass and the absorption at 2750 Å can be seen Fig (5) and (6) are taken from unpublished work by Nurnberger, Engström and Lindström

---

* The complete results will be published elsewhere by Nurnberger, Engström and Lindström

[5] Berek, *S B Ges Naturw Marbg*, 1927, **62**, 189

[6] Engström and Glick, *Science*, 1950, **111**, 379.

In (5) and (*6a* and *b*) a pair of nerve cells is photographed with ultra-violet light (wavelength 2750 Å) and X-rays. The good correlation between absorption at 2750 Å and by X-rays is well demonstrated. In the X ray pictures a general trend for mammalian cells can be traced. The cytoplasm has, in general, higher density than the nucleus but the nucleolus has the highest density. In nerve cells from the cat spinal cord the ratio for cytoplasm : nucleus : nucleolus is approximately 2 : 1 : 5. For certain plant cells the cytoplasm seems to have the lowest relative weight per volume unit.

The spinal cord from a cat was prepared in several ways: by freeze drying, fixation in formalin and Carnoy's solution. Sections of different thickness were cut (the thickness was estimated by microscope measurements) and X-ray and ultra-violet extinctions were measured. In this investigation, the results of which will be published in detail elsewhere (Nurnberger, Engström and Lindström) our aim was to see if there was any correlation between ultra-violet absorption and mass as well as to explore inter-relations between ultra-violet absorption, X-ray mass and thickness. The effects of different fixatives were also considered.

Fig. 2 shows the results of measuring X-ray and ultra-violet absorption at 2570 Å in nerve cell cytoplasm. In each case the measurements were integrated for whole cytoplasmic area. As can be seen from Fig. 2, there seems to be, up to relatively high extinction values, a fairly straight-line relationship between mass and ultra-violet extinction. Despite the errors inherent in the methods the distribution of the points as shown in Fig. 2 endows the curve with a high degree of statistical probability. The orientation effect postulated by Commoner[7] was in fact encompassed by the variability of the experimental results.

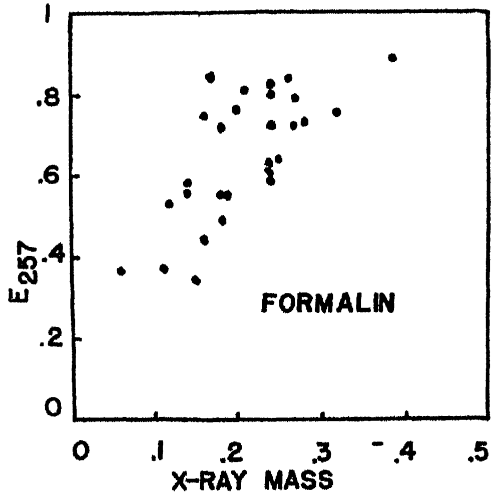

FIG. 2.— Extinction at 2570 Å as function of X-ray mass for nerve cell cytoplasm.

In general the best correlation was found between mass and ultra-violet absorption at 2750 Å. From the chemical composition and the response to which the treatment the nerve cells had been subjected (lipid solvents), it is obvious that the major part of cellular substance is accounted for by protein.

In giant chromosomes from *Chironomus*, X-ray absorption measurements showed that the bands had from 2 to 10 times a high mass per unit volume as the interband spaces. Striated muscle fibres had about twice as high a mass per unit volume in the anisotropic segments as in the isotropic.

Discussion

The investigation of a number of different tissues by the X-ray absorption technique for the determination of mass shows that there are large variations in density between different cells and also between different cell structures. This fact must be kept in mind when, for example, interpreting the results from dye-binding experiments or optical absorption measurements. A structure with a high density (high dry weight) has a high affinity for a dye and a high absorption in ultra-violet light, specific and unspecific. This is demonstrated in the difference in mass between the nucleus and cytoplasm in certain mammalian cells or in the giant chromosomes from *Chironomus*. In some experiments one gets the impression that the absorption of ultra-violet light reflects the variation in amount of dry substance of different cell structures. In other cases, like myelinated nerve fibres,[8] the strongly X-ray absorbing myelin sheath does not absorb ultra-violet light to a comparable extent. It appears important therefore to stress the significance of parallel studies of the density of cell structures before valid cytochemical conclusions can be drawn on the basis of evidence obtained by other techniques.

---

[7] Commoner, *Science*, 1950, 111, 68.

As the method of mass determination is based upon absorption measurements, the homogeneity of the area under analysis must be as carefully checked as in all types of optical microspectrography and densitometry. In connection with the homogeneity of the area measured, the granularity of the film used for recording the microradiogram is also of importance. Especially at higher magnifications associations of the submicroscopic grains in the Lippmann emulsion can cause an effect similar to that of a non-homogeneous field. A sufficient number of grains should be measured or counted with reference to the statistical nature of the photographic process.

The X-ray method for determination of mass suffers from the disadvantage in that living objects cannot be investigated since it is impossible to obtain an adequate contrast of an object immersed in a physiological salt solution. In order to secure good contrast extremely soft X-rays and work in high vacuum is necessary.

All errors which are included in the techniques for preparing smears or sections must be considered. Thickness measurements on microtome sections of nerve cells showed that the nucleus, cytoplasm and nucleolus all had different thicknesses even within the same cell, probably depending on different behaviour in sectioning. This finding also was confirmed by oblique metal shadow casting of sections.

The effects of fixation must also be investigated more carefully before applying cytochemical methods for solving different biological problems. The preliminary experiments reported here indicate that great losses of substance and changes in distribution of materials take place during different routine histological procedures for fixation, embedding, sectioning, etc.

In a structure like the nerve cell cytoplasm the molecular orientation effect in ultra-violet light,[6] is smaller than the experimental errors in recording mass and ultra-violet absorption. No experiments have as yet been reported on the correlation between ultra-violet absorption and mass in cell structures in which a strong orientation of the nucleic acids and proteins can be expected.

Department for Cell Research,
Karolinska Institutet,
Stockholm 60,
Sweden.

---

[8] Engström and Lüthy, *Expt. Cell. Res.*, 1950, 1, 81.

35836

SELF - RECORDING MICROSPECTROGRAPHY AND ITS APPLICATIONS ON PROBLEMS REGARDING THE ENDOCELLULAR FORMATION OF HAEMOGLOBIN

By Bo Thorell

Received 31*st July*, 1950

For studying the endocellular haemoglobin synthesis a single-beam recording microspectrograph, working in the short wavelength visible range, is described. The results of analysis on normal bone marrow cells reveal some data on the quantitative interplay between porphyrin compounds and haemoglobin during normal erythropoiesis.

Previous investigations[1, 2, 3] have shown that the endocellular haemin synthesis during red blood cell formation is separated from the earlier growth and division processes. Moreover, isotope studies[3, 4] on the metabolic behaviour of the different developmental stages showed that the synthesis of haemin in the later phases of erythropoiesis proceeds comparatively rapidly.

Thus, in the normal blood-forming organ, there is, at a given time, a relatively small number of cells with a maximum rate of haemin synthesis. From normal bone marrow, therefore, it seems unlikely that it would be possible to make macrochemical preparations of the intermediate steps in amounts large enough to permit analysis. If, however, the cells, which from earlier data can be concluded to possess the maximum rate of haemin synthesis, are investigated separately, the chance for detecting precursors is increased. Microspectrography offers favourable conditions in this case as the different prophyrin derivatives, conceivable as precursors, have characteristic absorption spectra.

This investigation will firstly reveal whether there are measureable amounts of porphyrin derivatives in the cytoplasm of the cells at certain stages during normal erythropoiesis. Secondly, in order to study the kinetics of the endocellular haemin synthesis in relation to the cytological behaviour of the erythroblasts, the ratio of possibly existing porphyrin compound to haemin at different stages of haemoglobinization will be determined.

The determination of haemoglobin in cytological preparations has been dealt with earlier.[1, 5, 6] Summarizing some recent results from this laboratory,[7] the haemoglobin in air-dried blood- (or bone marrow) smears after 72 hr. occurs in met- and oxy-form, the proportions varying between 40 and 60 %. This gives a complex absorption curve with a maximum at 412 mμ. Fairly independent of the above mentioned variation in met-haemoglobin formation, the extinction coefficient at the maximum is 8×10^3. The dry state does not affect this value. Lambert-Beer's law is followed without measurable deviations at concentrations below 30 % haemoglobin at the actual layer thicknesses.

[1] Thorell, *Acta Med. Scand.*, 1947, Suppl. 200.
[2] Thorell, *Cold Spring Harbor Symp. Quant. Biol.*, 1947, 12.
[3] Hammarsten, Thorell and Åquist (unpublished experiments).
[4] Thorell, *Nord. Med.* (*Swed.*), 1950, 43.
[5] Cole and Brackett, *Rev. Sci. Instr.*, 1940, 11, 419.
[6] Jope, *Haemoglobin*, ed. Roughton and Kendrew (London, 1949), p. 205.
[7] Thorell and Akerman, to be published in *Acta Chem. Scand.*, 1950

In this investigation, a great number of cells are being analysed with regard to cytoplasmic light absorption at the Soret band region (mainly 390-430 mμ). Also the total amount of absorbing substance per cell will be determined. For this purpose a single-beam recording microspectrograph was built.

Experimental and Results

Fig. 1 shows a block diagram. The source of light A is a tungsten lamp-fed from an accumulator battery. The tension (6·5 V) is controlled by a precision voltmeter. The light is dispersed by a prism monochromator B with 90° constant deflection angle. The band width at the slit apertures used is less than 3 Å. Stray light is filtered off with the Schott filter combination C. The optical path is so arranged that the monochromator exit slit functions as an illumination field slit, and the microscope condenser diaphragm as an aperture diaphragm.

The following were used in the beginning as microscope optics: an achromatic condenser with numerical aperture (N.A.) 1·0; an apochromatic × 60 objective with N.A. 1·0 and 2·9 mm. focal length; and as eyepiece a × 10 compensating ocular, D-F. In later experiments a reflecting condenser and objective were used, built with the help of instructions from Dr. W. E. Seeds and Dr. M. H. F. Wilkins.[8] These optics have a N.A. 0·55 and focal length 5 mm.

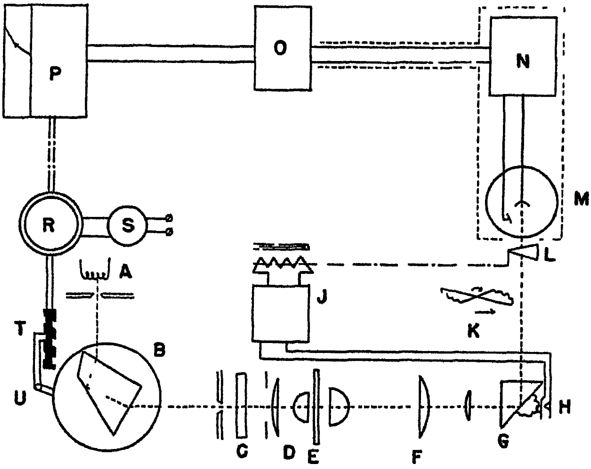

FIG 1

From the microscope the image is thrown by a 90° prism G towards the photocell aperture L. The prism can be moved in steps with a precision micrometer-screw around a horizontal axis. The contact H, the relay J and the shutter at L are used when measuring the total amount of absorbing substance in the cell (see later). K is a rotating sector for controlling the linearity of the intensity registration. The distance from the microscope to the photocell is so chosen that the photocell aperture corresponds to an object surface with a diameter of 0·2 μ.

The photocell M is a battery-fed RCA 931-A or 1P-21 multiplier tube shielded together with the pre-amplifier N, which is a D.C. amplifier with an input impedance of 5 megohm and 100 % feed-back. O is an effect amplifier and P the recording instrument, an Esterline-Angus recorder 0-5 mA.

When recording the spectrum in a certain wavelength range, the point to be measured is projected on to the photocell aperture and the drum T adjusted to the desired starting wavelength. The stop watch S with a circuit-breaker relay is set to the wavelength range required and the current switched on. Thereby, the synchronous motor R both drives the chart of the recording instrument and continuously changes the wavelength. The intensity of the incident unweakened light is obtained in the same manner but using a point in the immediate neighbourhood of the cell and projecting this on to the photocell aperture (Fig. 2a). This requires even illumination of the object, which is secured satisfactorily in the level of altitude of the monochromatic light image.

---

[8] Seeds and Wilkins, *Nature*, 1949, 164, 228.

When determining the total amount of absorbing substance per cell the image of the object is so adjusted that the diameter of the cell falls along a

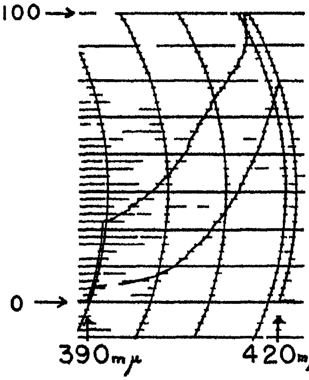

Fig 2a

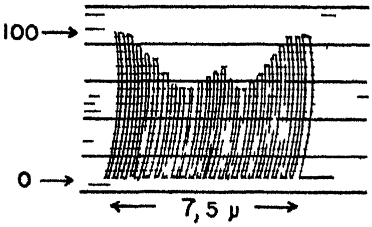

Fig 2b

vertical line through the photocell aperture. The prism G is then moved around its horizontal axis, whereby point after point along the diameter of the cell is projected into the photocell. The relay arrangement H J leaves the shutter I open only when each point is exactly in position; thus the recorded light intensity corresponds to definite points equidistantly distributed along the diameter of the cell (Fig 2b). The recorded peaks are connected and the enclosed area

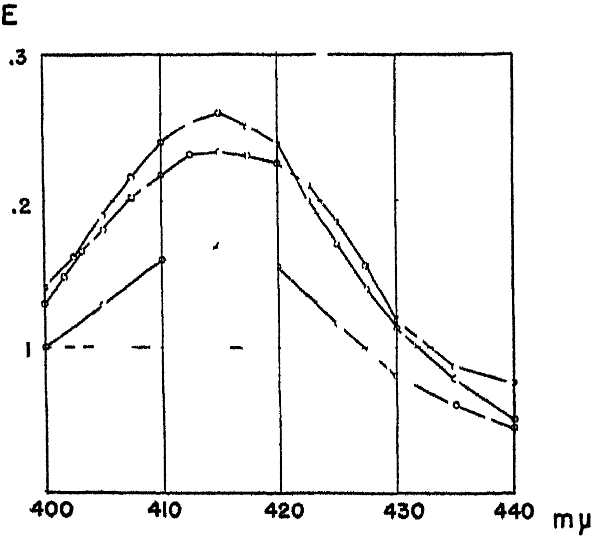

Fig 3

measured. In the case of the symmetrically built erythroblasts, the total extinction is then calculated by integration of the surface obtained. The accuracy of the method has been found to be 5-10 % of the calculated value.

Bone marrow cells from hens, rats and humans have been used as material for the investigation. Ordinary air-dried smears were made on object glasses, and the erythroblasts were investigated in the apparatus described after 1 to 72 hr

Fig 2a shows the primary records of an absorption spectrum between 300 400 mμ from a point in the cytoplasm of an erythroblast Fig 2b is an example of recording the light absorption at 41– mμ in points along the diameter of an erythroblast From the curve it can be seen directly how the absorption of the cytoplasm on both sides of the nucleus is high owing to the haemoglobin

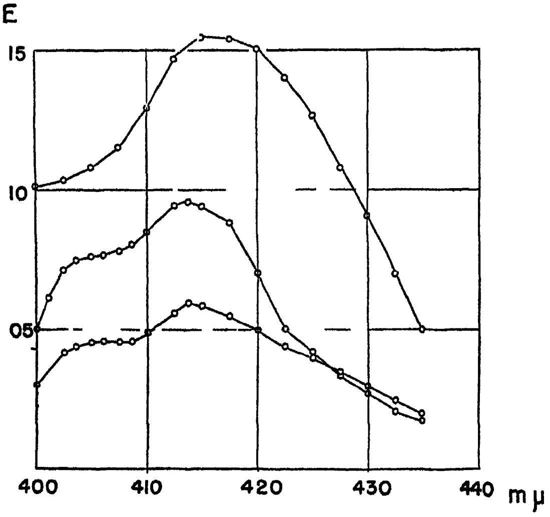

FIG 4

deposition Fig 3 shows calculated absorption curves from erythrocytes in a fresh smear preparation The curves have pure oxy-haemoglobin maxima

Fig 4 shows absorption spectra from a mature erythrocyte (top) and two erythroblasts containing about half the final amount of haemoglobin In the latter spectra there are two distinct and separate components (i) the met-oxyhaemoglobin mixture discussed above, and (ii) a specific absorption around 405 mμ This short wavelength absorption is no doubt due to a porphyrin

Table I shows some preliminary values of the ratio of porphyrin (calculated

TABLE 1

Cell Diameter μ	Total Amount of Hb in 10^{-6} μg	Ratio Porphyrin/haemoglobin (Hb)
9 0	2	—
7 8	10	0 2
7 5	15	0 25
7 5	22	0 1
6 5	25	0 0
Mature red cell	28	0 0

as protoporphyrin) to haemoglobin in rat erythroblasts at different stages of haemoglobinization From these values, the ratio appears to be highest in the cells which have reached around half the final amount of haemoglobin

Discussing the results, it can be stated firstly that during certain stages of haemoglobinization the normal erythroblast contains fairly large amounts of porphyrins Free protoporphyrin has earlier been found in iron deficiency and haemolytic anemia, in reticulocytes following increased red cell production, etc.[9, 10, 11, 12] The present results indicate porphyrin compounds to be a cellular constituent during normal erythropoiesis, and with great probability an intermediate compound in the synthesis of haemoglobin. Assuming this compound to be protoporphyrin, the absorption at 405 mμ suggests partly saturated side chains and probably that it is bound to (or formed on) the protein component.[13]

Concerning the kinetics of the endocellular haemoglobin synthesis, the finding of a maximal ratio of porphyrin to haemoglobin in the midst of the haemoglobinization process indicates a two step reaction with a slower second phase. The investigation is being continued, especially as regards the closer definition of the porphyrin compound.

This study is carried out under a grant from the Medical Research Council, Sweden.

Karolinska institutet,
Stockholm.

[9] Seggel, *Ergebn. inn. Med. u. Kinderh.*, 1940, **58**, 582.

[10] Watson and Clarke, *Proc. Soc. Expt. Biol. Med.*, 1937, **36**, 65.

[11] Watson, Grinstein and Hawkinson, *J. Clin. Invest.*, 1944, **23**, 69.

[12] Grinstein, Silva and Wintrobe, *ibid.*, 1948, **27**, 245.

[13] Lemberg and Legge, *Hematin Compounds and Bile Pigments* (Interscience, New York, 1949).

MICROSPECTROGRAPHIC STUDIES ON THE YELLOW PIGMENT IN NERVE CELLS

By Holger Hydén and Bo Lindström

Received 28th September, 1950

The results from a study with ultra-violet and X-ray microspectrography, fluorescence spectrography and cytochemical tests of the yellow pigment in human nerve cells are reported. This pigment, lipofuscin, is found in the cytoplasm of the nerve cell and increases in quantity with rising age.

Pentose nucleoproteins are a physiological constituent of all big nerve cells. They occur in great amounts in the cytoplasm and in smaller amounts in the nucleolus.[1-7] A production and consumption of the pentose nucleoproteins in the nerve cells has been shown to be a phenomenon accompanying adequate stimulation of the neuron.[5, 6, 8-10] The occurrence of the yellow pigment in the cytoplasm of human nerve cells thus makes a study of its composition a prerequisite for further investigations.

---

[1] Brachet, *C.R. Soc. Biol.*, 1940, **133-144**, 88.

[2] Brachet, *Enzymologia*, 1941, **10**, 87.

[3] Hydén (Landström), Caspersson and Wohlfart, *Z. mikr. anat. Forsch.*, 1941, 49.

[4] Hydén, *Nord. Med.*, 1941, **4**, 3048.

[5] Hydén, *Nord. Med.*, 1942, **1**, 144.

[6] Hydén, *Acta Physiol. Scand.*, 1943, Suppl. 17.

[7] Gersh and Bodian, *J. Cell Comp. Physiol.*, 1943, **21**, 253.

[8] Hydén and Hamberger, *Acta oto-laryng.*, 1945, Suppl. 61.

[9] Hydén and Hamberger, *Acta oto-laryng.*, 1949, Suppl. 75.

[10] Hydén and Hamberger, *Acta oto-laryng.*, 1949, Suppl. 75.

Cytological observations were early made on the incidence and frequency of the yellow pigment in the nerve cells. Between the age of 7 and 30 years only a limited number of nerve cells in the spinal cord and in the medulla oblongata contain yellow pigment whereas between the ages of 40 and 80 years it is present in nearly all the nerve cells in this area.[11-14] The substance can occupy the greater part of the cytoplasm, the nucleus then being displaced towards the periphery of the cell. Its distribution within different parts of the nervous system has also been described.[15, 16]

The lipofuscin contains a lipid part which is dissolved with organic solvents and another part which stains with basic dyes.[18, 19] The dye is not bound to the lipid-soluble part. The yellow pigment takes up basic dyes at a pH greater than 5·5. On this observation an elective staining procedure has been based.[20] The stained part of the yellow pigment is insoluble in acids, alkali and alcohol-ether. The colour remains after treatment with potassium permangate, sodium hydrogen sulphite and hydrogen peroxide.[18, 19, 22]

The yellow pigment in the nerve cells has frequently been interpreted as a slag product, impairing the function.[12, 23] Its occurrence at an early age and its large quantity in the cell on the other hand are against such an interpretation.[15]

Experimental

Material and Methods.—Anterior horn cells from the cervical intumescences of the spinal cord from individuals of varying ages, between 16 and 89 years, were studied. The material was taken 3 to 18 hours *post mortem* and fixed in liquid air according to the Altmann-Gersh freezing-drying method or in 10 % formaldehyde solution or in Carnoy's solution. Frozen sections of unfixed material were taken for fluorescence spectrography. To remove paraffin, chloroform was used which was followed by absolute alcohol. The section was immersed in glycerine for at least 2 hr. Before the ultra-violet measurements suitable cells were dissected free from adjoining tissue on one side to obtain a blank. Sections for fluorescence spectrography were only covered by glycerine and the cover slip or treated with chloroform and alcohol or with methanol-chloroform. This does not remove the yellow substance.

ABSORPTION SPECTRA were taken in the ultra-violet range and the visible part of the spectrum in various parts of the cells, using the apparatus constructed by Caspersson.[24] The cells were selected by means of photography at 2570 Å in the ultra-violet microscope constructed according to Köhler.

OPTICAL SYSTEM.—Zeiss quartz monochromates corrected for 2570 Å and for 2750 Å. *Objective*, 2·5 mm., numerical aperture 0·85. *Ocular*, × 10. *Condenser*, numerical aperture 0·65. Within the visible parts of the spectrum the optical system used was a Zeiss apochromate, numerical aperture 1·25 and compensation ocular × 10.

For a study of the ash content of the cells, *micro-incineration* was carried out at 500° C for 1 hr., after which the cells were photographed in the dark field. Sections were digested with ribonuclease, prepared according to Kunitz' method and recrystallized in alcohol three times, in a solution containing

[11] Obersteiner, *Arb. Neurol. Instit. Wiener Univer.*, 1903, **10**, 245.
[12] Mühlmann, *Verh. dtsh. path. Ges.*, 1900-1, **3-4**, 148.
[13] Mühlmann, *Arch. mikroskop. Anat. Entwicklungsgeschichte*, 1901, **58**, 231.
[14] Pilcz, *Arb. Anat. Physiol.*, 1895, **3**, 123.
[15] Altschul, *Virchow's Arch. path. Anat.*, 1938, **301**, 273.
[16] Altschul, *J. Comp. Neur.*, 1943, **78**, 45.
[17] Wolf and Pappenheimer, *J. Neuropath. Expt. Neurol.*, 1945, **4**, 402.
[18] Hueck, *Bietr. path. Anat. allgem. Path.*, 1912, **54**, 68.
[19] Bethe and Fluck, *Z. Zellforsch. mikroskop. Anat.*, 1937-38, **27**, 211.
[20] Volkmann, *Z. wissensch. Mikr. mikr. Technik.*, 1932, **49**, 457.
[21] Oberndorfer, *Zentr ges. Neurol. Psych.*, 1921, **26**, 1.
[22] Brahn and Schmidtmann, *Virchow's Arch. path. Anat.*, 1920, **227**, 137.
[23] Hett, *Z. Altersforch.*, 1941-4, **3-4**, 174.
[24] Caspersson, *J. Roy. Microsc. Soc.*, 1940, **60**, 8.

0.29 mg of ribonuclease/ml (pH 6.8). Microspectrography was carried out before and after digestion.

FLUORESCENCE SPECTROGRAPHY. Exciting radiation was obtained from an arc lamp using glass filters UG 1 and BG [illegible]. The radiation obtained in the ultra-violet region was limited to approximately 310–370 mμ.

Microscope optics. Zeiss achromatic, numerical aperture of 0.[illegible]. Quartz condenser with numerical aperture 1.[illegible] and [illegible] respectively. On the place of the ocular a Jena filter GG [illegible].

The spectra were taken on Ilford [illegible] plates. A Zeiss quartz Q[illegible] spectrograph was used. The image of the object was focused in the plane of the entrance slit, the magnification being 1.[illegible] times. The minimum slit width was 0.05 mm.

MASS DETERMINATIONS BY X-RAYS according to Engström and Lindström's method[25] was carried out for the purpose of studying the distribution of the dry substance in parts of the nerve cell containing yellow pigment as compared with those parts of the cells containing pentose nucleic acids and proteins. The method is based on the fact that the absorption of suitably selected continuous X-radiation is proportional to the total amount of substance per surface unit in the histological section. In our determination we used radiation generated at a tension of 3000 volts and filtered through a [illegible] μ thick aluminium foil, the wavelength then being approximately 8 Å. No element present in large quantities in the tissue has any disturbing absorption peak in this range.

Thick sections 6 to 10 μ of the cervical intumescence from a human spinal cord fixed in 10 % formaldehyde solution was photographed on a Lippmann film together with a reference system. This consisted of a wedge of collodion foils in steps approximately 0.1 μ thick. The film allows effective magnification up to 400 times. After developing in an alkaline hydroquinone developer, the picture of the tissue and the reference system was photographed in a microcamera at a magnification of 400 times. The density on the photographic plate within parts of the nerve cells containing yellow pigment or pentose nucleoproteins was measured with a Kipp and Zonen microphotometer.

Since both control cells and cells containing yellow pigment occurred in the same section and were photographed together with the reference system, those sources of error were eliminated that could be caused by differences in the density curve of the films and by the developing and fixation processes.

In order to control the cells after X-ray microphotography the same sections were stained with toluidine blue. This permitted a direct correlation of the results of the density determination with the cytological picture. In order to determine the thickness of the section within the part of the cell to be measured particles in the upper and lower surface of the section were focused and the focal length determined.

OPTICS.—Objective apochromatic 90, N.A. 1.32. Compensating ocular × 10. Staining of the cells with toluidine blue was also performed after absorption measurement in the ultra-violet and visible parts of the spectrum at pH 4, and also at pH greater than [illegible], with Gentian violet solution according to Bethe's and Volkmann's methods.[10, 20] Feulgen's nucleal reaction was used to demonstrate the presence of desoxypentose nucleic acids.

Nerve Cells containing Pentose Nucleoproteins (Controls). The control material consisted of anterior horn cells from a youth aged 18. Control cells and those containing yellow pigment were present in the same section on X-ray microphotography (see the foregoing). A microscopic control was first made of the cells selected for measurement to ensure that they contained no stained substances. A monochromator was used as the source of light.

ABSORPTION MEASUREMENTS. Motor anterior horn cells in man have been shown, by means of cytochemical methods, to contain considerable concentrations of pentose nucleic acids and protein substances. Quantitative determinations have shown a substantial content of nucleic acids, i.e. 1 to 2 %.[26, 20] The substance containing nucleoproteins is distributed in more or less well-defined agglomerations in the cytoplasm and in the dendrites, corresponding to the distribution of the basophil Nissl substance. Desoxypentose nucleic acids are only found in scanty amounts in the motor nerve cells and are confined to a small number of particles in the periphery of the nucleolus, comprising the so-called nucleolus-associated chromatin. No characteristic absorption maxima could be observed in the control material on measurements in the visible parts of the spectrum.

[25] Engström and Lindström, *Biochim. Biophys. Acta,* 1950, 4, 351.

[26] Hydén and Hartelius, *Acta psychiatr. neurol.*, Suppl. 48, 1948.

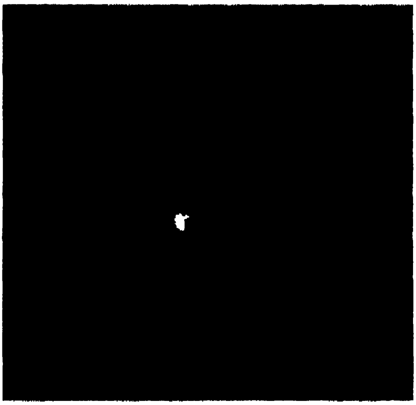

FIG. 1. Anterior horn cell from a human spinal cord. The cell contains pentose nucleic acids and proteins but no yellow pigment. Photographed on a Lippmann film with an acceleration tension of 5000 volts. The nucleolus and the nucleus have a considerable absorption compared with the nucleus.

[To face page 435

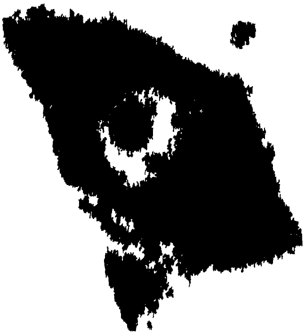

Fig. 2. Anterior horn cell from a human spinal cord photographed at 2570 A. The cytoplasm as a whole is characterized by a high absorption. Note that the absorbing substance of the right lower part of the cytoplasm has a fine granular appearance. This area contains yellow pigment.

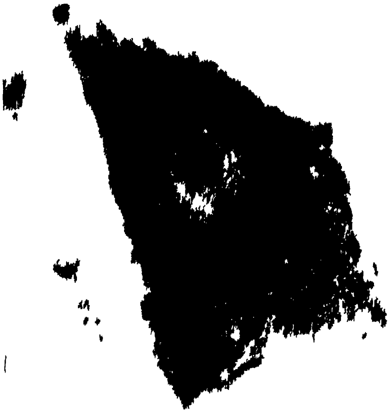

Fig. 3. The same nerve cell as in Fig. 2 stained with toluidine blue at pH 4. The right lower part of the cytoplasm which contains yellow pigment and absorbs strongly at 2570 A does not take the basic dye groups.

Fig. 4. The same nerve cell as in Figs. 2 and 3 microincinerated at 500° C and photographed in the dark field. In the right lower part of the cytoplasm containing yellow pigment the ash residue seems denser than in the remainder of the cell.

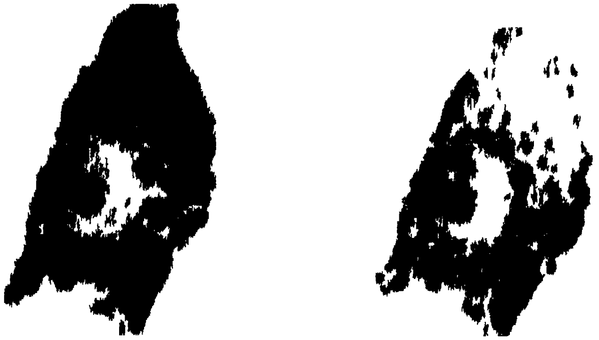

(*a*) (*b*)

FIG. 6.—Anterior horn cell containing yellow pigment from human spinal cord photographed at 2570 A (*a*) and after staining with toluidine blue at pH 4 (*b*).

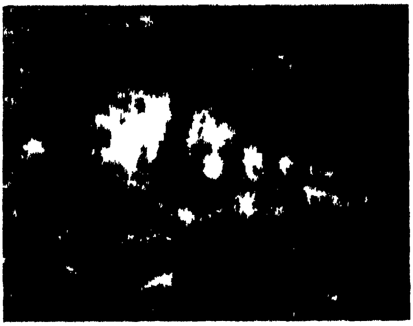

FIG. 7.—Anterior horn cell from human spinal cord. Photographed on a Lippmann film with an acceleration tension of 3000 volts. The area in the cytoplasm to the left of the left black line contains yellow pigment and stands out clearly due to its high absorption capacity. Cf. the nerve cell in Fig. 1.

MASS DETERMINATIONS BY X-RAYS.—Examples are given in the following of determinations of the total amount of substance in the nerve cells which contain no yellow pigment. The nucleolous stands out clearly in the cell in Fig. 1 by means of its more intense absorption compared with the remainder of the nucleus. A number of points in the nucleolus, the nucleus and the cytoplasm were measured on photometrical determinations. The relation between the total amount of substance in different parts of two control cells with the quantity of substance in the cytoplasm as a unit is given below. They are taken at the tension of 3000 volts. Each single figure is the mean figure of about ten determinations.

TABLE 1

Cytoplasm	Nucleus	Nucleolus
1	0·54	0·90
1	0·56	0·82

Nerve Cells containing Yellow Pigments.—ABSORPTION MEASUREMENTS—Fig. 2 shows an anterior horn cell, unstained and photographed at 2570 Å. The cytoplasm absorbs strongly. In the right-hand part the absorbing substance is not localized to distinct agglomerations but is diffusely distributed within the cytoplasm. Fig. 5 demonstrates absorption spectra taken within the ultra-violet range and the visible parts of the spectrum to 4600 Å at points in this area. A strong absorption maximum appears at 2600 Å. The absorption is also strong at 2800 Å indicating the presence of heterocyclic and aromatic amino acids (tryptophane, phenyl alanine and tyrosine) in the protein present. That part of the cytoplasm in the same nerve cells from which these absorption spectra were taken could not be stained with toluidine blue at pH 4 (Fig. 3).

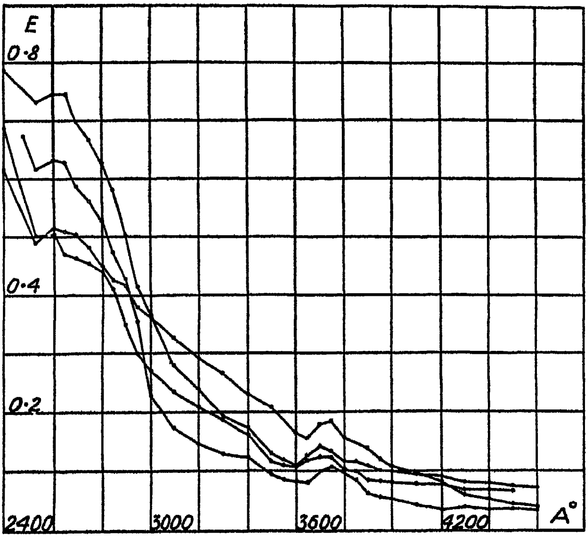

FIG. 5.—Absorption spectra taken between 2400 to 4600 Å in areas of anterior horn cells containing yellow pigment from human spinal cord.

Fig. 6(*a*) and (*b*) show another example. On the left of the figure is seen the cell photographed at 2570 Å. On the right it is stained with toluidine blue. The area nevertheless stained well with toluidine blue at pH greater than 6 or with Volkmann's Gentian violet solution, and contained much yellow pigment. The murexide reaction gave negative result.

On micro-incineration, this part of the cell yielded considerable ash (Fig. 4). A comparison with the remainder of the cytoplasm, which contains pentose nucleic acids and protein substances, showed that the ash had a substantially greater density in the area containing yellow pigment.

Experiments with digestion with ribonuclease revealed that it was not possible to remove that part of the cytoplasm containing yellow pigment with the help of the enzyme. The absorbing substance remained, and absorption spectra taken after digestion showed no differences in comparison with those taken before digestion. On the other hand, the pentose nucleic acids in the remainder of the cytoplasm were removed.

In view of the absorption maximum at 2600 Å and 3750 Å and the yellow colour of the pigment, it was easy to assume a flavin component. The tests prescribed by Warburg and Christian[27] were therefore made on the sections. These writers demonstrated that on illumination in an alkaline solution the composition of the yellow ferment is changed and after acidification can be extracted by chloroform. Our experiments did not, however, result in a disappearance of the yellow pigment in the nerve cell.

FLUORESCENCE SPECTRUM. The yellow pigment shows a yellowish fluorescence which is not changed or diminished after treatment of the section by acids, alkalis, chloroform, chloroform-methanol or irradiation.

Fluorescence spectra were taken on frozen, unfixed cells containing yellow pigment and on cells after the treatment described above. The photographic plate was also exposed without the cell but with the adjoining tissue in focus and also without the section. Spectra show a moderately strong fluorescence band between 440-460 mμ and another band between 530-560 mμ.

MASS DETERMINATION BY X-RAYS.—In order to make a direct comparison, measurements were taken of the control cells and the cells rich in pigment lying in the same section. Fig. 7 shows an example of a nerve cell containing both yellow pigment and nucleoproteins, photographed on a Lippmann film with an acceleration tension of 3000 volts. The area to the left of the left black line is seen to absorb particularly strongly. This contains yellow pigment. The right part of the cytoplasm on both sides of the black line contains pentose nucleic acids and proteins but no yellow pigment (see Table II).

TABLE II

Cytoplasm containing:	Weight in μg./μ²	Thickness in μ	% Dry Substance
Pentose nucleic acids and proteins	$4{\cdot}2 \times 10^{-6}$	11·3	37
Yellow pigment . . .	$5{\cdot}5 \times 10^{-6}$	9·8	50

Each determination is the mean figure of approximately 10 measurements. The results of these determinations thus show that the areas containing yellow pigment in the nerve cells have a considerably larger total quantity of dry substance than corresponding areas in the nerve cells containing pentose nucleic acids and proteins but no yellow pigment. Approximately 100 measurements, made on nerve cells with and without yellow pigment, have uniformly shown the same difference in the total quantity of substance per unit volume. In the examples of measurements series given, the figures show that, on an average, the area containing yellow pigment had 50 % more dry substance than corresponding areas containing nucleic acids and proteins.

Discussion

A survey of studies of the yellow pigment by optical methods reveals (i) absorption bands at 2600 Å and 3750 Å, (ii) fluorescence bands between 440-460 mμ and between 530-560 mμ, around 50 % larger quantity of dry substance than areas containing pentose nucleoproteins.

The absorption maximum at 2600 Å did not disappear after digestion with ribonuclease whereas the pentose nucleic acids present in the nerve cells could be removed by the enzyme. The specific band can be explained either by assuming the presence of substances other than nucleic acids or by assuming pentose nucleic acids in a chemical configuration which cannot be attacked by ribonuclease. The absorption data together with the fluorescence data suggest flavins or pterins.

---

[27] Warburg and Christian, *Naturwiss.*, 1932, **20**, 980.

The position of the absorption and the fluorescence bands with absorption at 260 mμ to 375 mμ and emission at 450 mμ and 550 mμ indicates the presence of a complex chromophore. Flavins, e.g. riboflavins can be excluded. The data obtained indicate more a substance belonging to the pterins. Standard spectra of pterins in solution, both xanthopterin and leucopterin, show two strong bands between 435 mμ and 540 mμ.[28] As the fluorescence spectrum of a pterin differs according to whether it is solid or in solution further data are required. The data obtained are, however, in favour of pterins as components of the yellow pigment.

The determinations by mass determinations by X-rays showed that the areas containing yellow pigment in the nerve cells had a considerably higher dry weight than areas containing pentose nucleoproteins. The difference was on an average 50 %. The difference in density of ash residue shown by micro-incineration was therefore in this case a true one.

Regarding the biological aspect of the results obtained the following reflections may be made. The data given show that the amount of pentose nucleic acids in the anterior horn cells decreases with rising age. The space occupied by them appears to be replaced by the complex yellow pigment. A partial change in the chemical structure of the nerve cells therefore takes place with increasing age.

Since this reconstruction of the nerve cell in rising age is so considerable a substantial reduction of function could be expected if the yellow pigment were a slag product due to the importance of the nucleic acids for the neuronal function. The reduction in motor function accompanying increasing age is not, however, proportional to the considerable chemical reconstruction of the nerve cell. The experiments reported thus are against the interpretation of the yellow pigment as a slag product.

From a general biological point of view it can be said that following the embryological period of growth and differentiation there occurs a further chemical differentiation of the nerve cell under the adult stage, apparently with maintained function.

Summary.—The yellow pigment lipofuscin, that is present in human nerve cells and increases in quantity with increasing age, is studied with ultra-violet, X-ray and fluorescence microspectrography, digestion with ribonuclease and micro-incineration. Absorption maxima are found at 2600 Å and 2800 Å indicating the presence of organic nitrogenous bases and protein substances. The strongly absorbing substance at 2600 Å cannot be removed by ribonuclease. Another absorption maximum is found at 3750 Å. Fluorescence bands are found between 4400 to 4600 Å and between 5300 to 5600 Å. The presence of flavins can be excluded. Data obtained indicate some possibility that the yellow substance belongs to pterins.

The mass determinations by X-rays show that the areas in the nerve cells that contain the yellow pigment have around 50 % greater quantity of dry substance than the areas containing pentose nucleoproteins. A partial chemical reconstruction of human nerve cells seems to take place with increasing age. The findings are not in favour of the view that the yellow pigment is a slag product.

The present investigation has been carried out with the aid of grants from Stiftelsen Therese and Johan Anderssons Minne and from the Swedish Medical Research Council.

Department of Histology,
Medical School,
Göteborg C.,
Sweden.

Department for Cell Research,
Karolinska Institutet,
Stockholm 60,
Sweden.

---

[28] Jacobson and Simpson, *Biochem. J.*, 1946, **40**, 3.

ULTRA-VIOLET MICROSPECTROGRAPHY OF LIVING TISSUE CULTURE CELLS

PART I. RADIATION MEASUREMENTS

By H. G. Davies

Received 26th July, 1950

The factors which determine the ultra-violet dosage received by cells when they are examined photomicrographically are discussed. Experimental determinations of the absolute sensitivity in the ultra-violet and visible spectrum of one film suitable for photomicrography, Kodak Microfile Panchromatic 35 mm., are described. The transmissions in this wavelength range of selected objectives are also measured. The dosage required for photomicrography is calculated from these data and also measured directly by a suitable thermopile. This dosage is compared with published data on the effects of ultra-violet radiation on chick fibroblasts in tissue culture. It is concluded that under the conditions described, only one or two photographs at 265 mμ of chick fibroblasts can be taken with no radiation effect, and that microspectrographic studies at a series of wavelengths should be carried out in as short a time as possible, since the dosage required will eventually produce cell damage.

Ultra-violet microscopy has been used extensively as a tool for cytochemical analysis.[1] The application of these methods to living cells is of especial interest, since artefacts due to the fixation process are then avoided. Furthermore, it would seem to present the possibility of studying the various stages in the metabolic activity of a single cell. However, it is well known that ultra-violet radiation damages living cells. This subject has been extensively reviewed.[2] The experiments described below were designed to investigate some of the factors which determine the ultra-violet dosage received by cells when they are examined by photomicrography. These factors are:

(i) film properties,
(ii) the absorption in any stage after the specimen,
(iii) the optical density of the specimen,
(iv) the amount of information which is obtained from the specimen.

In order to keep the dose at a minimum it is obvious that the cells should not be irradiated during focusing. This presents no difficulty with achromatic objectives, but with monochromats special methods have been devised.[3, 4, 5]

Serial photomicrographic study of cells is conveniently made by use of film. The choice of the best film can be approximately made from the data of Fraser,[6] who has measured the relative speeds and graininess of a number of films at a wavelength of 265 mμ. He has taken as an index of quality of an emulsion, the quantity S/G,[2] where S and G are the speed and grain size respectively relative to Kodak B. 20 Process Regular Plate. As is pointed out, the factor G is only an approximate index of film resolving power. The latter also depends on the gamma of the emulsion, and will increase with it. The effect of the other factor, turbidity of emulsion, on resolving power is unimportant under the conditions of use since high film densities and consequent spread of image are not necessary in the photography of living cells, which usually have a small density range. The speed S was measured by taking the exposure required to produce a density of 0·3 above fog, and comparing it with the standard B. 20 plate. Furthermore, at densities much in excess of 0·3, the high gamma films will show an increased relative sensitivity. It has been found that in order to obtain satisfactory photographs of living cells, films with high gammas should be used, and their use also increases the accuracy of subsequent microphotometry. The data[6] show that of the high gamma films Kodak Recording film 1372 (35 mm.) and Microfile Panchromatic (35 mm.) have about the same index of quality. The former has the higher gamma, about 1·8 under the conditions of measurement. Since data are not available for the absolute speeds of these films throughout the ultra-violet range of wavelengths, a series of measurements made on one of them (Kodak Microfile Panchromatic) is described below. Preliminary measurements of the radiation dose in photomicrography were made by the writer and Dr. R. C. Mellors independently, and the writer was glad to have the opportunity of discussing these results with him. Since then, the more thorough investigation has been made as described here, and by Mellors *et al.*[7]

---

[1] Caspersson, *Symp. Soc. Expt. Biol.*, 1947, **1**, 127.
[2] Giese, *Quart. Rev. Biol.*, 1947, **22**, 253.
[3] Barnard and Welch, *J. Roy. Micro. Soc. A*, 1936, **56**, 365.
[4] Wyckoff, Ebelung and ter Louw, *J. Morph.*, 1932, **53**, 189.
[5] Davies and Wilkins, *J. Roy. Micro. Soc.*, 1950 (in press).
[6] Fraser, *J. Sci. Instr.*, 1950, **27**, 106.

Experimental

The experiments were made with an ultra-violet microspectrographic apparatus described elsewhere.[8] It employed an automatic focusing monochromator in front of the microscope. A Thermal Syndicate 125-W medium pressure mercury arc was used as source. This arc is stabilized in position by two constrictions in the quartz envelope. The output was constant to a few per cent during the period of the experiment.

Film Measurements.—The film Kodak Microfile Pan. was exposed to a graded series of exposures at monochromatic wavelengths throughout the ultra-violet and visible spectrum. The output slit of the monochromator was imaged on to the film using a single quartz lens, and the camera moved to the position of correct focus. The energy was measured with a photocell (Cinema Television, Type QVA 38) which was calibrated at each wavelength against a calibrated thermopile (Hilger multi-junction thermopile). When used with a galvanometer with sensitivity 2600 mm./μA the deflection with light intensities small enough to blacken the film in easily measurable times, was not of sufficient magnitude for measurement to an accuracy of 1 %. The following procedure was therefore adopted. With light intensities which could be measured to the required accuracy, a series of filters calibrated at each wavelength in the spectrum were interposed in the beam prior to exposure of the film. Filters used in the ultra-violet were cellophane and partially aluminized quartz plates. Film densities were measured on a Hilger non-recording microphotometer. Processing was carried out in Kodak developer (formula D 19b) for 4 min. at 20° C.

Objective Transmission.—The simple method of measuring the ratio of the energy leaving the condenser to that leaving the objective did not yield consistent results. This was due to difficulties in measuring the highly divergent beam from the condenser. The following method was employed. Three objectives were used as objective and condenser alternately, and the total transmission of three combinations measured. The entrance and exit beams were approximately parallel and their apertures were controlled by suitably placed stops, so that they each fell on the same area of the photocathode. This latter condition is necessary since, as is well known, the sensitivity varies over the photosensitive surface. The values of the transmissions T_1, T_2, T_3 were calculated from the measured values of the products T_1T_2, T_2T_3, T_1T_3. A photocell was used in the visible and a photomultiplier (R.C.A. 931-A) in combination with a tungstate fluorescent screen in the ultra-violet.

It is convenient in biological experiments to measure directly the energy incident on the plane of the specimen. Measurements were made in this plane using a small thermopile (in air) of area 2·0 × 0·4 mm.², sensitivity 0·07 μA/μW (calibrated by an independent source from the calibrated thermopile used above), and resistance 12 ohms, with a Cambridge galvanometer (resistance 20 ohms sensitivity 140 mm./μA). The intensities in the ultra-violet were such that the deflections were small, and a telescope was used in recording them.

---

[7] Mellors, Berger and Streim, *Science*, 1950, **111**, 627.

[8] Walker and Davies (Part II), this Discussion.

Results

Fig. 1 shows the sensitivity data for the photocell (Type QVA 38) with a caesium-antimony cathode. This surface has a much higher quantum efficiency

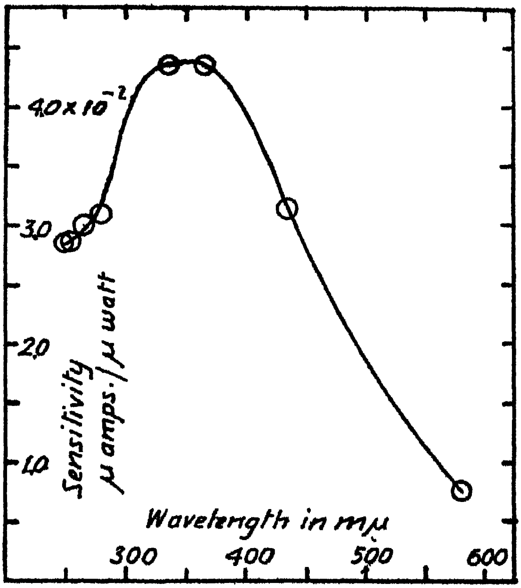

FIG. 1.—Calibration curve for Cinema Television photocell type QVA 38.

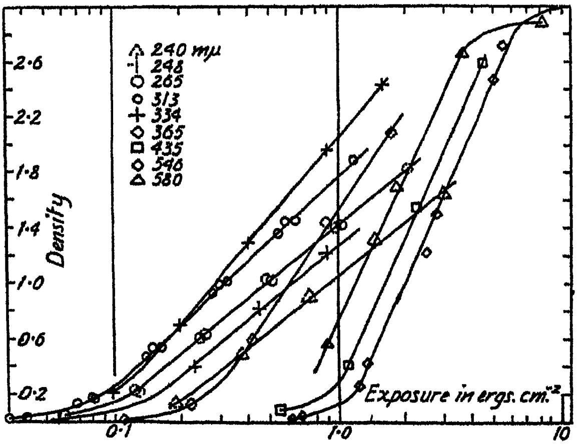

FIG. 2.—Characteristic curves for Kodak Microfile Panchromatic 35 mm. developed in D 19*b* for 4 min. at 20° C.

than any other photocathode. The characteristic curves for Kodak Microfile Pan. (developed as above) are shown in Fig. 2. From them the information on film speed and gamma is obtained. Film speed can be variously defined, but it has been taken here as the energy in erg cm.$^{-2}$ to produce a film density 0·6 above background. Fig. 3 shows how the speed varies with wavelength. The sensitivity is a maximum at about 325 mμ. Fig. 4 shows that the gamma

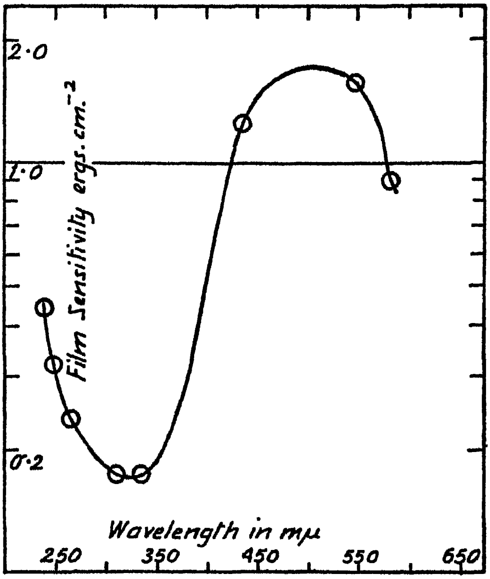

FIG. 3.—Film speed for Kodak Microfile: defined as the energy in erg cm.$^{-2}$ to produce a density 0·6 above fog.

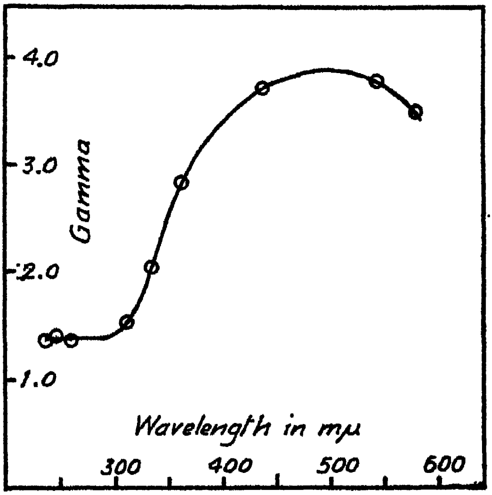

FIG. 4.—Variation of gamma with wavelength for Kodak Microfile Pan.

(the slope of the straight part of the characteristic curve and a measure of film contrast) decreases at shorter wavelengths and is approximately constant in the region 313 mμ-240 mμ. These latter results agree with those made on plates by Amstein.[9] The measured transmission data for two refracting and one reflecting objective[10] are shown in Fig. 5 (*a*, *b*, *c*). These results are a function of the particular media used in their construction and are expected to vary with objectives.[11] It is concluded that reflecting objectives have the highest transmission throughout the ultra-violet region and are therefore well suited for work on living cells, where the dosage must be kept at a minimum.

---

[9] Amstein, *J. Soc. Chem. Ind.*, 1944, **63**, 172.

An indication of the errors involved in the above measurements is obtained by comparing, at selected wavelengths, the dose to the specimen plane measured with the small thermopile with the value calculated from the objective transmission and film sensitivity, using eqn. (1) given later. The agreement is to within ± 5 %.

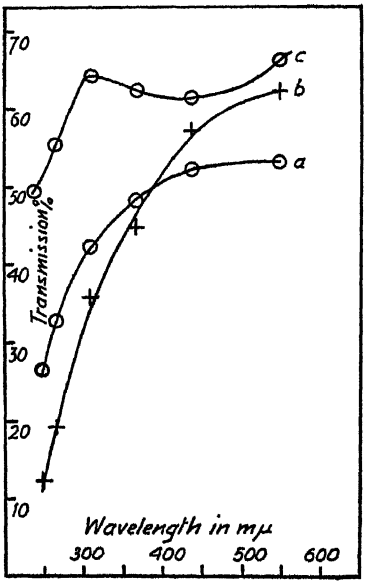

Fig. 5. Measured objective transmission :

(*a*) Monochromat quartz objective N.A. 1·15 constructed by Messrs. R. J. Beck Ltd.

(*b*) Lithium fluoride fused quartz achromat designed by R. J. Bracey (BSIRA), constructed by R. J. Beck; N.A. 1·24.

(*c*) Reflecting objective;[10] N.A. 0·6. Condenser N.A. used throughout,

Discussion

The above results can be used to calculate the dosage received by cells grown in tissue culture. Cultures grown in hanging drop preparation in liquid media (exudate from embryo extract and fowl plasma) produce cells which grow in close contact with the top quartz coverslip. These cells are well suited for photomicrographic study, since they grow in thin sheets with a negligible amount of absorbing media above them. The thickness of liquid medium in which they grow absorbs only about 50 % of the radiation at 265 mμ.

When the optimum film and objective have been chosen the other factors affecting the dosage to the cells are the optical density of the cell and the amount of information which is required. Thus, the density in the photographic negative of the most absorbing cell component should lie just at the bottom of the straight part of the characteristic curve (Fig. 2). Any smaller film density will reduce contrast and render microphotometry of this component less accurate. In the photography of resting chick fibroblasts the maximum optical density in the cell does not exceed about 0·3,[8] and it is sufficient to use a photographic density of about 0·6. Also, as is well known, if no resolved microscopic structure is to be lost in the photograph the magnification on to the film must be chosen so that its resolving power, or ability to show fine detail, is adequate

[10] Seeds and Wilkins, *Nature*, 1949, **164**, 248.

[11] Loofbourow, *J. Opt. Soc. Amer.*, 1950, **40**, 317.

to show this structure. Any greater magnification will involve an unnecessary irradiation of the specimen. It is clear that the maker's figures for the film resolving power, which are made under optimum conditions in visible light, will not apply in the ultra-violet where the gamma is considerably less. Furthermore, the detail resolved by the film will depend on the contrast in the subject. The proper magnification to be used should therefore be determined experimentally in the usual manner by varying the magnification on to the film and noting on suitable enlargements when the smallest structure is just resolved by the film. The resolving power of Kodak Microfile Pan. has not been thoroughly investigated. In photography of chick fibroblasts using Kodak Microfile Pan. with the Bracey Achromat (N.A. 1·24) a magnification of approximately × 100 seems adequate to resolve the fine structure in the cell. With films of lower resolving power correspondingly increased values of magnification are required. With the Kodak Recording film 1372 the increased magnification required is approximately balanced by the increased speed,[6] with the same dose to the specimen. However, with the latter film, as has been pointed out, there will be increased contrast in the negative. The limitations imposed by graininess, which produce noise in the microphotometric recordings of the smallest detail in the negative, requires further attention. It may well be that for accurate determinations of their density values magnifications considerably in excess of the above will be required. With objectives of lower numerical aperture less detail is contained in the final image. The magnification on to the film can be correspondingly reduced. The dose is reduced as the square of the numerical aperture (N.A.).

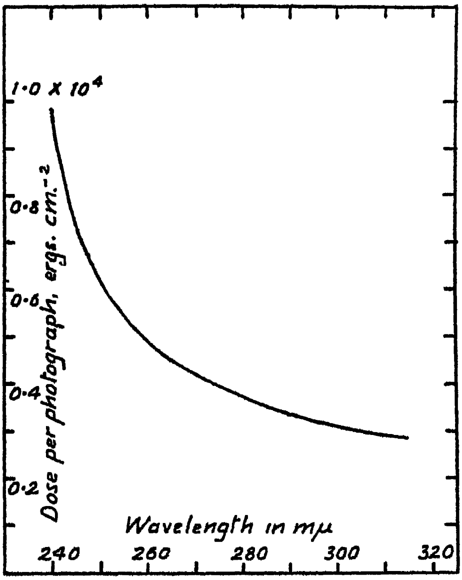

FIG. 6.—Ultra-violet dosage per photograph with reflecting objective (N.A. 1·3) × 100 on to Kodak Microfile Pan. 35 mm. for density 0·6.

The ultra-violet radiation dose received by the cells for a photograph of density d at wavelength λ is calculated from the formula

$$E_\lambda = m^2 F_\lambda^d T_\lambda^{-1} \quad . \quad . \quad . \quad . \quad . \quad (1)$$

where E_λ is the dose on the cells in erg cm.$^{-2}$ at wavelength λ, m the magnification on to the film, F_λ^d the film sensitivity in erg cm.$^{-2}$ for density d, and T_λ the objective transmission. The calculation is made for × 100 magnification on to Kodak Microfile Pan. at density 0·6 using the data from Fig. 3 and the transmission data for a reflecting objective N.A. 1·3 [12] (calculated from Fig. 5(*c*)) with an extra 4 % loss at the amici component : there is no loss at the cover slip due to reflection). The results (Fig. 6) are likely, with the materials at present available, to approach the optimum conditions for maximum information with minimum dose. The dose per photograph increases with decreasing wavelength due to lower film sensitivity and objective transmission.

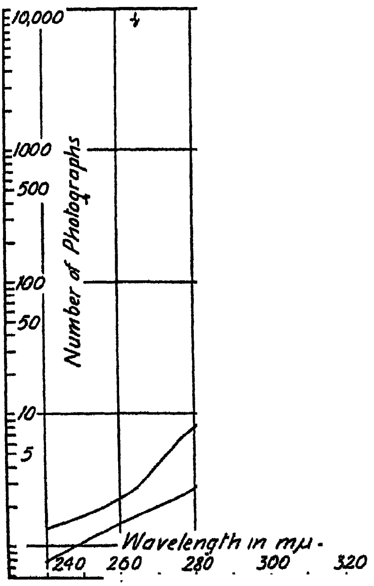

FIG. 7.—Graph showing number of photographs after which most sensitive cells are not injured (*a*) and after which most resistant cells are injured (*b*).

The data of Fig. 6 are now compared with the results of Mayer and Schreiber [13] who have investigated the effects of ultra-violet radiation at selected wavelengths throughout the ultra-violet spectrum on entire tissue cultures of chick fibroblasts. They used, as an indication of damage, the rate of growth as shown by area measurements. It has been pointed out [7] that the plasma embryo-extract medium in which the cultures were grown will exert a protective effect on the cells. However, under the conditions of irradiation, the cells, in particular the main layer, are only partly protected by that capillary layer of the medium which lies between them and the coverslip through which the radiation passes. This layer is small since chick fibroblasts (but not mammalian fibroblasts) liquefy the plasma-medium and will tend to grow near the coverslip for support. Thus it is unlikely that the results of Mayer and Schreiber are in serious error from this cause. Fig. 7 is obtained by dividing the dose per photograph (Fig. 6) into the radiation dose for cell injury as a function of wavelength obtained from the data summarized by Mayer.[14] Curve (*a*) shows the number of photographs that may be taken of the most sensitive cells without injury and curve (*b*) the number of photographs after which even the most resistant cells will be affected. The area between the two curves indicates the spread of sensitivity between cell cultures. This comparison assumes that a given dose will affect a group of cells photographed in any culture in the same way as the equivalent dose given to the culture as a whole. Furthermore, the spread indicated by the area may be slightly greater under the present conditions due, for example, to the most sensitive cultures containing a group of particularly sensitive cells which, if damaged, would not show any affect on the growth rate of the culture as a whole. It is concluded that at 265 mμ only one or two pictures, under conditions that approach the optimum, may be taken of these particular cells, chick fibroblasts, without any damage to the cells. At shorter wavelengths even one photograph may have an ultimate effect. The effects observed will vary from a decreased growth rate to complete cell inhibition. Thus a complete microspectrographic analysis in the ultra-violet at a series of wavelengths under these conditions cannot be performed photographically without eventual damage to the cell. It is important that such an analysis[9] is carried out quickly before the radiation damage has time to develop.

---

[12] Norris, this Discussion.

[13] Mayer and Schreiber, *Protoplasma*, 1934, **21**, 34.

[14] Mayer, *Tabulae Biol.*, 1939, **19**, 243.

I wish to thank the following for helpful discussions: Prof. J. T. Randall, F.R.S., Dr. H. B. Fell, Dr. M. H. F. Wilkins, R. D. B. Fraser and P. M. B. Walker. The small thermopile used in direct measurement of dose in the specimen plane was kindly loaned by T. R. E. Malvern and calibrated by them against their standard black body. I also wish to thank the Chemistry Dept., King's College, London, for facilities very generously provided for the calibration of the photocell Type QVA. 38. This photocell, and other apparatus, was loaned to the writer by Dr. W. C. Price and the quartz monochromat was kindly loaned by Mr. R. J. Bracey.

Medical Research Council Biophysics Unit,
King's College,
Strand, London, W.C.2.

ULTRA-VIOLET ABSORPTION SPECTRA OF STRUCTURES IN SURVIVING CELLS

By Barry Commoner

Received 24th July, 1950

The experimental and interpretive procedures necessary to obtain ultra-violet absorption spectra of structures in intact living cells are described. A simplified microspectrophotometer suitable for such studies has been constructed. It permits viewing of the object under visible light and yields absorption measurements with only a 10-sec. exposure to u.-v. Examples of u.-v. absorption spectra of surviving cells are presented. Because intact cells invariably present heterogeneous cross-sections to any given optical path, the u.-v. absorbing material is not necessarily uniformly distributed throughout the length of this path. Consequently, the position and height of the absorption maxima obtained from measurements at a single point in an intact cell can be assigned neither to a given structure nor to a specific substance. Procedures which determine the separate absorption spectra of various structures occurring in a light path through cells such as those of plant epidermal hairs are described. These are applied to the case of *Coleus* hair cells, and it is shown that the separate absorption spectrum of the vacuole contents, and of the thin protoplast layer can be derived from two absorption spectra taken at points of different thickness, or at different stages of partial plasmolysis. The spectra calculated by this procedure agree with the known composition of the vacuole, and with information concerning the absorbing materials likely to be present in the protoplast. By this method it is possible to obtain the actual absorption spectrum of the nucleus of an intact cell. To do this three absorption spectra must be measured. The absorption spectrum of a living tobacco hair cell nucleus obtained in this way is presented. Emphasis is placed on the fact that a single absorption spectrum through one point in an intact cell cannot be properly interpreted, and certainly should not be assigned to a given structure (such as the nucleus) which is included in the path. If the above considerations are kept in mind it is possible to select cells whose characteristics permit the determination of the actual absorption spectra of living cell structures.

Although ultra-violet absorption spectrometry has been most extensively applied to the problems of cytology, it also provides a valuable means of studying the physiological activity of single cells. It is apparent that data of unique significance might be obtained by determining at intervals the ultra-violet absorption spectra of individual cells undergoing various types of activity. To this end, it has been our purpose to develop experimental and analytical procedures suitable for the determination and interpretation of ultra-violet extinctions of single surviving cells.

This aim imposes a series of requirements on the method: (1) Absorption spectra must be obtained with an incident light intensity below the killing threshold. (2) The spectral band width of the incident light must be sufficient to resolve absorption bands encountered in various intracellular components, i.e. a maximum of about 2·5 mμ. (3) Since many intracellular structures are frequently in motion in living cells, the exposures required for absorption measurements must be of the order of seconds, and means must be provided for rapid visualization of the position of the object.

The application of ultra-violet spectrometry to single surviving cells also raises a number of analytical and interpretive problems: (1) Since intact cells almost always present heterogeneous cross sections to any given optical path, ways need to be found to assess the relative and absolute contributions of the different intracellular structures or regions which fall in the light path to the total absorption determined by measurement. (2) The validity of the so-called absorption laws must be ascertained for intracellular conditions. (3) Photochemical alterations in the composition of the cell during exposure to ultra-violet light must be guarded against or at least detected.

The present paper describes an effort to provide practical solutions to at least part of the problems cited above, and the application of these methods to the optical analysis of certain living plant cells.

Experimental and Results

The Apparatus. A new simplified microspectrophotometer, for the range 240–700 mμ which meets the above criteria has been constructed. It is based on an instrument described previously,[1] and differs from the latter in the following particulars.

The light source now used is a water-cooled high-pressure 1000-W mercury capillary lamp (General Electric Type AH6). The lamp transformer is supplied by a voltage stabilizer; light output is constant to about 0·2 %. A quartz condensing lens throws an image of the lamp on the entrance slit of the monochromator (Beckman, model DUR); the emerging beam is directed into an upright microscope by a front-surface aluminized mirror.

An auxiliary light source is provided. This is an ordinary microscope lamp with a green filter, focused on a second 45° mirror placed just above the mirror reflecting the monochromator beam. In this position the auxiliary light mirror blocks the monochromatic beam and illuminates the microscope with green light. Alternatively this mirror may be deflected (magnetically), thereby allowing the monochromatic beam to enter the system.

The microscope optics consist of a quartz condenser (Cooke, NA 1·25),* a Grey reflecting objective (Bausch and Lomb, ×53) and a ×10 quartz ocular. As in the instrument previously described, a side ocular is provided for direct observation of the object. The prism of this ocular may be deflected instantaneously, allowing the image of the object to fall on the photomultiplier tube. Since the Grey objective is essentially achromatic, it may be brought into focus for all wavelengths (including the ultra-violet) by focusing the object visually through the side ocular. Hence, all adjustments are made with the ultra-violet beam blocked, and exposure of the object thereby kept to a minimum.

The apparatus includes a combined signal detector and regulated voltage supply (designed by Mr. J. Townsend). The detector responds to an A.C. photomultiplier output obtained by placing a rotor in the exit beam of the monochromator. The detector responds selectively to the frequency with which the monochromator beam is chopped, and is relatively insensitive to all other signals emitted by the photomultiplier. This arrangement serves to discriminate against thermal noise and against stray light such as reflection from the cover glass. As a result, it is not necessary to provide a dark room for the instrument. The time-constant of the detector circuit is such as to give an accurate scale reading within a maximum of 10 sec., thus allowing for relatively rapid determination of absorption values.

---

[1] Commoner, *Ann. Mo. Bot. Gard.*, 1948, **35**, 239.

* Stopped down to N.A. of objective (0·72).

Signals are read on a microammeter with a 6″ scale divided in one-hundredths. Table I gives the monochromator slit widths required to give full-scale deflection with the instrument scanning an object circle 5·0 μ in diameter. It is apparent that at almost all wavelengths band half-widths of less than 2·5 mμ can be employed, thereby offering satisfactory spectral resolving power.

In summary it can be stated that the instrument meets the criteria of spectral resolving power and speed of measurement cited previously. That it also meets the requirement of yielding entire ultra-violet absorption spectra without killing cells can be seen from the data which follow.

Absorption Spectra of Surviving Cells.—Ultra-violet absorption spectra of areas in various living cells obtained with the above instrument are shown in Fig. 1, 2, 3, 4 and 5. In all cases the area scanned was a circle 5·0 μ in diameter, and the slit widths used are those given in Table I. The objects were exposed to the radiation for 8-15 sec. at each absorption measurement. For each cell objective evidence of survival was obtained.

Fig. 1 is the absorption spectrum of the cytoplasm of a living *Vorticella*. The readings were made while the organism maintained a steady position at the end of its extended stalk. The oral cilia continued to beat during the entire course of the determination, and the stalk responded to stimulation by coiling. The cell was observed for several hours after the spectrum was determined and showed no signs of diminished activity. In general, the spectrum appears to be that characteristic of nucleoprotein.

TABLE I.—SLIT WIDTHS REQUIRED FOR FULL-SCALE DEFLECTION; AREA SCANNED: 5 μ DIAM. CIRCLE

Wavelength mμ	Slit Width for Full-Scale Deflection mm.	Band Width mμ
700 to 300	Less than 0·10	Less than 0·6
290	0·17	0·6
280	0·20	0·6
270	0·30	0·9
260	1·00	2·5
254	0·84	1·5
250	0·66	1·5
245	1·25	2·5
240	1·50	2·9

Fig. 2 shows the absorption spectra of a region in the cytoplasm of a living *Euglena*, and through a neighbouring optical section which included the nucleus. The cell was somewhat immobilized by allowing the cover glass to compress it. During the measurements, the organism showed the characteristic flowing "euglenoid" motion but made only slight changes in position on the slide. Subsequent to the completion of the spectrum the cell was restored to full mobility by releasing the cover glass compression. The cytoplasm spectrum is similar to that for *Vorticella*, except that a significant absorption occurs at 300-310 mμ. This is probably due to the presence of plastid pigments. The interpretation of the spectrum taken through the section including the nucleus is complicated by factors which will be discussed below.

Fig. 3 represents two absorption spectra taken through an optical section of a living *Tradescantia* stamenal hair cell including the nucleus, and a third through a neighbouring cytoplasmic region. The cell was taken from an unopened flower bud and had not yet developed its characteristic anthocyanin pigment. Cyclosis is very easily observed in this type of cell, and it continued actively during the measurements which provided the spectra shown. The nucleus exhibited its normal slow movement in the protoplasmic stream during that time. The hair was mounted under a quartz cover glass in aerated distilled water which was continuously replenished during the observations. After the first absorption spectra (of the nuclear and cytoplasmic areas) were obtained, the slide was kept in a moist chamber for seven hours, at which time the cell was again brought into focus and the second spectrum through the nucleus obtained. Thus, the nucleus survived two ultra-violet absorption spectra 7 hr. apart. The two spectra are not significantly different, suggesting that the ultra-violet exposure did not alter the optical properties of the material. The spectra seem to show the typical presence of nucleoprotein. However, since in addition to the nucleus, these spectra also represent a section of the cell vacuole, the protoplast and wall, they must be interpreted according to the procedures described below.

Absorption spectra obtained from a more fully differentiated *Tradescantia* stamenal hair cell are shown in Fig. 4. This cell contained anthocyanin, and as can be seen from the spectrum taken through a cytoplasmic area, it also contained material absorbing in the region 300-350 mμ. The latter probably represents flavanoid compounds which are synthesized along with anthocyanin as the cell matures. It will be noted that this absorption does not occur in the less mature cell described in Fig. 3. The absorption spectrum taken through the nucleus shows a characteristic maximum in the region 260-280 mμ. Since the optical section including the nucleus contains a correspondingly reduced depth of vacuole fluid, the absorption apparently due to vacuole pigments is reduced as compared with that given by a neighbouring region not containing the nucleus. This cell exhibited active streaming during and after the measurements.

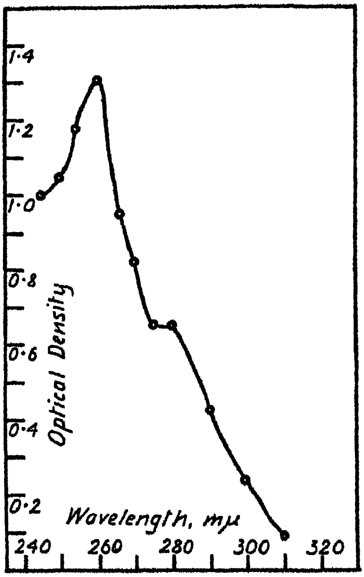

FIG. 1.—The absorption spectrum of an area in the cytoplasm of a living *Vorticella*. Cell dimensions: cylinder, 45 μ long, 22 μ diameter. Thickness of optical section scanned: 22 μ. Area scanned: circle, diameter 5 μ.

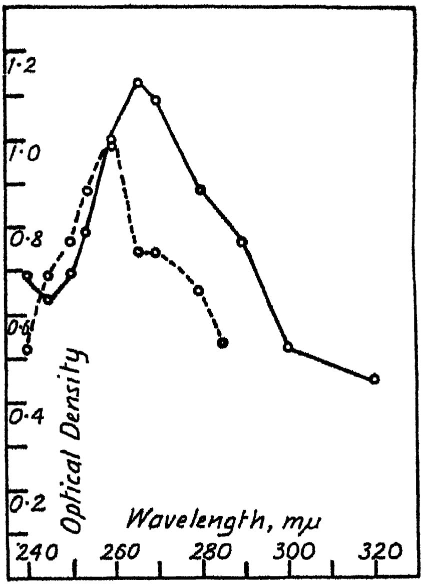

FIG. 2.—Absorption spectra of cytoplasmic area (solid line) and an optical section including the nucleus (broken line) in a living *Euglena*. Cell dimensions: approximately spherical, diameter 36 μ. Nucleus: sphere, diameter 8 μ. Thickness of optical sections scanned: 36 μ. Area scanned: circle, diameter 5 μ.

Fig. 5 shows absorption spectra taken through an optical section of a *Nicotiana tabacum* trichome including the nucleus and a neighbouring cytoplasmic region. That the cell survived the measurements was determined from the fact that cyclosis persisted. The cell was maintained in a film of aerated distilled water. Since the optical path also included part of the vacuole, the cell wall and protoplast, the absorption spectrum is not that of the nucleus itself and must be interpreted accordingly (see below).

The data show clearly that it is possible, by means of our instrument, to obtain detailed ultra-violet absorption spectra of surviving cells of certain types. It is notable that the nucleus may be exposed to sufficient irradiation to provide an absorption spectrum without killing the cell. The speed with which the individual measurements are made enables determination of the absorption of objects (such as a compressed *Euglena* or a *Tradescantia* nucleus) in relatively slow motion. Thus, it is apparent that at least for the cells thus

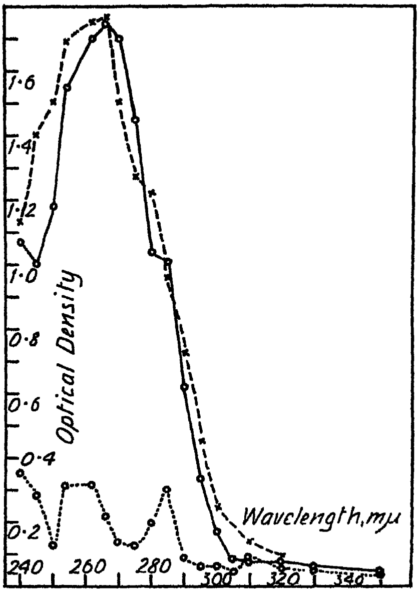

FIG. 3.—Absorption spectra of a living *Tradescantia* stamenal hair cell (non-pigmented). Lowermost curve: cytoplasmic area. Solid line: optical section including the nucleus. Broken line: second spectrum of nuclear area taken 7 hr. after the first. Cell dimensions: roughly spherical, diameter 40 μ. Nucleus: sphere, diameter 16 μ. Thickness of optical section scanned: 40 μ. Area scanned: circle, diameter 5 μ.

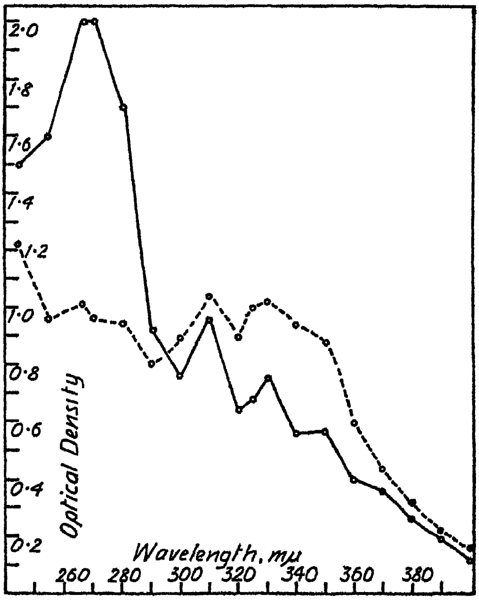

FIG. 4.—Absorption spectra of a living *Tradescantia* stamenal hair cell (pigmented). Solid line: optical section including the nucleus. Broken line: cytoplasmic area. Cell dimensions: cylinder, 350 μ long, diameter 60 μ. Nucleus: sphere, diameter 18 μ. Thickness of optical section scanned: 60 μ. Area scanned: circle, diameter 5 μ.

far studied, the instrument meets the criteria of providing ultra-violet absorption spectra without inducing the immediate death of the cell and of coping with normal rates of movement of the object.

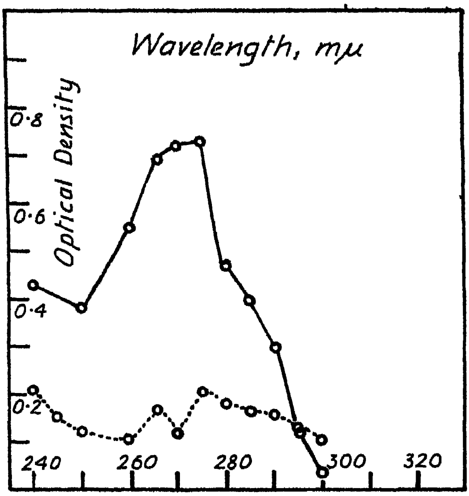

FIG. 5.—Absorption spectra of a living tobacco hair cell. Lower curve: cytoplasmic area. Upper curve: optical section including the nucleus. Cell dimensions: truncated cone, 190 μ long, end diameters 48 and 65 μ. Nucleus: approximately spherical, diameter 13 μ. Thickness of optical section: 58 μ (lower curve) and 52 μ (upper curve). Area scanned: circle, diameter 5 μ.

The Analysis and Interpretion of Absorption Spectra of Intact Cells.—As previously indicated, the application of microspectrometry to intact living cells raises certain new analytical problems. It is the aim of such measurements to ascertain the intracellular content of substances which can be identified with given absorption maxima. To do this, it is necessary (1) to detect these maxima in the cell's absorption spectrum and (2) to determine to what extent the Beer-Lambert laws hold in intracellular conditions.

Because of the structural heterogeneity of intact cells, such determinations are somewhat more complicated than the corresponding calibrations of solutions contained in the chemists' standard absorption vessels. In the latter case, the optical density of the object is a function of the thickness and concentration of a single absorbing element, the solution. While it is perhaps possible to isolate by appropriate sectioning a fragment of a *fixed* cell in which a given optical section contains but one light-absorbing element (e.g. the nucleus), this cannot be done with intact living cells. Consequently, the optical density of any given light path through an intact cell represents the additive absorption of several structures each characterized by a distinctive absorption spectrum.

Hence, without additional information it is not possible quantitatively to interpret the absorption spectrum of a given area of a cell, and indeed, as will be shown below, even the position of the maxima may be misleading. By the introduction of appropriate additional measurements, however, one can determine the specific absorption spectra of certain structures of intact living cells, ascertain to what degree they follow the so-called laws of absorption, and thereby arrive at estimations of the concentration of substances responsible for given absorption maxima.

The necessary procedures for this type of analysis may be derived from the following:

Consider a cell of the type shown in Fig. 6 (such as a mature plant cell). Let points 1 and 2 represent optical paths through two regions in the cytoplasm and point 3 an optical section including the nucleus. At points 1 and 2 the optical density D will represent the sum of the absorption due to the vacuole D^v and that due to the wall and protoplast layer D^p. Thus

$$D_1 = D_1^v + D_1^p, \text{ and } D_2 = D_2^v + D_2^p.$$

If the absorption due to the vacuole follows the Beer-Lambert laws, D^v is proportional to vacuole thickness d, and

$$D_1^v/D_2^v = d_1/d_2.$$

If we assume that the composition and thickness of the protoplast layer and wall are constant and that the concentration of vacuole solute is constant, these relationships give the equation:

$$D_1^v = \frac{D_1 - D_2}{1 - d_2/d_1}.$$

Since D_1 and D_2 are measured and d_1 and d_2 can also be obtained, the partial absorption due to the vacuole can be calculated. The partial absorption due to the non-variant structures can be obtained by difference from the observed value D_1.

In a similar way it is possible to determine D^v and D^p from measurements of the optical density of a cell brought to two different vacuole volumes (by plasmolysis), thereby achieving a corresponding known difference in concentration of vacuole solutes. If V_1 and V_2 are these two volumes, then, for equal values of d,

$$D_1^v = \frac{D_1 - D_2}{1 - V_1/V_2}.$$

Since V_1 and V_2 can be obtained from micrometer measurements, D_1^v (and by difference, D^p) can be calculated.

These equations show that it should be possible to derive the separate absorption spectra of the protoplast layer and of the vacuole from two absorption spectra taken at different diameters of the cell, or at different vacuole volumes. If in addition to two such measurements, a third set is obtained through an area of the cell (such as point 3, Fig. 6) including the nucleus, the absorption spectrum of the latter may be obtained. This is accomplished by subtracting from the density at this point the calculated value of D^v and the optical density of the depth of the vacuole not occupied by the nucleus. The latter value can be obtained from micrometer measurements of the nucleus and vacuole diameters, and from the value of D^v per unit vacuole thickness determined as outlined above.

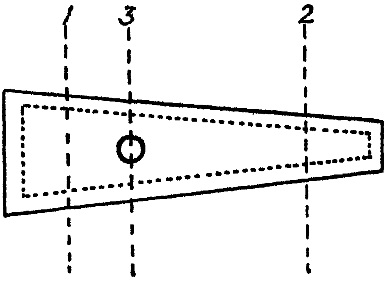

FIG. 6.—Diagram of mature plant cell showing three optical sections. The cell wall is represented by the outer solid line. The protoplast layer is represented by the space between the wall and the dotted line; the vacuole is the area enclosed by this line. The circle represents the nucleus.

The cells found in the epidermal hairs of certain plants offer convenient test objects for these relationships. In plants such as *Coleus* and tobacco, these cells are usually regular truncated cones of circular cross-section. Thus, optical sections of significantly different and measureable thicknesses can be found readily within the same cell. (These may also be obtained by reading different transects through the circular cross-section, but difficulties due to refraction arise.)

Fig. 7 shows an analysis of the absorption spectrum of a single *Coleus* hair cell. Readings were taken in the range 250-625 mμ through two diameters of the cell (32 and 44 mμ respectively) from which the separate absorption spectra of protoplast layer and vacuole were calculated. Protoplasmic streaming continued during the entire course of the measurements.

The absorption spectrum of the vacuole (broken line, Fig. 7) corresponds quite well with the known composition of the vacuole fluid. It has been possible by chromatographic separation to isolate four anthocyanins and two flavanols from *Coleus* leaves. The former have an absorption maximum in the visible (510-540 mμ) and a band at 260-270 mμ. The flavanols also have two maxima (separated by a shallow minimum) at 290-300 mμ and at 320-330 mμ. It has been shown previously[1] that the absorption maximum of *Coleus* hair cells at 540-560 mμ is due to anthocyanins; the peaks are somewhat shifted toward the longer wavelengths (as compared with extract solutions) by some type of intracellular complex formation. It can be seen from Fig. 7 that this maximum in the total absorption spectrum of the cell (uppermost curve) is due entirely to absorption occurring in the vacuole. On the other hand, the calculated absorption of the protoplast layer is zero (within the experimental error) at all wavelengths above 400 mμ, and this corresponds with the observation that these structures are colourless. It will also be noted that the calculated absorption spectrum of the vacuole shows the maxima expected from flavanols (300-330 mμ) and the u.-v. peak of the anthocyanins at 266-270 mμ.

The calculated absorption spectrum of the protoplast layer (solid line, Fig. 7) shows a sharp maximum at 280 mμ and a lower peak at 340 mμ. (The third maximum at 254 mμ is based on but two points and needs to be confirmed.) That these maxima are due entirely to the protoplast and not to the cell wall can be seen from the absorption spectrum of an empty cell wall (Fig. 8) which shows essentially zero values at all wavelengths. The band at 280 mμ may represent absorption due to aromatic amino acid residues in the protoplast protein, but it is possible that other substances also contribute, and further study is required. The maximum at 340 mμ cannot at present be assigned to any substance, but it is of some speculative interest that it coincides with the absorption band of reduced nicotinamide co-enzymes.

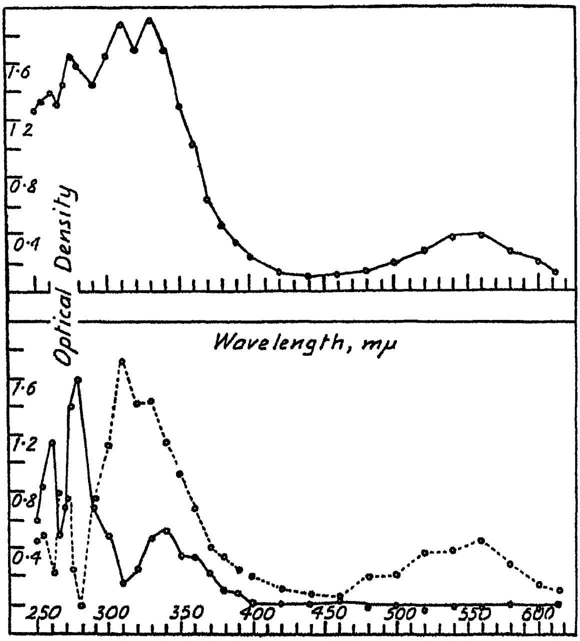

FIG. 7.—Differential analysis of the absorption spectrum of a living hair cell from a petiole of an anthocyanin-producing *Coleus*. Data based on differences between two absorption spectra taken through cytoplasmic areas 32 and 44 μ thick respectively. Upper curve: original absorption spectrum of 44 μ section. Lower dotted line: calculated absorption spectrum for the vacuole alone (44 μ thick). Lower solid line: calculated absorption spectrum for the protoplast layer alone. Cell dimensions: truncated cone 140 μ long, end diameters 48 and 30 μ. Area scanned: circle, diameter 5 μ.

The results described in Fig. 7 are confirmed by a corresponding analysis of the absorption spectrum of a *Coleus* hair cell based on comparison of the absorption spectrum of the living normal cell with that given by the same cell after reduction of vacuole volume (by plasmolysis). This cell was taken from an anthocyanin-free strain of *Coleus* which produced a small amount of the flavanols found in the red variety. The calculated absorption spectra of protoplast and vacuole (see Fig. 8, lower curves) show the expected maxima. While the vacuole contents are rather dilute, the flavanol absorption at 300-330 mμ is detectable. As anticipated from the absence of anthocyanin, the band at 266-270 mμ is absent. The calculated absorption spectrum of the protoplast is quite similar to that obtained from the red *Coleus* hair cell; the extinctions at 280 mμ correspond closely. The absorption of the empty wall of this cell (obtained by reading through the part of the plasmolyzed cell devoid of vacuole) is essentially zero at all wavelengths.

The data of Fig. 7 and 8 provide evidence that the analytical methods described above do actually yield separate absorption spectra of the protoplast and of the vacuole of intact living cells. Comparison of the calculated spectra with the original spectrum of the cell shows that the absorption maxima of the separate structures may be obscured in the total spectrum. Thus, the absorption maximum of the protoplast at 340 mμ does not appear in the original absorption spectrum shown in Fig. 7 because of the masking effect of the large flavanol concentration of the vacuole. It is notable that the analysis based on diameter differences and that based on volume differences agree with each other and correspond with what is known about the composition of the vacuole fluid and of the protoplast.

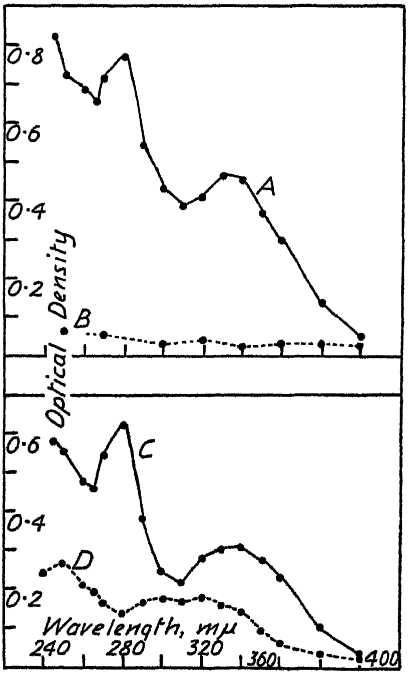

Fig. 8.—Differential analysis of the absorption spectrum of a living hair cell from a petiole of a colourless variety of *Coleus*. Data based on differences between absorption spectrum of a cytoplasmic area of the original cell (volume, 375,000 μ^3) and the spectrum of the cell contents plasmolyzed to a sphere with a volume of 65,200 μ^3. Curve A: original absorption spectrum of the cell. Curve B: absorption spectrum of the empty cell wall after plasmolysis. Curve C: calculated absorption spectrum of the protoplast layer alone. Curve D: calculated absorption spectrum of the vacuole alone. Original cell dimensions: truncated cone, 70 μ long, end diameters 22 and 28 μ. Plasmolyzed cell contents: sphere, diameter 24 μ. Thickness of optical sections scanned: 24 μ for both determinations. Area scanned: circle, diameter 5 μ.

Since a given maximum shown by an absorption spectrum of an optical section through an intact cell may represent contributions from more than one cytological structure, such a band cannot be ascribed to a single substance. Where such complex absorption occurs, it is not possible to describe the relative concentration of a given substance by the value of the extinction of the entire cell. For example, in the *Coleus* cells described above, that part of the optical density (at a given wavelength) due to the vacuole will vary proportionally with the cell diameter and with the reciprocal of the vacuole volume. On the other hand, that fraction of any given optical density due to an invariant structure such as the protoplast layer will remain constant for all cell diameters, and for all concentrations of vacuole solute. Consequently, the results obtained from tests of the Beer-Lambert laws will depend largely on the relative contributions made by each constituent to the density at the wavelength studied. This effect is shown in the data of Fig. 9 and 10, which represent the optical densities of a *Coleus* cell obtained at various cell diameters, and the extinctions for various vacuole volumes (achieved by gradual plasmolysis of the cell).

At 540 mμ the extinction due to the anthocyanins dissolved in the vacuole follows the Beer-Lambert laws closely, and the plots extrapolate to zero absorption at zero thickness and infinite dilution. Extinctions obtained at 280 mμ,

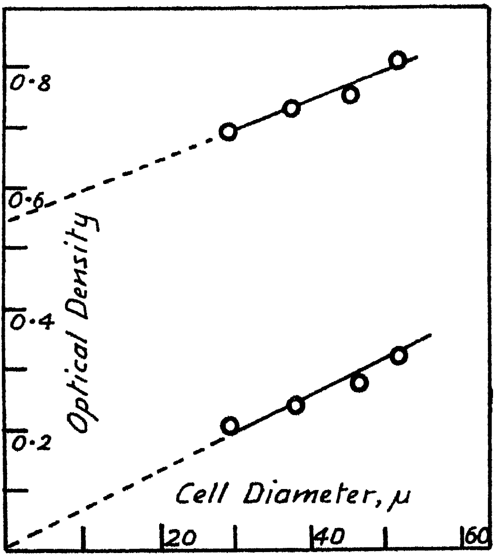

FIG. 9.—Optical density through various diameters of a conical pigmented *Coleus* cell. Upper line: 280 mμ. Lower line: 540 mμ. Area scanned: circle, diameter 5 μ.

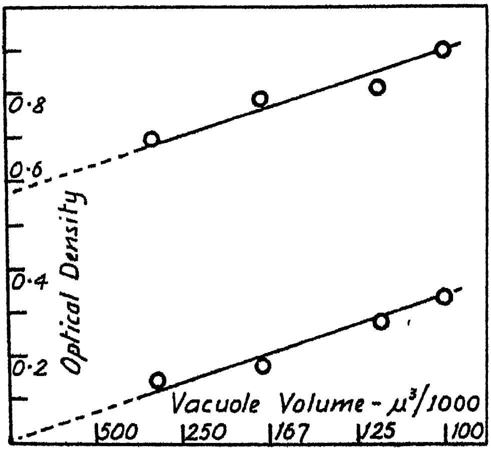

FIG. 10.—Optical density of a 35 μ section of a pigmented *Coleus* cell in various degrees of plasmolysis. The abscissa represents the reciprocals of the volume of the cell contents. Upper line: 280 mμ. Lower line: 540 mμ. Area scanned: circle, diameter 5 μ.

due largely to protoplast absorption, fall on plots which extrapolate to significant intercepts, and the slopes correspond to the variations due to that part of the extinction arising from vacuole material. Thus, for substances such as anthocyanins and flavanols, which are present in the cell in the dissolved state, the absorption laws hold, and estimation of concentration from extinction values is possible.

In order to arrive at a means of interpreting quantitatively the extinctions due to those parts of the cell which are not in the liquid state (such as the nucleus and protoplast) the relation between extinction and the number of molecules scanned must be similarly determined. As has been previously pointed out [2, 3] the structural arrangement of the absorbing material in non-liquid parts of the cell may cause serious alterations in the proportionalities which are anticipated from the Beer-Lambert laws.

The methods described above can be used to obtain the separate absorption spectrum of the nucleus of an intact living cell. This is shown in Fig. 11. The cell is from a tobacco trichome, and the method used was that of diameter differences. The cell survived the entire procedure; streaming and nuclear movement were noticeable at all times.

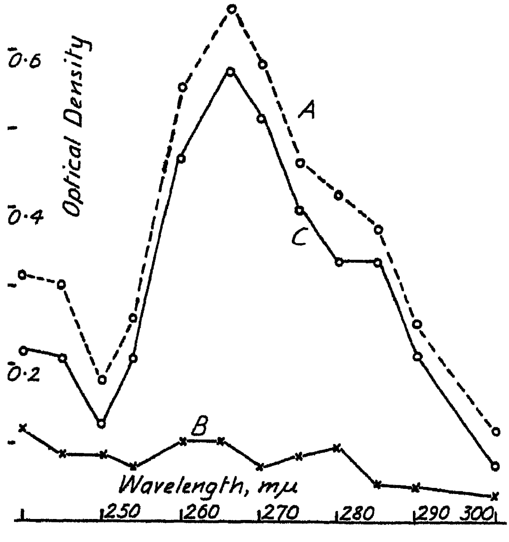

FIG. 11.—Absorption spectrum of a living tobacco hair cell nucleus. Curve A: absorption spectrum of optical section including the nucleus, 20 μ thick. Curve B: absorption spectrum of cytoplasmic area 22 μ thick. Curve C: absorption spectrum of the nucleus alone calculated from curves A and B and from a third spectrum taken through a smaller diameter (14 μ) of the cell. Cell dimensions: truncated cone, 62 μ long, end diameters 18 and 25 μ. Nucleus: sphere, diameter 15 μ. Area scanned: circle, diameter 5 μ.

The lowermost curve (B) is the absorption spectrum of an optical section through a part of the cell not including the nucleus, while the uppermost curve (A) is the absorption spectrum taken through a section centred on the nucleus. The centre curve (C) is the calculated absorption spectrum of the nucleus itself. The original spectrum taken through the section which included the nucleus is largely due to the absorption of the nucleus proper, the cytoplasmic absorption being relatively small. However, the calculated spectrum does reveal a definite plateau in the region 280-285 mμ (presumably representing aromatic amino acid residues of the protein) which is obscured in the original curve. In other respects the absorption spectrum of the living tobacco nucleus corresponds with previous curves obtained from fixed or otherwise killed nuclei of various types.[4]

---

[2] Commoner, *Science*, 1949, **110**, 31.

[3] Danielli, *Cold Spring Harbor Symp.*, 1949, **14**, 32.

[4] Caspersson, *Chromosoma*, 1940, **1**, 605.

Discussion

Recent studies have shown that the ultra-violet extinctions of living cells become significantly altered upon death.[5, 6] Analysis of this phenomena has been limited by the fact that it has hitherto been impossible to obtain complete ultra-violet absorption without exposing the cell to a lethal amount of irradiation. The results presented above show that the absorption spectra of certain surviving cells can be measured, and suggest new opportunities for the study of changes in extinction which occur on death.

It should be pointed out that certain of the plant cells studied thus far may be unusually protected against ultra-violet injury by the presence of absorbing materials in the vacuole fluid. On the other hand, tobacco hair cells, which frequently have high cytoplasmic transmissions, appear to be as resistant to irradiation as the pigmented cells of *Coleus* and *Tradescantia*.

It is also apparent that these cells have geometrical features which are unusually favourable for the determination of the absorption spectra of separate cell structures. It would be far more difficult to obtain the thickness measurements required for calculating the separate absorption spectrum of the nucleus of a living fibroblast (for example) than is the case in a tobacco hair cell.

Such measurements are, however, essential for ascertaining the actual absorption spectra of the separate parts of living cells. Further investigations of this type may need to depend on the selection of cells with dimensions suitable to the problem.

The optical properties of mature plants cells probably represent a special relatively simple case of the effects of structural heterogeneity on absorption. Analyses of the absorption spectra of animal cells (or of undifferentiated plant cells) corresponding to those described above might be considerably complicated by random changes in the intracellular distribution of ultra-violet-absorbing particles such as mitochondria and granules.

The present results suggest that an absorption spectrum based on measurements from a single optical section of a cell must be interpreted with caution. However, if the difficulties are recognized and material of appropriate characteristics selected for investigation, it does seem possible to carry out ultra-violet absorption analyses of the separate parts of intact surviving cells.

The Henry Shaw School of Botany,
Washington University,
St. Louis, Missouri.

---

[5] Larianov and Brumberg, *Compt. rend., U.S.S.R.*, 1946, N.S., **54**, 267.

[6] Mellors, Berger and Streim, *Science*, 1950, **111**, 627

ULTRA-VIOLET MICROSPECTROGRAPHY OF LIVING TISSUE CULTURE CELLS

PART II. MICROSPECTROGRAPHIC STUDIES OF LIVING CELLS AND ULTRAVIOLET-IRRADIATED CHICK FIBROBLASTS

By P. M. B. Walker and H. G. Davies

Received 26th July, 1950

A photographic method of microspectrography applicable to living cells is described. Absorption spectra and the total amounts of absorbing substance in living chick fibroblast nuclei are measured. It is concluded that the nucleic acid of the living cell nucleus is in a condition in which it can absorb, and that the absorption spectra are similar in form to those obtained by other workers on fixed material. The increase in absorption of chick fibroblast nuclei after irradiation with ultra-violet light at 265 mμ is a true increase in absorption and is accounted for by the decrease in projected nuclear area. The total amount of absorbing substance in the nucleus is actually found to decrease during irradiation. After certain assumptions have been made preliminary measurements of the total amount of desoxyribo-nucleic acid of individual fibroblast nuclei are obtained by the integration methods outlined. They are in approximate agreement with the results of other workers obtained by biochemical extraction.

The application of the techniques of microspectrography to living cells makes it possible to obtain data which will indicate the nature of some cellular components in their natural state. Furthermore, microspectrography may be linked with methods of obtaining a measure of the total amount of the absorbing substances in these components.

Photographic methods of obtaining this information offer certain advantages :[1]

(i) It is possible to record all the information regarding both the optical density and morphology of the specimen in one exposure at each wavelength.

(ii) The photograph shows whether the specimen has been properly focused.

(iii) Provided the exposure time is short, there is no difficulty in recording moving objects.

However, it is generally agreed that the photographic method of measuring extinctions is less accurate than the photoelectric. But errors in the former method are themselves small compared with errors due to the geometry and the state of the object examined.

There is, however, a problem basic to the use of biological material, which the photographic method may more easily overcome. It is difficult to measure the thickness of these specimens with the microscope, especially when they are in the living state. The information obtained by microspectrography cannot therefore be expressed as concentrations per unit volume. The photographic negative, recording both optical density and morphology, enables the total quantities of absorbing substances in certain cellular components to be measured by integration over the irregularly absorbing areas. This might be difficult with a purely photoelectric technique.

---

[1] Thorell, *Studies on the formation of cellular substances during blood cell production* (Henry Kimpton, London, 1947), p. 29.

This communication describes the first stages in the development of a photographic method of microspectrography, which has been applied to the study of normal and ultra violet irradiated fibroblast cells.

Experimental

Microspectrographic Apparatus. This apparatus was designed primarily for work on living cells grown in tissue culture. Its particular features are:

(*a*) The microscope is enclosed in a thermostatically controlled hot-box.

(*b*) Observation and focusing of cells is by visible phase contrast illumination.

(*c*) Immediately after focusing, photographs at selected wavelengths in the ultra-violet can be taken.

(*d*) Provision is made for film calibration at each wavelength.

The objective used is a new lithium fluoride fused quartz achromat (numerical aperture (N.A.) 1·24) designed by R. J. Bracey of the British Scientific Instruments Research Association, and constructed by R. and J. Beck. The focus varies by about 1 μ from 248 mμ to 313 mμ, and by about 3 μ from 313 mμ to 546 mμ. The objective was designed for use with an immersion fluid 60 % glycerine, 40 % water. The difficulties of using such a medium due to changes in refractive index are well known, and these difficulties are enhanced at the temperature used (37° C). Nonane was found to have the correct optical properties [2] in the wavelength range used, and was therefore employed as the immersion fluid. Nonane is a pure hydrocarbon so that the refractive index does not change during its slow evaporation. The condenser is a reflecting system [3] having N.A. 0·6 and 40 % central obstruction. Fig. 1 shows the

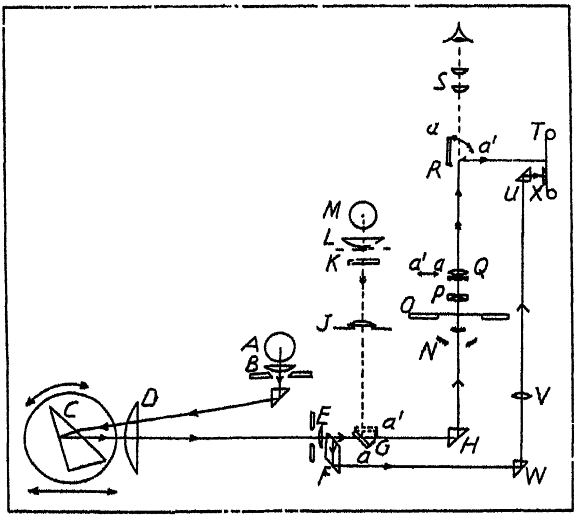

FIG. 1. Optical paths.

A, Ultraviolet light source. B, Monochromator input slip and Kohler lens. C, D, Monochromator prism and lens. E, Monochromator output slit and Köhler lens (u.-v. field stop). F, Prism. G, Movable mirror. H, Prism. J, Lens and visible field stop. K, Wratten filters 77A, 58. L, Phase-annulus and lens. M, Visible light source. N, Condenser. O, Specimen plane. P, Objective. Q, Auxiliary lens and phase annulus. R, Movable mirror. S, Viewing eyepiece. T, Cine camera. U, W, Prisms. V, Lens. X, Rhodium step wedge.

---

[2] Norris (unpublished).

[3] Seeds and Wilkins, *Nature*, 1949, **164**, 228.

optical paths in the apparatus. Focusing is performed in visible phase contrast using an auxiliary lens[4] and phase plate Q which can be removed from the light path above the objective. The numerical aperture of the viewing system is 0·85. The main purpose of the auxiliary lens is to correct for spherical aberration on the optic axis of the u.-v. achromatic objective, when used in green light. The phase annulus after imaging by lens J, condenser N and objective P is conjugate with the phase ring at Q. The visible light source M is a 250-W B.T.H. compact source mercury arc, from which the green line is isolated by Wratten filters 77 A and 58 (K). The ultra-violet light source A is a 125-W Thermal Syndicate mercury arc. Köhler illumination is used in the ultra-violet. It should be noted that with Köhler illumination even fields are obtained only after great care has been taken in optical alignment of the system and the first field lens (B) has been evenly illuminated. This latter requisite demands that there should be no obstruction to the equal emission of each point of the source in every direction. The prism F permits half the monochromator output slit to be imaged on to a rhodium step wedge X (A. Hilger). After accurate focusing in phase-contrast illumination the mirrors G, R are moved with the compensating lens Q to positions (*a′*), and an ultra-violet photograph is taken with its accompanying wedge shadow for calibration. The accurate centring and movement of the compensating lens and mirrors without vibration is achieved by a suitable mechanical system. A Littrow spectrograph has been converted so that it automatically aligns and focuses the spectral line on the output slit E. Stray light caused by reflection from the Littrow lens D is reduced at the output slit by slightly tilting this lens, a procedure legitimate with the wide slits used.

The following considerations decided the use of a rhodium step wedge as a method of film calibration :

(*a*) It is easily placed near the picture area inside the camera ; this avoids difficulties in imaging it on to the film ;

(*b*) it can be calibrated at each wavelength using the Beckman spectrophotometer ;

(*c*) it obviates the possibility of error due to the intermittency effect or reciprocity failure ;

(*d*) positioning near the picture area reduces errors due to uneven sensitivity and development along the length of the film.

The camera T, is a 35 mm. cine-camera specially designed for time-lapse photography.

Calibration.—A test object used for calibration was Cellophane sheets mounted in glycerine and water between quartz coverslips, together with the corresponding blank. Each slide was separately photographed at a series of wavelengths, the external light beam used for wedge calibration compensating for slight changes in lamp intensity. The two slides were also calibrated in the Beckman spectrophotometer. Fig. 2 shows comparative absorption curves for one series of measurements. No tests have yet been made on artificial

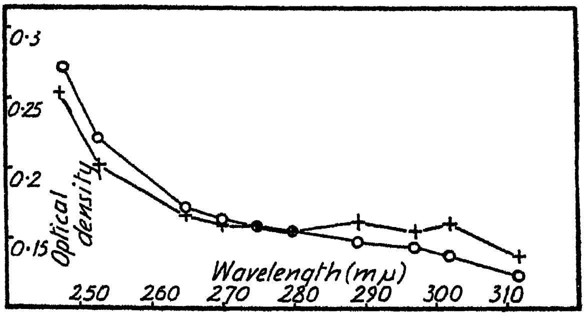

Fig. 2.—Calibration curves of Cellophane. ○ Beckman spectrophotometer. + Microspectrographic.

---

[4] Davies and Wilkins, *J. Roy. Micro. Soc.*, 1950 (in press).

bodies of known composition and absorption whose size is near that resolved by the microscope. However, absorption tests on a film of isotropic yeast nucleic acid comparable in area to the fibroblast nucleus gave a curve (Fig. 3) similar in shape to that measured on solutions with the Beckman spectrophotometer.

Techniques.– Two techniques have been used with this apparatus. Firstly, serial photographs have been taken at one wavelength; this has been used to investigate the changes that occur in living tissue culture cells during irradiation. Secondly, photographs have been taken at different wavelengths, from which spectrographic data have been calculated.

In serial photographs at one wavelength, electrical timing circuits have been made which control the following sequence of operations: (1) changing over from the visible focusing light train to the ultra-violet photographing light train, (2) opening the shutters before the specimen and in the camera, (3) closing the shutters and winding on the film after the appropriate exposure, (4) returning the optical system to the viewing position. This sequence can be initiated at variable intervals. It is thus possible to take sequences of photographs in the ultra-violet, focusing the microscope, if necessary, between each frame. This produces focused series of photographs. With films and the series on which measurements have been made, the time between the start of successive exposures has been 12 sec., and an exposure sufficient to give a density of 0·6 on the film (Kodak Microfile Pan. 35 mm.) has been used.

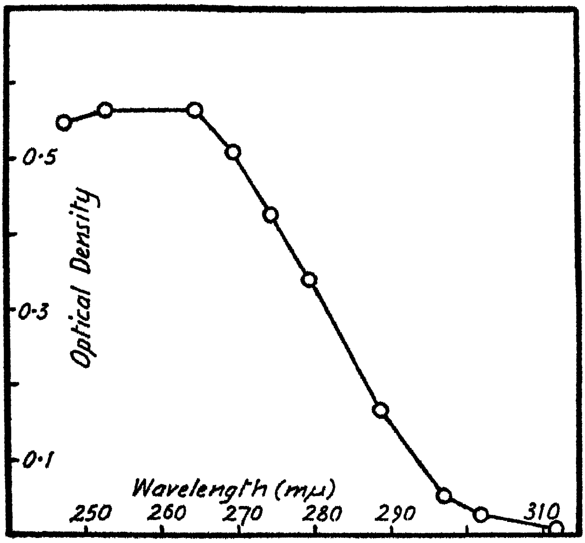

FIG. 3.—Calibration curve on ribonucleic acid film.

For microspectrography the following method is used. A cell is selected, which has a suitable clear region of medium around it. This cell is focused in green phase contrast illumination; the moving optical parts are then changed over to the ultra-violet illuminating train, which has been previously set to illuminate the field slit of the microscope at the wavelength of 312 mμ. A second timing mechanism now exposes the specimen and negative for a period appropriate to the intensity of the spectral line used and to the film sensitivity. On completion the film winds on and the prism table rotates and moves forward until the next selected spectral line is aligned with, and focused on, the field slit; a second exposure is now given corresponding to the new line. This cycle is repeated ten times until the 248 mμ line is reached. As explained above, the objective is not entirely achromatic; it is therefore necessary, by moving the microscope stage[5] to adjust the focus to predetermined positions over a range of about 1 μ during this procedure. On completion, the apparatus is returned to the visible focusing position and the focus checked. Exposing the ten negatives and moving the prism takes about 90 sec.

---

[5] Martin and Johnson, *J. Sci. Instr.*, 1930, 7, 1.

Table I shows the doses incident upon the cell for each wavelength to give a film density of 0·6 ; the output of the monochromator is monitored by a photocell. These values are higher than those given in Fig. 6 of Part I due to (i) the Bracey achromat having a low ultra-violet transmission, (ii) an aluminized mirror being used above the microscope, and (iii) the objective having been used at a magnification of × 114.

The heating effects in the cell for one photograph at 265 mμ may be calculated, if it is assumed that the average cell thickness is 2 μ and the optical density 0·15. The average temperature rise if no heat is lost during the exposure time is 0·75° C. The temperature rise varies inversely as thickness, so that it will be still greater for the small absorbing bodies. No attempt is made here to distinguish between photochemical changes and those due to heating effects.

TABLE I

No.	Wavelength (mμ)	Dose 10^4 ergs/cm.^{2}
1	312	0·85
2	302	1·0
3	297	1·2
4	289	1·25
5	280	1·5
6	275	1·6
7	270	1·8
8	265	2·1
9	253	3·4
10	248	5·4

Microphotometry—The measurement of total quantities of absorbing substances, by integration measurements over areas, requires a microphotometer which will rapidly and directly record photographic densities. An instrument incorporating the following features has been designed by one of us (P. M. B. W.).

(i) The recordings are made by pen on graph paper. The trace plots photographic density against linear displacement of the film.

(ii) The paper table and film carriage are so coupled as to make possible the accurate location of the morphological features on the trace. This is achieved by viewing the screen on which the image is projected.

The following method of recording densities is used. There are two light beams from a common source, one of which passes through the film to be measured and the other through a logarithmic density wedge. The two beams fall alternately on a photomultiplier. Any out-of-balance signal is then fed after amplification into a servo-motor driving the wedge in such a direction as to balance the intensities of the two beams. The pen is coupled to this density wedge.

The optical system allows a projected image (× 17) to fall on a screen in which a small circle limits the size of the spot recorded. A 1 mm. diameter circle has in general been used. This corresponds to a spot 0·06 mm. diameter on the film and 0·53 μ diameter on the biological specimen. The theoretical limit of resolution of the microscope optical system used at 265 m is about 0·16 μ. A smaller circle corresponding to this latter limit has also been used, but in this case irregularities in the grain clumping become noticeable in the trace, and it is difficult to determine their levels.

Evaluation of the traces are made in the following manner. Firstly, the morphological features (cell boundaries, nuclear membranes) are marked on the trace at the time of recording. Then the area under the microphotometer trace such as that shown in Fig. 4 for the nucleus, is obtained by a series of area measurements for each millimetre along the length of the trace. These readings can then be averaged to give the mean density for the area 0·53 μ wide, traced by the microphotometer spot across the structure. In integrating to give the total absorption of an area, parallel traces either spaced at 1 or 2 μ on the specimen have been used. From these values an average photographic density for the whole nucleus may be obtained if it is assumed that there is no great change in density between the areas measured and the adjacent unmeasured areas. Multiplication of this average density by the projected area of the structure will give a measure of the amount of absorbing substance present.

Where only comparisons of optical density in the cell are required, it is legitimate to compare the photographic densities provided that their range lies on the straight portion of the characteristic curve of the film. When optical densities are required as in the calculation of absorption curves, they are made conventionally as described below. The wedge shadows exposed by the side of each photograph give traces from which the characteristic curve relating density of the film and the logarithm of the transmission of the rhodium wedge can be plotted for each wavelength. The photographic density values from the negative for the area of interest and the clear background can now be converted to optical density using these characteristic curves. Curves relating optical density of the biological object to wavelength can then be drawn.

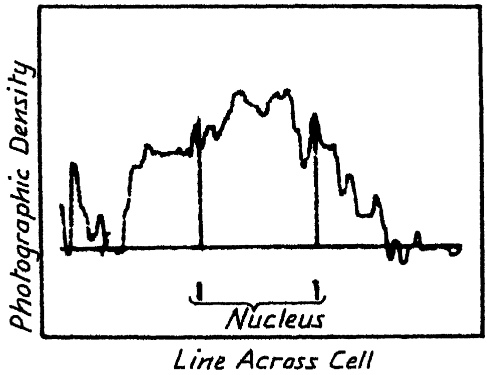

FIG. 4.—Microphotometer record across film negative of chick fibroblast at 265 mμ, showing position of nucleus.

Errors in the reproducibility of the microphotometer traces are less than those due to grain clumping and unevenness of field. It is estimated that the error from these causes for a single reading of density is about ± 0·01. The errors in the measurement of the total amount of absorbing material, due to that fraction which occurs in resolved particles smaller in size than the microphotometer spot, have been investigated. The errors will depend on the density difference between these particles and their background. Calculation shows that, provided the actual density differences are small, as in our material (chick fibroblasts), and that the product of the area traced by the microphotometer spot and apparent density is used as a measure of the amount of substance present in these particles, the errors will be small. These errors for density differences of 0·1 and 0·2 are 10 % and 20 % respectively with the microphotometer spot used. In the measurement of the total absorption for the whole structure, these errors may be neglected as the bulk of the absorption lies outside the particles.

Tissue Culture Technique.—The hanging drop method of tissue culture has been used in preparing cultures for ultra-violet micrography either by Miss S. Jackson or by one of us (P. M. B. W.). Explants from the ventricle of 9-12 day chick embryos were placed on the 0·1 mm. thick quartz coverslip together with a suitable nutrient medium, and were examined without further subculturing. The coverslip was supported by a 1 mm. thick stainless steel ring and the chamber was sealed off with a 0·5 mm. quartz window. Liquid medium, obtained as the exudate from embryo extract and fowl plasma, was used with or without a surrounding " horseshoe " of clotted plasma and extract. Liquid medium was found to give flat cells which only grew on the interface between medium and coverslip. Cultures showing normal growth and division after 36 hr. were used.

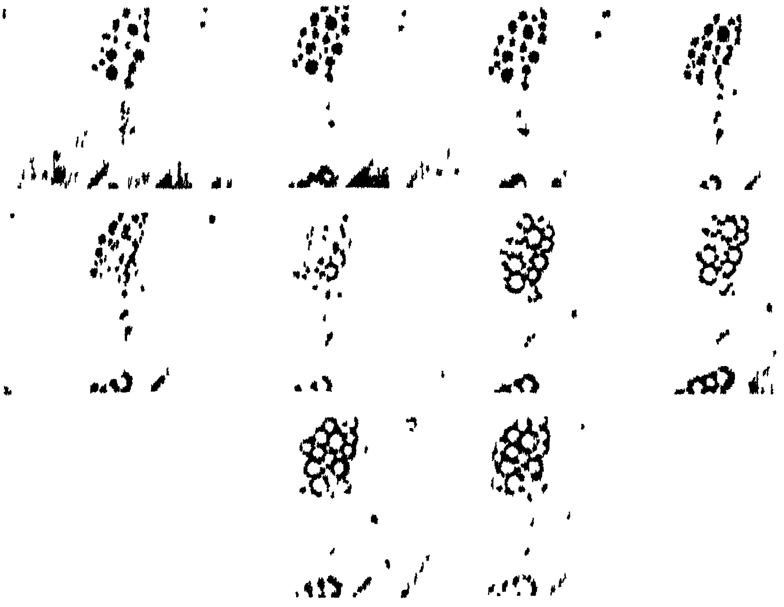

PLATE I.—Focusing range at approximately 0·1 μ intervals at 312 mμ. Objective N.A. 1·24. Condenser N.A. 0·6. × 114 on to Kodak Microfile Pan. Enlarged to × 975. Shows change in appearance of nucleolus and fat droplets during focusing.

[*To face page* 466

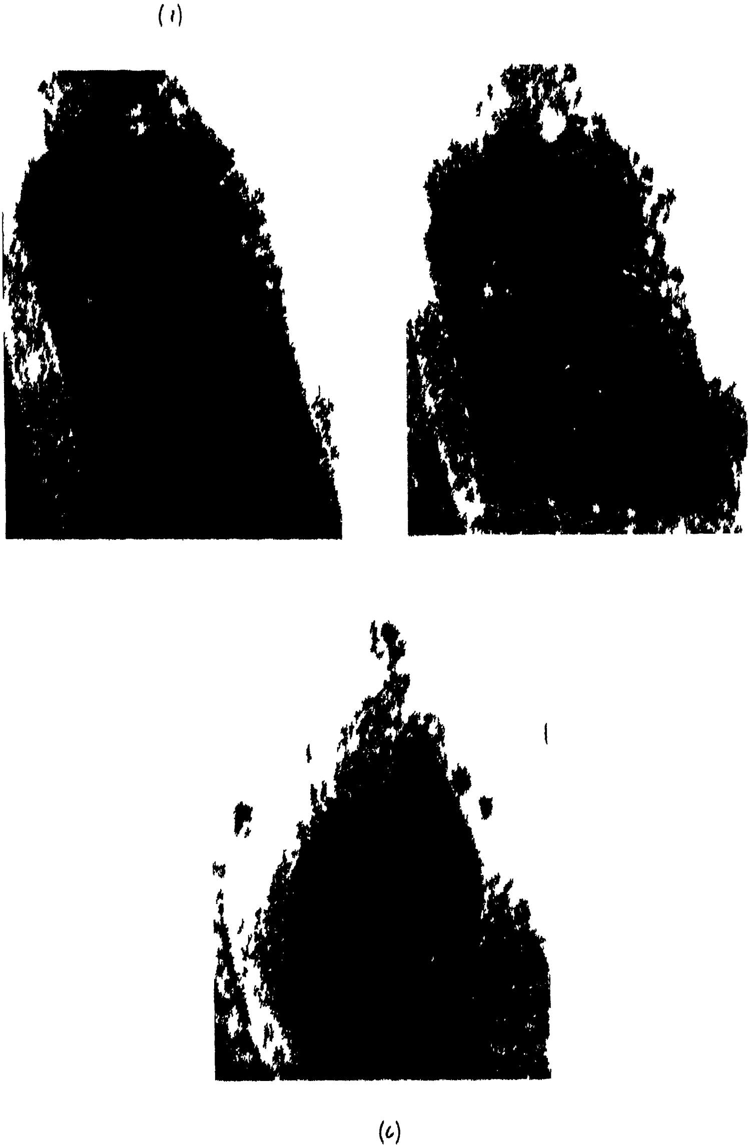

Plate II.—Chick fibroblast cells photographed at 265 mμ during radiation experiment (Fig. 6). Objective 1·24 N.A., condenser 0·6 N.A. × 114 on to Kodak Microfile Panchromatic. Enlarged to × 1950. (*a*) Exposure No. 1. (*b*) Exposure No. 28. (*c*) Exposure No. 200.

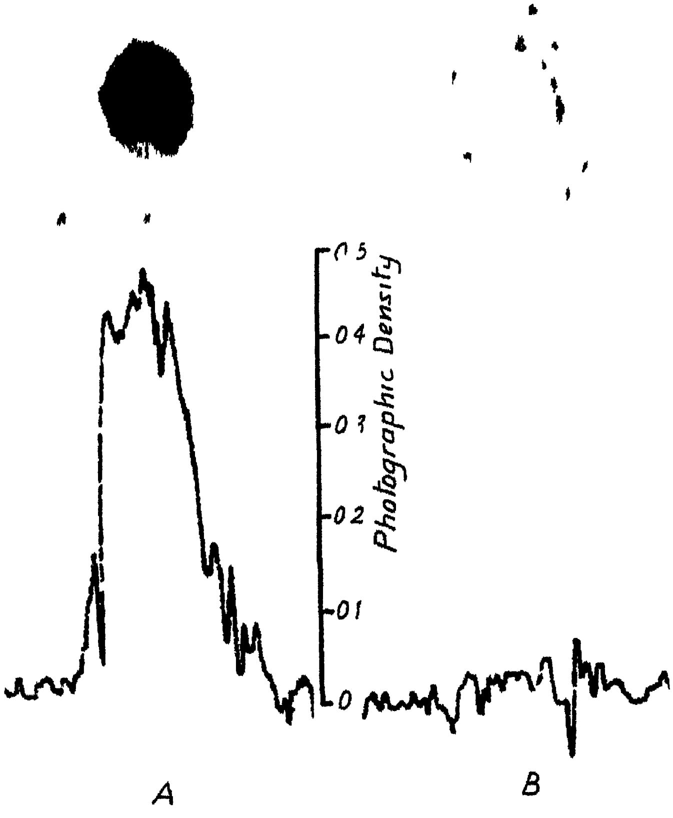

PLATE III — Chick fibroblast nuclei at end of radiation experiment (Fig. 6). Photographed at (*a*) 265 mμ, (*b*) 312 mμ (details Plate I). Accompanying microphotometer records across nucleus show negligible apparent absorption at 312 mμ.

Results

Normal Cells.- Fig. 5 is an example of the absorption spectra obtained for the nucleus (*a*) and nucleolus (*b*) of a living cell. The microphotometer trace was taken across the cell as shown in the figure and the average values of density for the structures have been used. Errors may occur in measuring the optical density of the smaller bodies in the cell. This is shown in Fig. 5 where negative density values for the nucleolus at 297 mμ and 302 mμ are obtained. These errors [6] are due to difficulties in obtaining proper focus for these small bodies and the effect is illustrated in the focusing range at 312 mμ through a normal cell (Plate I).

In the larger areas, such as the nucleus, these errors do not occur although, as in this cell, light diffracted outside the true area of the nucleolus may produce an artificially high value for the average density of the nucleus. Subject to these errors, the living material we have investigated shows negligible non-specific light loss as measured by the optical density at the longer wavelengths.

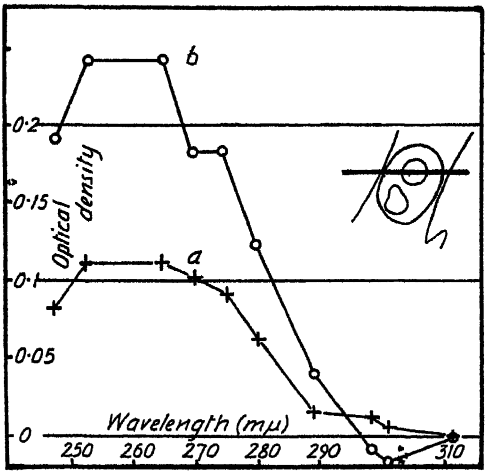

FIG. 5.—Absorption curves of nucleolus (○) and nucleus (+) of living intermitotic chick fibroblast.

Ultra-Violet Radiation Effects on Living Cells.- The general morphological changes when cells are irradiated have been often described.[7, 8, 9] Our results, obtained by the described irradiation procedure, and illustrated in Plate II, are in general agreement with those of other workers. The very first photograph at 265 mμ showed that the background of the nucleus is not homogeneous. There is no apparent change in the appearance of the nucleus in the first 20 exposures (duration 4 min.), but with further irradiation small absorbing bodies appear in the nuclear background. At about the 40th exposure the nuclear membrane is better defined and the nucleus becomes rounded, and thus appears as a smaller area on the photograph. At a stage during the shrinkage of the nucleus "blebs" containing much of the absorbing material from the cytoplasm are seen to appear at the cell boundary. These enlarge and eventually burst. An ultra-violet cine-film at 265 mμ illustrating these effects has been made.

Using the methods of integration described, we have investigated the quantitative changes that occur when living cells are irradiated. A complete analysis has been made on two cells. In these the degrees of shrinkage and the final average density of the nucleus were very different, but the total amount of absorbing substance measured by this method changed in a similar manner.

Fig. 6 illustrates the changes occurring in the nucleus of one of these cells.

[6] Wilkins, this Discussion.

[7] Bancher, *Protoplasma*, 1942, **36**, 607.

[8] Biebl, *ibid.*, 1942, **36**, 491.

[9] Larionov and Brumberg, *Compt. rend.*, *U.R.S.S.*, 1946, **54**, 267.

The average density of the nucleus remains fairly constant initially and then increases (curve *a*). This corresponds to the observed increase in absorption of the irradiated nucleus. The projected area also remains constant and then

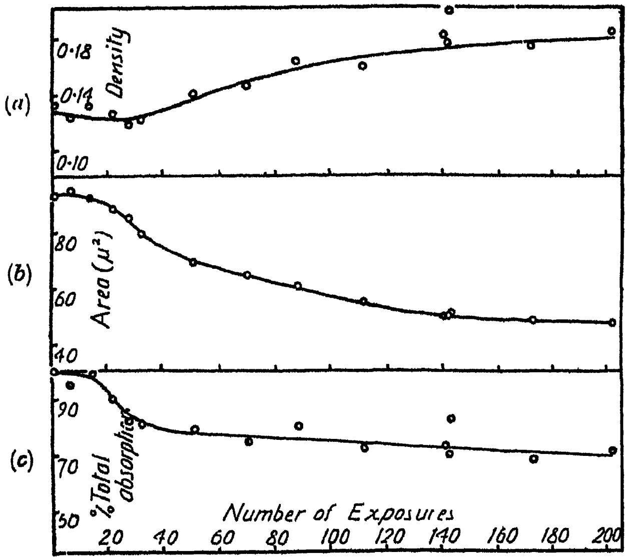

Fig. 6. Data from serial photographs of intermitotic chick fibroblast nucleus. Exposure time 2·4 sec., interval between exposures 12 sec. Duration of experiment 40 min. Total number of exposures 200. Curve *a* : average density of nucleus including nucleolus. Curve *b* : projected area of nucleus in μ^2. Curve *c* : variation in total amount of absorbing material, expressed as a percentage of initial amount and obtained from product of average density × area.

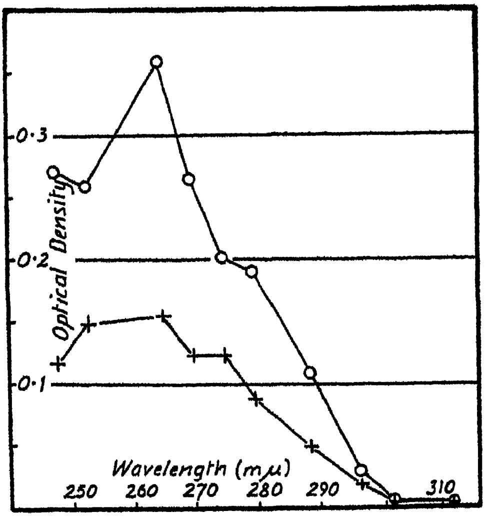

Fig. 7.—Absorption curve of chick fibroblast nucleus before (×) and after (O) irradiation as in Fig. 6.

decreases (curve *b*). The total amount of absorbing material present (the product of curves *a* and *b*) is found to decrease after irradiation to about 70 % of its initial value (curve (*c*)). The nucleolus has been included in the measurements of the average density of the nucleus. Microspectrographic errors due to differing light-path lengths are greater with the more rounded [1, 11] irradiated nucleus. A qualitative examination of these corrections shows that if they were made, the total amount of absorbing material after irradiation would be still further decreased.

Discussion

The Living Interphase Nucleus.—It has been suggested that the living interphase nucleus, except the nucleolus, is non-absorbing [9] at 265 mμ and optically homogeneous,[12] and that the absorption and structures that have been reported appear after injury by ultra-violet radiations [7, 8, 9] or other agents. Our results show that a photograph taken without previous irradiation has an optical density for the nucleus of chick fibroblasts of from 0·1 to 0·15. The optical density of the cytoplasm may be greater or less than this value. It is also found that the living nucleus is not homogeneous, but contains poorly-defined structures, other than the nucleolus, and similar to those seen in the phase microscope. Further small absorbing bodies become evident in our ultra-violet photographs after ultra-violet radiation.

Tissue culture cells are very sensitive to changes in medium and to mechanical injury, such as that produced by a smear technique. It is therefore necessary to emphasize that our photographs were taken of tissue culture cells growing in the normal manner, and that we found it unnecessary to add Ringer's solution, glucose or other reagent. Care is also taken to transfer the culture quickly from the incubator to the warm stage of the microscope. The unirradiated cells continue to grow and divide after the exposures have been made for the usual period of time for this type of culture. There is, therefore, no possibility of artefact due to injury of the cells during their preparation. Our results show conclusively that the nucleic acid of the living undamaged nucleus is in such a condition that it can absorb ultra-violet at 265 mμ.[13]

It is likely (Part I) that the exposures during the 90 sec. required to obtain an absorption series of photographs will eventually produce cell damage. We have carefully examined our cells before and immediately after this period with phase contrast illumination (N.A. 0·85) and find no detectable change.[14] The long filamentous mitochondria have neither changed their shape nor ceased moving, and the cytoplasmic processes have not been withdrawn. But cells examined an hour after one absorption series has been obtained, show variable signs of degeneration, such as clumping of the mitochondria and rounding up of the cells.

Results obtained by microspectrography of fixed material have been criticized by Larionov and Brumberg,[9] because the validity of this work has been partly based on a comparison of ultra-violet photographs of fixed material with those of living material, taken after prolonged irradiation during focusing and exposure. The form of the absorption curves we have obtained on living cells resemble those of Caspersson *et al.* for fixed material. However, in order to determine whether there has been any change in the quantity or distribution of absorbing substances on fixation, quantitative techniques should be applied to the same cell before and after fixation.

The Irradiated Interphase Nucleus.—Various explanations have been advanced to account for the increased optical density observed in nuclei irradiated with ultra-violet light at 265 mμ. Larionov and Brumberg [9] suggested that either there had been some change in the condition of the

[10] Wyckoff, Ebeling and Ter Louw, *J. Morph.*, 1932, **53**, 189.
[11] Caspersson, *Scand. Archiv. Physiol.*, 1936, Suppl. 8.
[12] Ris and Mirsky, *J. Gen. Physiol.*, 1949, **32**, 497.
[13] Ely and Ross, *Nature*, 1949, **163**, 906.
[14] Ludford and Smiles, *J. Roy. Micro. Soc.*, 1948, **68**, 1.

nucleic acid and its ability to absorb ultra-violet rays or that it was in some way connected with the reduced size of the nucleus. Ris and Mirsky [12] concluded from their experiments on chick fibroblasts that the increased density of the irradiated nucleus was due to increased structural light loss due to changes in refractive index. Their conclusion was based on ultra-violet photographs of cells before and after treatment with hot trichloracetic acid which removes nucleic acid. The appearance of their "chromatin" did not change after extraction. Our results also show that there is an increased optical density in the irradiated nucleus, but that this density is due to true light absorption and not structural light loss (Plate III and Fig. 7). The integration measurements (Fig. 6) show that this increased absorption is accounted for by a decrease in nuclear area as originally suggested by Larionov and Brumberg. There is in fact a decrease rather than an increase in the total amount of absorbing matter present after irradiation. This decrease in the total quantity may possibly be explained either by a loss of nucleotides through the nuclear membrane or by chemical changes due to ultra-violet radiation.[15]

We have outlined in this communication a method of quantitative comparison of absorbing substances in biological material which we must emphasize is in the early stages of its development. The method can be applied to other problems involving the comparison of cells in different states or metabolic conditions. Indeed, it is possible from the measurements of nuclear area and average nuclear density (excluding the nucleolus) already obtained to calculate the desoxyribo nucleic acid (DNA) content of individual living chick fibroblast nuclei. If the assumption is made that the measured absorption at 265 $m\mu$ is due entirely to DNA (neglecting the protein moiety) then the contents are for the two nuclei measured $3{\cdot}0$ and $5{\cdot}5 \times 10^{-12}$ g. These figures are similar in magnitude to the average DNA content per nucleus obtained by biochemical methods for fowl erythrocyte nuclei ($2{\cdot}62 \times 10^{-12}$ g.).[16, 17] The difference between our figures above is outside the limits of experimental error and one would not expect that in cells which are rapidly dividing, the DNA content of individual nuclei would be identical.

The main conclusions of the studies of chick fibroblasts are:

(i) The living interphase nucleus is heterogeneous in structure and the desoxyribo-nucleic acid is in a condition in which it can absorb.

(ii) The absorption curves of living cells are similar in form to those obtained by others on fixed material.

(iii) The increased optical density of nuclei irradiated at 265 $m\mu$ can be accounted for by their decreased projected area. There is in fact a decrease in the total amount of absorbing material.

We would like to thank the following for helpful discussions: Prof. J. T. Randall, F.R.S., Dr. H. B. Fell and Dr. M. H. F. Wilkins. We would also like to thank the following: Miss S. Jackson for preparing some of the tissue cultures, Miss H. Yates and Miss Ticehurst for help in preparing illustrations, P. Heaver for constructing the microphotometer, and C. Yhapp for general help in the construction of apparatus.

Medical Research Council Biophysics Unit,
King's College,
Strand, London, W.C.2.

---

[15] Heyroth and Loofbourow, *J. Amer. Chem. Soc.*, 1931, **53**, 3441.
[16] Davidson and Leslie, *Nature*, 1950, **165**, 49.
[17] Vendrely and Vendrely, *Experientia*, 1949, **5**, 327.

COMPONENTS OF NORMAL AND ABNORMAL LIVER CELLS STUDIED BY ULTRA-VIOLET MICROSCOPY AND BY DIFFERENTIAL CENTRIFUGATION *

By Hubert R. Catchpole and Isidore Gersh

Received, 18th July, 1950

Ultra-violet absorption was measured at 2652 A and 2804 Å in nuclei, nucleoli, and cytoplasm of cells in sections of normal rat livers, of hepatomas produced by feeding butter yellow, and of non-tumour portions of tumour bearing livers. Nucleic acids were determined chemically in cytoplasmic and nuclear fractions, obtained by differential centrifugalization, from the same and other livers and experimentally produced tumours. Comparison of the findings yielded a field of general agreement. Resolution of certain discrepancies led to deductions of (i) a lower state of aggregation of the nucleo-proteins of tumour nuclei, or an increased permeability of the nuclear membrane to them; (ii) a change in distribution of cytoplasmic nucleoproteins of tumours from more highly organized particulate states (large granules and microsomes) to smaller aggregates (sub-microsomes).

Numerous reports on nucleic acids and cell proteins in cells have been based on the use either of ultra-violet absorption or of conventional chemical methods applied to cells, or to their separated components. No single study making use of comparable material has appeared designed to take advantage of differences in the methodological assumptions implicit in the use of methods differing so markedly in technique. Such an attempt is the basis of the present paper.

Experimental Results

Material.—Female rats (Sprague-Dawley strain) weighing 80-120 g. at the start of the experiment were placed on Diet B † (Opie, 1944) [11] containing 0·06 % 4-dimethyl aminoazobenzene (butter yellow). Control rats, in groups of 5, were fed the same diet without dye, and received daily the same amount of food as was consumed by similar groups of animals on the butter yellow diet. In general, tumours were taken after 7 to 12 months on the diet.

Animals were killed by a blow on the head and were bled but not perfused. Pieces of liver or tumour tissue were frozen in *iso*pentane at −150° C. to −160° C., and dried *in vacuo* at about −30° C for histochemical study. Adjoining slices were fixed in formalin. Tumour tissue was freed from grossly necrotic and cystic tissue; this will be called tumour hepatoma tissue and the cells named correspondingly. Most generally, the right liver lobes showed preferential conversion to tumour, and frequently normal appearing, or hypertrophic tissue visually free of tumour could be obtained from the median and left lobes; this will be called non-tumour hepatoma tissue and the cells named correspondingly. In other cases, conversion to tumour was general. Tumour and non tumour heptoma tissues were processed separately where possible, and normal control tissues were taken at the same time. The tissues were weighed fresh and immediately chilled in the refrigerator.

Ultra-violet-Microscopy.‡—The frozen and dried blocks which had been embedded in paraffin were sectioned serially at 4 μ. A series of sections was

---

* This work was supported in part by a grant from the American Cancer Society recommended by the Committee on Growth of the National Research Council.

† 68·2 % fat, 21·1 % protein, adequate vitamins. This diet was reported to produce a high incidence of hepatomas without cirrhosis.

‡ In all measurements with the u.-v. microscope, we acknowledge with deep appreciation the assistance of Mr. Frank R. Vaughn.

passed through chloroform and absolute alcohol, transferred to a quartz slide and mounted. After preliminary experiments cited below, the mounting and clearing agent chosen was a 1·08 % solution of lanthanum nitrate $(LaNO_3)_3 . 6H_2O$ in 80 % aqueous glycerine. In order to reduce error due to section thickness, only two or three cells were measured in any one section, to reach a total of approximately twenty cells for each specimen. The cells measured were selected only for having the nucleolus, nuclear sap and cytoplasm unconfused by overlay or underlay. Measurements were taken the same day the preparations were made of a cylinder about 1 μ in diameter through a nucleolus, a nucleus free of visible particles, and cytoplasm at a distance of approximately 5 μ from the nuclear membrane. Simultaneous readings were made of monochromatic light transmitted through the object or clear space and the microscope, and of a beam reflected from the incident illumination. Measurements in any one cell at two wavelengths (2652 Å and 2804 Å) were completed in about 2 min., without undue exposure (see below).

The light source was a medium-high pressure water-cooled mercury arc. Zeiss quartz optics were used, except for a reflecting objective with a numerical aperture of approximately 0·6 and an initial magnification of 78. Other details are a quartz condenser, an ocular × 20, and distance to aperture approximately 75 cm. Amplification was by means of an electron multiplier tube and galvanometer.

Continued irradiation was accompanied by a fall in absorption (Fig. 1A), a phenomenon which was studied in detail on unfixed cells by Bradfield and Errera.[2] When illumination was interrupted, the absorption remained nearly constant during the time when the specimen was not irradiated (Fig. 1B). This phenomenon was noted in the nucleus, nucleolus and cytoplasm. There was a fall in absorption whether the object was fixed by freezing and drying, or by formalin, absolute alcohol, or aqueous or alcoholic mercuric chloride. The fall in absorption could be prevented for 3 or more minutes by using lanthanum glycerine as a mounting medium (Fig. 1C).

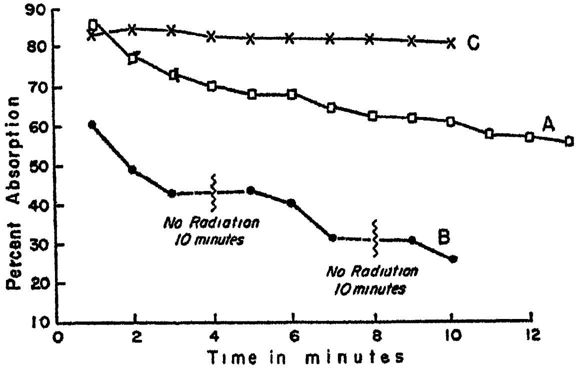

FIG. 1.

We were unable to test the applicability of Beer's law. Preliminary test of Lambert's law is based on the cytoplasmic absorption of 10 normal liver cells in sections 1, 2, 3 and 4 μ thick. Plotted as modified extinctions E_m, the mean values fall along a straight line (Fig. 2A, B). The ratios of E_m at 2652 Å and 2804 Å are nearly the same at all thicknesses. If the Lambert law for nucleoprotein and protein be represented (Fig. 2C, D) by straight lines passing through the origin, whose actual slope is not known, then deviations from them may be attributed, at least in part, to light scattering. It is suggested that these findings may provide a partial or alternative explanation of the phenomenon described by Commoner and Lipkin,[5, 6] in which a tendency for E

---

[1] Bensley, *Biol. Symp.*, 1943, **10**, 323.

[2] Bradfield and Errera, *Nature*, 1949, **164**, 532.

[3] Claude, *J. Expt. Med.*, 1946, **84**, 51, 61.

[4] Claude, *Science*, 1940, **91**, 77.

[5] Commoner and Lipkin, *ibid.*, 1949, **110**, 41.

[6] Commoner, *ibid.*, 1949, **110**, 31.

values to have a maximum frequency at 0·3 was interpreted as being due to orientation of nucleic acids. For, increasing downward displacement of expected E_m values (from curve C to curve A) at higher absorption levels would

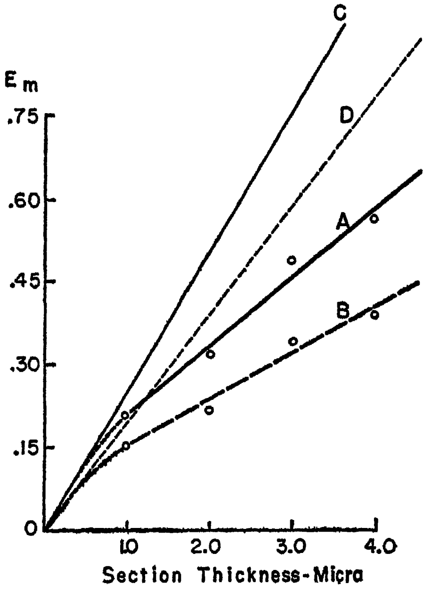

FIG. 2.

TABLE I.—MEAN E_m VALUES AT 2652 Å AND 2804 Å OF NUCLEUS, NUCLEOLUS AND CYTOPLASM OF HEPATOMA TUMOUR CELLS, OF NON-TUMOUR CELLS OF THE SAME AND SIMILAR RATS, AND OF NORMAL HEPATIC CELLS OF RATS FED THE SAME DIET MINUS BUTTER YELLOW, CALCULATED FROM ANIMALS IN EACH GROUP

		Tumour Hepatoma ($n = 7$)	Non-tumour Hepatoma ($n = 5$)	Normal Diet Control ($n = 11$)
2652 Å	Nucleus .	0·641 ±0·081	0·606 ±0·051	0·591 ±0·099
	Nucleolus .	0·779 ±0·126	0·728 ±0·046	0·713 ±0·109
	Cytoplasm .	0·831 ±0·118	0·796 ±0·037	0·694 ±0·115
2804 Å	Nucleus .	0·467 ±0·086	0·449 ±0·039	0·415 ±0·073
	Nucleolus .	0·572 ±0·134	0·523 ±0·039	0·508 ±0·053
	Cytoplasm .	0·627 ±0·101	0·614 ±0·039	0·530 ±0·060

Significance of difference between means calculated from animals in each group.

		Tumour Hepatoma and Non-tumour Hepatoma P Value	Tumour Hepatoma and Normal Diet Control P Value	Non-tumour Hepatoma and Normal Diet Control P Value
2652 Å	Nucleus .	$0·4 > P > 0·3$	$0·3 > P > 0·2$	$0·7 > P > 0·6$
	Nucleolus .	$0·4 > P > 0·3$	$0·3 > P > 0·2$	$0·8 > P > 0·7$
	Cytoplasm .	$0·5 > P > 0·4$	$0·05 > P > 0·02$	$0·02 > P > 0·01$
2804 Å	Nucleus .	$0·7 > P > 0·6$	$0·3 > P > 0·2$	$0·3 > P > 0·2$
	Nucleolus .	$0·4 > P > 0·3$	$0·3 > P > 0·2$	$0·6 > P > 0·5$
	Cytoplasm .	$0·8 > P > 0·7$	$0·05 > P > 0·02$	$0·1 > P > 0·05$

result in an apparent paucity of these higher values, and in a displacement of the extinction frequency curves to the left.

An examination of Table I shows a tendency for the absorption of nucleus, nucleolus and cytoplasm at both wavelengths to be lowest in normal cells, higher in non-tumour hepatoma cells and highest in tumour cells. This relationship is not statistically significant. However, when all values of all animals in each group (tumour, non-tumour, control) are treated as if they were from a single animal, and compared (Table II), a statistically significant difference appears between the various components of tumour hepatoma cells and those of normal cells, and also between cytoplasm of non-tumour hepatoma cells and normal cells. There is little doubt that if the absorption curves were corrected for light scattering and other regular errors (as has been done tentatively in Fig. 2c and D), more marked statistical differences would appear in the absorption of all three cell components of normal, tumour and non-tumour hepatoma cells.

TABLE II.—Mean Percentage Absorption at 2652 Å and 2804 Å of Nucleus, Nucleolus and Cytoplasm of Same Cells Treated in Table I, Calculated from the Values of all Absorptions by Groups

		Tumour Hepatoma (n = 13)	Non-tumour Hepatoma (n = 100)	Normal Diet Control (n = 94)
2652 Å	Nucleus .	77·0 ± 8·13	74·0 ± 6·24	73·8 ± 10·10
	Nucleolus .	82·9 ± 7·27	80·4 ± 4·03	70·6 ± 7·64
	Cytoplasm .	85·1 ± 5·66	81·2 ± 3·80	70·5 ± 8·40
2804 Å	Nucleus .	65·9 ± 11·66	64·2 ± 7·59	62·6 ± 11·10
	Nucleolus .	72·4 ± 11·70	70·0 ± 6·04	68·0 ± 9·08
	Cytoplasm .	75·6 ± 7·79	73·8 ± 5·65	70·3 ± 9·72

Significance of difference between means calculated for values of each group

		Tumour Hepatoma and Non-tumour Hepatoma P Value	Tumour Hepatoma and Normal Diet Control P Value	Non-tumour Hepatoma and Normal Diet Control P Value
2652 A	Nucleus .	0·05 > P > 0·02	P < 0·01	0·5 > P > 0·4
	Nucleolus .	P < 0·01	P < 0·01	0·3 > P > 0·2
	Cytoplasm .	0·2 > P > 0·1	P < 0·01	P < 0·01
2804 A	Nucleus .	0·2 > P > 0·1	P < 0·01	0·05 > P > 0·02
	Nucleolus .	0·05 > P > 0·02	P < 0·01	0·05 > P > 0·02
	Cytoplasm .	0·9 > P > 0·8	P < 0·01	P < 0·01

Volume Studies. Serial sections of the same material studied above were mounted on slides and stained with Toluidine Blue. Measurements were made with an ocular micrometer of the greatest and least dimensions of nucleolus, nucleus and cell body in the same cell, the criteria for selection of cells being the same as was used for ultra-violet microscopy. For calculation of volume, nucleoli were generally treated as spheres, nuclei and cells as ellipsoids. For practical purposes, the volume of cytoplasm may be regarded as that of the cell. It appears from Table III that only nucleoli of tumour hepatoma and non-tumour hepatoma cells have a significantly greater volume than those of normal hepatic cells. These differences may not be as great as indicated, since smaller nucleoli of normal cells were probably neglected. When the same basic data are treated as if pertaining to only three groups (tumour, non-tumour, normal), additional significant differences appear (Table IV). All three components of tumours are significantly, or possibly significantly, larger than those of normal cells and of non-tumour cells of the same or similar rats fed butter yellow. The nucleolus and cytoplasm, but not the nucleus of the latter, are larger than normal.

It would seem, then, that by a liberal, possibly justified analysis, the components of tumour cells have a greater absorption at 2652 Å and 2804 Å than normal cells, and that there is more absorbing material (nucleoprotein) in the former than in non-tumour cells of the same or similar livers of rats fed on a butter yellow diet. Also, as compared with normal, the cytoplasm of non-tumour hepatoma cells has a greater absorption at 2652 Å and at 2804 Å, and has more absorbing material (nucleoprotein). By a more conservative treatment of the same data, only the nucleoli of tumour and non-tumour cells of rats fed on butter yellow have a greater than normal amount of absorbing material (nucleoprotein). By either method of analysis, the absorption is least in nuclear sap, greatest in the cytoplasm, and intermediate in the nucleolus.

TABLE III. MEAN VOLUME OF NUCLEUS, NUCLEOLUS AND CYTOPLASM OF HEPATOMA TUMOUR CELLS, OF NON-TUMOUR CELLS OF THE SAME AND SIMILAR RATS, AND OF NORMAL HEPATIC CELLS OF RATS FED THE SAME DIET MINUS BUTTER YELLOW, CALCULATED FROM ANIMALS IN EACH GROUP

	Tumour Hepatoma ($n = 7$)	Non-tumour Hepatoma ($n = 5$)	Normal Diet Control ($n = 11$)
Nucleus (mm.$^3 \times 10^{-7}$) .	3·39 ± 0·91	2·46 ± 0·25	2·42 ± 0·37
Nucleolus (mm.$^3 \times 10^{-7}$) .	1·30 ± 0·45	0·79 ± 0·19	0·49 ± 0·11
Cytoplasm (mm.$^3 \times 10^{-4}$) .	2·50 ± 1·73	2·07 ± 1·46	1·76 ± 0·27

Significance of difference between means calculated from animals in each group.

	Tumour Hepatoma and Non-tumour Hepatoma P Value	Tumour Hepatoma and Normal Diet Control P Value	Non-tumour Hepatoma and Normal Diet Control P Value
Nucleus	$0{\cdot}05 > P > 0{\cdot}02$	$0{\cdot}02 > P > 0{\cdot}01$	$0{\cdot}9 > P > 0{\cdot}8$
Nucleolus	$0{\cdot}05 > P > 0{\cdot}02$	$P < 0{\cdot}01$	$P < 0{\cdot}01$
Cytoplasm	$0{\cdot}7 > P > 0{\cdot}6$	$0{\cdot}4 > P > 0{\cdot}3$	$0{\cdot}7 > P > 0{\cdot}6$

TABLE IV.—MEAN VOLUME OF NUCLEUS, NUCLEOLUS AND CYTOPLASM OF SAME CELLS TREATED IN TABLE III, CALCULATED FROM THE MEAN VALUES OF ALL VOLUMES BY GROUPS

	Tumour Hepatoma ($n = 220$)	Non-tumour Hepatoma ($n = 100$)	Normal Diet Control ($n = 240$)
Nucleus (mm.$^3 \times 10^{-7}$)	3·39 ± 1·34	2·46 ± 0·93	2·42 ± 0·52
Nucleolus (mm.$^3 \times 10^{-7}$)	1·30 ± 0·74	0·79 ± 0·47	0·46 ± 0·20
Cell volume (mm.$^3 \times 10^{-}$	2·75 ± 2·22	2·07 ± 0·90	1·76 ± 0·68

Significance of difference between means calculated from all values for each group.

	Tumour Hepatoma and Non-tumour Hepatoma P Value	Tumour Hepatoma and Normal Diet Control P Value	Non-tumour Hepatoma and Normal Diet Control P Value
Nucleus	$P < 0{\cdot}01$	$P < 0{\cdot}01$	$0{\cdot}7 > P > 0{\cdot}6$
Nucleolus . . .	$P < 0{\cdot}01$	$P < 0{\cdot}01$	$P < 0{\cdot}01$
Cytoplasm	$P < 0{\cdot}01$	$0{\cdot}05 > P > 0{\cdot}02$	$P < 0{\cdot}01$

Adverting to the theoretical considerations of Commoner and Lipkin, the phenomena attributed to nucleic acid orientation was not found by them with living cells (nucleic acid un-oriented), but only with material in which they believed some sort of alignment was produced by fixation distortion (nucleic acid oriented). It is likely that the cells used in the present study resembled the former in physical state, since freezing-drying under the conditions employed does not produce observable shrinkage or distortion. If, nevertheless, these arguments do apply to the material as fixed, then two possibilities seem to arise: (1) where no difference in absorption is seen, differences in fixation orientation might be obscuring an actual difference in concentration, (2) where a significant difference is found, this might be accompanied by an altered physical arrangement of the nucleic acids produced during fixation.

Preparation and Analysis of Liver and Tumour Particulates.—Manipulations were made at 0-4° C in a cold room. Centrifuges were operated "open", to obviate a temperature rise within the apparatus while spinning. Running times and speeds were standardized and the schedule was adhered to throughout the course of this work. An alkalinized saline suspension of the tissue (1 volume of tissue to 4 of saline) was made as in Claude's procedure.[3] This was centrifugalized 3 times at 1250 *g* for 3 min. each run to remove nuclei, cells and debris. The supernatant was then centrifugalized twice at 18,000 *g* for 5 min. each run to remove the large granule fraction. The large granules were pooled, re-sedimented, and then washed twice more with saline. The final preparation was frozen in liquid air and lyophilized. The large granule supernatant fraction was centrifugalized at 18,000 *g* for 90 min. to obtain the microsome pellet described by Claude[4] and by Bensley and Lazarow.[1] Microsomes were pooled and sedimented, and washed once with saline. The final preparation was lyophilized. These preparations were stored in a desiccator over Drierite. A limited number of preparations of isolated nuclei was made separately by the Dounce procedure,[8] using citric acid at pH 6·2, modified to deal with the relatively small amounts of tissue available from single animals (6-15 g.). In addition, whole tissues (normal, tumour and non-tumour hepatoma) were sampled following a preliminary grinding. The suspensions were weighed and lyophilized for dry weight and other determinations.

Weighed amounts of the dried whole tissue, or of the dried granules, were prepared for phosphorus analyses by the method of Schmidt and Thannhauser.[14] Following extraction of the lipid material, the preparations were hydrolyzed with 1·0 N KOH for 24 hr., and partition was made between the desoxyribosenucleic acid, phosphoprotein, and ribosenucleic acid phosphorus. Phosphoprotein phosphorus was removed by the method of Delory.[7] Phosphorus was estimated on all fractions by the method of Gomori.[9] Amino acids were determined on a few fractions by standard microbiological methods.

Results.—Whole Frozen-dried Liver Tissue (Table V).—There is no significant difference in total phosphorus or in ribonucleic acid of normal control and hepatoma. There is a possible significant increase in desoxyribonucleic acid in hepatoma.

TABLE V.—Whole Livers: Phosphorus per 1·0 g. Dry Tissue.
(Means and Standard Deviations)

	Normal Diet Control µM	Tumour Hepatoma µM
Total (non-lipid) . . .	(6) * 145 ± 13	(5) 148 ± 34
Desoxyribosenucleic acid . .	(6) 24 ± 4	(5) 36 ± 20
Phosphoprotein . . .	(6) 17 ± 11	(5) 5 ± 5
Ribosenucleic acid . . .	(6) 104 ± 12	(5) 107 ± 25

* Numbers in parentheses denote number of animals used.

Large Granules (Table VI).—There are no significant differences in total phosphorus and in ribo- and desoxyribonucleic acids of normal control, tumour and non-tumour hepatoma.

---

[7] Delory, *Biochem. J.*, 1938, **32**, 1161.
[8] Dounce, *J. Biol. Chem.*, 1943, **147**, 685.
[9] Gomori, *J. Lab. Clin. Med.*, 1941-2, **27**, 955.

MICROSOMES (Table VII).—As in the case of large granules, no significant differences in phosphorus containing components were noted in the three groups of animals.

NUCLEI (Table VIII).—The number of determinations made was limited owing to the poor success in obtaining nuclei preparations from small amounts of tissue. Values for total phosphorus and desoxyribosenucleic acid are low. This may have been due either to contamination with cytoplasmic components (which was not microscopically evident when the preparations were made) or to leaching of desoxyribosenucleic acid during the preparation. While the nuclei of control and non-tumour hepatoma (1 case only) livers are not different, there was a marked fall in desoxyribosenucleic acid of the tumour hepatomas, and a less marked fall in total phosphorus and ribonucleic acid.

TABLE VI.—LARGE GRANULES : PHOSPHORUS PER 1·0 G. DRY GRANULES

	Normal Liver µM	Non-tumour Hepatoma µM	Tumour Hepatoma µM
Total (non-lipid) . .	(6)* 161 ± 40	(6) 190 ± 30	(10) 167 ± 25
Desoxyribosenucleic acid .	(6) 28 ± 11	(6) 18 ± 3	(10) 19 ± 13
Phosphoprotein . .	(6) 6 ± 4	(6) 5 ± 4	(10) 4 ± 4
Ribosenucleic acid . .	(6) 128 ± 44	(6) 167 ± 21	(10) 145 ± 28

* Numbers in parentheses denote number of animals used.

TABLE VII.—MICROSOMES : PHOSPHORUS PER 1·0 G. DRY GRANULES

	Normal Liver µM	Non-Tumour Hepatoma µM	Tumour Hepatoma µM
Total (non-lipid) . .	(6)* 279 ± 65	(6) 242 ± 61	(10) 285 ± 51
Desoxyribosenucleic acid .	(6) 5 ± 3	(6) 5 ± 4	(10) 7 ± 6
Phosphoprotein . .	(6) 7 ± 7	(6) 10 ± 13	(10) 10 ± 9
Ribosenucleic acid . .	(6) 266 ± 60	(6) 227 ± 59	(10) 269 ± 50

* Numbers in parentheses denote number of animals used.

TABLE VIII.—NUCLEI : PHOSPHORUS PER 1·0 G. DRY NUCLEI. (MEANS AND RANGES)

	Normal Liver µM	Non-tumour Hepatoma µM	Tumour Hepatoma µM
Total (non-lipid) . .	(3)* 447 (400-477)	(1) 405	(4) 317 (248-385)
Desoxyribosenucleic acid	(3) 252 (220-295)	(1) 191	(4) 163 (100-251)
Phosphoprotein . .	(3) 35 (5-57)	(1) 52	(4) 44 (6-81)
Ribosenucleic acid . .	(3) 161 (138-175)	(1) 161	(4) 110 (50-138)

* Numbers in parentheses denote number of animals used.

DRY WEIGHT–WATER CONTENT (Table IX).—Water content increases significantly from normal to non-tumour hepatoma tissue, and a further significant increase is seen in tumour hepatoma as compared with non-tumour hepatoma.

GRANULE CONTENT (Table X).—Routine recoveries encountered using the standard methods of granule separation and washing may be considered at least to reflect the granule content of the whole tissues. When related to wet weight of original tissue, there was a marked fall in yield from normal to non-tumour hepatoma to tumour hepatoma, both for large granules and microsomes. Their relative proportions did not change markedly. On the basis of dry weight of original tissue, the differences were less marked, but still large enough to yield significant differences between the three types of tissue in most of the inter-group comparisons.

TABLE IX.—PERCENTAGE DRY WEIGHT OF NORMAL LIVERS AND TUMOUR AND NON-TUMOUR HEPATOMAS

	No. of Animal	Average Dry Weight %
Normal control livers	6	37·1 ± 1·7
Non-tumour hepatoma	18	34·0 ± 5·0
Tumour hepatoma	25	24·1 ± 6·0

Normal control—non-tumour hepatoma . . .	$0{\cdot}05 > P > 0{\cdot}02$
Tumour hepatoma—normal control	$P < 0{\cdot}01$
Tumour hepatoma—non-tumour hepatoma . . .	$P < 0{\cdot}01$

AMINO ACIDS. Of particular interest to this study was the possibility of changes in amino acids absorbing at 2804 A, which are largely responsible for the protein absorption in the ultra-violet. Large granule and microsome fractions obtained from a normal liver and a tumour are compared (Table XI), as well as a normal and tumour nuclear fraction obtained from another pair of animals. No. marked differences between the granules of normal liver and tumour were found for these amino acids, nor indeed for several other amino acids studied.

TABLE X.—RECOVERY OF GRANULES FROM NORMAL AND AFFECTED LIVERS AND HEPATOMAS

	No. of Animals	Weight of Dry Granules per 100 g. Wet Weight of Tissue		Weight of Dry Granules per 100 g. Dry Weight of Tissue	
		Large Granules g.	Microsomes g.	Large Granules g.	Microsomes g.
Normal control . .	5	5·5	2·8	15·1 ± 3·0	7·7 ± 1·1
Non-tumour hepatoma	8	4·2	1·0	12·8 ± 2·3	5·7 ± 0·9
Tumour hepatoma .	10	2·3	1·1	9·3 ± 2·0	4·2 ± 1·6

GROUP COMPARISONS (GRANULES PER 100 G. DRY WEIGHT OF TISSUE)

	Large Granules	Microsomes
Normal control—tumour hepatoma .	$0{\cdot}02 > P > 0{\cdot}01$	$P < 0{\cdot}01$
Normal control—non-tumour hepatoma	$0{\cdot}3 > P > 0{\cdot}2$	$P < 0{\cdot}01$
Non-tumour hepatoma—tumour hepatoma	$0{\cdot}02 > P > 0{\cdot}01$	$0{\cdot}02 > P > 0{\cdot}01$

An appreciable moiety of phosphorus was found in a fraction recovered as phosphoprotein by the Schmidt-Thannhauser procedure. This was found in whole liver and in all particulate fractions, agreeing in part with the protocolls given by Schneider.[15]

The presence of extra-nuclear desoxyribose nucleic acid is usually frowned upon by histochemists on the basis of the negative Feulgen reaction of cytoplasm. Its presence in separated granules has been affirmed and denied, and where found has been usually attributed to nuclear fragments. Preparations of large granules in sufficient quantity have given the Dische reaction.[10] This we have confirmed. The presence of desoxyribosenucleic acid in microsomes is harder to explain on the basis of nuclear fragments, which would be expected to sediment earlier. It is possible that both findings may represent adsorption of material leached from nuclei. In any case, this acid-insoluble fraction of cytoplasmic particulates has been labelled arbitrarily as desoxyribonucleic acid and reported as a positive finding.

TABLE XI. AMINO ACID COMPOSITION OF DRIED GRANULES AND NUCLEI OF LIVER AND TUMOUR TISSUE

	Large Granules			Microsomes			Nuclei		
	Liver g./100 g.	Tumour g./100 g.	Liver/Tumour	Liver g./100 g.	Tumour g./100 g.	Liver/Tumour	Liver g./100 g.	Tumour g./100 g.	Liver/Tumour
Phenylalanine	1·14	1·34	1·05	1·20	1·11	1·05	2·85	2·38	1·20
Tyrosine .	2·20	2·25	0·97	0·74	0·62	1·19	3·20	2·91	1·10
Tryptophane .	0·93	0·91	1·02	—	—	—	—	—	—

Discussion

It would be surprising if the results achieved by the two methods were identical, in view of the differences in the cell components analyzed by each (see Table XII) and in the substances analyzed. The microscopic method makes possible a survey of " nucleo-proteins ", while differentially separated cell components have been analyzed for total (non-lipid) phosphorus and for ribose- and desoxyribose nucleic acid and certain amino acids. Nevertheless, the results overlap to a certain extent and supplement each other. At this point it may be noted that the group of animals used for cytoplasmic analyses, normal and hepatomatous, was largely the same as that used for all u.-v. analyses. A different group of animals was used for isolated nuclei preparations.

By a conservative treatment of the data, the field of general agreement in the findings by the two methods is great: the constant composition of cytoplasmic components of normal, tumour and non-tumour hepatoma (large granules, microsomes) is matched by the uniform ultra-violet absorption of cytoplasm. The analysis of whole liver strengthens this summary statement. The points of disagreement are the normal, or possibly increased concentration of desoxyribonucleic acid of whole tumour hepatoma, the decreased concentration of total phosphorus, desoxyribonucleic acid and possibly the ribonucleic acid of isolated nuclei of tumour hepatoma, and the normal ultra-violet absorption of tumour nuclei and increased *amount* of nucleoprotein in nucleoli of these cells.

Some of these discrepancies are resolved by the more liberal statistical treatment of the ultra-violet absorption data. Thus, the *increased* amount and concentration of nucleoprotein in the tumour nucleus agrees with the possibly increased concentration of desoxyribonucleic acid of whole tumour tissue. But these findings are in marked contrast with the *lowered* concentration of desoxyribonucleic acid in *isolated* tumour nuclei. These divergent trends must mean that during the preparation of the isolated tumour nuclei, nucleic acid is leached out. This leads to the deduction that there may be a difference in the permeability of the nuclear membrane of normal and tumour nuclei under these conditions, or that the nucleic acid of tumour nuclei exists as smaller aggregates than in normal nuclei and are more readily extractable during the process of separation of nuclei.

---

[10] Huseby and Barnum, *Arch. Biochem.*, 1950, 26 187.

The more liberal statistical analysis has led to another major deduction dealing with the state of the cytoplasm of tumour cells. At first glance, the normal composition of large granules and microsomes of tumour cells stands in marked contrast with the increased concentration and amount of nucleoprotein found in the cytoplasm of these cells by ultra-violet absorption. This apparent contradiction is even more exaggerated by the decrease in the amount of particulate material in the cytoplasm of tumour cells. One should recall that the absorption of cytoplasm includes contributions of large granules, microsomes, and also a submicrosomal fraction which passes into the supernatant during the process of centrifugalization. One must conclude, then, that the cytoplasm of tumour hepatoma cells contains an increased amount of smaller nucleic acid containing aggregates (submicrosomes) than do normal cells. This agrees with the direct determinations of Price *et al.*[12, 13] Increased numbers of smaller molecular aggregates should cause an increase in cytoplasmic water, which is in fact observed to take place. In such an analysis the cytoplasm of non-tumour hepatoma cells occupies an intermediate position between normal and tumour cells.

TABLE XII.—COMPARISON OF CELL COMPONENTS MEASURED BY ULTRA-VIOLET ABSORPTION AND BY DIFFERENTIAL CENTRIFUGALIZATION

	Ultra-violet Microscopy	Centrifugalization
Cells	Hepatic cells only	Hepatic cells Biliary duct cells Connective tissue cells
Nucleus	Non-particulate chromatin nucleolus	Non-particulate chromatin Particulate chromatin Nucleolus Nuclear membrane Debris, cells and cytoplasmic contaminants
Cytoplasm	Large granules Microsomes Sub-microsomes	Large granules (with some microsomes, nuclear debris, extracellular debris) Microsomes (with some large granules, nuclear debris, extracellular debris)

Department of Pathology,
University of Illinois.

Department of Anatomy,
University of Chicago,
Illinois.

---

[11] Opie, *J. Expt. Med.*, 1944, **80**, 219.

[12] Price, Miller and Miller, *J. Biol. Chem.*, 1948, **173**, 345.

[13] Price, Miller, Miller and Weber, *Cancer Res.*, 1949, **9**, 398; 1950, **10**, 18.

[14] Schmidt and Thannhauser, *J. Biol. Chem.*, 1945, **161**, 83.

[15] Schneider, *ibid.*, 1946, **165**, 585.

THE ULTRA-VIOLET ABSORPTION OF LIVING CELLS

By J. R. G. Bradfield *

Received 31st July 1950

The ultra-violet absorption of small zones (1 to 5 μ diam.) in living cells in the region 2500 Å to 3000 Å has been followed for periods up to 20 min. after the cells were first irradiated, in order to determine whether the ultra-violet irradiation involved in measurement alters the absorption of the cells. Various conclusions regarding techniques have been drawn from the fact that, in different cells, all three possible results were obtained—an increase, a decrease and no change in absorption. The decrease in absorption (at 2650 Å) was prevented by the presence of reagents destroying sulphydryl groups and, since the decrease is probably due to loss of nucleotides, this observation suggests that the stability of nucleic acids may be affected by the condition of the sulphydryl groups in the proteins with which they are associated.

Some years have elapsed since the early examination of cells in ultra-violet by Kohler, Barnard, Wyckoff and Caspersson [1] and, later, many others and until recently it was generally accepted that living cells absorbed in a manner qualitatively similar to fixed cells, although most investigators agreed that living cells are soon damaged by ultra-violet irradiation. Brumberg and Larionow [2] have recently suggested, however, that undamaged living cells show only very low absorption around 2600 Å, which increases markedly after a few minutes' irradiation. The well-known photographs by Ludford, Smiles and Welch [3] of fresh cells of the Rb tumour and other work done here and in the United States have confirmed, on the other hand, that a variety of living cells possess marked nuclear and cytoplasmic absorption when first observed. The experiments described here aimed at discovering whether the ultra-violet absorption of living cells in the range 2400 Å to 3000 Å changes appreciably during the relatively short period required for absorption measurements and if so, at elucidating the nature and cause of such changes. It should be emphasized that the present work was not designed to investigate the general question of the effects of ultra-violet irradiation on cells—a subject about which there already exists a vast literature, as will be seen from reference to the reviews by Duggar,[4] Hollaender,[5] Loofbourow [6] and Giese.[7]

Experimental

The apparatus and procedure for making absorption measurements were developed from those of Gersh and Baker.[8] The light source (1, Fig. 1) is a water-cooled, high-pressure mercury discharge tube, used in conjunction with a quartz monochromator (2). The spectrum falls on a fluorescent screen (3), where a slit transmits a single wavelength. The monochromatic ultra-violet radiation is reflected into the microscope (6), which has all quartz lenses except in the fluorescent eyepiece; the latter can be swung in for visual inspection of the cells in the ultra-violet, or swung out for making absorption measurements by allowing the light emerging from the quartz eyepiece of the microscope to fall on the photomultiplier tube (7), the output of which is recorded by a moving mirror galvanometer. From the galvanometer reading on a "clear space" and on a particular cell area (down to 1 μ in diam., but usually about 3 μ), the absorption and extinction of that part of the cell can be calculated, the values being reproducible to within less than 1 %. The results include light loss by scattering, but as no attempt was made to deduce nucleotide concentrations, this was not felt to be unduly important. Cells were taken from freshly killed animals and mounted in buffered Ringer solution between quartz slide and cover slip; they could be examined within 2-3 min. of the death of the animal. A suitable field was selected with low intensity green light and the fine adjustment then rotated through a predetermined number of turns so as to bring the microscope into focus for a given wavelength of the ultra-violet (e.g. 12·7 turns for focusing at 2650 Å). The light source was then switched to ultra-violet and final focusing with the fluorescent eyepiece, if necessary at all, took only a few seconds. This eyepiece was then swung out and an absorption measurement obtained after the cell had been irradiated with ultra-violet for only about 10 sec. Apparatus for making highly accurate determinations of the light intensity

---

* Present address : Cavendish Laboratory, Cambridge.

[1] Caspersson, *Symp. Soc. Expt. Biol.*, 1947, **1**, 127.

[2] Brumberg and Larionow, *Nature*, 1947, **158**, 663.

[3] Ludford, Smiles and Welch, *Nature*, 1948, **162**, 650.

[4] Duggar, Ed., *Biological Effects of Radiation* (McGraw Hill, New York, 1st ed., 1936).

[5] Hollaender, *Physiol. Rev.*, 1946, **8**, 1.

[6] Loofbourow, *Growth Symposium*, 1948, **12**, 75.

[7] Giese, *Quart. Rev. Biol.*, 1947, **22**, 253.

[8] Gersh and Baker, *J. Cell. Comp. Physiol.*, 1943, **21**, 213.

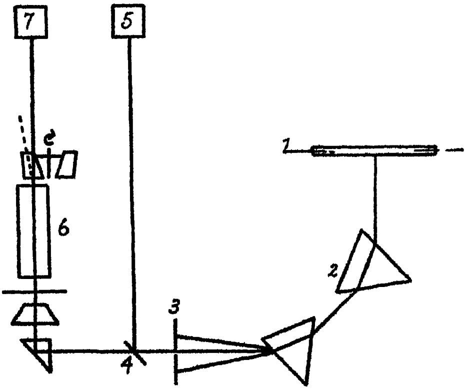

FIG. 1.—Apparatus used for the measurement of the ultra-violet absorption of small areas of living cells (for explanation, see text).

falling on the cells was not available, but application of the photochemical method of Leighton and Forbes[9] based on the photo-oxidation of uranyl oxalate indicated that the incident energy in most experiments was about 10,000 ergs/mm.^{2} sec. (In the absence of atmospheric absorption, the light energy falling on the earth from the sun would be about 14,000 ergs/mm.^{2} sec.) In fact, however, none of the experimental results described below was seriously modified by doubling or halving this intensity. During the observation of any one cell, the incident light intensity was kept constant to within 10 %. All cells were examined at room temperature. This varied on different days between 70 and 94° F, or 20 and 35° C, but the phenomena observed varied little over this range.

Material included stem cells of mammalian bone marrow, lymphocytes and thymocytes (all from the mouse), red blood corpuscles of frog, fowl, mouse and man and cells from two loose-cell sacromata of the mouse—all of which have been studied in some detail—together with chick fibroblasts, mouth epithelial cells and various invertebrates such as *Paramecium*, *Spirostomum* and *Rhabditis*—all of which were examined on only one or two occasions.

Results

From the moment when they were first illuminated by the ultra-violet, such cells showed absorption qualitatively similar to that found in fixed cells. This applied both to direct observation in the fluorescent eyepiece (which, when the

---

[9] Leighton and Forbes, *J. Amer. Chem. Soc.*, 1930, **52**, 3139.

FIG. 3. Frog erythrocyte at 2650 A after only 20-sec irradiation (including the photography). 2000

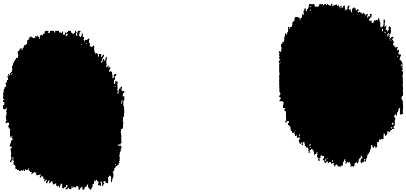

FIG. 4. Frog erythrocyte at 2650 A after 8 min irradiation at this wavelength, showing the considerable increase in nuclear and cytoplasmic absorption. As can be seen from the background, the print should have been made even darker to make it fully comparable with Fig. 3. 2000.

[*To face page* 482

Fig. 6.—Loose cell sarcoma, type OA. A smear in Ringer soln. photographed at 2650 Å showing cells in which absorption remains unchanged during 10-min. irradiation. × 750.

Fig. 7.—As Fig. 6, showing a late anaphase of mitosis (upper centre), and a metaphase plate (lower right). × 750.

microscope has been correctly prefocused, takes only the fraction of a second required for perception of the image by the eye) and to absorption measurement, which takes 5 to 15 sec. With continued irradiation, however, different cells behaved in all three possible ways: one large group—the stem cells of bone marrow, together with lymphocytes and thymocytes—showed a decrease in absorption; one rather specialized cell type, the vertebrate erythrocyte, showed an increase and, finally, the absorption in cells of two loose cell sarcomata remained approximately constant for many minutes. Most attention was directed to the group which showed a decrease in absorption and so the observations regarding the other two groups can be briefly summarized first.

Cells which undergo an increase in Absorption.—When first observed at 2650 or 2537 Å, the nucleated red blood corpuscles of frog and fowl absorb densely in the nucleus and only very little in the cytoplasm. As irradiation continues (at 2650 Å), there is a small, but constantly occurring fall in absorption, but later, after 1-1½ min., the absorption begins to rise sharply in nucleus and cytoplasm (Fig. 2) and soon the darkening becomes visible to the naked eye.

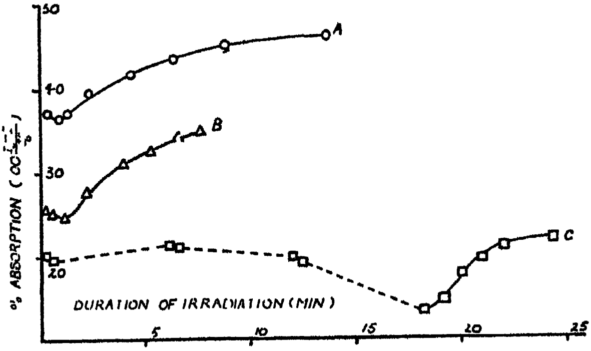

FIG. 2.—The increase in nuclear absorption (curve A) and cytoplasmic absorption (curve B) when frog erythrocytes are irradiated and measured at 2650 Å. Curve C illustrates the effect of a dark period (- - -) followed by continuous illumination (———) in the cytoplasm.

Fig. 3 (Plate I) was taken before irradiation and Fig. 4 (Plate I) after irradiation; from comparison of the two it is evident that the cells undergo considerable shrinkage. It is difficult to measure accurately any decrease in the already small cell thickness, but if this diminishes in proportion to cell length and breadth (which are easily measured), then the decrease in cell volume and consequent increase in concentration in all absorbing substances would account for the rise in absorption. There would be no need to postulate any changes in the molecular structure of absorbing substances (in this case mostly proteins and coenzymes in the cytoplasm, and desoxyribonucleic acid in the nucleus). The nucleus undergoes some shrinkage, but part of its increase in absorption may be due to the darkening of the thin layers of cytoplasm above and below it.

Except that they are anucleate, red blood cells of mouse and man react to irradiation (at 2650 Å) in almost exactly the same way as do those of frog and fowl, and all these erythrocytes show similar changes when irradiated at 2800 Å, the only other wavelength which was thoroughly investigated. The magnitude of those changes is not affected by the presence in the Ringer solution of any of the substances mentioned later in connection with bone marrow cells, viz.: sodium azide, cysteine, mercuric chloride, *p*-chlormercuribenzoate, iodosobenzoate, iodoacetamide, all in the concentrations mentioned later.

If frog erythrocytes are subjected to a dark period after 1 min. exposure to ultra-violet (2650 Å) (i.e. before the rise in absorption has begun) and then isolated absorption measurements are made at intervals of several minutes, the cells show a reaction quite different from that in continuous illumination. The initial slight decrease in absorption becomes more marked after several minutes (Fig. 2) until, as observed by Wyckoff, Ebeling and Ter Louw,[10] the cytoplasm is noticeably lighter than at the start of the experiment. Cell dimensions show little or no alteration during this process, but the marked shrinkage with accompanying rise in absorption can still be brought about if the cells are subjected to continuous irradiation, as illustrated at the end of the broken curve in Fig. 2.

---

[10] Wyckoff, Ebeling and Ter Louw, *J. Morph.*, 1932, **53**, 189.

Chick fibroblasts showed smaller increases than did erythrocytes both in nucleus and cytoplasm, but were much less satisfactory than erythrocytes because: (1) their very irregular shape makes it difficult to estimate their volume and hence to decide whether increases in absorption are due solely to shrinkage; (2) they have, in any case, highly variable and often very low initial absorptions, as is to be expected from the fact, demonstrated by Davidson and Waymouth,[11] that such cells undergo large fluctuations in nucleic acid content. For these reasons they were not studied in much detail, but it was clear that part of the increase in absorption shown in Fig. 5 was due to shrinkage.

Cells in which the Absorption undergoes little change. In smears of two loose cell sarcomata of the mouse (the OA and Earle HGW types) there was strong nuclear and considerable cytoplasmic absorption from the first (Fig. 6 and 7) and the absorption showed little change as irradiation (2650 Å) continued for several minutes (Fig. 5). There may well have been changes in the structure of cell constituents, but not in the overall ultra-violet absorption of the small areas of nucleus and cytoplasm selected for measurement.

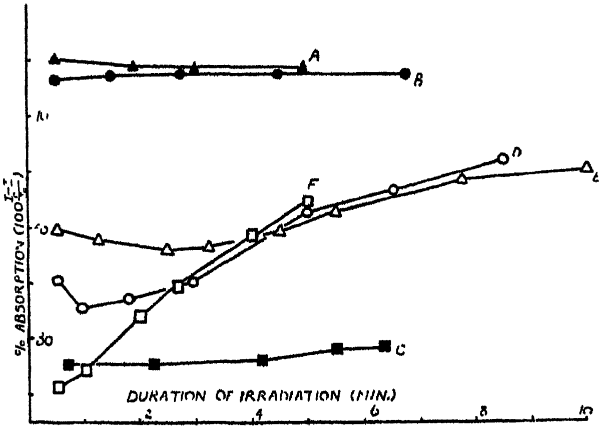

FIG. 5(*a*).– The absence of any change in absorption when nuclei (curves A and B) and cytoplasm (curve C) of mouse loose cell sarcoma (type OA) are irradiated and measured at 2650 Å. (*b*) The increase in absorption (due in part at least to shrinkage) when chick fibroblasts in tissue culture are irradiated and measured at 2650 Å (curves D, E, nucleus; curve F, cytoplasm).

Cells showing a Decrease in Nuclear Absorption.—The third and most interesting group of cells consisted of those in which there was a decrease in nuclear absorption, viz. mouse lymphocytes, thymocytes and stem cells of bone marrow and, to a smaller extent, epithelial cells from the human mouth and *Paramecium* (meganucleus). It did not seem practicable to distinguish rapidly the various young cell stages in unstained, living bone marrow and so we confined out attention to cells 10 to 12 μ in diam., with large spherical nuclei and sparse cytoplasm and refer to these as "stem cells". This group presumably included haemocytoblasts, myeloblasts, some myelocytes and erythroblasts, all of which showed fairly uniform behaviour.

The sort of change observed when these cells were irradiated at 2650 Å was a fall of 10 to 15 % in nuclear absorption, which began almost at once and was completed in 8 to 10 min. (Fig. 8, 10 and 11). This effect was observed in nearly 200 cells and less than 5 % of all those examined failed to show it. There was no simple relation between the magnitude of the fall and either the initial nuclear absorption or the intensity of the incident radiation (the latter over a four-fold range of variation). These results are not very surprising in view of the very inhomogeneous nature of the object measured and of the strong possibility (discussed later) that only one fraction of the total nuclear contents is affected.

---

[11] Davidson, *Cold Spring Harbor Symp.*, 1947, **12**, 51.

Similar changes occur when the cells are irradiated and measured at 2537 Å, which like 2650 Å is near the nucleic acid absorption peak. Less pronounced changes, though again of a similar nature, are produced when the cells are irradiated and measured at 2480 Å or 2800 Å. With the apparatus used it is difficult to measure absorption at several wavelengths before and after irradiation at a particular wavelength X, because the initial measurements (especially if they are in the region 2550 Å to 2650 Å) will themselves set off changes which will be superimposed on any changes caused subsequently by wavelength X. For this reason it is difficult to plot an accurate action spectrum, although such indications as have been obtained from attempts in this direction show that the action spectrum resembles that of a nucleoprotein. In two experiments the ultra-violet was switched on at 2800 Å and an absorption measurement made; the wavelength was then rapidly changed and a measurement obtained at 2650 Å not more than 20 sec. after irradiation had commenced. The cells were then followed at 2650 Å for about 10 min. (Fig. 8) and then a final measurement made at 2800 Å. Hence it was possible to plot (on the right of Fig. 8) the slope of the absorption curve between 2650 Å and 2800 Å before and after irradiation and in both experiments, the slope after irradiation was approximately parallel with the slope before irradiation. In terms of the explanation suggested later, this

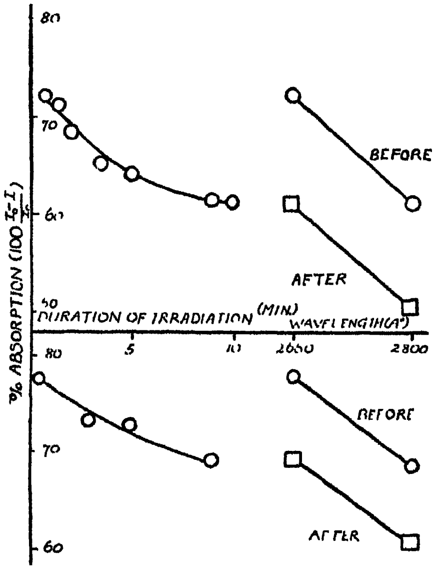

FIG. 8. (left). —The fall in nuclear absorption in two "stem cells" of mouse bone marrow, measured and irradiated at 2650 Å. (right) The slope of the absorption curve from 2650 Å to 2800 Å before and after irradiation for each nucleus.

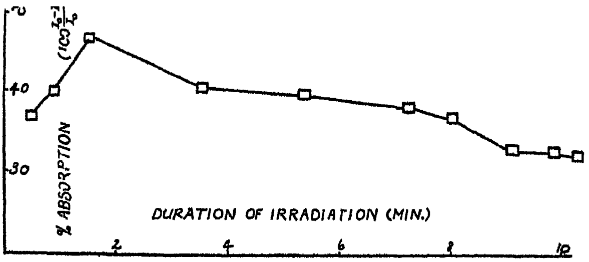

FIG. 9.—The variations in cytoplasmic absorption in a bone marrow stem cell irradiated and measured at 2650 Å (compare the fluctuations in nuclear absorption shown in Fig. 8, 10, 11).

would indicate that both nucleic acids (absorption peak near 2600 Å) and proteins (peak near 2800 Å) are being lost from the cell nuclei.

The possibility of such a loss focuses attention on the cytoplasm, since it ought to be possible to detect at least a transitory increase in absorption there if substances are leaking from the nucleus. The scanty cytoplasm in these cells is,

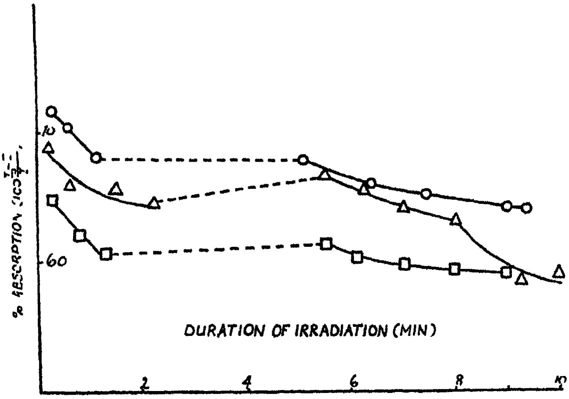

FIG. 10. The effect of a dark period (- - - -) on the fall in nuclear absorption in bone marrow stem cells measured and irradiated at 2650 Å.

however, only about 1 μ thick and must, moreover, be measured at the extreme edge of the cell, where, as a result of cell curvature, errors due to slight movement during measurement are at a maximum. It is, therefore, very difficult to obtain sound absorption measurements on the cytoplasm—although, as shown by the extensive researches of Thorell,[12] such cytoplasmic measurements can lead to very interesting conclusions regarding cell growth. We managed to obtain a few curves of cytoplasmic absorption against time, taking care in each case to check at the conclusion of the experiment that the cell had not moved relative to the diaphragm of the photocell. These showed that there often is an almost

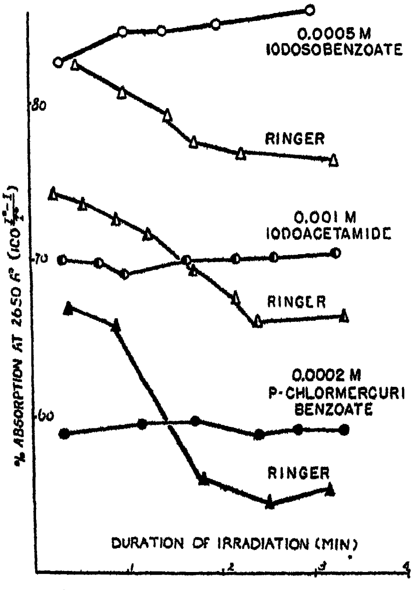

FIG. 11.—The changes in nuclear absorption at 2650 Å of bone marrow stem cells irradiated at 2650 Å in the presence and absence of various reagents destroying sulphydryl groups. (Each pair of curves represents cells from one mouse and the pairs shown above were selected from many similar curves for ease of representation on one figure).

---

[12] Thorell, *Acta Med. Scand.*, 1947, Suppl. 100.

immediate rise in cytoplasmic absorption (Fig. 9) at precisely the time when nuclear absorption is falling most sharply. The rapidity of the rise is not surprising since the first nuclear effects of the ultra-violet will be on the outermost chromatin, from which breakdown products could readily diffuse through the nuclear membrane into the cytoplasm to cause the observed rise in absorption. Later the cytoplasmic absorption returns to its original value, or even a little lower (Fig. 9), but it is clear that the fall in absorption observed when measurements are made on the nucleus cannot be due to decreasing absorption in the thin layers of cytoplasm above and below the nucleus and must be a true nuclear phenomenon.

In order to discover more about the nature of the fall in nuclear absorption the tests were repeated with two main kinds of alteration in experimental conditions : (i) introduction of a dark period ; (ii) incorporation of various substances into the Ringer solution. A dark period arrests the fall in absorption, but the latter is usually completed when the ultra-violet light is switched on again (Fig. 10). For the testing of various possible activators or inhibitors, the cells were mounted directly in Ringer solution, buffered to pH 7·6, containing an appropriate concentration of the test substance. Sodium azide (0·01M to 0·001M), which inactivates heavy metal enzymes and carriers, had no effect. Hence, as expected, none of these compounds is involved in bringing about the fall in absorption. Rather more surprising was the fact that that cysteine, over a similar range of concentrations, was also without effect ; the significance of this finding will be discussed below. On the contrary, the only substances which did prevent the fall in absorption were those which in some way destroy or alter sulphydryl (SH) groups, viz. : 0·0002M *p*-chlormercuribenzoate, 0·0002M mercuric chloride (both mercaptide-forming), 0·0005M iodosobenzoate (oxidizing), 0·001M iodoacetamide (alkylating). The cells were in contact with these substances for 3 to 10 min. before measurements were made and the observations were repeated on 10 to 20 cells for each substance. (Fig. 11).

Discussion

The most striking feature of the results described above is the great variation between the reactions of different cells to ultra-violet irradiation. This is not perhaps surprising between cells as different as stem cells of bone marrow and mature erythrocytes. The sarcoma cells, however, are rather similar to bone marrow stem cells, in that both possess large, heavily absorbing, but not pycnotic, nuclei, and on the other hand they have several general characteristics in common with fibroblasts. Yet their reactions to ultra-violet irradiation differ markedly from the reactions of both these cell types.

With regard to the condition of the cells, it should be stated that the bone marrow cells, lymphocytes, thymocytes and sarcoma cells which showed high absorption were neither pycnotic nor moribund at the commencement of the absorption measurements. It would have been better if (as Dr. C. O. Warren suggested to us) they had been mounted in mouse serum ultra-filtrate, but this unfortunately was not available. However, it is well known that bone marrow maintains its oxygen uptake in nutrient salt solutions *in vitro* for several hours. Moreover, tissue explants destined for cultivation *in vitro* survive similar periods in Ringer solution at room temperature—or even overnight in an ice-box. It is most unlikely, therefore, that the cells studied here, which were mounted in buffered Ringer solution and examined in most cases only 5 min. after the death of the mouse, had undergone any serious deterioration.

At the moment, no explanation can be offered of the striking increase in absorption of vertebrate red blood cells. Their membranes are not normally in a state of tension and during the ultra-violet induced shrinkage which often leaves a cell $\frac{1}{2}$ to $\frac{1}{4}$ of its original volume, the membrane sometimes (but by no means always) develops wrinkles. Very peculiar effects are often observed on the extreme periphery of the irradiated field, where the ultra-violet intensity is very low. Here cells may become spherical, or half a cell may shrink while the other half retains its normal dimensions.

Therefore, unless there can be very localized osmotic changes in the cells, the shrinkage must be due primarily to active shrinkage of the membrane.

As mentioned earlier, most attention was devoted to study of the fall in nuclear absorption caused by ultra-violet irradiation of lymphocytes, thymocytes and bone marrow stem cells. This fall may be due to one or more of at least five causes. (i) It might, firstly, be due to swelling of the nucleus, so that all absorbing substances became more dilute, but no evidence of swelling can be obtained from photographs taken before and after irradiation. (During the life-history of a red cell there is, therefore, a complete change in reaction to ultra-violet irradiation; in the same irradiated field of bone marrow cells, there will be erythroblasts which have undergone a fall in nuclear absorption, but remained constant in volume, and mature erythrocytes which have shrunk to less than half their original volume.) (ii) There might be some change in the molecular orientation of the nucleic acid of the kind discussed recently by Commoner[13] and by Pollister and Swift,[14] but in order for a fall in absorption to occur on this basis there would presumably have to be increased orientation in the fine structures containing nucleic acid as a result of ultra-violet irradiation and this seems rather unlikely. It also seems unlikely that the interesting shift in the absorption peak of yeast ribonucleic acid caused by ribonuclease depolymerization [15] is of sufficient magnitude to account for the present observations, though in view of the extensive changes in absorption spectra caused by various kinds of polymerization and aggregation (briefly reviewed by Commoner and Lipkin [16]), such effects cannot be altogether excluded here. (iii) Nucleoproteins, like other cell contents, are in dynamic equilibrium and it might be that the ultra-violet light inhibited the synthetic enzymes, but left unchecked the enzymes responsible for breakdown of nucleoproteins. The latter would then diminish in amount and the absorption would fall accordingly. Not only is the fall in absorption rather rapid to be enzyme-mediated, however, but the protective action of SH-inhibitors and the absence of any protection by cysteine also argue against this view, since enzyme inhibition by ultra-violet light is sometimes due to destruction of vital SH groups. If this were the case here, cysteine would prevent the inactivation of the synthetic enzymes and arrest the fall in absorption, but it has no such effect. (iv) The fall in nuclear absorption might be primarily due to a permeability change in the nuclear membrane, allowing leakage without much breakdown of nucleoprotein, but one would hardly expect this change to be reversed, and the leakage arrested, when the ultra-violet light is switched off. However, the fall in absorption does, in fact, appear to cease completely during dark periods of from 2½ to 5 min. (v) The fall in nuclear absorption might, as already suggested, be primarily due to a depolymerization of nuceoprotein by those wavelengths of ultra-violet close to the nucleic acid and protein absorption peaks, with immediate leakage of the breakdlown products. The changes detected in the cytoplasm are in favour of this view and it is noteworthy that if it is the true explanation, only a part of the nucleoprotein is so affected because the curve of absorption against time flattens out after about 10 min. Indeed, it may well be that only a part of the nuclear nucleoprotein is labile; studies [18] with ^{32}P as well as by direct analysis [19] show that there are several quite distinct nucleoprotein fractions in cell nuclei.

There are, moreover, numerous points from related work in favour of this last interpretation. Briefly, these show (i) that photo-chemical depolymerization of nucleic acids is possible *in vitro*; (ii) that the breakdown products can leak out of cells. Hollaender, Greenstein and Jenrette [20] found that solutions of desoxyribo-nucleic acid undergo a very considerable decrease in viscosity under the influence of prolonged ultra-violet irradiation and this is very probably due to extensive breakdown of the molecules. Loofbourow and his co-workers [6, 21] have shown in many papers that during ultra-violet irradiation of yeast, there diffuses out into the suspending medium a variety of proliferation-promoting substances, chief among them being various nucleotides which may well be breakdown products of nucleic acids. Hevesey and Zerahn [22] took yeast grown in the presence of ^{32}P, transferred it to normal medium and measured how much radio-phosphorous leaked out as the cells continued to metabolize. They then exposed the cells to ultra-violet light and found a large increase in the amount of acid-soluble ^{32}P, again probably nucleic acid breakdown products, which leaked out; X-rays caused no such increase. In the experiments described here, the fact that the absorption curve from 2650 Å to 2800 Å before irradiation is parallel with that after irradiation suggests that both nucleotides and peptides are escaping (as in Loofbourow's studies on yeast). Indeed it is highly probable that proteins or peptides are involved at some stage in the changes leading to the fall in absorption in view of the stabilizing effect of the sulphydryl inhibitors, since SH groups are absent from nucleic acids but common in proteins. (Nuclei contain many other proteins than simply the basic histones and protamines, and Gulick [23] has shown that they possess considerable amounts of sulphur.)

---

[13] Commoner, *Science*, 1949, **110**, 31, and 1950, **111**, 71.
[14] Pollister and Swift, *Science*, 1950, **111**, 68.
[15] Kunitz, *J. Biol. Chem.*, 1946, **164**, 563.
[16] Commoner and Lipkin, *Science*, 1949, **110**, 41.
[18] Marshak, *J. Cell. Comp. Physiol.*, 1948, **32**, 381.
[19] Mirsky and Ris, *J. Gen. Physiol.*, **31**, 1.

If this view based on depolymerization and leakage is correct, then it appears from the results with SH inhibitors that in the presence of certain SH groups some nucleoprotein is labile and susceptible to depolymerization by ultra-violet light, but that when these SH groups have been destroyed, this nucleoprotein becomes more stable and no longer is broken down by irradiation. In this respect there are also several previous studies worth recalling. Brachet [24] has shown that in the rapidly metabolizing, developing eggs of *Triton cristatus*, granules rich in ribonucleic acids are also rich in SH groups, which becomes understandable if the latter facilitate nucleoprotein breakdown and resynthesis. Chalkley [25] has shown an interesting fluctuation in the SH content of an Amoeba during mitosis. SH concentration is high in the non-dividing nucleus, when substances are passing between nucleus and cytoplasm, but at metaphase the chromosomes undergo a sharp fall in SH content, when as far as is known the nucleic acid is firmly bound to them. Hughes [26] has studied the effect of SH inhibitors on mitosis in tissue cultures and found not only inhibition of spindle formation, but also inability of chromosomes to resume their interphase condition and form nucleoli during telophase, which again is in accordance with the view that certain SH groups are essential for breakdown and building up of nucleoprotein complexes. Evidence of a rather different kind comes from study of bacterial nucleoprotein. Henry and Stacey [27] have stated that ribonucleotides removed from bacteria by treatment with bile salts can be recombined with the organisms provided the latter have been treated with a reducing agent. The significance of the reducing agent is not entirely clear, but among other things it will mean that SH groups will exist as such, rather than being in the oxidized SS form. A suggestive parallel at the level of mononucleotides instead of polynucleotides is seen in the effect of SH inhibitors on actomyosin.[28]

[20] Hollaender, Greenstein and Jenrette, *J. Nat. Canc. Inst.*, 1941, **2**, 23.

[21] Loofbourow, Oppenheim-Errera, Loofbourow and Yeats, *Biochem. J.*, 1947, **41**, 122.

[22] Hevesey and Zerahn, *Acta Radiol.*, 1946, **27**, 316.

[23] Gulick, *Proc. VIIth Int. Genet. Congr.*, 1939, p. 139.

[24] Brachet, *Embryologie Chimique*, (Desoeur, Liege, 1947, 2nd ed).

[25] Chalkley, *Protoplasma*, 1937, **28**, 489.

[26] Hughes, *J. Roy. Micr. Soc.*, 1949, **69**, 215.

[27] Henry and Stacey, *Proc. Roy. Soc. B*, 1946, **133**, 391.

[28] Bailey and Perry, *Biochim. Biophys. Acta*, 1947, **1**, 506.

If certain SH groups are destroyed in this enzymic muscle protein, it can no longer combine with and split its specific substrate, the mononucleotide adenosinetriphosphate. It may be that future work will prove these phenomena to have less in common than appears at the moment, but as far as can be judged at present, they all seem to be in agreement with the view that changes in the state of SH groups can have a marked affect on the ease with which nucleic acids and nucleotides can dissociate from, or recombine with, certain proteins. It must be remembered, however, that the fall in nuclear absorption may prove to have a different explanation from that developed above, in which case the stabilizing effect of SH inhibitors, though none the less interesting, would also have to be interpreted differently.

In conclusion, it is appropriate to review the three main problems raised earlier in this paper. Firstly, the extent to which ultra-violet microspectrography can be applied to living cells evidently varies from cell to cell. Under the conditions of these experiments, there was a safe period for observation of only a few seconds with the bone marrow cells, of about a minute with vertebrate erythrocytes and of many minutes with the mouse sarcoma cells. This does not necessarily mean that the sarcoma cells were living at the conclusion of the observations, but simply that absorption measurements could be made on them for several minutes without getting false values. The problem of making absorption measurements and keeping the cells in healthy condition so that they will go on living is obviously much more difficult, but should be facilitated by the reflecting microscope techniques described by Barer [29] and Mellors,[29] though it is doubtful whether the photographic recording used at present can ever be as accurate as photoelectric recording. On the second problem of to what extent fixation alters absorption, insufficient results have been collected to support definite conclusions and obviously this important subject requires extensive separate treatment. In frozen dried lymphocytes and bone marrow stem cells mounted in glycerol, however, nuclear absorption showed little change from that of living cells provided precautions were taken to prevent solution of the nucleo-proteins, which retain their normal solubility after freeze-drying. Finally, it is evident that although living cells do show appreciable and significant absorption from the earliest moment from which they can be observed, their absorption does, in some, but not all, cases undergo important changes as irradiation continues. Study of the nature of these changes in absorption may yield considerable information about conditions inside the cell. At the moment, the chief point which has emerged in this way is that certain sulphydryl groups appear to exert a marked effect on the stability of one fraction of the nuclear nucleoprotein in bone marrow stem cells.

I am much indebted to Dr. I. Gersh for allowing me the use of his ultra-violet equipment; to Dr. M. Errera (Facultés des Sciences, Université libre de Bruxelles) who participated in many of the experiments described; and to the Commonwealth Fund for a Fellowship which made the work possible.

Department of Pathology,
University of Illinois Medical School,
Chicago 12, *Ill.*

---

[29] This Discussion.

GENERAL DISCUSSION

Dr. R. Barer (*Oxford*) said : In view of the remarks made in Seeds and Wilkins's paper and in the discussion, I feel that I should say a few words in defence of the Weinstein spectrograph. Mr. Weinstein was commissioned by me to design a spectrograph specially suitable for some work I was doing with the Burch microscope. For this purpose I needed a spectrograph of high dispersion, but optically very well corrected, so that the image of a cytological specimen should not be distorted. It seems a little unreasonable to blame a spectrograph for the deficiencies of the mercury lamp (or any other source). It should also be pointed out that the use of any other spectrograph, no matter what its dispersion, would still not affect the characteristics of the source.

Dr. E. Schauenstein (*Graz*) (*communicated*) : Prof. M. Pestemer has drawn attention in connection with the paper by Beaven, Holiday and Jope to the publications of Schauenstein and co-workers of the University of Graz. During the last years, Schauenstein and co-workers (Bürgermeister, Fixl, Stanke and Treiber) have studied the ultra-violet absorption of fibre proteins.[1] They have found that the absorption of actomyosin, collagen and silk fibroin between 20000 and 42000 cm.$^{-1}$ is composed of (*a*) the absorption belonging to the chromophorous amino acids present, (*b*) an additional absorption due to the peptide grid. This additional band has the following properties :

(i) It has a very flat contour with a smeared-out maxima at about 25000 and 40000 cm.$^{-1}$. The intensity of absorption at 40000 cm.$^{-1}$ is comparable with that of proteins containing aromatic amino acids. At 35000 cm.$^{-1}$ the region of absorption maxima of tyrosine and tryptophane, the additional band, however, does not interfere with the method of Holiday for quantitative estimations of these amino acids.

(ii) The band disappears if the proteins are submitted to alkali or fermentation hydrolysis.

(iii) It shows a certain intensity even at low pH values and increases with increasing pH, in accord with the law of electrolytic dissociation. This effect is reversible.

(iv) The intensity of the band depends on mechanical deformation, i.e. it increases on stretching and decreases on contractions. These effects may be reversible (as in collagen) or irreversible (as in silk fibroin and actomyosin), according as the deformation is reversible or not.

(v) Measurements with polarized ultra-violet light offer the possibility of determining the position of regularly arranged chromophorous groups. Therefore, O. Kratky suggested an investigation of fibre proteins using this method. It was found by this means that in some exceptionally well crystallized samples of silk fibroin the main axis of absorption of the new chromophorus forms an angle of *ca.* 40° with the fibre axis.[2] In collagen [3] a composite arrangement was found, i.e. the main axis of absorption runs parallel in part to the fibre axis, and in part it forms an angle of *ca.* 50° with it. The structure of silk fibroin is already well known on the basis of X-ray measurements and is in good accord with the spectrographic result. In collagen the spectrographic measurements allows one to select from the number of proposed models the most probable structure which is in accord with the X-ray diagram as well as with the absorption spectrum.

(vi) The band is closely connected with the existence of interchain hydrogen bonds. A cleavage of these bonds leads to a decrease in absorption and the pH dependence disappears to the same extent. All these results point to the conclusion that Schauenstein and co-workers have observed the enolization of the peptide groups, i.e. the additional band may be ascribed to the $-\underset{\mathrm{HO}}{\overset{}{\mathrm{C}}}{=}\mathrm{N}-$ groups. This chromophorus group is not necessarily present in each protein but it can be formed if extended systems of hydrogen bonds render the enolization possible. Schauenstein has therefore suggested that this group be named the "peptenol" group and their ultra-violet absorption band, "peptenol" absorption.[4]

---

[1] See summarizing article by Schauenstein, *Monatsh.*, 1949, **80**, 821, 843.

[2] Schauenstein, Fixl and Kratky, *Monatsh.*, 1949, **80**, 143.

[3] Fixl, Kratky and Schauenstein, *Monatsh.*, 1949, **80**, 439.

Dr. G. H. Beaven and **Dr. E. R. Holiday** (*London Hospital*) (*partly communicated*) : Supplementing the remarks made in our paper on the value of the logarithmic-cam moving-plate technique for the study of fine structure in the ultra-violet absorption spectra of the aromatic amino acids and of polypeptides and proteins containing them, Fig. 1 and 2 are negative prints of some typical spectrograms obtained by this method. It should be noted that despite the use of high-contrast paper for preparing the prints, there is appreciable loss of detail on reproduction and additional fine structure features can easily be seen on the original plates (compare Fig. 1 (*a* and *b*) and the bands listed in Table III of our paper for phenyl alanine).

TABLE I.—FINE STRUCTURE BANDS IN THE ULTRA-

All substances examined at pH 6-8 by

Substances	Wave				
Foetal human haemoglobin . . .	—	—	—	2533±3	2588±5
Adult human haemoglobin . . .	—	—	—	2531±3	2588±3
Egg albumen (cryst.) .	—	—	—	2532	2591
Ox serum albumen (cryst.) . . .	—	—	—	2525	2585
Gelatin (sol) . .	—	—	—	2530	2581
Insulin . . .	—	—	—	2526	2585
Nucleohistone . .	—	—	—	—	—
Solubilized wool α-keratin . .	—	—	—	2523	2580
Lysozyme. . .	—	—	—	2521	2581
Chymotrypsin . .	—	—	—	2529	2581
Trypsin . . .	—	—	—	—	2583
Pepsin . . .	—	—	—	—	~2590
β-Phenylalanine .	(2350-66)*	2416±1	2466±1	2516-7	2575-6
Tyrosine . . .	—	—	—	—	—
Tryptophan . .	—	—	—	—	—

* Bands in parentheses are listed by McLaren (*loc. cit.*)

Comparison of (*a*) and (*b*) in Fig. 1 clearly shows the increased resolution of the band at 2610 Å at pH 12, which is present only as a very faint inflection at 2603 Å in acid and neutral solution. The spectrogram (*c*) for tyrosine at pH 6 shows the characteristic inflection at 2819 Å and the maximum at 2745 Å. The original plates also reveal a very slight inflection at *ca.* 2670 Å which has been observed by other workers (see McLaren (1949) for references). Fig. 1 (*d*) for tryptophan shows the well-resolved maximum at 2880 Å which is the most striking feature of logarithmic-cam spectrograms of polypeptides and proteins containing tryptophan, and which is very well suited for the study of the displacements to longer wavelengths which occur when the aromatic amino-acid residues are combined in peptide linkage and exist in certain molecular environments.

---

[4] Kratky and Schauenstein, *Z. Naturforsch.*, 1950, 5*b*, 281.

Table I gives the positions of the fine structure of a number of proteins, arranged to allow for comparison with the free aromatic amino acids. The correlation of the bands is fairly certain for phenylalanine, but less so for tyrosine and tryptophan due to overlapping in the 2700-2800 Å region. The long-wave maximum of tryptophan is easily identified, however, as it is well separated from the other tyrosine and tryptophan bands, both in the free amino acids and in proteins. The greatest long-wave shifts observed for this band are to 2916 Å in pepsin (Lavin and Northrop (1935) reported 2900 Å) and to 2914 Å for egg albumen (Coulter *et al.* (1936) reported 2923 Å). The discrepancies with the earlier results are most probably due to differences in experimental technique. In a very large number of observations with foetal and adult human haemoglobin, we have found it possible to locate the tryptophan fine-structure maximum with a precision of ± 1 Å, and we have been able to use the position of this maximum to estimate the proportions of adult- and foetal-type haemoglobins in foetal and early adult bloods.[5]

VIOLET ABSORPTION SPECTRA OF PROTEINS

the logarithmic-cam moving-plate method

length in Å

2618±2	2649±3	2686±6	2737±3	2787±5	2831±3	2898±1
2621±1	2649±2	2687±3	2739±2	2785±5	2835±10	2910±1
2622	2653	2691	2743	2803	2854	2914
—	2644	2682	2726	2781	2850	~2900
—	2639	2775	—	2755	2827	—
—	2645	2683	—	2762	2833	—
—	2642	2685	—	2755	2835	—
—	2641	2681	—	2759	2833	—
—	2635	2689	2741	—	2823	2911
2612	2640	2680	2741	—	2827	2911
—	2648	2687	—	—	2832	2909
—	~2655	—	—	—	~2840	2916
2603	2635	2673-4	(2715)	—	—	—
—	—	c2670	—	2745	2818	—
—	—	—	2710	—	2795	2880

but have not been observed in the present work

Supplementing the data in Table III of our paper on the effect of environment on the position of the tryptophan fine-structure maximum we have obtained the following results for a tryptophan dipeptide :

	λ_{max} (Å)
Tryptophan (free acid)	2880
Glycyl-tryptophan (in water) . . .	2890
,, ,, (in gelatin sol) . .	2890
,, ,, (in gelatin film) . .	2917

[5] Beaven, Hoch and Holiday, *Biochem. J.* (in press).

It is interesting to note that in a gelatin film the additional long-wave shift brings the tryptophan maximum to about the same position that it has in proteins.

Fig. 3 (*a*) shows the moving-plate spectrogram of a solution of egg albumen. The original plate reveals the fine-structure features of phenylalanine, tyrosine and tryptophan listed in Table I, and most of these are visible in the reproduction. For comparison, Fig. 5 (*b*) of our paper is a spectrogram of the same solution recorded on our automatic spectrophotometer, to show the superiority of the moving-plate method for the detection and location of fine structure.

With regard to the question of characteristic absorption by the "peptide grid", discussed by Prof. Schauenstein, we have given in our paper some evidence which, in our view, invalidates the earlier suggestion by Anslow on this subject. Some further criticisms of Anslow's more recent work are given in the Discussion on her contribution to this meeting. The evidence obtained by Schauenstein and his co-workers appears to be free from some of the experimental weaknesses of Anslow's work, but we are still not convinced that the alleged absorption of the polypeptide "fabric" or grid has been unequivocably demonstrated. For example, the net change in intensity of the "aromatic" absorption band of a protein on enzymic digestion is very small (and may be either positive or negative) even though the extent of degradation may be sufficient to cause a perceptible short-wave shift of the band, indicative of considerable reduction in complexity of the substrate relative to the nature protein. Such a change would be expected to result in considerable reduction in the "fabric" absorption.

In addition we suggest (for reasons given below) that the interpretation of ultra-violet absorption measurements of proteins in highly alkaline solution (pH 13) must be made with great caution, because of errors arising from apparent absorption caused by turbidity, which sometimes accompanies the slow alkaline denaturation that occurs under these conditions.

In view, however, of the importance of intra- and inter-chain hydrogen bonds in folded and extended proteins respectively (see Elliott and Ambrose, this Discussion, for references), and their role in the formation of the "peptenol" chromophore suggested by Schauenstein as the origin of the peptide "grid" absorption, we agree that the further investigation of this subject is of great importance.

In a personal discussion, Prof. Ketalaar stated that Havinga and Bruigom (Leiden, unpublished work) have observed that at pH 13 the absorption of some proteins increases with time, and pointed out that such behaviour could invalidate the spectrophotometric estimation of tyrosine and tryptophan in proteins. In our earlier analytical studies [6] such an effect was not observed, though it must be pointed out that the Spekker photometer used in this work was not well suited for the measurement of rapid changes in optical density at selected wavelengths, which can be done however with modern photo-electric spectrophotometers. In collaboration with Mr. R. G. S. Johns we are making a study of these time effects in the pH range 11-13.

The largest effects have so far been found for bovine plasma albumen, which in N/10 sodium hydroxide shows an apparent increase in optical density of *ca.* 12 % at 2900 Å and of *ca.* 17 % at 2800 Å during a period of 3 hr. at room temperature; simultaneously the low absorption outside the band, e.g. at 3500 Å, increases by some 30 %. Subsequently the absorption intensity within the band tends to decrease slightly while the low long-wave absorption continues to increase somewhat; filtration shows that a large proportion of this long-wave absorption is due to light-scattering by suspended material which was not present initially.

---

[6] Holiday and Ogston, *Biochem. J.*, 1938, **32**, 1166.

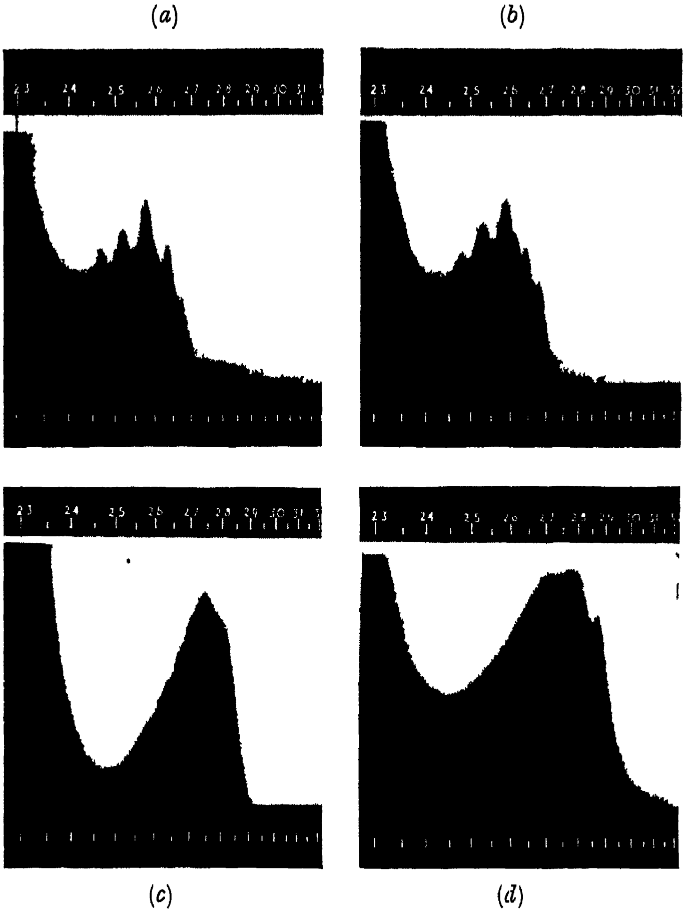

FIG. 1.—Logarithmic-cam, moving plate spectrograms.

(*a*) β-Phenylalanine (pH 6) (*c*) Tyrosine (pH 6)
(*b*) β-Phenylalanine (pH 12) (*d*) Tryptophan (pH 6)

Taken on Hilger medium quartz spectrograph (slit 0·15 mm.) with hydrogen arc source.

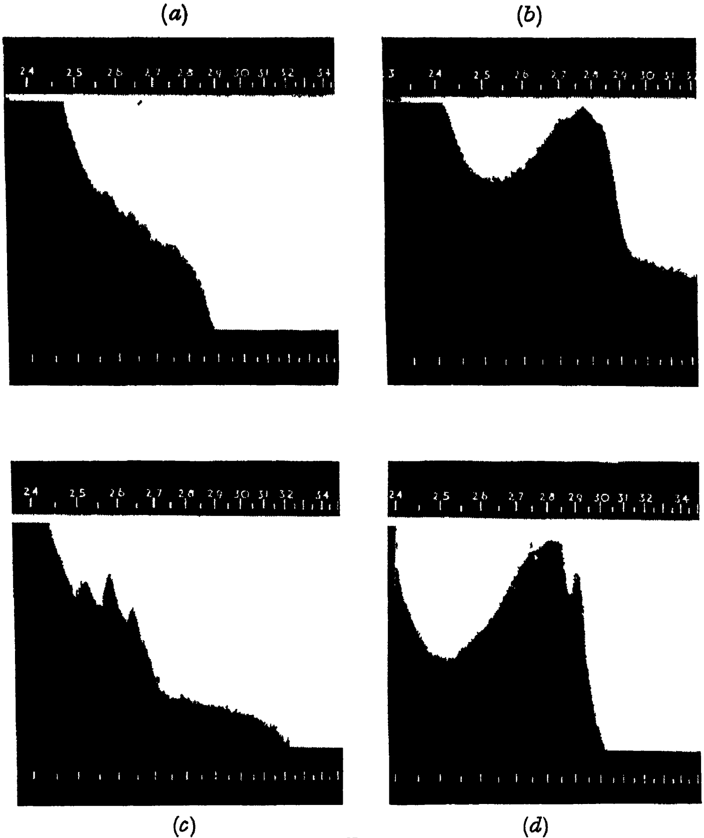

FIG. 2.

(a) Gelatin sol (pH 6)
(b) Insulin (pH 6)
(c) Polymyxin (pH 3)
(d) Gramicidin (in ethanol).

Experimental conditions as for Fig. 1.

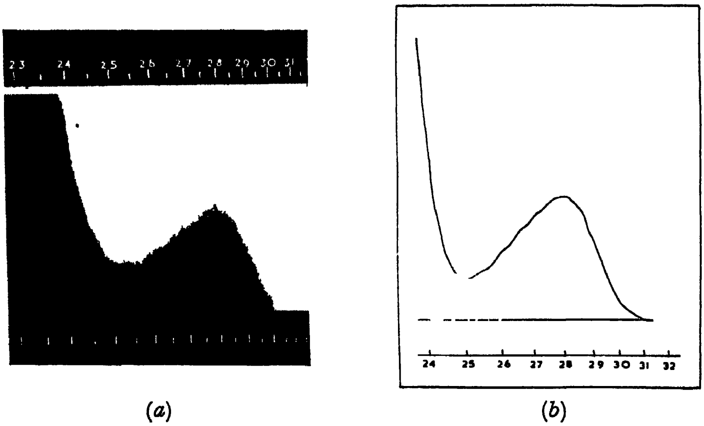

FIG. 3.—Egg albumen at pH 6.

(a) Logarithmic-cam, moving-plate spectrogram.

(b) Direct tracing of record from automatic spectrophotometer operated at 10 Å spectral band width. The ordinate of the record is linear in optical density and the abscissa is linear in wave number.

With bovine plasma albumen these time effects are very small at pH 10-11 but increase progressively at higher pH values ; above pH 12 the absorption probably increases significantly during the 1-2 min. required to make up the best solution and fill the cell.

Smaller time effects have been found with some other proteins ; at pH 13 and 2900 Å, horse serum albumen increases 3 % in 1 hr., and rabbit γ-globulin 5 % in 2 hr., both to steady values. Lysozyme does not alter at pH 13, and furthermore shows no low-intensity absorption outside the band.

Experiments with trypsin at pH 13 on an automatic recording spectrometer showed that the density at the maximum (2890 Å) does not increase more than 1 % up to 3 min. after mixing and then falls very slowly while the solution becomes visibly turbid.

Our tentative view is that these time effects are due to the breakdown of hydrogen bond structures involving tyrosine hydroxyl groups as envisaged by Neuberger and Crammer, on which are superposed more drastic irreversible changes associated with alkaline denaturation, such as the opening of S—S bonds which certainly occurs with bovine plasma albumen at pH 13. It is noteworthy that lysozyme, which shows no time effects at pH 13, is known to be very resistant to denaturation and its absorption spectrum changes with pH quite reversibly (up to N/10 alkali) provided that oxidation of the proteins does not occur.[7] In our experience this oxidation is revealed by the appearance of a new inflection in the alkaline absorption band at *ca.* 3030 Å, together with additional low-intensity absorption extending to the visible.

Further work will be required on other proteins to see if such alkaline time effects are of common occurrence and if they are of sufficient magnitude to invalidate the spectrophotometric estimation of tyrosine and tryptophan in nature proteins.

Prof. B. Commoner (*Washington University, Saint Louis*) said : The development by Dr. Engström of a method for determining the mass of cells and cell structures is an important contiibution to the problem of interpreting the data of visible and u.-v. absorption microspectrophotometry. Although microspectrophotometric measurements give estimates of the amount of certain substances present in an entire cell, it has until now been impossible to determine the proper denominator which should be used in comparing the content of two different cells. Concentration expressed as amount per unit cell volume is unsatifactory since in many cells the volume is subject to large alterations induced by osmotic phenomena. The obvious denominator required for such a quotient is dry weight, and until the development of Dr. Engstrom's elegant methods it was not possible to measure the dry weight of a cell *in situ*. Now by combining u.-v. and visible absorption measurements with X-ray absorption determinations it is possible to obtain for the first time a quotient which provides a valid means of comparing the composition of two different cells.

Dr. I. MacArthur (*Leeds University*) said : I would like to endorse Prof. Commoner's appreciation of the importance of Dr. Engström's work, which we at Leeds have followed with the greatest interest. In the alternative method of electron micro-analysis as developed by Ruthmann and by Hillier, a fine electron probe irradiates the specimen and the transmitted energy spectrum, resolved by a homogeneous magnetic *D*-analyzer, is found to be peaked by losses in positions (and magnitudes) indicating the atoms (and their concentrations) whose characteristic X-ray levels have been excited. *K* levels of C, N, O, Be, Al, Si and *L* and *M* levels of Fe are typical. While the technique was well advanced several years ago in respect of resolution, supply control, and minimal quantity assayable ($\sim 10^{-14}$ g.), I gather from Dr. Le Poole that Dr.

---

[7] Fromageot and Schnek, *Biochem. Biophys. Acta*, 1950, **6**, 113.

Hillier has some reservations as to its future and scope. At present Engström's method is quantitatively the more developed; one difficulty is to secure an X-ray λ spectrum to give maximum general efficiency.

Prof. B. Commoner (*Washington University, Saint Louis*) said: By failing to consider the effect of the geometry of living fibroblasts on the u.-v. absorption spectra of these cells, Walker and Davies have, I believe, fallen into errors which appear to invalidate certain of their quantitative conclusions.

The extinctions which they report for the nucleus and nucleolus of intact fibroblasts cannot with any degree of precision be assigned to these structures. Since the nucleus is embedded in the cytoplasm of the cell, the extinctions which they assign to the nucleus are in fact not due to that structure alone but to the added absorption of the nucleus and two layers of cytoplasm. The values reported by Walker and Davies as extinctions of the nucleolus are in actual fact the absorption due to the nucleolus plus the absorption of two layers of cytoplasm and the depth of the nucleus not occupied by the nucleolus. Consequently, the absorption spectra shown in their Fig. 5, which are supposed to represent the nucleus and nucleolus respectively, do not in fact describe the u.-v. absorption characteristics of these structures. Similarly, the absorption spectra shown in their Fig. 7 do not necessarily show the changes in the absorption characteristics of the nucleus induced by radiation. In the absence of additional information it would be of equal validity to ascribe the changes shown in this figure to differences in the absorption of the overlying cytoplasm before and after irradiation.

One may, of course, argue that since the tissue-cultured fibroblast is very flat, only a negligible amount of cytoplasm lies over and under the nucleus and that the absorption of this thin layer may be safely ignored. This is an unwarranted assumption. Since Walker and Davies have not obtained data on the distribution of the u.-v. absorbing material in a given optical section of the cytoplasm the possibility exists that a significant fraction of the total absorbing material in such a section is concentrated near the cell surface. They state that the optical density of the cytoplasm of a living fibroblast may be greater than that of the "nucleus" (actually, nucleus plus the surface cytoplasm layers) and the optical density of the cytoplasmic layers over and under the nucleus might therefore approach that of the nucleus itself. Walker and Davies conclude that the amount of u.-v. absorbing material in the nucleus decreases "to about 70 % of its initial value" after irradiation. From this statement, one must conclude that the authors feel that their values for the extinctions of nuclei are accurate to at least 30 % of the initial measurement. It seems to me that an error of at least 30 % may be involved in their neglect of the absorption due to the cytoplasmic layers, and that their conclusion concerning the changes due to irradiation is therefore open to serious question.

The errors in the extinctions which Walker and Davies ascribe to the nucleolus arising from their neglecting to consider geometric factors must be large indeed. In this case the nucleus contributes a depth of absorbing material equivalent to or greater than the nucleolus itself, and the extinctions attributed to the nucleolus must be too high by a factor of at least 50 %.

As has been pointed out in my own contribution to this Discussion, it is possible to obtain the actual absorption spectrum of the nucleus of certain intact living cells. This cannot be done as Walker and Davies have attempted to do, by measuring a single absorption spectrum through an optical section which includes the nucleus. *Three* absorption spectra must be measured to provide data which lead to the calculation of the absorption spectrum of the nucleus itself. A minimum of *five* absorption spectra would be required for determination of the absorption spectrum of the nucleolus.

Finally, it is even questionable these methods would be applicable to a cell such as the fibroblast in which accurate measurements of the thickness of various absorbing layers must be exceedingly difficult. The entire procedure might be defeated by random changes in the distribution of the u.-v. absorbing material in the cytoplasm. It might, in fact, be literally impossible to obtain from such a cell absorption spectra which can be validly ascribed to the nucleus or to the nucleolus.

This pessimistic conclusion raises a question which appears to me to merit serious discussion at this point in the development of the field of microspectrophotometry: What are the purposes of microspectrophotometric studies of cells and cell structures? It, as I have attempted to show, certain types of measurements can be made only on the relatively rare cells which are blessed with regular geometrical characteristics, then it may be necessary that the overall strategical aims of microspectrophotometry be approached in such a manner as to permit their being investigated in cells of this favourable type. On the other hand, re-examination of the aims of microspectrophotometry might reveal (as Dr. Barer has suggested) that in many instances only qualitative results are required. In such instances, measurements of the absorption of cells such as fibroblasts would be useful, but to avoid reaching unwarranted conclusions, we would need to make the frank admission that the data are only qualitative.

Mr. P. M. B. Walker (*Biophysics Res. Unit, King's College, London*) (*communicated*): The contributions to this Discussion illustrate the two aspects of an apparent dilemma with which we are faced in working with living cells. The thicker cells, such as those used by Commoner, give the possibility of accurately measuring the dimensions along the microscope axis, but the volume measured is less well defined in the plane at right-angles to the microscope axis, owing to the larger measuring spot consequent on the usually higher extinction and the biconical illuminating beam.[8] The very much thinner tissue-culture cell which we have used enables us to define more closely the dimensions in the object plane, at the expense of some uncertainty regarding the exact relative thicknesses. Living cells are, however, heterogeneous in all three dimensions and are in continual motion. It therefore seems likely that, although the shape of the absorption curves may give information about the kind of constituent, the exact value of the extinction at a particular wavelength for a small area of a cell cannot give any very valuable information *unless* it is clearly related spatially to the morphology of the cell, and temporally to stages in the cell's development which were not stated in our case. For these reasons we were careful to draw only two conclusions from absorption curves illustrated in our paper. These were that an extinction maximum near 265 mμ similar to that found in fixed material was also found in the living, and that there was negligible absorption at 312 mμ. Since the shape of the two curves were similar both to themselves and to that obtained for the cytoplasm (unpublished), neither of these conclusions are invalidated by considerations of relative path length.

A second criticism has been directed against our deliberate neglect of absorption due to the over- and under-lying cytoplasm in our integration measurements over the nucleus during irradiation. While it is very difficult to make accurate measurements of the thickness of these cytoplasmic layers the following observations lead us to believe that these are probably small compared to the thickness of the nucleus (see also Fell and Hughes [9]).

(i) Within the projected area of the nucleus, two thin layers containing a few small granules may be observed at the extreme focusing position, up and down, at which *any* material can be focused in the whole cell. Just within these extremes definite nuclear components such as the nucleolus may be focused.

---

[8] Thorell, this Discussion.

[9] Fell and Hughes, *Quart. J. Microsc. Soc.*, 1949, **90**, 362, 274.

(ii) The thickness of the cytoplasm measured near the projected area of the nucleus is similar to that measured through the nuclear area. The cytoplasmic thickness declines towards the periphery. Time lapse films show a relatively rigid nucleus surrounded by a more fluid cytoplasm which, together with its constituents, flows round the nuclear area. These three observations suggest the model of the rigid nucleus pushing apart the membranes of a more fluid cytoplasm, the whole cell growing on the interface of the quartz and liquid medium.

There remains the possibility that the bulk of the absorption measured in the cytoplasm resides near the cell membrane. This does not appear to be true as our measurements of absorption show a progressive decline towards the periphery, which can be correlated with the decrease in thickness measured in the phase microscope. A loss of 30 % of absorption within the nuclear projected area, due to loss in the over- and underlying cytoplasm, which might occur if the absorption was indeed residing near the cell boundary would be almost certainly reflected in the rest of the cytoplasm, and yet Plate II, Fig. *a* and *b*, and measurements, show no great change in the cytoplasm. However, it is precisely between these stages that the maximum change in nuclear absorption occurs. Furthermore, when the cytoplasmic absorption is lost to the " bleb " between exposures 40 and 90, no significant drop occurs in the amount of absorbing substance present within the nuclear projected area.

Finally, may we reiterate that the biological point we sought to establish was that no fundamental change in the chemical or physical state of the absorbing substances need be assumed to account for the great increase in optical density observed during irradiation, independent of any explanation assigned to the comparatively small decrease in the amount of absorbing substances in the area measured.

Dr. E. M. F. Roe (*Chester Beatty Res. Inst., London*) said : At the beginning of our discussions in this section it was stated that we wished to know the quantitative accuracy with which it is possible to carry out these investigations. I must confess that I am still no clearer than at the beginning, and that I share Dr. Commoner's puzzlement on this point. Is it a quantitative, a semi-quantitative or a qualitative picture which we can expect in such experiments ? Four years ago I spent some weeks in Prof. Caspersson's laboratory and since then have thought seriously about this apparatus, for as a chemical spectroscopist in the cancer field one is naturally interested in such a tool.

It seems clear that we should expect a number of limitations to the application of this technique. Firstly, the chemical spectroscopist who is accustomed to examining solutions of pure materials in a Beckman absorption cell can usually assign a particular band system to a particular molecular structure with some confidence. But our limited knowledge of the absorption spectroscopy of complexes and colloidal solutions, such as we expect to find in living tissue, should make us cautious in assigning absorption bands in cellular material to specific molecules. The classical studies of Sheppard and the more recent work of other investigators, exemplified by that described in Dr. Holiday's contribution, show that small or large wavelength shifts in bands may occur or entirely new bands may appear on complex, or micelle, formation. More work of this kind is needed. Secondly, our knowledge of the optical conditions necessary for accurate work in this field is still extremely limited ; optical theory lags behind desired applications. Dr. Barer's contribution was most valuable in raising the problem of the type of instrument needed for quantitative work ; we are waiting for objectives of the aspherized reflecting type as most likely to satisfy the optical requirements of this part of the apparatus. Thirdly, the object to be examined, in any biological investigation, limits the application of this technique and the accuracy attainable. It should be pointed out that Dr. Commoner's *Coleus* leaf hair cells and Dr. Wilkins' hexagonal tobacco mosaic virus crystals in the leaf hairs of the tobacco plant are rather special and relatively simple objects, and it by no means follows that conditions may be found for the investigation of most biological objects, as has been suggested. The kind of material in which we are interested is, e.g., the fresh cells from fowl tumour caused by Rous virus (u.-v. micrographs taken with 1·25 N.A. glycerine immersion quartz monochromat, corrected 2536 Å). The problems caused by the geometry of the cells, cytoplasmic material overlying the nucleus, differences in apparent absorption at nuclear boundaries and in cytoplasmic and nuclear structures where dimensions are of the order of the wavelength of light used, and which vary with the focus and may be due, at least in part, to changes in refractive index, or to diffraction or light scatter—all this makes it difficult to see clearly how to investigate, e.g. variations in purine-pyrimidine content in these cells. And they are by no means atypical biological objects.

On the other hand, there are trends in the results obtained by my friends from Caspersson's laboratory, e.g. in nucleic acid investigations in tissues, which make one wonder whether many of those errors actually cancel out in practice, or are much less important in practice than in theory. This is possible. Frankly, I do not know, but I am sure we must be cautious in the claims we make for the accuracy of results in this field.

Dr. B. Thorell (*Stockholm*) said: With the optics used by Commoner as stated in his paper (condenser aperture 1·25, grey objective × 53, N.A. 0·7) not all the light passing through the measurement area is collected. In the calculations on the differences in light path a cylindrical section has been assumed. But in measurements using a beam of light with an aperture as stated, there is a biconical form of the light beam passing through the cell. It can be calculated that with a circular area of 5 μ diameter scanned in the centre of a 30 μ thick part of the cell, the light beam passing through that area will section the upper and lower cell wall by an area of 50 μ in diameter.

In the curves obtained, for instance Fig. 7, from which Commoner had calculated the absorption spectrum for the vacuole and for the protoplast layer, it can be seen that the peaks consist of points differing by between 98·0 % and 98·7 % in absorption. If, now, the light output from the mercury lamp alone is varying about 2 %, is the accuracy of the measurement so high that one can calculate something from these maxima ?

Prof. B. Commoner (*Washington University, St. Louis*) (*communicated*): Dr. Thorell's comments concerning the light path in my measurements are based on the disparity between the N.A. of the condenser and the objective. In actual practice, of course, the condenser is stopped down to match the objective, and the difficulties described by Dr. Thorell are not encountered.

Dr. Thorell's statement that the light output of the mercury lamp varies by about 2 % does not coincide with the statement actually made in my contribution to this Discussion : the variation is 0·2 %. This is accomplished by use of a voltage stabilizer and selected lamps.

Dr. D. F. Cole (*Birmingham*) said: I must express my doubts as to the velocity of the second statistical method employed to estimate the significance of the results in Catchpole and Gersh's paper. On the second page of the paper the authors state that " when all values of all animals in each group . . . are treated as if they were from a single animal . . ." certain differences appear to be significant. It is not stated how large the groups in the class treated with butter-yellow were, but those in the central class were in groups of five. It seems doubtful whether it is justifiable to compound the intra-class variance with the group variances in such a way as to derive a larger number of degrees of freedom for the estimate of significance.

Unfortunately the details of the experimental grouping are not given and so it is not possible to say with certainty which of the two statistical methods is valid. Personally, it seems that this treatment which is referred to elsewhere as "more liberal" may not be valid.

Dr. B. Thorell (*Stockholm*) said: In the type of material used by Catchpole and Gersh, i.e. sectioned fixed tissue cells, the single extinction values at 2652 and 2804 Å mean very little as regards concentrations of nucleic acids. My experience from liver cells fixed with freeze-drying is that by far the greatest part of *E* is non-specific losses of light. Moreover, the inhomogenous distribution of absorbing substances within, for instance, the liver cytoplasm causes a serious departure from the photometric relationships, especially when using as large a measurement area as 1 μ diam. A simple calculation gives a 20-30 % difference simply due to inhomogenous distribution.

Also I cannot agree that these authors have tested Lambert's law, as the specific nucleic acid absorption is responsible for only a small part of the light losses measured in the 1-4 μ sections. What has been shown is that scattering, etc., plus nucleic acid absorption is roughly proportional to layer thickness from 1 to 4 μ.

As can be seen from the results, hepatoma tissue (solid cancer type) is an inconvenient material for this type of macrochemical analyses. Even with microscopical control it is hardly possible to state how much of a sample taken for analysis consists of actively growing, infiltrating cancer cells and how much consists of cells with degenerative changes. Even in an actively infiltrating cancer cord there are only two or three cell layers without morphological signs of degenerative changes. The results of these authors, viz., fall in desoxynucleic acid, higher water content, smaller cytoplasmic particles, etc., might be due to changes in the direction of necrobiosis.

Finally, I would like to say that there is no doubt that the approach to the analysis of intracellular nucleic acid distribution at different functional states, using cytochemical techniques, combined with biochemical procedures, is very valuable. Much work will have to be done along these lines in order to reveal the chemical organization of the cell.

Dr. H. R. Catchpole and **Dr. I. Gersh** (*University of Illinois*) (*communicated*): It is difficult, if not impossible, at the present time, to correct transmission readings for light scatter at 2652 Å and 2804 Å, in view of the indeterminate range of particle size. We have, however, nowhere been concerned with absolute values for nucleic acids or proteins. Consideration of light scatter, if this indeed be a large part of the apparent absorption, could enter into our comparisons in only two ways: (i) the increased values indicated in tumour cells must represent a change in the physical state of the protoplasm giving rise consistently to increased light scatter after freezing at − 150° C, drying in vacuum, embedding in paraffin, sectioning, and treatment with chloroform, alcohol and lanthanum-glycerol, or (ii) the "nucleoprotein" changes which we find in tumour cells are greater than indicated if the conditions responsible for light scatter remain the same for normal and tumour cells. We consider neither alternative very likely.

Material studied with the ultra-violet microscope was taken from the same masses chosen for biochemical studies. It was examined also by routine histological methods, and necrosis was not a prominent feature in the material used.

There seems to be some question as to the suitability of liver and hepatoma for this type of combined biochemical and ultra-violet absorption study. While we often wished that hepatoma would show some properties more dramatic than slow, inexorable growth, nevertheless, in our opinion it remains the most suitable organ for study because of the relative uniformity and simplicity of the cells and their contents.

Prof. B. Commoner (*Washington University, Saint Louis*) said: Dr.

Catchpole states that his tissue sections were 4 μ thick, that the average diameter of the nucleus was 5-6 μ, and that of the nucleolus about 1 μ. This being the case, it is apparent that absorption measurements made " through the nucleolus " must include in addition to the absorption of that structure, the absorption of about 3 μ of the nucleus. Yet, the extinctions of these complex sections are reported by Catchpole and Gersh (their Table I) as representing the extinction of the nucleolus alone. This is in my opinion not a valid interpretation of the extinctions which they have obtained. Without further data on the distribution of the absorbing material in the nucleus, it is not possible to decide what part of the absorption which they ascribe to the nucleolus is in fact due to that structure and what fraction arises from absorption by the nuclear material in which the nucleolus lies.

Dr. Bradfield states that the effect of the surrounding nuclear material on the supposed extinction of the nucleolus is negligible because the absorbing material of the nucleus is largely restricted to its surface layer, which is cut off by the planes of the 4 μ sections (the nucleus being 5-6 μ in diameter). Rather than answering the objection which I have raised Dr. Bradfield has, I fear, impaled himself on the other horn of the dilemma. If the large part of the absorbing material of the nucleus has been removed with the upper and lower sections cut away from the 5 μ sphere, then the meaning of the extinctions assigned by Catchpole and Gersh to the *nucleus* is very much in doubt. The point can be made, that the absorption of the nuclear sap is being measured, that the investigation was concerned with comparative measurements of normal and tumour nuclei, and that both types of nuclei have been subjected to the same sectioning procedure, thus allowing " relative " comparisons between them to be made. This procedure can hardly be expected to yield data of biological significance, for it is like throwing the baby away and analyzing the composition of the bath water.

Dr. H. R. Catchpole and **Dr. I. Gersh** (*University of Illinois*) (*communicated*) : The figures given to Dr. Commoner should be corrected as follows : the smallest nucleolus was about 4 μ and the smallest nucleus about 8 μ. It was entirely feasible to select cells in which the factor of overlay was negligible. Unlike the appearance of the nucleus after the use of fixatives, the nuclear contents in frozen-dried material are not concentrated around the nuclear membrane.

Dr. R. Barer (*Oxford*) said : The paper by Bradfield and that by Walker and Davies are interesting examples of how results of real biological value may be obtained by a qualitative approach. We now have a very good morphological picture of what may happen during u.-v. irradiation, and an excellent illustration of the difficulties of working on living cells.

In Bradfield's paper it should be pointed out that what is being measured is not strictly the *absorption* but the *transmission* of the specimen, i.e. no correction has been made for non-specific light-losses. It is possible to suggest another explanation for the observed effects in terms of variations in light scattering. If u.-v. irradiation results in a swelling, aggregation or coalescence of small particles into larger groups there may be an apparent decrease in absorption. If on the other hand large particles are broken down or formation of new granules occurs then there may be an apparent increase in absorption. Such an explanation would, I believe, fit in quite well with some of the effects observed. A change in refractive index, with or without a change in particle size, should also be considered.

Dr. I. MacArthur (*Leeds University*) said : Small-angle diffuse X-ray scattering might serve as an independent check on change in the refractive component. Variations in the two senses suggested by Dr. Barer (particle → subparticle → quasi-liquid structure) have been so revealed for vaccinia and in alginate cationic exchange.

Dr. B. Thorell (*Stockholm*) said : I would like to make some remarks in order to avoid misunderstanding of the part of my earlier work which Bradfield has cited in his paper. Dealing with the ultra-violet absorption of immature bone-marrow cells, the irradiation effect described by him was marked in many cases and much work on absorption measurements had to be discarded. As I remember, it was also stated in the text " that the object should not be illuminated unnecessarily, as then it is soon cytolyzed ", the term cytolysis including any discoverable change in morphology and optical properties during the irradiation which could be checked on the photographic plates. It is interesting, however, to have Bradfield's proper analyses of these (from my point of view) inconvenient effects, especially as he has thereby found a tool for studying the behaviour of SH-groups. It is a pity that he has not given the amount of energy falling on to the cell, or any data from which this could be roughly estimated.

Dr. J. R. G. Bradfield (*Cambridge*) (*communicated*) : I had not thought to put my comments in print, but find it necessary to reply to Prof. Commoner, Dr. Barer and Dr. Thorell.

Prof. Commoner's neo-Euclidean approach and his colourful analogies regarding infant ablutions are indeed refreshing. Like most colourful analogies, however, that of Prof. Commoner has little or no relevance to the supposed problem arising from the paper of Dr. Catchpole and Dr. Gersh. Nor indeed could it have, for the problem does not exist. Those who are not unduly cabined, cribbed and confined by geometry will know that it is quite easy to select those nucleoli in liver sections which are not obscured by overlying or underlying chromatin (as is clearly stated by Catchpole and Gersh). Moreover, even if the difficulty could not be readily overcome in this way, it would be simple to cut thin sections down to, say, $\frac{1}{2}\mu$ (with the thin-sectioning modification of the Cambridge rocking-microtome) and thus obtain unobjectionable sections through nucleoli. Similarly with regard to the other horn of the imaginary dilemma—either by selecting suitably sliced nuclei (which is what Catchpole and Gersh did), or by thin sections, one can readily surmount difficulties from which the mathematical mind turns helpless away.

Indeed, if anyone has impaled himself on the horns of a dilemma, it is Prof. Commoner. In order to prove that his cells were alive, Prof. Commoner emphasizes that *Euglena* maintained its characteristic flowing motion and that protoplasmic streaming continued in *Tradescantia* hairs throughout the eleven measurements at different wavelengths. In our experience, a very small cell movement completely invalidates any absorption measurements in progress, unless the area under study can be exactly returned to its previous position relative to the microscope. Exactly the same difficulty of re-examining the same spot applies to his 7-hr. time-lapse comparison in Fig. 3. Moreover it is noteworthy that measurements were made on areas 5 μ in diameter. In other words, 25 times more light was available for measurement than in studies on areas 1 μ in diameter, which may partly explain why absorption curves could be obtained without apparent protoplasmic damage. Where possible, low intensity measurements on large areas are obviously very desirable, but in a cylinder of protoplasm as large as 5 μ in diameter and 22-60 μ in depth there may well be all sorts of mutually-cancelling absorption changes during measurement. Possibly these difficulties regarding cell-movement and the like may eventually be overcome, but until then it seems that these procedures " can hardly be expected to yield data of biological significance "—unless the final absorption curves represent only statistical approximations for the nucleus as a whole or the cytoplasm as a whole, in which case Prof. Commoner would be knee-deep in bath water.

One admires the way in which Prof. Commoner has been able to distinguish between the absorptions of different components in certain plant cells, but as he points out elsewhere this approach becomes quite impossible with cells as inconveniently shaped as fibroblasts and the same is true of most cells which one wants to examine. It is easy to cut the Gordian knot, however, for the simple reason that the vast majority of animal cells must be examined in the *fixed* state; they cannot be satisfactorily kept alive *in vitro*. Examination of fixed material brings its own problems (some similar to those found with our own living bone-marrow cells, as Catchpole and Gersh point out), but at least Prof. Commoner's geometrical headaches can be dispelled by cutting suitable thin sections.

Dr. Barer is correct apropos of absorption and transmission and is right to emphasize the other possible explanations of our rise in nuclear transmission in bone-marrow cells, though I suspect that, in the present state of the evidence, William of Ockham's razor would wreak havoc among his suggestions. We listed five possibilities and only pointed out which of these was most completely in accordance with the experimental evidence. When there is a simultaneous rise in nuclear transmission and fall in cytoplasmic transmission and when one knows that nucleoproteins or their derivatives can pass through nuclear membranes and do leak from other cells after u.-v. irradiation, it seems reasonable to believe that leakage from nucleus to cytoplasm has in fact occurred. But whether leakage or aggregation proves to be correct, the conclusion that SH groups have a considerable effect on the behaviour of nucleoproteins remains unaffected.

As stated in the text, I have the highest regard for Dr. Thorell's studies on the growth of bone marrow cells. We studied these cells simply for convenience. It is indeed unfortunate that only photochemical and not photo-electric methods were available to us for measurement of light intensity. In any case, however, no thorough quantitative studies have been made *in vitro* of the u.-v. depolymerization of ribo- and desoxyribonucleoproteins, so that precise measurements of light intensity would not have helped us to elucidate the cell physiology underlying the changes observed—and this was of course our objective.

It is very appropriate that at a Discussion such as this there should be much debate regarding instruments and techniques, but since there has also been so much heart-searching as to the aims and *raison d'être* of microspectrography I must add that there seem to me to be a hundred and one important and interesting problems awaiting study by this method, which could be made to yield valid and significant biological results even with the limited techniques available at present.

AUTHOR INDEX[*]

Ambrose, E. J., 246, 324.
Anslow, Gladys A., 299, 333.
Axford, D. W. E., 210.
Barer, R., 369, 383, 391, 491, 501.
Barrow, R. F., 81.
Beaven, G. H., 406, 492.
Boyd, D. R. J., 154.
Bradfield, J. R. G., 481, 502.
Brown, J. K., 144, 261.
Burawoy, A., 70, 73, 78.
Burgess, A. R., 75.
Catchpole, H. R., 471, 500, 501.
Cave, W. T., 35.
Cole, D. F., 499.
Commoner, B., 395, 449, 495, 496, 499, 500.
Coté, G. L., 209.
Coulson, C. A., 1, 209.
Craig, D. P., 5, 69.
Cross, L. H., 235, 323.
Darmon, S. E., 251, 325.
Davies, H. G., 397, **442, 461.**
Davies, Mansel, 212, 325, 332, **335.**
Elliott, A., 246, 324.
Engström, Arne, 427.
Eyk, B. J. van, 291.
Franck, J., 73.
Fraser, R. D. B., 131, 378, 398.
Gersh, Isidore, 471, 500, 501.
Goldfinger, R., 81.
Gore, R. C., 138.
Guggenheimer, K. M., 221.
Hammond, V. J., 53.
Haszeldine, R. N., 78.
Herington, E. F. G., 26.
Herzberg, G., 80, **92,** 207.
Holiday, E. R., 332, **406,** 492.
Holliday, P., 325.
Hornig, D. F., 115, 209.
Hydén, Holger, 436.
Jones, A. Vallance, 281.
Jope, E. M., 406, 423.
Kasha, M., 14, 70, 74, 75.
Kastler, A., 69, 209.
Keohane, K. W., 388.
Ketelaar, J. A. A., 211, 213, **291,** 328, 333.
Kletz, T. A., 211, 393.
Leach, S., 81.
Lecomte, Jean, 125, 213, 215.
Lenormant, H., 319.
Liang, Ching-yu, 177.
Lindström, Bo, 436.
Longuet-Higgins, H. C., 131.
Lounsbury, Mackenzie, 196.
MacArthur, I., 495, 501.
McKean, D. C., 323.
Mathieu, Jean-Paul, 196.
Mecke, R., 75, **161,** 207, 213, 215, 327, 328.
Mellors, R. C., 398.
Minkoff, J. G., 320.
Nicholson, D. L., 222.
Nielsen, Harald H., 85.
Nielsen, J. Rudd, 78, **177,** 215
Nordheim, Gertrud P., 19.
Norris, K. P., 360.
Perutz, M. F., 423.
Pestemer, M., 213.
Pickett, Lucy W., 80.
Plyler, Earle K., 100.
Porter, George, 60, 81.
Price, W. C., 53, 131.
Pullman, Alberte, 46.
Pullman, Bernard, 46.
Ramsay, D. A., 80.
Randall, J. T., 353.
Rank, D. H., 187, 219.
Reynolds, J. G., 322.
Reid, C., 92.
Richards, R. B., 235.
Robin, S., 82.
Robinson, T. S., 131.
Roe, E. M. F., 498.
Romand, J., 214.
Rudall, K. M., 251.
Saksena, B. D., 187.
Salomon, G., 291, 329, 331.
Schauenstein, E., 491.
Schee, A. Chr. van der, 291.
Seeds, W. E., 394, **417.**
Sheppard, N., 144, 210, 216, **261,** 322, 328, 329, 331.
Short, L. N., 222.
Shull, E. R., 187.
Simpson, D. M., 216, **261,** 328.
Smith, D. C., 177.
Sponer, H., 19, 69, 76, 77.
Sutherland, G. B. B. M., 207, 216, **274, 281,** 319, 320, 324, 329.
Teegan, J. P., 53.
Thomas, Orville, 220, **335, 339.**
Thompson, H. W., 35, 77, **82, 154,** 208, 209, **222,** 327.
Thorell, Bo, 432, 499, 500, 502.
Torkington, P., 212, 319, 327, 328, 330, 331.
Ubbelohde, A. R., 213.
Vodar, B., 82, 214.
Walker, P. M. B., 461, 497.
Walsh, A. D., 53.
Wilkins, M. H. F., 360, 363, 390, 394, 396, **417.**
Williams, R., 154.
Willis, H. A., 235, 321.
Wilson, E. Bright, 108.

[*] The references in heavy type indicate papers submitted for discussion.